DRUGS AND THE PHARMACEUTICAL SCIENCES VOLUME 186

Handbook of Drug Metabolism

Second Edition

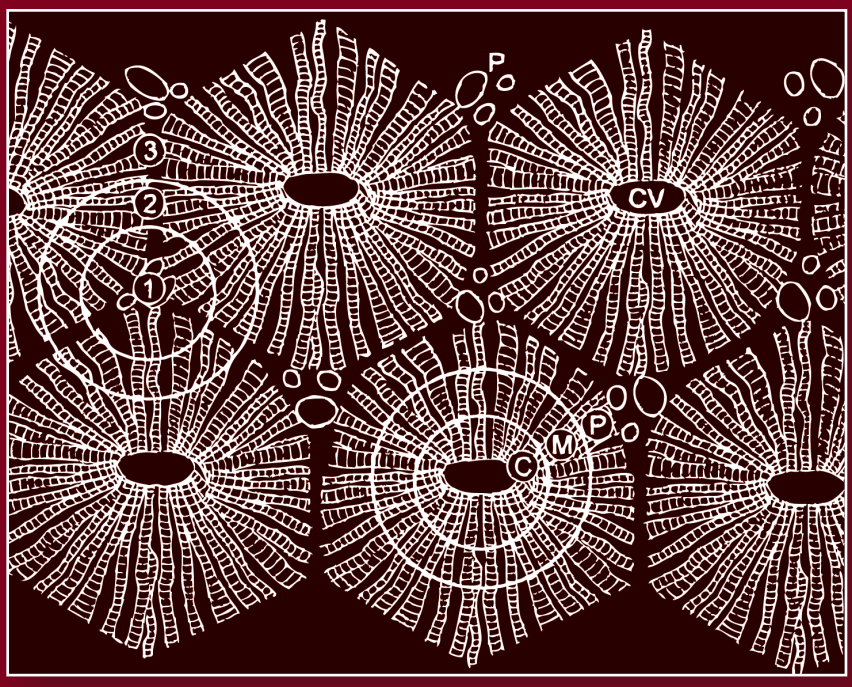

edited by
Paul G. Pearson
Larry C. Wienkers

informa
healthcare

Handbook of Drug Metabolism

DRUGS AND THE PHARMACEUTICAL SCIENCES
A Series of Textbooks and Monographs

Executive Editor

Advisory Board

1. Pharmacokinetics, *Milo Gibaldi and Donald Perrier*
2. Good Manufacturing Practices for Pharmaceuticals: A Plan for Total Quality Control, *Sidney H. Willig, Murray M. Tuckerman, and William S. Hitchings IV*
3. Microencapsulation, *edited by J. R. Nixon*
4. Drug Metabolism: Chemical and Biochemical Aspects, *Bernard Testa and Peter Jenner*
5. New Drugs: Discovery and Development, *edited by Alan A. Rubin*
6. Sustained and Controlled Release Drug Delivery Systems, *edited by Joseph R. Robinson*
7. Modern Pharmaceutics, *edited by Gilbert S. Banker and Christopher T. Rhodes*
8. Prescription Drugs in Short Supply: Case Histories, *Michael A. Schwartz*
9. Activated Charcoal: Antidotal and Other Medical Uses, *David O. Cooney*
10. Concepts in Drug Metabolism (in two parts), *edited by Peter Jenner and Bernard Testa*
11. Pharmaceutical Analysis: Modern Methods (in two parts), *edited by James W. Munson*
12. Techniques of Solubilization of Drugs, *edited by Samuel H. Yalkowsky*
13. Orphan Drugs, *edited by Fred E. Karch*
14. Novel Drug Delivery Systems: Fundamentals, Developmental Concepts, Biomedical Assessments, *Yie W. Chien*
15. Pharmacokinetics: Second Edition, Revised and Expanded, *Milo Gibaldi and Donald Perrier*
16. Good Manufacturing Practices for Pharmaceuticals: A Plan for Total Quality Control, Second Edition, Revised and Expanded, *Sidney H. Willig, Murray M. Tuckerman, and William S. Hitchings IV*
17. Formulation of Veterinary Dosage Forms, *edited by Jack Blodinger*
18. Dermatological Formulations: Percutaneous Absorption, *Brian W. Barry*
19. The Clinical Research Process in the Pharmaceutical Industry, *edited by Gary M. Matoren*
20. Microencapsulation and Related Drug Processes, *Patrick B. Deasy*
21. Drugs and Nutrients: The Interactive Effects, *edited by Daphne A. Roe and T. Colin Campbell*
22. Biotechnology of Industrial Antibiotics, *Erick J. Vandamme*
23. Pharmaceutical Process Validation, *edited by Bernard T. Loftus and Robert A. Nash*
24. Anticancer and Interferon Agents: Synthesis and Properties, *edited by Raphael M. Ottenbrite and George B. Butler*
25. Pharmaceutical Statistics: Practical and Clinical Applications, *Sanford Bolton*
26. Drug Dynamics for Analytical, Clinical, and Biological Chemists, *Benjamin J. Gudzinowicz, Burrows T. Younkin, Jr., and Michael J. Gudzinowicz*
27. Modern Analysis of Antibiotics, *edited by Adjoran Aszalos*
28. Solubility and Related Properties, *Kenneth C. James*
29. Controlled Drug Delivery: Fundamentals and Applications, Second Edition, Revised and Expanded, *edited by Joseph R. Robinson and Vincent H. Lee*
30. New Drug Approval Process: Clinical and Regulatory Management, *edited by Richard A. Guarino*
31. Transdermal Controlled Systemic Medications, *edited by Yie W. Chien*

32. Drug Delivery Devices: Fundamentals and Applications, *edited by Praveen Tyle*
33. Pharmacokinetics: Regulatory ● Industrial ● Academic Perspectives, *edited by Peter G. Welling and Francis L. S. Tse*
34. Clinical Drug Trials and Tribulations, *edited by Allen E. Cato*
35. Transdermal Drug Delivery: Developmental Issues and Research Initiatives, *edited by Jonathan Hadgraft and Richard H. Guy*
36. Aqueous Polymeric Coatings for Pharmaceutical Dosage Forms, *edited by James W. McGinity*
37. Pharmaceutical Pelletization Technology, *edited by Isaac Ghebre-Sellassie*
38. Good Laboratory Practice Regulations, *edited by Allen F. Hirsch*
39. Nasal Systemic Drug Delivery, *Yie W. Chien, Kenneth S. E. Su, and Shyi-Feu Chang*
40. Modern Pharmaceutics: Second Edition, Revised and Expanded, *edited by Gilbert S. Banker and Christopher T. Rhodes*
41. Specialized Drug Delivery Systems: Manufacturing and Production Technology, *edited by Praveen Tyle*
42. Topical Drug Delivery Formulations, *edited by David W. Osborne and Anton H. Amann*
43. Drug Stability: Principles and Practices, *Jens T. Carstensen*
44. Pharmaceutical Statistics: Practical and Clinical Applications, Second Edition, Revised and Expanded, *Sanford Bolton*
45. Biodegradable Polymers as Drug Delivery Systems, *edited by Mark Chasin and Robert Langer*
46. Preclinical Drug Disposition: A Laboratory Handbook, *Francis L. S. Tse and James J. Jaffe*
47. HPLC in the Pharmaceutical Industry, *edited by Godwin W. Fong and Stanley K. Lam*
48. Pharmaceutical Bioequivalence, *edited by Peter G. Welling, Francis L. S. Tse, and Shrikant V. Dinghe*
49. Pharmaceutical Dissolution Testing, *Umesh V. Banakar*
50. Novel Drug Delivery Systems: Second Edition, Revised and Expanded, *Yie W. Chien*
51. Managing the Clinical Drug Development Process, *David M. Cocchetto and Ronald V. Nardi*
52. Good Manufacturing Practices for Pharmaceuticals: A Plan for Total Quality Control, Third Edition, *edited by Sidney H. Willig and James R. Stoker*
53. Prodrugs: Topical and Ocular Drug Delivery, *edited by Kenneth B. Sloan*
54. Pharmaceutical Inhalation Aerosol Technology, *edited by Anthony J. Hickey*
55. Radiopharmaceuticals: Chemistry and Pharmacology, *edited by Adrian D. Nunn*
56. New Drug Approval Process: Second Edition, Revised and Expanded, *edited by Richard A. Guarino*
57. Pharmaceutical Process Validation: Second Edition, Revised and Expanded, *edited by Ira R. Berry and Robert A. Nash*
58. Ophthalmic Drug Delivery Systems, *edited by Ashim K. Mitra*
59. Pharmaceutical Skin Penetration Enhancement, *edited by Kenneth A. Walters and Jonathan Hadgraft*
60. Colonic Drug Absorption and Metabolism, *edited by Peter R. Bieck*

61. Pharmaceutical Particulate Carriers: Therapeutic Applications, *edited by Alain Rolland*
62. Drug Permeation Enhancement: Theory and Applications, *edited by Dean S. Hsieh*
63. Glycopeptide Antibiotics, *edited by Ramakrishnan Nagarajan*
64. Achieving Sterility in Medical and Pharmaceutical Products, *Nigel A. Halls*
65. Multiparticulate Oral Drug Delivery, *edited by Isaac Ghebre-Sellassie*
66. Colloidal Drug Delivery Systems, *edited by Jörg Kreuter*
67. Pharmacokinetics: Regulatory • Industrial • Academic Perspectives, Second Edition, *edited by Peter G. Welling and Francis L. S. Tse*
68. Drug Stability: Principles and Practices, Second Edition, Revised and Expanded, *Jens T. Carstensen*
69. Good Laboratory Practice Regulations: Second Edition, Revised and Expanded, *edited by Sandy Weinberg*
70. Physical Characterization of Pharmaceutical Solids, *edited by Harry G. Brittain*
71. Pharmaceutical Powder Compaction Technology, *edited by Göran Alderborn and Christer Nyström*
72. Modern Pharmaceutics: Third Edition, Revised and Expanded, *edited by Gilbert S. Banker and Christopher T. Rhodes*
73. Microencapsulation: Methods and Industrial Applications, *edited by Simon Benita*
74. Oral Mucosal Drug Delivery, *edited by Michael J. Rathbone*
75. Clinical Research in Pharmaceutical Development, *edited by Barry Bleidt and Michael Montagne*
76. The Drug Development Process: Increasing Efficiency and Cost Effectiveness, *edited by Peter G. Welling, Louis Lasagna, and Umesh V. Banakar*
77. Microparticulate Systems for the Delivery of Proteins and Vaccines, *edited by Smadar Cohen and Howard Bernstein*
78. Good Manufacturing Practices for Pharmaceuticals: A Plan for Total Quality Control, Fourth Edition, Revised and Expanded, *Sidney H. Willig and James R. Stoker*
79. Aqueous Polymeric Coatings for Pharmaceutical Dosage Forms: Second Edition, Revised and Expanded, *edited by James W. McGinity*
80. Pharmaceutical Statistics: Practical and Clinical Applications, Third Edition, *Sanford Bolton*
81. Handbook of Pharmaceutical Granulation Technology, *edited by Dilip M. Parikh*
82. Biotechnology of Antibiotics: Second Edition, Revised and Expanded, *edited by William R. Strohl*
83. Mechanisms of Transdermal Drug Delivery, *edited by Russell O. Potts and Richard H. Guy*
84. Pharmaceutical Enzymes, *edited by Albert Lauwers and Simon Scharpé*
85. Development of Biopharmaceutical Parenteral Dosage Forms, *edited by John A. Bontempo*
86. Pharmaceutical Project Management, *edited by Tony Kennedy*
87. Drug Products for Clinical Trials: An International Guide to Formulation • Production • Quality Control, *edited by Donald C. Monkhouse and Christopher T. Rhodes*

88. Development and Formulation of Veterinary Dosage Forms: Second Edition, Revised and Expanded, *edited by Gregory E. Hardee and J. Desmond Baggot*
89. Receptor-Based Drug Design, *edited by Paul Leff*
90. Automation and Validation of Information in Pharmaceutical Processing, *edited by Joseph F. deSpautz*
91. Dermal Absorption and Toxicity Assessment, *edited by Michael S. Roberts and Kenneth A. Walters*
92. Pharmaceutical Experimental Design, *Gareth A. Lewis, Didier Mathieu, and Roger Phan-Tan-Luu*
93. Preparing for FDA Pre-Approval Inspections, *edited by Martin D. Hynes III*
94. Pharmaceutical Excipients: Characterization by IR, Raman, and NMR Spectroscopy, *David E. Bugay and W. Paul Findlay*
95. Polymorphism in Pharmaceutical Solids, *edited by Harry G. Brittain*
96. Freeze-Drying/Lyophilization of Pharmaceutical and Biological Products, *edited by Louis Rey and Joan C. May*
97. Percutaneous Absorption: Drugs–Cosmetics–Mechanisms–Methodology, Third Edition, Revised and Expanded, *edited by Robert L. Bronaugh and Howard I. Maibach*
98. Bioadhesive Drug Delivery Systems: Fundamentals, Novel Approaches, and Development, *edited by Edith Mathiowitz, Donald E. Chickering III, and Claus-Michael Lehr*
99. Protein Formulation and Delivery, *edited by Eugene J. McNally*
100. New Drug Approval Process: Third Edition, The Global Challenge, *edited by Richard A. Guarino*
101. Peptide and Protein Drug Analysis, *edited by Ronald E. Reid*
102. Transport Processes in Pharmaceutical Systems, *edited by Gordon L. Amidon, Ping I. Lee, and Elizabeth M. Topp*
103. Excipient Toxicity and Safety, *edited by Myra L. Weiner and Lois A. Kotkoskie*
104. The Clinical Audit in Pharmaceutical Development, *edited by Michael R. Hamrell*
105. Pharmaceutical Emulsions and Suspensions, *edited by Francoise Nielloud and Gilberte Marti-Mestres*
106. Oral Drug Absorption: Prediction and Assessment, *edited by Jennifer B. Dressman and Hans Lennernäs*
107. Drug Stability: Principles and Practices, Third Edition, Revised and Expanded, *edited by Jens T. Carstensen and C. T. Rhodes*
108. Containment in the Pharmaceutical Industry, *edited by James P. Wood*
109. Good Manufacturing Practices for Pharmaceuticals: A Plan for Total Quality Control from Manufacturer to Consumer, Fifth Edition, Revised and Expanded, *Sidney H. Willig*
110. Advanced Pharmaceutical Solids, *Jens T. Carstensen*
111. Endotoxins: Pyrogens, LAL Testing, and Depyrogenation, Second Edition, Revised and Expanded, *Kevin L. Williams*
112. Pharmaceutical Process Engineering, *Anthony J. Hickey and David Ganderton*
113. Pharmacogenomics, *edited by Werner Kalow, Urs A. Meyer and Rachel F. Tyndale*

114. Handbook of Drug Screening, *edited by Ramakrishna Seethala and Prabhavathi B. Fernandes*
115. Drug Targeting Technology: Physical • Chemical • Biological Methods, *edited by Hans Schreier*
116. Drug–Drug Interactions, *edited by A. David Rodrigues*
117. Handbook of Pharmaceutical Analysis, *edited by Lena Ohannesian and Anthony J. Streeter*
118. Pharmaceutical Process Scale-Up, *edited by Michael Levin*
119. Dermatological and Transdermal Formulations, *edited by Kenneth A. Walters*
120. Clinical Drug Trials and Tribulations: Second Edition, Revised and Expanded, *edited by Allen Cato, Lynda Sutton, and Allen Cato III*
121. Modern Pharmaceutics: Fourth Edition, Revised and Expanded, *edited by Gilbert S. Banker and Christopher T. Rhodes*
122. Surfactants and Polymers in Drug Delivery, *Martin Malmsten*
123. Transdermal Drug Delivery: Second Edition, Revised and Expanded, *edited by Richard H. Guy and Jonathan Hadgraft*
124. Good Laboratory Practice Regulations: Second Edition, Revised and Expanded, *edited by Sandy Weinberg*
125. Parenteral Quality Control: Sterility, Pyrogen, Particulate, and Package Integrity Testing: Third Edition, Revised and Expanded, *Michael J. Akers, Daniel S. Larrimore, and Dana Morton Guazzo*
126. Modified-Release Drug Delivery Technology, *edited by Michael J. Rathbone, Jonathan Hadgraft, and Michael S. Roberts*
127. Simulation for Designing Clinical Trials: A Pharmacokinetic-Pharmacodynamic Modeling Perspective, *edited by Hui C. Kimko and Stephen B. Duffull*
128. Affinity Capillary Electrophoresis in Pharmaceutics and Biopharmaceutics, *edited by Reinhard H. H. Neubert and Hans-Hermann Rüttinger*
129. Pharmaceutical Process Validation: An International Third Edition, Revised and Expanded, *edited by Robert A. Nash and Alfred H. Wachter*
130. Ophthalmic Drug Delivery Systems: Second Edition, Revised and Expanded, *edited by Ashim K. Mitra*
131. Pharmaceutical Gene Delivery Systems, *edited by Alain Rolland and Sean M. Sullivan*
132. Biomarkers in Clinical Drug Development, *edited by John C. Bloom and Robert A. Dean*
133. Pharmaceutical Extrusion Technology, *edited by Isaac Ghebre-Sellassie and Charles Martin*
134. Pharmaceutical Inhalation Aerosol Technology: Second Edition, Revised and Expanded, *edited by Anthony J. Hickey*
135. Pharmaceutical Statistics: Practical and Clinical Applications, Fourth Edition, *Sanford Bolton and Charles Bon*
136. Compliance Handbook for Pharmaceuticals, Medical Devices, and Biologics, *edited by Carmen Medina*
137. Freeze-Drying/Lyophilization of Pharmaceutical and Biological Products: Second Edition, Revised and Expanded, *edited by Louis Rey and Joan C. May*
138. Supercritical Fluid Technology for Drug Product Development, *edited by Peter York, Uday B. Kompella, and Boris Y. Shekunov*

139. New Drug Approval Process: Fourth Edition, Accelerating Global Registrations, *edited by Richard A. Guarino*
140. Microbial Contamination Control in Parenteral Manufacturing, *edited by Kevin L. Williams*
141. New Drug Development: Regulatory Paradigms for Clinical Pharmacology and Biopharmaceutics, *edited by Chandrahas G. Sahajwalla*
142. Microbial Contamination Control in the Pharmaceutical Industry, *edited by Luis Jimenez*
143. Generic Drug Product Development: Solid Oral Dosage Forms, *edited by Leon Shargel and Isadore Kanfer*
144. Introduction to the Pharmaceutical Regulatory Process, *edited by Ira R. Berry*
145. Drug Delivery to the Oral Cavity: Molecules to Market, *edited by Tapash K. Ghosh and William R. Pfister*
146. Good Design Practices for GMP Pharmaceutical Facilities, *edited by Andrew Signore and Terry Jacobs*
147. Drug Products for Clinical Trials, Second Edition, *edited by Donald Monkhouse, Charles Carney, and Jim Clark*
148. Polymeric Drug Delivery Systems, *edited by Glen S. Kwon*
149. Injectable Dispersed Systems: Formulation, Processing, and Performance, *edited by Diane J. Burgess*
150. Laboratory Auditing for Quality and Regulatory Compliance, *Donald Singer, Raluca-Ioana Stefan, and Jacobus van Staden*
151. Active Pharmaceutical Ingredients: Development, Manufacturing, and Regulation, *edited by Stanley Nusim*
152. Preclinical Drug Development, *edited by Mark C. Rogge and David R. Taft*
153. Pharmaceutical Stress Testing: Predicting Drug Degradation, *edited by Steven W. Baertschi*
154. Handbook of Pharmaceutical Granulation Technology: Second Edition, *edited by Dilip M. Parikh*
155. Percutaneous Absorption: Drugs–Cosmetics–Mechanisms–Methodology, Fourth Edition, *edited by Robert L. Bronaugh and Howard I. Maibach*
156. Pharmacogenomics: Second Edition, *edited by Werner Kalow, Urs A. Meyer and Rachel F. Tyndale*
157. Pharmaceutical Process Scale-Up, Second Edition, *edited by Michael Levin*
158. Microencapsulation: Methods and Industrial Applications, Second Edition, *edited by Simon Benita*
159. Nanoparticle Technology for Drug Delivery, *edited by Ram B. Gupta and Uday B. Kompella*
160. Spectroscopy of Pharmaceutical Solids, *edited by Harry G. Brittain*
161. Dose Optimization in Drug Development, *edited by Rajesh Krishna*
162. Herbal Supplements-Drug Interactions: Scientific and Regulatory Perspectives, *edited by Y. W. Francis Lam, Shiew-Mei Huang, and Stephen D. Hall*
163. Pharmaceutical Photostability and Stabilization Technology, *edited by Joseph T. Piechocki and Karl Thoma*
164. Environmental Monitoring for Cleanrooms and Controlled Environments, *edited by Anne Marie Dixon*
165. Pharmaceutical Product Development: In Vitro-In Vivo Correlation, *edited by Dakshina Murthy Chilukuri, Gangadhar Sunkara, and David Young*

166. Nanoparticulate Drug Delivery Systems, *edited by Deepak Thassu, Michel Deleers, and Yashwant Pathak*
167. Endotoxins: Pyrogens, LAL Testing and Depyrogenation, Third Edition, *edited by Kevin L. Williams*
168. Good Laboratory Practice Regulations, Fourth Edition, *edited by Anne Sandy Weinberg*
169. Good Manufacturing Practices for Pharmaceuticals, Sixth Edition, *edited by Joseph D. Nally*
170. Oral-Lipid Based Formulations: Enhancing the Bioavailability of Poorly Water-soluble Drugs, *edited by David J. Hauss*
171. Handbook of Bioequivalence Testing, *edited by Sarfaraz K. Niazi*
172. Advanced Drug Formulation Design to Optimize Therapeutic Outcomes, *edited by Robert O. Williams III, David R. Taft, and Jason T. McConville*
173. Clean-in-Place for Biopharmaceutical Processes, *edited by Dale A. Seiberling*
174. Filtration and Purification in the Biopharmaceutical Industry, Second Edition, *edited by Maik W. Jornitz and Theodore H. Meltzer*
175. Protein Formulation and Delivery, Second Edition, *edited by Eugene J. McNally and Jayne E. Hastedt*
176. Aqueous Polymeric Coatings for Pharmaceutical Dosage Forms, Third Edition, *edited by James McGinity and Linda A. Felton*
177. Dermal Absorption and Toxicity Assessment, Second Edition, *edited by Michael S. Roberts and Kenneth A. Walters*
178. Preformulation Solid Dosage Form Development, *edited by Moji C. Adeyeye and Harry G. Brittain*
179. Drug-Drug Interactions, Second Edition, *edited by A. David Rodrigues*
180. Generic Drug Product Development: Bioequivalence Issues, *edited by Isadore Kanfer and Leon Shargel*
181. Pharmaceutical Pre-Approval Inspections: A Guide to Regulatory Success, Second Edition, *edited by Martin D. Hynes III*
182. Pharmaceutical Project Management, Second Edition, *edited by Anthony Kennedy*
183. Modified Release Drug Delivery Technology, Second Edition, Volume 1, *edited by Michael J. Rathbone, Jonathan Hadgraft, Michael S. Roberts, and Majella E. Lane*
184. Modified-Release Drug Delivery Technology, Second Edition, Volume 2, *edited by Michael J. Rathbone, Jonathan Hadgraft, Michael S. Roberts, and Majella E. Lane*
185. The Pharmaceutical Regulatory Process, Second Edition, *edited by Ira R. Berry and Robert P. Martin*
186. Handbook of Drug Metabolism, Second Edition, *edited by Paul G. Pearson and Larry C. Wienkers*

Handbook of Drug Metabolism

Second Edition

edited by

Paul G. Pearson

Pearson Pharma Partners
Westlake Village, California, USA

Larry C. Wienkers

Amgen, Inc.
Seattle, Washington, USA

informa
healthcare

New York London

Informa Healthcare USA, Inc.
52 Vanderbilt Avenue
New York, NY 10017

Informa Healthcare is an Informa business

No claim to original U.S. Government works
Printed in the United States of America on acid free paper
10 9 8 7 6 5 4 3 2 1

International Standard Book Number 10: 1 4200 7647 7(Hardcover)
International Standard Book Number 13: 978 1 4200 7647 9(Hardcover)

Library of Congress Cataloging-in-Publication Data

Handbook of drug metabolism. 2nd ed. / edited by Paul G. Pearson, Larry C. Wienkers.
p. ; cm. (Drugs and the pharmaceutical sciences; v. 186)
Includes bibliographical references and index.
ISBN 13: 978 1 4200 7647 9 (hardcover : alk. paper)
ISBN 10: 1 4200 7647 7 (hardcover : alk. paper)
1. Drugs Metabolism Handbooks, manuals, etc. I. Pearson, Paul G. (Paul Gerard), 1960 II. Wienkers, Larry C. III. Series.
[DNLM: 1. Pharmaceutical Preparations metabolism. W1 DR893B v.186 2008/QV 38 H23655 2008]
RM301.55.H36 2008
615′.7 dc22

2008035272

For Corporate Sales and Reprint Permissions call 212-520-2700 or write to: Sales Department, 52 Vanderbilt Avenue, 7th floor, New York, NY 10017.

Visit the Informa Web site at
www.informa.com

and the Informa Healthcare Web site at
www.informahealthcare.com

Preface

It is almost a decade since the first edition of the *Handbook of Drug Metabolism* was published. The goal of the first edition was to provide a comprehensive text to serve as a graduate course in Drug Metabolism, a useful reference for academic and industrial drug metabolism scientists, but also to serve as an important reference tool for those pursuing a career in drug metabolism. The second edition of the *Handbook of Drug Metabolism* has been completely updated to capture a decade of advances in our understanding of factors that impact the pharmacokinetics and metabolism of therapeutic agents in humans. Moreover, we have sought to include new chapters that reflect significant advances that have occurred in seven major areas, viz. analytical methodologies, pharmacokinetics, biotransformation reactions, molecular biology, pharmacogenetics, drug interactions, and transgenic animals.

The second edition of the *Handbook of Drug Metabolism* is organized into four parts. The first three parts capture scientific and experimental concepts around drug metabolism. Part I reviews fundamental aspects of drug metabolism, including a history of drug metabolism, a review of oxidative and nonoxidative biotransformation mechanisms, a review of liver structure and function, and pharmacokinetics of drugs metabolites. Part II details factors that impact drug metabolism including pharmacogenetics, drug-drug interactions, and the role of extrahepatic organs in drug biotransformation. Part III provides in depth insights into analytical technologies and methodologies to study drug metabolism at the molecular, subcellular, and cellular levels, and considerations of factors, viz. enzyme inhibition and induction that influence drug metabolism and therapeutic response. Part IV has been expanded substantially from the first edition to illustrate the highly integrated role of drug metabolism in drug discovery and drug development. In this regard, Part IV focuses on clinical and preclinical drug metabolism studies and safety considerations for drug metabolites (chemically reactive and nonreactive metabolites) in the selection and development of promising therapeutic candidates, and highlights the increased focus of regulatory agencies on safety considerations of drug metabolites.

This book is dedicated to two groups of exceptional individuals. First, we thank the distinguished academic and industrial leaders (many of whom have contributed to this book) who have trained a generation, or more, of high-quality drug metabolism scientists. Second, we thank the many graduate students, postdoctoral fellows, and industrial colleagues who have challenged us and enriched our lives over the last two decades. We thank all of you for advancing the field of drug metabolism; your efforts have enabled our

discipline to advance promising therapeutic agents with increased probability of success in finding medicines to treat serious illness.

Lastly, it has been a privilege to interact with this collection of expert authors, and we would like to express our sincere gratitude to them for their contributions to this second edition of the *Handbook of Drug Metabolism*.

Paul G. Pearson, Ph.D.
Larry C. Wienkers, Ph.D.

Contents

PART IV: APPLICATIONS OF METABOLISM STUDIES IN DRUG DISCOVERY AND DEVELOPMENT

Contributors

Upendra A. Argikar Novartis Pharmaceuticals, Cambridge, Massachusetts, U.S.A.

Thomas A. Baillie Department of Drug Metabolism and Pharmacokinetics, Merck Research Laboratories, Rahway, New Jersey, and West Point, Pennsylvania, U.S.A.

Jordan C. Bell Department of Biochemistry and Molecular Biology, The University of Texas Medical School at Houston, Houston, Texas, U.S.A.

Ian A. Blair Centers for Cancer Pharmacology and Excellence in Environmental Toxicology, Department of Pharmacology, University of Pennsylvania, Philadelphia, Pennsylvania, U.S.A.

Shu-Ying Chang Pharmaceutical Candidate Optimization, Bristol-Myers Squibb, Princeton, New Jersey, U.S.A.

Ann K. Daly Institute of Cellular Medicine, Newcastle University Medical School, Framlington Place, Newcastle upon Tyne NE2 4HH, U.K.

Felix A. de la Iglesia Department of Pathology, University of Michigan Medical School and Michigan Technology and Research Institute, Ann Arbor, Michigan, U.S.A.

Leslie J. Dickmann Pharmacokinetics and Drug Metabolism, Amgen Inc., Seattle, Washington, U.S.A.

Stacy L. Gelhaus Centers for Cancer Pharmacology and Excellence in Environmental Toxicology, Department of Pharmacology, University of Pennsylvania, Philadelphia, Pennsylvania, U.S.A.

F. Peter Guengerich Department of Biochemistry and Center in Molecular Toxicology, Vanderbilt University School of Medicine, Nashville, Tennessee, U.S.A.

Jeffrey R. Haskins Cellular Imaging & Analysis, Thermo Fisher Scientific, Pittsburgh, Pennsylvania, U.S.A.

Colin J. Henderson Cancer Research UK Molecular Pharmacology Unit, Biomedical Research Institute, University of Dundee, Ninewells Hospital and Medical School, Dundee, Scotland, U.K.

Kirk R. Henne Department of Pharmacokinetics and Drug Metabolism, Amgen Inc., South San Francisco, California, U.S.A.

Ronald N. Hines Departments of Pediatrics and Pharmacology and Toxicology, Medical College of Wisconsin, and Children's Research Institute, Children's Hospital and Health Systems, Milwaukee, Wisconsin, U.S.A.

Sanjeev Kumar Department of Drug Metabolism and Pharmacokinetics, Merck Research Laboratories, Rahway, New Jersey, U.S.A.

Lawrence H. Lash Department of Pharmacology, Wayne State University School of Medicine, Detroit, Michigan, U.S.A.

Jiunn H. Lin Department of Drug Metabolism and Pharmacokinetics, Merck Research Laboratories, West Point, Pennsylvania, U.S.A.

John C. Lindon Department of Biomolecular Medicine, Imperial College London, South Kensington, London, U.K.

Michael A. Mohutsky Lilly Research Laboratories, Eli Lilly & Company, Indianapolis, Indiana, U.S.A.

Carrie M. Mosher Department of Medicinal Chemistry, University of Washington, Seattle, Washington, U.S.A.

Patrick J. Murphy College of Pharmacy and Health Sciences, Butler University, Indianapolis, Indiana, U.S.A.

Jeremy K. Nicholson Department of Biomolecular Medicine, Imperial College London, South Kensington, London, U.K.

R. Scott Obach Department of Pharmacokinetics, Pharmacodynamics, and Drug Metabolism, Pfizer Global Research and Development, Groton, Connecticut, U.S.A.

Paul R. Ortiz de Montellano Department of Pharmaceutical Chemistry, School of Pharmacy, University of California, San Francisco, California, U.S.A.

Mary F. Paine Division of Pharmacotherapy and Experimental Therapeutics, School of Pharmacy, University of North Carolina, Chapel Hill, North Carolina, U.S.A.

William F. Pool Department of Pharmacokinetics, Dynamics, and Metabolism, Pfizer Global Research and Development, San Diego, California, U.S.A.

Thomayant Prueksaritanont Department of Drug Metabolism and Pharmacokinetics, Merck Research Laboratories, West Point, Pennsylvania, U.S.A.

Christopher A. Reilly Department of Pharmacology and Toxicology, University of Utah, Salt Lake City, Utah, U.S.A.

Rory P. Remmel Department of Medicinal Chemistry, College of Pharmacy, University of Minnesota, Minneapolis, Minnesota, U.S.A.

Allan E. Rettie Department of Medicinal Chemistry, University of Washington, Seattle, Washington, U.S.A.

Barbara J. Ring Lilly Research Laboratories, Eli Lilly & Company, Indianapolis, Indiana, U.S.A.

Dan Rock Department of Pharmacokinetics and Drug Metabolism, Amgen Inc., Seattle, Washington, U.S.A.

A. David Rodrigues Pharmaceutical Candidate Optimization, Bristol-Myers Squibb, Princeton, New Jersey, U.S.A.

Kevin L. Salyers Pharmacokinetics and Drug Metabolism, Amgen Inc., Thousand Oaks, California, U.S.A.

Nico Scheer TaconicArtemis GmbH, Cologne, Germany

Michael Schrag Department of Drug Metabolism, Array BioPharma Inc., Boulder, Colorado, U.S.A.

Michael W. Sinz Bristol-Myers Squibb Co., Wallingford, Connecticut, U.S.A.

J. Greg Slatter Pharmacokinetics and Drug Metabolism, Amgen Inc., Seattle, Washington, U.S.A.

Philip C. Smith School of Pharmacy, University of North Carolina at Chapel Hill, Chapel Hill, North Carolina, U.S.A.

Henry W. Strobel Department of Biochemistry and Molecular Biology, The University of Texas Medical School at Houston, Houston, Texas, U.S.A.

George R. Tonn Department of Pharmacokinetics and Drug Metabolism, Amgen Inc., South San Francisco, California, U.S.A.

Robert L. Walsky Department of Pharmacokinetics, Pharmacodynamics, and Drug Metabolism, Pfizer Global Research and Development, Groton, Connecticut, U.S.A.

Ying Wang Department of Biochemistry and Molecular Biology, The University of Texas Medical School at Houston, Houston, Texas, U.S.A.

Larry C. Wienkers Department of Pharmacokinetics and Drug Metabolism, Amgen Inc., Seattle, Washington, U.S.A.

Ian D. Wilson Departments of Clinical Pharmacology, Drug Metabolism and Pharmacokinetics, AstraZeneca, Macclesfield, Cheshire, U.K.

C. Roland Wolf Cancer Research UK Molecular Pharmacology Unit, Biomedical Research Institute, University of Dundee, Ninewells Hospital and Medical School, Dundee, Scotland, U.K.

Bradley K. Wong Department of Pharmacokinetics and Drug Metabolism, Amgen Inc., South San Francisco, California, U.S.A.

Steven A. Wrighton Lilly Research Laboratories, Eli Lilly & Company, Indianapolis, Indiana, U.S.A.

Ming Yao Pharmaceutical Candidate Optimization, Bristol-Myers Squibb, Princeton, New Jersey, U.S.A.

Garold S. Yost Department of Pharmacology and Toxicology, University of Utah, Salt Lake City, Utah, U.S.A.

Donglu Zhang Pharmaceutical Candidate Optimization, Bristol-Myers Squibb, Princeton, New Jersey, U.S.A.

Jin Zhou Department of Medicinal Chemistry, College of Pharmacy, University of Minnesota, Minneapolis, Minnesota, U.S.A.

Mingshe Zhu Pharmaceutical Candidate Optimization, Bristol-Myers Squibb, Princeton, New Jersey, U.S.A.

1

The Evolution of Drug Metabolism Research

Patrick J. Murphy
College of Pharmacy and Health Sciences, Butler University, Indianapolis, Indiana, U.S.A.

INTRODUCTION

Drug metabolism research has grown from a desire to understand the workings of the human body in chemical terms to a major force in the effort to develop drugs tailored to the individual. This essay will trace the beginnings of what are now major branches of drug metabolism to provide some background to the current state of the art represented in the many chapters of this book.

CHEMISTRY—MAJOR METABOLIC ROUTES

In 1828, the laboratory of Friedrich Woehler was abuzz with the synthesis of urea, the first "organic" synthetic achievement. Woehler then turned his attention to potential chemical transformations in the body. He had been interested in compounds found in urine since his undergraduate days, and when Liebig identified hippuric acid as a normal urinary product, Woehler suggested that it might be formed from benzoic acid and glycine in the body. His initial experiments in dogs, however, were inconclusive (1). Alexander Ure, a physician seeking a cure for gout, heard about Woehler's idea and reasoned that if it was correct then administration of benzoic acid to man might lead to a diminished excretion of urea due to the use of nitrogen in the glycine conjugate. Ure took benzoic acid and isolated hippuric acid from his urine (2). Woehler had his associate Keller repeat the experiment and confirmed that ingested benzoic acid was indeed excreted in the urine as hippuric acid (3).

These studies initiated a period lasting to the end of the century where scientists and their collaborators subjected themselves to interesting molecules to "see what would happen." Many of the studies followed logical extensions of the earlier work.

Erdmann and Marchand administered cinnamic acid to volunteers and isolated a product tentatively identified as hippuric acid (4,5). They proposed that the cinnamic acid was oxidized to benzoic acid and then conjugated with glycine. Woehler and Friederick Frerichs confirmed this transformation in dogs (6). They also showed that benzaldehyde was converted to hippuric acid in dogs and rabbits.

The oxidation of benzene to phenol was discovered by the clinician Bernhard Naunyn during the course of experimental treatment of stomach "fermentation" with benzene. He was surprised to find that phenol was excreted following the administration of benzene. Naunyn then collaborated with the chemist, Schultzen, to study the fate of a number of hydrocarbons, including toluene, xylene, and larger molecules (7). Aromatic hydroxylation, which had proven difficult for the chemists of the day, was readily accomplished in humans.

Studies on aromatic hydroxylation led Stadeler to discover conjugated phenols in human and animal urine (8). Munk, after ingesting varying amounts of benzene, monitored the excretion of "phenol-forming substance" in his urine by hydrolyzing the urine with acid and measuring the released phenol (9).

Baumann, using the color of indigo as his guide, purified an indigo-forming substance from urine and showed that upon hydrolysis both indigo and sulfate were released (10). Baumann made many pioneering studies on sulfates formed from a variety of compounds including, catechol, bromobenzene, indole, and aniline.

The surprising ability of the body to methylate compounds was discovered by His in 1887 when he was able to isolate and identify *N*-methyl pyridinium hydroxide from the urine of dogs dosed with pyridine (11). Over 60 years later, MacLagan and Wilkinson discovered the more significant *O*-methylation pathway using the phenol butyl-4-hydroxy 3,5 diiodobenzoate (12). This is the pathway that led Axelrod to his Nobel Prize related to the methylation of catecholamines.

N-Acetylation was first described by Cohn in his studies on the fate of m-nitrobenzaldehyde. The oxidized, reduced compound is acetylated and conjugated with glycine to yield the hippurate of *N*-acetyl m-aminobenzoic as a major metabolite (13).

Mercapturic acids were initially isolated in the laboratories of Baumann and Preuss studying the fate of bromobenzene and by Jaffe looking at chloro and iodobenzene (14,15). The actual structure of these acetyl cysteine conjugates was determined by Baumann in 1884 (16). The nature of the cofactors in the conjugation reactions would not be known until the 20th century.

A unique, primarily human, conjugation of glutamine with aryl acetic acids was discovered by Thierfelder and Sherwin in 1914 (17).

ACTIVE METABOLITES

By the early part of the 20th century the major drug-metabolizing reactions had been identified. A unifying theory on the role of metabolism was developed by John Paxson Sherwin. Sherwin was one of the most prominent Americans in the field of metabolism (18). A native of Bristol, Indiana, he was educated in Indiana and Illinois and then spent two years in Tubingen, Germany, before returning to the Midwest. He formulated the "chemical defense" theory elaborated in his reviews on drug metabolism in 1922, 1933, and 1935 (19 21). The latter two reviews carried the title "Detoxication Mechanisms." This same title was used by R.T. Williams in his groundbreaking summaries of drug metabolism in 1947 and 1959 (22). Although Williams was troubled with the general classification of all metabolic reactions as "detoxication," he accepted it as the most practical appellation. A mind-set that metabolism led to detoxication was so logical and

had so many examples that when a compound was actually made more active, it engendered disbelief. But even at this early stage of drug development the examples of activation began to accumulate.

The world's first major drug, arsphenamine (Fig. 1), an arsenical used for the treatment of syphilis, was ineffective in vitro (23). Twelve years after its launch, studies showing that the drug worked through an oxidation product were published by Voegtlin and coworkers (24). This compound, which evolved from the "magic bullet" concept of Ehrlich, set the stage for future worldwide "blockbusters."

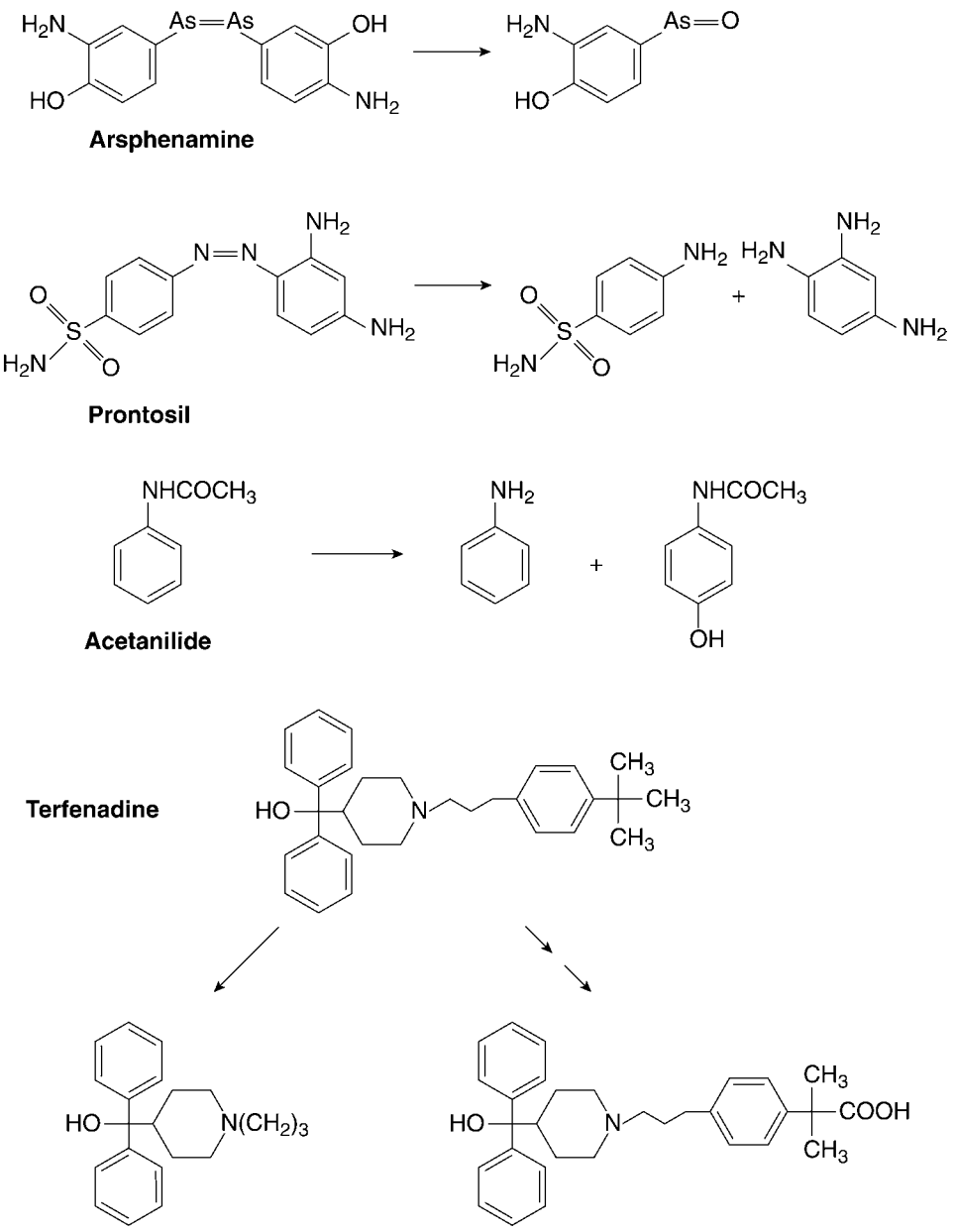

Figure 1 Examples of drug activation.

A more dramatic impact of metabolism occurred with the launch of prontosil (Fig. 1), the first major antibacterial agent. Prontosil was discovered in the early 1930s in the laboratories of I.G. Farben, the world's largest chemical company. G. Domagk and coworkers used the concept of Ehrlich, wherein compounds that could be shown to bind to tissues may lead to specific antagonists of infectious agents. The early work, therefore, concentrated on derivatives of azo dyes. After numerous failures they came across the compound prontosil, an azo dye containing a sulfonamide moiety (25). This molecule had striking activity and was an instant success. Launched initially in Europe, it quickly stormed the United States when President Roosevelt's son was cured by its administration (26). Domagk was awarded the Nobel Prize in 1939 for his work.

But, like arsphenamine, prontosil had very low activity in vitro. This puzzled workers in the laboratories of Trefouel in France. They proceeded to test both prontosil and the sulfonamide breakdown product and came to the conclusion that it was the metabolite formed by azo reduction that was the true antibacterial (27). This was confirmed by studies in England that showed the presence of aminobenzenesulfonamide in plasma and urine in patients treated with prontosil (28). Once it became clear that any derivative that would release the active sulfonamide in vivo could represent effective therapy, chemical companies around the world began making variations that would spawn the birth of the modern pharmaceutical industry.

Acetanilide (Fig. 1) provides a bridge from active to toxic metabolites. Brodie and Axelrod found that acetanilide was converted to aniline, which explained the methemoglobinemia, which had been observed at high doses and to acetaminophen, a superior analgesic (29). This study launched the illustrious career of Julius Axelrod in the field of metabolism.

There are numerous examples of prodrugs, either by fortune or design, that have to be activated for full pharmacological effect. Esters such as enalapril or clofibrate have to be hydrolyzed for activity. Methyl DOPA is decarboxylated and hydroxylated for activation, cyclophosphamide is hydroxylated for activation.

There are also many other examples where the metabolites had some or all of the activity designated for the parent. One of the most striking and significant of these is the antihistamine terfenadine (Fig. 1). The parent is oxidized to the active carboxylic acid and other metabolites by cytochrome P450 enzymes. When the P450s are inhibited, parent terfenadine reaches higher than normal levels (30,31). This interaction led to cardiovascular problems in patients taking terfenadine and ketoconazole or erythromycin. Because of this interaction, terfenadine was taken off the market and new regulatory guidelines were put in place by the Food and Drug Administration (FDA) to alert drug developers to the need for interaction studies before approval.

TOXIC AND REACTIVE METABOLITES

The products of metabolism are determined by reaction mechanism of the enzymes involved and by the chemical structure of the reactant. Whether a metabolic product is more or less active is independent of these two interacting forces. Humans have evolved over the years, whereby we have a certain capacity to handle whatever the environment and our diets present. Certain toxins, which cannot be handled metabolically, we learn to avoid. The time frame of evolution does not permit the type of adaptation necessary to dispose of every new compound in a safe and beneficial manner. It is impossible to estimate what percentage of new molecular entities are converted to active or toxic

metabolites, but it is clear that it has to be a higher percentage than we see just looking at marketed drugs. The fact is that if a toxic metabolite is produced during drug development, the candidate is usually eliminated from consideration. Therefore the number of compounds actually activated by metabolism is necessarily higher than the overall documented occurrences. With any new compound, there is a significant chance that metabolism will yield pharmacologically active derivatives.

REACTIVE INTERMEDIATES

The formation of reactive intermediates is of particular concern in the development of new agents. Guroff and coworkers found that during the course of aromatic hydroxylation the hydrogen on the position to be hydroxylated could shift to the adjacent position (32). This was termed the "NIH" shift and was subsequently explained by the formation of a reactive epoxide intermediate. The formation of "green pigments" during administration of 2-allyl-2-isopropylacetamide was shown by de Matteis to be due to destruction of P450 (33). Ethylene and other olefins had similar destructive properties (34). The most significant chemical moieties giving rise to reactive molecules and/or P450 inhibition have been reviewed (35). Many of these compounds will react with glutathione in an inactivation step. Excretion of mercapturic acids is often taken as a sign of the formation of the reactive species. In the absence of adequate levels of glutathione or when the kinetics are favorable for protein binding, the formation of chemical-protein conjugates can lead to systemic toxicity.

The prototypical reactive intermediate is the quinone-imine formed from metabolism of acetaminophen. In a classic series of papers, Brodie and coworkers revealed the metabolic fate of acetaminophen and its potential tissue-binding metabolite (36 39). While this compound is known to be hepatotoxic and readily binds to protein in vitro, it nonetheless remains a best-selling analgesic. Generally, at recommended doses, acetaminophen is efficiently removed by conjugation or, after oxidation, by glucuronidation and/or reaction with glutathione. At elevated doses or in conjunction with CYP2E1 induction, high levels of quinone-imine can lead to tissue damage (40).

BIOANALYTICAL

The progress in drug metabolism is paralleled by, indeed dependent on, the advances in bioanalytical techniques. For most of the first century of drug metabolism research, identification of metabolites involved isolation, purification, and chemical manipulation leading to characterization. At the end of World War II, new technology developed during the war came into use in metabolism research. A study on the distribution of radioactivity in the mouse after administration of ^{14}C-dibenzanthracene set new standards for metabolic research (41). The use of high-speed centrifuges to separate cellular components was another legacy of the Manhattan Project. The development of liquid-liquid partition chromatography by Martin and Synge (42) heralded the addition of new separation tools, including paper, thin layer, and gas chromatography. Spectrometry in biological media became routine with the Cary 14 spectrophotometer.

Mass spectrometry moved from the hands of specialists to the analytical laboratory with the launch of the LKB 9000 GC/MS. A crucial development for the eventual linking of mass spectrometry and liquid chromatography was the discovery of electrospray

ionization by Fenn in 1980 (43). LC/MS instruments from Sciex and Finnegan revolutionized the bioanalytical laboratories leading to increasingly more rapid and more efficient delineation of metabolic pathways. Newer analytical techniques permit the analysis of chemical bound to protein and the characterization of the proteins involved. For example, Shin and coworkers recently identified binding of electrophiles to 263 proteins in human microsomal incubations (44). Doss and Baillie (45) have suggested that drug developers use in vitro binding ability as a screen for potential reactive intermediates.

ENZYMOLOGY-MECHANISMS OF METABOLISM

Conjugation

The discovery of cofactor structures started with acetyl coA. This important cofactor, vital for intermediary metabolism, was identified using the acetylation of sulfanilamide as an assay. Lippman and coworkers painstakingly isolated and identified coenzyme A as the energy-containing component driving acetylation (46). The principle of active cofactors led researchers to solving the structures of 3′-phosphoadenosine-5′-phosphosulfate (PAPS) (47), uridinediphosphoglucuronic acid (UDPGA) (48), and *S*-adenosylmethionine (SAM) (49). Defining mercapturic acid formation took slightly longer because of the fact that the actual conjugating moiety was altered before elimination. The actual structure of mercapturic acids was solved when Baumann correctly identified the acetyl cysteine moiety (16). Glutathione, originally isolated by M.J. de Rey Pailhade (50), was fully characterized by Hopkins in 1929 (51). But it was not until 1959 when the relationship between glutathione conjugation and the formation of mercapturic acids was elucidated by Barnes and associates (52). In 1961, Booth, Boyland, and Sims published data on the enzymatic formation of glutathione conjugates (53). As a variation in the theme, it became clear that conjugation with amino acids such as glycine or glutamine involved initial activation of the substrate rather than the linking agent. The unique ability of humans and Old World monkeys to conjugate with glutamine was found to be due to the specificity of acyl transferase enzymes found in the mitochondria (54).

The structures of most of the human conjugating enzymes have now been elucidated, and in many cases, the enzymes have been cloned. Crystal structures have been slow to emerge for glucuronyl transferases because of the membrane-bound nature of these enzymes. There are 13 human sulfotransferases (55), 16 glucuronyl-transferases (56), multiple *N*-, *O*-, and *S*-methyl transferases, 2 *N*-acetyl transferases (57), and 24 glutathione transferases (58). The multiplicity of isozymes and overlapping specificities require extensive evaluation to understand which enzymes may be critical for a given drug.

Reduction

Some of the earliest in vitro experiments in metabolism dealt with enzymatic reduction. The importance of the azo derivatives of sulfanilamide led to initial experiments using neoprontosil as a model substrate. Bernheim reported the reduction of neoprontosil by liver homogenates (59). Mueller and Miller studied the metabolism of the carcinogen dimethylaminoazobenzene (DAB) and found that in rat liver homogenates DAB was hydroxylated and demethylated and the azo linkage was reduced (60). The reducing

enzyme was shown to require reduced nicotinamide adenine dinucleotide phosphate (NADPH) and to reside in the particulate portion of the fragmented cells (61).

Oxidation

The incorporation of oxygen into drugs and endogenous molecules was found to occur directly from molecular oxygen by the use of isotopically labeled oxygen (62,63). This led to the definition of a new category of oxidases termed "monooxygenases" by Hayaishi and "mixed-function oxidases" by Mason. These oxidases required oxygen and a reductant, usually NADPH.

IN VITRO METHODOLOGY/ENZYMOLOGY

The unraveling of the secrets of the cell began with the development of the techniques of gently breaking the cell developed by Potter and Elvejham and then fractionating the fragments and components of the cell by differential centrifugation (64). The first drug to be studied using these techniques was amphetamine. Axelrod examined the deamination of amphetamine and showed the activity to be dependent on oxygen and NADPH and to reside in the microsomal fraction of the cell (65). Brodie's laboratory quickly examined a number of drug substrates and found them to be metabolized by the same microsomal system (66).

Further examination of microsomes by Klingenberg and Garfinkel revealed the presence of a pigment that had some of the properties of a cytochrome and a peak absorbance after reduction in the presence of CO at 450 nm (67,68). The pigment was shown by Omura and Sato to be a cytochrome (69). Estabrook Cooper and Rosenthal used light activation of the CO-inhibited system to prove that cytochrome P450 was the terminal oxidase in the oxidation of many classes of drug substrates (70). The use of microsomes became standard practice in drug metabolism studies. However, the enzymes defied purification because of the fact that they were embedded in the membrane and solubilization inevitably led to denaturation.

Lu and Coon solved the problem of releasing the enzyme from the membrane using sodium deoxycholate in the presence of dithiotheitol and glycerol and our knowledge of multiple P450s rapidly expanded (71). Coon's laboratory, Wayne Levin and associates, and Fred Guengerich were among the pioneers in separation and purification of P450s (72). Nebert and coworkers developed a unifying nomenclature on the basis of the degree of similarity of the P450s, and the field began to blossom (73). The culmination of the efforts to define human P450s came with the sequencing of the human genome. At that point, it was clear that there were 57 variants of human P450. The major ones involved in drug metabolism have been well characterized, while there are still some isozymes whose function is yet to be defined (72).

The physical characteristics of the enzymes are rapidly being defined. The first P450 to be crystallized and the first structure determined were from a pseudomonad, *Pseudomonas putida* (74). This provided a blueprint for all the structures to come. Human P450s resisted crystallization until they were modified by shortening the amino terminus. It is this portion of the protein that binds the membrane, and by removing the amino terminal segment, it was possible to obtain a soluble, active P450 that could be crystallized and analyzed. The crystal structures of all of the major drug-metabolizing p450s now have been determined (75). The knowledge of the crystal structures has helped in our understanding of the broad specificity of this class of enzymes, helped to determine the

necessary properties of potential substrates, and led to the development of computer programs to predict whether a compound will be a substrate or not (76).

While the P450s have been the stars of drug metabolism, there are many other oxidative enzymes that can play a role, sometimes dominant, in the fate of new molecules. The flavin monooxygenases, which are often involved in the metabolism of heterocyclic amines, sulfur, or phosphorous-containing compounds, have been characterized and five forms identified (77). Aldehyde oxidase, a molybdenum-containing enzyme oxidizes nitrogen heterocycles and aldehydes (78), xanthine oxidase and xanthine dehydrogenase mainly involved in the production of uric acid (79), aldehyde dehydrogenase [3 classes, at least 17 genes (80)], and alcohol dehydrogenase (23 distinct human forms) (81) are among the enzymes most prominent in drug metabolism.

GENETIC CHARACTERISTICS OF DRUG-METABOLIZING ENZYMES

The drug-metabolizing enzymes showed early indications of genetic polymorphism on the basis of the individual variations in therapeutic effectiveness. The discovery of the utility of isoniazid in the treatment of tuberculosis was quickly followed by the realization that a significant portion of the patient population had elevated levels of isoniazid in the plasma. This was traced to a genetically determined deficiency in the *N*-acetyl transferase responsible for the inactivation of isoniazid (82). Similarly, genetic variations in serum cholinesterase led to altered susceptibility to the effects of the muscle-relaxant succinyl choline (83). A major breakthrough in the enzymes involved with drug oxidation came with the studies of Smith and coworkers on debrisoquine metabolism (84) and the work of Eichelbaum and coworkers on sparteine metabolism (85). These discoveries led to a broad range of population studies on debrisoquine hydroxylase, later to be identified as CYP450 2D6. The variation in blood levels of these agents could be traced to whether patients had diminished levels of CYP2D6 or, in some cases, enhanced levels of CYP2D6.

As we learned more about the role of the isozymes of P450, genetic variations became a major topic of study. Significant polymorphic variations in CYP2C9, CYP 2C19, CYP2A6, and CYP2B6 must be taken into account for substrates of these enzymes (86). Other oxidizing enzymes such as flavin monooxygenase (FMOs) (87) and dihydropyrimidine dehydrogenase (88) also show genetic variation leading to drug toxicity. Conjugating enzymes such as thiopurine methyltransferase, *N*-acetyl transferase, and glucuronyl transferase have variants that have been shown to be important in altered response to drugs (89).

The message for drug development is clear. It is vital to know the enzymes involved in the breakdown of the administered drug. If a specific isozyme is responsible for either the majority of the inactivation or for the activation of an agent, then appropriate studies are required to determine the efficacy and/or toxicity of the drug over a spectrum of the population, including the genetic variants.

INDUCTION-CONTROL MECHANISMS

One of the most striking features of drug-metabolizing enzymes is their ability to adapt to the substrate load. Early studies showed that ethanol administration to rats increased the ability of the kidney to metabolize ethanol (90), while borneol administration to dogs or

menthol administration to mice led to increased β-glucuronidase activity in these species (91). Conney et al. discovered enzyme induction by aromatic hydrocarbons (92), while Remmer and Merker reported phenobarbital induction of smooth endoplasmic reticulum in rabbits, rats, and dogs (93). Studies on the induction phenomenon eventually led to discovery of the Ah receptor (94). The mechanism of transcriptional regulation has been elucidated and forms the basis for our understanding of this superfamily of regulators (95). Other receptors integral to the initiation of induction include peroxisome proliferator activated receptor (PPAR) (96), constitutive androstane receptor (CAR), and pregnane X receptor (PXR). Interactions between CAR and PXR have recently been reviewed (97). The crystal structure of the human PXR ligand-binding domain in the presence and absence of ligands has been reported (98,99).

INHIBITORS

Compounds that had broad specificity as inhibitors of P450 played a major role in the understanding of this class of enzymes. The discovery of SKF525a in the laboratories of SKF and its expanded use by Brodie and coworkers defined the microsomal oxidases before the discovery of P450 (100,101). That one inhibitor could decrease the metabolism of so many diverse compounds argued for an enzyme with broad specificity or multiple enzymes with a common site of inhibition. Other inhibitors such as metyrapone, ketoconazole, and AIA were similarly employed. Attention was drawn to the role of inhibition in drug interactions when cimetidine, a popular proton pump inhibitor, was found to be a weak inhibitor of P450-catalyzed reactions (102). The observation that grapefruit juice had inhibitory properties stimulated the studies of endogenous and environmental inhibitors resulting in adverse drug reactions (103). Once the multiplicity of P450s was clear, specific inhibitors of individual isozymes were used to define activity (35). These inhibitors included antibodies with unique specificities (104). The field of specific inhibitors for targeted therapy is rapidly developing, as the roles of all 57 P450s are unraveled (105,106).

TRANSPORTERS

The discovery of p-glycoprotein (pgp or mdr1) in 1976 created an enhanced appreciation of the role of transporters in drug disposition (107). In addition to playing an important role in drug penetration through the intestine, pgp plays a significant role in controlling the penetration of many drugs into the brain (108). Umbenhauer and coworkers showed that a genetic deficiency in pgp was correlated with the penetration of avermectin into the brain in mice (109,110). Later studies showed a wide range of compounds controlled in a similar fashion. There are many other transporters that have yet to be characterized with regard to drug disposition. A total of 770 transporter proteins were predicted from analysis of the human genome. The ABC family, which contains pgp, consists of 47 members. The latest information and structural details on transporters can be found in the transporter protein analysis database (111). The first crystal structure of an S. Aureus ABC transporter was reported in 2007 (112). In the drug development process, knowledge as to whether the candidate compounds are substrates for transporters is crucial to predicting bioavailability.

DRUG METABOLISM RESEARCH IN DRUG DEVELOPMENT

The overall progression of drug metabolism from the determination of metabolic pathways to the current position in metabolic profiling is shown in Figure 2. The evolution of drug metabolism research has changed the role of the drug metabolism scientist in a most dramatic fashion. The modern day metabolism scientist must understand and evaluate not just the chemistry of metabolism but also the enzymatic, genetic, environmental, mechanistic, and interactive aspects of any new agent. The metabolism scientist must be able to develop a compound profile detailing all the nuances involved in proposed therapy. This profile, or metafile (Fig. 3), must encompass a breadth of understanding enabling the design of clinical studies that facilitates the tailoring of the new agent to the most appropriate patient population.

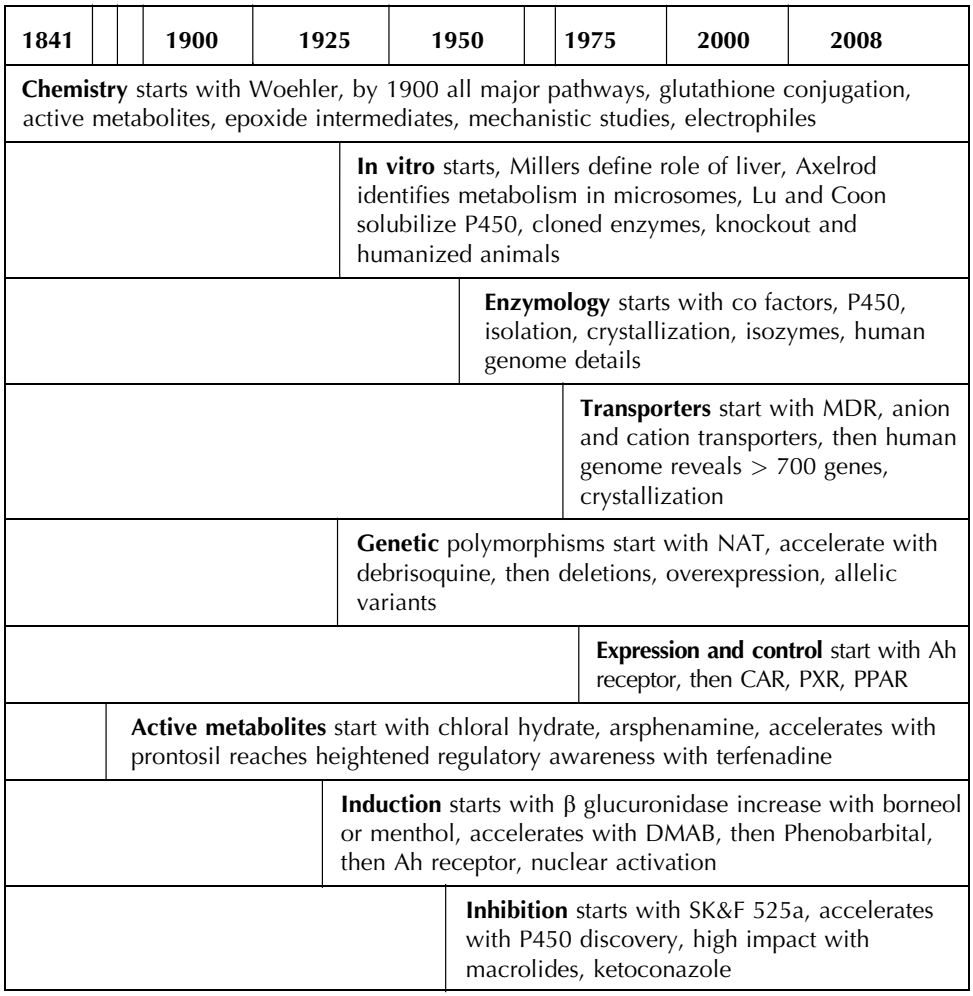

Figure 2 The evolution of drug metabolism research from the earliest days of discovery to the current broad ranging research effort. *Abbreviations*: Peroxisome proliferator activated receptor, PPAR; constitutive androstane receptor, CAR; pregnane X receptor, PXR.

Metabolic Profile (Metafile)	
Transformation products Identification Human in vitro/in vivo Animal in reference to efficacy models and toxicity models Activity Desirable Extraneous, adverse	**Genetics** Genotype for enzymes involved in metabolism/disposition Phenotype for enzymes Impact of genetic polymorphisms species comparisons
Bioavailability Methods of analysis parent/metabolites Pharmacokinetics	**Interactions** **Inhibition** by or of other drugs Parent, metabolites **Induction** potentiality Parent, metabolites
Enzymology Enzymes involved in metabolism Location of enzymes	**Transporters** Transporters involved in absorption and elimination

Figure 3 Summary of the research required for the creation of a compound profile. Many of these areas have greatly expanded in the last 25 years.

REFERENCES

1. Conti A, Bickel MH. History of drug metabolism. Discoveries of the major pathways in the 19th century. Drug Metab Rev 1977; 6:1 50.
2. Ure A. On gouty concretions; with a new method of treatment. Pharm J Transact 1841; 1:24.
3. Keller W. On the conversion of benzoic acid into hippuric acid. Ann Chem Pharm 1842; 43:108.
4. Erdmann OL, Marchand RF. Metabolism of cinnamic acid to hippuric acid in animals. Ann Chem Pharm 1842; 44:344.
5. Erdmann OL, Marchand RF. Umwandlung der Zimmtsäure in Hippursäure im thierishchen Organismus. J Prakt Chem 1842; 26:491 498.
6. Woehler F, Frerichs FT. Concerning the modifications which particular organic materials undergo in their transition to the urine. Ann Chem Pharm 1848; 63:335.
7. Schultzen O, Naunyn B. The behavior of benzene derived hydrocarbons in the animal organism. duBois Reymond's Arch Anat Physiol 1867:349.
8. Stadeler G. Ueber die flüchtigen Säuren des Harns. Ann Chem Liebigs 1851; 77:17 37.
9. Munk I. Zur Kenntniss der phenolbildenden Substanz im Harn. Arch Ges Physiol Pfluegers 1876; 12:142 151.
10. Baumann E. Concerning the occurrence of Brenzcatechin in the urine. Pfluger's Arch Physiol 1876; 12:69.
11. His W. On the metabolic products of pyridine. Arch exp Path Pharmak 1887; 22:253.
12. MacLagan NF, Wilkinson JH. The biological action of substances related to thyroxine. 7. The metabolism of butyl 4 hydroxy 3:5 diiodobenzoate. Biochem J 1954; 56:211 215.
13. Cohn R. Concerning the occurrence of acetylated conjugates following the administration of aldehydes. Z Physiol Chem 1893; 17:274.
14. Baumann E, and Preuss C. Concerning Bromophenylmercapturic acid. Ber deut chem Ges 1879; 12:806.
15. Jaffe M. Ueber die nach einfuhrung von brombenzol und chlorbenzol im organismus entstehenden schwefelhaltigen sauren. BerDeut Chem Ges 1879; 12:1092 1098.
16. Baumann E. Ueber cystin und cystein. Z Physiol Chem 1884; 8:299 305.

17. Thierfelder H, Sherwin CP. Phenylacetyl glutamin, ein Stoffwechsel Produkt des menschlichen Korpers nach Eingabe von Phenylessigsaure. Ber dtsch chem Ges 1914; 47:2630 2634.
18. Di Carlo FJ, Adams JD, Adams N. Carl paxson sherwin, american pioneer in drug metabolism. Drug Metab Rev 1992; 24:493 530.
19. Harrow B, Sherwin CP. Detoxication mechanisms. Annu Rev Biochem 1935; 4:263 278.
20. Ambrose AM, Sherwin CP. Detoxication mechanisms. Annu Rev Biochem 1933; 2:377 396.
21. Sherwin CP. The fate of foreign organic compounds in the animal body. Physiol Rev 1922; 2:238 276.
22. Williams RT. Detoxication Mechanisms. 2nd Edition ed. New York: John Wiley & Sons Inc., 1959.
23. Ehrlich P, Hata S. The Experimental Chemotherapy of Spirilloses. English ed. New York: Rebman Company, 1911.
24. Voegtlin C, Smith HW. Quantitative studies in chemotherapy III. The oxidation of arsphenamine. J Pharmacol Exp Ther 1920; 16:199 217.
25. Domagk G. A report on the chemotherapy of bacterial infections. Deut Med Woch 1935; lxi:250.
26. Hager T. The Demon Under The Microscope. New York: Harmony Books, 2006.
27. Trefouél J, Trefouél J, Nitti F, Bovet D. Activity of p aminophenylsulfamide in the experimental streptococcal infections of the mouse and rabbit. C R Seances Soc Biol 1935; 120:756.
28. Colebrook L, Kenny M. Treatment with prontosil of puerperal infections due to hemolytic streptococci. Lancet 1936; 1:1319.
29. Brodie BB, Axelrod J. The fate of acetanilide in man. J Pharmacol Exp Ther 1948; 94:29 38.
30. Monahan BP, Ferguson CL, Killeavy ES, Lloyd BK, Troy J, Cantilena LR Jr. Torsades de pointes occurring in association with terfenadine use. JAMA 1990; 264:2788 2790.
31. Jurima Romet M, Crawford K, Cyr T, Inaba T. Terfenadine metabolism in human liver. In Vitro Inhibition by Macrolide Antibiotics and Azole Antifungals. Drug Metab Dispos 1994; 22:849 856.
32. Guroff GDJ, Jerina DM, Renson J, Witkop B, Udenfriend S. Hydroxylation induced migration: the NIH shift. Recent experiments reveal an unexpected and general result of enzymatic hydroxylation of aromatic compounds. Science 1967; 157:1524 1530.
33. De Matteis F. Loss of haem in rat liver caused by the porphyrogenic agent 2 allyl 2 isopropylacetamide. Biochem J 1971; 124(4):767 777.
34. Ortiz de Montelano PR, Mico BA. Destruction of cytochrome P 450 by ethylene and other olefins. Mol Pharm 1980; 18:128 135.
35. Murray M, Reidy GF. Selectivity in the inhibition of mammalian cytochromes P 450 by chemical agents. Pharmacol Rev 1990; 42:85 101.
36. Jollow DJ, Mitchell JR, Potter WZ, Davis DC, Gillette JR, Brodie BB. Acetaminophen induced hepatic necrosis. II. Role of covalent binding in vivo. J Pharmacol Exp Ther 1973; 187(1):195 202.
37. Mitchell JR, Jollow DJ, Potter WZ, Davis DC, Gillette JR, Brodie BB. Acetaminophen induced hepatic necrosis. I. Role of drug metabolism. J Pharmacol Exp Ther 1973; 187(1):185 194.
38. Mitchell JR, Jollow DJ, Potter WZ, Gillette JR, Brodie BB. Acetaminophen induced hepatic necrosis. IV. Protective role of glutathione. J Pharmacol Exp Ther 1973; 187(1):211 217.
39. Potter WZ, Davis DC, Mitchell JR, Jollow DJ, Gillette JR, Brodie BB. Acetaminophen induced hepatic necrosis. III. Cytochrome P 450 mediated covalent binding in vitro. J Pharmacol Exp Ther 1973; 187(1):203 210.
40. Chen C, Krausz KW, Idle JR, Gonzalez FJ. Identification of novel toxicity associated metabolites by metabolomics and mass isotopomer analysis of acetaminophen metabolism in wild type and Cyp2e1 null mice. J Biol Chem 2008; 283:4543 4559.
41. Heidelberger C, Jones HB. The distribution of radioactivity in the mouse following administration of dibenzanthracene labeled in the 9 and 10 positions with carbon 14. Cancer 1948; 1:252 260.
42. Martin AJ, Synge RL. A new form of chromatogram employing two liquid phases: a theory of chromatography. 2. Application to the micro determination of the higher monoamino acids in proteins. Biochem J 1941; 35:1358 1368.

43. Fenn JB, Mann M, Meng CK, Wong SF, Whitehouse CM. Electrospray ionization for mass spectrometry of large biomolecules. Science 1989; 246:64 71.
44. Shin N, Liu Q, Stamer SL, Liebler DC. Protein targets of reactive electrophiles in human liver microsomes. Chem Res Toxicol 2007; 20:859 867.
45. Doss GA, Baillie TA. Addressing metabolic activation as an integral component of drug design. Drug Metab Rev 2006; 38:641 649.
46. Lipmann F. Acetylation of sulfanilamide by liver homogenates and extracts. J Biol Chem 1945; 160:173 190.
47. Robbins PW, Lipmann F. Isolation and identification of active sulfate. J Biol Chem 1957; 229:837 851.
48. Dutton GJ, Storey IDE. The isolation of a compound of uridine diphosphate and glucuronic acid from liver. Biochem J 1953; 53:37 38.
49. Cantoni GL. S adenosylmethionine; a new intermediate formed enzymatically from l methionine and adenosinetriphosphate. J Biol Chem 1953; 204:403 416.
50. De Rey Pailhade J. Sur un corps d'origine organique hydrogenant le soufre a froid. (On a body of organic origin hydrogenated cold sulfur.) Compte Rendus Hebdomadaire Séances de l'Académie des Sciences 1888;106:1683 4 (in French).
51. Hopkins FG. On Glutathione: A Reinvestigation. J Biol Chem 1929; 84:269 320.
52. Barnes MM, James SP, Wood PB. The formation of mercapturic acids. 1. Formation of mercapturic acid and the levels of glutathione in tissues. Biochem J 1959; 71:680 690.
53. Booth J, Boyland E, Sims P. An enzyme from rat liver catalysing conjugations with glutathione. Biochem J 1961; 79:516 524.
54. Webster LT, Siddiqui, U.A., Lucas, S.V., Strong, J.M., Mieyal, J.J. Identification of separate acyl CoA: glycine and acyl CoA:L glutamine N acyltransferase activities in mitochondrial fractions from liver of rhesus monkey and man. J Biol Chem 1976; 251:3352 3358.
55. Allali Hassani APP, Dombrovski L, Najmanovich R, Tempel W, Dong A, Loppnau P, Martin F, Thornton J, Edwards AM, Bochkarev A, Plotnikov AN, Vedadi M, Arrowsmith CH. Structural and chemical profiling of the human cytosolic sulfotransferases. PLoS Biol 2007; 5:e97.
56. Tukey RH, Strassburg CP. Human UDP glucuronosyltransferases: metabolism, expression and disease. Annu Rev Pharmacol Toxicol 2000; 40:581 616.
57. Wu H, Dombrovsky L, Tempel W, Martin F, Loppnau P, Goodfellow GH, Grant DM, Plotnikov AN. Structural basis of substrate binding specificity of human arylamine N acetyltransferases. J Biol Chem 2007; 282:30189 30197.
58. Hayes JD, Flanagan JU, Jowsey IR. Glutathione transferases. Annu Rev Pharmacol Toxicol 2005; 45:51 88.
59. Bernheim F. The reduction of neoprontosil by tissues in vitro. J Pharmacol Exp Ther 1941; 71:344 348.
60. Mueller GC, Miller JA. The metabolism of 4 dimethylaminoazobenzene by rat liver homogenates. J Biol Chem 1948; 176:535 544.
61. Mueller GC, Miller JA. The reductive cleavage of 4 dimethylaminoazobenzene by rat liver: the intracellular distribution of the enzyme system and its requirement for triphosphopyridine nucleotide. J Biol Chem 1949; 180(3):1125 1136.
62. Hayaishi O, Katagiri M, Rothberg S. J Am Chem Soc 1955; 77:5450.
63. Mason HS, Fowlks WL, Peterson E. Oxygen transfer and electron transport by the phenolase complex. J Am Chem Soc 1955; 77(10):2914 2915.
64. De Duve C, Beaufay H. A short history of tissue fractionation. J Cell Biol 1981; 9:293s 299s.
65. Axelrod J. The enzymatic deamination of amphetamine (benzedrine). J Biol Chem 1955; 214:753 763.
66. Brodie BB, Axelrod J, Cooper JR, Gaudette L, La Du B, Mitoma C, Udenfriend S. Detoxication of drugs and other foreign compounds by liver microsomes. Science 1955; 121:603 604.
67. Klingenberg M. Pigments of rat liver microsomes. Arch Biochem Biophys 1958; 75:376 386.
68. Garfinkel D. Studies on pig liver microsomes. I. Enzymic and pigment composition of different microsomal fractions. Arch Biochem Biophys 1958; 77:493 509.

69. Omura T, Sato R. A new cytochrome in liver microsomes. J Biol Chem 1962; 237:1375 1376.
70. Estabrook RW, Cooper DY, Rosenthal O. The light reversible carbon monoxide inhibition of the steroid C 21 hydroxylation system of the adrenal cortex. Biochem Z 1963; 338:741 755.
71. Lu AYH, Coon MJ. Role of hemoprotein P450 in fatty acid ω hydroxylation in a soluble enzyme system from liver microsomes. J Biol Chem 1968; 243:1331 1332.
72. Guengerich FP. Human Cytochrome P450 Enzymes. In: Paul R Ortiz de Montellano, ed. Cytochrome P450: Structure, Mechanism, and Biochemistry. 3rd ed. New York, NY: Kluwer Academic/Plenum Publishers, 2005:377 463.
73. Nebert DW, Adesnik M, Coon MJ, Estabrook RW, Gonzalez FJ, Guengerich FP, Gunsalus IC, Johnson EF, Kemper B, Levin W, Phillips IR, Sato R, Waterman MR. The P450 gene superfamily: recommended nomenclature. DNA 1987; 6:1 11.
74. Poulos TL, Finzel BC, Howard AJ. Crystal structure of substrate free Pseudomonas putida cytochrome P 450. Biochemistry 1986; 25:5314 5322.
75. Rowland P, Blaney FE, Smyth MG, Jones JJ, Leydon VR, Oxbrow AK, Lewis CJ, Tennant MG, Modi S, Eggleston DS, Chenery RJ, Bridges AM. Crystal structure of human cytochrome P450 2D6. J Biol Chem 2006; 281:7614 7622.
76. Yamashita F, Hashida M. In silico approaches for predicting ADME properties of drugs. Drug Metab Pharmacokinet 2004; 19:327 338.
77. Krueger SK, Williams DE. Mammalian flavin containing monooxygenases: structure/function, genetic polymorphisms and role in drug metabolism. Pharmacol Ther 2005; 106:357 387.
78. Garattini E, Mendel R, Romão MJ, Wright R, Terao M. Mammalian molybdo flavoenzymes, an expanding family of proteins: structure, genetics, regulation, function and pathophysiology. Biochem J 2003; 372(1):15 32.
79. Pacher P, Nivorozhkin A, Szabó C. Therapeutic effects of xanthine oxidase inhibitors: renaissance half a century after the discovery of allopurinol. Pharmacol Rev 2006; 58:87 114.
80. Vasiliou V, Pappa A, Estey T. Role of human aldehyde dehydrogenases in enobiotic and xenobiotic metabolism. Drug Metab Rev 2004; 36:279 299.
81. Agarwal DP, Goedde HW. Pharmacogenetics of alcohol dehydrogenase. In: Kalow W, ed. Pharmacogenetics of Drug Metabolism. New York: Pergammon, 1992; 263 280.
82. Evans DA, Manley KA, McKusick VA. Genetic control of isoniazid metabolism in man. Br Med J 1960; 2:485 491.
83. Kalow W. Butyrylcholine esterase in the blood serum of man and animal. Naunyn Schmiedebergs Arch Exp Pathol Pharmakol 1952; 215:370 377.
84. Mahgoub A, Idle JR, Dring LG, Lancaster R, Smith RL. Polymorphic hydroxylation of debrisoquine in man. Lancet 1977; 2:584 586.
85. Eichelbaum M, Spannbrucker N, Dengler HJ. A probably genetic defect of the metabolism of sparteine. In: Gorrod JW, ed. Biological Oxidation of Nitrogen. Amsterdam: Elsevier/North Hoiland Biomedical Press, 1978:113 118.
86. Ingelman Sundberg M, Sim SC, Gomez A, Rodriguez Antona C. Influence of cytochrome P450 polymorphisms on drug therapies: pharmacogenetic, pharmacoepigenetic and clinical aspects. Pharmacol Ther 2007; 116:496 526.
87. Koukouritaki SB, Poch MT, Henderson MC, Siddens LK, Krueger SK, VanDyke JE, Williams DE, Pajewski NM, Wang T, Hines RN. Identification and functional analysis of common human flavin containing monooxygenase 3 genetic variants. J Pharmacol Exp Ther 2007; 320:266 273.
88. Harris BE, Carpenter JT, Diasio RB. Severe 5 fluorouracil toxicity secondary to dihydropyrimidine dehydrogenase deficiency. A potentially more common pharmacogenetic syndrome. Cancer 1991; 68:499 501.
89. Gardiner SJ, Begg EJ. Pharmacogenetics, drug metabolizing enzymes, and clinical practice. Pharmacol Rev 2006; 58:521 590.
90. Leloir LF, Mufioz JM. Ethyl alcohol metabolism in animal tissues. Biochem J 1938; 32:299 307.
91. Fishman WH. Studies on β glucuronidase. III. The increase in β glucuronidase activity of mammalian tissues induced by feeding glucuronidogenic substances. J Biol Chem 1940; 136:229 236.
92. Conney AH, Miller EC, Miller JA. The metabolism of methylated aminoazo dyes. V. Evidence for induction of enzyme synthesis in the rat by 3 methylcholanthrene. Cancer Res 1956; 16:450 459.

93. Remmer H, Merker HJ. Drug induced changes in the liver endoplasmic reticulum: associaton with drug metabolizing enzymes. Science 1963; 142:1637 1638.
94. Poland A, Glover E, Kende AS. Stereospecific, high affinity binding of 2,3,7, 8 tetrachlorodibenzo p dioxin by hepatic cytosol. Evidence that the binding species is receptor for induction of aryl hydrocarbon hydroxylase. J Biol Chem 1976; 251:4936 4946.
95. McMillan BJ, Bradfield CA. The aryl hydrocarbon receptor sans xenobiotics: endogenous function in genetic model systems. Mol Pharmacol 2007; 72:487 498 (epub 2007, May 29).
96. Michalik L, Auwerx J, Berger JP, Chatterjee VK, Glass CK, Gonzalez FJ, Grimaldi PA, Kadowaki T, Lazar MA, O'Rahilly S, Palmer CN, Plutzky J, Reddy JK, Spiegelman BM, Staels B, Wahli W. International union of pharmacology. LXI. Peroxisome proliferator activated receptors. Pharmacol Rev 2006; 58:726 741.
97. Moreau A, Vilarem MJ, Maurel Pl. Xenoreceptors CAR and PXR activation and consequences on lipid metabolism, glucose homeostasis, and inflammatory response. Mol Pharm 2008; 5:35 41 (epub 2007, Dec 27).
98. Watkins RE, Wisely GB, Moore LB, Collins JL, Lambert MH, Williams SP, Willson TM, Kliewer SA, Redinbo MR. The human nuclear xenobiotic receptor PXR: structural determinants of directed promiscuity. Science 2001; 292:2329 2333.
99. Xue Y, Moore LB, Orans J, Peng L, Bencharit S, Kliewer SA, Redinbo MR. Crystal structure of the pregnane X receptor estradiol complex provides insights into endobiotic recognition. Mol Endocrinol 2007; 21:1028 1038.
100. Cooper JR, Axelrod J, Brodie BB. Inhibitory effects of β diethylaminoethyldiphenylpropyla cetate on a variety of drug metabolic pathways in vitro. J Pharmacol Exp Ther 1954; 112:55 63.
101. Axelrod J, Reichenthal J, Brodie BB. Mechanism of the potentiating action of β diethylaminoethyldiphenylpropylacetate. J Pharmacol Exp Ther 1954; 112:49 54.
102. Puurunen J, Pelkonen O. Cimetidine inhibits microsomal drug metabolism in the rat. Eur J Pharmacol 1979; 55:335 336.
103. Bailey DG, Spence JD, Munoz C, Arnold JM. Interaction of citrus juices with felodipine and nifedipine. Lancet 1991; 337:268 269.
104. Gelboin HV, Krausz K. Monoclonal antibodies and multifunctional cytochrome P450: drug metabolism as paradigm. J Clin Pharmacol 2006; 46:353 372.
105. Haining RL, Nichols Haining M. Cytochrome P450 catalyzed pathways in human brain: metabolism meets pharmacology or old drugs with new mechanism of action? Pharmacol Ther 2007; 113:537 545.
106. Schuster I, Bernhardt R. Inhibition of cytochromes p450: existing and new promising therapeutic targets. Drug Metab Rev 2007; 39:481 499.
107. Juliano RL, Ling V. A surface glycoprotein modulating drug permeability in Chinese hamster ovary cell mutants. Biochim Biophys Acta 1976; 455:152 162.
108. Schinkel AH, Smit JJ, van Tellingen O, Beijnen JH, Wagenaar E, van Deemter L, Mol CA, van der Valk MA, Robanus Maandag EC, te Riele HP, Berns AJ, Borst P. Disruption of the mouse mdr1a P glycoprotein gene leads to a deficiency in the blood brain barrier and to increased sensitivity to drugs. Cell 1994; 77:491 502.
109. Umbenhauer DR, Lankas GR, Pippert TR, Wise LD, Cartwright ME, Hall SJ, Beare CM. Identification of a p glycoprotein deficient subpopulation in the CF 1 mouse strain using a restriction fragment length polymorphism. Toxicol Appl Pharmacol 1997; 146:88 94.
110. Kwei GY, Alvaro RF, Chen Q, Jenkins HJ, Hop CE, Keohane CA, Ly VT, Strauss JR, Wang RW, Wang Z, Pippert TR, Umbenhauer DR. Disposition of ivermectin and cyclosporin A in CF 1 mice deficient in mdr1a P glycoprotein. Drug Metab Dispos 1999; 27:581 587.
111. Ren Q, Chen K, Paulsen IT. TransportDB: a comprehensive database resource for cytoplasmic membrane transport systems and outer membrane channels. Nucleic Acids Res 2007;35: D274 D279 (epub 2006, Nov 28).
112. Dawson RJ, Locher KP. Structure of the multidrug ABC transporter Sav1866 from Staphylococcus aureus in complex with AMP PNP. FEBS Lett 2007; 581:935 938 (epub 2007, Feb 7).

2
Pharmacokinetics of Drug Metabolites

Philip C. Smith
School of Pharmacy, University of North Carolina at Chapel Hill, Chapel Hill, North Carolina, U.S.A.

INTRODUCTION

Drug metabolites and their disposition in vivo are well recognized by scientists, clinicians, and regulatory agencies to be important when evaluating a new drug entity. In the past several decades, increased attention has been placed on drug metabolism for several reasons. Firstly, the number of drugs with active metabolites, by design (i.e., prodrugs) or by chance, has increased (1 3). This is exemplified by the transition from terfenadine to its active metabolite fexofenadine (3) and interest in the contributions of morphine-6-glucuronide (M6G) toward the analgesic activity of the age-old drug, morphine, and potential development of this active metabolite (4). In addition, with the advent of methods to establish the metabolic genotype and characterize the phenotype of individual patients (5,6) and the identification of specific isoforms of enzymes of metabolism, there is an increased appreciation of how elimination of a drug by metabolism can influence drug bioavailability and clearance, and ultimately affect its efficacy and toxicity. These rapidly evolving methods can be translated to permit cost-effective individual optimization of drug therapy on the basis of a subject's metabolic capability (5,6), just as renal creatinine clearance has been used for years to assess renal function and permits individualized dose adjustment for drugs cleared by the kidney (7). Finally, the well accepted, though still poorly understood role of bioactivation in the potential toxicity of drugs and other xenobiotics (8,9) requires that metabolites continue to be evaluated and scrutinized for possible contributions to adverse effects observed in vivo. Though the importance of drug metabolism is seldom questioned, the interpretation and use of pharmacokinetic data on the disposition of metabolites is not well understood or fully implemented by some investigators. The objective of this chapter is to provide a basis for the interpretation and use of metabolite pharmacokinetic data from preclinical and clinical investigations.

A number of previous authors have reviewed methods and theory for the analysis of metabolite pharmacokinetics, with literature based upon simple models, as early as 1963 by Cummings and Martin (10). Thorough theoretical analyses and reviews have been published, notably by Houston (11,12), Pang (13), and Weiss (14). The topic of metabolite kinetics is not found in commonly employed textbooks on pharmacokinetics

(15), though the topic is usually not presented or taught in a first, introductory course on pharmacokinetics. This chapter is not intended to present all aspects of basic pharmacokinetics that may be necessary for a thorough understanding of metabolite kinetics, and for this reason, motivated readers are recommended to consult other sources (15 19) if an introduction to basic pharmacokinetic principles is needed. This review will also not attempt to present or discuss all possible permutations of metabolite pharmacokinetics, but will make an effort to present and distinguish what can be assessed in humans and animals in vivo given commonly available experimental methods, which in some cases may be augmented by in vitro studies.

METABOLITE KINETICS FOLLOWING A SINGLE INTRAVENOUS DOSE OF PARENT DRUG

General Considerations in Metabolite Disposition

Much of the theory presented here will be based upon primary metabolites, as shown in Scheme 1, which are formed directly from the parent drug or xenobiotic whose initial dose is known. In contrast, secondary or sequential metabolites, as indicated in Scheme 2, are formed from one or more primary metabolites. The theory and resultant equations for the analysis of sequential metabolite kinetics are often more complex (see sect. "Sequential Metabolism") (13). Since most metabolites of interest are often primary metabolites, this review will focus on these, unless otherwise noted. Scheme 1 is the simplest model for one metabolite that can be measured in vivo, with other elimination pathways for the parent drug, either by metabolism or excretion (e.g., biliary or renal), represented as a combined first-order elimination term, k_{other}. Pharmacokinetic models will be presented here for conceptual reasons, but in the instances where model-independent or "non-compartmental" methods are appropriate, their applications will be discussed.

Here, $\boldsymbol{A}$ is the amount of drug or xenobiotic administered and $\boldsymbol{A}(\mathrm{m})$ is the amount of a particular metabolite present in the body with time. When sequential metabolism is occurring, metabolites are distinguished with a subscript; $\boldsymbol{A}(\mathrm{m}_1)$ is the amount of primary metabolite present with time and $\boldsymbol{A}(\mathrm{m}_2)$ is the amount of secondary, or sequential, metabolite formed with time. $\boldsymbol{A}(\mathrm{m})_{\mathrm{elim}}$ is the amount of the primary metabolite of interest that is excreted (e.g., biliary or renal) and/or further metabolized. It is assumed that once metabolite is excreted in the urine or bile, it is not subject to reabsorption or cycling. The

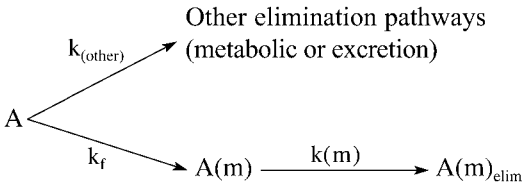

Scheme 1 Drug metabolism to a primary metabolite followed by urinary or biliary excretion with parallel elimination pathways. The arrows indicate irreversible processes.

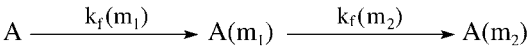

Scheme 2 Sequential metabolism to a secondary metabolite, m_2, from a primary metabolite, m_1.

parameter k_f is the first-order formation rate constant for the metabolite and k_{other} represent a first-order rate constant for the sum of formation of other metabolites and elimination via other pathways. The constant $k(m)$ is the elimination rate constant for the metabolite, whereas the sum of k_f and k_{other} is k, the total first-order rate constant for the overall elimination of the parent drug. With this simple model, and derivations from this, the following assumptions will be employed unless otherwise noted:

1. The elimination and distribution processes are first order, and thus linear, that is, they are not influenced by the concentration of drug or metabolite in the body. For example, saturation of enzyme and transport systems, co-substrate depletion, saturable plasma protein, or tissue binding does not occur.
2. All drug metabolism represents irreversible elimination of the parent drug, thus, there is no reversible metabolism, enterohepatic recycling, or bladder resorption.
3. For simplicity, a one-compartment model will be used, which assumes rapid distribution of parent drug and metabolite within the body.
4. There is no metabolism that results in metabolite being eliminated without first being presented to the systemic circulation.

From Scheme 1, the following equation is used to describe the rate of change in the amount of metabolite in the body at any time, which is equal to the rate of formation less the rate of elimination,

$$\frac{dA(m)}{dt} = k_f \cdot A - k(m) \cdot A(m) \qquad \text{(Eq. 1)}$$

This rate of input (i.e., formation) and output (i.e., elimination) is analogous to the form of the equation for first-order drug absorption and elimination (17). The amount of metabolite and parent drug present in the body upon initial intravenous bolus dosing of the drug is zero and the administered dose (D), respectively. The disposition of parent drug can be described with an exponential term, as shown in Eq. 2,

$$A = D \cdot e^{-k \cdot t} \qquad \text{(Eq. 2)}$$

Substitution of A into Eq. 1 permits solving for $A(m)$ as a function of time (17),

$$A(m) = \frac{k_f \cdot D}{k(m) - k}\left[e^{-k \cdot t} - e^{-k(m) \cdot t}\right] \qquad \text{(Eq. 3)}$$

Since amount of metabolite is often unknown, metabolite concentration, $C(m)$, is measured in plasma, which can be expressed by dividing both sides of Eq. 3 by the volume of distribution of the metabolite, $V(m)$, as follows,

$$C(m) = \frac{k_f \cdot D}{V(m) \cdot (k(m) - k)}\left[e^{-k \cdot t} - e^{-k(m) \cdot t}\right] \qquad \text{(Eq. 4)}$$

Eqs. 3 and 4 describe the amount and concentration, respectively, of a primary metabolite in the body over time after an intravenous bolus dose of the parent drug. Immediately after dosing there is no metabolite present, and the amount of metabolite will then reach a maximum when the rate of formation equals the rate of elimination of the metabolite. This peak occurs when $t_{m,peak} = \ln[k/k(m)]/[k \quad k(m)]$ (17). Here, k and $k(m)$ determine the shape of the drug and metabolite concentration versus time profiles, whereas k_f influences the fraction of the dose that is metabolized, thus affecting the magnitude of the metabolite concentration. It is apparent that the relative magnitude or

ratio of the two rate constants for the elimination of parent drug and metabolite determines the overall profile of the metabolite relative to that of the parent drug, with two limiting cases described below.

Formation Rate-Limited Metabolism

In the first case, if $k(\mathrm{m}) \gg k$, then the metabolite is eliminated by either excretion or further sequential metabolism much more rapidly than the rate at which the parent drug is eliminated. Since $k = k_{\mathrm{f}} + k_{\mathrm{other}}$, it also follows that $k(\mathrm{m}) \gg k_{\mathrm{f}}$. Under this condition, defined as formation rate-limited (FRL) metabolism, the exponential term describing metabolite elimination in Eqs. 3 and 4, $e^{-k(\mathrm{m})\cdot t}$, declines rapidly to zero relative to the exponential term describing parent drug elimination, $e^{-k\cdot t}$, and the term in the denominator, $[k(\mathrm{m}) - k]$, approaches the value $k(\mathrm{m})$. Thus, shortly after an intravenous bolus dose of parent drug, Eq. 3 simplifies to,

$$A(\mathrm{m}) = \frac{k_{\mathrm{f}} \cdot D}{k(\mathrm{m})}[e^{-k\cdot t}] \qquad \text{(Eq. 5)}$$

Equation 4 can be simplified similarly, and then, if one takes the natural log (ln) of both sides of Eq. 5, then the amount of metabolite in the body can be described by a linear relationship with respect to time,

$$\ln A(\mathrm{m}) = \ln\left(\frac{k_{\mathrm{f}} \cdot D}{k(\mathrm{m})}\right) - k \cdot t \qquad \text{(Eq. 6)}$$

A similar relationship to Eq. 6 can be derived from Eq. 4 using concentrations rather than amounts when FRL metabolism applies. This log-linear relationship, common to first-order systems, indicates that when $k(\mathrm{m}) \gg k$, the terminal half-life is measured for the metabolite amount or concentration versus time curves represent that of the parent drug, not that of the metabolite. This is shown below in Figures 1A and 2. Moreover, as $k(\mathrm{m})$ increases, the $t_{\mathrm{m,peak}}$ for the metabolite approaches zero. In this case, the metabolite will reach peak concentrations very quickly after a bolus dose of the parent drug.

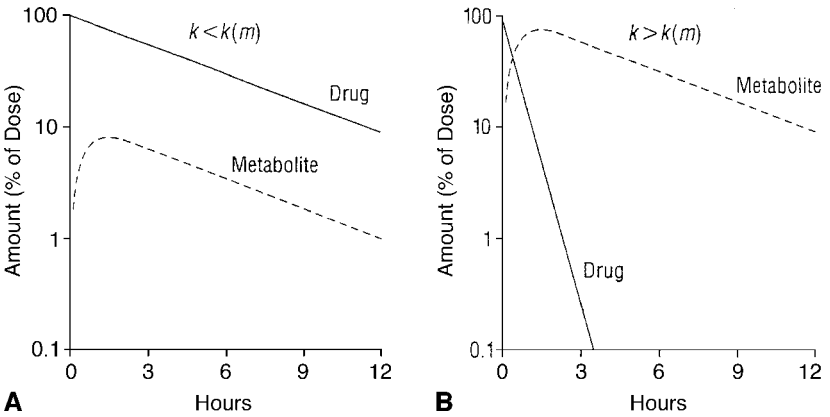

Figure 1 Drug and metabolite profiles simulated for the two common cases from Scheme 1. (**A**) Formation rate limited metabolism where $k(\mathrm{m}) > k$[k_{f}, k_{other}, and $k(\mathrm{m})$ are 0.2, 0, and 2, respectively]. (**B**) Elimination rate limited metabolism where $k(\mathrm{m}) < k$ [k_{f}, k_{other}, and $k(\mathrm{m})$ are 2, 0, and 0.2, respectively]. Shown are amounts expressed as percentage of the dose; if converted to concentrations of parent drug and metabolite, the relative ratios of the curves may change as determined by V and $V(\mathrm{m})$, respectively. *Source*: From Ref. 15.

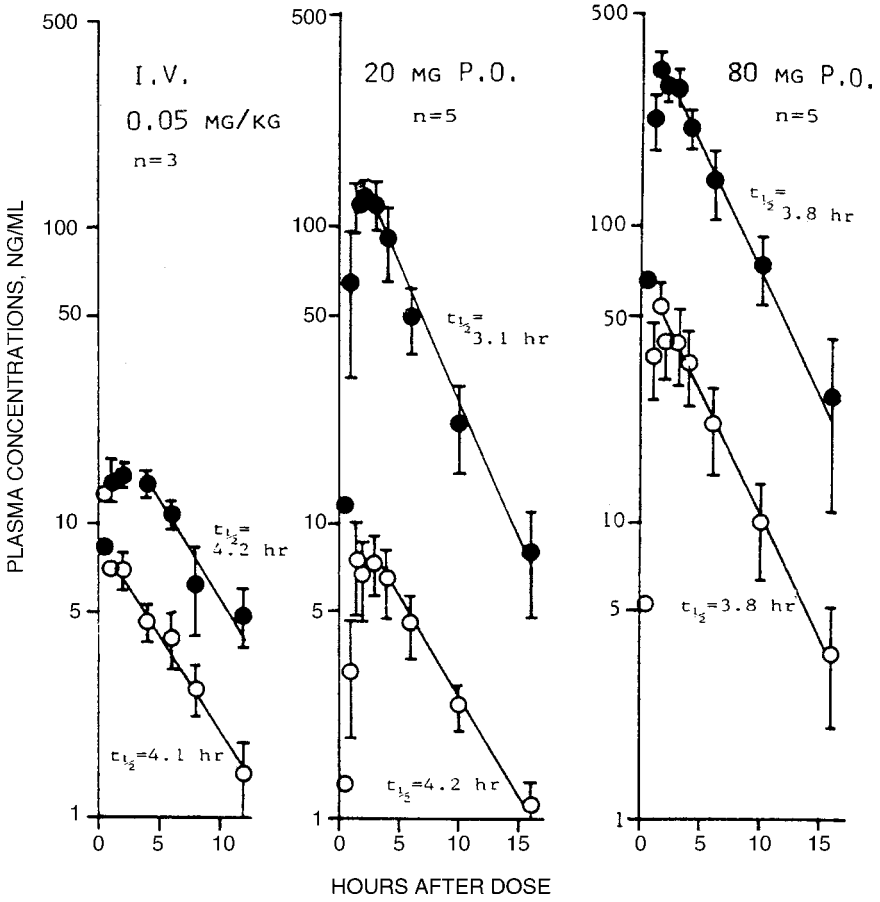

Figure 2 Plasma levels of NLA (●) and propranolol (o) (mean ± SEM) after single intravenous doses of propranolol in normal human subjects (20). NLA exhibits FRL metabolism with parallel half lives and rapid attainment of peak levels. The higher ratios of NLA/propranolol at equilibrium are due to a much low ratio of CL(m)/CL; however, $V(m)/V$ must be lower still (see Eq. 15) to provide $k(m)/k > 1$, characteristic of FRL metabolism. *Abbreviations*: NLA, naphthoxylacetic acid; FRL, formation rate limited. *Source*: From Ref. 20.

Equation 5 can also be rearranged to indicate that the rate of elimination of metabolite, $k(m) \cdot A(m)$, approximates its rate of formation from the parent drug, $k_f \cdot D \cdot [e^{-k \cdot t}] = k_f \cdot A$, where A is the amount of parent drug in the body at any time after the dose,

$$k(\mathrm{m}) \cdot A(\mathrm{m}) = k_f \cdot D \cdot e^{-k \cdot t} \qquad \text{(Eq. 7)}$$

Thus, with FRL metabolism, an apparent equilibrium exists between the formation and elimination of metabolite such that the ratio of metabolite to parent drug is approximately constant soon after a dose of the parent drug. Since the term "$D \cdot e^{-k \cdot t}$," describes the amount of parent drug in the body at any time, shortly after an intravenous bolus dose of the parent drug, the ratio of amount of metabolite to drug is,

$$A(\mathrm{m}) = \frac{k_f}{k(\mathrm{m})} \cdot A \qquad \text{(Eq. 8)}$$

Since the volume of distributions of parent drug (V) and metabolite [V(m)] are assumed constant, Eq. 8 can be rewritten by multiplying by volume terms to provide concentrations and clearance terms where $CL_f = k_f\ V$ and CL(m) = k(m) V(m), and the units of clearance are volume/time,

$$C(\mathrm{m}) = \frac{k_f \cdot V}{k(\mathrm{m}) \cdot V(\mathrm{m})} \cdot C = \frac{CL_f \cdot C}{CL(\mathrm{m})} \qquad \text{(Eq. 9)}$$

Though the metabolite concentration in the body, C(m), at any time after a dose of parent drug can be determined by assay of plasma samples, in this case where k(m) $\gg$ k, it is not possible to estimate k(m) unambiguously. An estimate of k(m) can only be determined by obtaining metabolite plasma concentration versus time data following an intravenous dose of the metabolite itself. These relationships do, however, indicate that the concentration ratio of metabolite versus parent drug will essentially be constant over time (Fig. 1A). This ratio will be useful when relationships of concentration and clearance are discussed below.

With FRL metabolism, the observed apparent half-life of metabolite from concentration versus time curves is related to a first-order elimination rate constant of the parent drug, $t_{1/2} = \ln 2/k$, and the elimination half-life of the parent drug is longer than that of the metabolite if the metabolite were dosed independently. Since the metabolite is eliminated much faster than it is formed, its true half-life is not apparent, and the concentration versus time profile of the metabolite follows that of the parent drug as shown in Figures 1A and 2, where the log of the amount or plasma concentration are plotted on the ordinate. For naphthoxylacetic acid, a metabolite of propranolol (Fig. 2), its plasma profile parallels that of propranolol whether the parent drug is given intravenously or orally (20). Even if the parent drug displayed more complex disposition characteristics with an initial distribution phase noted after an IV bolus dose (i.e., a two-compartment model) or perhaps secondary absorption peaks because of enterohepatic recycling, one would still expect to see a parallel profile for a metabolite subject to FRL metabolism. The observation of parallel metabolite and parent drug profiles after dosing the parent drug can also occur in cases of reversible metabolism, thus this possibility should also be considered (see sect. "Reversible Metabolism").

Elimination Rate-Limited Metabolism

The second limiting case is when k(m) $\ll$ k, that is, the elimination half-life of the metabolite is much longer than that of the parent drug. Here, the metabolite is eliminated by either excretion or sequential metabolism with a first-order rate constant that is much smaller than the rate constant for elimination of the parent drug ($k = k_f + k_{other}$), and this situation is defined as "elimination rate-limited" (ERL) metabolism. There is no requirement for the relative magnitude of k(m) and k_f. Because of the differences between k(m) and k, the exponential term $e^{-k \cdot t}$ in Eqs. 3 and 4 declines rapidly relative to the exponential term $e^{-k(m) \cdot t}$, and the term in the denominator, [k(m) $-$ k], approaches the value of k. Thus, when k(m) $\ll$ k, after most of the parent drug has been eliminated, Eq. 3, which describes an IV bolus of parent drug, simplifies to

$$A(\mathrm{m}) = \frac{k_f \cdot D}{k}[e^{-k(\mathrm{m})t}] \qquad \text{(Eq. 10)}$$

With ERL metabolism, Eq. 4 also simplifies to express metabolite concentration versus time after an intravenous dose of the parent drug. This simplification indicates that with ERL metabolism, a log-linear plot of amount or concentration of metabolite versus time would have a terminal slope reflecting the true elimination half-life for the

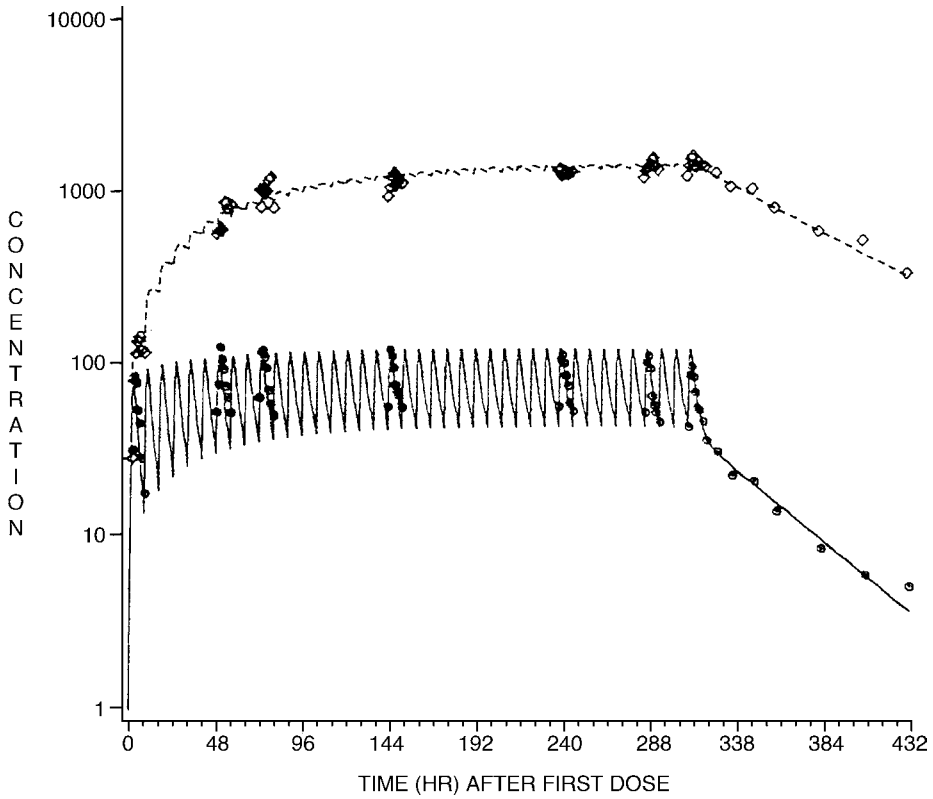

Figure 3 Plasma levels (ng/mL) of halazepam (⊙) and *N* desalkylhalazepam (◇) after 40 mg halazepam every 8 hours for 14 days showing characteristics of elimination rate limited metabolism (21). The estimated elimination half lives for halazepam and *N* desalkylhalazepam are 35 and 58 hours, repectively. Notable for the longer half lives of the metabolite are a longer time to achieve steady state than the parent drug and smaller fluctuations between doses as seen in the simulated fit of the data. *Source*: From Ref. 21.

metabolite, i.e., $t_{1/2} = \ln 2/k(\mathrm{m})$. This is shown in Figure 1B, and an example of this type of metabolite profile is exemplified by the disposition of *N*-desalkylhalazepam, a metabolite of halazepam shown in Figure 3 (21). Under the condition of ERL metabolism, the elimination half-life of the metabolite is unambiguously and clearly resolved from that of the parent drug. Prodrugs are generally designed to follow ERL metabolism where the prodrug is rapidly metabolized to the active moiety that persists in the body for a much longer time than the parent prodrug, e.g., aspirin forming salicylate or mycophenolate mofetil forming mycophenolic acid. Considerations of possible accumulation of metabolite under ERL metabolism after chronic dosing of parent drug will be addressed below.

Rates of Metabolite Elimination Approximately Equal to Rates of Elimination of Parent Drug

The above conditions of FRL and ERL metabolism permit simplification of the equations describing the disposition of the metabolite. However, in cases where $k(\mathrm{m})$ is close to the value of k, log-linear plots of metabolite concentration versus time do not, in theory,

become apparently linear in the terminal phase of a concentration versus time profile because neither exponential term of Eq. 3 nor of Eq. 4 will become negligible and drop out as time progresses. Error in the analysis of plasma concentrations will also contribute to inability to discern a value for k(m) from such a plot. Under these conditions, the use of log-linear plots to estimate k(m), and subsequently the elimination half-life of the metabolite, will lead to an underestimation of k(m) (12). Therefore, caution should be used when interpreting metabolite elimination rates and half-life data when clear distinction of k(m) from k cannot be made. In practice, when $k(\mathrm{m}) \cong k$, it is possible that noise in the data may make the terminal phase of the log concentration versus time plots appear reasonably log linear. A discussion of how to analyze data in instances where it appears that $k(\mathrm{m}) \cong k$ is presented in the earlier review by Houston (12).

Clearance and Volume of Distribution for Metabolites

Most of the above discussion dealt with amounts of drug and metabolite in the body and methods to simply distinguish FRL and ERL metabolism and also to estimate k(m) and half-life for a metabolite with ERL metabolism. However, in most instances, amounts are not known since concentrations of metabolite are determined in plasma or blood over time after dosing the parent drug. Since metabolites are seldom administered to humans [as an investigational new drug (IND) for the metabolite would require significant effort and expense], volume of distribution of the metabolite cannot be determined. Therefore, it is difficult for unambiguous conversion of observed metabolite concentrations to amount of metabolite in the body. It may be possible, given availability of metabolite(s), to administer metabolite to animals to determine relevant pharmacokinetic parameters; however, extrapolation of pharmacokinetic values from animals to humans is complex and problematic. In general, volume terms more often extrapolate between species when scaling than do clearance estimates. If the preformed metabolite can be administered to humans, relevant pharmacokinetic parameters can be determined as commonly employed for the parent drug (16 19). However, one needs to be considerate of the possibility that preformed metabolite dosed exogenously into the systemic circulation may behave differently than metabolite formed within specific tissues of the body such as the liver or kidney, as summarized by Smith and Obach (9) and Prueksaritanont and Lin in this book (Chapter 24). Although a position paper addressing metabolites and drug safety stated that radiolabeled ADME (absorption, distribution, metabolism, and excretion) studies were adequate to address metabolite exposures (22), the Food and Drug Administration (FDA) issued a guidance on "major metabolites" that suggest animal studies of exogenously administered metabolites (23). Thus, there will likely be considerable information on metabolite distribution and pharmacokinetics in animals in the future. Much of the discussion here will focus on basic clearance of concepts that are applicable to metabolites, given limited knowledge of their disposition in humans, and may provide insight into the disposition of the metabolite if some assumptions are made.

The mass balance relationship in Eq. 1 can be modified by multiplying k(m) by V(m) and then dividing A(m) by V(m), which provide the values of metabolite clearance CL(m) and C(m), respectively. Similarly, multiplying and dividing the other terms in Eq. 1 by the volume of distribution of the parent drug V provides $\mathrm{CL_f}$ ($k_\mathrm{f} \cdot V$) and C, respectively, where $\mathrm{CL_f}$ is the fractional clearance of parent drug to form the metabolite and C is the concentration of the parent drug. $\mathrm{CL_f}$ can also be expressed as the product, $f_\mathrm{m} \cdot \mathrm{CL}$, where f_m is the fraction ($f_\mathrm{m} = k_\mathrm{f}/k = \mathrm{CL_f}/\mathrm{CL}$) of systemically available dose of parent drug that is converted irreversibly to the metabolite of interest. For the purpose of the discussion here, it will be assumed that any metabolite formed is systemically available and not subject to

sequential metabolism or excretion without being presented to the systemic circulation. With this assumption and the above substitutions, Eq. 1 can be rewritten as

$$\frac{dA(\mathrm{m})}{dt} = \mathrm{CL_f} \cdot C - \mathrm{CL(m)} \cdot C(\mathrm{m}) \qquad \text{(Eq. 11)}$$

It is useful to consider the integration of Eq. 11 with respect to time from zero to infinity after an intravenous bolus of the parent drug. Since metabolite amounts in the body at times zero and infinity are zero and the terms of $\mathrm{CL_f}$ and CL(m) are assumed to be constant, the integral of concentration versus time is the area under the concentration versus time curve, AUC. The following relationship is obtained,

$$\mathrm{CL_f} \cdot \mathrm{AUC} = \mathrm{CL(m)} \cdot \mathrm{AUC(m)} \qquad \text{(Eq. 12)}$$

where AUC(m) and AUC are the area under the plasma concentration versus time curve for the metabolite and parent drug, respectively. Since the product of a clearance and an AUC term is an amount, $\mathrm{CL_f}$, AUC equals the amount of metabolite formed from the parent drug that reaches the systemic circulation, which for an intravenous dose equals f_m. The value of $\mathrm{CL_f}$ or f_m is usually not unambiguously known, but may be estimated in some cases with some assumptions, e.g., no sequential metabolism and all metabolite formed is excreted in the urine, or both urine and bile are collected in an animal model. Since $\mathrm{CL_f}$ is defined above as $f_\mathrm{m} \cdot \mathrm{CL}$, this can be substituted into Eq. 12 and then rearranged to provide,

$$\frac{f_\mathrm{m} \cdot \mathrm{CL}}{\mathrm{CL(m)}} = \frac{\mathrm{AUC(m)}}{\mathrm{AUC}} \qquad \text{(Eq. 13)}$$

This relationship indicates that the relative AUCs of the metabolite versus parent drug will be dictated by the elimination clearances of metabolite and parent drug and the magnitude of the fraction of the dose that is directed toward the particular metabolite. For example, the AUC of morphine-3-glucuronide (M3G) is much greater than the AUC of morphine (ratio, ~7.8). Since the value of f_m cannot exceed unity, and a collection of urine long enough to estimate total recovery indicated that M3G averages 44% of the IV dose, it is apparent that the ratio of CL/CL(m) must be much greater than 1 (~17). It was reported that the half-lives of M3G and morphine were 3.9 and 1.7 hours (24), respectively; thus M3G follows ERL metabolism, which is consistent with the much lower clearance of the metabolite contributing to its slow rate of elimination. With relative measures of clearance available from Eq. 13, one can also estimate the relative magnitude of the volume of distribution between metabolite and parent drug. Morphine being basic has a fairly large volume of distribution estimated to be 4 L/kg (24,25). In this case of ERL metabolism, where the relative values of k and k(m) can be determined, one can substitute the relationship, $\mathrm{CL} = k \cdot V$ into Eq. 13 and rearrange the equation to estimate relative values for the volumes of distribution,

$$\frac{V}{V(\mathrm{m})} = \frac{1}{f_\mathrm{m}} \cdot \frac{k(\mathrm{m}) \cdot \mathrm{AUC(m)}}{k \cdot \mathrm{AUC}} \qquad \text{(Eq. 14)}$$

Using the data presented in Figure 4 and associated data (20), Eq. 14 provides an estimate of V(m) for M3G of about 0.5 L/kg, which is roughly one-seventh the value for V of morphine in adults. M3G has not been administered to humans, however, following an infusion of a diamorphine (a prodrug of morphine) to infants, the V(m) of M3G was estimated to be 0.55 L/kg. Also, when its active analgetic isomer, M6G, was given to humans, it was determined to have a small volume of distribution of only 0.3 L/kg (26).

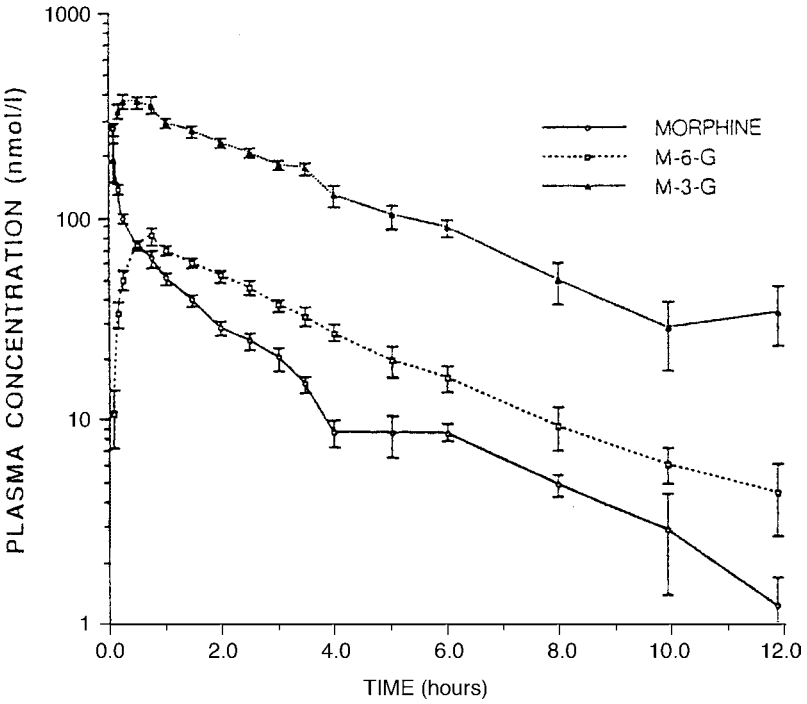

Figure 4 Plasma levels (mean ± SEM) for morphine, M6G and M3G in humans after a 5 mg intravenous bolus (24). The plot and associated data indicate that M3G has FRL metabolism, as its average half life is more than twofold longer than that of morphine. *Abbreviations*: M6G, morphine 6 glucuronide; M3G, morphine 3 glucuronide; FRL, formation rate limited. *Source*: From Ref. 24.

This example shows that the much larger AUC for M3G relative to morphine is due to a smaller clearance for the metabolite. The high peak M3G concentration is likely due to the rapid formation of the metabolite, which has a smaller volume of distribution because of its lower partitioning into tissues relative to the much more lipophilic parent drug, morphine.

The elimination rate constant, which is a parameter dependent on clearance and inversely dependent on the volume of distribution (i.e., $k = \mathrm{CL}/V$), is lower for M3G because of CL(m) being substantially smaller than CL. This relationship is summarized by the following equation,

$$\frac{k(\mathrm{m})}{k} = \frac{\mathrm{CL}(\mathrm{m}) \cdot V}{\mathrm{CL} \cdot V(\mathrm{m})} \qquad \text{(Eq. 15)}$$

In cases where metabolism is FRL, the value of k(m) cannot be estimated; thus, the relative volumes of distribution cannot be determined using Eq. 14, even when f_m is known. However, Eq. 13 is quite useful in estimating the important parameter, CL(m), which can be used to predict average concentrations of the metabolite upon chronic administration, as will be discussed below. From Eq. 13 and the example of naphthoxylacetic acid/propranolol shown in Figure 2, where AUC(m)/AUC is much greater than 1, it is apparent that the clearance of naphthoxylacetic acid is much smaller than that of its parent drug [CL(m)/CL $\ll$ 1]; since the value of f_m cannot exceed unity, propranolol forms other known metabolites, and only 14% of the dose was excreted in

urine as naphthoxylacetic acid. When Eq. 15 is then considered and since $k(m)/k$ must exceed the value of 1 for FRL metabolism, it is apparent that the ratio of $V/V(m)$ must be large to compensate for the small ratio of CL(m)/CL for naphthoxylacetic acid/propranolol. Thus, $V(m)$ must be much smaller than V, which is also confirmed by the high concentrations of naphthoxyacetic acid relative to that of propranol shown in Figure 2 soon after the dose.

Consideration of the two primary pharmacokinetic parameters, clearance and volume, in Eq. 15 also provides an understanding of why FRL is more common than ERL metabolism, i.e., $k(m)/k$ is greater than 1 for a majority of metabolites. Most metabolites are more polar than the parent drug because of oxidation, hydrolysis, or conjugation, thus they often distribute less extensively in the body [$V(m) < V$]. Exceptions to this may be metabolic products due to methylation or acetylation, which may be similar or more lipophilic than the respective parent drug. Most metabolites also have higher clearances than the parent drug, because of susceptibility to further phase II metabolism, enhanced biliary or renal secretion once a polar or charged functional group is added by biotransformation (e.g., oxidation to a carboxylic acid and conjugation with glucuronic acid, glycine, glutathione, or sulfate), or reduced protein binding, which may increase renal filtration clearance and increase clearance of metabolites with low extraction ratios. Together, these effects of a smaller volume and higher clearance, being the most commonly observed behavior for metabolites, result in FRL metabolism.

In the case of ERL metabolism, volume of distribution of a metabolite can be estimated using Eq. 14 if the parent drug can be administered as an intravenous dose to humans. As mentioned above, with FRL metabolism, $k(m)$ cannot often be unambiguously determined from plasma metabolite concentration versus time data in humans; therefore, $V(m)$ cannot be easily determined. However, volume of distribution for a metabolite in humans may be extrapolated from the values of $V(m)$ obtained in animals after intravenous dosing of the metabolite, if such data are available. Because volume is a parameter that is to a great extent dependent upon physiocochemical properties of a compound and binding to tissues, this parameter when corrected for differences in plasma protein binding tends to be more amenable to interspecies scaling than is clearance (27 29). With a prediction of $V(m)$ in humans based on interspecies scaling, Eq. 15 may be used to estimate $k(m)$ for cases of FRL metabolism if f_m or CL(m) is known.

Volume of distribution for a metabolite at steady-state [$V(m)_{ss}$] can also be estimated from mean residence time (MRT) measurements as discussed below.

Mean Residence Time for Metabolites after an Intravenous Dose of Parent Drug

MRT in the body is a measure of an average time that a molecule spends in the body after a dose and is a pharmacokinetic parameter that can be employed to describe metabolite disposition. MRT is considered a non-compartmental parameter on the basis of statistical moment theory (30); however, its use does assume that processes of metabolite formation and clearance are first order and linear, i.e., not dose or time dependent, the metabolite is formed irreversibly, and the metabolite is only eliminated from the sampling compartment, i.e., no peripheral tissues eliminate the metabolite by excretion or further metabolism. Hepatic and renal clearance are generally considered as part of the sampling compartment. There are more complex methods to estimate MRT that may accommodate reversible metabolism (31), though they are seldom employed or reported. MRT(m) is a time-average parameter, which is dependent on the disposition of the metabolite once formed. Thus, MRT(m) is of value in evaluating whether elimination and distribution of

the metabolite have changed when the shape of the plasma metabolite concentration versus time curve is altered in response to changes in the disposition of the parent drug. Also, the relationship, $V(m)_{ss} = CL(m) \cdot MRT(m)_{m,iv}$, is useful to determine $V(m)_{ss}$, if CL(m) can be determined (32).

When an intravenous bolus dose of preformed metabolite is administered, the $MRT(m)_{m,iv}$ is calculated as,

$$MRT(m)_{m,iv} = \frac{AUMC(m)_{m,iv}}{AUC(m)_{m,iv}} \quad \text{(Eq. 16)}$$

where AUMC is the area under the first moment of the concentration versus time curve from the time of dosing, then estimated to infinity (17,30 33). The subscripts indicate the compound and route administered. A similar relationship describes the MRT of the parent drug if given as an intravenous bolus. $MRT(m)_{m,iv}$ measured after a rapid intravenous bolus of the metabolite reflects a mean time in the body for elimination and distribution of the metabolite. Measures of AUMC can be subject to substantially more error than AUC, primarily because of the need to extrapolate a larger portion of the first moment from the last sampling time to infinity (17,30).

When the metabolite is formed after intravenous dosing of the parent drug, the measured mean residence time reflects not only the mean time of metabolite in the body but also the time required for its formation from the parent drug. Therefore, the MRT(m) is corrected for this contribution by subtracting the MRT of the parent drug,

$$MRT(m)_{m,iv} = \frac{AUMC(m)_{p,iv}}{AUC(m)_{p,iv}} - \frac{AUMC_{p,iv}}{AUC_{p,iv}} \quad \text{(Eq. 17)}$$

Here, the ratio $AUMC(m)_{p,iv}/AUC(m)_{p,iv}$ is sometimes referred to as the mean body residence time for the metabolite, MBRT(m), which reflects formation, distribution, and elimination processes, whereas the $MRT(m)_{m,iv}$ may be referred to as the mean disposition residence time, MDRT(m), reflecting only elimination and distribution (32). From Eq. 17, $MRT(m)_{m,iv}$ can be determined unambiguously from the plasma concentration versus time profiles of metabolite and parent drug after an intravenous dose of the parent drug, without the need for an intravenous dose of the metabolite (32,33). In a later section, $MRT(m)_{m,iv}$ will be derived following extravascular dosing of the parent drug.

METABOLITE KINETICS AFTER A SINGLE EXTRAVASCULAR DOSE OF PARENT DRUG

When a drug is not administered by an intravenous route, the rate of drug absorption from the site of extravascular administration, e.g., the gastrointestinal (GI) tract for peroral or the muscle for intramuscular adds additional complexity to understanding the disposition of the metabolite. There are several confounding factors to be considered, the most obvious being both the extent of availability, F, of the parent drug and its rate of absorption, k_a, as defined by a rate constant. Here, for simplicity, a first-order rate of absorption will be employed, though drug inputs that approximate zero-order process are also commonly found, especially with sustained or controlled release dosage forms. Additional considerations when extravascular administration is employed is estimating the fraction of the dose transformed into metabolite during absorption, which is referred to as "first-pass metabolite formation," and the fraction of metabolite that is formed during the absorption process reaching the plasma sampling site. These issues will be discussed

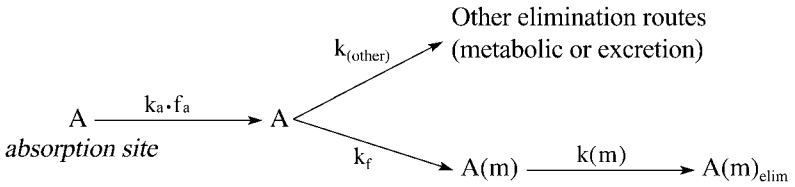

Scheme 3 Absorption of drug and its metabolism to a primary metabolite, with no first pass metabolism to the primary metabolite and parallel elimination pathways. Primary metabolite is eliminated by excretion or further metabolism.

later. It is instructive to first consider Scheme 3, which represents drugs with little or no first-pass metabolite formation, as commonly found for drugs with high oral availability. Again, for simplicity, it will be assumed that all metabolite formed after absorption of the parent compound reaches the systemic circulation prior to irreversible elimination, i.e., the availability of metabolite when formed in vivo, $F(\mathrm{m})$, is complete.

Metabolite Disposition After Extravascular Drug Administration with Limited Metabolite Formation During Absorption

Scheme 3 represents a drug where negligible metabolite forms during the absorption process. This scenario may be expected for drugs with high oral availability and low hepatic and gut wall metabolic clearance or drug administered by other extravascular administration routes where little or negligible metabolite may be formed during absorption, e.g., intramuscular administration. However, this scheme does not necessarily require high availability for the drug, but does assume that drug not reaching the systemic circulation is not because of biotransformation to the metabolite of interest, e.g., low availability may be due to poor dissolution, low GI membrane permeability, degradation at the site of absorption, or the formation of other metabolites. In this case, $F = f_a$, if no other first-pass metabolites are formed. Scheme 3 contains an absorption step, which was not present in Scheme 1. This catenary process with rate (k_a), drug elimination (k), and metabolite elimination [$k(\mathrm{m})$] in series will influence metabolite disposition depending on the step that is rate-limiting.

For a drug with first-order absorption and elimination, the following bi-exponential equation describes the disposition of the parent drug (17),

$$C = \frac{k_a \cdot F \cdot D}{V \cdot (k_a - k)} [e^{-k \cdot t} - e^{-k_a \cdot t}] \qquad \text{(Eq. 18)}$$

This equation is mathematically analogous to Eqs. 3 and 4 (above), and if multiplied by V provides amounts rather than concentrations. If Eq. 18 is substituted into Eq. 1 and solved for the concentration of metabolite over time, one obtains a relationship with three exponentials, since there are two steps prior to the metabolite reaching the systemic circulation and one step influencing its elimination

$$C(\mathrm{m}) = C_1 \cdot e^{-k \cdot t} + C_2 e^{-k(\mathrm{m}) \cdot t} + C_3 \cdot e^{-k_a \cdot t} \qquad \text{(Eq. 19)}$$

Here the constants C_1, C_2, and C_3 are complex terms derived from the model in Scheme 3, which include the bioavailability of the parent drug, F, and dose, D, in their respective numerators, as well as the volume of distribution of the metabolite in the denominator. The values for these constants in Eq. 19 may be estimated by computer

fitting of experimental data. Though the values of these constants have limited inherent utility themselves, the fitting process does provide a description of the time-dependent metabolite profile. Through the application of the superposition principle (17), the descriptive equation may be employed to estimate metabolite profiles at steady state after chronic dosing or following irregular multiple dosing regimens of the parent drug.

Since Scheme 3 does not have any reversible processes, it is a catenary chain with simple constants for each exponential term in Eq. 19, which are easily conceptualized from the schematic model. These exponential terms indicate that any one of the processes of absorption, parent drug elimination, or metabolite elimination may be rate determining. The rate constant associated with the rate-limiting step (i.e., the slowest step) corresponds to the slope observed for the log-linear concentration versus time curve of the metabolite in plasma, assuming that one of the three rate constants is distinctly smaller. For drugs with FRL metabolism, either k or k_a will correspond to the terminal slope (and subsequently the observed half-life) and knowledge of the rates of absorption and elimination of the parent drug may be employed to discern which process or step may control the apparent terminal half-life of the metabolite concentration in plasma. For ERL metabolism, the elimination half-life of the metabolite is by definition longer than the elimination half-life of the parent drug. Therefore, if absorption is rate limiting, then the absorption rate may not only govern the observed terminal half-life of the parent drug but may also dictate the observed apparent terminal half-life of the metabolite. This is shown in Figure 5 where the rate of absorption of morphine is decreased after administration of a slow release buccal formulation such that the elimination rate for morphine cannot be distinguished from that of its metabolites (24). Without administration of an intravenous dose or an immediate release tablet of morphine (Fig. 4), one could not discern from Figure 5 whether M3G follows ERL or FRL metabolism or whether the terminal half-life of Figure 5 is due to absorption.

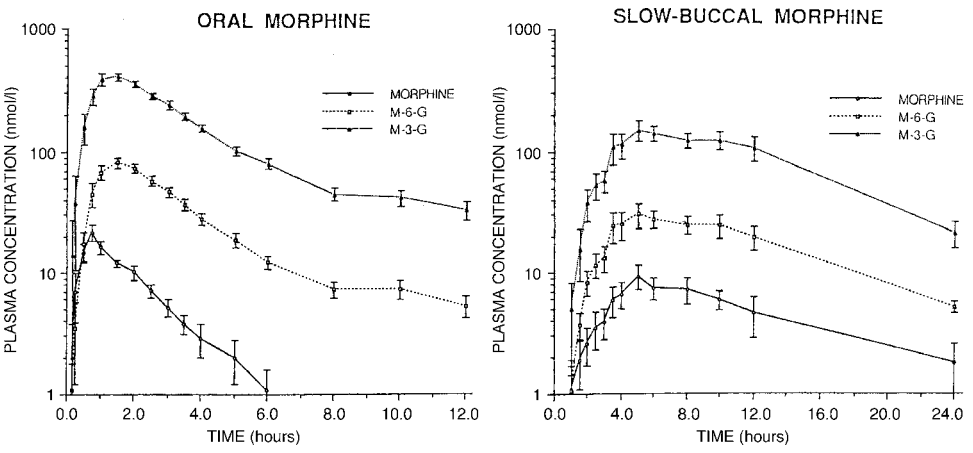

Figure 5 Comparison of immediate release oral (11.7 mg) versus slow release buccal (14.2 mg) adminstration of morphine in humans on the profile of morphine, M6G and M3G (24). The common terminal half life observed for parent drug and both metabolites shown for the slow release buccal formulation are longer than obtained after the immediate release dosage form, suggestive of absorption being rate limiting. *Abbreviations*: M6G, morphine 6 glucuronide; M3G, morphine 3 glucuronide. *Source*: From Ref. 24.

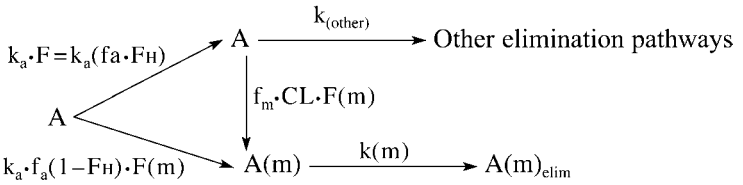

Scheme 4 Absorption of drug and metabolism to a primary metabolite with first pass formation of metabolite followed by excretion or metabolism.

Metabolite Disposition After Extravascular Drug Administration with Metabolite Formation During the Absorption Process

In numerous cases, as occurs for drugs with significant first-pass hepatic or gut wall metabolism, metabolite formed during absorption must be considered in characterizing the disposition of metabolite. Scheme 4 presents a model with one primary metabolite and other elimination pathways for the parent drug after absorption. Also introduced here is consideration of the availability of the metabolite once formed in vivo [F(m)].

Here the availability term, F, is the product of the fraction of dose of parent drug absorbed, f_a, and the fraction of dose reaching the liver that escapes biotransformation to metabolites (first-pass metabolism via the liver and/or GI tract) during first-pass absorption, F_H. As mentioned above, the term "f_a" includes drug not reaching the systemic circulation because of poor solubility, degradation, or low GI membrane permeability, and is often estimated by application of a mass balance approach after administration of radiolabeled drug. For example, if there is little radioactivity recovered in feces after an intravenous dose, then summation of the fraction of radiolabel in urine, tissues and expired breath after an oral dose of radiolabeled material would provide an estimate of f_a. The term "1 F_H" represents the fraction of drug absorbed that forms metabolites during the first-pass, which is also commonly defined as the extraction ratio across the organ, E. Also introduced here, is consideration of the availability of the metabolite, F(m), which is the fraction of metabolite formed that is subsequently systemically available, e.g., not subject to sequential metabolism, intestinal efflux, or biliary excretion. In practice, F(m) can only be determined unambiguously (assuming preformed metabolite behaves as does in situ generation of metabolite) after administration of the preformed metabolite by both the IV and extravascular routes, which is seldom possible in humans though may be feasible in animals (9). If other metabolites are also formed during absorption, then a fraction of the extraction ratio will represent the primary metabolite of interest (14). First-pass formation of metabolite via the gut wall is not considered separately here since the source of metabolite measured in the systemic circulation (either from the liver or GI wall) cannot be distinguished easily in human studies.

Assuming that there is no gut wall metabolism and that the fraction of metabolite formed during the first pass of drug through the liver is the same as subsequent passes (i.e., no saturable first-pass metabolism), then the amount of metabolite formed and presented to the systemic circulation is equal to the product of the AUC(m) and CL(m) (12),

$$f_a \cdot f_m \cdot F(\mathrm{m}) \cdot D_{po} = \mathrm{CL}(\mathrm{m}) \cdot \mathrm{AUC}(\mathrm{m})_{p,po} \qquad \text{(Eq. 20)}$$

where f_m is the fraction of dose that is converted to the metabolite of interest and the subscripts indicate that the parent drug was administered orally. A similar relationship exists for an intravenous dose of parent drug; however, f_a would be equal to unity. When the relationship of Eq. 20 is applied to both oral and intravenous doses of the parent drug (equal doses are used here, thus, doses cancel), the fraction of an oral dose of parent drug that is absorbed, f_a, can be estimated by measuring the metabolite exposure, AUC(m) (12),

$$f_a = \frac{\text{AUC(m)}_{p,po}}{\text{AUC(m)}_{p,iv}} \quad \text{(Eq. 21)}$$

With the assumption that first-pass loss of absorbed drug is only due to hepatic elimination, F_H can be estimated from the relationship, $F = f_a F_H$, where $F = \text{AUC}_{po}/\text{AUC}_{iv}$ if doses of parent drug are equal by both oral and intravenous routes. If the value of f_a as determined with Eq. 21 is greater than 1, this would suggest that GI wall metabolism is occurring. When the data of naphthoxylacetic acid/propranolol in Figure 2 is analyzed in this manner, f_a was estimated to be 0.98, which indicates that the absorption of propranolol is essentially complete and much of the formation of this metabolite is hepatic.

Estimating Fraction of Metabolite Formed and Formation Clearance

Commonly, values for f_m are reported for drugs administered to humans on the basis of collection of metabolite in urine after a dose of the parent drug. This, of course, assumes that all metabolite formed reaches the systemic circulation [i.e., $F(m) = 1$] and is then excreted into urine or that identification of sequential metabolites is accurate and they are also efficiently excreted in urine. If metabolite can be administered independently, then additional calculations of f_m can be employed. Dosing preformed metabolite intravenously provides $\text{AUC(m)}_{m,iv}$, which can be compared to metabolite exposure from an intravenous dose of parent drug (34),

$$f_m \cdot F(m) = \frac{\text{AUC(m)}_{p,iv} \cdot M}{[\text{AUC(m)}_{m,iv} \cdot D]} \quad \text{(Eq. 22)}$$

where M and D are molar doses of metabolite and parent drug, respectively. This relationship assumes that systemic clearance of the metabolite is independent of whether metabolite was dosed exogenously or formed from the parent drug in vivo. The term "F(m)" is present in Eq. 22 because availability of metabolite formed from intravenous parent drug may be less than complete. If the preformed metabolite was instead administered orally where it must also pass the liver before reaching the systemic circulation, then F(m) cancels (12),

$$f_m = \frac{\text{AUC(m)}_{p,iv} \cdot M}{[\text{AUC(m)}_{m,po} \cdot D]} \quad \text{(Eq. 23)}$$

The experimental approach of dosing the metabolite orally may be more easily performed, since it avoids the preparation and administration of an intravenous dose. However, use of Eq. 23 must now assume that the metabolite is well absorbed from the intestine, i.e., $f_a(m)$ is unity.

Once f_m is estimated, CL_f is simply the product of f_m and the total clearance of the parent drug, $CL_f = f_m\ CL$. An alternative approach to determine rate of metabolite formation and cumulative extent of formation is by the application of deconvolution analysis (35,36). With data from an intravenous dose of the metabolite, i.e., with a known input of the metabolite, the subsequent rate and extent of metabolite formation can be

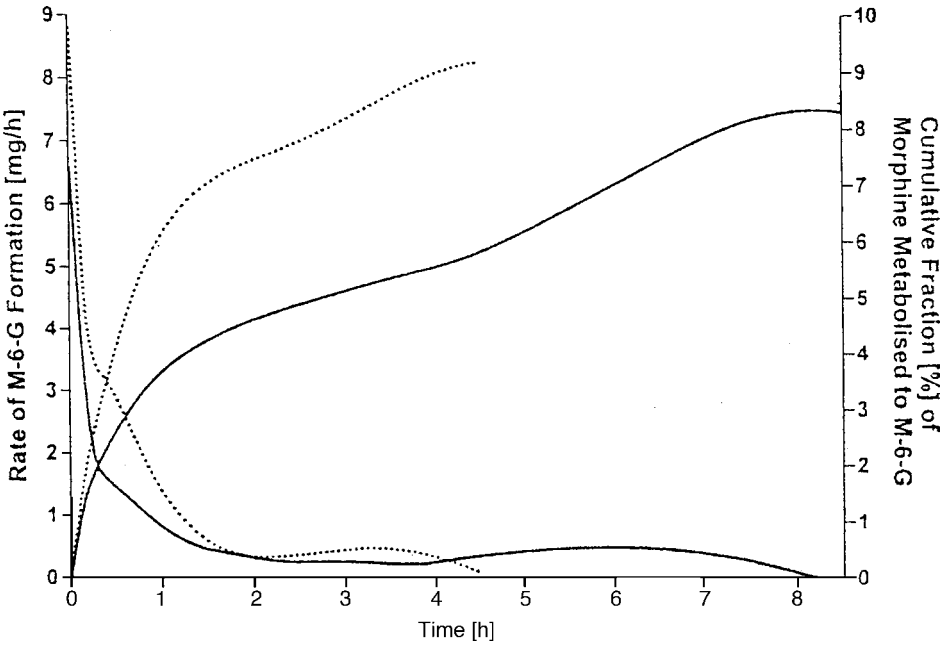

Figure 6 Deconvolution analysis of M6G/morphine to determine the rates of M6G formation (*left ordinate, decending lines*) and fraction of dose metabolized to M6G (*right ordinate, ascending lines*) after intravenous doses of morphine (26). Solid lines are data from a 0.13 mg/kg bolus followed by 0.005 mg/kg/hr infusion for 8 hours. Dotted lines are data from a 0.24 mg/kg bolus followed by 0.0069 mg/kg/hr infusion for 4 hours. *Abbreviation*: M6G, morphine 6 glucuronide. *Source*: From Ref. 26.

obtained by deconvolution (36) after any known input dose of the parent drug. This approach was applied to determine both metabolite formation rates and f_m for M6G after intravenous bolus and infusion doses of morphine, as shown in Figure 6 (26). The values of f_m when estimated by use of Eq. 22 [assuming $F(m) = 1$] and by deconvolution were 12 ± 2 (mean $\pm$ SD) and $9 \pm 1\%$ of the morphine dose, respectively, which is within anticipated experimental error (26). The advantage of the deconvolution approach is that it provides metabolite formation rates over time, which may be helpful in analyzing the system, and it has few assumptions for its application. A disadvantage of the method is that it requires an exogenous dose of the preformed metabolite and assumes that metabolite formed in vivo behaves similarly to that dosed as preformed metabolite.

MRT for Metabolite After an Extravascular Administration of Parent Drug

The $MRT(m)_{m,iv}$ can also be determined after an extravascular dose of the parent drug as long as the assumptions stated above in section "Mean Residence Time for Metabolites after an Intravenous Dose of Parent Drug" apply. The ability to obtain $MRT(m)_{m,iv}$ without an intravenous dose of the metabolite when there is no first-pass metabolism has been presented by several authors (32,33,37), and modifications to accommodate first-pass metabolite formation have been considered (38,39).

If there is no first-pass formation of metabolite during the absorption process, then $MRT(m)_{m,iv}$ can be determined by correction of the MRT of metabolite in the body for

contributions from the parent drug, which now include its absorption as well as distribution and elimination that were accounted for in Eq. 17,

$$\mathrm{MRT(m)_{m,iv}} = \frac{\mathrm{AUMC(m)_{p,po}}}{\mathrm{AUC(m)_{p,po}}} - \frac{\mathrm{AUMC_{p,po}}}{\mathrm{AUC_{p,po}}} \qquad \text{(Eq. 24)}$$

The ratio $\mathrm{AUMC_{p,po}/AUC_{p,po}}$ is defined as the $\mathrm{MRT_{po}}$ of the parent drug when given orally (or any other extravascular route) and is the sum of the $\mathrm{MRT_{iv}}$ and the mean absorption time (MAT) of the parent drug. Since the $\mathrm{MRT_{po}}$ is simply a ratio determined from observed plasma concentration profile of the parent drug after oral administration, $\mathrm{MRT(m)_{m,iv}}$ can be estimated without intravenous administration of either parent drug or metabolite. As mentioned above in section "Mean Residence Time for Metabolites after an Intravenous Dose of Parent Drug," $\mathrm{MRT(m)_{m,iv}}$ provides a parameter for the assessment of disposition (distribution and elimination) of the metabolite without consideration of its rate or time course of formation.

If there is first-pass formation of metabolite, then Eq. 24 may introduce significant error in determining $\mathrm{MRT(m)_{m,iv}}$ (38,39). To correct this error, the contribution of first-pass metabolism from an intravenous dose of the parent drug ($\mathrm{MRT_{p,iv}} = \mathrm{AUMC/AUC}$) and the fraction of the absorbed dose that escapes first-pass metabolism (F_H) need to be considered. Assuming that all metabolite formed from the first pass is due to a single metabolite,

$$\mathrm{MRT(m)_{m,iv}} = \frac{\mathrm{AUMC(m)_{p,po}}}{\mathrm{AUC(m)_{p,po}}} - \frac{\mathrm{AUMC_{p,po}}}{\mathrm{AUC_{p,po}}} + (1 - F_H) \cdot \mathrm{MRT_{p,iv}} \qquad \text{(Eq. 25)}$$

It is apparent that when first-pass metabolism is minimal, i.e., F_H is unity, then Eq. 25 collapses to Eq. 24. In addition, when $\mathrm{MRT_{p,iv}}$ is small relative to the other terms as occurs with transient prodrugs such as aspirin, then the last term of Eq. 25 is again insignificant. However, when there is substantial first-pass metabolism, then use of Eq. 24 would provide a value that underestimates $\mathrm{MRT(m)_{m,iv}}$. In practice, Eq. 24 may provide a value that is negative, indicating that there must be some first-pass metabolism occurring (39).

METABOLITE DISPOSITION AFTER CHRONIC ADMINISTRATION OF PARENT DRUG

Chronic administration of drugs by extravascular routes, multiple infusions, or continuous infusions is commonly employed in ambulatory and hospital settings. In these cases, active metabolites, toxic metabolites, or the impact of the metabolite on the disposition of the parent drug should be considered. Here, one needs to consider the accumulation of both the parent drug and metabolite to steady-state concentrations and the relationship between the steady-state characteristics of the parent drug relative to that of the metabolite, since these characteristics may differ from those observed after only a single dose of drug. The critical pharmacokinetic descriptors for the disposition of the metabolite on chronic drug administration are the time to achieve steady state, peak, trough, and average concentrations at steady state, the accumulation at steady state relative to a single dose of parent drug, and metabolite clearance. Volume of distribution is a parameter that has little contribution in achieving steady-state levels but does impact the swings from peak to trough concentrations at steady state because of its contribution in determining the half-life of parent drug and metabolite.

Time to Achieve Steady State for a Metabolite

Following chronic extravascular administration or intravenous infusion for a sufficiently long time, parent drug and metabolite will eventually achieve steady-state concentrations where the input of parent drug and metabolite (i.e., formation) into the systemic circulation on average equal their respective rates of elimination. The time to achieve such a steady state is dependent on the half-life of the parent drug or metabolite and, if first-order elimination processes occur, generally it takes about 3.3 half-lives to reach 90% of the ultimate steady-state level, and after 5 half-lives, a compound would achieve about 97% of the theoretical steady-state level. In the case of a primary metabolite formed from the parent drug, it will be the slowest, rate-limiting process that governs when a metabolite reaches steady-state levels in the body. Therefore, for metabolites with FRL metabolism, the elimination half-life of the parent compound will control the time to achieve steady-state levels of the metabolite, whereas for ERL metabolism, the longer half-life of the metabolite will dictate the time needed for the metabolite to reach steady-state levels. ERL metabolism is shown in Figure 7, where the two metabolites of morphine take as much as 30 hours to accumulate to steady-state concentrations after bolus injection and continuous intravenous infusion of diamorphine (a prodrug of morphine) to infants, even though morphine rapidly attained steady state (25). In this example, the mean elimination half-lives of the metabolites in 19 infants were estimated by the rate of attainment to steady state (17) to be 11.1 and 18.2 hours for M3G and M6G, respectively (25), whereas these metabolites have reported half-lives estimated to be only several hours in adults (24,26).

On discontinuation of chronic or repetitive parent drug administration, the rate of decline in metabolite concentration will again be dependent upon whether FRL or ERL metabolism is operative. In the case of FRL metabolism, the rate of decline for the concentrations of the metabolite will simply follow that of the parent drug. In contrast, for

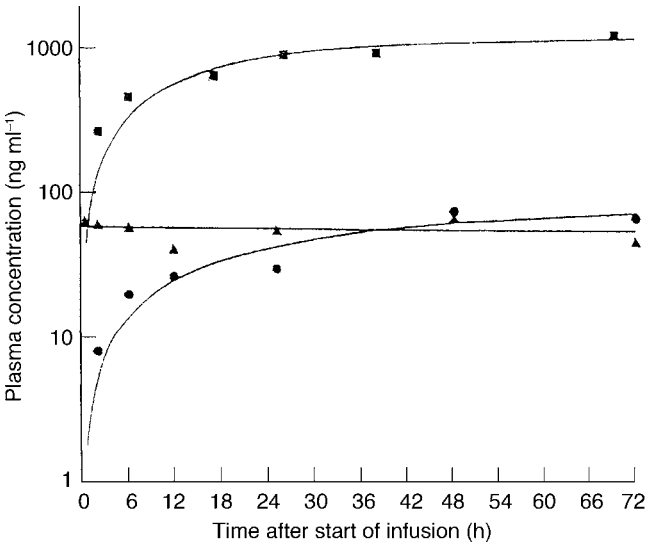

Figure 7 Disposition of morpine (▲), with the formation of M3G (■) and M6G (●), in a representative infant receiving diamorphine (prodrug of morphine) intravenous bolus followed by an infusion for 72 hours (25). The rate of attainment of steady state for the metabolites is determined by the slowest rate constant, which provides estimated half lives of 11 and 18 hours for M3G and M6G, respectively. *Abbreviations*: M6G, morphine 6 glucuronide; M3G, morphine 3 glucuronide. *Source*: From Ref. 25.

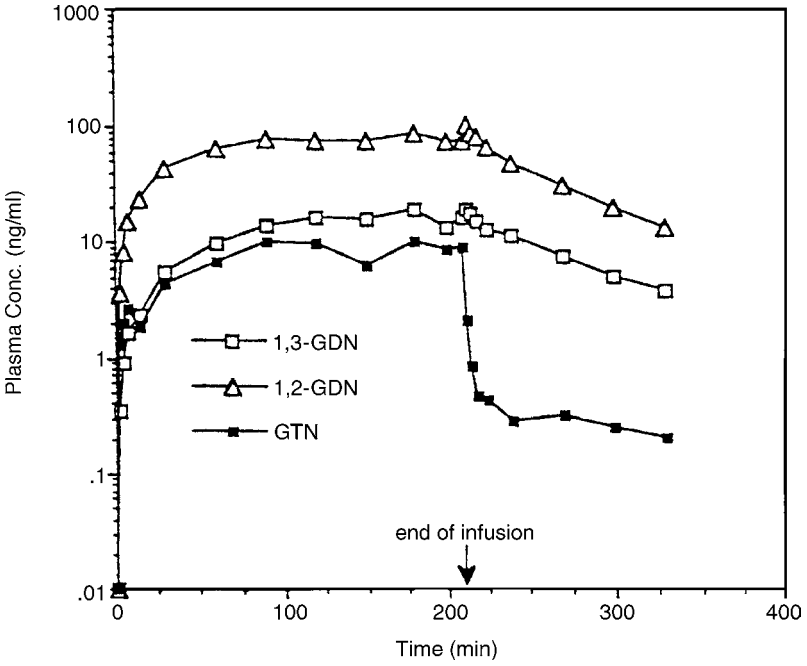

Figure 8 Plasma levels of GTN(■),1,2 GDN (△), and 1,3 GDN (□) following an intravenous infusion of 0.070 mg/min GTN to a dog (40). The half lives of the metabolites were much longer than the apparent half life of approximately four minutes for GTN after the end of the infusion, and data suggest that the prolonged activity of GTN may be due to the metabolites. The prolonged residual GTN at very low concentrations is not understood nor is its slower than anticipated rise to steady state. *Abbreviations*: GTN, glyceral trinitrate; GDN, glyceral dinitrate. *Source*: From Ref. 40.

ERL metabolism, metabolite levels will persist on the basis of their longer half-life as shown in Figure 8 for the metabolites of nitroglycerin (40).

Metabolite Concentrations at Steady State After Continuous Administration of Parent Drug

As mentioned above, at steady state for the metabolite, the rate of formation equals the rate of elimination of the metabolite, i.e., $\Delta A(\mathrm{m})/\Delta t = 0$. Considering the fraction of metabolite formed from the parent drug, f_{m}, and the systemic bioavailability of the metabolite once formed, $F(\mathrm{m})$, from Eq. 11, the following relationship is defined at steady state where the left term is the formation rate of metabolite that reaches the systemic circulation and the right term is its rate of elimination (11),

$$f_{\mathrm{m}} \cdot F(\mathrm{m}) \cdot \mathrm{CL} \cdot C_{\mathrm{ss}} = \mathrm{CL}(\mathrm{m}) \cdot C(\mathrm{m})_{\mathrm{ss}} \qquad \text{(Eq. 26)}$$

Since at steady state for the parent drug, CL C_{ss} is equal to the rate of infusion, R_{o}, this can be substituted into Eq. 26, which upon rearrangement provides the average concentration of metabolite at steady state, $C(\mathrm{m})_{\mathrm{ss.ave}}$.

$$C(\mathrm{m})_{\mathrm{ss,ave}} = \frac{f_{\mathrm{m}} \cdot F(\mathrm{m}) \cdot R_o}{\mathrm{CL}(\mathrm{m})} \qquad \text{(Eq. 27)}$$

This equation describes that $C(\mathrm{m})_{\mathrm{ss,ave}}$ will be proportional to the infusion rate of the parent drug. However, the difficulties in obtaining estimates of the other terms of the

equation without dosing of the metabolite limits the utility of Eq. 27. Alternatively, indirect approaches to estimate $C(\mathrm{m})_{\mathrm{ss,ave}}$ from AUC data obtained after a single dose of the parent drug will be addressed below.

If, instead of intravenous infusions, drug input is via regular and repetitive extravascular administration, the rate of input R_{o} in Eq. 27 is modified to reflect an average drug administered at each dosing interval, D/τ. There is also a correction for the fraction of extravascular dose absorbed, f_{a} (11),

$$C(\mathrm{m})_{\mathrm{ss,ave}} = \frac{f_{\mathrm{m}} \cdot F(\mathrm{m}) \cdot f_{\mathrm{a}} \cdot D}{\mathrm{CL}(\mathrm{m}) \cdot \tau} \qquad \text{(Eq. 28)}$$

Here, the average rate of drug input is $f_{\mathrm{a}} \cdot D/\tau$. The value of $C(\mathrm{m})_{\mathrm{ss,ave}}$ obtained reflects the average level at steady state, but gives no information of relative fluctuations from peak to trough metabolite concentrations, $C(\mathrm{m})_{\mathrm{ss,max}}/C(\mathrm{m})_{\mathrm{ss,min}}$, at steady state. The extent of this fluctuation for the metabolite levels will depend on whether FRL or ERL metabolism occurs. Assuming that absorption is not the rate-limiting process, for FRL metabolism, the metabolite rapidly equilibrates with the parent drug, thus the peak to trough metabolite concentration ratio, $C(\mathrm{m})_{\mathrm{ss,max}}/C(\mathrm{m})_{\mathrm{ss,min}}$, will be similar to $C_{\mathrm{ss,max}}/C_{\mathrm{ss,min}}$ obtained for the parent drug. In contrast, for ERL metabolism, the longer elimination half-life of the metabolite will dampen its concentration swings at steady state such that $C(\mathrm{m})_{\mathrm{ss,max}}/C(\mathrm{m})_{\mathrm{ss,min}} < C_{\mathrm{ss,max}}/C_{\mathrm{ss,min}}$.

Estimating Metabolite Levels at Steady State from a Single Dose

Superposition Principle to Estimate Metabolite Levels at Steady State

When the metabolite and parent drug follow linear processes that are independent of dose and concentrations, i.e., no saturable processes occur, then prediction of metabolite concentrations after multiple doses or with a change of dose can be estimated if the route of drug administration does not change. Under these conditions, the time course of the metabolites as well as their average concentrations can be estimated by the principle of superposition (17). However, if the route of drug administration is different between the single dose administration and the chronic dosing without a change in bioavailability (e.g., single dose is an intravenous bolus, whereas the chronic administration is an intravenous infusion), the average concentration of the metabolite at steady state can be predicted on the basis of relationships of clearance and AUC, as described below.

Superposition simply takes the plasma concentration versus time profile after a single dose and assumes that each successive dose would behave similarly, though the magnitude of concentration will vary proportionally with the dose administered. Thus, both the parent drug and metabolite profile can be summed over time. This can be done either by fitting the single dose data to appropriate mathematical functions as a sum of exponentials or polynomials and then summing this to infinity if the dosing regimen has a constant dosing interval (17), or alternatively, a more simple method, which is easily applied to even irregular dosing intervals, is to use a spreadsheet to sum the concentrations of metabolite from successive doses of the parent drug (15), making certain to have values or extrapolated metabolite concentrations for at least five elimination half-lives of metabolite or parent drug, whichever is longest.

Single Dose AUC Values to Predict Average Metabolite Levels at Steady State

If an estimate of the average concentration of metabolite at steady state is desired, then AUC(m) after a single dose can be employed effectively as shown by Lane and Levy (41).

This approach can also be used when the formulation of parent drug changed between single and chronic administration without altering availability of parent drug or fraction of metabolite formed (e.g., single dose is an oral suspension, whereas chronic administration is a sustained release capsule). From the relationship that the average rate of formation of metabolite is equal to its average rate of elimination at steady state, as provided in Eq. 26 above, these authors then used the relationships of AUC and CL in Eq. 12 to derive the following from AUC data collected after a single dose of the parent drug,

$$\frac{C(\mathrm{m})_{\mathrm{ss,ave}}}{C_{\mathrm{ss,ave}}} = \frac{\mathrm{AUC(m)}}{\mathrm{AUC}} \qquad \text{(Eq. 29)}$$

This relationship assumes linearity (i.e., constant clearance) for the parent drug and metabolite with respect to changes in dose and time. Eq. 29 is applicable to any route of administration but does require that the route used for the single dose measurements of AUC be the same as that to be employed for steady-state measurements of concentrations. This requirement usually ensures that availabilities of the parent drug and metabolite formed are the same between single and chronic doses. This provides a means to estimate the average metabolite concentrations at steady state from AUC(m)/AUC ratios from a single dose and knowledge of an estimated $C_{\mathrm{ss,ave}}$ for the parent drug. Though initially derived from a one-compartment model, Eq. 29 was later extended with fewer restrictions by Weiss (14) using a non-compartmental approach.

When the route of administration changes, which may alter availability of the parent drug, the relationship of Eq. 29 must consider this change. If the initial single dose data were obtained from an intravenous dose, then the ratio of metabolite to parent drug concentrations at steady state after oral dosing will be affected by fraction of parent drug systemically available (12,14). With an assumption that availability of the metabolite did not change with a change in the route of parent drug administration and there is no significant GI wall metabolism, the following relationship can be used,

$$\frac{C(\mathrm{m})_{\mathrm{ss,av}}}{C_{\mathrm{ss,ave}}} = \frac{\mathrm{AUC(m)_{iv}}}{\mathrm{AUC_{iv}}}\left(\frac{1}{F_{\mathrm{H}}}\right) \qquad \text{(Eq. 30)}$$

With regular doses and dosing intervals, τ, the AUC is equal to $C_{\mathrm{ss,ave}} \cdot \tau$; therefore, Eq. 29 can be rearranged and written more simply as,

$$C(\mathrm{m})_{\mathrm{ss,ave}} = \frac{\mathrm{AUC(m)}}{\tau} \qquad \text{(Eq. 31)}$$

where AUC(m) is determined after a single dose of parent drug. Under these conditions of regular dosing to steady state, data on the disposition of the parent drug are not necessarily required when estimating $C(\mathrm{m})_{\mathrm{ss,ave}}$, though most often the parent drug data are available.

In cases where a single intravenous bolus dose of parent drug was used to obtain measurement of AUC(m), but then a continuous infusion of rate, R_{o}, is later employed, one can also derive $C(\mathrm{m})_{\mathrm{ss,ave}}$ without complete knowledge of the disposition of parent drug. Since for continuous infusion, $C_{\mathrm{ss,ave}} = R_{\mathrm{o}}/\mathrm{CL}$, and for a single IV bolus dose of parent drug, $\mathrm{AUC} = D/\mathrm{CL}$, substitution of these well-known relationships into Eq. 29 and rearrangement provides (41),

$$C(\mathrm{m})_{\mathrm{ss}} = \frac{R_{\mathrm{o}} \cdot \mathrm{AUC(m)}}{D} \qquad \text{(Eq. 32)}$$

This relationship provides an actual level, since it is from an infusion where metabolite reaches a steady-state level. Only knowledge of the dose of drug employed for the single intravenous dose, D, and the resultant AUC(m) is needed.

SEQUENTIAL METABOLISM

A common scheme in drug metabolism is the concept of sequential metabolism where a parent drug is converted to one or more primary metabolites, which are then further converted to a secondary metabolite (Scheme 2, above). This process leads to two metabolites as shown in Figure 9, where propranolol is first oxidized to 4-hydroxy propranolol, which then undergoes sequential metabolism to 4-hydroxy propranolol glucuronide (42). Indeed, sequential metabolism formed the basis for the common nomenclature of phase I and phase II metabolism, coined by Williams (43). Another commonly observed sequence is that of parallel metabolism leading to a common metabolite as exemplified by the metabolism of dextromethorphan via CYP2D6 and CYP3A4 (44) shown in Scheme 5.

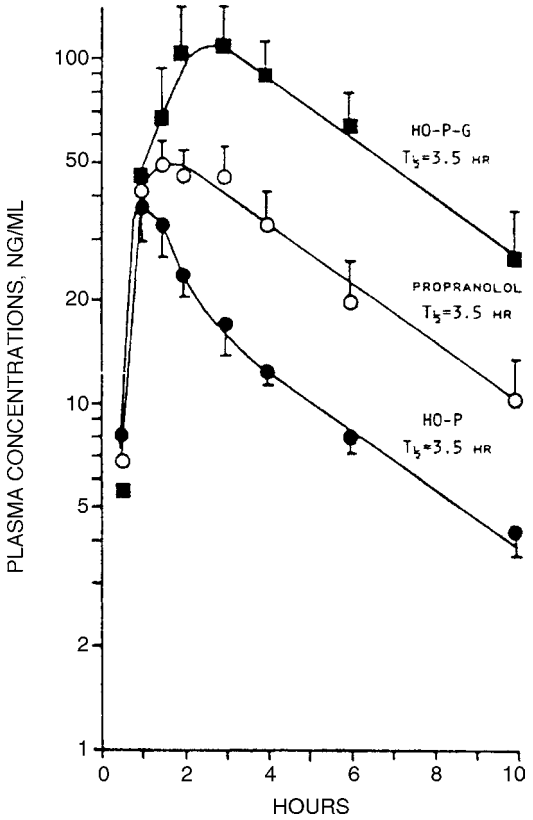

Figure 9 Disposition of propranol (o), its 4 OH metabolite (●), and sequential formation of its 4 OH glucuronide metabolite (■) in humans after a single 80 mg oral dose (42). Data are mean ± SEM, N = 6. The initial rapid increase in 4 OH propranolol is followed by a later peak concentration of 4 OH glucuronide due to sequential metabolism. The nonlinearity of the 4 OH metabolite immediately following its peak is likely due to significant formation of this metabolite during absorption, which takes time to distribute to tissues prior to equilibration with formation of the glucuronide. On the basis of urinary excretion data, most of the 4 OH propranolol is converted to propranolol glucuronide, and when Eq. 21 is applied to these two metabolites, the values of f_a are substantially greater than 1, suggestive of GI wall metabolism. *Source*: From Ref. 42.

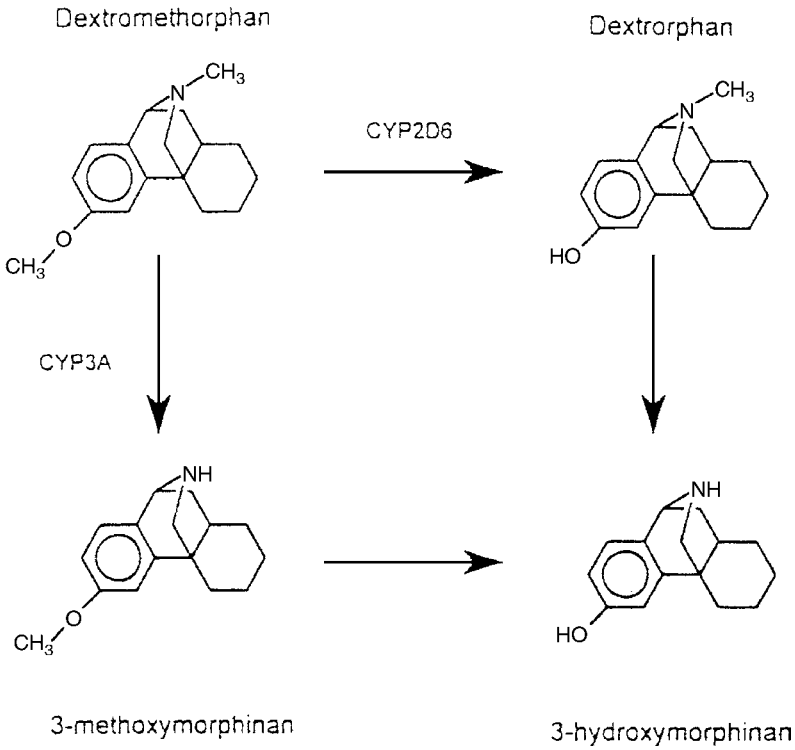

Scheme 5 Parallel metabolic pathways of dextromethorphan to a common metabolite (44).

For either of the two examples presented above, given that first-order processes apply, the equation that describes the disposition of the secondary metabolite would be complex polyexponential functions with the number of terms determined by the number of first-order processes leading to the penultimate metabolite of interest. Such processes may also include an absorption step (not shown in Scheme 5) if the parent compound is administered extravascularly. These processes can be dealt with by fitting the data with a polyexponential function or using other appropriate equations as presented by Eq. 19. A mathematical analysis of parallel and sequential systems has recently been developed (45). In the more simple, catenary chain represented by Scheme 2, the terminal apparent half-life of the secondary metabolite will be determined by the rate-limiting step, i.e., the step with the smallest rate constant among all steps describing the disposition of the metabolite. It is also possible in cases of sequential metabolism, depending on relative rates and competing pathways, that the primary metabolite (m_1 in Scheme 2) may not be observed at all, either in plasma or in urine.

Sequential metabolism is one of the primary reasons that the systemic availability $F(m)$, of a primary metabolite once formed may be less than complete (46,47), as exemplified by 4-OH propranolol, which forms the glucuronide in vivo (Fig. 9). Other factors impacting the systemic availability of a metabolite may include biliary and renal excretion of metabolites once formed in the liver and kidney, respectively, without access to the systemic circulation. Further complications arise when one considers the impact of sequential metabolism, intracellular access, and systemic availability of metabolites for evaluating the disposition of metabolite formed in vivo with that of preformed metabolite administered directly into the systemic circulation (41). To estimate actual pharmacokinetic parameters of metabolite, it is usually necessary to administer preformed

metabolite, preferably by the intravenous route. However, inherent assumptions with such experiments are that the above-mentioned factors are independent of the route of metabolite administration.

RENAL CLEARANCE OF METABOLITES

Many metabolites are eliminated to a significant extent or almost exclusively into the urine. Collection and analysis of urine samples have some advantages the primary one is that they are less invasive than blood sampling. Since urine production volume in a day or during a dosing interval is limited and usually a much smaller volume than V or V(m), urine concentrations of metabolite or parent drug are often a great deal higher than those seen in plasma and thus more easily measured. Urine can also be collected incrementally, usually in intervals of one or more hours from humans, though this is often more difficult for small children, infants, and the elderly. For larger animals, catheterization can be performed to obtain continuous urine samples, but for smaller animals such as the rat, this becomes an invasive procedure that may alter renal function. When incremental urine samples cannot be collected, complete collections over four to five half-lives after a single dose or during one dosing interval at steady state can be performed. Unfortunately, even though urine collection is noninvasive, urinary excretion data are all too often not included in clinical protocols, since these are considered as a secondary measure to plasma drug profiles. However, urinary metabolite excretion data can offer valuable information on the disposition of metabolites, especially when interpreting drug-drug interactions or the basis for altered pharmacokinetics in patient populations.

There are some assumptions that will be made in discussing renal clearance of metabolites that need to be considered. The first is that renal drug metabolism is not occurring, i.e., metabolite measured in plasma is what is filtered or transported into the renal tubule from the plasma, and parent drug does not convert to metabolite in the kidney. If renal drug metabolism does occur, the estimated renal clearance would be considered as an "apparent clearance," which is similar to estimating biliary clearance in a cannulated animal when hepatic metabolism of drug occurs without the metabolite being presented to the systemic circulation. Though the concept of drug metabolism in the liver prior to arrival of metabolite in the bile is well accepted, there appears to be a common, erroneous assumption that drug metabolism is unlikely to occur in the kidney. Another concern that is more easily tested is whether the metabolites are stable once excreted in the urine, since metabolites often reside in the bladder for periods of many hours prior to voiding. An example of this is the hydrolysis and acyl migration of ester glucuronides, which can be quite variable since it is a pH-dependent process (48,49). Finally, it is generally assumed that once a drug or metabolite arrives in the urinary bladder, it is irreversibly removed from the systemic circulation. However, studies have shown that resorption from the urinary bladder back into the systemic circulation can be significant for some compounds, and this phenomenon should be considered (50). For the purpose of discussion in this section, it will be assumed that these complicating factors are negligible, or if they are occurring, they are reproducible, thus permitting calculations that provide estimates of apparent pharmacokinetic parameters.

Determination of Renal Clearance for Metabolites

Renal clearance is one pharmacokinetic parameter that can be determined for most metabolites as well as the parent drug regardless of the route of administration, dosing regimens, formulations, or availability. The data needed are urinary excretion rates and

plasma concentrations. The following general equation applies to calculate renal clearance (CL_R) during a urine collection interval and is expressed for a metabolite (17),

$$CL_R(m) = \frac{\Delta A(m)_e / \Delta t}{C(m)_{ave}} \quad \text{(Eq. 33)}$$

Here, $\Delta A(m)_e$ is the amount of metabolite excreted into the urine during the collection interval, Δt is the collection interval, and $C(m)_{ave}$ is the average plasma metabolite concentration over the interval. Intervals are typically at least two or several hours long for studies in humans due to the difficulty in voiding more frequently. If frequent, short incremental collections of urine are desired, it is common practice to provide oral fluids so that adequate (but not excessive) urine production rates are maintained. The necessary collection interval makes the use of incremental renal clearance calculations difficult and less valuable for drugs with very short half-lives, such as less than an hour. The average plasma concentration is usually measured as the concentration at the midpoint of the collection interval or an average of the plasma concentrations at the beginning and end of a collection period.

An alternative calculation for incremental renal clearance is to rearrange Eq. 33, realizing that the product of the average plasma metabolite concentration and the time interval is the incremental AUC(m) for that collection period, i.e., $\Delta AUC(m) = C(m)_{ave} \cdot \Delta t$; thus,

$$CL_R(m) = \frac{\Delta A(m)_e}{\Delta AUC(m)} \quad \text{(Eq. 34)}$$

Either of the above incremental renal clearance calculations can be applied to any collection interval, without consideration for the method of drug administration. These can also be applied to chronic multiple dose regimens where it is common to measure total urinary output over the dosing interval τ.

Incremental renal clearance calculations should result in values that are approximately constant if $CL_R(m)$ is constant across the periods collected, i.e., linear or concentration-independent pharmacokinetics (15,17 19). If they are not similar, a useful approach is to examine a plot of excretion rate, $\Delta A(m)_e/\Delta t$, as a function of metabolite plasma concentration, $C(m)_{ave}$. The slope of such a plot is $CL_R(m)$, and any nonlinearities may become apparent if renal clearance increases or decreases as concentrations of metabolite change over time or parent drug competes for active renal clearance process, i.e., active secretion or reabsorption.

Measuring incremental renal clearance is not routinely performed as it requires multiple urine collection over several intervals, which adds expense due to processing and analysis costs, or it may not be feasible for studies with children, small animals, or drugs with very short half-lives. Alternatively, a measure of average renal clearance can be determined following a single dose of parent drug using the following equation (17),

$$CL_R(m) = \frac{A_e(m)_{0 \ \infty}}{AUC(m)_{0 \ \infty}} \quad \text{(Eq. 35)}$$

where $A_e(m)$ is the amount of metabolite excreted from initial time of dosing (time zero) to a later time, usually when almost all of the drug and metabolite have been eliminated from the body 4 or 5 elimination half-lives of parent or metabolite (whichever is rate limiting). AUC(m) is the area under the metabolite plasma concentration versus time curve for the same interval. For studies conducted with multiple doses to steady state, the interval for collection of urine and measurement of AUC should be the dosing interval τ.

Use of Metabolite Excretion to Assess Disposition of Drug and Metabolite

Use of Metabolite Excretion Rate to Assess the Profile of Metabolite in Plasma

As mentioned above, metabolite concentrations are often more easily measured in urine than in plasma where concentrations may be below detection limits of the available assay. Assuming that $CL_R(m)$ is constant, the excretion rate into urine should then parallel plasma concentrations of the metabolite as described by Eq. 33 (17). Since a fraction of the total systemic clearance of the metabolite, CL(m), may be due to renal excretion, $f_e(m) = CL_R(m)/CL(m)$, the rate of excretion can be expressed as,

$$\frac{\Delta A(m)_e}{\Delta t} = f_e(m) \cdot CL(m) \cdot C(m)_{ave} \qquad \text{(Eq. 36)}$$

Here, $C(m)_{ave}$ describes the average time course of plasma metabolite concentrations over time, whereas $f_e(m)$ and CL(m) are constant. Thus, urinary excretion data of metabolite when plotted versus time can characterize the profile of metabolite in plasma even when plasma concentrations of metabolite cannot be measured. This profile can be used to estimate the rates of initial increase in metabolite concentrations, the approximate time-to-peak metabolite levels in plasma, and the apparent elimination half-life of the metabolite.

Use of Metabolite Excretion Rates to Assess the Profile of the Parent Drug

For drugs exhibiting FRL metabolism, which is the most common situation, urinary excretion rates or fraction of dose excreted in the urine may be used to estimate the plasma profile of the parent drug. With FRL metabolism, the plasma profile of metabolite parallels that of the parent drug as shown in Eq. 9, which when substituted into Eq. 36 provides,

$$\frac{\Delta A(m)_e}{\Delta t} = f_e(m) \cdot CL_f \cdot C_{ave} \qquad \text{(Eq. 37)}$$

where C_{ave} is the average plasma concentration of parent drug over time. Thus, urinary excretion rate of the metabolite is directly proportional to the concentration of parent drug, which is expected under the conditions of FRL metabolism. Thus, a plot of metabolite excretion rates versus time provides a description of the parent drug profile and can be used to estimate the duration of the absorption phase, approximate time to peak concentration, and elimination half-life of the parent drug without the need to assay parent drug in plasma or urine. Also, evident from Eq. 37 is that with FRL metabolism when values of $f_e(m)$ and $F(m)$ are both unity, then the excretion rate of metabolite equals its rate of formation from the parent drug.

Use of Metabolite Excretion Rates to Assess Formation Clearance of the Metabolite

Where drug concentrations can be measured in plasma, and f_e is known, under FRL metabolism, Eq. 38 can be rearranged to estimate formation clearance of the metabolite CL_f,

$$CL_f = \frac{\Delta A(m)_e/\Delta t}{f_e(m) \cdot C_{ave}} \qquad \text{(Eq. 38)}$$

where C_{ave} is the average concentration of drug during the period of urine collection. The use of Eq. 38 assumes that $F(m)$ of the metabolite is unity, i.e., all metabolite formed reaches the systemic circulation, though it does not require f_e to be equal to unity, though in practice this relationship has been applied to metabolites that are primarily excreted in the urine.

Alternatively, one could use amounts of metabolite and drug rather than concentrations using the same assumptions,

$$k_f = \frac{\Delta A(m)_e/\Delta t}{f_e(m) \cdot A_{ave}} \quad \text{(Eq. 39)}$$

A classic example of the use of this approach is in Levy's studies of salicylate metabolism, which did not even require measurement of plasma salicylate concentrations (51). Salicylate has four major metabolites that are rapidly excreted in urine, so plasma concentrations of these metabolites were difficult to measure prior to the advent of modern liquid chromatography. Given that levels of metabolite in plasma were very low and urinary metabolites accounted for almost all of the salicylate dose, Levy estimated the amount of salicylate remaining in the body by using a mass balance approach where the amount remaining to be excreted at a given time interval represented A_{ave}. By evaluating urinary excretion rates versus A_{ave}, using a linear transformation of the Michaelis Menton equation, the formation of the salicyluric acid and the phenol glucuronide metabolites were found to be saturable, and Michaelis Menton constants, K_m and V_m, were determined, while the metabolism to gentisic acid and the acyl glucuronide were nonsaturable with constant k_f values over a large range of amounts of salicylate in the body.

When incremental collections of urine are not obtained, but the urine collection is for a sufficient number of elimination half-lives to approximate a complete collection of metabolite in the urine, then Eq. 37 can be rearranged and the integral of $C_{ave} \cdot \Delta t$ is the AUC for the parent drug,

$$CL_f = \frac{A(m)_e}{f_e(m) \times AUC} \quad \text{(Eq. 40)}$$

The use of Eq. 40 is not dependent on rapid elimination of metabolite upon formation; thus, it is applicable to both conditions of FRL and ERL metabolism as long as urine is collected for a sufficient duration to account for all the metabolite formed after a single dose. The relationship is also applicable for the analysis of excretion data after chronic dosing to steady state where amount of metabolite in urine and AUC is measured over the dosing interval τ. This equation, as written, does assume that $F(m)$ of the metabolite is unity for the CL_f value to be accurate, though use of an apparent CL_f may be adequate for comparative experiments if $F(m)$ is constant between experiments.

Assessment of Renal Metabolism

Using pharmacokinetic analysis to assess or quantify the extent of renal metabolism in vivo is difficult and not often employed. Renal and biliary clearance calculations employ the same equations and are both subject to errors if formation of metabolite occurs in the organ with subsequent excretion of metabolite without presentation of all metabolite to the systemic circulation. Biliary clearances of a metabolite can be determined by collection of bile in animals, but rarely in humans, and then are often referred to as *apparent* clearances because of the understanding that hepatic metabolism is likely occurring. In contrast, seldom are renal clearances of metabolites reported as *apparent* clearances; thus, there is an inherent assumption that none of the metabolite excreted in the urine is formed by the kidney and immediately excreted in the urine. Though there is little information to determine how often this assumption is valid, given the lower metabolic capability of the kidney relative to the liver for most substrates that have been examined, this assumption is usually accepted for renal clearance calculations. In contrast,

such an assumption would probably be challenged if made for calculating biliary clearance of a metabolite.

If Eqs. 33 to 35 (above) are applied to metabolite excreted in the urine and the value of renal clearance based upon blood concentrations was very high, exceeding renal blood flow, then one may suspect that renal metabolism is occurring. This requires the use of clearance values on the basis of blood concentrations, which can be calculated from clearance in plasma and measurement of the blood/plasma concentration ratio, by the relationship, $CL\ C = CL_B\ C_B$, where the subscript B refers to blood. Therefore, ratios of metabolite concentration in blood relative to plasma need to be obtained and are easily determined in vitro. This phenomenon was reviewed by Vree et al. (52) in human studies. It is easy to conceptualize this phenomenon if one obtains extensive excretion of metabolite in urine when a very sensitive assay cannot even measure the metabolite in plasma. If the plasma concentration of metabolite is assigned a value of zero, then $CL_R(m)$ from the above equations is infinity, an unlikely event; therefore, renal metabolism should considered. It would be more appropriate to conservatively assign the concentration of metabolite in plasma to a value just below the assay quantification limit rather than zero and then compare the clearance value on the basis of blood concentration to known renal blood flow.

An alternative, though more complex and invasive approach to assess renal metabolism was proposed and evaluated by Riegelman and coworkers (53,54), where parent drug and radiolabeled metabolite were infused simultaneously to estimate the renal clearance of the metabolite and formation rates. Contributions of hepatic metabolism to metabolite excreted in urine were determined with the assumption that the metabolism was FRL and $F(m)$ of metabolite formed in the liver was unity, i.e., these metabolites were not excreted in the bile or subject to sequential metabolism. The labeled dose of metabolite provides information supporting renal metabolism because the ratio of labeled to unlabelled metabolite in plasma versus urine will be different if parent drug is converted to metabolite when passing through the kidney. This approach revealed that 60% to 70% of salicyluric acid metabolite produced from salicylate in a human subject was formed in the kidney (54). With the current availability of liquid chromatography-mass spectrometry, this method could be adapted to use stable isotope tracers of metabolites rather than radiolabeled material.

BILIARY CLEARANCE AND ENTEROHEPATIC RECYCLING OF METABOLITES

Biliary clearance is an excretory route of elimination, in many ways similar to renal clearance discussed above. For some drugs, xenobiotics and metabolites, excretion into the bile can represent the major route for elimination. The mechanisms of bile formation, hepatobiliary transport, and excretion processes have been reviewed (55 57). Drugs can be eliminated in the bile by direct excretion without biotransformation; however, many drugs are excreted after metabolism to more polar, charged metabolites, often by conjugation with sulfate, glucuronic acid, or glutathione. Excretion via the bile can be an irreversible route of elimination for a drug if its metabolites have poor permeability (e.g., glucuronide or sulfate conjugates), the drug molecule is poorly absorbed, or the drug is subject to degradation or complexation in the intestinal contents. In contrast, there are numerous examples of conjugated (phase II) metabolites, which are excreted in the bile, cleaved to yield the parent drug, and then the parent drug is reabsorbed into the systemic circulation, i.e., enterohepatic recycling (EHC). The factors influencing EHC can be quite complex and have been reviewed (58).

Measurement of Biliary Clearance

Bile collection can occasionally be obtained from humans, such as in patients treated for biliary obstruction or post liver transplant. Animal studies of biliary excretion are quite common, often conducted to provide insight into mechanistic processes of drug and metabolite disposition. When bile is collected after administration of the parent drug, *apparent* biliary clearance of metabolite can be determined using Eqs. 33 to 35 above, where the excretion rate of bile is substituted for that of urine. The term "*apparent*" is usually used because it is often the case that drug entering the hepatocyte is first metabolized and then the metabolite is excreted in the bile without subsequent access to the systemic circulation. If a preformed metabolite is administered directly, the same equations can be applied, but may provide many different values for biliary clearance of the metabolite than that the values determined when parent drug is administered since the metabolite need not be formed in the hepatocyte prior to excretion in the bile. Because of potential rate-limiting steps involving active uptake or diffusion into the hepatocyte, metabolism in the hepatocyte and active transport from the hepatocyte into the bile, which may vary when parent drug versus metabolite is administered, the absolute value for metabolite biliary clearance using Eqs. 33 to 35 may not be that informative when preformed metabolite is administered directly.

More commonly employed when metabolite is formed in the hepatocyte and subsequently excreted in bile with negligible plasma levels is the measurement of excretion rate of metabolite and/or parent drug in the bile as a function of parent drug concentration in plasma, which provides a measure of *apparent* biliary clearance,

$$\Delta A_{bile}/\Delta t = CL_{bile} \cdot C_{ave} \qquad \text{(Eq. 41)}$$

where ΔA_{bile} can include both parent drug and metabolite, though often metabolite(s) is (are) dominant, and C_{ave} refers to average plasma concentrations of the parent drug during the collection interval. If only metabolite is present in bile, but no metabolite is measurable in plasma, and metabolite once formed in the hepatocyte is not released into the systemic circulation, the term "CL_{bile}" represents an apparent formation clearance ($CL_{f,bile}$) for the metabolite in the liver. This relationship can be rewritten in terms of an AUC, either during an interval or until all drug is eliminated after a single dose, where the subscript *bc* refers the AUC obtained with an exteriorized bile cannula,

$$\Delta A_{bile} = CL_{bile} \cdot \Delta AUC_{bc} \qquad \text{(Eq. 42)}$$

Enterohepatic Recycling

EHC recycling via metabolites is considered as a "futile cycle" because of the inefficiency of the metabolic process. The existence of EHC can be proven on the basis of several criteria as summarized by Duggan and Kwan (59). It can be proven unequivocally in animal studies by (*i*) linked experiments where the bile from a donor animal is infused into a recipient, (*ii*) a gradual establishment of a portal:systemic plasma concentration gradient after intravenous dosing of parent drug, and (*iii*) an increase in systemic clearance when there is irreversible bile diversion. In contrast, in most human studies, only suggestive evidence of EHC can be obtained. These include observations such as the presence of secondary peaks in plasma concentration versus time curves, often coincident with gallbladder discharge in response to a meal, or the presence of drug-derived material in the feces after administration via routes other than oral or rectal. It should be noted that secondary peaks due to EHC seen in humans would not initially be expected in the rat,

which lacks a gallbladder. However, if reabsorption in the intestine is delayed because of regional distributions of β-glucuronidase or sulfatase, time-dependent hydrolysis of conjugates or site-specific permeability, secondary peaks may also be seen in the rat. Thus, secondary peaks in humans may be due to reasons other than EHC, such as delayed or irregular oral absorption.

When bile is diverted in animals, the AUC in plasma of parent drug will decrease relative to that obtained without diversion when enterohepatic recycling is operative. CL_{bile} determined with bile diversion using Eq. 43 can then be employed to estimate total biliary exposure or the total amount of drug/metabolite subject to EHC when cycling is operative without bile diversion (59),

$$\Sigma A_{bile} = CL_{bile} \cdot AUC \qquad \text{(Eq. 43)}$$

where AUC is the exposure to parent drug in plasma in an animal without biliary diversion and ΣA_{bile} is the estimated sum of all parent drug and metabolite that may be excreted in bile when EHC is operative, i.e., it is the cumulative drug exposure to the intestine. This measure of cumulative drug/metabolite exposure to the intestine due to EHC can result in an amount exceeding the intravenous dose when EHC is very extensive and efficient. For example as shown in Table 1, indomethacin exposure in bile of the dog had an estimated 362% of the dose cycled, and the extent of cycling was inversely correlated with observed toxic doses across the species (59).

EHC can be very efficient, resulting in futile cycling. When this occurs, the metabolite formed and excreted in the bile does not represent an irreversible loss, instead the EHC process represents a distribution process with bile/intestine as a peripheral distribution compartment (58). One measure of the efficiency of EHC was provided by Tse et al. (60). From two experiments, conducted with and without bile collection, and AUC for the parent drug in plasma, which is measured in each treatment after a single intravenous dose, one can calculate the fraction of drug dose excreted in the bile as parent

Table 1 Species Differences in Indomethacin Biliary Exposure and Toxicity[a]

	Clearance (mL/min/kg)			Area (μg·mL)		Plasma gradient, $C_p^{port}\,dt / C_p^{ven}$	Total exposure, $\Sigma_{bile}^{\%}$	Minimum toxic dosage (mg/kg/day)
Species	Plasma, $\dot{V}_{cl,p}$	Urine, $\dot{V}_{cl,r}$	Bile, $\dot{V}_{cl,b}$	Venous, $\int_0^\infty C_p^{ven}\,dt$	Portal, $\int_0^\infty C_p^{port}\,dt$			
Dog	8.2	<0.1	13.3	122	310[b]	2.54[b]	362	0.5
Rat	0.32	0.01	0.39	3074	3535	1.15	134	0.75
Monkey	8.3	3.0	2.2	121	121	1.0	26	1.0
Guinea pig	6.25	1.85	1.20	158	181	1.15	21	6.0
Rabbit	3.62	1.09	0.40	278	334	1.20	13	20.0
Man	1.79	0.22	0.16[c]	592	592	1.0[d]	9.5	

Portal/venous concentration ratios greatly exceeded 1 in the dog, and there was a strong inverse correlation between total biliary exposure and minimum toxic dosage.

[a]All disposition data for single intravenous dosage of 1 mg/kg, except man, for whom 25 mg total dosage normalized to 1 mg/kg.

[b]Based on complete 0 to 2 hr portal and systemic plasma profiles; for all other species, mean of more than five measurements at interval specified in text.

[c]Calculated from f_{bile} 0.09 (H. B. Hucker, unpublished).

[d]Assumed.

Source: From Ref. 59.

drug and metabolites that are subject to possible cycling, $F_{b.}$ From this information, and the definition that the amount of drug that is reabsorbed from the first cycle is $F_a \cdot F_b \cdot D$, together with the assumption that this fraction is constant with all subsequent cycles, the following relationship can be derived (60),

$$F_a = [1 - AUC_{bc}/AUC]/F_b \quad \text{(Eq. 44)}$$

where AUC_{bc} for the parent drug is measured with bile cannulation and drainage. The value of F_a obtained is a measure of the fraction of the sum of drug and metabolite excreted in the bile, which is then reabsorbed. When using this relationship, only metabolites that could be recycled (i.e., they are reversible to parent drug in the GI tract) would be included when estimating F_b. When F_b is a significant part of the dose, but AUC_{bc} is equivalent to AUC, it is apparent that bile diversion did not influence the amount of drug reaching the systemic circulation, and thus F_a is zero. In contrast, when a significant part of the dose is excreted in bile and AUC_{bc} is much less than AUC, then recycling is significant and F_a can approach a value of 1.

REVERSIBLE METABOLISM

Reversible metabolism occurs when a metabolite or biotransformation product and the parent drug undergo interconversion in both directions as shown in Scheme 6. The scheme can also be written in terms of concentrations and clearance terms rather than amounts and rate constants, respectively, as shown in Scheme 6B using the common convention in the literature where the drug is considered in compartment 1 and the metabolite in compartment 2. These compartments are not to be confused with physiological spaces. Here, the "metabolite" may be the pharmacologically active species in the case of administration of a prodrug, an active metabolite, or an inactive metabolite. Generally, enzyme-catalyzed chiral inversion reactions are not reversible, such as the R- to S- conversion of ibuprofen (61,62), and these are not considered here. In contrast, chemical catalysis of the chiral inversion of thalidomide (63) would be expected to behave similarly to reversible metabolism, and the pharmacokinetic modeling would be the same.

Though reversible metabolism is less often addressed in reviews of drug metabolite kinetics (12), there are numerous examples occurring across a wide variety of compounds as noted in a recent review by Cheng and Jusko (64). These include phase I metabolic pathways for amines such as imipramine, alcohols such as corticosteroids and estradiol, lactones, and sulfides/sulfoxides such as captopril and sulindac. Examples for phase II

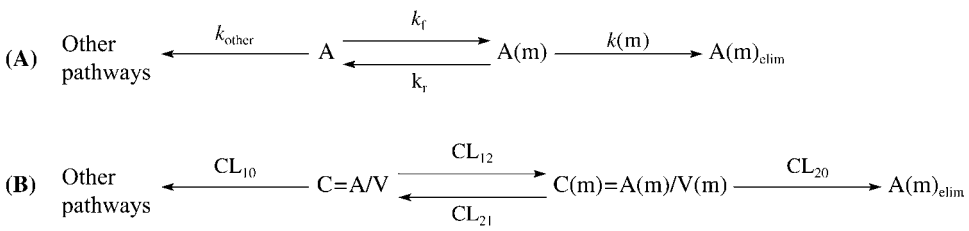

Scheme 6 Reversible conversion between metabolite and drug with parallel elimination pathways for the parent drug and metabolite.

metabolic pathways include carboxylic acids to their glucuronides as in the case of ibuprofen, sulfation of phenols such as estrone, and acetylation of amines such as procainamide (64). Pharmacokinetic methods for the analysis of reversible metabolism are well described (64 67). More recently, considerations of statistical moment analysis as applied to reversible systems have also been addressed by Cheng (68,69).

Reversible metabolism is often ignored when analyzing the pharmacokinetic data of compounds that undergo metabolite interconversion. The pharmacokinetic parameter estimates so obtained using methods or approaches that do not consider the reversible nature of the system are not true estimates of pharmacokinetic parameters and should be considered *apparent* parameter values. Indeed, regulatory agencies may not require rigorous evaluation of the true reversible metabolic parameters because the critical parameters of clearance, volume of distribution, and bioavailability can only be unambiguously obtained after direct administration of the preformed metabolite, which is usually not feasible in humans because of the need to secure an IND for the intravenous administration of the metabolite. Moreover, in many cases of reversible metabolism, the metabolite may only achieve low concentrations relative to the parent drug or is inactive; thus, a great deal of effort to fully elucidate its pharmacokinetics may be difficult or not justified on the basis of the considerable costs and efforts. There are, however, a number of common disease states such as renal or hepatic impairment, which may dramatically alter the disposition of the metabolite, thus significantly influencing the disposition of the parent drug, and these should be addressed. When a metabolite is active or of toxicological relevance, or when altered disposition of the metabolite substantially modifies the pharmacokinetic profile of the parent drug, efforts to more fully investigate reversible metabolism are warranted.

Determination of Primary Pharmacokinetic Parameters for Reversible Metabolic Systems

The primary pharmacokinetic parameters of clearance, volume, and availability as well as commonly employed secondary parameters of half-life and MRT will be discussed here. Discussion of less commonly employed parameters can be found in other literature (64 69). However, difficulties in estimating parameters involving reversible metabolism, due to either the need to dose the metabolite directly or inherent errors in the complex equations employed, generally limit the utility of estimating some parameters. Other parameters unique to reversible metabolic systems are descriptors of the reversibility of the process that include the recycling numbers, recycled fraction, and exposure enhancement, which will be discussed below.

Half-Life in Reversible Metabolism Systems

As shown in Figure 10 for the interconversion of methylprednisone and methylprednisolone, which undergo the reversible metabolism of ketone/alcohol common with steroids, after the parent drug and metabolite reach equilibrium, the two compounds decline in parallel when either is administered intravenously (70). Because the terminal half-life reflects a hybrid of the clearance terms for the overall reversible system and the volumes of distribution of parent drug and metabolite, estimating changes in the half-life in response to an altered clearance or volume term is difficult. Although the use of "sojourn times" have been proposed as a measure of time a drug or metabolite is in the body before being eliminated or transformed in reversible systems (57), in practice most often an *apparent* half-life is reported with the understanding that it may be subject to change in response to alterations of the disposition of parent drug or metabolite.

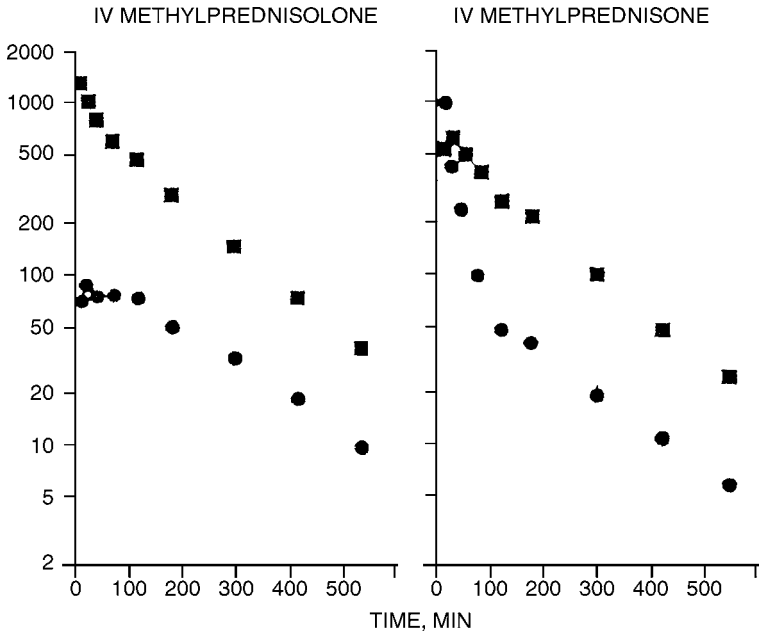

Figure 10 The reversible metabolism of methylprednisolone (■) and methylprednisone (●) when each is given on separate occasions as a 1.25 mg/kg intravenous bolus to a rabbit (70). The parallel profiles, constant concentration ratios at equilibrium, and formation of both compounds when either, is administered, are characteristics of reversible metabolism. *Source*: From Ref. 70.

The fact that the terminal half-life of parent drug and metabolite are parallel when parent drug is administered could lead to an erroneous assumption that FRL metabolism is operative when in fact reversible metabolism is occurring. Confirmation of reversibility can be made by identifying formation of the parent drug after administration of the metabolite; however, such an experiment may not be feasible in humans. Therefore, in vitro studies with human tissues or animal studies may be necessary to infer reversible metabolism in humans.

Clearance Parameters in Reversible Metabolism Systems

For a reversible system as shown in Scheme 6B the following relationships can be derived (64,65) for determining clearance values after collection of AUC data from an intravenous bolus dose of parent drug or metabolite on two separate occasions. These relationships assume that clearance and distribution processes are linear for both parent drug and metabolite, i.e., independent of concentration.

$$CL_{10} = \frac{Dose^{p} \cdot AUC_{m}^{m} - Dose^{m} \cdot AUC_{m}^{p}}{AUC_{p}^{p} \cdot AUC_{m}^{m} - AUC_{m}^{p} \cdot AUC_{p}^{m}} \quad \text{(Eq. 45)}$$

$$CL_{20} = \frac{Dose^{m} \cdot AUC_{p}^{p} - Dose^{p} \cdot AUC_{p}^{m}}{AUC_{p}^{p} \cdot AUC_{m}^{m} - AUC_{m}^{p} \cdot AUC_{p}^{m}} \quad \text{(Eq. 46)}$$

$$CL_{21} = \frac{Dose^{m} \cdot AUC_{m}^{p}}{AUC_{p}^{p} \cdot AUC_{m}^{m} - AUC_{m}^{p} \cdot AUC_{p}^{m}} \quad \text{(Eq. 47)}$$

$$CL_{21} = \frac{Dose^{p} \cdot AUC_{p}^{m}}{AUC_{p}^{p} \cdot AUC_{m}^{m} - AUC_{m}^{p} \cdot AUC_{p}^{m}} \quad \text{(Eq. 48)}$$

Here the superscript indicates the dose administered as being from the parent drug or metabolite, whereas the subscript refers to the compound that is measured in plasma. AUC is the total area under the plasma concentration versus time curve extrapolated to infinity. Similar equations can be derived when the compounds are infused to steady state (67) where the values needed are infusion rates and steady-state concentrations. These relationships are not unique, as the model has also been applied to other two compartment pharmacokinetic systems with elimination occurring from each compartment, such as the reversible distribution and elimination from the maternal-fetal unit (71).

If apparent clearance terms are used for parent drug or metabolite, these will overestimate the true values for CL_{10} and CL_{20}, respectively. The magnitude of the error is a complex relationship of all the clearance terms as discussed by Ebling and Jusko (65) and is shown here for CL_{app} of the parent drug,

$$CL_{app} = \frac{D}{AUC} = CL_{10} + CL_{12}\left[\frac{CL_{20}}{CL_{21} + CL_{20}}\right] \quad \text{(Eq. 49)}$$

Ebling and Jusko (65) defined the term "$CL_{20}/(CL_{21} + CL_{20})$" an efficiency parameter because it is a fraction that defines the extent of drug clearance by metabolite formation (CL_{12}), resulting in metabolite that does not return or interconvert back to the parent drug, i.e. an irreversible loss. Similar relationships have been determined for $CL(m)_{app}$; however, if the metabolite cannot be administered, then only the term "CL_{app}" will usually be reported.

It is also evident from Eq. 49 that CL_{app} will underestimate the total elimination capacity for the parent drug, i.e., $CL_{10} + CL_{12}$, where CL_{12} is a measure of metabolite formation clearance, CL_f. Therefore, estimating the formation clearance of a metabolite from in vivo studies using $CL_f = CL_{app} \quad CL_{10}$ (where CL_{10} is determined from the other clearance pathways) may grossly underestimate total metabolic capability for the particular metabolic pathway in vivo.

Volume of Distribution in Reversible Metabolism Systems

Volume of distribution at steady state for parent drug and metabolite in reversible metabolic systems are independent, but the equations to calculate the values necessitate consideration of the disposition of both parent drug and metabolite. Indeed, given the structural changes from parent drug to metabolites, as well as potential differences in protein binding and lipophilicity between the parent drug and metabolites, it is reasonable to expect that distribution in the body could be quite different, as previously mentioned for morphine and M6G. In the absence of interconversion, volume of distribution at steady state [$V(m)_{ss,app}$] is calculated with the following equation for the metabolite,

$$V(m)_{ss,app} = \frac{M \cdot AUMC_{m}^{m}}{(AUC_{m}^{m})^{2}} \quad \text{(Eq. 50)}$$

where AUMC(m) is the first moment of the plasma concentration versus time curve for the metabolite (17). This equation for apparent V_{ss} is in error if applied to reversible metabolism systems, since $V(m)_{ss,app}$ will overestimate the real $V(m)_{ss}$ because the parent drug reverts back to the metabolite (65). Moreover, $V(m)_{ss,app}$ is not independent of clearance processes as is the true $V(m)_{ss}$; thus, changes in clearance terms of either parent drug or metabolite will modify the value of $V(m)_{ss,app}$ in reversible metabolism systems.

The relationship between the apparent and real parameter is described for the metabolite as follows (65),

$$V(\mathrm{m})_{\mathrm{ss,App}} = V(\mathrm{m}) + V_{\mathrm{ss}}\left[\frac{\mathrm{CL}_{12} \times \mathrm{CL}_{21}}{(\mathrm{CL}_{12} + \mathrm{CL}_{10})^2}\right] \quad \text{(Eq. 51)}$$

The complexities of these relationships for volume and clearance combine, such that the following equation for $V(\mathrm{m})_{\mathrm{ss}}$ is dependent on dose of metabolite and measured AUC and AUMC data (65),

$$V_{\mathrm{ss}}(\mathrm{m}) = \frac{M[(\mathrm{AUC}_{\mathrm{p}}^{\mathrm{p}})^2 \times \mathrm{AUMC}_{\mathrm{m}}^{\mathrm{m}} - \mathrm{AUC}_{\mathrm{p}}^{\mathrm{m}} \times \mathrm{AUC}_{\mathrm{m}}^{\mathrm{p}} \times \mathrm{AUMC}_{\mathrm{p}}^{\mathrm{p}}]}{(\mathrm{AUC}_{\mathrm{p}}^{\mathrm{p}} \times \mathrm{AUC}_{\mathrm{m}}^{\mathrm{m}})^2 - (\mathrm{AUC}_{\mathrm{m}}^{\mathrm{p}} \times \mathrm{AUC}_{\mathrm{p}}^{\mathrm{m}})^2} \quad \text{(Eq. 52)}$$

Measures of AUMC used for Eqs. 50 and 52 are often criticized for the potential error that may be introduced when extrapolating the first-moment curve to infinity. Alternative equations derived for application of data obtained from infusions of metabolite and parent drug to steady state may reduce some of the errors (67). Given the limited ability to dose preformed metabolite to humans and the potential error in determining $\mathrm{V_{ss}}$ for parent drug or metabolite within reversible systems, true values for the pharmacokinetic parameters in reversible metabolism systems have been determined in humans for very few compounds. Instead, it is more common to report $V_{\mathrm{ss,app}}$ values, with an understanding that such values are inaccurate and subject to change if clearance is altered.

Bioavailability in Reversible Metabolism Systems

Interconversion of parent drug and metabolite also complicates the measures of bioavailability and consideration of this has led to the development of equations that assess absorption processes independent of clearance (64,72). However, the increased complexity of the relationships and the need to dose metabolite independently to assess the values have restricted their application. Thus, apparent bioavailability is often employed ignoring the contributions of reversible metabolism.

Measures of Reversibility in Drug Metabolism

Unique to reversible systems are measures defined as recycled fraction (RF), number of recyclings through the reversible process (R_{I}), as well as other terms (64,65). RF is a measure of the likelihood of a molecule going back and forth through the reversible system, i.e., being converted in both directions, and is a value between 0 and 1 determined from the relative values of clearance,

$$RF = \frac{CL_{12} \cdot CL_{21}}{CL_{11} \cdot CL_{22}} \quad \text{(Eq. 53)}$$

where $\mathrm{CL_{11}} = \mathrm{CL_{10}} + \mathrm{CL_{12}}$ and $\mathrm{CL_{22}} = \mathrm{CL_{20}} + \mathrm{CL_{21}}$.

The number of recyclings, $\mathrm{R_I}$, can exceed 1 and provides a measure of how exposure to parent or metabolite is enhanced by the interconversion process,

$$R_I = \frac{CL_{12} \cdot CL_{21}}{CL_{11} \cdot CL_{22} - CL_{12} \cdot CL_{21}} \quad \text{(Eq. 54)}$$

Influence of Altered Metabolite Clearances on the Disposition of Parent Drug

Because metabolite and parent drug can interconvert, altered irreversible clearance of the metabolite (CL_{20}) can influence the disposition of the parent drug, causing changes in CL_{app}, i.e., Eq. 49. Examples of this include the nonsteroidal anti-inflammatory drugs where renal clearance of labile ester glucuronide metabolite is reduced by renal dysfunction (73). For example, though diflunisal and other carboxylic acid containing drugs are eliminated almost entirely by metabolism, simulation results shown in Table 2 show that when clearances that directly affect acyl glucuronides are altered, the AUC of both parent drug and metabolite can in some cases be significantly and seemingly unpredictably modified (74). This has potential clinical significance, since hepatobiliary

Table 2 Relative Values of AUC for Acidic Drugs and Their Acyl Glucuronide Metabolites in Animals Obtained by Simulation Using the Model Shown When Individual Clearance Terms in the Scheme for Reversible Metabolism are Reduced to 10% of Their Initial Value

Clearance terms altered	Percentage of noral AUC for parent compound (%)[b]					
	DF	S ET	R ET	VPA	S	Z
Cl_{10}	241	380	242	477	791	850
Cl_{12}	146	119	146	112	103	102
Cl_{20}	144	117	141	111	103	102
Cl_{21}	75	99	99	96	83	100
Cl_{23}	93	89	79	96	100	94
Clearance terms altered	Percentage of noral AUC for acyl glucuronide (%)[b]					
	DFG	S ETG	R ETG	VPAG	SG	ZG
Cl_{10}	241	380	242	477	791	850
Cl_{12}	15	12	15	11	10	10
Cl_{20}	186	202	248	181	104	103
Cl_{21}	147	106	102	130	664	116
Cl_{23}	114	152	139	129	101	386

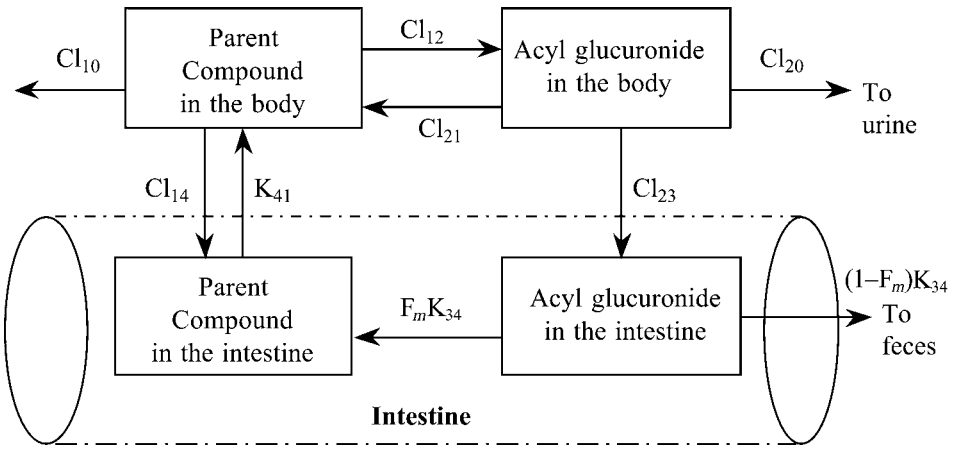

The clearance terms are defined in the figure. Baseline value is 100. Data were obtained by Monte Carlo simulation using initial values obtained in animals (74).
Abbreviation: AUC, area under the curve.
Source: From Ref. 74.

or renal disease may alter clearance pathways of the metabolite and cause unanticipated alterations in the disposition of the parent drug, even though the parent drug itself is not eliminated directly into bile or into the urine.

NONLINEAR PROCESSES AND METABOLITE DISPOSITION

Metabolite disposition is subject to the same sources of nonlinearity that can occur with parent drug (17). These may include saturable enzymic metabolism, co-substrate depletion in phase II metabolism, saturable transport for biliary or renal excretion, saturable active uptake into hepatocytes, or saturable protein binding. In summary, metabolite disposition can be affected by nonlinearities involving both the rate of input (i.e., formation), rate of output (i.e., elimination), and distribution. Any nonlinearity in disposition of the parent drug, which is the precursor for the metabolite, will lead to increased complexities in predicting metabolite disposition; thus, the correlation between exposure to parent drug and exposure to the metabolite will not be predictable as dose is varied or may vary with time when dosing chronically. In this section, the most common source of nonlinearity will be considered and discussed, assuming that only one clearance parameter is nonlinear at a given time. However, one should realize that multiple nonlinearities may occur simultaneously, especially in animal toxicology studies where drug doses are intentionally pushed to levels much greater than those employed later in humans.

Michaelis–Menton Formation Vs. Elimination of the Metabolite

The assumption that metabolite formation and elimination occur as first-order processes with constant CL_f and CL(m) generally holds true for typical enzyme or active transport systems when concentrations of drug or metabolite, respectively, are below their K_m [Michaelis Menton constant where the rate is half of the maximum velocity, V_m) (17) values. In cases where Michaelis Menton kinetics apply for metabolite formation and elimination, with only a single pathway formation and elimination of metabolite, Eq. 11 can be rewritten as,

$$\frac{dA(\mathrm{m})}{dt} = \frac{V_{\mathrm{m,f}} \cdot C}{\left(K_{\mathrm{m,f}} + C\right)} - \frac{V_{\mathrm{m}}(\mathrm{m}) \cdot C(\mathrm{m})}{[K_{\mathrm{m}}(\mathrm{m}) + C(\mathrm{m})]} \qquad \text{(Eq. 55)}$$

It is apparent that CL(m) and k(m) are now functions of K_m(m) and V_m(m),

$$\mathrm{CL}(\mathrm{m}) = \frac{V_{\mathrm{m}}(\mathrm{m})}{K_{\mathrm{m}}(\mathrm{m}) + C(\mathrm{m})} \qquad \text{(Eq. 56)}$$

$$k(\mathrm{m}) = \frac{\frac{V_{\mathrm{m}}(\mathrm{m})}{V(\mathrm{m})}}{[K_{\mathrm{m}}(\mathrm{m}) + C(\mathrm{m})]} \qquad \text{(Eq. 57)}$$

and similar relationships exist for CL_f and k_f. When $C \ll K_m$ and $C(\mathrm{m}) \ll K_m(\mathrm{m})$, then both right-hand terms of Eq. 55 simplify, yielding first-order processes, since clearance of formation and the rate constant of elimination of the metabolite are essentially constant. However, if the elimination of the metabolite is saturable, i.e., when $C(\mathrm{m}) > K_m(\mathrm{m})$, both CL(m) and k(m) become variable with CL(m) and k(m) decreasing as C(m) increases, thus the apparent half-life of the metabolite increases as C(m) increases. When saturation of CL(m) occurs, and CL_f is constant (i.e., formation of metabolite is not saturable in the concentration range of drug), then $C(\mathrm{m})/C$ and AUC(m)/AUC will increase as the drug dose increases. Typically, plots of metabolite levels normalized to drug dose should be

superimposable, but with saturable elimination, the dose-normalized metabolite concentrations will increase with dose level. Even under conditions of FRL metabolism, saturation of metabolite elimination will increase these ratios as dose increases, though the metabolite concentration profile may still appear to be parallel to that of the parent drug profile. However, because the formation clearance (CL_f) of the metabolite did not change with dose, f_m would remain constant. Thus, for a metabolite that is primarily excreted in the urine, the percentage of the dose recovered in the urine as metabolite would be independent of dose.

For metabolites subject to ERL metabolism, saturable metabolite elimination may be noticeable from a profile of metabolite concentration versus time when parent drug is rapidly administered or absorbed. A semilog plot of metabolite concentrations versus time profile may show the classical concave shape at higher concentrations and then become loglinear at lower concentrations (15).

In contrast, if the metabolite formation clearance (CL_f) is saturable, while the elimination of metabolite is not, then $C(m)/C$ and AUC(m)/AUC will decrease as drug dose increases. In this case, f_m will decline as the dose increases, assuming that there are other parallel pathways for drug elimination besides formation of the metabolite of interest. With FRL metabolism, the apparent half-life of the metabolite will increase if the saturable pathway of metabolism is a significant fraction of the overall elimination of parent drug, since the half-life of parent drug will increase. For ERL metabolism [$k(m) \ll k$], the profile of the metabolite after escalating single doses of parent drug may not be altered significantly, unless the elimination half-life of the parent drug increased significantly at higher doses such that value of k decreases to the extent that it approaches that of $k(m)$. In this case of saturable metabolite formation clearance, plotting metabolite concentration versus time profiles normalized to dose would show a decline in the AUC of the profiles as dose increased.

MRT concepts can also be applied to metabolites subject to Michaelis Menton metabolism (31,69,75). Though there has been some debate about using MRT in nonlinear systems, a review addressed these concerns and with simulations showed that the values of MRT, V_{ss}, V_m and K_m could be determined accurately (76). A potential advantage of MRT concepts for evaluating nonlinear systems is that they do not require multiple trials of various compartmental models normally employed when determining Michaelis Menton parameters (76).

CONCLUSIONS

Even if some of the commonly employed mathematical relationships for performing pharmacokinetic analysis of parent drug are also applicable to metabolites, because metabolites are formed in vivo, there are some unique methods applicable to describing metabolite disposition and an effort was made in this chapter to identify those methods. Many of the difficulties in analyzing metabolite pharmacokinetics stem from limited information about the rate and extent of their formation in the body, i.e., the input into the body is usually not known. Thus, many of the relationships described in this review are based upon derivations that do not require knowledge of the rate of metabolite input, but often make informed estimates of the extent of metabolite formation from the parent drug or assume that the extent of formation is constant between treatments or linear with dose. In many instances, especially when estimating levels after chronic administration of the parent drug, the extent of metabolite formed is more important than the rate at which it was formed. When possible, exogenous administration of preformed metabolite by a known input rate circumvents these limitations. However, due to the potential different

behavior of preformed metabolite and that formed at tissue sites within the body (9,46,47), new assumptions arise that may be difficult to validate. One of the primary advantages of MRT approaches for describing metabolite pharmacokinetics is the fewer assumptions made for their application, but a lack of thorough understanding of their theory has limited their use by some investigators. Whatever approach is used, there is much to be gained from a better understanding of the pharmacokinetics of metabolites. Although data obtained in animals by administration of preformed metabolites will have to be interpreted with caution (9), the FDA guidance suggesting toxicology studies in animals with "major metabolites" (23) will in the future lead to substantially more data reported on metabolite disposition. Careful analysis of these data from exogenously administered metabolites relative to metabolites generated in situ from the parent drug should provide insight into whether such extraordinary efforts and cost can provide valuable information beyond that presently obtained by radiolabeled tracer studies.

This chapter did not present extensive derivations of some of the mathematical relationships provided. Earlier reviews on the pharmacokinetics of metabolites (12,14) or the primary literature cited should be consulted together with this chapter for further insight and understanding of the derivations and assumptions of the equations presented. In addition, some basic concepts in pharmacokinetics are needed for the full implementation of some of the relationships provided, and these can be found in textbooks on the topic (15 19). The pharmacokinetics and rates of metabolism are not necessarily limited by the metabolic step, and considerations of uptake and efflux transporters need to be considered when interpreting in vivo data. Topics such as reversible metabolism and MRT concepts are now better understood because of more recent work, and original literature should be consulted where appropriate. This review should provide a foundation for understanding how the complexities of metabolite formation and elimination may be analyzed. In conjunction with other later chapters in this text, this should assist scientists in the design of in vitro experiments, in vivo animal studies, and clinical trials to characterize the metabolism of drugs and other xenobiotics such that optimal information can be obtained about the disposition of metabolites in the body with as few assumptions as possible.

ACKNOWLEDGMENTS

The assistance and patience of Dr. Laurene Wang in reading, commenting, and editing this chapter is greatly appreciated.

REFERENCES

1. Atkinson AJ, Strong JM. Effect of active drug metabolites on plasma level response relationships. J Pharmacokinet Biopharm 1977; 5:95 109.
2. Sutfin TA, Jusko WJ. Compendium of active drug metabolites. In: Wilkinson GR, Rawlins MD, eds. Drug Metabolism and Disposition: Considerations in Clinical Pharmacology. Boston: MTP Press, 1985:91 159.
3. Fura A. Role of pharmacologically active metabolites in drug discovery and development. Drug Discov Today 2006; 11:133 142.
4. Penson RT, Joel SP, Robert M, Gloyne A, Beckwith S, Slevin ML. The bioavailability and pharmacokinetics of subcutaneous, nebulized and oral morphine 6 glucuronide. Br J Clin Pharmacol 2002; 53:347 354.
5. Fuhr U, Jetter A, Kirchheiner J. Appropriate phenotyping procedures for drug metabolizing enzymes and transporters in humans and their simultaneous use in the "cocktail" approach. Clin Pharmacol Ther 2007; 81:270 283.

6. Relling MV, Giacomini KM. Pharmacogenomics. In: Burnton LL, Lazo JS, Parker KL, eds. Goodman and Gillman's, The Pharmacological Basis of Therapeutics. 11th ed. New York: McGraw Hill, 2006:93 115.
7. Matzke GR, Comstock TJ. Influence of renal function and dialysis on drug disposition. In: Burton ME, Shaw LM, Schentag JJ, et al., eds. Applied Pharmacokinetics and Pharmacody namics. 4th ed. New York: Lippincott Williams and Wilkins, 2006:187 212.
8. Uetrecht J. Idiosyncratic drug reactions: past, present and future. Chem Res Toxicol 2008; 21:84 92.
9. Smith DA, Obach RS. Metabolites and safety: what are the concerns, and how should we address them? Chem Res Toxicol 2006; 19:1570 1579.
10. Cummings AJ, Martin BK. Excretion and accrual of drug metabolites. Nature (London) 1963; 200:1296 1297.
11. Houston JB, Taylor G. Drug metabolite concentration time profiles: influence of route of drug administration. Br J Clin Pharmacol 1984; 17:385 394.
12. Houston JB. Drug metabolite kinetics. Pharmacol Ther 1982; 15:521 552.
13. Pang KS. A review of metabolite kinetics. J Pharmacokinet Biopharm 1985; 13:632 662.
14. Weiss M. A general model of metabolite kinetics following intravenous and oral administration of the parent drug. Biopharm Drug Dispos 1988; 9:159 176.
15. Rowland M., Tozer TN. Clinical Pharmacokinetics. Baltimore: Lea and Febiger, 1995.
16. Buxton ILO. Pharmacokinetics and pharmacodynamics: the dynamics of drug absorption, disposition, action and elimination. In: Burnton LL, Lazo JS, Parker KL, eds. Goodman and Gillman's, The Pharmacological Basis of Therapeutics. 11th ed. New York: McGraw Hill, 2006:1 39.
17. Gibaldi M, Perrier D. Pharmacokinetics. 2nd ed. New York: Marcel Dekker, 1982.
18. Gibaldi M. Biopharmaceutics and Clinical Pharmacokinetics, 4th ed. Philadelphia: Lea Febiger, 1991.
19. Shargel L, Wu Pong S, Yu ABC. Applied Biopharmaceutics and Pharmacokinetics. 5th ed. New York: McGraw Hill, 2005.
20. Walle T, Conradi EC, Walle UK, Fagan TC, Gaffrey TE. Naphthoxylacetic acid after single and long term doses of propranolol. Clin Pharmacol Ther 1979; 26:548 554.
21. Chung JM, Hilbert RP, Gural E, Radwanski S, Symchowicz S, Zampaglione N. Multiple dose halazepam kinetics. Clin Pharmacol Ther 1984; 35:838 842.
22. Baillie TA, Cayen MN, Fouda H, Gerson RJ, Green JD, Grossman SJ. Klunk LJ, LeBlanc B, Perkins DG, Shipley LA. Drug metabolites in safety testing. Toxicol Appl Pharmacol 2002; 182:188 196.
23. Food and Drug Administration. Guidance for Industry: Safety testing of drug metabolites. Available at: www.fda.gov/cder/guidance/6897fnl.htm 02 14 2008.
24. Osborne S, Joel D, Trew D, Slevin M. Morphine and metabolite behavior after different routes of morphine administration: demonstration of the importance of the active metabolite morphine 6 glucuronide. Clin Pharmacol Ther 1990; 47:12 19.
25. Barret DA, Barker DP, Rutter N, Pawula M, Shaw PN. Morphine, morphine 6 glucuronide and morphine 3 glucuronide pharmacokinetics in newborn infants receiving diamorphine infusions. Br J Clin Pharmacol 1996; 41:531 537.
26. Lotsch J, Stockmann A, Kobal G, Brune K, Waibel R, Schmidt N, Geisslinger G. Pharmacokinetics of morphine and its glucuronides after intravenous infusion of morpine and morphine 6 glucuronide in healthy volunteers. Clin Pharmacol Ther 1996; 60:316 325.
27. Rowland M. Physiological pharmacokinetic models and interanimal species scaling. Pharmacol Ther 1985; 29:49 68.
28. Boxenbaum H. Interspecies scaling, allometry, physiological time, and the ground plan for pharmacokinetics. J Pharmacokinet Biopharm 1982; 10:201 227.
29. Mahmood I. Application of allometric principles for the prediction of pharmacokinetics in human and veterinary drug development. Adv Drug Deliv Rev 2007; 59:1177 1192.
30. Riegelman S, Collier P. The application of statistical moment theory to the evaluation of in vivo dissolution time and absorption time. J Pharmacokinet Biopharm 1980; 8:509.

31. Cheng H, Jusko WJ. Mean residence times and distribution volumes for drugs undergoing linear reversible metabolism and tissue distribution and linear or nonlinear elimination from the central compartment. Pharm Res 1991; 8:508 511.
32. Weiss M. Drug metabolite kinetics: noncompartmental analysis. Br J Clin Pharmacol 1985; 19:855 856.
33. Veng SA Pedersen, Gillespie WR. A method for evaluating the mean residence times of metabolites in the body, systemic circulation, and the peripheral tissue not requiring separate i.v. administration of the metabolite. Biopharm Drug Dispos 1987; 8:395 401.
34. Kaplan, Jack ML, Cotler S, Alexander K. Utilization of area under the curve to elucidate the disposition of an extensively biotransformed drug. J Pharmacokinet Biopharm 1973; 1:201 215.
35. Cutler DJ. Linear system analysis in pharmacokinetics. J Pharmacokinet Biopharm 1978; 6:265 282.
36. Karol MD and Goodrich S. Metabolite formation pharmacokinetics: rate and extent determined by deconvolution. Pharm Res 1988; 5:347 351.
37. Murai Y, Nakagawa T, Yamaoka K, Uno T. High performance liquid chromatographic determination and moment analysis of urinary excretion of flucloxacillin and its metabolites in man. Int J Pharm 1983; 15:309 320.
38. Weiss M. Metabolite residence time: influence of the first pass effect. Br J Clin Pharmacol 1986; 22:121 122.
39. Chan KKH, Gibaldi M. Effects of first pass metabolims and metabolite mean residence time determination after oral administration of parent drug. Pharm Res 1990; 7:59 63.
40. Lee FW, Salmonson T, Benet LZ. Pharmacokinetics and pharmacodynamics of nitroglycerin and its dinitrate metabolites in conscious dogs: intravenous infusion studies. J Pharmacokinet Biopharm 1993; 21:533 550.
41. Lane EA, Levy RH. Prediction of steady state behavior of metabolite from dosing of parent drug. J Pharm Sci 1980; 69:610 612.
42. Walle T, Conradi EC, Walle UK, Fagan TC, Gaffney TE. 4 Hydroxypropranolol and its glucuronide after single and long term doses of propranolol. Clin Pharmacol Ther 1980; 27:22 31.
43. Williams RT. Detoxification Mechanisms. The Metabolism of Drugs and Allied Organic Compounds. New York: Wiley, 1947.
44. Jones D, Gorski C, Haehner BD, O'Mara EM, Hall SD. Determination of cytochrome P450 3A4/5 activity in vivo with dextromethorphan N demethylation. Clin Pharmacol Ther 1996; 60:374 384.
45. Pang KS. Kinetics of sequential metabolism. Drug Metab Dispos 1995; 23:166 177.
46. Pang KS, Gillette JR. Sequential first pass elimination of a metabolite derived from its precursor. J Pharmacokinet Biopharm 1979; 7:275 290.
47. Tirona RG, Pang KS. Sequestered endoplasma reticulum space for sequential metabolism of salicylamide: coupling of hydroxylation and glucuronidation. Drug Metab Dispos 1996; 24:821 833.
48. Upton RA, Buskin JN, Williams RL, Holford NHG, Riegelman S. Negligible excretion of unchanged ketoprofen, naproxen and probenecid in urine. J Pharm Sci 1980; 69:1254 1257.
49. Smith PC, Hasegawa J, Langendijk PNJ, Benet LZ. Stability of acyl glucuronides in blood, plasma and urine: studies with zomepirac. Drug Metab Dispos 1985; 13:110 112.
50. Dalton JT, Weintjes ME, Au JL. Effects of bladder reabsorption on pharmacokinetic data analysis. J Pharmacokinet Biopharm 1994; 22:183 205.
51. Levy G, Tsuchiya T, Amsel LP. Limited capacity for salicyl phenolic glucuronide formation and its effect on the kinetics of salicylate elimination in man. Clin Pharmacol Ther 1972; 13:258 268.
52. Vree TB, Hekster YA, Anderson PG. Contribution of the human kidney to the metabolic clearance of drugs. Ann Pharmacother 1992; 26:1421 1428.
53. Wan SH, Riegelman S. Renal contribution to overall metabolism of drugs I: conversion of benzoic acid to hippuric acid. J Pharm Sci 1972; 61:1278 1284.

54. Lihmann BV, Wan SH, Riegelman S, Becker C. Renal contribution to overall metabolism of drugs IV: biotransformation of salicylic acid to salicyluric acid in man. J Pharm Sci 1973; 62:1483 1486.
55. Bohan A, Boyer JL. Mechanisms of hepatic transport of drugs: implications for cholestatic drug reactions. Semin Liver Dis 2002; 22:123 136.
56. Chandra P, Brouwer KL. The complexities of hepatic drug transport: current knowledge and emerging concepts. Pharm Res 2004; 21:719 735.
57. Shitara Y, Sato H, Sugiyama Y. Evaluation of drug drug interaction in the hepatobiliary and renal transport of drugs. Annu Rev Pharmacol Toxicol 2005; 45:689 723.
58. Roberts MS, Magnusson BM, Burczynski FJ, Weiss M. Enterohepatic circulation: physiolog ical, pharmacokinetic and clinical implications. Clin Pharmacokinet 2002; 41:751 790.
59. Duggan DE, Kwan KC. Enterohepatic recirculation of drugs as a determinant of therapeutic ratio. Drug Metab Rev 1979; 9:21 41.
60. Tse FLS, Ballard F, Skinn J. Estimating the fraction reabsorbed in drugs undergoing enterohepatic circulation. J Pharmacokinet Biopharm 1982; 10:455 461.
61. Hutt AJ, Caldwell J. The metabolic chiral inversion of 2 arylpropionic acids a novel route with pharmacological consequences. J Pharm Pharmacol 1983; 35:693 704.
62. Baillie TA, Adams WJ, Kaiser DG, Olanoff LS, Halstead GW, Harpootlian H, Van Giessen GJ. Mechanistic studies of the metabolic chiral inversion of (R) ibuprofen in humans. J Pharmacol Exp Ther 1989; 249:517 523.
63. Reist M, Carrupt PA, Francotte E, Testa B. Chiral inversion and hydrolysis of thalidomide: mechanisms and catalysis by bases and serum albumin, and chiral stability of teratogenic metabolites. Chem Res Toxicol 1998; 11:1521 1528.
64. Cheng H, Jusko WJ. Pharmacokinetics of reversible metabolic systems. Biopharm Drug Dispos 1993; 14:721 766.
65. Ebling WF, Jusko WF. The determination of essential clearance, volume and residence time parameters of recirculating metabolic systems: the reversible metabolism of methylpredniso lone and methylprednisone in rabbits. J Pharmacokinet Biopharm 1986; 14:557 599.
66. Wagner JG, DiSanto AR, Gillespie WR, Albert KS. Reversible metabolism and pharmacoki netics: applications to prednisone prednisolone. Res Commun Chem Pathol Pharmacol 1981; 32: 387 405.
67. Cheng H, Jusko WJ. Constant rate intraneous infusion methods for estimating steady state volumes of distribution and mean residence times in the body for drugs undergoing reversible metabolism. Pharm Res 1990; 7:628 632.
68. Cheng H. A method for calculating the mean transit times and distribution rate parameters of interconversion metabolites. Biopharm Drug Dispos 1993; 14:635 641.
69. Cheng H. Mean residence time of drugs administered non instantaneously and undergoing linear tissue distribution and reversible metabolism and linear or non linear elimination from the central compartment. Biopharm Drug Dispos 1995; 16:259 267.
70. Ebling WF, Szefler SJ, Jusko WJ. Methylprednisolone disposition in rabbits. Analysis, prodrug conversion, reversible metabolism. Drug Metab Dispos 1985; 13:296 301.
71. Wang LH, Rudolph AM, Benet LZ. Pharmacokinetic studies of the disposition of acetaminophen in the sheep maternal fetal unit. J Pharmacol Exp Ther 1986; 238:198 205.
72. Hwang SS, Bayne WF. General method for assessing bioavailability of drugs undergoing reversible metabolism in a linear system. J Pharm Sci 1986; 75:820 821.
73. Faed EM. Decreased clearance of diflunisal in renal insufficiency an alternative explanation. Br J Clin Pharmacol 1980; 10:185.
74. Liu JH, Smith PC. Predicting the pharmacokinetics of acyl glucuronides and their parent compounds in disease states. Curr Drug Metab 2006; 7:147 163.
75. Cheng H, Jusko WJ. Mean residence time for drugs showing simultaneous first order and Michaelis Menton elimination kinetics. Pharm Res 1989; 6:258 261.
76. Cheng H, Gillespie WR, Jusko WJ. Mean residence time concepts for nonlinear systems. Biopharm Drug Dispos 1995; 15:627 641.

3

Hepatic Architecture: Functional and Subcellular Correlates

Felix A. de la Iglesia
Department of Pathology, University of Michigan Medical School and Michigan Technology and Research Institute, Ann Arbor, Michigan, U.S.A.

Jeffrey R. Haskins
Cellular Imaging & Analysis, Thermo Fisher Scientific, Pittsburgh, Pennsylvania, U.S.A.

INTRODUCTION

This chapter will provide the reader with a morphological and functional overview of the liver in relation to the many biochemical and enzymatic reactions that take place in the organ. The liver has a major role in drug metabolism and toxicity, and the integrity of the individual cellular elements is essential to maintain homeostasis and essential detoxifying mechanisms. Different cell types and organelles within cells interact with each other and participate in basic metabolic reactions, protein synthesis, and biotransformation of xenobiotics. Although a significant portion of liver activity involves providing the proteins, lipoproteins, and carriers necessary for normal function, the protective effect of the liver is reflected in its ability to detoxify foreign compounds, metabolize drugs, and provide compensatory mechanisms for diverse reactions that may compromise cell survival. Liver cells constitute individual elementary reactors with separate compartments that synthesize, hydrolyze, conjugate, or oxidize exogenous and endogenous chemicals. Therefore, the study of liver cells is of primary interest to scientists interested in hepatic drug metabolism. The delicate architecture of the hepatocyte must be renewed frequently so that it can perform effectively in response to adverse effects or injury. Above all, numerous anabolic or catabolic activities are under control from the nucleus, which houses all the replicative and messaging functions necessary for structural integrity. The use of combined microscopic and functional approaches can provide an integrated view on drug metabolism and biotransformation. This approach offers some advantages over the uncertainties that can emerge from studies that disrupt the normal cell architecture, as occurs with techniques of isolation and separation of cellular components.

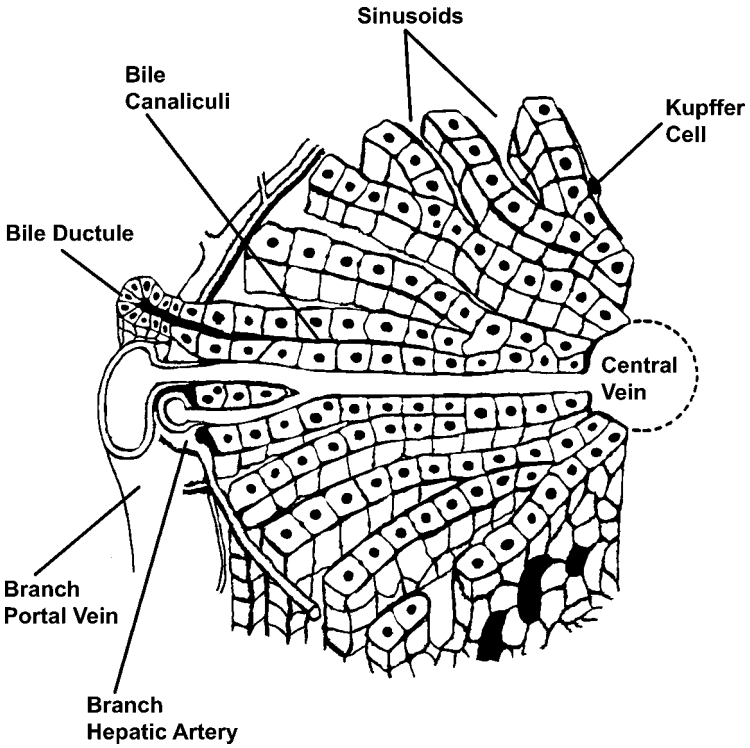

Figure 1 Diagram representing the anatomical structure of the liver lobule. The chords of hepatocytes radiate toward the central vein, which receives sinusoidal blood flowing from the hepatic artery and the portal vein in the periportal area, thus establishing an oxygenation gradient; the bile flows toward the portal space, which contains the interlobular collecting bile ductules.

GENERAL ANATOMICAL CONSIDERATIONS

Lobule Vs. Acinar View of Hepatic Architecture

The arrangement of liver cells is in the form of intertwined trabecular plates or cords, and the tissue architecture is a disposition designed for optimal contact with the blood (Fig. 1). Two primary views of the basic architecture of the liver have arisen over the years.

The earliest concept, described by Kiernan (1), was based on plain morphological terms that defined the basic functional unit of the liver as a lobule (Fig. 2). The Kiernan lobule consists of a hexagonal cluster of hepatocytes centered on a hepatic venule, known as the central vein, and each corner of the hexagon, called the portal triad, grouping a hepatic arteriole, a portal venule, and a bile ductule. The area surrounding the central vein is known as the centrilobular region, and the region surrounding the portal triad is known as the periportal region, with the area in between described simply as the midzone. This classification neatly fits the morphology of the liver, and this lobular terminology is most frequently used in defining the location of pathological lesions in the liver.

The second classification of liver architecture revolves around the concept of the hepatic acinus introduced by Rappaport (2) and is based on the blood circulation pattern rather than on morphology, exclusively. The basic unit of hepatic architecture in this view is the acinus, and follows the direction of the blood flow within the liver (Fig. 2). At the center of the acinus are the portal venules and hepatic arterioles from which blood flows,

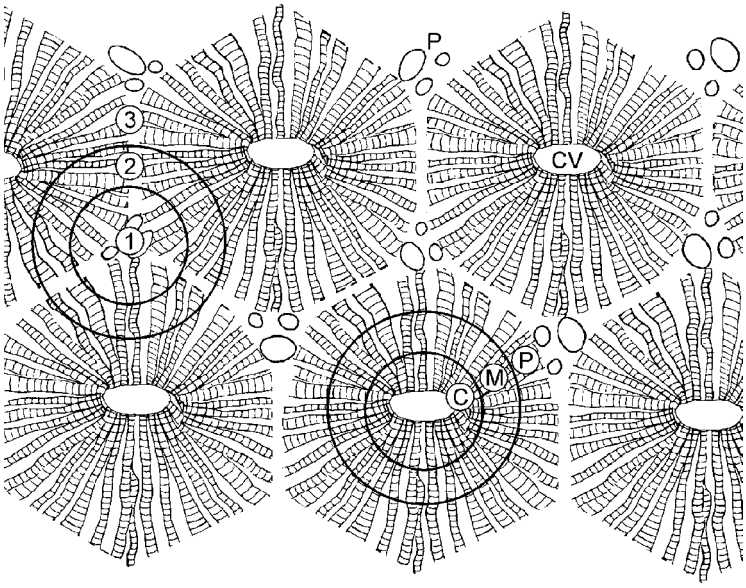

Figure 2 Schematic representation of the lobular architecture of the liver. The cords of hepatocytes radiate away from the central vein (CV) to the portal space (P), which contains a branch of the portal vein and hepatic artery and a bile ductule. The concentric circles around the central vein depict the classic lobular architecture, with centrilobular (C), midzonal (M), and periportal (P) areas. At top left, the circles centered on the portal space represent the vascular zonation according to Rappaport zones 1, 2, and 3, with the outermost blood irrigation toward the central vein.

percolating in three-dimensional space through cords of hepatocytes to distal central veins in which the blood is collected and distributed to the systemic circulation. The acinus is divided into three zones, on the basis of their proximity to the hepatic blood supply: zone 1 is closest to the portal venules and hepatic arterioles, zone 3 lies closest to the central vein, whereas zone 2 lies in between. These "zonal" subdivisions of the acinus correspond to the periportal, centrilobular, and midzonal regions of the lobule, respectively.

Liver Cell Types

Hepatic Parenchymal Cells

Hepatic parenchymal cells, or hepatocytes, are endodermal in origin, arising from outgrowths of the hepatic diverticulum early in prenatal development. In humans, hepatic α-fetoprotein synthesis is evident as early as 25 days after conception, with bile acid synthesis and secretion established by the end of the third month in utero. However, canalicular transport and hepatic excretory function is not completely developed until after birth (3,4), when the system becomes fully functional (i.e., evidence of glucuronidation).

In the adult liver, hepatic parenchymal cells are polyhedral or spherical, are between 28 and 35 μm in diameter, and are approximately 4500 to 5500 μm^3 in volume. Hepatocytes account for 60% of the cells in the liver and represent 80% or more of the total volume. The human liver contains about 27×10^9 hepatocytes, and the rat liver contains approximately 100 times fewer hepatocytes in absolute numbers. A schematic view of the hepatocyte with the different intracellular organelles is shown in Figure 3.

There are two primary views on the life cycle for the renewal of hepatocytes, which have a life span of approximately 200 days in the rat. The cell-streaming view holds that

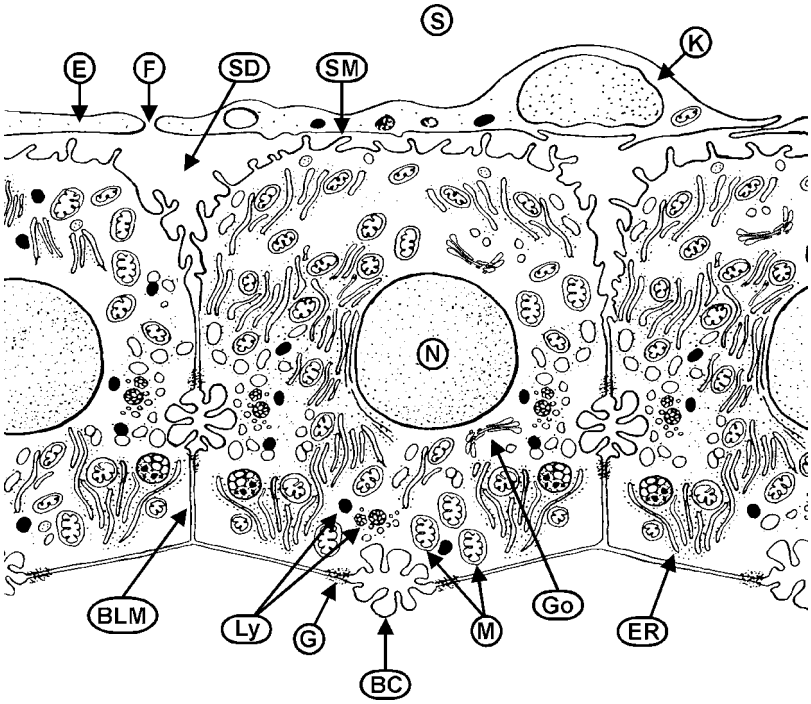

Figure 3 Idealized schematic of an electron microscopic image of a normal liver cell cytoplasm is shown for interpretative purposes. Speckles in the cytoplasm (*unlabeled*) represent free ribosome and glycogen particles. *Abbreviations*: BC, bile canaliculus membrane; BLM, basolateral membrane; E, endothelial cell; ER, endoplasm reticulum; F, foramen or fenestra; G, gap junctions; Go, Golgi apparatus; K, Kupffer cell; Ly, lysosomes; M, mitochondria; N, hepatocyte nucleus with granular chromatin; SD, space of Disse between endothelium and hepatocyte; SM, sinusoidal liver.

hepatocytes are produced from stem cells in periportal regions and move as continuous sheets of cells toward the region of the central vein, where the cells undergo apoptosis (5,6). An alternative approach is that all hepatocytes are capable of cell division, and newly formed cells stay in place with populations of cells growing by clonal expansion in response to various stimuli (7 10).

Hepatocyte cords are bordered by sinusoidal spaces through which blood from the portal and hepatic arteries percolates on its journey to the central vein. The sinusoidal space is lined by a layer of endothelial cells, called sinusoidal cells, which along with the space of Disse, located between the hepatocytes and the sinusoidal cells, serve as a barrier between the sinusoidal space and the hepatocyte cytoplasm. The bile canaliculi provide the route for formed bile to return to the bile ductule, and eventually to the common bile duct. The canaliculi, as their name implies, are not walled vessels, but represent a canal formed by specialized membrane junctions of adjacent hepatocytes.

A discussion of the many functions of the hepatocyte is beyond the scope of this review, but some can be summarized in general terms. Portal circulation exposes the liver to various dietary constituents and hence is a primary site of protein synthesis and carbohydrate and lipid metabolism and the primary site for phase I and phase II reactions in xenobiotic metabolism.

Sinusoidal Endothelial Cells

Sinusoids range in diameter from 10 to 25 μm, and they are lined with a continuous sheet of endothelial cells that is punctuated with numerous perforations named fenestrae. Little, if any basement membrane backs the sheet of endothelial cells, so the fenestrae provide a direct microconduit from the sinusoid to the space of Disse. These fenestrae are approximately 0.1 to 0.2 μm in diameter and exhibit lobular gradients with increasing pore diameter and pore number from periportal to centrilobular regions. The fenestrae play an important role in the filtration of lipoproteins by the liver, with the pores blocking passage of chylomicrons while allowing passage of smaller chylomicron remnants (11,12). Additionally, the diameter of fenestrae may respond to either endogenous neurohumoral factors or to toxicants or even to osmosis (13,14). Modification of pore diameter by toxicants may play a role in the etiology of fatty liver by altering the lipoprotein-filtering capacity of the fenestrae (15). Alcohol reduces the number and size of fenestrae, together with the development of a subendothelial basal lamina with collagen matrix deposition in the space of Disse (16). The sinusoidal cells themselves exhibit marked endocytotic activity leading to significant lysosomal degradation of taken-up materials, including proteins and lipoproteins (17). The sinusoidal cells are active in the synthesis and release of prostaglandins, endothelin, and various cytokines (18). Sinusoidal endothelial disruption is an important factor in the toxicity of compounds such as acetaminophen paracetamol and carbon tetrachloride (19,20).

Kupffer Cells

Kupffer cells are hepatic resident macrophages attached to the luminal surface of sinusoidal endothelial cells, or they may lie within the endothelial cell layer itself. Kupffer cells represent the largest population of fixed macrophages in the human and most other vertebrates (21). The origin of Kupffer cells is uncertain, but they may derive from monocytic precursor cells in the bone marrow (22,23), or they may represent a replicating population of fixed histiocytes (24). Kupffer cells exhibit many of the functions of circulating macrophages and are active in endocytotic removal of particulate, infective, and toxic substances from portal blood (25). Their location within the trabecular structure makes them ideally suited for removal of bacteria and bacterial endotoxins from blood arriving from the intestine (26). The importance of this function is amply demonstrated by the marked proliferation of Kupffer cells in animals experimentally exposed to endotoxin or other inflammatory mediators (27 29). Kupffer cells also have significant secretory functions and are an important source of biologically active mediators, including eicosanoids, cytokines, proteases, tumor necrosis factor (TNF), reactive oxygen species, and nitric oxide (30). The secretory actions of Kupffer cells may play an important role in the regulation of hepatocyte function. The release of cytokines can lead to hepatocyte production of acute-phase reactants (31). Overproduction of these mediators, particularly free radicals and proteases, can lead to hepatocyte dysfunction and necrosis, as observed in severe sepsis (32). Vitamin A may exacerbate carbon tetrachloride toxicity by augmenting the release of active oxygen species from Kupffer cells (33). Hepatocytes may also affect Kupffer cell function, such as the production of prostaglandin E_2 (34,35). Acetaminophen acts on Kupffer cells by interaction with the hepatocytes, releasing active mediators, including superoxide, from the Kupffer cells, leading to hepatocyte dysfunction (36).

Ito Cells

The Ito cell is also known as the fat-storing cell, or the stellate cell. Ito cells are located in the space of Disse between the sinusoid endothelium and the liver cell cords and were originally thought to be a type of Kupffer cell. In 1952, Ito and Nemoto recognized these

stellate-shaped cells as a separate cell population (37) that they believed actively internalized fat. It was later discovered that the cells do not actually take up fat, but store fat synthesized from glycogen (38). Although representing only 5% to 8% of liver cells (39), Ito cells are regularly dispersed along the hepatocyte chords, and their distribution may be sufficient to permit interactions with the entire hepatic sinusoidal network (40). Extended cytoplasmic processes from Ito cells give the cells their stellate appearance. These processes are in contact with multiple hepatocytes, and a single Ito cell may provide connecting processes to more than one neighboring sinusoid (41). Ito cells express smooth muscle α-actin, suggesting that they are contractile, possibly playing a role in regulation of blood flow through the sinusoid (42). Desmin, an intermediate filament protein, has been proposed as an in vivo marker for Ito cells in rats (43). Ito cells are a primary storage site for vitamin A, storing up to 300 times more retinyl ester per milligram of protein than the amount found in hepatocytes (44). Abundant intracytoplasmic vitamin A droplets are distinguishing morphological features of these cells. The morphology of Ito cells exhibits lobular heterogeneity, with midzonal cells exhibiting the greatest concentration of vitamin A droplets; periportal Ito cells are smaller than in other zones, and centrilobular cells display longer processes and very little vitamin A (38).

In vivo, Ito cells can be activated by hepatotoxic compounds such as carbon tetrachloride (38), and appear to play a key role in hepatic fibrosis (45 47). Ito cells proliferate in and around areas of acute focal hepatocyte injury, and their normal physiological role appears to be aiding tissue repair (41). However, chronic liver insult may lead to phenotypic and morphological modulation of Ito cells. The cells change progressively in shape from quiescent compact cells, through a spread transitional stage, with myofilaments and receding vitamin A droplets, eventually resembling a myofibroblast. These phenotypic myoblast or fibroblast spindled cells have pronounced myofilaments and lack vitamin A droplets (40). The fibroblast-like Ito cells are characteristic in experimental animal models of cirrhosis as well as in human disease (15,48), and are believed to play a key role in alcoholic fibrosis and cirrhosis (49,50).

BLOOD CIRCULATION, PATHWAY OF BILE

Hepatic Vasculature

The liver receives about 25% of the total cardiac output, representing only 25% of the body weight, making liver parenchymal cells the most richly perfused cells in the body (51). Portal blood supplies about two-thirds of the total blood flow to the organ, and arterial blood flow accounts for the remainder. The liver does not directly control hepatic portal blood flow; therefore, its intrinsic or extrinsic control occurs through changes in the diameter of the hepatic artery lumen. There is no conclusive agreement about how homogeneous portal versus arterial blood flow is across the sinusoids and exquisite control of sinusoidal circulation appears to exist (52). However, blood flow within the normal liver remains remarkably homogeneous, and compounds entering the liver either through the portal vein or the hepatic artery are equally distributed (53,54).

Microcirculation

Within the liver, the portal vein subdivides into smaller and smaller branches, eventually ending in terminal portal venules that are approximately 20 to 40 μm in diameter and open into the hepatic sinusoids. Portal blood flow across the sinusoids can be controlled by neurohumoral factors, such as norepinephrine, angiotensin, or histamine, which can

activate hepatic venous sphincters at either end of the hepatic sinusoids (51,55). These anatomical structures are more pronounced and easily observable in dog liver. After percolating through the sinusoids, the blood flows into the hepatic venule and out into systemic circulation via the suprahepatic veins. Arterial blood is supplied to the liver through the hepatic artery. Hepatic arteries terminate in either the periportal plexus, which distributes around the branches of the portal vein; the peribiliary plexus, which supplies blood to the bile ducts; or into terminal hepatic arterioles. All three branches drain primarily into the hepatic sinusoids.

The Biliary System

Bile is a complex, dense viscous fluid, with many organic and inorganic components including bile acids, phospholipids, cholesterol, glutathione, proteins, metals, and ions (56). Bile serves two primary purposes. First, bile aids in the digestion and absorption of lipids from the intestine, and second, bile serves as a major route of elimination for many endogenous products as well as various xenobiotics and metabolites. Bile salts are the major constituent of bile, with concentrations ranging from 2 to 45 mM (57). The amphiphilic nature of bile salts permits the formation of micelles with lipid components, which allows a greater concentration of the latter in bile than it would be anticipated on the basis of aqueous solubility. Bile salts are critical to bile flow because their presence in the fluid creates an osmotic gradient pulling water into the bile, thereby creating downstream bile flow. Bile salts are synthesized in the liver from cholesterol and subsequently secreted into the bile and eliminated into the small intestine.

Intestinal reabsorption of bile salts leads back to systemic circulation. Systemic bile salts are rapidly and actively taken up by hepatocytes. In humans, approximately 450 mL of canalicular bile is produced each day (58). Whether synthesized or imported, bile salts exit the hepatocyte at the canalicular membrane. The surface of the hepatocyte membrane forming the bile canaliculi is covered with microvilli, which are folded finger-like projections of the cell membrane. The pericanalicular region of the hepatocyte is largely free of cytoplasmic organelles, but rich in ATP and microfilaments (59). The bile canaliculi meshwork can be visualized using a histochemical stain for ATPase (Fig. 4). The tight junctions between hepatocytes were once thought to be impermeable, but subsequently have been demonstrated to provide a route, known as paracellular diffusion, where substances pass from the sinusoids to the bile without going through hepatocytes. Water, neutrally charged organic molecules, and some ions may enter the bile canaliculi by this route as well (60,61).

The canaliculi themselves form a converging network of anastomotic connections. The ductal system initiates at the canals of Hering, an interface structure where ductal cells symmetrically connect with hepatocytes (62). These ductules anastomose into larger ducts, eventually leading to the larger common bile duct. Far from being a passive drain out of the liver, the biliary epithelial cells in the duct wall modify bile and contribute significantly to bile flow (63,64). Additionally, bile acids or organic molecules may be reabsorbed from the bile duct and recirculate through the liver by way of the peribiliary plexus (65,66). This pattern of redistribution contributes to the intrahepatic drug metabolism.

LOBULAR GRADIENTS

Considerable functional and cellular heterogeneity exists within the context of the liver lobule or acinus. Metabolic and oxygenation zonations are evident across the lobule in a fashion similar to morphological and phenotypic variations found among cell types within

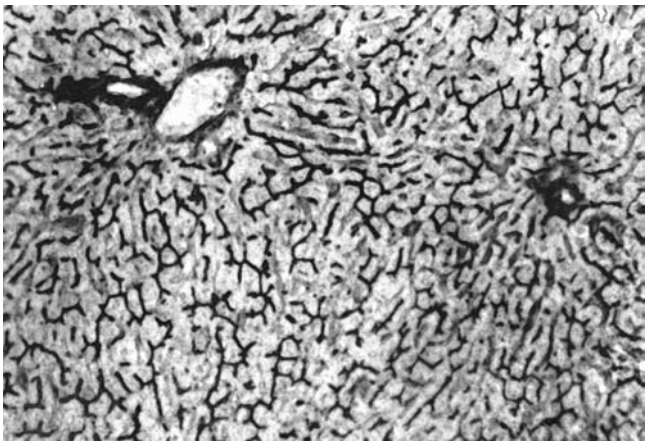

Figure 4 Histochemical reaction for membrane bound ATPase in a frozen liver section demonstrating the network of biliary canals in the liver lobule with confluence toward the portal space (*top left*). The reaction product is within the bile canaliculus, which is formed by the plasma membrane contribution from two adjacent hepatocytes.

different zones. The metabolic differences can contribute to these gradients, on the basis of the intrinsic requirements for excretion of polar metabolites.

Oxygen Gradients

Perhaps the most obvious example of lobular heterogeneity is for oxygen and nutrients along the lateral dimension of the lobule. Cells in the periportal region or acinar zone 1 are exposed to blood high in oxygen and nutrient content. Thus, hepatocytes at the end of the trabecular cords in the centrilobular or acinar zone 3 have to adapt to lower blood oxygen tension and nutrient supply left from the pass over the periportal cells. Periportal oxygen concentrations range from 9% to 13%, which diminish to 4% to 5% by the time blood reaches the central vein (67). These changes in oxygenation may influence the extraction of xenobiotics from the circulation and cause a particular lobular distribution for cellular lesions.

Metabolic Gradients

Although the reasons for regional differences in oxygen tension are obvious, less apparent are the zonal differences in cellular enzyme distribution. Significant lobular heterogeneity exists in activities of enzymes involved in carbohydrate, ammonia, lipid, and xenobiotic metabolism (68 71). In general, in the rat, zonation is described by a periportal prevalence of enzymes involved in gluconeogenesis, fatty acid oxidation, urea formation, and albumin synthesis, whereas glycolysis, fatty acid synthesis, glutamine formation, and xenobiotic metabolism are most prevalent in the centrilobular region (72). In humans, a similar zonation appears to exist, although differences in zonal distribution of lipid synthesis, glutamine formation, and ketone formation have been reported (73 75). The reasons for such functional zonation are unclear, but are likely to involve regional differences in substrate exposure and distribution of oxygen tensions. Lobular variations in hepatocyte transport of drugs and bile formation are also evident (76). The observed differences are at least partially due to the positioning of cells along the sinusoid, with

decreasing oxygen gradients and substrate or drug concentrations as blood moves from periportal regions toward the central vein. Real differences in transport capacity based on cellular localization have been demonstrated.

Intralobular variations of the cytochrome P450s (CYP) have been well documented, with centrilobular hepatocytes having a greater concentration of the hemoproteins (68). Correspondingly, centrilobular hepatocytes have more smooth endoplasmic reticulum (SER) than do periportal hepatocytes. However, more heterogeneity is anticipated if consideration is given to the number of CYP isozymes. In rats, CYP2E and CYP3A are more prominent in centrilobular areas, whereas CYP1A and CYP2B are equally distributed across the lobule (77,78). CYP distribution across the lobule also changes with age (79). In addition, sensitivity of isozymes to inducing agents also appears to vary across the lobule, in some cases normalizing isozyme activity across the lobule (78,80).

Phenotypic and Morphological Heterogeneity of Hepatocytes

On morphological examination, either by light or electron microscopy, hepatocytes appear surprisingly homogeneous in view of the multitude of metabolic functions that run simultaneously in the cytoplasm. Routine stains reveal well-ordered arrays of trabecular cords of hepatocytes radiating from the periportal to the central area. The administration of foreign compounds results in a striking, particular disposition of lesions within the liver lobule. For example, carbon tetrachloride administration produces centrilobular damage as a result of the reductive metabolism by hepatocytes in this area. The early phases of the process of enzyme induction by barbiturates starts in the pericentral hepatocytes, eventually extending to the midzones and periportal zones (81,82). The production of albumin can be a good indicator of protein synthesis by which to follow this induction process. The production of albumin in the rat is about 0.4 mg/hr/g. Michaelson (83), using immunofluorescent tagging, demonstrated that albumin production is confined to about one-tenth of 1% of all hepatocytes. It is obvious that this albumin secretion must be programmed in hepatocytes that appear to be at random within the liver lobule, whereas other hepatocytes secrete proteins of diverse molecular weights. This functional diversity was demonstrated in the increase of fibrinogen production by parenchymal cells following turpentine injection (84). The increased production of fibrinogen is based on the clonal expansion of fibrinogen-producing hepatocytes after mitotic division. This individualized secretion of serum proteins from hepatocytes is also noticeable during neonatal development. The number of liver cells producing α-fetoprotein decreases with age, whereas the number of cells producing albumin, fibrinogen, and other proteins increases (83).

SUBCELLULAR ORGANIZATION OF THE HEPATOCYTE: BASIS FOR ORGANELLE PATHOLOGY

According to the level of microscopic visualization, the liver reveals different orders of structural arrangement. For example, the study of liver tissue by routine transmitted light microscopy provides a survey of well-arranged trabecular parenchymal cells, with a repeating pattern with apparent uniformity. In contrast, the electron microscope reveals a seemingly heterogeneous population of organelles in a diverse network of membrane-bound sacks, vesicles, and microtubules dispersed at random in the cytoplasm. However, there are specific cytoplasmic regions where the Golgi apparatus can be seen and lysosomes congregate near the bile canaliculus. The resemblance between hepatocytes

from different species is uncanny, although it is recognized that similar organelles do not have similar functionalities on a comparative basis. Recent knowledge, gained with embedment-free electron microscopy, suggests unique aspects of the cytoskeleton structure (85). Previously, an approximation of the cytoplasmic infrastructure was described after using high-voltage electron microscopy of unembedded cells (86). Such cytoskeletal network reveals a very important framework akin to a scaffold for organelle interaction and intracytoplasmic motion.

Work at Subramani's laboratory (87) showed that peroxisomes possess bimodal kinetic properties within the hepatocytes. In one mode, peroxisomes display a slow Brownian movement, and in a second or fast mode, these subcellular particles zigzag through the cytoplasm. These studies were achieved by means of fluorescence-specific analysis combined with real-time kinetic imaging and high-resolution tracing of organelle movements. With use of agents that modulate the stability of microfilaments, it was shown that peroxisomes are closely associated with the microfibrillar network. These advances were made feasible by the application of converging technologies employing high-resolution fluorescence microscopy and molecular biology.

The Plasma Membrane: The Blood-Cytoplasm Interface

The plasma membrane envelopes the hepatic parenchymal cells and constitutes the interface barrier with the surrounding microenvironment. A specialized structure of the plasma membrane can be anticipated on the basis of different functions and specific areas that are dedicated to absorption, secretion, and excretion. In a single liver cell, part of the hepatocyte plasma membrane faces the sinusoid, adjoining areas share surfaces with other hepatocytes, and other areas form the biliary canaliculus. Structurally, the bilayer membrane facing each opposing hepatocyte contributes one half of all specialized structures, such as desmosomes and tight junctions. Each individual hepatocyte has an estimated surface area of 1650 to 1950 μm^2, depending on whether the idealized stereological model is based on a dodecahedron or a sphere, respectively. The applicability of these models in tissue sections is based on the closest statistical fit and on the correspondence with different measures that contribute to establishing the final shape factor (88). Hepatocytes contribute about 70% of their plasma membrane surface to the sinusoidal interface in the space of Disse; this space is delineated between the hepatocyte and the inner surface of the Kupffer or sinusoid endothelial cells. The remaining membrane is approximately divided between the portion contributing to the bile canalicular tree and that contributing to the hepatocyte-hepatocyte interface or basolateral membrane. The membrane exposed to the sinusoid provides specialized transporters to move solutes and nutrients from the blood into the cell cytoplasm. If a substance is actively transported, it can traverse various membrane interfaces, ranging from the sinusoidal aspect of the endothelial cell to the hepatocyte facing the space of Disse. The integrity of this membrane transport is responsible in part for the elimination time of drugs from the circulation. Potential routes for solute transport in and out of the liver cell are schematized in Figure 5. This absorption process is also supported by active endocytotic activity, which occasionally includes receptor internalization. The microvilli that characterize this aspect of the membrane contribute to a significant increase of the extent of surface exposed to the plasma. In contrast, the biliary aspect of the plasma membrane directs excretion products, such as metabolites, bile salts, phospholipids, and cholesterol, across the membrane to a highly concentrated, surface-active environment within the lumen of the bile canaliculus. In turn, the basolateral membrane, because of the

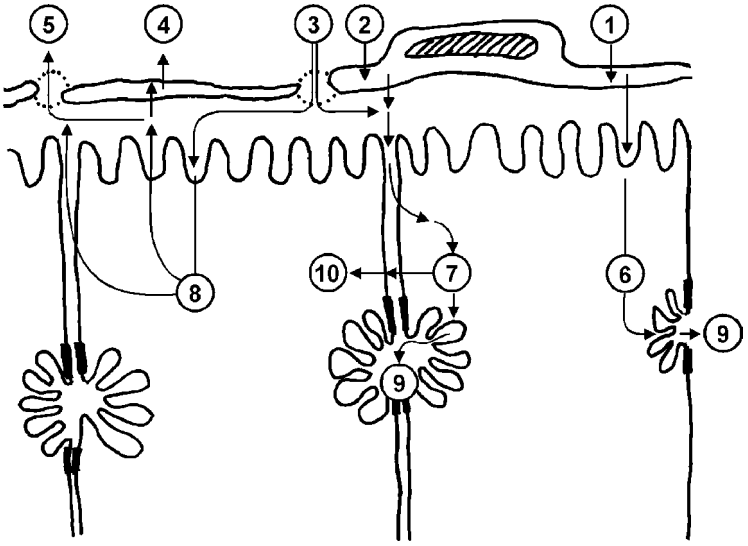

Figure 5 Schematic drawing of the different pathways (*in circled numbers*) that a substance, either conjugated drugs or metabolites, may traverse from the sinusoid into the hepatocyte during absorption; (*circles 6 and 7*). Compounds may reach liver cells either by passage through the foramen (*circle 3*) of endothelial and Kupffer cells or through the cell cytoplasm (*circles 1 and 2*). Different cytoplasmic interactions may influence the route of excretion (circles 4, 5, and 8). Substances may also be excreted into the bile canaliculus (*circle 9*) or the basolateral membrane (*circle 10*) into neighboring cells.

tight junctions, provides a dynamic area where contractile microfilaments rhythmically pulsate the cell membrane, thereby contributing to downstream biliary flow. The biliary cell membrane also contains digital projections that enhance the extent of surface area available for excretory functions. In addition, cilia have been found in the lumen of collecting biliary ductules, and their function or purpose is not clearly known. Because of their paucity, cilia were attributed chemosensory functions and sometimes a streaming role in biliary flow.

The identification of constitutive elements of the liver cell membrane has progressed significantly (89), and specialized canalicular P-glycoproteins were identified having a role in multidrug resistance. These P-glycoproteins are ATP-dependent transport proteins that pump a variety of substances with significantly heterogeneous anionic strength. The mdr-2 P-glycoprotein is a phospholipid flippase, with a key role in the elimination of lipids into bile (90). Models of biliary excretion have been evaluated by Elferink et al. (91) in homozygous variants of the *mdr-2* gene in mice. This approach contributed to the understanding of the physiological basis for bile synthesis and transport and other important functions that modulate drug metabolism and excretion of conjugated products.

The Endoplasmic Reticulum: A Membrane-Based Reactor

The endoplasmic reticulum (ER) is the most critical organelle in hepatocytes for metabolism of drugs. It consists of a labyrinth of tubules and flattened sacs that extend throughout the cytoplasm. The membrane is a continuous sheet that surrounds a common interluminal space called the cisternal space. The ER is the primary location for protein

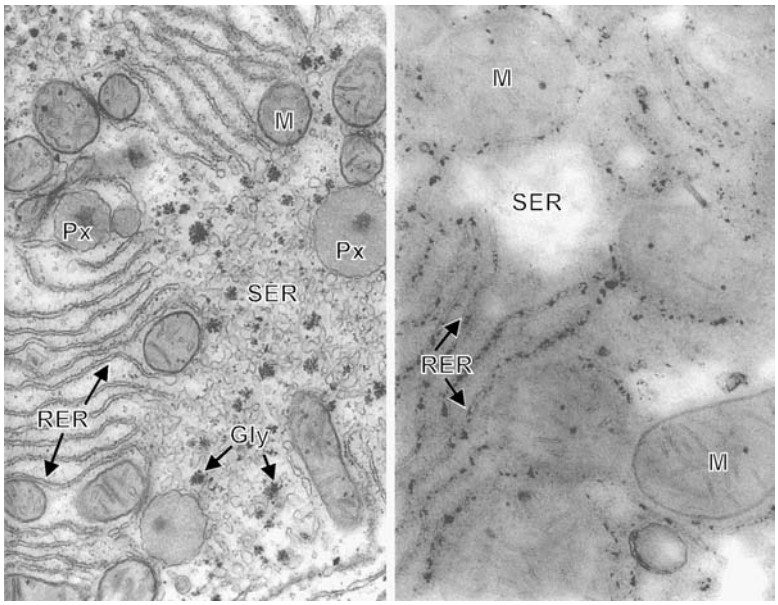

Figure 6 Conventional electron microscopy appearance of a liver cell cytoplasm with lead and uranium contrast (*left*). Electron microscopy cytochemistry for inosinediphosphatase from an unstained liver cell revealed by the dark reaction product within the RER cisternae (*right*). *Abbreviations*: M, mitochondria; RER, rough endoplasmic reticulum; Px, peroxisome; Gly, glycogen particle; SER, smooth endoplasmic reticulum.

synthesis within the hepatocyte and is responsible for the synthesis of all transmembrane proteins. It is also the primary site of lipid and lipoprotein synthesis and metabolism within the hepatocyte, as well as the immediate site for xenobiotic metabolism. The ER consists of two distinct membrane populations; the rough ER (RER), which is characterized by a ribosome-studded cytosolic surface, and the smooth ER (SER), which lacks the ribosomes (Fig. 6). ER membranes can appear as stacks of lamellae as in the rough ER or as furled clumps, characteristic of the SER. Extensive ER connections exist with the Golgi apparatus, which has also specialized functions for protein processing. Within the hepatocyte, the SER constitutes approximately 40% of the total ER membrane. The cytosolic surface of the ER is contiguous with the outer nuclear membrane. The ER is the largest single organelle component within the hepatocyte (92) comprising over 24,000 m^2 of membrane surface area in the adult human liver and approximately 160 to 200 m^2 of surface area in the adult rat liver (93). Quantitative morphometric investigations of ER synthesis and assembly suggest that ER membranes increase at a rate of 17 cm^2/hr from the postnatal period to maturity, at which time, barring physiological or exogenous stimuli, the membrane content is maintained at a relatively constant level (94). Turnover of ER membranes is rapid, with rates ranging from 20 to 50 cm^2/hr for membrane lipids and from 40 to 140 cm^2/hr for membrane proteins (95). CYP inducers can increase the rate of membrane synthesis up to 320 cm^2/hr, whereas removal of the stimuli for induction can cause an acceleration of membrane elimination up to 330 cm^2/hr, which plateaus at the point where the normal physiological membrane content is achieved (96,97). Within the hepatocyte, the ER content is closely regulated, and the capacity for the liver to generate membrane appears to decline with age, indicating that the elderly may be at risk of hepatic dysfunction (98). The CYP enzymes

are located preferentially in the SER, which may explain why, compared with other cell types, hepatocytes have a higher percentage of cellular membranes in the SER configuration. SER membranes proliferate rapidly in response to inducing agents, and this phenomenon is due to a significant buildup in membrane synthesis and not to a decrease in membrane turnover (96). Membrane proliferation in response to induction is a unique phenomenon that may be associated with adaptive synthesis of drug-metabolizing enzymes, but may occur with no concurrent increase in enzyme activity, the so-called hyperplastic hypofunctional ER (94,99). Phospholipids are key components of the ER membrane and maintain a fixed proportion of the membrane components. Systemic phospholipidosis by amphiphilic drugs can cause morphological and functional changes within the membrane and, consequently, alterations in microsomal and lysosomal enzymatic activity (100,101).

Mitochondria: Energy Engines and More

Other than the nucleus, the mitochondria are the most prominent morphological feature of the normal hepatocyte (Fig. 7). This organelle has received significant attention because of its critical role in cell respiration, apoptosis, and cell renewal. There are approximately 1000 mitochondria per liver cell, and they occupy approximately 20% of the cell volume, or approximately 1000 to 1400 μm^3 per hepatocyte. Mitochondria have a half-life of approximately 10 days, and this includes a large synthesis effort if one considers the total number of hepatocytes in the liver. The mitochondrial volume fraction within hepatocytes appears to be consistent across several species, including humans (88,94,102,103). However, lobular heterogeneity in the size and distribution of mitochondria exists. In rats, mitochondria are smaller and more numerous in centrilobular regions (104), although the total mitochondrial volume fraction is similar across the lobule (105). The volume of an average rat hepatic mitochondrion is approximately 0.27 μm^3, with an inner membrane surface area of approximately 65 μm^2 (106). The mitochondrial envelope consists of an inner and outer membrane that encases the intermembranous space. The inner membrane is characterized by numerous folds, called cristae, which greatly increase the available

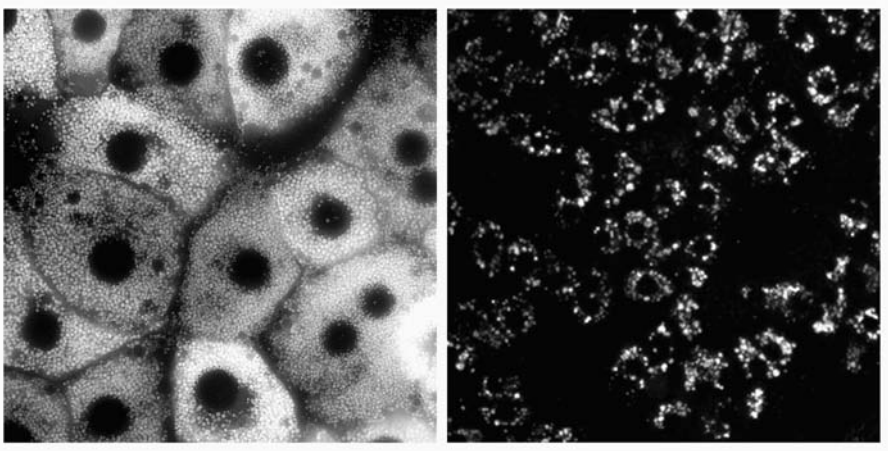

Figure 7 Fluorescence microscopy image of isolated hepatocytes in culture, showing rhodamine 123 uptake into mitochondria (*left*) and FTTC dextran into lysosomes (*right*). This technique allows the quantitative evaluation of hepatocyte uptake under real time conditions by recording the cell changes over a period of time and serially computing the fluorescence over a specified time interval.

surface area for reaction purposes. In the hepatocyte, approximately two-thirds of the mitochondrial protein is located in the mitochondrial matrix, whereas 20% is in the inner membrane, with the remainder found in the intermembranous space. In contrast with the static electron micrographic depictions of mitochondria, mitochondria are mobile within the hepatocyte cytoplasm and can fuse, split, and rapidly change their shape. Although they are usually thought of as independent organelles, it has been suggested that in the hepatocyte, most, if not all, mitochondria may be associated with the RER, with the ER serving as a framework to cluster similarly sized mitochondria. Furthermore, these clusters of mitochondria appear to exhibit functional heterogeneity (107). Mitochondrial morphology by electron microscopy may show changes caused by tissue preparation, fixation, and embedding techniques (108). Morphological alterations of hepatic mitochondria are frequent sequelae of toxicity. Chronic alcoholism, drugs that interfere with copper metabolism, ethionine, orotic acid, hypolipidemic agents, and cortisone, all produce enlarged mitochondria (109). Even though hypolipidemic agents cause large mitochondria, the process of forming large mitochondria results in correspondingly fewer mitochondria (110), suggesting that fusion of preexisting mitochondria may lead to the appearance of the enlarged organelle. Mitochondrial dysfunction has been mechanistically implicated in the liver toxicity of the pesticide endosulfan (111), allyl alcohol (112), the bidentate phosphine gold antineoplastic agent SKF 104524 (113), acetaminophen (114), and the Alzheimer's drug tacrine (115). The mitochondrial impairment induced by acetaminophen is related to the compound's propensity to covalently bind aldehyde dehydrogenase (116).

A main function of mitochondria is to convert energy from carbohydrates and fats into usable forms, primarily ATP. Insight into mitochondrial function can be gleaned from the application of transport-dependent fluorophores, and rhodamine 123 is an example of such a compound that has been used to estimate mitochondrial functional integrity (117) (Fig. 7). Enzymes involved in the β-oxidation of fatty acids and those of the citric acid and urea cycles are found in the mitochondrial matrix, whereas proteins associated with electron transport and oxidative phosphorylation are primarily associated with the inner membrane. The mitochondrial transmembrane potential is the best index for mitochondrial integrity when using fluorescence analysis. A mitochondrion contains its own genome with about five to ten copies per organelle. In humans, mitochondrial DNA (mtDNA) is a circular molecule of 16,569 base pairs, which exclusively code for protein components of the oxidative phosphorylation pathway (118), and most protein components of the mitochondrion are encoded in nuclear DNA and imported into the organelle. mtDNA lacks many of the protective histones of nuclear DNA and is constantly subjected to exposure to oxygen radicals generated during oxidative phosphorylation. These effects are coupled with an inefficient DNA repair system found in mitochondria that makes them susceptible to a high mutation rate, estimated to be up to ten times higher than the rate for nuclear DNA (119). Mitochondrial mutations play a role in several human disease states, primarily involving the skeletal muscle or nervous system. No evidence of human liver disease has been reported to date as a result of mitochondrial mutations. The antiviral nucleoside analogue fialuridine (FIAU) inhibits mtDNA polymerase-γ (120), and the compound caused clinically severe hepatic toxicity and liver failure (121). The woodchuck has been proposed as a model for the study of FIAU-induced hepatic injury (122). This raises the intriguing possibility that toxicant-induced mtDNA changes, or a subset of naturally occurring mitochondrial mutations, may make hepatic mitochondria more susceptible to xenobiotic-induced toxicity. This mechanism has been proposed as a plausible explanation for the hepatotoxicity of the acridine derivative, tacrine (115).

Lysosomes and Cellular Waste

A primary role of the lysosome is disposal or elimination of exogenous or endogenous substances by degradation or solubilization. The organelles contain various esterases, phosphatases, and hydrolases that are active at different pH levels. The average hepatocyte contains approximately 250 lysosomes, occupying about 1% of the total cell volume, and can be tracked by the use of fluorophores under fluorescence microscopy (Fig. 7). These pleiotropic organelles can vary substantially in size and shape, and certain physiological or pathological conditions can drastically increase the number of lysosomes within the hepatocytes. Accumulation of lysosomes after exposure to drugs or ethanol may represent an adaptive response to impaired catabolic processes (94). Long-term oral contraceptive administration increases the number of lysosomes in humans (123), and amphiphilic drugs causing phospholipidosis are frequently associated with accumulation of lysosomes resembling myeloid bodies with high osmium affinity (101). With aging, lysosomes accumulate oxidized fat products, resulting in deposition of lipofuscin or ceroid, the wax-like wear-and-tear pigment (124).

Peroxisomes: Fatty Acid Oxidation and Other Enzymes

Peroxisomes constitute unique subcellular organelles, seen ubiquitously in the cytoplasm of hepatocytes and either in clusters or singly intermeshed in the ER network (125). In conventional transmission electron micrographs, peroxisomes appear as single, scalloped, membrane-bound structures between 0.2 and 0.5 μm, and they are frequently observed containing nucleoids made up of crystalline urate oxidase in many species. Human peroxisomes rarely exhibit a nucleoid probably because of preferential uric acid excretion. A similar spheroidal shape of peroxisomes is observed from the study of pelleted subcellular gradient fraction isolates under the electron microscope (126). These organelles are considered vestigial in terms of evolution because their occurrence is seen in unicellular and multicellular orders, including plants (i.e., glyoxisomes) and higher mammals, with functions genetically modulated according to the level of organization (127). Mature hepatic peroxisomes in mammals contain upward of 40 to 50 enzymes of intermediary metabolism. The main enzyme component by protein weight is catalase, with preferential β-oxidation of short-chain fatty acids. In higher mammals, peroxisomes may play a role in lipoprotein metabolism (128). Approximately 500 to 600 peroxisomes are found in the normal hepatocyte, although higher values, up to 1000, were reported in human liver. The peroxisome population within liver cells is rather stable and seems constant across species, with minor differences because of lobular disposition. Although there is a normal turnover of peroxisomes, their assembly can proceed very quickly after exposure to certain chemicals, particularly after administration of cholesterol biosynthesis inhibitors (128). Such proliferation is transcription dependent, and several proteins are targeted to the membrane or to the matrix of the peroxisome (129). A certain degree of specificity to the proliferative reaction is appreciable, particularly in rats in which peroxisomal enzymes are induced preferentially, whereas urate oxidase, constitutive of the core, is not. Such preferential enzyme synthesis accounts for changes in ratios of nucleated to nonnucleated peroxisomes in rodent liver. Quantitative morphometry has been used to study the dynamics of peroxisome replication. Proliferation is triggered from a baseline turnover rate of 78 to 185 peroxisomes assembled every hour in every one of the 179×10^6 hepatocytes per gram of liver, equivalent to a 20% to 25% increase over the normal baseline in the cell population. Chemical structure and lipid-regulating activity affect the degree of the response, and

once a stimulus is eliminated, the peroxisome population quickly recedes at the same rate as when peroxisomes accumulated. The proliferative response that follows the signal is receptor mediated (130), and the nuclear receptor involved belongs to the steroid receptor superfamily, recognized as the peroxisome proliferator activated receptor (PPAR). Different receptor subtypes have been identified, and PPARα is largely responsible for the proliferation of peroxisomes after dimerization with the retinoid X receptor (RXR). Peroxisome proliferation shows significant species specificity, in parallel with the prevalence of α, δ, or γ subtypes. PPARα is well characterized and mediates a florid response in rodent liver. PPARα requires dimerization with the RXR receptor for downstream activation and binding, a process that is not yet entirely clear. The nucleotide sequence of the peroxisome proliferator response element (PPRE) appears to have highly conserved species specificity. This may explain the lack of peroxisome proliferation in humans and to a certain extent in nonhuman primates administered drugs that otherwise cause profound proliferation in rodents. PPARγ has different affinity and localization in organs and tissues, and its activation may play a role in insulin signaling and carbohydrate metabolism (131). Whereas peroxisome proliferation does not appear to be observable in humans (94), the lack of one or more peroxisomal functions evokes significant abnormalities in autosomal recessive clinical conditions (129). The most severe forms of peroxisome deficiency constitute the loss of multiple enzymes. Among these diseases is the Zellweger syndrome, neonatal adrenoleukodystrophy, Refsum disease, and hyper-pipecolic academia, and patients so affected rarely survive to 10 years of age. Other forms of peroxisomal disorders include the lack of one or more enzymes affecting different steps of intermediate metabolism, each with different clinical prognosis.

Correlating Organelle Integrity: Multiprobe Fluorescence Analysis

Fluorescence analysis has become an ever present method of study in biology for the past two to three decades. The advent of multiprobe fluorescence with multimode microscopy to monitor subcellular events in live liver cells represents an ideal technology for assessing the integrity of cellular elements and possibly identifying toxic molecules (132,133). The methodology of multiprobe fluorescence analysis allows the selection of panels of fluorophores functionally linked to track specific intracellular organelles taking advantage of different excitation/emission spectral properties. The multiple, simultaneous tracking of functional changes within live cells over time leads to a better and clearer understanding when comparing with "single" point assays using cell fractions. Usually, a group of fluorochromes is selected to target a group of parameters addressing basic hepatocyte functions. The panel can include the simultaneous tracking of the intracellular flow of Ca^{2+} with Fura-2, the mitochondrial membrane potential with Mito Tracker Green, the permeability of the plasma membrane/cytoskeleton integrity with Texas Red-phalloidin, and the nucleus integrity (or apoptosis in case of injury) with Hoechst blue 33342. An example of this type of multiprobe fluorescence approach was used with troglitazone, an antidiabetic agent that caused severe idiosyncratic liver dysfunction and damage. To investigate whether or not the toxicity was related to the intact moiety, to different segments of the molecule, or to the metabolites, the panel of probes described above was used (134). The study included human and animal hepatocytes, and the sequential changes were a prompt and significant decline of the mitochondrial transmembrane potential, increased membrane permeability, cytoskeleton disruption, increased intracellular calcium and apoptotic nuclei caused by the intact compound (Fig. 8). The findings were reproducible in peripheral white blood cells by flow cytometry mimicking the multimode microscopy. This methodology represents an important tool for understanding adverse

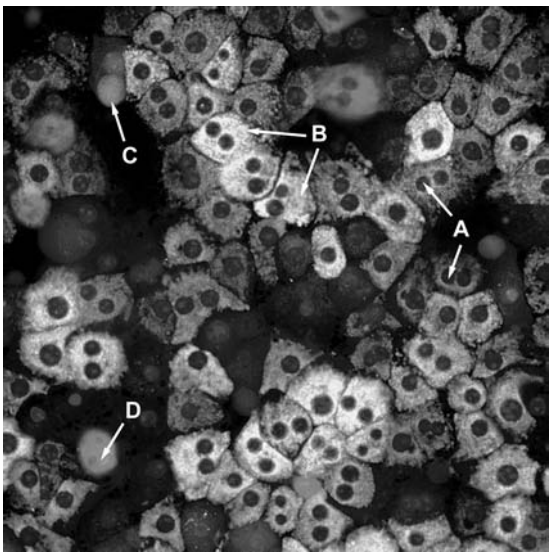

Figure 8 Multiprobe coherent fluorescent microscopy of live hepatocytes. This image is a composite of the simultaneously recorded images with different fluorophores over a period of time. (**A**) Hoechst 33342 for DNA, (**B**) TMRE for mitochondrial transmembrane potential, (**C**) Fluo4 for free calcium, and (**D**) Bodipy phalloidin for membrane permeability. For the explanation of observed events, see text.

cellular events that can predict potential clinical toxicity or impaired metabolism of discrete molecules.

CONCLUDING REMARKS

The liver is a central organ for a variety of anabolic and catabolic functions, and as such, it plays a significant role in drug metabolism and toxicity. Central to its polyfacetic functions is the liver architecture, which commands a large role in the physiology of blood clearance and excretion of degradation products. Although hepatocytes appear to represent similarly repeating functional reactors, their diversity is becoming obvious, and it is possible that functions are closely integrated with cell replication. Within liver cells, the different organelles, although having close interrelations, represent functionally discrete compartments, and significant species differences influence their basic metabolic activities. These subcellular compartments reveal unique responses to metabolic or pathological stimuli, lobular blood flow gradients modulate these responses, and zonation may relate to nutrient availability or to reactive metabolism. The most important account is the high turnover of structural protein and enzymes contained in these organelles requiring large amounts of energy. The different relationships between hepatocytes and non-parenchymal cells are not yet fully discerned, but they reveal a very close metabolic interdependence between different cell populations. This brief functional-anatomical overview may help explain pharmacodynamic, genetic, and physiological correlations that significantly influence drug metabolism. Most importantly, the authors hope that this bird's eye view of liver function and metabolism may encourage younger scientists to gain further knowledge into the intricate problems leading to adverse drug interactions, impaired metabolism, and injurious toxicity.

ACKNOWLEDGMENT

Many of the concepts elaborated in this chapter where the subject of challenging discussions with debate and hypotheses testing taking place over many years. We wish to extend our great appreciation to many of those who worked in our "skunk" laboratories, Ramin Rhabari, Paul Rowse, Tim Braden, Greg Urda, John Lucas, and Doug Plymale. We recognize the valuable contributions from Michael Bleavins, Jeff Theiss, David Monteith, Jennifer Sturgess, Hiroshi Masuda, Ted McGuire, and Bob Gray. We dedicate this chapter to the memory of George Feuer, Akira Takada, and José Mosquera, who were great colleagues, contributors, tireless scientists, emotional intellectuals, and most of all, our teaching allies and mentors.

REFERENCES

1. Kiernan F. The anatomy and physiology of the liver. Phil Trans Roy Soc London B Biol Sci 1833; 123:711 770.
2. Rappaport AM, Borowy ZJ, Lougheed WM, Lotto WN. Subdivision of hexagonal liver lobules into a structural and function unit. Role in hepatic physiology and pathology. Anat Rec 1954; 119:11 33.
3. Dubois AM. The embryonic liver. In: Rouiller CL, ed. The Liver. New York: Academic Press, 1963:1 39.
4. Suchy FJ, Buscuvalas JC, Novak DA. Determinants of bile formation during development: ontogeny of hepatic bile acid metabolism and transport. Semin Liver Dis 1987; 7:77 84.
5. Zajicek G, Oren R, Weinreb M. The streaming liver. Liver 1985; 5:293 300.
6. Bralet M P, Branchereau S, Brechot C, Ferry N. Cell lineage study in the liver using retroviral mediated gene transfer. Evidence against the streaming of hepatocytes in normal liver. Am J Pathol 1994; 144:896 905.
7. Arber N, Zajicek GI, Ariel I. The streaming liver. II Hepatocyte life history. Liver 1988; 8:80 87.
8. Grisham JW. Migration of hepatocytes along hepatic plates and stem cell fed hepatocyte lineages. Am J Pathol 1994; 144:849 854.
9. Sell S. Liver stem cells. Mod Pathol 1994; 7:105 112.
10. Kennedy S, Rettinger S, Flye MW, Ponder KP. Experiments in transgenic mice show that hepatocytes are the source for postnatal liver growth and do not stream. Hepatology 1995; 22:160 168.
11. Wisse E. An electron microscopic study of the fenestrated endothelial lining of rat liver sinusoids. J Ultrastruct Res 1970; 31:125 150.
12. Fraser R, Bowler L, Day W. The filtration of lipoproteins by the liver. N Z Med J 1975; 82:352.
13. Mak KM, Lieber CS. Alterations in endothelial fenestration in liver sinusoids of baboons fed alcohol. A scanning electron microscopic study. Hepatology 1984; 4:386 391.
14. Arias IM. The biology of hepatic endothelial fenestrae. Prog Liver Dis 1990; 9:11 26.
15. Fraser R, Day WA, Fernando NS. The liver sinusoidal cells. Their role in disorders of the liver, lipoprotein metabolism and atherogenesis. Pathology 1986; 18:5 11.
16. Witte MH, Borgs P, Way DL, Ramirez G Jr, Bernas MJ, Witte CL. Alcohol, hepatic sinusoidal microcirculation, and chronic liver disease. Alcohol 1992; 9:473 480.
17. Wisse E, De Leeuw AM. Structural elements determining transport and exchange processes in the liver. In: Pharmaceutical, Immunological and Medical Aspects. Amsterdam: Elsevier, 1984:1 23.
18. Reider H, Meyer zum Bushenfelde KH, Ramadori G. Functional spectrum of sinusoidal endothelial liver cells. Filtration, endocytosis, synthetic capacities and intercellular commu nication. J Hepatol 1992; 15:237 250.
19. Walker RM, Racz WJ, McElligott TF. Scanning electron microscopic examination of acetaminophen induced hepatotoxicity and congestion in mice. Am J Pathol 1983; 113:321 330.

20. Rouiller C, Colombey N, Haenni B. Modifications of the capillary sinusoids of the liver in acute experimental poisoning. Rev Int Hepatol 1965; 15:437 453.
21. Singer JM, Adlersberg L, Hoenig EM, Ende E, Tchorsch Y. Radiolabeled latex particles in the investigation of phagocytosis in vivo: clearance curves and histological observations. J Reticuloendothel Soc 1969; 6:561 589.
22. Gale RP, Sparkes RS, Golde DW. Bone marrow origin of hepatic macrophages. Kupffer cells in humans. Science 1978; 201:937 938.
23. van Furth R. Monocyte origin of Kupffer cells. Blood Cells 1980; 6:87 92.
24. Bouwens L, Baekeland M, Wisse E. Importance of local proliferation in the expanding Kupffer cell population of rat liver after zymosan stimulation and partial hepatectomy. Hepatology 1984; 4:213 219.
25. McCuskey RS, McCuskey PA. Fine structure and function of Kupffer cells. J Electron Microsc Tech 1990; 14:237 246.
26. Liehr H, Grun M. Clinical aspects of Kupffer cell failure in liver diseases. In: Wisse E, Knook DL, eds. Kupffer Cells and Other Liver Sinusoidal Cells. Amsterdam: Elsevier/North Holland Biomedical, 1977:427 436.
27. Bouwens L, Wisse E. Proliferation, kinetics, and fate of monocytes in rat liver during a zymosan induced inflammation. J Leukoc Biol 1985; 37:531 543.
28. Bouwens L, Knook DL, Wisse E. Local proliferation and extrahepatic recruitment of liver macrophages Kupffer cells in partial body irradiated rats. J Leukoc Biol 1986; 39:687 975.
29. Pilaro AM, Laskin DL. Accumulation of activated mononuclear phagocytes in the liver following lipopolysaccharide treatment of rats. J Leukoc Biol 1986; 40:29 41.
30. Winwood PJ, Arthur MJ. Kupffer cells: their activation and role in animal models of liver injury and human liver disease. Semin Liver Dis 1993; 13:50 59.
31. Billiar TR, Curran RD. Kupffer cell and hepatocyte interactions: a brief overview. JPEN J Parenter Enteral Nutr 1990; 14:175s 180s.
32. Ghezzi P, Saccardo B, Bianchi M. Role of reactive oxygen intermediates in the hepatotoxicity of endotoxin. Immunopharmacology 1986; 12:241 244.
33. elSisi AE, Earnest DL, Sipes IG. Vitamin A potentiation of carbon tetrachloride hepatotoxicity: role of liver macrophages and active oxygen species. Toxicol Appl Pharmacol 1993; 119:295 301.
34. Billiar TR, Lysz TW, Curran R D, Bentz BG, Machiedo W, Simmons PL. Hepatocyte modulation of Kupffer cell prostaglandin E_2 production in vitro. J Leukoc Biol 1990; 47: 305 311.
35. Harbrecht BG, Billiar TR. The role of nitric oxide in Kupffer cell hepatocyte interactions. Shock 1995; 3:79 87.
36. Laskin DL. Nonparenchymal cells and hepatotoxicity. Semin Liver Dis 1990; 10:293 304.
37. Ito T, Nemoto W. Uber die kupffersche sternzellen und die fettspeicherungszellen fatstoring cell in der blutkapillarwand der menschlichen leber. Okajamas Folia Anat Jpn 1952; 24:243 258.
38. Wake K. Perisinusoidal stellate cells fat storing cells, interstitial cells, lipocytes, their related structure in and around the liver sinusoids, and vitamin A storing cells in extrahepatic organs. Int Rev Cytol 1980; 66:303 353.
39. Giampieri MP, Jezequel AM, Orlandi F. The lipocytes in normal human liver A quantitative study. Digestion 1981; 22:165 169.
40. Pinzani M. Novel insights into the biology and physiology of the Ito cell. Pharmacol Ther 1995; 66:387 412.
41. Ramadori G. The stellate cell Ito cell, fat storing cell, lipocyte, perisinusoidal cell of the liver. New insights into pathophysiology of an intriguing cell. Virchows Arch B 1991; 61:147 158.
42. Ito T, Itoshima T, Ukida M, Tobe K, Kiyotoshi S, Kawaguchi K, Ogawa H, Yamamoto H, Hattori S, Kitadai M, Mizutani S, Tsuchiya T, Kita K, Tanaka R, Nagasima H. Scanning electron microscopy of Ito's fat storing cells in the rat liver. Acta Med Okayama 1984; 38:1 9.
43. Yokoi Y, Namihisa T, Kuroda H, Komatsu I, Miyasaki A, Watanabe S, Usui K. Immunocytochemical detection of desmin in fatstoring cells Ito cells. Hepatology 1984; 4: 709 714.

44. Hendriks HF, Verhoofstad WA, Brouwer A, de Leuw AM, Knook DL. Perisinusoidal fat storing cells are the main vitamin A storage sites in rat liver. Exp Cell Res 1985; 160:138 149.
45. Friedman SL. Cellular sources of collagen and regulation of collagen production in liver. Semin Liver Dis 1990; 10:20 29.
46. Gressner AM, Bachem MG. Cellular sources of noncollagenous matrix proteins: role of fat storing cells in fibrogenesis. Semin Liver Dis 1990; 10:30 46.
47. Maher JJ, McGuire RF. Extracellular matrix gene expression increases preferentially in rat lipocytes and sinusoidal endothelial cells during hepatic fibrosis in vivo. J Clin Invest 1990; 86:1641 1648.
48. Lissoos TW, Davis BH. Pathogenesis of hepatic fibrosis and the role of cytokines. J Clin Gastroenterol 1992; 15:63 67.
49. Nakano M, Worner TM, Lieber CS. Perivenular fibrosis in alcoholic liver injury: ultrastructure and histologic progression. Gastroenterology 1982; 83:777 785.
50. French SW, Miyamoto K, Wong, Jui L, Briere L. Role of the Ito cell in liver parenchymal fibrosis in rats fed alcohol and a high fat low protein diet. Am J Pathol 1988; 132:73 85.
51. Lautt WW, Greenway CV. Conceptual review of the hepatic vascular bed. Hepatology 1987; 7:952 963.
52. McCuskey RS and Reilly FD. Hepatic microvasculature: Dynamic structure and its regulation. Semin Liver Dis 1992,13:1 12.
53. Greenway CV, Oshiro G. Intrahepatic distribution of portal and hepatic arterial blood flows in anaesthetized cats and dogs and the effects of portal occlusion, raised venous pressure and histamine. J Physiol 1972; 227:473 485.
54. Lautt WW, Legare DJ, Daniels TR. The comparative effect of administration of substances via the hepatic artery or portal vein on hepatic arterial resistance, liver blood volume and hepatic extraction in cats. Hepatology 1984; 4:927 932.
55. McCuskey RS. A dynamic and static study of hepatic arterioles and hepatic sphincters. Am J Anat 1966; 119:455 478.
56. Klaassen CD, Watkins JBD. Mechanisms of bile formation, hepatic uptake, and biliary excretion. Pharmacol Rev 1984; 36:1 67.
57. Angelin B, Bjorkhem I, Einarsson K, Ewerth S. Hepatic uptake of bile acids in man. Fasting and postprandial concentrations of individual bile acids in portal venous and systemic blood serum. J Clin Invest 1982; 70:724 731.
58. Strange RC. Hepatic bile flow. Physiol Rev 1984; 64:1055 1102.
59. Arias IM, Che M, Gatmaitan, Leveille C, Nishida T, St. Pierre M. The biology of the bile canaliculus. Hepatology 1993; 17:318 329.
60. Layden TJ, Elias E, Boyer JL. Bile formation in the rat: the role of the paracellular shunt pathway. J Clin Invest 1978; 62:1375 1385.
61. Bradley SE, Herz R. Permselectivity of biliary canalicular membrane in rats: clearance probe analysis. Am J Physiol 1978; 235:E570 E576.
62. MacSween RNM, Scothorne RF. Developmental anatomy and normal structure. In: MacSween RNM, Anthony PP, Scheuer PJ, et al. eds. Pathology of the Liver. 3rd ed. Edinburgh: Churchill Livingstone, 1994:1 49.
63. Alpini G, Roberts S, Kuntz SM, Ueno Y, Gubba S, Podila PV, Lesage G, LaRusso NF. Morphological, molecular and functional heterogeneity of cholangiocytes from normal rat liver. Gastroenterology 1996; 110:1636 1643.
64. Nathanson MH, Boyer JL. Mechanisms and regulation of bile secretion. Hepatology 1991; 14:551 566.
65. Yoon YB, Hagey LR, Hofmann AF, Gurantz D, Michelotti EL, Steinbach JH. Effect of side chain shortening on the physiological properties of bile acids: hepatic transport and effect on the biliary reaction of 23 urodeoxycholate in rodents. Gastroenterology 1986; 90:837 852.
66. Lamri Y, Erlinger S, Dumont M, Roda A, Feldmann G. Immunoperoxidase localisation of urodeoxycholic acid in rat biliary epithelial cells evidence for a cholehepatic circulation. Liver 1992; 12:351 354.

67. Moslen MT. Toxic responses of the liver. In: Klaassen CD, ed. Toxicology, the Basic Science of Poisons. 5th ed. New York: McGraw Hill, 1996:403 416.
68. Jungermann K, Katz N. Functional specialization of different hepatocyte populations. Physiol Rev 1989; 69:708 764.
69. Gumucio JJ. Hepatocyte heterogeneity: the coming of age from the description of a biological curiosity to a partial understanding of its physiological meaning and regulation. Hepatology 1989; 9:154 160.
70. Haussinger D, Lamers WH, Moorman AF. Hepatocyte heterogeneity in the metabolism of amino acids and ammonia. Enzyme 1992; 46:72 93.
71. Gebhardt R. Metabolic zonation of the liver: regulation and implications for liver function. Pharmacol Ther 1992; 53:275 354.
72. Jungermann K. Zonal liver cell heterogeneity. Enzyme 1992; 46:5 7.
73. Hoffmann GE, Andres H, Weiss L, Kreisel C, Sander R. Properties and organ distribution of ATP citrate pro 3S lyase. Biochim Biophys Acta 1980; 620:151 158.
74. Moorman AF, Vermeulen JL, Charles R, Lamers WH. Localization of ammonia metabolizing enzymes in human liver: ontogenesis of heterogeneity. Hepatology 1989; 9:367 372.
75. Racine Samson L, Scoazec JY, D'Errico A, Fiorentino M, Christa L, Moreau A, Roda C, Grigioni WF, Feldman G. The metabolic organization of the adult human liver: a comparative study of normal, fibrotic, and cirrhotic liver tissue. Hepatology 1996; 24:104 113.
76. Groothuis GM, Meijer DK. Hepatocyte heterogeneity in bile formation and hepatobiliary transport of drugs. Enzyme 1992; 46:94 138.
77. Tsutsumi M, Lasker JM, Shimizu M, Rosman AS, Lieber CS. The intralobular distribution of ethanol inducible P450IIE1 in rat and human liver. Hepatology 1989; 10:437 446.
78. Serasinghe P, Yamazaki H, Nishiguchi K, Serasinghe S, Nakanishi S. Intralobular localization of different cytochrome P 450 form dependent monooxygenase activities in the liver of normal and inducer treated rats. Int J Biochem 1992; 24:959 965.
79. Ratanasavanh D, Beaune P, Morel F, Flinois JP, Guengerich FP, Guillouzo A. Intralobular distribution and quantitation of cytochrome P 450 enzymes in human liver as a function of age. Hepatology 1991; 13:1142 1151.
80. Buhler R, Lindros KO, Nordling A, Johansson I, Ingelman Sundberg M. Zonation of cytochrome P450 isozyme expression and induction in rat liver. Eur J Biochem 1992; 204:407 412.
81. Lindamood C. Xenobiotic biotransformation. In: Meeks RG, Harrison SD, Bull RJ, eds. Hepatotoxicology. Boca Raton: CRC Press, 1991:139 180.
82. Gumucio JJ, May M, Dvorak C, Chianale J, Massey V. The isolation of functionally heterogeneous hepatocytes of the proximal and distal half of the liver acinus in the rat. Hepatology 1986; 6:932 944.
83. Michaelson J. Cellular selection in the genesis of multicellular organization. Lab Invest 1993; 69:136 151.
84. Schreiber G, Tsykin A, Aldred AR, Thomas T, Fung WP, Dickson PW, Cole T, Birch H, De Jong FA, Milland J. The acute phase response in the rodent. Ann N Y Acad Sci 1989; 557:61 85.
85. Penman S. Rethinking cell structure. Proc Natl Acad Sci U S A 1995; 92:5251 5257.
86. Porter KR. The cytomatrix: a short history of its study. J Cell Biol 1984; 99:3s 12s.
87. Wiemer EA, Wenzel T, Deerinck TJ, Ellisman MH, Subramani S. Visualization of the peroxisomal compartment in living mammalian cells: dynamic behavior and association with microtubules. J Cell Biol 1997; 136:71 80.
88. Weibel ER, Staubli W, Gnagi HR, Hess FA. Correlated morphometric and biochemical studies on the liver cell. I. Morphometric model, stereologic methods and normal morphometric data for rat liver. J Cell Biol 1969; 42:68 91.
89. Keppler D, Arias IM. Hepatic canalicular membrane introduction: transport across the hepatocyte canalicular membrane. FASEB J 1997; 11:15 18.
90. Elferink RP, Groen AK. The mechanism of biliary lipid secretion and its defects. Gastroenterol Clin North Am 1999; 28:59 74.

91. Elferink RP, Tytgat GN, Groen AK. Hepatic canalicular membrane. 1: The role of mdr2 P glycoprotein in hepatobiliary lipid transport. FASEB J 1997; 11:19 28.
92. Feuer G, Cooper SD, de la Iglesia FA, Lumb G. Microsomal phospholipids and drug action. Quantitative biochemical and electron microscopic studies. Int Z Klin Pharmakol Ther Toxikol 1972; 5:389 396.
93. de la Iglesia FA, Sturgess JM, Feuer G. New approaches for the assessment of hepatotoxicity by means of quantitative functional morphological interrelationships. In: Dixon RL, Hewitt WR, Plaa GL, eds. Target Organ Toxicology Series Toxicology of the Liver. New York: Raven Press, 1982:47 102.
94. Feuer G, de la Iglesia FA. Subcellular biochemical and pathological correlates in experimental models of hepatotoxicity. In: Cameron R, Feuer G, de la Iglesia FA, eds. Drug Induced Hepatotoxicity. Heidelberg: Springer Verlag, 1996:43 73.
95. Dallner G, Ericsson JLE. Molecular Structure and Biological Implication of the Liver Endoplasmic Reticulum. New York: Grune & Stratton, 1976:35 50.
96. Bolender RP, Weibel ER. A morphometric study of removal of phenobarbital induced membranes from hepatocytes after cessation of treatment. J Cell Biol 1973; 51:746 776.
97. Staubli W, Hess R, Weibel ER. Correlated morphometric and biochemical studies on the liver cell. II. Effects of phenobarbital on rat hepatocytes. J Cell Biol 1969; 42:92 112.
98. Schmuckler DL. Age related changes in hepatic fine structure: a quantitative analysis. J Gerontol 1976; 31:135 143.
99. Feuer G, DiFonzo CJ. Intrahepatic cholestasis: a review of biochemical pathological mechanisms. Drug Metabol Drug Interact 1992; 10:1 161.
100. de la Iglesia FA, Feuer G, Takada A, Matsuda Y. Morphologic studies on secondary phospholipidosis in human liver. Lab Invest 1974; 30:539 549.
101. de la Iglesia FA, Feuer G, McGuire EJ, Takada A. Morphological and biochemical changes in the liver of various species in experimental phospholipidosis after diethylaminoethoxyhex estrol treatment. Toxicol Appl Pharmacol 1975; 34:28 44.
102. Hess FA, Weibel ER, Preisig R. Morphometry of dog liver: normal base line data. Virchows Arch B Cell Pathol 1973; 12:303 317.
103. David H. Quantitative Ultrastructural Data of Animal and Human Cell. Stuttgart: Fisher, 1977.
104. Blouin A, Bolender RP, Weibel ER. Distribution of organelles and membranes between hepatocytes and nonhepatocytes in the rat liver parenchyma. A stereological study. J Cell Biol 1977; 72:441 455.
105. Schmuckler DL, Mooney JS, Jones AL. Stereological analysis of hepatic fine structure in the fischer 344 rat. Influence of sublobular location and animal age. J Cell Biol 1978; 78:319 337.
106. Schwerzmann K, Cruz Orive LM, Eggman R, Sanger A, Weibel ER. Molecular architecture of the inner membrane of mitochondria from rat liver: a combined biochemical and stereological study. J Cell Biol 1986; 102:97 103.
107. Cascarano J, Chambers PA, Schwartz E, Poorkaj P, Gondo RE. Organellar clusters formed by mitochondrial rough endoplasmic reticulum associations: an ordered arrangement of mitochondria in hepatocytes. Hepatology 1995; 22:837 846.
108. Candipan RC, Sjostrand FS. An analysis of the contribution of the preparatory techniques to the appearance of condensed and orthodox conformations of the liver mitochondria. J Ultrastruct Res 1984; 89:281 294.
109. Smith RA, Ord MJ. Mitochondrial form and function relationships in vivo: their potential in toxicology and pathology. Am J Pathol 1983; 83:63 134.
110. McGuire EJ, Haskins JR, Lucas JA, de la Iglesia FA. Hypolipidemic induced quantitative microscopic changes in rat liver mitochondria. In: VII International Congress of Toxicology, Seattle, WA, 1995; 7:47 P 7 (abstr.).
111. Dubey RK, Beg MU, Singh J. Effects of endosulfan and its metabolites on rat liver mitochondrial respiration and enzyme activities in vitro. Biochem Pharmacol 1984; 33:3405 3410.
112. Jacobs JM, Rutkowski JV, Roebuck BD, Smith RP. Rat hepatic mitochondria are more sensitive to allyl alcohol than are those of mice. Toxicol Lett 1987; 38:257 264.

113. Smith PF, Hoke GD, Alberts DW, Bugelski PJ, Lupo S, Mirabelli CK, Rush GF. Mechanism of toxicity of an experimental bidentate phosphine gold complexed antineoplastic agent in isolated rat hepatocytes. J Pharmacol Exp Ther 1989; 249:944 950.
114. Donnelly PJ, Walker RM, Racz WJ. Inhibition of mitochondrial respiration in vivo is an early event in acetaminophen induced hepatotoxicity. Arch Toxicol 1994; 68:110 118.
115. Robertson DG, Braden TK, Urda ER, Lalwani NL, de la Iglesia FA. Elucidation of mitochondrial effects by the tetra hydroaminoacridine tacrine in rat, dog, monkey and human hepatic parenchymal cells. Arch Toxicol 1998; 72:362 371.
116. Landin JS, Cohen SD, Khairallah EA. Identification of a 54 kDa mitochondrial acetaminophen binding protein as aldehyde dehydrogenase. Toxicol Appl Pharmacol 1996; 141:299 307.
117. Monteith DK, Theiss JC, Haskins JR, de la Iglesia FA. Functional and subcellular organelle changes in isolated rat and human hepatocytes induced by tetrahydroaminoacridine. Arch Toxicol 1998; 72:147 156.
118. Wallace DC. Mitochondrial DNA sequence variation in human evolution and disease. Proc Natl Acad Sci U S A 1994; 91:8739 8746.
119. LeDoux SP, Wilson GL, Bohr VA. Mitochondrial DNA repair and cell injury. In: Lash LH, Jones DP, eds. Methods in Toxicology. Mitochondrial Dysfunction. Vol. 2. New York: Academic Press, 1993:461 476.
120. Lewis W, Meyer RR, Simpson J F, Colacino JM, Perrino FW. Mammalian DNA polymerases alpha, beta, gamma, delta, and epsilon incorporate fialuridine FIAU monophosphate into DNA and are inhibited competitively by FIAU triphosphate. Biochemistry 1994; 33:14620 14624.
121. Lewis W, Dalakas MC. Mitochondrial toxicity of antiviral drugs. Nat Med 1995; 51:417 422.
122. Lewis W, Griniuviene B, Tankersley KO, Levine ES, Montione R, Engelman L, de Courten Myers G, Ascenzi MA, Hombuckle WE, Gerrin JL. Depletion of mitochondrial DNA, destruction of mitochondria, and accumulation of lipid droplets result from fialuridine treatment in woodchucks Marmota monax. Lab Invest 1997; 76:77 87.
123. Stahl K, Themann H, Verhagen A. Ultrastructural morphometric investigations on liver biopsies. The influence of oral contraceptives on the human liver. Arch Gynakol 1977; 223:205 211.
124. Miyai K. Structural Organization of the Liver. Boca Raton: CRC Press, 1991:1 66.
125. Yamamoto K, Fahimi H. Three dimensional reconstruction of a peroxisomal reticulum in regenerating rat liver: evidence of interconnections between heterogeneous segments. J Cell Biol 1987; 105:713 722.
126. Afzelius BA. The occurrence and structure of microbodies. J Cell Biol 1965; 26:835 841.
127. de Duve C. The peroxisome in retrospect. Ann N Y Acad Sci 1996; 804:1 10.
128. McGuire EJ, Lucas JA, Gray RH, de la Iglesia FA. Peroxisome induction potential and lipid regulating activity in rats. Quantitative microscopy and chemical structure activity relation ships. Am J Pathol 1991; 39:217 229.
129. Subramani S. Protein import into peroxisomes and biogenesis of the organelle. Annu Rev Cell Biol 1993; 9:445 478.
130. Lemberger T, Desvergne B, Wahli W. Peroxisome proliferator activated receptors: a nuclear receptor signaling pathway in lipid physiology. Annu Rev Cell Dev Biol 1996; 12:335 363.
131. Saltiel AR, Olefsky JM. Thiazolidinediones in the treatment of insulin resistance and type II diabetes. Diabetes 1996; 45:1661 1669.
132. Plymale D, Haskins JR, de la Iglesia FA. Monitoring Subcellular events in vitro by means of coherent multiprobe fluorescence. Nat Med 1999; 5:351 355.
133. Plymale DR, de la Iglesia FA. Acridine induced subcellular and functional changes in isolated human hepatocytes in vitro. J Appl Toxicol 1999; 19:31 38.
134. Haskins JR, Rowse P, Rahbari R, de la Iglesia FA. Thiazolidinedione toxicity to isolated hepatocytes revealed by coherent multiprobe fluorescence microscopy and correlated with multiparameter flow cytometry of peripheral leukocytes. Arch Toxicol 2001; 75:425 438.

4

The Cytochrome P450 Oxidative System

Paul R. Ortiz de Montellano
Department of Pharmaceutical Chemistry, School of Pharmacy, University of California, San Francisco, California, U.S.A.

INTRODUCTION TO THE CYTOCHROME P450 SYSTEM

The cytochrome P450 (P450) enzymes play essential roles in the biosynthesis of sterols, eicosanoids, and other physiologically important intermediates. Conversely, they are also critical for the metabolism of fatty acids and other lipophilic endogenous substrates and of most drugs and xenobiotics. The cytochrome P450 catalytic function is uniquely suited to the introduction of polar functionalities into systems as difficult to oxidize as saturated hydrocarbons. The oxidative introduction of such functions is particularly critical for the metabolism and elimination of lipophilic compounds without polar functional groups suitable for conjugation reactions. On the darker side, the oxidative power of cytochrome P450 enzymes not infrequently transforms an innocuous substrate into a chemically reactive, toxic metabolite.

The P450 enzymes involved in nonbiosynthetic transformations are widely distributed, with particularly high concentrations in the endoplasmic reticulum of the liver, kidney, lung, nasal passages, and gut and with significant concentrations in most other tissues (1). In contrast, the sterol biosynthetic enzymes are primarily found in steroidogenic tissues such as the adrenals and testes. The mammalian P450 enzymes are all membrane bound and the solubilization, purification, and reconstitution of the pure enzymes are technically challenging. However, all the relevant enzymes can be heterologously expressed in *Eschericia coli*, *Saccharomyces cerevisiae*, or baculovirus/insect cell systems. Each of these expression systems has advantages and disadvantages, but the bacterial and baculovirus systems are routinely used for the commercial production of mammalian P450 enzymes.

CYTOCHROME P450 GENE FAMILY

Analysis of the human genome has identified a total of 57 human P450 enzymes, several of which were previously unknown and some of which have yet to be significantly characterized (Table 1). The sequences of thousands of cytochrome P450 enzymes are

Table 1 The Complement of Human Cytochrome P450 Enzymes

1A1	2J2	4F11	11B2
1A2	2R1	4F12	17A1
1B1	2S1	4F22	19A1
2A6	2U1	4V2	20A1
2A7	2W1	4X1	21A2
2A13	3A4	4Z1	24A1
2B6	3A5	5A1	26A1
2C8	3A7	7A1	26B1
2C9	3A43	7B1	26C1
2C19	4A11	8A1	27A1
2D6	4A22	8B1	27B1
2E1	4B1	11A1	27C1
2F1	4F2	11B1	39A1

now known, and the number of additional sequences, particularly those of bacterial, insect, and plant origin, increases monthly (http://drnelson.utmem.edu/CytochromeP450.html). This flood of sequence information has required the development of a rational nomenclature on the basis of the premise that the extent of sequence and functional identity decreases as a function of evolutionary distance from a common precursor. In consequence, the new nomenclature groups P450 enzymes according to probable structural and functional similarity rather than, as in earlier days, on the basis of properties such as electrophoretic mobility, absorption spectrum, or substrate specificity. Although the cutoff lines are somewhat arbitrary, enzymes with more than 40% sequence identity are considered as members of the same family, and those with more than 55% identity are assigned to the same subfamily (2). P450 enzymes are thus identified by a number denoting the family, a letter denoting the subfamily, and a number (and sometimes subsequent letters) identifying the specific member of the subfamily (Table 1). The identifying numbers can be associated with the term P450, as in P450 3A4, or more formally with the term cytochrome P (CYP), as in CYP3A4. Thus, cytochrome P450 1A2 (CYP1A2) is the second member of subfamily A of family 1, and P450 3A4 is the fourth member of subfamily A of family 3. The trivial names of some substrate-specific enzymes continue to be widely used (e.g., aromatase for CYP19), but the P450 enzymes primarily involved in drug metabolism are now known by their systematic names.

The cytochrome P450-dependent metabolism of drugs and xenobiotics in humans is primarily mediated by enzymes of the CYP1, CYP2, CYP3, and CYP4 families (Table 2). In humans, CYP3A4 is the most abundant isoform, representing approximately 30% of the cytochrome P450 in the liver, while CYP1A2 represents approximately 13%, CYP2A6 approximately 4%, the CYP2C enzymes approximately 20%, CYP2D6 approximately 2%, and CYP2E1 approximately 7% of the total (1,3). The importance of the individual enzymes in drug metabolism depends not only on their abundance but also on the extent to which their substrate specificity coincides with the spectrum of drugs and xenobiotics to which the individual is exposed. As suggested by Table 2, CYP3A4, CYP2D6, and the CYP2C enzymes are responsible for the bulk of drug metabolism, although other isoforms can play critical roles with specific substrates. In practice, CYP3A5/CYP3A5 are thought to account for approximately 50% of all P450-dependent drug metabolism, CYP2D6 and CYP2C9 for approximately 15% each, and the remaining enzymes, notably CYP2E1, CYP2C19, CYP2C8, CYP2B6, CYP2A6, CYP1B1, CYP1A2, and CYP1A1, for small percentages of the remaining total (4). Furthermore,

Table 2 Human Cytochrome P450 Isoforms Largely Responsible for Drug Metabolism and a Partial List of Their Substrates (1)

Enzyme	Substrates	Enzyme	Substrates
CYP1A1	benzo[a]pyrene	CYP2E1	caffeine
	acetylaminofluorene		chlorzoxazone
CYP1A2	caffeine		*N* nitrosodimethylamine
	ethoxyresorufin		acetaminophen
	2 acetylaminofl uorene		aflatoxin
	acetaminophen		aniline
	phenacetin	CYP2F1	naphthylamine
	aflatoxin B_1	CYP3A4	aldrin
CYP2A6	coumarin		quinidine
	N nitrosodiethylamine		cyclosporin A
CYP2B6	7 ethoxycoumarin		warfarin
CYP2C9	benzphetamine		erythromycin
	aminopyrene		17β estradiol
	tienilic acid		lidocaine
	hexobarbital		dapsone
	tolbutamide		sterigmatocystin
CYP2C19	mephenytoin		cortisol
CYP2D6	bufuralol		taxol
	debrisoquine		nifedipine
	desipramine		alfentanil
	sparteine		diltiazem
	propranolol		ethynylestradiol
	dextromethorphan	CYP4A11	arachidonic acid

the relative importance of the different enzymes depends on the genetics of the individual and on the history of exposure to environmental factors such as alcohol or drugs. Certain P450 enzymes, notably CYP2C19 and CYP2D6, are polymorphically distributed in the human population (1,4). Thus, CYP2D6 levels are low in approximately 7% of the Caucasian population, and the ability in this subgroup to metabolize substrates such as debrisoquine is partially compromised (5). CYP2C19 is in low titer in only 4% of the Caucasian population, but in 20% of the Asian population, as reflected by the relatively low ability of the latter subgroup to metabolize substrates such as mephenytoin (6). A number of criteria are required to unambiguously determine the role of a given P450 enzyme in the in vivo metabolism of a given agent. These include (*i*) demonstration that the purified enzyme has the required activity, (*ii*) correlation of the activity in question in liver samples with the activities of substrates considered to be markers for individual P450 enzymes, and (*iii*) inhibition of the activity by isoform-selective or specific inhibitors, antibodies, or, in vivo, by silent interfering RNA (*si* RNA) or gene-silencing techniques.

STRUCTURE OF THE MAMMALIAN P450 ENZYMES

Until recently, the insolubility and propensity to aggregate of the membrane-bound P450 proteins precluded the determination of their crystal structures. In contrast, the bacterial cytochrome P450 enzymes are generally soluble, and the structures of many of them have been determined. Among the earliest bacterial P450 structures to be elucidated were those of $P450_{cam}$ (CYP101) (7), $P450_{BM\text{-}3}$ (CYP102) (8), and $P450_{eryF}$ (CYP107A1) (9), and

much of our current understanding of P450 structure and mechanism stems from this early crystallographic work. The structure of the first mammalian P450, rabbit CYP2C5, was reported in 2000 (10), and since that time, the same general approach has been used to determine the structures of CYP1A2 (11), CYP2A6 (12), CYP2A13 (13), CYP2B4 (14), CYP2C8 (15), CYP2C9 (16,17), CYP2D6 (18), CYP2R (19), and CYP3A4 (20,21) in the presence and absence of diverse ligands. In terms of mechanism, these human P450 structures by and large confirm the conclusions derived from those of the bacterial P450 enzymes.

The mammalian cytochrome P450 enzymes are roughly triangular prisms in which 12 helical segments account for a large proportion of the amino acid residues (10 21). The heme prosthetic group is generally anchored by at least three interactions: (*i*) the pincer action of two helices on the heme, (*ii*) hydrogen bonds to the heme propionic acid groups, and (*iii*) coordination of a cysteine thiolate ligand to the iron. A cysteine thiolate (Cys—S–), rather than the protonated thiol (Cys—SH), is the proximal iron ligand in all active P450 enzymes. The active-site cavity is generally lined with hydrophobic residues, as might be expected of an enzyme designed for the metabolism of lipophilic substrates. A few residues on the distal (substrate binding) side of the heme are highly, but not universally, conserved throughout the P450 family. The most important of these is a catalytic threonine, Thr252 in $P450_{cam}$, which helps to stabilize the ferrous-dioxy (Fe^{II}—OO–) complex and to promote heterolysis of the dioxygen bond in the subsequent ferric peroxide (Fe^{III}—OOH) intermediate. The threonine is conserved in all the human P450 enzymes, but it is not absolutely essential because it is absent in the bacterial $P450_{eryF}$ (9). Nevertheless, it is important because its replacement by non-hydrogen-bonding residues alters catalysis. Thus, mutation of Thr252 in $P450_{cam}$ greatly increases the degree of uncoupled turnover (22,23), and mutation of the corresponding residue (Thr319) to an alanine in CYP1A2 suppresses the ability of the enzyme to oxidize benzphetamine but not 7-ethoxycoumarin (24). In $P450_{eryF}$, the hydrogen-bonding role of the threonine is satisfied by a hydroxyl group on the substrate itself (9).

Before the crystal structures of mammalian P450 enzymes were available, six domains of the primary sequences of P450 enzymes, known as sequence recognition sequences (SRS), were proposed to be particularly important in determining substrate specificity (25). These SRS were based on sequence alignments of the mammalian proteins with the sequences in the $P450_{cam}$ structure that interacted with the substrate. The recent determination of multiple mammalian P450 crystal structures now makes it possible to more reliably address the questions of substrate specificity, hydroxylation regiochemistry, and allosteric effects. This has led to extensive efforts to use computational docking of potential ligands into the P450 active sites to predict which compounds will be substrates for which enzyme (26 28), as this might provide an efficient in silico screening method for potential drug-drug interactions at an early stage in the drug discovery process. These computational efforts were previously carried out with sequence-based homology models constructed by aligning the sequences of the human enzymes with those of P450 enzymes of known structure. The crystal structures now available indicate that these models are only approximately correct and are not sufficiently reliable for the analysis of substrate specificity. As more structures have become available, it has become clear that P450 enzymes are subject to a high degree of both minor and major conformational adjustments in response to the binding of specific ligands. For example, the crystal structure of CYP2C9 with warfarin bound in the active site places the substrate more than 10 Å away from the heme iron atom, whereas the structure of this enzyme with flurbiprofen positions the substrate close to the iron atom (16,17). Substantial conformational differences are found in the two active sites. A similar

conformational mobility has been found in the bacterial enzymes. For example, the binding of imidazole and phenylimidazole to CYP119 causes a major internal rearrangement of an active-site peptide (29). The widespread observation of substrate-dependent active-site conformational adjustments seriously complicates efforts to predict substrate specificity by computational docking. Resolution of this problem will require further technological or computational advances.

As found originally for $P450_{cam}$ (7), the heme group and the substrate in P450 enzymes are buried deep within the protein. In the case of $P450_{cam}$, the camphor substrate is positioned approximately 4 Å above the heme iron atom by a hydrogen bond between the ketone oxygen and a tyrosine residue (Tyr-96) as well as by contacts with a variety of active-site residues. A weakening of the interactions that position the substrate, either by mutation of the active-site residues or alteration of the substrate itself, decreases the regiospecificity of the hydroxylation reaction and the extent to which catalytic turnover is coupled to substrate oxidation (22,23). Given its final location, the binding of a substrate requires the transient opening of a channel into the active site. A crystal structure has been obtained of the structure of unligated CYP2B4 that reveals an open state of the entrance channel (14). On complexation with 4-(4-chlorophenyl)imidazole, the protein closes by movement of a protein domain with intact secondary structure (i.e., essentially like a lid) to give a structure similar to that of the closed stage of other P450 enzymes (30). A similar change in which a large domain of the protein shifts to enable access to the heme crevice has been observed with other P450 enzymes.

SPECTROSCOPIC PROPERTIES OF CYTOCHROME P450 ENZYMES

The cytochrome P450 chromophore provides information on the nature of the iron ligands, the iron oxidation state, and the properties of the heme environment (31,32). The defining P450 spectrum is that of the ferrous-CO complex, which has an absorption maximum at 447 to 452 nm, indicative of a thiolate-ligated hemoprotein. The thiolate ligand actually gives rise to a split Soret absorption with maxima at approximately 450 and 370 nm. Denaturation of the enzyme is associated with a shift of the absorption maximum of the ferrous-CO complex to approximately 420 nm, a value similar to that for the ferrous-CO complex of imidazole-ligated proteins such as myoglobin (32). The enzyme with the 420-nm ferrous-CO absorbance maximum is inactive, and formation of this 420-nm species is one of the earliest indicators of P450 denaturation.

The absorption spectrum of ferric cytochrome P450 depends on the ligation state of the iron (31,32). The ferric low-spin state associated with the presence of two strong axial iron ligands has an absorption maximum at approximately 416 to 419 nm. The high-spin state in which one of the two coordination sites of the iron is either unoccupied or occupied by a weak ligand exhibits an absorption maximum at 390 to 416 nm. Cytochrome P450 enzymes commonly exist in an equilibrium mixture of the high- and low-spin states. In the P450 enzymes for which crystal structures are available, including the membrane-bound human enzymes, the ligand opposite to the cysteine thiolate, if one is present, is a water molecule (7 21). The binding of a noncoordinating substrate, as illustrated by the binding of camphor to cytochrome $P450_{cam}$, is accompanied by extrusion of water from the active site, loss of the distal water ligand, and a general decrease in the active-site polarity (7). The loss of the distal ligand causes a shift from the hexacoordinated to a pentacoordinated iron state, which in turn results in a shift from the low- to the high-spin state. This transition is evidenced by a shift in the absorption

maximum from 419 to 390 nm. The spectroscopic shift is usually determined from a difference spectrum in which the absorption of a solution containing everything except the compound of interest is subtracted from a similar sample that does contain the compound (31). The binding of noncoordinating substrates gives rise to what is known as a type I difference spectrum with a maximum at 385 to 390 nm and a trough at approximately 420 nm. However, if the substrate can coordinate strongly to the iron atom, a type II difference spectrum is observed with a maximum at approximately 425 to 435 nm and a trough at 390 to 405 nm. If the substrate only coordinates weakly to the iron, a variant of the type II spectrum with a maximum at 420 nm and a trough at 388 to 390 nm is obtained. This latter spectrum is known as a type III difference spectrum. Substrate and inhibitor binding to P450 enzymes can thus be monitored spectroscopically, although compounds are known that bind without significantly perturbing the spin-state equilibrium and therefore do not give rise to a difference spectrum. An example of this is the binding of 2-isopropyl-4-pentenamide to microsomes from phenobarbital pretreated rats (33), or the binding of noncoordinating ligands to CYP1A2, which unusually does not have a water molecule coordinated to the heme iron in the ligand-free state (11).

CYTOCHROME P450 REDUCTASE AND CYTOCHROME b_5

In contrast to most bacterial P450 enzymes, whose catalytic turnover is supported by electrons provided by the coordinated action of a flavoprotein and an iron-sulfur protein, the electrons required for catalytic turnover of the human xenobiotic-metabolizing cytochrome P450 enzymes are provided by reduced nicotinamide adenine dinucleotide phosphate (NADPH) cytochrome P450 reductase (Fig. 1) (34). This reductase is a 78-kDa protein that is anchored to the membrane by an N-terminal hydrophobic domain. Cytochrome P450 reductase binds one flavin mononucleotide (FMN) and one flavin dinucleotide (FAD) as prosthetic groups and is reduced by NADPH but not nicotinamide adenine dinucleotide, reduced (NADH). NADPH transfers a hydride to the FAD group, which in turn uncouples the two associated electrons and transfers them to the heme via the FMN group. The reductase can be reduced by up to four electrons, but under normal turnover conditions, it cycles between the one- and three-electron-reduced forms, both of which can transfer electrons to cytochrome P450. Limited tryptic digestion of liver microsomes releases a 72-kDa cytosolic reductase domain that binds NADPH and reduces cytochrome c but is no longer able to reduce cytochrome P450. The structure of the heterologously expressed cytochrome P450 reductase without the membrane-binding domain has been determined (35).

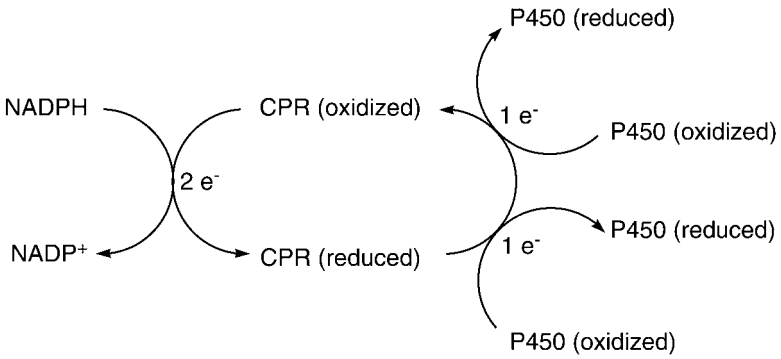

Figure 1 CPR transfers electrons from NADPH to cytochrome P450 enzymes in the mammalian endoplasmic reticulum. *Abbreviation*: CPR, cytochrome P450 reductase.

In some instances, the catalytic turnover of mammalian cytochrome P450 enzymes can be synergistically increased or modified by cytochrome b_5 (36,37). Cytochrome b_5, which can be reduced by either NADH and cytochrome b_5 reductase or NADPH-cytochrome P450 reductase, with few exceptions is able to deliver the second but not the first electron required for catalytic turnover of cytochrome P450. The synergistic effect of cytochrome b_5 is due, at least in part, to an increase in the coupling of reduced pyridine nucleotide and oxygen use to product formation (i.e., to a decrease in uncoupled reduction of oxygen to give H_2O_2 or water rather than substrate oxidation). However, in some situations, cytochrome b_5 alters P450 catalysis by allosteric mechanisms independent of its ability to donate electrons. One example of this is the demonstration that apo-cytochrome b_5 can stimulate the nifedipine oxidation and testosterone 6β-hydroxylation activities of CYP3A4 (36,38).

CATALYTIC CYCLE OF CYTOCHROME P450

The catalytic cycle of cytochrome P450 has been most thoroughly defined for the bacterial cytochrome $P450_{cam}$ (39), but the same cycle has been confirmed in its essential features for the mammalian P450 enzymes (Fig. 2). In $P450_{cam}$, the spin-state change triggered by the binding of a noncoordinating substrate alters the redox potential of the heme and makes it possible for the electron-donor partner to transfer an electron to the iron. The redox potential shift from −300 to −170 mV on binding of camphor to $P450_{cam}$ enables its reduction by the iron-sulfur protein putidaredoxin ($E_{1/2} = -196$ mV) (40). Catalytic turnover of the protein is thus initiated by substrate binding, a strategy that helps to control uncoupled turnover of the protein. Although studies of the mammalian enzymes in detergent and artificial lipid mixtures suggested that a similar spin-state-redox potential correlation did not hold in those proteins (41), a recent study using a nanodisc environment that more closely resembles the environment in normal membranes has demonstrated that a similar correlation exists for at least CYP3A4 (42).

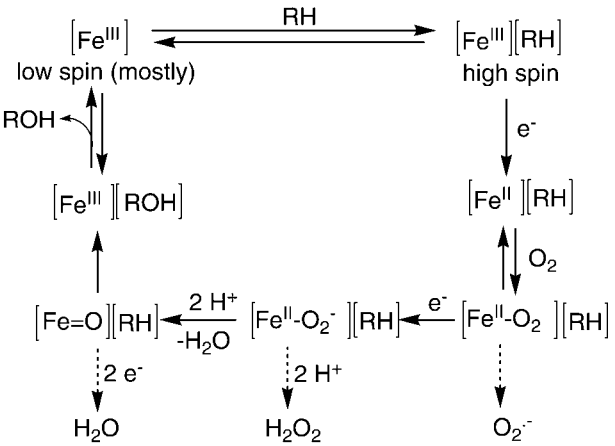

Figure 2 The cytochrome P450 catalytic cycle. The iron in brackets represents a cytochrome P450 prosthetic heme group and RH represents a substrate with an oxidizable C H bond. The first electron is provided by CPR and the second by CPR or cytochrome b_5. The sites at which the catalytic cycle can be uncoupled to produce O_2^-, H_2O_2, or H_2O rather than oxidized substrate (ROH) are indicated. *Abbreviation*: CPR, cytochrome P450 reductase.

Reduction of iron is followed by binding of oxygen to give the ferrous-dioxy P450 complex, an intermediate that is unstable but has been observed under a variety of conditions. A further one-electron reduction of the ferrous-dioxy complex produces the highly unstable ferric hydroperoxide complex that has only been observed in cryogenic studies with $P450_{cam}$ (43). The formation of this intermediate is consistent with the finding that one of the products of uncoupled turnover of P450 is H_2O_2. It is also consistent with the fact that catalytic turnover of many P450 enzymes can be supported to some extent by exogenous H_2O_2 in the absence of cytochrome P450 reductase and NADPH. Heterolytic cleavage of the dioxygen bond in the ferric hydroperoxide complex concomitant with the uptake of two protons and the loss of a molecule of water produces the ferryl intermediate that is thought to be the species that oxidizes most substrates (39,44). The ferryl, two oxidation states above the ferric state, is formally an $Fe^{V}=O$, but it is more appropriately represented by an $Fe^{IV}=O$ coupled to a porphyrin radical cation. The ferryl species is the most transient of the catalytic intermediates, and even now, it is unclear whether it has been directly observed (43). In most, but not all, instances, the ferryl oxygen is transferred to the substrate to give an oxygenated metabolite. If the substrate is resistant to oxidation, the ferryl species can be reduced to a water molecule by further electrons from cytochrome P450 reductase or cytochrome b_5. To the extent that superoxide, H_2O_2 and water are produced at the expense of substrate oxidation during the catalytic turnover of cytochrome P450, the reaction is said to be uncoupled.

The possibility that substrate oxidation is mediated by intermediates in oxygen activation prior to the ferryl species is currently under discussion. It is generally accepted that the ferric peroxy anion (Fe^{III}—OO–) can add as a nucleophile to aldehydes (and perhaps other highly electrophilic groups), resulting after homolytic cleavage of the dioxygen bond in carbon-carbon bond cleavage and loss of the aldehyde carbon atom (44). This reaction underlies the action of the biosynthetic P450 enzymes that catalyze lanosterol 14-demethylation (CYP51), removal of the progesterone side chain to produce androstenedione (CYP17), and the 19-demethylation and aromatization of testosterone that yields estradiol (CYP19). However, more controversial is the proposal that the ferric hydroperoxide intermediate (Fe^{III}—OOH) can insert into CH bonds. At this time, there is no compelling evidence for this type of reactivity in normal P450 turnover, although there is evidence that active-site mutations can alter the reactivity of the oxidizing species (45). If the ferric hydroperoxide plays any role in normal catalysis, it is likely to be in the oxidation of readily oxidized sulfur or nitrogen functionalities.

CYTOCHROME P450–CATALYZED REACTIONS

Cytochrome P450 catalyzed reactions produce a diversity of metabolites, many of which are formed by secondary, nonenzymatic decomposition of the initial products formed by the P450 reaction. Although the already large list of reactions catalyzed by P450 continues to expand, most of the reactions involve (*i*) insertion of an oxygen atom into the bond between a hydrogen and a carbon or other heavy atom (hydroxylation), (*ii*) addition of an oxygen atom to a π-bond (epoxidation), or (*iii*) addition of an oxygen atom to the electron pair on a heteroatom (heteroatom oxidation) (44). All three of these reactions are illustrated in the metabolism of strychnine (Fig. 3) (46). Cytochrome P450 enzymes also catalyze reductive reactions under conditions of low oxygen tension. The oxidative catalytic process can be viewed as consisting of two stages: activation of molecular oxygen to the reactive (ferryl) oxidizing species followed by its reaction with the substrate. The cytochrome P450 catalytic machinery is primarily required for the first

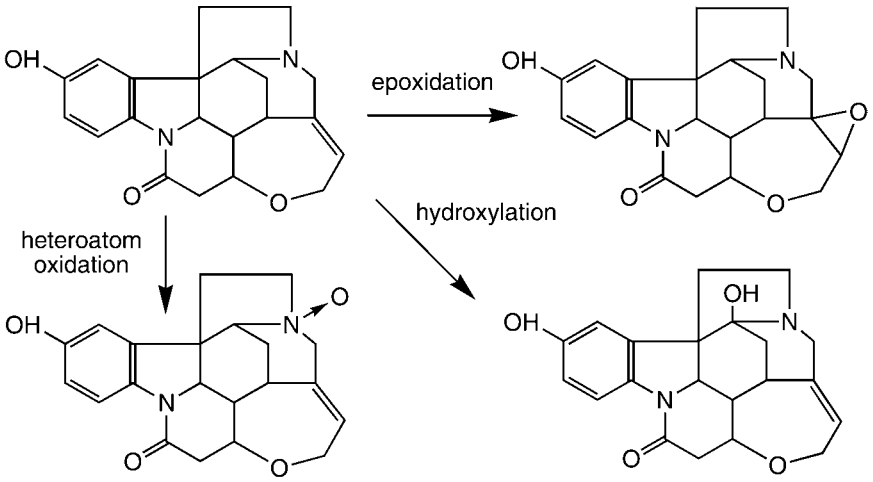

Figure 3 Hydroxylation, π bond oxidation, and heteroatom oxidation, the three fundamental cytochrome P450 catalyzed reactions, are illustrated in the metabolism of strychnine (46).

phase of this two-stage process. In contrast, the enzyme appears to contribute little to the reaction of the activated oxygen with the substrate beyond providing an appropriate environment for the reaction and, by only binding the substrate in certain orientations, limiting the sites on the substrate exposed to the activated oxygen. The outcome of the catalytic process is therefore largely determined by the relative reactivities of the functionalities on the substrate that are accessible to the activated oxygen in the enzyme-substrate complex.

HYDROXYLATION

Carbon Hydroxylation

The regio- and stereoselective hydroxylation of unactivated hydrocarbon functionalities is one of the most common but most difficult reactions catalyzed by cytochrome P450. Isotope effects provide direct evidence that the reaction outcome depends on the reactivity of the accessible C—H bonds. Thus, hydroxylation of the undeuterated carbon is strongly favored in the oxidation of [1,1-$^2H_2$]-1,3-diphenylpropane (i.e., $C_6H_5CH_2CD_2C_6H_5$), a symmetric molecule in which the hydrogens are replaced by deuteriums on one of the two, otherwise identical, methylene groups. A large isotope effect ($k_H/k_D = 11$) is observed in the intramolecular preference for hydroxylation of the undeuterated methylene, even though only a small kinetic isotope effect is observed on the net rate of hydroxylated product formation (47). The large intramolecular isotope effect indicates that the enzyme is sensitive to the differential energies required to break C—H and C—D bonds and is able to choose between the competing sites. Only a relatively small kinetic isotope effect is usually observed on the actual rate of product formation because the rate is determined by steps other than insertion of the oxygen into the C—H bond (48).

The relationship between bond strength and susceptibility to oxidation is confirmed by the finding that the P450-catalyzed insertion of an oxygen into hydrocarbon C—H bonds decreases in the order of tertiary > secondary > primary (49), a preference confirmed by computational studies (28,50). The intrinsic higher reactivity of weaker C—H bonds is often masked by steric effects or by the protein-imposed orientation of the substrate with respect to

Table 3 Bond Strengths of Selected C H Bonds

Bond	kcal/mol	Bond	kcal/mol
CH_3 H	104	$HC{=}CCH_2$ H	88
Me_2CH H	95	$HOCH_2$ H	94
Me_3C H	92	H_2NCH_2 H	89
$CH_2{=}CH_2CH_2$ H	89	$CH_2{=}CH$ H	108
$C_6H_5CH_2$ H	85		

the activated ferryl species. If these factors are minimized, however, the intrinsic reactivity of the C—H bonds becomes evident, as illustrated by the hydroxylation of small hydrocarbons whose movement within the P450 active site is less restricted. Thus, the microsomal oxidation of *tert*-butane [$CH(CH_3)_3$] yields 95% *tert*-butanol [$HOC(CH_3)_3$] and only 5% 2-methylpropanol [$CH_3CH(CH_3)CH_2OH$] (49). The sterically hindered but weaker tertiary C—H bond is oxidized in preference to the nine relatively unhindered but primary C—H bonds. The bond strengths of C—H bonds (Table 3) provide a good first approximation of the intrinsic reactivity of a C—H bond in a substrate molecule.

The relationship of bond strength to enzymatic hydroxylation indicates that reactivity is related to the homolytic C—H bond scission energy, an inference consistent with a nonconcerted "oxygen-rebound" mechanism in which hydrogen abstraction by the activated oxygen is followed by recombination of the resulting radical species to give the hydroxylated product (44):

$$[Fe^{V}{=}O] + R_3C{-}H \rightarrow [Fe^{IV}{-}OH] + R_3C\cdot \rightarrow [Fe^{III}] + R_3C{-}OH$$

As already noted, the $Fe^{V}{=}O$ in the above reaction sequence is likely to be an $Fe^{IV}{=}O$ coupled to a porphyrin radical cation. If a substrate radical is formed as a transient species, it should be possible to detect it in substrates in which the radical can undergo a sufficiently rapid rearrangement prior to recombination to give the hydroxylated product. Indeed, the hydroxylation of *exo*-tetradeuterated norbornane yields, among other products, the *endo*-deuterated alcohol metabolite (51). This inversion of the deuterium stereochemistry requires the formation of either a radical or cationic intermediate in which the geometry of the tetrahedral carbon can be inverted. Numerous other examples are known of reactions that proceed with loss of stereo- or regiochemistry, including the allylic rearrangement that accompanies the P450-catalyzed hydroxylation of taxa-4(5),11(12)-diene during the biosynthesis of taxol (Fig. 4) (52).

Another approach to demonstrating the intervention of a substrate radical is to incorporate a radical clock into the substrate. A radical clock is a structure, commonly a cyclopropyl methylene group, for which the radical rearranges at a known rate. The use of this approach has led to controversial results, initially confirming the role of a substrate radical in catalysis (53) but subsequently suggesting that the radical would be too short

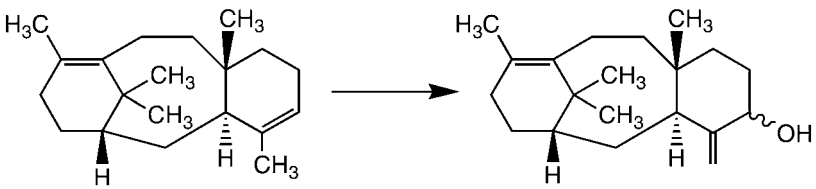

Figure 4 Rearrangement of the double bond accompanying the cytochrome P450 catalyzed oxidation of an intermediate in the biosynthesis of taxol (52).

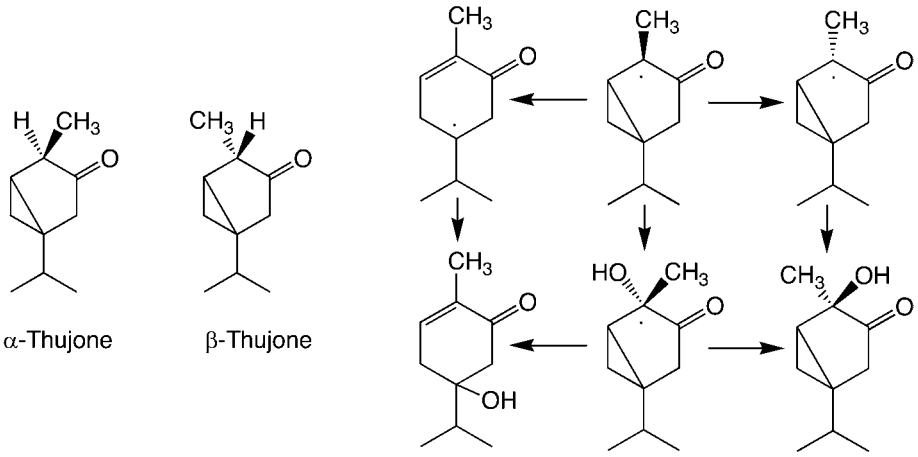

Figure 5 P450 oxidation of the radical clock substrates α and β thujone produces a C4 radical in which the methyl substituted ring carbon can undergo both stereochemical inversion and cyclopropyl ring opening, two independent indicators of a radical intermediate (55).

lived and might be closer to a transition state (54). More recent results appear to confirm the radical nature of the reaction. Thus, β-thujone, a two-zone clock in that the radical can be revealed by both a methyl group inversion and opening of the cyclopropyl ring (Fig. 5), supports the proposal that a radical rather than cation intermediate is involved in the reaction (55). Computational results suggest that the discrepancies in the clock reactions may be related to the existence of the ferryl species in multiple-spin states (50).

The cytochrome P450-catalyzed hydroxylation of hydrocarbon chains commonly occurs at the terminal (ω) carbon or at the carbon adjacent to it (ω−1), although the hydroxylation can occur at internal sites in the hydrocarbon chain. ω-Hydroxylation is disfavored with respect to ω-1 hydroxylation by the higher strength of a primary than a secondary C—H bond. Except for the CYP4 family of enzymes, which are specifically designed as fatty acid ω-hydroxylases, P450 enzymes preferentially catalyze ω-1 hydroxylation of hydrocarbon chains. Of course, this reaction must compete with other favored reactions, such as allylic or benzylic hydroxylation. The hydroxylation of C—H bonds that are stronger than those of a terminal methyl group is essentially not observed. Thus, the direct oxidation of vinylic, acetylenic, or aromatic C—H bond is negligible, although the π-bonds themselves are readily oxidized (see the section "Carbon Hydroxylation Followed by Heteroatom Elimination").

Carbon Hydroxylation Followed by Heteroatom Elimination

Hydroxylation adjacent to a heteroatom or a π-bond is highly favored by the weaker bond strength of C—H bonds adjacent to conjugating functionalities. In the case of sulfur, and particularly nitrogen, the availability of alternative mechanisms that lead to the same reaction outcome also enhances the reactivity at those positions. Allylic or benzylic hydroxylation normally produces a stable alcohol product, but the product of hydroxylation adjacent to a heteroatom readily eliminates the heteroatom to give two fragments, one containing a carbonyl group, and the other retaining the heteroatom (Fig. 6). Thus, oxidation adjacent to an oxygen normally results in O-dealkylation, adjacent to a nitrogen in N-dealkylation, adjacent to a sulfur in S-dealkylation, and adjacent to a halogen in oxidative dehalogenation (Fig. 7).

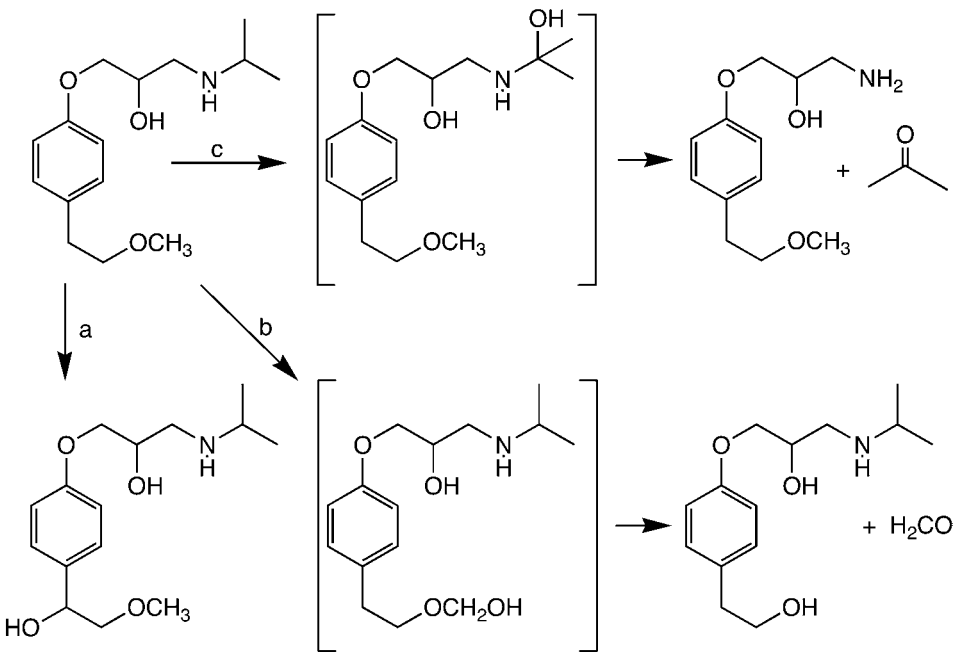

Figure 6 The oxidations of metoprolol illustrate (**a**) benzylic hydroxylation, (**b**) hydroxylation adjacent to an oxygen followed by elimination (O dealkylation), and (**c**) hydroxylation adjacent to a nitrogen followed by elimination (N dealkylation).

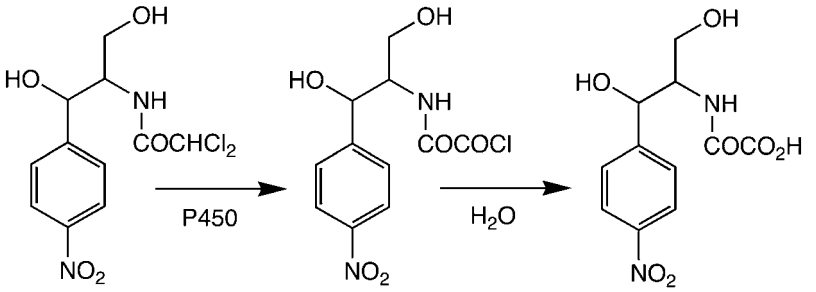

Figure 7 Hydroxylation adjacent to a halogen followed by elimination (oxidative dehalogenation), as illustrated by the oxidation of chloramphenicol. The acyl chloride produced from the dihalogenated carbon by the P450 reaction can react with water, as shown, or with other cellular nucleophiles.

Heteroatom Hydroxylation

The mechanism of cytochrome P450-catalyzed amine hydroxylation is ambiguous because the reaction can proceed via insertion of an oxygen into the N—H bond or oxidation of the nitrogen to a nitroxide, followed by proton tautomerization to give the hydroxylamine. A similar ambiguity exists in the hydroxylation of sulfhydryl groups. N-hydroxylation via insertion into the N—H bond, as illustrated by the hydroxylation of *p*-chloroacetanilide, is favored in situations where the nitrogen electron pair is highly delocalized and therefore reacts poorly as an electron donor (Fig. 8) (56).

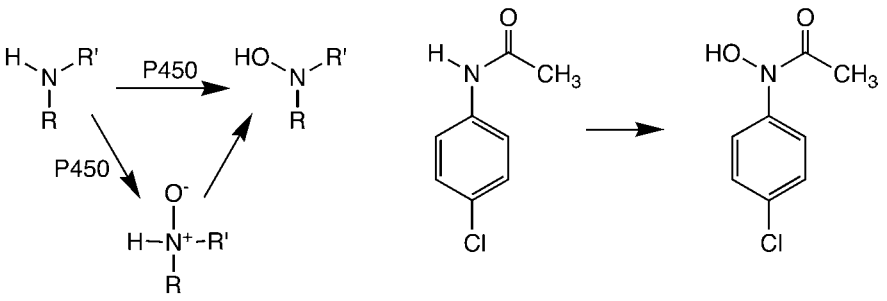

Figure 8 The "hydroxylation" of a nitrogen bearing a hydrogen atom can involve direct insertion into the N H bond or transfer of the oxygen to the nitrogen followed by proton tautomerization. Insertion into the N H bond is favored in amides. The hydroxylation of *p* chloroacetanilide is shown as an example.

π-Bond Oxidation

Oxidation of Aliphatic π-Bonds

Cytochrome P450 enzymes normally oxidize double bonds to the corresponding epoxides (Fig. 9). Retention of the olefin stereochemistry, as well illustrated by the oxidation of *cis*-1-deuterated styrene without loss of stereochemistry (57), suggests that the two carbon-oxygen bonds of the epoxide are formed without traversing an intermediate that allows rotation about the carbon-carbon bond. This strongly implies that both bonds are formed at the same time, if not necessarily at the same rate. In general, the epoxidation of electron-rich double bonds is favored over that of electron-deficient double bonds because the ferryl species are electron deficient. Carbonyl products formed by migration of a hydrogen or halide from the carbon to which the oxygen is added to the adjacent carbon of the double bond are occasionally obtained as minor metabolites. An example of this is the formation of trichloroacetaldehyde (CCl_3CHO) from 1,1,2-trichloroethylene ($CHCl{=}CCl_2$) (59). The 1,2-migration of a hydrogen or halide indicates that a positive charge develops at the carbon toward which the migration occurs. Carbonyl products thus appear to result from π-bond oxidations in which the two carbon-oxygen bonds are not simultaneously formed. Although this is a negligible reaction pathway for most olefinic substrates, it is an important reaction when the π-bond is part of an aromatic ring (see the section "Oxidation of Aromatic Rings"). Formation of epoxides by concerted oxygen insertion but carbonyl products by non-concerted oxygen transfer implies either that there are two independent reaction pathways or a single reaction manifold with a branch point leading to concerted (epoxide) versus non-concerted (carbonyl) products. Computational studies support the existence of a single pathway with a branchpoint determined by the spin state of the reactive species (50).

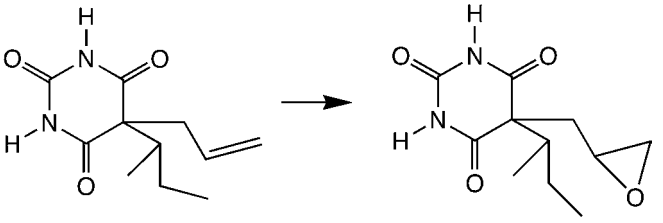

Figure 9 The cytochrome P450 catalyzed epoxidation of secobarbital (58).

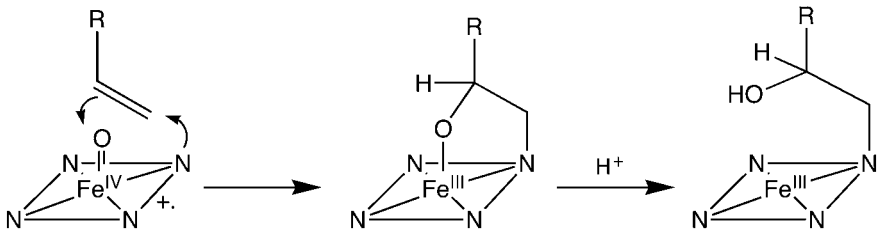

Figure 10 N alkylation of the cytochrome P450 prosthetic heme group during terminal olefin oxidation. The P450 heme is represented by the square of nitrogen atoms surrounding an iron atom. The heme is shown in the proposed hypervalent activated state.

The oxidation of terminal, unconjugated olefins often results not only in olefin epoxidation but also in inactivation of the cytochrome P450 enzyme (60,61). In some instances, inactivation results from reaction of the epoxide metabolite with the protein, but in others, inactivation involves alkylation of a pyrrole nitrogen of the prosthetic heme group by a catalytically activated form of the olefin (Fig. 10). Characterization of the heme adducts shows that alkylation is initiated by oxygen transfer from the enzyme to the double bond but is not due to reaction with the actual epoxide metabolite. Heme alkylation thus involves an asymmetric, non-concerted olefin oxidation pathway that may be part of the same manifold of reactions that produces the epoxide and carbonyl metabolites. In these heme alkylation reactions, the oxygen is added to the internal carbon of the double bond and the terminal carbon to the pyrrole nitrogen atom. Terminal acetylenes can participate in an analogous reaction in which ferryl oxygen transfer to the terminal carbon of the triple bond produces a ketene, whereas addition of the oxygen to the internal carbon leads to alkylation of a nitrogen of the heme group (61).

The reaction manifold that leads to the formation of epoxides, carbonyl products, and heme alkylation has not been definitively elucidated. It is likely that an initial complex involving some degree of charge transfer between the ferryl oxygen and the π-bond decomposes by (*i*) what appears to be a concerted pathway leading to epoxide formation, (*ii*) a free radical pathway that can lead to heme alkylation, and (*iii*) a cationic pathway that leads to the observed 1,2-shifts of the olefin substituents (Fig. 11). The computational studies suggest that the initial complex exists in indifferent spin states, and that these states determine which pathway is followed in the reaction (50).

Oxidation of Aromatic Rings

The cytochrome P450-catalyzed processing of aromatic systems is a special case of π-bond oxidation. In its simplest form, the oxidation is analogous to the oxidation of an isolated double bond and gives the same product, i.e., the epoxide. However, the epoxides derived from aromatic systems are unstable and readily rearrange to give phenols. The steps in this reaction are (*i*) heterolytic scission of one of the strained epoxide carbon-oxygen bonds, (*ii*) migration of the hydrogen (or rarely some other substituent) on the carbon that retains the epoxide oxygen to the adjacent carbocation to give a ketone, and (*iii*) proton tautomerization to rearomatize the structure, giving the phenol metabolite (Fig. 12). The net result is oxidation of an aromatic ring via an epoxide to the hydroxylated product that would formally result from insertion of oxygen into one of the aromatic C-H bonds. This aromatic "hydroxylation" mechanism is known as the NIH shift because it was discovered at that institution (62). The National Institutes of Health (NIH) shift of an epoxide can yield two different phenolic products, depending on

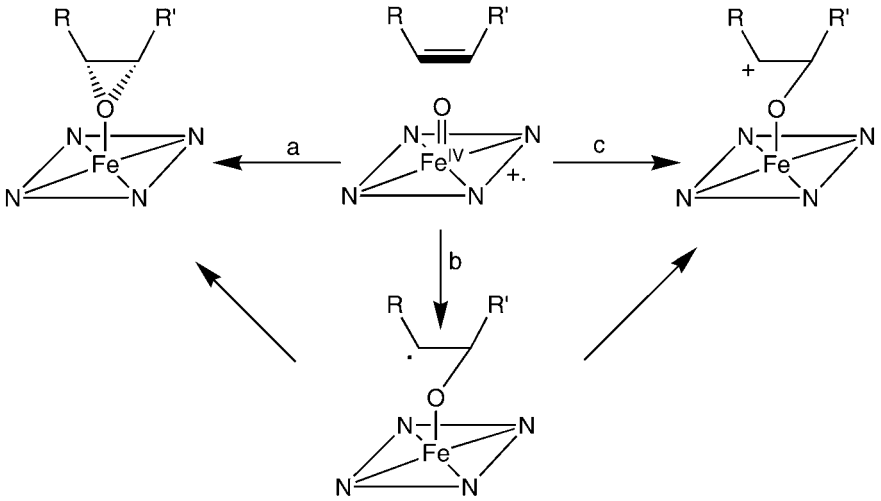

Figure 11 Reaction manifold in the cytochrome P450 catalyzed oxidation of olefins. Formation of a charge transfer complex may be followed by (**a**) apparently concerted epoxide formation, (**b**) nonconcerted oxygen transfer to give a radical, or (**c**) nonconcerted oxygen transfer to give a cation. The radical intermediate could give rise to both the epoxide and cation metabolites, but the retention of stereochemistry indicates it would have to be a very short lived radical.

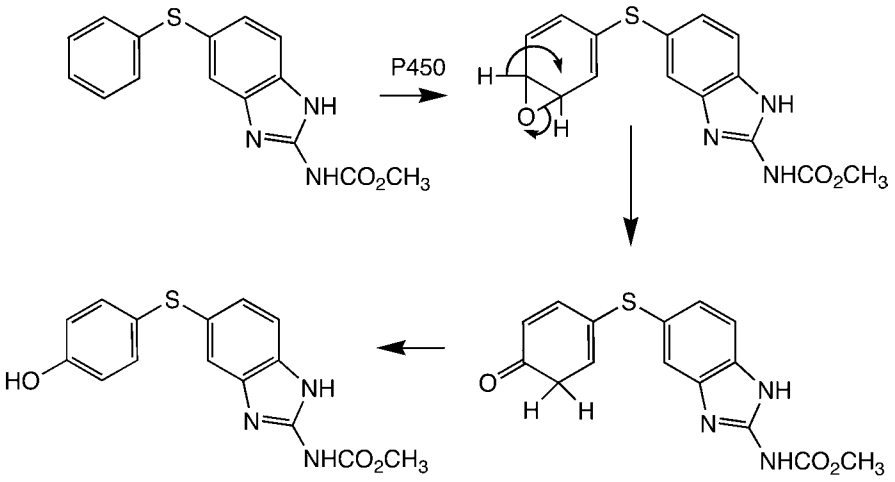

Figure 12 Cytochrome P450 catalyzed oxidation of fenbendazole illustrating the NIH shift mechanism for aromatic "hydroxylation" (63).

which of the two epoxide carbon-oxygen bonds is broken. If the cation formed by breaking one of the bonds is significantly more stable than that obtained by breaking the other, the phenol produced by the lower energy pathway predominates. Substitution of an electron-donating group (e.g., alkoxy) promotes formation of the *ortho*- or *para*-hydroxy metabolite, whereas a strong electron-withdrawing substituent (e.g., nitro) favors formation of the *meta*-hydroxy metabolite.

Aromatic π-bond oxidation is subject to mechanistic ambiguities comparable to those for the oxidation of simple olefins. Although the epoxides of some aromatic

substrates have been isolated and shown to undergo the NIH shift, in some instances, the epoxide is not a true intermediate in the reaction trajectory that produces the NIH shift. Asymmetric transfer of the ferryl oxygen to the aromatic π-bond may directly give a cation similar to that expected from cleavage of one of the epoxide carbon-oxygen bonds. This intermediate then flows directly into the NIH shift (Fig. 13). The reaction manifold can be diverted toward other reaction outcomes. An example of this is the oxidation of pentafluorophenol to 2,3,5,6-tetrafluoroquinone (64). It appears that one-electron abstraction from the polyfluorinated phenol produces a phenoxy radical that combines with the ferryl oxygen at the carbon *para* to the oxygen. The resulting *para*-hydroxylated intermediate eliminates fluoride to give the quinone (Fig. 14). As always, the reaction with the lowest energy barrier predominates!

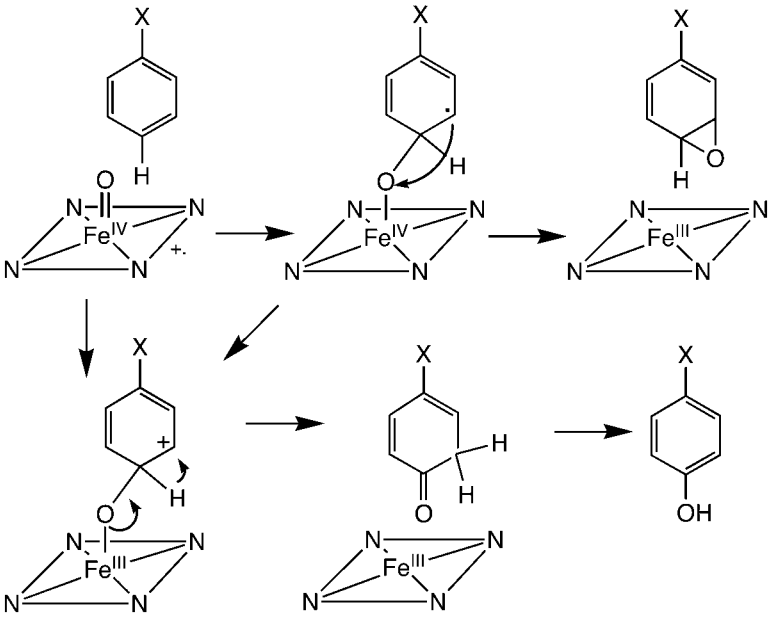

Figure 13 Hydroxylation of aromatic rings may occur without the formation of an epoxide intermediate. The putative cytochrome P450 heme reactive species is abbreviated as before.

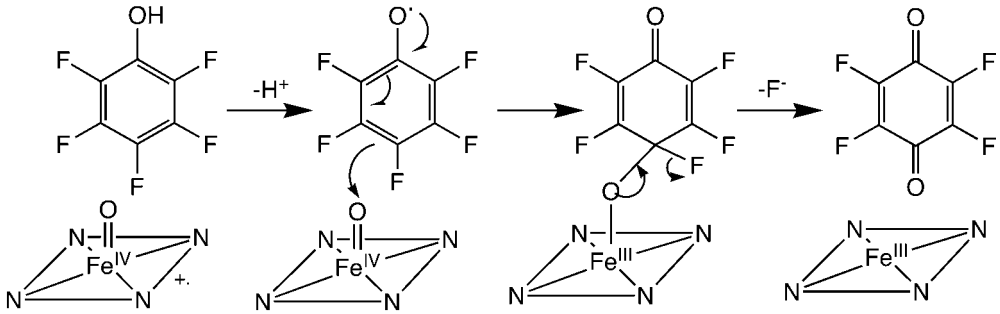

Figure 14 Proposed mechanism for the oxidation of pentafluorophenol resulting in fluoride elimination to give tetrafluoro *p* quinone without the formation of an epoxide intermediate.

HETEROATOM OXIDATION

The cytochrome P450 ferryl species is electron deficient and therefore has a propensity to react with the electron pairs on nitrogen and sulfur atoms. A similar reaction is not observed with oxygen electron pairs because of the much higher electronegativity of this atom. Halogen atoms, like oxygen, are highly electronegative and difficult to oxidize, but their oxidation can occur in special circumstances. A recent example is the oxidation of the chloride atom in 12-chlorododecanoic acid by CYP4A1, an enzyme that specifically oxidizes the terminal atom of a chain (65).

Nitrogen Oxidation

Tertiary amines can be oxidized to the corresponding *N*-oxides by both the cytochrome P450 enzymes and the flavin monooxygenases (Fig. 15). In general, but not always (66), cytochrome P450 enzymes preferentially catalyze the N-dealkylation of alkyl amines rather than the formation of an *N*-oxide. The flavin monooxygenases can only form the *N*-oxide. It is not possible to attribute the formation of an *N*-oxide to either the P450 or flavoprotein monooxygenase system without evidence that specifically implicates one or the other of these two enzyme systems.

The dealkylation of alkyl amines, ethers, thioethers, and other alkyl-substituted heteroatoms is catalyzed by cytochrome P450 but not by the flavin monooxygenase. As already described, this reaction can be viewed as proceeding via introduction of a hydroxyl group adjacent to the heteroatom followed by intramolecular elimination of the heteroatom (Fig. 6). The final products are therefore an aldehyde or ketone and a heteroatom-containing substrate fragment. This conventional carbon hydroxylation mechanism operates in the case of ethers and halides. However, the lower electronegativity of nitrogen makes possible an alternative mechanism triggered by initial electron abstraction from the nitrogen atom by the ferryl species (Fig. 15). Subsequent removal of a proton from the adjacent carbon by the partially reduced ferryl species, followed by recombination of the iron-bound hydroxyl group with the resulting radical, completes an indirect route to hydroxylation of the carbon adjacent to the nitrogen. Evidence is available for both reaction pathways, and the pathway may be substrate dependent (44,67).

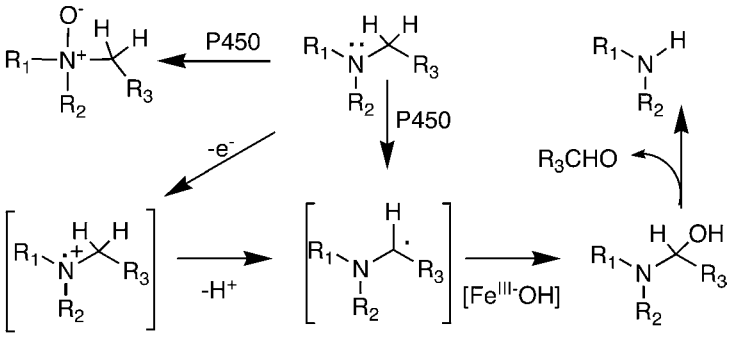

Figure 15 Cytochrome P450 can either oxidize a trisubstituted nitrogen to an *N* oxide or introduce a hydroxyl adjacent to the nitrogen. The latter reaction can involve insertion of the oxygen into the adjacent C H bond or a reaction initiated by abstraction of an electron from the nitrogen followed by loss of a proton. [Fe^{III} OH] represents the heme of P450 with a hydroxyl group on the ferric iron.

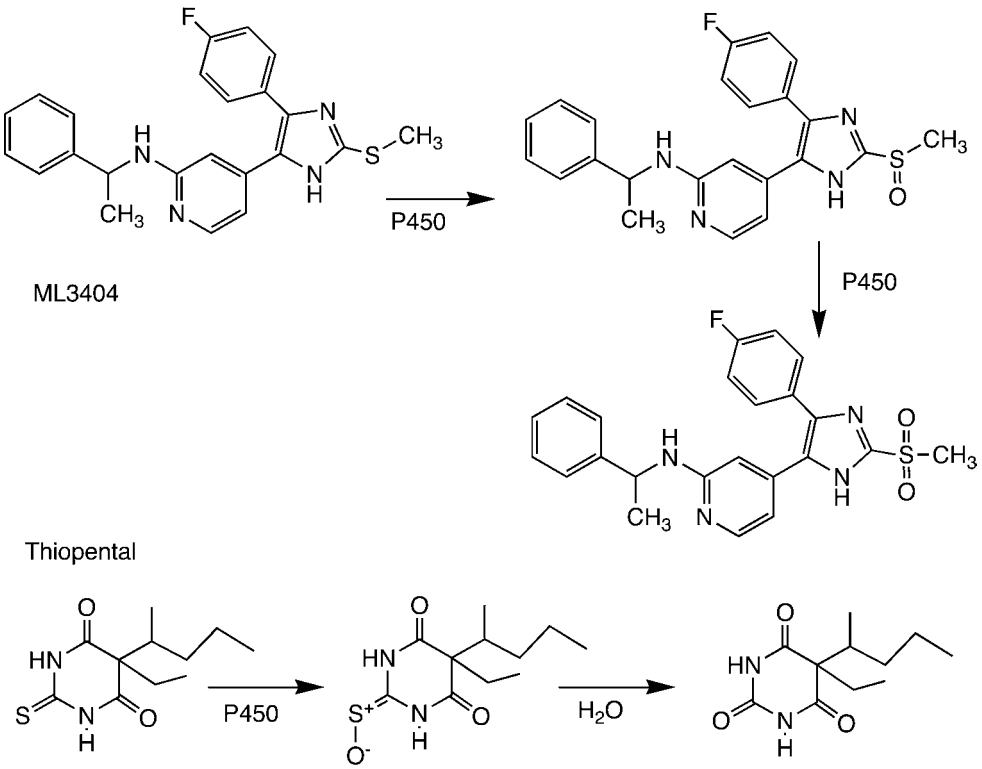

Figure 16 The P450 catalyzed oxidation of thioethers and thiocarbonyl groups as illustrated by the oxidations of ML3404 and thiopental (68).

Sulfur Oxidation

The oxidation of thioethers to sulfoxides and the dealkylation of alkyl thioethers are subject to the same considerations as the metabolism of alkylamines. Sulfoxidation, as illustrated by the oxidation of ML3403 (Fig. 16) (68), can be catalyzed by both the P450 enzymes and flavin monooxygenases. A thioether can be oxidized twice, first to the sulfoxide and then to the sulfone. The second oxidation is more difficult as the sulfur is more electron deficient after the first oxidation. S-dealkylation, like N- and O-dealkylations (Fig. 6), is really a carbon hydroxylation reaction mediated by cytochrome P450 in which hydroxylation on the carbon adjacent to the sulfur is followed by extrusion of the heteroatom.

The P450-catalyzed oxidation of thiocarbonyl groups, as represented by the oxidation of thiopental (Fig. 16), is unusual in that it leads to elimination of the sulfur to yield a simple carbonyl moiety. Transfer of the ferryl oxygen to the sulfur of the thiocarbonyl group produces an unsaturated sulfoxide that decomposes to the carbonyl product. The sulfur is eliminated, probably as HSOH, via a hydrolytic mechanism that may be assisted by glutathione (69).

UNUSUAL OXIDATIVE REACTIONS

The range of reactions catalyzed by cytochrome P450 continues to grow, although some of the more novel reactions only occur in low yields or in special circumstances. One of these P450-catalyzed reactions is the desaturation of hydrocarbon functionalities. The

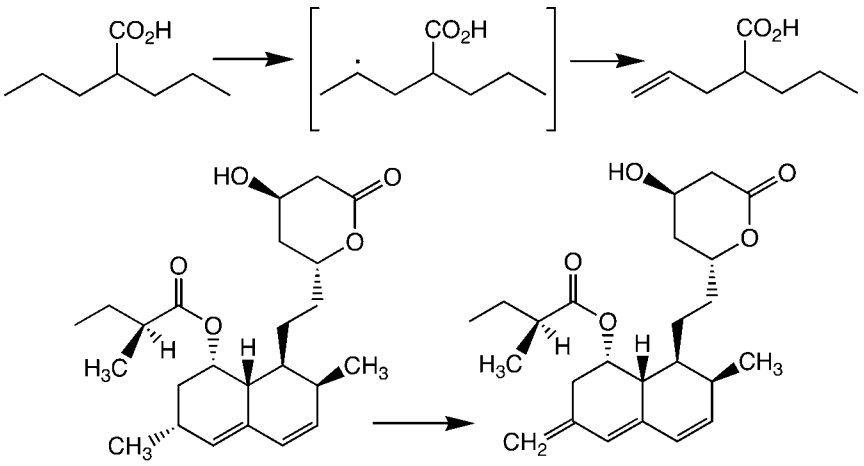

Figure 17 Cytochrome P450 catalyzed desaturation of valproic acid (*above*) and lovostatin (*below*). Isotope effects suggest that a radical intermediate, as shown for valproic acid, is involved in the reaction.

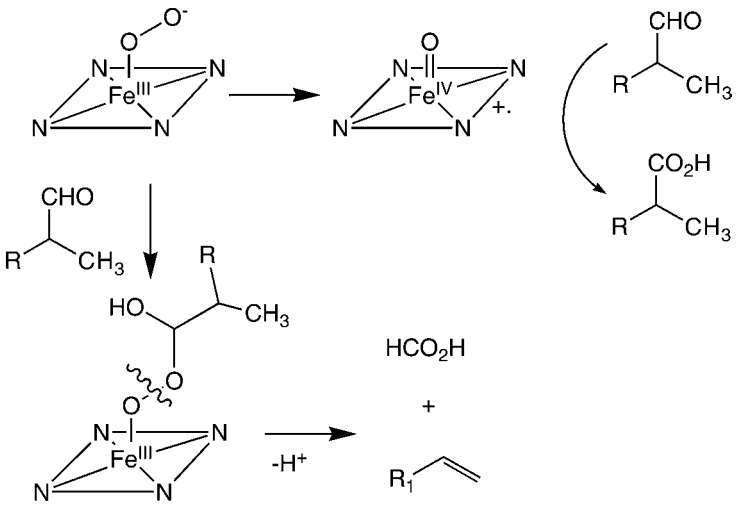

Figure 18 Aldehydes are generally oxidized by cytochrome P450 to the corresponding acids, but in some instances, reaction of the aldehyde with the [Fe^{III} OO] intermediate results in loss of the aldehyde group as formic acid and formation of an unsaturated hydrocarbon.

most extensively characterized of these reactions is the desaturation of valproic acid to give the terminal olefin (Fig. 17) (70). Isotope effect studies indicate that this reaction is initiated by hydrogen abstraction from the ω-1 position. This abstraction is followed either by recombination to give the 4-hydroxy metabolite or, alternatively, by a second hydrogen atom abstraction from the terminal carbon to give the olefin. Other examples of desaturation reactions catalyzed by mammalian cytochrome P450 enzymes are the $\Delta^{6,7}$-desaturation of testosterone (71) and the desaturation of lovastatin (72).

The reaction of aldehydes with cytochrome P450 can follow one of two divergent pathways (Fig. 18). The more common reaction is oxidation of the aldehyde to give a carboxylic acid, as illustrated by the metabolism of losartan (73), but the other is a process

that results in elimination of the aldehyde group as formic acid (74). The carbon-carbon bond cleavage reaction finds strong precedent in the reactions catalyzed by the biosynthetic P450 enzymes lanosterol demethylase, aromatase, and sterol $C^{17,20}$-lyase. Cleavage of a carbon-carbon bond in the reaction catalyzed by each of these three enzymes appears to involve the reaction of a substrate carbonyl group with the ferrous-dioxy species of cytochrome P450 (75). A similar mechanism is proposed for the reactions of simple aldehydes with hepatic P450 enzymes, with the difference that the carbon-carbon bond cleavage process is the major or exclusive reaction in the biosynthetic enzymes but is often a minor reaction in the metabolism of xenobiotic aldehydes.

REDUCTIVE REACTIONS

In addition to oxidative reactions, cytochrome P450 is known to catalyze reductive reactions (76). These reductive reactions are particularly relevant under anaerobic conditions but, under some aerobic conditions, can compete with oxidative reactions. A major reductive reaction catalyzed by cytochrome P450 is the dehalogenation of alkyl halides. Cytochrome P450 and sometimes cytochrome P450 reductase by itself are also involved in reactions such as the reduction of azo and nitro compounds. Two examples of these reactions are the bioactivation of the anticancer prodrug AQ4N to the topoisomerase II inhibitor AQ4 by cytochrome P450 (77) and the bioactivation of the anticancer drug tirapazamine by electron transfer from cytochrome P450 reductase (78) (Fig. 19). The important catalytic species in the P450-dependent reaction is presumably the ferrous-deoxy intermediate in which the reduced iron has an open coordination position. Reductive reactions thus compete with the binding and activation of oxygen, a fact that explains the oxygen sensitivity of the pathway.

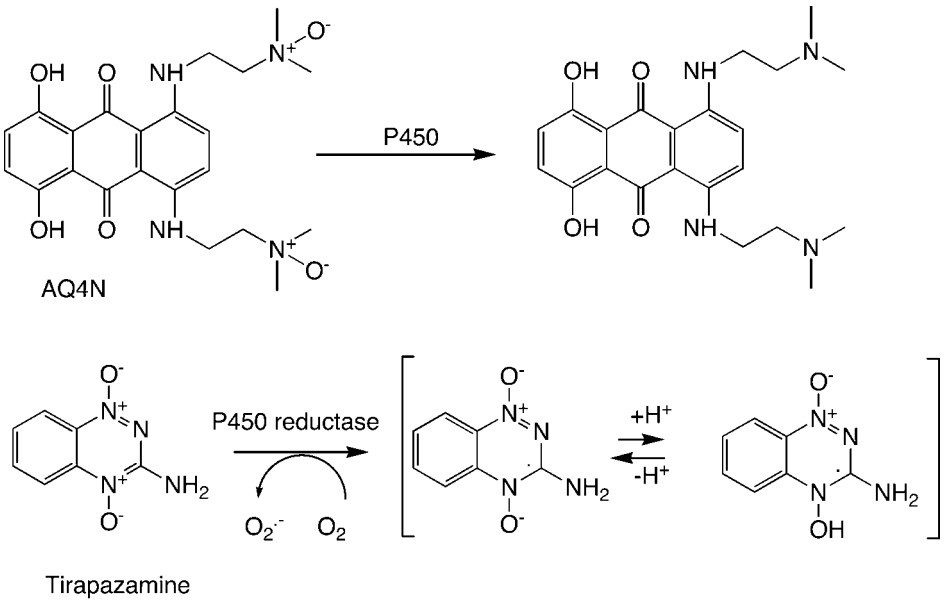

Figure 19 Reductive activation of the anticancer agents AQ4N and tirapazamine, the former by cytochrome P450 and the latter primarily by electron transfer from CPR. *Abbreviation*: CPR, cytochrome P450 reductase.

REFERENCES

1. Guengerich FP. Human cytochrome P450 enzymes. In: Ortiz de Montellano PR, ed. Cytochrome P450: Structure, Mechanism, and Biochemistry. 3rd ed. New York: Kluwer/ Plenum, 2005:377 530.
2. Nelson, D, Koymans L, Kamataki T, Stegeman JJ, Feyereisen R, Waxman DJ, Waterman MR, Gotoh O, Coon MJ, Estabrook RW, Gunsalus IC, Nebert DW. P450 superfamily: update on new sequences, gene mapping, accession numbers and nomenclature. Pharmacogenetics 1996; 6: 1 42.
3. Shimada T, Yamazaki H, Mimura M, Inui Y, Guengerich FP. Interindividual variations in human liver cytochrome P450 enzymes involved in the oxidation of drugs, carcinogens, and toxic chemicals: studies with liver microsomes of 30 Japanese and 30 Caucasians. J Pharmacol Exp Ther 1994; 270:414 423.
4. Evans WE, Relling MV. Pharmacogenomics: translating function genomics into rational therapeutics. Science 1999; 286:487 491.
5. Nakamura K, Goto F, Ray WA, McAllister CB, Jacqz E., Wilkinson GR, Branch RA. Interethnic differences in genetic polymorphism of debrisoquine and mephenytoin hydrox ylation between Japanese and Caucasian populations. Clin Pharmacol Ther 1987; 38:402 408.
6. Kalow W. Genetics of drug transformation. Clin Biochem 1986; 19:76 82.
7. Poulos TL, Finzel BC, Howard AJ. High resolution crystal structure of cytochrome $P450_{cam}$. J Mol Biol 1987; 195:687 700.
8. Ravichandran KG, Boddupalli SS, Hasemann CA, Peterson JA, Deisenhofer, J. Crystal structure of hemoprotein domain of P450BM 3, a prototype for microsomal P450s. Science 1993; 261:731 736.
9. Cupp Vickery JR, Poulos TL. Structure of cytochrome P450eryF involved in erythromycin biosynthesis. Struct Biol 1995; 2:144 153.
10. Williams PA, Cosme J, Sridhar V, Johnson EF, McRee DE. Mammalian microsomal cytochrome P450 monooxygenase: structural adaptations for membrane binding and functional diversity. Mol Cell 2000; 5:121 131.
11. Sansen S, Yano JK, Reynald RL, Schoch GA, Griffin KJ, Stout CD, Johnson EF. Adaptations for the oxidation of polycyclic aromatic hydrocarbons exhibited by the structure of human P450 1A2. J Biol Chem 2007; 282:14348 14355.
12. Yano JK, Hsu M, Griffin KJ, Stout CD, Johnson EF. Structures of human microsomal cytochrome P450 2A6 complexed with coumarin and methoxsalen. Nat Struct Mol Biol 2005; 12:822 823.
13. Smith BD, Sanders JL, Porubsky PR, Lushington GH, Stout CD, Scott EE. Structure of the human lung cytochrome P450 2A13. J Biol Chem 2007; 282:17306 17313.
14. Scott EE, He YA, Wester MR, White MA, Chin CC, Halpert JR, Johnson EF, Stout CD. An open conformation of mammalian cytochrome P450 2B4 at 1.6 Å resolution. Proc Natl Acad Sci U S A 2003; 100:13196 13201.
15. Schoch GA, Yano YK, Wester MR, Griffin KJ, Stout CD, Johnson EF. Structure of human microsomal cytochrome P450 2C8. Evidence for a peripheral fatty acid binding site. J Biol Chem 2004; 279:9497 9503.
16. Williams PA, Cosme J, Ward A, Angove HC, Matak Vinkovic D, Jhoti, H. Crystal structure of human cytochrome P450 2C9 with bound warfarin. Nature 2003; 424:464 468.
17. Wester MR, Yano JK, Schoch GA, Yang C, Griffin KJ, Stout CD, Johnson EF. The structure of human cytochrome P450 2C9 complexed with flurbiprofen at 2.0 Å resolution. J Biol Chem 2004; 279:35630 35637.
18. Rowland P, Blaney FE, Smyth MG, Jones JJ, Leydon VR, Oxbrow AK, Lewis CJ, Tennant MG, Modi S, Eggleston DS, Chenery RJ, Bridges AM. Crystal structure of human cytochrome P450 2D6. J Biol Chem 2006; 281:7614 7622.
19. Strushkevich NV, Min J, Loppnau P, Tempel W, Arrowsmith CH, Edwards AM, Sundstrom M, Weigelt J, Bochkarev A, Plotnikov AN, Park H. Structural analysis of CYP2R1 in complex with vitamin D. J Mol Biol 380:95 106.

20. Williams PA, Cosme J, Vincovic VM, Ward A, Angove HC, Day PJ, Vonrhein, C., Tickle IJ, Jhoti H. Crystal structures of human cytochrome P450 3A4 bound to metyrapone and progesterone. Science 2004; 305:683 686.
21. Yano JK, Wester MR, Schoch GA, Griffin KJ, Stout CD, Johnson EF. The structure of human microsomal cytochrome P450 3A4 determined by X ray crystallography to 2.05 Å resolution. J Biol Chem 2004; 279:38091 38094.
22. Atkins WM, Sligar SG. Molecular recognition in cytochrome P450: alteration of regioselective alkane hydroxylation via protein engineering. J Am Chem Soc 1989; 111:2715 2717.
23. Atkins WM, Sligar SG. The roles of active site hydrogen bonding in cytochrome P 450_{cam} as revealed by site directed mutagenesis. J Biol Chem 1988; 263:18842 18849.
24. Furuya H, Shimizu T, Hirano K, Hatano M, Fujii Kuriyama Y, Raag R, Poulos TL. Site directed mutagenesis of rat liver cytochrome P 450d: catalytic activities toward benzphetamine and 7 ethoxycoumarin. Biochemistry 1989; 28:6848 6857.
25. Gotoh O. Substrate recognition sites in cytochrome P450 family 2 (CYP2) proteins inferred from comparative analyses of amino acid and coding nucleotide sequences. J Biol Chem 1992; 267:83 90.
26. Crivori P, Poggesi I. Computational approaches for predicting CYP related metabolism properties in the screening of new drugs. Eur J Med Chem 2006; 41:795 808.
27. Cruciani G, Carosati E, De Boeck B, Ethirajulu K, Mackie C, Howe T, Vianello R. MetaSite: understanding metabolism in human cytochromes from the perspective of the chemist. J Med Chem 2005; 48:6970 6979.
28. Afzelius L, Arnby CH, Broo A, Carlsson L, Isaksson C, Jurva U, Kjellander B, Kolmodin K, Nilsson K, Raubacher F, Weidolf L. State of the art tools for computational site of metabolism predictions: comparative analysis, mechanistical insights, and future applications. Drug Metab Rev 2007; 39:61 86.
29. Yano YK, Koo LS, Schuller DJ, Li H, Ortiz de Montellano PR, Poulos TL. Crystal structure of a thermophilic cytochrome P450 from the archaeon *Sulfolobus solfataricus*. J Biol Chem 2000; 275:31086 31092.
30. Scott EE, White MA, He YA, Johnson EF, Stout CD, Halpert JR. Structure of mammalian cytochrome P450 2B4 complexed with 4 (4 chlorophenyl)imidazole at 1.9 Å resolution. J Biol Chem 2004; 279:27294 27301.
31. Schenkman JB, Sligar SG, Cinti DL. Substrate interaction with cytochrome P450. In: Schenkman JB, Kupfer D, eds. Hepatic Cytochrome P 450 Monooxygenase System. New York: Pergamon Press, 1982:587 615.
32. Dawson JH, Sono M. Cytochrome P450 and chloroperoxidase: thiolate ligated heme enzymes. Spectroscopic determination of their active site structures and mechanistic implications of thiolate ligation. Chem Rev 1987; 87:1255 1276.
33. Sweeney GD, Rothwell JD. Spectroscopic evidence of interaction between 2 allyl 2 isopropylacetamide and cytochrome P 450 of rat liver microsomes. Biochem Biophys Res Commun 1973; 55:798 804.
34. Murataliev MB, Feyereisen R, Walker A. Electron transfer by diflavin reductases. Biochim Biophys Acta Proteins & Proteomics 2004; 1698:1 26.
35. Wang M, Roberts DL, Paschke R, Shea TM, Masters BS, Kim JJ. Three dimensional structure of NADPH cytochrome P450 reductase: prototype for FMN and FAD containing enzymes. Proc Natl Acad Sci U S A 1997; 94:8411 8416.
36. Schenkman JB, Jansson I. The many roles of cytochrome b_5. Pharmacol Ther 2003; 97:139 152.
37. Porter TD. The roles of cytochrome b_5 in cytochrome P450 reactions. J Biochem Mol Toxicol 2002; 16:311 316.
38. Yamazaki H, Johnson WW, Ueng JF, Shimada T, Guengerich FP. Lack of electron transfer from cytochrome b_ε in stimulation of catalytic activities of cytochrome P450 3A4. Characterization of a reconstituted cytochrome P450 3A4/NADPH cytochrome P450 reductase system and studies with apo cytochrome b_5. J Biol Chem 1996; 271:27438 27444.
39. Makris TM, Denisov I, Schlichting I, Sligar SG. Activation of molecular oxygen by cytochrome P450. In: Ortiz de Montellano PR, ed. Cytochrome P450: Structure, Mechanism, and Biochemistry New York: Kluwer/Plenum, 2005:149 182.

40. Sligar SG. Coupling of spin, substrate and redox equilibria in cytochrome P 450, Biochemistry 1976; 15:5399 5406.
41. Guengerich FP. Oxidation reduction properties of rat liver cytochromes P 450 and NADPH cytochrome P 450 reductase related to catalysis in reconstituted systems. Biochemistry 1983; 22:2811 2820.
42. Das A, Grinkova YV, Sligar SG. Redox potential control by drug binding to cytochrome P450 3A4. J Am Chem Soc 2007; 129:13778 13779.
43. Schlichting I, Berendzen J, Chu K, Stock AM, Maves SA, Benson DE, Sweet RM, Ringe D, Pesko GA, Sligar SG. The catalytic pathway of cytochrome $P450_{cam}$ at atomic resolution. Science 2000; 287:1615 1622.
44. Ortiz de Montellano PR, De Voss JJ. Substrate oxidation by cytochrome P450 enzymes. In: Ortiz de Montellano PR, ed. Cytochrome P450: Structure, Mechanism, and Biochemistry, New York: Kluwer/Plenum, 2005:183 245.
45. Vaz A, McGinnity D, Coon M. Epoxidation of olefins by cytochrome P450: evidence from site specific mutagenesis for hydroperoxo iron as an electrophilic oxidant. Proc Nat Acad Sci USA 1998; 95:3555 3560.
46. Oguri K, Tanimoto Y, Yoshimura H. Metabolite fate of strychnine in rats. Xenobiotica 1989; 19:171 178.
47. Hjelmeland LM, Aronow L, Trudell JR. Intramolecular determination of primary kinetic isotope effects in hydroxylations catalyzed by cytochrome P 450. Biochem Biophys Res Commun 1977; 76:541 549.
48. Foster AB. Deuterium isotope effects in the metabolism of drugs and xenobiotics: implications for drug design. Adv Drug Res 1985; 14:2 40.
49. Frommer U, Ullrich V, Staudinger H. Hydroxylation of aliphatic compounds by liver microsomes. 1. The distribution of isomeric alcohols. Hoppe Seylers Z Physiol Chem 1970; 351:903 912.
50. Shaik S, Visser SP. Computational approaches to cytochrome P450 function. In: Ortiz de Montellano PR, ed. Cytochrome P450: Structure, Mechanism, and Biochemistry. New York: Kluwer/Plenum, 2005:45 85.
51. Groves JT, McClusky GA, White RE, Coon MJ. Aliphatic hydroxylation by highly purified liver microsomal cytochrome P 450. Evidence for a carbon radical intermediate. Biochem Biophys Res Commun 1978; 81:154 160.
52. Hefner J, Rubenstein SM, Ketchum RE, Gibson DM, Williams RM, Croteau R. Cytochrome P450 catalyzed hydroxylation of taxa 4(5),11(12) diene to taxa 4(20),11(12)dien 5α ol: the first oxygenation step in taxol biosynthesis. Chem Biol 1996; 3:479 489.
53. Ortiz de Montellano PR, Stearns RA. Timing of the radical recombination step in cytochrome P 450 catalysis with ring strained probes. J Am Chem Soc 1987; 109:3415 3420.
54. Newcomb M, Hollenberg PF, Coon MJ. Multiple mechanisms and multiple oxidants in P450 catalyzed hydroxylations. Arch Biochem Biophys 2003; 409:72 79.
55. Jiang Y, He X, Ortiz de Montellano PR. Radical intermediates in the catalytic oxidation of hydrocarbons by bacterial and human cytochrome P450 enzymes. Biochemistry 2006; 45:533 542.
56. Hinson JA, Mitchell JR, Jollow DJ. N Hydroxylation of *p* chloroacetanilide in hamsters. Biochem Pharmacol 1975; 25:599 601.
57. Ortiz de Montellano PR, Mangold BLK, Wheeler C, Wheeler C, Kunze KL, Reich NO. Stereochemistry of cytochrome P 450 catalyzed epoxidation and prosthetic heme alkylation. J Biol Chem 1983; 258:4208 4213.
58. Harvey DJ, Glazener L, Johnson DB, Butler CM, Horning MG. Comparative metabolism of four allylic barbiturates and hexobarbital by rat and guinea pig. Drug Metab Dispos 1977; 5:527 546.
59. Miller RE, Guengerich FP. Oxidation of trichloroethylene by liver microsomal cytochrome P 450: evidence for chlorine migration in a transition state not involving trichloroethylene oxide. Biochemistry 1982; 21:1090 1097.
60. Correia MA, Ortiz de Montellano PR. Inhibition of cytochrome P450 enzymes. In: Ortiz de Montellano PR, ed. Cytochrome P450: Structure, Mechanism, and Biochemistry. New York: Kluwer/Plenum, 2005:247 322.

61. Kunze KL, Mangold BLK, Wheeler C, Beilan HS, Ortiz de Montellano PR. The cytochrome P 450 active site. Regiospecificity of the prosthetic heme alkylation by olefins and acetylenes. J Biol Chem 1983; 258:4202 4207.
62. Jerina DM, Daly JW. Arene oxides: a new aspect of drug metabolism. Science 1974; 185: 573 582.
63. Barker SA, Hsieh LC, McDowell TR, Short CR. Short, qualitative and quantitative analysis of the anthelminthic febendazole and its metabolites in biological matrices by direct exposure probe mass spectrometry. Biomed Environ Mass Spectrom 1987; 14:161 165.
64. Den Besten, C, van Bladeren PJ, Duizer E, Vervoort J, Rietjens IM. Cytochrome P450 mediated oxidation of pentafluorophenol to tetrafluorobenzoquinone as the primary reaction product. Chem Res Toxicol 1993; 6:674 680.
65. He X, Cryle MJ, De Voss JJ, Ortiz de Montellano PR. Calibration of the channel that determines the ω hydroxylation regiospecificity of cytochrome P4504A1. Catalytic oxidation of 12 halododecanoic acids. J Biol Chem 2005; 280:22697 22705.
66. Seto Y, Guengerich FP. Partitioning between N dealkylation and N oxygenation in the oxidation of N,N dialkylarylamines catalyzed by cytochrome P450 2B1. J Biol Chem 1993; 268:9986 9997.
67. Karki SB, Dinnocenzo JP, Jones JP, Korzekwa KR. Mechanism of oxidative amine dealkylation of substituted N,N dimethylanilines by cytochrome P 450: application of isotope effect profiles. J Am Chem Soc 1995; 117:3657 3664.
68. Kammerer B, Scheible H, Albrecht W, Bleiter CH, Laufer S. Pharmacokinetics of ML3403 ({4 [5 (4 fluorophenyl) 2 methylsulfanyl 3*H* imidazol 4 yl]pyridine 2 yl} (1 phenylethyl) amine, a 4 pyridinylimidazole type p38 mitogen activated protein kinase inhibitor. Drug Metab Dispos 2007; 35:875 883.
69. Madan A, Williams TD, Faiman MD. Glutathione and glutathione S transferase dependent oxidative desulfuration of the thione xenobiotic diethyldithiocarbamate methyl ester. Mol Pharmacol 1994; 46:1217 1225.
70. Rettie AE, Boberg M, Rettenmeier AW, Baillie TA. Cytochrome P 450 catalyzed desaturation of valproic acid *in vitro*. Species differences, induction effects, and mechanistic studies. J Biol Chem 1988; 263:13733 13738.
71. Korzekwa KR, Trager WF, Nagata K, Parkinson A, Gillette JR. Isotope effect studies on the mechanism of the cytochrome P450IIA1 catalyzed formation of Δ^6 testosterone from testosterone. Drug Metab Dispos 1990; 18:974 979.
72. Vyas KP, Kari PH, Prakash SR, Duggan DE. B. Biotransformation of lovastatin. II. *In vitro* metabolism by rat and mouse liver microsomes and involvement of cytochrome P 450 in dehydrogenation of lovastatin. Drug Metab Dispos 1990; 18:218 222.
73. Stearns RA, Chakravarty PK, Chen R, Chiu SH. Biotransformation of losartan to its active carboxylic acid metabolite in human liver microsomes. Role of cytochrome P4502C and 3A subfamily members. Drug Metab Dispos 1995; 23:207 215.
74. Roberts ES, Vaz AD, Coon MJ. Catalysis by cytochrome P 450 of an oxidative reaction in xenobiotic aldehyde metabolism: deformylation with olefin formation. Proc Natl Acad Sci U S A 1991; 88:8963 8966.
75. Akhtar M, Njar VCO, Wright JN. Mechanistic studies on aromatase and related C C bond cleaving P 450 enzymes. J Steroid Biochem Molec Biol 1993; 44:375 387.
76. Goeptar AR, Scheerens H, Vermeulen NPE. Oxygen and xenobiotic reductase activities of cytochrome P450. Crit Rev Toxicol 1995; 25:25 65.
77. Patterson LH. Bioreductively activated antitumor N oxides: the case of AQ4N, a unique approach to hypoxia activated cancer chemotherapy. Drug Metab Rev 2002; 34:581 592.
78. Saunders MP, Patterson AV, Chinje EC, Harris AL, Stratford IJ. NADPH:cytochrome c (P450) reductase activates tirapazamine (SR4233) to restore hypoxic and oxic cytotoxicity in anaerobic resistant derivative of the A549 lung cancer cell line. Br J Cancer 2000; 82:651 656.

5

Transformation Enzymes: Oxidative; Non-P450

Carrie M. Mosher and Allan E. Rettie
Department of Medicinal Chemistry, University of Washington, Seattle, Washington, U.S.A.

GENERAL INTRODUCTION

As noted in earlier chapters, P450 monooxygenases dominate oxidative enzymatic reactions that metabolize drugs and other xenobiotics to facilitate their excretion. Indeed, it is estimated that P450 pathways contribute significantly to the clearance of about two-thirds of all drugs that depend on metabolism (1). However, complete reliance on P450 clearance pathways can precipitate adverse drug reactions if plasma concentrations are elevated either because of competition of multiple coadministered drugs for the same P450 isoforms or because the P450 clearance pathway is polymorphic. Consequently, during drug discovery and development, distribution of a drug's clearance pathways over multiple P450 isoforms and/or non-P450 enzymes is often considered beneficial.

Many non-P450 oxidative enzymes, including aldehyde dehydrogenase (ALDH), monoamine oxidase, and semicarbazide-sensitive amine oxidase, are capable of carrying out xenobiotic oxidation, but generally their quantitative contribution to drug metabolism is too low, or our present knowledge of their basic biochemistry is insufficiently comprehensive, to warrant detailed discussion here. However, interested readers are directed toward some recent excellent reviews on the dehydrogenases (2) and amine oxidases (3). This chapter will focus on three mammalian nonheme oxygenases, which can conveniently be categorized by the nature of their active centers as either *flavin-containing* or *molybdenum-containing enzymes*. The flavin-containing monooxygenase (FMO) isoforms are located predominantly in the microsomal cell fraction, whereas the molybdenum-containing enzymes, aldehyde oxidase (AO) and xanthine oxidoreductase (XOR), are both located in the soluble fraction. Each of the three enzymes will be discussed in terms of their catalytic mechanism, multiplicity, tissue distribution, enzyme regulation, biotransformation reactions, and relevance to human drug metabolism.

MICROSOMAL FLAVIN-CONTAINING MONOOXYGENASE

Microsomal FMOs have been categorized as class B flavoprotein monooxygenases, along with the sequence-related Baeyer Villiger monooxygenases and microbial N-hydroxylating monooxygenases (4). All three enzymes exhibit common characteristics of a tightly bound FAD cofactor, two glycine-rich dinucleotide-binding domains (Rossman folds) for FAD and NADPH, and maintenance of bound NADPH/$NADP^+$ throughout catalysis. Microsomal FMOs activate molecular oxygen in order to function as sulfur, nitrogen, phosphorus, and selenium oxygenases (5), and in this regard, as well as in their dependence on NADPH, they are indistinguishable from P450s, which can carry out many of the same catalytic reactions. Moreover, both FMOs and P450s are localized in the endoplasmic reticulum of the cell, and so it is of interest to be able to distinguish between catalysis by these two monooxygenases in microsomal membranes. To accomplish this, investigators can take advantage of the increased thermolability of FMO relative to P450, human liver microsomes that have been phenotyped for FMO-selective substrate activity and/or immunochemical content, as well as commercially available recombinant preparations of FMO (and P450) isoforms. Examples of these various approaches can be found in several publications (6 10).

Catalytic Mechanism

The simplest catalytic cycle consistent with available experimental data involves the initial transfer of the *pro*-R hydrogen from NADPH to reduce FAD, followed by dioxygen binding to the reduced flavin to generate a C-4a-hydroperoxide (FAD-OOH in Fig. 1A) (11,12). Substrate nucleophiles (e.g., trimethylamine) attack the distal oxygen of this hydroperoxide with resultant oxygen transfer to the substrate and the generation of a hydroxyflavin (FAD-OH) species. The rate-limiting step in FMO catalysis is considered to be decomposition of the hydroxyflavin and/or release of $NADP^+$ (5). Because the rate-limiting step follows transfer of oxygen to the substrate, it provides a rationalization for the observation that the V_{max} for FMO-dependent reactions is relatively constant (13).

Recently, the crystal structures of *Saccharomyces pombe* FMO bound with NADPH and the substrate methimazole (Fig. 1B) have been solved (14). However, the quaternary complex of enzyme-FAD-NADP(H)-methimazole was not obtained, and in the two ternary complexes, methimazole bound in the same location as NADPH. These observations prompted the authors to suggest that substrate competes with NADPH and replaces the cofactor during the catalytic cycle of the yeast enzymes; however, no kinetic studies have yet been reported in support of this alternate mechanism. Yeast and mammalian FMOs share only 21% to 25% sequence similarity, but contain a highly conserved asparagine residue (Asn91 yeast; Asn61 FMO3), which is implicated in catalysis by yeast FMO, where it is proposed to be involved in oxygen binding (14). A homology model of human FMO3 based on the yeast FMO template also locates Asn61 at the catalytic center (15). Moreover, site-directed mutagenesis of this residue, while maintaining enzyme expression and FAD binding, greatly diminished enzymatic activity for all substrates examined, consistent with a critical role for this residue in catalysis by human FMO3 (15,16).

Multiplicity, Tissue Distribution, and Species Differences

Multiplicity

Molecular biology techniques have revealed the existence of 11 human *FMO* genes located on chromosome 1, 5 of which encode functional enzymes that are expressed in all mammalian species examined to date. These functional enzymes are FMO1, FMO2,

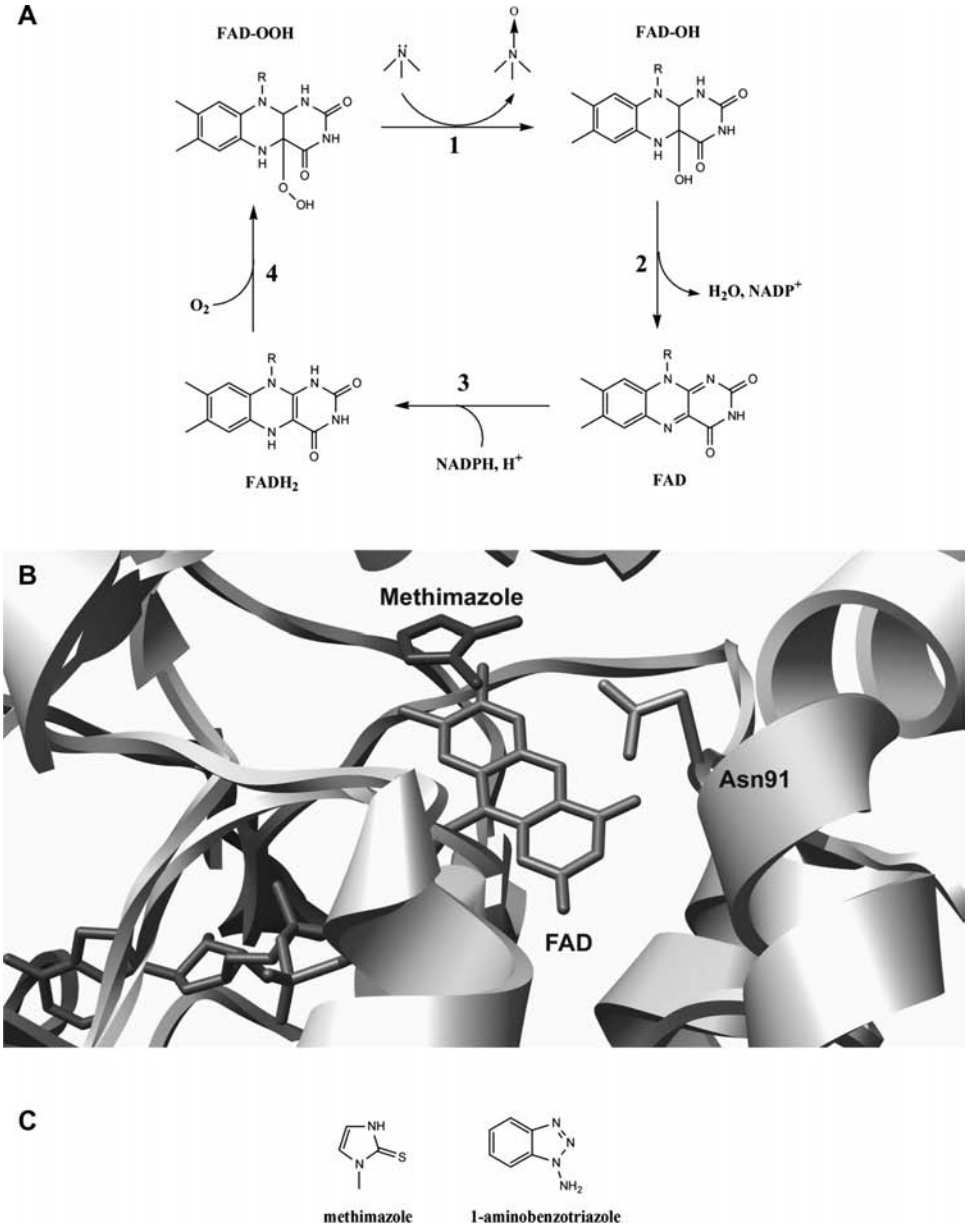

Figure 1 (**A**) Catalytic cycle for FMO dependent oxygenation. Step 1 illustrates reaction of the prototypical substrate trimethylamine with the enzyme's activated oxygen species resulting in the formation of trimethylamine *N* oxide. Step 2 involves decomposition of the pseudobase FAD OH, with loss of water and release of $NADP^+$. Steps 3 and 4 are sequential reductions of the oxidized enzyme by NADPH and reaction of $FADH_2$ with molecular oxygen to once again generate the reactive oxygen species FAD OOH. (**B**) Crystal structure of the yeast FMO (pdb 2GVC) active site. The flavin cofactor, a residue involved in the catalytic mechanism (Asn91), and the inhibitor methimazole are highlighted. (**C**) Compounds used to elucidate FMO metabolic involvement via inhibition of FMO (methimazole) or P450s (1 aminobenzotriazole) as discussed within. *Abbrevia tion*: FMO, flavin containing monooxygenase.

FMO3, FMO4, and FMO5, which share 50% to 55% sequence identity (17). Human *FMO6* mRNA is subject to alternative splicing that results in nonfunctional protein (18). Three additional, possibly functional, *FMO* genes (*FMO9*, *FMO12*, and *FMO13*) exist in mice and rats, but apparently not in humans (19).

Tissue Distribution

On the basis of mRNA expression, the major forms of FMO expressed are FMO3 and FMO5 in human liver, FMO1 in human kidney, FMO2 in human lung, and FMO5 in human intestine (20,21). However, it should be noted that mRNA expression and protein expression are not always well correlated. Moreover, the human FMO enzymes differ substantially in their catalytic capabilities, and so this must also be factored into consideration of their contribution to drug or xenobiotic clearance in any given tissue.

In terms of human drug metabolism, FMO3 is clearly the most important isoform because it is highly expressed in the liver (22) at protein levels 2 to 10 times greater than FMO5 (23), which contrasts with the mRNA data for these two enzymes (20,21). Human liver FMO1 protein expression is prominent in fetal liver, but is silenced within a few days after birth (24). In human kidney, FMO1 appears to be the functionally dominant form, present at protein levels that are 2 to 3 times higher than reported for fetal liver (25). As in nearly all animal species, human FMO2 is a pulmonary enzyme, but it is inactive in most human populations because of a polymorphism that results in a premature stop codon (26). FMO4 is the least well studied of the human FMO enzymes, perhaps because expression of the recombinant protein has proved challenging (27). FMO5 is a quantitatively important hepatic FMO enzyme in humans and many experimental animals, but has attracted little attention because of its narrow substrate specificity (28).

Species Differences

As a general rule, FMO1 and FMO3 are expressed in the liver of most preclinical animal species, with the FMO1 isoform usually dominating FMO-dependent activity, a situation that contrasts strongly with that found in humans. While no gender differences in hepatic FMO activity have been reported in humans, a sex difference does exist in mice, as female mice exhibit higher liver FMO activity than males. The basis for this appears to be a combination of increased FMO1 levels in female mice and ablated FMO3 expression in male mice (29). Whereas FMO-mediated benzydamine clearance in cryopreserved rat hepatocytes was a good predictor of in vivo clearance, this was not true for cryopreserved human hepatocytes (30). Therefore, because tissue expression profiles and the substrate specificities of the individual FMO isoforms can differ across species, it is important to exercise caution when attempting to extrapolate liver microsomal data for FMO catalysis from experimental animals to humans.

Enzyme Regulation

Unlike the cytochrome P450s, the FMO system is not induced by exogenously administered xenobiotics, such as the barbiturates or polycyclic hydrocarbons. However, as noted above, the FMOs are subject to developmental, hormonal, and genetic regulation, all of which can influence FMO3 and/or FMO1 activity in humans.

Developmental Expression

The most striking example of developmental control concerns the selective expression of FMO1 in fetal human liver and FMO3 in adult human liver. Temporal expression patterns of human FMO1 and FMO3 protein have been investigated in human liver microsomal preparations representing ages from 8-week gestation to 18 years, using antibodies selective for each enzyme (24). FMO1 expression was highest in the embryo, whereas suppression occurred within three days postpartum in a process tightly coupled to birth. The onset of FMO3 expression was variable; most individuals failed to express this isoform during the neonatal period, but significant levels of FMO3 were generally detectable by one to two years of age. The authors concluded that birth is necessary, but not sufficient, for the onset of FMO3 expression. Hines and coworkers have undertaken additional studies to probe the trigger mechanism(s) for these events and recently identified that Pbx2 and Hox transcription factors are important to FMO3 developmental regulation (31).

Hormonal Regulation

Sex steroids have long been recognized to influence FMO activity, with induction of rabbit lung microsomal *N,N*-dimethylaniline N-oxygenase during pregnancy an early example of this phenomenon (32). Subsequently, upregulation of rabbit lung FMO2 was shown to correlate with plasma levels of progesterone and cortisol in pregnant animals (33). Human FMO3 may also be induced in pregnancy (34). In male mice, sex steroids play an important role in hepatic FMO1 and FMO3 expression, with testosterone acting as a negative regulator of FMO3 in male mice (29). Finally, menstruation can be associated with a transient trimethylaminuria (35) (see following section), possibly because of changes in hormone levels affecting FMO3 expression and/or the presence of common genetic polymorphisms with independently modest effects on activity.

Genetic Polymorphism

Rare polymorphisms in the *FMO3* gene that abolish functional activity cause the metabolic disorder trimethylaminuria, also known as fish-odor syndrome. Affected individuals are unable to metabolize trimethylamine for urinary excretion and resort, in part, to eliminating the compound unchanged in the sweat and exhaled breath (36,37). This is a consequence of the fact that FMO3 is the most efficient of all the human FMO enzymes for the conversion of dietary-derived trimethylamine to its non-odoriferous *N*-oxide metabolite (38).

Whereas the human *FMO3* gene contains over 40 common single nucleotide polymorphisms (SNPs), common polymorphic variation in human *FMO1* appears relatively minimal (39), suggestive perhaps of a critical endogenous role for this enzyme. In *FMO3*, the coding region polymorphisms, E158K, V257M, and E308G, are each expressed at an allele frequency of greater than 5% in a variety of racial populations (16). These common coding region variants maintain variable degrees of FMO3 activity, which may impact human drug metabolism to some degree, depending on the nature of the substrate (15,40,41).

Transformation Reactions

The wide panoply of metabolic transformations of which mammalian FMOs are capable is exemplified by the substrate specificity of pig liver FMO1, the first FMO enzyme to be described (42). This enzyme catalyzes the oxidative metabolism of a huge array of

amines, hydrazines, thiols, sulfides, thioamides, thiocarbamides, as well as numerous organic compounds bearing nucleophilic selenium and phosphorus atoms (43). Extensive structure-function studies with this enzyme have shown that, in principle, any soft nucleophile that gains access to the active site of FMO will be oxygenated (13,44); however, access can be modulated by substrate charge and size (45). Presumably, differences in the dimensions and charge neutralization capabilities of FMO enzyme active sites and/or their access channels underlie the general view that mammalian FMO substrate specificity decreases in the order FMO1 > FMO3 > FMO2 > FMO5 (5).

A few illustrative examples of FMO-catalyzed oxidation at nitrogen and sulfur centers the most commonly encountered nucleophilic sites in drug molecules are presented below, together with discussion of methodology that can be used to discriminate between FMO and P450-dependent catalysis.

Oxidation at Nitrogen Centers

A very large number of nitrogen-containing functionalities are found in drugs and other xenobiotics. Given the nucleophilic mechanism of FMO catalysis, it might be expected that substrates for the enzyme would exhibit a minimum basicity requirement. Indeed, FMO catalyzes *N*-oxide formation on the pyrrolidine ring of nicotine (pK_a of protonated nitrogen = 8), but not on the pyridine ring (pK_a = 3). However, predictions of substrate specificity based on pK_a alone do not accommodate all of the experimental observations (10), and it is clear that steric and electronic effects of the substrates themselves and the relative expression levels of specific FMO and P450 isoforms in a given species will determine the nature of the enzyme system involved in vivo. Regardless, xenobiotics that contain a basic sp^3-hybridized nitrogen are generally good substrates for FMO.

A major group of substrates for the FMOs are the tertiary acyclic and cyclic amines. Substrates such as trimethylamine (Fig. 1), clozapine (Fig. 2), benzydamine, and guanethidine are converted to stable *N*-oxides. However, the levels of *N*-oxide metabolite formed may often be underestimated owing to relatively facile reduction back to the parent amine. Although cytochrome P450s tend to preferentially N-dealkylate tertiary amines, P450-dependent formation of *N*-oxides is well documented (46,47). FMOs also catalyze the metabolism of secondary and primary amines (13), but are usually not involved in the oxidation of amides, heteroaromatic amines, benzamidines, guanidines, or diamines.

Oxidation at Sulfur Centers

FMOs readily catalyze the oxidation of thioethers to sulfoxides, often with a high degree of stereoselectivity, and the further metabolism of sulfoxides to sulfones. Thioethers, such as tazarotenic acid (Fig. 2), are generally better substrates for FMO than the tertiary amines discussed above, owing to the enhanced nucleophilicity of the sulfur atom. Relative nucleophilicity also explains why thioamides are excellent substrates and sulfoxides are usually poorer substrates for FMO. However, oxidation of sulfur-containing compounds is also carried out readily by cytochrome P450s. The relative participation of these two monooxygenase systems in sulfur oxidation will depend on their levels of expression in the metabolizing tissue and the substrate specificity of the FMO isoforms involved.

Diagnostic Substrates and Inhibitors

Approaches to the differentiation of P450-mediated and FMO-dependent catalysis may capitalize on the availability of (partially) selective substrates and inhibitors for both

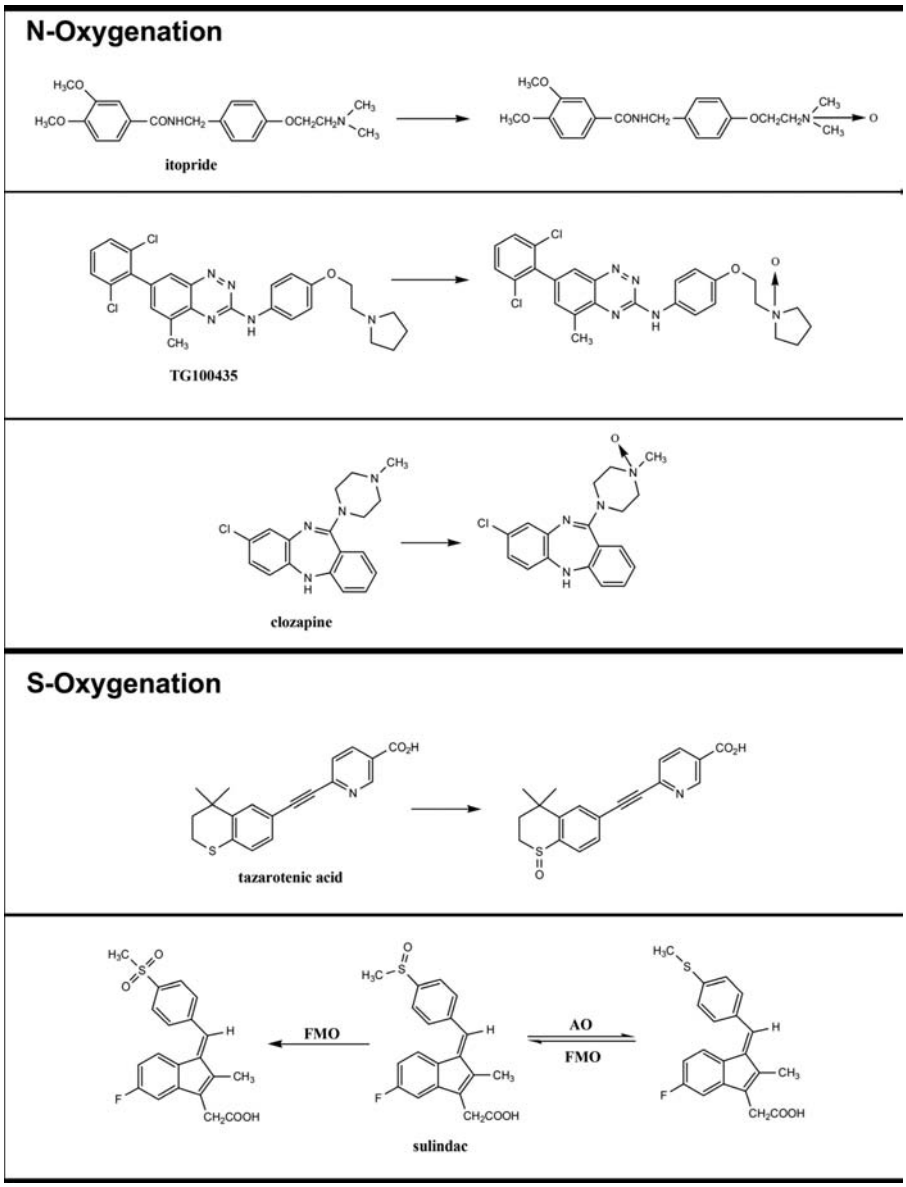

Figure 2 Typical N and S oxygenation reactions catalyzed by FMO. Redox interconversions of sulindac illustrate the metabolic interplay of FMO and AO enzymes discussed in this review. *Abbreviations*: FMO, flavin containing monooxygenase; AO, aldehyde oxidase.

enzyme systems. For example, the conversion of *N,N*-dimethylaniline to its *N*-oxide is one of the most widely used indicators of FMO catalysis in microsomal preparations, and as long as reactions are carried out at pH 8.5 to 9, only FMO(s) are likely to be involved. However, at physiological pH, even this most diagnostic of substrates may be turned over, in part, by cytochrome P450s. A useful FMO substrate is the anti-inflammatory drug benzydamine (48) because several FMO enzymes, including human FMO3, form the

highly fluorescent *N*-oxide metabolite. This has permitted the development of a simple, sensitive, LC-based metabolite assay for FMO activity (49,50).

Chemical inhibitors suffer from the disadvantage that they are rarely, if ever, specific for FMO. Unfortunately, no mechanism-based inhibitors of FMO have been identified, and antibodies raised against purified enzymes do not significantly inhibit the activity of microsomal FMOs. However, 1-aminobenzotriazole (Fig. 1C), a suicide inhibitor of most P450s at high substrate concentrations, is a useful indirect indicator of FMO catalysis if preincubation with this compound does not decrease the reaction rate that is being monitored. Methimazole (Fig. 1C) is a widely used inhibitor of FMOs, but it also competitively inhibits human CYP2B6, CYP2C9, and CYP3A4 at the relatively low substrate concentrations of 40 to 100 μM (51). *n*-Octylamine, an activator of FMO1, is an inhibitor of human FMO3 (52). Therefore, it is prudent to employ a battery of "selective" inhibition methods (6) when evaluating the in vitro role of FMO in a given oxidative pathway.

Relevance to Human Drug Metabolism

The conversion of lipophilic tertiary amines to polar *N*-oxides can be considered the prototypic FMO xenobiotic reaction pathway, and so it is not surprising that FMO has been implicated in the metabolism of a variety of tertiary amine-containing drugs. However, although FMOs are clearly responsible for the N-oxygenation of widely used agents like nicotine and tamoxifen (53,54), this pathway does not dictate their metabolic clearance. Nonetheless, there are a number of examples where FMO-dependent metabolism is a significant contributor to drug clearance in vivo.

N-oxygenation is the major metabolic pathway for the gastroprokinetic agent itopride (Fig. 2), and FMO3 is the main catalyst of this pathway in human liver microsomes (55). More recently, an investigational Src kinase inhibitor TG100435 (Fig. 2) was shown to rely on FMO3 for metabolism to its major, active *N*-oxide metabolite (56). Ranitidine, benzydamine, and olanzapine provide additional examples of marketed drugs where FMO plays a significant role in their metabolic elimination through formation of *N*-oxide metabolites (7,49,57).

Sulfoxides are quantitatively significant human metabolites of therapeutic agents such as the anti-inflammatory sulindac sulfide (Fig. 2), and tazarotenic acid, the major circulating metabolite of the topical antipsoriatic agent tazarotene. The former drug is administered as a sulfoxide prodrug and relies on metabolic reduction for its pharmacological activity. In vitro microsomal studies indicate that human liver FMO(s) S-oxygenate both sulindac sulfide (58) and tazarotenic acid (59).

An interesting variation on FMO-dependent S-oxygenation processes can occur following S-methylation of thiol precursors. In this regard, FMO catalysis has been documented for *S*-methyl metabolites of the alcohol aversion drug disulfiram (60), as well as MK0767, an investigational peroxisome proliferator-activated receptor (PPAR) dual agonist that initially undergoes thiazolidine ring scission to unmask the thiol (61). Figure 3 provides an example of this reductive scission reaction involving the antipsychotic drug ziprasidone, which can be catalyzed by molybdenum-containing hydroxylases.

XANTHINE OXIDASE/ALDEHYDE OXIDASE

The molybdenum hydroxylases are a family of homodimeric, 300-kDa enzymes that include AO, xanthine dehydrogenase (XDH), and xanthine oxidase (XOD). XDH and XOD are two forms of the same enzyme and are often collectively referred to as XOR.

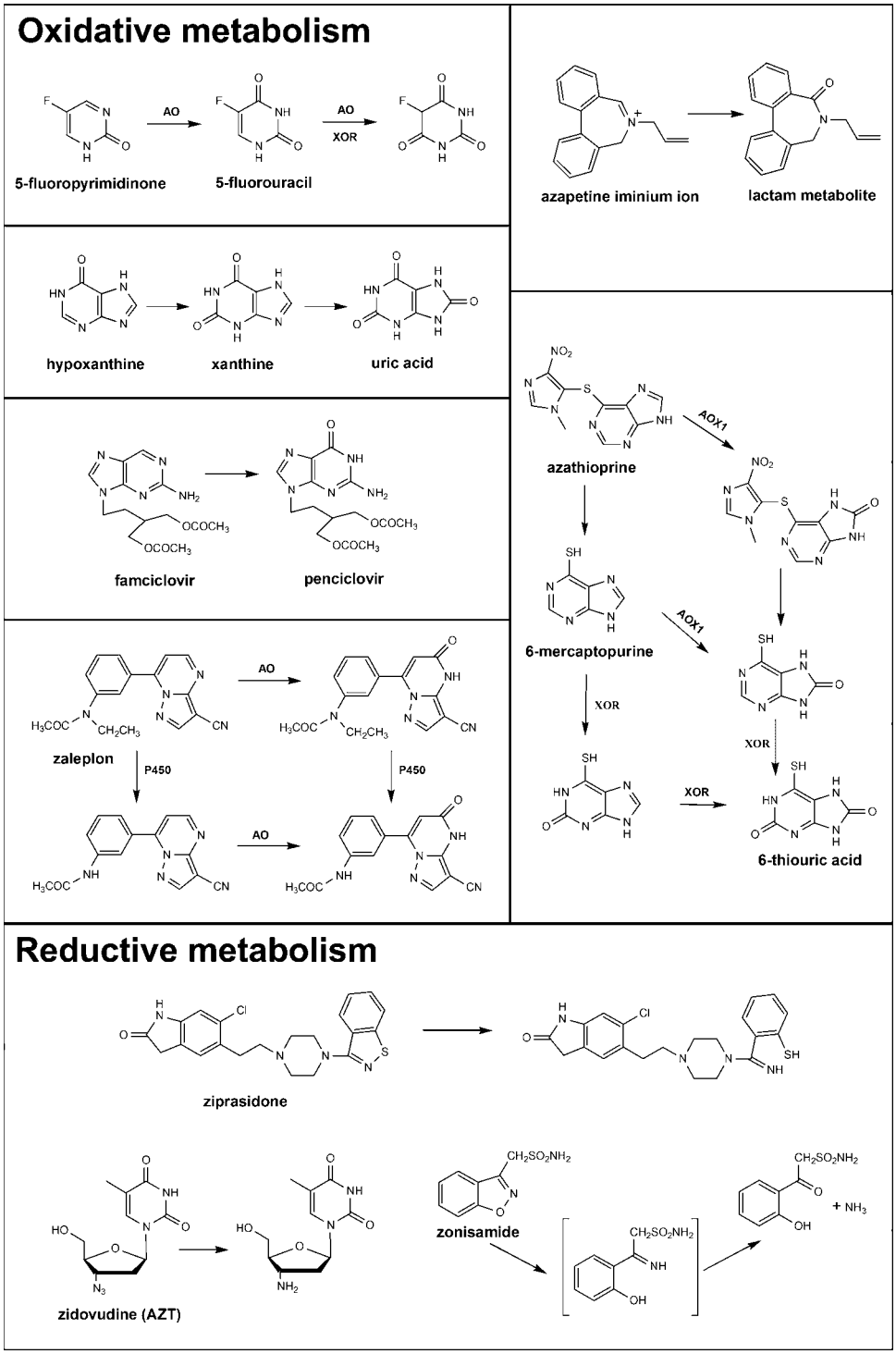

Figure 3 Typical oxidative and reductive reactions catalyzed by XOR and AO. *Abbreviations*: XOR, xanthine oxidoreductase; AO, aldehyde oxidase.

While there is no "alternative" form of AO, several homologs have been identified in certain species (see below). More information is available for XOR than AO, although extensive characterization of the human enzyme is still lacking for both. The physiological role of the mammalian molybdenum hydroxylases has yet to be elucidated; however, these enzymes are involved in human health, and AO has an increasingly important role in human xenobiotic metabolism (62,63).

Catalytic Mechanism

Each 150-kDa subunit of a mammalian molybdozyme has a tripartite structure consisting of a 20-kDa N-terminal domain containing two nonidentical Fe_2S_2 redox centers, a central 40-kDa flavin-containing region, and an 85-kDa C-terminal domain containing the molybdenum cofactor and substrate-binding sites (62). The molybdenum atom is anchored to its active site via a covalent bond to an organic pyranopterin dithiolene cofactor (often called molybdopterin) (64). This molybdopterin cofactor is essential to the chemistry of the molybdozymes, which catalyze the general reaction in Eq. 1,

$$RH + H_2O \rightarrow ROH + 2e \quad + 2H^+ \qquad \text{(Eq. 1)}$$

where RH is the substrate and ROH is the hydroxylated metabolite. Most of the details of the catalytic mechanism have been worked out with bovine XOR and then extrapolated to the orthologous XORs and to AO.

Crystallization of the first molybdenum hydroxylase structure, the AO enzyme from the bacterium *Desulfovibrio gigas*, confirmed that the molybdenum catalytic center had pentacoordinate geometry, with three sulfur ligands and two oxygen ligands, supporting the postulate that catalysis requires base-assisted proton abstraction from Mo-OR (64,65). Later studies showed that the catalytically labile active site center is present in the form of Mo-OH in the resting-state enzyme, and a universally conserved active site glutamate residue (66), Glu1261 in the bovine structure, is indeed positioned to be involved in proton abstraction (Fig. 4B) (67,68). Ensuing nucleophilic attack on an electron-deficient sp^2 carbon with concomitant hydride transfer to the Mo=S of the molybdenum center results in simple, end-on coordination of product to the molybdopterin cofactor (Fig. 4A) (67,69). The bound product is then displaced by a solvent hydroxide ion, and electrons and protons are transferred out of the molybdenum center to the FAD, returning the molybdopterin to its resting state (70). The specific sequence of these latter events appears to vary with the substrate used and reaction conditions (71).

The two iron-sulfur centers appear to be involved in electron transfer from molybdenum to FAD as well as acting as an electron sink to provide electrons to FAD (72). The ultimate electron acceptors are either NAD^+ (XDH form of the enzyme) or molecular oxygen (either XDH or XOD forms, and AO) (73). It is important to note that both the dehydrogenase and oxidase forms of XOR can transfer electrons to molecular oxygen, although the affinity for XDH is much lower (74). Further work is needed to verify the mechanism in both human XOR and AO. Unfortunately, the only crystal structure available for AO is of the *D. gigas* enzyme, which lacks an FAD domain and is only distantly related to the human enzyme (64). However, sequence alignment, homology modeling, and spectroscopic experiments suggest a high degree of homology and structural similarity in the cofactor and apoprotein environments of XOR and AO (75,76), as well as a strict conservation of the Glu1261 residue among all molybdenum hydroxylases (62). Taken together, it is highly likely that the proposed XOR mechanism also applies to AO.

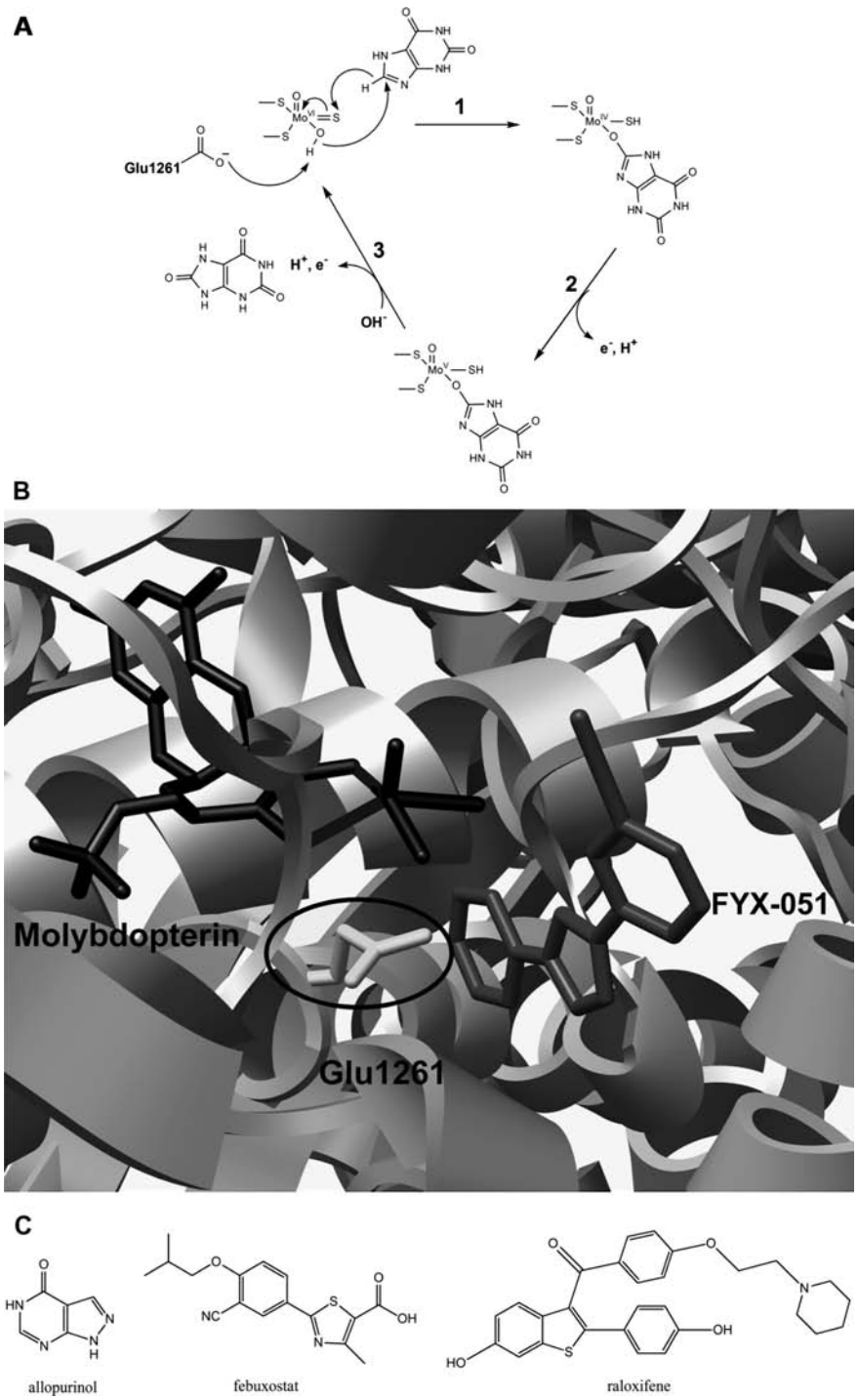

Figure 4 (**A**) Catalytic cycle for XOR dependent oxygenation. Step 1 illustrates the reaction with the prototypic substrate xanthine by base assisted nucleophilic attack with concomitant hydride transfer to the sulfur ligand. Step 2 shows oxidation of the molybdenum center. Step 3 illustrates displacement of the uric acid product by water and reoxidation of the molybdenum. (**B**) Crystal structure of bovine milk XDH (pdb 1V97) active site. The molybdopterin cofactor, the residue involved in the catalytic mechanism (Glu1261, circled), and the inhibitor FYX 051 are shown. (**C**) Inhibitors of XOR and AO. *Abbreviations*: XOR, xanthine oxidoreductase; XDH, xanthine dehydrogenase; AO, aldehyde oxidase.

Multiplicity, Tissue Distribution, and Species Differences

Multiplicity

Whereas only one *XOR* gene appears to exist, multiple genes encoding AO activity have been identified in various species. In humans, AO activity results from expression of a single *AOX1* gene (77), while the mouse and rat genomes consist of four genes [*AOX1*, *AOH1* (aldehyde oxidase homologue 1), *AOH2*, and *AOH3*]. These all contribute to rodent AO activity, although more work is needed to define the individual substrate specificities of the different homologues (62). The human *AOX1* and *XOR* loci both map to chromosome 2; the *AOX1* gene located on chromosome 2q32.3-2q33.1, while *XOR* maps to 2p22 (77). The overall structure of the human *AOX1* gene is nearly identical to the *XOR* gene, with only one less exon and conservation of the position and type of exon-intron junctions (78).

Tissue Distribution

The molybdenum hydroxylases are considered to be cytosolic enzymes, although milk XOR is associated with lipid globules (79,80). While there is a general consensus that the highest levels of XOR and AO are found in the liver (62), both enzymes are widely distributed in mammalian tissues (81). Some differences do exist, however, in their expression patterns. Notably, only XOR appears to be expressed in the small intestine of humans (21) and, therefore, would be implicated in first-pass metabolism to a greater extent than is AO.

Species Differences

There are significant differences in molybdozyme substrate specificity for the orthologous isoforms across species. Dogs lack functional liver *AOX1*, but do express active orthologues of *AOH2* and *AOH3*; therefore, low AO activity is sometimes detected (77). AO activity in humans is generally high compared with other species, complicating extrapolation of drug disposition studies from preclinical species to humans (82).

In rodents, variation in AO activity, both between strains and within strains, is well documented. The predominant form of AO protein expressed in mouse (and likely rat) strains is AOH1, and different strains express different ratios of AOH1:AOX1 in hepatic tissues (62). Two mouse strains, DBA/2 and CBA, were recently identified as having selective deficits in the expression of AOH1 and AOH2, which may present the opportunity to more specifically study AOX1 metabolism in mice (83). Ultrarapid, extensive, and poor metabolizer phenotypes that have been identified in Donryu rats are due to a gene mutation in poor metabolizers that leads to loss of AO dimer formation (84). In addition, different rat strains showed a range of AO dimer:monomer ratios, which correlated with reported intrastrain variation in enzyme activities (84,85). The authors cautioned that rat studies of new drug candidates primarily metabolized by AO should be performed using strains with high activity and low interindividual variation (84).

Human AO activity does not vary as much as in rat or mice (86,87), although due to the lability of the human AO enzyme, which results in significant decreases in activity upon homogenization and storage, the true extent of variation is still unknown. The ability of AO from several species to metabolize aldehydes of varying size provided an estimate of the relative volumes of their substrate-binding sites that were ranked in the order rabbit < guinea pig < baboon < human (88,89). From these studies, it would appear that baboon would be the best animal model for human AO metabolism, although guinea pig has also been suggested as a useful alternative (90).

Enzyme Regulation

Compared with other biological hydroxylation systems, a substantial amount of reactive oxygen species (ROS), superoxide anion and hydrogen peroxide, are formed during molybdozyme catalysis, especially from XOR. Indeed, both XOR and AO appear to be involved in an increasing number of biological processes and toxicities characterized by oxygen radical-induced tissue damage, and so there is a growing interest in understanding the regulation of these enzymes.

Disease States and XOR Regulation

The prototypic XOR-involved disease state is ischemia-reperfusion injury, which appears to promote formation of the oxidase form (91). A number of steps involved in the conversion from XDH to XOD have recently been elucidated in detail. The exact mechanism of switching between these two forms is beyond the scope of this discussion, but in brief, cysteine oxidation or proteolysis ultimately results in structural changes around the FAD that block the approach of NAD^+ and increase the reactivity toward O_2 (92,93). The newly formed oxidase is thought to act on the substantial amounts of hypoxanthine that are known to accumulate because of the breakdown of ATP during ischemia, producing ROS (94). However, there has been considerable debate over the necessity and reasonability of the XDH to XOD transition in vivo, which is discussed in several reviews (95,96).

The wider substrate specificity of AO (see sect. "Transformation Reactions") and the increased cellular aldehyde levels during ischemia could mean that this enzyme is an important basal source of ROS under normal conditions as well as under oxidative stress. Unfortunately, most of the research on ROS damage by the molybdenum hydroxylases has been conducted with XOR, and while it is likely that AO plays an additional role, this is an area that needs to be better elucidated.

Consonant with its role in ROS production, XOR appears to be upregulated in a number of inflammatory-based diseases, particularly those with pulmonary complications (74). It was noted that inflammation was induced by cytokine and corticosteroid production, which also transcriptionally activated XOR activity (97). XOR also has a role in immunity and bacterial infection, and is implicated in lipopolysaccharide-induced cytotoxicity, mainly due to modulation of the gene transcript (98). Conversely, XOR has been hypothesized to be a conserved part of the innate immune system due to its antimicrobial effects via the production of ROS (99). XOR and/or AO appear also to be upregulated in other disease states, including ethanol-induced hepatotoxicity (100), breast cancer (101,102), atherosclerosis and coronary heart disease (103,104), and obesity (105).

Regulation by AhR and PPAR

In addition to the endogenous compounds mentioned above, molybdozyme levels are also induced by the environmental contaminant dioxin (106,107). Dioxin increases transcription via the aryl hydrocarbon receptor (AhR), analogous to the induction of CYP1 enzymes. In contrast, AOX1 mRNA and protein expression are suppressed by PPARα agonists, such as adiponectin and fenofibrate (108).

Hormonal Regulation

Steroid hormones also appear to influence the gender differences in molybdenum hydroxylase activity observed in mice. Mature females have about half the XOR activity of males, and it was initially hypothesized that there were different sex-specific isoforms (109).

However, further studies suggested that the differences were not due to distinct isoforms, but rather sex-related regulation of protein synthesis and redox potential (110,111). Estrogens appear to regulate AO at the transcriptional level, possibly by influencing the secretory pattern of growth hormone by the hypothalamus-pituitary system (112). Androgens seem to exert transcriptional control, which also may be influenced by other hormones or growth factors (62). The lower AO activity of female mice appears to be due to much lower protein levels (although similar mRNA levels) than males, which can be equalized by the addition of testosterone (111). In addition, female rats contain a more oxidized form of AO than do males, resulting in kinetically distinct enzymes (110). There are few studies examining sex differences in humans. However, neither in vivo studies employing caffeine metabolite ratios nor in vitro studies involving human liver tissue revealed a substantial sex difference in XOR or AO activity, although small sample sizes may have rendered this assessment difficult (86,113,114).

Developmental Regulation

In addition to sex-based differences, expression changes are evident throughout development. AO activity begins to increase soon after birth before reaching a plateau at four weeks in rats or one year in humans (115,116). There also appears to be an increase in XOR expression upon aging; XOR activity and expression was higher in cardiac and skeletal muscle tissue samples from old rats than in younger counterparts, and this same correlation between XOR activity and age was found in human plasma (117). Females also exhibit mammary gland tissue- and stage-dependent expression of XOR. During the final stage of pregnancy and all through lactation, prominent induction of XOR via an increase in transcript levels by lactogenic hormones is observed (75).

Genetic Regulation

Both the human *AOX1* and *XOR* genes possess a large number of SNPs, and the functional consequences of these alleles/haplotypes are still under investigation (118,119). Patients with rheumatoid arthritis exhibited two phenotypes for methotrexate hydroxylation, possibly indicating two *AOX1* genotypes, posttranslational modification of a single gene product to two AO proteins, or activity from extrahepatic enzymes (118).

Xanthinuria, a rare genetic disorder, causes loss of either XOR activity alone (type I) or dual loss of XOR and AO activity (type II), depending on the source of the genetic mutation. Mutations in *XOR* result in a loss of enzyme activity, termed "type I classical xanthinuria" (120 122), but do not affect AO activity. Unlike other molybdoproteins, AO and XOR require posttranslational sulfuration of the molybdopterin center to become catalytically active (62), and mutations in the enzyme (human molybdenum cofactor sulfurase) that carries out this activation result in loss of functional XOR and AO enzymes, called "type II classical xanthinuria" (123). This sulfuration process, as well as the many cofactors of the molybdozymes, has limited the ability to express recombinant protein, although expression of AO in *Escherichia coli* and XOR in a baculovirus-insect cell system has been reported (124,125). These technical difficulties have restricted the study of transformation reactions catalyzed by the molybdozymes to impure cytosolic preparations of enzymes purified from convenient tissue sources.

Transformation Reactions

The molybdenum hydroxylases carry out oxidation of electron-deficient sp^2-hybridized carbon atoms found, most commonly, in nitrogen heterocycles such as purines and

pyrimidines. The lowest electron density in these substrates usually occurs at carbons adjacent to the nitrogen atom(s), and so XOR-mediated metabolism of purine leads sequentially to the formation of hypoxanthine, xanthine, and ultimately, uric acid (Fig. 4). The initial hydroxyimine products are seldom isolated and normally tautomerize to α-aminoketone. Because of the high specificity of XOR for hypoxanthine and xanthine and the much more relaxed substrate selectivity of AO, most of the substrate specificity studies with mammalian forms of the molybdenum hydroxylases have been conducted with AO (62). AO is characterized by turnover numbers up to 4100 min^{-1} and a wide variety of K_m values from the low μM to low mM range (126).

Metabolism of Xenobiotics and Endogenous Compounds

AO has been suggested to be the cytosolic equivalent of the microsomal cytochrome P450 drug-metabolizing system, and indeed the enzyme often acts in concert with P450s to activate or detoxify various types of xenobiotics (62). The substrate specificities of various mammalian AO enzymes have been examined with a diverse range of substrates (79) and in a systematic fashion with a series of substituted phthalazines and quinazolines (88,127). In general, substrate substituents that increase electronegativity are favored, as evidenced by enhanced V_{max} values, because of the reduced electron density on the site of hydroxylation (127). Substituents that enhance lipophilicity generally increase affinity for AO. Although molecular orbital calculations and density functional theory methods can often predict the regiochemistry of hydroxylation by the molybdenum hydroxylases in terms of relative electronegativity at the various oxidizable positions, steric factors as well as electronic factors can influence the site of hydroxylation, and AO metabolism can be more accurately predicted than can products from xanthine oxidase catalysis (128).

Both molybdozymes (AO to a greater extent than XOR) are capable of oxidizing aldehydes to the corresponding carboxylic acids. In vivo, this reaction is carried out preferentially by ALDH; however, AO appears to have a broader aldehyde specificity than do the ALDH enzymes and is capable of metabolizing aromatic aldehydes that are not ALDH substrates (129). AO has been implicated recently in the metabolism of several important endogenous compounds that were originally considered to be metabolized by ALDH, including 5-hydroxyindoleacetaldehyde, pyridoxal, nicotinamide, and retinaldehyde (62). In fact, rabbit liver retinal oxidase, which is the enzyme responsible for the biosynthesis of retinoic acid, has been characterized and found to be identical to rabbit liver AO (130). Conceivably, tissue AO concentrations play a role in regulating cellular growth, differentiation, and morphogenesis through the modulation of retinoic acid levels.

Diagnostic Substrates and Inhibitors

Because XOR and AO have overlapping, but not identical, substrate and product specificities, it has been possible to identify both substrates and inhibitors that are selective for either of these two molybdozymes. XOR converts 1-methylxanthine, a secondary metabolite of caffeine, to 1-methyluric acid, and the urinary ratio of these two metabolites is used as an in vivo index of XOR activity (131). Allopurinol (Fig. 4C), a drug administered to patients suffering from gout, is metabolized by both XOR and AO to oxypurinol (alloxanthine), a potent, selective, tight-binding inhibitor of XOR. Allopurinol-dependent inhibition, in vitro or in vivo, can be used to evaluate XOR-dependent biotransformation because it only modestly inhibits AO (132). Recently, allopurinol derivatives have been identified as potent XOR inhibitors that also prevent the production of ROS (133). While oxypurinol is a type of mechanism-based inactivator of

XOR, febuxostat (Fig. 4C), a novel, selective non-purine inhibitor of XOR being investigated for treatment of gout (134), is a "structure-based" inhibitor that functions by filling the access channel and preventing substrate binding (135). In addition, there are hybrid-type inhibitors, such as FYX-051 (Fig. 4B), which have features of both mechanism-based and structure-based inhibitors.

A recent survey of 239 drugs demonstrated that the most potent inhibitor of AO to date is an uncompetitive inhibitor, the selective estrogen receptor modulator raloxifene (Fig. 4C) (136). Other estrogen derivatives, tamoxifen, menadione, β-carboline, isovanillin, hydralazine, and chlorpromaxine, are also reasonably selective inhibitors of AO (62). Menadione is perhaps the most widely used in vitro inhibitor of AO, and can be used together with allopurinol to discriminate between AO and XOR-catalyzed reactions (137).

Relevance to Human Drug Metabolism

AO, and to a lesser extent XOR, have been implicated in the metabolism of a growing number of therapeutic agents. Because XOR is expressed in relatively high levels in human liver and small intestine, it is involved in the first-pass metabolism and reduced bioavailability of a number of xenobiotics. While AO is not expressed significantly in human small intestine, it too appears to be involved in first-pass metabolism in the liver, and this has been utilized for the bioactivation of several prodrugs. A comprehensive review of XOR and AO involvement in drug metabolism has recently been published (63); therefore, this discussion will focus on select drugs that are substrates for these enzymes.

Anticancer and Antiviral Prodrug Oxidative Metabolism

A number of anticancer compounds are metabolized by AO and/or XOR, including members of the antimetabolite, topoisomerase inhibitor, and immunosuppressant classes of compounds. 5-Fluorouracil (5-FU) is one of the most commonly used antineoplastic agents; however, it is rapidly inactivated in the gastrointestinal tract (126). Therefore, to overcome this poor bioavailability, the prodrug 5-fluoro-pyrimidinone (Fig. 3), which lacks the keto group at ring position 4, was tested (138). Hepatic AO introduces the ring keto group, producing 5-FU, and allows for greater targeting toward liver cancers (125,137). The use of the oral prodrug also facilitates outpatient treatment as compared with intravenous 5-FU administration. Ethynyluracil is a mechanism-based inhibitor of dihydropyrimidine dehydrogenase that is often coadministered with 5-FU to prevent the latter's breakdown (126). The derivative, 5-ethynyl-2(1*H*)-pyrimidinone, was developed as a liver-selective prodrug that is rapidly oxidized to 5-ethynyluracil by AO (139).

The immunosuppressant compound 6-mercaptopurine (6-MP) must be converted to nucleotides intracellularly to be cytotoxic, and therefore exhibits competing pathways: the anabolic pathway converting 6-MP to the active nucleotide forms of the drug, and the catabolic pathways that ultimately convert 6-MP to 6-thiouric acid (Fig. 3), the major plasma and urinary metabolite (140). There are two possible routes to 6-thiouric acid, with either 8-hydroxy-6-MP (141) or 6-thioxanthine (142) as intermediates. It appears that both of these paths are employed by both molybdenum hydroxylases, and the ratio of ultimate metabolites may differ depending on route of administration or the relative activities of XOR and AO. XOR appears to have a greater propensity for producing the 6-thioxanthine intermediate, while hydroxylation at the 8-position is catalyzed primarily by AO (140). Coadminstration of purine-derivative XOR inhibitors with 6-MP decreases its inactivation, and may be a combination chemotherapy option (143). Azathioprine (Fig. 3),

a prodrug of 6-MP used to treat inflammatory bowel disease, is inactivated by AO to 8-hydroxyazathiopurine (144). After bioactivation to 6-MP, sequential metabolism by XOR occurs, ultimately forming 6-thiouric acid.

Antiviral prodrugs can also be (in)activated by the molybdenum hydroxylases. Acyclovir is a nucleoside analogue of deoxyguanosine whose oral absorption is slow and variable, requiring administration of high doses (145). Therefore, prodrugs such as famciclovir (Fig. 3), which is activated to penciclovir, were developed (146). Such prodrugs are activated by XOR and/or AO and often inactivated by the latter enzyme; e.g., AO metabolizes acyclovir to its 8-hydroxy-metabolite (63).

Whether xenobiotics are activated or inactivated by the molybdenum hydroxylases, the variability in the rates of XOR and AO metabolism must be taken into account. A patient was recently identified who formed no detectable active nucleotide metabolites upon administration of azathioprine, even though there appeared to be no deficiencies in any of her anabolic enzymes (147). The complete inactivation of azathioprine was due to very high XOR activity. In addition, the use of the molybdenum hydroxylases to activate prodrugs is not ideal for organ targeting because of their widespread distribution, and there are large differences in substrate specificity and activities between species. It was suggested that the best model for prodrug activation would be optimization using human AO in vitro before testing the efficacy in vivo in transgenic animals expressing the human enzyme (126).

CNS Drug Oxidative Metabolism

A number of drugs that act on the central nervous system are substrates for the molybdenum hydroxylases. The quinine-related racemic compound RS-8359, a reversible MAO-A inhibitor antidepressant, is metabolized by AO to its 2-keto-derivative in a stereoselective manner (148). AO had remarkable selectivity for the (*S*)-enantiomer, similar to its preference for the (9*R*)-configuration of cinchona alkaloids, such as quinine (90). Zaleplon, a sedative-hypnotic, is metabolized by P450s and AO (Fig. 3). There are three major metabolites: the P450-derived *N*-desethyl-zaleplon, the AO-derived 5-oxo-zaleplon, and the combined metabolite *N*-desethyl-5-oxo-zaleplon (149). In human tissue samples, it was shown that the oxygen atom inserted into the metabolites originated in radiolabeled water, not molecular oxygen, further implicating AO (149). AO is also thought to be the major hepatic enzyme involved in the detoxification of the neurotoxin 1-methyl-4-phenyl-1,2,3,6-tetrahydropyridine (MPTP) (150).

Iminium Ion Oxidation

AO can also act on nonaromatic iminium metabolites produced by the cytochrome P450 system from drugs such as prolintane and azapetine (Fig. 3), which are oxidized further to γ- and ε-lactam metabolites, respectively (63). The classic example of iminium ion oxidation is the AO-catalyzed metabolism of nicotine. P450s convert nicotine into nicotine-$\Delta^{1'(5')}$-iminium ion, which is then metabolized by AO to cotinine, and in the absence of the enzyme, the iminium ion accumulates (151). A nicotine derivative, N^1-methylnicotinamide (NMN), is also a common marker substrate for AO. However, it shows significant species differences in its metabolite profile; mice form approximately equal amounts of the metabolites N^1-methyl-2-pyridone-5-carboxamide (2-PY) and N^1-methyl-4-pyridone-3-carboxamide (4-PY), while humans produce mainly 2-PY (152). Recently, chimeric mice in which the liver is almost completely composed of human hepatocytes have been produced (153). On administration of NMN to these humanized

mice, 2-PY was the dominant product, demonstrating that this mouse model is valid for cytosolic AO as well as microsomal enzymes (152).

Reductive Metabolism

Both XOR and AO can catalyze reductive reactions in the presence of an adequate electron donor, such as 2-hydroxypyrimidine (AO) or xanthine (XOR) (154). Although both AO and XOR are capable of performing a number of reductive reactions, such as converting *N*-oxide derivatives to amines, many are relatively obscure reactions (63). However, there are several pharmacologically relevant drugs in which molybdenum hydroxylase catalyzed reductive metabolism is a significant biotransformation pathway. As was seen with oxidative metabolism, reductive metabolism by either enzyme can activate prodrugs, such as the anti-inflammatory sulfoxide prodrug, sulindac (Fig. 2), which is converted to the active sulfide by AO (155). XOR can also bioactivate the quinone-containing antineoplastic antibiotics doxorubicin (156) and mitomycin C, which is reduced to 2,7-diaminomitosene, a DNA-alkylating metabolite (157).

AO was also recently implicated in the metabolism of the antiretroviral drug zidovudine (AZT) (Fig. 3) (158). Whereas the reductive pathway was previously attributed to microsomal enzymes, even though inhibition by isoform-specific P450 inhibitors did not affect the formation of aminothymidine (159), the cytosolic AO-catalyzed pathway was, in fact, more active than the microsomal fraction (158). Therefore, there is potential for treating HIV infection or AIDS by coadministering an effective amount of AZT in combination with AO inhibitor(s). The anticonvulsant zonisamide (1,2-benzisoxazole-3-methanesulfonamide) is reduced to 2-sulfamoylacetyl-phenol by AO in humans, monkeys, and rabbits (Fig. 3), illustrating that (*i*) the reductive ability of AO is not species-specific and (*ii*) electron donors need to be included in order to correctly identify cytosolic metabolites (154,160).

A recently approved atypical antipsychotic agent, ziprasidone (Fig. 3), is primarily converted by AO-catalyzed reduction to ring-cleaved *S*-methyldihydroziprasidone, a pathway that accounts for two-thirds of the drug's metabolism (161). Interestingly, a study investigating AO inhibition of ziprasidone metabolism demonstrated that potent inhibitors of oxidative metabolism, such as raloxifene (K_i = 0.87 1.4 nmol/L), did not affect ziprasidone reduction, and of the over 200 drugs previously tested, many of which were potent AO inhibitors (136), only three inhibited the ring-cleavage reaction (162). Such variable inhibition of oxidative versus reductive metabolism could lessen the risk of drug-drug interactions for reductively metabolized drugs coadministered with other AO ligands (136).

CONCLUSION

While the majority of xenobiotics are detoxified via cytochrome P450-based pathways, the characterization of non-P450 routes is becoming increasingly important. Other oxidative enzymes, including FMO, XOR, and AO, may play significant roles in drug metabolism. Like P450s, these enzymes can be inducible and/or polymorphic, and their clinical relevance may be underestimated. For the enzymes discussed here (except XOR), the physiological roles are not well understood. However, like XOR, an involvement in endogenous processes may result in interactions between drugs and endogenous compounds. Although many sites of oxidative metabolism are common between both

P450 and non-P450 enzymes, the differences can be exploited for drug activation and/or targeting (145). The complementarity between these systems can also be useful in drug design to increase the number of oxidative enzymes that act on a xenobiotic, thereby decreasing the drug interaction risk, which is reported to be low in non-P450 enzymes. The development of selective inhibitors for the mammalian FMOs and molybdozymes, as well as improved recombinant systems for the latter enzymes, would provide useful tools to aid these endeavors.

ACKNOWLEDGMENTS

CMM was supported by NIH Training Grant GM07750.

REFERENCES

1. Williams JA, Hyland R, Jones BC, Smith DA, Hurst S, Goosen TC, Peterkin V, Koup JR, Ball SE. Drug drug interactions for UDP glucuronosyltransferase substrates: a pharmacokinetic explanation for typically observed low exposure (AUCi/AUC) ratios. Drug Metab Dispos 2004; 32:1201 1208.
2. Vasiliou V, Nebert DW. Analysis and update of the human aldehyde dehydrogenase (ALDH) gene family. Hum Genomics 2005; 2:138 143.
3. Strolin Benedetti M, Tipton KF, Whomsley R. Amine oxidases and monooxygenases in the in vivo metabolism of xenobiotic amines in humans: has the involvement of amine oxidases been neglected? Fundam Clin Pharmacol 2007; 21:467 480.
4. van Berkel WJ, Kamerbeek NM, Fraaije MW. Flavoprotein monooxygenases, a diverse class of oxidative biocatalysts. J Biotechnol 2006; 124:670 689.
5. Krueger SK, Williams DE. Mammalian flavin containing monooxygenases: structure/function, genetic polymorphisms and role in drug metabolism. Pharmacol Ther 2005; 106:357 387.
6. Grothusen A, Hardt J, Brautigam L, Lang D, Bocker R. A convenient method to discriminate between cytochrome P450 enzymes and flavin containing monooxygenases in human liver microsomes. Arch Toxicol 1996; 71:64 71.
7. Ring BJ, Catlow J, Lindsay TJ, Gillespie T, Roskos LK, Cerimele BJ, Swanson SP, Hamman MA, Wrighton SA. Identification of the human cytochromes P450 responsible for the in vitro formation of the major oxidative metabolites of the antipsychotic agent olanzapine. J Pharmacol Exp Ther 1996; 276:658 666.
8. Usmani KA, Karoly ED, Hodgson E, Rose RL. In vitro sulfoxidation of thioether compounds by human cytochrome P450 and flavin containing monooxygenase isoforms with particular reference to the CYP2C subfamily. Drug Metab Dispos 2004; 32:333 339.
9. Vyas PM, Roychowdhury S, Koukouritaki SB, Hines RN, Krueger SK, Williams DE, Nauseef WM, Svensson CK. Enzyme mediated protein haptenation of dapsone and sulfamethoxazole in human keratinocytes: II. Expression and role of flavin containing monooxygenases and peroxidases. J Pharmacol Exp Ther 2006; 319:497 505.
10. Yanni SB, Annaert PP, Augustijns P, Bridges A, Gao Y, Benjamin DK Jr., Thakker DR. Role of flavin containing monooxygenase in oxidative metabolism of voriconazole by human liver microsomes. Drug Metab Dispos 2008; 36:1119 1125.
11. Beaty NB, Ballou DP. The oxidative half reaction of liver microsomal FAD containing monooxygenase. J Biol Chem 1981; 256:4619 4625.
12. Beaty NB, Ballou DP. The reductive half reaction of liver microsomal FAD containing monooxygenase. J Biol Chem 1981; 256:4611 4618.
13. Ziegler DM. Flavin containing monooxygenases: catalytic mechanism and substrate specificities. Drug Metab Rev 1988; 19:1 32.
14. Eswaramoorthy S, Bonanno JB, Burley SK, Swaminathan S. Mechanism of action of a flavin containing monooxygenase. Proc Natl Acad Sci U S A 2006; 103:9832 9837.

15. Yeung CK, Adman ET, Rettie AE. Functional characterization of genetic variants of human FMO3 associated with trimethylaminuria. Arch Biochem Biophys 2007; 464:251 259.
16. Koukouritaki SB, Poch MT, Henderson MC, Siddens LK, Krueger SK, VanDyke JE, Williams DE, Pajewski NM, Wang T, Hines RN. Identification and functional analysis of common human flavin containing monooxygenase 3 genetic variants. J Pharmacol Exp Ther 2007; 320:266 273.
17. Lawton MP, Cashman JR, Cresteil T, Dolphin CT, Elfarra AA, Hines RN, Hodgson E, Kimura T, Ozols J, Phillips IR, Philpot RM, Poulsen LL, Rettie AE, Shephard EA, Williams DE, Ziegler DM. A nomenclature for the mammalian flavin containing monooxygenase gene family based on amino acid sequence identities. Arch Biochem Biophys 1994; 308:254 257.
18. Hines RN, Hopp KA, Franco J, Saeian K, Begun FP. Alternative processing of the human FMO6 gene renders transcripts incapable of encoding a functional flavin containing monooxygenase. Mol Pharmacol 2002; 62:320 325.
19. Hernandez D, Janmohamed A, Chandan P, Phillips IR, Shephard EA. Organization and evolution of the flavin containing monooxygenase genes of human and mouse: identification of novel gene and pseudogene clusters. Pharmacogenetics 2004; 14:117 130.
20. Zhang J, Cashman JR. Quantitative analysis of FMO gene mRNA levels in human tissues. Drug Metab Dispos 2006; 34:19 26.
21. Nishimura M, Naito S. Tissue specific mRNA expression profiles of human phase I metabolizing enzymes except for cytochrome P450 and phase II metabolizing enzymes. Drug Metab Pharmacokinet 2006; 21:357 374.
22. Haining RL, Hunter AP, Sadeque AJ, Philpot RM, Rettie AE. Baculovirus mediated expression and purification of human FMO3: catalytic, immunochemical, and structural characterization. Drug Metab Dispos 1997; 25:790 797.
23. Overby LH, Carver GC, Philpot RM. Quantitation and kinetic properties of hepatic microsomal and recombinant flavin containing monooxygenases 3 and 5 from humans. Chem Biol Interact 1997; 106:29 45.
24. Koukouritaki SB, Simpson P, Yeung CK, Rettie AE, Hines RN. Human hepatic flavin containing monooxygenases 1 (FMO1) and 3 (FMO3) developmental expression. Pediatr Res 2002; 51:236 243.
25. Yeung CK, Lang DH, Thummel KE, Rettie AE. Immunoquantitation of FMO1 in human liver, kidney, and intestine. Drug Metab Dispos 2000; 28:1107 1111.
26. Whetstine JR, Yueh MF, McCarver DG, Williams DE, Park CS, Kang JH, Cha YN, Dolphin CT, Shephard EA, Phillips IR, Hines RN. Ethnic differences in human flavin containing monooxygenase 2 (FMO2) polymorphisms: detection of expressed protein in African Americans. Toxicol Appl Pharmacol 2000; 168:216 224.
27. Itagaki K, Carver GT, Philpot RM. Expression and characterization of a modified flavin containing monooxygenase 4 from humans. J Biol Chem 1996; 271:20102 20107.
28. Fisher MB, Lawton MP, Atta Asafo Adjei E, Philpot RM, Rettie AE. Selectivity of flavin containing monooxygenase 5 for the (*S*) sulfoxidation of short chain aralkyl sulfides. Drug Metab Dispos 1995; 23:1431 1433.
29. Falls JG, Ryu DY, Cao Y, Levi PE, Hodgson E. Regulation of mouse liver flavin containing monooxygenases 1 and 3 by sex steroids. Arch Biochem Biophys 1997; 342:212 223.
30. Fisher MB, Yoon K, Vaughn ML, Strelevitz TJ, Foti RS. Flavin containing monooxygenase activity in hepatocytes and microsomes: in vitro characterization and in vivo scaling of benzydamine clearance. Drug Metab Dispos 2002; 30:1087 1093.
31. Klick DE, Hines RN. Mechanisms regulating human FMO3 transcription. Drug Metab Rev 2007; 39:419 442.
32. Devereux TR, Fouts JR. Effect of pregnancy or treatment with certain steroids on N,N dimethylaniline demethylation and N oxidation by rabbit liver or lung microsomes. Drug Metab Dispos 1975; 3:254 258.
33. Lee MY, Smiley S, Kadkhodayan S, Hines RN, Williams DE. Developmental regulation of flavin containing monooxygenase (FMO) isoforms 1 and 2 in pregnant rabbit. Chem Biol Interact 1995; 96:75 85.

34. Hukkanen J, Dempsey D, Jacob P III, Benowitz NL. Effect of pregnancy on a measure of FMO3 activity. Br J Clin Pharmacol 2005; 60:224 226.
35. Shimizu M, Cashman JR, Yamazaki H. Transient trimethylaminuria related to menstruation. BMC Med Genet 2007; 8:2.
36. Dolphin CT, Janmohamed A, Smith RL, Shephard EA, Phillips IR. Missense mutation in flavin containing mono oxygenase 3 gene, FMO3, underlies fish odour syndrome. Nat Genet 1997; 17:491 494.
37. Zhou J, Shephard EA. Mutation, polymorphism and perspectives for the future of human flavin containing monooxygenase 3. Mutat Res 2006; 612:165 171.
38. Lang DH, Yeung CK, Peter RM, Ibarra C, Gasser R, Itagaki K, Philpot RM, Rettie AE. Isoform specificity of trimethylamine N oxygenation by human flavin containing monoox ygenase (FMO) and P450 enzymes: selective catalysis by FMO3. Biochem Pharmacol 1998; 56:1005 1012.
39. Hines RN, Luo Z, Hopp KA, Cabacungan ET, Koukouritaki SB, McCarver DG. Genetic variability at the human FMO1 locus: significance of a basal promoter yin yang 1 element polymorphism (FMO1*6). J Pharmacol Exp Ther 2003; 306:1210 1218.
40. Cashman JR, Akerman BR, Forrest SM, Treacy EP. Population specific polymorphisms of the human FMO3 gene: significance for detoxication. Drug Metab Dispos 2000; 28:169 173.
41. Stormer E, Roots I, Brockmoller J. Benzydamine *N* oxidation as an index reaction reflecting FMO activity in human liver microsomes and impact of FMO3 polymorphisms on enzyme activity. Br J Clin Pharmacol 2000; 50:553 561.
42. Poulsen LL, Ziegler DM. The liver microsomal FAD containing monooxygenase. Spectral characterization and kinetic studies. J Biol Chem 1979; 254:6449 6455.
43. Ziegler DM. The 1990 Bernard B. Brodie Award Lecture. Unique properties of the enzymes of detoxication. Drug Metab Dispos 1991; 19:847 852.
44. Ziegler DM. Recent studies on the structure and function of multisubstrate flavin containing monooxygenases. Annu Rev Pharmacol Toxicol 1993; 33:179 199.
45. Ziegler DM. An overview of the mechanism, substrate specificities, and structure of FMOs. Drug Metab Rev 2002; 34:503 511.
46. Seto Y, Guengerich FP. Partitioning between *N* dealkylation and *N* oxygenation in the oxidation of *N,N* dialkylarylamines catalyzed by cytochrome P450 2B1. J Biol Chem 1993; 268:9986 9997.
47. Ballard JE, Prueksaritanont T, Tang C. Hepatic metabolism of MK 0457, a potent aurora kinase inhibitor: interspecies comparison and role of human cytochrome P450 and flavin containing monooxygenase. Drug Metab Dispos 2007; 35:1447 1451.
48. Lang DH, Rettie AE. In vitro evaluation of potential in vivo probes for human flavin containing monooxygenase (FMO): metabolism of benzydamine and caffeine by FMO and P450 isoforms. Br J Clin Pharmacol 2000; 50:311 314.
49. Kawaji A, Ohara K, Takabatake E. An assay of flavin containing monooxygenase activity with benzydamine *N* oxidation. Anal Biochem 1993; 214:409 412.
50. Yeung CK, Rettie AE. Benzydamine *N* oxygenation as a measure of flavin containing monooxygenase activity. Methods Mol Biol 2006; 320:157 162.
51. Guo Z, Raeissi S, White RB, Stevens JC. Orphenadrine and methimazole inhibit multiple cytochrome P450 enzymes in human liver microsomes. Drug Metab Dispos 1997; 25:390 393.
52. Adali O, Carver GC, Philpot RM. Modulation of human flavin containing monooxygenase 3 activity by tricyclic antidepressants and other agents: importance of residue 428. Arch Biochem Biophys 1998; 358:92 97.
53. Park SB, Jacob P III, Benowitz NL, Cashman JR. Stereoselective metabolism of (*S*) ( ) nicotine in humans: formation of trans (*S*) ( ) nicotine *N* 1′ oxide. Chem Res Toxicol 1993; 6:880 888.
54. Parte P, Kupfer D. Oxidation of tamoxifen by human flavin containing monooxygenase (FMO) 1 and FMO3 to tamoxifen *N* oxide and its novel reduction back to tamoxifen by human cytochromes P450 and hemoglobin. Drug Metab Dispos 2005; 33:1446 1452.
55. Mushiroda T, Douya R, Takahara E, Nagata O. The involvement of flavin containing monooxygenase but not CYP3A4 in metabolism of itopride hydrochloride, a gastroprokinetic agent: comparison with cisapride and mosapride citrate. Drug Metab Dispos 2000; 28:1231 1237.

56. Kousba A, Soll R, Yee S, Martin M. Cyclic conversion of the novel Src kinase inhibitor [7 (2,6 dichloro phenyl) 5 methyl benzo[1,2,4]triazin 3 yl] [4 (2 pyrrolid in 1 yl ethoxy) phenyl] amine (TG100435) and Its *N* oxide metabolite by flavin containing monoxygenases and cytochrome P450 reductase. Drug Metab Dispos 2007; 35:2242 2251.
57. Chung WG, Park CS, Roh HK, Lee WK, Cha YN. Oxidation of ranitidine by isozymes of flavin containing monooxygenase and cytochrome P450. Jpn J Pharmacol 2000; 84:213 220.
58. Hamman MA, Haehner Daniels BD, Wrighton SA, Rettie AE, Hall SD. Stereoselective sulfoxidation of sulindac sulfide by flavin containing monooxygenases. Comparison of human liver and kidney microsomes and mammalian enzymes. Biochem Pharmacol 2000; 60:7 17.
59. Attar M, Dong D, Ling KH, Tang Liu DD. Cytochrome P450 2C8 and flavin containing monooxygenases are involved in the metabolism of tazarotenic acid in humans. Drug Metab Dispos 2003; 31:476 481.
60. Pike MG, Martin YN, Mays DC, Benson LM, Naylor S, Lipsky JJ. Roles of FMO and CYP450 in the metabolism in human liver microsomes of S methyl N,N diethyldithiocarbamate, a disulfiram metabolite. Alcohol Clin Exp Res 1999; 23:1173 1179.
61. Karanam BV, Hop CE, Liu DQ, Wallace M, Dean D, Satoh H, Komuro M, Awano K, Vincent SH. In vitro metabolism of MK 0767 [(±) 5 [(2,4 dioxothiazolidin 5 yl)methyl] 2 methoxy *N* [[(4 trifluoromethyl) phenyl]methyl]benzamide], a peroxisome proliferator activated recep tor α/γ agonist. I. Role of cytochrome P450, methyltransferases, flavin monooxygenases, and esterases. Drug Metab Dispos 2004; 32:1015 1022.
62. Garattini E, Fratelli M, Terao M. Mammalian aldehyde oxidases: genetics, evolution and biochemistry. Cell Mol Life Sci 2008; 65:1019 1048.
63. Kitamura S, Sugihara K, Ohta S. Drug metabolizing ability of molybdenum hydroxylases. Drug Metab Pharmacokinet 2006; 21:83 98.
64. Romão MJ, Archer M, Moura I, Moura JJ, LeGall J, Engh R, Schneider M, Hof P, Huber R. Crystal structure of the xanthine oxidase related aldehyde oxido reductase from *D. gigas*. Science 1995; 270:1170 1176.
65. Huber R, Hof P, Duarte RO, Moura JJ, Moura I, Liu MY, LeGall J, Hille R, Archer M, Romão MJ. A structure based catalytic mechanism for the xanthine oxidase family of molybdenum enzymes. Proc Natl Acad Sci U S A 1996; 93:8846 8851.
66. Doonan CJ, Stockert A, Hille R, George GN. Nature of the catalytically labile oxygen at the active site of xanthine oxidase. J Am Chem Soc 2005; 127:4518 4522.
67. Okamoto K, Matsumoto K, Hille R, Eger BT, Pai EF, Nishino T. The crystal structure of xanthine oxidoreductase during catalysis: implications for reaction mechanism and enzyme inhibition. Proc Natl Acad Sci U S A 2004; 101:7931 7936.
68. Xia M, Dempski R, Hille R. The reductive half reaction of xanthine oxidase. Reaction with aldehyde substrates and identification of the catalytically labile oxygen. J Biol Chem 1999; 274:3323 3330.
69. Truglio JJ, Theis K, Leimkuhler S, Rappa R, Rajagopalan KV, Kisker C. Crystal structures of the active and alloxanthine inhibited forms of xanthine dehydrogenase from *Rhodobacter capsulatus*. Structure 2002; 10:115 125.
70. Pauff JM, Hemann CF, Junemann N, Leimkuhler S, Hille R. The role of arginine 310 in catalysis and substrate specificity in xanthine dehydrogenase from *Rhodobacter capsulatus*. J Biol Chem 2007; 282:12785 12790.
71. Choi EY, Stockert AL, Leimkuhler S, Hille R. Studies on the mechanism of action of xanthine oxidase. J Inorg Biochem 2004; 98:841 848.
72. Nishino T, Okamoto K. The role of the [2Fe 2S] cluster centers in xanthine oxidoreductase. J Inorg Biochem 2000; 82:43 49.
73. Harris CM, Massey V. The reaction of reduced xanthine dehydrogenase with molecular oxygen. Reaction kinetics and measurement of superoxide radical. J Biol Chem 1997; 272:8370 8379.
74. Boueiz A, Damarla M, Hassoun PM. Xanthine oxidoreductase in respiratory and cardiovas cular disorders. Am J Physiol Lung Cell Mol Physiol 2008; 294:L830 L840.

75. Garattini E, Mendel R, Romao MJ, Wright R, Terao M. Mammalian molybdo flavoenzymes, an expanding family of proteins: structure, genetics, regulation, function and pathophysiology. Biochem J 2003; 372:15 32.
76. Turner NA, Doyle WA, Ventom AM, Bray RC. Properties of rabbit liver aldehyde oxidase and the relationship of the enzyme to xanthine oxidase and dehydrogenase. Eur J Biochem 1995; 232:646 657.
77. Terao M, Kurosaki M, Barzago MM, Varasano E, Boldetti A, Bastone A, Fratelli M, Garattini E. Avian and canine aldehyde oxidases. Novel insights into the biology and evolution of molybdo flavoenzymes. J Biol Chem 2006; 281:19748 19761.
78. Terao M, Kurosaki M, Demontis S, Zanotta S, Garattini E. Isolation and characterization of the human aldehyde oxidase gene: conservation of intron/exon boundaries with the xanthine oxidoreductase gene indicates a common origin. Biochem J 1998; 332:383 393.
79. Beedham C. Molybdenum hydroxylases: biological distribution and substrate inhibitor specificity. Prog Med Chem 1987; 24:85 127.
80. Vorbach C, Scriven A, Capecchi MR. The housekeeping gene xanthine oxidoreductase is necessary for milk fat droplet enveloping and secretion: gene sharing in the lactating mammary gland. Genes Dev 2002; 16:3223 3235.
81. Moriwaki Y, Yamamoto T, Yamakita J, Takahashi S, Higashino K. Comparative localization of aldehyde oxidase and xanthine oxidoreductase activity in rat tissues. Histochem J 1998; 30:69 74.
82. Strolin Benedetti M, Whomsley R, Baltes E. Involvement of enzymes other than CYPs in the oxidative metabolism of xenobiotics. Expert Opin Drug Metab Toxicol 2006; 2:895 921.
83. Vila R, Kurosaki M, Barzago MM, Kolek M, Bastone A, Colombo L, Salmona M, Terao M, Garattini E. Regulation and biochemistry of mouse molybdo flavoenzymes. The DBA/2 mouse is selectively deficient in the expression of aldehyde oxidase homologues 1 and 2 and represents a unique source for the purification and characterization of aldehyde oxidase. J Biol Chem 2004; 279:8668 8683.
84. Itoh K, Masubuchi A, Sasaki T, Adachi M, Watanabe N, Nagata K, Yamazoe Y, Hiratsuka M, Mizugaki M, Tanaka Y. Genetic polymorphism of aldehyde oxidase in Donryu rats. Drug Metab Dispos 2007; 35:734 739.
85. Al Salmy HS. Inter strain variability in aldehyde oxidase activity in the mouse. Comp Biochem Physiol C Toxicol Pharmacol 2002; 132:341 347.
86. Al Salmy HS. Individual variation in hepatic aldehyde oxidase activity. IUBMB Life 2001; 51:249 253.
87. Sugihara K, Kitamura S, Tatsumi K, Asahara T, Dohi K. Differences in aldehyde oxidase activity in cytosolic preparations of human and monkey liver. Biochem Mol Biol Int 1997; 41:1153 1160.
88. Beedham C, Bruce SE, Critchley DJ, Rance DJ. 1 substituted phthalazines as probes of the substrate binding site of mammalian molybdenum hydroxylases. Biochem Pharmacol 1990; 39:1213 1221.
89. Beedham C, Critchley DJ, Rance DJ. Substrate specificity of human liver aldehyde oxidase toward substituted quinazolines and phthalazines: a comparison with hepatic enzyme from guinea pig, rabbit, and baboon. Arch Biochem Biophys 1995; 319:481 490.
90. Beedham C, al Tayib Y, Smith JA. Role of guinea pig and rabbit hepatic aldehyde oxidase in oxidative in vitro metabolism of cinchona antimalarials. Drug Metab Dispos 1992; 20:889 895.
91. McCord JM. Oxygen derived free radicals in postischemic tissue injury. N Engl J Med 1985; 312:159 163.
92. Kuwabara Y, Nishino T, Okamoto K, Matsumura T, Eger BT, Pai EF. Unique amino acids cluster for switching from the dehydrogenase to oxidase form of xanthine oxidoreductase. Proc Natl Acad Sci U S A 2003; 100:8170 8175.
93. Nishino T, Okamoto K, Kawaguchi Y, Hori H, Matsumura T, Eger BT, Pai EF. Mechanism of the conversion of xanthine dehydrogenase to xanthine oxidase: identification of the two cysteine disulfide bonds and crystal structure of a non convertible rat liver xanthine dehydrogenase mutant. J Biol Chem 2005; 280:24888 24894.

94. Hille R, Nishino T. Flavoprotein structure and mechanism. 4. Xanthine oxidase and xanthine dehydrogenase. FASEB J 1995; 9:995 1003.
95. Harrison R. Structure and function of xanthine oxidoreductase: Where are we now? Free Radic Biol Med 2002; 33:774 797.
96. Maia L, Duarte RO, Ponces Freire A, Moura JJ, Mira L. NADH oxidase activity of rat and human liver xanthine oxidoreductase: potential role in superoxide production. J Biol Inorg Chem 2007; 12:777 787.
97. Pfeffer KD, Huecksteadt TP, Hoidal JR. Xanthine dehydrogenase and xanthine oxidase activity and gene expression in renal epithelial cells. Cytokine and steroid regulation. J Immunol 1994; 153:1789 1797.
98. Kurosaki M, Li Calzi M, Scanziani E, Garattini E, Terao M. Tissue and cell specific expression of mouse xanthine oxidoreductase gene in vivo: regulation by bacterial lipopolysaccharide. Biochem J 1995; 306(pt 1):225 234.
99. Vorbach C, Harrison R, Capecchi MR. Xanthine oxidoreductase is central to the evolution and function of the innate immune system. Trends Immunol 2003; 24:512 517.
100. Shaw S, Jayatilleke E. The role of aldehyde oxidase in ethanol induced hepatic lipid peroxidation in the rat. Biochem J 1990; 268:579 583.
101. Seymour KJ, Roberts LE, Fini MA, Parmley LA, Oustitch TL, Wright RM. Stress activation of mammary epithelial cell xanthine oxidoreductase is mediated by p38 MAPK and CCAAT/ enhancer binding protein β. J Biol Chem 2006; 281:8545 8558.
102. Page S, Powell D, Benboubetra M, Stevens CR, Blake DR, Selase F, Wolstenholme AJ, Harrison R. Xanthine oxidoreductase in human mammary epithelial cells: activation in response to inflammatory cytokines. Biochim Biophys Acta 1998; 1381:191 202.
103. Guzik TJ, Sadowski J, Guzik B, Jopek A, Kapelak B, Przybylowski P, Wierzbicki K, Korbut R, Harrison DG, Channon KM. Coronary artery superoxide production and Nox isoform expression in human coronary artery disease. Arterioscler Thromb Vasc Biol 2006; 26:333 339.
104. Vendrov AE, Madamanchi NR, Hakim ZS, Rojas M, Runge MS. Thrombin and NAD(P)H oxidase mediated regulation of CD44 and BMP4 Id pathway in VSMC, restenosis, and atherosclerosis. Circ Res 2006; 98:1254 1263.
105. Cheung KJ, Tzameli I, Pissios P, Rovira I, Gavrilova O, Ohtsubo T, Chen Z, Finkel T, Flier JS, Friedman JM. Xanthine oxidoreductase is a regulator of adipogenesis and PPARγ activity. Cell Metab 2007; 5:115 128.
106. Sugihara K, Kitamura S, Yamada T, Ohta S, Yamashita K, Yasuda M, Fujii Kuriyama Y. Aryl hydrocarbon receptor (AhR) mediated induction of xanthine oxidase/xanthine dehydrogenase activity by 2,3,7,8 tetrachlorodibenzo p dioxin. Biochem Biophys Res Commun 2001; 281:1093 1099.
107. Rivera SP, Choi HH, Chapman B, Whitekus MJ, Terao M, Garattini E, Hankinson O. Identification of aldehyde oxidase 1 and aldehyde oxidase homologue 1 as dioxin inducible genes. Toxicology 2005; 207:401 409.
108. Neumeier M, Weigert J, Schaffler A, Weiss TS, Schmidl C, Buttner R, Bollheimer C, Aslanidis C, Scholmerich J, Buechler C. Aldehyde oxidase 1 is highly abundant in hepatic steatosis and is downregulated by adiponectin and fenofibric acid in hepatocytes in vitro. Biochem Biophys Res Commun 2006; 350:731 735.
109. Beedham C. Molybdenum hydroxylases as drug metabolizing enzymes. Drug Metab Rev 1985; 16:119 156.
110. Wright RM, Clayton DA, Riley MG, McManaman JL, Repine JE. cDNA cloning, sequencing, and characterization of male and female rat liver aldehyde oxidase (rAOX1). Differences in redox status may distinguish male and female forms of hepatic APX. J Biol Chem 1999; 274:3878 3886.
111. Kurosaki M, Demontis S, Barzago MM, Garattini E, Terao M. Molecular cloning of the cDNA coding for mouse aldehyde oxidase: tissue distribution and regulation in vivo by testosterone. Biochem J 1999; 341(pt 1):71 80.
112. Yoshihara S, Tatsumi K. Involvement of growth hormone as a regulating factor in sex differences of mouse hepatic aldehyde oxidase. Biochem Pharmacol 1997; 53:1099 1105.

113. Relling MV, Lin JS, Ayers GD, Evans WE. Racial and gender differences in N acetyltransferase, xanthine oxidase, and CYP1A2 activities. Clin Pharmacol Ther 1992; 52:643 658.
114. Guerciolini R, Szumlanski C, Weinshilboum RM. Human liver xanthine oxidase: nature and extent of individual variation. Clin Pharmacol Ther 1991; 50:663 672.
115. Tayama Y, Miyake K, Sugihara K, Kitamura S, Kobayashi M, Morita S, Ohta S, Kihira K. Developmental changes of aldehyde oxidase activity in young Japanese children. Clin Pharmacol Ther 2007; 81:567 572.
116. Tayama Y, Moriyasu A, Sugihara K, Ohta S, Kitamura S. Developmental changes of aldehyde oxidase in postnatal rat liver. Drug Metab Pharmacokinet 2007; 22:119 124.
117. Aranda R, Domenech E, Rus AD, Real JT, Sastre J, Vina J, Pallardo FV. Age related increase in xanthine oxidase activity in human plasma and rat tissues. Free Radic Res 2007; 41:1195 1200.
118. Baggott JE, Bridges SL, Morgan SL. Evidence for two phenotypes in the metabolism of methotrexate to 7 hydroxymethotrexate in patients with rheumatoid arthritis. Arthritis Rheum 2005; 52:356 358.
119. Kudo M, Moteki T, Sasaki T, Konno Y, Ujiie S, Onose A, Mizugaki M, Ishikawa M, Hiratsuka M. Functional characterization of human xanthine oxidase allelic variants. Pharmacogenet Genomics 2008; 18:243 251.
120. Gok F, Ichida K, Topaloglu R. Mutational analysis of the xanthine dehydrogenase gene in a Turkish family with autosomal recessive classical xanthinuria. Nephrol Dial Transplant 2003; 18:2278 2283.
121. Ichida K, Amaya Y, Kamatani N, Nishino T, Hosoya T, Sakai O. Identification of two mutations in human xanthine dehydrogenase gene responsible for classical type I xanthinuria. J Clin Invest 1997; 99:2391 2397.
122. Levartovsky D, Lagziel A, Sperling O, Liberman U, Yaron M, Hosoya T, Ichida K, Peretz H. XDH gene mutation is the underlying cause of classical xanthinuria: a second report. Kidney Int 2000; 57:2215 2220.
123. Peretz H, Naamati MS, Levartovsky D, Lagziel A, Shani E, Horn I, Shalev H, Landau D. Identification and characterization of the first mutation (Arg776Cys) in the C terminal domain of the human molybdenum cofactor sulfurase (HMCS) associated with type II classical xanthinuria. Mol Genet Metab 2007; 91:23 29.
124. Adachi M, Itoh K, Masubuchi A, Watanabe N, Tanaka Y. Construction and expression of mutant cDNAs responsible for genetic polymorphism in aldehyde oxidase in Donryu strain rats. J Biochem Mol Biol 2007; 40:1021 1027.
125. Nishino T, Amaya Y, Kawamoto S, Kashima Y, Okamoto K. Purification and characterization of multiple forms of rat liver xanthine oxidoreductase expressed in baculovirus insect cell system. J Biochem 2002; 132:597 606.
126. Rooseboom M, Commandeur JN, Vermeulen NP. Enzyme catalyzed activation of anticancer prodrugs. Pharmacol Rev 2004; 56:53 102.
127. Ghafourian T, Rashidi MR. Quantitative study of the structural requirements of phthalazine/quinazoline derivatives for interaction with human liver aldehyde oxidase. Chem Pharm Bull (Tokyo) 2001; 49:1066 1071.
128. Torres RA, Korzekwa KR, McMasters DR, Fandozzi CM, Jones JP. Use of density functional calculations to predict the regioselectivity of drugs and molecules metabolized by aldehyde oxidase. J Med Chem 2007; 50:4642 4647.
129. Wroczyński P, Wierzchowski J. Aromatic aldehydes as fluorogenic indicators for human aldehyde dehydrogenases and oxidases: substrate and isozyme specificity. Analyst 2000; 125:511 516.
130. Tomita S, Tsujita M, Ichikawa Y. Retinal oxidase is identical to aldehyde oxidase. FEBS Lett 1993; 336:272 274.
131. Miners JO, Birkett DJ. The use of caffeine as a metabolic probe for human drug metabolizing enzymes. Gen Pharmacol 1996; 27:245 249.
132. Pacher P, Nivorozhkin A, Szabo C. Therapeutic effects of xanthine oxidase inhibitors: renaissance half a century after the discovery of allopurinol. Pharmacol Rev 2006; 58:87 114.

133. Tamta H, Kalra S, Mukhopadhyay AK. Biochemical characterization of some pyrazolopyrimidine based inhibitors of xanthine oxidase. Biochemistry (Mosc) 2006; 71(suppl 1):S49 S54.
134. Yu K H. Febuxostat: a novel non purine selective inhibitor of xanthine oxidase for the treatment of hyperuricemia in gout. Recent Patents Inflamm Allergy Drug Discov 2007; 1:69 75.
135. Okamoto K, Nishino T. Crystal structures of mammalian xanthine oxidoreductase bound with various inhibitors: allopurinol, febuxostat, and FYX 051. J Nippon Med Sch 2008; 75:2 3.
136. Obach RS, Huynh P, Allen MC, Beedham C. Human liver aldehyde oxidase: inhibition by 239 drugs. J Clin Pharmacol 2004; 44:7 19.
137. Ueda O, Kitamura S, Ohashi K, Sugihara K, Ohta S. Xanthine oxidase catalyzed metabolism of 2 nitrofluorene, a carcinogenic air pollutant, in rat skin. Drug Metab Dispos 2003; 31:367 372.
138. LoRusso PM, Prakash S, Wozniak A, Flaherty L, Zalupski M, Shields A, Sands H, Parchment R, Jasti B. Phase I clinical trial of 5 fluoro pyrimidinone (5FP), an oral prodrug of 5 fluorouracil (5FU). Invest New Drugs 2002; 20:63 71.
139. Porter DJ, Harrington JA, Almond MR, Lowen GT, Zimmerman TP, Spector T. 5 ethynyl 2 (1H) pyrimidinone: aldehyde oxidase activation to 5 ethynyluracil, a mechanism based inactivator of dihydropyrimidine dehydrogenase. Biochem Pharmacol 1994; 47:1165 1171.
140. Rashidi MR, Beedham C, Smith JS, Davaran S. In vitro study of 6 mercaptopurine oxidation catalysed by aldehyde oxidase and xanthine oxidase. Drug Metab Pharmacokinet 2007; 22:299 306.
141. Rowland K, Lennard L, Lilleyman JS. In vitro metabolism of 6 mercaptopurine by human liver cytosol. Xenobiotica 1999; 29:615 628.
142. Keuzenkamp Jansen CW, DeAbreu RA, Bokkerink JP, Lambooy MA, Trijbels JM. Metabolism of intravenously administered high dose 6 mercaptopurine with and without allopurinol treatment in patients with non Hodgkin lymphoma. J Pediatr Hematol Oncol 1996; 18:145 150.
143. Kalra S, Jena G, Tikoo K, Mukhopadhyay AK. Preferential inhibition of xanthine oxidase by 2 amino 6 hydroxy 8 mercaptopurine and 2 amino 6 purine thiol. BMC Biochem 2007; 8:8.
144. Ding TL, Benet LZ. Comparative bioavailability and pharmacokinetic studies of azathioprine and 6 mercaptopurine in the rhesus monkey. Drug Metab Dispos 1979; 7:373 377.
145. Beedham C. The role of non P450 enzymes in drug oxidation. Pharm World Sci 1997; 19:255 263.
146. Clarke SE, Harrell AW, Chenery RJ. Role of aldehyde oxidase in the in vitro conversion of famciclovir to penciclovir in human liver. Drug Metab Dispos 1995; 23:251 254.
147. Wong DR, Derijks LJ, den Dulk MO, Gemmeke EH, Hooymans PM. The role of xanthine oxidase in thiopurine metabolism: a case report. Ther Drug Monit 2007; 29:845 848.
148. Itoh K, Yamamura M, Muramatsu S, Hoshino K, Masubuchi A, Sasaki T, Tanaka Y. Stereospecific oxidation of the (S) enantiomer of RS 8359, a selective and reversible monoamine oxidase A (MAO A) inhibitor, by aldehyde oxidase. Xenobiotica 2005; 35:561 573.
149. Lake BG, Ball SE, Kao J, Renwick AB, Price RJ, Scatina JA. Metabolism of zaleplon by human liver: evidence for involvement of aldehyde oxidase. Xenobiotica 2002; 32:835 847.
150. Yoshihara S, Harada K, Ohta S. Metabolism of 1 methyl 4 phenyl 1,2,3,6 tetrahydropyridine (MPTP) in perfused rat liver: involvement of hepatic aldehyde oxidase as a detoxification enzyme. Drug Metab Dispos 2000; 28:538 543.
151. Hukkanen J, Jacob P III, Benowitz NL. Metabolism and disposition kinetics of nicotine. Pharmacol Rev 2005; 57:79 115.
152. Kitamura S, Nitta K, Tayama Y, Tanoue C, Sugihara K, Inoue T, Horie T, Ohta S. Aldehyde oxidase catalyzed metabolism of N^1 methylnicotinamide in vivo and in vitro in chimeric mice with humanized liver. Drug Metab Dispos 2008; 36:1202 1205.
153. Tateno C, Yoshizane Y, Saito N, Kataoka M, Utoh R, Yamasaki C, Tachibana A, Soeno Y, Asahina K, Hino H, Asahara T, Yokoi T, Furukawa T, Yoshizato K. Near completely humanized liver in mice shows human type metabolic responses to drugs. Am J Pathol 2004; 165:901 912.
154. Sugihara K, Kitamura S, Tatsumi K. Involvement of mammalian liver cytosols and aldehyde oxidase in reductive metabolism of zonisamide. Drug Metab Dispos 1996; 24:199 202.

155. Lee SC, Renwick AG. Sulphoxide reduction by rat and rabbit tissues in vitro. Biochem Pharmacol 1995; 49:1557 1565.
156. Yee SB, Pritsos CA. Reductive activation of doxorubicin by xanthine dehydrogenase from EMT6 mouse mammary carcinoma tumors. Chem Biol Interact 1997; 104:87 101.
157. Pritsos CA, Gustafson DL. Xanthine dehydrogenase and its role in cancer chemotherapy. Oncol Res 1994; 6:477 481.
158. Inaba T, Fayz S, Stewart DJ. Aldehyde oxidase inhibitors for treatment of AIDS. US Patent 6040434, 2000.
159. Pan Zhou XR, Cretton Scott E, Zhou XJ, Yang MX, Lasker JM, Sommadossi JP. Role of human liver P450s and cytochrome b_5 in the reductive metabolism of 3′ azido 3′ deoxythymidine (AZT) to 3′ amino 3′ deoxythymidine. Biochem Pharmacol 1998; 55:757 766.
160. Kitamura S, Ohashi KNK, Sugihara K, Hosokawa R, Akagawa Y, Ohta S. Extremely high drug reductase activity based on aldehyde oxidase in monkey liver. Biol Pharm Bull 2001; 24:856 859.
161. Beedham C, Miceli JJ, Obach RS. Ziprasidone metabolism, aldehyde oxidase, and clinical implications. J Clin Psychopharmacol 2003; 23:229 232.
162. Obach RS, Walsky RL. Drugs that inhibit oxidation reactions catalyzed by aldehyde oxidase do not inhibit the reductive metabolism of ziprasidone to its major metabolite, S methyldihydroziprasidone: an in vitro study. J Clin Psychopharmacol 2005; 25:605 608.

6
UDP-Glucuronosyltransferases

Rory P. Remmel and Jin Zhou
Department of Medicinal Chemistry, College of Pharmacy, University of Minnesota, Minneapolis, Minnesota, U.S.A.

Upendra A. Argikar
Novartis Pharmaceuticals, Cambridge, Massachusetts, U.S.A.

INTRODUCTION

The uridine diphosphate (UDP)-glycosyltransferases (EC2.4.21.17) are a group of enzymes that catalyze the transfer of sugars (glucuronic acid, glucose, and xylose) to a variety of acceptor molecules (aglycones). The sugars may be attached at aromatic and aliphatic alcohols, carboxylic acids, thiols, primary, secondary, tertiary, and aromatic amino groups, and acidic carbon atoms. In vivo, the most common reaction occurs by transfer of glucuronic acid moiety from UDP glucuronic acid (UDPGA) to an acceptor molecule. This process is termed either *glucuronidation* or *glucuronosylation.* When the enzymes catalyze this reaction, they are also referred to as UDP-glucuronosyltransferases (UGTs). The structure and function of the enzymes have been the subject of several reviews (1 4). This chapter reviews the role of these enzymes in drug-drug interactions that occur in humans.

Glucuronidation is an important step in the elimination of many important endogenous substances from the body, including bilirubin, bile acids, steroid hormones, thyroid hormones, retinoic acids, and biogenic amines such as serotonin. Many of these compounds are also substrates for sulfonyltransferases (SULTs) (2). The interplay between glucuronidation and sulfonylation (sulfation) of steroid and thyroid hormones and the corresponding hydrolytic enzymes, β-glucuronidase and sulfatase, may play an important role in development and regulation. The UGTs are expressed in many tissues, including liver, kidney, intestine, colon, adrenals, spleen, lung, skin, testes, ovaries, olfactory glands, and brain. Interactions between drugs at the enzymatic level are most likely to occur during the absorption phase in the intestine and liver or systemically in the liver, kidney, or intestine.

Given the broad array of substrates and the variety of molecular diversity, it is not surprising that there are multiple UGTs. The UGTs have been divided into two families (UGT1 and UGT2) on the basis of their sequence homology. All members of a family have at least 50% sequence identity to one another (3). The UGT1A family is encoded by

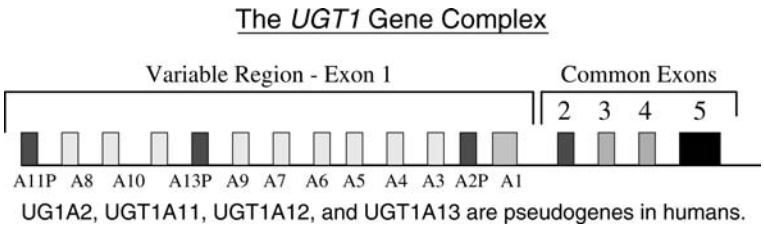

Figure 1 The *UGT1* gene complex.

a gene complex located on chromosome 2. The large UGT1A gene complex contains 13 variable region exons that are spliced onto four constant region exons that encode for amino acids on the C-terminus of the enzyme. Consequently, all enzymes in the UGT1 family have an identical C-terminus (encoding for the UDPGA binding site), but the N-terminus is highly variable, with a sequence homology of only 24 49% (3). The UGT1A enzymes are generally named in order of their proximity to the four constant region exons, i.e., UGT1A1 through UGT1A13. The arrangement (Fig. 1) appears to be conserved across all mammalian species studied to date (5). In humans, all of the gene products are functions except for pseudogenes UGT1A2, UGT1A11, UGT1A12, and UGT1A13. Pseudogenes encoding for inactive proteins vary from species to species. For example, UGT1A6 is a pseudogene in cats (6), whereas UGT1A3 and UGT1A4 are pseudogenes in rats and mice. The *UGT1A* gene complex is located on human chromosome 2 at 2q.37. Nomenclature for these enzymes in other species can be found on the UGT Web site at http://som.flinders.edu.au/FUSA/ClinPharm/UGT/.

The UGT2A subfamily represents olfactory UGTs and will not be discussed further in this review. Human UGT2A was originally cloned by Burchell and coworkers (7). The UGT2B subfamily is encoded in a series of complete UGT genes located at 4q12 on chromosome 4. Like the UGT1A enzymes, the C-terminus is highly conserved among all members of the *UGT2B* genes, with greater variation in the N-terminal half of the protein. Several human UGT2B enzymes have been cloned, expressed, and characterized for a variety of substrates. The nomenclature for the UGT2B genes has been assigned on the basis of the order of their discovery and submission to the nomenclature committee similar to that for CYP2 and CYP3 family enzymes. The human UGT2B enzymes are UGT2B4, UGT2B7, UGT2B10, UGT2B11, UGT2B15, UGT2B17, and UGT2B43.

Inhibitory interactions involving glucuronidation have been described in a number of clinical and in vitro studies and have been recently reviewed (8). Apparent decreases in the amount of glucuronide excreted in urine or bile or apparent increases in the AUC (decreased clearance) have been demonstrated in clinical studies. These apparent effects on glucuronidation could occur via several different mechanisms as follows:

1. Direct inhibition of the enzyme by competition with substrate or with UDPGA
2. Induction of the individual UGT enzymes resulting in increased clearance
3. Depletion of the UDPGA cofactor
4. Inhibition of the transport of UDPGA into the endoplasmic reticulum (ER)
5. Inhibition of the renal excretion of the glucuronide, with subsequent reconversion to the parent aglycone by β-glucuronidases (futile cycling)
6. Alteration of ER transport, sinusoidal membrane transport, or bile canalicular membrane transport of the glucuronides
7. Inhibition of the intestinal microflora, resulting in interruption of enterohepatic recycling and increased fecal excretion of the glucuronide metabolite.

Major interactions involving individual UGT enzymes will be discussed in detail along with a brief discussion of the function of each enzyme. A table of substrates, inducers, and inhibitors for the UGT enzymes is provided in the appendix to this chapter.

UGT1A1

UGT1A1 is an important enzyme that is primarily responsible for the glucuronidation of bilirubin in the liver. Cloned, expressed UGT1A1 is a glycosyltransferase that is also capable of catalyzing the formation of bilirubin xylosides and glycosides in the presence of UDP-xylose and UDP-glucose, respectively (9). In vivo, glucuronidation predominates, but bilirubin xylosides and glucosides have been identified in human bile. Polymorphisms in the UGT1A1 gene have been extensively studied because of a rare inborn error of bilirubin metabolism resulting in Crigler-Najjar syndrome. Type I Crigler-Najjar patients typically require liver transplantation, whereas Type II patients can be treated with UGT1A1 inducers such as phenobarbital. Gilbert's syndrome is an asymptomatic unconjugated hyperbilirubinemia that is most often caused by a genetic polymorphism in the promoter region of the UGT1A1 gene in Caucasians and Africans. Decreased expression of UGT1A1 in Gilbert's patients is a result of the presence of a $(TA)_7TAA$ allele (*UGT1A1*28*) in place of the more prevalent $(TA)_6TAA$ allele (10,11). Persons who are homozygous for the $(TA)_7TAA$ express approximately 70% less UGT1A1 enzyme in the liver. A second mutation at 3279 C>T in a phenobarbital response enhancer module (PBREM) also is linked with Gilbert's syndrome and is often in linkage disequilibrium with UGT1A1*28 in Caucasians and Japanese (12 14). Larger screening studies have demonstrated that this regulatory defect occurs in approximately 2 19% of various populations (11). In Asian patients, other mutations in the *UGT1A1* gene besides the $(TA)_7TAA$ genotype contribute significantly to hyperbilirubinemia, including *UGT1A1*6* (211 G>A, G71R) (15,16). Drugs that are substrates for or inhibit UGT1A1 may cause a further increase of unconjugated bilirubin concentrations, especially in patients with Gilbert's syndrome. For example, the HIV protease inhibitors atazanavir and indinavir are known to increase bilirubin levels (17). Lankisch et al. recently found that atazanavir treatment increased median bilirubin concentrations from 10 to 41 μM ($p = 0.001$) (18). Bilirubin levels exceeding 43 μM were observed in 37% of the 106 patients. Hyperbilirubinemia >43 μM was significantly associated with three non-1A1 mutations UGT1A3-66C, UGT1A7-57G, and *UGT1A7*2* along with *UGT1A1*28*, although these variants are not typically in linkage disequilibrium in other populations. Six patients expressing all four mutations had bilirubin levels >87 μM, a level that may require discontinuation or dosage adjustment. UGT1A3 is a weak catalyst of bilirubin glucuronidation, whereas UGT1A7 would not be expected to contribute given its extrahepatic tissue distribution.

Older studies in persons with mild hyperbilirubinemia (meeting the criteria for Gilbert's syndrome, but not genetically determined) demonstrated a decreased clearance rate for drugs that are glucuronidated. Clearance of acetaminophen (APAP; also catalyzed by other UGT enzymes, especially UGT1A5) was decreased by 30% in six subjects with Gilbert's syndrome (19). In contrast, a small study by Ullrich et al. demonstrated no difference in the APAP-glucuronide/acetaminophen ratio in urine of 11 persons with Gilbert's syndrome (20). A more recent study in genotyped patients also found no difference in the glucuronide/acetaminophen urinary ratio (21). Racemic (*S*/*R*) lorazepam clearance (catalyzed by UGT2B7 and UGT2B15) was 30 40% lower in persons with Gilbert's syndrome (22). A modest decrease (32%) in lamotrigine oral clearance was

observed in persons with Gilbert's syndrome (23). However, lamotrigine is glucuronidated by cloned, expressed UGT1A3 and UGT1A4, but not by UGT1A1 (24,25). In general, these studies were conducted in a small number of Gilbert's syndrome subjects. A distinct heterogeneity may be present in persons exhibiting mild hyperbilirubinemia that could include patients with Crigler-Najjar Type II syndrome who have mutations in the *UGT1A1*-coding region, persons who are homozygous for *UGT1A1*28*, or in patients with a higher than normal breakdown of heme.

The role of *UGT1A1*28* polymorphism and irinotecan toxicity has been extensively investigated in Japan by Ando et al. (26) and in the United States by Innocenti et al. (27). Irinotecan is a prodrug that is rapidly converted by esterases to active phenolic compound, SN-38. SN-38 glucuronidation is catalyzed primarily by UGT1A1 in studies with cloned, expressed enzymes. Iyer et al. compared the liver microsomal glucuronidation rate of SN-38 and bilirubin in 44 patients genotyped for the $(TA)_7TAA$ allele (*UGT1A1*28*) and found a high correlation ($r = 0.9$) (28). Patients with the *UGT1A1*28* allele who take irinotecan have a significantly higher risk for neutropenia, and the FDA has recently recommended that patients should be genotyped prior to use of irinotecan.

Evidence for drug-drug or herb-drug interactions involving UGT1A1 and irinotecan are limited (29). Case reports have suggested that inducers (e.g., phenytoin, carbamazepine, or rifampin) acting via the constitutive androstane receptor (CAR) or pregnenolone-16α-nitrile-X-receptor (pregnane-X-receptor; PXR) reduce exposure to SN-38; however, this could be due to enhanced CYP3A4-mediated metabolism of irinotecan to 7-ethyl-10-[4-N-[(5-aminopentanoic acid)-1-piperidino]-carbonyloxy-camptothecin (APC) (30) or by glucuronidation (31,32). Similar findings by Mathijssen et al. have implicated induction of SN-38 metabolism by St. John's wort (contains hyperforin, a potent PXR ligand) (33); however, evidence of increased glucuronidation in humans is lacking even though UGT1A1 is inducible by both PXR and CAR activation. Milk thistle (sylibinin) had no effect on SN-38 or SN-38 glucuronide levels (34). Sylibinin is metabolized by UGT1A1, but bioavailability is low and circulating levels are probably not high enough to affect glucuronidation. Gefitinib enhances irinotecan (SN-38) bioavailability in mice apparently via inhibition of the ABCG2 transporter (BCRP) (35). In a small study of etoposide and irinotecan, Ohtsu reported that all three patients receiving the combination had grade 3 or 4 toxicities (one neutropenia, one hepatotoxicity, and one hyperbilirubinemia) (36). Etoposide was recently shown to be a UGT1A1 substrate (37,38), so this combination should be avoided. In a single patient case report, an interaction between lopinavir/ritonavir and irinotecan was reported resulting in increased SN-38 AUC, most likely because of inhibition of CYP3A4 to APC (29,39). No reports of interactions between atazanavir or indinavir (known inhibitors of UGT1A1) and irinotecan have surfaced.

UGT1A3 AND UGT1A4

UGT1A3 and UGT1A4 appear to be important enzymes involved in the catalysis of many tertiary amine or aromatic heterocycles to form quaternary ammonium glucuronides (24,25). UGT1A3, UGT1A4, and UGT1A5 share a high nucleic acid sequence homology of 93 94% in the first variable-region exon and probably have arisen by gene duplication. The first exon of this group of enzymes appears to have diverged considerably from UGT1A1 (58% homology to 1A4), UGT1A5, and UGT1A7-10. UGT1A4 is expressed in human liver, intestine, and colon, although the level of expression of UGT1A4 mRNA is lower than that of UGT1A1 mRNA. UGT1A3 is expressed in liver, biliary epithelium,

colon, and gastric tissue. UGT1A4 has low activity for bilirubin compared with UGT1A1 and has sometimes been designated as a minor bilirubin form. Although the N-glucuronidation of UGT1A3 and UGT1A4 for a variety of tertiary amines such as imipramine, cyproheptadine, amitriptyline, tripelennamine, and diphenhydramine overlaps (K_m = 0.2 2 mM), some differences have been observed. UGT1A3 catalyzes the glucuronidation of buprenorphine, norbuprenorphine (low K_m values), morphine (3-position only), and naltrexone. Only UGT1A3 is capable of forming carboxyl-linked glucuronides of bile acids and nonsteroidal anti-inflammatory drugs (NSAIDs) (25). Fulvestrant appears to be a highly selective substrate for this enzyme (40). In contrast, N-glucuronidation of trifluoperazine and tamoxifen are selectively catalyzed by UGT1A4 and the steroidal sapogenins, hecogenin, and tigogenin are low K_m substrates (7 20 μM) for 1A4, but not 1A3. UGT1A4 has good activity for progestins, especially 5α-pregnane-3α,20α-diol and androgens such as 5α-androstane-3α,17β-diol.

Assuming that UGT1A3 and UGT1A4 are primarily responsible for the glucuronidation of tertiary amine antihistamines and antidepressants, significant drug interactions involving glucuronidation with these substrates have not been reported. This is not unexpected because <25% of the dose is excreted as a direct quaternary ammonium glucuronide in urine. The formation of quaternary ammonium glucuronides appears to be highly species specific, with the highest activity in humans and monkeys. Rats and mice are generally incapable of forming quaternary ammonium glucuronides (UGT1A3 and UGT1A4 are pseudogenes in these rodents). Lamotrigine, a novel triazine anticonvulsant, is extensively glucuronidated at the 2-position of the triazine ring in humans (>80% of the dose is excreted in human urine) (41). It is not significantly glucuronidated in rats or dogs, but 60% of the dose is excreted in guinea pig urine as the 2-*N*-glucuronide (42). Several significant interactions have been reported for lamotrigine in humans. Lamotrigine glucuronidation is induced in patients taking phenobarbital, phenytoin, or carbamazepine (CAR inducers), resulting in a twofold decrease in apparent half-life from 25 hours to approximately 12 hours (43). In contrast, valproic acid inhibits lamotrigine glucuronidation resulting in a two- to threefold increase in half-life (44). Valproic acid is a weak substrate for UGT1A4 and UGT1A3 (U Argikar, PhD thesis, University of Minnesota, 2006), but has higher affinity for UGT2B7. Lamotrigine had a small, but significant effect (25% increase) on the apparent oral clearance of valproic acid (44). This increase could be due to induction of the UGTs responsible for valproic acid glucuronidation, since chronic treatment with lamotrigine results in autoinduction. The interaction between APAP and lamotrigine has also been studied. Surprisingly, APAP decreased the lamotrigine AUC by approximately 20% after multiple oral doses in human volunteers. Lamotrigine clearance was 32% lower in seven patients with Gilbert's syndrome compared with persons with normal bilirubin levels, but it does not appear to be a substrate for UGT1A1 (23).

Polymorphisms have been identified in both UGT1A3 and UGT1A4. Iwai et al. identified four nonsynonymous single-nucleotide polymorphisms (SNPs) in the *UGT1A3* sequence of a Japanese population (n = 100) at Q6R, W11R, R45W, and V47A (45). Five allele combinations with frequencies of 0.055 to 0.13 were identified. The intrinsic clearances of estrone glucuronidation for the cloned, expressed variants were determined and the only significant difference was in the W11R-V47A variant (*UGT1A3*2*) that showed an increase of 369% due to a fivefold lower K_m value (allele frequency = 0.125). In contrast, Ehmer et al. reported that the W11R and V47A variants were much more common in German Caucasians (allele frequency = 0.65 and 0.58, respectively) (46). Chen et al. extended this work and examined activities of the variants with several other flavonoid substrates, including quercetin, luteolin, and kaempferol, and also found increased activity (47). They found that the R45W variant had 3.5 to 4.7 times higher

intrinsic clearance toward the flavonoids, whereas for estrone, activity was reduced to 70% of control (47). Regioselectivity in the glucuronidation of quercetin was also altered between variants. Two common variants in the UGT1A4 gene have also been identified, but the effect on activity appears to vary depending on the substrate. Ehmer et al. found two major variants at P24T and L48V (allele frequencies of 0.07 0.1 in Caucasians). The L48V mutant completely lost dihydrotestosterone glucuronidation activity (46), but was more efficient for 4-(methylnitrosamino)-1-(3-pyridyl)-1-butanol (NNAL) (48) and clozapine compared with wild-type UGT1A4 (49). Catalytic efficiencies for substrates such as *trans*-androsterone, imipramine, cyproheptadine, and tigogenin also changed (49).

Regulation of UGT1A4 and UGT1A3 has been recently investigated in a transgenic human UGT1A knock-in mouse model (50). UGT1A3 bile acid glucuronidation was highly upregulated by peroxisome proliferator activated receptor (PPAR)-α agonists (51). UGT1A4 activity and mRNA expression was inducible by PXR and CAR agonists. Consequently, induction interactions are likely to occur and have been demonstrated in humans as demonstrated by lamotrigine interactions with inducing anticonvulsants.

UGT1A6

UGT1A6 is the most important enzyme for the conjugation of planar phenols and amines. It displays high activity for a variety of aromatic alcohols, including 1-naphthol, 4-nitrophenol, 4-methylumbelliferone, and APAP. However, these planar phenols are substrates for several other UGT enzymes. Immunoinhibition studies with an antibody raised against the 120 amino acid N-terminal region UGT1A6 peptide fused to *Staphylococcus aureus* protein A revealed that approximately 50% of the 1-naphthol glucuronidation activity in human liver microsomes (HLMs) could be inhibited (52). Cats are highly susceptible to APAP liver toxicity because UGT1A6 is a pseudogene in this species (6). Serotonin appears to be a highly selective endogenous substrate for this enzyme (53). The first exon sequence of UGT1A6 is divergent from other UGT1A sequences, being most similar to UGT1A9 with only a 54% homology. In rats, UGT1A6 is inducible by polycyclic aromatic hydrocarbons (PAH). UGT1A6 was also induced in human hepatocytes by β-naphthoflavone and in some, but not all, hepatocyte preparations by rifampin. APAP glucuronidation appears to be increased in smokers, perhaps due to PAH-mediated induction of UGT1A6. Serotonin glucuronidation was doubled in microsomes from persons with moderate-to-heavy alcohol use (54).

Krishnaswamy discovered several variants in the UGT1A6 gene (55). The UGT1A6*2 variant (S7A/T181A/R184S) showed a twofold higher activity (lower K_m) for several substrates (serotonin 4-nitrophenol, APAP, valproic acid) when cloned and expressed in HEK-293 cells compared with wild-type enzyme; however, the K_m was higher than wild type in (*2/*2) HLMs (54). Allele frequencies in Caucasians for the S7A, T181A, and R184S variants were 0.32 to 0.37. In Japanese, the frequency of these mutations is somewhat lower (0.22) (56). Response elements for HNF1-α, Nrf-2, AhR, PXR/CAR have been identified in the regulatory region of this gene (55). In a small study of 15 β-thalassemia/hemoglobin E patients, those subjects with a *UGT1A6*2* variant without *UGT1A1*28* showed a significant, lower AUC of APAP, APAP-glucuronide, and APAP-sulfate than those of the patients with wild-type UGT1A1 and UGT1A6 (57).

Interactions involving APAP and its glucuronidation are listed in Table 1. Approximately 50% of a typical dose of APAP is glucuronidated (58). UGT1A1, UGT1A6, and UGT1A9 are the principal UGTs involved in glucuronidation. UGT1A6 is a high-affinity ($K_m = 2.2$ mM), low-capacity enzyme. UGT1A1 has intermediate affinity

Table 1 Interactions Affecting APAP Glucuronidation

Precipitant drug	Object drug	Effect	Comments	Reference
Propranolol	APAP		Fractional clearance to the glucuronide reduced by 27%. Overall CL decreased by 14%	59
Oral contraceptives	APAP		Oral metabolic clearance increased 22 61% due to increased glucuronidation	60
Phenytoin	APAP		CL increased by 46%, half life decreased by 28% glucuronide/ APAP ratio in urine increased by 41%	61,62
Probenecid	APAP		Renal elimination of glucuronide decreased from 260 to 84 mg/day	63
Rifampin	APAP		Glucuronide/APAP ratio increased by 37%	61,64

(9 mM) with high capacity, and UGT1A9 is a low-affinity, high-capacity enzyme (21 mM) (58). With a kinetic model, Court et al. estimated that at typical therapeutic concentrations (0.05 5 mM), UGT1A9 was the most important enzyme (>55% of total activity). Consequently, the mechanism of induction of APAP glucuronidation by oral contraceptives, phenytoin, and rifampin is unclear and may involve multiple enzymes.

UGT1A7, UGT1A8, UGT1A9, AND UGT1A10

There is a 93 94% sequence homology in the first exon of UGT1A7 to UGT1A10; however, these enzymes show great variation in the level of tissue expression. This group of UGT1A enzymes is highly divergent from UGT1A3 to UGT1A5 with approximately 50% identity in the first exon compared with UGT1A9. UGT1A9 is expressed in human hepatic and kidney tissues, whereas UGT1A7, UGT1A8, and UGT1A10 are expressed extrahepatically. Liver expression appears to be controlled by the presence of an HNF4-α response element at 372 to 360, that is present only in UGT1A9 and a distal response element to HNF-1 (65,66). UGT1A8 and UGT1A10 are intestinal forms (and UGT1A7 is expressed in esophagus and gastric epithelium). In both rat and rabbit, UGT1A7 is expressed in liver. The rabbit (legomorph) enzyme (UGT1A7l) displays high activity for a variety of small phenolic compounds such as 4-methylumbelliferone, p-nitrophenol, vanillin, 4-*tert*-butylphenol, and octylgallate. In addition, the rabbit enzyme is capable of catalyzing the N-glucronidation of imipramine to a quaternary ammonium glucuronide, similar to UGT1A4 (67). Rat UGT1A7 catalyzes the glucuronidation of benzo(a)pyrene phenols and is inducible by both 3-methylcholanthrene (3-MC) and oltipraz. Ciotti demonstrated that human UGT1A7 has very high activity for the glucuronidation of 7-ethyl-10-hydroxycamptothecin (SN-38), the active metabolite of irinotecan, and therefore may play a role in the gastrointestinal first-pass metabolism of this drug along with UGT1A8 and UGT1A10 (68).

UGT1A8 mRNA is expressed in human jejunum, ileum, and colon, but not in the liver or kidney. Intestinal expression of both UGT1A8 and UGT1A10 appears to be due to a caudal-related homeodomain protein (Cdx2) consensus site in the respective promoters (69). UGT1A8 catalyzes the glucuronidation of a variety of planar and bulky phenols, coumarins, flavonoids, anthroquinones, and primary aromatic amines (70). It also catalyzes the glucuronidation of several endogenous compounds, including dihydrotestosterone, 2-OH and 4-OH-estrone, estradiol, hypocholic acid, *trans*-retinoic acid, and 4-OH-retinoic acid. Several drugs are also substrates, including opioids (e.g., buprenorphine, morphine, naloxone, and naltrexone), ciprofibrate, diflunisal, furosemide, mycophenolic acid (MPA), phenolphthalein, propofol, raloxifene, 4-OH-tamoxifen, and tolcapone (70). Cloned, expressed UGT1A8 has high intrinsic clearance for the conjugation of flavonoids such as apigenin and narigenin; thus, drug-food interactions are possible, particularly if the drugs display extensive first-pass metabolism in the intestine (70).

UGT1A9 is expressed in human liver, kidney, and colon. UGT1A9 is expressed in greater amounts in kidney than in liver and is the most prevalent UGT in renal tissue. UGT1A9 is largely responsible for the glucuronidation of a variety of bulky phenols, e.g., *tert*-butylphenol and the anaesthetic agent, propofol (2,6-diisopropylphenol, commonly used as a marker substrate). Propofol is a selective substrate for UGT1A8 and UGT1A9, but extrahepatic metabolism of propofol appears to be important because propofol glucuronide is formed in substantial amounts in patients during the anhepatic phase of liver transplantation (71,72). Propofol clearance is greater than liver blood flow, also suggesting that extrahepatic metabolism is important for this compound. It is glucuronidated in vitro by human kidney and small intestinal microsomes. The V_{max} was 3 to 3.5 times higher in human kidney microsomes compared with liver or small intestine microsomes on a milligram per microsomal protein basis. A number of pharmacodynamic interactions have been reported between propofol and benzodiazepines or opoids such as fentanyl and alfentanil (73 75). Pharmacokinetic interaction studies in humans with fentanyl or alfentanil revealed a modest decrease in propofol clearance (20 50%).

UGT1A9 also catalyzes the glucuronidation of clofibric acid *S*-oxazepam, propranolol, raloxifene, valproic acid, *cis*-4-OH-tamoxifen, and several NSAIDs. These acidic drugs appear to be glucuronidated at a much faster rate by cloned, expressed UGT2B7 than by UGT1A9 on a milligram protein basis (assuming equivalent levels of expression). Formation of the phenolic ether glucuronide of MPA is catalyzed by UGT1A8 and UGT1A9, whereas the acyl glucuronide formation of MPA (a minor metabolite in HLMs) is attributable to UGT2B7. The 7-*O*-glucuronide is the predominant conjugate formed in vivo and is the major excretory metabolite of mycophenolate (90% of the dose in human urine). Tacrolimus and cyclosporine (agents commonly used with mycophenolate in transplant patients) have been shown to inhibit mycophenolate glucuronidation in vitro (76) and were later shown to be substrates for intestinal UGT2B7 (77). In renal transplant patients, cyclosporine increased MPA AUC by 1.8-fold, and sirolimus increased the AUC by 1.5-fold (78). Several investigators suggested that the effect of cyclosporine was due to inhibition of biliary excretion of the glucuronide metabolites by inhibition of organic anion transporters such as MRP2 (78 80). Relatively few clinical drug interactions with NSAIDs have been reported, although probenecid may inhibit glucuronidation directly and cause modest increases in NSAIDs concentrations (see sec. IX on probenecid).

UGT1A9 is an inducible enzyme. In a case study report, rifampin decreased MPA AUC by greater than twofold and increased the AUC of both the phenolic and acyl glucuronides (81), suggesting that there is a PXR response element in the human *UGT1A9* gene. Klaassen et al. had previously shown that mouse Ugt1a9 is upregulated by PXR

Table 2 Polymorphisms in the UGT1A8 gene

Allele	Sequence change	Amino acid substitution	Frequency
*UGT1A8*1*			0.551
*UGT1A8*1a*	765A>G	T255T	0.282
*UGT1A8*2*	518C>G	A173G	0.145
*UGT1A8*3*	830G>A	C277Y	0.022

Table 3 Polymorphisms in the UGT1A9 gene

Allele	Sequence change	Amino acid substitution	Frequency ($n = 288$) (%)
*UGT1A9*1*			97.8 (Caucasians)
*UGT1A9*2*	8G>A	C3Y	2.5 (Africans) 0 (Caucasians)
*UGT1A9*3*	98T>C	M33T	2.2 3.6 (Caucasians)
*UGT1A9*4*	726T>G	(Truncated protein)	
*UGT1A9*5*	766G>A	D256N	1.7 (Asians)

agonists (82). In rat, phenobarbital is a good general inducer of the glucuronidation of bulky phenols catalyzed by UGT1A9. UGT1A9 along with UGT1A6 were inducible by 10 μM tetrachlorodibenzodioxin (TCDD) in Caco-2 cells, a human-derived colon carcinoma cell line (83).

Four genotypes of UGT1A8 have been identified but one mutation is silent (T^{255} A>G, *UGT1A8*1a*), while the other mutations lead to base pair changes: $A^{173}C^{277}$ (UGT1A8*1), $G^{173}C^{277}$ (*UGT1A8*2*), and $A^{173}Y^{277}$ (UGT1A8*3) (84). Allele frequencies are: *1 = 0.551, *1a = 0.282, *2 = 0.145, *3 = 0.022 (Table 2). UGT1A8*1 and 1A8*2 appear to exhibit similar activities toward a variety of substrates (e.g., estrone, 4-methylumbelliferone, 17α-ethinylestradiol, hydroxybenzo(a)pyrene (all positions), benzo(a)pyrene *cis*- and *trans*-diols, and hydroxyacetylaminofluorenes). However, little activity toward any substrate was noted with the *3 variant (85). Thibaudeau et al. also found substantially lower activity with 4-OH-estradiol (2- to 3-fold lower intrinsic clearance) and 4-OH-estrone (8- to 13-fold lower intrinsic clearance) in vitro with this variant enzyme (84).

Several polymorphisms in the UGT1A9 gene have been identified (see http://galien.pha.ulaval.ca/alleles/UGT1A/UGT1A9.htm). Coding region mutants and relative frequencies are shown in Table 3. Allele frequencies for the coding region mutations are relatively uncommon (<5%). Functionally, expressed UGT1A9.3 had a drastically reduced intrinsic clearance for SN-38 glucuronidation (Table 4) (86).

A small sequencing study of Japanese cancer patients ($n = 61$) was carried out to examine the role of potential UGT1A9 polymorphisms on irinotecan metabolism. Jinno et al. reported that one patient carried a genetic variant 766 G>A, resulting in a nonsynonymous mutation of D256N (87). This variant protein was expressed in COS cells and was

Table 4 Kinetic Constants for SN 38 Glucuronidation of Wild type UGT1A9 Vs. 256N Variant

UGT1A9 variant	K_m (μM)	V_{max}[a] (pmol/min/mg protein)	Normalized V_{max}/K_m (nL/min/mg protein)
Wild type 256D	19.3	2.94	153
256N variant	44.4	0.24	7.1

[a] V_{max} and V_{max}/K_m ratios normalized for expression differences.

characterized with regard to SN-38 glucuronidation. Expression of the protein was slightly lower in COS-1 cells relative to wild type. Kinetic characterization showed large differences in SN-38 glucuronidation.

In vitro studies have indicated that two regulatory region mutations at 275 T>A and 2152 C>T may result in increased expression of UGT1A9 (81). The role of these mutations has been studied in addition to a more rare (<5% allele frequency) coding region mutation, *UGT1A9*3*, (T98C) on MPA kinetics in kidney transplant patients. The two regulatory region mutations are more common appearing in >15% of Caucasians and may result in increased protein expression. In a population of 95 kidney transplant recipients, (88) 16/95 carried only the 275 T>A mutation, 12/95 had only the 2152 C>T mutation, and 11/95 carried both mutations, although Innocenti et al. reported far lower frequencies, 0.04 and 0.03, respectively, in 132 Caucasians (89). The kinetics of MPA were not significantly altered at a 1-g dose, but in a smaller number of patients at the 2-g dose, the CL/*F* (apparent oral clearance) was increased (decreased AUC) suggesting that these regulatory region mutations increased enzyme or mRNA expression. In three heterozygote patients with a *UGT1A9*3* allele, MPA AUC increased in accordance with the low activity observed in vitro (88). Innocenti reported a linkage disequilibrium between the two regulatory mutations of UGT1A9 and the 53 $(TA)_7$ mutation of UGT1A1 (89). Glucuronidation of 4-OH-catechol estrogens was not affected in the UGT1A9.2 enzyme, but the Thr33Met mutation resulted in a 9- to 12-fold decrease in intrinsic clearance for 4-OH-estrone glucuronidation and a four- to sixfold decrease in intrinsic clearance in 4-OH-estradiol glucuronidation due to a dramatic decrease in V_{max} (86).

Like UGT1A1, there is also a common TATA box polymorphism in the UGT1A9 gene. The *UGT1A9*22* mutation contains a AT(10)AT [$118(T)_{9>10}$] repeat instead of the more common AT_9AT repeat (90). Allele frequencies were 60% in Japanese ($n = 87$), 39% in Caucasians ($n = 50$), and 44% in African Americans ($n = 50$). Innocenti found similar frequencies [53% in Asians ($n = 200$) and 39% in Caucasians ($n = 254$)] (89). When transfected into HepG2 cells, the expression level of UGT1A9.22 by Western blotting was 2.6-fold higher. Further studies will be needed to determine if this is true in vivo.

UGT1A10

UGT1A10 is expressed in intestine and kidney and is closely related to UGT1A7 to UGT1A9. Mojarrabi and Mackenzie cloned the cDNA from human colon, and it was 90% homologous to UGT1A9 (91). It is an important enzyme in the extrahepatic metabolism of estrogens (estrone and estradiol) as well as the catechol estrogens with much higher activity than other UGT1 enzymes (92). The binding motif of F90-M91-V92-F93 in UGT1A10 is essential for enzyme activity toward estrogens. When tranfected into COS-7 cells, the enzyme was very active in the conjugation of MPA, the major active metabolite of the prodrug, mycophenolate mofetil, an immunosuppressant agent used for the treatment of allograft rejection and bone marrow transplants. In vitro, the enzyme was shown to catalyze conjugation at both the phenolic hydroxyl at the 7-position and the carboxylic acid moiety to form an acyl glucuronide. Zucker et al. studied the interaction between tacrolimus and MPA in vitro and demonstrated that MPA glucuronidation was 100-fold higher in human kidney microsomes compared with HLMs (76). With a partially purified preparation of the kidney UGT, tacrolimus was found to be a potent inhibitor of MPA glucuronidation ($K_i = 27.3$ ng/mL compared with 2158 ng/mL for cyclosporin A). Both UGT1A9 and UGT1A10 are expressed in human kidney. Tacrolimus would also be

expected to affect first-pass metabolism of MPA in the intestine and liver, resulting in an increased C_{max} and AUC. Intestinal first-pass metabolism may be more attributable to UGT1A8 than UGT1A10 because Cheng et al. reported that the formation of MPA-glucuronide was 1900 pmol/min/mg protein for UGT1A8 versus 93 pmol/min/mg protein for UGT1A10 (93). UGT1A10 appears to be less active than UGT1A8 for flavonoids such as alizarin and scopoletin, but further studies will be needed to determine the relative expression levels of the enzymes in the gut. UGT1A10 has not been as extensively examined for other metabolic activities, but it may be an important enzyme in the extrahepatic metabolism of other drugs such as propofol and dobutamine. Compared with UGT1A9, a surprising opposite stereoselectivity for propranolol enantiomers was observed. UGT1A9 prefers *S*-propranolol as a substrate, whereas UGT1A10 prefers *R*-propranolol with relatively equal affinity between the two enzymes. Consequently, HLMs glucuronidate *S*-propranolol selectively, and human intestinal microsomes selectively glucuronidate the R isomer (94). Raloxifene 4-O-glucuronidation is the predominant metabolite formed by both UGT1A10 and human intestinal microsomes (95). In contrast, the 6-*O*-glucuronide of raloxifene was the major metabolite formed in Caco-2 cell lysate and no UGT1A10 mRNA was found in Caco-2 cells. These data suggest that the Caco-2 cell system may not be the optimal model to predict small intestinal glucuronidation. The very low bioavailability of raloxifene in humans (2%) is therefore attributable to UGT1A10 as well as UGT1A9 in the liver (95). Structure-activity relationships for the regioselectivity of UGT1A10 for bioflavonoids were recently studied by Lewinsky et al. (96). Thirty-four out of 42 bioflavonoids tested were UGT1A10 substrates and the 6- and 7-OH groups on the A ring were the preferred sites for glucuronidation. Thus, food-drug interactions may be problematic with substrates of this enzyme.

Variants in *UGT1A10* gene have been recently identified. Lazarus et al. have shown that the Glu139Lys mutant (*UGT1A10*2*) had significantly lower activity for *p*-nitrophenol and phenols of PAH (97). The allele frequency of this variant is rare in Caucasians (0.01%) and more prevalent but also rare in African-Americans (0.05%). Two other coding region SNPs (T202I and M59I) with a frequency of 2.1% were identified in a Japanese population (98). The V_{max} values for the M59I variant were about half of wild type for 17β-estradiol glucuronidation with a similar K_m value (98,99).

UGT2B7

UGT2B7 is an important enzyme involved in the glucuronidation of several drug substrates, including NSAIDs, morphine, 3-OH-benzodiazepines, and zidovudine (ZDV). UGT2B7 has 82% sequence homology to UGT2B4, but has <50% homology to the UGT1A family enzymes. UGT2B4 has limited activity for drug substrates such as 3-O-glucuronidation of morphine and ZDV-5′-O-glucuronidation, but is the primary catalyst for hyodeoxycholic acid glucuronidation. Ritter et al. initially cloned and expressed UGT2B7(H), a protein with a His at amino acid 268 (100). This enzyme had activity toward several steroidal substrates, including estriol and androsterone, with low activity for the bile acid and hyodeoxycholic acid. Jin et al. cloned and expressed a polymorphic variant from the same cDNA library, UGT2B7(Y), with a His268Tyr substitution. UGT2B7(Y) was expressed in COS-7 cells and was more extensively characterized for activity against a variety of drug substrates (101). The enzyme catalyzed the conjugation of several NSAIDs (naproxen, ketoprofen, ibuprofen, fenoprofen, zomipirac, diflunisal, and indomethacin) and 3-OH-benzodiazepines (temazepam, lorazepam, and oxazepam). Tephly et al. demonstrated that UGT2B7 catalyzed both the 3-O- and 6-O-glucuronidation of morphine, 6-O-glucuronidation of codeine, and the conjugation of several other opiods (102).

This group also compared the activities of UGT2B7(Y) and UGT2B7(H) that were stably expressed in HEK293 cells. Both isoforms displayed similar activity for a range of compounds. Endogenous substrates for UGT2B7(H) include 4-OH estrone, hyodeoxycholic acid, estriol, androsterone, and epitestosterone. Testosterone is a poor substrate. Other xenobiotic substrates for UGT2B7 are listed below:

Phenols and aliphatic alcohols: abacavir, APAP, almokalant, carvedilol, chloramphenicol, epirubicin, 1′-OH-estragole, 5-OH-rofecoxib, lorazepam, menthol, 4-methylumbelliferone, 1-naphthol (low), 4-nitrophenol, octylgallate, *R*-oxazepam, propranolol, temazepam, ZDV

Carboxylic acid containing drugs: a variety of NSAIDs, chloramphenicol, ciprofibrate, clofibric acid, dimethylxanthenone-4-acetic acid (DMXAA), MPA (acyl glucuronide), pitavastatin, simvastatin acid, tiaprofenic acid, and valproic acid

Other drugs: almokalant, carvedilol, carbamazepine (N-glucuronidation), clonixin, cyclosporin A, epirubicin, ezetimibe, Maxipost, tacrolimus

On the basis of the substrate activity for a variety of important drugs, one might expect that several interactions could result from competition for UGT2B7. Morphine glucuronidation has been well studied; however, relatively few clinical drug-drug interaction with morphine have been reported. In HLMs, the 3-O-glucuronidation of morphine is biphasic with a high K_m of 2 to 7 μM and a low K_m of 700 to 1600 μM. UGT2B7 is the only human UGT expressed in liver that has been shown to glucuronidate morphine to its pharmacologically active metabolite, morphine-6-glucuronide. Morphine-6-glucuronide is much more potent in binding to the μ receptor in the CNS than morphine (30- to 50-fold more potent). However, morphine-6-glucuronide has poor ability to cross the blood-brain barrier, with a permeability coefficient in rats that 1/57 that of morphine. Morphine-6-glucuronide has potency similar to the analgesic effects of morphine when administered to rats on a mg/kg basis. Since rats are unable to make morphine-6-glucuronide, this reflects a balance of poor permeability and higher CNS potency. In humans, both morphine-3-glucuronide (lacking analgesic activity) and morphine-6-glucuronide are present in higher concentrations in plasma than morphine at steady state. Competitive inhibition with other UGT2B7 substrate may not result in a significant effect on analgesic efficiency of morphine, since morphine levels would rise while morphine-6-glucuronide levels would fall. Morphine glucuronidation is inhibited by various benzodiazepines in vitro in rats, and oxazepam (20 mg/kg PO) was shown to lower the morphine-3-glucuronide/morpine ratio in urine. In vitro, the 6-O-glcuronidation of codeine in HLMs is inhibited by morphine, amitriptyline, diazepam, probenecid, and chloramphenicol with K_i values of 3.5, 0.13, 0.18, 1.7, and 0.27 mM, respectively.

Benzodiazepines containing a hydroxyl group at the 3-position, such as lorazepam, oxazepam, and temazepam, are glucuronidated by UGT2B7. (*S*)-oxazepam is a better substrate for glucuronidation in HLMs than the R isomer with a V_{max}/K_m ratio of 1.125 mL/(min·mg) protein versus 0.25 mL/(min·mg) protein. Inhibition studies with racemic ketoprofen in HLMs demonstrated competitive inhibition for (*S*)-oxazepam, with weaker inhibition of (*R*)-oxazepam glucuronidation. The data did not fit to a simple hyperbolic fit expected of a competitive inhibitor of single enzyme. (*S*)-oxazepam glucuronidation was inhibited (in order of potency) by hyodeoxycholic acid, estriol, (*S*)-naproxen, ketoprofen, ibuprofen, fenoprofen, and clofibric acid. Since these initial findings, Court et al. demonstrated that UGT2B15 is the primary catalyst for (*S*)-oxazepam glucuronidation (103). Drug interaction studies with lorazepam and clofibric acid in humans have been reported and are summarized in Table 5. A number of clinical drug-drug interactions with

Table 5 Interactions Involving UGT2B7 Substrates

Precipitant drug	Object drug	Effect	Comments	Reference
Valproate	Lorazepam	⇑	20% increase in lorazepam AUC, 31% decrease in formation CL of lorazepam glucuronide; 40% decrease in lorazepam CL	104,105
Probenecid	Lorazepam	⇑	Lorazepam CL decreased twofold, half life increased from 14 to 33 hr	63
Neomycin + Cholestyramine	Lorazepam	⇓	Half life decreased 19 26%, 34% increase in free oral CL/F, effect attributed to decreased enterohepatic circulation	106
Probenecid	Clofibric acid	⇑	Nonrenal CL decreased by 72%, free clofibric acid C_{ss} increased 3.6 fold	107
Probenecid	Diflunisal	⇑	Formation CL of phenol glucuronide and acyl glucuronide decreased 45% and 54%, respectively	108
Probenecid	Zomepirac	⇑	Zomepirac CL declined by 64%, zomepirac glucuronide CL formation decreased by 71%, urinary excretion of zomepirac glucuronide decreased from 72% to 58%	109
Probenecid	Naproxen	⇑	Decreased naproxen CL	110
Oral contraceptives	Clofibric acid	⇓	Clofibric acid CL increased 48% in women receiving oral contraceptives	111

Abbreviations: CL, clearance. C_{ss}, concentration at steady state. AUC, area under the concentration time curve.

ZDV, another selective UGT2B7 substrate, have also been reported and are discussed in a separate section X. Kiang et al. have recently reviewed the literature concerning drug-drug interactions for several UGT2B7 substrates and readers are referred to this extensive review as an additional source of information (8).

A highly prevalent polymorphism has been observed in UGT2B7. The variant of UGT2B7 with a tyrosine at position 268 instead of a histidine (UGT2B7.2) appears to affect the activity of the enzyme toward some substrates, but not all, and is highly prevalent in Caucasians and Asians. Polymorphisms for three UGT2B enzymes UGT2B4 (D458E), UGT2B7 (H268Y), and UGT2B15 (D85Y) have been identified and are shown in Table 6.

Miners et al. reported an ethnic difference in the His268Tyr (802 C>T) variant (112). In 91 Caucasians, the allele frequency for *UGT2B7*2* (802 C>T) was 0.482 versus 0.268 for 84 Japanese subjects. Patel et al. reported a potential polymorphism in the ratio

Table 6 Allele Frequency of UGT2B Variants in Caucasians and Asians

UGT2B variant	Frequency in Caucasians ($n = 202$)	Frequency in Asians ($n = 32$)	Percent homozygous for variant protein
UGT2B4 (D458)	0.75	1.00	Caucasian = 8.4 Asian = 0
UGT2B7 (H268)	0.46	0.73	Caucasian = 29.2 Asians = 9.4
UGTB15 (D85)	0.45	0.64	Caucasian = 32.2 Asians = 18.7

Source: From Ref. 113.

Table 7 Kinetics of Buprenorphine and Morphine 3 O glucuronidation in UGT2B7 Variants

	Buprenorphine		Morphine 3 O glucuronidation	
UGT2B7 variant	K_m (μM)	V_{max} (pmol/min/mg protein)	K_m (μM)	V_{max} (pmol/min/mg protein)
UGT2B7(H) (UGT2B7.1)	22 ± 6	400 ± 40	633, 331	4779, 3054
UGT2B7(Y) (UGT2B7.2)	3, 1	580, 900	458, 490	5050, 5900

of (*R*)- and (*S*)-oxazepam glucuronides in urine (114). While (*R*)-oxazepam is a substrate for UGT2B7, the turnover is very low and there was no difference between the UGT2B7 variants in terms of stereoselectivity (112). More recent data indicates that (*S*)-oxazepam is a UGT2B17 substrate.

The Tyr268 variant, UGT2B7(Y), glucuronidates menthol and androsterone, compounds not glucuronidated by UGT2B7(H) (or UGT2B7.1). UGT2B7(Y), and UGT2B7(H) have similar activities toward opioid and catechol estrogen substrates, except for normorphine, buprenorphine, and norbuprenorphine (115). The location of this amino acid change is near the junction of the variable and constant regions (112). Court et al. found no difference in enzyme kinetics for ZDV, morphine, or codeine between UGT2B7.1 and UGT2B7.2 (Table 7) (116). However, UGT2B7.1 had an 11-fold higher intrinsic clearance (V_{max}/K_m) for aldosterone glucuronidation compared with UGT2B7.2 (117).

Holthe et al. screened 239 Norwegian cancer patient for sequence variation in the coding and regulatory region of UGT2B7 (118). The impact of genetic variant of morphine glucuronidation was studied in 175 patients receiving oral morphine. They found 12 SNPs (only one of which was in the coding region H268Y). There was no functional polymorphism observed for seven common genotypes and the three main haplotypes with regard to the morphine-6-glucuronide/morphine ratio. The authors concluded that factors other than UGT2B7 polymorphisms are responsible for the variability in morphine glucuronidation (119). A similar study on the effect of polymorphisms on morphine kinetics was done in the United States by Sawyer et al. (120). They found that the 802 C>T variant (*UGT2B7*2*) was in complete linkage disequilibrium with a 161 C>T mutation in the regulatory region of UGT2B7. In this study, morphine-6-glucuronide and morphine-3-glucuronide concentrations were significantly lower in C/C patients (120).

UGT2B10, UGT2B15, AND UGT2B17

UGT2B10 was first cloned in 1993 by Miners, Mackenzie, and coworkers in Australia, but no substrates were identified (121). The first endogenous substrates were identified in 2003 by Belanger's group in Quebec and consisted of several arachidonic acid metabolites, including 12- and 15-HETE, 13-HODE, and leukotriene B4. Recently, Lazarus and coworkers reported that UGT2B10 was capable of catalyzing the N-glucuronidation of several xenobiotic compounds in tobacco, including nicotine, cotinine, and the tobacco nitrosamines NNAL and NNK (122). This group also identified a common polymorphic variant (Asp67Tyr) for UGT2B10 (122) that results in dramatically lower substrate activity in human liver microsomes.

UGT2B15 and UGT2B17 (96% homologous) were initially identified by screening for UGT androgen glucuronidation activity in prostate cells by Belanger et al. (123). *UGT2B17* cDNA was first cloned in 1996, and mRNA was also detected in liver and kidney (124). UGT2B15 specifically catalyzes the conjugation at the 17-OH position of 5α-androgens (dihydrotestosterone, androstane-3α-17β-diol), but can also catalyze the glucuronidation of hydroxy-androgens with high to moderate K_m values. Also, 2- and 4-OH-catechol estrogens are substrates, but with low efficiency. UGT2B17 glucuronidates at both the 3- and the 17-OH positions of androgens as well as (*S*)-oxazepam (103).

UGT2B15 and UGT2B17 are major UGTs in human prostate. UGT2B15 is expressed in adipose tissue, and clearance of racemic oxazepam is faster in obese patients (125) and in women compared to lean men. UGT2B17 is also expressed in liver, kidney, skin, brain, mammary gland ovaries, and uterus. The UGT2B gene cluster is located on chromosome 4q13. Androgens, epidermal growth factor, and interleukin-1 downregulate UGT2B15 and UGT2B17 expression in LnCAP cells (prostate cancer cell line) (126).

A polymorphism has been observed in UGT2B15 (Table 8). The common allele, *UGT2B15*2* results in approximately 50% lower activity in genotyped microsomes with the substrate *S*-oxazepam (see Table 9), but shows increased activity with androgens (127). In contrast, the rare variant, *UGT2B15*6*, may result in a more active or efficient enzyme. No significant difference in velocity was observed in the *UGT2B15*4* variant enzyme (see Table 9) (127). The UGT2B15*2 variant (D85Y) is more prevalent in Asians than in Caucasians (113). Court et al. also identified a gender difference in human liver microsomal samples. Median rates of glucuronidation were 65 pmol/min/mg protein in male samples (25 75% range of 49 112, $n = 38$) versus 39 in females (25 75% range of 30 72, $n = 16$), $p = 0.042$ (127).

Wilson et al. have determined that in some DNA samples, no UGT2B17 DNA could be identified. Further investigation found that a 170 kB stretch of DNA encompassing the entire UGT2B17 locus was deleted in some individuals (*UGT2B17*2*) (128).

Table 8 Frequency of UGT2B15 Variants in Caucasians and Asians

UGT2B15 variant	Frequency in Caucasians ($n = 48$)	Frequency in Asians ($n = 32$)	Alleles (%)
*UGT2B15*2* (D85Y)	0.55	0.72	Caucasian = 27
*UGT2B15*3* (L86S)			Japanese < 1
*UGTB15*4* (K523T)	0.35	0.64	Caucasian = 11
*UGT2B15*5* (D85Y/K523T)			Caucasians = 14
*UGT2B15*6* (T352I)	0.02	0.73	Caucasian = 2

*UGT2B15*1* represented 17% of alleles.
Source: Adapted from Ref. 127.

Table 9 Kinetics of *S* oxazepam in UGT2B15 Variants

UGT2B7 variant	*S* oxazepam mean velocity (pmol/min/mg protein)
UGT2B15.1 (85D/D)	131
UGT2B15.2 (85Y/Y)	49
UGT2B15.1 (352T/T)	64
UGT2B15.1/6 (352T/I)	135 and 210
UGT2B15.4 (523 K/K)	77
UGT2B15.1 (523 T/T)	65

Source: Adapted from Ref. 127.

INTERACTIONS WITH PROBENECID

Probenecid is a uricosuric agent that is used in the treatment of gout. Probenecid inhibits the active tubular secretion of a number of organic anions, including uric acid and glucuronides of several different drugs. Detailed studies of clinical interactions between prebenecid and several drugs, including clofibric acid, ZDV, and NSAIDs, have demonstrated that the rate of excretion of glucuronides into the urine is decreased, which coincides with the known effects of probenecid upon organic anion transport. Clinical interactions between probenecid and clofibric acid (107), diflunisal, (108), ketoprofen (129), indomethacin (130), carprofen (131,132), isofezolac (133), naproxen (110), zomepirac (109), and ZDV (134) have been described. In addition to the expected effect of a decreased rate of glucuronide excretion, these studies have also revealed that the clearance of the parent aglycone is also decreased. In several cases, it has been demonstrated that probenecid affects both the nonrenal and renal clearance of the parent aglycones, suggesting that there are multiple mechanisms for the probenecid effect. The apparent decrease in clearance of the parent drugs has been attributed to three basic mechanisms: (1) inhibition of the renal clearance of the parent drug, (2) direct inhibition of the UGT enzyme responsible for the glucuronidation of the parent drugs, and (3) inhibition of the active secretion of the glucuronide and subsequent hydrolysis of the glucuronide back to the aglycone, resulting in reversible metabolism. Several interactions between NSAIDs and probenecid have been reported (referenced above). Inhibition of direct renal excretion may occur but probably does not significantly contribute, since the urinary excretion of unchanged NSAIDs is negligible (129). Consequently, alternate mechanisms have been proposed. Probenecid has been shown to inhibit the formation clearance of zomepirac glucuronide by 78% in humans, suggesting a direct effect on the UGT enzyme responsible for glucuronidation. Similarly, both the phenolic and acyl glucuronide formation clearance of diflunisal was reduced by approximately 50% (108). Glucuronidation of NSAIDs is catalyzed by several UGT enzymes, including UGT1A9 and UGT2B7, although UGT1A9 may be the most important enzyme for these drugs. An alternate mechanism involving hydrolysis of the glucuronide back to the parent aglycone has also been proposed. The reversible metabolism (futile cycle) hypothesis has been well studied with clofibric acid in a uranyl nitrate induced renal failure model in rabbits (135).

The interaction between ZDV and probenecid has been extensively studied in vitro and in several species. The interaction is complex. Probenecid inhibits the renal tubular secretion of both ZDV and ZDV glucuronide. Probenecid also directly affects the

glucuronidation step, thus decreasing the nonrenal clearance of ZDV. For example, the nonrenal clearance of ZDV was significantly decreased from 10.5 ± 2.1 mL/min/kg to 7.8 ± 3.3 mL/min/kg by probenecid in a rabbit model. Probenecid has been demonstrated to be a direct inhibitor of the glucuronidation of ZDV in HLMs. In freshly isolated rat hepatocytes, probenecid decreased ZDV glucuronide by 10-fold. Probenecid also appears to inhibit the efflux of ZDV from the brain, presumably at the choroid plexus.

INTERACTIONS WITH ZIDOVUDINE

Zidovudine (3-azido-deoxythymidine, AZT or ZDV) is an important nucleoside used in the treatment of AIDS. It was the first drug approved for the treatment of AIDS, and as such there is a number of in vitro and in vivo drug interaction studies conducted with this compound. Zidovudine (ZDV) is eliminated in humans primarily by glucuronidation; approximately 75% of the dose is excreted as the glucuronide, with the rest excreted unchanged in urine. A small portion of the drug is reduced to 3′-amino-3′-deoxythymidine, a reaction catalyzed by CYP3A4. The enzyme responsible for ZDV glucuronidation is UGT2B7 with a small contribution of UGT2B4 (116,136). HLMs from Crigler-Najar Type I patients and Gunn rat liver microsomes did not show diminished ZDV glucuronidation rates, suggesting that the enzyme responsible was not a member of the UGT1A family of enzymes. In rats, ZDV glucuronidation was inducible by phenobarbital, but not by 3-MC or clofibrate and the activity was inhibited by morphine. The enzyme responsible for ZDV glucuronidation in human is UGT2B7 with a small contribution of UGT2B4 and the activity was inhibited by morphine and probenecid in human liver microsomes (137).

Several in vitro drug interaction studies have been conducted in HLMs. In HLMs, the K_m for ZDV glucuronidation is approximately 2 to 3 mM, a concentration well above the typical therapeutic concentration of 0.5 to 2 μM (138). Turnover of the substrate is also quite slow, which belies the relatively high clearance observed in vivo. On the basis of the determination of K_i in *N*-octyl-β-D-glucoside solubilized HLMs and comparison to therapeutic concentrations in plasma, Resetar et al. predicted potential interactions of more than 10% with probenecid, chloramphenicol, and (+)-naproxen out of 17 drugs tested (138). Rajaonarison et al. examined the inhibitory potential of 55 different drugs on ZDV glucuronidation (139). By comparison of the relevant therapeutic concentrations, interactions were predicted for cefoperazone, penicillin G, amoxicillin, piperacillin, chloramphenicol, vancomycin, miconazole, rifampicin, phenobarbital, carbamezepine, phenytoin, valproic acid, quinidine, phenylbutazone, ketoprofen, probenecid, and propofol. Interactions with β-lactam antibiotics and vancomycin are not likely to be significant because these compounds do not penetrate into cells well and are excreted primarily by direct renal elimination, except for cefoperazone. A similar study was conducted by Sim et al. (140). Indomethacin, naproxen, chloramphenicol, probenecid, and ethinylestradiol decreased the glucuronidation of ZDV (2.5 mM) by over 90% at supratherapeutic concentrations of 10 mM. Other compounds producing some inhibition of ZDV conjugation were oxazepam, salicylic acid, and acetylsalicyclic acid. More recently, Trapnell et al. examined the inhibition of ZDV at a more relevant concentration of 20 μM in bovine serum albumin (BSA)-activated microsomes by atovaquone, methadone, fluconazole, and valproic acid at therapeutically relevant concentrations (141). Both fluconazole and valproic acid inhibited ZDV glucuronidation by more than 50% at therapeutic concentrations. Clinical interaction studies have been conducted with methadone, fluconazole, naproxen, probenecid, rifampicin, and valproic acid (see Table 10).

Table 10 Clinical Interactions Affecting ZDV Glucuronidation

Precipitant drug	Object drug	Effect	Comments	Reference
Atovaquone	ZDV	⇑	ZDV CL/F decreased by 25%, $AUC_{(m)}/AUC_p$ ratio declined from 4.48 ± 1.94 to 3.12 ±1.1 with atovaquone	142
Fluconazole (400 mg)	ZDV	⇑	Decreased CL/F by 46%, decreased ZDV G CL_f by 48%, $A_{e(m)}/A_e$ decreased by 34%	143
Methadone	ZDV	⇑	Oral AUC increased by 41%, IV AUC by 19%, Chronic methadone decreased CL by 26%, ZDV G CL_f decreased by 17%	144
ZDV	Methadone	N. S.	No significant change in methadone levels	144
Naproxen	ZDV	N. S.	No alteration in ZDV pharmacokinetics, ZDV G AUC significantly decreased by 21%	145
Probenecid	ZDV	⇑	ZDV AUC significantly increased more than twofold	134
Rifampicin	ZDV	⇓	Decreased AUC of ZDV by 2 to 4 fold ($n = 4$), AUC ratio of ZDV G/ZDV increased in three patients, ratio returned to baseline in one patient discontinuing rifampin	146
Valproate	ZDV	⇑	ZDV AUC increased twofold, $A_{e(m)}/A_e$ in urine decreased by >50%	147

Abbreviations: ZDV, zidovudine; AUC, area under concentration time curve; CL, clearance; CL_f, formation clearance; $AUC_{(m)}$, AUC of the metabolite; AUC_p, AUC of parent; A_e, amount excreted unchanged in urine; $A_{e(m)}$, amount of metabolite excreted in urine; ZDV G, zidovudine glucuronide.

IN VITRO APPROACHES TO PREDICTION OF DRUG-DRUG INTERACTIONS

UGTs are membrane-bound enzymes located intracellularly in the endoplasmic reticulum (ER). Unlike cytochrome P450, the active site is located in the lumen of the ER, and there is good evidence for the existence of an ER transporter for UDPGA, the polar, charged cofactor that is produced in the cytosol. Similarly, the polar glucuronides that are formed in the lumen may require specific transporters for drug efflux from the ER. Microsomes maintain this membrane integrity, and thus both UDPGA and substrate access may be limited in incubations. Consequently, a variety of techniques have been used to "active enzyme" or to "remove enzyme latency" in vitro. The previously cited in vitro studies with ZDV can be used to illustrate these approaches.

ZDV glucuronidation has been stimulated by the addition of detergents such as asoleoyl lysophosphatidylcholine (0.8 mg/mg protein optimal), Brij 58 (0.5 mg/mg protein), and *N*-octyl-β-D-glucoside (0.05%) (148). Trapnell et al. reported a 15-fold increase in ZDV glucuronidation rate with 2.25% BSA (141). In our laboratory, we have used a pore-forming antibiotic, alamethacin, to stimulate the glucuronidation of ZDV in HLMs. The advantage of alamethacin is that isozyme-dependent inhibition by detergents can be avoided, but it is still important to determine the optimal concentration for activation for an individual substrate. In our hands, alamethacin stimulated ZDV glucuronidation activity three- to fourfold, to a slightly higher extent than Fraction V BSA (Remmel RP and Streich JA, unpublished data). Addition of BSA to alamethacin did not substantially increase activation. When low-endotoxin, fatty acid free BSA was used, almost no activation was observed, suggesting that endotoxin or fatty acids may be

involved in a detergent-like effect. Recently, Rowland et al. reported that long-chain free fatty acids acted as inhibitors of ZDV or 4-methylumbelliferone glucuronidation resulting in higher K_m/S50 values (148). Alamethacin is now used routinely by many investigators in the field to overcome latency and allow access of UDPGA into the interior of microsomal vescicles (149,150).

INHIBITION SCREENING OF UGTs

Unlike the situation with cytochrome P450, specific and selective inhibitors of individual UGT enzymes may not be available. Furthermore, inhibitory antibodies have not been developed because of the high similarity in amino acid content (identical in all UGT1 enzymes) in the constant region containing the UDPGA-binding site. Consequently, at this time, the only method available to identify isozyme selectivity is to conduct studies with cloned, expressed enzymes. Fortunately, many of these enzymes have recently been commercially available as microsomes prepared from lymphocytes, mammalian cells, insect cells, or have been expressed in bacteria. Procedures for "activation" of UGT activity in cloned, expressed cell systems also vary, but freeze-thawed or sonicated whole-cell lysates or preparations of microsomes from insect cells (Supersomes®) or mammalian cells have been commonly used as a convenient preparation for screening. When microsomes are used, the pore-forming antibiotic, alamethacin, is preincubated for 30 minutes at ~50 μg/mg protein at 4°C. This allows entry of UDPGA and polar substrates to the UGT active site in the interior of the ER vesicles (150). Another potential problem in microsomal incubations is the presence of long-chain free fatty acids that are substrates for several UGT enzymes, most notably UGT1A9 and UGT2B7 (148). Addition of 2% fatty acid free bovine or human serum albumin markedly reduces the K_m values for typical UGT2B7 substrates, such as zidovudine, by apparent removal of the inhibitory long-chain fatty acids (oleic, linoleic, arachinodic acid). However, correction for substrate binding to the serum albumin that was added to each incubation should be determined as there is no albumin present inside of the endoplasmic reticulum.

One must be aware that the protein expression and relative variability in expression in the liver or other tissues is not known. Thus, normalizing the data with a relative activity factor (RAF) as is typically done with P450s is not currently possible. The problem of quantitating protein expression levels may soon be overcome by proteomics approaches. Recently, Smith and coworkers, at North Carolina, developed and evaluated a quantitative proteomic digestion LC-MS method with the use of stable labeled synthetic peptide internal standards for UGT1A1 and UGT1A6 (Personal communication, Smith PC). UGT1A1 (7.8 52 pmol/mg protein) was generally expressed in higher amounts in human liver microsomes than UGT1A6 (2.6 7.9 pmol/mg protein) with a mean 1A1/1A6 ratio of 5.2 to 6.9 in 10 different HLM samples.

Enzyme selective substrates and inhibitors have been widely used to distinguish individual cytochrome P450 activities, but this has been problematic for glucuronidation because of the overlapping substrate specificity for some of these enzymes. This is especially true for the closely homologous enzymes UGT1A3 and UGT1A4, and UGT1A7 to UGT1A10. However, selective substrates for some of the enzymes have been fairly well characterized (Table 11).

UGT1A3 and UGT1A4 are >95% homologous and share many common substrates, especially tertiary amine substrates. There are some substrate differences. The general UGT substrate 4-methyl-umbelliferone is a substrate for 1A3, but not for 1A4. Bile acid conjugation at the 24-COOH group is much more efficiently catalyzed by 1A3 versus

Table 11 Selective Substrates for Individual UGTs

Enzyme	Substrate	Reported K_m	Reference
UGT1A1	Bilirubin	5 μM	
UGT1A1	Estradiol or	23 μM	6
	ethinylestradiol	In liver only	28
	(3 O glucuronidation)	(UGT1A8 also active)	
UGT1A3	Lithocholic acid	NR	29
	(24 COO glucuronidation)	Also a UGT2B7 rxn	
UGT1A3	Fulvestrant	5.4 μM	28
UGT1A4	Trifluoperazine	6 μM	30
UGT1A4	Hecogenin	10 μM	30, 31
UGT1A6	Serotonin	6 μM	32
UGT1A9 (in liver)	Propofol	300 μM	
UGT1A9 (in liver)	Entecapone	10 μM	33
UGT2B7	Diclofenac	25 μM	151
UGT2B7[a]	Zidovudine	439 μM	148
		52 μM (with FAF HSA)	
UGT2B10	Nicotine	470 μM	122
		290 μM	152
UGT2B15	*S* oxazepam	30 μM	34

[a]With FAF BSA, fatty acid free bovine serum albumin to remove free fatty acids (148).
Abbreviation: FAF HAS, fatty acid free human serum albumin.

1A4, whereas trifluoperazine, hecogenin, and tamoxifen-N-glucuronidation appear to be selective for 1A4. UGT1A3 not only has a 10-fold higher V_{max} than UGT1A4 for fulvestrant 3-O-glucuronidation, but also has a 10-fold higher K_m (UGT1A4 K_m = 0.5 μM) (40). At higher concentrations, it appears to be a selective substrate. Trifluoperazine may be somewhat problematic due to nonspecific binding to microsomal proteins and surfaces. Olanzapine and tamoxifen-N-glucuronidation may be more appropriate in vitro markers. UGT1A7, 1A8, 1A9, and 1A10 are highly homologous (>90%) and have overlapping substrate selectivity for a number of phenolic substrates, but differ by their tissue distribution. UGT1A9 is expressed highly in the liver and kidney, but not in the intestine. UGT1A7 is expressed in the esophagus and gastric epithelium, but not in the liver. Both UGT1A8 and UGT1A10 are expressed in the intestine, but not the liver. UGT1A8 is also expressed in the lung. In liver tissue, propofol and entacapone are selective substrates for 1A9, but 1A8 and 1A10 can also glucuronidate these bulky phenolic compounds. Entecapone is more selective for UGT1A9 due to a lower K_m and may be preferred, but is not widely available. Zidovudine (AZT, azidothymidine) appears to be fairly selective for UGT2B7, but is also turned over by UGT2B4 with similar K_m values (139). Carbamazepine N-glucuronidation appears to be a UGT2B7 selective substrate, but has a high K_m (36). Androsterone is a selective endogenous UGT2B7.1 substrate. Several of these compounds can be employed as selective inhibitors for screening purposes, such as bilirubin for 1A1, hecogenin for UGT1A4, serotonin for 1A6, etc., but they should be employed at proper concentrations (2 4 times greater than than Km) as they may affect other enzymes at higher concentrations. Fluconazole, a nonsubstrate, appears to be a selective inhibitor of UGT2B7. Valproic acid and probenecid inhibit multiple UGTs and may be useful as general inhibitors, but are not selective.

There is evidence that some of the enzymes may have multiple binding sites (similar to CYP3A4). For example, buprenorphine, a UGT1A1 substrate, does not inhibit

estradiol glucuronidation. Our group has recent evidence for at least two binding sites in UGT1A4 based on detailed kinetic studies with lamotrigine, tamoxifen, dihydrotestosterone, and *trans*-androsterone (Zhou and Remmel, Glucuronidation Workshop, Quebec City, 2008), and Miners and coworkers have demonstrated atypical two-site kinetics for UGT1A9. Thus, for some enzymes, multiple probe substrates may be required to evaluate potential inhibitors.

INTERACTIONS INVOLVING DEPLETION OF UDPGA

An alternate mechanism of drug-drug interactions involving glucuronidation may involve depletion of the required cofactor, UDPGA. Several drugs and chemicals have been shown to deplete UDPGA in the rat, including D-galactosamine, diethylether, ethanol, and APAP. In the mouse, Howell et al. demonstrated that valproic acid, chloramphenicol, and salicylamide depleted hepatic UDPGA by >90% at doses of 1 to 2 mmol/kg. Maximal decreases were noted at 7 to 15 minutes after injection, but rebounded toward control levels by two to four hours after injection (153). Once depleted, UDPGA levels will be replaced by the breakdown of glycogen stores in the liver. For drugs that are glucuronidated but are given at relatively low doses, UDPGA depletion is not likely to be of major importance. Extrahepatic glucuronidation may be more susceptible to depletion of UDPGA, since UDPGA concentrations in liver (279 μmol/kg) were reportedly 15 times higher than intestine, kidney, or lung (154). However, in patients receiving high doses of certain drugs, such as the NSAIDs, ethanol, APAP, and valproate, depletion of UDPGA stores may influence the rate of glucuronidation, especially if glycogen stores are low. For example, lamotrigine clearance is decreased two- to threefold in patients also taking valproic acid (44). Lamotrigine has shown to be glucuronidated by UGT1A4 and may also be a substrate for UGT1A3, which also catalyzes the glucuronidation of many tertiary amine drugs. Valproic acid is a slow substrate for UGT1A3 and is weak inhibitor of lamotrigine glucuronidation in microsomes containing excess UDPGA (155). The maximum recommended dose of valproic acid is 60 mg/kg/day (4200 mg/day), which is equivalent to a dose of 0.14 mmol/kg. Thus, it is conceivable that UDPGA depletion may play a role in interactions involving valproic acid. A similar case could be made for patients taking high dose of APAP, although in the case of lamotrigine, coadministration of APAP resulted in an unexpected 20% decrease in lamotrigine AUC. Evidence for UDPGA depletion by any drug in humans is lacking, and thus the clinical relevance of this mechanism is unclear.

INTERACTIONS INVOLVING INDUCTION OF UGT ENZYMES

Regulation of the UGT enzymes has been well studied in animals, especially in the rat. It is clear that many of the enzymes involved in metabolism of xenobiotics share common regulatory sequences (response elements) in the 5′ promoter region that respond to classic inducers such as 3-MC, phenobarbital, clofibrate, dexamethasone, and rifampin. Treatment of rats with PAH, such as β-naphthoflavone (β-NF), or 3-MC has been shown to increase the transcription of *UGT1A6*, an enzyme that conjugates a variety of planar phenols, such as 1-naphthol. UGT1A6, the PAH-inducible cytochrome P450 enzymes, CYP1A1 and CYP1A2, glutathione transferase Ya (GSTA1-1), NAD(P)H-menadione oxidoreductase, and class 3 aldehyde reductase (ALDH3) are members of an Ah-receptor gene battery because all of the genes encoding these enzyme contain a xenobiotic response element (XRE) in their 5′ promoter regions. In humans, omeprazole and cigarette smoking have been shown to induce CYP1A1/2. Cigarette smoking modestly

induces the glucuronidation of APAP, codeine, mexiletine, and propranolol. In smokers or patients receiving omeprazole treatment, the in vitro glucuronidation of 4-methylumbelliferone (a general substrate for UGT activity) was not significantly induced in duodenal mucosal biopsies. 1-Naphthol glucuronidation (a marker substrate for UGT1A6) was induced fourfold by β-NF in Caco-2 cells, a human colon carcinoma cell line. In contrast, CYP1A1 activity (ethoxyresorufin-deethylation) was induced by more than 100-fold in the same cell line. 1-Naphthol glucuronidation was not affected by the addition of rifampin or clofibrate. Induction of UGT1A6 mRNA and 1-naphthol glucuronidation by β-NF was observed in MZ-Hep-1 cells, another human hepatocarcinoma line. Rifampin (100 μM) significantly increased this activity in MZ-Hep-1 cells, but not in KYN-2 cells. A variable response to induction by rifampin and β-NF was also observed in cultured hepatocyes isolated from five different donors. Fabre et al. also reported that inducibility of glucuronidation of 1-naphthol by β-NF in human hepatocytes was variable (156).

Induction of glucuronidation by anticonvulsant drugs such as phenobarbital, phenytoin, and carbamazepine has been demonstrated for a number of different drugs, including APAP, chloramphenicol, irinotecan, lamotrigine, valproic acid, and ZDV. HLMs obtained from patients treated with phenytoin or phenobarbital displayed two or three times higher activity for the glucuronidation of bilirubin, 4-methylumbelliferone, and 1-naphthol compared with control HLMs. Less is known about the response to induction of the mRNA concentrations of individual genes, but Sutherland et al. (157) reported that the UGT1A1 mRNA was elevated in livers from individuals treated with phenytoin and phenobarbital. Bilirubin conjugation is also elevated in microsomes prepared from patients taking phenobarbital and phenytoin, and rat bilirubin UGT activity was inducible by phenobarbital and clofibrate in H4IIE rat hepatoma cells. However, when a proximal 611 bp UGT1A1 promoter/luciferase reporter gene construct was transfected into H4IIE cells, no induction was observed upon treatment with phenobarbital. Retinoic acid and a combination of retinoic acid and WY 14643 (a potent PPAR-α ligand) both increased luciferase activity. Patients with Crigler-Najjar Type II syndrome (a genetic deficiency in UGT1A1) have been treated with phenobarbital or clofibrate in order to increase bilirubin glucuronidation. The beneficial effect could arise either by increasing the transcription of a poorly expressed UGT1A1 or by inducing UGT1A4 (the minor builirubin enzyme). Lamotrigine, a triazine anticonvulsant that metabolizes to a quaternary ammonium is increased approximately twofold in patients taking other inducing anticonvulsants, suggesting that UGT1A4 is inducible by CAR activators such as phenobarbital, phenytoin, and carbamazepine.

Induction of the glucuronidation of several drugs, including lamotrigine by oral contraceptive steroids (OCSs), has been observed (158). The formation clearance to the acyl glucuronide of diflunisal increased from 3.01 mL/min in control women compared with 4.81 mL/min in OCS users (159). The urinary recovery of phenprocoumon glucuronide was 14% of the dose in age-matched controls compared with 21% of the dose in OCS users. Ethinylestradiol doubled the fraction of propranolol metabolized to the glucuronide without affecting total body clearance (160). Oral contraceptives have also been shown to induce the metabolism of APAP, clofibric acid, and temazepam.

Rifampin is a potent inducer of several cytochrome P450 enzymes via PXR activation and also appears to be an inducer of several UGTs such as UGT1A1, UGT1A4, UGT1A9, and UGT2B7. Several case reports have documented an induction of methadone withdrawal symptoms upon introduction of antituberculosis therapy that included rifampin. Fromm et al. studied the effect of rifampin (600 mg/day for 18 days) on morphine analgesia and pharmacokinetics in healthy volunteers (161). Morphine CL/F was increased from 3.58 ± 0.97 L/min initially to 5.49 ± 2.97 L/min during rifampin treatment. The AUC of both

morphine-6-glucuronide (an active metabolite) and morphine-3-glucuronide were significantly reduced, although the ratio of the morphine AUC/AUCs of the glucuronide was not significantly increased. Since the metabolite/parent ratios in blood were not affected, the authors suggested that rifampin may have affected the absorption of morphine, perhaps by induction of MDR1 (P-glycoprotein) or an alternate pathway of metabolism or excretion was enhanced, since the urinary recovery of both the glucuronide was decreased. The area under the pain threshold time curve (cold pressor test) was also significantly reduced by rifampin treatment. Both methadone and morphine are reported substrates for UGT2B7. Rifampicin has also been shown to double the oral clearance of lamotrigine, a UGT1A4 substrate (162). Rifampin appears to significantly increase the glucuronidation of zidovudine (ZDV) in humans (146). Burger et al. reported a higher CL/F and significantly increased ratio of ZDV-glucuronide/ZDV in plasma in four AIDS patients on rifampin compared with untreated controls (163). In one patient, who had stopped rifampin, the metabolite/parent AUC ratio also decreased. Rifabutin, a new rifamycin analog, has been reported to decrease ZDV C_{max} and AUC by 48% and 37%, respectively. However, Gallicano et al. reported that 300 mg of rifabutin/day for 7 or 14 days had no significant effect on ZDV pharmacokinetics, except for a statistically significant decrease in half-life from 1.5 to 1.1 hours (146). Culture of human hepatocytes with 15-μM rifabutin for 48 hours modestly increased the rate of ZDV glucuronidation (28% increase) in one of two donors, but no significant induction was observed with either rifampin or rifapentine, which were more potent inducers of CYP3A4 and CYP2C8/9 in vitro.

METABOLIC SWITCHING AND INHIBITION OF GLUCURONIDATION

Glucuronidation is normally a primary detoxification pathway. In cases where glucuronidation becomes saturated or inhibited, metabolic switching to form reactive metabolites (typically catalyzed by cytochrome P450 enzymes) can occur. APAP is the classic example of a drug that at high doses is hepatotoxic because saturation of phase II pathways (glucuronidation and sulfation) due to metabolic switching to a CYP2E1-mediated pathway to form *N*-acetylbenzoquinoneimine. Our laboratory has recently shown that inhibition of naltrexone metabolism by NSAIDs can lead to hepatotoxicity. In vitro experiments have revealed that naltrexone is metabolized by CYP3A4 to form a catechol metabolite that is rapidly oxidized to a quinone and quinonemethide as evidenced by the formation of two glutathione conjugates in a microsomal incubation (Kalyanaraman, Kim, and Remmel, unpublished). Naltrexone glucuronidation was inhibited by NSAIDs, especially fenamates, and the reduction to β-naltrexol (the primary metabolic pathway) is also inhibited by NSAIDs (164). Glucuronides can also be substrates for cytochrome P450 enzymes. Gemfibrozil glucuronide was shown to be a potent inhibitor of CYP2C8 (141), and inhibition of CYP2C8 and competition of the UGT-catalyzed lactonization of statins is the mechanism for the interaction between cerivastatin and gemfibrozil (142). This interaction was an important factor in the removal of cerivastatin (Baycol®) from the market.

CONCLUSIONS

It is clear from the examples just discussed that interactions involving glucuronidation are possible, especially for drugs that extensively excreted as glucuronides. Because of the overlapping substrate specificity among different UGTs, most interactions (particularly with phenolic substrates) are likely to be relatively modest. Prediction of

interactions is possible in HLMs, but it is important to conduct these studies at relevant therapeutic concentrations. With the availability of cloned, expressed enzymes, detailed kinetic studies of inhibitory interactions may be carried out. Induction potential may be accomplished in human hepatocytes or perhaps by utilization of a reporter gene assay similar to studies conducted with cytochrome P450 enzymes. While outside the scope of this review, interactions involving glucuronide transport may be important as well.

REFERENCES

1. Burchell B, Brierley CH, Rance D. Specificity of human UDP glucuronosyltransferases and xenobiotic glucuronidation. Life Sci 1995; 57(20):1819 1831.
2. Burchell B, Coughtrie MW. Genetic and environmental factors associated with variation of human xenobiotic glucuronidation and sulfation. Environ Health Perspect 1997; 105(suppl 4): 739 747.
3. Mackenzie PI, Owens IS, Burchell B, et al. The UDP glycosyltransferase gene superfamily: recommended nomenclature update based on evolutionary divergence. Pharmacogenetics 1997; 7(4):255 269.
4. Tukey RH, Strassburg CP. Human UDP glucuronosyltransferases: metabolism, expression, and disease. Annu Rev Pharmacol Toxicol 2000; 40:581 616.
5. Burchell B, Brierley CH, Monaghan G, et al. The structure and function of the UDP glucuronosyltransferase gene family. Adv Pharmacol 1998; 42:335 338.
6. Court MH, Greenblatt DJ. Molecular genetic basis for deficient acetaminophen glucuronidation by cats: UGT1A6 is a pseudogene, and evidence for reduced diversity of expressed hepatic UGT1A isoforms. Pharmacogenetics 2000; 10(4):355 369.
7. Jedlitschky G, Cassidy AJ, Sales M, et al. Cloning and characterization of a novel human olfactory UDP glucuronosyltransferase. Biochem J 1999; 340(pt 3):837 843.
8. Kiang TK, Ensom MH, Chang TK. UDP glucuronosyltransferases and clinical drug drug interactions. Pharmacol Ther 2005; 106(1):97 132.
9. Senafi SB, Clarke DJ, Burchell B. Investigation of the substrate specificity of a cloned expressed human bilirubin UDP glucuronosyltransferase: UDP sugar specificity and involve ment in steroid and xenobiotic glucuronidation. Biochem J 1994; 303(pt 1):233 240.
10. Monaghan G, Ryan M, Seddon R, et al. Genetic variation in bilirubin UPD glucuronosyltransferase gene promoter and Gilbert's syndrome [see comments]. Lancet 1996; 347(9001):578 581.
11. Guillemette C. Pharmacogenomics of human UDP glucuronosyltransferase enzymes. Pharmacogenomics J 2003; 3(3):136 158.
12. Kitagawa C, Ando M, Ando Y, et al. Genetic polymorphism in the phenobarbital responsive enhancer module of the UDP glucuronosyltransferase 1A1 gene and irinotecan toxicity. Pharmacogenet Genomics 2005; 15(1):35 41.
13. Ferraris A, D'Amato G, Nobili V, et al. Combined test for UGT1A1 3279T >G and A(TA) nTAA polymorphisms best predicts Gilbert's syndrome in Italian pediatric patients. Genet Test 2006; 10(2):121 125.
14. Costa E. Hematologically important mutations: bilirubin UDP glucuronosyltransferase gene mutations in Gilbert and Crigler Najjar syndromes. Blood Cells Mol Dis 2006; 36(1): 77 80.
15. Urawa N, Kobayashi Y, Araki J, et al. Linkage disequilibrium of UGT1A1 *6 and UGT1A1 *28 in relation to UGT1A6 and UGT1A7 polymorphisms. Oncol Rep 2006; 16(4): 801 806.
16. Akaba K, Kimura T, Sasaki A, et al. Neonatal hyperbilirubinemia and mutation of the bilirubin uridine diphosphate glucuronosyltransferase gene: a common missense mutation among Japanese, Koreans and Chinese. Biochem Mol Biol Int 1998; 46(1):21 26.
17. Rotger M, Taffe P, Bleiber G, et al. Gilbert syndrome and the development of antiretroviral therapy associated hyperbilirubinemia. J Infect Dis 2005; 192(8):1381 1386.

18. Lankisch TO, Moebius U, Wehmeier M, et al. Gilbert's disease and atazanavir: from phenotype to UDP glucuronosyltransferase haplotype. Hepatology 2006; 44(5):1324 1332.
19. de Morais SM, Uetrecht JP, Wells PG. Decreased glucuronidation and increased bioactivation of acetaminophen in Gilbert's syndrome. Gastroenterology 1992; 102(2):577 586.
20. Ullrich D, Sieg A, Blume R, et al. Normal pathways for glucuronidation, sulphation and oxidation of paracetamol in Gilbert's syndrome. Eur J Clin Invest 1987; 17(3):237 240.
21. Rauchschwalbe SK, Zuhlsdorf MT, Wensing G, et al. Glucuronidation of acetaminophen is independent of UGT1A1 promotor genotype. Int J Clin Pharmacol Ther 2004; 42(2):73 77.
22. Herman RJ, Chaudhary A, Szakacs CB. Disposition of lorazepam in Gilbert's syndrome: effects of fasting, feeding, and enterohepatic circulation. J Clin Pharmacol 1994; 34(10): 978 984.
23. Posner J, Cohen AF, Land G, et al. The pharmacokinetics of lamotrigine (BW430C) in healthy subjects with unconjugated hyperbilirubinaemia (Gilbert's syndrome). Br J Clin Pharmacol 1989; 28(1):117 120.
24. Green MD, Tephly TR. Glucuronidation of amines and hydroxylated xenobiotics and endobiotics catalyzed by expressed human UGT1.4 protein. Drug Metab Dispos 1996; 24(3):356 363.
25. Green MD, King CD, Mojarrabi B, et al. Glucuronidation of amines and other xenobiotics catalyzed by expressed human UDP glucuronosyltransferase 1A3. Drug Metab Dispos 1998; 26:507 512.
26. Ando Y, Saka H, Asia G, et al. UGT1A1 genotypes and glucuronidation of SN 38, the active metabolite of irinotecan. Ann Oncol 1998; 9(8):845 847.
27. Innocenti F, Ratain MJ. Pharmacogenetics of irinotecan: clinical perspectives on the utility of genotyping. Pharmacogenomics 2006; 7(8):1211 1221.
28. Iyer L, King CD, Whitington PF, et al. Genetic predisposition to the metabolism of irinotecan (CPT 11). Role of uridine diphosphate glucuronosyltransferase isoform 1A1 in the glucuronidation of its active metabolite (SN 38) in human liver microsomes. J Clin Invest 1998; 101(4):847 854.
29. Toffoli G, Cecchin E, Corona G, et al. The role of UGT1A1*28 polymorphism in the pharmacodynamics and pharmacokinetics of irinotecan in patients with metastatic colorectal cancer. J Clin Oncol 2006; 24(19):3061 3068.
30. Murry DJ, Cherrick I, Salama V, et al. Influence of phenytoin on the disposition of irinotecan: a case report. J Pediatr Hematol Oncol 2002; 24(2):130 133.
31. Mathijssen RH, Verweij J, Loos WJ, et al. Irinotecan pharmacokinetics pharmacodynamics: the clinical relevance of prolonged exposure to SN 38. Br J Cancer 2002; 87(2):144 150.
32. Kuhn JG. Influence of anticonvulsants on the metabolism and elimination of irinotecan. A North American Brain Tumor Consortium preliminary report. Oncology (Williston Park) 2002; 16(8 suppl 7):33 40.
33. Mathijssen RH, Verweij J, de Bruijn P, et al. Effects of St. John's wort on irinotecan metabolism. J Natl Cancer Inst 2002; 94(16):1247 1249.
34. van Erp NP, Baker SD, Zhao M, et al. Effect of milk thistle (Silybum marianum) on the pharmacokinetics of irinotecan. Clin Cancer Res 2005; 11(21):7800 7806.
35. Stewart CF, Leggas M, Schuetz JD, et al. Gefitinib enhances the antitumor activity and oral bioavailability of irinotecan in mice. Cancer Res 2004; 64(20):7491 7499.
36. Ohtsu T, Sasaki Y, Igarashi T, et al. Unexpected hepatotoxicities in patients with non Hodgkin's lymphoma treated with irinotecan (CPT 11) and etoposide. Jpn J Clin Oncol 1998; 28(8):502 506.
37. Wen Z, Tallman MN, Ali SY, et al. UDP glucuronosyltransferase 1A1 is the principal enzyme responsible for etoposide glucuronidation in human liver and intestinal microsomes: structural characterization of phenolic and alcoholic glucuronides of etoposide and estimation of enzyme kinetics. Drug Metab Dispos 2007; 35(3):371 380.
38. Watanabe Y, Nakajima M, Ohashi N, et al. Glucuronidation of etoposide in human liver microsomes is specifically catalyzed by UDP glucuronosyltransferase 1A1. Drug Metab Dispos 2003; 31(5):589 595.
39. Corona G, Vaccher E, Cattarossi G, et al. Potential hazard of pharmacokinetic interactions between lopinavir ritonavir protease inhibitors and irinotecan. Aids 2005; 19(17):2043 2044.

40. Chouinard S, Tessier M, Vernouillet G, et al. Inactivation of the pure antiestrogen fulvestrant and other synthetic estrogen molecules by UDP glucuronosyltransferase 1A enzymes expressed in breast tissue. Mol Pharmacol 2006; 69(3):908 920.
41. Sinz MW. Animal model systems for the study of selected antiepileptic drug interactions. In: Ph.D thesis. Minneapolis: University of Minnesota, 1991.
42. Remmel RP, Sinz MW. A quaternary ammonium glucuronide is the major metabolite of lamotrigine in guinea pigs. In vitro and in vivo studies. Drug Metab Disp 1991; 19(3):630 636.
43. Jawad S, Yuen WC, Peck AW, et al. Lamotrigine: single dose pharmacokinetics and initial 1 week experience in refractory epilepsy. Epilepsy Res 1987; 1(3):194 201.
44. Anderson GC, Yau MK, Gidal BE, et al. Bidirectional interaction of valproate and lamotrigine in healthy subjects. Clin Pharmacol Ther 1996; 60:145 156.
45. Iwai M, Maruo Y, Ito M, et al. Six novel UDP glucuronosyltransferase (UGT1A3) polymorphisms with varying activity. J Hum Genet 2004; 49(3):123 128.
46. Ehmer U, Vogel A, Schütte JK, et al. Variation of hepatic glucuronidation: Novel functional polymorphisms of the UDP glucuronosyltransferase UGT1A4. Hepatology 2004; 39(4):970 977.
47. Chen Y, Chen S, Li X, et al. Genetic variants of human UGT1A3: functional characterization and frequency distribution in a Chinese Han population. Drug Metab Dispos 2006; 34(9):1462 1467.
48. Wiener D, Doerge DR, Fang JL, et al. Characterization of N glucuronidation of the lung carcinogen 4 (methylnitrosamino) 1 (3 pyridyl) 1 butanol (NNAL) in human liver: importance of UDP glucuronosyltransferase 1A4. Drug Metab Dispos 2004; 32(1): 72 79.
49. Mori A, Maruo Y, Iwai M, et al. UDP glucuronosyltransferase 1A4 polymorphisms in a Japanese population and kinetics of clozapine glucuronidation. Drug Metab Dispos 2005; 33(5): 672 675.
50. Chen S, Beaton D, Nguyen N, et al. Tissue specific, inducible, and hormonal control of the human UDP glucuronosyltransferase 1 (UGT1) locus. J Biol Chem 2005; 280(45):37547 37557.
51. Senekeo Effenberger K, Chen S, Magdalou J, et al. Expression of the human UGT1 locus in transgenic mice by 4 chloro 6 (2,3 xylidino) 2 pyrimidinylthioacetic acid (WY 14643) and implications on drug metabolism through peroxisome proliferator activated receptor alpha activation. Drug Metab Dispos 2007; 35(3): 419 427.
52. Ouzzine M, Pillot T, Fournel Gigleux S, et al. Expression and role of the human liver UDP glucuronosyltransferase UGT1*6 analyzed by specific antibodies raised against a hybrid protein produced in Escherichia coli. Arch Biochem Biophys 1994; 310(1):196 204.
53. Krishnaswamy S, Duan SX, von Moltke LL, et al. Validation of serotonin (5 hydroxtryptamine) as an in vitro substrate probe for human UDP glucuronosyltransferase (UGT) 1A6. Drug Metab Dispos 2003; 31(1):133 139.
54. Krishnaswamy S, Hao Q, Al Rohaimi A, et al. UDP glucuronosyltransferase (UGT) 1A6 pharmacogenetics: I. Identification of polymorphisms in the 5′ regulatory and exon 1 regions, and association with human liver UGT1A6 gene expression and glucuronidation. J Pharmacol Exp Ther 2005; 313(3):1331 1339.
55. Krishnaswamy S, Hao Q, Al Rohaimi A, et al. UDP glucuronosyltransferase (UGT) 1A6 pharmacogenetics: II. Functional impact of the three most common nonsynonymous UGT1A6 polymorphisms (S7A, T181A, and R184S). J Pharmacol Exp Ther 2005; 313(3):1340 1346.
56. Saeki M, Saito Y, Jinno H, et al. Genetic polymorphisms of UGT1A6 in a Japanese population. Drug Metab Pharmacokinet 2005; 20(1):85 90.
57. Tankanitlert J, Morales NP, Howard TA, et al. Effects of combined UDP Glucuronosyltransferase (UGT) 1A1*28 and 1A6*2 on paracetamol pharmacokinetics in beta thalassemia/HbE. Pharmacology 2007; 79(2):97 103.
58. Court MH, Duan SX, von Moltke LL, et al. Interindividual variability in acetaminophen glucuronidation by human liver microsomes: identification of relevant acetaminophen UDP glucuronosyltransferase isoforms. J Pharmacol Exp Ther 2001; 299(3):998 1006.
59. Baraka OZ, Truman CA, Ford JM, et al. The effect of propranolol on paracetamol metabolism in man. Br J Clin Pharmacol 1990; 29(2):261 264.
60. Miners JO, Attwood J, Birkett DJ. Influence of sex and oral contraceptive steroids on paracetamol metabolism. Br J Clin Pharmacol 1983; 16(5):503 509.

61. Miners JO, Attwood J, Birkett DJ. Determinants of acetaminophen metabolism: effect of inducers and inhibitors of drug metabolism on acetaminophen's metabolic pathways. Clin Pharmacol Ther 1984; 35(4):480 486.
62. Bock KW, Bock Hennig BS. Differential induction of human liver UDP glucuronosyltransferase activities by phenobarbital type inducers. Biochem Pharmacol 1987; 36(23):4137 4143.
63. Abernethy DR, Greenblatt DJ, Ameer B, et al. Probenecid impairment of acetaminophen and lorazepam clearance: direct inhibition of ether glucuronide formation. J Pharmacol Exp Ther 1985; 234(2):345 349.
64. Bock KW, Wiltfang J, Blume R, et al. Paracetamol as a test drug to determine glucuronide formation in man. Effects of inducers and of smoking. Eur J Clin Pharmacol 1987; 31(6):677 683.
65. Barbier O, Girard H, Inoue Y, et al. Hepatic expression of the UGT1A9 gene is governed by hepatocyte nuclear factor 4alpha. Mol Pharmacol 2005; 67(1):241 249.
66. Gardner Stephen DA, Mackenzie PI. Hepatocyte nuclear factor1 transcription factors are essential for the UDP glucuronosyltransferase 1A9 promoter response to hepatocyte nuclear factor 4alpha. Pharmacogenet Genomics 2007; 17(1):25 36.
67. Bruck M, Li Q, Lamb JG, et al. Characterization of rabbit UDP glucuronosyltransferase UGT1A7: tertiary amine glucuronidation is catalyzed by UGT1A7 and UGT1A4. Arch Biochem Biophys 1997; 348(2):357 364.
68. Ciotti M, Basu N, Brangi M, et al. Glucuronidation of 7 ethyl 10 hydroxycamptothecin (SN 38) by the human UDP glucuronosyltransferases encoded at the UGT1 locus. Biochem Biophys Res Commun 1999; 260(1):199 202.
69. Gregory PA, Lewinsky RH, Gardner Stephen DA, et al. Coordinate regulation of the human UDP glucuronosyltransferase 1A8, 1A9, and 1A10 genes by hepatocyte nuclear factor 1alpha and the caudal related homeodomain protein 2. Mol Pharmacol 2004; 65(4):953 963.
70. Cheng Z, Radominska Pandya A, Tephly TR. Cloning and expression of human UDP glucuronosyltransferase (UGT) 1A8. Arch Biochem Biophys 1998; 356(2):301 305.
71. Veroli P, O'Kelly B, Bertrand F, et al. Extrahepatic metabolism of propofol in man during the anhepatic phase of orthotopic liver transplantation. Br J Anaesth 1992; 68(2):183 186.
72. Takizawa D, Sato E, Hiraoka H, et al. Changes in apparent systemic clearance of propofol during transplantation of living related donor liver. Br J Anaesth 2005; 95(5):643 647.
73. Pavlin DJ, Coda B, Shen DD, et al. Effects of combining propofol and alfentanil on ventilation, analgesia, sedation, and emesis in human volunteers. Anesthesiology 1996; 84(1):23 37.
74. Cockshott ID, Briggs LP, Douglas EJ, et al. Pharmacokinetics of propofol in female patients. Studies using single bolus injections. Br J Anaesth 1987; 59(9):1103 1110.
75. Gepts E, Camu F, Cockshott ID, et al. Disposition of propofol administered as constant rate intravenous infusions in humans. Anesth Analg 1987; 66(12):1256 1263.
76. Zucker K, Tsaroucha A, Olson L, et al. Evidence that tacrolimus augments the bioavailability of mycophenolate mofetil through the inhibition of mycophenolic acid glucuronidation. Ther Drug Monit 1999; 21(1):35 43.
77. Strassburg CP, Barut A, Obermayer Straub P, et al. Identification of cyclosporine A and tacrolimus glucuronidation in human liver and the gastrointestinal tract by a differentially expressed UDP glucuronosyltransferase: UGT2B7. J Hepatol 2001; 34(6):865 872.
78. Picard N, Premaud A, Rousseau A, et al. A comparison of the effect of ciclosporin and sirolimus on the pharmokinetics of mycophenolate in renal transplant patients. Br J Clin Pharmacol 2006; 62(4):477 484.
79. Westley IS, Brogan LR, Morris RG, et al. Role of Mrp2 in the hepatic disposition of mycophenolic acid and its glucuronide metabolites: effect of cyclosporine. Drug Metab Dispos 2006; 34(2):261 266.
80. Hesselink DA, van Hest RM, Mathot RA, et al. Cyclosporine interacts with mycophenolic acid by inhibiting the multidrug resistance associated protein 2. Am J Transplant 2005; 5(5):987 994.
81. Naesens M, Kuypers DR, Streit F, et al. Rifampin induces alterations in mycophenolic acid glucuronidation and elimination: implications for drug exposure in renal allograft recipients. Clin Pharmacol Ther 2006; 80(5):509 521.

82. Kuypers DR, Naesens M, Vermeire S, et al. The impact of uridine diphosphate glucuronosyltransferase 1A9 (UGT1A9) gene promoter region single nucleotide polymorphisms T 275A and C 2152T on early mycophenolic acid dose interval exposure in de novo renal allograft recipients. Clin Pharmacol Ther 2005; 78(4):351 361.
83. Chen C, Staudinger JL, Klaassen CD. Nuclear receptor, pregname X receptor, is required for induction of UDP glucuronosyltranferases in mouse liver by pregnenolone 16 alpha carbonitrile. Drug Metab Dispos 2003; 31(7):908 915.
84. Huang YH, Galijatovic A, Nguyen N, et al. Identification and functional characterization of UDP glucuronosyltransferases UGT1A8*1, UGT1A8*2 and UGT1A8*3. Pharmacogenetics 2002; 12(4):287 297.
85. Munzel PA, Schmohl S, Heel H, et al. Induction of human UDP glucuronosyltransferases (UGT1A6, UGT1A9, and UGT2B7) by t butylhydroquinone and 2,3,7,8 tetrachlorodibenzo p dioxin in Caco 2 cells. Drug Metab Dispos 1999; 27(5):569 573.
86. Thibaudeau J, Lepine J, Tojcic J, et al. Characterization of common UGT1A8, UGT1A9, and UGT2B7 variants with different capacities to inactivate mutagenic 4 hydroxylated metabolites of estradiol and estrone. Cancer Res 2006; 66(1):125 133.
87. Girard H, Court MH, Bernard O, et al. Identification of common polymorphisms in the promoter of the UGT1A9 gene: evidence that UGT1A9 protein and activity levels are strongly genetically controlled in the liver. Pharmacogenetics 2004; 14(8):501 515.
88. Jinno H, Saeki M, Saito Y, et al. Functional characterization of human UDP glucuronosyl transferase 1A9 variant, D256N, found in Japanese cancer patients. J Pharmacol Exp Ther 2003; 306(2):688 693.
89. Innocenti F, Liu W, Chen P, et al. Haplotypes of variants in the UDP glucurnosyltransferase1A9 and 1A1 genes. Pharmacogenet Genomics 2005; 15(5):295 301.
90. Yamanaka H, Nakajima M, Katoh M, et al. A novel polymorphism in the promoter region of human UGT1A9 gene (UGT1A9*22) and its effects on the transcriptional activity. Pharmacogenetics 2004; 14(5):329 332.
91. Mojarrabi B, Mackenzie PI. The human UDP glucuronosyltransferase, UGT1A10, glucuronidates mycophenolic acid. Biochem Biophys Res Commun 1997; 238(3):775 778.
92. Starlard Davenport A, Xiong Y, Bratton S, et al. Phenylalanine(90) and phenylalanine(93) are crucial amino acids within the estrogen binding site of the human UDP glucuronosyltransferase 1A10. Steroids 2007; 72(1):85 94.
93. Cheng Z, Radominska Pandya A, Tephly TR. Studies on the substrate specificity of human intestinal UDP lucuronosyltransferases 1A8 and 1A10. Drug Metab Dispos 1999; 27(10):1165 1170.
94. Sten T, Qvisen S, Uutela P, et al. Prominent but reverse stereoselectivity in propranolol glucuronidation by human UDP glucuronosyltransferases 1A9 and 1A10. Drug Metab Dispos 2006; 34(9):1488 1494.
95. Jeong EJ, Liu Y, Lin H, et al. Species and disposition model dependent metabolism of raloxifene in gut and liver: role of UGT1A10. Drug Metab Dispos 2005; 33(6):785 794.
96. Lewinsky RH, Smith PA, Mackenzie PI. Glucuronidation of bioflavonoids by human UGT1A10: structure function relationships. Xenobiotica 2005; 35(2):117 129.
97. Elahi A, Bendaly J, Zheng Z, et al. Detection of UGT1A10 polymorphisms and their association with orolaryngeal carcinoma risk. Cancer 2003; 98(4):872 880.
98. Saeki M, Ozawa S, Saito Y, et al. Three novel single nucleotide polymorphisms in UGT1A10. Drug Metab Pharmacokinet 2002; 17(5):488 490.
99. Jinno H, Saeki M, Tanaka Kagawa T, et al. Functional characterization of wild type and variant (T202I and M59I) human UDP glucuronosyltransferase 1A10. Drug Metab Dispos 2003; 31(5):528 532.
100. Ritter JK, Chen F, Sheen YY, et al. Two human liver cDNAs encode UDP glucuronosyltransferases with 2 log differences in activity toward parallel substrates including hyodeoxycholic acid and certain estrogen derivatives. Biochemistry 1992; 31(13):3409 3414.
101. Jin C, Miners JO, Lillywhite KG, et al. Complementary deoxyribonucleic acid cloning and expression of a human liver uridine diphosphate glucuronosyltransferase glucuronidating carboxylic acid containing drugs. J Pharmacol Exp Ther 1993; 264(1):475 479.

102. Coffman BL, Rios GR, King CD, et al. Human UGT2B7 catalyzes morphine glucuronidation. Drug Metab Dispos 1997; 25(1):1 4.
103. Court MH, Duan SX, Guillemette C, et al. Stereoselective conjugation of oxazepam by human UDP glucuronosyltransferases (UGTs): S oxazepam is glucuronidated by UGT2B15, while R oxazepam is glucuronidated by UGT2B7 and UGT1A9. Drug Metab Dispos 2002; 30(11): 1257 1265.
104. Samara EE, Granneman RG, Witt GF, et al. Effect of valproate on the pharmacokinetics and pharmacodynamics of lorazepam. J Clin Pharmacol 1997; 37(5):442 450.
105. Anderson GD, Gidal BE, Kantor ED, et al. Lorazepam valproate interaction: studies in normal subjects and isolated perfused rat liver. Epilepsia 1994; 35(1):221 225.
106. Herman RJ, Van Pham JD, Szakacs CB. Disposition of lorazepam in human beings: enterohepatic recirculation and first pass effect. Clin Pharmacol Ther 1989; 46(1):18 25.
107. Veenendaal JR, Brooks PM, Meffin PJ. Probenecid clofibrate interaction. Clin Pharmacol Ther 1981; 29(3):351 358.
108. Macdonald JI, Wallace SM, Herman RJ, et al. Effect of probenecid on the formation and elimination kinetics of the sulphate and glucuronide conjugates of diflunisal. Eur J Clin Pharmacol 1995; 47(6):519 523.
109. Smith PC, Langendijk PN, Boss JA, et al. Effect of probenecid on the formation and elimination of acyl glucuronides: studies with zomepirac. Clin Pharmacol Ther 1985; 38(2):121 127.
110. Runkel R, Mroszczak E, Chaplin M, et al. Naproxen probenecid interaction. Clin Pharmacol Ther 1978; 24(6):706 713.
111. Miners JO, Robson RA, Birkett DJ. Gender and oral contraceptive steroids as determinants of drug glucuronidation: effects on clofibric acid elimination. Br J Clin Pharmacol 1984; 18(2): 240 243.
112. Bhasker CR, McKinnon W, Stone A, et al. Genetic polymorphism of UDP glucuronosyltransferase 2B7 (UGT2B7) at amino acid 268: ethnic diversity of alleles and potential clinical significance. Pharmacogenetics 2000; 10(8):679 685.
113. Lampe JW, Bigler J, Bush AC, et al. Prevalence of polymorphisms in the human UDP glucuronosyltransferase 2B family: UGT2B4(D458E), UGT2B7(H268Y), and UGT2B15 (D85Y). Cancer Epidemiol Biomarkers Prev 2000; 9(3):329 333.
114. Patel M, Tang BK, Kalow W. (S)oxazepam glucuronidation is inhibited by ketoprofen and other substrates of UGT2B7. Pharmacogenetics 1995; 5(1):43 49.
115. Coffman BL, King CD, Rios GR, et al. The glucuronidation of opioids, other xenobiotics, and androgens by human UGT2B7Y(268) and UGT2B7H(268). Drug Metab Dispos 1998; 26(1): 73 77.
116. Court MH, Krishnaswamy S, Hao Q, et al. Evaluation of 3′ azido 3′ deoxythymidine, morphine, and codeine as probe substrates for UDP glucuronosyltransferase 2B7 (UGT2B7) in human liver microsomes: specificity and influence of the UGT2B7*2 polymorphism. Drug Metab Dispos 2003; 31(9):1125 1133.
117. Girard C, Barbier O, Veilleux G, et al. Human uridine diphosphate glucuronosyltransferase UGT2B7 conjugates mineralocorticoid and glucocorticoid metabolites. Endocrinology 2003; 144(6):2659 2668.
118. Holthe M, Rakvag TN, Klepstad P, et al. Sequence variations in the UDP glucuronosyltransferase 2B7 (UGT2B7) gene: identification of 10 novel single nucleotide polymorphisms (SNPs) and analysis of their relevance to morphine glucuronidation in cancer patients. Pharmacogenomics J 2003; 3(1):17 26.
119. Holthe M, Klepstad P, Zahlsen K, et al. Morphine glucuronide to morphine plasma ratios are unaffected by the UGT2B7 H268Y and UGT1A1*28 polymorphisms in cancer patients on chronic morphine therapy. Eur J Clin Pharmacol 2002; 58(5):353 356.
120. Sawyer MB, Innocenti F, Das S, et al. A pharmacogenetic study of uridine diphosphate glucuronosyltransferase 2B7 in patients receiving morphine. Clin Pharmacol Ther 2003; 73(6): 566 574.
121. Jin CJ, Miners JO, Lillywhite KJ, et al. cDNA cloning and expression of two new members of the human liver UDP glucuronosyltransferase 2B subfamily. Biochem Biophys Res Commun 1993; 194:496 503.

122. Chen G, Blevins Primeau AS, Dellinger RW, et al. Glucuronidation of nicotine and cotinine by UGT2B10: loss of function by the UGT2B10 Codon 67 (Asp>Tyr) polymorphism. Cancer Res 2007; 67:9024 9029.
123. Belanger A, Pelletier G, Labrie F, et al. Inactivation of androgens by UDP glucuronosyltransferase enzymes in humans. Trends Endocrinol Metab 2003; 14(10):473 479.
124. Beaulieu M, Levesque E, Hum DW, et al. Isolation and characterization of a novel cDNA encoding a human UDP glucuronosyltransferase active on C19 steroids. J Biol Chem 1996; 271(37):22855 22862.
125. Abernethy DR, Greenblatt DJ, Divoll M, et al. Enhanced glucuronide conjugation of drugs in obesity: studies of lorazepam, oxazepam, and acetaminophen. J Lab Clin Med 1983; 101(6): 873 880.
126. Chouinard S, Pelletier G, Bélanger A, et al. Isoform specific regulation of uridine diphosphate glucuronosyltransferase 2B enzymes in the human prostate: differential consequences for androgen and bioactive lipid inactivation. Endocrinology 2006; 147(11): 5431 5442.
127. Court MH, Hao Q, Krishnaswamy S, et al. UDP glucuronosyltransferase (UGT) 2B15 pharmacogenetics: UGT2B15 D85Y genotype and gender are major determinants of oxazepam glucuronidation by human liver. J Pharmacol Exp Ther 2004; 310(2):656 665.
128. Wilson W III, Pardo Manuel de Villena F, Lyn Cook BD, et al. Characterization of a common deletion polymorphism of the UGT2B17 gene linked to UGT2B15. Genomics 2004; 84(4):707 714.
129. Upton RA, Buskin JN, Williams RL, et al. Negligible excretion of unchanged ketoprofen, naproxen, and probenecid in urine. J Pharm Sci 1980; 69(11):1254 1257.
130. Baber N, Halliday L, Sibeon R, et al. The interaction between indomethacin and probenecid. A clinical and pharmacokinetic study. Clin Pharmacol Ther 1978; 24(3):298 307.
131. Yu TF, Perel J. Pharmacokinetic and clinical studies of carprofen in gout. J Clin Pharmacol 1980; 20(5 6 pt 1):347 351.
132. Spahn H, Spahn I, Benet LZ. Probenecid induced changes in the clearance of carprofen enantiomers: a preliminary study. Clin Pharmacol Ther 1989; 45(5):500 505.
133. Bannier A, Comet F, Soubeyrand J, et al. Effect of probenecid on isofezolac kinetics. Eur J Clin Pharmacol 1985; 28(4):433 437.
134. de Miranda P, Good SS, Yarchoan R, et al. Alteration of ZDV pharmacokinetics by probenecid in patients with AIDS or AIDS related complex. Clin Pharmacol Ther 1989; 46(5): 494 500.
135. Meffin PJ, Zilm DM, Veenendaal JR, et al. A renal mechanism for the clofibric acid probenecid interaction. J Pharmacol Exp Ther 1983; 227(3):739 742.
136. Barbier O, Turgeon D, Girard C, et al. 3′ azido 3′ deoxythimidine (ZDV) is glucuronidated by human UDP glucuronosyltransferase 2B7 (UGT2B7). Drug Metab Dispos 2000; 28(5):497 502.
137. Haumont M, Magdalou J, Lafaurie C, et al. Phenobarbital inducible UDP glucuronosyltransferase is responsible for glucuronidation of 3′ azido 3′ deoxythymidine: characterization of the enzyme in human and rat liver microsomes. Arch Biochem Biophys 1990; 281(2):264 270.
138. Resetar A, Spector T. Glucuronidation of 3′ azido 3′ deoxythymidine: human and rat enzyme specificity. Biochem Pharmacol 1989; 38(9):1389 93.
139. Rajaonarison JF, Lacarelle B, De Sousa G, et al. In vitro glucuronidation of 3′ azido 3′ deoxythymidine by human liver. Role of UDP glucuronosyltransferase 2 form. Drug Metab Dispos 1991; 19(4):809 815.
140. Sim SM, Back DJ, Breckenridge AM. The effect of various drugs on the glucuronidation of ZDV (azidothymidine; ZDV) by human liver microsomes. Br J Clin Pharmacol 1991; 32(1):17 21.
141. Trapnell CB, Klecker RW, Jamis Dow C, et al. Glucuronidation of 3′ azido 3′ deoxythymidine (ZDV) by human liver microsomes: relevance to clinical pharmacokinetic interactions with atovaquone, fluconazole, methadone, and valproic acid. Antimicrob Agents Chemother 1998; 42(7):1592 1596.
142. Lee BL, Tauber MG, Sadler B, et al. Atovaquone inhibits the glucuronidation and increases the plasma concentrations of ZDV. Clin Pharmacol Ther 1996; 59(1):14 21.
143. Sahai J, Gallicano K, Pakuts A, et al. Effect of fluconazole on ZDV pharmacokinetics in patients infected with human immunodeficiency virus. J Infect Dis 1994; 169(5):1103 1107.

144. McCance Katz EF, Rainey PM, Jatlow P, et al. Methadone effects on ZDV disposition (AIDS Clinical Trials Group 262). J Acquir Immune Defic Syndr Hum Retrovirol 1998; 18(5):435 443.
145. Barry M, Howe J, Back D, et al. The effects of indomethacin and naproxen on ZDV pharmacokinetics. Br J Clin Pharmacol 1993; 36(1):82 85.
146. Gallicano KD, Sahai J, Shukla VK, et al. Induction of ZDV glucuronidation and amination pathways by rifampicin in HIV infected patients. Br J Clin Pharmacol 1999; 48(2):168 179.
147. Lertora JJ, Rege AB, Greenspan DL, et al. Pharmacokinetic interaction between zidovudine and valproic acid in patients infected with human immunodeficiency virus. Clin Pharmacol Ther 1994; 56(3):272 278.
148. Rowland A, Gaganis P, Elliot J, et al. Binding of inhibitory fatty acids is responsible for the enhancement of UDP glucuronosyltransferase 2B7 activity by albumin: implications for in vitro in vivo extrapolation. J Pharmacol Exp Ther 2007; 321(1):137 147.
149. Boase S, Miners JO. In vitro in vivo correlations for drugs eliminated by glucuronidation: investigations with the model substrate ZDV. Br J Clin Pharmacol 2002; 54(5):493 503.
150. Soars MG, Ring BJ, Wrighton SA. The effect of incubation conditions on the enzyme kinetics of udp glucuronosyltransferases. Drug Metab Dispos 2003; 31(6):762 767.
151. Hara Y, Nakajima M, Miyamoto K, et al. Morphine glucuronosyltransferase activity in human liver microsomes is inhibited by a variety of drugs that are co administered with morphine. Drug Metab Pharmacokinet 2007; 22(2):103 112.
152. Kaivosaari S, Toivonen P, Hesse LM, et al. Nicotine glucuronidation and the human UDP glucuronosyltransferase UGT2B10. Mol Pharmacol 2007; 72(3):761 768.
153. Howell SR, Hazelton GA, Klaassen CD. Depletion of hepatic UDP glucuronic acid by drugs that are glucuronidated. J Pharmacol Exp Ther 1986; 236(3):610 614.
154. Cappiello M, Giuliani L, Pacifici GM. Distribution of UDP glucuronosyltransferase and its endogenous substrate uridine 5′ diphosphoglucuronic acid in human tissues. Eur J Clin Pharmacol 1991; 41(4):345 350.
155. Argikar U. Effects of age, induction, regulation and polymorphisms on the metabolism of antiepileptic drugs. In: PhD. thesis. Minneapolis: University of Minnesota, 2006.
156. Fabre G, Combalbert J, Berger Y, et al. Human hepatocytes as a key in vitro model to improve preclinical drug development. Eur J Drug Metab Pharmacokinet 1990; 15(2):165 171.
157. Sutherland L, Ebner T, Burchell B. The expression of UDP glucuronosyltransferases of the UGT1 family in human liver and kidney and in response to drugs. Biochem Pharmacol 1993; 45(2): 295 301.
158. Sabers A, Ohman I, Christensen J, et al. Oral contraceptives reduce lamotrigine plasma levels. Neurology 2003; 61(4):570 571.
159. Macdonald JI, Herman RJ, Verbeeck RK. Sex difference and the effects of smoking and oral contraceptive steroids on the kinetics of diflunisal. Eur J Clin Pharmacol 1990; 38(2):175 179.
160. Walle T, Fagan TC, Walle UK, et al. Stimulatory as well as inhibitory effects of ethinyloestradiol on the metabolic clearances of propranolol in young women. Br J Clin Pharmacol 1996; 41(4):305 309.
161. Fromm MF, Eckhardt K, Li S, et al. Loss of analgesic effect of morphine due to coadministration of rifampin. Pain 1997; 72(1 2):261 267.
162. Ebert U, Thong NQ, Oertel R, et al. Effects of rifampicin and cimetidine on pharmacokinetics and pharmacodynamics of lamotrigine in healthy subjects. Eur J Clin Pharmacol 2000; 56(4):299 304.
163. Burger DM, Meenhorst PL, Koks CH, et al. Pharmacokinetic interaction between rifampin and ZDV. Antimicrob Agents Chemother 1993; 37(7):1426 1431.
164. Kalyanaraman N. Inhibition of naltrexone metabolism by NSAIDs leading to metabolic switching and reactive metabolite formation. In: MS. thesis. Minneapolis: University of Minnesota, 2004.
165. Prueksaritanont T, Subramanian R, Fang X, et al. Glucuronidation of statins in animals and humans: a novel mechanism of statin lactonization. Drug Metab Dispos 2002; 30(5):505 512.
166. Ogilvie BW, Zhang D, Li W, et al. Glucuronidation converts gemfibrozil to a potent, metabolism dependent inhibitor of CYP2C8: implications for drug drug interactions. Drug Metab Dispos 2006; 34(1):191 197.

Appendix

Isoenzyme	Trivial names	Tissue expression	Endogenous substrates	Drug or xenobiotic substrates	Inducers	Inhibitors
UGT1A1	HP3 HUG_{Br-1} UGTBr1	Liver, small intestine, mammary glands	Bilirubin, estradiol (3-OH), 2-OH-estrone, 2-OH-estradiol *trans*-retinoic acid, Catechol estrogens (2-OH & 4-OH)15-OH-eicosa-tetraenoic acid, 20-OH-eicosa-tetraenoic acid, arachidonic acid, prostaglandin B1	Ethinyl estradiol, buprenorphine ferulic acid, genistein naltrexone (low), naloxone (low), SN-38 (active metabolite of irinotecan) alizarin, quinalizarin, retigabine	Bilirubin, chlorophenoxypropionic acid, chrysin, clofibrate, 3-MC, oltipraz, phenylpropionic acid, phenobarbital, clotrimazole, rifampin, and St John's wort WY-14643 Response elements for AhR, CAR, GR, PPAR-α, PXR, Nrf2 (antioxidant response element) have been identified	Atazanavir, indinavir, ketoconazole ($K_i = 3$ μM)
UGT1A2		Pseudogene in humans	–	–	–	–
UGT1A3		Liver (lower), small intestine, kidney, prostate, testes	*Bile acids*: (carboxyl functional group), e g, lithocholic acid, chenodeoxycholic acid Bilirubin (low) *Catechol estrogens*: (2-OH > 4-OH), 2-OH-estrone, 2-OH-estradiol, decanoic acid, dodecanoic acid, 15-OH-eicosatetraenoic acid, arachidonic acid	Afloqualone, alizarin, buprenorphine, norbuprenorphine, bropirimine, cyproheptadine, diphenylamine, diprenorphine, emodin, esculetin, eugenol, ezetimibe, fulvestrant, fisetin, genistein, 5,6,7,3′,4′,5′-hexamethoxyflavone, 3-hydroxydesloratadine, 7-hydroxyflavone, hydromorphone, 4-methylumbelliferone, morphine, nalorphine, naloxone, naltrexone, naringenin, quercetin (3->4-> 3′- >7-glucuronide), scopoletin, thymol, umbelliferone	β-Naphthoflavone, rifampin, WY-14643 Response elements for AhR, PPAR-α, PXR, have been identified Fibrates are potent inducers	Bile acids

				Substrates with carboxyl groups: clofibrate, ciprofibrate, etodolac, fenoprofen, ibuprofen, ketoprofen, naproxen (racemic > S), valproic acid and formation of simvastatin and atorvastatin lactones via an intermediate acyl glucuronide, (fourfold lower turnover by UGT2B17)		
UGT1A4	HUG_{Br-2}	Liver, small intestine	*Estrogens:* 2-OH-estrone, 2-OH estradiol, 4-OH catechol estrogens (low), estriol *Progestins*: 5α-pregnan-3α,20α-diol, 16α-hydroxy-pregnenolone, 19-hydroxy- and 21-hydroxy-pregnenolone, pregnenolone, androsterone, epiandrosterone, etiocholanone *Androgens:* dehydroepiandrosterone, dihydrotestosterone, epitestosterone, testostereone, 5α-androstan-3α, 17β-diol, 5β-androstan-3α,11α,17β-triol; bilirubin (very low), F_6-1α,23S,25$(OH)_3D_3$—a hexafluorinated Vit D_3 analog, 15-OH-eicosatetraenoic acid, 20-OH-eicosatetraenoic acid, arachidonic acid	*Tertiary amines:* Afloqualone, amitriptyline, chlorpheniramine, chlorpromazine, clozapine, cyproheptadine, diphenylamine, doxepin, imipramine, ketotifen, loxapine, olanzapine, promethazine, tamoxifen, tripelennamine, trifluoperazine *Aromatic heterocyclic amines:* croconazole, lamotrigine, nicotine (30X> velocity than UGT1A3), 1-phenylimidazole, posaconazole, retigabine *Primary and secondary amines*: 2- and 4-aminobiphenyl, diphenylamine, desmethylclozapine *Alcoholic and phenolic substrates:* borneol, carveol, carvacrol diosgenin, hecogenin, isomenthol, menthol, neomenthol, 1- and 2-naphthol (low), *p*-nitrophenol (low), nopol, tigogenin	Phenobarbital, phenytoin, and carbamazepine, TCDD, PCN (transgenic mice), WY-14643 (weak) In vivo induction experiments indicate response elements are present for CAR, PXR, and PPAR-α ligands	Hecogenin Trifluoroperazine

(*Continued*)

Appendix (*Continued*)

Isoenzyme	Trivial names	Tissue expression	Endogenous substrates	Drug or xenobiotic substrates	Inducers	Inhibitors
UGT1A5				4-Methyl-umbelliferone (low), scopoletin (low), 1-hydroxypyrene	Rifampin, 3-methylchloranthrene	
UGT1A6	HP1 HlugP1 UGT1-6	Liver, kidney, intestine, brain, ovaries, testes, skin, spleen	Serotonin, 3-hydroxy-methyl DOPA	*Phenols:* APAP, 2-amino-5-nitro-4-trifluoromethylphenol (flutamide metabolite), BHA, BHT, 7-hydroxy-coumarin, 4-hydroxy-coumarin (low), dobutamine, 4-ethylphenol, 3-ethylphenol, 4-fluorocatechol, 2-OH-biphenyl, 4-iodophenol, 4-isopropylphenol (low), 4-methylcatechol, 4-methylphenol, methylsalicylate, 4-methylumbelliferone, 4-nitrophenol, 4-nitrocatechol, octylgallate, phenol, 4-propylphenol (low), *cis*-resveratrol, salicylate, 4-*tert*-butylphenol (low), tetrachlorocatechol, vanillin *Amines:* 4-aminobiphenyl, 1-naphthylamine >2-naphthylamine, *N*-OH-2-naphthylamine *Drugs:* APAP, β-blocking adrenergic agents (low activity) such as atenolol, labetolol, metoprolol, pindolol, propranolol, naproxen (R≫S for rat 1A6), salicylate, valproic acid	TCDD, β-naphthoflavone, 3-MC Response elements for AhR have been identified	α-napthol, 4-*tert*-butyl phenol, 4-methyl-umbelliferone, 7-hydroxy–coumarin

UGT1A7		Gastric epithelium, oesophagus	Estriol, 2-OH-estradiol, 4-OH-estrone	*Flavonoids:* chrysin, 7-hydroxyflavone, naringenin Benzo(a)pyrene phenols (7-OH≫9-OH>3-OH), benzo (a)pyrene-*tert*-7,8-dihydrodiol (7R-glucuronide, low affinity), 2-OH-biphenyl, 4-methylumbelliferone, 1- and 2-naphthol, 4-nitrophenol, octylgallate, vanillin	TCDD
UGT1A8	HP4	Liver, kidney, ovaries, testes, skin, spleen, oesophagus	2-OH-estrone, 4-OH-estrone, 2-OH-estradiol, 4-OH-estradiol, estrone, dihydrotestosterone, *trans*-retinoic acid, 4-hydroxy-retinoic acid, hyocholic acid, hyodeoxycholic, testosterone, LTB4	Alizarin, anthraflavic acid, apigenin, benzo(a)pyrene-*tert*-7, 8-dihydrodiol (7*R*- and 8*S*-glucuronides), emodin, fisetin, flavoperidol, genistein, naringenin, quercetin, quinalizarin, 4-methylumbelliferone, scopoletin, carvacrol, eugenol, 1-naphthol, *p*-nitrophenol, 4-aminobiphenyl, 2-OH-, 3-OH-, and 4-OH-biphenyl, buprenorphine (low), morphine (low), naloxone, naltrexone, ciprofibrate, diflunisal, diphenylamine, furosemide, MPA (high), phenolphthalein, propofol, valproic acid, nandrolone, 1-methyl-5α-androst-1-en-17β-ol-3-one (metabolite of metenolone), 5α-androstane-3α,17β-diol (metabolite of testosterone), (-)-epigallocatechin gallate (tea phenol), SN-38 (low) (metabolite of irinotecan), troglitazone (moderate), raloxifene (both 6β- and 4′-β-glucuronides), quercetin, luteolin	3-Methyl-cholanthrene

(*Continued*)

Appendix (*Continued*)

Isoenzyme	Trivial names	Tissue expression	Endogenous substrates	Drug or xenobiotic substrates	Inducers	Inhibitors
UGT1A9		Intestine, oesophagus	Retinoic acid, thyroxine (T4), tri-iodothyronine (T3; minor), 4-OH-estrone, 4-OH-estradiol (major), 15-OH-eicosatetraenoic acid, arachidonic acid, prostaglandin B1	*Planar Phenols:* Phenol, APAP, 2-OH-biphenyl, 4-iodophenol, 4-propylphenol, 4-isopropylphenol (low), 4-ethylphenol, 3-ethylphenol, 4-methylphenol, 4-nitrophenol, methylsalicylate, salicylate, mono(ethylhexyl) phthalate, BHA, BHT, vanillin,7-hydroxy-coumarin, 4-hydroxy-coumarin (low), 4-methyl-umbelliferone *Bulky Phenols:* Phenol red, phenolphthalein, fluorescein 4-*tert*-butylphenol (low), propofol (2,6-di-isopropylphenol) *Simple catechols:* Octyl gallate, propyl gallate *Primary amines:* 4-Aminobiphenyl *Xenobiotics:* APAP, bumetanide, carbidopa, clofibric acid, ciprofibric acid, dobutamine, dopamine, entacapone, ethinyl estradiol–(minor), fenofibric acid, furosemide, gemfibrozil, levodopa, MPA, propofol, atenolol, labetolol, metoprolol, pindolol, propranolol, *R*-oxazepam, *p*-HPPH (phenytoin metabolite), raloxifene, retigabine, SN-38 (active metabolite	TCDD, tetrabutyl hydroquinone, clofibric acid	High concentrations of propofol, flurbiprofen

			of irinotecan), troglitazone, *NSAIDs*: (Low activity against all NSAIDs) diflunisal, fenoprofen, flurbiprofen, ibuprofen, ketoprofen, mefenamic acid, naproxen *Flavonoids:* Emodin, chrysin, 7-hydroxyflavone, galangin, naringenin, quercetin carveol, nopol, citronellol, 6-hydroxychrysene, retigabine, quercetin (3->7->3′->4′-glucuronide)		
UGT1A10	Intestine	2-OH-estrone (low), 4-OH estrone (low), dihydrotestosterone, testosterone, 15-OH-eicosatetraenoic acid, arachidonic acid, prostaglandin B1	Alizarin, anthraflavic acid, apigenin, benzo(a)pyrene-*tert*-7,8-dihydrodiol (7*R*- and 8*S*-glucuronides, high affinity), emodin, fisetin, genistein, naringenin, quercetin, quinalizarin, 4-methylumbelliferone, scopoletin, carvacrol, eugenol, MPA, 17β-methyl-5β-androst-4-ene-3α,17α-diol (metabolite of metadienone), nandrolone, 1-methyl-5α-androst-1-en-17β-ol-3-one (metabolite of metenolone), 5α-androstane-3a, 17β-diol (metabolite of testosterone), SN-38 (minor), raloxifene (4′-β-glucuronide only)		
UGT1A11	pseudogene		–	–	–
UGT1A12	pseudogene		–	–	–

(*Continued*)

Appendix (*Continued*)

Isoenzyme	Trivial Names	Species	Human Counter-part	Tissue Expression	Endogenous Substrates	Drug or Xenobiotic Substrates	Inducers	Inhibitors
UGT2B4		Human, variant of UGT2B11, 82% homologous with UGT2B7		Liver, small intestine, aerodigestive tract (tongue, mouth)	6α-hydroxy bile acids, 3α-hydroxy pregnanes, 3α-, 16α-, 17β-androgens, metabolites of PUFA, arachidonic and linoleic acids, estriol, 2-OH-estriol, 4-OH-estrone	*Phenols:* Eugenol, 4-nitrophenol, 2-aminophenol, 4-methylumbelliferone, morphine, zidovudine (low)	Fenofibric acid, chenodeoxycholic acid activated Response elements for FXR and PPAR-α have been identified	
UGT2B7		Human		Liver, kidney, intestine, brain (cerebellum), esophagus, mammary gland	*Arachidonic acid metabolites*: Arachidonic acid, LTB4, 5-HETE, 12-HETE, 15-HETE, 20-HETE, and 13-HODE) *Bile acids*: hyodexycholic acid *Estrogens*: Estriol, estradiol (17β-hydroxy),4-OH-estrone (high) 2-OH-estrone, 2-OH-estriol *Pregnanes:* 3α-hydroxy pregnanes *Androgens*: 3α -, 16α -, 17β-androgens *Others*: 5α- and 5β-dihydroaldosterone,	*R*-oxazepam, naproxen, menthol, abacavir, APAP, almokalant, carbamazepine, carvedilol, chloramphenicol, epirubicin, 1′-OH-estragole, gemcabene, 5-OH-rofecoxib, lorazepam, menthol, 4-methylumbelliferone, Maxipost, 1-naphthol (low), 4-nitrophenol, octylgallate, propranolol, temazepam zidovudine *Carboxylic acid-containing drugs*: benoxaprofen, ciprofibrate, clofibric acid, diflunisal, DMXAA, fenoprofen, ibuprofen, indomethacin,	Rifampin, phenobarbital, HNF1α	*R*-oxazepam and zidovudine (competitive), flunitrazepam relatively potent (K_i ∼50–90 μM), but also inhibits UGT1A3 (K_i = 20–30 μM for 2-OH-estrogens) and UGT1A1 (K_i > 200 μM), diclofenac, etonitazenyl

			trans-retinoic acid, prostaglandin B1	ketoprofen, naproxen, pitavastatin, simvastatin acid, tiaprofenic acid, valproic acid, zaltoprofen, zomepirac, *S*-flurbiprofen *Opioids*: morphine 3-OH>6-OH, buprenorphine, nalorphine, naltrexone, codeine (low), and naloxone	
UGT2B10	Humans	Liver, kidney, lung, small intestine, spleen, mammary gland, testis, prostate, placenta	*Arachidonic acid metabolites*: Arachidonic acid, LTB4, 5-HETE, 12-HETE, 15-HETE, 20-HETE, and HODE		
UGT2B11	Humans 91% identical to UGT2B10, 76% identical to UGT2B15 and UGT2B17	Liver, kidney, prostrate, lungs, mammary gland, skin, adipose tissue, adrenal glands	*Arachidonic acid metabolites*: Arachidonic acid, LTB4, HETE, 12-HETE, 15-HETE, 20-HETE, and HODE		
UGT2B15	Human	Liver, prostate, testes, adipose tissue	*Steroids:* UGT2B17 glucuronidates preferentially at the 17-OH positions of androgens (>3OH) Aldosterone, 5α- and 5β-dihydroaldosterone, androsterone (low),	*S*-oxazepam, temazepam, S-OH-rofecoxib, E-4-OH-tamoxifen, eugenol, nansroline, phenolphthalein	Androgens, epidermal growth factor, and IL-1α downregulate UGT2B15 and UGT2B17 expression in LnCAP cells

(*Continued*)

Appendix (*Continued*)

Isoenzyme	Trivial Names	Species	Human Counter-part	Tissue Expression	Endogenous Substrates	Drug or Xenobiotic Substrates	Inducers	Inhibitors
					dihydrotestosterone (3 and 17-O-glucuronidation), androstane-3α-17β-diol (17-O-glucuronidation), 3α-, 16α-, 17β–OH-androgens, 3α-hydroxypregnanes; estriol, 4-OH-estrone (high) 2-OH-estrone, 2-OH estriol *Bile acids*: hyodeoxycholic acid (hydroxyl glucuronide), lithocholic acid (hydroxyl>carboxyl) Retinoic acid			(prostate cancer cell line)
UGT2B17		Human		Liver, kidney, prostrate, testes, placenta, uterus, mammary glands, skin, adrenal glands	Dihydrotestosterone, Testosterone, androsterone UGT2B17 glucuronidates at both the 3- and the 17-OH positions of androgens	Ibuprofen *Anthraquinones, coumarins, flavonoids, and terpenoids*: alizarin, anthraflavic acid, borneol, chrysin, emodin, eugenol, 4-ethylphenol, galangin, 7-hydroxyflavone, menthol (low), 4-methylumbelliferone (low), 1-naphthol, naringen (low), 4-nitrophenol, phenol		Androgens, epidermal growth factor, and IL-1α downregulate UGT2B15 and UGT2B17 expression in LnCAP cells (prostate cancer cell line)

		red, 4-propylphenol, scopoletin, and umbelliferone (low) Alizarin, borneol, galangin, and scopoletin are higher turnover compounds

AhR activators in humans—TCDD, β-naphthoflavone, 3-methylcloranthrene
PXR activators in rodents—PCN, dexamethasone
PXR activators in humans—clotrimazole, rifampin, and St John's wort
CAR activators in humans—3-MC, phenylpropionic acid, phenobarbital, phenytoin, carbamazepine
PPARα activator in humans—clofibric acid, fenofibric acid, pirinixic acid (WY-14643)
PPARα activator in humans—rosiglitazone
FXR activators in humans—chenodeoxycholic acid
Underlined substrates denote the most commonly used probes for enzymatic activity
Abbreviations: AhR, aromatic hydrocarbon receptor; TCDD, tetrachlorodibenzodioxin; PXR, pregnenolone-16α-nitrile-X-receptor; PCN, pregnenolone-16α-nitrile; CAR, constitutive androstane receptor; MC, methylcholanthrene; PPARα, peroxisome proliferated-activated receptor-α; FXR, farnesoid-X-receptor; LXR, liver-X-receptor; RXR, retinod-X-receptor; 5-HETE, 5-OH-eicosatetraenoic acid; LTB4, leukotriene B4; 13-HODE, hydroxyoctadecadienoic acid; DMXAA, dimethylxanthenone-4-acetic acid

7
Pharmacogenetics

Ann K. Daly
Institute of Cellular Medicine, Newcastle University Medical School, Framlington Place, Newcastle upon Tyne NE2 4HH, U.K.

INTRODUCTION

Pharmacogenetics can be defined as the study of genetically determined variations that are revealed by the effects of drugs and other xenobiotics (1). The subject includes both the areas of drug biotransformation and responses of cells or tissues to drugs, but this chapter is concerned only with the pharmacogenetics of human drug biotransformation. Interindividual variability in drug metabolism can be determined by a number of different factors but polymorphisms in the genes encoding metabolizing enzymes and in genes regulating their transcription are important factors. Genetic polymorphisms with functional effects on drug metabolism were detected initially on the basis of discontinuous variation in phenotype where phenotype represented either levels of the enzyme or rate of metabolism (1). This approach originally led to the detection of a variety of relatively common polymorphisms. However, other sources of genetic variation in drug metabolism such as polygenic effects where the variation is controlled by a number of different genes or rarer genetic defects that occur at a frequency of less than 1 in 100 were not necessarily detected. More detailed studies on DNA sequence variation are now routine and have resulted in the detection of a wide range of polymorphisms affecting drug metabolism (2–5).

Pharmacogenetic polymorphisms in genes encoding xenobiotic metabolizing enzymes may have a number of effects, depending on both the type of reaction catalyzed and the type of substrate. In the case of drugs, the consequences of a polymorphism may be toxic plasma concentrations if there is a deficiency in metabolizing enzymes or lack of response if activation by a polymorphic enzyme is required for biological activity or if higher than normal levels of a metabolizing enzyme result in too rapid a rate of elimination (3). Whether absence of a metabolizing enzyme results in toxicity will depend on a number of factors, including the therapeutic margin of safety versus activity and, in particular, the contribution the polymorphic enzyme makes to total metabolism.

With recent studies on variability in the human genome such as those involving the single nucleotide polymorphism (SNP) consortium and the HapMap as well as continuing studies more specifically on pharmacogenetics of drug metabolism, it is now recognized that all genes that contribute to human drug metabolism are subject to genetic

polymorphism (6,7). However, the functional consequences of these polymorphisms vary greatly. In some cases, the result is absence of enzyme activity in significant numbers of individuals whereas, in other cases, the effects of polymorphism are relatively small and not of major importance in terms of drug treatment. In view of the vast amount of pharmacogenetic data now available, the emphasis in this chapter is on those genes that are currently recognized to have well-established roles in the metabolism of licensed drugs and where pharmacogenetic knowledge is extensive.

PHASE I POLYMORPHISMS

Among phase I enzymes, the cytochrome P450 superfamily is the most important group of enzymes in terms of both numbers of drugs metabolized (see chap. 4) and understanding of the effects of pharmacogenetic polymorphisms. For this reason, the emphasis in this section is on cytochrome P450 polymorphisms.

Cytochrome P450 Polymorphisms

A range of polymorphisms have been described in the 50 or more genes encoding human cytochromes P450. Many of these are functionally significant, possibly reflecting the nonessential nature of many P450 reactions as well as the overlapping substrate specificity of these enzymes. In the case of four different isoforms, CYP2D6, CYP2C19, CYP2A6, and CYP3A5, there is complete absence of active enzyme in significant numbers of individuals (Table 1). In addition, polymorphisms resulting in either decreased or increased activity are common in most isoforms involved in drug metabolism (Table 1). For at least three separate CYP genes, higher than normal activity due to the existence of copy number variants can also occur.

CYP1 Family

The three isoforms in this family, CYP1A1, CYP1A2, and CYP1B1, have been well studied pharmacogenetically but only CYP1A2 has a well-established role in hepatic drug metabolism.

CYP1A2. CYP1A2 substrates include the antipsychotics clozapine and olanzapine as well as caffeine, *R*-warfarin, melatonin, and theophylline. As with other CYP1 family

Table 1 CYP Genes and Polymorphic Drug Metabolism

Gene	Nature of polymorphism
CYP1A2	No absence of activity reported. Some variation
CYP2A6	Absence of activity common. Some ultrarapid metabolizers
CYP2B6	No absence of activity reported. Some variation
CYP2C8	No absence of activity reported. Some variation
CYP2C9	Very low activity in some individuals.
CYP2C19	Absence of activity common. Some ultrarapid metabolizers
CYP2D6	Absence of activity common. Some ultrarapid metabolizers
CYP2E1	No absence of activity reported. Some variation
CYP3A4	No absence of activity reported. Some variation
CYP3A5	Absence of activity common
CYP3A7	Absence of activity common

members, CYP1A2 is inducible by a range of compounds via the Ah receptor. Though a few coding region polymorphisms have been identified (8), with the exception of one amino acid substitution found at reasonable frequencies in Chinese (9), other polymorphisms are very rare and therefore unlikely to be population risk factors for adverse drug reactions or disease even if functionally significant. More common polymorphisms have been detected in upstream sequences and in intron 1 in an area upstream of the translation start site (C-163A polymorphism termed *CYP1A2*1F*). In phenotyping studies, smokers positive for certain variants (*CYP1A2*1C* and *CYP1A2*1F*) showed significantly higher enzyme activity compared with smokers positive only for the wild-type sequences suggesting that these polymorphisms may affect inducibility (10,11). Screening for two polymorphisms (C-163A and T-2467del) allows the identification of the five most common haplotypes in Caucasians. There is no evidence of any significant differences in CYP1A2 activity/inducibility between the various haplotypes but the number of subjects studied was relatively small (12). *CYP1A2*1K*, a relatively rare variant of *CYP1A2*1F*, has been found in African populations (13). This allele includes C-729T as well as C-163T, with T-729 abolishing a binding site for a transcription factor of the Ets family that results in decreased CYP1A2 expression and caffeine metabolism.

Though there are continuing reports of considerable variation in CYP1A2 activity in phenotypic studies that mainly use caffeine as a probe drug, a clear relationship between phenotype and genotype is still lacking. However, a number of studies indicate a contribution of *CYP1A2*1F* to higher inducibility (11,14) though not to slower metabolism as was suggested incorrectly in a recent study (15,16). As stated recently, "CYP1A2 metabolic phenotyping by a DNA test cannot yet be performed with any degree of reliability" (17), and this is also true for genotyping.

CYP2 Family

This family includes the largest number of isoforms that contribute to drug metabolism, including three where complete absence of activity is seen commonly in populations.

CYP2A6. CYP2A6 is a mainly hepatic P450 with a limited range of xenobiotic substrates. Examples of specific substrates are nicotine, coumarin, pilocarpine, the antiplatelet drug SM-12502, and the prodrug tegafur (18). Evidence for the existence of genetic polymorphism in this gene emerged during cDNA cloning studies when an apparently inactive allelic variant with a single base difference resulting in an amino acid substitution was isolated in addition to a wild-type cDNA (19). In parallel with this study, evidence of considerable interindividual variation in human coumarin metabolism in vivo was reported (20,21). Over 20 distinct CYP2A6 alleles have now been described and additional minor variants of certain of these also occur (8). Some individuals also appear to have an additional copy of the wild-type allele (22,23) and may therefore show unusually fast metabolism, though further studies on this copy number variation are needed. Most variant alleles so far identified appear to be associated with absent or decreased activity. The most common variant allele *CYP2A6*4* has all or part of CYP2A6 deleted and is seen at an allele frequency of approximately 15% to 20% in East Asians but more rarely in Europeans with an allele frequency of approximately 3% (24,25). On the other hand, the original allelic variant *CYP2A6*2*, which is associated with absence of activity due to an amino acid substitution, occurs at an allele frequency of approximately 3% in Europeans but has not been detected in East Asians (25,26). In a recent study, a common variant (*CYP2A6*1B*) with a gene conversion to CYP2A7 in the 3′-noncoding

region has been shown to be associated with higher enzyme activity in vivo, probably because of increased mRNA stability (27). The contribution of CYP2A6 to nitrosamine activation as well as its role in nicotine metabolism makes it a good candidate as a susceptibility gene for cancers related to tobacco smoking as well as to adverse drug reactions relating to other substrates (28,29). However, it seems likely that such an effect will only be detectable in East Asians and that the population frequency of variant alleles in other ethnic groups will be too low for any consistent associations to emerge, even though it is possible that it will be an individual risk factor.

CYP2B6. CYP2B6 was originally regarded as an enzyme of minor importance except when its expression was induced by exposure to phenobarbital-type inducers. However, it is now recognized that levels of expression in uninduced livers are higher than previously thought (30,31). Since CYP2B6 has a role in the biotransformation of several clinically important drugs including cyclophosphamide, bupropion, and efavirenz as well as a range of xenobiotics including various nitrosamines, the existence of polymorphism in this gene is of considerable interest especially since there is evidence of variability in enzyme activity (32). Approximately 30 different alleles, mainly showing nonsynoymous mutations, have now been described and in addition to the wild-type *CYP2B6*1*, several of the variants occur at high population frequencies (33). The functional significance of the various polymorphisms is still not completely clear, and generally effects on enzyme activity may be small. A recent report on a new variant named *CYP2A6*29*, a hybrid between CYP2B6 and the neighboring CYP2B7 gene, showed that this variant was associated with significant impaired metabolism of efavirenz in vivo (34), but the population frequency of this allele is low compared with many of the other known variants. In general, further studies on CYP2B6 pharmacogenetics, especially in vivo, would be helpful.

CYP2C8. CYP2C8 was one of the first human cytochromes P450 with a major role in drug metabolism to be cloned (35). Its minor though important role in drug metabolism is now well recognized with drug substrates including paclitaxel, all-*trans* retinoic acid, cerivastatin, rosiglitazone, repaglinide, and amodiaquine (36). In addition to the wild-type allele, at least nine variant alleles with nonsynonymous base substitutions together with two other variants showing frameshifts are known to exist (8). The variants associated with frameshifts and one with a premature stop codon are associated with absence of activity. Several of the nonsynonymous variants appear to show decreased activity, though this has been suggested to be substrate dependent. For example, in the case of *CYP2C8*3* that codes for two nonsynoymous polymorphisms, there are indications that the variant allele shows decreased activity with paclitaxel but increased activity with repaglinide and rosiglitazone (37 40). A haplotype that includes several different intron polymorphisms has also been suggested to be associated with decreased activity toward paclitaxel (41). Several of the nonsynoymous or frameshift-encoding variants occur at very low population frequencies but *CYP2C8*2*, *CYP2C8*3*, and *CYP2C8*4* are relatively common, at least in some ethnic groups. *CYP2C8*2* occurs at a frequency of 0.18 among African Americans but is very rare in Europeans with the opposite true of *CYP2C8*3* that has a frequency of 0.13 in Europeans and 0.02 in African Americans (37). In the case of *CYP2C8*4*, the frequency among Europeans is 0.075 but the allele appears rare in African Americans (38). In general, though there have been no reports of individuals with complete absence of CYP2C8 activity, based on our current knowledge of variant alleles, this is a rare possibility. Our understanding of polymorphism in CYP2C8 is now good in terms of reports of variant alleles but the importance of all these

polymorphisms in clinical response is still poorly understood, mainly due to most patient-based studies involving small numbers.

CYP2C9. In the 1960s and 1970s, reports appeared on the existence of individuals with an impaired ability to hydroxylate the drugs phenytoin and tolbutamide (42,43). Subsequent purification and cDNA cloning experiments resulted in the identification of CYP2C9 as the enzyme responsible for tolbutamide and phenytoin hydroxylation (35,44 46). It is now recognized that CYP2C9 is responsible for approximately 20% of all cytochrome P450 mediated oxidations of prescribed drugs (47). Therapeutically important CYP2C9 substrates include *S*-warfarin, other coumarin anticoagulants, phenytoin, and a range of nonsteroidal anti-inflammatory drugs (48). Evidence for the possible existence of variant CYP2C9 alleles was obtained from alignment of a number of cDNA sequences, and population studies confirmed that two of these variants (*CYP2C9*2* and *CYP2C9*3*) occurred in vivo (49). At least 27 additional variant alleles have now been identified (8). With the exception of one of these (*CYP2C9*6*), all other CYP2C9 variant alleles described so far are associated with a single nonsynonymous base change. The two most common variant alleles are *CYP2C9*2* and *CYP2C9*3* and, among Northern Europeans, over 30% of the population are positive for one or two of these alleles. An overall allele frequency for *CYP2C9*2* of 0.10 compared with 0.08 for *CYP2C9*3* was found in Europeans (50,51). Both *CYP2C9*2* and *CYP2C9*3* occur more rarely in other ethnic groups including East Asians and African Americans, and the other variant alleles are all seen at population frequencies in the order of 1% (33).

CYP2C9 polymorphisms are particularly relevant to the metabolism of drug substrates with narrow therapeutic indices where adverse drug reactions are common such as warfarin and phenytoin. In the case of warfarin, individualization of dose on the basis of drug response is a standard procedure but a large number of studies have now found a consistent relationship between warfarin dose requirement and CYP2C9 genotype (52). An example of data showing the relationship between CYP2C9 genotype and warfarin dose requirement is shown in Figure 1 (53). There is also evidence that individuals with

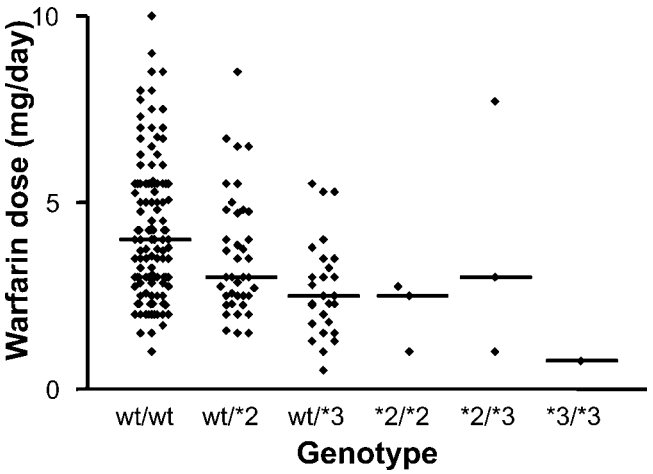

Figure 1 Relationship between CYP2C9 genotype and warfarin dose requirement for 200 randomly selected Caucasian individuals. Samples were genotyped for *CYP2C9*2* and *CYP2C9*3*. The median dose for each genotype is indicated by horizontal bars. There was a significant difference in dose requirements between genotype groups ($p = 0.0002$; Kruskal Wallis test). *Source*: From Ref. 53.

one or more "low-activity" CYP2C9 alleles may be at increased risk of bleeding problems especially during initiation of treatment. In the United States, FDA guidelines now suggest that genotyping for CYP2C9 and the warfarin target VKORC1 should be performed prior to prescription of warfarin (54). In general, studies suggest that CYP2C9 genotype contributes between 10% and 20% of the variability in warfarin dose requirement compared with a 20% to 30% contribution from VKORC1 genotype (55). Up to the present, clinical trials on genotyping for CYP2C9 prior to warfarin prescription, in some cases with VKORC1 genotyping included as well, have generally not shown a benefit (56 58). However, the statistical power of these studies may not have been adequate to detect an effect in relation to bleeding.

Other CYP2C9 substrates including nonsteroidal anti-inflammatory drugs are also frequently associated with adverse drug reactions. Some recent reports suggest that CYP2C9 genotype may predict susceptibility to NSAID-related gastrointestinal bleeding (59,60). One study found an increased incidence of *CYP2C9*3* heterozygotes in patients with bleeding undergoing endoscopy (60). There are some limitations with this study, including small numbers of patients and concerns about genotype frequencies among controls and classification of NSAIDs as CYP2C9 substrates, but further larger studies would be helpful to increase our understanding of the relevance of CYP2C9 to this common adverse reaction (61,62).

CYP2C19. A phenotypic polymorphism affecting the metabolism of the anticonvulsant drug mephenytoin was described in the early 1980s (63). Some individuals appeared to be unable to hydroxylate the *S*-enantiomer of this compound, and the deficiency appeared to be more common among East Asians than Europeans, affecting approximately 20% of East Asians and 3% of Europeans. Though it was soon established that *S*-mephenytoin hydroxylation was catalyzed by a cytochrome P450 enzyme, identification of the precise isoform involved proved quite difficult, probably mainly due to the protein being expressed at a lower level in human liver than most drug-metabolizing P450s (64). It is now known that the enzyme responsible for *S*-mephenytoin hydroxylation is encoded by the CYP2C19 gene. Two relatively common variant alleles together with five other rarer alleles associated with absence of enzyme activity have been identified (8). The two common alleles are associated with production of truncated proteins though absence of activity can also arise due to amino acid substitutions (64). Individuals with the CYP2C19 deficiency have two variant alleles present. Heterozygotes may show impaired metabolism. CYP2C19 is responsible for the metabolism of a relatively small number of commonly prescribed drugs, including the proton pump inhibitor omeprazole. Individuals with an absence of CYP2C19 activity show a better response to treatment of peptic ulcer with this drug compared with those with one or two normal alleles (65), apparently due to higher drug levels in the poor metabolizer group. Several recent studies indicate that the antiplatelet agent clopidogrel is less effective in individuals with at least one variant CYP2C19 allele probably because of a major role for CYP2C19 in activation of this prodrug (66 69). Some benzodiazepines including diazapam and clobazam are CYP2C19 substrates, and individuals defective in CYP2C19 may be at risk of toxicity such as oversedation (70). The antidepressants citalopram and escipalopram are mainly metabolized by CYP2C19, and patients heterozygous for variant alleles show higher serum levels of the parent drug (71). Voriconazole, a second-generation triazole antifungal agent, is a CYP2C19 substrate with contributions by other P450s, particularly CYP3A4, to its metabolism (72). The U.S. drug label mentions that individuals heterozygous for CYP2C19 have on average twofold higher exposure levels than

homozygous wild-type individuals, but this is currently for information only with no requirement for genotyping prior to prescription (54).

The variant allele *CYP2C19*17* includes an upstream polymorphism that apparently increases transcription levels and is associated with higher levels of gene expression (73). This variant appears to be associated with faster than normal metabolism of omeprazole and the antidepressant escitalopram (74,75).

CYP2D6. In the mid-1970s, 5% to 10% of individuals were found to be unable to metabolize the drugs debrisoquine and sparteine efficiently apparently due to a genetic defect (debrisoquine-sparteine polymorphism) (76,77). Further studies showed that metabolism of certain other drugs, mainly antidepressants, antipsychotic agents, and β-blockers, was also defective in these individuals. It was then established that the enzyme responsible for human debrisoquine metabolism was a cytochrome P450, which is now termed CYP2D6 (78). Subsequently, following isolation of cDNA and genomic clones, the molecular basis of the defect was determined (79,80). It is now well established that in the region of 5% of Europeans and 1% of East Asians, known as poor metabolizers, lack CYP2D6 activity. Individuals showing impaired activity (often referred to as intermediate metabolizers) and particularly high levels of activity (ultrarapid metabolizers) have also been described (81). Those with activity in the normal range are known as extensive metabolizers. CYP2D6 is responsible for the metabolism in the region of 25% of all prescribed drugs that are subject to metabolism by cytochrome P450 (47).

Over 80 different allelic variants of *CYP2D6* have been identified and characterized (8). Approximately 95% of European poor metabolizers will have two copies of any combination of four alleles termed *CYP2D6*3*, *CYP2D6*4*, *CYP2D6*5*, and *CYP2D6*6*, which each encode defective forms of CYP2D6 (Table 2) (82,83). The remaining 5% of poor metabolizers are homozygous or heterozygous for a range of different "loss of function" alleles, with each individual allele relatively rare. The majority of inactivating mutations in *CYP2D6* are either point mutations resulting in splicing defects or deletions that lead to either a truncated protein or no protein at all being synthesized. However, two separate polymorphisms introducing amino acid substitutions have also been shown to be inactivating (8).

Many individuals fall into the category of intermediate metabolizers, which is particularly common among East Asians and in certain African regions. Intermediate metabolizers may be either heterozygous for one of the inactivating mutations or homozygous for alleles associated with impaired metabolism. The best-studied alleles associated with impaired metabolism are *CYP2D6*10*, which is common in Eastern Asia and *CYP2D6*17*, which is common in African populations. Both alleles have nonsynonymous polymorphisms that result in a less catalytically active gene product. A recent study has examined the activity of the variant enzymes with a range of common

Table 2 CYP2D6 Phenotype Genotype Relationships for Individual Alleles

Phenotype	Allele
Ultrarapid metabolism	CYP2D6*1×N, CYP2D6*2×N
Extensive metabolism	CYP2D6*1, CYP2D6*2
Intermediate metabolism	CYP2D6*9, CYP2D6*10, CYP2D6*17, CYP2D6*41
Poor metabolism	CYP2D6*3, CYP2D6*4, CYP2D6*5, CYP2D6*6

Alleles listed are the most common and widely studied examples. Other alleles are also associated with these phenotypes. For full details, see Ref. 8.

substrates and found that the extent of difference in catalytic acivity between these isoforms and the reference "wild-type" variant depends on the individual substrate (84). In European populations, two alleles associated with impaired metabolism, *CYP2D6*9* and *CYP2D6*41*, are relatively common. *CYP2D6*9* encodes a protein with an amino acid deleted. *CYP2D6*41* includes several different polymorphisms, including two nonsynoymous mutations that are also seen in the *CYP2D6*2* allele, an upstream polymorphism at position -1584 and a base substitution in intron 6. The nonsynonymous polymorphisms characteristic of *CYP2D6*2* are now generally considered not to affect enzyme activity, but the intron 6 polymorphism has been demonstrated to be associated with altered RNA splicing leading to lower levels of protein (85).

Ultrarapid metabolizers were originally identified on the basis of their extremely fast clearance of the antidepressant desmethylimipramine. Some individuals in this category have 13 copies of *CYP2D6* arranged as tandem repeats but a single-gene duplication event is more commonly associated with the ultrarapid phenotype (81). Depending on the precise country of origin, 1% to 8% of Europeans have one extra copy of the *CYP2D6*1* or *CYP2D6*2* alleles resulting in faster than average metabolism (86,87). Subjects with three to five tandem copies of *CYP2D6*2* have also been detected, mainly in African populations (88).

Despite the fact that the CYP2D6 polymorphism was initially identified almost 30 years ago, and it has been possible to identify most of those with the genetic deficiency for the last 15 years, CYP2D6 genotyping has so far failed to enter routine clinical practice. There are a number of possible reasons for this. These include the general difficulty of introducing pharmacogenotyping into clinical practice, the fact that a number of key CYP2D6 substrates have been withdrawn from the market due to the problems experienced by poor metabolizers (e.g., phenformin, perhexiline) and that certain types of CYP2D6 substrates are less commonly used than when the polymorphism was first described. Guidelines for dose adjustment for antidepressant drugs on the basis of CYP2D6 genotype have been formulated but have not yet been tested in clinical trials (89). The FDA-approved labels for atomoxetine and fluoxetine now include mention of CYP2D6. The label for atomoxetine, specificially mentioning the possibility of higher plasma concentrations in poor metabolizers, is for information only and a test is neither ''required'' nor ''recommended'' currently (54). However, there is now increasing new evidence that CYP2D6 genotype may be relevant to outcome of treatment with codeine and with tamoxifen.

The very widely used analgesic drug codeine is an important CYP2D6 substrate. It is activated to morphine exclusively by CYP2D6, and this is generally accepted to be essential to achieve analgesia. Two case reports concerning excessive activation of codeine in ultrarapid metabolizers with one additional copy of CYP2D6 have appeared. In the first, a patient prescribed a cough medicine containing codeine suffered life-threatening opioid intoxication (90). This individual had at least three copies of CYP2D6 on genotyping. The second concerned the death of a breast-fed baby 13 days after birth (91). His mother was prescribed codeine for pain postdelivery. Postmortem examination of stored breast milk samples showed a morphine level at least four times higher than expected, and the mother was found to have a CYP2D6 gene duplication with the infant, an extensive metabolizer. A study involving codeine administration to healthy volunteers of known CYP2D6 genotype showed that ultrarapid metabolizers were significantly more likely than extensive metabolizers to suffer sedation (92). It therefore appears that CYP2D6 genotyping in patients requiring treatment with codeine and related compounds could be beneficial both in avoiding dangerous intoxication and lack of response. However, there is a possibility that high levels of morphine described in some case reports

could result from concurrent intake of codeine and heroin rather than a problem CYP2D6 genotype (93).

Tamoxifen is an extremely successful and widely used treatment for hormone receptor positive breast cancer. Its metabolism is complex, but it has been recently recognized that CYP2D6 produces a 4-hydroxy-*N*-desmethyltamoxifen metabolite (endoxifen) (94). Endoxifen is found at high plasma levels in many patients and appears to bind strongly to estrogen receptors, suggesting it is important in the biological response to tamoxifen (95,96). Evidence is now emerging that patients positive for one or two CYP2D6 poor metabolizer alleles show an increased incidence of breast cancer relapse (97,98). As mentioned by the FDA (12,54), tamoxifen is also a substrate for CYP3A and CYP2C9, and it may be necessary to consider the effect of additional polymorphisms on tamoxifen metabolism before comprehensive recommendations can be formulated. In view of the availability of other effective treatments such as aromatase inhibitors, CYP2D6 genotyping may be of value in determining the most appropriate treatment for hormone receptor positive breast cancer (99).

CYP2E1. CYP2E1 is an ethanol-inducible cytochrome P450 that metabolizes mainly low molecular weight compounds such as acetone, ethanol, benzene, and nitrosamines. Due to the nature of its substrate specificity, CYP2E1 is of most interest in relation to its role in toxicology, but it also has a minor role in drug metabolism and is one of several cytochromes P450 demonstrated to convert acetaminophen to toxic quinones in overdose (100). Other drug substrates include isoniazid and the anesthetics halothane and enflurane. There is evidence of approximately 20-fold interindividual variation in expression of the enzyme in human livers, though phenotyping studies using the muscle relaxant chlorzoxazone as probe in Caucasian populations have demonstrated only two- to threefold variation in levels of activity (101). A number of genetic polymorphisms in *CYP2E1* have been reported but the majority of these occur in either upstream sequences or introns and mostly appear to lack functional significance. Polymorphisms affecting coding sequences are rare, but three nonsynonymous polymorphisms have been described. One of these, R76H encoded by *CYP2E1*2*, is associated with decreased catalytic activity and occurs at a low frequency in a Chinese population but has not been detected in other ethnic groups (102). It has been suggested that a polymorphism in the 5′-flanking region within a putative HNF-1-binding site may be of functional significance (103). This variant allele (*CYP2E1*5*) occurs at a frequency of 0.27 in Japanese but only 0.02 in Caucasians (104). In vitro studies suggest that this allele shows approximately 10-fold higher transcriptional activity than the wild type, but a study on phenotype-genotype relationships did not find any evidence for increased activity in vivo in those heterozygous for the polymorphism (101). However, an association between *CYP2E1*5* and susceptibility to nasopharyngeal cancer and alcoholic liver disease points to possible functional significance (105 107). A recent report suggests that those negative for CYP2E1 variants are more likely to develop isoniazid-induced hepatotoxicity (108). There is a need for further studies on the molecular basis of interindividual variation in CYP2E1 expression and also on the possibility that there is interindividual variability in ability to induce this enzyme, as reported in a study on ethanol induction of CYP2E1 (109).

CYP3 Family

CYP3A4 is the most abundant cytochrome P450 in most human livers and is also the cytochrome P450 with the widest range of drug substrates (110). Levels of CYP3A4

activity vary considerably between individuals and, in addition, the closely related gene, *CYP3A5*, shows a polymorphism with detectable expression in only 10% to 20% of individuals (111). A third *CYP3A* gene, *CYP3A7*, is universally expressed in fetal liver but is also expressed in some adult livers. Another CYP3A gene, CYP3A43, is expressed in extrahepatic tissues but does not appear to contribute to drug metabolism.

CYP3A4. A substantial number of variant CYP3A4 alleles have now been described including some associated with nonsynonymous mutations. Several of these give rise to alterations in catalytic activity (8). However, all the nonsynonymous mutations described up to the present are seen at very low population frequencies and therefore seem unlikely to be able to fully explain interindividual variation in CYP3A4 activity. A number of upstream polymorphisms have also been detected with one (A-392G in *CYP3A4*1B*), being common in a number of ethnic groups. The precise functional significance of these polymorphisms remains somewhat unclear, but one study has found significantly lower metabolism of quinine in carriers of this allele compared with wild-type individuals. This may be due to decreased binding of nuclear proteins to the sequence in the region of the polymorphism (112). There are also reports of disease associations, particularly with respect to prostate cancer, with *CYP3A4*1B* (110). It is possible that interindividual variation in levels of CYP3A4 in liver could be explained in part by polymorphisms in one of its transcriptional regulators PXR. Some of the observed interindividual variability in CYP3A4 levels could be due to both interindividual variation in levels of endogenous PXR ligands and interindividual variation in ability to induce CYP3A4 as a result of polymorphisms in PXR. Studies on polymorphism in PXR have identified several SNPs that may affect individual ability to induce CYP3A4 (113).

CYP3A5. Polymorphisms in CYP3A5 that explain the basis of the variation in expression of this gene have been well studied. In particular, a polymorphic site in intron 3 results in an A6986G polymorphism. Individuals positive for G (*CYP3A5*3* allele) at this position do not express CYP3A5 due to the creation of a cryptic splice site, which results in the incorporation of intron sequence in the mature mRNA leading to production of a truncated protein (114). This allele is very common in all ethnic groups examined up to the present. The rarer alleles *CYP3A5*6*, which also results in abnormal splicing, and *CYP3A5*7*, which has a frameshift present, also explain the absence of CYP3A5 expression in some African Americans (114). It is now possible to predict whether an individual will express hepatic CYP3A5, but it is still unclear whether variable expression of CYP3A5 can explain the wide interindividual variation seen in CYP3A activity toward a number of substrates. Individuals with a *CYP3A5*1* allele may show more rapid than average metabolism of CYP3A substrates since a number of CYP3A4 substrates are also efficiently metabolized by CYP3A5. There is some disagreement between studies regarding the activity of CYP3A5 with certain compounds and in some cases, actual kinetic constants. To some extent, this could be due to the use of different expression systems in kinetic studies. A number of studies comparing the contributions of CYP3A4 and CYP3A5 to clinically important drug substrates have now been performed both in vitro and in vivo (115). In general, the best-studied drugs have been midazolam and tacrolimus. For midazolam, despite early reports suggesting an important role for CYP3A5 in metabolism, most recent studies suggest that there is little difference in clearance of this drug between individuals of CYP3A5-expressor genotypes and nonexpressors (116 118). The situation with tacrolimus is different. As reviewed recently (119), a large number of published studies show that transplant patients positive for one or two alleles associated with CYP3A5 expression have a higher dose requirement for this

drug than nonexpressors. This appears to be the case regardless of the type of organ transplant or ethnic origin. In vitro studies indicate that CYP3A5 expression in human liver is associated with higher levels of production of several major tacrolimus metabolites (120). The increased metabolism in CYP3A5 expressors is also seen for the related immunosuppressant sirolimus but not for cyclosporine (119). It seems likely that further examples of drugs where CYP3A5 expression is clearly associated with faster metabolism will emerge in the future.

CYP3A7. In addition to variable CYP3A5 expression, there is evidence that some adults continue to express the normally fetal-specific CYP3A7. The presence of a low-frequency variant allele *CYP3A7*1C* that has a series of polymorphisms in linkage disequilibrium in the promoter region correlates well with CYP3A7 mRNA expression in adult liver and could be an additional contributor to high overall CYP3A activity (114). The clinical significance of CYP3A7 expression in adults is still unclear though both all-*trans* and 13-*cis* retinoic acid appear to be more efficiently oxidized by CYP3A7 than by either CYP3A4 or CYP3A5 (121,122). Retinoic acid has an important role in developmental processes. The finding for CYP3A7-mediated metabolism may reflect the endogenous nature of this substrate more than a general role for this isoform in drug metabolism in adults.

Non-Cytochrome P450 Phase I Polymorphisms

A number of polymorphisms of pharmacogenetic relevance occur in non-cytochrome P450-mediated phase I reactions. In general, these are either relatively common but not of great importance in drug metabolism or rare and important only in the metabolism of a restricted range of drugs. There is one example of a dehydrogenase enzyme that has an important role in metabolism of the anticancer drug 5-fluorouracil and is subject to a common well-studied pharmacogenetic polymorphism.

Dihydropyrimidine Dehydrogenase

Dihydropyrimidine dehydrogenase (DPD) has a biochemical role in the catabolism of uracil and thymine and is not primarily a drug-metabolizing enzyme. However, this enzyme is also responsible for the phase I metabolism of the anticancer drug 5-fluorouracil and related compounds such as capecitabine. Interindividual variation in the metabolism of this drug has been correlated with levels of DPD in peripheral blood mononuclear cells (123). Complete deficiency of DPD has been linked to various physiological abnormalities. It is estimated that up to 3% of the population may be heterozygous for the deficiency and, although they do not suffer physiological abnormalities, it appears that these individuals are at increased risk of serious toxic effects if given 5-fluorouracil treatment. The FDA suggests that "rarely, unexpected, severe toxicity (e.g., stomatitis, diarrhea, neutropenia, and neurotoxicity) associated with 5-fluorouracil has been attributed to a deficiency of DPD activity. A link between decreased levels of DPD and increased, potentially fatal toxic effects of 5-fluorouracil therefore cannot be excluded" (12,54). A number of polymorphisms that give rise to DPD deficiency have been identified, but these do not appear to explain all cases of low DPD activity indicating the complex nature of genetics of this enzyme (124 126). Measurement of DPD levels in peripheral blood mononuclear cells may therefore be a more useful predictor of 5-fluorouracil toxicity than genotyping.

PHASE II POLYMORPHISMS

UDP-Glucuronosyltransferases

Glucuronidation is the most common conjugation reaction in drug metabolism. The importance of pharmacogenetic variation in the UDP-glucuronosyltransferases (UGTs) is still unclear, and studies are made difficult by various factors such as the overlapping substrate specificities of these enzymes but some reports of interindividual variation in activity in the general population have appeared. UGT1A1, which is subject to a common polymorphism giving rise to Gilbert's syndrome, has received the most attention from a pharmacogenetic perspective, though it only contributes to the metabolism of a small number of prescribed drugs. Polymorphisms have also been described in both coding and noncoding sequences of UGT1A6, UGT1A7, UGT1A9, UGT2B4, UGT2B7, and UGT2B15. Their importance has been reviewed in detail elsewhere (5). Currently, the most relevant polymorphisms to prescribed drugs appear to be those in UGT1A1 and UGT2B7, and both are considered here as they have been relatively well studied.

UGT1A1

UGT1A1 is the main enzyme responsible for the glucuronidation of bilirubin but also metabolizes the active metabolite (SN-38) of the topoisomerase I inhibitor irinotecan (127). Gilbert's syndrome, which is characterized by a raised serum bilirubin, is due to genetic defects in UGT1A1 (128). The most common polymorphism associated with this syndrome is a 2 base pair TA insertion in the promoter region (*UGT1A1*28* allele), but certain polymorphisms that result in amino acid substitutions can also give rise to the Gilbert's phenotype (5). Individuals homozygous or heterozygous for polymorphisms associated with Gilbert's syndrome appear to be at increased risk of toxicity with irinotecan (127). It has now been recommended in the FDA-approved drug label for the United States that genotyping should be performed prior to administration of this drug due to the increased risk of neutropenia in patients with Gilbert's syndrome (54). The FDA has also licensed a genotyping test for *UGT1A1*28*. However, there are still some issues that need to be addressed regarding the value of UGT1A1 genotyping in patients receiving irinotecan. A review of all published studies linking UGT1A1 genotype and either irinotecan pharmacokinetics or irinotecan-associated toxicity has recently been performed (127). In particular, the majority of pharmacokinetic studies found that possession of either *UGT1A1*28* or another "Gilbert's" allele was associated with a lower SN38-glucuronide over SN38 ratio as expected due to lower rates of glucuronide formation. However, the various studies disagreed on whether *UGT1A1*28* was a risk factor for either severe diarrhea or neutropenia though there was some indication that *UGT1A1*28* might be associated with an increased risk of neutropenia but with a decreased risk of diarrhea. A possible reason for lack of agreement could be due to each study involving less than 100 patients in total resulting in few patients with variant alleles being present. In addition, some of the studies involved more than one tumor type and drug regimens that included additional agents to irinotecan such as 5-fluorouracil. Also, other members of the UGT1A family can glucuronidate SN38. Associations between toxicity and other UGT1A genotypes including UGT1A6, UGT1A7, UGT1A9 have also been reported (129,130). Strong linkage disequilibrium within the UGT1A locus complicates interpretation of these studies but it is possible that genotyping for additional SNPs may provide a better prediction of susceptibility to toxicity. Irinotecan is a second-line therapy for metastatic colorectal cancer in Europe as well as the United States but

there is still a need for additional larger studies on the association between UGT1A genotype and toxicity. The frequency of *UGT1A1*28* is lower in non-European populations but a number of other polymorphisms that give rise to the same phenotype are more common in those of non-European ethnic origin (131). The current licensed genotyping assay does not detect these other alleles and ideally needs to be modified to ensure that all ethnic groups can benefit equally.

UGT2B7

UGT2B7 is one of major hepatic UGTs and is responsible for metabolism of a range of prescribed drugs including morphine, zidovudine, and various NSAIDs (5). The coding region of UGT2B7 has a common polymorphism (C802T) that results in a His268Tyr substitution (132). This polymorphism is in apparent complete linkage disequilibrium with an upstream C-161T polymorphism together with a number of additional upstream SNPs (133,134). In Caucasians, five haplotypes are known to occur at frequencies above 1% but two of these are very rare, while one other differs from the most common haplotype by only a single nonsynonymous base change at codon 145 (133). The two major haplotypes correspond broadly to the alleles designated *UGT2B7*1* and *UGT2B7*2*, which encode the His268 and Tyr268 forms, respectively and occur at approximately similar frequencies in European populations. Whether *UGT2B7*1* and *UGT2B7*2* differ functionally remains controversial. Expression of the two cDNA sequences in mammalian cell lines showed no difference in kinetics or substrate specificity for a small group of substrates (135). More recently, a well-controlled study found that when normalization for protein expression was performed, the *UGT2B7*2* gene product showed significantly higher catalytic activity with both 4-hydroxyestradiol and 4-hydroxyestrone compared with *UGT2B7*1* (136). At least some of the discrepancies between studies could be due to the coding region polymorphisms being associated with substrate-dependent effects on catalytic activity (136). Using reporter gene constructs, some evidence for a higher transcription rate for *UGT2B7*2* compared with *UGT2B7*1* has been obtained but only when sequences upstream from -551 were included in the construct (137). Together these in vitro studies point to a higher enzyme activity associated with *UGT2B7*2*, but recent in vivo studies on patients taking mycophenolate are not consistent with this. Two independent investigations found that *UGT2B7*2* was associated with slower glucuronidation of this compound and showed differences between homozygotes that may be clinically relevant (138,139). Another clinical study found that *UGT2B7*2* was significantly overrepresented in patients suffering diclofenac-induced hepatotoxicity (140). This finding could reflect either faster or slower glucuronidation of diclofenac by the *UGT2B7*2* gene product as several possible mechanisms for the toxicity have been proposed. It seems clear that UGT2B7 is pharmacogenetically important, but further studies to clarify the precise differences between the gene products and the possibility that there may be substrate-specific differences are needed.

Acetyltransferases

Acetylation of amino, hydroxyl, and sulfhydryl groups is catalyzed in humans by two *N*-acetyltransferases termed *N*-acetyltransferase 1 (NAT1) and *N*-acetyltransferase 2 (NAT2) (141). The existence of a polymorphism in NAT2 has been known since the 1950s but NAT1, which was previously often referred to as the monomorphic *N*-acetyltransferase, is also polymorphic. The polymorphism in NAT2 is the more

significant of the two with substantial numbers of individuals completely deficient in this enzyme activity and unable to acetylate a range of drugs including dapsone, isoniazid, procainide, and sulfamethoxazole (1,141).

NAT2

The *NAT2* gene is subject to extensive polymorphism with many individuals who are usually termed slow acetylators unable to acetylate a range of drugs (141). A number of different polymorphisms in NAT2 give rise to amino acid substitutions, and these have been demonstrated to result in absence of catalytic activity in vitro. Screening for three variant alleles (*NAT2*5*, *NAT2*6*, and *NAT2*7*) results in the detection of the vast majority of Caucasian slow acetylators, though additional alleles are also common in some other ethnic groups (141). The precise percentage of slow acetylators also varies with ethnic origin, ranging from 90% in North Africans to less than 10% in many Asian populations, with a frequency of 50% in Caucasians.

Relatively few NAT2 substrates are widely used in modern medicine though isoniazid remains an important drug in the treatment of tuberculosis, and sulfamethoxazole is used in the treatment of secondary infections in AIDS patients. With respect to isoniazid, the FDA states that "slow acetylation may lead to higher blood levels of the drug, and thus an increase in toxic reactions" (54). It is well established that slow acetylators are more likely to suffer side effects when prescribed isoniazid, though there is also evidence that these individuals' overall response to therapy may be better due to being exposed to higher drug levels for longer (141). Therefore, while offering genotyping for NAT2 is likely to be feasible, determining guidelines for dosage recommendations for slow and fast acetylators may not be completely straightforward, though some proposals for this have been put forward (142).

Methyltransferases

Methyltransferases are a large group of enzymes that contribute to specific reactions of both endogenous compound and xenobiotic metabolism. The main member of this family with a clear role in the biotransformation of prescribed drugs is thiopurine methyltransferase. Pharmacogenetic aspects of the gene encoding this enzyme are well understood, probably both because complete deficiency of this enzyme can occur, and the drugs metabolized by it show a narrow therapeutic window.

Thiopurine Methyltransferase

Thiopurine *S*-methyltransferase (TPMT) metabolizes the cytotoxic drug 6-mercaptopurine, widely used in treatment of childhood acute lymphoblastic leukemia, together with azathioprine, a 6-mercaptopurine precursor used as an immunosuppressant. It is the metabolic polymorphism where the most progress has been made in performing testing prior to prescription with the FDA recommending testing though the test is not yet mandatory (54). Approximately 0.3% of Europeans have undetectable activity and 11% intermediate levels (143). If an individual lacks TPMT, high concentrations of thioguanine nucleotides will be formed resulting in toxicities such as myelosuppression, which can be life-threatening (144). The molecular basis of the deficiency is now well understood with two main alleles associated with absence of enzyme activity identified (145). The most common defective allele *TPMT*3* results in two amino acid substitutions that either together or separately result in complete absence of activity and accounts for

approximately 75% of defective alleles. The clinical importance of this polymorphism has been demonstrated in a number of studies. For example, in one large study, individuals who were either homozygous or heterozygous for variant alleles were demonstrated to be at significantly increased risk of toxicity when treated with 6-mercaptopurine (146). TPMT deficiency has also been linked to an increased risk of second malignancies among patients with acute lymphoblastic leukemia (147). In the U.S., drug labels for both 6-mercaptopurine and azathioprine now include information on the TPMT polymorphism and recommend determining patient phenotype or genotype prior to drug treatment (54). Azathioprine is used in treatment of several immune-related diseases including atopic eczema, Crohn's disease, and autoimmune liver disease and, because these diseases are relatively common compared with childhood leukemia, is used more widely than 6-mercaptopurine (148,149).

TPMT status can be determined either by genotyping or by phenotyping, which involves measurement of enzyme levels in erythrocytes, prior to treatment. Appropriate dose adjustment can then be performed. Though generally 6-mercaptopurine is very useful in combination therapy of childhood leukemia, providing dosage is adjusted to take account of TPMT genotype, response to azathioprine is more variable. It appears that while dose adjustment on the basis of TPMT genotype should prevent serious hematological toxicity, therapeutic response to azathioprine is rather unpredictable, suggesting that other factors, possibly additional genetic polymorphisms, also contribute (148). Reports in the literature suggest that TPMT testing prior to initiation of treatment with either 6-mercaptopurine or azathioprine is now common in many centers, but this does not appear to be universal (150,151). Nevertheless, TPMT is the best current example of a pharmacogenetic polymorphism where a test involving determination of host genotype is already in use clinically.

CONCLUDING REMARKS

Genetic polymorphisms have now been identified in the genes encoding all the main cytochrome P450 isoforms that contribute to drug and other xenobiotic metabolism as well as the main phase II conjugating enzymes. Many of the polymorphisms have also been demonstrated to show functional significance but in some cases the significance is still not completely clear, especially with regard to all substrates. Most of the current literature is concerned with polymorphisms in Caucasian, African-American, and East Asian populations but far less is known about other ethnic groups, and there is a need for further studies in this area. The availability of information on the existence and significance of polymorphisms together with the development of effective methods for rapid high-throughput genotyping means that it is likely that it will be possible to individualize drug selection and dosage on the basis of drug metabolism genotype in the near future. Drug regulators are increasingly considering pharmacogenetic data (54), and it is likely that this will be an important contributor to the more widespread adoption of genotyping prior to drug prescription in the near future.

REFERENCES

1. Evans DAP. Genetic Factors in Drug Therapy. Clinical and Molecular Pharmacogenetics. Cambridge: Cambridge University Press, 1993.
2. Roden DM, Altman RB, Benowitz NL, Flockhart DA, Giacomini KM, Johnson JA, Krauss RM, McLeod HL, Ratain MJ, Relling MV, Ring HZ, Shuldiner AR, Weinshilboum RM,

Weiss ST. Pharmacogenomics: challenges and opportunities. Ann Intern Med 2006; 145(10): 749 757.
3. Kirchheiner J, Seeringer A. Clinical implications of pharmacogenetics of cytochrome P450 drug metabolizing enzymes. Biochim Biophys Acta 2007; 1770(3):489 494.
4. Nowell S, Falany CN. Pharmacogenetics of human cytosolic sulfotransferases. Oncogene 2006; 25(11):1673 1678.
5. Guillemette C. Pharmacogenomics of human UDP glucuronosyltransferase enzymes. Pharmacogenomics J 2003; 3(3):136 158.
6. Gibbs JR, Singleton A. Application of genome wide single nucleotide polymorphism typing: simple association and beyond. PLoS Genet 2006; 2(10):e150.
7. Marsh S, McLeod HL. Pharmacogenomics: from bedside to clinical practice. Hum Mol Genet 2006; 15 Spec No 1:R89 R93.
8. Human Cytochrome P450 (CYP) Allele Nomenclature Committee. Allele nomenclature for Cytochrome P450 enzymes. Available at: http://www.cypalleles.ki.se/. Accessed March 2008.
9. Huang JD, Guo WC, Lai MD, Guo YL, Lambert GH. Detection of a novel cytochrome P 450 1A2 polymorphism (F21L) in Chinese. Drug Metab Dispos 1999; 27(1):98 101.
10. Nakajima M, Yokoi T, Mizutani M, Kinoshita M, Funayama M, Kamataki T. Genetic polymorphism in the 5′ flanking region of human CYP1A2 gene: effect on the CYP1A2 inducibility in humans. J Biochem 1999; 125(4):803 808.
11. Sachse C, Brochmoller J, Bauer S, Roots I. Functional significance of a C > A polymorphism in intron I of the cytochrome P450 CYP1A2 gene tested with caffeine. Br J Clin Pharmacol 1999; 47(4):445 449.
12. Sachse C, Bhambra U, Smith G, Lightfoot TJ, Barrett JH, Scollay J, Garner RC, Boobis AR, Wolf CR, Gooderham NJ. Polymorphisms in the cytochrome P450 CYP1A2 gene (CYP1A2) in colorectal cancer patients and controls: allele frequencies, linkage disequilibrium and influence on caffeine metabolism. Br J Clin Pharmacol 2003; 55(1):68 76.
13. Aklillu E, Carrillo JA, Makonnen E, Hellman K, Pitarque M, Bertilsson L, Ingelman Sundberg M. Genetic polymorphism of CYP1A2 in Ethiopians affecting induction and expression: characterization of novel haplotypes with single nucleotide polymorphisms in intron 1. Mol Pharmacol 2003; 64(3):659 669.
14. Ghotbi R, Christensen M, Roh HK, Ingelman Sundberg M, Aklillu E, Bertilsson L. Comparisons of CYP1A2 genetic polymorphisms, enzyme activity and the genotype phenotype relationship in Swedes and Koreans. Eur J Clin Pharmacol 2007; 63(6):537 546.
15. Cornelis MC, El Sohemy A, Kabagambe EK, Campos H. Coffee, CYP1A2 genotype, and risk of myocardial infarction. JAMA 2006; 295(10):1135 1141.
16. Ingelman Sundberg M, Sim SC, Nebert DW. Coffee, myocardial infarction, and CYP nomenclature. JAMA 2006; 296(7):764 765; author reply 765 766.
17. Jiang Z, Dragin N, Jorge Nebert LF, Martin MV, Guengerich FP, Aklillu E, Ingelman Sundberg M, Hammons GJ, Lyn Cook BD, Kadlubar FF, Saldana SN, Sorter M, Vinks AA, Nassr N, von Richter O, Jin L, Nebert DW. Search for an association between the human CYP1A2 genotype and CYP1A2 metabolic phenotype. Pharmacogenet Genomics 2006; 16(5): 359 367.
18. Xu C, Goodz S, Sellers EM, Tyndale RF. CYP2A6 genetic variation and potential consequences. Adv Drug Deliv Rev 2002; 54(10):1245 1256.
19. Yamano S, Tatsuno J, Gonzalez FJ. The *CYP2A3* gene product catalyses coumarin 7 hydroxylation in human liver microsomes. Biochemistry 1990; 29:1322 1329.
20. Cholerton S, Idle ME, Vas A, Gonzalez FJ, Idle JR. Comparison of a novel thin layer chromatographic flourescence detection method with a spectrofluorometric method for the determination of 7 hydroxycoumarin in human urine. J Chromatogr 1992; 575:325 330.
21. Rautio A, Kraul H, Kojo A, Salmela E, Pelkonen O. Interindividual variation of coumarin 7 hydroxylase in healthy volunteers. Pharmacogenetics 1992; 2:227 233.
22. Rao YS, Hoffmann E, Zia M, Bodin L, Zeman M, Sellers EM, Tyndale RF. Duplications and defects in the CYP2A6 gene: identification, genotyping, and in vivo effects on smoking. Mol Pharmacol 2000; 58(4):747 755.

23. Fukami T, Nakajima M, Yamanaka H, Fukushima Y, McLeod HL, Yokoi T. A novel duplication type of CYP2A6 gene in African American population. Drug Metab Dispos 2007; 35(4):515 520.
24. Nunoya K, Yokoi T, Takahashi Y, Kimura K, Kinoshita M, Kamataki T. Homologous unequal cross over within the human CYP2A gene cluster as a mechanism for the deletion of the entire CYP2A6 gene associated with the poor metabolizer phenotype. J Biochem 1999; 126(2):402 407.
25. Oscarson M. Genetic polymorphisms in the cytochrome P450 2A6 (CYP2A6) gene: implications for interindividual differences in nicotine metabolism. Drug Metab Dispos 2001; 29(2):91 95.
26. Chen GF, Tang YM, Green B, Lin DX, Guengerich FP, Daly AK, Caporaso NE, Kadlubar FF. Low frequency of CYP2A6 gene polymorphism as revealed by a one step polymerase chain reaction method. Pharmacogenetics 1999; 9(3):327 332.
27. Mwenifumbo JC, Lessov Schlaggar CN, Zhou Q, Krasnow RE, Swan GE, Benowitz NL, Tyndale RF. Identification of novel CYP2A6*1B variants: the CYP2A6*1B allele is associated with faster in vivo nicotine metabolism. Clin Pharmacol Ther 2008; 83(1):115 121.
28. Fujieda M, Yamazaki H, Saito T, Kiyotani K, Gyamfi MA, Sakurai M, Dosaka Akita H, Sawamura Y, Yokota J, Kunitoh H, Kamataki T. Evaluation of CYP2A6 genetic polymorphisms as determinants of smoking behavior and tobacco related lung cancer risk in male Japanese smokers. Carcinogenesis 2004; 25(12):2451 2458.
29. Farinola N, Piller NB. CYP2A6 polymorphisms: is there a role for pharmacogenomics in preventing coumarin induced hepatotoxicity in lymphedema patients? Pharmacogenomics 2007; 8(2):151 158.
30. Code EL, Crespi CL, Penman BW, Gonzalez FJ, Chang TKH, Waxman DJ. Human cytochrome P4502B6 interindividual hepatic expression, substrate specificity, and role in procarcinogen activation. Drug Metab Dispos 1997; 25(8):985 993.
31. Ekins S, Wrighton SA. The role of CYP2B6 in human xenobiotic metabolism. Drug Metab Rev 1999; 31(3):719 754.
32. Turpeinen M, Raunio H, Pelkonen O. The functional role of CYP2B6 in human drug metabolism: substrates and inhibitors in vitro, in vivo and in silico. Curr Drug Metab 2006; 7(7):705 714.
33. Solus JF, Arietta BJ, Harris JR, Sexton DP, Steward JQ, McMunn C, Ihrie P, Mehall JM, Edwards TL, Dawson EP. Genetic variation in eleven phase I drug metabolism genes in an ethnically diverse population. Pharmacogenomics 2004; 5(7):895 931.
34. Rotger M, Saumoy M, Zhang K, Flepp M, Sahli R, Decosterd L, Telenti A. Partial deletion of CYP2B6 owing to unequal crossover with CYP2B7. Pharmacogenet Genomics 2007; 17(10): 885 890.
35. Kimura S, Pastewka J, Gelboin HV, Gonzalez FJ. cDNA and amino acid sequences of 2 members of the human P450IIC gene subfamily. Nucleic Acids Res 1987; 15(23):10053 10054.
36. Totah RA, Rettie AE. Cytochrome P450 2C8: substrates, inhibitors, pharmacogenetics, and clinical relevance. Clin Pharmacol Ther 2005; 77(5):341 352.
37. Dai D, Zeldin DC, Blaisdell JA, Chanas B, Coulter SJ, Ghanayem BI, Goldstein JA. Polymorphisms in human CYP2C8 decrease metabolism of the anticancer drug paclitaxel and arachidonic acid. Pharmacogenetics 2001; 11(7):597 607.
38. Bahadur N, Leathart JBS, Mutch E, Steimel Crespi D, Dunn SA, Gilissen R, Van Houdt J, Hendrickx J, Mannens G, Bohets H, Williams FM, Armstrong M, Crespi CL, Daly AK. CYP2C8 polymorphisms in Caucasians and their relationship with paclitaxel 6± hydroxylase activity in human liver microsomes. Biochemical Pharmacology 2002; 64:1579 1589.
39. Kirchheiner J, Thomas S, Bauer S, Tomalik Scharte D, Hering U, Doroshyenko O, Jetter A, Stehle S, Tsahuridu M, Meineke I, Brockmoller J, Fuhr U. Pharmacokinetics and pharmacodynamics of rosiglitazone in relation to CYP2C8 genotype. Clin Pharmacol Ther 2006; 80(6):657 667.
40. Niemi M, Leathart JB, Neuvonen M, Backman JT, Daly AK, Neuvonen PJ. Polymorphism in CYP2C8 is associated with reduced plasma concentrations of repaglinide. Clin Pharmacol Ther 2003; 74(4):380 387.

41. Saito Y, Katori N, Soyama A, Nakajima Y, Yoshitani T, Kim SR, Fukushima Uesaka H, Kurose K, Kaniwa N, Ozawa S, Kamatani N, Komamura K, Kamakura S, Kitakaze M, Tomoike H, Sugai K, Minami N, Kimura H, Goto Y, Minami H, Yoshida T, Kunitoh H, Ohe Y, Yamamoto N, Tamura T, Saijo N, Sawada J. CYP2C8 haplotype structures and their influence on pharmacokinetics of paclitaxel in a Japanese population. Pharmacogenet Genomics 2007; 17(7): 461 471.
42. Kutt H, Wolk M, Scherman R, McDowell F. Insufficient parahydroxylation as a cause of diphenylhydantoin toxicity. Neurology 1964; 14:542 548.
43. Scott J, Poffenbarger PL. Pharmacogenetics of tolbutamide metabolism in humans. Diabetes 1978; 28:41 51.
44. Yasumori T, Kawano S, Nagata K, Shimada M, Yamazoe Y, Kato R. Nucleotide sequence of a human liver cytochrome P450 related to the rat male specific form. J Biochem 1987; 102:493 501.
45. Umbenhauer DR, Martin MV, Lloyd RS, Guengerich FP. Cloning and sequence determination of a complementary DNA related to human liver microsomal cytochrome P450 S mephenytoin 4 hydroxylase. Biochemistry 1987; 26:1094 1099.
46. Meehan RR, Gosden JR, Rout D, Hastie ND, Friedberg T, Adesnik M, Buckland R, van Heyningen V, Fletcher J, Spurr NK, Sweeney J, Wolf CR. Human cytochrome P450 PB 1: a multigene family involved in mephenytoin and steroid oxidations that maps to chromosome 10. Am J Hum Genet 1988; 42:26 37.
47. Evans WE, Relling MV. Pharmacogenomics: translating functional genomics into rational therapeutics. Science 1999; 286:487 491.
48. Kirchheiner J, Brockmoller J. Clinical consequences of cytochrome P450 2C9 polymorphisms. Clin Pharmacol Ther 2005; 77(1):1 16.
49. Stubbins MJ, Harries LW, Smith G, Tarbit MH, Wolf CR. Genetic analysis of the human cytochrome P450 CYP2C9 locus. Pharmacogenetics 1996; 6(5):429 439.
50. Aithal GP, Day CP, Kesteven PJL, Daly AK. Association of polymorphisms in the cytochrome P450 CYP2C9 with warfarin dose requirement and risk of bleeding complications. Lancet 1999; 353(9154):717 719.
51. Scordo MG, Aklillu E, Yasar U, Dahl ML, Spina E, Ingelman Sundberg M. Genetic polymorphism of cytochrome P4502C9 in a Caucasian and a black African population. Br J Clin Pharmacol 2001; 52(4):447 450.
52. Daly AK, King BP. Contribution of CYP2C9 to variability in vitamin K antagonist metabolism. Expert Opin Drug Metab Toxicol 2006; 2(1):3 15.
53. Daly AK, King BP. Pharmacogenetics of oral anticoagulants. Pharmacogenetics 2003; 13(5): 247 252.
54. U.S. Food and Drug Administration. Table of Valid Genomic Biomarkers in the Context of Approved Drug Labels. Available at: http://www.fda.gov/cder/genomics/genomic biomarkers table.htm. Accessed March 2008.
55. Wadelius M, Pirmohamed M. Pharmacogenetics of warfarin: current status and future challenges. Pharmacogenomics J 2007; 7(2):99 111.
56. Anderson JL, Horne BD, Stevens SM, Grove AS, Barton S, Nicholas ZP, Kahn SF, May HT, Samuelson KM, Muhlestein JB, Carlquist JF. Randomized trial of genotype guided versus standard warfarin dosing in patients initiating oral anticoagulation. Circulation 2007; 116(22):2563 2570.
57. Caraco Y, Blotnick S, Muszkat M. CYP2C9 genotype guided warfarin prescribing enhances the efficacy and safety of anticoagulation: a prospective randomized controlled study. Clin Pharmacol Ther 2008; 83(3):460 470.
58. Wen MS, Lee M, Chen JJ, Chuang HP, Lu LS, Chen CH, Lee TH, Kuo CT, Sun FM, Chang YJ, Kuan PL, Chen YF, Charng MJ, Ray CY, Wu JY, Chen YT. Prospective study of warfarin dosage requirements based on CYP2C9 and VKORC1 genotypes. Clin Pharmacol Ther 2008; 84(1):83 89.
59. Blanco G, Martinez C, Ladero JM, Garcia Martin E, Taxonera C, Gamito FG, Diaz Rubio M, Agundez JA. Interaction of CYP2C8 and CYP2C9 genotypes modifies the risk for nonsteroidal anti inflammatory drugs related acute gastrointestinal bleeding. Pharmacogenet Genomics 2008; 18(1):37 43.

60. Pilotto A, Seripa D, Franceschi M, Scarcelli C, Colaizzo D, Grandone E, Niro V, Andriulli A, Leandro G, Di Mario F, Dallapiccola B. Genetic susceptibility to nonsteroidal anti inflammatory drug related gastroduodenal bleeding: role of cytochrome P450 2C9 poly morphisms. Gastroenterology 2007; 133(2):465 471.
61. Agundez JA, Martinez C, Garcia Martin E, Ladero JM. Cytochrome P450 CYP2C9 polymorphism and NSAID related acute gastrointestinal bleeding. Gastroenterology 2007; 133(6):62071 2072; author reply 2072 2073.
62. van Oijen MG, Laheij RJ. Impact of CYP2C9 genotype on pharmacokinetics: are all NSAIDs the same? Gastroenterology 2007; 133(6):2073 2074; author reply 2074 2075.
63. Kupfer A, Preisig R. Pharmacogenetics of mephenytoin: a new drug hydroxylation polymorphism in man. Eur J Clin Pharmacol 1984; 26:753 759.
64. Goldstein JA. Clinical relevance of genetic polymorphisms in the human CYP2C subfamily. Br J Clin Pharmacol 2001; 52(4):349 355.
65. Furuta T, Ohashi K, Kamata T, Takashima M, Kosuge K, Kawasaki T, Hanai H, Kubota T, Ishizaki T, Kaneko E. Effect of genetic differences in omeprazole metabolism on cure rates for Helicobacter pylori infection and peptic ulcer. Ann Intern Med 1998; 129(12):1027 1030.
66. Hulot JS, Bura A, Villard E, Azizi M, Remones V, Goyenvalle C, Aiach M, Lechat P, Gaussem P. Cytochrome P450 2C19 loss of function polymorphism is a major determinant of clopidogrel responsiveness in healthy subjects. Blood 2006; 108(7):2244 2247.
67. Brandt JT, Close SL, Iturria SJ, Payne CD, Farid NA, Ernest CS 2nd, Lachno DR, Salazar D, Winters KJ. Common polymorphisms of CYP2C19 and CYP2C9 affect the pharmacokinetic and pharmacodynamic response to clopidogrel but not prasugrel. J Thromb Haemost 2007; 5(12):2429 2436.
68. Giusti B, Gori AM, Marcucci R, Saracini C, Sestini I, Paniccia R, Valente S, Antoniucci D, Abbate R, Gensini GF. Cytochrome P450 2C19 loss of function polymorphism, but not CYP3A4 IVS10 + 12G/A and P2Y12 T744C polymorphisms, is associated with response variability to dual antiplatelet treatment in high risk vascular patients. Pharmacogenet Genomics 2007; 17(12):1057 1064.
69. Kim K, Park P, Hong S, Park JY. The effect of CYP2C19 polymorphism on the pharmacokinetics and pharmacodynamics of clopidogrel: a possible mechanism for clopidogrel resistance. Clin Pharmacol Ther 2008; 84(2):236 242.
70. Desta Z, Zhao X, Shin JG, Flockhart DA. Clinical significance of the cytochrome P450 2C19 genetic polymorphism. Clin Pharmacokinet 2002; 41(12):913 958.
71. Rudberg I, Hendset M, Uthus LH, Molden E, Refsum H. Heterozygous mutation in CYP2C19 significantly increases the concentration/dose ratio of racemic citalopram and escitalopram (S citalopram). Ther Drug Monit 2006; 28(1):102 105.
72. Mikus G, Schowel V, Drzewinska M, Rengelshausen J, Ding R, Riedel KD, Burhenne J, Weiss J, Thomsen T, Haefeli WE. Potent cytochrome P450 2C19 genotype related interaction between voriconazole and the cytochrome P450 3A4 inhibitor ritonavir. Clin Pharmacol Ther 2006; 80(2):126 135.
73. Sim SC, Risinger C, Dahl ML, Aklillu E, Christensen M, Bertilsson L, Ingelman Sundberg M. A common novel CYP2C19 gene variant causes ultrarapid drug metabolism relevant for the drug response to proton pump inhibitors and antidepressants. Clin Pharmacol Ther 2006; 79(1):103 113.
74. Baldwin RM, Ohlsson S, Pedersen RS, Mwinyi J, Ingelman Sundberg M, Eliasson E, Bertilsson L. Increased omeprazole metabolism in carriers of the CYP2C19*17 allele; a pharmacokinetic study in healthy volunteers. Br J Clin Pharmacol 2008; 65(5):767 774. [Epub 2008, Feb 20].
75. Rudberg I, Mohebi B, Hermann M, Refsum H, Molden E. Impact of the ultrarapid CYP2C19*17 allele on serum concentration of escitalopram in psychiatric patients. Clin Pharmacol Ther 2008; 83(2):322 327.
76. Mahgoub A, Idle JR, Dring LG, Lancaster R, Smith RL. Polymorphic hydroxylation of debrisoquine in man. Lancet 1977; 2:584 586.
77. Eichelbaum M, Spannbrucker N, Steincke B, Dengler HJ. Defective N oxidation of sparteine in man: a new pharmacogenetic defect. Eur J Clin Pharmacol 1979; 17:153 155.

78. Distelrath LM, Reilly PEB, Martin MV, Davis GG, Wilkinson GR, Guengerich FP. Purification and characterisation of the human liver cytochromes P450 involved in debrisoquine 4 hydroxylation and phenacetin O deethylation, two prototypes for genetic polymorphism in oxidative drug metabolism. J Biol Chem 1985; 260:9057 9067.
79. Gough AC, Miles JS, Spurr NK, Moss JE, Gaedigk A, Eichelbaum M, Wolf CR. Identification of the primary gene defect at the cytochrome P450 *CYP2D* locus. Nature 1990; 347:773 776.
80. Kagimoto M, Heim M, Kagimoto K, Zeugin T, Meyer UA. Multiple mutations of the human cytochrome P450IID6 gene (CYP2D6) in poor metabolisers of debrisoquine. J Biol Chem 1990; 265:17209 17214.
81. Johansson I, Lundqvist E, Bertilsson L, Dahl M L, Sjoqvist F, Ingelman Sundberg M. Inherited amplification of an active gene in the cytochrome P450 *CYP2D* locus as a cause of ultrarapid metabolism of debrisoquine. Proc Natl Acad Sci U S A 1993; 90:11825 11829.
82. Sachse C, Brockmoller J, Bauer S, Roots I. Cytochrome P450 2D6 variants in a Caucasian population: allele frequencies and phenotypic consequences. Am J Hum Genet 1997; 60: 284 295.
83. Gaedigk A, Simon SD, Pearce RE, Bradford LD, Kennedy MJ, Leeder JS. The CYP2D6 activity score: translating genotype information into a qualitative measure of phenotype. Clin Pharmacol Ther 2008; 83(2):234 242.
84. Shen H, He MM, Liu H, Wrighton SA, Wang L, Guo B, Li C. Comparative metabolic capabilities and inhibitory profiles of CYP2D6.1, CYP2D6.10, and CYP2D6.17. Drug Metab Dispos 2007; 35(8):1292 1300.
85. Toscano C, Klein K, Blievernicht J, Schaeffeler E, Saussele T, Raimundo S, Eichelbaum M, Schwab M, Zanger UM. Impaired expression of CYP2D6 in intermediate metabolizers carrying the *41 allele caused by the intronic SNP 2988G>A: evidence for modulation of splicing events. Pharmacogenet Genomics 2006; 16(10):755 766.
86. Dahl ML, Johansson I, Bertilsson L, Ingelmansundberg M, Sjoqvist F. Ultrarapid hydroxylation of debrisoquine in a Swedish population analysis of the molecular genetic basis. J Pharmacol Exp Ther 1995; 274(1):516 520.
87. Lovlie R, Daly AK, Molven A, Idle JR, Steen VM. Ultrarapid metabolizers of debrisoquine: characterization and PCR based detection of alleles with duplication of the CYP2D6 gene. FEBS Lett 1996; 392(1):30 34.
88. Aklillu E, Persson I, Bertilsson L, Johansson I, Rodrigues F, Ingelman Sundberg M. Frequent distribution of ultrarapid metabolizers of debrisoquine in an Ethiopian population carrying duplicated and multiduplicated functional *CYP2D6* alleles. J Pharmacol Exp Ther 1996; 278:441 446.
89. Kirchheiner J, Brosen K, Dahl ML, Gram LF, Kasper S, Roots I, Sjoqvist F, Spina E, Brockmoller J. CYP2D6 and CYP2C19 genotype based dose recommendations for antidepressants: a first step towards subpopulation specific dosages. Acta Psychiatr Scand 2001; 104(3):173 192.
90. Gasche Y, Daali Y, Fathi M, Chiappe A, Cottini S, Dayer P, Desmeules J. Codeine intoxication associated with ultrarapid CYP2D6 metabolism. N Engl J Med 2004; 351(27): 2827 2831.
91. Koren G, Cairns J, Chitayat D, Gaedigk A, Leeder SJ. Pharmacogenetics of morphine poisoning in a breastfed neonate of a codeine prescribed mother. Lancet 2006; 368(9536):704.
92. Kirchheiner J, Schmidt H, Tzvetkov M, Keulen JT, Lotsch J, Roots I, Brockmoller J. Pharmacokinetics of codeine and its metabolite morphine in ultra rapid metabolizers due to CYP2D6 duplication. Pharmacogenomics J 2007; 7(4):257 265.
93. He YJ, Brockmoller J, Schmidt H, Roots I, Kirchheiner J. Short communication: CYP2D6 ultrarapid metabolism and morphine/codeine ratios in blood: was it codeine or heroin? J Anal Toxicol 2008; 32(2):178 182.
94. Desta Z, Ward BA, Soukhova NV, Flockhart DA. Comprehensive evaluation of tamoxifen sequential biotransformation by the human cytochrome P450 system in vitro: prominent roles for CYP3A and CYP2D6. J Pharmacol Exp Ther 2004; 310(3):1062 1075.

95. Jin Y, Desta Z, Stearns V, Ward B, Ho H, Lee KH, Skaar T, Storniolo AM, Li L, Araba A, Blanchard R, Nguyen A, Ullmer L, Hayden J, Lemler S, Weinshilboum RM, Rae JM, Hayes DF, Flockhart DA. CYP2D6 genotype, antidepressant use, and tamoxifen metabolism during adjuvant breast cancer treatment. J Natl Cancer Inst 2005; 97(1):30 39.
96. Lim YC, Li L, Desta Z, Zhao Q, Rae JM, Flockhart DA, Skaar TC. Endoxifen, a secondary metabolite of tamoxifen, and 4 OH tamoxifen induce similar changes in global gene expression patterns in MCF 7 breast cancer cells. J Pharmacol Exp Ther 2006; 318(2): 503 512.
97. Goetz MP, Rae JM, Suman VJ, Safgren SL, Ames MM, Visscher DW, Reynolds C, Couch FJ, Lingle WL, Flockhart DA, Desta Z, Perez EA, Ingle JN. Pharmacogenetics of tamoxifen biotransformation is associated with clinical outcomes of efficacy and hot flashes. J Clin Oncol 2005; 23(36):9312 9318.
98. Goetz MP, Kamal A, Ames MM. Tamoxifen pharmacogenomics: the role of CYP2D6 as a predictor of drug response. Clin Pharmacol Ther 2008; 83(1):160 166.
99. Goetz MP, Loprinzi CL. Aromatase inhibitors and tamoxifen: where do we go from here? Nat Clin Pract Oncol 2007; 4(11):626 627.
100. Patten CJ, Thomas PE, Guy RL, Lee M, Gonzalez FJ, Guengerich FP, Yang CS. Cytochrome P450 enzymes involved in acetaminophen activation by rat and human liver microsomes and their kinetics. Chem Res Toxicol 1993; 6:511 518.
101. Kim RB, O'Shea D, Wilkinson GR. Interindividual variability of chlorzoxazone 6 hydroxylation in men and women and its relationship to *CYP2E1* genetic polymorphisms. Clin Pharmacol Ther 1995; 57:645 655.
102. Hu Y, Oscarson M, Johansson I, Yue QY, Dahl ML, Tabone M, Arinco S, Albano E, IngelmanSundberg M. Genetic polymorphism of human CYP2E1: characterization of two variant alleles. Mol Pharmacol 1997; 51(3):370 376.
103. Hayashi S, Watanabe J, Kawagiri K. Genetic polymorphisms in the 5′ flanking region change transcriptional regulation of the human cytochrome P450IIE1 gene. J Biochem 1991; 110: 559 565.
104. Kato S, Shields PG, Caporaso NE, Hoover RN, Trump BF, Sugimura H, Weston A, Harris CC. Cytochrome P450IIE1 genetic polymorphisms, racial variation, and lung cancer risk. Cancer Res 1992; 52:6712 6715.
105. Pirmohamed M, Kitteringham NR, Quest LJ, Allott RL, Green VJ, Gilmore IT, Park BK. Genetic polymorphism of cytochrome P4502E1 and risk of alcoholic liver disease in Caucasians. Pharmacogenetics 1995; 5(6):351 357.
106. Hildesheim A, Anderson LM, Chen CJ, Cheng YJ, Brinton LA, Daly AK, Reed CD, Chen IH, Caporaso NE, Hsu MM, Chen JY, Idle JR, Hoover RN, Yang CS, Chhabra SK. CYP2E1 genetic polymorphisms and risk of nasopharyngeal carcinoma in Taiwan. J Natl Cancer Inst 1997; 89(16):1207 1212.
107. Grove J, Brown ASM, Daly AK, Bassendine MF, James OFW, Day CP. The RsaI polymorphism of CYP2E1 and susceptibility to alcoholic liver disease in Caucasians: effect on age of presentation and dependence on alcohol dehydrogenase genotype. Pharmacogenetics 1998; 8(4):335 342.
108. Vuilleumier N, Rossier MF, Chiappe A, Degoumois F, Dayer P, Mermillod B, Nicod L, Desmeules J, Hochstrasser D. CYP2E1 genotype and isoniazid induced hepatotoxicity in patients treated for latent tuberculosis. Eur J Clin Pharmacol 2006; 62(6):423 429.
109. Dupont I, Lucas D, Clot P, Menez C, Albano E. Cytochrome P4502E1 inducibility and hydroxyethyl radical formation among alcoholics. J Hepatol 1998; 28(4):564 571.
110. Wojnowski L, Kamdem LK. Clinical implications of CYP3A polymorphisms. Expert Opin Drug Metab Toxicol 2006; 2(2):171 182.
111. Aoyama T, Yamano S, Waxman DJ, Lapenson DP, Meyer UA, Fischer V, Tyndale R, Inaba T, Kalow W, Gelboin HV, Gonzalez FJ. Cytochrome P450 hPCN3, a novel cytochrome P450 IIA gene product that is differentially expressed in adult human liver. J Biol Chem 1989; 264:10388 10395.

112. Rodriguez Antona C, Sayi JG, Gustafsson LL, Bertilsson L, Ingelman Sundberg M. Phenotype genotype variability in the human CYP3A locus as assessed by the probe drug quinine and analyses of variant CYP3A4 alleles. Biochem Biophys Res Commun 2005; 338(1):299 305.
113. Zhang J, Kuehl P, Green ED, Touchman JW, Watkins PB, Daly A, Hall SD, Maurel P, Relling M, Brimer C, Yasuda K, Wrighton SA, Hancock M, Kim RB, Strom S, Thummel K, Russell CG, Hudson JR, Schuetz EG, Boguski MS. The human pregnane X receptor: genomic structure and identification and functional characterization of natural allelic variants. Pharmacogenetics 2001; 11(7):555 572.
114. Kuehl P, Zhang J, Lin Y, Lamba J, Assem M, Schuetz J, Watkins PB, Daly A, Wrighton SA, Hall SD, Maurel P, Relling M, Brimer C, Yasuda K, Venkataramanan R, Strom S, Thummel K, Boguski MS, Schuetz E. Sequence diversity in CYP3A promoters and characterization of the genetic basis of polymorphic CYP3A5 expression. Nat Genet 2001; 27(4):383 391.
115. Daly AK. Significance of the minor cytochrome P450 3A isoforms. Clin Pharmacokinet 2006; 45(1):13 31.
116. Fromm MF, Schwilden H, Bachmakov I, Konig J, Bremer F, Schuttler J. Impact of the CYP3A5 genotype on midazolam pharmacokinetics and pharmacodynamics during intensive care sedation. Eur J Clin Pharmacol 2007; 63(12):1129 1133.
117. Kharasch ED, Walker A, Isoherranen N, Hoffer C, Sheffels P, Thummel K, Whittington D, Ensign D. Influence of CYP3A5 genotype on the pharmacokinetics and pharmacodynamics of the cytochrome P4503A probes alfentanil and midazolam. Clin Pharmacol Ther 2007; 82(4): 410 426.
118. He P, Court MH, Greenblatt DJ, von Moltke LL. Factors influencing midazolam hydroxylation activity in human liver microsomes. Drug Metab Dispos 2006; 34(7):1198 1207.
119. Anglicheau D, Legendre C, Beaune P, Thervet E. Cytochrome P450 3A polymorphisms and immunosuppressive drugs: an update. Pharmacogenomics 2007; 8(7):835 849.
120. Dai Y, Hebert MF, Isoherranen N, Davis CL, Marsh C, Shen DD, Thummel KE. Effect of CYP3A5 polymorphism on tacrolimus metabolic clearance in vitro. Drug Metab Dispos 2006; 34(5):836 847.
121. Marill J, Capron CC, Idres N, Chabot GG. Human cytochrome P450s involved in the metabolism of 9 cis and 13 cis retinoic acids. Biochem Pharmacol 2002; 63(5):933 943.
122. Marill J, Cresteil T, Lanotte M, Chabot GG. Identification of human cytochrome P450s involved in the formation of all trans retinoic acid principal metabolites. Mol Pharmacol 2000; 58(6):1341 1348.
123. Gonzalez FJ, Fernandez Salguero P. Diagnostic analysis, clinical importance and molecular basis of dihydropyrimidine dehydrogenase deficiency. Trends Pharmacol Sci 1995; 16(10): 325 327.
124. Collie Duguid ES, Etienne MC, Milano G, McLeod HL. Known variant DPYD alleles do not explain DPD deficiency in cancer patients. Pharmacogenetics 2000; 10(3):217 223.
125. van Kuilenburg AB. Screening for dihydropyrimidine dehydrogenase deficiency: to do or not to do, that's the question. Cancer Invest 2006; 24(2):215 217.
126. van Kuilenburg AB, Muller EW, Haasjes J, Meinsma R, Zoetekouw L, Waterham HR, Baas F, Richel DJ, van Gennip AH. Lethal outcome of a patient with a complete dihydropyrimidine dehydrogenase (DPD) deficiency after administration of 5 fluorouracil: frequency of the common IVS14+1G>A mutation causing DPD deficiency. Clin Cancer Res 2001; 7(5): 1149 1153.
127. Nagar S, Blanchard RL. Pharmacogenetics of uridine diphosphoglucuronosyltransferase (UGT) 1A family members and its role in patient response to irinotecan. Drug Metab Rev 2006; 38(3):393 409.
128. Monaghan G, Ryan M, Seddon R, Hume R, Burchell B. Genetic variation in bilirubin UDP glucuronosyltransferase gene promoter and Gilbert's syndrome. Lancet 1996; 347:578 581.
129. Carlini LE, Meropol NJ, Bever J, Andria ML, Hill T, Gold P, Rogatko A, Wang H, Blanchard RL. UGT1A7 and UGT1A9 polymorphisms predict response and toxicity in colorectal cancer patients treated with capecitabine/irinotecan. Clin Cancer Res 2005; 11(3):1226 1236.

130. Girard H, Villeneuve L, Court MH, Fortier LC, Caron P, Hao Q, von Moltke LL, Greenblatt DJ, Guillemette C. The novel UGT1A9 intronic I399 polymorphism appears as a predictor of 7 ethyl 10 hydroxycamptothecin glucuronidation levels in the liver. Drug Metab Dispos 2006; 34(7):1220 1228.
131. Hall D, Ybazeta G, Destro Bisol G, Petzl Erler ML, Di Rienzo A. Variability at the uridine diphosphate glucuronosyltransferase 1A1 promoter in human populations and primates. Pharmacogenetics 1999; 9(5):591 599.
132. Jin C, Miners JO, Lillywhite KJ, Mackenzie PI. Complementary deoxyribonucleic acid cloning and expression of a human liver uridine diphosphate glucuronosyltransferase glucuronidating carboxylic acid containing drugs. J Pharmacol Exp Ther 1993; 264(1):475 479.
133. Holthe M, Rakvag TN, Klepstad P, Idle JR, Kaasa S, Krokan HE, Skorpen F. Sequence variations in the UDP glucuronosyltransferase 2B7 (UGT2B7) gene: identification of 10 novel single nucleotide polymorphisms (SNPs) and analysis of their relevance to morphine glucuronidation in cancer patients. Pharmacogenomics J 2003; 3(1):17 26.
134. Sawyer MB, Innocenti F, Das S, Cheng C, Ramirez J, Pantle Fisher FH, Wright C, Badner J, Pei D, Boyett JM, Cook E Jr., Ratain MJ. A pharmacogenetic study of uridine diphosphate glucuronosyltransferase 2B7 in patients receiving morphine. Clin Pharmacol Ther 2003; 73(6):566 574.
135. Coffman BL, King CD, Rios GR, Tephly TR. The glucuronidation of opioids, other xenobiotics, and androgens by human UGT2B7Y(268) and UGT2B7H(268). Drug Metab Dispos 1998; 26(1):73 77.
136. Thibaudeau J, Lepine J, Tojcic J, Duguay Y, Pelletier G, Plante M, Brisson J, Tetu B, Jacob S, Perusse L, Belanger A, Guillemette C. Characterization of common UGT1A8, UGT1A9, and UGT2B7 variants with different capacities to inactivate mutagenic 4 hydroxylated metabolites of estradiol and estrone. Cancer Res 2006; 66(1):125 133.
137. Duguay Y, Baar C, Skorpen F, Guillemette C. A novel functional polymorphism in the uridine diphosphate glucuronosyltransferase 2B7 promoter with significant impact on promoter activity. Clin Pharmacol Ther 2004; 75(3):223 233.
138. Levesque E, Delage R, Benoit Biancamano MO, Caron P, Bernard O, Couture F, Guillemette C. The impact of UGT1A8, UGT1A9, and UGT2B7 genetic polymorphisms on the pharmaco kinetic profile of mycophenolic acid after a single oral dose in healthy volunteers. Clin Pharmacol Ther 2007; 81(3):392 400.
139. Djebli N, Picard N, Rerolle JP, Le Meur Y, Marquet P. Influence of the UGT2B7 promoter region and exon 2 polymorphisms and comedications on Acyl MPAG production in vitro and in adult renal transplant patients. Pharmacogenet Genomics 2007; 17(5):321 330.
140. Daly AK, Aithal GP, Leathart JB, Swainsbury RA, Dang TS, Day CP. Genetic susceptibility to diclofenac induced hepatotoxicity: contribution of UGT2B7, CYP2C8, and ABCC2 genotypes. Gastroenterology 2007; 132(1):272 281.
141. Dupret JM, Rodrigues Lima F. Structure and regulation of the drug metabolizing enzymes arylamine N acetyltransferases. Curr Med Chem 2005; 12(3):311 318.
142. Kinzig Schippers M, Tomalik Scharte D, Jetter A, Scheidel B, Jakob V, Rodamer M, Cascorbi I, Doroshyenko O, Sorgel F, Fuhr U. Should we use N acetyltransferase type 2 genotyping to personalize isoniazid doses? Antimicrob Agents Chemother 2005; 49(5):1733 1738.
143. Weinshilboum R, Sladek SL. Mercaptopurine pharmacogenetics: monogenic inheritance of erythrocyte thiopurine methyltransferase activity. Am J Hum Genet 1980; 32:651 662.
144. Lennard L, Gibson BES, Nicole T, Lilleyman JS. Congenital thiopurine methyltransferase deficiency and 6 mercaptopurine toxicity during treatment for acute lymphoblastic leukemia. Arch Dis Child 1993; 69(5):577 579.
145. Szumlanski C, Otterness D, Her C, Lee D, Brandriff B, Kelsell D, Spurr N, Lennard L, Wieben E, Weinshilboum R. Thiopurine methyltransferase pharmacogenetics: human gene cloning and characterization of a common polymorphism. DNA Cell Biol 1996; 15:17 30.
146. Relling MV, Hancock ML, Rivera GK, Sandlund JT, Ribeiro RC, Krynetski EY, Pui CH, Evans WE. Mercaptopurine therapy intolerance and heterozygosity at the thiopurine S methyltransferase gene locus. J Natl Cancer Inst 1999; 91(23):2001 2008.

147. Relling MV, Rubnitz JE, Rivera GK, Boyett JM, Hancock ML, Felix CA, Kun LE, Walter AW, Evans WE, Pui CH. High incidence of secondary brain tumours after radiotherapy and antimetabolites. Lancet 1999; 354(9172):34 39.
148. Meggitt SJ, Gray JC, Reynolds NJ. Azathioprine dosed by thiopurine methyltransferase activity for moderate to severe atopic eczema: a double blind, randomised controlled trial. Lancet 2006; 367(9513):839 846.
149. Heneghan MA, Allan ML, Bornstein JD, Muir AJ, Tendler DA. Utility of thiopurine methyltransferase genotyping and phenotyping, and measurement of azathioprine metabolites in the management of patients with autoimmune hepatitis. J Hepatol 2006; 45(4):584 591.
150. Gardiner SJ, Begg EJ. Pharmacogenetic testing for drug metabolizing enzymes: is it happening in practice? Pharmacogenet Genomics 2005; 15(5):365 369.
151. Woelderink A, Ibarreta D, Hopkins MM, Rodriguez Cerezo E. The current clinical practice of pharmacogenetic testing in Europe: TPMT and HER2 as case studies. Pharmacogenomics J 2006; 6(1):3 7.

8
Inhibition of Drug Metabolizing Enzymes

F. Peter Guengerich
Department of Biochemistry and Center in Molecular Toxicology, Vanderbilt University School of Medicine, Nashville, Tennessee, U.S.A.

INTRODUCTION

The topic of inhibition of the enzymes of drug metabolism is of great interest to enzymologists, chemists, pharmacologists, and clinicians. Two major practical applications of knowledge of inhibition are important in the pharmaceutical industry. One is drug-drug interaction, i.e., one drug may inhibit the biotransformation of another when two are taken concurrently (1). Such interactions can be fatal, and the possibilities are scrutinized by regulatory agencies. The other major interest in enzyme inhibition is based on the selection of enzymes as targets for drug action. For instance, monoamine oxidase and some of the cytochrome P450 (P450) enzymes are targets because the products of their normal reactions can be deleterious under certain conditions. However, the focus of this chapter will be on inhibition of drug metabolism as opposed to drug discovery.

BASIC MECHANISMS OF ENZYME INHIBITION

The general treatments presented here in this update of the first edition (2) are rather introductory, and the reader is referred to more comprehensive treatments of the subject (3 6). Classifications used here are oriented toward major mechanisms known for the enzymes of drug metabolism. Inhibition has its basis in the enzymology itself, including the field of enzyme kinetics. Overviews of major mechanisms and their principles will be presented, followed by a few prominent examples involving various enzymes, particularly the P450s.

Competitive Inhibition

The classic view of competitive inhibition is that the inhibitor shares structural similarity with the normal substrate (although defining a "normal" substrate for many of the

enzymes under consideration is not always easy). The inhibitor may or may not be a substrate itself; i.e., be transformed to a product by the enzyme:

$$\mathrm{E + S} \underset{k_{-1}}{\overset{k_1}{\rightleftharpoons}} \mathrm{ES} \underset{k_{-2}}{\overset{k_2}{\rightleftharpoons}} \mathrm{ES^*} \underset{k_{-3}}{\overset{k_3}{\rightleftharpoons}} \mathrm{EP} \underset{k_{-4}}{\overset{k_4}{\rightleftharpoons}} \mathrm{E + P}$$

$$\mathrm{E + I} \underset{k'_{-1}}{\overset{k'_1}{\rightleftharpoons}} \mathrm{EI},$$

where an intermediate ES* may or may not be present. Sometimes k_1, k'_1, and k_{-1} are termed "k_{on}" and k_{-1}, k'_{-1}, and k_4 are "k_{off}" rates. In classic competitive inhibition, the steady-state $K_{m,apparent}$ value (for the reaction with the "typical" substrate) increases when the inhibitor is present, and examination of steady-state kinetics with increasing concentrations of inhibitor and concomitant increasing $K_{m,apparent}$ values allow estimation of an inhibition constant K_i because they are related by the expression

$$v = \frac{V_{max}}{K_m(1 + [I]/K_i + [S])}$$

where $K_{m,apparent} = K_m\,(1 + [I]/K_i)$. (Recall that $V_{max} = k_{cat} \times$ enzyme concentration/mg protein; k_{cat} will be used in this discussion.) This behavior is readily identified by a common intersection point (ordinate) in a Lineweaver Burk (1/v vs. 1/S) plot or various characteristics of other linear transformations of the Michaelis Menten equation.

The classic approach to characterization of competitive inhibition and the associated parameters is to do enzyme assays with varying concentrations of both the substrate S and inhibitor I, fitting to the above equations or their derivatives. An alternative method is the Dixon plot, in which 1/v is plotted versus S (6). Historically, linear transforms were used to do fitting "by eye" or linear regression. All of the linear plots have some weighting deficiencies (4), and many convenient and useful nonlinear regression programs are now commercially available. However, screening for inhibition is very common in the pharmaceutical industry today, and new approaches have been introduced to handle the increased load of drug candidates. One statistical experimental approach is usually termed "virtual kinetics" (7).

In principle, K_i is an actual binding constant, as opposed to K_m, which is usually not. When the inhibitor is a substrate itself, the two substrates show competitive inhibition of each other. In ideal cases, if the $K_m \sim K_d$, then $K_m \sim K_i$. However, there are many reasons why such a relationship may not be seen with a complex enzyme system.

Competitive inhibition is a relatively commonly encountered phenomenon in drug metabolism work, and there are means of characterizing in vivo situations through pharmacokinetic parameters (8 10). Many of the enzymes under consideration have multiple drug substrates (e.g., P450s 2C9, 2D6, 3A4) that can compete with each other. Drug-drug interactions of this sort can be expected in individuals who are administered several drugs simultaneously.

Noncompetitive Inhibition

In classic noncompetitive inhibition, the inhibitor binds to the enzyme at a site distinct from that of the substrate. The expected result is that a decrease in k_{cat} or (V_{max}) is observed without a change in K_m. For instance, one might expect an electrophilic inhibitor to poison the enzyme in such a manner. Although this example is often presented in

introductory biochemistry courses, clear examples of such inhibition are not very common and are not often encountered in studies with enzymes of drug metabolism. In vitro, one might expect such results by adding heavy metals to or heating an enzyme. What is often encountered is "mixed inhibition," where it is usually the case that k_{cat} decreases and K_m increases. The physical meaning of such changes may vary. For example, such behavior might be observed if one were dealing with two different enzymes in a population (e.g., microsomes) that both catalyzed a reaction, and one was inhibited competitively while the other was being inactivated by mechanistic inactivation. Interpretation of such results must be done with a single enzyme system.

A comprehensive discussion of all the features of competitive and noncompetitive inhibition is beyond the scope of this chapter. Competitive inhibition is commonly considered to reflect a single site, but the potential for compounds binding to different parts of a larger active site is also possible. For more on the complex possibilities for competitive (and noncompetitive and uncompetitive) inhibition see Segel (3).

Uncompetitive Inhibition

As in the case of noncompetitive inhibition, classic uncompetitive inhibition is defined but seldom seen. The principle is that the inhibitor binds only to the enzyme-substrate complex. Both k_{cat} and K_m are decreased proportionately and the ratio k_{cat}/K_m remains constant. For instance, in a Lineweaver Burk plot, parallel lines should be seen in the absence and presence of the inhibitor. The enzyme efficiency (and, by extension, the intrinsic clearance of the drug substrate) would not really change. However, there are few clear examples of this phenomenon in the field.

Product Inhibition

In some cases, a product of a reaction of a drug-metabolizing enzyme may inhibit the reaction. For instance, oxidized nicotinamide adenine nucleotide phosphate ($NADP^+$) is a competitive inhibitor of reduced nicotinamide adenine nucleotide phosphate (NADPH)-P450 reductase (11). [For this reason, an NADPH-generating system (12) is preferred to a bolus of NADPH as a cofactor in in vitro incubations.] In a cellular system, this case would not exist because there are reduction systems that work well on the oxidized cofactor. However, in other cases the product may not have physical characteristics very different from the substrate and competitively inhibits, sometimes being further transformed. For instance, benzene is oxidized by P450 2E1 to phenol and then on to hydroquinone (13). Thus, benzene and phenol compete with each other. Polycyclic aromatic hydrocarbons and their dihydrodiols compete for P450 1 family enzymes (14,15).

Transition-State Analogs

Transition-state analogs are tight-binding, non-covalently bound inactivators that resemble the transition state for the enzymatic reaction, i.e., the transient complex formed in a single step within the catalytic cycle with the maximum free energy. The axiom that the enzyme has the highest affinity for this putative entity (which cannot be directly observed) was developed by Haldane (16) and Pauling (17) and is the basis for the development

$$E + I \underset{k_{off}}{\overset{k_{on}}{\rightleftharpoons}} E - I$$

of catalytic antibodies (18). The k_{on} rate is rapid and k_{off} is slow. Inactivation is rapid, and no time dependence is observed under typical assay conditions. Enzyme activity can, at

least in principle, be restored by removal of inhibitor using dialysis, gel filtration, centrifugal concentration, etc. (19).

Slow, Tight-Binding Inhibitors

These compounds are characterized by relatively slow (apparent) k_{on} rates and even slower k_{off} rates. The binding can be non-covalent or covalent, but due to the slowness of binding, the loss of activity may be time dependent and mistaken for mechanism-based inactivation. The initial interaction is, of course, diffusion-limited, but other steps complicate the apparent "k_{on}" rate. Removal of the inhibitor by dialysis, etc., will restore enzyme activity, although the process may be slow.

An example of a characterized slow, tight-binding inhibitor of testosterone 5α-reductase is finasteride (Proscar®), which binds to the enzymes at a slow rate, competitively inhibits, and effectively irreversibly inactivates the enzyme by covalently binding NADPH (20). Another example involves "coxib" prostaglandin synthase (COX-2) inhibitors (21). Possible causes for the slow, tight binding include a conformational change of the enzyme imposed by binding, a change in the protonation state of the enzyme, displacement of a water molecule at the active site, or reversible formation of a covalent bond (19).

Mechanism-Based Enzyme Inactivators

Silverman (19) has stated that a broad definition of this term includes any inactivators that use the enzyme mechanism but invokes a stricter definition, one that will be adhered to in this chapter. The definition is "an unreactive compound whose structure resembles that of either the substrate or the product of the target enzyme, and which undergoes a catalytic transformation by the enzyme to a species that, prior to release from the active site, inactivates the enzyme" (19). A key point here is the need to inactivate the enzyme before leaving the active site. The definition, taken as a whole, restricts the grouping from transition state analogs, affinity labels, and slow, tight-binding inhibitors.

Mechanism-based inactivation is sometimes encountered inadvertently with existing drugs. There are several major intentional uses of these compounds, and this group will be covered in some detail (5,19,22 27). Mechanism-based inactivators have been of considerable interest because of their usefulness in the delineation of enzyme mechanisms. They are also of interest in the design of new drugs because, in principle, only the target enzyme will be attenuated. Many of the better diagnostic inhibitors of the drug-metabolizing enzymes are mechanism-based inactivators. For instance, these can be used to gain valuable in vitro information about which of the P450s are involved in a particular reaction (28,29).

The relevant scheme for mechanism-based inactivation is

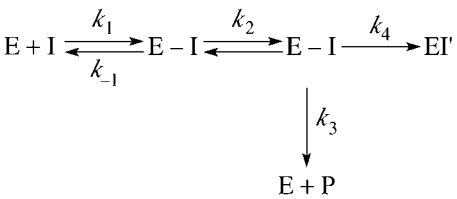

where I is the mechanism-based inactivator, E-I* is an intermediate derived by transformation of the initial complex, EI′ is an inactivated enzyme, and P is a stable product that leaves the enzyme. Sometimes these inhibitors are called "suicide inactivators," although the term is not generally accepted by purists. It is the enzyme, not the inhibitor, that is dying.

Several parameters are experimentally determined and used to describe these inhibitors. The ratio k_3/k_4 is the "partition ratio," which can be thought of as the number of times that the enzyme must cycle, on the average, for one inactivation to occur. However, the ratio can range from several thousand to less than one, even approaching zero.

The inactivation process shows first-order kinetics, i.e., a plot of the logarithm of the remaining enzyme activity versus time gives a straight line (first order, or single exponential kinetics). The half-life, $t_{1/2}$, can be determined at each inhibitor concentration used and used to calculate k, using the relationship $t_{1/2} = \frac{0.693}{k_{\text{inact}}} + \frac{0.6932K_{\text{I}}}{k_{\text{inact}} \cdot \text{I}}$ (19). The plot of k versus [I] is hyperbolic, and a linear transformation (e.g., plot of $1/k$ vs. $1/[\text{I}]$) yields k_{inact}, the maximum rate of inactivation, and K_{I}, the concentration of inhibitor required for half-maximal inhibition. In the above scheme, $k_{\text{inact}} = k_2$ if k_2 is rate limiting in the overall reaction. K_{I} is a complex expression of microscopic rate constants but is useful in estimating the potential usefulness of an inhibitor.

A number of criteria can be used to determine if mechanism-based inactivation is actually occurring. Although not all these tests are applicable to every situation, the case for mechanism-based inactivation is stronger when several can be demonstrated.

One of the simplest tests is whether or not the typical cofactors are required. For instance, in a P450-dependent reaction, is pre-incubation with NADPH necessary to see inhibition by the compound under consideration? In most cases, a mechanism-based inactivator also has a strictly competitive component, and results can be misleading. The generally accepted way of discerning the two aspects is to pre-incubate the concentrated enzyme with cofactors and a certain concentration of the inhibitor and then, at a certain time, to dilute this enzyme (e.g., 50-fold) into a solution containing a non-inhibitory substrate (and cofactors) and assay product formation, either continuously, if possible, or after a set time.

One characteristic of mechanism-based inactivation is the first-order kinetic pattern mentioned above. In practice, aliquots are withdrawn at indicated times from an incubation of enzyme, the inhibitor, and any necessary cofactors are diluted into excess substrate as mentioned above. The rate of inactivation (k) should increase when the experiment is repeated with a higher concentration of inhibitor, as mentioned above (Fig. 1). In a plot of the logarithm of residual enzyme activity versus time, the intercept ($t = 0$) indicates the extent of inhibition that is of a competitive nature.

The enzyme should be protected from inactivation by a "normal" (non-inhibitory) substrate. Of course, this criterion may not distinguish a mechanism-based inhibitor from a competitive one, unless the time dependence of inhibition is examined.

Another criterion is irreversibility. However, in some cases a slow reactivation is seen, usually occurring over a period of days. Exactly what time period of reactivation does or does not constitute mechanism-based inactivation is not specifically defined. In practice, one usually removes excess inhibitor from the enzyme (e.g., dialysis, gel filtration, centrifugal filtration) and assays the activity of the enzyme to determine if it has been restored.

The inhibitor is usually covalently bound to the enzyme in mechanism-based inactivation, either to the protein or a prosthetic group. The stoichiometry of binding should be unimolecular; i.e., only one molecule should be bound per enzyme (subunit). The extent of labeling should be correlated with the degree of inactivation; for example, a ratio of 0.7-labeled inhibitor bound per enzyme subunit should correspond to a 70% loss of activity (corrected for any competitive inhibition). Further, labeling should be specific in the sense that "scavenger" nucleophiles [e.g., glutathione (GSH)] and other proteins (that do have access to the enzyme-active site) are not labeled. A general rule of thumb is that a specific radioactivity of 0.5 Ci (^{14}C)/nmol is needed for labeling studies of this

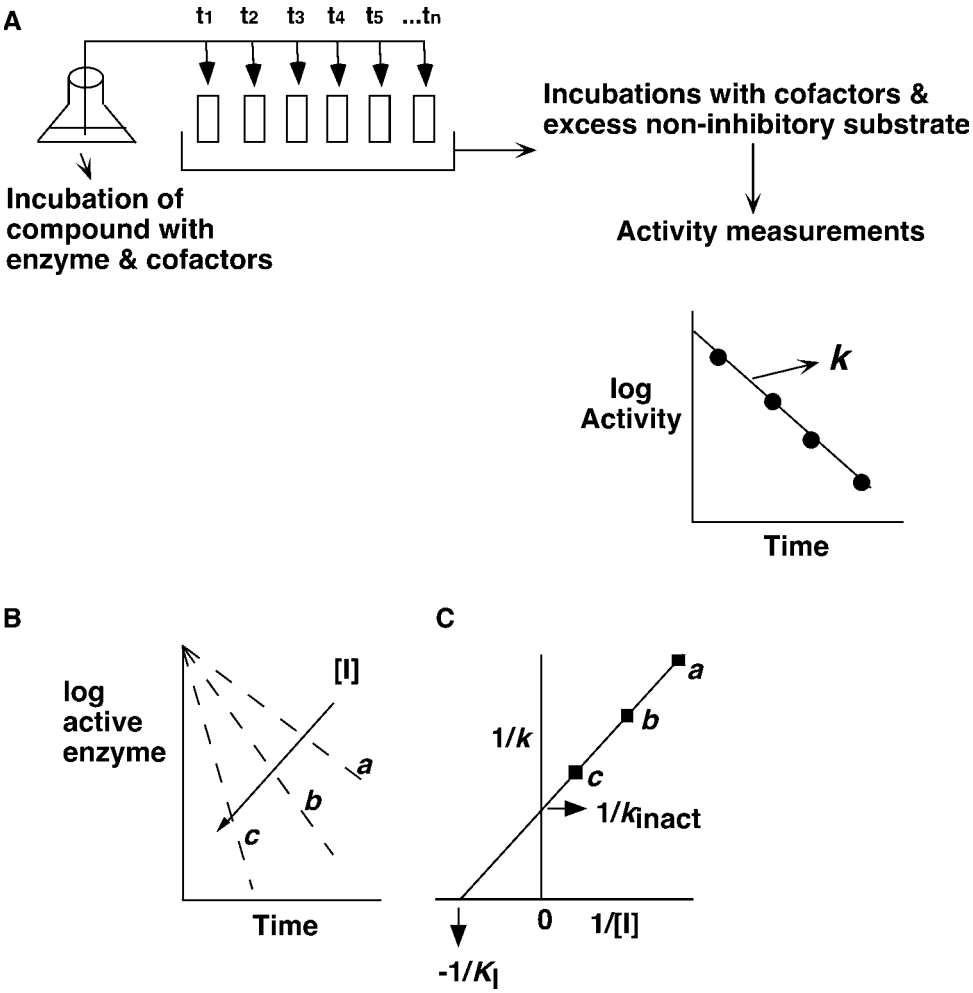

Figure 1 Determination of k_{inact} for a mechanism based inactivator. (**A**) The compound under investigation is incubated with the enzyme (plus all relevant cofactors); at various timepoints, the solution is diluted into an excess of (non inhibitory) substrate to determine the amount of remaining "active enzyme." (**B**) Plots of $\log_{10}$ (active enzyme) versus time give the plots designated ***a***, ***b***, and ***c*** at various concentrations of the inhibitory substrate I. ***a***, ***b***, and ***c*** have constants, k, defined by the slopes ($k = 0.693/t_{1/2}$). (**C**) The values of k from lines ***a***, ***b***, and ***c*** are related to [I] in the double reciprocal "Kitz Wilson" plot. The intercept on the ordinate in this plot gives k_{inact}, the extrapolated rate of inactivation at infinite inhibitor concentration, and the intercept on the x axis gives K_I, the inhibitor concentration at which a half maximal rate of inactivation is seen.

type to obtain sufficient counts for analysis (using liquid scintillation counting or similar drug methods). Other isotopes can be used; tritium is acceptable if the hydrogen is stable in all involved processes. In some cases, it is possible to use other labels such as fluorescent chromophores or mass spectrometry.

True mechanism-based inactivators use the same catalytic step in partitioning between product formation and inactivation. Thus, both should show the same cofactor requirements, and any kinetic isotope effects (e.g., deuterium) should be common to both.

More extensive treatments of the theory and practice of mechanism-based inactivation have appeared elsewhere (5,19,22,23,26,27), as well as examples of applications to various enzymes (19,22 25,30,31).

Inhibitors That Generate Reactive Products That Are Covalently Attached to the Enzyme

This group of compounds is often grouped with the mechanism-based inactivators discussed above. Many of the same criteria apply, such as the need for cofactors and the irreversible nature of the inactivation. However, labeling may be more extensive and less specific. Also, careful analysis of the kinetics may show critical differences from linearity in plots of log (enzyme activity) versus time (19). For instance, there might be a lag in the inhibition and then an apparent first-order plot, as the concentration of reactive product increases. If fresh enzyme is added to the mixture at this point, then no lag will be observed because of the buildup of electrophilic product in the medium. However, it should be emphasized that discerning deviations from pseudo-first-order kinetics may not be easy, especially if the assays are subject to error or if relatively few data points are collected.

Experiments in which mechanism-based inactivation and inhibition of the type discussed here need not be restricted to purified enzymes. They can be done with relatively crude preparations, e.g., microsomes or cytosolic fractions, if appropriate caveats are used. Labeling studies can be done with such preparations to examine the specificity of the process.

INHIBITORS OF VARIOUS ENZYMES

This section is intended not to be comprehensive but to provide some examples of the previously discussed types of enzyme inhibition, as they relate to several of the enzymes involved in the biotransformation of drugs and xenobiotics. The reader is referred to other articles for more comprehensive lists of inhibitors (29).

Monoamine Oxidase

There are two forms of monoamine oxidase, termed "A" and "B" (32). These have long been recognized to show differences in inhibition by various drugs and are recognized to be the products of different genes. Mechanism-based inactivation is common among many of the inhibitors of these enzymes, and drugs have been developed to treat problems related to the nervous system (19,33).

Monoamine oxidase A oxidizes biogenic amines and is selectively inhibited by the mechanism-based inactivator clorgyline. The B form of the enzyme is involved in the oxidation of non-catecholamines and is inhibited by pargyline and deprenyl, also mechanism-based inactivators. These compounds all contain an *N*-propynyl (propanyol) group (N COC CH_3), which leads to a covalent adduct (19).

Another inhibitor of monoamine oxidase is the anticonvulsant milacemide, $CH_3(CH_2)_4NHCH_2CONH_2$, which is also a substrate (19). The compound is thought to be oxidized to an aminium radical (1-electron oxidation) with attack on an α-carbon to generate a protein adduct (19).

Another popular group of inhibitors has been ring-strained cycloalkylamines, which rearrange to reactive products following one-electron oxidation (34,35). The

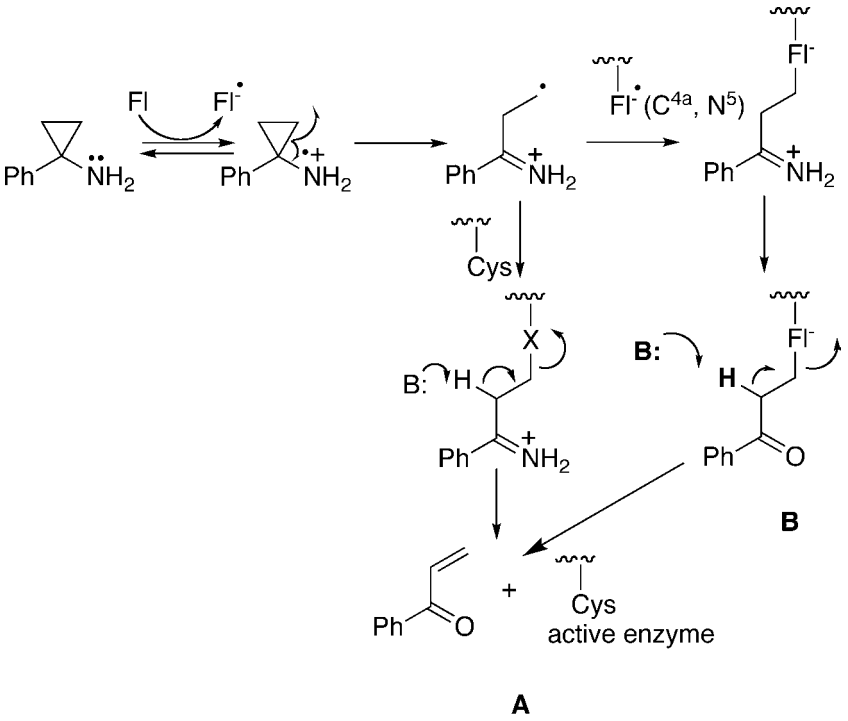

Figure 2 Proposed scheme for oxidation of 1 phenylcyclopropylamine by monoamine oxidase, with both pathways leading to inactivation by binding to a (**A**) cysteine and (**B**) flavin (19). In the case of the flavin, both the C 4a and N 5 adducts are formed (36,37).

antidepressant tranylcypromine was one of the first compounds in this class. Postulated mechanisms for some of these are shown in Figure 2. There are two paths (Figs. 2A, B). One leads to modification of the flavin prosthetic group, either at the C-4a or N-5 atom (36,37). The other pathway leads to modification of a protein Cys group. This appears to be a reversible process, with the enzyme losing the group after 24 hours (see the section "Mechanism-Based Inactivation" for discussion of the issue of reversibility). A series of cyclopropyl derivatives of *N*-methyl-4-phenyl-1,2,5,6-tetrahydropyridine have been studied (38,39).

Cytochrome P450

Inhibitors of P450s have been studied with regard to several aspects. Some aspects are quite basic. First, many different P450 enzymes are found in humans, and experimental animals and diagnostic inhibitors have been used to ascertain the roles of individual P450s in catalysis of reactions (29). Because of the overlapping catalytic specificity of many of the P450s, inhibitors are usually not totally selective. Nevertheless, the selectivity can be examined, and the use of diagnostic inhibition of individual P450s is possible, with appropriate caveats (40,41). A list of generally accepted "probe" inhibitors is presented in Table 1 (29). Further, inhibitors have provided considerable insight into function, both in terms of chemical aspects of catalysis and structural details of the proteins that contribute to selectivity (47).

Other aspects of P450 inhibition are more practical (48). For instance, one prominent strategy in therapy of estrogen-dependent tumors is the inhibition of P450

Table 1 Some Diagnostic Inhibitors of Human P450 Enzymes[a]

P450	Inhibitor	Apparent mechanism
1A1	7,8 benzoflavone	Competitive[b]
	Ellipticine	Competitive
1A2	7,8 benzoflavone	Competitive[b]
	Fluvoxamine	Competitive
	Furafylline	Mechanism based
2A6	Diethyldithiocarbamate	Mechanism based
	Pyridine analogs of nicotine	Competitive[c]
2C9	Sulfaphenazole	Competitive[d]
	Tienilic acid	Mechanism based
2D6	Quinidine, several others[e]	Competitive[f]
2E1	4 methylpyrazole	Competitive
	Diethyldithiocarbamate	Mechanism based[b]
	Many organic solvents	Competitive[b]
3A4, 3A5	Troleandomycin	Conversion to heme ligand
	Erythromycin	Conversion to heme ligand
	Gestodene	Mechanism based

[a](29).
[b]Known to be oxidized by the enzyme. Also, some of the results with these compounds reported in (42) are not supported in subsequent work (40,41).
[c](43).
[d]Apparently not a heme ligand (44).
[e](45).
[f]Apparently not oxidized (46).

19A1, the "aromatase" that catalyzes the three-step conversion of androgens to estrogens (49). Aminoglutethimide is a classic but not an ideal inhibitor, and numerous efforts are in progress to design better drugs (50). Another target in yeast and fungal infections is P450 51, the lanosterol 14α-demethylase (51). Many "azoles" (e.g., ketoconazole) are used as drugs in this regard (52). Selectivity for the fungal enzyme is observed, but these drugs can also inhibit mammalian P450 51A1 and other P450s at higher concentrations (53,54). Another example of a P450 inhibitor is piperonyl butoxide, which is used as an insecticide "synergist" to block the detoxication of chemicals by insect P450s (Fig. 3) (55). As more information becomes available about the P450s present in noxious insects, the design and development of pesticides (and synergists) with more selectivity for the insect enzymes should be possible.

Another practical area where the development of better inhibitors of P450s may be useful is in cancer prevention. Some inhibitors (e.g., ethynyls) can block rodent and

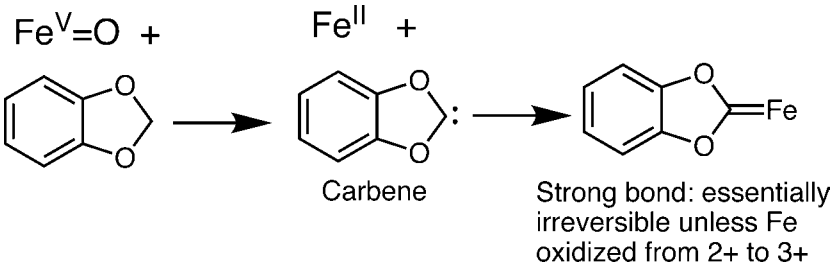

Figure 3 Oxidation of piperonyl butoxide by P450 to a carbene that yields a stable ferrous ligand (55).

human P450s that activate carcinogens (56) and can be shown to block carcinogen-induced cancers in rodents (57). The drug oltipraz and the natural compound sulforophane have been studied in cancer prevention studies because of their abilities to induce conjugation enzymes (e.g., GSH S-transferase, quinone reductase) (58,59). More importantly, perhaps, they have both been shown to block P450s involved in the activation of carcinogens, e.g., aflatoxin B_1 (60).

Several types of inhibition are seen for the P450s. A relatively common mechanism is competitive inhibition. For instance, quinidine and most other P450 2D6 inhibitors seem to act in this way (61); a basic nitrogen in the inhibitor seems to bind in the same site as the substrates in most, but not all, cases (45,62,63). Azoles have already been mentioned and are one example of nitrogen heterocycles that ligand to the heme iron (52,64). Sulfaphenazole is a competitive inhibitor of P450 2C9 and has selectivity (compared with other P450 2C enzymes) (65,66). Many organic solvents inhibit P450 2E1 by competing as substrates (67,68), so care must be taken in experimental designs (esp. in vitro).

Another group of inhibitors are not particularly effective themselves but are oxidized to "metabolic intermediates" that bind tightly to the heme and prevent further involvement of the iron atom in catalysis. For instance, some amines are oxidized to *C*-nitroso derivatives (e.g., troleandomycin) (69,70), and piperonyl butoxide (*vide supra*) yields a carbene (Fig. 3) (71). This process might be termed "mechanism-based inactivation," but perhaps a better description would be transformation by the enzyme(s) to very tight-binding inhibitors. The linkages are not covalent in the usual sense, since addition of a strong oxidant [e.g., $Fe(CN)_6^{3-}$] oxidizes such a ferrous complex to ferric and releases the ligand.

Mechanism-based inactivators have been studied extensively, primarily from a basic standpoint (28,72). Many vinyl and acetylenic inhibitors have been characterized as yielding heme and/or protein adducts (Fig. 4). Some of these have practical consequences with drugs [e.g., secobarbital (72)]. A dihalomethylene group (74) can also be involved in mechanism-based inactivation, although it is not clear whether chloramphenicol should be classified in this group or among the inhibitors that are converted to a reactive product (75). Inhibition by cyclopropylamines is considered to involve oxidation to an aminium

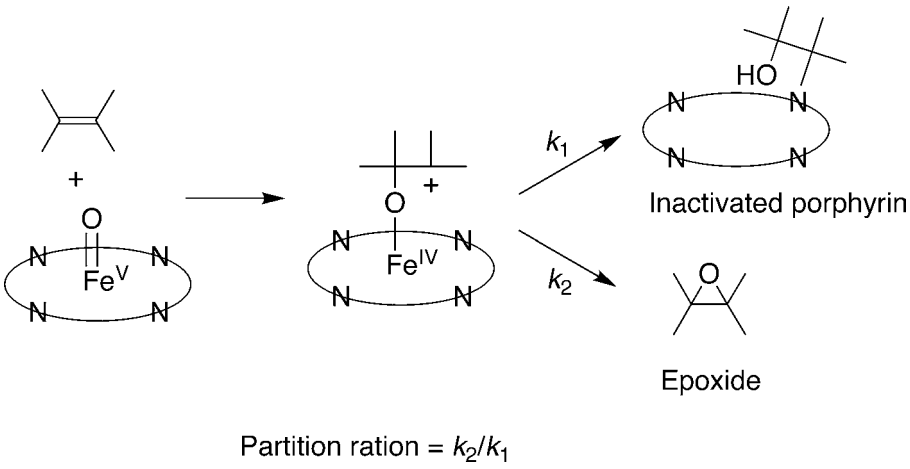

Figure 4 Mechanism based inactivation of P450 by heme destruction during the epoxidation of an olefin (73). The partition ratio is given by k_2/k_1. Several of the *N* alkyl porphyrin adducts arising from the heme have been vigorously characterized by NMR and mass spectrometry. *Abbreviation*: NMR, nuclear magnetic resonance.

radical that rearranges to a reactive methylene radical, as in the case of the postulated mechanism for monoamine oxidase (Fig. 2), although adducts remain to be characterized (76 78).

4-Alkyl-1,4-dihydropyridines are readily oxidized by P450s by one-electron oxidation (79). Rearrangement of the putative aminium radical to the pyridine generates an alkyl radical, which modifies a pyrrole nitrogen of the prosthetic heme (80). If an aromatic group is at the 4-position, it is retained, and such compounds are used as drugs (81). This is, strictly speaking, not an example of mechanism-based inactivation, since (*i*) alkyl radicals can react with spin traps outside of the protein (79) and (*ii*) other P450s that cannot oxidize the 4-alkyl-1,4-dihydropyridines can also be inactivated when an enzyme capable of oxidation (e.g., P450 3A4) is also present. Ortiz de Montellano and his associates have also characterized other compounds (e.g., 1-aminobenztriazole) that are oxidized by P450s to yield covalent heme adducts (46,82,83). Interestingly, Meschter et al. (84) have reported that it is possible to use 1-aminobenztriazole to lower total hepatic P450 levels in rats to $<30\%$ that of the normal for 13 weeks without significant physiological effects.

Mechanism-based inhibition is of considerable inhibition of P450s, in the context of leading to drug-drug interactions, particularly with P450 3A4 (85). Collectively, these inhibitors may be grouped into several families of effects: (*i*) oxidation to compounds that bind heme reversibly but very tightly (i.e., methylene dioxyphenyls compounds, *vide supra*), amines that are oxidized to *C*-nitroso derivatives (70); (*ii*) oxidation to intermediates that react with P450 heme and generate porphyrin derivatives (72,85); (*iii*) oxidation to products that react with the (apo) protein (as opposed to heme); and (*iv*) oxidation to products that cross-link the heme to the protein (85). A list of some of the chemical moieties that have demonstrated mechanism-based inactivation includes olefins, acetylenes (and proparyls), thiophenes, furans, strained cycloalkylamines, some thiols and thionosulfurs, and dihalomethylenes (85).

Most of the compounds that have been studied fall into classes (*ii*) and (*iii*). Some mechanisms are shown in Figure 4. At this time, prediction of whether an olefin or acetylene will act as a mechanism-based inactivator is not really possible nor is the prediction as to whether heme modification, protein modification, or a mixture of both may occur. Few examples of group (*iv*), with heme-protein cross-linking, have been characterized in detail.

During the time elapsed since the first edition of this monograph was published (2), a number of examples of P450-based inactivation have been characterized in some detail (Table 2). In some cases, the specific P450 residues involved in covalent binding have been identified (99,101). Although we have a reasonably good understanding of the chemistry involved in some of these processes (*vide supra*), there are several chemicals for which the chemistry involved in inhibition/binding is not well understood (e.g., imines, piperazines).

NADPH-P450 Reductase

This flavoprotein is involved in the transfer of electrons from NADPH to P450s (103). The enzyme also functions in electron transfer to some other hemoproteins, e.g., heme oxygenase (104).

Inhibition has not been studied extensively. The oxidation product $NADP^+$ is a competitive inhibitor (11). The 2′-phosphate group is important in binding; 2′-AMP is also a competitive inhibitor, and the enzyme is the basis for the use of 2,5′-ADP affinity chromatography in purification (105).

Table 2 P450 Mechanism Based Inhibitors[a]

Compound	Putative activated moiety	P450	Mode of binding	Ref.
L 754,394	Furan	3A4	Protein (?)	86
Zafirlukast	3 Methylindole	3A4	Protein (?)	87
Raloxifene	Quinonemethide (?)	3A4	Protein (?)	88
Phencyclidine	Iminium ion	2B1	Protein	89
9 Ethynylphenathrene	Acetylene	2B1	Protein	90, 91
Deprenyl	Acetylene	2B1	Heme	92
Clorgyline	Acetylene	2B1	Iron complex	92, 93
tert Butylisothiocyanate	Isothiocyamate	2E1	Heme (?)	94
Xanthates	Dithiocarbonic acid	2B1, 2B6	(?)	95, 96
7 ethynylcoumarin	Acetylene	2B1	Protein	97
Phencyclidine	Acetylene	2B6	Protein	98
tert butylacetylene	Acetylene	2B4	Heme	99
Phenyldiaziridines	Aziridines	2B6	Protein (?)	100
17*a* ethynylestradiol	Acetylene	2B6, 3A5	Protein and heme	101, 102

[a]Concentrated on results published since 1995. For earlier and more information see Refs. 72, 85.

Diphenyliodonium has been reported to be a mechanism-based inactivator of the enzyme (106). The mechanism is postulated to involve one-electron reduction of the iodonium to give an iodide/flavin radical pair that combines to give an N^5-phenylflavin adduct, along with a labeled amino acid (Trp 419).

Flavin-Containing Monooxygenase

In contrast to the flavoprotein monoamine oxidase, little is known about inhibitors of this enzyme. Some are known but have poor affinities (107). No mechanism-based inactivators have been characterized. The various substrates seem to inhibit each other, at least insofar as they are substrates for the same form of the enzyme (at least 5 forms can exist in a single animal species) (108,109).

Aldehyde Oxidase

Aldehyde oxidase and the related molybdenum-flavin-iron sulfur protein xanthine oxidoreductase are involved in the oxidation of a number of drugs, particularly heterocycles (110). The mechanism differs clearly from P450 and other mixed-function oxidases in that electrons are removed from a substrate and transferred to an electron donor, generally NAD^+ or O_2 (111). The oxygen atom incorporated into the substrate is derived from H_2O, not O_2.

Allopurinol is a reversible inhibitor that can be used to distinguish between the involvement of aldehyde oxidase and xanthine oxidoreductase in vitro or in vivo, preferentially inhibiting the latter enzyme. Aldehyde oxidase is preferentially inhibited by isovanillin.

Recently the neonicotinoid insecticide imidacloprid has been shown to be reduced from a nitro to a nitroso substitution. The nitroso compound, in turn, is an irreversible, mechanism-based inactivator of rabbit aldehyde oxidase, as judged by several kinetic and other criteria, including covalent binding (112).

Carbonyl Dehydrogenases and Reductases

Disulfiram is a well-known inhibitor of aldehyde dehydrogenase. This drug, Antabuse®, has been given to recovering alcoholics to produce unpleasant physiological effects when the individuals consume ethanol. Disulfiram is reduced to diethyldithiocarbamate, which seems to be bound to an enzyme Cys in disulfide linkage (113). Diethyldithiocarbamate is also an inhibitor of some P450s (esp. 2E1, 2A6) (114). It may have a mechanism-based action, at least as judged by the kinetics seen in limited investigations (13). In vivo, diethyldithiocarbamate is methylated and then oxygenated to yield a more effective inhibitor (115,116).

The sedative chloral (2,2,2-trichloroacetaldehyde) is a competitive inhibitor of aldehyde dehydrogenase, with a K_i of 1 to 10 mM. Apparently a stable thiohemiacetal is formed with Cys 302. Because of the electronegativity of the chlorine atoms, transfer of a hydride ion is effectively blocked.

Similarly, aldose reductase is a target for inhibition in the treatment of certain types of diabetes. The drugs sorbinil, alrestatin, and tolrestat seem to be effective in diabetic rats but have not been as useful in humans (117).

Esterases and Amidases

The mechanisms of inhibition of acetylcholinesterase have long been of interest because chemical warfare agents (nerve gases) and organophosphate insecticides can interfere with cholinergic transmission and lead to respiratory failure. The basic principles have been known for some time and involve nucleophilic attack by a Ser in the active site (118) (Fig. 5).

In contrast to most of the examples of drug inhibition, this is a "noncompetitive" mechanism where reaction with an active site Ser occurs. The reaction is somewhat reversible in that hydrolysis can occur to reactivate the enzyme. However, a rearrangement, usually referred to as "aging," can occur to fix the damage by generation of a nonhydrolyzable linkage (118).

Epoxide Hydrolase

The epoxide hydrolases are now recognized to be a subfamily of the α-, β-lyase family that have certain features that make epoxides good substrates (119). In recent years, the discovery that a covalent ester intermediate is formed has had considerable implication for mechanistic studies (120). Modes of inhibition need to be reexamined in this context.

A number of supposedly competitive inhibitors of microsomal epoxide hydrolase have been reported (121). Of these, 3,3,3-trichloropropylene oxide has historically been considered the most diagnostic, although it seems to have disappeared from the commercial market because of unknown regulatory issues. However, if an ester intermediate is formed, the rate of hydrolysis of this may be the issue, and this may be better classified as a slow, tight-binding inhibitor. The "soluble" epoxide hydrolase has inhibitors with lower K_i values, particularly among the chalcone oxides (122).

Glutathione S-Transferases

These enzymes are very abundant (123), and the crystal structures of many are now known (124). Some hydrophobic compounds are good ligands [hence one of the original names, "ligandin" (125)], which probably act as competitive inhibitors (123). GSH has a K_d for several of the GSH transferases of approximately 20 μM, facilitating the use

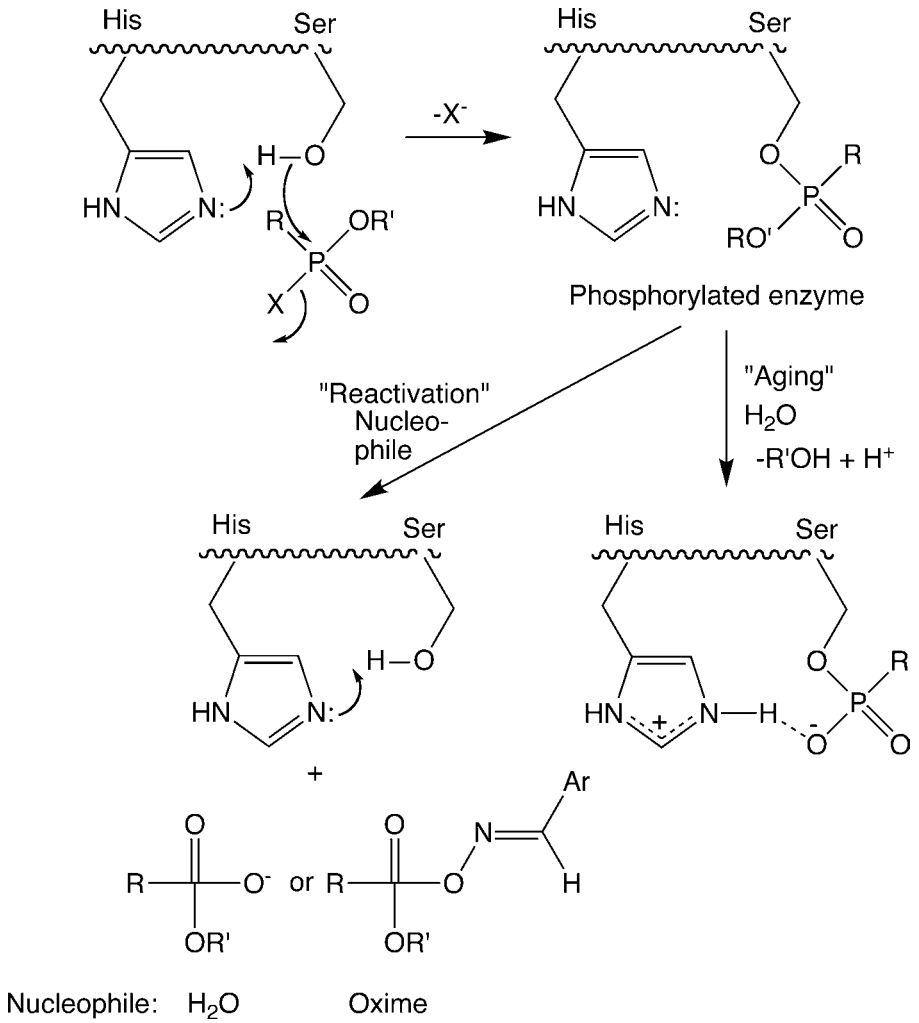

Figure 5 Inactivation of acetylcholinesterase by organophosphates and enzyme reactivation and "aging" (118).

of affinity chromatography for purification (126). Replacement of the CH CH_2S (CH CH_2 SH) moiety of GSH with CH CO_2 provides an analog of a key intermediate, which has a K_i of 0.9 μM (127). A somewhat similar approach was used by Mulder, who replaced the entire L-Cys-Gly moiety with D-aminoadipate (128) (K_i 8 μM, GST 4-4). Also, a Meisenheimer complex of GSH with 1,3,5-trinitrobenzene appears to behave as a transition state analog (129). Product complexes can also be used as inhibitors (130). For instance, S-(3′-iodobenzyl) GSH had a K_i of 0.2 μM and was used to solve the structure of GST 3-3, as a source of a heavy atom in diffraction studies. Some GSH conjugates have been used as affinity labels (131). The GSH conjugate 2-(*S*-glutathionyl)-3,5,6-trichloro-1,4-benzoquinone is an effective irreversible inhibitor ($Ki < 1$ μM, k_{inact} 0.3 min^{-1}) and modifies active site Tyr groups (132). Since GSH transferases are generally beneficial, the question can be raised as to why they should be targets for inhibition. The antischistosomal drug praziquantel is used to inhibit the parasite *Schistosoma japonica* (133). It appears to compete by binding to a hydrophobic substrate site near the subunit

interface of the dimer. Also, GSH S-transferase over-expression may contribute to multiple drug resistance in cancer cells and is a potential therapeutic target (133).

Sulfotransferases

The phenols 2,6-dichloro-4-nitrophenol and pentachlorophenol have been described as competitive, "dead-end" inhibitors (134). This is a family of enzymes that is growing in complexity, and the selectivity of these interactions is still a matter of investigation.

UDP-Glucuronosyl Transferases

Many drugs have been characterized as competitive inhibitors of the steroid-, bilirubin-, and drug-conjugation activities of uridine diphosphate (UDP)-glucuronosyl transferases [see Table 7 of ref. (135)]. The roles of these interactions in practical drug metabolism issues are largely unexplored. Both transition-state analog inhibitors (136) and photo-affinity labels (137 139) have been designed and used to characterize these enzymes (135).

EXAMPLES OF RELEVANCE OF INHIBITION TO DRUG-DRUG INTERACTIONS

Clinical aspects of drug-drug interaction are covered elsewhere in this book and, therefore, only a few classical examples of in vivo problems will be mentioned here. The reader is also referred to other treatments of the subject (140).

As mentioned already, in some cases the enzymes are targets and inhibition is intended. In other cases, some inhibition may be expected on the basis of preliminary in vitro assays. Nevertheless, most pharmaceutical companies would rather not put a drug with the potential for interaction problems on the market, if another that did not have such potential were available.

What one would like to avoid is the development of a potential inhibition/interaction problem with a drug already on the market (or heavily invested in the developmental process). A few examples will be mentioned.

The H_2 receptor antagonist cimetidine has been widely prescribed for ulcers. This compound can inhibit P450-catalyzed reactions, although it is a relatively weak inhibitor (141). Nevertheless, a considerable market share was lost to the noninhibitory alternative ranitidine through advertising, on the basis of the prospect of drug-drug interactions.

Terfenadine was the first non-sedating antihistamine on the market and has been highly successful. Nevertheless, some adverse incidents have been reported, and the basis of some seems to be related to metabolism. Terfenadine is usually extensively oxidized, and in most individuals, none of the parent drug is found circulating in plasma. One of the two main oxidation routes yields the inactive N-dealkylation products. The product of the other oxidation route, a carboxylic acid, retains its ability to block the histamine receptor. The acid is actually a zwitterion and does not readily cross the blood-brain barrier, so it is non-sedating. If P450 3A4 is inhibited, then terfenadine can accumulate and may cause arrythmias (142,143). Adverse effects had been reported (144), and now the Food and Drug Administration (FDA) has withdrawn registration, mainly on the basis of experiences with the concurrent use of known P450 3A4 inhibitors, e.g., erythromycin and ketoconazole (145).

Another example of P450 3A4 inhibition involves the progestin gestodene, which has been used with the estrogen 17α-ethynylestradiol in some oral contraceptive formulations. All 17α-acetylenic steroids seem to have some inherent capability of acting as P450 mechanism-based inactivators (146,147), but gestodene appears to be more

effective than many others (148). The inhibition of P450 3A4 might explain some of the thrombolytic problems attributed to gestodene (149), because inhibition of 17β-estradiol and 17α-ethynylestradiol oxidation (catalyzed by P450 3A4) could raise estrogen levels, a known factor in thrombolytic problems. However, the levels of gestodene ingested daily do not seem high enough to account for destruction of a substantial fraction of the P450 3A4 pool (148), and the in vivo significance of these phenomena is not yet clear.

CONSIDERATIONS OF ENZYME INHIBITION IN MEDICINAL CHEMISTRY AND DRUG DEVELOPMENT

Today many pharmaceutical companies routinely screen libraries of new chemical entities for inhibition early in the drug development process, sometimes even as a part of drug discovery. The major concern is inhibition of P450 enzymes and the potential for drug-drug interactions. Five P450 enzymes 1A2, 2C9, 2C19, 2D6, and 3A4 account for approximately 95% of all P450 metabolism of drugs, and these are used in initial screens (49). One strategy is to use individual recombinant P450s; the other is to use human liver microsomes. With either, one can use either model fluorescent or luminescent substrates for individual P450s or diagnostic marker reactions (29), usually with liquid chromatography-mass spectrometry (LC-MS) methods. The fluorescence/luminescence assays have the advantage of higher throughput, but in recent years several pharmaceutical companies have moved in favor of the LC-MS approaches because of better predictability of interactions with company compounds.

Reversible inhibition can be analyzed rapidly. In general, IC_{50} values of >10 μM are considered unimportant, IC_{50} values <1 μM are considered problematic, and IC_{50} values of 1 to 10 μM are considered possible issues, depending upon the predicted plasma or tissue C_{max} (150,151).

Compounds that are still of interest are further examined for the contribution of preincubation with NADPH on metabolism of P450 diagnostic substrates. The consideration of mechanism-based inactivation is more complex. For a list of some of the typical chemical moieties associated with P450 mechanism-based inactivation see Table 2. One approach is to experimentally obtain in vitro parameters for inhibition in human liver microsomes, purified human P450 systems, or human hepatocytes. The parameters of most interest are the partition coefficient, $k_{inactivation}$, and K_i (Fig. 1). The ratio $k_{inactivation}/K_i$ is perhaps the most useful parameter, being rather analogous to k_{cat}/K_m for oxidation, which is prediction of Cl_{int} in vivo.

The ratio $k_{inactivation}/K_i$ does not give a definite answer regarding whether a drug candidate will be a problem in vivo. The dose will be one issue, as will the partition ratio. However, a very useful strategy is to compare $k_{inactivation}/K_i$ (and other parameters) with drugs already used in practice and experience with those. For instance, $k_{inactivation}/K_i$ varies from 2 (17α-ethynylestradiol) to 126,000 (ritonavir) (152). The former compound is generally not considered to be a problem due to low doses, but the latter is recognized as producing major in vivo drug interactions. Further development of databases such as this should help guide decisions about prediction of drug-drug interactions.

CONCLUSIONS

Inhibition of the enzymes usually associated with drug metabolism is a subject of both basic and practical interest. Basic studies involve studies of mechanisms of catalysis and the use of selective inhibitors of individual forms of enzymes in multigene families.

Practical aspects of inhibition include drug-drug interactions and enzymes as therapeutic targets. Among the more common modes of enzyme inhibition seen are competitive inhibition, product inhibition, slow, tight-binding inhibition, mechanism-based inactivation, and products that become covalently attached. Discrimination among these is necessary for a proper understanding of action. However, in some cases the classification into a particular mode may not be obvious. A better understanding of inhibition mechanisms and selectivity has led to more efficient screening for drug-drug interactions in the pharmaceutical industry and appreciation of the phenomenon in the regulatory agencies.

ACKNOWLEDGMENTS

Research in the author's laboratory has been supported by USPHS grants R37 CA090426 and P30 ES000267. Thanks are extended to K. Trisler for assistance in preparation of the manuscript.

REFERENCES

1. Guengerich FP. Role of cytochrome P450 in drug interactions. Adv Pharmacol 1997; 43:7 35.
2. Guengerich FP. Inhibition of drug metabolizing enzymes: molecular and biochemical aspects. In: Woolf TF, ed. Handbook of Drug Metabolism. New York: Marcel Dekker, 1999:203 227.
3. Segel IH. Enzyme Kinetics. New York: Wiley, 1975.
4. Cornish Bowden A. Analysis of Enzyme Kinetics. Oxford: Oxford Univ Press, 1995.
5. Silverman RB. Mechanism based Enzyme Inactivation: Chemistry & Enzymology. Boca Raton, FL: CRC Press, 1988.
6. Kuby SA. A Study of Enzymes, Vol. I, Enzyme Catalysis, Kinetics, and Substrate Binding. Boca Raton, FL: CRC Press, 1991.
7. Bronson DD, Daniels DM, Dixon JT, Redick CC, Haaland PD. Virtual kinetics: using statistical experimental design for rapid analysis of enzyme inhibitor mechanisms. Biochem Pharmacol 1995; 50:823 831.
8. Renwick AG. Toxicokinetics. In: Hayes AW, ed. Principles and Methods of Toxicology. 5th ed. New York: Raven Press, 2007:179 230.
9. von Moltke LL, Greenblatt DJ, Duan SX, et al. *In vitro* prediction of the terfenadine ketoconazole pharmacokinetic interaction. J Clin Pharmacol 1994; 34:1222 1227.
10. Black DJ, Kunze KL, Wienkers LC, Gidal BE, Seaton TL, Mcdonnell ND, Evans JS, Bauwens JE, Trager WF. Warfarin fluconazole II. A metabolically based drug interaction: *in vivo* studies. Drug Metab Dispos 1996; 24:422 428.
11. Vermilion JL, Coon MJ. Purified liver microsomal NADPH cytochrome P 450 reductase: spectral characterization of oxidation reduction states. J Biol Chem 1978; 253:2694 2704.
12. Guengerich FP, Bartleson CJ. Analysis and characterization of enzymes and nucleic acids. In: Hayes AW, ed. Principles and Methods of Toxicology. 5th ed. Boca Raton, FL: CRC Press, 2007:1981 2048.
13. Guengerich FP, Kim D H, Iwasaki M. Role of human cytochrome P 450 IIE1 in the oxidation of many low molecular weight cancer suspects. Chem Res Toxicol 1991; 4:168 179.
14. Shimada T, Guengerich FP. Inhibition of human cytochrome P450 1A1, 1A2, and 1B1 mediated activation of procarcinogens to genotoxic metabolites by polycyclic aromatic hydrocarbons. Chem Res Toxicol 2006; 19:288 294.
15. Shimada T, Murayama N, Okada K, Funae Y, Yamazaki H, Guengerich FP. Different mechanisms for inhibition of human cytochromes P450 1A1, 1A2 and 1B1 by polycyclic aromatic inhibitors. Chem Res Toxicol 2007; 20:489 496.
16. Haldane JBS. Enzymes. London: Longmans, Green, 1930.

17. Pauling L. Chemical achievement and hope for the future. Am Sci 1948; 36:51 58.
18. Lerner RA, Benkovic SJ. Principles of antibody catalysis. BioEssays 1988; 9:107 112.
19. Silverman RB. Mechanism based enzyme inactivators. Methods Enzymol 1995; 249:240 283.
20. Tian GC, Mook RA, Moss ML, Frye SV. Mechanism of time dependent inhibition of 5 alpha reductases by delta(1) 4 azasteroids: Toward perfection of rates of time dependent inhibition by using ligand binding energies. Biochemistry 1995; 34:13453 13459.
21. Marnett LJ. Cyclooxygenase mechanisms. Curr Opin Chem Biol 2000; 4:545 552.
22. Abeles RH, Maycock AL. Suicide enzyme inactivators. Acc Chem Res 1976; 9:313 319.
23. Rando RR. Mechanism based enzyme inactivators. Pharmacol Rev 1984; 36:111 142.
24. Walsh CT. Suicide substrates, mechanism based enzyme inactivators: recent developments. Annu Rev Biochem 1984; 53:493 535.
25. Abeles RH and Alston TA. Enzyme inhibition by fluoro compounds. J Biol Chem 1990; 265:16705 16708.
26. Waley SG. Kinetics of suicide substrates. Biochem J 1980; 185:771 773.
27. Waley SG. Kinetics of suicide substrates: practical procedures for determining parameters. Biochem J 1985; 227:843 849.
28. Halpert JR, Guengerich FP. Enzyme inhibition and stimulation. In: Guengerich FP, ed. Biotransformation, Vol. 3, Comprehensive Toxicology. 1st ed. Oxford: Elsevier, 1997:21 35.
29. Correia MA. Human and rat liver cytochromes P450: functional markers, diagnostic inhibitor probes, and parameters frequently used in P450 studies. In: Ortiz de Montellano PR, ed. Cytochrome P450: Structure, Mechanism, and Biochemistry. 3rd ed. New York: Plenum Press, 2005:619 657.
30. Xiao X, Prestwich GD. 29 Methylidene 2,3 oxidosqualene: a potent mechanism based inactivator of oxidosqualene cyclase. J Am Chem Soc 1991; 113:9673 9674.
31. Schechter PJ, Sjoerdsma A. Therapeutic utility of selected enzyme activated irreversible inhibitors. In: Enzymes as Targets for Drug Design. New York: Academic Press, 1990: 201 210.
32. Bach AWJ, Lan NC, Johnson DL, et al. cDNA cloning of human liver monoamine oxidase A and B: molecular basis of differences in enzymatic properties. Proc Natl Acad Sci U S A 1988; 85:4934 4938.
33. Dostert PL, Benedetti MS, Tipton KF. Interactions of monoamine oxidase with substrates and inhibitors. Med Res Rev 1989; 9:45 89.
34. Silverman RB. Mechanism of inactivation of monoamine oxidase by *trans* 2 phenyl cyclopropylamine and the structure of the enzyme inactivator adduct. J Biol Chem 1983; 258:14766 14769.
35. Silverman RB, Ding CZ. Chemical model for a mechanism of inactivation of monoamine oxidase by heterocylic compounds. Electronic effects on acetal hydrolysis. J Am Chem Soc 1993; 115:4571 4576.
36. Mitchell DJ, Nikolic D, Rivera E, Sablin SO, Choi S, van Breemen RB, Singer TP, Silverman RB. Spectrophotometric evidence for the flavin 1 phenylcyclopropylamine inactivator adduct with monoamine oxidase N. Biochemistry 2001; 40:5447 5456.
37. Mitchell DJ, Nikolic D, van Breemen RB, Silverman RB. Inactivation of monoamine oxidase B by 1 phenylcyclopropylamine: Mass spectral evidence for the flavin adduct. Bioorg Med Chem Lett 2001; 11:1757 1760.
38. Tipton KF, McCrodden JM, Youdim MBH. Oxidation and enzyme activated irreversible inhibition of rat liver monoamine oxidase B by 1 methyl 4 phenyl 1,2,3,6 tetrahydropyridine (MPTP). Biochem J 1986; 240:379 383.
39. Rimoldi JM, Wang YX, Nimkar SK, Kuttab SH, Anderson AH, Burch H, Castagnoli N Jr. Probing the mechanism of bioactivation of MPTP type analogs by monoamine oxidase B: structure activity studies on substituted 4 phenoxy , 4 phenyl , and 4 thiophenoxy 1 cyclo propyl 1,2,3,6 tetrahydropyridines. Chem Res Toxicol 1995; 8:703 710.
40. Newton DJ, Wang RW, Lu AYH. Cytochrome P450 inhibitors: evaluation of specificities in the *in vitro* metabolism of therapeutic agents by human liver microsomes. Drug Metab Dispos 1994; 23:154 158.

41. Bourrié M, Meunier V, Berger Y, Fabre G. Cytochrome P450 isoform inhibitors as a tool for the investigation of metabolic reactions catalyzed by human liver microsomes. J Pharmacol Exp Ther 1996; 277:321 332.
42. Chang TKH, Gonzalez FJ, Waxman DJ. Evaluation of triacetyloleandomycin, a naphtho flavone and diethyldithiocarbamate as selective chemical probes for inhibition of human cytochrome P450. Arch Biochem Biophys 1994; 311:437 442.
43. Denton TT, Zhang X, Cashman JR. 5 substituted, 6 substituted, and unsubstituted 3 heteroaromatic pyridine analogues of nicotine as selective inhibitors of cytochrome P 450 2A6. J Med Chem 2005; 48:224 239.
44. Mancy A, Dijols S, Poli S, Guengerich FP, Mansuy D. Interaction of sulfaphenazole derivatives with human liver cytochromes P450 2C: molecular origin of the specific inhibitory effects of sulfaphenazole on CYP 2C9 and consequences for the substrate binding topology. Biochemistry 1997; 35:16205 16212.
45. Strobl GR, von Kruedener S, Stöckigt J, Guengerich FP, Wolff T. Development of a pharmacophore for inhibition of human liver cytochrome P 450 2D6: molecular modeling and inhibition studies. J Med Chem 1993; 36:1136 1145.
46. Guengerich FP, Müller Enoch D, Blair IA. Oxidation of quinidine by human liver cytochrome P 450. Mol Pharmacol 1986; 30:287 295.
47. Halpert JR. Structural basis of selective cytochrome P450 inhibition. Annu Rev Pharmacol Toxicol 1995; 35:29 53.
48. Vanden Bossche H, Koymans L, Moereels H. P450 inhibitors of use in medical treatment: focus on mechanisms of action. Pharmacol Ther 1995; 67:79 100.
49. Guengerich FP. Human cytochrome P450 enzymes. In: Ortiz de Montellano PR, ed. Cytochrome P450: Structure, Mechanism, and Biochemistry. 3rd ed. New York: Plenum Press, 2005:377 530.
50. Brodie AMH. Aromatase, its inhibitors and their use in breast cancer treatment. Pharmacol Ther 1993; 60:501 515.
51. Aoyama Y, Yoshida Y, Nishino T, Katsuki H, Maitra US, Mohan VP, Sprinson DB. Isolation and characterization of an altered cytochrome P 450 from a yeast mutant defective in lanosterol 14α demethylation. J Biol Chem 1987; 262:14260 14264.
52. Vanden Bossche H. Inhibitors of P450 dependent steroid biosynthesis: from research to medical treatment. J Steroid Biochem Mol Biol 1992; 43:1003 1021.
53. Sonino N. The use of ketoconazole as an inhibitor of steroid production. New Engl J Med 1987; 317:812 818.
54. Baldwin SJ, Bloomer JC, Smith GJ, Ayrton AD, Clarke SE, Chenery RJ. Ketoconazole and sulphaphenazole as the respective selective inhibitors of P4503A and 2C9. Xenobiotica 1995; 25:261 270.
55. Casida JE. Mixed function oxidase involvement in the biochemistry of insecticide synergists. J Agric Food Chem 1970; 18:753 772.
56. Hammons GJ, Alworth WL, Hopkins NE, Guengerich FP, Kadlubar FF. 2 Ethynylnaphthalene as a mechanism based inactivator of the cytochrome P 450 catalyzed N oxidation of 2 naphthylamine. Chem Res Toxicol 1989; 2:367 374.
57. Viaje A, Lu JYL, Hopkins NE, Nettikumara AN, DiGiovanni J, Alworth WL, Slaga TJ. Inhibition of the binding of 7,12 dimethylbenz[*a*]anthracene and benzo[*a*]pyrene to DNA in mouse skin epidermis by 1 ethynylpyrene. Carcinogenesis 1990; 11:1139 1143.
58. Davidson NE, Egner PA, Kensler TW. Transcriptional control of glutathione S transferase gene expression by the chemoprotective agent 5 (2 pyrazinyl) 4 methyl 1,2 dithiole 3 thione (oltipraz) in rat liver. Cancer Res 1990; 50:2251 2255.
59. Zhang Y, Talalay P, Cho CG, Posner GH. A major inducer of anticarcinogenic protective enzyme from broccoli: isolation and elucidation of structure. Proc Natl Acad Sci U S A 1992; 89:2399 2403.
60. Langouët S, Coles B, Morel F, Becquemont L, Beaune PH, Guengerich FP, Ketterer B, Guillouzo A. Inhibition of CYP1A2 and CYP3A4 by oltipraz results in reduction of aflatoxin B_1 metabolism in human hepatocytes in primary culture. Cancer Res 1995; 55:5574 5579.

61. Koymans L, Vermeulen NPE, van Acker SABE, te Koppele JM, Heykants JJP, Lavrijsen K, Meuldermans W, Donné Op den Kelder GM. A predictive model for substrates of cytochrome P450 debrisoquine (2D6). Chem Res Toxicol 1992; 5:211 219.
62. Wolff T, Distlerath LM, Worthington MT, Groopman JD, Hammons GJ, Kadlubar FF, Prough RA, Martin MV, sGuengerich FP. Substrate specificity of human liver cytochrome P 450 debrisoquine 4 hydroxylase probed using immunochemical inhibition and chemical modeling. Cancer Res 1985; 45:2116 2122.
63. Guengerich FP, Miller GP, Hanna IH, Martin MV, Léger S, Black C, Chauret N, Silva JM, Trimble L, Jergey JA, Nicoll Griffith DA. Diversity in the oxidation of substrates by cytochrome P450 2D6. Lack of an obligatory role of aspartate 301 substrate electrostatic bonding. Biochemistry 2002; 41:11025 11034.
64. Murray M and Wilkinson CF. Interactions of nitrogen heterocycles with cytochrome P 450 and monooxygenase activity. Chem Biol Interact 1984; 50:267 275.
65. Brian WR, Srivastava PK, Umbenhauer DR, Lloyd RS, Guengerich FP. Expression of a human liver cytochrome P 450 protein with tolbutamide hydroxylase activity in *Saccha romyces cerevisiae*. Biochemistry 1989; 28:4993 4999.
66. Miners JO, Smith KJ, Robson RA, McManus ME, Veronese ME, Birkett DJ. Tolbutamide hydroxylation by human liver microsomes: kinetic characterisation and relationship to other cytochrome P 450 dependent xenobiotic oxidations. Biochem Pharmacol 1988; 37:1137 1144.
67. Yoo JSH, Cheung RJ, Patten CJ, Wade D, Yang CS. Nature of *N* nitrosodimethylamine demethylase and its inhibitors. Cancer Res 1987; 47:3378 3383.
68. Chauret N, Gauthier A, Nicoll Griffith DA. Effect of common organic solvents on in vitro cytochrome P450 mediated metabolic activities in human liver microsomes. Drug Metab Dispos 1998; 26:1 4.
69. Danan G, Descatoire V, Pessayre D. Self induction by erythromycin of its own transformation into a metabolite forming an inactive complex with reduced cytochrome P 450. J Pharmacol Exp Ther 1981; 218:509 514.
70. Jönsson KH, Lindeke B. Cytochrome P 455 nm complex formation in the metabolism of phenylalkylamines. XII. Enantioselectivity and temperature dependence in microsomes and reconstituted cytochrome P 450 systems from rat liver. Chirality 1992; 4:469 477.
71. Murray M, Wilkinson CF, Marcus C, Dubé CE. Structure activity relationships in the interactions of alkoxymethylenedioxybenzene derivatives with rat hepatic microsomal mixed function oxidases in vivo. Mol Pharmacol 1983; 24:129 136.
72. Ortiz de Montellano PR, Correia MA. Suicidal destruction of cytochrome P 450 during oxidative drug metabolism. Annu Rev Pharmacol Toxicol 1983; 23:481 503.
73. Ortiz de Montellano PR, Reich NO. Inhibition of cytochrome P 450 enzymes. In: Ortiz de Montellano PR, ed. Cytochrome P 450: Structure, Mechanism, and Biochemistry, 1st ed., New York: Plenum Press, 1986:273 314.
74. Halpert JR, Balfour C, Miller NE, Kaminsky LS. Dichloromethyl compounds as mechanism based inactivators of rat liver cytochromes P 450 in vitro. Mol Pharmacol 1986; 30:19 24.
75. Miller NE, Halpert J. Analogues of chloramphenicol as mechanism based inactivators of rat liver cytochrome P 450: modifications of the propanediol side chain, the p nitro group, and the dichloromethyl moiety. Mol Pharmacol 1986; 29:391 398.
76. Macdonald TL, Zirvi K, Burka LT, Peyman P, Guengerich FP. Mechanism of cytochrome P 450 inhibition by cyclopropylamines. J Am Chem Soc 1982; 104:2050 2052.
77. Hanzlik RP, Tullman RH. Suicidal inactivation of cytochrome P 450 by cyclopropylamines. Evidence for cation radical intermediates. J Am Chem Soc 1982; 104:2048 2050.
78. Bondon A, Macdonald TL, Harris TM, Guengerich FP. Oxidation of cycloalkylamines by cytochrome P 450. Mechanism based inactivation, adduct formation, ring expansion, and nitrone formation. J Biol Chem 1989; 264:1988 1997.
79. Augusto O, Beilan HS, Ortiz de Montellano PR. The catalytic mechanism of cytochrome P 450: spin trapping evidence for one electron substrate oxidation. J Biol Chem 1982; 257:11288 11295.

80. Ortiz de Montellano PR, Beilan HS, Kunze KL. N Alkylprotoporphyrin IX formation in 3, 5 dicarbethoxy 1,4 dihydrocollidine treated rats: transfer of the alkyl group from the substrate to the porphyrin. J Biol Chem 1981; 256:6708 6713.
81. Böcker RH, Guengerich FP. Oxidation of 4 aryl and 4 alkyl substituted 2,6 dimethyl 3,5 bis (alkoxycarbonyl) 1,4 dihydropyridines by human liver microsomes and immunochemical evidence for the involvement of a form of cytochrome P 450. J Med Chem 1986; 29: 1596 1603.
82. Lukton D, Mackie JE, Lee JS, Marks GS, Ortiz de Montellano PR. 2,2 Dialkyl 1, 2 dihydroquinolines: cytochrome P 450 catalyzed N alkylporphyrin formation, ferrochelatase inhibition, and induction of 5 aminolevulinic acid synthase activity. Chem Res Toxicol 1988; 1:208 215.
83. Stearns RA, Ortiz de Montellano PR. Inactivation of cytochrome P 450 by a catalytically generated cyclobutadiene species. J Am Chem Soc 1985; 107:234 240.
84. Meschter CL, Mico BA, Mortillo M, Feldman D, Garland WA, Riley JA, Kaufman LS. A 13 week toxicologic and pathologic evaluation of prolonged cytochromes P450 inhibition by 1 aminobenzotriazole in male rats. Fundam Appl Toxicol 1994; 22:369 381.
85. Correia MA, Ortiz de Montellano PR. Inhibition of cytochrome P450 enzymes. In: Ortiz de Montellano PR, ed. Cytochrome P450: Structure, Mechanism, and Biochemistry. 3rd ed. New York: Kluwer Academic/Plenum Publishers, 2005:247 322.
86. Sahali Sahly Y, Balani SK, Lin JH, Baillie TA. In vitro studies on the metabolic activation of the furanopyridine L 754,394, a highly potent and selective mechanism base inhibitor of cytochrome P450 3A4. Chem Res Toxicol 1996; 9:1007 1012.
87. Kassahun K, Skordos K, McIntosh I, Slaughter D, Doss GA, Baillie TA, Yost GS. Zafirlukast metabolism by cytochrome P450 3A4 produces an electrophilic alpha,beta unsaturated iminium species that results in the selective mechanism based inactivation of the enzyme. Chem Res Toxicol 2005; 18:1427 1437.
88. Chen Q, Ngui JS, Doss GA, Wang RW, Cai X, DiNinno FP, Blizzard TA, Hammond ML, Stearns RA, Evans DC, Baillie TA, Tang W. Cytochrome P450 3A4 mediated bioactivation of raloxifene: irreversible enzyme inhibition and thiol adduct formation. Chem Res Toxicol 2002; 15:907 914.
89. Crowley JR, Hollenberg PF. Mechanism based inactivation of rat liver cytochrome P4502B1 by phencyclidine and its oxidative product, the iminium ion. Drug Metab Dispos 1995; 23:786 793.
90. Roberts ES, Hopkins NE, Zaluzec EJ, Gage DA, Alworth WL, Hollenberg PF. Mechanism based inactivation of cytochrome P450 2B1 by 9 ethynylphenanthrene. Arch Biochem Biophys 1995; 323:295 302.
91. Roberts ES, Ballou DP, Hopkins NE, Alworth WL, Hollenberg PF. Mechanistic studies of 9 ethynylphenanthrene inactivated cytochrome P450 2B1. Arch Bioche Biophys 1995; 323: 303 312.
92. Sharma U, Roberts ES, Hollenberg PF. Inactivation of cytochrome P4502B1 by the monoamine oxidase inhibitors *R* ( ) deprenyl and clorgyline. Drug Metab Dispos 1996; 24:669 675.
93. Sharma U, Roberts ES, Hollenberg PF. Formation of a metabolic intermediate complex of cytochrome P4502B1 by clorgyline. Drug Metab Dispos 1996; 24:1247 1253.
94. Kent UM, Roberts ES, Chun J, Hodge K, Juncaj J, Hollenberg PF. Inactivation of cytochrome P450 2E1 by *tert* butylisothiocyanate. Chem Res Toxicol 1998; 11:1154 1161.
95. Yanev S, Kent UM, Pandova B, Hollenberg PF. Selective mechanism based inactivation of cytochromes P 450 2B1 and P 450 2B4 by a series of xanthates. Drug Metab Dispos 1999; 27:600 604.
96. Kent UM, Yanev S, Hollenberg PF. Mechanism based inactivation of cytochromes P450 2B1 and P450 2B6 by *n* propylxanthate. Chem Res Toxicol 1999; 12:317 322.
97. Regal KA, Schrag ML, Kent UM, Wienkers LC, Hollenberg PF. Mechanism based inactivation of cytochrome P450 2B1 by 7 ethynylcoumarin: verification of apo P450 adduction by electrospray ion trap mass spectrometry. Chem Res Toxicol 2000; 13:262 270.

98. Jushchyshyn MI, Kent UM, Hollenberg PF. The mechanism based inactivation of human cytochrome P450 2B6 by phencyclidine. Drug Metab Dispos 2003; 31:46 52.
99. Blobaum AL, Harris DL, Hollenberg PF. P450 active site architecture and reversibility: inactivation of cytochromes P450 2B4 and 2B4 T302A by tert butyl acetylenes. Biochemistry 2005; 44:3831 3844.
100. Kobayashi Y, Sridar C, Kent UM, Puppali SG, Rimoldi JM, Zhang H, Waskell L, Hollenberg PF. Structure activity relationship and elucidation of the determinant factor(s) responsible for the mechanism based inactivation of cytochrome P450 2B6 by substituted phenyl diaziridines. Drug Metab Dispos 2006; 34:2102 2110.
101. Kent UM, Lin HL, Mills DE, Regal KA, Hollenberg PF. Identification of 17 alpha ethynylestradiol modified active site peptides and glutathione conjugates formed during metabolism and inactivation of P450s 2B1 and 2B6. Chem Res Toxicol 2006; 19:279 287.
102. Lin HL and Hollenberg PF. The inactivation of cytochrome P450 3A5 by 17α ethynylestradiol is cytochrome b_5 dependent: metabolic activation of the ethynyl moiety leads to the formation of glutathione conjugates, a heme adduct, and covalent binding to the apoprotein. J Pharmacol Exp Ther 2007; 321:276 287.
103. Masters BSS. The role of NADPH cytochrome *c* (P 450) reductase in detoxication. In: Jakoby WB, ed. Enzymatic Basis of Detoxication, Vol. I. New York: Academic Press, 1980:183 200.
104. Yoshida T, Takahashi S, Kikuchi G. Partial purification and reconstitution of the heme oxygenase system from pig spleen microsomes. J Biochem 1974; 75:1187 1191.
105. Yasukochi Y, Masters BSS. Some properties of a detergent solubilized NADPH cytochrome *c* (cytochrome P 450) reductase purified by biospecific affinity chromatography. J Biol Chem 1976; 251:5337 5344.
106. Tew DG. Inhibition of cytochrome P450 reductase by the diphenyliodonium cation. Kinetic analysis and covalent modifications. Biochemistry 1993; 32:10209 10215.
107. Clement B, Weide M, Ziegler DM. Inhibition of purified and membrane bound flavin containing monooxygenase 1 by (*N,N* dimethylamino)stilbene carboxylates. Chem Res Toxicol 1996; 9:599 604.
108. Hines RN, Cashman JR, Philpot RM, Williams DE, Ziegler DM. The mammalian flavin containing monooxygenases: molecular charcterization and regulation of expression. Toxicol Appl Pharmacol 1994; 125:1 6.
109. Cashman JR. Monoamine oxidase and flavin containing monooxygenases. In: Guengerich FP, ed. Biotransformation, Vol. 3, Comprehensive Toxicology. 1st ed. Oxford: Elsevier, 1997: 69 96.
110. Panoutsopoulos GI, Kouretas D, Beedham C. Contribution of aldehyde oxidase, xanthine oxidase, and aldehyde dehydrogenase on the oxidation of aromatic aldehydes. Chem Res Toxicol 2004; 17:1368 1376.
111. Rajagopalan KV. Xanthine dehydrogenase and aldehyde oxidase. In: Guengerich FP, ed. Biotransformation, Vol. 3, Comprehensive Toxicology. 1st ed. Oxford: Elsevier, 1997:165 178.
112. Dick RA, Kanne DB, Casida JE. Nitroso imidacloprid irreversibly inhibits rabbit aldehyde oxidase. Chem Res Toxicol 2007; 20:1942 1946.
113. Petersen D, Lindahl R. Aldehyde dehydrogenases. In: Guengerich FP, ed. Biotransformation, Vol. 3, Comprehensive Toxicology. 1st ed. Oxford: Elsevier, 1997: 97 118.
114. Yamazaki H, Inui Y, Yun C H, Mimura M, Guengerich FP, Shimada T. Cytochrome P450 2E1 and 2A6 enzymes as major catalysts for metabolic activation of *N* nitrosodialkylamines and tobacco related nitrosamines in human liver microsomes. Carcinogenesis 1992; 13:1789 1794.
115. Hart BW, Faiman MD. Bioactivation of *S* methyl *N,N* diethylthiolcarbamate to *S* methyl *N, N* diethylthiolcarbamate sulfoxide. Biochem Pharmacol 1993; 46:2285 2290.
116. Madan A, Parkinson A, Faiman MD. Identification of the human and rat P450 enzymes responsible for the sulfoxidation of *S* methyl *N,N* diethylthiolcarbamate (DETC Me): the terminal step in the bioactivation of disulfiram. Drug Metab Dispos 1995; 23:1153 1162.
117. Flynn TG, Kubiseski TJ. Aldo ketoreductases: structure, mechanism, and function. In: Guengerich FP, ed. Biotransformation, Vol. 3, Comprehensive Toxicology. 1st ed. Oxford: Elsevier, 1997:133 147.

118. Quinn DM. Esterases of the α/β hydrolase fold family. In: Guengerich FP, ed. Biotransformation, Vol. 3, Comprehensive Toxicology. 1st ed. Oxford: Elsevier, 1997:243 264.
119. Lacourciere GM, Armstrong RN. Microsomal and soluble epoxide hydrolases are members of the same family of C X bond hydrolase enzymes. Chem Res Toxicol 1994; 7:121 124.
120. Lacourciere GM, Armstrong RN. The catalytic mechanism of microsomal epoxide hydrolase involves an ester intermediate. J Am Chem Soc 1993; 115:10466 10467.
121. Oesch F. Purification and specificity of a human microsomal epoxide hydratase. Biochem J 1974; 139:77 88.
122. Hammock BD, Grant DF, Storms DH. Epoxide hydrolases. In: Guengerich FP, ed. Biotransformation, Vol. 3, Comprehensive Toxicology. 1st ed. Oxford: Elsevier, 1997:283 305.
123. Jakoby WB, Habig WH. Glutathione transferases. In: Jakoby WB, ed. Enzymatic Basis of Detoxication, Vol. 2. New York: Academic Press, 1980:63 94.
124. Armstrong RN. Glutathione S transferases: reaction mechanism, structure, and function. Chem Res Toxicol 1991; 4:131 140.
125. Litwack G, Ketterer B, Arias IM. Ligandin: a hepatic protein which binds steroids, bilirubin, carcinogens, and a number of exogenous anions. Nature 1971; 234:466 467.
126. Simons PC, Vander Jagt DL. Purification of glutathione *S* transferases from human liver by glutathione affinity chromatography. Anal Biochem 1977; 82:334 341.
127. Graminski GF, Kubo Y, Armstrong RN. Spectroscopic and kinetic evidence for the thiolate anion of glutathione at the active site of glutathione S transferase. Biochemistry 1989; 28:3562 3568.
128. Adang AEP, Brussee J, van der Gen A, Mulder GJ. Inhibition of rat liver glutahione *S* transferase isoenzymes by peptides stabilized against degradation by γ glutamyl trans peptidases. J Biol Chem 1991; 266:830 836.
129. Graminski GF, Zhang P, Sesay MA, Ammon HL, Armstrong RN. Formation of the 1 (*S* glutathionyl) 2,4,6 trinitrocyclohexadienate anion at the active site of glutathione S transferase: evidence for enzymic stabilization of s complex intermediates in nucleophilic aromatic substitution reactions. Biochemistry 1989; 28:6252 6258.
130. Armstrong RN. Glutathione transferases. In: Guengerich FP, ed. Biotransformation, Vol. 3, Comprehensive Toxicology. 1st ed. Oxford: Elsevier, 1997:307 327.
131. Katusz RM, Bono B, Colman RF. Affinity labeling of Cys^{111} of glutathione S transferase, isoenzyme 1 1, by *S* (4 bromo 2,3 dioxobutyl)glutathione. Biochemistry 1992; 31:8984 8990.
132. Ploemen JHTM, Johnson WW, Jespersen S, Vanderwall D, van Ommen B, van der Greef J, van Bladeren PJ, Armstrong RN. Active site tyrosyl residues are targets in the irreversible inhibition of a class mu glutathione transferase by 2 (*S* glutathionyl) 3,5,6 trichloro 1,4 benzoquinone. J Biol Chem 1994; 269:26890 26897.
133. McTigre MA, Williams DR, Tainer JA. Crystal structures of a Schistomal drug vaccine target: Glutathione S transferase from *Schistoma japonica* and its complex with the leading antischistosomal drug praziquantel. J Mol Biol 1995; 246:21 27.
134. Duffel MW. Sulfotransferases. In: Guengerich FP, ed. Biotransformation, Vol. 3, Compre hensive Toxicology. 1st ed. Oxford: Elsevier, 1997:365 383.
135. Burchell B, McGurk K, Brierly CH, Clarke DJ. UDP glucuronosyltransferases. In: Guengerich FP, ed. Biotransformation, Vol. 3, Comprehensive Toxicology. 1st ed. Oxford: Elsevier, 1997: 401 435.
136. Noort D, Coughtrie MWH, Burchell B, van der Morel GA, van Boom JH, van der Gen A, Mulder GJ. Inhibition of UDP glucuronosyltransferase activity by possible transition state analogues in rat liver microsomes. Eur J Biochem 1990; 281:170.
137. Radominska A, Paul P, Treat S, Towbin H, Pratt C, Little J, Magdalou J, Lester R, Drake R. Photoaffinity labeling for evaluation of uridinyl analogs as specific inhibitors of rat liver UDP glucuronosyltransferase. Biochim Biophys Acta 1994; 1205:336.
138. Thomassin J, Tephly TR. Photoafinity labeling of rat liver microsomal morphine UDP glucuronosyltransferase by [^{3}H]flunitrazepam. Mol Pharmacol 1990; 38:294 298.
139. Xiong Y, Bernardi D, Bratton S, Ward MD, Battaglia E, Finel M, Drake RR, Radominska Pandya A. Phenylalanine 90 and 93 are localized within the phenol binding site of human

UDP glucuronosyltransferase 1A10 as determined by photoaffinity labeling, mass spectrom etry, and site directed mutagenesis. Biochemistry 2006; 45:2322 2332.
140. Li AP, ed. Drug Interactions: Scientific and Regulatory Perspectives (Adv. Pharmacol. Series). San Diego: Academic Press, 1996.
141. Knodell RG, Browne D, Gwodz GP, Brian WR, Guengerich FP. Differential inhibition of human liver cytochromes P 450 by cimetidine. Gastroenterology 1991; 101:1680 1691.
142. Yun C H, Okerholm RA, Guengerich FP. Oxidation of the antihistaminic drug terfenadine in human liver microsomes: role of cytochrome P450 3A(4) in N dealkylation and C hydroxylation. Drug Metab Dispos 1993; 21:403 409.
143. Kivistö KT, Neuvonen PJ, Klotz U. Inhibition of terfenadine metabolism: pharmacokinetic and pharmacodynamic consequences. Clin Pharmacokin 1994; 27:1 5.
144. Woosley RL, Chen Y, Freiman JP, Gillis RA. Mechanism of the cardiotoxic actions of terfenadine. J Am Med Assoc 1993; 269:1532 1536.
145. Stinson SC. Uncertain climate for antihistamines. Chem Eng News 1997; 75:43 45.
146. Ortiz de Montellano PR, Kunze KL, Yost GS, Mico BA. Self catalyzed destruction of cytochrome P 450: covalent binding of ethynyl sterols to prosthetic heme. Proc Natl Acad Sci U S A 1979; 76:746 749.
147. Guengerich FP. Oxidation of 17α ethynylestradiol by human liver cytochrome P 450. Mol Pharmacol 1988; 33:500 508.
148. Guengerich FP. Mechanism based inactivation of human liver cytochrome P 450 IIIA4 by gestodene. Chem Res Toxicol 1990; 3:363 371.
149. Jung Hoffmann C, Kuhl H. Pharmacokinetics and pharmacodynamics of oral contraceptive steroids: factors influencing steroid metabolism. Am J Obstet Gynecol 1990; 163:2183 2197.
150. Houston JB, Galetin A. Progress towards prediction of human pharmacokinetic parameters from in vitro technologies. Drug Metab Rev 2003; 35:393 415.
151. Shiran MR, Proctor NJ, Howgate EM, Rowland Yeo K, Tucker GT, Rostami Hodjegan A. Prediction of metabolic drug clearance in humans: in vitro in vivo extrapolation vs allometric scaling. Xenobiotica 2006; 36:567 580.
152. Zhou S, Yung Chan S, Cher Goh B, Chan E, Duan W, Huang M, McLeod HL. Mechanism based inhibition of cytochrome P450 3A4 by therapeutic drugs. Clin Pharmacokinet 2005; 44:279 304.

9

The Ontogeny of Drug Metabolizing Enzymes/Pediatric Exclusivity

Ronald N. Hines
Departments of Pediatrics and Pharmacology and Toxicology, Medical College of Wisconsin, and Children's Research Institute, Children's Hospital and Health Systems, Milwaukee, Wisconsin, U.S.A.

INTRODUCTION

Pharmacokinetic changes occur during human development, which contribute substantially to differences in therapeutic efficacy and adverse drug events (1,2). Although there are many factors that contribute to these changes, maturation of drug-metabolizing enzyme (DME) expression constitutes a major component (3,4). Important advances in our understanding of DME ontogeny have been made that improve our ability to predict therapeutic dosing and avoid adverse events. Yet, knowledge gaps remain. Several challenges to extending our understanding of human developmental pharmacology exist. Of major importance are ethical and logistical problems associated with obtaining suitable tissue samples for in vitro studies as well as the design and recruitment of appropriate and sufficient volunteers for clinical trials. Adding to the significance of these problems, substantial species differences exist in both DME primary structure and regulatory mechanisms, necessitating caution in extrapolating data from animal model systems to the human and limiting the utility of such model systems. Furthermore, dynamic changes in gene expression occur during different stages of ontogeny. Thus, studies must be designed to avoid the use of a small number of tissue samples representing a narrow time window, or the pooling of samples across wide time windows. The use of such study designs in the past has led to data from which it is difficult or impossible to draw general conclusions.

This chapter will provide an overview of our current understanding of DME ontogeny and knowledge gaps that remain as well as provide some regulatory perspective that has helped drive the field. Most of our existing knowledge is restricted to enzyme developmental expression in the liver, and as such, this chapter largely will be restricted to discussion of this organ.

OVERVIEW OF EXPERIMENTAL APPROACHES

Several approaches have been used to characterize and better understand the underlying mechanisms controlling DME ontogeny. Early investigations sought to characterize specific enzymatic activities in autopsy tissue samples using specific or semi-specific probe substrates. Although these data were certainly useful in characterizing trends, many were limited by the sensitivity of the assays, unknown or poorly characterized substrate specificity, and restrictions on the amount of available tissue, particularly those of fetal origin. With the development of highly specific antibody probes, sensitive chemiluminescent detection techniques, as well as recombinant protein standards, more recent studies have been successful in characterizing age-dependent changes in specific protein content [see Ref. (5) for an example]. Of course, questions regarding the correlation between protein levels and enzyme activity remain, as do concerns regarding tissue quality. In vitro activity studies also have been enhanced by the development of more sensitive detection methods, such as high-performance liquid chromatography coupled with tandem mass spectrometry. Furthermore, investigators have become more sophisticated in data analysis, incorporating multiple linear regression models that take advantage of data generated with purified enzyme preparations to tease apart the relative contributions of specific enzymes to a given metabolic reaction [see Ref. (16) for an example]. A paradigm shift also has occurred with regard to in vivo pharmacokinetic studies in pediatric patients. Unless unusual and extenuating circumstances exist, investigators remain restricted to taking advantage of probe substrates prescribed for normal clinical care. However, the same improvements in detection techniques that have benefited in vitro studies have also been a boon for in vivo studies, allowing accurate measurements on much smaller biospecimens often more appropriate for pediatric volunteers. Perhaps more importantly, the realization that the use of off-label drug use in children was tantamount to poorly designed experimentation has resulted in a greater acceptance of pediatric clinical trials and efforts to ensure that appropriate infrastructure and guidance is in place to facilitate such studies [see Ref. (6) for a recent example]. Finally, the emergence of information on DME ontogeny has begun to be incorporated into increasingly sophisticated modeling systems that hopefully will allow better prediction of drug disposition and response during different early-life stages and prove useful for both drug development and therapeutic decision making (7).

DME ONTOGENY

Although somewhat oversimplified, our growing knowledge of DME ontogeny suggests that individual developmental expression patterns can be binned into one of three classes (Table 1). The first class consists of enzymes expressed at relatively high levels during the first trimester and either remain high or decrease during gestation but are silenced or expressed at low levels within a few days to as long as two years after birth. Enzymes belonging to the second class are expressed at relatively constant levels throughout gestation. Moderate postnatal increases in expression are observed for some, but not all, within the first year. Enzymes in the third class are not expressed or are expressed at low levels in the fetus. For some, the onset of expression can be seen in either the second or third trimester. Substantial increases in expression usually are observed within the first one to two years after birth, however for some, full maturation does not occur until postpuberty. This third category appears to include the largest number of enzymes, although this might change as our knowledge expands. Examples of enzymes belonging to each of these three classes and that illustrate salient features of each expression pattern are discussed below.

Table 1 Categorization of DMEs Based on Developmental Expression Patterns

Class 1	Class 2	Class 3
ADH1A	CYP2C19	ADH1B and 1C
CYP1A1	CYP3A5	AOX
CYP3A7	EPHX1	CYP1A2
FMO1	EPHX2	CYP2A6
GSTP	GSTA	CYP2C9
SULT1E1	SULT1A1	CYP2D6
		CYP2E1
		CYP3A4
		FMO3
		PON1
		SULT2A1
		UGT1A1
		UGT1A6
		UGT2B7

Abbreviations: DME, drug metabolizing enzyme; ADH, alcohol dehydrogenase; SULT, sulfotransferase; CYP, cytochrome P450; FMO, flavin containing monooxygenase; GST, glutathione S transferase; EPHX, epoxide hydrolase; AOX, aldehyde oxidase; PON, paraoxonase; UGT, UDP glucuronosyl transferase.

Cytochrome P4503A Ontogeny

The cytochrome P4503A (*CYP3A*) subfamily consists of four genes, *CYP3A4*, *3A5*, *3A7*, and *3A43*, encoded at an approximate 270-kbp locus on human chromosome 7q21.1. CYP3A43 has minimal, if any, drug-metabolizing activity and is expressed at low levels where detectable. In contrast, CYP3A4, 3A5, and 3A7 are collectively the most abundant hepatic members of the cytochrome P450-dependent monooxygenase family and account for nearly 46% of the oxidative metabolism of clinically relevant drugs (8). Although these three enzymes share at least 85% sequence identity, a property that has proven an obstacle to independent measurement, they exhibit considerable different but overlapping substrate specificities and expression patterns. In adult liver, CYP3A4 comprises 10% to 50% of total cytochrome P450 (9). CYP3A5 levels can exceed CYP3A4, subject to the presence of the *CYP3A5*1* allele (10,11). CYP3A7 is the dominant enzyme in fetal liver, but can be expressed at substantial levels in some adults (10 40% of total CYP3A levels), dependent on the presence of the *CYP3A7*1C* allele (12). These three members of the CYP3A family are representative of all three classes of DME ontogeny.

Multiple metabolic probes have been used to measure CYP3A-dependent metabolic activity in fetal liver tissue, including codeine, dextromethorphan, and imipramine *N*-demethylation, retinioic acid 4-hydroxylation, and dehydroepiandrosterone (DHEA) 16α-hydroxylation (13 16). However, only the latter two reactions are preferentially catalyzed by CYP3A7, and thus, the interpretation of these data is challenging. For example, CYP3A4 has the greatest activity toward the *N*-demethylation of dextromethorphan, but below a substrate concentration of 1 mM, both CYP3A7 and 3A5 exhibit activities that are approximately 33% and 17%, respectively, of that exhibited by CYP3A4 (Drs. Robin E. Pearce and J. Steven Leeder, Children's Mercy Hospital, Kansas City, MO; personal communication). Yet, both western blotting and reverse transcriptase-coupled polymerase chain reaction DNA amplification approaches have been used to confirm the expression of CYP3A7 and, to a much lesser extent, CYP3A5, but not CYP3A4, in fetal liver as early as seven to eight weeks' gestation. In contrast, CYP3A4 was clearly the dominant CYP3A family member in adult liver (14,17,18). All of these

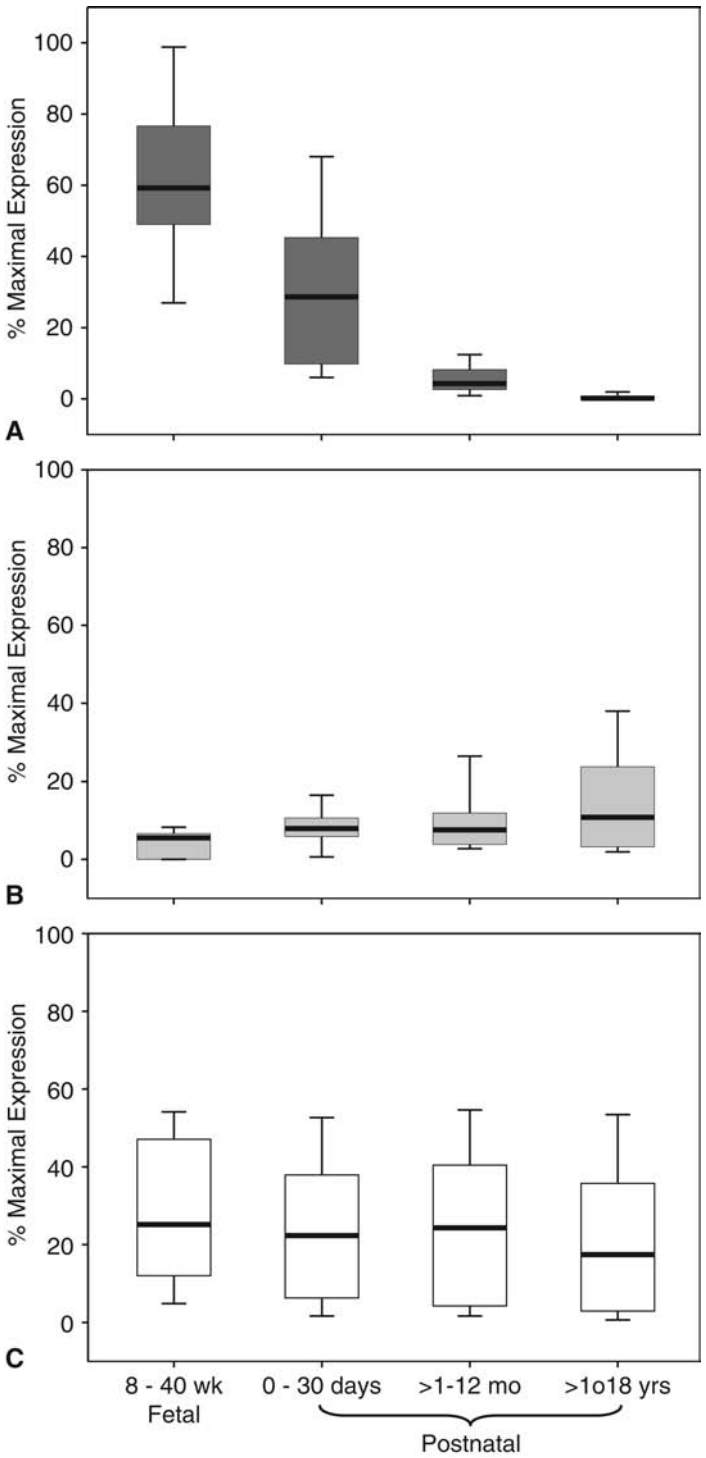

Figure 1 Human hepatic CYP3A ontogeny. (**A**) CYP3A7, (**B**) 3A4, and (**C**) 3A5 expression levels were determined using metabolic probe substrates and/or quantitative western blotting with hepatic microsomal preparations obtained from fetal (8 40 weeks estimated gestational age), neonatal (0 30 days after birth), >1 month to 12 months postnatal age, and >1 to 18 years postnatal

(*continued*)

early studies suffered from limited sample numbers and age ranges. Thus, the dynamics of the transition between CYP3A7 and 3A4 was not apparent from the resulting data.

The development of more robust tissue repositories and the use of multiple metrics, including quantitative western blotting to measure protein levels, hybridization with specific probes to measure transcript levels, and the preferential catalysis of DHEA 16α-hydroxylation by CYP3A7 and testosterone 6β-hydroxylation or DHEA 7β-hydroxylation by CYP3A4, has led to a much better understanding of CYP3A ontogeny (15,16,19). Extending the use of preferential substrates, Stevens et al. (16) applied a multiple regression model to extrapolate individual protein content and minimize the problems associated with overlapping substrate specificity (Fig. 1). CYP3A7 expression was confirmed to dominate in the fetal liver with expression levels that exhibited considerable interindividual variation, but remained relatively constant throughout gestation (Fig. 1A). DHEA 16α-hydroxylase activity (CYP3A7) ranged from 0.48 to 1.31 nmol/min/mg microsomal protein in fetal samples, while median protein content was determined to be 279.5 pmol/mg microsomal protein (range = 122.2 471.9 pmol/mg microsomal protein). In contrast, testosterone 6β hydroxylase activity (CYP3A4) ranged from only 0.004 to 0.008 nmol/min/mg microsomal protein in fetal samples and median protein levels were only 4.4 pmol/mg microsomal protein (range = 0 6.5 pmol/mg microsomal protein), nearly 50-fold lower than that reported in adult liver (15,16).

A progressive decrease in CYP3A7 expression was observed after birth (Fig. 1A). In neonatal liver samples, DHEA 16α-hydroxylation was 50% of that observed in fetal samples and consistent with a similar drop in mean CYP3A7 protein levels. Activity and protein levels continued to decline in tissue samples from infants aged 1 to 3 months and children aged 3 to 12 months. In adults, DHEA 16α-hydroxylation was determined to be only 0.07 nmol/min/mg microsomal protein, again consistent with median CYP3A7 protein levels in older pediatric samples of 1.3 pmol/mg microsomal protein (range = 0−20.8 pmol/mg microsomal protein) (Fig. 1A).

In contrast to CYP3A7, a progressive age-dependent increase in CYP3A4 expression was observed, although using multiple linear regression modeling to extrapolate protein levels suggested a somewhat delayed increase in CYP3A4 relative to what was reported by measuring activity alone (Fig. 1B). Little or no change from mean fetal enzyme levels was observed in neonatal samples, while only a modest increase was observed in infant samples aged between 1 and 12 months. Further, hepatic CYP3A4 levels in samples from children aged between 1 and 10 years remained well below adult levels (13.1 ± 17.5 pmol/mg microsomal protein vs. 128.9 ± 99.9 pmol/mg microsomal protein). Thus, these studies would suggest that in many individuals, CYP3A7 remains the dominant CYP3A enzyme in many children up to one year after birth and that CYP3A4 expression increases steadily, but does not reach adult levels until well after one year of age. These conclusions regarding CYP3A4 postnatal ontogeny are consistent with an in vivo, longitudinal study of dextromethorphan *N*-demethylase activity (6,20) as well as a metabolic study of amprenavir disposition in fetal and postnatal liver samples (21).

Consistent with the known frequency of the *CYP3A5*1* allele, fetal CYP3A5 protein was observed in approximately 50% of samples at a mean level of 6.0 ± 5.2 pmol/mg

age donors (16). Data are plotted as medians (*bars*), interquartile values (*boxes*), and 10th to 90th percentiles (*whiskers*) of the maximum expression levels observed in the entire data set. For clarity, data outliers are not shown. Maximum CYP3A4, 3A5, and 3A7 protein levels were 78.7, 24.5, and 472.0 pmol/mg microsomal protein, respectively. The lower than expected median CYP3A4 levels in the oldest age bracket is likely due to the weighting of this data set to early ages; the median age of the samples within this age bracket was eight years. *Abbreviation*: CYP, cytochrome P450.

microsomal protein for those samples with detectable protein. No age-dependent changes were observed in either the pre- or postnatal samples, consistent with this enzyme belonging to the class 2 developmental expression pattern (Fig. 1C).

The clinical implications of the CYP3A7/3A4 transition is illustrated by studies on the pharmacokinetics and pharmacodynamics of cisapride, a gastroprokinetic agent that was commonly used in pediatric patients presenting with symptoms associated with gastroesophageal reflux. Because of a higher than acceptable incidence of cisapride-related prolonged QT syndrome in adult patients that was associated with excessive dose or high plasma levels of parent drug, cisapride was removed from the general market and its use limited through an access program for specific diseases, including neonatal gastroesophageal reflux. However, a prospective study in this latter patient population demonstrated a significant increase in prolonged QT syndrome not associated with the risk factors identified in adults (22). Given the evidence for CYP3A4-dependent cisapride metabolic inactivation, but an absence of activity with either CYP3A5 or 3A7 (23), it was hypothesized that neonates would show deficient metabolic ability. Consistent with this hypothesis, cisapride oxidation was low or absent in microsomal preparations from fetal or neonatal liver aged less than seven days (24). Furthermore, the cisapride terminal elimination rate constant was shown to increase from approximately 0.02 hour ^{1} in 30-week postconceptional age patients to 0.20 hour ^{1} in 52-week postconceptional age patients (25). Thus, the differential substrate specificities exhibited by the CYP3A enzymes toward cisapride, combined with the developmental expression pattern described above, illustrates the significant impact DME ontogeny can have on the risk for adverse drug events in pediatric patients.

Flavin-Containing Monooxygenase Ontogeny

The flavin-containing monooxygenase (FMO) family of enzymes (EC 1.14.13.8) is important for the oxidative metabolism of a variety of therapeutics containing nucleophilic nitrogen, sulfur, selenium, or phosphorous heteroatoms. Common substrates include tamoxifen, itopride, benzydamine, olopatidine, and xanomeline (26). Eleven human FMO genes have been identified: *FMO1*, *2*, *3*, *4*, and *6P* contained within a cluster at chromosome 1q24.3; *FMO5* outside this cluster and in the opposite orientation at 1q21.1; and a second five-gene cluster at 1q24.2 that in the human, but not mouse, consists entirely of pseudogenes (*FMO7P-11P*) (27). The human FMO enzymes active in xenobiotic metabolism include FMO1, 2, and 3, although the role of FMO2 is limited because of the high prevalence of a premature stop codon resulting in a truncated, inactive protein (26).

FMO ontogeny was recently reviewed by Hines (28). Measurement of FMO transcript levels in a limited number of fetal and adult liver, kidney, and lung tissue samples provided the first evidence for a developmental transition from FMO1 to FMO3 in the liver, but not other tissues. The restriction of FMO1 expression to the fetal liver was confirmed using immunological approaches wherein mean FMO1 protein levels were determined to be 14.4 $\pm$ 3.5 pmol/mg microsomal protein, but were undetectable adult liver. Consistent with the earlier studies measuring transcript levels, FMO1 protein levels were highest in the adult kidney, 47 $\pm$ 9 pmol/mg microsomal protein, but also were observed in the adult small intestine (2.9 $\pm$ 1.9 pmol/mg microsomal protein). However, similar to the early study on CYP3A, the dynamics of the transition from fetal hepatic FMO1 to adult FMO3 were unclear.

Employing an immunological approach with monospecific antibodies together with a much more robust tissue sample set, the highest level of hepatic FMO1 expression was

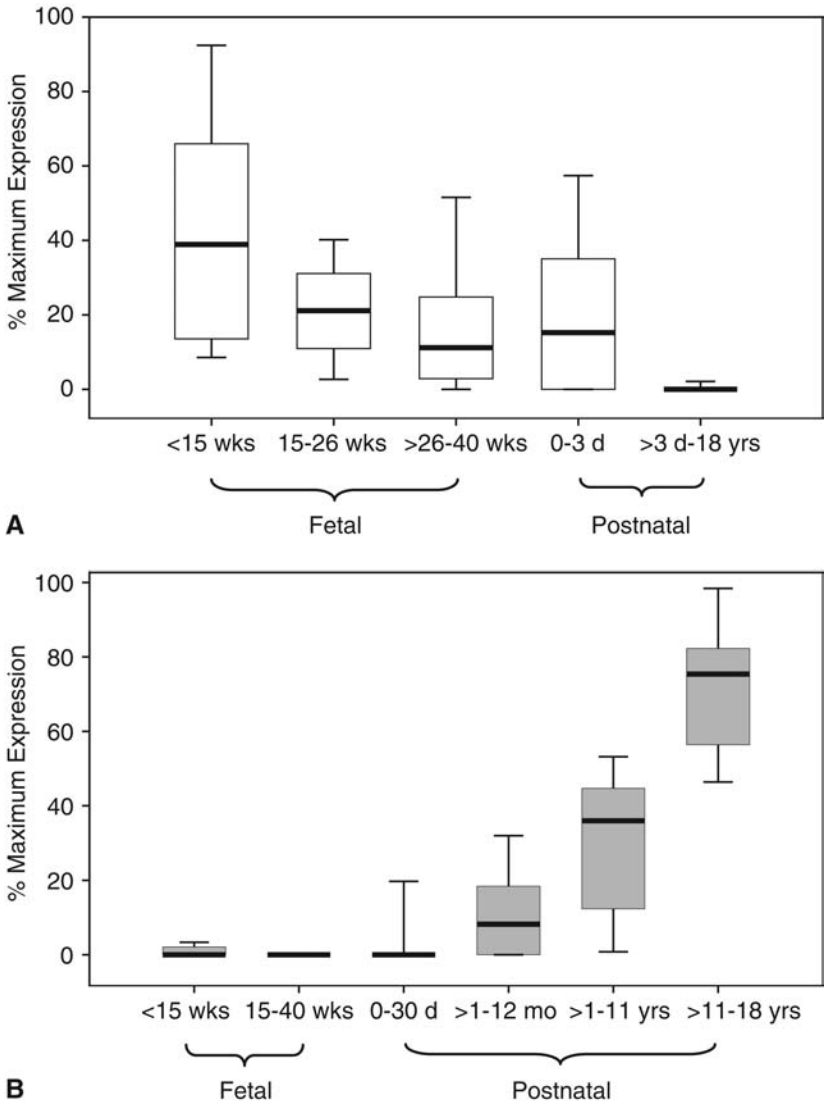

Figure 2 Human hepatic FMO ontogeny. (**A**) FMO1 and (**B**) FMO3 expression levels were determined using quantitative western blotting with hepatic microsomal preparations obtained from <15 week fetal, 15 to 26 week fetal, >26 to 40 week fetal, 0 to 3 days postnatal, neonatal (0 30 days after birth), >1 month to 12 months postnatal, >1 to 11 years postnatal, and >11 to 18 years postnatal age donors (50). Data are plotted as medians (*bars*), interquartile values (*boxes*), and 10th to 90th percentiles (*whiskers*) of the maximum expression levels observed in the entire data set. For clarity, data outliers are not shown. Maximum FMO1 and FMO3 protein levels were 18.5 and 38.5 pmol/mg microsomal protein, respectively. *Abbreviation*: FMO, flavin containing monooxygenase.

observed and in the greatest percentage of samples at gestational ages less than 15 weeks (96%) (Fig. 2A). FMO1 protein levels subsequently declined by approximately 50% in each subsequent trimester (90% and 70% of samples with detectable levels, respectively), and expression was essentially silenced within three days after parturition in a birth-, rather than gestational age dependent process. Interestingly, low FMO3 expression levels (<1 pmol/mg microsomal protein) were detectable in about 15% of first trimester fetal

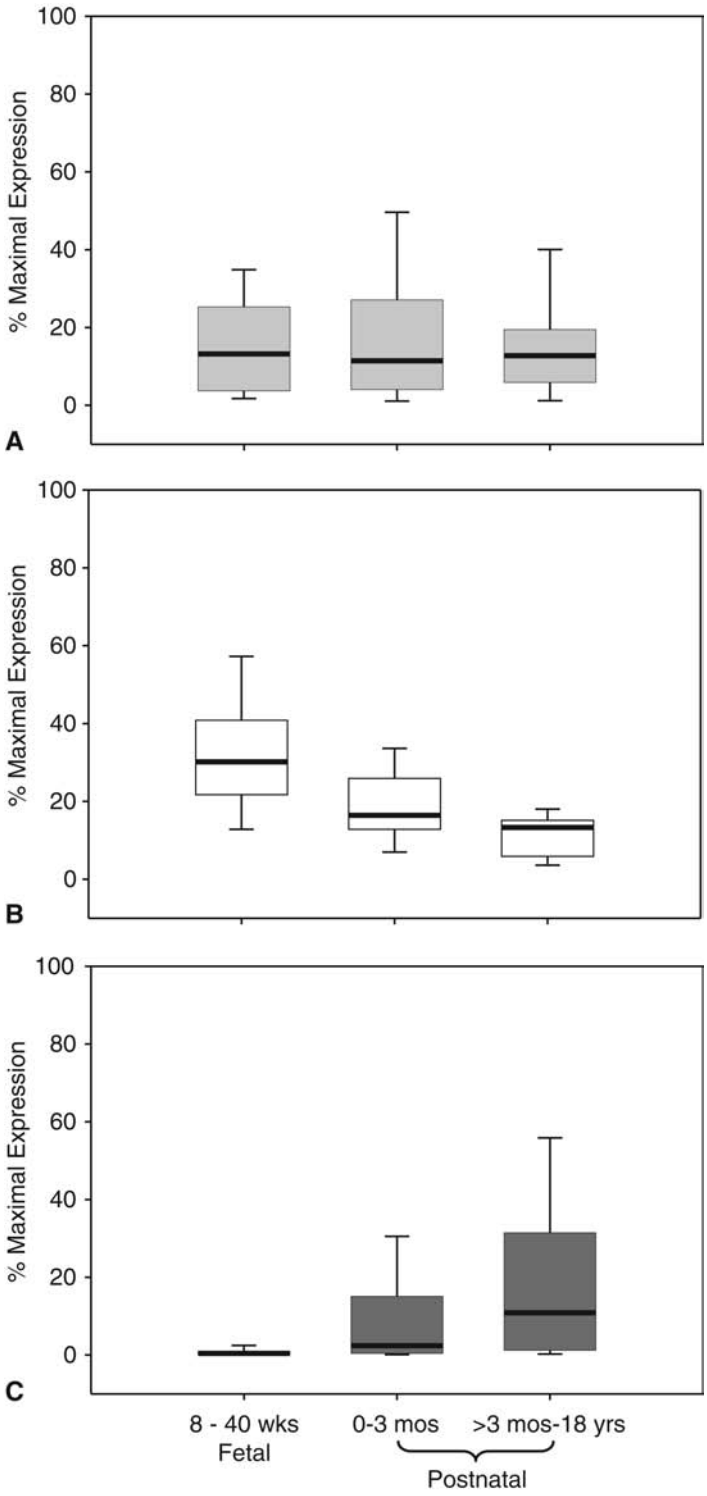

Figure 3 Human hepatic SULT ontogeny. (**A**) SULT1A1, (**B**) 1E1, and (**C**) 2A1 expression levels were determined using metabolic probe substrates and/or quantitative western blotting with hepatic microsomal preparations obtained from fetal (8 40 weeks estimated gestational age), 0 to 3 months

(*continued*)

liver samples, but was non-detectable throughout the remaining prenatal period (Fig. 2B). Low FMO3 expression levels were observed in approximately 25% of the neonatal liver samples. However, it was only between 1 month and 12 months of age that detectable FMO3 was observed in most samples. These data suggested that birth is necessary, but not sufficient for the onset of FMO3 expression. Intermediate FMO3 expression was observed in samples from donors between the ages of 1 and 11 years but in postpuberty samples, increased in a gender-independent, age-dependent manner to levels approaching those measured in adults. Taken together, the above studies suggested that not only is the ontogeny of hepatic FMO1 and FMO3 regulated independently, but that the ontogeny of FMO1 itself is regulated differently in different tissues; a hypothesis that has been confirmed (29,30). FMO1 and FMO3 clearly can be considered class 1 and class 3 enzymes with regard to developmental expression patterns, respectively.

Sulfotransferase Ontogeny

The family of sulfotransferase (SULT) enzymes (EC 2.8.2.1) catalyzes the conjugation of a sulfonate moiety donated by 3′-phosphoadenosine-5′-phosphosulfate to a wide variety of electrophilic substrates, generally resulting in inactivation and facilitating elimination from the body. The human SULT enzymes are encoded by three gene families on the basis of divergent evolution and function, the phenol SULTs (*SULT1*), the hydroxysteroid SULTs (*SULT2*), and a more recently discovered brain-specific SULT (*SULT4*). The *SULT1* family is subdivided into four subfamilies consisting of seven genes (S*ULT1A1 1A3/4*; *SULT1B1*, *SULT1C2,* and *SULT1C4*; and *SULT1E1*) and the *SULT2* family into two subfamilies consisting of two genes (*SULT2A1* and *2B1*). A single gene encodes the only known brain-specific SULT, *SULT4A1* (31). No information is available regarding the ontogeny of SULT1A2, 1B1, 1C4, 2B1, or 4A1.

Although early studies with a nonspecific probe substrate suggested the possibility of an age-dependent increase in hepatic SULT1A1 during development, more recent reports using both immunological approaches and the use of more specific substrates are consistent with little or no age-dependent change in SULT1A1 expression (32 35) (Fig. 3A). Thus, SULT1A1 can be categorized as a class 2 enzyme with regard to its developmental expression pattern. However, all these studies need to be reconsidered in the context of the findings recently reported by Hebbring et al. (36) in which a SULT1A1 copy number polymorphism was described that occurs with different frequencies in different population groups. In addition, Richard et al. (32) demonstrated predominant SULT1A1 expression in fetal hematopoietic stem cells versus fetal hepatocytes in contrast to expression only in hepatocytes in adult liver. During peak multilineage hematopoiesis at around 15 weeks' gestation, hematopoietic stem cells and precursors account for nearly 50% of the total cells in the developing liver. The percentage of these stem cells then declines throughout the remaining prenatal period such that in the perinatal and adult liver, parenchymal hepatocytes dominate (37). Taken together, these observations would suggest a decline in hematopoietic stem cell specific SULT1A1 expression during the prenatal period and a corresponding increase in hepatocyte-specific SULT1A1 expression. A similar cell-specific expression pattern has been reported for several glutathione

postnatal age, and >3 months to 18 years postnatal age donors (34). Data are plotted as medians (*bars*), interquartile values (*boxes*), and 10th to 90th percentiles (*whiskers*) of the maximum expression levels observed in the entire data set. For clarity, data outliers are not shown. Maximum SULT1A1, 1E1, and 2A1 protein levels were 311.1, 30.5, and 1,531.4 pmol/mg microsomal protein, respectively. *Abbreviation*: SULT, sulfotransferase.

S-transferase enzymes which was largely restricted to fetal liver hepatocytes (38). Clearly, cell-specific expression plays an important role in the ontogeny of hepatic DME.

Preliminary data suggesting a decrease in SULT1E1 protein levels between fetal and adult liver (33) were confirmed using a more robust tissue sample set in which a progressive decrease in SULT1E1 expression was observed in fetal liver from the first to third trimester, from the prenatal to the perinatal period (0 3 months after birth), and finally, between the perinatal samples and samples from older children (34) (Fig. 3B). Higher expression levels also were demonstrated in male versus female fetal liver tissue, which the authors speculated might protect the male fetus from excessive estrogen levels. Thus, this enzyme can be categorized as a class 1 enzyme with regard to developmental expression.

Barker et al. (39) used DHEA sulfation to demonstrate relatively low levels of SULT2A1 activity in fetal liver, but substantially increased levels in postnatal samples and adults, suggestive of a class 3 enzyme. Furthermore, there seemed to be a relatively good correlation between activity and protein levels as determined by immunological analysis. Subsequent studies by this same group (33) and others (34) confirmed low but detectable SULT2A1 enzyme activity and protein in fetal liver with a significant increase in samples from the perinatal period and a further increase to adult expression levels in older samples (Fig. 3C). Thus, like the CYP3A gene family, these three members of the SULT multigene family exhibit developmental expression patterns representing all three ontogeny classes.

CHANGES IN PHYSIOLOGICAL FACTORS

Although changes in relative DME levels are now widely recognized as having a profound impact on pharmacokinetic differences in children versus adults, these changes must be considered within the context of other changing physiological parameters [see Ref. (2) for a recent review]. For examples, intragastric pH is elevated in the neonate relative to later-life stages, resulting in lower bioavailability of weakly acidic drugs. There also are age-dependent changes in body composition that impact the volume of drug distribution, and thus, overall disposition. Drug distribution also is impacted by age-dependent changes in the major plasma drug-binding proteins (40). However, anatomical and functional changes in the liver and kidney appear to have a quantitatively more important influence on pharmacokinetics.

The ratio of liver to body mass is not constant during development, being considerably greater in infants and young children. This difference can account for a substantial portion of the developmental differences observed in drug metabolism between adults and children (41,42). Scaling by normalizing to a 70-kg individual using a 3/4 power allometric rule (Eq. 1) is sometimes used to adjust for the differences in liver size relative to body mass in pediatric versus adult individuals.

$$\text{Activity}_{70\ \text{kg}} = \text{Activity}/(\text{Weight}/70\ \text{kg})^{0.75} \qquad \text{(Eq. 1)}$$

Recent studies have determined that microsomal protein content also changes with age. Although there is considerable interindividual variability, at birth, mean microsomal content was 28 mg/g liver and increased to a maximum of 40 mg/g liver around the age of 28 years with a subsequent decline to 29 mg/g liver for the average 65-year-old (43) (Barter et al. *Drug Metab Disp*, submitted). Data from the author's laboratory are consistent with this observation and, furthermore, would suggest significantly less microsomal content in the fetal liver (44). Interestingly, for drugs undergoing microsomal enzyme-dependent metabolism, the age-dependent change in microsomal content

between pediatric and adult patients would affect drug disposition in a direction opposite to that of the changes in liver size relative to body mass.

The maturation of kidney structure and function also has a profound impact on those drugs that depend on renal clearance for elimination and/or termination of pharmacological action (45). Although nephrogenesis is complete by 36-weeks' gestation, vasoconstriction and reduced renal blood flow result in a substantially diminished glomerular filtration rate in the term infant versus the adult. With parturition and the resulting decrease in vascular resistance and increase in cardiac output and renal blood flow, the glomerular filtration rate increases rapidly and approaches adult levels by the first year of life. Tubular secretion and reabsorption also play an important role in overall renal drug clearance. At birth, the renal tubules are not yet mature, either structurally or functionally, leading to activity that is only 20% to 30% of adult values. Increases to adult levels of tubular secretion are attained by seven to eight months.

REGULATORY PERSPECTIVE

Unfortunately, it took several therapeutic misadventures to highlight the differences in drug disposition and response between children and adults and drive changes in regulation. The administration of chloramphenicol to neonates at doses that were extrapolated from those found effective and safe in adult patients is an often-cited example. These children exhibited symptoms of emesis, abdominal distension, abnormal respiration, cyanosis, and cardiovascular collapse and death that were referred to as gray baby syndrome. An immature uridine diphosphate glucuronosyl transferase system, resulting in impaired metabolism and clearance, subsequently was shown to be primarily responsible (46). These events were major impetuses for legislative changes to encourage pediatric clinical trials both in the United States (the 1997 FDA Modernization Act, the 2002 Best Pharmaceuticals for Children Act, and the 2007 FDA Revitalization Act) and in Europe (Regulation EC No. 1901/2006 on Medicinal Products for Paediatric Use). Simultaneously, as illustrated by the examples above, there has been a concerted effort to better understand life-stage-dependent changes in drug metabolism and disposition that would facilitate and improve drug development, clinical trial design, and ultimate therapeutic use.

A major component of the legislation in the United States has been an extended exclusivity to incentivize pediatric clinical trials. The Federal Drug Administration (FDA) may issue a written request for pediatrics studies prior to approval of a new drug application, or to holders of approved applications, if use of the drug in the pediatric population may produce health benefits. However, applicants also can propose that the FDA issue a written request. Upon receipt of the written request, completion of the studies detailed, and submission of an appropriate report that meets both the time frame and terms of the written request, pediatric exclusivity can be granted that applies to all of the applicant's formulations, dosage forms, and indications. As of 13 February 2008, a total of 142 product label changes had been approved by the FDA and pediatric exclusivity granted. Although the use of off-label drugs remains a problem, particularly in the pediatric intensive care setting (47), there is little doubt these legislative actions and the incentives they provide have been highly successful.

SUMMARY AND CONCLUSION

An overview of the existing knowledge regarding hepatic DME ontogeny reveals common developmental expression patterns, permitting the categorization of the various enzymes into one of three classes. As typified by CYP3A7, FMO1, and SULT1E1, the

class 1 enzymes are expressed at their highest level during the first trimester, and they either remain at high concentrations or decrease during gestation, but are silenced or expressed at low levels within one to two years after birth. This expression pattern causes one to question whether or not these enzymes might have an important endogenous function during hepatic development. CYP3A5 and SULT1A1 are examples of enzymes that can be categorized into class 2. These enzymes are expressed at relatively constant levels throughout gestation. Moderate postnatal increases in expression are observed for some of these enzymes [e.g., CYP2C19 (5)], but not all, including the examples presented in this chapter. CYP3A4, FMO3, and SULT2A1 are the examples provided for class 3 enzymes that are not expressed or are expressed at low levels in the fetus. For many, the onset of expression can be seen in either the second or third trimester. However, substantial increases in expression are observed within the first one to two years after birth. This third category of ontogeny represents the largest number of DMEs. Most importantly, the categorization of the enzymes into one of these three classes is highly tissue specific.

For those class 3 DMEs, i.e., those that undergo a perinatal onset or significant increase in hepatic expression, most, if not all, exhibit greater interindividual variability during this time frame. As an example, both CYP2C9 (5) and 2E1 (48) exhibited an approximate 100-fold range of expression in the perinatal period, which was approximately two times greater than that observed within any other age bracket. This largely is explained by what appears to be variability in the postnatal onset or increase in expression for many of the class 3 enzymes. Thus, during the neonatal period, nearly 50% of the samples exhibited CYP2C9 and 2E1 expression levels that were no different than those observed in the fetal third trimester samples, while the remaining samples exhibited CYP2C9 and 2E1 expression levels that were similar or approached the maximum observed over the entire sample set. In the case of FMO3, interindividual differences in the onset of expression during the first years of life are likely a major cause for the case reports of transient trimethylaminuria in children (49). However, the observation of perinatal hypervariability also can be extended to some class 1 enzymes. Thus, the largest variation in CYP3A7 expression (>100-fold) was observed in infant samples, likely explained by variation in the silencing or suppression of this gene during this period of time. Thus, there are windows of hypervariability during the ontogeny of many of the DMEs that would have a significant impact on the risk for adverse drug events in this population, but would not be predicted on the basis of pharmacogenetic studies in adults.

For multiple enzyme families with members belonging to both class 1 and class 3, the term "developmental switch" has been used to describe the transition between the predominant fetal to the predominant adult enzyme form. Such a developmental switch within the CYP3A family, wherein hepatic CYP3A7 expression dominates in the fetus while hepatic CYP3A4 expression dominates in the adult, has long been recognized (15). A similar phenomenon occurs within the FMO family between FMO1 and FMO3 (50) and within the CYP2C family between CYP2C19 and 2C9 (5). However, in none of these systems is there any evidence for coordinated inverse regulation between these "fetal" and "adult" enzymes, suggesting that the term developmental switch is a misnomer and that developmental transition is a more appropriate description of this process.

Despite recent advances in our understanding of DME ontogeny, several important knowledge gaps remain. Additional studies are needed to define the true ontogeny of many of the enzyme systems, particularly in extrahepatic tissues. Too much of our current knowledge is based on in vitro or in vivo studies that used samples or recruited patients, respectively, representing narrow windows of time or omitting what would appear to be critical time windows. Conclusions drawn from such studies can be contradictory and

misleading. Finally, the mechanisms regulating DME ontogeny remain poorly understood. Associations between specific transcription factor ontogeny and DME ontogeny have been made, but such associations hardly offer definitive proof for control mechanisms. A better understanding of regulation hopefully would provide insight into the mechanism or mechanisms whereby the increase or onset of expression of many of the class 3 enzymes are linked to the birth process, independent of gestational age, and the underlying cause for the interindividual variation in this process. Despite these knowledge gaps, the field has progressed to a point that has permitted the development of robust physiologically based pharmacokinetic models that provide a much improved means of predicting age-specific drug disposition (7,51). Further advances in the field will only improve these valuable tools.

REFERENCES

1. Alcorn J, McNamara PJ. Pharmacokinetics in the newborn. Adv Drug Deliv Rev 2003; 55(5): 667 686.
2. Kearns GL, Abdel Rahman SM, Alander SW, Blowey DL, Leeder JS, Kauffman RE. Developmental pharmacology drug disposition, action, and therapy in infants and children. N Engl J Med 2003; 349(12):1157 1167.
3. Hines RN, McCarver DG. The ontogeny of human drug metabolizing enzymes: phase I oxidative enzymes. J Pharmacol Exp Ther 2002; 300(2):355 360.
4. McCarver DG, Hines RN. The ontogeny of human drug metabolizing enzymes: phase II conjugation enzymes and regulatory mechanisms. J Pharmacol Exp Ther 2002; 300(2):361 366.
5. Koukouritaki SB, Manro JR, Marsh SA, Stevens JC, Rettie AE, McCarver DG, Hines RN. Developmental expression of human hepatic CYP2C9 and CYP2C19. J Pharmacol Exp Ther 2004; 308(3):965 974.
6. Blake MJ, Gaedigk A, Pearce RE, Bomgaars LR, Christensen ML, Stowe C, James LP, Wilson JT, Kearns GL, Leeder JS. Ontogeny of dextromethorphan O and N demethylation in the first year of life. Clin Pharmacol Ther 2007; 81(4):510 516.
7. Johnson TN, Rostami Hodjegan A, Tucker GT. Prediction of the clearance of eleven drugs and associated variability in neonates, infants and children. Clin Pharmacokinet 2006; 45(9):931 956.
8. Williams JA, Hyland R, Jones BC, Smith DA, Hurst S, Goosen TC, Peterkin V, Koup JR, Ball SE. Drug drug interactions for UDP glucuronosyltransferase substrates: a pharmacokinetic explanation for typically observed low exposure (AUCi/AUC) ratios. Drug Metab Dispos 2004; 32(11):1201 1208.
9. Shimada T, Yamazaki H, Mimura M, Inui Y, Guengerich FP. Interindividual variations in human liver cytochrome P 450 enzymes involved in the oxidation of drugs, carcinogens and toxic chemicals: studies with liver microsomes of 30 Japanese and 30 Caucasians. J Pharmacol Exp Ther 1994; 270:414 423.
10. Kuehl P, Zhang J, Lin Y, Lamba J, Assem M, Schuetz J, Watkins PB, Daly A, Wrighton SA, Hall SD, Maurel P, Relling M, Brimer C, Yasuda K, Venkataramanan R, Strom S, Thummel K, Boguski MS, Schuetz E. Sequence diversity in *CYP3A* promoters and characterization of the genetic basis of polymorphic CYP3A5 expression. Nat Genet 2001; 27:383 391.
11. Lin YS, Dowling ALS, Quigley SD, Farin FM, Zhang J, Lamba J, Schuetz EG, Thummel KE. Co regulation of CYP3A4 and CYP3A5 and contribution to hepatric and intestinal midazolam metabolism. Mol Pharmacol 2002; 62(1):162 172.
12. Sim SC, Edwards RJ, Boobis AR, Ingelman Sundberg M. CYP3A7 protein expression is high in a fraction of adult human livers and partially associated with the CYP3A7*1C allele. Pharmacogenet Genomics 2005; 15(9):625 631.
13. Ladona MG, Lindström B, Thyr C, Dun Ren P, Rane A. Differential foetal development of the *O* and *N* demethylation of codeine and dextromethorphan in man. Br J Clin Pharmacol 1991; 32:295 302.

14. Chen H, Fantel AG, Juchau MR. Catalysis of the 4 hydroxylation of retinoic acids by CYP3A7 in human fetal hepatic tissues. Drug Metab Dispos 2000; 28(9):1051 1057.
15. Lacroix D, Sonnier M, Moncion A, Cheron G, Cresteil T. Expression of CYP3A in the human liver. Evidence that the shift between CYP3A7 and CYP3A4 occurs immediately after birth. Eur J Biochem 1997; 247:625 634.
16. Stevens JC, Hines RN, Gu C, Koukouritaki SB, Manro JR, Tandler PJ, Zaya MJ. Developmental expression of the major human hepatic CYP3A enzymes. J Pharmacol Exp Ther 2003; 307(2):573 582.
17. Schuetz EG, Beach DL, Guzelian PS. Selective expression of cytochrome P450 CYP3A mRNAs in embryonic and adult human liver. Pharmacogenetics 1994; 4:11 20.
18. Hakkola J, Raunio H, Purkunen R, Saarikoski S, Vahakangas K, Pelkonen O, Edwards RJ, Boobis AR, Pasanen M. Cytochrome P450 3A expression in the human fetal liver: evidence that CYP3A5 is expressed in only a limited number of fetal livers. Biol Neonate 2001; 80(3):193 201.
19. Leeder JS, Gaedigk R, Marcucci KA, Gaedigk A, Vyhlidal CA, Schindel BP, Pearce RE. Variability of CYP3A7 expression in human fetal liver. J Pharmacol Exp Ther 2005; 314(2): 626 635.
20. Johnson TN, Tucker GT, Rostami Hodjegan A. Development of CYP2D6 and CYP3A4 in the First Year of Life. Clin Pharmacol Ther 2008; 83(5):670 671.
21. Treluyer J M, Bowers G, Cazali N, Sonnier M, Rey E, Pons G, Cresteil T. Oxidative metabolism of amprenavir in the human liver, effect of the CYP3A maturation. Drug Metab Dispos 2003; 31(3):275 281.
22. Bernardini S, Semama DS, Huet F, Sgro C, Gouyon JB. Effects of cisapride on QTc interval in neonates. Arch Dis Child Fetal Neonatal Ed 1997; 77(3):F241 F243.
23. Pearce RE, Gotschall RR, Kearns GL, Leeder JS. Cytochrome P450 involvement in the biotransformation of cisapride and racemic norcisapride in vitro: differential activity of individual CYP3A isoforms. Drug Metab Dispos 2001; 29(12):1548 1554.
24. Treluyer J M, Rey E, Sonnier M, Pons G, Cresteil T. Evidence of impaired cisapride metabolism in neonates. Br J Clin Pharmacol 2001; 52:419 425.
25. Kearns GL, Robinson PK, Wilson JT, Wilson Costello D, Knight GR, Ward RM, van den Anker JN. Cisapride disposition in neonates and infants: in vivo reflection of cytochrome P450 3A4 ontogeny. Clin Pharmacol Ther 2003; 74(4):312 325.
26. Krueger SK, Williams DE. Mammalian flavin containing monooxygenases: structure/function, genetic polymorphisms and role in drug metabolism. Pharmacol Ther 2005; 106(3):357 387.
27. Hernandez D, Janmohamed A, Chandan P, Phillips IR, Shephard EA. Organization and evolution of the flavin containing monooxygenase genes of human and mouse: identification of novel gene and pseudogene clusters. Pharmacogenetics 2004; 14(2):117 130.
28. Hines RN. Developmental and tissue specific expression of human flavin containing monooxygenase 1 and 3. Expert Opin Drug Metab Toxicol 2006; 2(1):41 49.
29. Zhang J, Cashman JR. Quantitative analysis of FMO gene mRNA levels in human tissues. Drug Metab Dispos 2006; 34(1):19 26.
30. Shephard EA, Chandan P, Stevanovic Walker M, Edwards M, Phillips IR. Alternative promoters and repetitive DNA elements define the species dependent tissue specific expression of the FMO1 genes of human and mouse. Biochem J 2007; 406(3):491 499.
31. Blanchard RL, Freimuth RR, Buck J, Weinshilboum RM, Coughtrie MW. A proposed nomenclature system for the cytosolic sulfotransferase (SULT) superfamily. Pharmacogenetics 2004; 14(3):199 211.
32. Richard K, Hume R, Kaptein E, Stanley EL, Visser TJ, Coughtrie MW. Sulfation of thyroid hormone and dopamine during human development: ontogeny of phenol sulfotransferases and arylsulfatase in liver, lung, and brain. J Clin Endocrinol Metab 2001; 86(6):2734 2742.
33. Stanley EL, Hume R, Coughtrie MW. Expression profiling of human fetal cytosolic sulfotransferases involved in steroid and thyroid hormone metabolism and in detoxification. Mol Cell Endocrinol 2005; 240(1 2):32 42.

34. Duanmu Z, Weckle A, Koukouritaki SB, Hines RN, Falany JL, Falany CN, Kocarek TA, Runge Morris M. Developmental expression of aryl, estrogen, and hydroxysteroid sulfotrans ferases in pre and postnatal human liver. J Pharmacol Exp Ther 2006; 316(3):1310 1317.
35. Adjei AA, Gaedigk A, Simon SD, Weinshilboum RM, Leeder JS. Interindividual variability in acetaminophen sulfation by human fetal liver: implications for pharmacogenetic investigations of drug induced birth defects. Birth Defects Res A Clin Mol Teratol 2008; 82(3):155 165.
36. Hebbring SJ, Adjei AA, Baer JL, Jenkins GD, Zhang J, Cunningham JM, Schaid DJ, Weinshilboum RM, Thibodeau SN. Human SULT1A1 gene: copy number differences and functional implications. Hum Mol Genet 2007; 16(5):463 470.
37. Morrison SJ, Uchida N, Weissman IL. The biology of hematopoietic stem cells. Annu Rev Cell Dev Biol 1995; 11:35 71.
38. Shao J, Stapleton PL, Lin YS, Gallagher EP. Cytochrome p450 and glutathione s transferase mRNA expression in human fetal liver hematopoietic stem cells. Drug Metab Dispos 2007; 35 (1):168 175.
39. Barker EV, Hume R, Hallas A, Coughtrie MWH. Dehydroepiandrosterone sulfotransferase in the developing human fetus: quantitative biochemical and immunological characterization of the heptatic, renal, and adrenal enzymes. Endocrinology 1994; 134(2):982 989.
40. McNamara PJ, Alcorn J. Protein binding predictions in infants. AAPS PharmSci 2002; 4(1):E4.
41. Murry DJ, Crom WR, Reddick WE, Bhargava R, Evans WE. Liver volume as a determinant of drug clearance in children and adolescents. Drug Metab Dispos 1995; 23(10):1110 1116.
42. Noda T, Todani T, Watanabe Y, Yamamoto S. Liver volume in children measured by computed tomography. Pediatr Radiol 1997; 27(3):250 252.
43. Barter ZE, Bayliss MK, Beaune PH, Boobis AR, Carlile DJ, Edwards RJ, Houston JB, Lake BG, Lipscomb JC, Pelkonen OR, Tucker GT, Rostami Hodjegan A. Scaling factors for the extrapolation of in vivo metabolic drug clearance from in vitro data: reaching a consensus on values of human microsomal protein and hepatocellularity per gram of liver. Curr Drug Metab 2007; 8(1):33 45.
44. Hines RN. Ontogeny of Drug Metabolism Enzymes and Implications for Adverse Drug Reactions. Pharamcol Ther 2008; 118(2):250 267.
45. Alcorn J, McNamara PJ. Ontogeny of hepatic and renal systemic clearance pathways in infants: part I. Clin Pharmacokinet 2002; 41(12):959 998.
46. Weiss CF, Glazko AJ, Weston JK. Chloramphenicol in the newborn infant: a physiological explanation of its toxicity when given in excessive doses. N Engl J Med 1960; 262(16):787 794.
47. Cuzzolin L, Atzei A, Fanos V. Off label and unlicensed prescribing for newborns and children in different settings: a review of the literature and a consideration about drug safety. Expert Opin Drug Saf 2006; 5(5):703 718.
48. Johnsrud EK, Koukouritaki SB, Divakaran K, Brunengraber L, Hines RN, McCarver DG. Human hepatic CYP2E1 expression during development. J Pharmacol Exp Ther 2003; 307(1): 402 407.
49. Mayatepek E, Kohlmüeller D. Transient trimethylaminuria in childhood. Acta Paediatr 1998; 87:1205 1207.
50. Koukouritaki SB, Simpson P, Yeung CK, Rettie AE, Hines RN. Human hepatic flavin containing monooxygenase 1 (*FMO1*) and 3 (*FMO3*) developmental expression. Pediatric Res 2002; 51(2):236 243.
51. Ginsberg G, Hattis D, Russ A, Sonawane B. Physiologically based pharmacokinetic (PBPK) modeling of caffeine and theophylline in neonates and adults: implications for assessing children's risks from environmental agents. J Toxicol Environ Health A 2004; 67(4):297 329.

10

Sites of Extra Hepatic Metabolism, Part I: Lung

Christopher A. Reilly and Garold S. Yost
Department of Pharmacology and Toxicology, University of Utah, Salt Lake City, Utah, U.S.A.

INTRODUCTION

Metabolism of xenobiotic compounds in pulmonary tissues is complex and incompletely understood. Despite years of research, the precise mechanisms and factors that determine pulmonary-specific metabolism and associated consequences for xenobiotic disposition in man remain relatively undefined. Several excellent reviews highlight this burgeoning field (1–8).

The complexity associated with pulmonary metabolism of xenobiotics arises, in part because of the many different cell types (over 40), diverse cellular functions, and differences in gene expression patterns that exist for each cell type (9). Lung cell types range from secretory cells with cilia, designed to move foreign particles up the tracheobronchial tract, to epithelial and endothelial cells that line the alveoli and pulmonary vasculature and comprise the junction between vascular fluids and the external environment. The drug-metabolizing functions of many of these cells have not been fully investigated, but accumulating scientific literature indicates that significant differences exist among different cell types, particularly differences in the expression and action of xenobiotic-metabolizing enzymes (1–9).

Metabolic processes in the lung are often studied using whole-lung homogenates. These studies are plentiful in the scientific literature and have been reasonably helpful to evaluate the overall metabolic capacity of the lung. These studies usually conclude that lung tissues are far less active in the metabolism of xenobiotics compared with the liver, exhibiting both a decrease in the overall ability to clear xenobiotics and a loss of metabolic diversity due to limited expression of many xenobiotic-metabolizing enzymes. However, studies using lung homogenates are overly simplistic, because they fail to accurately illustrate the gamut of unique interactions that occur between xenobiotics and lung cells. In many instances, erroneous conclusions about the susceptibility of the lung and selected lung cell types to toxic insult or the capability of certain cells or regions of the tracheobronchial tract to metabolize xenobiotics have been drawn from such studies.

As a general rule, pulmonary metabolism of xenobiotics plays only a minor role in determining the overall bioavailability and distribution of xenobiotics in humans. The

majority of xenobiotic metabolism occurs in other organs such as the liver, although significant first-pass metabolism by the lung can be observed for selected agents that are delivered via inhalation, actively sequestered by lung cells, or selectively acted upon by drug-metabolizing enzymes expressed solely in the lung. Examples of physiological compounds that are subject to accumulation or metabolic clearance by the lung include eicosanoids (10,11) and endogenous oligoamines such as spermine (6). The accumulation of nitrogen-containing drugs, such as paraquat (6,12,13), propranolol (6,14,15), fentanyl and related agents (16 18), ipomeanol (6,19), amioderone (20), and imipramine (21 23) by first-pass retention has also been observed. A prototypical example of selective metabolism of a xenobiotic by lung tissues is the metabolism of inhaled butadiene for which both the monoxide and diepoxide metabolites were found at higher concentrations in lung tissues than in liver tissues of mice, presumably because of metabolism in the lung and not by selective accumulation of the metabolites by lung cells (24,25).

Xenobiotic metabolism in respiratory tissues can be examined by looking at the chemical classes that are metabolized or by focusing on the enzymes responsible for the biotransformations. This review will focus on the expression of pulmonary drug-metabolizing enzymes and associated consequences. Frequently, genes coding for critical xenobiotic-metabolizing enzymes including cytochrome P450s (CYPs), flavin-containing monooxygenases (FMOs), and glucuronosyltransferases are solely expressed in the respiratory tract, where they play definitive roles in determining the ultimate actions of xenobiotics in respiratory cells and the respiratory tract as a whole.

REDOX ENZYMES

NADPH Cytochrome P450 Reductase

NADPH CYP reductase is a flavoprotein enzyme that catalyzes the transfer of electrons from NADPH to the heme of CYP enzymes. NADPH CYP reductase is required for P450 enzyme function and ultimately substrate oxidation. Only one gene product has been identified for NADPH CYP reductase, and its expression is generally considered ubiquitous. Although the reductase enzyme is assumed to be tightly coupled to P450 enzymes within the endoplasmic reticulum, reductase has not been immunochemically detected in all cells within the lung, including type I alveolar cells and vascular endothelial cells that possess demonstrable P450 protein (26 29). Therefore, it is doubtful that the P450 enzymes in these cells are catalytically active. Similar localizations of the reductase in bronchiolar and bronchial epithelial cells, Clara cells, and alveolar type II cells have been demonstrated in human lung tissues (30).

Because NADPH CYP reductase is tightly coupled with P450 enzyme function, its individual contribution to xenobiotic metabolism is often overlooked. A classic example of pulmonary xenobiotic metabolism by NADPH CYP reductase is the NADPH-dependent bioactivation and toxicity of paraquat in pneumocytes (12,13). Paraquat is actively accumulated in alveolar type II cells via polyamine transporters. NADPH CYP reductase catalyzes the one-electron reduction of paraquat to form the highly reducing paraquat cation radical, a potent cytotoxicant by virtue of its ability to readily reduce molecular oxygen (O_2) to form the superoxide anion radical (O_2). Superoxide ultimately dismutates (enzymatically or spontaneously) to form hydrogen peroxide (H_2O_2) and through the Fenton reaction with ferrous iron (Fe^{2+}) produces the hydroxyl radical (·OH), a potent oxidant that reacts with cellular nucleophiles at diffusion-limited rates. Metabolism of paraquat by NADPH CYP reductase has been shown to promote cell death through the depletion of reducing agents, lipid peroxidation, and DNA and protein

oxidation. Paraquat is an example of how NADPH CYP reductase dependent metabolism directly influences the disposition of a selected agent in the lung.

Cytochrome P450

CYP enzymes are a family of heme-containing proteins that catalyze a variety of oxidative metabolic processes. There are 57 unique P450 genes in humans, and each gene product exhibits unique distribution and function, including selective expression in tissues and the ability or inability to metabolize a given endogenous or xenobiotic agent (31). Various aspects of P450 enzymes have been reviewed in recent years (32 38). The classic example of a P450-catalyzed reaction is the addition of oxygen to a carbon-carbon bond to render the molecule more water soluble and amenable to conjugation reactions that further hasten the excretion of the xenobiotic from the body via specific excretion mechanisms. The oxidation of a hydrocarbon substrate by P450 is represented by the following equation: $RH + O_2 + NADPH + H^+ \rightarrow ROH + H_2O + NADP^+$. P450-catalyzed reactions are not limited to hydrocarbon hydroxylation/oxygenation; heteroatom (O-, N-, and S-) dealkylation, dehydrogenation/desaturation, aliphatic and aromatic epoxidation, heteroatom (O-, N-, and S-) oxidation, hydrolysis (amide and ester), decarboxylation, and dehalogenation reactions are all possible for P450 enzymes, depending on the chemical properties of the substrate and the specific P450 enzyme.

P450 enzymes are expressed to varying degrees throughout the human body, with the greatest concentration in the liver. The P450 content in whole-lung microsomal fractions ranges from 0.01 nmol/mg microsomal protein for humans (39,40) to 1.04 nmol/mg protein for goats (41). These values are one-tenth of the P450 content of hepatic microsomes from the same species (2). Therefore, key factors governing significant contributions of P450 enzymes in respiratory tract pharmacology and toxicology of xenobiotics include the concentration of specific enzymes in certain cells or regions of the respiratory tract and the concentration of the agent in metabolically competent lung cells. Examples of these phenomena were mentioned previously.

The number of P450 enzymes that are known to be expressed as functional proteins in respiratory tissues has increased in recent years as more studies have investigated xenobiotic metabolism in lung tissue. P450 genes that have been identified in human respiratory tissue using either mRNA analysis, immunohistology, or functional assays include CYP1A1, 1A2, 1B1, 2A6, 2A13, 2B6, 2C8, 2C18, 2D6, 2E1, 2F1, 2J2, 2S1, 3A4, 3A5, and 4B1 (3,5,8,42 46). These gene products are generally expressed in the lung in addition to other organs. However, some P450 genes are selectively expressed in the human trachea and lung, including (but likely not limited to) CYP2A13, 2F1, 4B1, and 2S1 (5,8,43). In general, similar properties and expression profiles are observed for P450 orthologues, thus allowing many studies of pulmonary xenobiotic metabolism to be performed in rodents and other animal models. Despite this commonality, researchers are cautioned when extrapolating results across species since definite differences exist in overall metabolic potential, P450 enzyme selectivity and catalytic efficiency, and interactions occurring between multiple enzymes.

The selective expression and catalytic participation of certain P450 enzymes in human lung cells is a major factor for the pneumotoxicity and/or carcinogenicity of several xenobiotics (7,47) including naphthalene (48), 4-ipomeanol (49 52), 3-methylindole (3MI) (53 58), butylated hydroxytoluene (BHT) (59,60), 1,1-dichloroethylene (DCE) (61,62), and 4-(methylnitrosamino)-l-(3-pyridyl)-l-butanone (NNK) (63 65). Examples of several of these toxicants and their putative reactive intermediates and P450 enzymes that catalyze the bioactivation processes are shown in Figures 1 to 4.

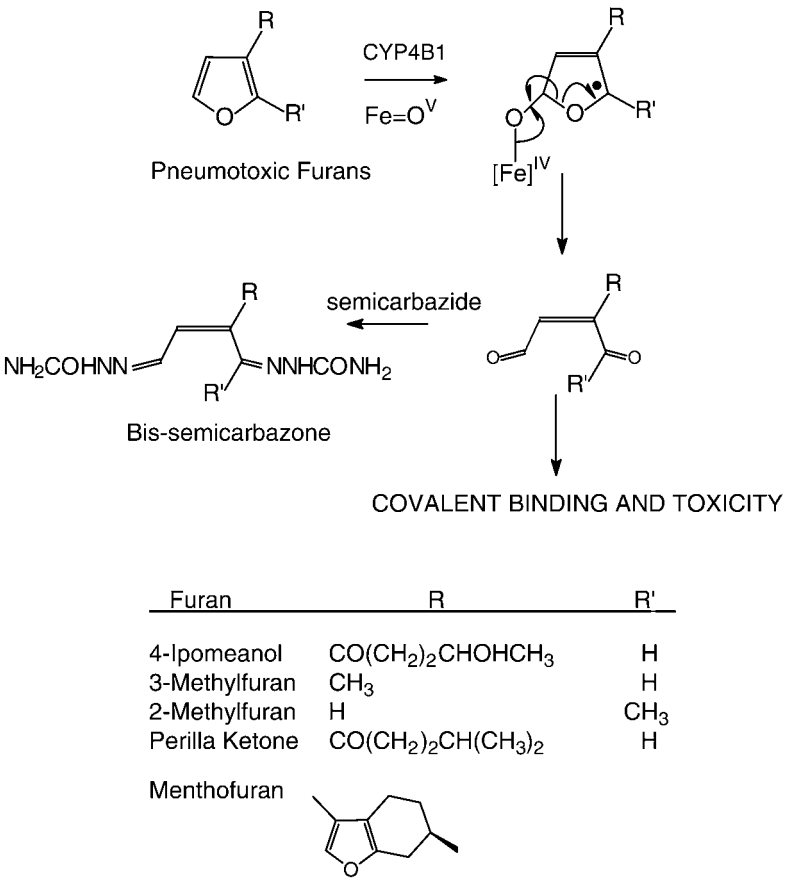

Furan	R	R'
4-Ipomeanol	$CO(CH_2)_2CHOHCH_3$	H
3-Methylfuran	CH_3	H
2-Methylfuran	H	CH_3
Perilla Ketone	$CO(CH_2)_2CH(CH_3)_2$	H

Menthofuran

Figure 1 Pneumotoxic furans are bioactivated through formation of highly reactive unsaturated bis carbonyl intermediates. The furans are usually toxic to hepatic cells in addition to lung cells. The glutathione adducts of these intermediates are highly unstable, so they were trapped and identified as their semicarbazone adducts.

Many examples of regional and/or cell type specific expression of P450s exist. For example, in humans, the expression of CYP1A1 gene is primarily restricted to the bronchial and alveolar epithelial and capillary endothelial cells of the lung, while the expression of 2A6, 2A13, 2B6, 2C, 2J2, 2S1, and 3A genes is observed throughout the nasal mucosa, trachea, and lung tissues (5,8,43,66,67). In rabbits, CYP2A10, 2A11, and 2G1 enzymes are specifically expressed in nasal tissues, particularly the olfactory epithelium, where CYP2A10 and CYP2A11 constitute over 90% of total P450 in this anatomical region. In addition, the 2B4 and 4B1 enzymes constitute over 90% of the total P450 content of rabbit lung (68), and the orthologues of these enzymes in other species often appear to be major contributors to the P450 contents and catalytic activities of lung tissues. Similarly, the 2F subfamily genes are selectively expressed in human and some animal lung tissues and human placenta (43,66,69). It is important to highlight that for each P450 enzyme selective toxicities can be observed in the cells and tissue regions that express unique P450 enzymes.

The enzymes from the 2B and 4B subfamilies are often expressed to a much higher extent in the lung than in the liver, and higher expression often leads to enhanced

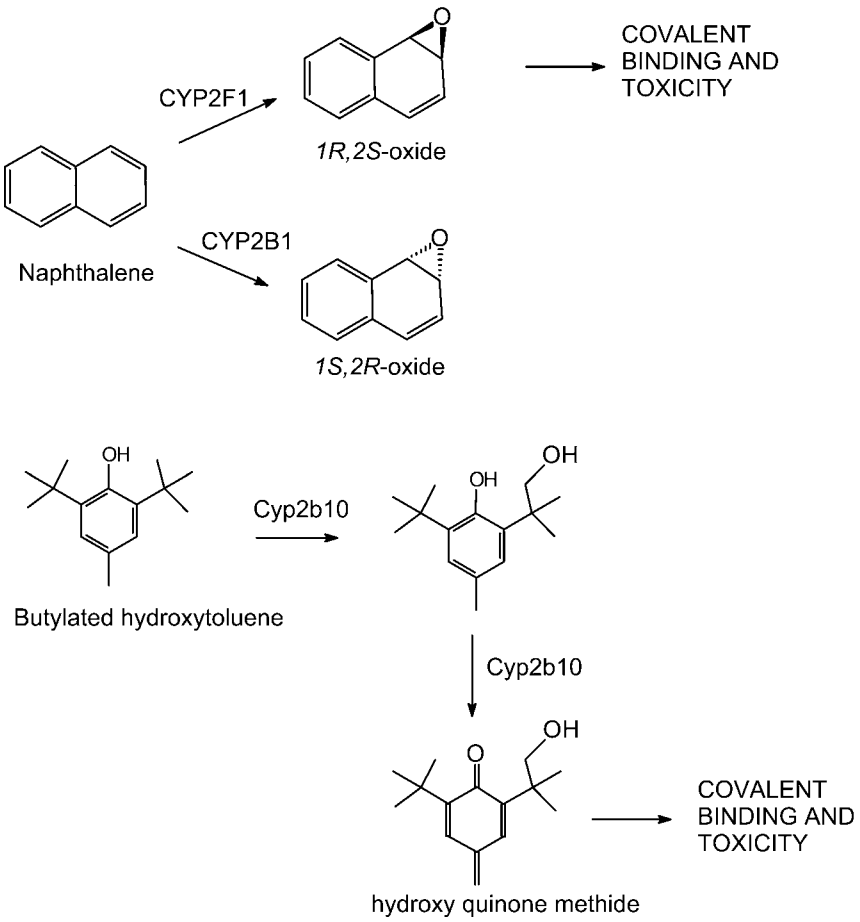

Figure 2 Bioactivation of naphthalene and butylated hydroxytoluene by CYP enzymes from the CYP2B and CYP2F subfamilies. The postulated ultimate reactive intermediates of each toxicant are shown. *Abbreviation*: CYP, cytochrome P450.

bioactivation of xenobiotics. Mouse lung Cyp2b10 is highly expressed in Clara cells, and this enzyme oxidizes BHT by subsequent hydroxylation and dehydrogenation steps to produce the ultimate pneumotoxic quinone methide (Fig. 2) (59,60). This enzyme is not expressed extensively in mouse liver unless the animals are pretreated with phenobarbital to induce hepatic expression.

A unique mechanism has been established for the tumor-promoting activity of BHT (70,71). Presumably, Cyp2b10 first oxygenates BHT on one of the methyl groups to form 6-*tert*-butyl-2-(1′,1′-dimethyl-2′-hydroxy)ethyl-4-methylphenol, and subsequently dehydrogenates the hydroxylated intermediate to form a potent electrophilic quinone methide. This electrophile then alkylates cysteine or histidine residues on crucial protective enzymes, including peroxiredoxin 6 and superoxide dismutase 1, and possibly other antioxidant enzymes in mouse lung. Inactivation of these vital enzymes leads to high levels of reactive oxygen species and inflammation, conditions that facilitate tumor promotion in the mouse lung.

CYP4B1 is selectively expressed in rat lung, not liver, and this enzyme efficiently catalyzes the bioactivation of 4-ipomeanol (6,48 51) to a pneumotoxic unsaturated

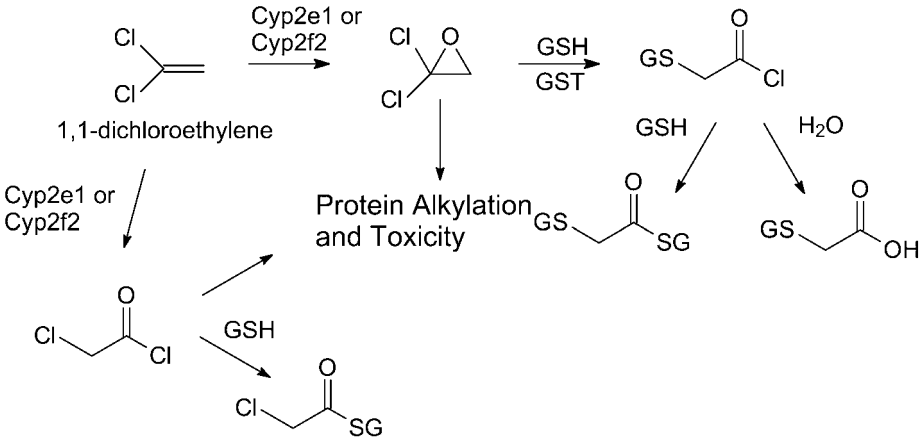

Figure 3 1,1 Dichloroethylene is a pneumotoxicant in mice, and its bioactivation by the mouse Cyp2f2 and Cyp2e1 enzymes is remarkably complex for such a simple small molecule. The epoxide and two putative acyl halide reactive intermediates are shown, along with glutathione adducts of the electrophiles. The glutathione adducts and the mercapturates that are the excreted forms of the adducts have been used in vitro and in vivo as biomarkers of alkylation events. *Abbreviations*: Cyp, cytochrome P450; GSH, glutathione; GST, glutathione *S* transferase.

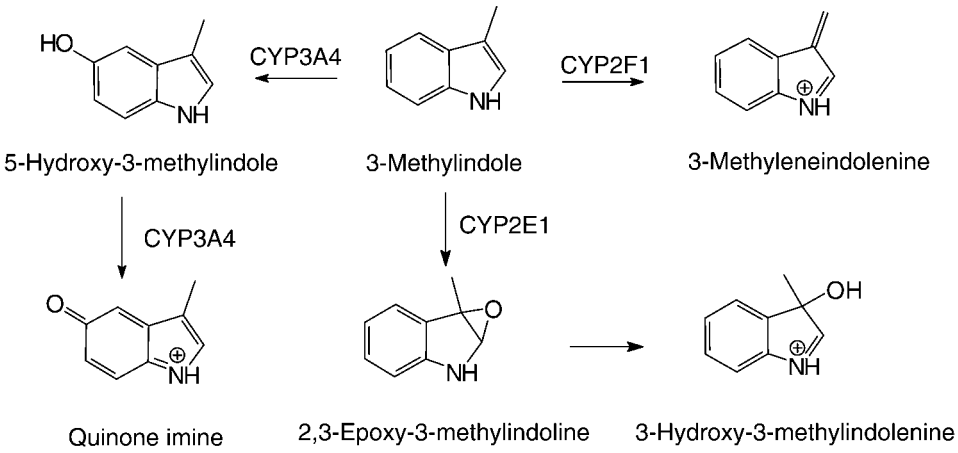

Figure 4 The prototypical pulmonary toxin 3MI is bioactivated by CYP enzymes by human CYP2F1, CYP2E1, and CYP3A4. Four reactive intermediates that may participate in the pneumotoxicity of 3MI are 3 methyleneindolenine, 2,3 epoxy 3 methylindoline, 3 hydroxy 3 methyleneindolenine, and the quinone imine of 5 hydroxy 3 methylindole. The quinone imine of 5 hydroxy 3 methylindole was identified from incubations of 3MI with human liver microsomes, and CYP3A4 is implicated as the most likely mediator of this bioactivation pathway. Oxidation of 3MI in the respiratory tract can proceed through two distinctly different pathways, dehydrogenation and ring oxygenation that appear to be predominantly mediated by different CYP enzymes. However, the results of multiple experiments implicate the dehydrogenated intermediate, 3 methyleneindolenine, as the most likely toxic culprit. *Abbreviations*: CYP, cytochrome P450; 3MI, 3 methylindole.

bis-carbonyl electrophile. Several other substituted furans are bioactivated in similar manner (Fig. 1), and most are pneumotoxic, and usually hepatotoxic as well. Likewise, CYP4B2 is selectively transcribed in lung tissues of goats (54), and most of the bioactivation of 3MI to the electrophilic 3-methyleneindolenine intermediate is catalyzed

by this enzyme (53,56,72,73). The goat 4B2 enzyme uniquely oxidized 3MI at the methyl group to form the methylene imine and indole-3-carbinol, without detectable production of 3-methyloxindole or any other oxygenated product (74). All other enzymes either produced the methylene imine (CYP2F1 and CYP2F3), only ring-oxygenated products (CYP2E1), or oxygenated products and the methylene imine (CYP1A1 and CYP1A2) (73). Additional discussions about the expression and metabolism of xenobiotics by pulmonary P450 enzymes are provided below for each enzyme.

The human CYP1 family contains three genes, CYP1A1, 1A2, and 1B1. These P450s are expressed to varying degrees in the human respiratory tract. CYP1A1 is the major extrahepatic gene, and it is ubiquitously expressed at trace levels in many cell types including bronchiolar and alveolar cells of the peripheral airways (<1 mm in diameter) of the human lung (8,43,75 78). CYP1A1 is highly induced by several compounds in tobacco smoke [polycyclic aromatic hydrocarbons (PAHs) and aromatic amines] (75,79,80), and by TCDD (81,82) via activation of the aryl hydrocarbon receptor (AhR). CYP1A1 metabolizes PAHs including benzo[a]pyrene (83), 5- and 6-methylchrysene (84), and aromatic amines (85). The sequential two-step metabolism of benzo[a]pyrene to the benzo[a]pyrene-7,8-diol-9,10-epoxide is a prototypical example of how a P450 enzyme can determine the toxicity, in this case, carcinogenicity, of an otherwise inactive agent in the lung. CYP1A1 expression levels are directly correlated with aryl hydrocarbon hydroxylase bioactivation in human tissues (86 88). CYP1A1 expression levels are correlated with increased risk for lung cancer in humans, and higher levels of expression or the expression of the T3801C (Msp1) and Ile462Val allelic variants drastically increase risks for developing lung cancer (89 92).

Like CYP1A1, CYP1A2 is expressed in human lung peripheral tissue, primarily in smokers (5,8,93,94). Recent evaluations of human lung samples routinely list CYP1A1 and CYP1B1 as the most highly transcribed P450 enzymes (8,66). CYP1A2 likely plays a role in the pulmonary metabolism of aromatic and heterocyclic amines, nitroaromatic compounds, mycotoxins, and estrogens in lungs of smokers (5,8).

CYP1B1 is expressed in bronchial and alveolar epithelial cells as well as in alveolar macrophages (8). Like CYP1A1 and 1A2, 1B1 is induced by tobacco smoke (95) and TCDD (43,96). CYP1B1 catalyzes the 2- and 4-hydroxylation of 17β-estradiol as well as the bioactivation of numerous PAHs, including benzo[a]pyrene, nitroarenes, arylarenes, and aromatic and aryl amines (8,97,98). There is some evidence that differences in CYP1B1 variant expression influence susceptibility to lung cancer (99).

A number of *CYP2A* gene products are expressed in animal and human respiratory tracts (100 102). *CYP2A6* and *CYP2A13* genes are expressed in the human respiratory tract, particularly in the nasal epithelium (103). CYP2A6 is expressed in nasal, tracheal, and bronchial epithelial cells (8,101), while CYP2A13 is also expressed at low levels in alveolar epithelial cells (104). Mouse CYP2a5 appears to have similar tissue and cellular distribution (105). There is strong evidence that CYP2A enzymes, particularly CYP2A13, play critical roles in the metabolic bioactivation of tobacco-specific nitrosamines, the major procarcinogenic substances in cigarette smoke. CYP2A6 efficiently catalyzes the 7-hydroxylation of coumarin (106), the metabolism of nicotine to cotinine (107,108), and is responsible, in part, for the bioactivation of NNK (109 111), the tobacco-specific procarcinogenic nitrosamine. CYP2As also metabolize the nasal carcinogen hexamethylphosphoramide (102). The genetic polymorphism CYP2A6*4C variant of CYP2A6 has been shown to correlate with a decreased odds ratio for lung cancer, suggesting a key role for catalytically active CYP2A6 in the development of lung cancer by environmental pneumotoxicants (112,113). Furthermore, CYP2A6 expression may influence smoking behavior (113,114).

CYP2A13 is active toward a number of chemical agents and lung carcinogens including aflatoxin B1 (115), hexamethylphosphoramide (102), 2′-methoxyacetophenone, N,N′-dimethylanaline, *N*-nitrosodiethylamine, *N*-nitrosomethylphenylamine, 2,6-dichlorobenzonitrile (116), NNK (117,118), naphthalene (119), styrene (119), and toluene (119). Recent studies have led to the conclusion that CYP2A13 is the most efficient catalyst of NNK bioactivation (120), and expression of the R257C variant form of CYP2A13, which exhibits reduced turnover efficiency for NNK, was associated with a decreased risk for lung adenocarcinoma in heavy smokers (120). The contribution of other CYP2A13 polymorphisms to risks for developing lung cancer has yet to be established (121). CYP2A6 is capable of bioactivating the cigarette smoke component 3-methyindole to electrophiles (122), and CYP2A13 bioactivates 3MI to 3-methyleneindolenine, the putative toxic electrophile of 3MI (unpublished observations).

CYP2B6 is expressed in Clara and bronchial epithelial cells of the human lung as an inactive splice variant called CYP2B7 (76,123,124). CYP2B6 has also been implicated in the bioactivation of NNK in the lung (109,125).

CYP2C8 and CYP18 may also be expressed in human lungs (94), possibly localized to the serous cells of bronchial glands (126). CYP2C8 may participate in the regulation of vascular and bronchial tone via the synthesis of endothelium-derived hyperpolarizing factor (127 129).

The expression of CYP2D6 in lung is debated (8), although there is support for low-level expression in bronchial mucosal cells. CYP2D6 is a highly polymorphic enzyme, and the expression of the "extensive metabolizer" phenotype is associated with increased risk for lung cancer in heavy smokers (89). CYP2D6 metabolizes a number of pharmaceutical agents, including basic amine-containing drugs, nicotine, opiates, and structurally related substances. CYP2D6 may also bioactivate NNK and other carcinogens (130,131).

CYP2E1 is ubiquitously expressed in lung tissue, particularly in Clara, bronchial, bronchiolar, alveolar epithelial, and endothelial cells . Some studies have suggested that this enzyme can be induced by ethanol (132) or pyridine (133) in lung tissues and in nasal tissues. The CYP2E1 enzyme is primarily active toward small halogenated hydrocarbons (134 138), and several of these chemicals cause Clara cell damage in animals via the formation of electrophilic intermediates. CYP2E1 bioactivates ethyl carbamate, urethane (139,140), and nitrosamines (141) to produce carcinogenic electrophiles. CYP2E1 catalyzes the epoxidation of DCE to its ultimate electrophilic intermediates (Fig. 3) (61,62). Pulmonary damage elicited by CYP2E1-induced processes is typically not as selective for lung tissue damage as for liver toxicity because 2E1 is usually expressed more extensively in the liver, but the selective necrosis of Clara cells indicates that expression of 2E1 in Clara cells is the primary mechanism of toxicity for several pneumotoxicants. Indeed, the toxicity of DCE to Clara cells has been linked specifically to the expression of Cyp2e1 in mice (138), although recent evidence suggests that Cyp2f2 may be more important than Cyp2e1 in the observed metabolism-dependent toxicity for DCE (61,62). Metabolism of DCE by 2e1 and 2f2 produces both chloral and the epoxide of DCE, 1,1-dichlorooxirane. Studies have quantified the formation of the glutathione adduct of DCE epoxide in vitro and in vivo and have demonstrated that the primary ultimate electrophile in the cytotoxic process is the epoxide (61,62). CYP2E1 is also most likely the catalyst for the oxidation of 1,1-dichloro-2,2-bis(*p*-chlorophenyl) ethane (DDD) to a reactive acyl halide intermediate that causes necrosis in isolated Clara cells and human bronchial epithelial cells (141,142).

An example of P450 enzymes that are selectively expressed in pulmonary tissues is a CYP2F subfamily enzyme. Four members of this subfamily have been identified from

human (69), mouse (143), goat (56), and rat (144). Rabbits, rats, goats, and humans show high selectivity for transcription in pulmonary tissues (54,69). CYP2F1, the human enzyme, catalyzes the metabolism of ethoxycoumarin, propoxycoumarin, and pentoxyresorufin (69), and the bioactivation of benzene (145,146), 3MI (147), naphthalene, styrene, DCE, and NNK (56,72,73,148). CYP2F1 is expressed in alveolar macrophages, epithelial and endothelial cells in the lung (8,149). The production of 3-methyleneindolenine, the putative pneumotoxic electrophilic intermediate of 3MI (Fig. 4), has been shown to be highest for CYP2F1 compared with 11 other human P450 enzymes, including CYP4B1, 1A2, 3A4, and 2E1 (147). Production of the methylene imine intermediate of 3MI by CYP2F1 has been shown to induce DNA damage and apoptosis in human bronchial epithelial cells expressing CYP2F1 (53), and covalent binding of the methylene imine intermediate to cellular nucleophiles in lung tissues is directly correlated with the expression and action of CYP2F enzymes (69). 3-Methyleneindolenine alkylates both DNA (150) and proteins (41,55), and the electrophile is potent enough to cause mechanism-based inactivation of both CYP2F1 and CYP2F3 (58). The goat 2F3 enzyme has also been cloned and characterized (56). Similar to CYP2F1, 2F3 demonstrated catalytic specificity for the dehydrogenation of 3MI, without detectable formation of any oxygenated products. Thus, the organ-selective toxicity of 3MI for the lung appears to be predominantly explained by the selective expression of the CYP2F enzyme and its efficient production of the toxic methylene imine intermediate.

Similar to CYP2F1 and CYP2F3, the mouse Cyp2f2 enzyme is an efficient catalyst of 3MI dehydrogenation and DCE epoxidation (61,62). Cyp2f2 is also the primary stereoselective catalyst of the *1R,2S*-naphthalene oxide (Fig. 2), the putative reactive epoxide that produces Clara cell necrosis in mice. This enzyme is highly localized to the Clara cells in distal bronchioles of mouse lung (151), and the production of the reactive epoxide was much higher in the microdissected distal airways from mice than from hamsters or rats, two species with less susceptibility to naphthalene toxicity.

CYP2J2 is another extrahepatic P450 expressed in the lung, particularly in ciliated epithelial cells of the human airway (152). CYP2J2 catalyzes the epoxidation of arachidonic acid to bioactive epoxyeicosatrienoic acids (EETs) and is believed to play a key role in modulating airway smooth muscle tone and cellular ion homeostasis (153 157). CYP2J2 has not been shown to act on traditional xenobiotic P450 substrates (43).

CYP2S1 mRNA is highly expressed in epithelial cells of the nasal passages, trachea, bronchi, and bronchioles, with limited expression in alveolar cells (158,159). CYP2S1 expression can be induced by TCDD binding to the AhR receptor (160), as well as by all-*trans* retinoic acid (161), UV light (161), and carcinogenic PAHs present in coal tar (160). CYP2S1 also appears to be upregulated in tumor cells (162), leading some to believe that it is integral in the metabolism of endogenous substrates involved in cell cycle control. To date, specific substrates for CYP2S1 have not been identified despite extensive screening efforts (163,164), although claims have been made that this enzyme can bioactivate naphthalene (165) and metabolize retinoic acid by hydroxylation and epoxidation (161).

CYP3A4 and 3A5 are expressed in human lungs. The dominant CYP3A isoform expressed in human lungs is CYP3A5, and expression is highest in bronchial and alveolar epithelial cells, alveolar macrophages, and bronchial glands (8,166,167). Many studies reported a lack of evidence for the expression of CYP3A4 in human lung (66,168 170), but one report indicated that CYP3A4 was expressed in about 20% of individuals (166). However, 3A5 is almost always found in human lung samples. CYP3A5 expression in the lung is dramatically induced by glucocorticoids through binding to the glucocorticoid receptor in human adenocarcinoma cells, and is repressed by cigarette smoke (171).

CYP3A4 expression appears to be repressed in lung cells by differential binding of transcription factors including pregnane X receptor (PXR) and the constitutive androstane receptor (CAR) (170) as well as a yet unidentified lung-selective factor that binds to a specific 57 base pair region in the promoter region of CYP3A4, but not 3A5, because CYP3A5 lacks this motif (168). CYP3A enzymes are prolific and have the broadest substrate selectivity of all P450 enzymes, often showing little limitation in their ability to metabolize a chemical (43). Bioactivation of aflatoxin B1 to its carcinogenic epoxide (172,173) has been attributed to CYP3A4 expression in the lung, and CYP3A5 may bioactivate NNK (109). In general, however, few differences in substrate selectivity have been documented for these enzymes, and differential toxicity due to CYP3A activity is primarily due to differences in enzyme expression.

CYP4B1 mRNA is routinely detected in human lung samples, although the expression of a functional enzyme in human lung tissue is controversial (8,174). The prototypical substrate for the CYP4B1 enzyme from rabbit lung is 2-aminofluorene (175), and 4-ipomeanol, a classic pneumotoxicant, is metabolized effectively by this enzyme in rabbit and rat lung tissues. Recombinant human 4B1 did not bioactivate 4-ipomeanol, although the rabbit enzyme expressed in the same system was an efficient catalyst of 4-ipomeanol bioactivation (176). The rabbit cDNA has been expressed in mouse C3H/10T1/2 cells, and in these cells, the enzyme bioactivated 4-ipomeanol to a cytotoxic intermediate (177). CYP4B1 also metabolized 2-aminoanthracene in these cells to produce cytotoxicity. Recombinant goat CYP4B2 was expressed primarily in the lung and catalyzed the oxygenation of 2-aminofluorene, the prototype substrate for CYP4B1 enzymes, as well as preferential dehydrogenation of 3MI to the pneumotoxic methylene imine metabolite (74). It is possible that CYP4B2 is a major contributor to the pneumotoxicity of 3MI in goats.

Prostaglandin Synthases/Cyclooxygenases

Prostaglandin endoperoxide synthases or cyclooxygenases PGHS1/COX1 and PGHS2/COX2 are another important group of xenobiotic-metabolizing enzymes present in the lung. These enzymes are responsible for the biosynthesis of prostaglandins and thromboxanes (178 181). Recently, COX3 and partial COX1 (PCOX1) have been described (182). *bis*-dioxygenation of arachidonic acid by the cyclooxygenase function of PGH synthases yields the hydroperoxide-endoperoxide PGG_2. Subsequent two-electron reduction of the hydroperoxide by the peroxidase function of PGH synthases produces PGH_2. PGH_2 is the precursor of other prostaglandins (D_2, E_2, $F_{2\alpha}$, and I_2) and thromboxane A_2. Arachidonic acid metabolites have been shown to be produced by human alveolar type II cells (183).

The peroxidase function of PGH synthases is similar in nature to that of other heme peroxidases that metabolize xenobiotics. PGH synthases form activated iron-oxo intermediates analogous to compounds I and II of horseradish peroxidase and exhibit relatively broad substrate specificity, reducing alkyl and lipid hydroperoxides as well as H_2O_2 (184,185). The relatively high oxidation potentials of the intermediate iron-oxo heme compounds that form during PGH synthase turnover can often facilitate the cooxidation of xenobiotics, including the one-electron oxidation of potentially pneumotoxic phenols and aromatic amines like 2-aminofluorene and benzidine, a potent bladder carcinogen (186,187). Products of PGH synthase mediated cooxidation reactions are frequently shown to be identical to those produced by P450- and peroxidase-catalyzed reactions (188). Classic examples of PGH synthase mediated cooxidation of human lung toxicants and carcinogens are aflatoxin B1 metabolism (189 191) and the conversion of

benzo[*a*]pyrene 7,8-dihydrodiol to the genotoxic benzo[a]pyrene-7,8-diol-9,10-epoxide metabolite via hydroperoxide-dependent mechanisms (192,193). Epoxidation of the benzo[*a*]pyrene 7,8-dihydrodiol is predominantly catalyzed by PGH synthase, not P450s, in type II alveolar cells from rats (194). PGH synthase has also been shown to catalyze the epoxidation of the diol to tetrols (after hydrolysis of the epoxide) at approximately half the rate of P450-mediated turnover in hamster trachea and human lung explants (192).

Flavin-Containing Monooxygenases

The FMOs are another class of xenobiotic-metabolizing enzymes. The participation of the FMO enzymes in the metabolism of xenobiotics has been well documented, but the contribution of FMOs to oxidative metabolism is limited relative to P450 enzymes. However, in some instances, metabolism by FMOs is dominant, especially for the oxidation of *N*-, *P*-, and *S*-containing chemicals. In humans, the *FMO* family consists of six genes whose protein products catalyze N-, P-, and S-oxidation of nucleophilic small-molecule xenobiotics to the corresponding *N*-, *P*-, and *S*-oxides (195,196). The active site of FMOs is an activated C(4a)-hydroperoxide flavin generated by addition of oxygen to reduced flavin adenine dinucleotide ($FADH_2$) (197). This intermediate is relatively stable and FMOs typically reside in the activated form until a suitable substrate enters the enzyme active site (198,199). Primary and secondary amines are good substrates for FMOs, but several other unusual substrates, such as secondary and tertiary amines, hydrazines, phosphines, iodides, and sulfides, are oxidized by these enzymes (195,196). Recently, FMO3 has been shown to catalyze the N-oxidation of indoline to form *N*-hydroxyindole, *N*-hydroxyindoline, and an interesting novel dimer of indoline, [1,4,2,5] dioxadiazino[2,3-*a*:5,6-*a*′]diindole (200). Similar to P450 enzymes, FMOs generally convert lipophilic xenobiotics to more polar, oxygenated metabolites that are more readily excreted.

The expression of FMO1, FMO2, FMO2.1, and FMO3 and FMO5 are generally considered to be organ selective (195,196,201). In the human lung, FMO2 is the primary FMO enzyme. Quantitative PCR analysis has shown that FMO2 mRNA is present at 50-fold higher concentrations than FMO3 and FMO5 and 150-fold higher than FMO1 and FMO4 (201). In mice, FMO2 is also the dominant lung enzyme. However, FMO1 is also expressed at moderate levels, representing ~34% of the total FMO transcripts, compared with the expression of approximately 59% for FMO2 (202). FMO6 is also expressed at low levels in the human lung, but *FMO6* is a nonfunctional pseudogene (195,196). Similarly, the *FMO2* gene (the FMO2*2 allele) in Caucasians and Asians codes for a prematurely truncated protein that is readily degraded. FMO2.1, the full-length and functional form of FMO2 arising from the *FMO2*1* genotype, is expressed in ~13% to 26% of African Americans (196,203,204) and ~5% of Hispanics (99,196,204). Currently, the significance of FMO2.1 expression in human lungs remains incompletely defined, but African Americans or Hispanics are likely to be significantly more susceptible to thiourea-mediated pneumotoxicity.

FMO-dependent metabolism is generally considered protective, and it typically reduces both the toxicological and pharmacological potency of substrates (8,196). However, examples of bioactivation of xenobiotics to electrophiles have been demonstrated. Examples include the conversion of thioureas like phenylthiourea (Fig. 5) to its sulfenic acid and in a subsequent oxidation step to the sulfinic acid (205,206). The toxicity of the thiourea was postulated to occur by redox cycling of the sulfenic acid with the parent thiourea, coupled to the oxidation of glutathione to its dimer. The pulmonary-selective FMO2.1 protein is functional and catalytically unique compared with the other

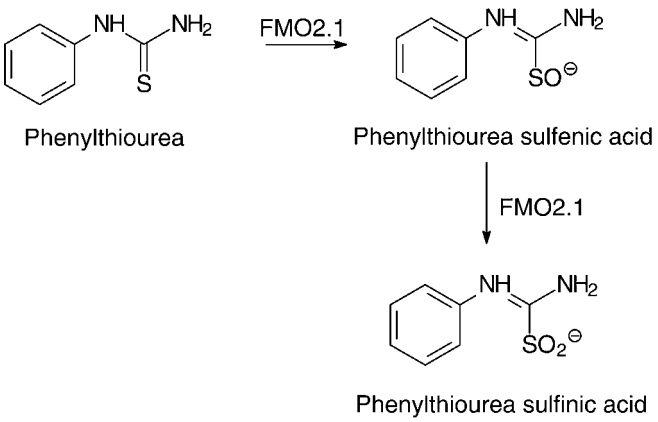

Figure 5 The functional FMO2.1 enzyme is not present in Caucasians and Asians, who have the *FMO**2 allele that codes for a prematurely truncated protein. The functional enzyme is only present in respiratory cells of approximately 13% to 26% of African Americans and 5% of Hispanics. Oxidation of phenylthiourea to its sulfenic acid metabolite and reduction back to the thiourea by glutathione oxidation to its disulfide leads to potent acute lung injury by reactive oxygen species and NADPH depletion. FMO2.1 also catalyzes the subsequent oxidation to the sulfinic acid metabolite. *Abbreviation*: FMO, flavin containing monooxygenases.

FMOs, in that it exhibits significant thermal stability and more stringent substrate selectivity, presumably due to a restricted substrate access channel. FMO2.1 readily catalyzes the N-oxidation of primary alkyl amines, including *n*-dodecylamine, to produce *N*-hydroxy primary amines, which can be oxidized to oximes (195,196,201). Human FMO2.1 also catalyzes the oxidation of lipoic acid (195,196,201) and organophosphate insecticides, including the efficient oxidation of phorate, disulfoton (204), and the lung toxicant, ethylenethiourea (205).

Finally, the physiological role of FMO enzymes has also been explored, particularly the role of FMOs in the metabolism of endogenous cysteamine to regulate cellular thiol status and H_2O_2 levels, as well as their metabolism of farnesylated proteins, and trimethylamine (195,196). As such, it is possible that FMO2.1 may contribute significantly to pulmonary homeostasis during oxidative stress induced by selected pneumotoxic xenobiotics in addition to having a direct role in the metabolic modification of selected substrates. Whether differential expression of FMO2 and FMO2.1 plays a major role in determining individual differences in susceptibility to selected pneumotoxicants remains to be determined.

HYDROLYSIS AND CONJUGATION ENZYMES

Epoxide Hydrolases

Epoxide hydrolases (EPHX1 and EPHX2) catalyze the hydration of arene, alkene, and aliphatic epoxides of PAHs and aromatic amines to form *trans*-dihydrodiols. EPHX1 is the endoplasmic reticulum localized form, while EPHX2 is cytosolic. EPHXs contribute to both bioactivation and detoxification processes, depending on the substrate and cellular context. The levels of these enzymes are lower in lung homogenates relative to liver preparations, however, EPHX expression and function are detectable. Recently, it has

been shown that 3-methylcholanthrene induces microsomal EPHX1 activity in both rat lung and liver, albeit induction in the lung was ~50% of that of the liver (207). Furthermore, analysis of EPHX1 and EPHX2 gene expression in primary lung parenchymal cells confirmed the expression of both EPHX1 and EPHX2 as well as a number of CYP genes (169). EPHX1 was expressed at a level similar to that for cryopreserved hepatocytes, while EPHX2 was ~50% (169).

However, as stated above, the cellular distribution of most drug-metabolizing enzymes is highly variable in the lung. EPHX-mediated hydrolysis of styrene oxide was highest in the distal airways of beagle dog lungs, and the observed levels were twice that of liver preparations (208). High EPHX activities in the distal airways corresponded to increases in Clara cell abundance, and EPHX activity was significantly higher in isolated Clara cells versus alveolar type II cells (209) and presumably other epithelial cell types. As such, it seems that EPHXs are expressed more abundantly in more metabolically competent cells that generate higher amounts of reactive cytotoxic or genotoxic epoxides. Here EPHXs likely play critical roles in the detoxication of potentially deleterious electrophilic epoxide intermediates generated by the P450 enzymes. This concept is supported by findings that EPHX1 expression was markedly induced in bronchoalveolar lavage samples of smokers but repressed in bronchial biopsy samples taken from anterior portions of the lung; BAL samples consisted primarily of macrophages, but bronchial biopsy samples were comprised of epithelial cells (95). The authors speculated that repression of EPHX1 in smokers was potentially beneficial in the context of bioactivation of benzo[a]pyrene. However, it is likely that reduced EPHX1 expression may have other adverse consequences in smokers, as discussed below.

The balance between bioactivation and detoxification is the principal determinant of metabolism-dependent toxicities and ultimately in the frequency of formation of neoplastic lesions. EPHXs are a double-edged sword. A direct role for epoxide hydrolase in pulmonary drug toxicities is demonstrated by the hydration of benzo[a]pyrene-7,8-epoxide following oxidation of benzo[a]pyrene by selected P450 enzymes. The product of epoxide hydrolysis is the benzo[a]pyrene-7,8-diol, which can be readily conjugated and detoxified by conjugation enzymes. However, subsequent oxidation of the benzo[a] pyrene-7,8-diol to the benzo[a]pyrene-7,8-diol-9,10-epoxide by P450s represents the principal mechanism leading to DNA mutations and lung cancer. Despite the role of pulmonary EPHXs in the detoxification of selected epoxide intermediates, elevated EPHX1 activity has been associated with an increased risk for lung cancer (210), particularly when CYP1A1 expression is high (211), while decreased EPHX1 activity, either through low levels of expression or through the expression of poor-functioning polymorphic variants (i.e., Y113H and H139R), has been associated with slightly decreased risks for lung cancer (212).

Uridine Diphosphate Glucuronosyltransferases

Uridine diphosphate glucuronosyltransferases (UGT) are a superfamily of microsomal xenobiotic-metabolizing enzymes that catalyze the addition of uridine diphosphate (UDP)-glucuronic acid to small hydrophobic molecules with highly diverse structures. UGTs provide a primary mechanism of protection against the accumulation of unfolded proteins in the endoplasmic reticulum (213) and toxic xenobiotics and/or their oxidative products to render potentially toxic substances inactive and amenable for excretion (214). The *UGT* family of genes is divided into two subfamilies, *UGT1* and *UGT2* (215 217). The human *UGT1* subfamily is distinctively derived from a single gene locus and consists

of *UGT1A1, 1A3, 1A4, 1A5, 1A6, 1A7, 1A8, 1A9*, and *1A10*. The UGT2 subfamily is comprised of multiple, similar genes that have evolved from gene duplication. The *UGT2* family is comprised of *UGT2A1, 2A2, 2B4, 2B7, 2B10, 2B11, 2B15, 2B17*, and *2B28*. The different UGT enzymes often exhibit overlapping substrate profiles (218), but UGT2B proteins exhibit reduced capacity to metabolize phenolic and heterocyclic compounds, such as the known carcinogens and procarcinogens found in cigarette smoke (215). Conversely, UGT1 enzymes are highly active toward these substances.

UGT1A1, 1A3, 1A4, 1A6-1, 1A9, 2B4, 2B7, and 2B11 transcripts are considerably more abundant in human liver, while UGT1A6-2, 1A7, 1A8, 1A10, and 2A1 are primarily extrahepatic UGTs that are expressed at moderate levels in human pulmonary tissues (169,219 221). Transcripts for UGT1A1, 1A3, 1A5, 1A7, 1A8, and 2B12 were amplified from rat lung (220), while UGT1A1, 1A4, 1A6-1 and 1A6-2, 2A1, 2B4, 2B7, and 2B11 were detected in human lung samples and in most upper aerodigestive tract tissues including the mouth and tongue (169,221). In general, the overall extent of glucuronidation of xenobiotics by pulmonary tissues is considered to be minimal, but not insignificant with respect to xenobiotic toxicology. For example, 4-nitrophenol glucuronidation in rat lung microsomes is only 30% of the rat liver microsomal rate of glucuronidation (222). However, cell type selective differences in metabolic capacity were observed, because rat Clara cells glucuronidated 4-methylumbelliferone to a greater extent than did isolated alveolar type II cells (223). Again, the overall metabolic capacity of Clara cells is generally higher than that of other cells in the lung. Recently it has been shown that a mixture of PAHs was able to induce the expression of rat lung UGT1A6 and 1A9. However, the glucuronidation activities of UGT1A6 and 1A9 were considerably lower and were highly variable in human lungs (224). Unfortunately, other UGT activities were not evaluated in this study, but the authors (169) showed similar results using multiple probe substrates. In 2002, no member of the UGT1A genes had been found to be expressed in human lung tissue (221), but the recent studies described above confirm the low-level expression of a number of UGT1 enzymes. In contrast, UGT2A1, 2B4, 2B7, 2B10, 2B11, 2B15, and 2B17 are expressed in human and animal nasal epithelium and lung at levels equal to or even greater than that in liver (169,221,225,226). In fact, UGT2A1 appears to be selectively expressed at high levels in the nasal epithelium (220,225) and to a lesser extent in the whole lung, albeit still higher than that in hepatocytes (169). Recombinant UGT2A1 gene expressed in mammalian cells has broad substrate selectivity, and it shows activity toward a number of phenolic, aliphatic, and monoterpenoid alcohols, selected steroids and androgens, and carcinogens (225). It is therefore possible that this enzyme plays a direct role in the inactivation of odorants such as eugenol (227).

Examples of bioactivation of xenobiotics to toxins by UGTs are limited, and contributions to toxicity are typically due to a lack of efficient detoxification of xenobiotics by UGT enzymes rather than a gain of toxicity. A mechanism (Fig. 6) for the pneumotoxicity and pulmonary carcinogenicity of trichloroethylene has been proposed to be mediated by deficient UGT activities in lung Clara cells (228). The authors showed that isolated Clara cells from mice did not possess sufficient UGT activity to glucuronidate trichloroethanol, while isolated hepatocytes efficiently formed this inactive metabolite. The lack of glucuronidation of trichloroethanol was proposed to lead to the buildup of the cytotoxic P450-generated intermediate, chloral, in the Clara cells. Thus, the lack of detoxication by glucuronidation in susceptible cells was proposed as an operative mechanism for the toxicity of trichloroethylene. It is also possible that bioactivation by glucuronidation may produce toxicities to respiratory tissues, by mechanisms analogous to acyl-linked glucuronide toxicities to hepatic tissues (229) and renal tissues (230).

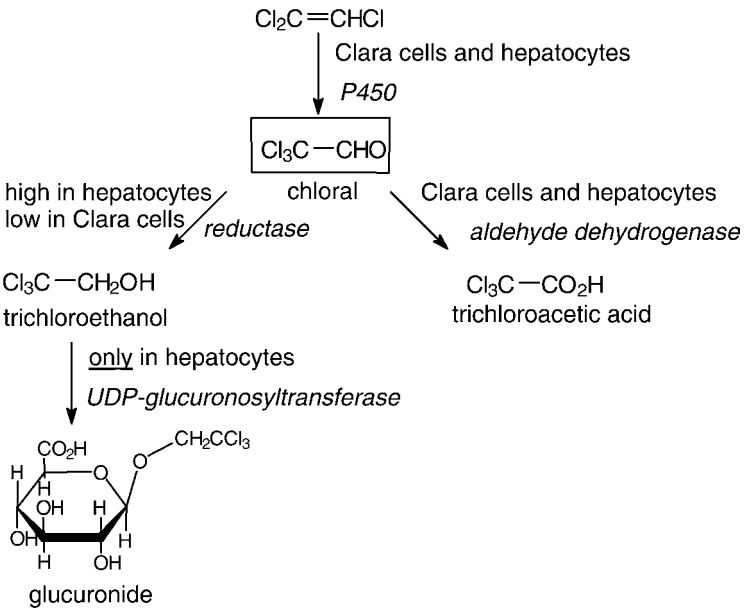

Figure 6 Mechanism of selective Clara cell damage by trichloroethylene, caused by the lack of detoxification. Although chloral, the putative toxic intermediate from trichloroethylene can be formed in both mouse lung Clara cells and in hepatocytes; efficient detoxication of this aldehyde by reductase and by UGT is lacking in the lung epithelial cells. *Abbreviation*: UGT, uridine diphosphate glucuronosyltransferases.

Glutathione *S*-Transferases

Glutathione *S*-transferases (GSTs) catalyze the nucleophilic addition of reduced glutathione to hydrophobic compounds that contain electrophilic carbon, nitrogen, and sulfur atoms. Prototypical substrates include halogen or nitrobenzenes [e.g., 1-chloro-2,4-dinitrobenzene (CDNB)], arene oxides, quinones, and α,β-unsaturated carbonyls. Furthermore, GSTs catalyze the isomerization of unsaturated compounds and participate in the synthesis of various prostaglandins and leukotrienes (231 233). Cytosolic, microsomal, and mitochondrial forms of GST exist. Cytosolic GSTs are the largest family of enzymes and are comprised of two subunits of 199 to 244 amino acids each. Cytosolic GSTs are divided into the following seven major subclasses: alpha (GSTA1 through A5), mu (GSTM1 through M5), kappa (GSTK1), theta (GSTT1 and T2), omega (GSTO1 and O2), pi (GSTP1), sigma (GSTS1), and zeta (GSTZ1), on the basis of amino acid similarities and antibody cross-reactivity. At least 16 different cytosolic GSTs are expressed by humans, due in part to the fact that alpha and mu class GST subunits form heterodimers (231). Mitochondrial GSTs are dimeric enzymes comprised of 226 amino acid kappa class subunits. Microsomal GSTs are now referred to as membrane-associated proteins in eicosanoid and glutathione metabolism (MAPEGs), highlighting the key role of these enzymes in eicosanoid biosynthesis (231,232).

The expression of GSTs in respiratory tissues has been evaluated in animals and in humans. The precise elucidation of which GSH transferase exists in which cells of the respiratory system has not been accurately determined, because most studies simply determine the aggregate CDNB activities of gene expression in lung homogenates or

Table 1 Xenobiotic-Metabolizing Enzymes in the Respiratory Tract

Enzyme	Species	Substrate	Localization
Cytochrome P450 Enzymes			
1A1	All	Ethoxyresorufin, polycyclic aromatic hydrocarbons	Olfactory epithelium, Clara cells, type II cells, induced macrophages
1B1	Rat, mouse, human	Polycyclic aromatic hydrocarbons	Unknown
2A3	Rat	Unknown	Unknown
2A6/13	Human	Diethylnitrosamine, aflatoxin B_1, 4-(methylnitrosamino)-l-(3-pyridyl)-l-butanone	Trachea, olfactory mucosa, lung
2B1/4/6	Rabbit, rat, human	Arachidonic acid, butylated hydroxytoluene	Clara cells
2E1	All	4-Nitrophenol, dimethylnitrosamine, dichloroethylene	Nasal tissues
2F1/2/3/4	All	Ethoxycoumarin, naphthalene, 3-methylindole	Clara cells, trachea
2G1	Rabbit	Testosterone	Olfactory mucosa
2J2	All	Arachidonic acid	Ciliated epithelial
2S1	All	Retinoic acid	Epithelial cells
3A5	Human	Benzo[a]pyrene-7,8-diol, testosterone	Bronchial and alveolar epithelium
4B1/2	All	2-Aminoflourene, 4-ipomeanol, valproic acid	Clara cells
Prostaglandin H synthase	All	Benzo[a]pyrene-7,8-diol	Endothelial and epithelial cells
Flavin-containing monooxygenases	All	Amines, phosphines, sulfides	Entire respiratory system
Epoxide hydrolases	All	Polycyclic aromatic hydrocarbon epoxides	Clara cells
Uridine diphosphate glucuronosyltransferases	All	1-Naphthol, 4-methylumbelliferone, eugenol	Clara cells
Glutathione *S*-transferases	All	1-Chloro-2,4-dinitrobenzene, benzopyrene epoxide	Clara cells and ciliated cells

mixed populations of cells. CDNB activity distribution in the lung was slightly higher in proximal airways than in distal airways of the mouse and monkey (234). It appears that at least the alpha, mu, and pi classes are expressed in rat (235) and human (236) lung samples. It has been shown that the pi, mu, and alpha classes of GSTs represent approximately 94%, 3%, and 3%, respectively, of the total human lung activity toward CDNB (237), although differences in the ability to catalyze CDNB conjugation likely confounded determination of the true ratios of enzyme expression. Regardless, immunochemical staining of GST enzymes in human lungs demonstrated expression of the alpha and pi forms in large- and small-airway epithelial tissues (236), and recent studies of BAL and bronchial biopsy samples from smokers and nonsmokers confirmed the expression of GSTP1, GSTA2, and GSTM1. Cytosolic GST alpha was mildly induced by 3-methylcholanthere in rat lungs (207). As with many other drug-metabolizing enzymes, Clara cells tend to have considerably higher GST activity than alveolar type II cells, using CDNB as a probe (223,238), consistent with the expected elevated production of reactive electrophiles by resident P450 (and other) enzymes in Clara cells.

Conjugation of xenobiotics by GST enzymes is typically considered protective. GSTs, particularly GSTP1, are overexpressed during lung cancer, rendering the cancer cells less susceptible to some anticancer drugs. Several studies have attempted to link polymorphisms of the mu class of GSTs in human lung tissues with susceptibility to lung cancer induced by cigarette smoking (239). A particularly strong association has been shown between genetic polymorphisms in the CYP1A1 gene and a deficient genotype of GSTM1, relative to lung cancer induced by cigarette smoking (240). Individuals with both genetic alterations had elevated risks for lung cancer from smoking.

Similarly, GSTA4-null mice have been shown to be more sensitive to the pneumotoxicant paraquat and to exhibit a reduced capacity to conjugate the toxic α,β-unsaturated aldehyde 4-hydroxynonenal (241). Conjugation with GSH has been shown to be protective in the lung against toxicities elected by DCE (61,135), naphthalene (242 244), 3MI (55), and isocyanates (245,246). However, there are some instances where conjugation promotes toxicity, such as that observed with formation of the unstable electrophilic DNA-modifying agent *S*-chloromethylglutathione from dichloromethane (247,248) or the depletion of intracellular GSH stores via recycling of selected isothiocyanate conjugates (i.e., thiocarbamates).

CONCLUSIONS

This chapter has attempted to provide a brief overview of the metabolic enzymes that exist in respiratory tissues, and has made an effort to distinguish this organ system from other anatomical regions that participate to a greater or lesser extent in the metabolism of xenobiotics. The lung should not be viewed as a metabolic organ with lower activities than liver, but rather as an active, dynamic, and often highly selective metabolic tissue with important contributions to xenobiotic disposition and toxicity. The complexity of cellular distribution and function in respiratory tissues provides a unique paradigm for scientists involved in drug metabolism, toxicology, and risk assessment. As we learn more about the mechanisms of selective gene expression in certain lung cells and the functional consequences of the enzymology of the gene products, predictions of metabolic processes and toxicological consequences will become possible.

REFERENCES

1. Bond JA. Metabolism of xenobiotics by the respiratory tract. In: Gardner DE, Crapo JD, McClellan RO, eds. Toxicology of the Lung. New York: Raven Press, 1993:187 215.
2. Buckpitt AR, Cruikshank MK. Biochemical function of the respiratory tract: metabolism of xenobiotics. In: Sipes IG, McQueen CA, Gandolfi AJ, eds. Comprehensive Toxicology. New York: Elsevier Science, 1997:159 186.
3. Castell JV, Donato MT, Gomez Lechon MJ. Metabolism and bioactivation of toxicants in the lung. The in vitro cellular approach. Exp Toxicol Pathol 2005; 57(suppl 1):189 204.
4. Dahl AR, Lewis JL. Respiratory tract uptake of inhalants and metabolism of xenobiotics. Annu Rev Pharmacol Toxicol 1993; 33:383 407.
5. Ding X, Kaminsky LS. Human extrahepatic cytochromes P450: function in xenobiotic metabolism and tissue selective chemical toxicity in the respiratory and gastrointestinal tracts. Annu Rev Pharmacol Toxicol 2003; 43:149 173.
6. Foth H. Role of the lung in accumulation and metabolism of xenobiotic compounds implications for chemically induced toxicity. Crit Rev Toxicol 1995; 25:165 205.
7. Yost GS. Bioactivation and selectivity of pneumotoxic chemicals. In: Neumann H G, Dekant W, eds. Tissue Specific Toxicity: Biochemical Mechanisms. London: Academic Press; 1992: 195 220.
8. Zhang JY, Wang Y, Prakash C. Xenobiotic metabolizing enzymes in human lung. Curr Drug Metab 2006; 7:939 948.
9. Yost GS. Sites of metabolism: lung. In: Wolf TF, ed. Handbook of Drug Metabolism. New York: Marcel Dekker, Inc., 1999:263 278.
10. Weissmann N, Seeger W, Conzen J, Kiss L, Grimminger F. Effects of arachidonic acid metabolism on hypoxic vasoconstriction in rabbit lungs. Eur J Pharmacol 1998; 356:231 237.
11. Yaghi A, Webb CD, Scott JA, Mehta S, Bend JR, McCormack DG. Cytochrome P450 metabolites of arachidonic acid but not cyclooxygenase 2 metabolites contribute to the pulmonary vascular hyporeactivity in rats with acute Pseudomonas pneumonia. J Pharmacol Exp Ther 2001; 297:479 488.
12. Dinis Oliveira RJ, Duarte JA, Sanchez Navarro A, Remiao F, Bastos ML, Carvalho F. Paraquat poisonings: mechanisms of lung toxicity, clinical features, and treatment. Crit Rev Toxicol 2008; 38:13 71.
13. Gram TE. Chemically reactive intermediates and pulmonary xenobiotic toxicity. Pharmacol Rev 1997; 49:297 341.
14. Howell RE, Lanken PN. Pulmonary accumulation of propranolol in vivo: sites and physiochemical mechanism. J Pharmacol Exp Ther 1992; 263:130 135.
15. Vestal RE, Kornhauser DM, Shand DG. Active uptake of propranolol by isolated rabbit alveolar macrophages and its inhibition by other basic amines. J Pharmacol Exp Ther 1980; 214:106 111.
16. Waters CM, Krejcie TC, Avram MJ. Facilitated uptake of fentanyl, but not alfentanil, by human pulmonary endothelial cells. Anesthesiology 2000; 93:825 831.
17. Waters CM, Avram MJ, Krejcie TC, Henthorn TK. Uptake of fentanyl in pulmonary endothelium. J Pharmacol Exp Ther 1999; 288:157 163.
18. Boer F, Olofsen E, Bovill JG, Burm AG, Hak A, Geerts M, Wetselaar KE. Pulmonary uptake of sufentanil during and after constant rate infusion. Br J Anaesth 1996; 76:203 208.
19. Larsson P, Tjalve H. Tracing tissues with 4 ipomeanol metabolizing capacity in rats. Chem Biol Interact 1988; 67:1 24.
20. Antonini JM, Reasor MJ. Accumulation of amiodarone and desethylamiodarone by rat alveolar macrophages in cell culture. Biochem Pharmacol 1991; 42(suppl):S151 S156.
21. Suhara T, Sudo Y, Yoshida K, Okubo Y, Fukuda H, Obata T, Yoshikawa K, Suzuki K, Sasaki Y. Lung as reservoir for antidepressants in pharmacokinetic drug interactions. Lancet 1998; 351:332 335.
22. Yoshida H, Okumura K, Hori R. Subcellular distribution of basic drugs accumulated in the isolated perfused lung. Pharm Res 1987; 4:50 53.

23. Junod AF. Accumulation of 14 C imipramine in isolated perfused rat lungs. J Pharmacol Exp Ther 1972; 183:182 187.
24. Himmelstein MW, Acquavella JF, Recio L, Medinsky MA, Bond JA. Toxicology and epidemiology of 1,3 butadiene. Crit Rev Toxicol 1997; 27:1 108.
25. Himmelstein MW, Asgharian B, Bond JA. High concentrations of butadiene epoxides in livers and lungs of mice compared to rats exposed to 1,3 butadiene. Toxicol Appl Pharmacol 1995; 132:281 288.
26. Lee MJ, Dinsdale D. The subcellular distribution of NADPH cytochrome P450 reductase and isoenzymes of cytochrome P450 in the lungs of rats and mice. Biochem Pharmacol 1995; 49:1387 1394.
27. Overby L, Nishio SJ, Lawton MP, Plopper CG, Philpot RM. Cellular localization of flavin containing monooxygenase in rabbit lung. Exp Lung Res 1992; 18:131 144.
28. Overby LH, Nishio S, Weir A, Carver GT, Plopper CG, Philpot RM. Distribution of cytochrome P450 1A1 and NADPH cytochrome P450 reductase in lungs of rabbits treated with 2,3,7,8 tetrachlorodibenzo p dioxin: ultrastructural immunolocalization and in situ hybridization. Mol Pharmacol 1992; 41:1039 1046.
29. Serabjit Singh CJ, Wolf CR, Philpot RM, Plopper CG. Cytochrome p 450: localization in rabbit lung. Science 1980; 207:1469 1470.
30. Hall PM, Stupans I, Burgess W, Birkett DJ, McManus ME. Immunohistochemical localization of NADPH cytochrome P450 reductase in human tissues. Carcinogenesis 1989; 10:521 530.
31. Nelson DR, Zeldin DC, Hoffman SM, Maltais LJ, Wain HM, Nebert DW. Comparison of cytochrome P450 (CYP) genes from the mouse and human genomes, including nomenclature recommendations for genes, pseudogenes and alternative splice variants. Pharmacogenetics 2004; 14:1 18.
32. Guengerich FP. Cytochromes P450, drugs, and diseases. Mol Interv 2003; 3:194 204.
33. Guengerich FP. Cytochrome P450: what have we learned and what are the future issues? Drug Metab Rev 2004; 36:159 197.
34. Guengerich FP. Mechanisms of cytochrome P450 substrate oxidation: MiniReview. J Biochem Mol Toxicol 2007; 21:163 168.
35. Nebert DW, Dalton TP. The role of cytochrome P450 enzymes in endogenous signalling pathways and environmental carcinogenesis. Nat Rev Cancer 2006; 6:947 960.
36. Nebert DW, Russell DW. Clinical importance of the cytochromes P450. Lancet 2002; 360:1155 1162.
37. Hodgson E, Rose RL. Human metabolic interactions of environmental chemicals. J Biochem Mol Toxicol 2007; 21:182 186.
38. Omura T. Mitochondrial P450s. Chem Biol Interact 2006; 163:86 93.
39. Wheeler CW, Guenthner TM. Spectroscopic quantitation of cytochrome P 450 in human lung microsomes. J Biochem Toxicol 1990; 5:269 272.
40. Wheeler CW, Guenthner TM. Cytochrome P 450 dependent metabolism of xenobiotics in human lung. J Biochem Toxicol 1991; 6:163 169.
41. Ruangyuttikarn W, Skiles GL, Yost GS. Identification of a cysteinyl adduct of oxidized 3 methylindole from goat lung and human liver microsomal proteins. Chem Res Toxicol 1992; 5:713 719.
42. Hukkanen J, Hakkola J, Anttila S, Piipari R, Karjalainen A, Pelkonen O, Raunio H. Detection of mRNA encoding xenobiotic metabolizing cytochrome P450s in human bronchoalveolar macrophages and peripheral blood lymphocytes. Mol Carcinog 1997; 20:224 230.
43. Hukkanen J, Pelkonen O, Hakkola J, Raunio H. Expression and regulation of xenobiotic metabolizing cytochrome P450 (CYP) enzymes in human lung. Crit Rev Toxicol 2002; 32:391 411.
44. Hukkanen J, Pelkonen O, Raunio H. Expression of xenobiotic metabolizing enzymes in human pulmonary tissue: possible role in susceptibility for ILD. Eur Respir J Suppl 2001; 32:122s 126s.
45. Piipari R, Savela K, Nurminen T, Hukkanen J, Raunio H, Hakkola J, Mantyla T, Beaune P, Edwards RJ, Boobis AR, Anttila S. Expression of CYP1A1, CYP1B1 and CYP3A, and

polycyclic aromatic hydrocarbon DNA adduct formation in bronchoalveolar macrophages of smokers and non smokers. Int J Cancer 2000; 86:610 616.
46. Raunio H, Hakkola J, Hukkanen J, Lassila A, Paivarinta K, Pelkonen O, Anttila S, Piipari R, Boobis A, Edwards RJ. Expression of xenobiotic metabolizing CYPs in human pulmonary tissue. Exp Toxicol Pathol 1999; 51:412 417.
47. Yost GS. Mechanisms of cytochrome P450 mediated formation of pneumotoxic electrophiles. In: Snyder R, ed. Biological Reactive Intermediates V. New York: Plenum Press, 1996:221 229.
48. Buckpitt A, Boland B, Isbell M, Morin D, Shultz M, Baldwin R, Chan K, Karlsson A, Lin C, Taff A, West J, Fanucchi M, Van Winkle L, Plopper C. Naphthalene induced respiratory tract toxicity: metabolic mechanisms of toxicity. Drug Metab Rev 2002; 34:791 820.
49. Baer BR, Rettie AE, Henne KR. Bioactivation of 4 ipomeanol by CYP4B1: adduct characterization and evidence for an enedial intermediate. Chem Res Toxicol 2005; 18:855 864.
50. Plopper CG, Weir AJ, Nishio SJ, Chang A, Voit M, Philpot RM, Buckpitt AR. Elevated susceptibility to 4 ipomeanol cytotoxicity in immature Clara cells of neonatal rabbits. J Pharmacol Exp Ther 1994; 269:867 880.
51. Verschoyle RD, Philpot RM, Wolf CR, Dinsdale D. CYP4B1 activates 4 ipomeanol in rat lung. Toxicol Appl Pharmacol 1993; 123:193 198.
52. Chen LJ, DeRose EF, Burka LT. Metabolism of furans in vitro: ipomeanine and 4 ipomeanol. Chem Res Toxicol 2006; 19:1320 1329.
53. Nichols WK, Mehta R, Skordos K, Mace K, Pfeifer AM, Carr BA, Minko T, Burchiel SW, Yost GS. 3 methylindole induced toxicity to human bronchial epithelial cell lines. Toxicol Sci 2003; 71:229 236.
54. Ramakanth S, Thornton Manning JR, Wang H, Maxwell H, Yost GS. Correlation between pulmonary cytochrome P450 transcripts and the organ selective pneumotoxicity of 3 methylindole. Toxicol Lett 1994; 71:77 85.
55. Thornton Manning JR, Nichols WK, Manning BW, Skiles GL, Yost GS. Metabolism and bioactivation of 3 methylindole by Clara cells, alveolar macrophages, and subcellular fractions from rabbit lungs. Toxicol Appl Pharmacol 1993; 122:182 190.
56. Wang H, Lanza DL, Yost GS. Cloning and expression of CYP2F3, a cytochrome P450 that bioactivates the selective pneumotoxins 3 methylindole and naphthalene. Arch Biochem Biophys 1998; 349:329 340.
57. Yan Z, Easterwood LM, Maher N, Torres R, Huebert N, Yost GS. Metabolism and bioactivation of 3 methylindole by human liver microsomes. Chem Res Toxicol 2007; 20:140 148.
58. Kartha JS, Yost GS. Mechanism based inactivation of lung selective cytochrome P450 CYP2F enzymes. Drug Metab Dispos 2008; 36:155 162.
59. Bolton JL, Thompson JA, Allentoff AJ, Miley FB, Malkinson AM. Metabolic activation of butylated hydroxytoluene by mouse bronchiolar Clara cells. Toxicol Appl Pharmacol 1993; 123:43 49.
60. Witschi H, Malkinson AM, Thompson JA. Metabolism and pulmonary toxicity of butylated hydroxytoluene (BHT). Pharmacol Ther 1989; 42:89 113.
61. Simmonds AC, Ghanayem BI, Sharma A, Reilly CA, Millen B, Yost GS, Forkert PG. Bioactivation of 1,1 dichloroethylene by CYP2E1 and CYP2F2 in murine lung. J Pharmacol Exp Ther 2004; 310:855 864.
62. Simmonds AC, Reilly CA, Baldwin RM, Ghanayem BI, Lanza DL, Yost GS, Collins KS, Forkert PG. Bioactivation of 1,1 dichloroethylene to its epoxide by CYP2E1 and CYP2F enzymes. Drug Metab Dispos 2004; 32:1032 1039.
63. Akopyan G, Bonavida B. Understanding tobacco smoke carcinogen NNK and lung tumorigenesis. Int J Oncol 2006; 29:745 752.
64. Hecht SS. Recent studies on mechanisms of bioactivation and detoxification of 4 (methylnitrosamino) 1 (3 pyridyl) 1 butanone (NNK), a tobacco specific lung carcinogen. Crit Rev Toxicol 1996; 26:163 181.
65. Nishikawa A, Mori Y, Lee IS, Tanaka T, Hirose M. Cigarette smoking, metabolic activation and carcinogenesis. Curr Drug Metab 2004; 5:363 373.

66. Bieche I, Narjoz C, Asselah T, Vacher S, Marcellin P, Lidereau R, Beaune P, de Waziers I. Reverse transcriptase PCR quantification of mRNA levels from cytochrome (CYP)1, CYP2 and CYP3 families in 22 different human tissues. Pharmacogenet Genomics 2007; 17:731 742.
67. Nishimura M, Yaguti H, Yoshitsugu H, Naito S, Satoh T. Tissue distribution of mRNA expression of human cytochrome P450 isoforms assessed by high sensitivity real time reverse transcription PCR. Yakugaku Zasshi 2003; 123:369 375.
68. Domin BA, Devereux TR, Philpot RM. The cytochrome P 450 monooxygenase system of rabbit lung enzyme components, activities, and induction in the nonciliated bronchiolar epithelial (Clara) cell, alveolar type II cell, and alveolar macrophage. Mol Pharmacol 1986; 30:296 303.
69. Nhamburo PT, Kimura S, McBride OW, Kozak CA, Gelboin HV, Gonzalez FJ. The human CYP2F gene subfamily: identification of a cDNA encoding a new cytochrome P450, cDNA directed expression, and chromosome mapping. Biochemistry 1990; 29:5491 5499.
70. Kupfer R, Dwyer Nield LD, Malkinson AM, Thompson JA. Lung toxicity and tumor promotion by hydroxylated derivatives of 2,6 di tert butyl 4 methylphenol (BHT) and 2 tert butyl 4 methyl 6 iso propylphenol: correlation with quinone methide reactivity. Chem Res Toxicol 2002; 15:1106 1112.
71. Meier BW, Gomez JD, Kirichenko OV, Thompson JA. Mechanistic basis for inflammation and tumor promotion in lungs of 2,6 di tert butyl 4 methylphenol treated mice: electrophilic metabolites alkylate and inactivate antioxidant enzymes. Chem Res Toxicol 2007; 20:199 207.
72. Lanza DL, Code E, Crespi CL, Gonzalez FJ, Yost GS. Specific dehydrogenation of 3 methylindole and epoxidation of naphthalene by recombinant human CYP2F1 expressed in lymphoblastoid cells. Drug Metab Dispos 1999; 27:798 803.
73. Lanza DL, Yost GS. Selective dehydrogenation/oxygenation of 3 methylindole by cytochrome p450 enzymes. Drug Metab Dispos 2001; 29:950 953.
74. Carr BA, Ramakanth S, Dannan GA, Yost GS. Characterization of pulmonary CYP4B2, specific catalyst of methyl oxidation of 3 methylindole. Mol Pharmacol 2003; 63:1137 1147.
75. Wheeler CW, Park SS, Guenthner TM. Immunochemical analysis of a cytochrome P 450IA1 homologue in human lung microsomes. Mol Pharmacol 1990; 38:634 643.
76. Willey JC, Coy E, Brolly C, Utell MJ, Frampton MW, Hammersley J, Thilly WG, Olson D, Cairns K. Xenobiotic metabolism enzyme gene expression in human bronchial epithelial and alveolar macrophage cells. Am J Respir Cell Mol Biol 1996; 14:262 271.
77. Willey JC, Coy EL, Frampton MW, Torres A, Apostolakos MJ, Hoehn G, Schuermann WH, Thilly WG, Olson DE, Hammersley JR, Crespi CL, Utell MJ. Quantitative RT PCR measurement of cytochromes p450 1A1, 1B1, and 2B7, microsomal epoxide hydrolase, and NADPH oxidoreductase expression in lung cells of smokers and nonsmokers. Am J Respir Cell Mol Biol 1997; 17:114 124.
78. Saarikoski ST, Husgafvel Pursiainen K, Hirvonen A, Vainio H, Gonzalez FJ, Anttila S. Localization of CYP1A1 mRNA in human lung by in situ hybridization: comparison with immunohistochemical findings. Int J Cancer 1998; 77:33 39.
79. McLemore TL, Adelberg S, Liu MC, McMahon NA, Yu SJ, Hubbard WC, Czerwinski M, Wood TG, Storeng R, Lubet RA, et al. Expression of CYP1A1 gene in patients with lung cancer: evidence for cigarette smoke induced gene expression in normal lung tissue and for altered gene regulation in primary pulmonary carcinomas. J Natl Cancer Inst 1990; 82:1333 1339.
80. Anttila S, Hietanen E, Vainio H, Camus AM, Gelboin HV, Park SS, Heikkila L, Karjalainen A, Bartsch H. Smoking and peripheral type of cancer are related to high levels of pulmonary cytochrome P450IA in lung cancer patients. Int J Cancer 1991; 47:681 685.
81. Wei C, Caccavale RJ, Weyand EH, Chen S, Iba MM. Induction of CYP1A1 and CYP1A2 expressions by prototypic and atypical inducers in the human lung. Cancer Lett 2002; 178:25 36.
82. Hukkanen J, Lassila A, Paivarinta K, Valanne S, Sarpo S, Hakkola J, Pelkonen O, Raunio H. Induction and regulation of xenobiotic metabolizing cytochrome P450s in the human A549 lung adenocarcinoma cell line. Am J Respir Cell Mol Biol 2000; 22:360 366.
83. Shou M, Korzekwa KR, Crespi CL, Gonzalez FJ, Gelboin HV. The role of 12 cDNA expressed human, rodent, and rabbit cytochromes P450 in the metabolism of benzo[a]pyrene and benzo[a]pyrene trans 7,8 dihydrodiol. Mol Carcinog 1994; 10:159 168.

84. Koehl W, Amin S, Staretz ME, Ueng YF, Yamazaki H, Tateishi T, Guengerich FP, Hecht SS. Metabolism of 5 methylchrysene and 6 methylchrysene by human hepatic and pulmonary cytochrome P450 enzymes. Cancer Res 1996; 56:316 324.
85. Hammons GJ, Milton D, Stepps K, Guengerich FP, Tukey RH, Kadlubar FF. Metabolism of carcinogenic heterocyclic and aromatic amines by recombinant human cytochrome P450 enzymes. Carcinogenesis 1997; 18:851 854.
86. Anttila S, Vainio H, Hietanen E, Camus AM, Malaveille C, Brun G, Husgafvel Pursiainen K, Heikkila L, Karjalainen A, Bartsch H. Immunohistochemical detection of pulmonary cytochrome P450IA and metabolic activities associated with P450IA1 and P450IA2 isozymes in lung cancer patients. Environ Health Perspect 1992; 98:179 182.
87. Bartsch H, Castegnaro M, Rojas M, Camus AM, Alexandrov K, Lang M. Expression of pulmonary cytochrome P4501A1 and carcinogen DNA adduct formation in high risk subjects for tobacco related lung cancer. Toxicol Lett 1992; 64 65 Spec No:477 483.
88. Chang KW, Lee H, Wang HJ, Chen SY, Lin P. Differential response to benzo[A]pyrene in human lung adenocarcinoma cell lines: the absence of aryl hydrocarbon receptor activation. Life Sci 1999; 65:1339 1349.
89. Vineis P. The relationship between polymorphisms of xenobiotic metabolizing enzymes and susceptibility to cancer. Toxicology 2002; 181 182:457 462.
90. Mollerup S, Berge G, Baera R, Skaug V, Hewer A, Phillips DH, Stangeland L, Haugen A. Sex differences in risk of lung cancer: expression of genes in the PAH bioactivation pathway in relation to smoking and bulky DNA adducts. Int J Cancer 2006; 119:741 744.
91. Kawajiri K, Nakachi K, Imai K, Watanabe J, Hayashi S. The CYP1A1 gene and cancer susceptibility. Crit Rev Oncol Hematol 1993; 14:77 87.
92. Nakachi K, Hayashi S, Kawajiri K, Imai K. Association of cigarette smoking and CYP1A1 polymorphisms with adenocarcinoma of the lung by grades of differentiation. Carcinogenesis 1995; 16:2209 2213.
93. Wei C, Caccavale RJ, Kehoe JJ, Thomas PE, Iba MM. CYP1A2 is expressed along with CYP1A1 in the human lung. Cancer Lett 2001; 171:113 120.
94. Bernauer U, Heinrich Hirsch B, Tonnies M, Peter Matthias W, Gundert Remy U. Character isation of the xenobiotic metabolizing Cytochrome P450 expression pattern in human lung tissue by immunochemical and activity determination. Toxicol Lett 2006; 164:278 288.
95. Thum T, Erpenbeck VJ, Moeller J, Hohlfeld JM, Krug N, Borlak J. Expression of xenobiotic metabolizing enzymes in different lung compartments of smokers and nonsmokers. Environ Health Perspect 2006; 114:1655 1661.
96. Jiang H, Shen YM, Quinn AM, Penning TM. Competing roles of cytochrome P450 1A1/1B1 and aldo keto reductase 1A1 in the metabolic activation of (+/) 7,8 dihydroxy 7,8 dihydro benzo [a]pyrene in human bronchoalveolar cell extracts. Chem Res Toxicol 2005; 18:365 374.
97. McFadyen MC, Murray GI. Cytochrome P450 1B1: a novel anticancer therapeutic target. Future Oncol 2005; 1:259 263.
98. Tsuchiya Y, Nakajima M, Yokoi T. Cytochrome P450 mediated metabolism of estrogens and its regulation in human. Cancer Lett 2005; 227:115 124.
99. Aklillu E, Ovrebo S, Botnen IV, Otter C, Ingelman Sundberg M. Characterization of common CYP1B1 variants with different capacity for benzo[a]pyrene 7,8 dihydrodiol epoxide formation from benzo[a]pyrene. Cancer Res 2005; 65:5105 5111.
100. Peng HM, Ding X, Coon MJ. Isolation and heterologous expression of cloned cDNAs for two rabbit nasal microsomal proteins, CYP2A10 and CYP2A11, that are related to nasal microsomal cytochrome P450 form a. J Biol Chem 1993; 268:17253 17260.
101. Su T, Sheng JJ, Lipinskas TW, Ding X. Expression of CYP2A genes in rodent and human nasal mucosa. Drug Metab Dispos 1996; 24:884 890.
102. Thornton Manning JR, Nikula KJ, Hotchkiss JA, Avila KJ, Rohrbacher KD, Ding X, Dahl AR. Nasal cytochrome P450 2A: identification, regional localization, and metabolic activity toward hexamethylphosphoramide, a known nasal carcinogen. Toxicol Appl Pharmacol 1997; 142:22 30.

103. Chen Y, Liu YQ, Su T, Ren X, Shi L, Liu D, Gu J, Zhang QY, Ding X. Immunoblot analysis and immunohistochemical characterization of CYP2A expression in human olfactory mucosa. Biochem Pharmacol 2003; 66:1245 1251.
104. Zhu LR, Thomas PE, Lu G, Reuhl KR, Yang GY, Wang LD, Wang SL, Yang CS, He XY, Hong JY. CYP2A13 in human respiratory tissues and lung cancers: an immunohistochemical study with a new peptide specific antibody. Drug Metab Dispos 2006; 34:1672 1676.
105. Piras E, Franzen A, Fernandez EL, Bergstrom U, Raffalli Mathieu F, Lang M, Brittebo EB. Cell specific expression of CYP2A5 in the mouse respiratory tract: effects of olfactory toxicants. J Histochem Cytochem 2003; 51:1545 1555.
106. Pelkonen O, Rautio A, Raunio H, Pasanen M. CYP2A6: a human coumarin 7 hydroxylase. Toxicology 2000; 144:139 147.
107. Messina ES, Tyndale RF, Sellers EM. A major role for CYP2A6 in nicotine C oxidation by human liver microsomes. J Pharmacol Exp Ther 1997; 282:1608 1614.
108. Murphy SE, Johnson LM, Pullo DA. Characterization of multiple products of cytochrome P450 2A6 catalyzed cotinine metabolism. Chem Res Toxicol 1999; 12:639 645.
109. Smith GB, Bend JR, Bedard LL, Reid KR, Petsikas D, Massey TE. Biotransformation of 4 (methylnitrosamino) 1 (3 pyridyl) 1 butanone (NNK) in peripheral human lung micro somes. Drug Metab Dispos 2003; 31:1134 1141.
110. Tiano HF, Wang RL, Hosokawa M, Crespi C, Tindall KR, Langenbach R. Human CYP2A6 activation of 4 (methylnitrosamino) 1 (3 pyridyl) 1 butanone (NNK): mutational specificity in the gpt gene of AS52 cells. Carcinogenesis 1994; 15:2859 2866.
111. Hecht SS. Biochemistry, biology, and carcinogenicity of tobacco specific N nitrosamines. Chem Res Toxicol 1998; 11:559 603.
112. Kamataki T, Fujieda M, Kiyotani K, Iwano S, Kunitoh H. a. Genetic polymorphism of CYP2A6 as one of the potential determinants of tobacco related cancer risk. Biochem Biophys Res Commun 2005; 338:306 310.
113. Fujieda M, Yamazaki H, Saito T, Kiyotani K, Gyamfi MA, Sakurai M, Dosaka Akita H, Sawamura Y, Yokota J, Kunitoh H, Kamataki T. Evaluation of CYP2A6 genetic polymorphisms as determinants of smoking behavior and tobacco related lung cancer risk in male Japanese smokers. Carcinogenesis 2004; 25:2451 2458.
114. Malaiyandi V, Sellers EM, Tyndale RF. Implications of CYP2A6 genetic variation for smoking behaviors and nicotine dependence. Clin Pharmacol Ther 2005; 77:145 158.
115. He XY, Tang L, Wang SL, Cai QS, Wang JS, Hong JY. Efficient activation of aflatoxin B1 by cytochrome P450 2A13, an enzyme predominantly expressed in human respiratory tract. Int J Cancer 2006; 118:2665 2671.
116. Su T, Bao Z, Zhang QY, Smith TJ, Hong JY, Ding X. Human cytochrome P450 CYP2A13: predominant expression in the respiratory tract and its high efficiency metabolic activation of a tobacco specific carcinogen, 4 (methylnitrosamino) 1 (3 pyridyl) 1 butanone. Cancer Res 2000; 60:5074 5079.
117. Wong HL, Zhang X, Zhang QY, Gu J, Ding X, Hecht SS, Murphy SE. Metabolic activation of the tobacco carcinogen 4 (methylnitrosamino) (3 pyridyl) 1 butanone by cytochrome P450 2A13 in human fetal nasal microsomes. Chem Res Toxicol 2005; 18:913 918.
118. Jalas JR, Ding X, Murphy SE. Comparative metabolism of the tobacco specific nitrosamines 4 (methylnitrosamino) 1 (3 pyridyl) 1 butanone and 4 (methylnitrosamino) 1 (3 pyridyl) 1 butanol by rat cytochrome P450 2A3 and human cytochrome P450 2A13. Drug Metab Dispos 2003; 31:1199 1202.
119. Fukami T, Katoh M, Yamazaki H, Yokoi T, Nakajima M. Human cytochrome P450 2A13 efficiently metabolizes chemicals in air pollutants: naphthalene, styrene, and toluene. Chem Res Toxicol 2008; 21:720 725.
120. Wang H, Tan W, Hao B, Miao X, Zhou G, He F, Lin D. Substantial reduction in risk of lung adenocarcinoma associated with genetic polymorphism in CYP2A13, the most active cytochrome P450 for the metabolic activation of tobacco specific carcinogen NNK. Cancer Res 2003; 63:8057 8061.

121. Wang SL, He XY, Shen J, Wang JS, Hong JY. The missense genetic polymorphisms of human CYP2A13: functional significance in carcinogen activation and identification of a null allelic variant. Toxicol Sci 2006; 94:38 45.
122. Thornton Manning J, Appleton ML, Gonzalez FJ, Yost GS. Metabolism of 3 methylindole by vaccinia expressed P450 enzymes: correlation of 3 methyleneindolenine formation and protein binding. J Pharmacol Exp Ther 1996; 276:21 29.
123. Gervot L, Rochat B, Gautier JC, Bohnenstengel F, Kroemer H, de Berardinis V, Martin H, Beaune P, de Waziers I. Human CYP2B6: expression, inducibility and catalytic activities. Pharmacogenetics 1999; 9:295 306.
124. Mace K, Bowman ED, Vautravers P, Shields PG, Harris CC, Pfeifer AM. Characterisation of xenobiotic metabolising enzyme expression in human bronchial mucosa and peripheral lung tissues. Eur J Cancer 1998; 34:914 920.
125. Dicke KE, Skrlin SM, Murphy SE. Nicotine and 4 (methylnitrosamino) 1 (3 pyridyl) butanone metabolism by cytochrome P450 2B6. Drug Metab Dispos 2005; 33:1760 1764.
126. Yokose T, Doy M, Taniguchi T, Shimada T, Kakiki M, Horie T, Matsuzaki Y, Mukai K. Immunohistochemical study of cytochrome P450 2C and 3A in human non neoplastic and neoplastic tissues. Virchows Arch 1999; 434:401 411.
127. Fisslthaler B, Fleming I, Busse R. EDHF: a cytochrome P450 metabolite in coronary arteries. Semin Perinatol 2000; 24:15 19.
128. Fisslthaler B, Hinsch N, Chataigneau T, Popp R, Kiss L, Busse R, Fleming I. Nifedipine increases cytochrome P4502C expression and endothelium derived hyperpolarizing factor mediated responses in coronary arteries. Hypertension 2000; 36:270 275.
129. Vriens J, Owsianik G, Fisslthaler B, Suzuki M, Janssens A, Voets T, Morisseau C, Hammock BD, Fleming I, Busse R, Nilius B. Modulation of the Ca2 permeable cation channel TRPV4 by cytochrome P450 epoxygenases in vascular endothelium. Circ Res 2005; 97:908 915.
130. Bouchardy C, Benhamou S, Dayer P. The effect of tobacco on lung cancer risk depends on CYP2D6 activity. Cancer Res 1996; 56:251 253.
131. Laforest L, Wikman H, Benhamou S, Saarikoski ST, Bouchardy C, Hirvonen A, Dayer P, Husgafvel Pursiainen K. CYP2D6 gene polymorphism in caucasian smokers: lung cancer susceptibility and phenotype genotype relationships. Eur J Cancer 2000; 36:1825 1832.
132. Ding XX, Coon MJ. Induction of cytochrome P 450 isozyme 3a (P 450IIE1) in rabbit olfactory mucosa by ethanol and acetone. Drug Metab Dispos 1990; 18:742 745.
133. Carlson GP, Day BJ. Induction by pyridine of cytochrome P450IIE1 and xenobiotic metabolism in rat lung and liver. Pharmacology 1992; 44:117 123.
134. Raucy JL, Kraner JC, Lasker JM. Bioactivation of halogenated hydrocarbons by cytochrome P4502E1. Crit Rev Toxicol 1993; 23:1 20.
135. Forkert PG. Mechanisms of 1,1 dichloroethylene induced cytotoxicity in lung and liver. Drug Metab Rev 2001; 33:49 80.
136. Forkert PG, Boyd SM, Ulreich JB. Pulmonary bioactivation of 1,1 dichloroethylene is associated with CYP2E1 levels in A/J, CD 1, and C57BL/6 mice. J Pharmacol Exp Ther 2001; 297:1193 1200.
137. Lee RP, Forkert PG. In vitro biotransformation of 1,1 dichloroethylene by hepatic cytochrome P 450 2E1 in mice. J Pharmacol Exp Ther 1994; 270:371 376.
138. Lee RP, Forkert PG. Pulmonary CYP2E1 bioactivates 1,1 dichloroethylene in male and female mice. J Pharmacol Exp Ther 1995; 273:561 567.
139. Forkert PG, Kaufmann M, Black G, Bowers R, Chen H, Collins K, Sharma A, Jones G. Oxidation of vinyl carbamate and formation of 1,N6 ethenodeoxyadenosine in murine lung. Drug Metab Dispos 2007; 35:713 720.
140. Hoffler U, El Masri HA, Ghanayem BI. Cytochrome P450 2E1 (CYP2E1) is the principal enzyme responsible for urethane metabolism: comparative studies using CYP2E1 null and wild type mice. J Pharmacol Exp Ther 2003; 305:557 564.
141. Nichols WK, Covington MO, Seiders CD, Safiullah S, Yost GS. Bioactivation of halogenated hydrocarbons by rabbit pulmonary cells. Pharmacol Toxicol 1992; 71:335 339.

142. Nichols WK, Terry CM, Cutler NS, Appleton ML, Jesthi PK, Yost GS. Oxidation at C 1 controls the cytotoxicity of 1,1 dichloro 2,2 bis(p chlorophenyl)ethane by rabbit and human lung cells. Drug Metab Dispos 1995; 23:595 599.
143. Ritter JK, Owens IS, Negishi M, Nagata K, Sheen YY, Gillette JR, Sasame HA. Mouse pulmonary cytochrome P 450 naphthalene hydroxylase: cDNA cloning, sequence, and expression in Saccharomyces cerevisiae. Biochemistry 1991; 30:11430 11437.
144. Baldwin RM, Shultz MA, Buckpitt AR. Bioactivation of the pulmonary toxicants naphthalene and 1 nitronaphthalene by rat CYP2F4. J Pharmacol Exp Ther 2005; 312:857 865.
145. Powley MW, Carlson GP. Cytochromes P450 involved with benzene metabolism in hepatic and pulmonary microsomes. J Biochem Mol Toxicol 2000; 14:303 309.
146. Sheets PL, Yost GS, Carlson GP. Benzene metabolism in human lung cell lines BEAS 2B and A549 and cells overexpressing CYP2F1. J Biochem Mol Toxicol 2004; 18:92 99.
147. Thornton Manning JR, Ruangyuttikarn W, Gonzalez FJ, Yost GS. Metabolic activation of the pneumotoxin, 3 methylindole, by vaccinia expressed cytochrome P450s. Biochem Biophys Res Commun 1991; 181:100 107.
148. Smith TJ, Guo Z, Gonzalez FJ, Guengerich FP, Stoner GD, Yang CS. Metabolism of 4 (methylnitrosamino) 1 (3 pyridyl) 1 butanone in human lung and liver microsomes and cytochromes P 450 expressed in hepatoma cells. Cancer Res 1992; 52:1757 1763.
149. Baldwin RM, Jewell WT, Fanucchi MV, Plopper CG, Buckpitt AR. Comparison of pulmonary/nasal CYP2F expression levels in rodents and rhesus macaque. J Pharmacol Exp Ther 2004; 309:127 136.
150. Regal KA, Laws GM, Yuan C, Yost GS, Skiles GL. Detection and characterization of DNA adducts of 3 methylindole. Chem Res Toxicol 2001; 14:1014 1024.
151. Buckpitt A, Chang AM, Weir A, Van Winkle L, Duan X, Philpot R, Plopper C. Relationship of cytochrome P450 activity to Clara cell cytotoxicity. IV. Metabolism of naphthalene and naphthalene oxide in microdissected airways from mice, rats, and hamsters. Mol Pharmacol 1995; 47:74 81.
152. Zeldin DC, Foley J, Ma J, Boyle JE, Pascual JM, Moomaw CR, Tomer KB, Steenbergen C, Wu S. CYP2J subfamily P450s in the lung: expression, localization, and potential functional significance. Mol Pharmacol 1996; 50:1111 1117.
153. Capdevila JH, Falck JR, Harris RC. Cytochrome P450 and arachidonic acid bioactivation. Molecular and functional properties of the arachidonate monooxygenase. J Lipid Res 2000; 41:163 181.
154. Scarborough PE, Ma J, Qu W, Zeldin DC. P450 subfamily CYP2J and their role in the bioactivation of arachidonic acid in extrahepatic tissues. Drug Metab Rev 1999; 31:205 234.
155. Spiecker M, Liao JK. Vascular protective effects of cytochrome p450 epoxygenase derived eicosanoids. Arch Biochem Biophys 2005; 433:413 420.
156. Xiao YF. Cyclic AMP dependent modulation of cardiac L type Ca2+ and transient outward K+ channel activities by epoxyeicosatrienoic acids. Prostaglandins Other Lipid Mediat 2007; 82:11 18.
157. Zeldin DC. Epoxygenase pathways of arachidonic acid metabolism. J Biol Chem 2001; 276:36059 36062.
158. Rylander T, Neve EP, Ingelman Sundberg M, Oscarson M. Identification and tissue distribution of the novel human cytochrome P450 2S1 (CYP2S1). Biochem Biophys Res Commun 2001; 281:529 535.
159. Saarikoski ST, Wikman HA, Smith G, Wolff CH, Husgafvel Pursiainen K. Localization of cytochrome P450 CYP2S1 expression in human tissues by in situ hybridization and immunohistochemistry. J Histochem Cytochem 2005; 53:549 556.
160. Rivera SP, Saarikoski ST, Hankinson O. Identification of a novel dioxin inducible cytochrome P450. Mol Pharmacol 2002; 61:255 259.
161. Smith G, Wolf CR, Deeni YY, Dawe RS, Evans AT, Comrie MM, Ferguson J, Ibbotson SH. Cutaneous expression of cytochrome P450 CYP2S1: individuality in regulation by therapeutic agents for psoriasis and other skin diseases. Lancet 2003; 361:1336 1343.

162. Downie D, McFadyen MC, Rooney PH, Cruickshank ME, Parkin DE, Miller ID, Telfer C, Melvin WT, Murray GI. Profiling cytochrome P450 expression in ovarian cancer: identification of prognostic markers. Clin Cancer Res 2005; 11:7369 7375.
163. Wu ZL, Sohl CD, Shimada T, Guengerich FP. Recombinant enzymes overexpressed in bacteria show broad catalytic specificity of human cytochrome P450 2W1 and limited activity of human cytochrome P450 2S1. Mol Pharmacol 2006; 69:2007 2014.
164. Wang SL, He XY, Hong JY. Human cytochrome p450 2s1: lack of activity in the metabolic activation of several cigarette smoke carcinogens and in the metabolism of nicotine. Drug Metab Dispos 2005; 33:336 340.
165. Karlgren M, Miura S, Ingelman Sundberg M. Novel extrahepatic cytochrome P450s. Toxicol Appl Pharmacol 2005; 207:57 61.
166. Anttila S, Hukkanen J, Hakkola J, Stjernvall T, Beaune P, Edwards RJ, Boobis AR, Pelkonen O, Raunio H. Expression and localization of CYP3A4 and CYP3A5 in human lung. Am J Respir Cell Mol Biol 1997; 16:242 249.
167. Raunio H, Hakkola J, Hukkanen J, Pelkonen O, Edwards R, Boobis A, Anttila S. Expression of xenobiotic metabolizing cytochrome P450s in human pulmonary tissues. Arch Toxicol Suppl 1998; 20:465 469.
168. Biggs JS, Wan J, Cutler NS, Hakkola J, Uusimaki P, Raunio H, Yost GS. Transcription factor binding to a putative double E box motif represses CYP3A4 expression in human lung cells. Mol Pharmacol 2007; 72:514 525.
169. Somers GI, Lindsay N, Lowdon BM, Jones AE, Freathy C, Ho S, Woodrooffe AJ, Bayliss MK, Manchee GR. A comparison of the expression and metabolizing activities of phase I and II enzymes in freshly isolated human lung parenchymal cells and cryopreserved human hepatocytes. Drug Metab Dispos 2007; 35:1797 1805.
170. Raunio H, Hakkola J, Pelkonen O. Regulation of CYP3A genes in the human respiratory tract. Chem Biol Interact 2005; 151:53 62.
171. Hukkanen J, Vaisanen T, Lassila A, Piipari R, Anttila S, Pelkonen O, Raunio H, Hakkola J. Regulation of CYP3A5 by glucocorticoids and cigarette smoke in human lung derived cells. J Pharmacol Exp Ther 2003; 304:745 752.
172. Aoyama T, Yamano S, Guzelian PS, Gelboin HV, Gonzalez FJ. Five of 12 forms of vaccinia virus expressed human hepatic cytochrome P450 metabolically activate aflatoxin B1. Proc Natl Acad Sci U S A 1990; 87:4790 4793.
173. Kelly JD, Eaton DL, Guengerich FP, Coulombe RA Jr. Aflatoxin B1 activation in human lung. Toxicol Appl Pharmacol 1997; 144:88 95.
174. Nhamburo PT, Gonzalez FJ, McBride OW, Gelboin HV, Kimura S. Identification of a new P450 expressed in human lung: complete cDNA sequence, cDNA directed expression, and chromosome mapping. Biochemistry 1989; 28:8060 8066.
175. Wolf CR, Szutowski MM, Ball LM, Philpot RM. The rabbit pulmonary monooxygenase system: characteristics and activities of two forms of pulmonary cytochrome P 450. Chem Biol Interact 1978; 21:29 43.
176. Czerwinski M, McLemore TL, Philpot RM, Nhamburo PT, Korzekwa K, Gelboin HV, Gonzalez FJ. Metabolic activation of 4 ipomeanol by complementary DNA expressed human cytochromes P 450: evidence for species specific metabolism. Cancer Res 1991; 51:4636 4638.
177. Smith PB, Tiano HF, Nesnow S, Boyd MR, Philpot RM, Langenbach R. 4 Ipomeanol and 2 aminoanthracene cytotoxicity in C3H/10T1/2 cells expressing rabbit cytochrome P450 4B1. Biochem Pharmacol 1995; 50:1567 1575.
178. Lipsky PE. Role of cyclooxygenase 1 and 2 in health and disease. Am J Orthop 1999; 28:8 12.
179. Marnett LJ. Cyclooxygenase mechanisms. Curr Opin Chem Biol 2000; 4:545 552.
180. Marnett LJ. Structure, function and inhibition of cyclo oxygenases. Ernst Schering Res Found Workshop 2000; (31):65 83.
181. Simmons DL, Botting RM, Hla T. Cyclooxygenase isozymes: the biology of prostaglandin synthesis and inhibition. Pharmacol Rev 2004; 56:387 437.
182. Chandrasekharan NV, Dai H, Roos KL, Evanson NK, Tomsik J, Elton TS, Simmons DL. COX 3, a cyclooxygenase 1 variant inhibited by acetaminophen and other analgesic/

antipyretic drugs: cloning, structure, and expression. Proc Natl Acad Sci U S A 2002; 99: 13926 13931.
183. van Overveld FJ, Jorens PG, De Backer WA, Rampart M, Bossaert L, Vermeire PA. Release of arachidonic acid metabolites from isolated human alveolar type II cells. Prostaglandins 1992; 44:101 110.
184. Samokyszyn VM, Marnett LJ. Hydroperoxide dependent cooxidation of 13 cis retinoic acid by prostaglandin H synthase. J Biol Chem 1987; 262:14119 14133.
185. Samokyszyn VM, Sloane BF, Honn KV, Marnett LJ. Cooxidation of 13 cis retinoic acid by prostaglandin H synthase. Biochem Biophys Res Commun 1984; 124:430 436.
186. Wise RW, Zenser TV, Davis BB. Prostaglandin H synthase metabolism of the urinary bladder carcinogens benzidine and ANFT. Carcinogenesis 1983; 4:285 289.
187. Yamazoe Y, Miller DW, Weis CC, Dooley KL, Zenser TV, Beland FA, Kadlubar FF. DNA adducts formed by ring oxidation of the carcinogen 2 naphthylamine with prostaglandin H synthase in vitro and in the dog urothelium in vivo. Carcinogenesis 1985; 6:1379 1387.
188. Zenser TV, Lakshmi VM, Hsu FF, Davis BB. Metabolism of N acetylbenzidine and initiation of bladder cancer. Mutat Res 2002; 506 507:29 40.
189. Donnelly PJ, Stewart RK, Ali SL, Conlan AA, Reid KR, Petsikas D, Massey TE. Biotransformation of aflatoxin B1 in human lung. Carcinogenesis 1996; 17:2487 2494.
190. Liu L, Massey TE. Bioactivation of aflatoxin B1 by lipoxygenases, prostaglandin H synthase and cytochrome P450 monooxygenase in guinea pig tissues. Carcinogenesis 1992; 13:533 539.
191. Massey TE, Smith GB, Tam AS. Mechanisms of aflatoxin B1 lung tumorigenesis. Exp Lung Res 2000; 26:673 683.
192. Reed GA, Grafstrom RC, Krauss RS, Autrup H, Eling TE. Prostaglandin H synthase dependent co oxygenation of (+/) 7,8 dihydroxy 7,8 dihydrobenzo[a]pyrene in hamster trachea and human bronchus explants. Carcinogenesis 1984; 5:955 960.
193. Reed GA, Marnett LJ. Metabolism and activation of 7,8 dihydrobenzo[a]pyrene during prostaglandin biosynthesis. Intermediacy of a bay region epoxide. J Biol Chem 1982; 257:11368 11376.
194. Sivarajah K, Jones KG, Fouts JR, Devereux T, Shirley JE, Eling TE. Prostaglandin synthetase and cytochrome P 450 dependent metabolism of (+/)benzo(a)pyrene 7,8 dihydrodiol by enriched populations of rat Clara cells and alveolar type II cells. Cancer Res 1983; 43:2632 2636.
195. Cashman JR, Zhang J. Human flavin containing monooxygenases. Annu Rev Pharmacol Toxicol 2006; 46:65 100.
196. Krueger SK, Williams DE. Mammalian flavin containing monooxygenases: structure/ function, genetic polymorphisms and role in drug metabolism. Pharmacol Ther 2005; 106:357 387.
197. Massey V. Activation of molecular oxygen by flavins and flavoproteins. J Biol Chem 1994; 269:22459 22462.
198. Beaty NB, Ballou DP. Transient kinetic study of liver microsomal FAD containing monooxygenase. J Biol Chem 1980; 255:3817 3819.
199. Williams DE, Ziegler DM, Nordin DJ, Hale SE, Masters BS. Rabbit lung flavin containing monooxygenase is immunochemically and catalytically distinct from the liver enzyme. Biochem Biophys Res Commun 1984; 125:116 122.
200. Sun H, Ehlhardt WJ, Kulanthaivel P, Lanza DL, Reilly CA, Yost GS. Dehydrogenation of indoline by cytochrome P450 enzymes: a novel "aromatase" process. J Pharmacol Exp Ther 2007; 322:843 851.
201. Zhang J, Cashman JR. Quantitative analysis of FMO gene mRNA levels in human tissues. Drug Metab Dispos 2006; 34:19 26.
202. Siddens LK, Henderson MC, Vandyke JE, Williams DE, Krueger SK. Characterization of mouse flavin containing monooxygenase transcript levels in lung and liver, and activity of expressed isoforms. Biochem Pharmacol 2008; 75:570 579.
203. Whetstine JR, Yueh MF, McCarver DG, Williams DE, Park CS, Kang JH, Cha YN, Dolphin CT, Shephard EA, Phillips IR, Hines RN. Ethnic differences in human flavin containing

monooxygenase 2 (FMO2) polymorphisms: detection of expressed protein in African Americans. Toxicol Appl Pharmacol 2000; 168:216 224.
204. Henderson MC, Krueger SK, Siddens LK, Stevens JF, Williams DE. S oxygenation of the thioether organophosphate insecticides phorate and disulfoton by human lung flavin containing monooxygenase 2. Biochem Pharmacol 2004; 68:959 967.
205. Henderson MC, Krueger SK, Stevens JF, Williams DE. Human flavin containing monooxygenase form 2 S oxygenation: sulfenic acid formation from thioureas and oxidation of glutathione. Chem Res Toxicol 2004; 17:633 640.
206. Smith PB, Crespi C. Thiourea toxicity in mouse C3H/10T1/2 cells expressing human flavin dependent monooxygenase 3. Biochem Pharmacol 2002; 63:1941 1948.
207. Kondraganti SR, Jiang W, Jaiswal AK, Moorthy B. Persistent induction of hepatic and pulmonary phase II enzymes by 3 methylcholanthrene in rats. Toxicol Sci 2008; 102:337 344.
208. Bond JA, Harkema JR, Russell VI. Regional distribution of xenobiotic metabolizing enzymes in respiratory airways of dogs. Drug Metab Dispos 1988; 16:116 124.
209. Devereux TR, Diliberto JJ, Fouts JR. Cytochrome P 450 monooxygenase, epoxide hydrolase and flavin monooxygenase activities in Clara cells and alveolar type II cells isolated from rabbit. Cell Biol Toxicol 1985; 1:57 65.
210. Park JY, Chen L, Elahi A, Lazarus P, Tockman MS. Genetic analysis of microsomal epoxide hydrolase gene and its association with lung cancer risk. Eur J Cancer Prev 2005; 14:223 230.
211. Lin P, Wang SL, Wang HJ, Chen KW, Lee HS, Tsai KJ, Chen CY, Lee H. Association of CYP1A1 and microsomal epoxide hydrolase polymorphisms with lung squamous cell carcinoma. Br J Cancer 2000; 82:852 857.
212. Kiyohara C, Yoshimasu K, Takayama K, Nakanishi Y. EPHX1 polymorphisms and the risk of lung cancer: a HuGE review. Epidemiology 2006; 17:89 99.
213. Arnold SM, Fessler LI, Fessler JH, Kaufman RJ. Two homologues encoding human UDP glucose:glycoprotein glucosyltransferase differ in mRNA expression and enzymatic activity. Biochemistry 2000; 39:2149 2163.
214. Burchell B, Soars M, Monaghan G, Cassidy A, Smith D, Ethell B. Drug mediated toxicity caused by genetic deficiency of UDP glucuronosyltransferases. Toxicol Lett 2000; 112 113: 333 340.
215. Tukey RH, Strassburg CP. Human UDP glucuronosyltransferases: metabolism, expression, and disease. Annu Rev Pharmacol Toxicol 2000; 40:581 616.
216. Mackenzie PI, Bock KW, Burchell B, Guillemette C, Ikushiro S, Iyanagi T, Miners JO, Owens IS, Nebert DW. Nomenclature update for the mammalian UDP glycosyltransferase (UGT) gene superfamily. Pharmacogenet Genomics 2005; 15:677 685.
217. Mackenzie PI, Owens IS, Burchell B, Bock KW, Bairoch A, Belanger A, Fournel Gigleux S, Green M, Hum DW, Iyanagi T, Lancet D, Louisot P, Magdalou J, Chowdhury JR, Ritter JK, Schachter H, Tephly TR, Tipton KF, Nebert DW. The UDP glycosyltransferase gene superfamily: recommended nomenclature update based on evolutionary divergence. Pharmacogenetics 1997; 7:255 269.
218. Batt AM, Magdalou J, Vincent Viry M, Ouzzine M, Fournel Gigleux S, Galteau MM, Siest G. Drug metabolizing enzymes related to laboratory medicine: cytochromes P 450 and UDP glucuronosyltransferases. Clin Chim Acta 1994; 226:171 190.
219. Strassburg CP, Oldhafer K, Manns MP, Tukey RH. Differential expression of the UGT1A locus in human liver, biliary, and gastric tissue: identification of UGT1A7 and UGT1A10 transcripts in extrahepatic tissue. Mol Pharmacol 1997; 52:212 220.
220. Shelby MK, Cherrington NJ, Vansell NR, Klaassen CD. Tissue mRNA expression of the rat UDP glucuronosyltransferase gene family. Drug Metab Dispos 2003; 31:326 333.
221. Zheng Z, Fang JL, Lazarus P. Glucuronidation: an important mechanism for detoxification of benzo[a]pyrene metabolites in aerodigestive tract tissues. Drug Metab Dispos 2002; 30:397 403.
222. Yoshimura T, Tanaka S, Horie T. Species difference and tissue distribution of uridine diphosphate glucuronyltransferase activities toward E6080, 1 naphthol and 4 hydroxybiphenyl. J Pharmacobiodyn 1992; 15:387 393.

223. Jones KG, Holland JF, Foureman GL, Bend JR, Fouts JR. Xenobiotic metabolism in Clara cells and alveolar type II cells isolated from lungs of rats treated with beta naphthoflavone. J Pharmacol Exp Ther 1983; 225:316 319.
224. Elovaara E, Mikkola J, Stockmann Juvala H, Luukkanen L, Keski Hynnila H, Kostiainen R, Pasanen M, Pelkonen O, Vainio H. Polycyclic aromatic hydrocarbon (PAH) metabolizing enzyme activities in human lung, and their inducibility by exposure to naphthalene, phenanthrene, pyrene, chrysene, and benzo(a)pyrene as shown in the rat lung and liver. Arch Toxicol 2007; 81:169 182.
225. Jedlitschky G, Cassidy AJ, Sales M, Pratt N, Burchell B. Cloning and characterization of a novel human olfactory UDP glucuronosyltransferase. Biochem J 1999; 340(pt 3):837 843.
226. Turgeon D, Carrier JS, Levesque E, Hum DW, Belanger A. Relative enzymatic activity, protein stability, and tissue distribution of human steroid metabolizing UGT2B subfamily members. Endocrinology 2001; 142:778 787.
227. Lazard D, Zupko K, Poria Y, Nef P, Lazarovits J, Horn S, Khen M, Lancet D. Odorant signal termination by olfactory UDP glucuronosyl transferase. Nature 1991; 349:790 793.
228. Odum J, Foster JR, Green T. A mechanism for the development of Clara cell lesions in the mouse lung after exposure to trichloroethylene. Chem Biol Interact 1992; 83:135 153.
229. Hargus SJ, Martin BM, George JW, Pohl LR. Covalent modification of rat liver dipeptidyl peptidase IV (CD26) by the nonsteroidal anti inflammatory drug diclofenac. Chem Res Toxicol 1995; 8:993 996.
230. McGurk KA, Remmel RP, Hosagrahara VP, Tosh D, Burchell B. Reactivity of mefenamic acid 1 o acyl glucuronide with proteins in vitro and ex vivo. Drug Metab Dispos 1996; 24:842 849.
231. Hayes JD, Flanagan JU, Jowsey IR. Glutathione transferases. Annu Rev Pharmacol Toxicol 2005; 45:51 88.
232. Jakobsson PJ, Morgenstern R, Mancini J, Ford Hutchinson A, Persson B. Common structural features of MAPEG a widespread superfamily of membrane associated proteins with highly divergent functions in eicosanoid and glutathione metabolism. Protein Sci 1999; 8:689 692.
233. Khojasteh Bakht SC, Nelson SD, Atkins WM. Glutathione S transferase catalyzes the isomerization of (R) 2 hydroxymenthofuran to mintlactones. Arch Biochem Biophys 1999; 370:59 65.
234. Duan X, Buckpitt AR, Plopper CG. Variation in antioxidant enzyme activities in anatomic subcompartments within rat and rhesus monkey lung. Toxicol Appl Pharmacol 1993; 123: 73 82.
235. Lee MJ, Dinsdale D. Immunolocalization of glutathione S transferase isoenzymes in bronchiolar epithelium of rats and mice. Am J Physiol 1994; 267:L766 L774.
236. Anttila S, Hirvonen A, Vainio H, Husgafvel Pursiainen K, Hayes JD, Ketterer B. Immunohistochemical localization of glutathione S transferases in human lung. Cancer Res 1993; 53:5643 5648.
237. Singhal SS, Saxena M, Ahmad H, Awasthi S, Haque AK, Awasthi YC. Glutathione S transferases of human lung: characterization and evaluation of the protective role of the alpha class isozymes against lipid peroxidation. Arch Biochem Biophys 1992; 299:232 241.
238. Forkert PG, Geddes BA, Birch DW, Massey TE. Morphological changes and covalent binding of 1,1 dichloroethylene in Clara and alveolar type II cells isolated from lungs of mice following in vivo administration. Drug Metab Dispos 1990; 18:534 539.
239. Nakajima T, Elovaara E, Anttila S, Hirvonen A, Camus AM, Hayes JD, Ketterer B, Vainio H. Expression and polymorphism of glutathione S transferase in human lungs: risk factors in smoking related lung cancer. Carcinogenesis 1995; 16:707 711.
240. Nakachi K, Imai K, Hayashi S, Kawajiri K. Polymorphisms of the CYP1A1 and glutathione S transferase genes associated with susceptibility to lung cancer in relation to cigarette dose in a Japanese population. Cancer Res 1993; 53:2994 2999.
241. Engle MR, Singh SP, Czernik PJ, Gaddy D, Montague DC, Ceci JD, Yang Y, Awasthi S, Awasthi YC, Zimniak P. Physiological role of mGSTA4 4, a glutathione S transferase

metabolizing 4 hydroxynonenal: generation and analysis of mGsta4 null mouse. Toxicol Appl Pharmacol 2004; 194:296 308.
242. Phimister AJ, Lee MG, Morin D, Buckpitt AR, Plopper CG. Glutathione depletion is a major determinant of inhaled naphthalene respiratory toxicity and naphthalene metabolism in mice. Toxicol Sci 2004; 82:268 278.
243. Phimister AJ, Nagasawa HT, Buckpitt AR, Plopper CG. Prevention of naphthalene induced pulmonary toxicity by glutathione prodrugs: roles for glutathione depletion in adduct formation and cell injury. J Biochem Mol Toxicol 2005; 19:42 51.
244. Phimister AJ, Williams KJ, Van Winkle LS, Plopper CG. Consequences of abrupt glutathione depletion in murine Clara cells: ultrastructural and biochemical investigations into the role of glutathione loss in naphthalene cytotoxicity. J Pharmacol Exp Ther 2005; 314:506 513.
245. Wisnewski AV, Lemus R, Karol MH, Redlich CA. Isocyanate conjugated human lung epithelial cell proteins: a link between exposure and asthma? J Allergy Clin Immunol 1999; 104:341 347.
246. Wisnewski AV, Liu Q, Liu J, Redlich CA. Glutathione protects human airway proteins and epithelial cells from isocyanates. Clin Exp Allergy 2005; 35:352 357.
247. Guengerich FP, McCormick WA, Wheeler JB. Analysis of the kinetic mechanism of haloalkane conjugation by mammalian theta class glutathione transferases. Chem Res Toxicol 2003; 16:1493 1499.
248. Wheeler JB, Stourman NV, Thier R, Dommermuth A, Vuilleumier S, Rose JA, Armstrong RN, Guengerich FP. Conjugation of haloalkanes by bacterial and mammalian glutathione transferases: mono and dihalomethanes. Chem Res Toxicol 2001; 14:1118 1127.

11

Sites of Extra Hepatic Metabolism, Part II: Gut

Mary F. Paine
Division of Pharmacotherapy and Experimental Therapeutics, School of Pharmacy, University of North Carolina, Chapel Hill, North Carolina, U.S.A.

INTRODUCTION

The oral route remains as the most common, convenient, economical, and generally safest means of drug administration. However, for systemically acting drugs, this route is not always the most efficient because of the numerous anatomic and physiologic barriers that drugs can encounter from the time of ingestion until the time of entry into the general circulation. As a consequence, before the drug enters the circulation and elicits its effects in the target tissue(s), significant loss of the original dose can occur as it passes, sequentially, through the gastrointestinal (GI) tract, the liver, and the cardiopulmonary system. For some drugs, these barriers can preclude their use as oral agents. Isoproterenol, dihydroergotamine, lidocaine, nitroglycerin, fentanyl, and naloxone are examples of drugs that suffer from a high *first-pass effect*, which refers to the loss of drug as the dose passes, for the first time, through organs of elimination during transit from the site of administration to the systemic circulation (1). Processes known to cause significant loss of active drug during first-pass include incomplete release from the dosage form, degradation in the GI lumen, poor permeation through the GI wall, active export into the GI lumen, biliary excretion, and metabolism. Of these processes, only metabolism can take place in all of the aforementioned organs.

A survey of the top 200 prescribed drugs indicated that metabolism represents the major means by which the body eliminates drugs (2). Enzymatic modification of the drug generally produces inactive metabolites with increased polarity and water solubility to enhance excretion. For several drugs, the extent of conversion to inactive metabolites can be large enough so that circulating concentrations of active drug are reduced significantly, which in turn can cause a significant decrease in pharmacologic activity and, ultimately, a reduced clinical response. Drugs with a narrow therapeutic window that undergo extensive first-pass metabolism are particularly vulnerable to a reduced clinical response. Moreover, the extent of first-pass metabolism can vary substantially between individuals, further hampering the optimization of oral drug therapy.

Of the first-pass organs of drug elimination, the liver is the most often implicated, in large part, because it expresses the highest specific contents of drug-metabolizing enzymes. Next to the liver, the small intestinal mucosa is undoubtedly the most important extrahepatic site of drug metabolism (3). While the role of the relevant enzymes in the liver has been established for some time, relatively less is known about the complement of enzymes in the small intestine. Nevertheless, much progress has been made in the last two decades regarding the identification and characterization of different subfamilies and individual isoforms. In parallel, the potential impact of intestinal first-pass metabolism on drug disposition has become increasingly recognized. Before discussing the various enzymes and their clinical implications, an understanding of drug movement through the GI wall is warranted.

DRUG MOVEMENT THROUGH THE GI WALL

The GI tract represents the first in the sequence of organs that drugs encounter when taken orally. Most drugs are given as solid dosage forms. As such, dissolution of the dosage form must occur in the lumen before the molecules are absorbed through the GI wall. Several physicochemical properties of both the drug and the GI environment govern the rate of dissolution. Drug properties include solubility, particle size, salt form, complexation, and crystal form; environmental properties include pH and lumenal stirring (4). Following dissolution of the dosage form, the drug molecules must then traverse the contents of the lumen (e.g., water, food, bacteria) and a mucous layer before they are absorbed through the epithelial layer into the lamina propria, which contain the capillaries that eventually lead to the portal vein. Most drugs are weak acids or weak bases and are absorbed by passive diffusion. On the basis of the pH partition hypothesis, which assumes that only unionized drug can traverse biological membranes, weak acids are predicted to be absorbed more rapidly from the stomach (pH 1 3) than from the small intestine (pH 6 8) or large intestine (pH 6 7) (1,5); the converse is predicted for weak bases. Contrary to this hypothesis, the majority of drugs, whether a weak acid or weak base, and whether in the unionized or ionized form, are absorbed predominately in the small intestine. These apparent inconsistencies can be explained by the small intestine being favored over the stomach and large intestine in terms of surface area and permeability, two key anatomic/physiologic factors that govern the rate and extent of drug absorption.

The adult small intestine, which has an anatomical length (i.e., length at autopsy or after surgical removal) that measures approximately 500 cm (6), is divided into three segments: the duodenum, jejunum, and ileum. The duodenum measures 25 to 30 cm in length, begins just distal to the pyloric sphincter of the stomach and ends at the ligament of Treitz (7). Whereas the ligament of Treitz distinguishes the duodenum from the jejunum, no such anatomical landmark distinguishes the jejunum from the ileum; however, the jejunum is generally assumed to represent the proximal two-fifths and the ileum the distal three-fifths of the remainder of the small intestine (~200 and 300 cm, respectively). In comparison, the length of the entire large intestine is approximately 160 cm (6).

The major function of the small intestine is to absorb nutrients. The unique morphology of the mucosal surface facilitates this task. A cross-section of the small intestine shows extensive folding (folds of Kerckering) (Fig. 1). The folds of Kerkering, or plicae circulares, are circular folds created by mucosal/submucosal invaginations into the lumen. These circular folds, which are predominant in the duodenum and jejunum and essentially absent by middle ileum, are lined with finger-like projections or villi. At the base of the villi are the crypts of Lieberkuhn, which consist of undifferentiated (crypt)

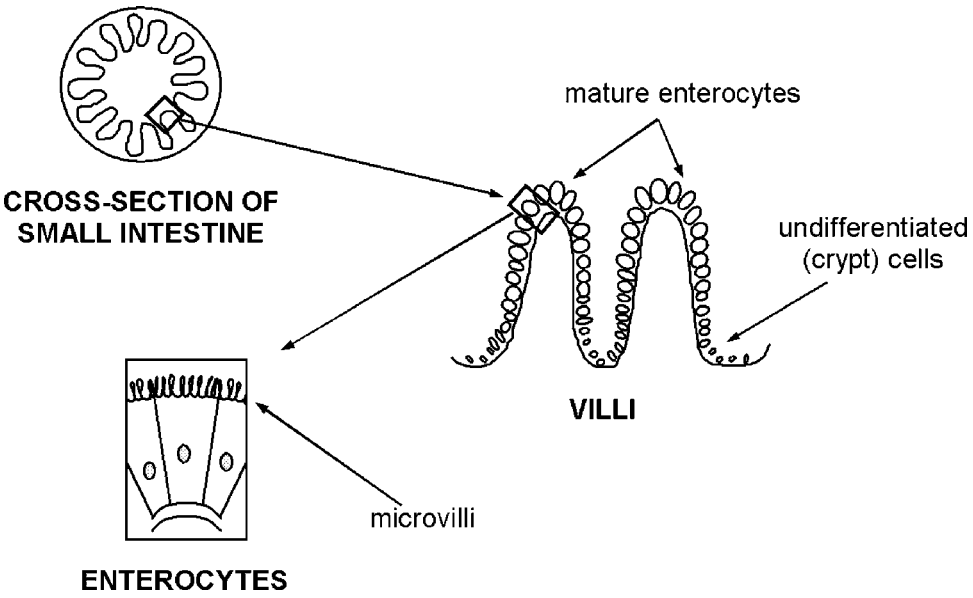

Figure 1 Morphology of the human small intestine. Invaginations in the lumen are lined with villi, which are lined with a single layer of absorptive columnar epithelial cells (enterocytes), which are further lined with microvilli. From Ref. 8.

cells. Over the course of two to three days, crypt cells migrate to the villous tips while maturing into various cell types, including mucus-secreting goblet cells, enteroendocrine cells, and absorptive cells (enterocytes); after three more days, the mature cells of the villous tips are shed into the lumen (7). Enterocytes, which are the predominant cell types that compose the single layer of epithelial cells lining the villi, are further lined with microvilli. Taken together, this combination of circular folds, villi and microvilli creates a tremendous absorptive surface area. In adults, this area has been estimated at 200 m^2, which is roughly the size of a tennis court. In comparison, the surface area of the stomach is approximately 0.053 m^2 and that of the large intestine is approximately 0.35 m^2 (6).

The small intestine has not only a much greater surface area than the stomach and large intestine, but it is also more permeable, due in part to having both a relatively thin epithelial layer and a lower electrical resistance (1). Thus, as with nutrients, the small intestine is the prime site for the absorption of drugs. Moreover, because surface area and permeability decline from proximal to distal regions, it can be argued that, at least for immediate-release formulations, drug absorption occurs predominately in the duodenum and jejunum.

Absorption of drug molecules through the small intestinal epithelial layer occurs via paracellular or transcellular mechanisms. That is, the molecule can either passively diffuse between enterocytes (paracellular) or passively diffuse or be actively transported through the apical (lumenal) and basolateral membranes of enterocytes (transcellular). Most hydrophilic, polar drugs are absorbed by the paracellular route (exceptions are polar drugs that are actively transported across the epithelial cell), whereas most lipophilic, nonpolar drugs are absorbed by the transcellular route (9). For drugs absorbed by the latter route, the opportunity exists for first-pass metabolism, as the relevant enzymes are located intracellularly, predominantly in the endoplasmic reticulum or cytosol of enterocytes. Indeed, evidence has amassed that the small intestine can contribute significantly to the overall first-pass metabolism of drugs, the extent of which can have clinical ramifications.

CLINICAL IMPLICATIONS OF INTESTINAL FIRST-PASS METABOLISM

Many commonly prescribed drugs undergo extensive first-pass metabolism upon oral administration (Table 1). For those listed in Table 1, at least 45% of the original dose is lost, on average, before entering the systemic circulation. That is, all have a low average *oral bioavailability* (F_{oral}), which refers to the fraction of the oral dose that reaches the systemic circulation in the unchanged form. Since metabolism is frequently the major source of first-pass drug elimination, F_{oral} is often used to assess the extent of first-pass metabolism. F_{oral} can be calculated from the ratio of the area under the blood or plasma concentration-time curve following oral administration (AUC_{oral}) to that following intravenous administration (AUC_{iv}) after correcting for dose:

$$F_{oral} = \frac{AUC_{oral}}{AUC_{iv}} \times \frac{Dose_{iv}}{Dose_{oral}}$$

Table 1 Selected Drugs with Low and Variable Oral Bioavailability Believed to Be Due in Part to Intestinal First Pass Metabolism

Drugs	Intestinal enzyme(s)	Oral bioavailability (%) (average ± SD)
Alfentanil	CYP3A (10)	43 ± 19
Amiodarone	CYP3A	46 ± 22
Atorvastatin	CYP3A	12
Buspirone	CYP3A	3.9 ± 4.3
Cyclosporine	CYP3A	28 ± 18
Diclofenac	CYP2C9	54 ± 2
Dihydroergotamine	CYP3A (11)	0.5 ± 0.1 (12)
Diltiazem	CYP3A	38 ± 11
Erythromycin	CYP3A	35 ± 25
Ethinylestradiol	CYP3A, SULT1E1, UGT1A1(13,14,15,16)	42 (15)
Felodipine	CYP3A	15 ± 8
Fluvastatin	CYP2C9	29 ± 18
Irinotecan	CYP3A, CES2 (17,18,19)	8 (19)
Isoproterenol	SULT1A3 (13,14)	28 (13)
Lidocaine	CYP3A	35 ± 11
Losartan	CYP2C9, CYP3A	36 ± 16
Lovastatin	CYP3A	≤5
Midazolam	CYP3A	44 ± 17
Nicardipine	CYP3A	18 ± 11
Nifedipine	CYP3A	50 ± 13
Omeprazole	CYP2C19, CYP3A	53 ± 29
Oxybutinin	CYP3A	1.6 10.9
Raloxifene	UGT1A1, UGT1A8, UGT1A10 (20)	2
Saquinavir	CYP3A	4 13
Sirolimus	CYP3A	15
Tacrolimus	CYP3A	25 ± 10
Terbutaline	SULT1A3 (14)	14 ± 2
Triazolam	CYP3A	44
Verapamil	CYP3A, CYP2C9	22 ± 8

Enzyme(s) and bioavailability values are from Ref. 21 unless indicated otherwise.

When drug-metabolizing organs are arranged sequentially, such as the small intestine and liver, F_{oral} may be viewed as the product of the fractions of the dose that escape first-pass metabolism by each organ:

$$F_{oral} = F_{abs} \times F_I \times F_L$$

where F_{abs} is the fraction of an oral dose absorbed intact through the apical membrane of the enterocyte, and F_I and F_L are the fractions of the absorbed dose that escape metabolism by the intestine (enterocytes) and liver, respectively. This simple equation illustrates the impact of a second presystemic site of metabolism on F_{oral}. For example, if the entire dose is absorbed intact into the enterocytes ($F_{abs} = 1$), has an F_I of 60% and an F_L of 40%, then an F_{oral} of 24% is predicted. If only first-pass metabolism by the liver is considered ($1 \times 1 \times 40\%$), then an F_{oral} of 40% is predicted. Thus, omission of the intestinal component would result in an overestimation of F_{oral}, which could potentially lead to suboptimal dosing and ineffective concentrations at the site(s) of action. For drugs that have a wide therapeutic window, this situation can be rectified simply by increasing the dose. However, for drugs that have a narrow therapeutic window, optimization of oral dosing regimens becomes more challenging. Moreover, factors that significantly alter metabolism, including other xenobiotics that induce or inhibit drug-metabolizing enzymes, thus altering F_I and/or F_L, present further challenges to optimal oral drug therapy.

The above equation also illustrates the potential impact of a second presystemic site of metabolism on the interindividual variation in F_{oral}. For example, if a drug has an F_I that varies from 30% to 60% (2-fold range), an F_L that varies from 20% to 80% (4-fold range), and the extraction efficiencies of the gut and liver vary independently, then F_{oral} will vary from 6% to 48% (8-fold range), resulting in a 100% increase in the variation in F_{oral} (if only F_L were considered initially). Indeed, data collected from 143 pharmacokinetic studies showed a significant inverse correlation between F_{oral} and the interindividual variation in F_{oral}, as measured by the coefficient of variation in F_{oral} (22). This relationship indicated that the greater the extent of first-pass elimination, the greater the variation in F_{oral}. Accordingly, knowledge of the degree and variation in the expression of the major drug-metabolizing enzymes in the human intestine is essential, as these enzymes can represent a key determinant of not only the extent of first-pass metabolism but also the interindividual variation in F_{oral} and the probability and magnitude of drug-xenobiotic interactions (23).

DRUG-METABOLIZING ENZYMES IN THE GUT WALL

The human GI tract shares several of the same drug-metabolizing enzymes as the liver and includes both phase I and phase II enzymes (Table 2). As with enzymes in the hepatocyte, enzymes in the enterocyte generally reside in either the microsomal or cytosolic fraction (Table 2). Compared with enzymes in the liver, research on the expression and catalytic properties of the complement of enzymes in the GI tract has lagged, largely due to a limited supply of high-quality tissue as well as the lack of sensitive methods to detect the low expression levels/catalytic activity relative to the liver. Over the past decade, however, a variety of human intestine derived tissue preparations have become available, including subcellular fractions (microsomes, cytosol), precision-cut tissue slices, shed enterocytes, Ussing chamber preparations, and intestinal cell lines (24,25). Thus, through the application of the same molecular biological techniques as for hepatic enzymes, coupled with the ongoing identification of selective catalytic probe

Table 2 Drug Metabolizing Enzymes in the Human Small Intestine That Are Known to be Expressed at the Protein Level and to Have Catalytic Activity

Enzyme	Location in subcellular fraction
Phase I	
Cytochromes P450 (CYPs)	Microsomes
Carboxylesterases (CESs)	Microsomes, cytosol
Epoxide hydrolases (EHs)	Microsomes, cytosol
Flavin monooxygenases (FMOs)	Microsomes
Phase II	
Sulfotransferases (SULTs)	Cytosol
UDP glucuronosyl transferases (UGTs)	Microsomes
N acetyltransferases (NATs)	Cytosol
Glutathione *S* transferases (GSTs)	Cytosol

substrates and inhibitors and improved methods of detection, a rigorous characterization of the various intestinal enzymes has become more feasible.

Phase I Enzymes

Cytochromes P450

The cytochromes P450 (CYPs) are the most prominent of the enteric phase I enzymes. The existence of CYP protein and associated monooxygenase activity (7-ethoxycoumarin *O*-deethylation) in the human small intestine was first reported in 1979 by Hoensch et al. (26), who determined total CYP content in a small number of surgical specimens. Average (±SD) content, as measured by carbon monoxide difference spectra, declined from proximal to distal regions and ranged from 93 ± 19 to 35 ± 4 pmol/mg microsomal protein; 7-ethoxycoumarin *O*-deethylase activity paralleled this pattern. Similar values were reported later by other investigators (27,28). Thus, on a per microgram microsomal protein basis, total CYP content in the average adult small intestine ranges from approximately 10% to 30% of that in the average human liver. Almost a decade following the report by Hoensch et al. (26), a series of pivotal in vitro and in vivo studies by Watkins and coworkers identified CYP3A as the major CYP subfamily expressed in human enterocytes.

CYP3A.

In Vitro Studies. Utilizing mucosae isolated from jejunal sections from four surgical patients, Watkins et al. identified a CYP enzyme and associated mRNA that were recognized selectively by an anti-CYP3A1 murine monoclonal antibody (which detected all human CYP3A forms) and HLp (CYP3A4) cDNA, respectively (29). Using purified HLp as the reference standard, average (±SD) CYP3A protein content in microsomes prepared from the specimens was comparable to that for liver microsomes prepared from four separate organ donors/surgical patients (70 ± 20 vs. 65 ± 20 pmol/mg). Moreover, the average CYP3A-catalyzed rate of erythromycin *N*-demethylation in jejunal microsomes was comparable to that for liver microsomes and was inhibited by anti-CYP3A1. Three years later, de Waziers et al. (30) quantified, by immunoblot analysis, the levels of various CYP isoforms/subfamilies in microsomes prepared from the following human extrahepatic tissues: esophagus, stomach, duodenum, jejunum, ileum, colon, and kidney. These investigators reported that, next to the liver, the duodenum was the highest with respect to immunoreactive CYP3A protein, followed by the jejunum and then by the

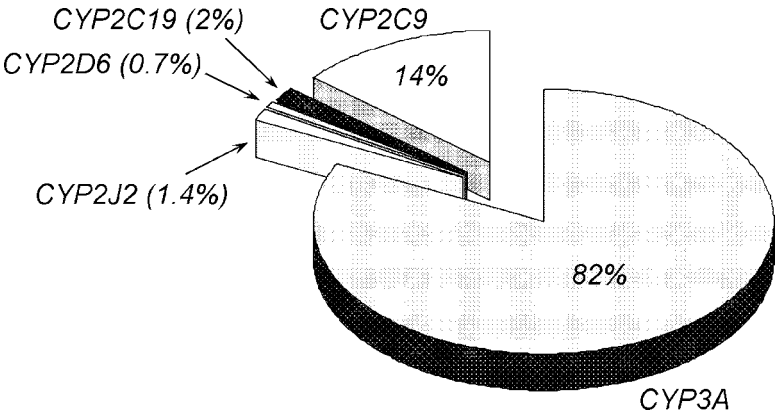

Figure 2 The average human proximal small intestinal cytochrome P450 "pie." The percent contributions of individual enzymes are based on average total immunoquantified CYP content (61 pmol/mg). Adapted from Ref. 31.

ileum. Average duodenal, jejunal, and ileal CYP3A content represented approximately 50%, 30%, and 10%, respectively, of average hepatic CYP3A content. Corresponding values for the remaining extrahepatic organs were less than 5%. Consistent with the report by Watkins et al., CYP3A was the dominant CYP expressed in all three regions of the small intestine. More recently, a comprehensive analysis of microsomes prepared from the duodenal/proximal jejunal portion of 31 unrelated human donor small intestines demonstrated CYP3A as the major "piece" of the intestinal CYP "pie," representing approximately 80% of total immunoquantified CYP protein (31) (Fig. 2). Subsequent to the earlier in vitro studies, the significance of intestinal CYP3A to first-pass drug metabolism in vivo was demonstrated.

In Vivo Studies. The widely used immunosuppressive agent, cyclosporine, is notorious for having a large interindividual variation in F_{oral}, which has been reported to range from 5% to 89% for the conventional formulation (Sandimmune) (32) and from 21% to 73% for the microemulsion formulation (Neoral) (33 36). This property, coupled with a narrow therapeutic window, can lead to an under- or overdosing of the patient, which in turn can lead to graft rejection or toxicity. The low and unpredictable F_{oral} of cyclosporine was believed initially to result from erratic absorption through the intestinal lumen coupled with variable hepatic first-pass metabolism (i.e., a low and variable F_{abs} and F_L). However, Kolars et al. (37), after instilling cyclosporine into the duodenum of two patients during the anhepatic phase of their liver transplant operations, measured appreciable concentrations of two CYP3A-mediated primary metabolites in hepatic portal and systemic blood. The investigators concluded that the extrahepatic site of metabolism was the gut because organs other than the gut (i.e. kidney and lung) express low levels of CYP3A, and portal metabolite concentrations exceeded systemic concentrations at the end of the anhepatic phase. These observations provided direct evidence that the small intestine can contribute significantly to the first-pass metabolism of a CYP3A substrate. A subsequent pharmacokinetic analysis of cyclosporine AUC after oral and intravenous administration suggested that the intestine, rather than the liver, was largely responsible for the first-pass elimination of cyclosporine (38). However, cyclosporine is now known to be a substrate for the efflux transporter P-glycoprotein (P-gp), which is expressed on the apical membranes of enterocytes and other cell types. As such, this indirect approach would not distinguish between intestinal CYP3A-mediated metabolism and P-gp-mediated efflux.

The sedative-hypnotic agent and CYP3A substrate midazolam has been shown not to be a substrate for P-gp (39) and thus should serve as a "clean" in vivo CYP3A probe. Using a study design similar to that for the cyclosporine study, the disposition of midazolam and primary metabolite, 1′-hydroxymidazolam, were examined in a larger group of anhepatic transplant recipients following either intravenous ($n = 5$) or intraduodenal ($n = 5$) administration (40). Blood was collected simultaneously from the hepatic portal vein and a peripheral artery during the approximately one-hour anhepatic phase. Using the difference between the arterial and hepatic portal venous midazolam AUCs (intravenous) or between the hepatic portal venous and arterial midazolam and 1′-hydroxymidazolam AUCs (intraduodenal), an average (±SD) extraction fraction of 8 ± 12% and 43 ± 18% was calculated for subjects who received midazolam by the intravenous and intraduodenal route, respectively. The low and variable extraction fraction following intravenous administration indicated that the intestine contributed somewhat to the systemic metabolism of midazolam. Importantly, the fivefold greater value following intraduodenal administration was identical to the average intestinal extraction ratio estimated in healthy volunteers (43 ± 24%) (41). Moreover, these values were essentially identical to the average hepatic extraction ratio estimated in the healthy volunteer study (44 ± 14%) (410). These data strongly indicated that the small intestine is a major determinant of the overall extent of the first-pass metabolism of midazolam and can rival the liver.

By the indirect approach, enteric CYP3A also has been shown to contribute significantly to the first-pass metabolism of the calcium channel blockers nifedipine (42) and verapamil (43). The comparable contributions of the intestine and liver (mean extraction ratio of 49% and 48%, respectively) to the overall first-pass elimination of verapamil was confirmed subsequently using a method involving a multilumen intestinal perfusion technique and stable isotope-labeled drug (44). This method demonstrated the importance of the intestine not only to the first-pass metabolism of verapamil but also to the secretion of verapamil metabolites, some of which are substrates for P-gp and possibly multidrug resistance associated protein 2 (MRP2), another efflux transporter known to be expressed on the apical membranes of enterocytes. Indeed, intestinal secretion was shown to be as important as biliary excretion for the elimination of the metabolites.

For all of the aforementioned drugs, significant intestinal first-pass metabolism occurred despite that total CYP3A content of the entire gut mucosa has been estimated to be approximately 1% of total hepatic CYP3A content (70 vs. 5490 nmol) (27,45). Of apparently more importance than total enzyme mass is the comparable intracellular enzyme concentration (enterocyte vs. hepatocyte) and the obligatory nature of drug passage through the enterocyte (if transcellular absorption is operative). Thus, a more appropriate comparison might be microsomal intrinsic activities. Indeed, mean CYP3A-mediated rates of erythromycin *N*-demethylation (29), tacrolimus *O*-demethylation (46), midazolam 1′-hydroxylation (27), and testosterone 6β-hydroxylation (47) in small intestinal (duodenal/jejunal) microsomes were 45% to 120% of corresponding metabolic rates in hepatic microsomes. On the basis of these data, mean intestinal mucosal intrinsic clearances may be within two- to threefold of corresponding hepatic intrinsic clearances. Whether a similarity in vivo for a given drug will occur is more difficult to predict, as total oral dose, enzyme saturability, and absorption rate become relevant. Should the dose be large enough, and the K_m of the drug for the enzyme active site be low enough, it is possible that the majority of absorbed drug could escape intestinal first-pass metabolism. Some of the HIV protease inhibitors (e.g., indinavir, saquinavir, and ritonavir) may represent such drugs.

CYP3A4 vs. CYP3A5. As in the liver, CYP3A4 protein appears to be expressed constitutively in the small intestine of all individuals, whereas CYP3A5 expression is polymorphic. Immunoreactive CYP3A5 protein was detected readily at a frequency of 20% to 30% in intestinal tissue obtained from adult Caucasians (27,48,49). Moreover, if detected, the enzyme was expressed along the length of the small intestinal tract (27). As has been shown for the liver (50), the frequency of CYP3A5 expression in the small intestine varies among different racial/ethnic groups (49). With the advent of specific, commercially available antibodies and suitable reference standards for immunoblot analysis, CYP3A5 has been shown to constitute from 3% to 80% of total intestinal CYP3A (CYP3A4+CYP3A5) protein content (31,51). Accordingly, like hepatic CYP3A5 (50,52), enteric CYP3A5 may have a significant role in the first-pass metabolism of drugs in some individuals. Identification of a selective in vivo CYP3A5 probe substrate is needed to test this hypothesis.

Significant expression of CYP3A4 in the GI tract appears to be restricted to the small intestine. In mucosa of the stomach and colon, both CYP3A5 mRNA and protein were more prominent than corresponding CYP3A4 measures (53,54). Consistent with these observations, in two full-length human donor small intestines that were CYP3A5-positive, the ratio of CYP3A5 to CYP3A4 immunoreactive protein decreased from duodenum to jejunum, then increased in distal ileum to values comparable to or greater than those observed for the duodenum (55). Finally, Gervot et al. (56) detected CYP3A5 protein, but not CYP3A4 protein, in colonic mucosa from 40 unrelated and uninduced tissue donors. The authors suggested that any CYP3A4 in colonic tissue is likely to be a consequence of prior treatment of the donor with an enzyme inducer.

Localization. CYP3A4 protein expression along the length of the small intestine is not uniform. Enzyme content is generally highest from duodenum to middle jejunum then declines progressively to distal ileum (27,28,30). In microsomes prepared from mucosal scrapings obtained from 20 donor small intestines, median CYP3A4 content decreased from 31 to 23 to 17 pmol/mg protein in duodenum, jejunum, and ileum, respectively (27). CYP3A-catalyzed midazolam 1′-hydroxylation activity paralleled this pattern (27). Likewise, erythromycin *N*-demethylase activity decreased from proximal to distal regions (28). These data suggest that the extent of CYP3A-mediated first-pass metabolism may depend in part on the site of absorption.

CYP3A4 expression from the crypt to the tip of the small intestinal villus also is not uniform. By immunohistochemical analysis, CYP3A4 protein was not detected in the crypt cells or goblet cells but was readily detected in enterocytes, with the most intense staining evident in the mature enterocytes lining the villous tips (53,57). By in situ hybridization, a similar pattern was reported for CYP3A4 mRNA (54). Within the enterocyte, CYP3A4 protein was located predominately at the apex of the cell, adjacent to the microvillous border (54). The strategic location of CYP3A4 in mature enterocytes further highlights the small intestine as uniquely suited for the task of first-pass drug metabolism.

Modifying Agents and Conditions. Localization of CYP3A within only the mature enterocytes of the small intestinal mucosa is consistent with a wider pattern of differentiation of cell function as cells formed within the crypts migrate toward the villus tip and are eventually shed. Total CYP3A content even within a defined region of the small intestine varies considerably. CYP3A protein content measured in duodenal pinch biopsies obtained from CYP3A inducer/inhibitor-free healthy volunteers has been reported to vary approximately 10-fold (48,49). Even greater variability (>30-fold) was reported for CYP3A protein content and catalytic activity in duodenal, jejunal, and ileal mucosal scrapings obtained from 20 organ donors (27). Although some of the extreme

variability in the latter study could have been due to events preceding organ procurement (e.g., reduced nutritional intake, antibiotic administration, brain death, and ischemia), these observations suggest that CYP3A is remarkably sensitive to a variety of modifying factors or conditions that can alter enzyme expression.

Dietary Factors. One of the most extensively studied dietary substances in terms of CYP3A-mediated drug metabolism is grapefruit juice, which, when consumed in usual volumes, has been shown to elevate systemic concentrations of a variety of drugs by inhibiting intestinal, but not hepatic, CYP3A-mediated first-pass metabolism (58 61). The lack of an effect on hepatic CYP3A has been attributed to dilution of the causative ingredients in portal blood to concentrations below their effective inhibitory concentrations (K_i or IC_{50}) and/or to avid binding of the causative ingredients to plasma and/or cellular proteins in portal blood (62,63). The magnitude of the grapefruit juice effect can be large enough to cause untoward effects, such as severe muscle pain with some HMG-CoA reductase inhibitors (statins) (64,65) and hypotension/dizziness with some calcium channel antagonists (66). Accordingly, the labeling of several drug products contains precautionary statements regarding the concomitant intake of grapefruit juice. Using a "furanocoumarin-free" grapefruit juice suitable for human consumption and the CYP3A probe substrate felodipine, furanocoumarins were demonstrated unequivocally as major causative ingredients, several of which are potent reversible and mechanism-based inhibitors of enteric CYP3A catalytic activity (60,67). In addition, the pioneering study by Lown et al. (68) showed that grapefruit juice significantly reduced average enteric CYP3A4 immunoreactive protein (measured in duodenal pinch biopsies) by 60% in 10 healthy volunteers; the lack of a decrease in corresponding mRNA suggested a posttranscriptional mechanism. In vitro studies involving CYP3A4-expressing Caco-2 cells confirmed that two candidate furanocoumarins (bergamottin and 6′,7′-dihydroxybergamottin) reduced CYP3A4 protein by accelerating enzyme degradation without affecting enzyme synthesis (69). The list of drugs shown to interact with grapefruit and related citrus juices is expansive and is described in several comprehensive reviews (58 61).

Therapeutic Agents. Therapeutic agents that have been shown to inhibit intestinal CYP3A in vivo include the azole antifungals ketoconazole (70) and fluconazole (71); the macrolide antibiotics erythromycin (72), troleandomycin (10), and clarithromycin (73,74); and the calcium channel antagonist diltiazem (75). Exposure of human subjects to the enzyme inducer rifampin (7 10 days) and to the popular herbal medicine St. John's wort (14 days) increased average duodenal CYP3A protein content by $\geq$4- and 1.5-fold, respectively, relative to baseline (43,57,76). Moreover, a comparison of the effect of rifampin on the systemic and apparent oral clearance of the CYP3A probes midazolam (10,77), triazolam (78), verapamil (43), nifedipine (42), and alfentanil (10) suggested that the inducer increased enteric enzyme levels to an extent greater than hepatic levels. The greater effect of enzyme inhibitors and inducers on enteric CYP3A activity compared with hepatic CYP3A activity may be due to higher intracellular concentrations and greater receptor occupancy in the enterocyte that occurs during absorption of the modifying agent.

Pathophysiologic Conditions. Although less is known about the effect of disease on enteric CYP3A relative to hepatic CYP3A, some human studies have shown that pathophysiologic conditions can markedly alter enteric CYP3A protein expression/catalytic activity. For example, Lang et al. (79) reported that adult patients with celiac

disease had reduced levels of jejunal mucosal CYP3A protein as a consequence of widespread epithelial cell destruction. Treatment with a gluten-free diet reversed this aberration. Similar observations have been reported for pediatric patients with celiac disease (80). In the pediatric patients, after gluten rechallenge, a further decrease in enteric CYP3A expression was observed. Chalasani et al. (81) compared the disposition of midazolam between cirrhotic patients, cirrhotic patients with transjugular intrahepatic portosystemic shunts (TIPS), and healthy volunteers. The significantly higher mean F_{oral} in the cirrhotic patients with TIPS compared with the cirrhotic patients and healthy volunteers (0.76 vs. 0.27 and 0.30) was largely due to the significantly higher F_I in the TIPS patients compared with the cirrhotic and healthy subjects (0.83 vs. 0.32 and 0.42). The markedly lower extent of midazolam first-pass metabolism in the TIPS patients was concluded to result from diminished enteric CYP3A activity.

Intestinal vs. Hepatic CYP3A. In view of the many differing responses between enteric and hepatic CYP3A to various regulatory factors, including those aforementioned, it follows that intestinal and hepatic CYP3A appear to be regulated independently. Such noncoordinate regulation was first demonstrated by Lown et al. (48), who reported that neither duodenal CYP3A protein content nor catalytic activity correlated with hepatic CYP3A activity in 20 healthy subjects. Likewise, other investigators found no rank order correlation between intestinal and hepatic CYP3A protein content or midazolam 1′-hydroxylation activity in microsomes prepared from eight matched intestine-liver donor pairs (27). Finally, independent groups of investigators found no correlation between the F_I and F_L of midazolam in healthy volunteers (41,73). This noncoordinate regulation between intestinal and hepatic CYP3A indicates that a measure of one should not be used to predict the other. However, the possibility of overlapping mechanisms of constitutive and inducible CYP3A expression cannot be excluded.

CYP1A1. CYP1A1 is expressed predominantly in extrahepatic tissues, including the lungs (82 84), placenta (85,86), stomach, and small intestine (31,87 89). In two independent investigations in which duodenal biopsies were obtained from healthy volunteers, CYP1A1 mRNA was expressed constitutively in all specimens; as with other CYP isoforms, large interindividual variation was evident among the specimens, at least sixfold (88,90). CYP1A1 protein and/or catalytic (ethoxyresorufin *O*-deethylase or EROD) activity were undetectable or low. Following treatment with the CYP1A inducers omeprazole (88) or chargrilled meat (90), enteric CYP1A1 protein and catalytic activity became readily detectable. Similarly, median duodenal EROD activity was higher in smokers and omeprazole-treated patients compared with nonsmoking control subjects (2.1 vs. 1.1 vs. 0.5 pmol/min/mg homogenate protein) (89).

Characterization of a bank of microsomes prepared from the proximal region of 18 human donor small intestines showed measurable rates of ethoxyresorufin *O*-deethylation in one-third of the donors, with a median and range (23.7 and 1.4 124 pmol/min/mg, respectively) (55) comparable to those reported for CYP1A2-catalyzed EROD activity in human liver microsomes (39.4 and 10.1 224 pmol/min/mg, respectively) (91). Median CYP1A1 protein content for the three preparations in which immunoreactive CYP1A1 was detected readily (5.6 pmol/mg) (31) was 14% of the average CYP1A2 protein content reported for a large panel of human liver microsomes (41 pmol/mg) (92). The differing protein contents between enteric CYP1A1 and hepatic CYP1A2 despite comparable EROD activities were attributed to CYP1A1 having a greater catalytic efficiency than CYP1A2 toward the *O*-deethylation of ethoxyresorufin, as evidenced by recombinant CYP1A1 having both a lower K_m and a higher V_{max} compared with recombinant CYP1A2

(87 nM and 7.6/min vs. 240 nM and 1.9/min) (93). A greater catalytic efficiency for CYP1A1 compared with CYP1A2 also has been demonstrated for ethoxycoumarin *O*-deethylation and benzo(*a*)pyrene hydroxylation (94). In contrast, the catalytic efficiency of CYP1A1 toward the CYP1A drug substrates caffeine (95), theophylline (96), phenacetin (97), and *R*-warfarin (98) has been shown to be much lower than that compared with CYP1A2. Consistent with these observations, to date, there are no examples reported in the literature describing enteric CYP1A1 as having a significant role in the first-pass metabolism of drugs.

CYP2C9. Although CYP2C mRNAs have been detected in a number of human extrahepatic tissues (e.g., kidney, testes, adrenal gland, prostate, brain, duodenum), significant protein expression appears to be limited to the small intestinal tract (30,99). de Waziers et al. (30) first detected what was described as "CYP2C8-10" in small intestinal microsomes, which, like CYP3A, was expressed predominantly in the proximal region. Other investigators later confirmed the descending pattern of expression of a CYP2C enzyme along the length of the small intestine (28). However, in both studies, it was unclear which enzyme (CYP2C8, CYP2C9, or CYP2C19) was detected. On the basis of the relative amount of each CYP2C enzyme in human liver, the intestinal form identified was most likely CYP2C9. From an analysis of 31 duodenal/jejunal microsomal preparations, two proteins were detected that reacted with a CYP2C-selective anti-CYP2C19 antibody and that comigrated with recombinant CYP2C9 and CYP2C19 protein standards (31). CYP2C9 protein content varied ninefold among the different preparations, with a mean specific content (8.4 pmol/mg) that was nearly one-tenth of reported average hepatic microsomal specific content (73 pmol/mg protein) (100).

With respect to intestinal CYP2C9 catalytic activity, Prueksaritanont et al. (101) reported a >20-fold variation in tolbutamide methylhydroxylase activity (<0.5 9.8 pmol/min/mg) for five duodenal/jejunal microsomal preparations; average (±SD) activity (5.1 ± 3.8 pmol/min/mg) was at least one-tenth of the hepatic counterpart. Other investigators subsequently reported a similarly large interindividual variation in CYP2C9-catalyzed diclofenac 4′-hydroxylase activity (7.3 129 pmol/min/mg) for 10 human jejunal microsomal preparations; median activity was 55 pmol/min/mg (47), which was roughly one-sixth of that reported for a panel of 16 human liver microsomal preparations (~320 pmol/min/mg) (102). Collectively, these in vitro data suggest that the small intestine would have minimal contribution to the first-pass metabolism of drugs. However, due to the wide range in both specific content and activity, enteric CYP2C9 could be important in some individuals for substrates with a low oral bioavailability, for example, fluvastatin (103). In addition, the low expression/catalytic activity of CYP2C9 in the intestine relative to the liver does not preclude the potential importance of enteric CYP2C9 to the first-pass metabolism of substrates ingested in trace amounts, for example, pesticides (104,105).

CYP2C19. CYP2C19 immunoreactive protein content for the aforementioned 31 human duodenal/jejunal microsomal preparations ranged from <0.6 to 3.9 and averaged 1.0 pmol/mg (31), which was one-fifteenth of average hepatic microsomal content (14 pmol/mg) (100). Large interindividual variation in enteric CYP2C19 catalytic activity also has been reported. CYP2C19-catalyzed *S*-mephenytoin 4′-hydroxylase activity varied from 0.8 to 13.1 pmol/min/mg in the same panel of human small intestinal microsomal preparations that were analyzed previously for CYP2C9 activity (47). Average enteric catalytic activity (5.2 pmol/min/mg) was approximately one-tenth of the average activity reported for a panel of 10 human liver microsomal preparations (~45 pmol/min/mg) (106). As with

enteric CYP2C9, these data suggest a minimal role for enteric CYP2C19 in the first-pass metabolism of drugs. The scarcity of CYP2C19 drug substrates with a low oral bioavailability supports this contention. Again, the low enteric CYP2C19 expression/activity relative to hepatic CYP2C19 does not preclude the potential importance of enteric CYP2C19 to the first-pass metabolism of substrates ingested in trace amounts, for example, pesticides and insect repellents (105,107).

CYP2D6. CYP2D6 expression in the human intestine was first reported in 1990 by de Waziers et al. (30). Like CYP3A4, CYP2D6 protein was most concentrated in the proximal region and was localized in the enterocytes. The enzyme was not detected in ileum or colon. Prueksaritanont et al. later confirmed the expression of CYP2D6 protein in microsomes prepared from the proximal portion of two (108) and five (101) human donor small intestines. Moreover, CYP2D6-catalyzed (+)-bufuralol 1′-hydroxylation activity was measurable in all preparations. From a comprehensive comparison involving 19 human jejunal and 31 human liver microsomal preparations, CYP2D6 immunoreactive protein was detected readily in 18 of the intestinal preparations, with a median specific content (0.9 pmol/mg) that was one-fifteenth of the median content measured in the liver preparations (12.8 pmol/mg) (109). Median catalytic activity, as assessed by the intrinsic clearance of metoprolol oxidation, was also much lower in jejunal compared with hepatic microsomes (0.7 vs. 19.7 μl/min/mg). Likewise, the predicted average in vivo intestinal extraction ratio for metoprolol was negligible compared with the predicted average hepatic extraction ratio (0.01 vs. 0.48). The authors concluded that, unless a CYP2D6 substrate has a long residence time in the intestinal mucosa or undergoes futile cycling via an efflux transporter, enteric CYP2D6 would be expected to contribute minimally to the first-pass metabolism of drugs. However, enteric CYP2D6 may become clinically relevant if it mediates the formation of a cytotoxic metabolite that could cause mucosal damage (109).

CYP2J2. CYP2J2 is a relatively newly identified human CYP that is expressed predominately in extrahepatic tissues (110). Although most abundant in the heart, CYP2J2 is also expressed at appreciable levels (both mRNA and immunoreactive protein) in the GI tract (111). Immunoreactive CYP2J2 protein has been detected in microsomes prepared from the human esophagus, stomach, small intestine, and colon. Unlike other small intestinal CYPs, CYP2J2 expression was qualitatively highest in the esophagus and slightly lower but relatively uniform throughout the remainder of the GI tract (111). Moreover, there was little interindividual variation in CYP2J2 expression in jejunal microsomes. Although the role of CYP2J2 in drug metabolism remains largely unknown, in vitro studies have suggested that intestinal CYP2J2 contributes to the first-pass metabolism of the non-sedating antihistamines astemizole and ebastine.

Using human intestinal and liver microsomes, Matsumoto et al. (112) showed *O*-demethylation as the primary metabolic pathway for astemizole, with the average (±SD) rate in enteric microsomes being approximately one-third of that in liver microsomes (170 ± 57 vs. 480 ± 88 pmol/min/mg). With recombinant CYP2J2 as the reference standard, immunoreactive CYP2J2 protein in microsomes prepared from five human small intestines averaged 2.1 (±0.6) pmol/mg, consistent with that measured in a larger number of small intestinal microsomal preparations (1.0 ± 0.1 pmol/mg; $n = 31$) (31). These observations are comparable to average CYP2J2 content measured in liver microsomes from 20 Japanese and 29 Caucasian donors (2.0 ± 1.5 and 1.2 ± 2.1 pmol/mg, respectively) (113). A role of intestinal CYP2J2 in the *O*-demethylation of astemizole was supported further by the excellent correlation between CYP2J2 protein content and *O*-demethylastemizole formation rate in intestinal microsomes ($r = 0.90$, $p < 0.05$), as

well as the strong inhibition of *O*-demethylastemizole formation by the CYP2J2 substrates ebastine and arachidonic acid. Using similar strategies, along with an inhibitory anti-CYP2J2 antibody, Hashizume et al. (114) demonstrated CYP2J2 as the major ebastine hydroxylase in human intestinal microsomes. Whether intestinal CYP2J2 contributes to the first-pass metabolism of astemizole, ebastine, and other drugs in vivo awaits further investigation.

CYP4F. CYP4F enzymes catalyze the biotransformation of several endogenous compounds, including arachidonic acid and its derivatives, such as leukotrienes, prostaglandins, lipoxins, and hydroxyeicosatetraenoic acids (115). Accordingly, the CYP4Fs are important regulators of vascular tone and inflammation, as well as other physiologic functions. In addition to their role in the biotransformation of endogenous compounds, the CYP4Fs have been reported to metabolize some drugs. For example, CYP4F12 was shown to be expressed, by RT-PCR, in human liver and small intestine (116). Yeast-expressing CYP4F12 was capable of catalyzing the hydroxylation of ebastine, suggesting that CYP4F12 in the small intestine (and liver) may have a role in the first-pass metabolism of this drug. However, as reported subsequently by the same investigators, intestinal CYP2J2 was shown to be the predominate enzyme involved in this pathway (114). Most recently, Wang and coworkers identified CYP4Fs as the major enzymes in human proximal small intestinal microsomes that catalyze the initial *O*-demethylation of the antiparasitic agent pafuramidine (117). However, the much lower average intrinsic clearance of this reaction (0.3 mL/min/mg; $n = 9$) relative to that in pooled liver microsomes (7.6 mL/min/mg) suggested that enteric CYP4Fs do not contribute significantly to the initial *O*-demethylation of pafuramidine during first-pass. A role of enteric CYP4F in subsequent *O*-demethylation reactions remains to be determined. Interestingly, quantitative Western blot analysis of these intestinal preparations indicated appreciable CYP4F protein expression in the small intestine, with a mean (range) of 7 pmol/mg (3 18), which was comparable to that for CYP2C9. This observation suggested that CYP4F could represent an appreciable portion of the human intestinal CYP pie (117).

Other CYPs. Other CYP enzymes shown to be expressed in the human small intestine at the mRNA level include CYP1A2, but only after treatment with omeprazole (88), CYP1B1 (28), and CYP2C8 and CYP2C18 (99). The importance of these enzymes in vivo remains to be determined. By immunoblot analysis, and with prolonged exposure, CYP2A6, CYP2B6, CYP2C8, CYP2E1, and CYP4A11 either were not detected or were expressed in only trace amounts (30,31,117,118). The roles of these enzymes in enteric drug metabolism are likely to be negligible.

Other Phase I Enzymes

Other phase I enzymes reported to be expressed in the human intestine include carboxylesterases (CESs) (119), epoxide hydrolases (30,120), and flavin monooxygenases (FMOs) (121). Of these enzymes, the CESs have been implicated in the first-pass metabolism of some drugs. Whereas the CES1 family predominates in the liver, the CES2 family predominates in the small intestine (119). Human intestinal microsomes have been shown to catalyze the hydrolysis of betamethasone valerate and aspirin at comparable (aspirin) or greater (betamethasone valerate) rates than human liver microsomes (119). Likewise, intestinal biopsy tissues were as proficient as liver biopsy tissues in converting the prodrug irinotecan to the active chemotherapeutic metabolite, SN-38 (17,18).

Approximately one-third of an intravenous radiolabeled dose of irinotecan has been detected in human bile as unchanged drug (122). Therefore, because the bile duct empties into the duodenum, direct conversion of the prodrug to SN-38 could occur in the intestine, as well as bacterial β-glucuronidase-mediated deconjugation of SN-38 glucuronide, leading to accumulation of SN-38 in the intestine and the potential for toxicity (i.e., severe diarrhea). Moreover, the large interindividual variability in the systemic exposure of irinotecan and SN-38 following oral administration of irinotecan has been attributed in part to interindividual variation in the extent of intestinal CES-mediated first-pass metabolism (123).

Epoxide hydrolases have been detected in the human small intestine, but protein levels and catalytic activity were much lower ($\leq$6%) relative to the liver (30,120). Although a significant role for intestinal epoxide hydrolases in the first-pass metabolism of drugs has not been described, these enzymes could play a protective role in the detoxification of procarcinogenic epoxides generated from environmental xenobiotics (13). Like epoxide hydrolases, FMOs (to date only FMO1) have been detected in the human small intestine, but the much lower catalytic activity (*p*-tolyl methyl sulfoxidation) relative to the liver (0.11 $\pm$ 0.04 vs. 2.8 $\pm$ 1.4 nmol/min/mg microsomal protein, respectively) indicates a minimal role for these enzymes in the first-pass metabolism of drugs (121,124).

Phase II Enzymes

Sulfotransferases

At least four sulfotransferases (SULTs) are known to be expressed and to have functional activity in the human GI tract: SULT1A1, SULT1A3, SULT1E1, and SULT2A1. Using cytosolic fractions prepared from the stomach, small intestine, and colon of 23 unrelated organ donors, Chen et al. (125) showed the stomach and colon to have low sulfation activity toward 2-naphthol (SULT1A1) and dopamine (SULT1A3) and to have very low to no activity toward estradiol (SULT1E1) and dehydroepiandrosterone (DHEA) (SULT2A1). Comparatively, sulfation activity toward all probe substrates was higher in the small intestine. Given the much greater surface area of the small intestine, sulfation activity in this section of the GI tract is undoubtedly the most important with respect to drug metabolism. Average ($\pm$SD) small intestinal SULT1A1 and SULT2A1 activities were less than one-half and approximately one-fifth, respectively, of the corresponding activities measured in four human liver cytosolic preparations (2.1 $\pm$ 1.4 vs. 5.3 $\pm$ 1.0 nmol/min/mg and 32 $\pm$ 33 vs. 140 $\pm$ 28 pmol/min/mg, respectively) (125). In contrast, small intestinal SULT1A3 and SULT1E1 activities were approximately threefold higher than and comparable to, respectively, the corresponding hepatic activities (0.45 $\pm$ 0.25 vs. 0.17 $\pm$ 0.05 nmol/min/mg and 3.3 $\pm$ 0.9 vs. 2.6 $\pm$ 1.6 pmol/min/mg, respectively) (125). Intestinal sulfation activity toward all probe substrates showed large interindividual variation, as exemplified by coefficients of variation of at least 60%, consistent with an earlier report involving 62 human jejunal preparations analyzed for SULT1E1 and SULT2A1 immunoreactive protein (126). SULT activity along the length of the small intestine varied among different donors; some donors showed higher activity in the proximal portion, while others showed higher activity in the distal portion (125). Age, sex, underlying pathology, and time of tissue storage appeared not to influence SULT activity and/or protein expression (125,126). No significant correlation was evident between any of these enzymes with respect to catalytic activity or protein expression, suggesting the enzymes are regulated independently (125,126).

Of the aforementioned intestinal SULTs, SULT1A3 and SULT1E1 have been implicated to contribute significantly to the first-pass metabolism of some drugs. Intestinal SULT1A3-mediated metabolism likely contributes to the low oral bioavailability of the β-adrenergic agents isoproterenol and terbutaline (14,127,128) (Table 1). SULT1E1 is likely the major intestinal SULT involved in the first-pass metabolism of ethinyl estradiol (126,129,15) (Table 1).

UDP-Glucuronosyl Transferases

The UDP-glucuronosyl transferases (UGTs) are ubiquitous in a number of extrahepatic tissues, including the GI tract (130,131). As with sulfation activity, relative to the small intestine, glucuronidation activity in general appears to be much lower in the stomach and colon (and esophagus) (130). Also like the SULTs, the expression of a relatively small number of UGTs has been confirmed in the small intestine by multiple laboratories using the same or different approaches: UGT1A1, UGT1A3, UGT1A8, UGT1A10, and UGT2B7 (132). In addition, selective expression of UGT1A8 and UGT1A10 mRNAs in the small intestine and/or colon vs. the liver has been reported by multiple investigators (132). Of all of these enzymes, only UGT1A1 and UGT2B7 have been detected at the protein level in small intestinal microsomes (131); specific antibodies are not yet available for the remaining enzymes (132). Using microsomes prepared from the three regions of three unrelated donor intestines, Fisher and coworkers showed UGT1A1 activity, as measured by estradiol 3-glucuronidation, to be generally much higher than that in pooled human liver microsomes (0.2 3.9 vs. 0.4 nmol/min/mg) (131), suggesting an important role for intestinal UGT1A1 in the first-pass metabolism of relevant drug substrates. In contrast, intestinal UGT2B7 activity, as measured by morphine 3-glucuronidation, was at most one-fifth of that measured in the pooled liver microsomes (0 0.5 vs. 2.3 nmol/min/mg), suggesting a minor role for intestinal UGT2B7 in the first-pass metabolism of morphine and other UGT2B7 substrates. Multiple investigators have shown many enteric UGTs to have large interindividual variation in expression level and/or catalytic activity (132,133). Moreover, UGT activity along the length of the small intestine appears to vary with substrate/UGT isoform (132,134). For example, UGT activity toward testosterone (a UGT2B substrate) increased gradually from proximal jejunum to colon, whereas that toward bilirubin (a UGT1A1 substrate) decreased sharply from proximal to distal intestine (132).

Of the aforementioned intestinal UGTs, several of the UGT1As have been implicated to contribute significantly to the extensive first-pass metabolism, and hence low oral bioavailability, of some drugs. For example, evidence suggests that enteric UGT1A1, in addition to enteric CYP3A and SULT1E1, may contribute to the first-pass metabolism of ethinyl estradiol (129,16) (Table 1). The intestine-specific forms, UGT1A8 and UGT1A10, likely are the major contributors to the low oral bioavailability of raloxifene (20,135,136) (Table 1). Enteric UGT1As (e.g., UGT1A1, UGT1A3) may influence the efficiency of the enterohepatic cycling of SN-38 (137) and ezetimibe (138,139).

Other Phase II Enzymes

Other phase II enzymes that have been identified in the human GI tract include members of the *N*-acetyltransferase (NAT) and glutathione *S*-transferase (GST) families (30,133,140 142). Mesalazine (5-aminosalicylic acid), indicated for the treatment of inflammatory bowel disease, undergoes extensive first-pass acetylation, and intestinal

NAT, most likely NAT1 (141), is believed to contribute to this process (143). Although both NAT1 and NAT2 have been detected and to have functional activity in the small intestine, NAT1 activity, as measured by *p*-aminobenzoic acid acetylation, was always higher than NAT2 activity, as measured by sulfamethazine acetylation (141). Moreover, the ratio of NAT1:NAT2 activities varied from 2- to 70-fold. Among four human donor small intestines, NAT1 activity was relatively uniform or increased slightly, whereas NAT2 activity tended to decrease, from the duodenum to the rectum.

The GSTs are commonly implicated in the detoxification or bioactivation of environmental toxins, carcinogens, and some chemotherapeutic agents. Using cytosolic fractions prepared from the GI tracts (stomach to colon) of 16 organ donors, Coles et al. showed GSTP1, GSTA1, and GSTA2 to be the major GST proteins expressed in the small intestine (142). For all three of these enzymes, large interindividual variation was observed in all regions of the GI tract. Despite the high degree of interindividual variability, consistent patterns of expression along the length of the GI tract were evident. Specifically, GSTP1 was expressed throughout the GI tract and decreased progressively from stomach to colon. In contrast, GSTA1 and GSTA2 were expressed at very low levels in the stomach and colon relative to the small intestinal regions, where levels were high in the duodenum and decreased to distal ileum. Similar differences in expression between stomach and duodenum for GSTA and GSTP were reported by other investigators who examined antral and duodenal biopsy specimens obtained from 202 patients (144). It has been speculated that the low levels of GSTA in the stomach and colon contribute to the greater susceptibility of these GI tissues to some cancers compared with the small intestine (133,142). With respect to chemotherapeutic agents, Gibbs and coworkers, using cytosol prepared from 12 small intestines and 23 livers, reported comparable busulfan conjugation intrinsic clearances (GSTA activity) between the two organs (0.17 ± 0.07 vs. 0.18 ± 0.09 μL/min/mg), suggesting a role for intestinal GSTA in the first-pass metabolism of busulfan (140).

SUMMARY AND PERSPECTIVE

Most drugs are taken orally. For those intended to act systemically, a significant fraction of the dose can be eliminated during its first passage through a sequence of organs prior to entering the systemic circulation. For some drugs, the extent of first-pass elimination can be large enough so that oral bioavailability is reduced significantly, with the consequent potential for a reduced clinical response. Next to the liver, the small intestine can represent a major organ of first-pass drug elimination, the means of which occurs primarily via metabolism.

Like the liver, the small intestinal mucosa is replete with a myriad of drug biotransformation enzymes, including both phase I and phase II enyzmes. Of all these enzymes, the CYPs are the most extensively studied. Of the CYP enzymes, CYP3A is the most extensively studied and represents, on average, approximately 80% of total immunoquantified CYP content in the proximal human small intestine. In addition, microsomal CYP3A catalytic activity and immunoreactive protein content in the proximal region (duodenum to mid-jejunum) are within the ranges reported for human liver microsomes. These in vitro observations are consistent with clinical studies demonstrating that the intestinal contribution to the low and variable F_{oral} of some CYP3A substrates can rival the hepatic contribution. However, because intestinal and hepatic CYP3A appear to be regulated independently, and thus do not correlate, CYP3A activity measured in one organ will not necessarily predict CYP3A activity in the other. Taken together, the

development/refinement of in vivo methods capable of delineating intestinal from hepatic first-pass metabolism, as well as capable of delineating CYP3A-mediated metabolism from transporter-mediated efflux, is of clinical importance. This is an ongoing and active area of research, as the successful prediction of intestinal first-pass metabolism could aid in the therapeutic management of drugs with a low and variable F_{oral}, particularly those with a narrow therapeutic window.

Other human enteric CYP enzymes have been identified and characterized in vitro (CYP1A1, CYP2C9, CYP2C19, CYP2D6, CYP2J2, CYP4F), but their role in drug disposition in vivo remains to be determined. Regarding other enteric phase I enzymes, CESs have been implicated in the first-pass metabolism of some drugs, whereas roles for the epoxide hydrolases and FMOs remain to be determined. Regarding phase II enzymes, while a number of such families have been known to be expressed in the human intestine for some time (e.g., SULTs, UGTs, NATs, GSTs), progress on the identification and quantification of individual isoforms has lagged behind that of the CYPs. With the increasing availability of quality human intestinal tissue, along with the ongoing identification of selective probe substrates, inhibitors, and antibodies, it is anticipated that a comprehensive characterization of these enzymes will soon become achievable. Meanwhile, further refinement of human intestinal cell culture models and/or the identification of an appropriate animal model should improve our understanding of the unique nature of intestinal drug-metabolizing enzymes and allow us not only to better predict the impact of the intestine on the overall first-pass elimination of existing drugs but also to improve the drug selection process during preclinical development.

REFERENCES

1. Rowland M, Tozer TN. Clinical Pharmacokinetics. Concepts and Applications. 3rd ed. Philadelphia: Lippincott Williams & Wilkins, 1995.
2. Wienkers LC, Heath TG. Predicting in vivo drug interactions from in vitro drug discovery data. Nat Rev Drug Discov 2005; 4:825 833.
3. Lin JH, Lu AY. Interindividual variability in inhibition and induction of cytochrome P450 enzymes. Annu Rev Pharmacol Toxicol 2001; 41:535 567.
4. Aungst B, Shen DD. Gastrointestinal absorption of toxic agents. In: Rozman K, Hanninen O, eds. Gastrointestinal Toxicology. Amsterdam: Elsevier Science Publishers B.V., 1986:29 56.
5. Nugent SG, Kumar D, Rampton DS, Evans DF. Intestinal luminal pH in inflammatory bowel disease: possible determinants and implications for therapy with aminosalicylates and other drugs. Gut 2001; 48:571 577.
6. DeSesso JM, Jacobson CF. Anatomical and physiological parameters affecting gastrointestinal absorption in humans and rats. Food Chem Toxicol 2001; 39:209 228.
7. Rubin DC. Small intestine: anatomy and structural anomalies. In: Yamada T, Alpers DH, Kaplowitz N, et al., eds. Textbook of Gastroenterology. 4th ed. Philadelphia: Lippincott Williams & Wilkins, 2003:1466 1485.
8. Paine MF, Thummel KE. Role of Intestinal Cytochromes P450 in Drug Disposition. In: Obach RS, Lee JS, Fisher MB, eds. Cytochrome P450 and Other Enzymes in Drug Metabolism and Pharmaceutical Research. Lausanne, Switzerland: FontisMedia, 2003:421 451.
9. Meunier V, Bourrie M, Berger Y, Fabre G. The human intestinal epithelial cell line Caco 2; pharmacological and pharmacokinetic applications. Cell Biol Toxicol 1995; 11:187 194.
10. Kharasch ED, Walker A, Hoffer C, Sheffels P. Intravenous and oral alfentanil as in vivo probes for hepatic and first pass cytochrome P450 3A activity: noninvasive assessment by use of pupillary miosis. Clin Pharmacol Ther 2004; 76:452 466.
11. Delaforge M, Riviere R, Sartori E, Doignon JL, Grognet JM. Metabolism of dihydroergot amine by a cytochrome P 450 similar to that involved in the metabolism of macrolide antibiotics. Xenobiotica 1989; 19:1285 1295.

12. Little PJ, Jennings GL, Skews H, Bobik A. Bioavailability of dihydroergotamine in man. Br J Clin Pharmacol 1982; 13:785 790.
13. Thummel KE, Kunze KL, Shen DD. Enzyme catalyzed processes of first pass hepatic and intestinal drug extraction. Adv Drug Deliv Rev 1997; 27:99 127.
14. Glatt H, Boeing H, Engelke CE, Ma L, Kuhlow A, Pabel U, Pomplun D, Teubner W, Meinl W. Human cytosolic sulphotransferases: genetics, characteristics, toxicological aspects. Mutat Res 2001; 482:27 40.
15. Schrag ML, Cui D, Rushmore TH, Shou M, Ma B, Rodrigues AD. Sulfotransferase 1E1 is a low K_m isoform mediating the 3 *O* sulfation of ethinyl estradiol. Drug Metab Dispos 2004; 32:1299 1303.
16. Ebner T, Remmel RP, Burchell B. Human bilirubin UDP glucuronosyltransferase catalyzes the glucuronidation of ethinylestradiol. Mol Pharmacol 1993; 43:649 654.
17. Khanna R, Morton CL, Danks MK, Potter PM. Proficient metabolism of irinotecan by a human intestinal carboxylesterase. Cancer Res 2000; 60:4725 4728.
18. Gupta E, Vyas V, Ahmed F, Sinko P, Cook T, Rubin E. Pharmacokinetics of orally administered camptothecins. Ann N Y Acad Sci 2000; 922:195 204.
19. Garcia Carbonero R, Supko JG. Current perspectives on the clinical experience, pharmacology, and continued development of the camptothecins. Clin Cancer Res 2002; 8:641 661.
20. Kemp DC, Fan PW, Stevens JC. Characterization of raloxifene glucuronidation in vitro: contribution of intestinal metabolism to presystemic clearance. Drug Metab Dispos 2002; 30:694 700.
21. Thummel KE, Shen DD, Isoherranen N, Smith HE. Appendix II. Design and optimization of dosage regimens: pharmacokinetic data. In: Brunton LL, Lazo JS, Parker KL, eds. Goodman & Gilman's The Pharmacological Basis of Therapeutics. 11th ed. New York: McGraw Hill, 2006:1917 2024.
22. Hellriegel ET, Bjornsson TD, Hauck WW. Interpatient variability in bioavailability is related to the extent of absorption: implications for bioavailability and bioequivalence studies. Clin Pharmacol Ther 1996; 60:601 607.
23. George CF. Drug metabolism by the gastrointestinal mucosa. Clin Pharmacokinet 1981; 6:259 274.
24. Fisher MB, Labissiere G. The role of the intestine in drug metabolism and pharmacokinetics: an industry perspective. Curr Drug Metab 2007; 8:694 699.
25. van de Kerkhof EG, de Graaf IA, Groothuis GM. In vitro methods to study intestinal drug metabolism. Curr Drug Metab 2007; 8:658 675.
26. Hoensch HP, Hutt R, Hartmann F. Biotransformation of xenobiotics in human intestinal mucosa. Environ Health Perspect 1979; 33:71 78.
27. Paine MF, Khalighi M, Fisher JM, Shen DD, Kunze KL, Marsh CL, Perkins JD, Thummel KE. Characterization of interintestinal and intraintestinal variations in human CYP3A dependent metabolism. J Pharmacol Exp Ther 1997; 283:1552 1562.
28. Zhang QY, Dunbar D, Ostrowska A, Zeisloft S, Yang J, Kaminsky LS. Characterization of human small intestinal cytochromes P 450. Drug Metab Dispos 1999; 27:804 809.
29. Watkins PB, Wrighton SA, Schuetz EG, Molowa DT, Guzelian PS. Identification of glucocorticoid inducible cytochromes P 450 in the intestinal mucosa of rats and man. J Clin Invest 1987; 80:1029 1036.
30. de Waziers I, Cugnenc PH, Yang CS, Leroux JP, Beaune PH. Cytochrome P 450 isoenzymes, epoxide hydrolase and glutathione transferases in rat and human hepatic and extrahepatic tissues. J Pharmacol Exp Ther 1990; 253:387 394.
31. Paine MF, Hart HL, Ludington SS, Haining RL, Rettie AE, Zeldin DC. The human intestinal cytochrome P450 "pie". Drug Metab Dispos 2006; 34:880 886.
32. Ptachcinski RJ, Venkataramanan R, Burckart GJ. Clinical pharmacokinetics of cyclosporin. Clin Pharmacokinet 1986; 11:107 132.
33. Wallemacq PE, Reding R, Sokal EM, de Ville de Goyet J, Clement de Clety S, Van Leeuw V, De Backer M, Otte JB. Clinical pharmacokinetics of Neoral in pediatric recipients of primary liver transplants. Transpl Int 1997; 10:466 470.

34. Chueh SC, Kahan BD. Pretransplant test dose pharmacokinetic profiles: cyclosporine microemulsion versus corn oil based soft gel capsule formulation. J Am Soc Nephrol 1998; 9: 297 304.
35. Ku YM, Min DI, Flanigan M. Effect of grapefruit juice on the pharmacokinetics of microemulsion cyclosporine and its metabolite in healthy volunteers: does the formulation difference matter? J Clin Pharmacol 1998; 38:959 965.
36. Lee M, Min DI, Ku YM, Flanigan M. Effect of grapefruit juice on pharmacokinetics of microemulsion cyclosporine in African American subjects compared with Caucasian subjects: does ethnic difference matter? J Clin Pharmacol 2001; 41:317 323.
37. Kolars JC, Awni WM, Merion RM, Watkins PB. First pass metabolism of cyclosporin by the gut. Lancet 1991; 338:1488 1490.
38. Hebert MF, Roberts JP, Prueksaritanont T, Benet LZ. Bioavailability of cyclosporine with concomitant rifampin administration is markedly less than predicted by hepatic enzyme induction. Clin Pharmacol Ther 1992; 52:453 457.
39. Kim RB, Wandel C, Leake B, Cvetkovic M, Fromm MF, Dempsey PJ, Roden MM, Belas F, Chaudhary AK, Roden DM, Wood AJ, Wilkinson GR. Interrelationship between substrates and inhibitors of human CYP3A and P glycoprotein. Pharm Res 1999; 16:408 414.
40. Paine MF, Shen DD, Kunze KL, Perkins JD, Marsh CL, McVicar JP, Barr DM, Gillies BS, Thummel KE. First pass metabolism of midazolam by the human intestine. Clin Pharmacol Ther 1996; 60:14 24.
41. Thummel KE, O'Shea D, Paine MF, Shen DD, Kunze KL, Perkins JD, Wilkinson GR. Oral first pass elimination of midazolam involves both gastrointestinal and hepatic CYP3A mediated metabolism. Clin Pharmacol Ther 1996; 59:491 502.
42. Holtbecker N, Fromm MF, Kroemer HK, Ohnhaus EE, Heidemann H. The nifedipine rifampin interaction. Evidence for induction of gut wall metabolism [see comments]. Drug Metab Dispos 1996; 24:1121 1123.
43. Fromm MF, Busse D, Kroemer HK, Eichelbaum M. Differential induction of prehepatic and hepatic metabolism of verapamil by rifampin. Hepatology 1996; 24:796 801.
44. von Richter O, Greiner B, Fromm MF, Fraser R, Omari T, Barclay ML, Dent J, Somogyi AA, Eichelbaum M. Determination of in vivo absorption, metabolism, and transport of drugs by the human intestinal wall and liver with a novel perfusion technique. Clin Pharmacol Ther 2001; 70:217 227.
45. Yang J, Tucker GT, Rostami Hodjegan A. Cytochrome P450 3A4 expression and activity in the human small intestine. Clin Pharmacol Ther 2004; 76:391.
46. Lampen A, Christians U, Guengerich FP, Watkins PB, Kolars JC, Bader A, Gonschior AK, Dralle H, Hackbarth I, Sewing KF. Metabolism of the immunosuppressant tacrolimus in the small intestine: cytochrome P450, drug interactions, and interindividual variability. Drug Metab Dispos 1995; 23:1315 1324.
47. Obach RS, Zhang QY, Dunbar D, Kaminsky LS. Metabolic characterization of the major human small intestinal cytochrome P450s. Drug Metab Dispos 2001; 29:347 352.
48. Lown KS, Kolars JC, Thummel KE, Barnett JL, Kunze KL, Wrighton SA, Watkins PB. Interpatient heterogeneity in expression of CYP3A4 and CYP3A5 in small bowel. Lack of prediction by the erythromycin breath test. Drug Metab Dispos 1994; 22:947 955. Erratum in: Drug Metab Dispos 1995; 23(3): following table of contents.
49. Paine MF, Ludington SS, Chen ML, Stewart PW, Huang SM, Watkins PB. Do men and women differ in proximal small intestinal CYP3A or P glycoprotein expression? Drug Metab Dispos 2005; 33:426 433.
50. Kuehl P, Zhang J, Lin Y, Lamba J, Assem M, Schuetz J, Watkins PB, Daly A, Wrighton SA, Hall SD, Maurel P, Relling M, Brimer C, Yasuda K, Venkataramanan R, Strom S, Thummel K, Boguski MS, Schuetz E. Sequence diversity in CYP3A promoters and characterization of the genetic basis of polymorphic CYP3A5 expression. Nat Genet 2001; 27:383 391.
51. Lin YS, Dowling AL, Quigley SD, Farin FM, Zhang J, Lamba J, Schuetz EG, Thummel KE. Co regulation of CYP3A4 and CYP3A5 and contribution to hepatic and intestinal midazolam metabolism. Mol Pharmacol 2002; 62:162 172.

52. Isoherranen N, Ludington SR, Givens RC, Lamba JK, Pusek SN, Dees EC, Blough DK, Iwanaga K, Hawke RL, Schuetz EG, Watkins PB, Thummel KE, Paine MF. The influence of CYP3A5 expression on the extent of hepatic CYP3A inhibition is substrate dependent: an in vitro in vivo evaluation. Drug Metab Dispos 2008; 36:146 154.
53. Kolars JC, Lown KS, Schmiedlin Ren P, Ghosh M, Fang C, Wrighton SA, Merion RM, Watkins PB. CYP3A gene expression in human gut epithelium. Pharmacogenetics 1994; 4:247 259.
54. McKinnon RA, Burgess WM, Hall PM, Roberts Thomson SJ, Gonzalez FJ, McManus ME. Characterisation of *CYP3A* gene subfamily expression in human gastrointestinal tissues. Gut 1995; 36:259 267.
55. Paine MF, Schmiedlin Ren P, Watkins PB. Cytochrome P 450 1A1 expression in human small bowel: interindividual variation and inhibition by ketoconazole. Drug Metab Dispos 1999; 27:360 364.
56. Gervot L, Carriere V, Costet P, Cugnenc PH, Berger A, Beaune PH, de Waziers I. CYP3A5 is the major cytochrome P450 3A expressed in human colon and colonic cell lines. Environ Toxicol Pharmacol 1996; 2:381 388.
57. Kolars JC, Schmiedlin Ren P, Schuetz JD, Fang C, Watkins PB. Identification of rifampin inducible P450IIIA4 (CYP3A4) in human small bowel enterocytes. J Clin Invest 1992; 90:1871 1878.
58. Bailey DG, Arnold JMO, Spence JD. Grapefruit juice drug interactions. Br J Clin Pharmacol 1998; 46:101 110.
59. Satoh H, Yamashita F, Tsujimoto M, Murakami H, Koyabu N, Ohtani H, Sawada Y. Citrus juices inhibit the function of human organic anion transporting polypeptide OATP B. Drug Metab Dispos 2005; 33:518 523.
60. Paine MF, Oberlies NH. Clinical relevance of the small intestine as an organ of drug elimination: drug fruit juice interactions. Expert Opin Drug Metab Toxicol 2007; 3:67 80.
61. Mertens Talcott SU, De Castro WV, Manthey JA, Derendorf H, Butterweck V. Poly methoxylated flavones and other phenolic derivates from citrus in their inhibitory effects on P glycoprotein mediated transport of talinolol in Caco 2 cells. J Agric Food Chem 2007; 55: 2563 2568.
62. Paine MF, Criss AB, Watkins PB. Two major grapefruit juice components differ in intestinal CYP3A4 inhibition kinetic and binding properties. Drug Metab Dispos 2004; 32: 1146 1153.
63. Paine MF, Criss AB, Watkins PB. Two major grapefruit juice components differ in time to onset of intestinal CYP3A4 inhibition. J Pharmacol Exp Ther 2005; 312:1151 1160.
64. Karch AM. The grapefruit challenge: the juice inhibits a crucial enzyme, with possibly fatal consequences. Am J Nurs 2004; 104:33 35.
65. Dreier JP, Endres M. Statin associated rhabdomyolysis triggered by grapefruit consumption. Neurology 2004; 62:670.
66. Bailey DG, Dresser GK. Interactions between grapefruit juice and cardiovascular drugs. Am J Cardiovasc Drugs 2004; 4:281 297.
67. Paine MF, Widmer WW, Hart HL, Pusek SN, Beavers KL, Criss AB, Brown SS, Thomas BF, Watkins PB. A furanocoumarin free grapefruit juice establishes furanocoumarins as the mediators of the grapefruit juice felodipine interaction. Am J Clin Nutr 2006; 83:1097 1105.
68. Lown KS, Bailey DG, Fontana RJ, Janardan SK, Adair CH, Fortlage LA, Brown MB, Guo W, Watkins PB. Grapefruit juice increases felodipine oral availability in humans by decreasing intestinal CYP3A protein expression [see comments]. J Clin Invest 1997; 99:2545 2553.
69. Malhotra S, Schmiedlin Ren P, Paine MF, Criss AB, Watkins PB. The furocoumarin 6′,7′ dihydroxybergamottin (DHB) accelerates CYP3A4 degradation via the proteasomal pathway. Drug Metab Rev 2001; 2001:97.
70. Tsunoda SM, Velez RL, von Moltke LL, Greenblatt DJ. Differentiation of intestinal and hepatic cytochrome P450 3A activity with use of midazolam as an in vivo probe: effect of ketoconazole. Clin Pharmacol Ther 1999; 66:461 471.
71. Ahonen J, Olkkola KT, Neuvonen PJ. Effect of route of administration of fluconazole on the interaction between fluconazole and midazolam. Eur J Clin Pharmacol 1997; 51:415 419.

72. Olkkola KT, Aranko K, Luurila H, Hiller A, Saarnivaara L, Himberg JJ, Neuvonen PJ. A potentially hazardous interaction between erythromycin and midazolam. Clin Pharmacol Ther 1993; 53:298 305.
73. Gorski JC, Jones DR, Haehner Daniels BD, Hamman MA, O'Mara EM Jr, Hall SD. The contribution of intestinal and hepatic CYP3A to the interaction between midazolam and clarithromycin. Clin Pharmacol Ther 1998; 64:133 143.
74. Pinto AG, Wang YH, Chalasani N, Skaar T, Kolwankar D, Gorski JC, Liangpunsakul S, Hamman MA, Arefayene M, Hall SD. Inhibition of human intestinal wall metabolism by macrolide antibiotics: effect of clarithromycin on cytochrome P450 3A4/5 activity and expression. Clin Pharmacol Ther 2005; 77:178 188.
75. Pinto AG, Horlander J, Chalasani N, Hamman M, Asghar A, Kolwankar D, Hall SD. Diltiazem inhibits human intestinal cytochrome P450 3A (CYP3A) activity in vivo without altering the expression of intestinal mRNA or protein. Br J Clin Pharmacol 2005; 59: 440 446.
76. Durr D, Stieger B, Kullak Ublick GA, Rentsch KM, Steinert HC, Meier PJ, Fattinger K. St John's Wort induces intestinal P glycoprotein/MDR1 and intestinal and hepatic CYP3A4. Clin Pharmacol Ther 2000; 68:598 604.
77. Backman JT, Olkkola KT, Neuvonen PJ. Rifampin drastically reduces plasma concentrations and effects of oral midazolam. Clin Pharmacol Ther 1996; 59:7 13.
78. Villikka K, Kivisto KT, Backman JT, Olkkola KT, Neuvonen PJ. Triazolam is ineffective in patients taking rifampin. Clin Pharmacol Ther 1997; 61:8 14.
79. Lang CC, Brown RM, Kinirons MT, Deathridge MA, Guengerich FP, Kelleher D, O'Briain DS, Ghishan FK, Wood AJ. Decreased intestinal CYP3A in celiac disease: reversal after successful gluten free diet: a potential source of interindividual variability in first pass drug metabolism. Clin Pharmacol Ther 1996; 59:41 46.
80. Johnson TN, Tanner MS, Taylor CJ, Tucker GT. Enterocytic CYP3A4 in a paediatric population: developmental changes and the effect of coeliac disease and cystic fibrosis. Br J Clin Pharmacol 2001; 51:451 460.
81. Chalasani N, Gorski JC, Patel NH, Hall SD, Galinsky RE. Hepatic and intestinal cytochrome P450 3A activity in cirrhosis: effects of transjugular intrahepatic portosystemic shunts. Hepatology 2001; 34:1103 1108.
82. Wheeler CW, Park SS, Guenthner TM. Immunochemical analysis of a cytochrome P 450IA1 homologue in human lung microsomes. Mol Pharmacol 1990; 38:634 643.
83. Shimada T, Yun CH, Yamazaki H, Gautier JC, Beaune PH, Guengerich FP. Characterization of human lung microsomal cytochrome P 450 1A1 and its role in the oxidation of chemical carcinogens. Mol Pharmacol 1992; 41:856 864.
84. Ding X, Kaminsky LS. Human extrahepatic cytochromes P450: function in xenobiotic metabolism and tissue selective chemical toxicity in the respiratory and gastrointestinal tracts. Annu Rev Pharmacol Toxicol 2003; 43:149 173.
85. Hakkola J, Pelkonen O, Pasanen M, Raunio H. Xenobiotic metabolizing cytochrome P450 enzymes in the human feto placental unit: role in intrauterine toxicity. Crit Rev Toxicol 1998; 28:35 72.
86. Syme MR, Paxton JW, Keelan JA. Drug transfer and metabolism by the human placenta. Clin Pharmacokinet 2004; 43:487 514.
87. Peters WH, Kremers PG. Cytochromes P 450 in the intestinal mucosa of man. Biochem Pharmacol 1989; 38:1535 1538.
88. McDonnell WM, Scheiman JM, Traber PG. Induction of cytochrome P450IA genes (CYP1A) by omeprazole in the human alimentary tract. Gastroenterology 1992; 103:1509 1516.
89. Buchthal J, Grund KE, Buchmann A, Schrenk D, Beaune P, Bock KW. Induction of cytochrome P4501A by smoking or omeprazole in comparison with UDP glucuronosyl transferase in biopsies of human duodenal mucosa. Eur J Clin Pharmacol 1995; 47:431 435.
90. Fontana RJ, Lown KS, Paine MF, Fortlage L, Santella RM, Felton JS, Knize MG, Greenberg A, Watkins PB. Effects of a chargrilled meat diet on expression of CYP3A, CYP1A, and P glycoprotein levels in healthy volunteers. Gastroenterology 1999; 117:89 98.

91. Pelkonen O, Pasanen M, Kuha H, Gachalyi B, Kairaluoma M, Sotaniemi EA, Park SS, Friedman FK, Gelboin HV. The effect of cigarette smoking on 7 ethoxyresorufin O deethylase and other monooxygenase activities in human liver: analyses with monoclonal antibodies. Br J Clin Pharmacol 1986; 22:125 134.
92. Shimada T, Yamazaki H, Mimura M, Inui Y, Guengerich FP. Interindividual variations in human liver cytochrome P 450 enzymes involved in the oxidation of drugs, carcinogens and toxic chemicals: studies with liver microsomes of 30 Japanese and 30 Caucasians. J Pharmacol Exp Ther 1994; 270:414 423.
93. Penman BW, Chen L, Gelboin HV, Gonzalez FJ, Crespi CL. Development of a human lymphoblastoid cell line constitutively expressing human CYP1A1 cDNA: substrate specificity with model substrates and promutagens. Carcinogenesis 1994; 15:1931 1937.
94. Miners JO, McKinnon RA. CYP1A. In: Levy RH, Thummel KE, Trager WF, et al., eds. Metabolic Drug Interactions. Philadelphia: Lippincott Williams & Wilkins, 2000:61 73.
95. Tassaneeyakul W, Mohamed Z, Birkett DJ, McManus ME, Veronese ME, Tukey RH, Quattrochi LC, Gonzalez FJ, Miners JO. Caffeine as a probe for human cytochromes P450: validation using cDNA expression, immunoinhibition and microsomal kinetic and inhibitor techniques. Pharmacogenetics 1992; 2:173 183.
96. Ha HR, Chen J, Freiburghaus AU, Follath F. Metabolism of theophylline by cDNA expressed human cytochromes P 450. Br J Clin Pharmacol 1995; 39:321 326.
97. Tassaneeyakul W, Birkett DJ, Veronese ME, McManus ME, Tukey RH, Quattrochi LC, Gelboin HV, Miners JO. Specificity of substrate and inhibitor probes for human cytochromes P450 1A1 and 1A2. J Pharmacol Exp Ther 1993; 265:401 407.
98. Kaminsky LS, Zhang ZY. Human P450 metabolism of warfarin. Pharmacol Ther 1997; 73:67 74.
99. Klose TS, Blaisdell JA, Goldstein JA. Gene structure of CYP2C8 and extrahepatic distribution of the human CYP2Cs. J Biochem Mol Toxicol 1999; 13:289 295.
100. Galetin A, Houston JB. Intestinal and hepatic metabolic activity of five cytochrome P450 enzymes: impact on prediction of first pass metabolism. J Pharmacol Exp Ther 2006; 318:1220 1229.
101. Prueksaritanont T, Gorham LM, Hochman JH, Tran LO, Vyas KP. Comparative studies of drug metabolizing enzymes in dog, monkey, and human small intestines, and in Caco 2 cells. Drug Metab Dispos 1996; 24:634 642.
102. Bort R, Mace K, Boobis A, Gomez Lechon MJ, Pfeifer A, Castell J. Hepatic metabolism of diclofenac: role of human CYP in the minor oxidative pathways. Biochem Pharmacol 1999; 58:787 796.
103. Scripture CD, Pieper JA. Clinical pharmacokinetics of fluvastatin. Clin Pharmacokinet 2001; 40:263 281.
104. Hu Y, Krausz K, Gelboin HV, Kupfer D. CYP2C subfamily, primarily CYP2C9, catalyses the enantioselective demethylation of the endocrine disruptor pesticide methoxychlor in human liver microsomes: use of inhibitory monoclonal antibodies in P450 identification. Xenobiotica 2004; 34(2):117 132.
105. Usmani KA, Karoly ED, Hodgson E, Rose RL. In vitro sulfoxidation of thioether compounds by human cytochrome P450 and flavin containing monooxygenase isoforms with particular reference to the CYP2C subfamily. Drug Metab Dispos 2004; 32(3):333 339.
106. Pearce RE, McIntyre CJ, Madan A, Sanzgiri U, Draper AJ, Bullock PL, Cook DC, Burton LA, Latham J, Nevins C, Parkinson A. Effects of freezing, thawing, and storing human liver microsomes on cytochrome P450 activity. Arch Biochem Biophys 1996; 331:145 169.
107. Tang J, Cao Y, Rose RL, Brimfield AA, Dai D, Goldstein JA, Hodgson E. Metabolism of chlorpyrifos by human cytochrome P450 isoforms and human, mouse, and rat liver microsomes. Drug Metab Dispos 2001; 29(9):1201 1204.
108. Prueksaritanont T, Dwyer LM, Cribb AE. (+) bufuralol 1′ hydroxylation activity in human and rhesus monkey intestine and liver. Biochem Pharmacol 1995; 50:1521 1525.
109. Madani S, Paine MF, Lewis L, Thummel KE, Shen DD. Comparison of CYP2D6 content and metoprolol oxidation between microsomes isolated from human livers and small intestines. Pharm Res 1999; 16:1199 1205.

110. Scarborough PE, Ma J, Qu W, Zeldin DC. P450 subfamily CYP2J and their role in the bioactivation of arachidonic acid in extrahepatic tissues. Drug Metab Rev 1999; 31:205 234.
111. Zeldin DC, Foley J, Goldsworthy SM, Cook ME, Boyle JE, Ma J, Moomaw CR, Tomer KB, Steenbergen C, Wu S. CYP2J subfamily cytochrome P450s in the gastrointestinal tract: expression, localization, and potential functional significance. Mol Pharmacol 1997; 51:931 943.
112. Matsumoto S, Hirama T, Matsubara T, Nagata K, Yamazoe Y. Involvement of CYP2J2 on the intestinal first pass metabolism of antihistamine drug, astemizole. Drug Metab Dispos 2002; 30:1240 1245.
113. Yamazaki H, Okayama A, Imai N, Guengerich FP, Shimizu M. Inter individual variation of cytochrome P4502J2 expression and catalytic activities in liver microsomes from Japanese and Caucasian populations. Xenobiotica 2006; 36:1201 1209.
114. Hashizume T, Imaoka S, Mise M, Terauchi Y, Fujii T, Miyazaki H, Kamataki T, Funae Y. Involvement of CYP2J2 and CYP4F12 in the metabolism of ebastine in human intestinal microsomes. J Pharmacol Exp Ther 2002; 300:298 304.
115. Kalsotra A, Strobel HW. Cytochrome P450 4F subfamily: at the crossroads of eicosanoid and drug metabolism. Pharmacol Ther 2006; 112(3):589 611.
116. Hashizume T, Imaoka S, Hiroi T, Terauchi Y, Fujii T, Miyazaki H, Kamataki T, Funae Y. cDNA cloning and expression of a novel cytochrome p450 (cyp4f12) from human small intestine. Biochem Biophys Res Commun 2001; 280:1135 1141.
117. Wang MZ, Wu JQ, Bridges AS, Zeldin DC, Kornbluth S, Tidwell RR, Hall JE, Paine MF. Human enteric microsomal CYP4F enzymes O demethylate the antiparasitic prodrug pafuramidine. Drug Metab Dispos 2007; 35:2067 2075.
118. Mouly S, Lown KS, Kornhauser D, Joseph JL, Fiske WD, Benedek IH, Watkins PB. Hepatic but not intestinal CYP3A4 displays dose dependent induction by efavirenz in humans. Clin Pharmacol Ther 2002; 72:1 9.
119. Imai T, Taketani M, Shii M, Hosokawa M, Chiba K. Substrate specificity of carboxylesterase isozymes and their contribution to hydrolase activity in human liver and small intestine. Drug Metab Dispos 2006; 34:1734 1741.
120. Krishna DR, Klotz U. Extrahepatic metabolism of drugs in humans. Clin Pharmacokinet 1994; 26:144 160.
121. Yeung CK, Lang DH, Thummel KE, Rettie AE. Immunoquantitation of FMO1 in human liver, kidney, and intestine. Drug Metab Dispos 2000; 28:1107 1111.
122. Slatter JG, Schaaf LJ, Sams JP, Feenstra KL, Johnson MG, Bombardt PA, Cathcart KS, Verburg MT, Pearson LK, Compton LD, Miller LL, Baker DS, Pesheck CV, Lord RS 3rd. Pharmacokinetics, metabolism, and excretion of irinotecan (CPT 11) following I.V. infusion of [(14)C]CPT 11 in cancer patients. Drug Metab Dispos 2000; 28:423 433.
123. Soepenberg O, Dumez H, Verweij J, Semiond D, deJonge MJ, Eskens FA, ter Steeg J, Selleslach J, Assadourian S, Sanderink GJ, Sparreboom A, van Oosterom AT. Phase I and pharmacokinetic study of oral irinotecan given once daily for 5 days every 3 weeks in combination with capecitabine in patients with solid tumors. J Clin Oncol 2005; 23:889 898.
124. Haining RL, Hunter AP, Sadeque AJ, Philpot RM, Rettie AE. Baculovirus mediated expression and purification of human FMO3: catalytic, immunochemical, and structural characterization. Drug Metab Dispos 1997; 25:790 797.
125. Chen G, Zhang D, Jing N, Yin S, Falany CN, Radominska Pandya A. Human gastrointestinal sulfotransferases: identification and distribution. Toxicol Appl Pharmacol 2003; 187:186 197.
126. Her C, Szumlanski C, Aksoy IA, Weinshilboum RM. Human jejunal estrogen sulfotransferase and dehydroepiandrosterone sulfotransferase: immunochemical characterization of individual variation. Drug Metab Dispos 1996; 24:1328 1335.
127. Hochhaus G, Mollmann H. Pharmacokinetic/pharmacodynamic characteristics of the beta 2 agonists terbutaline, salbutamol and fenoterol. Int J Clin Pharmacol Ther Toxicol 1992; 30:342 362.
128. Hartman AP, Wilson AA, Wilson HM, Aberg G, Falany CN, Walle T. Enantioselective sulfation of beta 2 receptor agonists by the human intestine and the recombinant M form phenolsulfotransferase. Chirality 1998; 10:800 803.

129. Back DJ, Breckenridge AM, MacIver M, Orme M, Purba HS, Rowe PH, Taylor I. The gut wall metabolism of ethinyloestradiol and its contribution to the pre systemic metabolism of ethinyloestradiol in humans. Br J Clin Pharmacol 1982; 13:325 330.
130. Tukey RH, Strassburg CP. Genetic multiplicity of the human UDP glucuronosyltransferases and regulation in the gastrointestinal tract. Mol Pharmacol 2001; 59:405 414.
131. Fisher MB, Paine MF, Strelevitz TJ, Wrighton SA. The role of hepatic and extrahepatic UDP glucuronosyltransferases in human drug metabolism. Drug Metab Rev 2001; 33:273 297.
132. Ritter JK. Intestinal UGTs as potential modifiers of pharmacokinetics and biological responses to drugs and xenobiotics. Expert Opin Drug Metab Toxicol 2007; 3:93 107.
133. Kaminsky LS, Zhang QY. The small intestine as a xenobiotic metabolizing organ. Drug Metab Dispos 2003; 31:1520 1525.
134. Strassburg CP, Barut A, Obermayer Straub P, Li Q, Nguyen N, Tukey RH, Manns MP. Identification of cyclosporine A and tacrolimus glucuronidation in human liver and the gastrointestinal tract by a differentially expressed UDP glucuronosyltransferase: UGT2B7. J Hepatol 2001; 34:865 872.
135. Hochner Celnikier D. Pharmacokinetics of raloxifene and its clinical application. Eur J Obstet Gynecol Reprod Biol 1999; 85:23 29.
136. Snyder KR, Sparano N, Malinowski JM. Raloxifene hydrochloride. Am J Health Syst Pharm 2000; 57:1669 1675; quiz 1676 1668.
137. Gagne JF, Montminy V, Belanger P, Journault K, Gaucher G, Guillemette C. Common human UGT1A polymorphisms and the altered metabolism of irinotecan active metabolite 7 ethyl 10 hydroxycamptothecin (SN 38). Mol Pharmacol 2002; 62:608 617.
138. Ghosal A, Hapangama N, Yuan Y, Achanfuo Yeboah J, Iannucci R, Chowdhury S, Alton K, Patrick JE, Zbaida S. Identification of human UDP glucuronosyltransferase enzyme(s) responsible for the glucuronidation of ezetimibe (Zetia). Drug Metab Dispos 2004; 32:314 320.
139. Kosoglou T, Statkevich P, Johnson Levonas AO, Paolini JF, Bergman AJ, Alton KB. Ezetimibe: a review of its metabolism, pharmacokinetics and drug interactions. Clin Pharmacokinet 2005; 44:467 494.
140. Gibbs JP, Yang JS, Slattery JT. Comparison of human liver and small intestinal glutathione S transferase catalyzed busulfan conjugation in vitro. Drug Metab Dispos 1998; 26:52 55.
141. Hickman D, Pope J, Patil SD, Fakis G, Smelt V, Stanley LA, Payton M, Unadkat JD, Sim E. Expression of arylamine N acetyltransferase in human intestine. Gut 1998; 42:402 409.
142. Coles BF, Chen G, Kadlubar FF, Radominska Pandya A. Interindividual variation and organ specific patterns of glutathione S transferase alpha, mu, and pi expression in gastrointestinal tract mucosa of normal individuals. Arch Biochem Biophys 2002; 403:270 276.
143. Vree TB, Dammers E, Exler PS, Sorgel F, Bondesen S, Maes RA. Liver and gut mucosa acetylation of mesalazine in healthy volunteers. Int J Clin Pharmacol Ther 2000; 38:514 522.
144. Hoensch H, Morgenstern I, Petereit G, Siepmann M, Peters WH, Roelofs HM, Kirch W. Influence of clinical factors, diet, and drugs on the human upper gastrointestinal lglutathione system. Gut 2002; 50:235 240.

12

Sites of Extra Hepatic Metabolism, Part III: Kidney

Lawrence H. Lash
Department of Pharmacology, Wayne State University School of Medicine, Detroit, Michigan, U.S.A.

INTRODUCTION

Although the kidneys only comprise 1% to 2% of total body weight, they can play an important, if not critical, role in overall drug metabolism in the body. There are several factors that are responsible for the ability of the kidneys to play such a disproportionately important role. First, despite their weight, the kidneys receive approximately 25% of the cardiac output, thereby delivering a large proportion of blood-borne chemicals to the renal circulation. A second major factor is that by multiple mechanisms that are a central, underlying part of the basic physiology of the kidneys, drugs and chemicals may become concentrated within renal epithelial cells to levels that are often markedly higher than those to which the tissue is exposed. These concentrating mechanisms include glomerular filtration, the countercurrent circulatory system that operates in the distal nephron and has the physiological function of concentrating the tubular fluid severalfold over that in the plasma, and the existence of a large array of transporters for organic anions and cations on the basolateral membrane (BLM) and luminal membrane of renal epithelial cells. A third reason for the importance of the kidneys in drug metabolism is that once inside the renal cell, many of the same enzymes that have been classically studied in liver are also present, enabling metabolism to occur. A review of many of these enzymes, as well as some that are unique to the kidneys or that have unique characteristics compared with those in other organs because of renal morphology or physiology, is the primary area of focus for this chapter.

In studying renal drug metabolism, it is critical to consider the impact of nephron heterogeneity (1,2). The mammalian kidney is complex and can be structurally and functionally subdivided into multiple, distinct parts. At the simplest level, kidneys are subdivided into cortex, outer medulla (further subdivided into inner stripe and outer stripe), and inner medulla (or papilla). The nephron, which is the basic building block of the kidney, can exist as either short-looped or long-looped types, the frequency of which varies among species. To understand the importance of this suborganellar organization, one can compare nephron segment specific differences in metabolism, cellular energetics,

Table 1 Selected Biochemical, Morphological, and Functional Properties of Some Key Nephron Segments of Mammalian Kidney

Nephron Cell type	Morphology	Physiology	Metabolism
Proximal tubule	Tall, prominent microvilli on luminal membrane; cuboidal shape; extensive basolateral infoldings; high density of mitochondria	Active Na^+ reabsorption; organic anion and cation secretion; most glucose and amino acid reabsorption; passive water and Cl reabsorption	Oxidative phosphorylation, citric acid cycle, gluconeogenesis; substrates = fatty acids, ketone bodies, lactate, glutamine, pyruvate, citrate, acetate; drug metabolism: high CYP, FMO, UGT, SULT, GSH dependent
Thick ascending limb	Extensive interdigitations; large number of elongated, rod shaped mitochondria	Water impermeable; Na^+ K^+ 2Cl cotransport; active Ca^{2+} and Mg^{2+} transport; dilution of hyperosmotic tubular urine	Oxidative phosphorylation and glycolysis; substrates = lactate, glucose, ketone bodies, fatty acids, acetate; drug metabolism: low CYP, FMO, UGT, SULT; high PGS (mTAL)
Distal tubule (distal convoluted tubule and cortical collecting duct)	DCT: appears bright under microscope; numerous, long mitochondria. CCT: appears granular under microscope; wider than DCT.	High rates of Na^+ reabsorption; thiazide inhibitable Na^+ Cl cotransport; K^+ Cl cotransport; Ca^{2+} reabsorption; DCT: water impermeable; CCT: vasopressin dependent water channel	Glycolysis; substrates = glucose, lactate, β hydroxybutyrate, fatty acids (CCT only); drug metabolism: generally all low

Abbreviations: CCT, cortical collecting duct; CYP, cytochrome P450; DCT, distal convoluted tubule; FMO, flavin containing monooxygenase; mTAL, medullary thick ascending limb; PGS, prostaglandin synthetase; SULT, sulfotransferase; UGT, UDP glucuronosyltransferase.

and other parameters of physiological function (Table 1). The different segments of the nephron, three of which are highlighted here, provide a perfect example of form corresponding with function. In terms of morphology, the proximal tubule is ideally suited for extensive reabsorption and secretion of anions, cations, and metabolites because of the large surface area provided by the microvilli on the luminal membrane or brush-border plasma membrane (BBM) and the extensive infoldings on the serosal or basolateral plasma membrane. Mitochondrial density is high in nephron segments that exhibit particularly high activities of energy-dependent processes such as active transport and biosynthetic reactions.

Of particular interest for the primary focus of this chapter is that significant segment-specific differences exist in pathways of drug metabolism. For the majority of reactions that are of interest for drugs and other xenobiotics, the highest amounts of the key reaction pathways are present in the proximal tubules. It should be noted, however, that certain enzymatic pathways in other nephron segments also play a critical role for the bioactivation of certain drugs and chemicals. For the majority of drugs and chemicals of interest, it is the proximal tubules that are the primary sites of metabolism. As listed in Table 1, the various phase I and phase II pathways as well as enzymes such as the cysteine conjugate β-lyase (CCBL) are predominantly localized in the proximal tubules.

EXPERIMENTAL MODELS TO STUDY KIDNEY DRUG METABOLISM

The segment-specific distribution of many drug metabolism enzymes sometimes makes it difficult to properly study or even detect certain reaction pathways. This is particularly true for pathways that are present at relatively low activities. For clinical studies, one is of course limited to noninvasive methods to determine metabolism. Metabolites of certain chemicals in either blood or urine can be considered as biomarkers for the presence of a particular enzyme. It is often difficult, however, to distinguish renal metabolism from the more prominent hepatic metabolism. Moreover, the subsequent action of additional enzymes that generate reactive and unstable metabolites may make detection of metabolism difficult.

A suitable alternative to in vivo study of metabolism can be the use of a variety of in vitro models. A key advantage of using such models is that renal metabolism can be measured separately from hepatic metabolism. When in vitro models are used to measure renal metabolism, however, care is needed in choosing the model because of the selective distribution of drug metabolism enzymes and transporters along the nephron. Thus, a model that contains multiple nephron cell types may result in either measurement of low metabolic rates or failure to detect metabolism because of dilution of the pathway enzymes due to the presence of cell types that do not express them.

A detailed discussion of the various in vitro models that are available to study renal drug metabolism is beyond the scope of this chapter. The reader is referred to two reviews (3,4) that describe various model systems and consider their advantages, disadvantages, primary uses, and limitations. A few comments will be made here, with the focus being on their applicability for the study and quantitation of drug metabolism reactions.

The simplest in vitro model in terms of its preparation is that of the isolated perfused kidney. It has the advantage that extrarenal metabolism is eliminated. As with many of the freshly isolated in vitro models, its use is limited to relatively short time periods because of gradual and progressive functional impairment. Another limitation for study of drug metabolism is that one cannot always distinguish processes that occur in specific nephron segments (the dilution effect mentioned above). The isolated perfused kidney is also relatively expensive in that a single animal (typically the rat) is used for all measurements.

Renal slices are a convenient and relatively simple model that enables better assessment of metabolism occurring in specific nephron segments. Substrate transport is conveniently measured as the slice-to-medium ratio and is often used as an assessment of tubular viability when actively transported substrates are used. While slices are easy to prepare and have relatively low cost, they are limited by a relatively short lifetime, the potential for collapsed lumens and poor oxygenation, and the presence of multiple cell

populations despite the ability to prepare slices from discrete regions of the kidney (i.e., cortex, outer stripe, and inner stripe of the outer medulla and inner medulla).

The most convenient in vitro models to enable measurement of drug metabolism pathways in specific nephron cell types, thereby minimizing the "dilution effect," are freshly isolated tubular fragments and isolated cells. Both can be prepared from specific nephron segments using various physical separation methods, such as microdissection, density-gradient centrifugation, or electrophoresis. Enzymatic digestion with collagenase and/or hyaluronidase is often used as a first step prior to separation of cell types. Although both methods can provide similar data, it is usually easiest to prepare tubular fragments from rabbits and isolated cells from rats. As with the isolated perfused kidney and renal slices, isolated tubular fragments and isolated cells can only be maintained in a viable state for a limited time period, which is typically up to four hours.

While the relatively short lifetime of isolated tubular fragments or isolated cells is not a limitation if one wants to simply quantify metabolism, other types of assays such as enzyme induction or study of gene regulation require models that retain viability for longer periods of time. To accomplish this, many investigators have established primary cultures of renal epithelial cells from the proximal tubule (3,5 19) and distal tubule and thick ascending limb (14,20,21) of rat, mouse, or rabbit. The advantage of primary cultures is that they can be maintained in a viable state for at least four-to five days and are derived directly from the in vivo tissue. Unfortunately, primary cell cultures, particularly those from epithelial cells, tend to lose some of their differentiated functions during the course of culture. Expression of drug metabolism enzymes is particularly prone to being lost during culture. To combat this problem, investigators have used serum-free, hormonally defined media with limited success.

Another important issue about the experimental model used concerns the known species-dependent differences in drug metabolism enzymes, which will be discussed in the sections below. Inasmuch as we are primarily interested in drug metabolism in the human kidney, the availability of human kidneys or human kidney slices (e.g., surgical waste) has enabled investigators to use freshly isolated renal cells or primary cultures of proximal tubular cells from the primary species of interest (22 28). Primary cultures of human proximal tubular cells also suffer from the same potential problem of dedifferentiation as do those from rats, mice, or rabbits.

A final type of in vitro renal cellular model is that of continuous or immortalized cell lines. Distinct advantages with use of these cell lines are that they are easy to use and are reproducible. Renal cell lines that are commonly used in study of metabolism, transport, and toxicity derive from various species and multiple nephron segments, including the glomerulus, proximal tubule, medullary thick ascending limb, and distal tubule. As discussed elsewhere (29), these cell lines, by being immortalized, have undergone genotypic and phenotypic changes that may make them questionable as models of in vivo renal metabolism. As compared with primary cell cultures, immortalized cell lines possess even more uncertainties as to their value for in vivo drug metabolism.

MEMBRANE TRANSPORT

Although membrane transport processes are not, strictly speaking, a part of drug metabolism, no discussion of the renal handling of drugs can be complete without some consideration of how drugs gain access to enzymes in renal epithelial cells. Figure 1 schematically summarizes some of the major carrier proteins on the BLM and BBM of renal proximal tubular cells that are important in the renal tubular uptake or efflux of

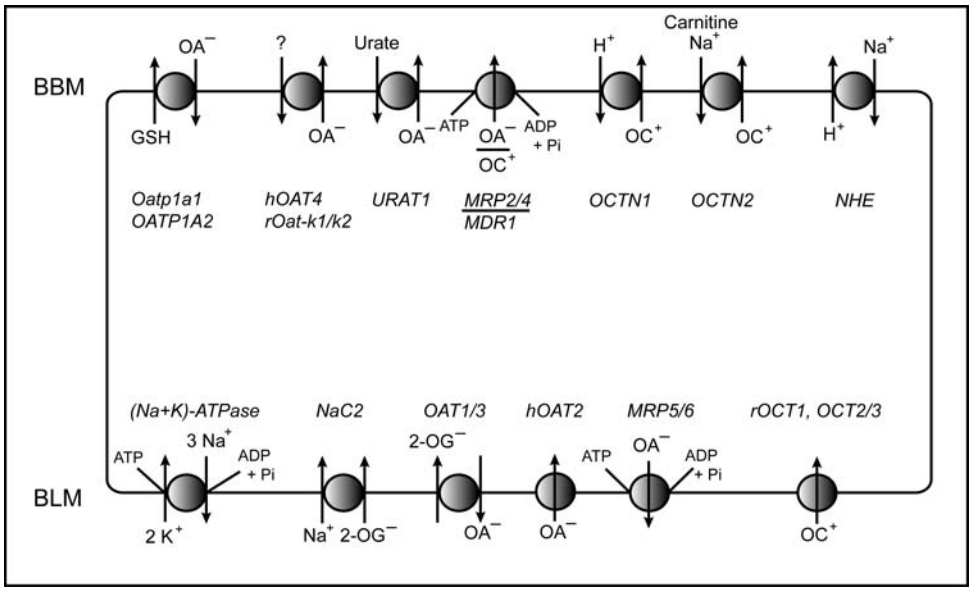

Figure 1 *Organic anion and cation transport in renal proximal tubule.* This scheme illustrates the major transporters found on the BLM and BBMs that mediate the uptake or efflux of OA and OC^+. Also shown are the (Na^++K^+) stimulated ATPase, the NaC2 carrier, and the NHE, which provide the driving force for many of the carriers involved in the transport of drugs. Note that when the carrier name is preceded by "h" or "r," this indicates that it is only found in human or rat, respectively. *Abbreviations*: BLM, basolateral membrane; BBM, brush border membrane; OA , organic anions; NaC2, sodium dicarboxylate 2; OC^+, organic cations ATPase, adenosine 5′ triphosphatase; NHE, Na^+/H^+ exchanger; GSH, glutathione; MDR, multiple drug resistance protein; MRP, multidrug resistance associated protein; OAT, organic anion transporter; OCT, organic cation transporter; Oat k1/2, kidney specific organic anion transporter; OATP, organic anion transporting polypeptide; 2 OG , 2 oxoglutarate; URAT, urate transporter.

organic anions and organic cations. Most drugs of interest for therapeutics or toxicology studies are charged, so that the carrier proteins shown are responsible for the majority of their transport in the renal proximal tubule.

The various carriers are primary, secondary, or tertiary active or facilitated transporters. Primary active transporters are those that directly couple adenosine-5′-triphosphate (ATP) hydrolysis to the movement of substrate; relevant examples include the multidrug resistance-associated proteins (MRPs), the multiple drug resistance protein (MDR1) (also known as P-glycoprotein), the (Na^++K^+)-stimulated ATPase, and the Na^+/H^+ exchanger (NHE). Secondary active transporters are those that couple or exchange substrate with an ion (generally either Na^+ or H^+ ion) whose gradient is generated by a primary active transporter. These include the sodium-dicarboxylate 2 (NaC2) carrier and the organic cation transporters (OCTs) N1 and N2. Tertiary active transporters include the organic anion transporters (OATs) 1 and 3, which couple uptake of organic anions, bile salts, and some organic cations with efflux of 2-oxoglutarate ($2\text{-}OG^-$), which is generated by NaC2. The remaining carriers are either facilitated exchangers or uniporters. Similar to many of the drug metabolism enzymes that are discussed below [particularly the cytochrome P450s (CYPs)], the various OATs, OCTs, MRPs, and MDR1s have broad and often overlapping substrate specificities, resulting in some degree of functional redundancy. However, there are some discrete substrate specificities for the various carriers. Readers are

referred to several recent reviews on the identity, function, and regulation of mammalian renal organic anion and cation transporters (30 38).

PHASE I METABOLISM IN THE KIDNEYS

The major phase I or oxidative metabolism enzymes in the kidneys exhibit similar biochemistry as those in the liver, although there are significant differences based on patterns of expression and nephron heterogeneity (39,40). This section will review three major enzyme systems, CYPs, flavin-containing monooxygenases (FMO), and prostaglandin synthetase (PGS). The focus will be to describe the patterns of expression of the different enzymes among cell types of the nephron and sex- and species-dependent differences that are known to exist. The species-dependent differences have important implications for the use of metabolism data from laboratory animals for making predictions for metabolism in humans. In some cases, particularly for some drugs and chemicals that are bioactivated to reactive intermediates that elicit nephrotoxicity, metabolic pathways in rats or mice cannot be used to make predictions for humans.

Cytochrome P450

The most obvious difference between the better-studied CYP enzymes in the liver and those in the kidney is that overall expression of CYP enzymes in the kidney is generally only 5% to 20% of those in the liver. Another difference is that CYP enzymes are not uniformly distributed throughout the nephron but exhibit discrete localizations (cf. Table 1). The pattern of expression of CYP enzymes differs in the two tissues, with the liver exhibiting a more extensive array of enzymes, particularly in humans. Further, substrate specificity and inducibility of some CYP enzymes that are expressed in both the liver and kidney differ, suggesting that regulation of enzyme activity differs (39 42).

Table 2 summarizes some key properties of the major CYP enzymes in the kidneys of rodents and humans. As in the liver, the kidneys contain four major families of CYP

Table 2 Selected CYP Enzymes Expressed in Rodent and Human Kidney

CYP enzyme	Rats and/or mice	Humans
CYP1A1/2	Low constitutive; CYP1A1 inducible	Not detected or poorly inducible
CYP1B1/2	Present at modest levels	Present at modest levels
CYP2A	Present in mice; not detected in rats	Not detected
CYP2B1/2	Inducible by clofibrate in rats	Not detected
CYP2C11 (CYP2C19)	Constitutive; sex and developmental differences	Not detected
CYP2D6	Low levels?	Low levels
CYP2E1	Present; inducible	Not detected
CYP3A1/2 (CYP3A4/5)	Primarily in glomerulus	Glomerulus, proximal tubule; genetic polymorphisms
CYP4A2/3 (CYP4A11)	Proximal tubule; inducible by fibrates	Proximal tubule; inducible by ethanol, dexamethasone

The major CYP enzymes that are important in drug metabolism or in renal physiology are listed for rats, mice, and where applicable, the human orthologue is listed in parentheses.
Abbreviation: CYP, cytochrome P450.

enzymes that are important in drug metabolism (CYP1, CYP2, CYP3) or renal physiological function (CYP4). It should be apparent from this brief consideration that there are significant differences based on tissue (liver vs. kidney), sex, and species (rat vs. mouse vs. human) with regard to level of expression (ranging from not detectable to high), inducibility, and nephron cell type localization.

An example that highlights some of the tissue- and species-dependent differences in CYP is that of the environmental contaminant trichloroethylene (TRI). Adverse effects of TRI are all associated with metabolism, and TRI is metabolized to a large range of products by both CYP ("oxidative" pathway) or glutathione *S*-transferase (GST) ("conjugation" pathway), although CYP-dependent metabolism predominates at all but the highest substrate concentrations (43). CYP2E1 is the primary CYP enzyme that metabolizes small halogenated solvents such as TRI. CYP2C11 in the rat or CYP2C19 in humans is also reasonably active toward TRI. TRI has several potential target organs, which vary according to sex, species, and dose, and is considered a "probable human carcinogen" by the National Toxicology Program (NTP) (44). All the adverse effects of TRI in the kidneys are linked solely to its glutathione (GSH)-dependent metabolism (43,45). CYP-dependent metabolism of TRI in either the liver or kidneys may, however, influence GSH-dependent metabolism, which can have both a hepatic and a renal component even though the terminal products are formed in the kidneys. Thus, we find that rat kidney readily metabolizes TRI to its oxidative metabolites as both CYP2E1 and CYP2C11 are expressed at fairly high levels in the proximal tubules (46). In contrast to this situation, little or no detectable oxidative metabolism of TRI occurs in the human kidney (23), which is consistent with the inability to detect either CYP2E1 or CYP2C19 in human proximal tubular cells (24,47). Hence, we can modulate GSH-dependent metabolism and toxicity of TRI in rat proximal tubular cells by altering CYP status (48). This is an example of a case where metabolism data cannot be extrapolated from rodents to humans at all because of species-dependent differences.

As suggested by its broad substrate specificities, enzymes of the CYP2 family are a diverse set of enzymes. Differences exist between species and tissues in a given species. As summarized in Table 2, CYP2A enzymes are expressed in mouse kidney but not in rat or human kidney (39). CYP2B1/2 illustrates both species and tissue differences. Whereas CYP2B1/2 is inducible by phenobarbital in rat liver, it is not induced by it in rat kidney and is undetectable in human kidney. As mentioned above, CYP2C enzymes and CYP2E1 also demonstrate significant species differences. Whereas CYP2E1 is readily detected in rat and mouse kidney (42,49), its expression has not been detected in human kidney (23,24,47,50). In rat and mouse kidney, CYP2E1 expression is under androgenic control, and males have significantly more enzyme than females. A consequence of this gender-dependent difference is that male mice are markedly more susceptible than female mice to nephrotoxicity caused by certain CYP2E1 substrates (51).

The CYP3 gene family is highly expressed in kidneys of both rodents and humans, although there may be some difference in nephron localization across species, with a higher proportion being expressed in the glomerulus versus the proximal tubules in rodent kidney and the reverse in human kidney (49,52,53). The human orthologue of rodent CYP3A1/2 is CYP3A4/5; it is readily detected in microsomes from human kidney cortex homogenates (47,53) but appears to exhibit a high degree of variability among human kidney samples (47), consistent with the known genetic polymorphisms for CYP3A4 and other CYP enzymes (54,55).

Enzymes of the CYP4A family are primarily involved in metabolism of fatty acids, such as arachidonic acid, and are prominently expressed in the kidneys (56 58). Although the CYP4A family does not metabolize drugs and other xenobiotics, it is mentioned here

because its expression is strongly influenced by hypolipidemic drugs, such as the fibrates, and other drugs that are known to cause peroxisome proliferation. One should note, however, that the effectiveness of such peroxisome proliferators is much greater in liver than in kidney and in rats than in humans.

Flavin-Containing Monooxygenase

Like the CYPs, FMOs are a multigene family of enzymes found in the endoplasmic reticulum and are highly expressed in not only the liver but also in extrahepatic tissues, including the kidneys (59,60). While there are five active isoforms (FMO1-5) that have been identified in mammals, they are not ubiquitously expressed, with significant species-, sex-, tissue-, and developmental-dependent differences (61 64). Although the FMOs have a fairly broad substrate specificity, they are most active in catalyzing the oxidation of sulfur-, selenium-, and nitrogen-containing drugs and xenobiotics. While many FMO substrates are also metabolized by various CYPs, there are several types of substrates that are restricted to FMO.

In contrast to human liver, which expresses primarily FMO3 as well as several other FMO enzymes, human kidney (in particular, the proximal tubules) expresses primarily FMO1, somewhat lower levels of FMO5, and very low levels of FMO3 (65). Similarly, Nishimura and Naito (66) assessed profiles of FMO messenger ribonucleic acid (mRNA) expression in human kidney and found that FMO1 mRNA was the most abundantly expressed form, whereas FMO2, FMO3, FMO4, and FMO5 mRNAs were expressed at 4%, 0.09%, 25%, and 13%, respectively, of the levels found for FMO1. Another interesting finding was that FMO1 protein levels varied considerably in a limited number of samples of human kidney, consistent with the existence of genetic polymorphisms (65). Moreover, single nucleotide polymorphisms and splicing variants have been identified for all the FMOs in several human tissues, including the kidneys (59).

It has been known for many years that sulfoxides are stable, urinary metabolites of many cysteine *S*-conjugates. It was only with the studies of Elfarra and colleagues (67 69) that it became apparent that these sulfoxide metabolites may play a different role than just being a stable end-product. In the kidneys, in particular, many of the studies over the past nearly two decades have focused on the role of FMOs in the bioactivation of nephrotoxic cysteine *S*-conjugates, which are converted to reactive sulfoxides (23,67 72). The function of FMOs in bioactivation of cysteine *S*-conjugates and the role of this in nephrotoxicity are discussed further, in the sections on the GSH conjugation pathway and in the example of how TRI and perchloroethylene (Perc) cause nephrotoxicity.

Prostaglandin Synthase

Prostaglandins play a number of critical roles in renal physiology and pathophysiology, involving volume and sodium homeostasis, with the various lipid-derived products functioning as important signaling molecules (73,74). The biosynthesis of prostaglandins involves a two-step process, catalyzed by the bifunctional prostaglandin H synthase (PHS): the cyclooxygenase-dependent oxidation of a polyunsaturated fatty acid, such as arachidonic acid, to a hydroperoxy endoperoxide, prostaglandin G_2 (PGG_2) and the subsequent reduction to a hydroxy endoperoxide prostaglandin H_2 (PGH_2) (Fig. 2). In the kidneys, PHS is localized in the microsomal fraction of cells of the inner and outer medulla (75,76).

Although the primary focus of studies on this pathway has been that of subsequent products (e.g., various eicosanoids) that influence renal function, it was realized in the late

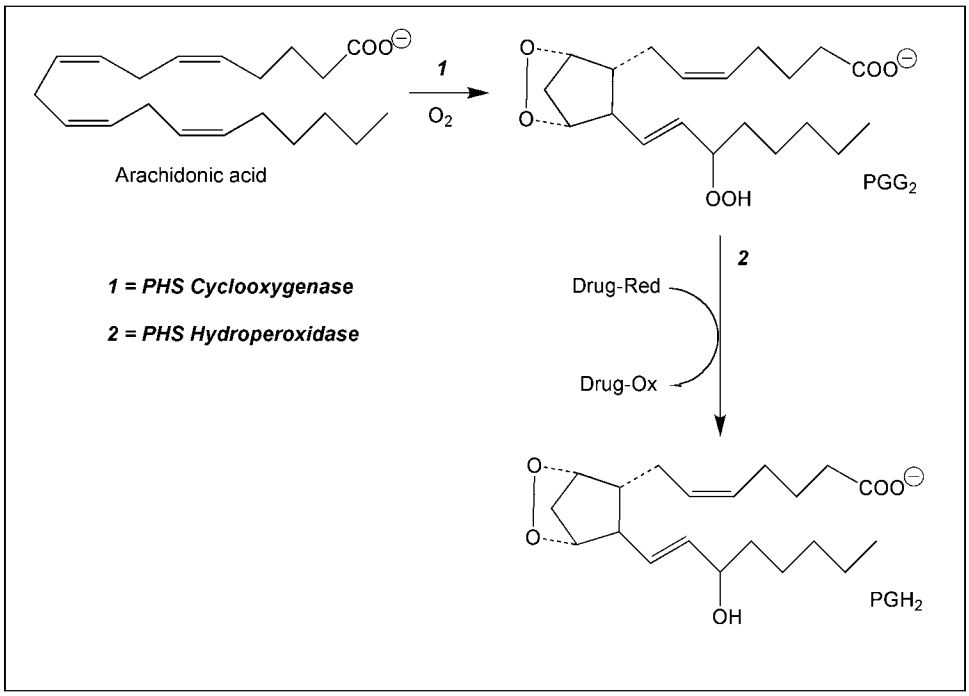

Figure 2 *Prostaglandin synthase reaction pathway for drug co oxidation.* Scheme showing how certain drugs are oxidized during the hydroperoxidase step of the PHS reaction. *Abbreviation*: PHS, prostaglandin synthase.

1970s that a number of drugs can undergo co-oxidation in the hydroperoxidase step of the PHS reaction (77,78). The diverse group of drugs that can be oxidized in this manner include analgesics such as acetaminophen (APAP) and aminopyrene and carcinogens such as benzidine and benzo(a)pyrene. PHS-catalyzed oxidation of benzidine has been associated with increased risk of bladder cancer (78 81).

PHASE II METABOLISM IN THE KIDNEYS

Phase II metabolism reactions include the various conjugation reactions, such as glucuronidation, sulfation, and GSH conjugation. A drug or xenobiotic is linked by a covalent bond to an endogenous group through a functional group (e.g., hydroxyl or amino group) that is either present in the parent molecule or is introduced by a phase I reaction (e.g., CYP- or FMO-catalyzed oxidation, reduction, or hydrolysis). While these pathways occur in the liver, they are also present in select regions of the kidney, although isozyme patterns differ. Although it is generally true that the conjugates formed by phase II reactions are highly water soluble and are readily excreted in either bile or urine, there are some notable exceptions, particularly for renal metabolism; some of these exceptions will be discussed below in the section on specific examples.

Glucuronidation

This phase II reaction is catalyzed by a family of enzymes called the UDP-glucuronosyltransferases (UGTs), which are localized in the endoplasmic reticulum and are expressed in most tissues, but in varying amounts. Glucuronidation is an Sn2 reaction

in which an acceptor group on the substrate (nucleophile) attacks an electrophilic carbon on the glucuronic acid moiety. Glucuronides may form on N-, S-, and C-groups of both endogenous and xenobiotic substrates. The glucuronidation pathway occurs in three steps, the first two for formation of UDP-glucuronic acid (UDPGA) from glucose-1-phosphate and uridine-5′-triphosphate (UTP) with NAD^+-dependent oxidation and the third for formation of the conjugate. UDPGA is considered to be limiting in extrahepatic tissues, whereas ample substrate levels are usually present in the liver (40).

UGTs were originally divided into two gene families, UGT1 and UGT2, on the basis of sequence homology. Recently, the nomenclature used for the UDP-glycosyltransferases, which include the UGTs, was updated (82). Thus, the mammalian UGT gene superfamily, as of October 2005, has 117 members that are divided into four gene families, UGT1, UGT2, UGT3, and UGT8. UGTs from the UGT1 and UGT2 family are the most efficient at using UDPGA as donor substrate, so are thus the ones that are of most interest in drug metabolism. The sugar specificity of the UGT3 members is unclear, as this group has only recently been identified. The UGT8 family is a single gene that encodes UDP-galactose ceramide galactosyltransferase and is not likely to be involved in drug metabolism.

Substrates for the UGTs include a broad range of both endogenous (e.g., steroid hormones, bile acids, biogenic amines) and xenobiotic chemicals (e.g., fat-soluble vitamins, carcinogens, APAP, salicylic acid). Klaassen and colleagues (83) studied the mRNA expression of several members of the UGT1 and UGT2 gene families in several rat tissues. As summarized by Shelby et al. (83), UGT1 family members are encoded from a single gene that has multiple first exons followed by four common exons. Individual UGT1A gene products are formed by the splicing of one of the first exons with the four common exons. Identification of distinct gene promoter regions for the multiple first exon is consistent with tissue-specific patterns of expression and inducibility of specific UGT1A isoforms. In the rat, nine different first exons have been identified, generating UGT1A1 through UGT1A9, although UGT1A4 and UGT1A9 are pseudogenes (i.e., they do not encode for functional proteins). Members of the UGT2 gene family, in contrast to those of the UGT1, are encoded from individual genes, with each gene containing six exons. The UGT2 gene family is further subdivided into two subfamilies, UGT2A and UGT2B. In humans, a total of 17 UGTs have been characterized as of a 2004 review (84). The potential importance of UGTs in human health and disease was also emphasized in that review. A check of the UGT homepage (http://som.flinders.edu.au/FUSA/ClinPharm/UGT/) in April 2008 shows 21 human UGTs.

Renal UGTs are microsomal enzymes of 54- to 56-kDa molecular weight and are found predominantly in the proximal tubules. Comparison of UGT activities in liver and kidney microsomes from several species shows that rates of metabolism are invariably higher in the liver than in the kidney, sometimes by $>$ 10-fold, and those in rodents were generally higher than those in humans (40). Similar to the situation with several CYPs, renal and hepatic UGTs exhibit different patterns of inducibility; in some cases, certain inducers are just more effective in the liver, whereas in other cases, chemicals may induce in one tissue and not at all in the other.

The studies of Shelby et al. (83) showed that individual genes of both the UGT1 and UGT2 families exhibit distinct patterns of expression that vary with both tissue and gender. mRNA expression was determined in the liver, kidney, lung, stomach, small intestine (duodenum, jejunum, ileum), colon, and brain (cerebellum, cerebral cortex). Of the seven functional UGT1A gene products, UGT1A1 mRNA was detected in all tissues studied and was found at similar levels for both males and females, with the exception of lung tissue, which was relatively low. UGT1A2, UGT1A3, and UGT1A7 were detected

primarily in the gastrointestinal tract with no significant gender differences for the former and possibly some for the latter. UGT1A5 mRNA was primarily limited to the liver with higher levels in females. UGT1A6 mRNA was found in most tissues, but was highest in the kidneys and large intestine; expression in rat kidney from females was significantly higher than that in males. UGT1A8 mRNA was detected almost exclusively in the liver and kidney and was about twofold higher in females in both tissues. Thus, from the UGT1 gene family, rat kidney expresses primarily UGT1A1, UGT1A6, and UGT1A8. In human kidneys, Nishimura and Naito (66) found UGT1A6 and UGT1A9 (a pseudogene) to be the major mRNA species detected. Lash et al. (47) detected UGT1A1 and UGT1A6 proteins in primary cultures of human proximal tubular cells.

Shelby et al. (83) found more prominent tissue-specific differences in mRNA expression for members of the UGT2 gene family. UGT2A1 was detected almost exclusively in the nasal epithelium, whereas UGT2B1 and UGT2B2 were detected almost exclusively in the liver with $>$ twofold higher levels found in female rats as compared with male rats. UGT2B3 mRNA was found predominantly in the liver with 10% to 20% as much found in the small intestine. UGT2B6 mRNA was also predominantly expressed in the liver with low levels ($<$10% of liver) detected in the small intestine and brain. The only isoform mRNAs detected in the kidney were those for UGT2B8 (very low levels) and UGT2B12. The latter was found ubiquitously but was most prominent in the kidney and liver. In human kidney, relatively low levels of mRNA for UGT2B10, UGT2B15, and UGT2B17 were detected (66). In primary cultures of human proximal tubular cells, UGT2B7 protein was readily detected as well (47). UGT8 mRNA was also detected in human kidney (66), but its function has not yet been characterized.

Sulfation

The sulfation pathway results in the sulfonation of a broad range of drugs, hormones, and neurotransmitters. As with the glucuronidation pathway, the sulfation pathway occurs in three steps, the first two being those that activate the donor substrate, forming 3′-phosphoadenosine-5′-phosphosulfate (PAPS), and the third being the sulfonation or sulfation reaction, which is catalyzed by a family of cytoplasmic enzymes called the sulfotransferases (SULTs). The known gene products are spread across six gene families (SULT1 6), although SULT3 is only found in mice and rabbits and SULT5a1 is only found in mice (85,86). Thus, there are 13 human cytosolic SULTs currently known that include members of the SULT1, SULT2, SULT4, and SULT6 gene families. Only those SULT enzymes that are found in the kidneys will be briefly discussed below. Much like other major drug metabolism enzyme systems, genetic polymorphisms and single nucleotide polymorphisms have been found for the SULTs (87), suggesting that individual variations in SULT activity may both contribute to disease or sensitivity to toxic chemicals or may be used to individualize new therapeutic approaches.

Products of the SULT1 family have a broad substrate specificity and can sulfonate simple, small planar phenols, such as estradiol, thyroid hormones, and a broad variety of drugs and environmental chemicals. SULT1A1 is the major adult liver SULT1A subfamily member and is also found in the kidneys. Both SULT1A1 and SULT1A3 are reported to be abundant in fetal liver and kidney, but the latter one is said to disappear in the adult, although expression of SULT1A3 protein was recently reported in primary cultures of human proximal tubular cells (47) and both SULT1A1 and SULT1A3 mRNA were reported in adult kidney (66), with SULT1A1 being by far the most highly expressed. Although SULT1A2 mRNA is found in several tissues, including the liver and kidneys, the consensus is that it is not translated into a functional protein in humans and is

thus likely a pseudogene. SULT1E1 is also expressed in the kidneys (47,66,85), but is primarily active with phenols such as estradiol.

SULT2 family members are most active in the sulfonation of hydroxyl groups of steroids such as androsterone. SULT2A1 has been localized to the kidney by immunostaining and was found not only in the proximal tubules but also in several more distal nephron segments. SULT2A1 protein was readily detected in primary cultures of human proximal tubular cells (47). SULT2B1 exists as two variants and has been found in human kidney (66,85). Thus, enzymes of the SULT2 family do not seem to have a major role in drug metabolism.

GSH Conjugation

Mercapturate Pathway

Along with glucuronidation and sulfation, GSH conjugation functions as a major detoxification pathway for many drugs and other xenobiotics. In the classical view, GSH *S*-transferases (GSTs) catalyze the conjugation of reactive electrophiles with GSH in the initial step of a detoxication pathway that ultimately results in formation of *N*-acetylcysteine conjugates (mercapturates), which are ultimately excreted in urine (Fig. 3). Although GSTs are expressed in most cell types, including renal tubular epithelial cells, hepatocytes express the highest levels of any organ.

In mammals, multiple families of GSTs are found in cytoplasm, mitochondria, and endoplasmic reticulum (microsomes). Isoforms of importance for renal drug metabolism are those found in the cytoplasm and microsomes. Cytoplasmic GSTs are dimers with subunits of 199 to 244 amino acids in length and are divided into seven families on the basis of amino acid sequence (i.e., $>$40% homology). These families are designated as α, μ, π, σ, τ, and ζ. The convention is to refer to rodent GSTs by Greek letters (i.e., GSTα, GSTμ, GST π, GST σ, GST τ, and GST ζ) and human GSTs by capital Arabic letters (i.e., GSTA, GSTM, GSTP, S, GSTT, GSTO, and GSTZ). At present, 16 cytoplasmic GST subunits are known in humans. The mature protein can exist as a variety of homo- and heterodimers, indicating that a large variety of isoenzymes are ultimately generated.

Three families of cytoplasmic GSTs are expressed in rat kidney: GSTα, GSTπ, and GSTμ. Immunolocalization (88) and Western blot analyses in renal tissue and isolated renal proximal and distal tubular cells (89) showed selective localization of GSTα in proximal tubules, whereas GSTπ and GSTμ are expressed in the distal nephron. In human kidney, the GST isoenzyme expression pattern is quite different from that in the rat kidney; renal proximal tubular cells express GSTA, GSTP, and GSTM (24,47). Because of the broad and often overlapping substrate specificities of the different GST isoforms, it is difficult to assess the impact of this difference in expression pattern when extrapolating renal metabolism data from rats to humans.

The other cytoplasmic GST family found in the kidneys is the Zeta class, which was discovered in the late-1990s using a bioinformatics approach with human-expressed sequence tag databases (90 92). GSTZs are widely distributed in eukaryotes and are identical to maleylacetoacetate isomerase, a key catalyst in tyrosine catabolism. Unlike the other cytoplasmic GSTs, GSTZs lack significant activity toward the prototypical substrate 1-chloro-2,4-dinitrobenzene. An important substrate class is the α-haloacids such as dichloroacetic acid (DCA), which is metabolized to glyoxylic acid. Metabolism of DCA is important because DCA is used in the clinical management of congenital lactic acidosis, is a common drinking water contaminant, and is a metabolite of the environmental contaminant and probable human carcinogen TRI (43). Four polymorphic variants of GSTZ have been described thus far in humans, and these have distinct catalytic activities.

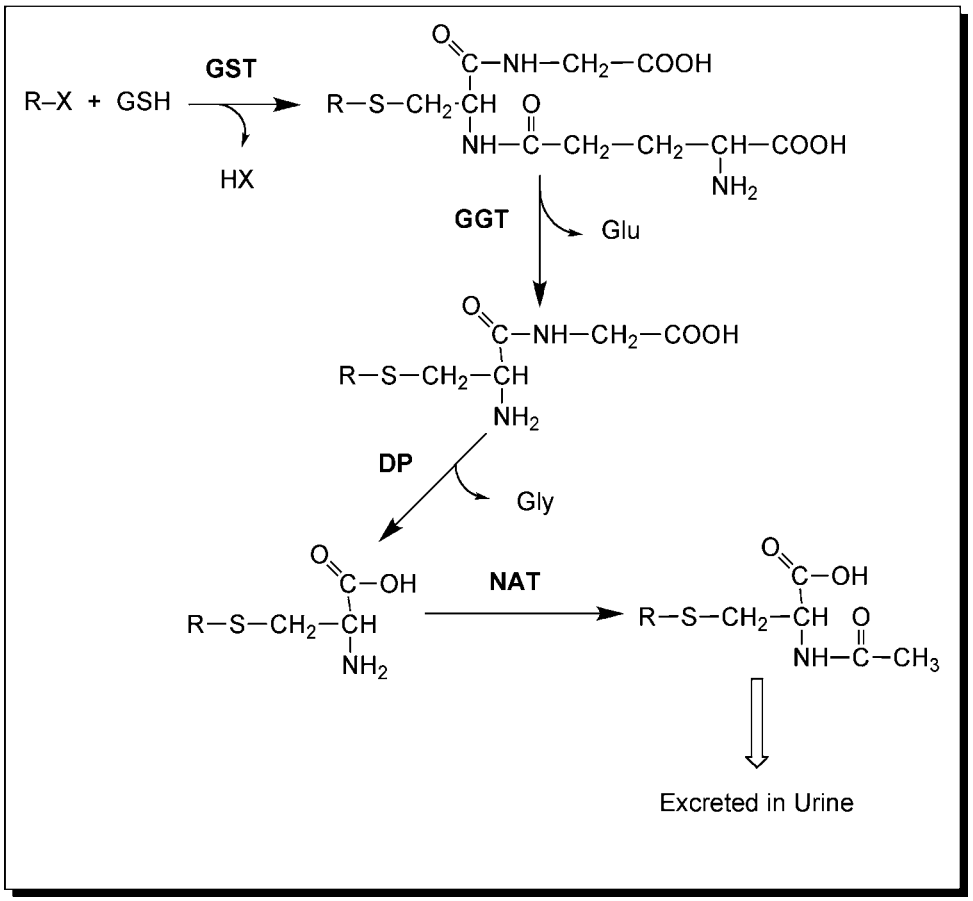

Figure 3 *Classical mercapturic acid pathway for drug detoxication.* Drugs (R X; X is a good leaving group) are conjugated with GSH to form the GSH conjugate, either in the liver or kidney. Subsequent reactions occur in the kidneys and include hydrolysis of the γ glutamyl isopeptide bond by GGT and the cysteinylglycine peptide bond by DP activity to yield the cysteine conjugate. The cysteine conjugate undergoes *N* acetylation by the cysteine conjugate NAT to form the *N* acetylcysteine conjugate, or mercapturate. The mercapturate, because of its polarity, is readily excreted into the urine. *Abbreviations*: GGT, γ glutamyltransferase; DP, dipeptidase; NAT, *N* acetyltransferase.

The other family of renal GSTs that is important for drug metabolism are the MAPEG (membrane-associated proteins in eicosanoid and glutathione metabolism) proteins, which are a unique family of GSTs that share no sequence identity with either the cytoplasmic or mitochondrial GSTs. While a distinctive function includes their involvement in eicosanoid metabolism, MAPEG proteins are also important in drug metabolism. Of the different MAPEG members, MGST1 (microsomal GSH *S*-transferase 1) seems to function exclusively as a detoxication enzyme, whereas MGST2 and MGST3 are involved in both drug metabolism and leukotriene C_4 synthesis (93). Although the precise role of MAPEG proteins in GSH-dependent bioactivation is unclear, MGSTs have been immunolocalized to several rat tissues, including the kidneys (94), and chemicals such as TRI are readily metabolized to their respective GSH conjugates in the presence of GSH and liver or kidney microsomal fractions from rats or humans (95 97).

Regardless of whether the GSH conjugation reaction occurs within the kidneys themselves or in the liver, the subsequent reactions of the mercapturic acid pathway occur predominantly in the kidneys. The next two steps in the metabolism of GSH conjugates, regardless of whether they are undergoing the classic detoxication pathway to ultimately yield the mercapturate or whether they are being bioactivated, involve successive cleavage of the γ-glutamyl isopeptide and cysteinylglycyl peptide bonds to yield the corresponding cysteine conjugate. These steps are catalyzed by two BBM enzymes, γ-glutamyltransferase (GGT) and various dipeptidases (DPs). Although GGT and DP activities are found on several extrarenal tissues, such as the hepatic canalicular plasma membrane and the jejunal BBM, their activities are by far the highest on the BBM of renal proximal tubules (98). The overall, quantitative significance of these pathways in metabolism and turnover of GSH (and by analogy GSH conjugates) is illustrated by the profound glutathionuria that occurs when GGT activity is inhibited (99).

In the classic mercapturate pathway, cysteine conjugates are subsequently *N*-acetylated by the microsomal cysteine conjugate *N*-acetyltransferase (NAT) to yield the mercapturate. For most chemicals, the mercapturates function as highly polar metabolites that are readily excreted in urine. Many mercapturates, however, can be acted on by a deacetylase (or aminoacylase) activity to regenerate the cysteine conjugate. The significance of this for those cysteine conjugates that may also undergo bioactivation (see below) is evident from the observations that *N*-acetyl-L-cysteine-*S*-conjugates of nephrotoxic haloalkenes and haloalkanes may be deacetylated and exhibit toxicity in a manner similar to the corresponding cysteine conjugates (100–102).

CCBL and Bioactivation Pathways

Although most chemicals that undergo GSH conjugation and processing to form cysteine conjugates are ultimately metabolized to mercapturates that are excreted in the urine, several classes of chemicals are converted to cysteine conjugates that are substrates for a CCBL activity that results in bioactivation rather than detoxication (Fig. 4). Substrates are cysteine conjugates of chemicals such as halogenated alkenes and alkanes, which include numerous environmental contaminants, such as the metal degreasing agent TRI (47), the analogue Perc, which is used in dry cleaning (103), and chlorofluorocarbons that have been used as refrigerants (104).

CCBL activities are found in both cytoplasm and mitochondria and in numerous tissues besides the kidneys (105). In the kidneys, two proteins, each dually localized in the cytoplasm and mitochondria, have been identified as catalyzing CCBL activity. The first is glutamine transaminase K (GTK) (EC 2.6.1.64), which exists as a homodimer of 45-kDa subunit molecular weight; the second activity has not been extensively characterized, but has been identified as a high molecular weight β-lyase of 330 kDa. Abraham et al. (106,107) have suggested that, at least in mitochondria, this high molecular weight form is the primary enzyme catalyzing CCBL activity. Both GTK and the high molecular weight CCBL contain pyridoxal-5′-phosphate (PLP) as prosthetic group and can catalyze either a direct β-elimination to yield a reactive thiolate (Fig. 5, pathway B) or a transamination (Fig. 5, pathway A), which yields an unstable α-keto acid. Because of the ability to undergo a transamination reaction, maximal CCBL activity often requires the presence of an α-keto acid in the reaction mixture as a cosubstrate (108,109).

A third potential pathway for bioactivation of cysteine *S*-conjugates is catalyzed by FMO (Fig. 5, pathway C), as described above. Although most studies on cysteine conjugate nephrotoxicity have focused on the role of CCBL, some studies in human

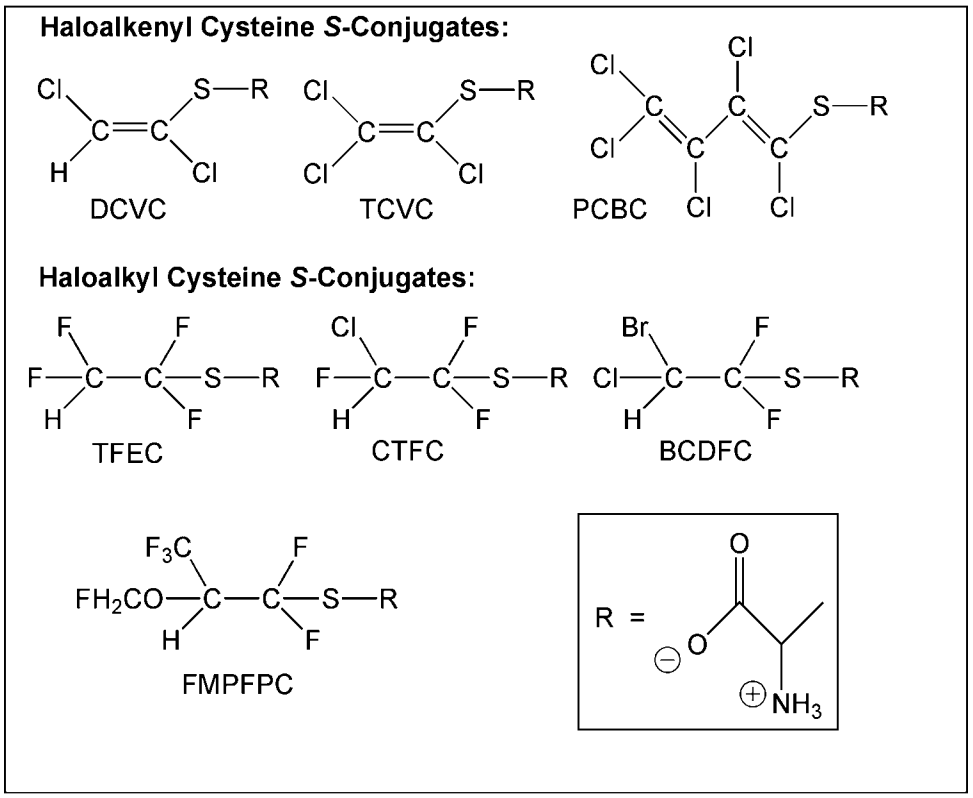

Figure 4 *Structures of selected cysteine conjugates that undergo bioactivation. Abbreviations*: BCDFC, *S* (1 bromo 1 chloro 2,2 difluoroethyl) L cysteine; CTFC, *S* (1 chloro 1,2,2 trifluor oethyl) L cysteine; DCVC, *S* (1,2 dichlorovinyl) L cysteine; FMPFPC, *S* (1 fluoromethoxy 1,1,1 trifluoro 3,3 difluoropropyl) L cysteine; PCBC, *S* (1,1,2,3,4 pentachlorobutadienyl) L cysteine; TFEC, *S* (1,1,2,2 tetrafluoroethyl) L cysteine; TCVC, *S* (1,2,2 trichlorovinyl) L cysteine.

kidney suggest that FMO may have a more significant role than CCBL; the opposite appears to be the case in rats, where the CCBL is more prominent than FMO (23,71,72).

GSH Conjugates as Prodrugs

Because of the unique position that the kidneys play in overall GSH and GSH conjugate metabolism, investigators have taken advantage of these properties to synthesize prodrugs that are targeted to the kidneys whereupon they become bioactivated to their therapeutic form. Examples include selenocysteine compounds that are selectively accumulated by the kidneys and converted to selenol compounds (110), *N*-acetyl-γ-glutamyl derivatives that are also selectively accumulated by the kidneys and then metabolized to their active forms (111,112), and various cysteine or GSH conjugates of purine derivatives that are metabolized to antitumor agents within the kidneys (113 117).

An example of taking advantage of the unique properties of transport and metabolism to selectively deliver renal prodrugs to their primary target cell (i.e., the proximal tubules) is illustrated in Figure 6. In this study (118), which was an in vitro study of transport, metabolism, and toxicity based on the in vivo studies from Elfarra and colleagues (113 117), the importance of each of the three major steps, leading from

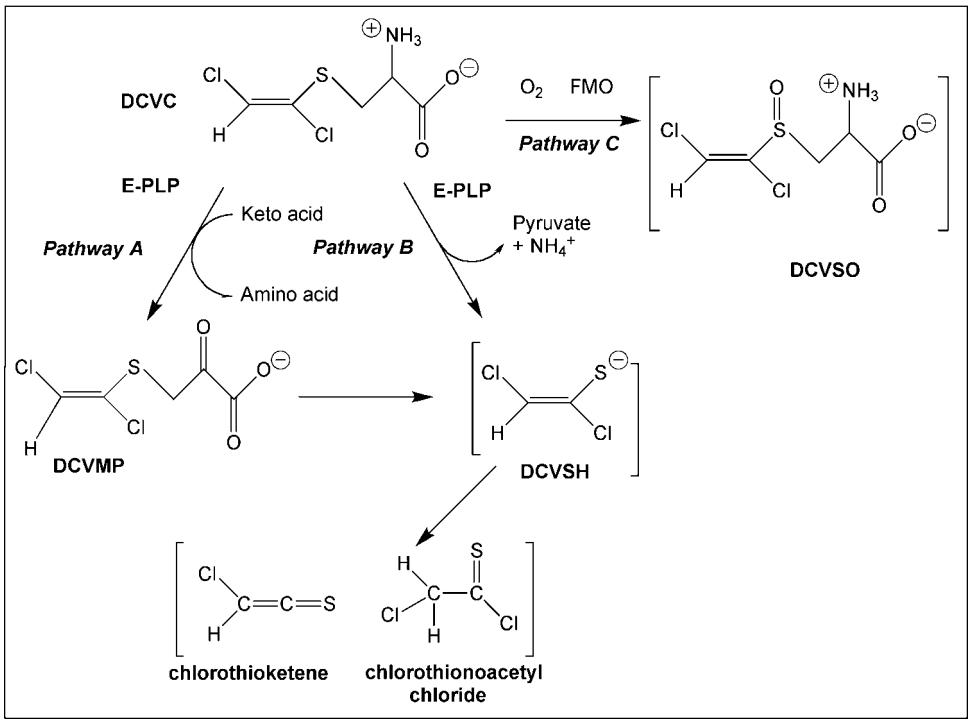

Figure 5 *Bioactivation pathway for DCVC.* DCVC undergoes bioactivation by either the PLP containing CCBL, which occurs by either transamination (pathway A) or β elimination (pathway B), or the FMO (pathway C). Products of the three pathways include DCVMP, DCVSH, and DCVSO, respectively. *Abbreviations*: DCVC, *S* (1,2 Dichlorovinyl) L cysteine; PLP, pyridoxal 5′ phosphate; FMO, flavin containing monooxygenase; DCVMP, *S* (1,2 dichlorovinyl) mercaptopropionic acid; DCVSH, *S* (1,2 dichlorovinyl) thiol; DCVSO, DCVC sulfoxide; CCBL, cysteine conjugate β lyase.

administration of prodrug to generation of toxicant, was probed by the use of selective inhibitors. Thus, inhibition of uptake of the GSH conjugate prodrug (6-purinylglutathione, 6-PG) was inhibited with probenecid, thereby inhibiting subsequent steps [i.e., metabolism to generate 6-mercaptopurine (6-MP) and toxicity]. Probenecid is a well-known inhibitor of organic anion transport and of GSH and GSH *S*-conjugate transport across the renal BLM (119). Similar to earlier studies in renal proximal tubular cells to demonstrate the function of each step in TRI bioactivation (45), inhibition of GGT with acivicin or CCBL with aminooxyacetic acid (AOAA) resulted in decreased formation of 6-MP and decreased cytotoxicity. Additionally, inhibition of xanthine oxidase (XO) with allopurinol prevented cytotoxicity, demonstrating that this is the key step in generating the cytotoxic species.

EXAMPLES ILLUSTRATING UNIQUE FUNCTIONS OF THE KIDNEYS IN DRUG METABOLISM

Acetaminophen

Although APAP is a widely used analgesic that is considered very safe to use under normal conditions, it can exhibit significant organ toxicity under overdose conditions. Moreover, it is a frequent cause of poisoning due to overdose. The liver is the initial site

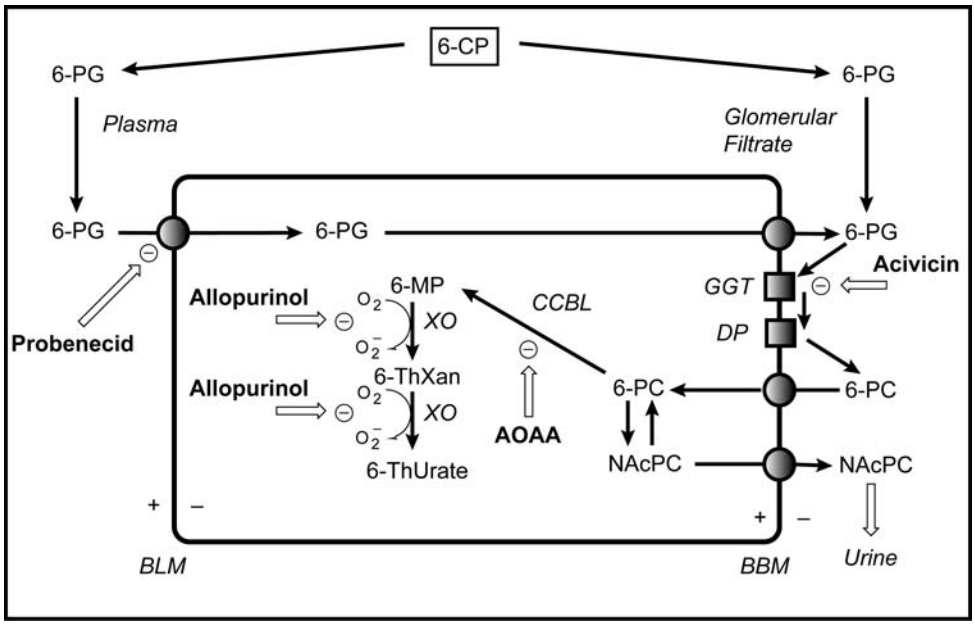

Figure 6 *Handling of a GSH conjugate prodrug by the renal proximal tubular cell.* This scheme summarizes the renal delivery, transport, and metabolism of a GSH conjugate prodrug by the renal proximal tubular cell. The parent compound, 6 CP was administered to rats and converted to the prodrug 6 PG. 6 PG undergoes either glomerular filtration or enters the renal periplasmic space, where it can be taken up in the proximal tubular cell by transport across the BLM. Intracellular 6 PG is secreted into the tubular lumen where it, along with filtered 6 PG, undergoes degradation by GGT and DP activities on the BBM to yield the cysteine conjugate 6 PC. 6 PC is transported into the proximal tubular cell where it can either be converted to the mercapturate, NAcPC, or undergo metabolism by the CCBL, which generates the chemotherapeutic agent 6 MP. The NAcPC can either be deacetylated to regenerate 6 PC or transported into the lumen for excretion in the urine. 6 MP can be further metabolized by XO to generate 6 ThXan and 6 ThUrate. The importance of some of these steps was demonstrated by use of selective inhibitors, such as probenecid, allopurinol, acivicin, and AOAA. *Abbreviations*: 6 CP, 6 chloropurine; 6 PG, 6 purinylglutathione; BLM, basolateral (plasma) membrane; GGT, γ glutamyltransferase; DP, dipeptidase; BBM, brush border (plasma) membrane; 6 PC, 6 purinyl L cysteine; NacPC, *N* acetyl 6 purinyl L cysteine; CCBL, cysteine conjugate β lyase; 6 MP, 6 mercaptopurine; XO, xanthine oxidase; 6 ThXan, 6 thioxanthine; 6 ThUrate, 6 thiourate; AOAA, aminooxyacetic acid.

of damage after APAP overdose, and the kidneys are secondary sites due to their significant ability to metabolize APAP to both detoxication and bioactivation products (120), the latter resulting in analgesic nephropathy (121). The major pathways for metabolism of APAP in either the liver or renal cortex (Fig. 7) show the presence of competing detoxification and bioactivation reactions. Under normal dose conditions (i.e., therapeutic doses), the primary flux of metabolism is generation of glucuronide or sulfate conjugate, which are both readily excreted in urine. Once the capacity of these phase II enzymes is exceeded as occurs in an acute overdose, however, significant activity with CYP (primarily CYP2E1, but also CYP1A2 and CYP3A4/5 in humans or CYP3A1/2 in rodents) can occur, resulting in formation of a reactive quinoneimine, *N*-acetyl-*p*-benzoquinoneimine (NAPQI). Under nonstressed conditions in which ample amounts of GSH are present, NAPQI forms a GSH conjugate, which has generally been considered a detoxification product, leading to formation of a readily excreted mercapturate. When

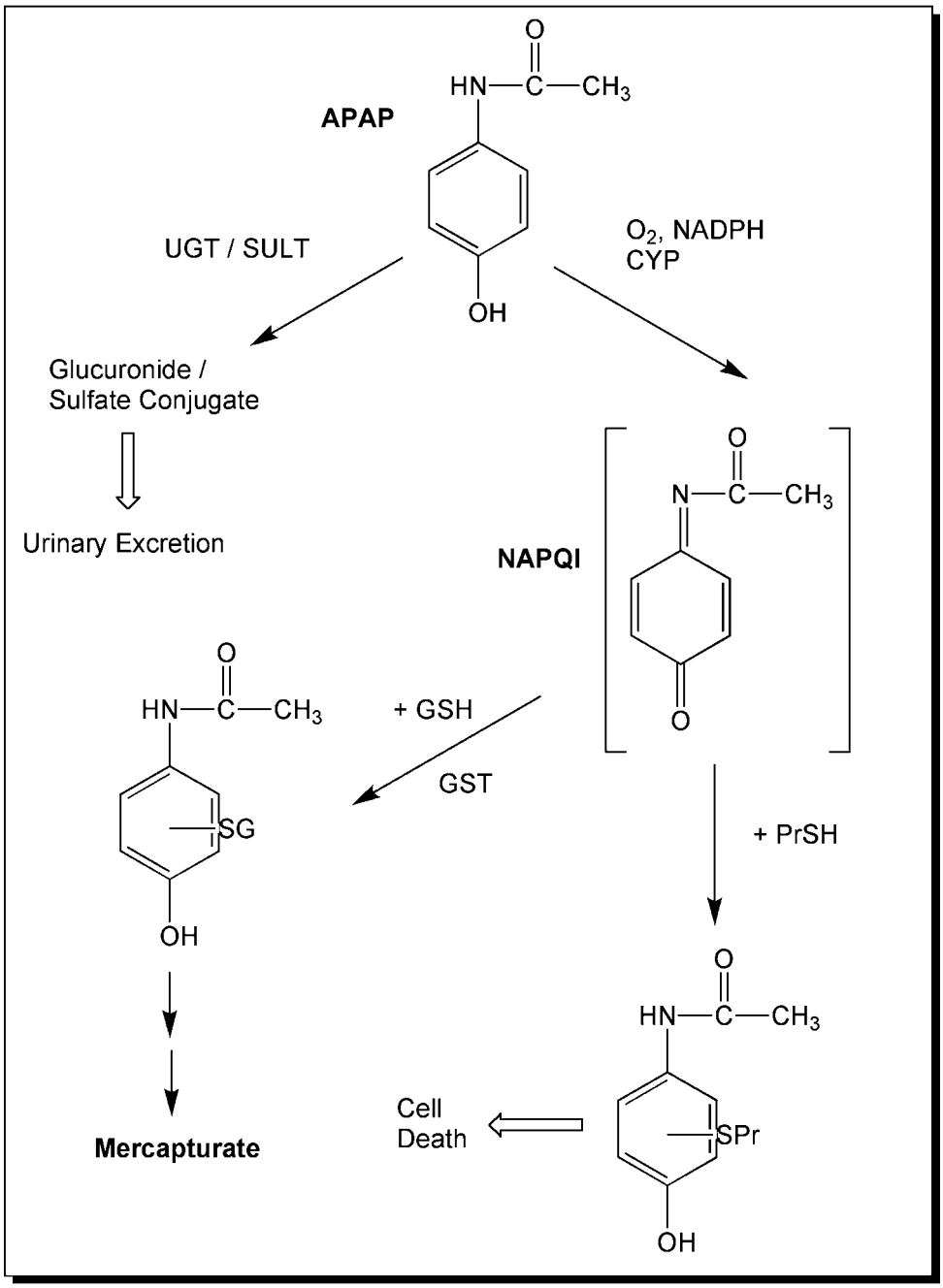

Figure 7 *Metabolism of APAP.* APAP primarily undergoes conjugation by either a UGT or SULT to form a readily excreted, highly polar product. When these reactions are saturated, APAP may be metabolized by CYP to form a reactive intermediate, NAPQI, which reacts with either GSH via GST catalysis to ultimately form a mercapturate, or with PrSH groups. The latter reaction can lead to cytotoxicity. *Abbreviations*: APAP, acetaminophen; UGT, UDP glucuronosyltransferase; SULT, sulfotransferase; CYP, cytochrome P450; NAPQI, *N* acetyl *p* benzoquinoneimine; GST, GSH *S* transferase; PrSH, protein sulfhydryl.

GSH is depleted, however, NAPQI can react with other nucleophiles, such as protein sulfhydryl groups, leading to cell damage and cytotoxicity. APAP may also undergo deacetylation to form *p*-aminophenol (PAP), which can then be metabolized by similar reactions to produce a reactive quinoneimine (122). Thus, acute nephrotoxicity due to APAP overdosage is characterized by tubular necrosis, largely confined to the proximal tubules of the renal cortex and outer stripe of the outer medulla.

Because of the potential for chronic abuse of APAP, renal injury due to long-term exposures to moderate doses is also a problem. The chronic ingestion of APAP can be associated with the so-called analgesic nephropathy, which is characterized by papillary necrosis and interstitial fibrosis. Thus, in contrast to acute overdose, which is associated with damage to the proximal tubules and is associated with CYP-dependent formation of NAPQI and GSH depletion, chronic exposure is due to the one-electron co-oxidation of APAP by PGS in the renal medulla to initially produce a phenoxyl radical, which is further oxidized to yield the reactive NAPQI (123). This distinct pattern of injury is due to accumulation of APAP in the inner medulla and the presence of PGS in that nephron region.

Cephaloridine

Cephaloridine (CPH), which is a first-generation cephalosporin antibiotic, is limited in its therapeutic efficacy by dose-limiting nephrotoxicity (124). The CPH molecule possesses two functional groups besides the characteristic β-lactam ring, giving the molecule three potential sites of bioactivation (Fig. 8). A thiophene ring on one end of the molecule can undergo CYP-dependent oxidation to yield a reactive epoxide, whereas the pyridinium ring on the other end of the molecule is thought to undergo redox cycling similar to paraquat, thereby generating superoxide anions and an oxidative stress. The β-lactam ring, however, appears to be the primary site at which interactions occur that lead to cytotoxicity. In a series of studies, Tune and colleagues (125 129) showed that the β-lactam ring can open and selectively form adducts with substrate transporters on the mitochondrial inner membrane, thereby inhibiting mitochondrial function. Similarly, Lash et al. (130) showed that mitochondria are selective targets for CPH and provided additional data suggesting that besides the β-lactam ring, metabolism at the thiophene ring may also play a significant role in nephrotoxicity (131).

Another point that is critical for CPH-induced nephrotoxicity and that illustrates a general principle that contributes to many forms of drug-induced nephrotoxicity is that CPH is efficiently and selectively transported into proximal tubular cells by organic anion carriers but is poorly secreted, thereby leading to high intracellular concentrations. This accumulated drug is then metabolized by either CYPs or undergoes nonenzymatic redox cycling or hydrolysis of the β-lactam ring, thereby leading to the various toxic effects.

GSH Conjugates of TRI and Perc

TRI and Perc provide additional examples of chemicals that are selectively nephrotoxic and whose mode of action takes advantage of some of the unique features of renal proximal tubular function with respect to GSH conjugates. These features include both transport and metabolism, as illustrated in Figure 6 for the GSH conjugate prodrugs. For both chemicals, while there can be intrarenal GSH conjugation, most of the GST reaction occurs in the liver, and the GSH conjugate thus formed is transported out of the liver into

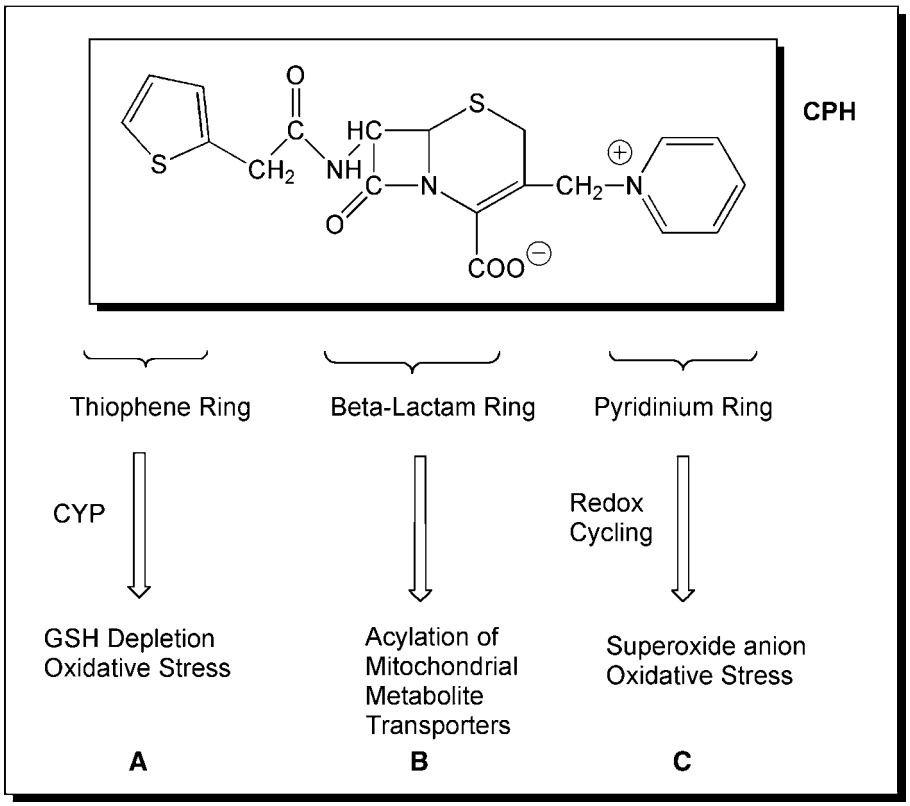

Figure 8 *Structure of CPH showing potential sites of bioactivation.* CPH has three regions that can be sites of metabolism: (**A**) a thiophene ring that can undergo CYP dependent oxidation; (**B**) the β lactam ring, which may undergo a ring opening reaction that results in acylation of mitochondrial transporter proteins; and (**C**) a pyridinium ring that may undergo redox cycling to generate superoxide anion. *Abbreviations*: CPH, cephaloridine; CYP, cytochrome P450.

bile or plasma (43,45,103). It eventually reaches the renal circulation as either the GSH conjugate or the cysteine conjugate. The presence of a large array of amino acid and OATs, primarily in the proximal tubules, enables the kidney to accumulate these chemicals and metabolize them further. It is quite telling that although other tissues have CCBL activity, such as the liver, the kidneys are the predominant, if not sole, target organ (45,103).

CONCLUSION

The kidneys possess most of the same drug-metabolizing enzymes as the much more studied liver. Significant differences exist between tissues, however, in terms of isoenzyme expression, overall amount of enzyme activity, regulation of enzyme expression and activity, and cell type distribution. Hence, for most of the enzymes that are of interest for drug metabolism, the highest levels of expression in the kidneys are found in the proximal tubules. These include enzymes of so-called phase I metabolism, the CYPs and FMOs, and conjugation enzymes of phase II metabolism, the UGTs, SULTs, and GSTs. The most notable exception is that of PGS, which is found predominantly in the inner medulla. Another important feature of renal function that

correlates with metabolism is transport. Plasma membrane transporters for organic anions and cations are localized predominantly in the proximal tubules as well and serve to deliver substrates to their sites of metabolism. Significant species differences also exist in the renal expression of several classes of drug metabolism enzymes, making extrapolation from experimental animals to humans very difficult when renal metabolism is involved.

A few selected examples were cited of drugs whose renal metabolism illustrates unique aspects of renal function. For example, the cephalosporin antibiotics (as exemplified by CPH) were discussed as an example of a class of drugs whose nephrotoxicity is enhanced by accumulation in proximal tubular cells due to efficient uptake and poor efflux. Different classes of prodrugs that either possess a selenocysteine, γ-glutamyl, or GSH moiety were discussed. These prodrugs take advantage of the unique manner in which the kidneys, and in particular the proximal tubules, handle these various *S*-conjugates and GSH derivatives to effect selective delivery to the proximal tubules. The case of APAP is instructive in showing that distinct patterns of cellular accumulation and metabolism occur, depending on whether exposure is acute or chronic.

REFERENCES

1. Walker LA, Valtin H. Biological importance of nephron heterogeneity. Annu Rev Physiol 1982; 44:203 219.
2. Guder WG, Ross BD. Enzyme distribution along the nephron. Kidney Int 1984; 26:101 111.
3. Lash LH. Use of freshly isolated and primary cultures of proximal tubular and distal tubular cells from rat kidney. In: Zalups RK, Lash LH, eds. Methods in Renal Toxicology. Boca Raton, FL: CRC Press, 1996:189 215.
4. Lash LH. In vitro methods of assessing renal damage. Toxicol Pathol 1998; 26:33 42.
5. Chung SD, Alavi N, Livingston D, Hiller S, Taub M. Characterization of primary rabbit kidney cultures that express proximal tubule functions in a hormonally defined medium. J Cell Biol 1982; 95:118 126.
6. Taub ML, Yang IS, Wang Y. Primary rabbit kidney proximal tubule cell cultures maintain differentiated functions when cultured in a hormonally defined serum free medium. In Vitro Cell Dev Biol 1989; 25:770 775.
7. Aleo MD, Taub ML, Nickerson PA, Kostyniak PJ. Primary cultures of rabbit renal proximal tubule cells: I. Growth and biochemical characteristics. In Vitro Cell Dev Biol 1989; 25:776 783.
8. Nowak G, Schnellmann RG. Improved culture conditions stimulate gluconeogenesis in primary cultures of renal proximal tubule cells. Am J Physiol 1995; 268:C1053 C1061.
9. Blumenthal SS, Lewand DL, Buday MA, Mandel NS, Mandel GS, Kleinman JG. Effect of pH on growth of mouse renal cortical tubule cells in primary culture. Am J Physiol 1989; 257: C419 C426.
10. Boogaard PJ, Zoeteweij JP, van Berkel TJC, van't Noordende JM, Mulder GJ, Nagelkerke JF. Primary culture of proximal tubular cells from normal rat kidney as an in vitro model to study mechanisms of nephrotoxicity: toxicity of nephrotoxicants at low concentrations during prolonged exposure. Biochem Pharmacol 1990; 39:1335 1345.
11. Chen TC, Curthoys NP, Lagenaur CF, Puschett JB. Characterization of primary cell cultures derived from rat renal proximal tubules. In Vitro Cell Dev Biol 1989; 25:714 722.
12. Elliget KA, Trump BF. Primary cultures of normal rat kidney proximal tubule epithelial cells for studies of renal cell injury. In Vitro Cell Dev Biol 1991; 27A:739 748.
13. Hatzinger PB, Stevens JL. Rat kidney proximal tubule cells in defined medium: the roles of cholera toxin, extracellular calcium and serum in cell growth and expression of γ glutamyltransferase. In Vitro Cell Dev Biol 1989; 25:205 212.
14. Lash LH, Tokarz JJ, Pegouske DM. Susceptibility of primary cultures of proximal tubular and distal tubular cells from rat kidney to chemically induced toxicity. Toxicology 1995; 103:85 103.

15. Miller JH. Restricted growth of rat kidney proximal tubule cells cultured in serum supplemented and defined media. J Cell Physiol 1986; 129:264 272.
16. Rosenberg MR, Michalopoulos G. Kidney proximal tubular cells isolated by collagenase perfusion grow in defined media in the absence of growth factors. J Cell Physiol 1987; 131:107 113.
17. Sakhrani LM, Badie Dezfooly B, Trizna W, Mikhail N, Lowe AG, Taub M, Fine LG. Transport and metabolism of glucose by renal proximal tubular cells in primary culture. Am J Physiol 1984; 246:F757 F764.
18. Taub ML, Yang IS, Wang Y. Primary rabbit kidney proximal tubule cell cultures maintain differentiated functions when cultured in a hormonally defined serum free medium. In Vitro Cell Dev Biol 1989; 25:770 775.
19. Toutain H, Vauclin Jacques N, Fillastre J P, Morin J P. Biochemical, functional, and morphological characterization of a primary culture of rabbit proximal tubule cells. Exp Cell Res 1991; 194:9 18.
20. Pizzonia JH, Gesek FA, Kennedy SM, Coutermarsh BA, Bacskal BJ, Friedman PA. Immunomagnetic separation, primary culture, and characterization of cortical thick ascending limb plus distal convoluted tubule cells from mouse kidney. In Vitro Cell Dev Biol 1991; 27A:409 416.
21. Scott DM, Zierold K, Kinne R. Development of differentiated characteristics in cultured kidney (thick ascending loop of Henle) cells. Exp Cell Res 1986; 162:521 529.
22. Courjault Gautier F, Chevalier J, Abbou CC, Chopin DK, Toutain HJ. Consecutive use of hormonally defined serum free media to establish highly differentiated human renal proximal tubule cells in primary culture. J Am Soc Nephrol 1995; 5:1949 1963.
23. Cummings BS, Lash LH. Metabolism and toxicity of trichloroethylene and S (1,2 dichlorovinyl) L cysteine in freshly isolated human proximal tubular cells. Toxicol Sci 2000; 53:458 466.
24. Cummings BS, Lasker JM, Lash LH. Expression of glutathione dependent enzymes and cytochrome P450s in freshly isolated and primary cultures of proximal tubular cells from human kidney. J Pharmacol Exp Ther 2000; 293:677 685.
25. Detrisac CJ, Sens MA, Garvin AJ, Spicer SS, Sens DA. Tissue culture of human kidney epithelial cells of proximal tubule origin. Kidney Int 1984; 25:383 390.
26. Rodilla V, Miles AT, Jenner W, Hawksworth GM. Exposure of cultured human proximal tubular cells to cadmium, mercury, zinc and bismuth: toxicity and metallothionein induction. Chem Biol Interact 1998; 115:71 83.
27. Trifillis AL, Regec AL, Trump BF. Isolation, culture and characterization of human renal tubular cells. J Urol 1985; 133:324 329.
28. Van Der Biest I, Nouwen EJ, Van Dromme SA, De Broe ME. Characterization of pure proximal and heterogeneous distal human tubular cells in culture. Kidney Int 1994; 45:85 94.
29. Lash LH. Principles and methods for renal toxicology. In: Hayes AW, ed. Principles and Methods in Toxicology. 5th ed. Boca Raton, FL: CRC Press, 2008:1508 1540.
30. Berkhin EB, Humphreys MH. Regulation of renal tubular secretion of organic compounds. Kidney Int 2001; 59:17 30.
31. Burckhardt G, Bahn A, Wolff NA. Molecular physiology of renal *p* aminohippurate secretion. News Physiol Sci 2001; 16:114 118.
32. Hagenbuch B, Peier PJ. Organic anion transporting polypeptides of the OATP/SLC21 family: phylogenetic classification as OATP/SLCO superfamily, new nomenclature and molecular/ functional properties. Pflugers Arch 2004; 447:653 665.
33. Inui K I, Masuda S, Saito H. Cellular and molecular aspects of drug transport in the kidney. Kidney Int 2000; 58:944 958.
34. Koepsell H, Endou H. The SLC22 drug transporter family. Pflugers Arch 2004; 447:666 676.
35. Lee W, Kim RB. Transporters and renal drug elimination. Annu Rev Pharmacol Toxicol 2004; 44:137 166.
36. Robertson EE, Rankin GO. Human renal organic anion transporters: characteristics and contributions to drug and drug metabolite excretion. Pharmacol Ther 2006; 109:399 412.

37. Russel FGM, Masereeuw R, van Aubel RAMH. Molecular aspects of renal anionic drug transport. Annu Rev Physiol 2002; 64:563 594.
38. Wright SH, Dantzler WH. Molecular and cellular physiology of renal organic cation and anion transport. Physiol Rev 2004; 84:987 1049.
39. Lock EA, Reed DJ. Renal xenobiotic metabolism. In: Goldstein RS, ed. Comprehensive Series in Toxicology, Vol. 7: Kidney Toxicology. Oxford: Elsevier, 1997:77 97.
40. Lohr JW, Willsky GR, Acara A. Renal drug metabolism. Pharmacol Rev 1998; 50:107 141.
41. Jones DP, Orrenius S, Jakobson SW. Cytochrome P 450 linked monooxygenase systems in the kidney. In: Gram TE, ed. Extrahepatic Metabolism of Drugs and Other Foreign Compounds. New York: Spectrum Publications, 1980:123 158.
42. Ronis MJJ, Huang J, Longo V, Tindberg N, Ingelman Sundberg M, Badger TM. Expression and distribution of cytochrome P450 enzymes in male rat kidney: effects of ethanol, acetone and dietary conditions. Biochem Pharmacol 1998; 55:123 129.
43. Lash LH, Fisher JW, Lipscomb JC, Parker JC. Metabolism of Trichloroethylene. Environ Health Perspec 2000; 108(suppl 2):177 200.
44. National Toxicology Program (NTP). Report on Carcinogens, 11th ed., Research Triangle Park, NC: U.S. Department of Heath and Human Services, Public Health Service, National Toxicology Program, 2005.
45. Lash LH, Parker JC, Scott CS. Modes of action of trichloroethylene for kidney tumorigenesis. Environ Health Perspec 2000; 108(suppl 2):225 240.
46. Cummings BS, Parker JC, Lash LH. Cytochrome P450 dependent metabolism of trichloro ethylene in rat kidney. Toxicol Sci 2001; 60:11 19.
47. Lash LH, Putt DA, Cai H. Drug metabolism enzyme expression and activity in primary cultures of human proximal tubular cells. Toxicology 2008; 244:56 65.
48. Lash LH, Putt DA, Huang P, Hueni SE, Parker JC. Modulation of hepatic and renal metabolism and toxicity of trichloroethylene and perchloroethylene by alterations in status of cytochrome P450 and glutathione. Toxicology 2007; 235:11 26.
49. Cummings BS, Zangar RC, Novak RF, Lash LH. Cellular distribution of cytochromes P 450 in the rat kidney. Drug Metab Dispos 1999; 27:542 548.
50. Amet Y, Berthou F, Fournier G, Dréano Y, Bardou L, Cledes J, Ménez J F. Cytochrome P450 4A and 2E1 expression in human kidney microsomes. Biochem Pharmacol 1997; 53: 765 771.
51. Hu JJ, Rhoten WB, Yang CS. Mouse renal cytochrome P450IIE1: immunocytochemical localization, sex related differences and regulation by testosterone. Biochem Pharmacol 1990; 40:2597 2602.
52. Bebri K, Boobis AR, Davies DS, Edward RJ. Distribution and induction of CYP3A1 and CYP3A2 in rat liver and extrahepatic tissue. Biochem Pharmacol 1995; 50:2047 2056.
53. Schuetz EG, Schuetz JD, Grogan WM, Naray Fejes Toth A, Fejes Toth G, Raucy J, Guzelian P, Gionela K, Watlington CO. Expression of cytochrome P450 3A in amphibian, rat, and human kidney. Arch Biochem Biophys 1992; 294:206 217.
54. Guengerich FP. Polymorphism of cytochrome P 450 in humans. Trends Pharmacol Sci 1989; 10:107 109.
55. Haener BD, Gorski JC, Vandenbranden M, Wrighton SA, Janardan SK, Watkins PB, Hall SD. Bimodal distribution of renal cytochrome P450 3A activity in humans. Mol Pharmacol 1996; 50:52 59.
56. Ito O, Alonso Galicia M, Hopp KA, Roman RJ. Localization of cytochrome P 450 4A isoforms along the rat nephron. Am J Physiol 1998; 274:F395 F404.
57. Okita JR, Johnson SB, Castle PJ, Dezellem SC, Okita RT. Improved separation and immunodetection of rat cytochrome P450 4A forms in liver and kidney. Drug Metab Dispos 1997; 25:1008 1012.
58. Stec DE, Flasch A, Roman RJ, White JA. Distribution of cytochrome P 450 4A and 4F isoforms along the nephron in mice. Am J Physiol 2003; 284:F95 F102.
59. Cashman JR, Zhang J. Human flavin containing monooxygenases. Annu Rev Pharmacol Toxicol 2006; 46:65 100.

60. Ziegler DM. Recent studies on the structure and function of multisubstrate flavin containing monooxygenases. Annu Rev Pharmacol Toxicol 1993; 33:179 199.
61. Dolphin CT, Beckett DT, Janmohamed A, Cullingford TE, Smith RL, Shephard EA, Phillips IR. The flavin containing monooxygenase 2 gene (FMO2) of humans, but not of other primates, encodes a truncated, nonfunctional protein. J Biol Chem 1998; 273:30599 30607.
62. Hines RN, Cashman JR, Philpot RM, Williams DE, Ziegler DM. The mammalian flavin containing monooxygenases: molecular characterization and regulation of expression. Toxicol Appl Pharmacol 1994; 125:1 6.
63. Koukouritaki SB, Simpson P, Yeung CK, Rettie AE, Hines RN. Human hepatic flavin containing monooxygenase 1 (FMO1) and 3 (FMO3) developmental expression. Pediatr Res 2002; 51:236 243.
64. Ripp SL, Itagak IK, Philpot, RM, Elfarra AA. Species and sex differences in expression of flavin containing monooxygenase form 3 in liver and kidney microsomes. Drug Metab Dispos 1999; 27:46 52.
65. Krause RJ, Lash LH, Elfarra AA. Human kidney flavin containing monooxygenases and their potential roles in cysteine S conjugate metabolism and nephrotoxicity. J Pharmacol Exp Ther 2003; 304:185 191.
66. Nishimura M, Naito S. Tissue specific mRNA expression profiles of human phase I metabolizing enzymes except cytochrome P450 and phase II metabolizing enzymes. Drug Metab Pharmacokinet 2006; 21:357 374.
67. Sausen PJ, Elfarra AA. Cysteine conjugate S oxidase: characterization of a novel enzymatic activity in rat hepatic and renal microsomes. J Biol Chem 1990; 265:6139 6145.
68. Sausen PJ, Elfarra AA. Reactivity of cysteine S conjugates sulfoxides: formation of S [1 chloro 2 (S glutathionyl)vinyl] L cysteine sulfoxide by the reaction of S (1,2 dichlorovinyl) L cysteine sulfoxide with glutathione. Chem Res Toxicol 1991; 4:655 660.
69. Sausen PJ, Duescher RJ, Elfarra AA. Further characterization and purification of the flavin dependent S benzyl L cysteine S oxidase activities of rat liver and kidney microsomes. Mol Pharmacol 1993; 43:388 396.
70. Elfarra AA, Krause RJ. *S* (1,2,2 Trichlorovinyl) L cysteine sulfoxide, a reactive metabolite of *S* (1,2,2 trichlorovinyl) L cysteine formed in rat liver and kidney microsomes, is a potent nephrotoxicant. J Pharmacol Exp Ther 2007; 321:1095 1101.
71. Lash LH, Sausen PJ, Duescher RJ, Cooley AJ, Elfarra AA. Roles of cysteine conjugate β lyase and *S* oxidase in nephrotoxicity: studies with *S* (1,2 dichlorovinyl) L cysteine and *S* (1,2 dichlorovinyl) L cysteine sulfoxide. J Pharmacol Exp Ther 1994; 269:374 383.
72. Lash LH, Putt DA, Hueni SE, Krause RJ, Elfarra AA. Roles of necrosis, apoptosis, and mitochondrial dysfunction in *S* (1,2 dichlorovinyl) L cysteine sulfoxide induced cytotoxicity in primary cultures of human renal proximal tubular cells. J Pharmacol Exp Ther 2003; 305:1163 1172.
73. Hao C M, Breyer MD. Physiologic and pathophysiologic roles of lipid mediators in the kidney. Kidney Int 2007; 71:1105 1115.
74. Nasrallah R, Clark J, Hébert RL. Prostaglandins in the kidney: developments since Y2K. Clin Sci 2007; 113:297 311.
75. Schlondorff D, Zanger R, Satriano JA, Folkert, VW, Eveloff J. Prostaglandin synthesis by isolated cells from the outer medulla and from the thick ascending loop of Henle of rabbit kidney. J Pharmacol Exp Ther 1982; 223:120 124.
76. Bonventre JV, Nemenoff R. Renal tubular arachidonic acid metabolism. Kidney Int 1991; 39:438 449.
77. Zenser TV, Davis BB. Enzyme systems involved in the formation of reactive metabolites in the renal medulla: cooxidation via prostaglandin H synthase. Fundam Appl Toxicol 1984; 4:922 929.
78. Zenser TV, Cohen SM, Mattammal MB, Wise RW, Rapp NS, Davis BB. Prostaglandin hydroperoxidase catalyzed activation of certain N substituted aryl renal and bladder carcinogens. Environ Health Perspec 1983; 49:33 41.

79. Wise RW, Zenser TV, Rice JR, Davis BB. Peroxidatic metabolism of benzidine by intact tissue: a prostaglandin H synthase mediated process. Carcinogenesis 1986; 7:111 115.
80. Zenser TV, Mattammal MB, Davis BB. Cooxidation of benzidine by renal medullary prostaglandin cyclooxygenase. J Pharmacol Exp Ther 1979; 211:460 464.
81. Zenser TV, Mattammal MB, Wise RW, Rice JR, Davis BB. Prostaglandin H synthase catalyzed activation of benzidine: a model to assess pharmacologic intervention of the initiation of chemical carcinogenesis. J Pharmacol Exp Ther 1983; 227:545 550.
82. Mackenzie PI, Bock KW, Burchell B, Guillemette C, Ikushiro S, Iyanagi T, Miners JO, Owens IS, Nebert DW. Nomenclature update for the mammalian UDP glycosyltransferase (UGT) gene superfamily. Pharmacogenet Genomics 2005; 15:677 685.
83. Shelby MK, Cherrington NJ, Vansell NR, Klaassen CD. Tissue mRNA expression of the rat UDP glucuronosyltransferase gene family. Drug Metab Dispos 2003; 31:326 333.
84. Wells PG, Mackenzie PI, Chowshury JR, Guillemette C, Gregory PA, Ishii Y, Hansen AJ, Kessler FK, Kim PM, Chowdhury NR, Ritter JK. Glucuronidation and the UDP glucuronosyltransferases in health and disease. Drug Metab Dispos 2004; 32:281 290.
85. Gamage N, Barnett A, Hempel N, Duggleby RG, Windmill KF, Martin JL, McManus ME. Human sulfotransferases and their role in chemical metabolism. Toxicol Sci 2006; 90:5 22.
86. Lindsay J, Wang LL, Li Y, Zhou SF. Structure, function and polymorphism of human cytosolic sulfotransferases. Curr Drug Metab 2008; 9:99 105.
87. Nowel S, Falany CN. Pharmacogenetics of human cytosolic sulfotransferases. Oncogene 2006; 25:1673 1678.
88. Rozzel B, Hansson H A, Guthenberg C, Tahir MK, Mannervik B. Glutathione transferases of classes α, μ and π show selective expression in different regions of rat kidney. Xenobiotica 1993; 23:835 849.
89. Cummings BS, Parker JC, Lash LH. Role of cytochrome P450 and glutathione *S* transferase α in metabolism and cytotoxicity of trichloroethylene in rat kidney. Biochem Pharmacol 2000; 59:531 543.
90. Board PG, Anders MW. Human glutathione transferase Zeta. Methods Enzymol 2005; 401:61 77.
91. Board PG, Baker RT, Chelvanayagam G, Jermiin LS. Zeta, a novel class of glutathione transferases in a range of species from plants to humans. Biochem J 1997; 328:929 935.
92. Board PG, Chelvanayagam G, Jermiin LS, Tetlow N, Tzeng HF, Anders MW, Blackburn AC. Identification of novel glutathione transferases and polymorphic variants by expressed sequence tag database analysis. Drug Metab Dispos 2001; 29:544 547.
93. Jakobsson P J, Morgenstern R, Mancini J, Ford Hutchinson A, Persson B. Common structural features of MAPEG a widespread superfamily of membrane associated proteins with highly divergent functions in eicosanoid and glutathione metabolism. Protein Sci 1999; 8: 689 692.
94. Otieno MA, Baggs RB, Hayes JD, Anders MW. Immunolocalization of microsomal glutathione *S* transferases in rat tissues. Drug Metab Dispos 1997; 25:12 20.
95. Lash LH, Lipscomb JC, Putt DA, Parker JC. Glutathione conjugation of trichloroethylene in human liver and kidney: kinetics and individual variation. Drug Metab Dispos 1999; 27:351 359.
96. Lash LH, Qian W, Putt DA, Jacobs K, Elfarra AA, Krause RJ, Parker JC. Glutathione conjugation of trichloroethylene in rats and mice: sex , species , and tissue dependent differences. Drug Metab Dispos 1998; 26:12 19.
97. Lash LH, Xu Y, Elfarra AA, Duescher RJ, Parker JC. Glutathione dependent metabolism of trichloroethylene in isolated liver and kidney cells of rats and its role in mitochondrial and cellular toxicity. Drug Metab Dispos 1995; 23:846 853.
98. Hinchman CA, Ballatori N. Glutathione degrading capacities of liver and kidney in different species. Biochem Pharmacol 1990; 40:1131 1135.
99. Griffith OW, Meister A. Translocation of intracellular glutathione to membrane bound γ glutamyl transpeptidase as a discrete step in the γ glutamyl cycle: glutathionuria after inhibition of transpeptidase. Proc Natl Acad Sci U S A 1979; 76:268 272.

100. Birner G, Werner M, Rosner E, Mehler C, Dekant W. Biotransformation, excretion, and nephrotoxicity of the hexachlorobutadiene metabolite (E) N acetyl S (1,2,3,4,4 pentachlor obutadienyl) L cysteine sulfoxide. Chem Res Toxicol 1998; 11:750 757.
101. Wolfgang GHI, Gandolfi AJ, Stevens JL, Brendel K. N Acetyl S (1,2 dichlorovinyl) L cysteine produces a similar toxicity to S (1,2 dichlorovinyl) L cysteine in rabbit renal slices: differential transport and metabolism. Toxicol Appl Pharmacol 1989; 101:205 219.
102. Zhang G, Stevens JL. Transport and activation of S (1,2 dichlorovinyl) L cysteine and N acetyl S (1,2 dichlorovinyl) L cysteine in rat kidney proximal tubules. Toxicol Appl Pharmacol 1989; 100:51 61.
103. Lash LH, Parker JC. Hepatic and renal toxicities associated with perchloroethylene. Pharmacol Rev 2001; 53:177 208.
104. Yin H, Jones JP, Anders MW. Metabolism of 1 fluoro 1,1,2 trichloroethane, 1,2 dichloro 1, 1 difluoroethane, and 1,1,1 trifluoro 2 chloroethane. Chem Res Toxicol 1995; 8:262 268.
105. Cooper AJL, Pinto JT. Cysteine S conjugate β lyases. Amino Acids 2006; 30:1 15.
106. Abraham DG, Patel PP, Cooper AJL. Isolation from rat kidney of a cytosolic high molecular weight cysteine S conjugate β lyase with activity toward leukotriene E_4. J Biol Chem 1995; 270:180 188.
107. Abraham DG, Thomas RJ, Cooper AJL. Glutamine transaminase K is not a major cysteine S conjugate β lyase of rat kidney mitochondria: evidence that a high molecular weight enzyme fulfills this role. Mol Pharmacol 1995; 48:855 860.
108. Elfarra AA, Lash LH, Anders MW. Alpha keto acids stimulate rat renal cysteine conjugate β lyase activity and potentiate the cytotoxicity of S (1,2 dichlorovinyl) L cysteine. Mol Pharmacol 1987; 31:208 212.
109. Stevens JL, Robbins JD, Byrd RA. A purified cysteine conjugate β lyase from rat kidney cytosol: requirement for an α keto acid or an amino acid oxidase for activity and identity with soluble glutamine transaminase K. J Biol Chem 1986; 261:15529 15537.
110. Andreadou I, Menge WMPB, Commandeur JNM, Worthington EA, Vermeulen NPE. Synthesis of novel se substituted selenocysteine derivatives as potential kidney selective prodrugs of biologically active selenol compounds: evaluation of kinetics of β elimination reactions in rat renal cytosol. J Med Chem 1996; 39:2040 2046.
111. Drieman JC, Thijssen HHW, Struyker Boudier HAJ. Renal selective N acetyl γ glutamyl prodrugs. II. Carrier mediated transport and intracellular conversion as determinants in the renal selectivity of N acetyl γ glutamyl sulfamethoxazole. J Pharmacol Exp Ther 1990; 252:1255 1260.
112. Drieman JC, Thijssen HHW, Struyker Boudier HAJ. Renal selective N acetyl L γ glutamyl prodrugs: studies on the selectivity of some model prodrugs. Br J Pharmacol 1993; 108: 204 208.
113. Elfarra AA, Hwang IY. Targeting of 6 mercaptopurine to the kidneys: metabolism and kidney selectivity of S (6 purinyl) L cysteine analogs in rats. Drug Metab Dispos 1993; 21:841 845.
114. Elfarra AA, Duescher RJ, Hwang IY, Sicuri AR, Nelson JA. Targeting 6 thioguanine to the kidney with S (guanin 6 yl) L cysteine. J Pharmacol Exp Ther 1995; 274:1298 1304.
115. Hwang Y, Elfarra AA. Cysteine S conjugates may act as kidney selective prodrugs: formation of 6 mercaptopurine by the renal metabolism of S (6 purinyl) L cysteine. J Pharmacol Exp Ther 1989; 251:448 454.
116. Hwang IY, Elfarra AA. Kidney selective prodrugs of 6 mercaptopurine: biochemical basis of kidney selectivity of S (6 purinyl) L cysteine and metabolism of new analogs in rats. J Pharmacol Exp Ther 1991; 258:171 177.
117. Hwang IY, Elfarra AA. Detection and mechanisms of formation of S (6 purinyl)glutathione and 6 mercaptopurine in rats given 6 chloropurine. J Pharmacol Exp Ther 1993; 264:41 46.
118. Lash LH, Shivnani A, Mai J, Chinnaiyan P, Krause RJ, Elfarra AA. Renal cellular transport, metabolism and cytotoxicity of S (6 purinyl)glutathione, a prodrug of 6 mercaptopurine, and analogues. Biochem Pharmacol 1997; 54:1341 1349.
119. Lash LH. Role of glutathione transport processes in kidney function. Toxicol Appl Pharmacol 2005; 204:329 342.

120. Newton JF, Braselton WE, Kuo C H, Kluwe WM, Gemborys MW, Mudge GH, Hook JB. Metabolism of acetaminophen by the isolated perfused kidney. J Pharmacol Exp Ther 1982; 221:76 79.
121. Duggin GG. Mechanisms in the development of analgesic nephropathy. Kidney Int 1980; 18: 553 561.
122. Klos C, Koob M, Kramer C, Dekant W. *p* Aminophenol nephrotoxicity: biosynthesis of toxic glutathione conjugates. Toxicol Appl Pharmacol 1992; 115:98 106.
123. West PR, Harman LS, Josephy PD, Mason RP. Acetaminophen: enzymatic formation of a transient phenoxyl free radical. Biochem Pharmacol 1984; 33:2933 2936.
124. Tune BM. The nephrotoxicity of cephalosporin antibiotics Structure activity relationships. Comments Toxicol 1986; 1:145 170.
125. Tune BM, Hsu C Y. The renal mitochondrial toxicity of cephalosporins: specificity of the effect on anionic substrate uptake. J Pharmacol Exp Ther 1990; 252:65 69.
126. Tune BM, Hsu C Y. Effects of nephrotoxic β lactam antibiotics on the mitochondrial metabolism of monocarboxylic substrates. J Pharmacol Exp Ther 1995; 274:194 199.
127. Tune BM, Hsu C Y. Toxicity of cephalosporins to fatty acid metabolism in rabbit renal cortical mitochondria. Biochem Pharmacol 1995; 49:727 734.
128. Tune BM, Sibley RK, Hsu C Y. The mitochondrial respiratory toxicity of cephalosporin antibiotics. An inhibitory effect on substrate uptake. J Pharmacol Exp Ther 1988; 245: 1054 1059.
129. Tune BM, Fravert D, Hsu C Y. Oxidative and mitochondrial toxic effects of cephalosporin antibiotics in the kidney: a comparative study of cephaloridine and cephaloglycin. Biochem Pharmacol 1989; 38:795 802.
130. Lash LH, Tokarz JJ, Woods EB. Renal cell type specificity of cephalosporin induced cytotoxicity in suspensions of isolated proximal tubular and distal tubular cells. Toxicology 1994; 94:97 118.
131. Lash LH, Tokarz JJ. Oxidative stress and cytotoxicity of 4 (2 thienyl)butyric acid in isolated rat renal proximal tubular and distal tubular cells. Toxicology 1995; 103:167 175.

13

Sites of Extra Hepatic Metabolism, Part IV: Brain

Ying Wang, Jordan C. Bell, and Henry W. Strobel
Department of Biochemistry and Molecular Biology, The University of Texas Medical School at Houston, Houston, Texas, U.S.A.

INTRODUCTION

Drug metabolism in brain tissue has been the subject of several reviews over the recent past emphasizing differing aspects of the topic including Phase I and Phase II metabolism, transporters, regional and cellular enzyme distribution, regulation of metabolic activities, and range of substrates metabolized by brain (1–7). The earlier reviews (1–4) focused on summarizing the evidence that the cytochromes P450 (CYPs) were actually expressed in brain and were catalytically competent in brain tissue, a view held then to be controversial possibly because the question was addressed primarily from a drug clearance point of view. Indeed the levels of CYPs reported (1–5) were low compared with the liver and intestine. Subsequent reviews focused the question of CYP function more squarely on activation/metabolism of drugs whose target functions were in brain.

Brain is a unique organ in that it is remarkably isolated from many compounds present in the general circulation. While this makes the brain a privileged organ, it poses difficulties for the design and development of drugs targeted for treatment of diseases or malfunctions of brain. This is mainly due to the blood-brain barrier (BBB). In contrast to other tissues, brain endothelial cells have continuous tight junctions, few fenestrations, and exhibit very low pinocytotic activity (8). Brain endothelial cells are also surrounded by a basal membrane and extracellular matrix, as well as pericytes and astrocyte foot processes, which further contribute to the BBB and mediate its permeability. Astrocyte end feet cover over 90% of the endothelial cell surface, and the permeability of the BBB is partially under control of these associated brain cells (9). Astroglia can also release chemical factors and signals that modulate the permeability of the main endothelium (10). It is also important to understand that the endothelium of the brain and spinal cord lack the pores found in the periphery because the endothelial cells of brain capillaries are sealed together by continuous tight junctions produced by the interaction of several

transmembrane proteins that project into and seal the paracellular pathway (11,12). These junctional proteins block the free diffusion of polar solutes from blood along these potential paracellular pathways so that there is no access to the brain interstitial fluid (4). This leaves access to the brain very exclusive, mainly to molecules that are small and lipophilic or those that enter the brain through an active transport mechanism for essential nutrients, precursors, and cofactors (4).

Given the complexity and efficacy of the BBB, it is striking how many drugs actually penetrate the barrier and exert important effects on brain functions. Such drugs account for a significant revenue source for companies expending the effort and resources to develop brain-active drugs. The top five brain-active drugs and their revenues as reported in 2001 were olanzapine, a CYP2D6-metabolized serotonin receptor target drug, $3.1 billion; paroxetine, a CYP2D6-metabolized serotonin reuptake inhibitor antidepressant, $2.7 billion; sertraline, a serotonin reuptake inhibitor metabolized by CYPs 2D6, 2C9, 2B6, and 3A4, $2.4 billion; and risperadone, an antischizophrenic medication metabolized by CYP2D6, 1.8 billion (13).

Alavijeh et al. (4) reviewed the role of the BBB with emphasis on the role of transporters, which can and do transport drugs, which enter by passive diffusion or leave by specific efflux processes out of brain cells and back into the circulation. Haining and Nichols-Haining (5) extend this theme focusing on the inhibition of brain P450 catalyzed processes by other CYP products. Upton (6) has cast light on the uptake of drugs in brain, making an effort to link uptake in brain with clinical efficacy. In a very comprehensive review, Deeken and Löscher (7) have emphasized an integrated approach of pharmacokinetics, metabolism, and transport-facilitated efflux of products in the blood and/or cerebrospinal fluid in the evaluation of drugs and drug candidates for brain cancer. This review summarizing the background of efforts to date also articulates nicely the problems facing drug discovery and development of therapeutic agents for brain diseases in general by centering their argument around treatment of brain cancers.

CYTOCHROMES P450

In this review, we focus on the major drug-metabolizing CYP families, namely 1, 2, 3, and 4. We will emphasize distribution and function of the human isoforms with wide reference to forms present in animal models. While in the liver, most CYPs are located primarily in the endoplasmic reticulum or microsomal cell fraction, in the brain, it has been observed that some of the CYP activity is found in the mitochondrial subcellular fraction (7). A number of studies have shown the presence, inducibility, and activity of several forms of drug-metabolizing CYPs in the brain mitochondrial membrane fractions. Two mitochrondrial-specific functional forms of CYP1A1 have been identified in the liver (14) and brain (15). The protein structure of these P450MT2 forms are altered, allowing for specific targeting of the CYP forms to the mitochondrial membrane. It was also shown that expression of CYP enzyme in neuronal processes devoid of endoplasmic reticular membranes, particularly in the dendritic trees of Purkinje cells in the cerebellum (16), is localized in mitochondria. On the other hand, many of the characteristics of brain CYP isoforms are the same as liver forms. For instance, many brain CYPs can be induced by the same compounds that induce the corresponding hepatic CYPs (17,18).

CYP1 Family

The CYP1 family consists of three known isoforms that have been shown to be expressed in the human brain. These isoforms include 1A1, 1A2, and 1B1. CYP1A1 is a major extrahepatic enzyme that is expressed in many different regions of the brain including

cortex, cerebellum, basal ganglia, hippocampus, substantia nigra, pons, and other areas. This protein was shown to localize predominantly in neurons of cerebral cortex, Purkinje cells, and granule cells in dentate gyrus and pyramidal neurons of the CA1, CA2, and CA3 subfields of the hippocampus and reticular neurons in midbrain. CYP1A1 is known for its contributions to the toxicity of many carcinogens, mainly polycyclic aromatic hydrocarbons because of its role as the primary enzyme that bioactivates hydrocarbons into DNA-binding reactive metabolites (7). CYP1A1's expression in brain could play a role in initiating carcinogenesis because of the ability of lipophilic polycyclic aromatic hydrocarbons to cross the BBB (19). It was shown in several epidemiological studies carried out on workers in the petroleum industry and on smokers, both of which are exposed to polycyclic aromatic hydrocarbons, that there was a high association of exposure with brain tumor incidence (7). The Ravindranath laboratory has shown that in some humans, there is a splice variant of the CYP1A1 enzyme that excludes exon 6, is brain specific, and has markedly reduced abilities to form DNA-binding hydroxylated polyaromatic hydrocarbons (19).

CYP1A2 has been shown to metabolize endogenous and exogenous compounds such as linoleic acid, tryptophan, melatonin, caffeine, polycyclic and polyaromatic hydrocarbons, heterocyclic amines, nitrosamines, and arylamines. It is the most active metabolizer of xenobiotics in the CYP1 family. Shimada et al. reported that this enzyme accounts for approximately 13% of the total P450 in the human liver (20). Reverse transcriptase- polymerase chain reaction (RT-PCR) and immunoblotting have identified this enzyme in many different regions of the brain including all the regions in which CYP1A1 was found. One of the most commonly encountered compounds metabolized by CYP1A2 is caffeine. 90% of caffeine is metabolized by CYP1A2, while the remaining 10% is metabolized by CYP2E1 and CYP3A4/5 (21). Caffeine like alcohol, nicotine, and antidepressants can easily cross the blood-brain barrier. In the brain, caffeine acts as an antagonist of adenosine receptors, leading to increased activity of dopamine (22). Also, CYP1A2 is important for the metabolism of a tacrine, which is a drug used to treat Alzheimer's disease (23).

CYP1B1 is involved in xenobiotic detoxification, in activation of procarcinogens and promutagens, and in metabolism of sterol substrates (24,25). RT-PCR data have shown that CYP1B1 expression is localized in many different regions of the brain including cortex, cerebellum, basal ganglia, hippocampus, substantia nigra, and medulla oblongata (24). Muskhelishvili et al. showed that CYP1B1 protein is strongly expressed in the nuclei of a majority of astrocytes and neurons in the brain cortex. Rieder et al. reported that in the temporal lobe, the 1B1 protein lines the blood-brain barrier and thus may play an important role in brain xenobiotic metabolism (25). They suggest that by localizing at the interface between blood and brain, CYP1B1 may act as an enzymatic barrier preventing the entry of chemicals into adjacent brain parenchyma (25). Of note is the higher activity of CYP1B1 for activation of various promutagens over CYP1A1 and CYP1A2 (26). 1B1 is also known to have endogenous substrates along with its ability to catalyze xenobiotic metabolism. Studies with human CYP1B1 expressed in *Saccharomyces cerevisiae* (27) or *Escherichia coli* (28) have confirmed that CYP1B1 is highly selective toward estradiol 4-hydroxylase and that it is inefficient in catalyzing the 2-hydroxylation of estradiol (26).

CYP2 Family

In the human, the CYP2A family includes CYP2A6, CYP2A7, and CYP2A13 (29,30). The CYP2A7 protein is nonfunctional because of its inability to incorporate heme (31).

CYP2A6 was first purified as a coumarin (the precursor of several anticoagulants) 7-hydroxylase (32). While CYP2A6 is predominantly expressed in human liver, its expression and activity have also been detected in the brain (33). CYP2A6 has gained growing interest as a major enzyme responsible for the metabolism of nicotine, a major constituent of tobacco, to cotinine by C-oxidation (34), and further to *trans*-3′-hydroxycotinine by 3′-hydroxylation (35). Other studies also reported that CYP2A6, together with CYP2B6, is involved in nornicotine formation from nicotine via N-demethylation, a relatively minor pathway of total nicotine metabolism (33,36). Although only 1.6% of nornicotine was detected in 24-hr urine in human, experimental animal studies revealed that nornicotine is present in brain at significant levels (approximately 20% of the total amount of nicotine and its metabolites) (37 39), indicating that nornicotine is a major metabolite of nicotine in rat and monkey brain. CYP2A6 mRNA expression has been detected in various regions of human brain (40) and its nicotine *N*-demethylase activity has been confirmed in human brain striatum (33). Therefore, CYP2A6 expressed in human brain contributes to the local metabolism of nicotine (33,40). Furthermore, CYP2A6 can metabolically activate aflatoxin B_1 and tobacco-specific nitrosamines such as 4-(methylnitrosoamino)-1-(3-pyridyl)-1-butanone (NNK) and *N*-nitrosodiethylamine (41). A recent study demonstrated that recombinant CYP2A6 protein activity can be inhibited by several neurotransmitters and steroids including tryptamine, serotonin, dopamine, histamine, noradrenaline, adrenaline, estrogen, androgen, and corticosterone (42). This study indicates a potential role for various neurotransmitters in the regulation of drug metabolism in the brain.

CYP2A13 mRNA expression has been detected in human brain (43). Activity studies indicated that CYP2A13 is a more efficient enzyme than CYP2A6 toward the N-demethylation of nicotine (33,36). Heterologously expressed CYP2A13 can also catalyze the C-oxidation of nicotine and the 3′-hydroxylation of cotinine (44). Furthermore, CYP2A13 shows high activity in the metabolism of NNK, a nicotine-derived carcinogen. Although CYP2A13 shows high potential in drug metabolism in brain, detectable levels of human brain CYP2A13 protein have not yet been reported. Therefore, the in vivo function of CYP2A13 in human brain remains to be determined.

The CYP2B subfamily is comprised of 17 different members in several different species (45). CYP2B1 and CYP2B2 are the primary isoforms expressed in rats. RT-PCR and in situ hybridization experiments provided evidence for the presence of rat CYP2B1 and CYP2B2 mRNA in rat brain and demonstrated the predominant expression of these two isoforms in neurons (46). The same study also detected to some extent the mRNA expression of CYP2B1 and CYP2B2 in astrocytes of corpus callosum and olfactory bulb (46). CYP2B6 is the major human CYP2B isoform. Its protein expression has been identified in human brain (16,47). Similar to the rat CYP2B isoforms, CYP2B6 expression also varies among brain regions, and has been found primarily in neurons but also in astrocytes in specific brain regions (16).

CYP2B6 metabolizes multiple drugs including nicotine, bupropion, l-deprenyl, and many toxins and carcinogens (48,49). Nicotine N-demethylation produces nornicotine, which is the major nicotine metabolite in the brain. CYP2B6 exhibited the highest nicotine *N*-demethylase activity, followed by CYP2A6. A further study in human liver microsomes indicated that the contributions of CYP2A6 and CYP2B6 to the nicotine N-demethylation would be significant at low and high substrate concentrations, respectively (33). In addition, CYP2B6 can also inactivate nicotine to its non-psychoactive metabolite cotinine via C-oxidation (50). Experimental animal studies revealed that nicotine induces CYP2B expression in rat brain (51). An analogous study also demonstrated that CYP2B6 protein expression in human brain is clearly higher in

smokers and alcoholics (16,52). Since CYP2B6 also metabolizes many other drugs of abuse, such as cocaine, phencyclidine, and amphetamines to neurotoxic metabolites (53 55), it is highly possible that smoking and alcoholism may increase the risk of neurotoxic effects of those xenobiotics and alter sensitivity to some centrally acting drugs such as bupropion. Moreover, drug-drug interaction also influences brain CYP2B6 levels. Chronic phenobarbital treatment in monkeys resulted in increased in vivo nicotine disposition and induced brain CYP2B6 protein level (56). On the other hand, drugs like phencyclidine, xanthates, and 2-phenyl-2-(1-piperidinyl) propane can inhibit CYP2B activity (53,57 59), which may consequently reduce nicotine metabolism in brain. A recent study suggests the induction of in vivo nicotine deposition and CYP2B6 protein expression in brain by chronic phenobarbital treatment in monkeys (56). In addition, genetic polymorphisms also alter CYP2B6 level in brain, which in turn affects smoking cessation rates in humans (16,60).

Bupropion is an antidepressive agent, which blocks dopamine uptake. It has been used in smoking cessation treatment. According to the study of Hesse et al. on human liver microsomes, CYP2B6 is reported to be responsible for 95% of bupropion hydroxylation, producing hydroxybupropion, which is a pharmacologically active metabolite (61). The same group indicated that bupropion hydroxylation was inhibited by a number of antidepressants such as venlafaxine, *O*-desmethylvenlafaxine, citalopram, and desmethyl-citalopram (61). Since bupropion is often coadministrated with other antidepressants, the in vitro inhibition of bupropion hydroxylation by antidepressants suggests the potential for clinical drug-drug interactions. L-deprenyl, a drug against Parkinson's disease, can also be metabolized by recombinant CYP2B6 via N-demethylation (49).

CYP2B6 also mediates the stereoselective metabolism of methadone by N-demethylation (62,63). Methadone is a synthetic opioid currently used against opiate addiction and acute and chronic pain. Another opioid analgesic meperidine is also a substrate for CYP2B6. In vitro experiments using human liver microsome have indicated that CYP2B6, together with CYP3A4 and CYP2C19, catalyzes the N-demethylation of meperidine to normeperidine (64). Although at present, few studies have reported that brain methadone or meperidine metabolism is mediated by CYP2B6, it is not unreasonable to speculate the potential role of CYP2B6 in the regulation of brain methadone levels and the potential interaction between methadone and other CYP2B6 substrates in the brain.

The CYP2C subfamily consists of four members in humans (CYP2C8, CYP2C9, CYP2C18, and CYP2C19). CYP2C8 and CYP2C18 mRNA expression has been detected in human brain by RT-PCR, whereas CYP2C9 and CYP2C19 expression was barely detectable in the same samples (65).

CYP2C8 has multiple substrates. The primary endogenous substrate of CYP2C8 is arachidonic acid (AA) (66), an unsaturated essential fatty acid found in many organs including the brain. AA is known to be the precursor of many eicosanoids (such as prostaglandins, leukotrienes, and thromboxanes) concerned with aspects of the inflammation process. In addition, AA seems related to depression. Studies on depressed patients reveal that the AA-eicosapentaenoic acid ratio in blood correlates positively with clinical symptoms of depression (67). Experimental animal work also revealed that rats exhibiting the signs of depression had increased brain levels of AA (68). CYP2C8 is able to catalyze the olefin epoxidation of AA and formation of 11(R)-, 12(S)- and 14(R)-, 15(S)-epoxyeicosatrienoic acids (69). Therefore, brain CYP2C8 may have a role in pathophysiological processes such as brain inflammation and depression.

Diazepam, an antianxiety drug that binds to a specific subunit on the γ-aminobutytic acid (GABA) type A receptor, is a substrate for CYP2C18 in brain (70). Diazepam is also

a substrate of CYP2C19 (71). Diazepam may influence neurosteroid metabolism, which in turn affects the functions of the brain. Recombinant CYP2C18 catalyzes the N-demethylation of diazepam. However, diazepam N-demethylation catalyzed by CYP2C18 is negligible compared with CYP2C19 and CYP3A4 in human liver microsomes (71). CYP2C18 and CYP2C19 can also catalyze 4′-hydroxylation of mephenytoin, an anticonvulsant, but here again, the activity of CYP2C18 is not as high as that of CYP2C19 (72). CYP2C18 activity in the brain is an area of continuing study.

Although CYP2C9 and CYP2C19 isozymes have not yet been identified in brain, these isoforms are involved in the metabolism of some fatty acids, psychoactive drugs, and neurotransmitters. For example, recombinant CYP2C9 and CYP2C19 metabolize AA (73), 5-hydroxytryptamine (74), and progesterone, a neuroprotective steroid with potential function for memory and cognitive ability (75). CYP2C9 is involved in the metabolism of several important psychoactive drugs such as tetrahydrocannabinol, fluoxetine, amitriptyline, and phenytoin (76,77). CYP2C19 metabolizes amitriptyline (78,79), clomipramine (80), diazepam (81), imipramine (82), phenytoin (83), citalopram (84), mephobarbital (85), and hexobarbital (86). Endogenous compounds such as neurotransmitters and hormones (5-hydroxytryptamine, adrenaline, and melatonin) can modulate CYP2C9 activity (87,88), raising the possibility that a hypothetical local activity of brain CYP2C9 would be susceptible to regulatory mechanisms. Studies in Japan demonstrate that CYP2C19 polymorphism affects personality traits, possibly influenced by neurotransmitters (89). This may indicate that CYP2C19 also metabolizes endogenous substrates important for central nervous system (CNS) function, and that potential activities and functions of CYP2C19 in human brain need to be explored in the future for drug development possibilities.

As for CYP2D family, six isoforms (CYP2D1, CYP2D2, CYP2D3, CYP2D4, CYP2D5, and CYP2D18) have been reported in rat. Rat CYP2D2 is weakly expressed within neurons of the subthalamic nucleus, substantia nigra, and interpeduncular nucleus as well as in the hippocampus, dentate gyrus, red nucleus, and pontine nucleus (90). CYP2D2 is able to catalyze O-demethylation of dextromethorphan, an *N*-methyl-D-aspartate (NMDA) receptor antagonist with cough-suppressing effects (91,92). The human CYP2D subfamily consists of CYP2D6, CYP2D7, and CYP2D8. CYP2D7 and CYP2D8 are designated as pseudogenes, and CYP2D6 is recognized as the active human isoform in this subfamily. This single isoenzyme is responsible for 20% to 30% of the oxidation of all pharmaceutics used by humans (93). CYP2D6 mRNA expression was detected in all regions of human brain, and the highest level was detected in the cerebellum (94,95). Western blotting experiments showed the presence of CYP2D6 protein in many regions of human brain, including cortex, cerebellum, midbrain, striatum, and thalamus (95). Immunohistochemical studies demonstrated the presence of CYP2D6 protein in neuronal soma and dentrites of Purkinje and cortical neurons (95).

The substrates of CYP2D6 include many psychoactive compounds and drugs acting on the CNS, which are shown in Table 1. A previous study has reported that the known CYP2D6 substrate dextromethorphan was metabolized to dextrorphan in rat brain microsomes and was inhibited by quinidine and by a polyclonal antibody against CYP2D6 (96). An analogous study indicated that another CYP2D6 substrate bufuralol can also be metabolized by rat brain microsomal fraction (97). The presence of CYP2D6 in human brain highly suggests the possible direct metabolism of these drugs by CYP2D6 in or near neurons in the brain.

CYP2D6 can also metabolize the neurotransmitters tryptamine and tyramine (98,99). The metabolism of tyramine by CYP2D6 results in the formation of dopamine (99). CYP2D6 also metabolizes the neurotoxin 1-methyl-4-phenyl-1,2,3,6-tetrahydropyridine

Table 1 Drugs Metabolized by CYP2D6

Drug[a]	Metabolizing reaction by CYP2D6	Pharmacological action[a]
Amitriptyline (191,192)	*N* demethylation	Tricyclic antidepressant drugs (TCA)
Clomipramine (80)	2 and 8 Hydroxylation	
Desipramine (193)	Hydroxylation	
Imipramine (194)	2 Hydroxylation	
Mianserin (195)	*O* demethylation	
Nortriptyline (196)	2 hydroxylation	
Fluoxetine (196)	*N* demethylation	Selective serotonin reuptake inhibitors (SSRI)
Fluvoxamine (197)	Demethylation	
Paroxetine (198)	Demethylation	
Haloperidol (199)	*N* dealkylation	Antiemetics, antipsychotic agent, dopamine antagonist, anti dyskinesia agent
Codeine (200)	*O* demethylation	Analgesics, opioid, antitussive agent
Chlorpromazine (201)	*N* demethylation	Phenothiazine antipsychotic
Dextromethorphan (201)	*O* demethylation	Antitusive agent
Tramadol (202)	*O* and *N* demethylation	Opioid, analgesic
Venlafaxine (203,204)	*O* and *N* demethylation	Antidepressant, serotonin norepeinephrine reuptake inhibitor
Ondansetron (205)	*O* demethylation	Serotonin 5 HT_3 receptor antagonist
Promethazine (112)	*N* demethylation	H1 receptor antagonist, antihistamine
Perphenazine (206)	*N* dealkylation	Antipsychotic
Amphetamine (207)	*N* dealkylation	CNS stimulant
Ethylmorphine (208)	*N* demethylation, *O* deethylation	Opioid
Metoclopramide (209)	*N* dealkylation	Dopamine receptor agonist
Aripiprazole (210)	Hydroxylation	Atypical antipsychotic
Debrisoquine (211)	Hydroxylation	Antihypertension agent
Thioridazine (211)	*O* demethylation	Piperidine antipsychotic
Risperidone (212)	9 Hydroxylation	Antipsychotic
Ibogaine (213)	*O* demethylation	Psychoactive alkaloid

KEGG website of cytochrome P450 substrates (http://www.genome.jp/kegg bin/get htext?br08105.keg) is referred for the list of drugs and relative pharmacological actions.

(MPTP), a chemical resulting in Parkinson's disease symptoms (100). The metabolism of neurotransmitters and neurotoxins by CYP2D6 partially explains the clinical association of this enzyme and Parkinson's disease as demonstrated in many studies (98,101 104). Additionally, CYP2D6 has been shown to catalyze the metabolism of progesterone (105), a neuroprotective neurosteroid affecting synaptic functioning and myelinization (106). CYP2D6 activity is also related to personality traits, which suggests that CYP2D6 enzyme may have more endogenous neuroactive substrates or products (107).

CNS-active drugs are able to affect CYP2D6 activity. A number of studies indicate that antidepressants fluoxetine, paroxetine, sertraline, venlafaxine, and citalopram, known as selective serotonin (5-hydroxytryptamine) reuptake inhibitors (SSRIs), are able to inhibit CYP2D6 activity (108 110). In addition, the histamine H1 antagonist promethazine can inhibit CYP2D6-catalyzed bulfuralol 1′-hydroxylation in human liver microsomes (111). On the other hand, it has been demonstrated that alcoholics have higher CYP2D6 levels compared with nonalcoholic individuals (94). CYP2D levels are also induced in rat brain by chronic nicotine treatment (112). Induction of CYP2D4 in rat

brain was detected by clozapine and toluene treatment (113), indicating the possible induction of CYP2D6 in human brain by neuroactive compounds. The CYP2D6 gene is highly polymorphic, causing absent, decreased, normal, or increased enzyme activity due to the presence of two or more copies of a functional CYP2D6 allele existing in tandem on the same chromosome (114,115). Therefore, both genetic and enviromental factors result in the functional diversity of CYP2D6 activity among individuals.

CYP2D7 has long been considered a pseudogene. Ravindranath and colleagues described an indel polymorphism (CYP2D7 138delT) that causes a frameshift generating an open reading frame and functional protein. This polymorphism was observed in an Indian population. Individuals with the 138delT polymorphism expressed CYP2D7 protein from a brain-specific, alternatively spliced transcript (116). However, to date, no further evidence for functional CYP2D7 transcripts has been observed in Asian, Caucasian, or African-American individuals (117,118).

CYP2E1 is an ethanol-metabolizing enzyme expressed constitutively in both rodent and human brains. This enzyme is used as a secondary pathway for the oxidation of ethanol (119). When plasma/tissue levels of ethanol are low, the classic class I alcohol dehydrogenases are the most important catalysts for oxidative biotransformation of ethanol (120). The alcohol dehydrogenase enzymes represent a high-affinity/low-capacity system, while the CYP2E1 enzymes represent a low-affinity/high-capacity system (120). Such studies have shown that at high blood alcohol concentrations and in chronic users, CYP2E1 plays a major role in oxidizing ethanol in adults because of the saturation of the dehydrogenase system at relatively low ethanol concentrations and because of the induction of CYP2E1 by chronic ethanol exposure (119,121). The Ravindranath laboratory showed that in the rat brain, CYP2E was heterogeneously expressed among brain regions and prominent in neurons of the cerebral cortex, denatate, gyrus, and the CA1, CA2, and CA3 regions of the hippocampus and in Purkinje cells in the cerebellum (122). The Ravindranath laboratory was also able to localize human CYP2E1 mRNA in brain regions and showed that the expression pattern was similar to that of the rat brain. CYP2E1 was also found in dopaminergic cells of the rat substantia nigra (123).

Knowing the expression patterns of CYP2E1 may prove important because Juchau et al. have suggested that CYP2E1 expression and its catalytic function of oxidizing ethanol with the associated generation of several reactive chemical species could contribute significantly to the etiology of neuroembryotoxic effects of prenatal ethanol exposure (120). They later suggested that ethanol induced CYP2E1 expression in the fetal brain. Further, Juchau concluded that CYP2E1 could be dangerous because of the leaky properties it possesses, which results in the production of highly detrimental reactive oxygen species (124).

CYP2E1 not only oxidizes ethanol, but it also metabolizes many other endogenous and exogenous compounds. These include caffeine, chloroform, acetaldehyde, chloromethane, and benzene. Recently the Engberg laboratory reported that CYP2E1 may play a role in the dopamine metabolism, because they found that when the CYP2E1 enzymes were inhibited, there was a subsequent increase in available dopamine levels (125). Table 2 shows different xenobiotics that have brain-specific affects and are catalyzed by CYP2E1.

Other CYP2 isoenzymes detected in human brain include CYP2J2, CYP2S1, and CYP2U1. CYP2J2 was detected in human brain at a very low level (126). This enzyme is known to metabolize AA to 20-hydroxyeicosatetraenoic acid (20-HETE) and epoxyeicosatrienoic acids (EETs) (127), indicating that CYP2J2 might be involved in the regulation of normal brain function. The known xenobiotic substrates of CYP2J2 are limited in number. Little evidence has been presented to confirm whether CYP2J2 is able to metabolize any neurotrophic drugs. CYP2S1 gene is the sole member of the CYP2S subfamily. In human

Table 2 Drugs Metabolized by CYP2E1

Drug[a]	Metabolizing reaction by CYP2E1	Pharmacological action[a]
Benzene (214)	1,4 Hydroxylation	Organic chemical compound, precursor to drugs
Acetaminophen (215)	*N* Alkylation	Analgesic
Halothane (216)	Oxidation	General anesthetic
Enflurane (217)	Oxidation	Anesthetic
Methoxyflurane (218)	Oxidation	Inhalational anesthetic
Chlorzoxazone1 (219)	6 Hydroxylation	Muscle relaxant
Isoflurane (218)	Oxidation	Anesthetic

[a]KEGG website of cytochrome P450 substrates (http://www.genome.jp/kegg bin/get htext?br08105.keg) is referred for the list of drugs and relative pharmacological actions.

brain tissue, weak CYP2S1 expression was detected in the nuclei of the white matter by in situ hybridization to mRNA and immunohistochemistry (128). The substrates identified for recombinant CYP2S1 include both xenobiotics and endobiotics (129,130), although the function of CYP2S1 in the brain has not been clarified. CYP2U1 is a novel human thymus- and brain-specific CYP (131). CYP2U1 mRNA was detected at a high level in the cerebellum, and this enzyme catalyzes ω- and (ω-1)-hydroxylation of fatty acids including AA and docosahexaenoic acid (131), suggesting a specific but yet unidentified physiological role for CYP2U1 in the brain (131).

CYP3 Family

The CYP3 family includes the CYP3A, CYP3B, and CYP3C subfamilies (132,133). Members of the CYP3A subfamily represent the dominant CYP3 forms expressed in vertebrates. The human CYP3A subfamily consists of four functional genes, CYP3A4, CYP3A5, CYP3A7, CYP3A43, and two pseudogenes, CYP3A5P1 and CYP3A5P2. The CYP3A isoforms account for as much as 30% of total P450 content in liver and have an important role in the metabolism of endogenous steroids and at least 50% of all currently prescribed drugs (134,135).

The most abundant CYP3A isoform expressed in liver and gut is CYP3A4 (136). CYP3A4 gene is also expressed in human brain, although the expression level is much lower compared with that in the liver. RT-PCR experiments performed by McFayden et al. revealed the presence of CYP3A4 mRNAs in specific areas including basal ganglia and frontal cortex of normal human brain (137). CYP3A5 mRNA was also detected by RT-PCR in brain areas including midbrain, basal ganglia, and frontal cortex (137). Immunoblot analysis of microsomal protein from human brain regions using CYP3A4 antiserum suggested the expression of CYP3A protein in cortex, cerebellum, striatum, and hippocampus (138). Furthermore, in situ hybridization and immunohistochemical analysis show that CYP3A is predominantly localized in neurons of both rat and human brain (138). CYP3A7 is the major CYP isoform in the fetus but not in adults. It accounts for at least 50% of the total P450 in human fetal liver, but it is expressed at much lower levels in adult liver (139,140) and undetectable level in adult brain. A recent unpublished study by Ravindranath and colleagues in India indicated that CYP3A43 mRNA is expressed at a high level in the brain of a group of brain samples (personal communication).

To date, CYP3A4 appears to be the most potent drug-metabolizing enzyme. A number of substrates of CYP3A4 are psychoactive compounds, which are listed in Table 3. Many exogenous CYP3A4 substrates such as alprazolam (ALP), l-deprenyl, amitriptyline,

Table 3 Drugs Metabolized by CYP3A4

Drug[a]	Metabolizing reaction by CYP3A4	Pharmacological action in brain[a]
Codeine (218), ethylmorphine (208), methadone (63,219)	*N* demethylation	Analgesics, opioid, antitussive agents, narcotics
Buprenorphine (220), fentanyl (221)	*N* dealkylation	Analgesics, opioid
Alprazolam (165,222)	4 and α hydroxylation	Hypnotics and sedatives, antianxiety agents, GABA modulator
Diazepam (223)	*N* demethylation, 3 hydroxylation	
Midazolam (224)	1′ and 4 Hydroxylation	
Nordazepam (225)	3 Hydroxylation	
Triazolam (226)	1 and 4 Hydroxylation	
Zaleplon (227)	*N* deethylation	
Zolpidem (228,229)	Hydroxylation	
Dextromethorphan (230)	*N* demethylation	Antitussive agents, excitatory amino acid antagonists
Citalopram (84)	*N* demethylation	Antidepressive agents, serotonin uptake inhibitors
Clomipramine (231)	*N* demethylation	
Trazodone (232)	*N* dealkylation	
Venlafaxine (204)	*N* and *O* demethylation	
Buspirone (233)	N dealkylation, N oxidation, 3′, 5 and 6′ hydroxylation	Anti anxiety agents, serotonin agonists
Amiodarone (234)	*N* deethylation	Neurotoxic agents
Parathion (235)	Oxidation	
Cyclosporine (236 238)	Oxidation	
Amitriptyline (191,239)	*N* demethylation	Antidepressive agents, non narcotic analgesics
Tetrahydrocannabinol (240,241)	11 , 8 , and 7 Hydroxylation, 9α and 10α epoxidation	
Carbamazepine (153)	10 and 11 Epoxidation	Anticonvulsants, antimanic agent, non narcotic analgesics
Cilostazol (242)	Hydroxylation	Neuroprotective agents
Dapsone (243,244)	*N* hydroxylation	
Dexamethasone (245)	6 Hydroxylation	
Diltiazem (246,247)	*N* demethylation	
Statins (atorvastatin, lovastatin, imvastatin) (248 250)	Oxidation	
Tacrolimus (251,252)	Hydroxylation	
Caffeine (253,254)	8 Hydroxylation	Central nervous system stimulant, phosphodiesterase inhibitor
Zonisamide (255,256)	Reduction	Anticonvulsants, antioxidants
Phencyclidine (257)	*N* dealkylation	Hallucinogens, NMDA receptor antagonists
Aripiprazole (258)	Dehydroxylation	Antipsychotic agent
Domperidone (259)	*N* dealkylation, aromatic hydroxylation	Antiemetics, antipsychotic agents, dopamine antagonists
Haloperidol (199,260)	*N* dealkylation, dehydration, oxidation	

Table 3 Drugs Metabolized by CYP3A4 (*Continued*)

Drug[a]	Metabolizing reaction by CYP3A4	Pharmacological action in brain[a]
Terfenadine (261)	*C* hydroxylation, *N* demethylation	Nonsedating antihistamine
Cocaine (262)	*N* demethylation	Anesthetics, vasoconstrictor agent, dopamine uptake inhibitor
Vitamin D (263,264)	24 and 25 hydroxylation	Neurotrophic factors biosynthesis, nitric oxide synthase inhibition, glutathione levels inhibition

[a]KEGG website of cytochrome P450 substrates (http://www.genome.jp/kegg bin/get htext?br08105.keg) was consulted for the list of drugs and relative pharmacological actions.

imipramine, and aminopyrine have been shown to be metabolized by brain microsomal fractions from mouse, rat, monkey, and human (96,138,141 143). Therefore, cerebral CYP3A4 has a high potential to be involved in the in situ activation or deactivation of CYP3A4-metabolized drugs targeted in the brain. CYP3A4 is also responsible for the metabolism of endogenous compounds. It has been reported that CYP3A4 is involved in the metabolism of steroid hormones and prohormones such as cortisol (144), testosterone (145), 17β-estradiol (146), progesterone (75), and dehydroepiandrosterone (147), all of which play important roles in brain.

Many drugs, including CNS drugs, are inhibitors or inducers of CYP3A4 activity. Nefazodone, an antidepressant, has been shown to inhibit the CYP3A4 activity both in vivo (148) and in vitro (149). Fluoxetine, a potent CYP2D6 inhibitor, can also mildly inhibit CYP3A4 activity (150). Other known inhibitors of CYP3A4 include diltiazem, verapamil, delavirdine, indinavir, erythromycin, clarithromycin, mifepristone, and so on (151,152). Carbamazepine can activate CYP3A4 activity in human liver microsomes (151,153). Other known CYP3A4 activators include phenobarbital, phenytoin, clotrimazole, rifampicin, dexamethasone, sulfinpyrazone, sulfadimidine, troglitazone, efavirenz, nevirapine, and taxol (154 156). The induction of CYP3A4 is primarily mediated by nuclear receptors including pregnane X receptor (PXR) and constitutive androstane receptor (CAR) (157,158). It is noteworthy that some of these activators and inhibitors can cross the BBB even though they are not psychoactive drugs. Although the regulation of CYP3A4 activity in the brain remains unidentified, the above xenobiotic CYP3A4 regulators strongly indicate the effects of drugs on CYP3A4 and the presence of drug-drug interaction in the brain. In vitro experiments using human liver microsomes demonstrated that endogenous substances such as neurotransmitters and steroids can also modulate CYP3A4 activity. Adrenaline, serotonin, and 5-hydroxytriptofol are inhibitors of CYP3A4 enzyme activity (159). Endogenous androgens, such as androstenedione, testosterone, and dehydroepiandrosterone, can activate triazolam 4-hydroxylation and the metabolism of nevirapine and carbamazepine by CYP3A4, while triazolam 1′-hydroxylation and the metabolism of erythromycin and zonisamide by CYP3A4 are inhibited by the same androgens (160). Therefore, brain CYP3A activity can be modulated by some neurotransmitters and steroids and their precursors. CYP3A4 levels can differ greatly among individuals. Hepatic expression of CYP3A4 varies by more than 50-fold among individuals and in vivo CYP3A4 enzymatic activity varies by at least 20-fold (161). This variability is probably due to a combination of genetic factors (161) and environmental influences such as drug-drug interaction and drug-enzyme interaction (162). Whether there is a significant difference in the brain CYP3A4 activity remains to be clarified.

CYP3A5 has generally been considered to contribute less than CYP3A4 to drug metabolism because of its relatively lower hepatic level and overlapping substrate specificity. However, the product regioselectivity and rate of formation catalyzed by CYP3A5 can differ. RT-PCR experiments in human brain demonstrated the presence of cerebral CYP3A5 mRNA in some regions (137). In addition, studies on human liver microsomes indicate that CYP3A5 is capable of metabolizing many psychoactive drugs including midazolam, lidocaine, dextromethorphan, carbamazepine, ethylmorphine, flunitrazepam, and ALP (163,164). Therefore, the function of CYP3A5 in the brain is a promising area for further study.

CYP3A43 is a recently discovered P450 enzyme (165). The expression of CYP3A43 in the human liver is 0.1% of CYP3A4 and 2% of CYP3A5 (166). However, studies from Ravindranath and colleagues have revealed much higher CYP3A43 levels in human brain than that in liver (personal communication). The same study also indicated that recombinant CYP3A43 is capable of metabolizing ALP, an antianxiety drug. ALP is metabolized dominantly to 4-OH ALP by recombinant CYP3A4, while recombinant CYP3A43 metabolizes ALP to both α and 4-OHALP in equal amounts. The metabolic activity of CYP3A43 toward ALP is similar to that of CYP3A5, which has a relatively lower expression level in human brain. Therefore, the presence of relatively higher amount of CYP3A43 in human brain might also contribute to the metabolism of other psychoactive drugs that metabolize by CYP3A enzymes.

CYP4 Family

While CYPs play a major role in the drug metabolism, they also play a very important role in the metabolism of key endogenous compounds that have important physiological functions. Previous studies have shown that 20-HETE, the ω-hydroxylation product of AA, is the principal AA metabolite formed in tubular and vascular structures of the rat renal cortex and outer medulla (167). 20-HETE is a primary eicosanoid in the microcirculation where it helps in the regulation of vascular tone by sensitizing the smooth muscle cells to constrictor stimuli (168), and contributes to myogenic, mitogenic, and angiogenic responses (169). The synthesis of 20-HETE is catalyzed by enzymes of the CYP4A family (169). This vascular regulation and function is important in the human brain where neuronal activity evokes localized changes in blood flow supplying oxygen and nutrients to active neurons (170). Roy and Sherrington termed this relationship neurovascular coupling (171). As important as this regulation of vascular function is, the cellular mechanism is not fully understood (172,173). It has been suggested that glial cells are well suited to mediate this response because of their close proximity to both neurons and blood vessels (174,175). Metea and Newman (2006) showed that light- and glial-evoked constriction is mediated by ω-hydroxylase production of 20-HETE (170). Most of these reactions described are catalyzed in human brain by CYP4A11, the best characterized member of the 4A subfamily. It is also important to note here that although there is only one 4A member found in human, some of the seven members of the CYP4F family also contribute to the metabolism of AA into 20-HETE.

To date, four CYP4F isoforms (CYP4F1, CYP4F4, CYP4F5, and CYP4F6) have been detected in rat, and five (Cyp4f13, Cyp4f14, Cyp4f15, Cyp4f16, and Cyp4f18) in mouse. Among the four rat isoforms, CYP4F4, CYP4F5, and CYP4F6 were originally isolated from rat brain (170). Although CYP4F1 was cloned from a cDNA library of a 2-acetylaminofluorene-induced transplantable rat hepatic tumor (176); the expression of this isoform was also detected in the rat brain (177). Current study in our laboratory indicates that CYP4Fs are widely distributed in rat brain (unpublished data). The

Table 4 CYP4Fs Expression and Distribution in Rat Brain

Brain regions	Frontal lobe	Occipital lobe	Hippocampus	Cerebellum	Striatum	Midbrain	Medulla	Detect technique
CYP4F1	+	+	+	+	+	+	+	qRT PCR
	+	+						western blot
CYP4F4	+	+	+	+	+	+	+	qRT PCR
	+	+	+	+	+	+	+	western blot
CYP4F5	+	+	+	+	+	+	+	qRT PCR
	+	+	+		+			western blot
CYP4F6	+	+	+	+	+	+	+	qRT PCR
	+	+	+	+	+	+		western blot

distribution pattern of rat CYP4Fs is shown in Table 4. According to mRNA levels detected by quantitative reverse transcriptase PCR (qRT-PCR), CYP4F6 is the most dominantly expressed one in rat brain, followed by CYP4F1, whereas CYP4F4 and CYP4F5 mRNA expression levels are much lower in rat brain (178). All rat CYP4F isoforms are able to catalyze the metabolism of endogenous bioproducts such as eisosanoids via the ω-hydroxylation reaction (179,180). However, the xenobiotic substrates of rat CYP4Fs are less well known than those of human CYP4Fs. So far, psychotropic drugs are the major known xenobiotic substrates for rat CYP4Fs. CYP4F4 and CYP4F5 are able to catalyze the N-demethylation and S-oxidation of chlorpromazine (181). In addition, recombinant CYP4F6 has been shown to convert imipramine to its 10-hydroxy product (182).

Although little has been reported about the enzymatic functions of mouse Cyp4f isoforms against drugs, considerable effort has been focused on their tissue expression and distribution, which is necessary for the further study of potential drug metabolism activities of these enzymes. No Cyp4f13 mRNA has been detected in the brain till present time. Cyp4f14, the mouse counterpart of rat CYP4F1, was first cloned from mouse liver by Kikuta et al., and Cyp4f14 mRNA was also detected in the mouse brain by the same group using RT-PCR (183). Cui et al. detected the mRNA expression of Cyp4f15 and Cyp4f16 in mouse brain (184). Cyp4f18 is the functional orthologue of human polymorphonuclear leukocytes (PMN) CYP4F3A, however, Cyp4f18 mRNA was barely detectable in the mouse brain (185).

The human 4F subfamily consists of seven isoforms, two of which have been shown to metabolize xenobiotics. CYP4F12 was cloned from small intestine and liver by two different groups (186,187), respectively. Hashizume's group later showed that CYP4F12 was capable of metabolizing an antihistamine, ebastine, which has two major pathways for metabolism, hydroxylation and N-dealkylation (188). CYP4F12 protein has not been reported to be expressed in human brain, but current RTQPCR studies reveal that CYP4F12 is expressed in human brain tissue (unpublished data). CYP4F11 was characterized by Kalsotra et al. and was shown to be the main drug metabolizer of the human CYP4F subfamily (189). CYP4F11 was reported to be expressed in human liver, kidney, heart, skeletal muscle, and brain. Table 5 shows the turnover rate of both CYP4F11 and CYP4F3 for various clinically relevant drugs. CYP4F isoforms like those of CYP4A subfamily are also reported to produce 19- and 20-HETE (190). Most of the recent studies reported on CYP4F have been concerned with their ability to metabolize AA and AA metabolites such as prostoglandins and leukotrienes, which are potent inflammatory mediators. It is now known that the main pathway for leukotriene metabolism is through the CYP4 family, and as such, the possibility to use CYP4F expression as a way to address traumatic brain injury is now being studied.

Table 5 Human CYP4F11 and CYP4F3A Drug Metabolism

Drug	CYP4F11	CYP4F3A
Amitriptyline	28.46 ± 3.53	95.31 ± 18.8
Benzphetamine	253.3 ± 25.4	56.0 ± 6.41
Chlorpromazine	58.0 ± 6.30	Not detected
Erythromycin	807.6 ± 11.6	70.33 ± 9.87
Ehylmorphine	175.0 ± 38.7	84.0 ± 6.93
Imipramine	274.2 ± 8.16	79.46 ± 13.9
Pirenzepine	16.55 ± 2.33	122.3 ± 2.90
Theophylline	260.7 ± 8.69	31.0 ± 9.64
Verapamil	110.8 ± 6.92	98.32 ± 15.3

Source: Adapted from Ref. 189.

DISCUSSION

It is clear from the foregoing descriptions that the existence of single nucleotide polymorphisms in the CYP can have a considerable, sometimes deleterious, impact on the metabolism and, therefore, efficacy of therapeutic agents. It has been primarily through many careful population studies of CYP2D6-dependent metabolism of drugs that we have come to understand the impact of ultrarapid, extensive, moderate, and slow metabolizer phenotypes on the utility of many drugs and, more importantly, the variations in risk of side effects for these populations. In addition to CYP2D6, polymorphisms have been reported in other CYP subfamilies (e.g., CYP2B6).

In addition to single nucleotide polymorphisms, other variant CYP isoforms arising by different mechanisms have been shown to play a role in substrate preference, product profile, and turnover, which may increasingly be of concern in drug design and development approaches. Exon switching/selection has been shown by Christmas et al. to occur in CYP4A3 to produce two different protein products CYP4A3A and CYP4A3B by the expression of either exon 3 (CYP4F3A) or exon 4 (CYP4F3B), but not the alternate exon in transcription of its messenger RNA. The results of this exon selection event produces active enzyme with quite different substrate specificities; CYP4F3A prefers AA as its substrate producing the biological signal molecule 20-HETE, while CYP4F3B prefers leukotriene B_4 inactivating it to 20-OH leukotriene B_4.

The formation of splice variants has also been shown to occur. The Ravindranath laboratory has reported that in a certain segment of the South Indian population, the pseudogene CYP2D7 is expressed because of a single-base deletion of position 138, resulting in a polypeptide containing a 19 amino acid insert. This insert has been shown to be expressed in brain regions and catalyzes the conversion of codeine to morphine as its almost exclusive product in contrast to CYP2D6, which converts codeine to morphine and norcodeine in a 30% to 70% product balance.

Similarly, Chinta et al. have reported the expression of a CYP1A1 splice variant, in which bases of exon 6 are deleted in its mRNA trading to a protein with an 87 base pair deletion. This active enzyme exhibits reduced ethoxycoumarin activity (about 50% as much as wild-type 1A1) and, more significantly, does not produce benzo[a]pyrene products capable of binding DNA. This CYP1A1 variant is expressed in brain (19).

Thus, various processes modifying the protein product of CYP genes in brain as well as other tissues affect metabolic activities. Consequently, additional pathways for disposition of drugs as well as endogenous compounds are a clear reality with the potential of multiplying exploitable drug target opportunities on the one hand and

increasing the possibilities for unfavorable drug-drug interactions on the other. Perhaps here also lies another possibility for investigation/explanation of idiosyncratic drug reactions, which seem most notable for their effects on specific individuals within a population rather than on a larger segment of a population.

REFERENCES

1. Hedlund E, Gustafsson JA, Warner M. Cytochrome P450 in the brain; a review. Curr Drug Metab 2001; 2(3):245 263.
2. Miksys SL, Tyndale RF. Drug metabolizing cytochrome P450s in the brain. J Psychiatry Neurosci 2002; 27(6):406 415.
3. Strobel HW, Thompson CM, Antonovic L. Cytochromes P450 in brain: function and significance. Curr Drug Metab 2001; 2(2):199 214.
4. Alavijeh MS, Chishty M, Qaiser MZ, Palmer AM. Drug metabolism and pharmacokinetics, the blood brain barrier, and central nervous system drug discovery. NeuroRx 2005; 2(4):554 571.
5. Haining RL, Nichols Haining M. Cytochrome P450 catalyzed pathways in human brain: metabolism meets pharmacology or old drugs with new mechanism of action? Pharmacol Ther 2007; 113(3):537 545.
6. Upton RN. Cerebral uptake of drugs in humans. Clin Exp Pharmacol Physiol 2007; 34(8):695 701.
7. Dutheil F, Beaune P, Loriot MA. Xenobiotic metabolizing enzymes in the central nervous system: Contribution of cytochrome P450 enzymes in normal and pathological human brain. Biochimie 2008; 90(3):426 436.
8. Wolburg H, Lippoldt A. Tight junctions of the blood brain barrier: development, composition and regulation. Vascul Pharmacol 2002; 38(6):323 337.
9. Deeken JF, Loscher W. The blood brain barrier and cancer: transporters, treatment, and Trojan horses. Clin Cancer Res 2007; 13(6):1663 1674.
10. Abbott NJ, Ronnback L, Hansson E. Astrocyte endothelial interactions at the blood brain barrier. Nat Rev Neurosci 2006; 7(1):41 53.
11. Ballabh P, Braun A, Nedergaard M. The blood brain barrier: an overview: structure, regulation, and clinical implications. Neurobiol Dis 2004; 16(1):1 13.
12. Abbott NJ. Dynamics of CNS barriers: evolution, differentiation, and modulation. Cell Mol Neurobiol 2005; 25(1):5 23.
13. Zambrowicz BP, Sands AT. Knockouts model the 100 best selling drugs will they model the next 100? Nat Rev Drug Discov 2003; 2(1):38 51.
14. Addya S, Anandatheerthavarada HK, Biswas G, Bhagwat SV, Mullick J, Avadhani NG. Targeting of NH2 terminal processed microsomal protein to mitochondria: a novel pathway for the biogenesis of hepatic mitochondrial P450MT2. J Cell Biol 1997; 139(3):589 599.
15. Boopathi E, Anandatheerthavarada HK, Bhagwat SV, Biswas G, Fang JK, Avadhani NG. Accumulation of mitochondrial P450MT2, NH(2) terminal truncated cytochrome P4501A1 in rat brain during chronic treatment with beta naphthoflavone. A role in the metabolism of neuroactive drugs. J Biol Chem 2000; 275(44):34415 34423.
16. Miksys S, Lerman C, Shields PG, Mash DC, Tyndale RF. Smoking, alcoholism and genetic polymorphisms alter CYP2B6 levels in human brain. Neuropharmacology 2003; 45(1):122 132.
17. Anandatheerthavarada HK, Shankar SK, Ravindranath V. Rat brain cytochromes P 450: catalytic, immunochemical properties and inducibility of multiple forms. Brain Res 1990; 536(1 2):339 343.
18. Ghersi Egea JF, Walther B, Perrin R, Minn A, Siest G. Inducibility of rat brain drug metabolizing enzymes. Eur J Drug Metab Pharmacokinet 1987; 12(4):263 265.
19. Chinta SJ, Kommaddi RP, Turman CM, Strobel HW, Ravindranath V. Constitutive expression and localization of cytochrome P 450 1A1 in rat and human brain: presence of a splice variant form in human brain. J Neurochem 2005; 93(3):724 736.
20. Shimada T, Gillam EM, Sandhu P, Guo Z, Tukey RH, Guengerich FP. Activation of procarcinogens by human cytochrome P450 enzymes expressed in Escherichia coli. Simplified bacterial systems for genotoxicity assays. Carcinogenesis 1994; 15(11):2523 2529.

21. Faber MS, Jetter A, Fuhr U. Assessment of CYP1A2 activity in clinical practice: why, how, and when? Basic Clin Pharmacol Toxicol 2005; 97(3):125 134.
22. Fisone G, Borgkvist A, Usiello A. Caffeine as a psychomotor stimulant: mechanism of action. Cell Mol Life Sci 2004; 61(7 8):857 872.
23. Fontana RJ, deVries TM, Woolf TF, Knapp MJ, Brown AS, Kaminsky LS, Tang BK, Foster NL, Brown RR, Watkins PB. Caffeine based measures of CYP1A2 activity correlate with oral clearance of tacrine in patients with Alzheimer's disease. Br J Clin Pharmacol 1998; 46(3):221 228.
24. Muskhelishvili L, Thompson PA, Kusewitt DF, Wang C, Kadlubar FF. In situ hybridization and immunohistochemical analysis of cytochrome P450 1B1 expression in human normal tissues. J Histochem Cytochem 2001; 49(2):229 236.
25. Rieder CR, Parsons RB, Fitch NJ, Williams AC, Ramsden DB. Human brain cytochrome P450 1B1: immunohistochemical localization in human temporal lobe and induction by dimethylbenz (a)anthracene in astrocytoma cell line (MOG G CCM). Neurosci Lett 2000; 278(3):177 180.
26. Murray GI, Melvin WT, Greenlee WF, Burke MD. Regulation, function, and tissue specific expression of cytochrome P450 CYP1B1. Annu Rev Pharmacol Toxicol 2001; 41:297 316.
27. Hayes CL, Spink DC, Spink BC, Cao JQ, Walker NJ, Sutter TR. 17 beta estradiol hydroxylation catalyzed by human cytochrome P450 1B1. Proc Natl Acad Sci U S A 1996; 93(18):9776 9781.
28. Shimada T, Wunsch RM, Hanna IH, Sutter TR, Guengerich FP, Gillam EM. Recombinant human cytochrome P450 1B1 expression in Escherichia coli. Arch Biochem Biophys 1998; 357(1):111 120.
29. Fernandez Salguero P, Hoffman SM, Cholerton S, Mohrenweiser H, Raunio H, Rautio A, Pelkonen O, Huang JD, Evans WE, Idle JR, Gonzalez FJ. A genetic polymorphism in coumarin 7 hydroxylation: sequence of the human CYP2A genes and identification of variant CYP2A6 alleles. Am J Hum Genet 1995; 57(3):651 660.
30. Hoffman SM, Fernandez Salguero P, Gonzalez FJ, Mohrenweiser HW. Organization and evolution of the cytochrome P450 CYP2A 2B 2F subfamily gene cluster on human chromosome 19. J Mol Evol 1995; 41(6):894 900.
31. Yamano S, Tatsuno J, Gonzalez FJ. The CYP2A3 gene product catalyzes coumarin 7 hydroxylation in human liver microsomes. Biochemistry 1990; 29(5):1322 1329.
32. Yun CH, Shimada T, Guengerich FP. Purification and characterization of human liver microsomal cytochrome P 450 2A6. Mol Pharmacol 1991; 40(5):679 685.
33. Yamanaka H, Nakajima M, Fukami T, Sakai H, Nakamura A, Katoh M, Takamiya M, Aoki Y, Yokoi T. CYP2A6 AND CYP2B6 are involved in nornicotine formation from nicotine in humans: interindividual differences in these contributions. Drug Metab Dispos 2005; 33(12): 1811 1818.
34. Nakajima M, Yamamoto T, Nunoya K, Yokoi T, Nagashima K, Inoue K, Funae Y, Shimada N, Kamataki T, Kuroiwa Y. Role of human cytochrome P4502A6 in C oxidation of nicotine. Drug Metab Dispos 1996; 24(11):1212 1217.
35. Nakajima M, Yamamoto T, Nunoya K, Yokoi T, Nagashima K, Inoue K, Funae Y, Shimada N, Kamataki T, Kuroiwa Y. Characterization of CYP2A6 involved in 3′ hydroxylation of cotinine in human liver microsomes. J Pharmacol Exp Ther 1996; 277(2):1010 1015.
36. Murphy SE, Raulinaitis V, Brown KM. Nicotine 5′ oxidation and methyl oxidation by P450 2A enzymes. Drug Metab Dispos 2005; 33(8):1166 1173.
37. Nordberg A, Hartvig P, Lundqvist H, Antoni G, Ulin J, Långström B. Uptake and regional distribution of (+) (R) and ( ) (S) N [methyl 11C] nicotine in the brains of rhesus monkey. An attempt to study nicotinic receptors in vivo. J Neural Transm Park Dis Dement Sect 1989; 1(3):195 205.
38. Plowchalk DR, Andersen ME, deBethizy JD. A physiologically based pharmacokinetic model for nicotine disposition in the Sprague Dawley rat. Toxicol Appl Pharmacol 1992; 116(2): 177 188.
39. Crooks PA, Li M, Dwoskin LP. Metabolites of nicotine in rat brain after peripheral nicotine administration. Cotinine, nornicotine, and norcotinine. Drug Metab Dispos 1997; 25(1):47 54.
40. Miksys S, Tyndale RF. The unique regulation of brain cytochrome P450 2 (CYP2) family enzymes by drugs and genetics. Drug Metab Rev 2004; 36(2):313 333.

41. Nakajima M, Kuroiwa Y, Yokoi T. Interindividual differences in nicotine metabolism and genetic polymorphisms of human CYP2A6. Drug Metab Rev 2002; 34(4):865 877.
42. Higashi E, Nakajima M, Katoh M, Tokudome S, Yokoi T. Inhibitory effects of neurotransmitters and steroids on human CYP2A6. Drug Metab Dispos 2007; 35(4):508 514.
43. Su T, Bao Z, Zhang QY, Smith TJ, Hong JY, Ding X. Human cytochrome P450 CYP2A13: predominant expression in the respiratory tract and its high efficiency metabolic activation of a tobacco specific carcinogen, 4 (methylnitrosamino) 1 (3 pyridyl) 1 butanone. Cancer Res 2000; 60(18):5074 5079.
44. Bao Z, He XY, Ding X, Prabhu S, Hong JY. Metabolism of nicotine and cotinine by human cytochrome P450 2A13. Drug Metab Dispos 2005; 33(2):258 261.
45. Omiecinski CJ, Remmel RP, Hosagrahara VP. Concise review of the cytochrome P450s and their roles in toxicology. Toxicol Sci 1999; 48(2):151 156.
46. Rosenbrock H, Hagemeyer CE, Ditter M, Knoth R, Volk B. Expression and localization of the CYP2B subfamily predominantly in neurones of rat brain. J Neurochem 2001; 76(2):332 340.
47. Gervot L, Rochat B, Gautier JC, Bohnenstengel F, Kroemer H, de Berardinis V, Martin H, Beaune P, de Waziers I. Human CYP2B6: expression, inducibility and catalytic activities. Pharmacogenetics 1999; 9(3):295 306.
48. Ekins S, Wrighton SA. The role of CYP2B6 in human xenobiotic metabolism. Drug Metab Rev 1999; 31(3):719 754.
49. Hidestrand M, Oscarson M, Salonen JS, Nyman L, Pelkonen O, Turpeinen M, Ingelman Sundberg M. CYP2B6 and CYP2C19 as the major enzymes responsible for the metabolism of selegiline, a drug used in the treatment of Parkinson's disease, as revealed from experiments with recombinant enzymes. Drug Metab Dispos 2001; 29(11):1480 1484.
50. Yamazaki H, Inoue K, Hashimoto M, Shimada T. Roles of CYP2A6 and CYP2B6 in nicotine C oxidation by human liver microsomes. Arch Toxicol 1999; 73(2):65 70.
51. Anandatheerthavarada HK, Williams JF, Wecker L. The chronic administration of nicotine induces cytochrome P450 in rat brain. J Neurochem 1993; 60(5):1941 1944.
52. Miksys S, Tyndale RF. Nicotine induces brain CYP enzymes: relevance to Parkinson's disease. J Neural Transm Suppl 2006(70):177 180.
53. Chun J, Kent UM, Moss RM, Sayre LM, Hollenberg PF. Mechanism based inactivation of cytochromes P450 2B1 and P450 2B6 by 2 phenyl 2 (1 piperidinyl)propane. Drug Metab Dispos 2000; 28(8):905 911.
54. Kreth K, Kovar K, Schwab M, Zanger UM. Identification of the human cytochromes P450 involved in the oxidative metabolism of "Ecstasy" related designer drugs. Biochem Pharmacol 2000; 59(12):1563 1571.
55. Pellinen P, Kulmala L, Konttila J, Auriola S, Pasanen M, Juvonen R. Kinetic characteristics of norcocaine N hydroxylation in mouse and human liver microsomes: involvement of CYP enzymes. Arch Toxicol 2000; 74(9):511 520.
56. Lee AM, Miksys S, Tyndale RF. Phenobarbital increases monkey in vivo nicotine disposition and induces liver and brain CYP2B6 protein. Br J Pharmacol 2006; 148(6):786 794.
57. Jushchyshyn MI, Kent UM, Hollenberg PF. The mechanism based inactivation of human cytochrome P450 2B6 by phencyclidine. Drug Metab Dispos 2003; 31(1):46 52.
58. Yanev SG, Kent UM, Roberts ES, Ballou DP, Hollenberg PF. Mechanistic studies of cytochrome P450 2B1 inactivation by xanthates. Arch Biochem Biophys 2000; 378(1):157 166.
59. Kent UM, Yanev S, Hollenberg PF. Mechanism based inactivation of cytochromes P450 2B1 and P450 2B6 by n propylxanthate. Chem Res Toxicol 1999; 12(4):317 322.
60. Related Articles, LinksLerman C, Shields PG, Wileyto EP, Audrain J, Pinto A, Hawk L, Krishnan S, Niaura R, Epstein L. Pharmacogenetic investigation of smoking cessation treatment. Pharmacogenetics 2002; 12(8):627 634.
61. Hesse LM, Venkatakrishnan K, Court MH, von Moltke LL, Duan SX, Shader RI, Greenblatt DJ. CYP2B6 mediates the in vitro hydroxylation of bupropion: potential drug interactions with other antidepressants. Drug Metab Dispos 2000; 28(10):1176 1183.
62. Totah RA, Allen KE, Sheffels P, Whittington D, Kharasch ED. Enantiomeric metabolic interactions and stereoselective human methadone metabolism. J Pharmacol Exp Ther 2007; 321(1):389 399.

63. Gerber JG, Rhodes RJ, Gal J. Stereoselective metabolism of methadone N demethylation by cytochrome P4502B6 and 2C19. Chirality 2004; 16(1):36 44.
64. Ramírez J, Innocenti F, Schuetz EG, Flockhart DA, Relling MV, Santucci R, Ratain MJ. CYP2B6, CYP3A4, and CYP2C19 are responsible for the in vitro N demethylation of meperidine in human liver microsomes. Drug Metab Dispos 2004; 32(9):930 936.
65. Klose TS, Blaisdell JA, Goldstein JA. Gene structure of CYP2C8 and extrahepatic distribution of the human CYP2Cs. J Biochem Mol Toxicol 1999; 13(6):289 295.
66. Lundblad MS, Stark K, Eliasson E, Oliw E, Rane A. Biosynthesis of epoxyeicosatrienoic acids varies between polymorphic CYP2C enzymes. Biochem Biophys Res Commun 2005; 327 (4):1052 1057.
67. Adams PB, Lawson S, Sanigorski A, Sinclair AJ. Arachidonic acid to eicosapentaenoic acid ratio in blood correlates positively with clinical symptoms of depression. Lipids 1996; 31(suppl):S157 161.
68. Green P, Gispan Herman I, Yadid G. Increased arachidonic acid concentration in the brain of Flinders Sensitive Line rats, an animal model of depression. J Lipid Res 2005; 46(6):1093 1096.
69. Zeldin DC, DuBois RN, Falck JR, Capdevila JH. Molecular cloning, expression and characterization of an endogenous human cytochrome P450 arachidonic acid epoxygenase isoform. Arch Biochem Biophys 1995; 322(1):76 86.
70. Sieghart W. Pharmacology of benzodiazepine receptors: an update. J Psychiatry Neurosci 1994; 19(1):24 29.
71. Jung F, Richardson TH, Raucy JL, Johnson EF. Diazepam metabolism by cDNA expressed human 2C P450s: identification of P4502C18 and P4502C19 as low K(M) diazepam N demethylases. Drug Metab Dispos 1997; 25(2):133 139.
72. Romkes M, Faletto MB, Blaisdell JA, Raucy JL, Goldstein JA. Cloning and expression of complementary DNAs for multiple members of the human cytochrome P450IIC subfamily. Biochemistry 1991; 30(13):3247 3255.
73. Bylund J, Ericsson J, Oliw EH. Analysis of cytochrome P450 metabolites of arachidonic and linoleic acids by liquid chromatography mass spectrometry with ion trap MS. Anal Biochem 1998; 265(1):55 68.
74. Fradette C, Yamaguchi N, Du Souich P. 5 Hydroxytryptamine is biotransformed by CYP2C9, 2C19 and 2B6 to hydroxylamine, which is converted into nitric oxide. Br J Pharmacol 2004; 141(3):407 414.
75. Yamazaki H, Shimada T. Progesterone and testosterone hydroxylation by cytochromes P450 2C19, 2C9, and 3A4 in human liver microsomes. Arch Biochem Biophys 1997; 346 (1):161 169.
76. Dahl ML. Cytochrome p450 phenotyping/genotyping in patients receiving antipsychotics: useful aid to prescribing? Clin Pharmacokinet 2002; 41(7):453 470.
77. Miners JO, Birkett DJ. Cytochrome P4502C9: an enzyme of major importance in human drug metabolism. Br J Clin Pharmacol 1998; 45(6):525 538.
78. Olesen OV, Linnet K. Metabolism of the tricyclic antidepressant amitriptyline by cDNA expressed human cytochrome P450 enzymes. Pharmacology 1997; 55(5):235 243.
79. Venkatakrishnan K, Greenblatt DJ, von Moltke LL, Schmider J, Harmatz JS, Shader RI. Five distinct human cytochromes mediate amitriptyline N demethylation in vitro: dominance of CYP 2C19 and 3A4. J Clin Pharmacol 1998; 38(2):112 121.
80. Nielsen KK, Brøsen K, Hansen MG, Gram LF. Single dose kinetics of clomipramine: relationship to the sparteine and S mephenytoin oxidation polymorphisms. Clin Pharmacol Ther 1994; 55(5):518 527.
81. Desta Z, Zhao X, Shin JG, Flockhart DA. Clinical significance of the cytochrome P450 2C19 genetic polymorphism. Clin Pharmacokinet 2002; 41(12):913 958.
82. Madsen H, Rasmussen BB, Brosen K. Imipramine demethylation in vivo: impact of CYP1A2, CYP2C19, and CYP3A4. Clin Pharmacol Ther 1997; 61(3):319 324.
83. Bajpai M, Roskos LK, Shen DD, Levy RH. Roles of cytochrome P4502C9 and cytochrome P4502C19 in the stereoselective metabolism of phenytoin to its major metabolite. Drug Metab Dispos 1996; 24(12):1401 1403.

84. Kobayashi K, Chiba K, Yagi T, Shimada N, Taniguchi T, Horie T, Tani M, Yamamoto T, Ishizaki T, Kuroiwa Y. Identification of cytochrome P450 isoforms involved in citalopram N demethylation by human liver microsomes. J Pharmacol Exp Ther 1997; 280(2):927 933.
85. Kobayashi K, Kogo M, Tani M, Shimada N, Ishizaki T, Numazawa S, Yoshida T, Yamamoto T, Kuroiwa Y, Chiba K. Role of CYP2C19 in stereoselective hydroxylation of mephobarbital by human liver microsomes. Drug Metab Dispos 2001; 29(1):36 40.
86. Saito K, Dan H, Masuda K, Katsu T, Hanioka N, Yamamoto S, Miyano K, Yamano S, Narimatsu S. Stereoselective hexobarbital 3′ hydroxylation by CYP2C19 expressed in yeast cells and the roles of amino acid residues at positions 300 and 476. Chirality 2007; 19(7):550 558.
87. Gervasini G, Martínez C, Agúndez JA, García Gamito FJ, Benítez J. Inhibition of cytochrome P450 2C9 activity in vitro by 5 hydroxytryptamine and adrenaline. Pharmacogenetics 2001; 11(1):29 37.
88. Facciolá G, Hidestrand M, von Bahr C, Tybring G. Cytochrome P450 isoforms involved in melatonin metabolism in human liver microsomes. Eur J Clin Pharmacol 2001; 56(12):881 888.
89. Yasui Furukori N, Kaneda A, Iwashima K, Saito M, Nakagami T, Tsuchimine S, Kaneko S. Association between cytochrome P450 (CYP) 2C19 polymorphisms and harm avoidance in Japanese. Am J Med Genet B Neuropsychiatr Genet 2007; 144(6):724 727.
90. Riedl AG, Watts PM, Edwards RJ, Schulz Utermoehl T, Boobis AR, Jenner P, Marsden CD. Expression and localisation of CYP2D enzymes in rat basal ganglia. Brain Res 1999; 822 (1 2):175 191.
91. Di Marco A, Yao D, Laufer R. Demethylation of radiolabelled dextromethorphan in rat microsomes and intact hepatocytes. Eur J Biochem 2003; 270(18):3768 3777.
92. Kobayashi K, Urashima K, Shimada N, Chiba K. Substrate specificity for rat cytochrome P450 (CYP) isoforms: screening with cDNA expressed systems of the rat. Biochem Pharmacol 2002; 63(5):889 896.
93. Evans WE, Relling MV. Pharmacogenomics: translating functional genomics into rational therapeutics. Science 1999; 286(5439):487 491.
94. Miksys S, Rao Y, Hoffmann E, Mash DC, Tyndale RF. Regional and cellular expression of CYP2D6 in human brain: higher levels in alcoholics. J Neurochem 2002; 82(6):1376 1387.
95. Chinta SJ, Pai HV, Upadhya SC, Boyd MR, Ravindranath V. Constitutive expression and localization of the major drug metabolizing enzyme, cytochrome P4502D in human brain. Brain Res Mol Brain Res 2002; 103(1 2):49 61.
96. Voirol P, Jonzier Perey M, Porchet F, Reymond MJ, Janzer RC, Bouras C, Strobel HW, Kosel M, Eap CB, Baumann P. Cytochrome P 450 activities in human and rat brain microsomes. Brain Res 2000; 855(2):235 243.
97. Coleman T, Spellman EF, Rostami Hodjegan A, Lennard MS, Tucker GT. The 1′ hydroxylation of Rac bufuralol by rat brain microsomes. Drug Metab Dispos 2000; 28(9):1094 1099.
98. Martínez C, Agúndez JA, Gervasini G, Martín R, Benítez J. Tryptamine: a possible endogenous substrate for CYP2D6. Pharmacogenetics 1997; 7(2):85 93.
99. Hiroi T, Imaoka S, Funae Y. Dopamine formation from tyramine by CYP2D6. Biochem Biophys Res Commun 1998; 249(3):838 843.
100. Gilham DE, Cairns W, Paine MJ, Modi S, Poulsom R, Roberts GC, Wolf CR. Metabolism of MPTP by cytochrome P4502D6 and the demonstration of 2D6 mRNA in human foetal and adult brain by in situ hybridization. Xenobiotica 1997; 27(1):111 125.
101. Armstrong M, Daly AK, Cholerton S, Bateman DN, Idle JR. Mutant debrisoquine hydroxylation genes in Parkinson's disease. Lancet 1992; 339(8800):1017 1018.
102. Kurth MC, Kurth JH. Variant cytochrome P450 CYP2D6 allelic frequencies in Parkinson's disease. Am J Med Genet 1993; 48(3):166 168.
103. Agúndez JA, Jiménez Jiménez FJ, Luengo A, Bernal ML, Molina JA, Ayuso L, Vázquez A, Parra J, Duarte J, Coria F, et al. Association between the oxidative polymorphism and early onset of Parkinson's disease. Clin Pharmacol Ther 1995; 57(3):291 298.
104. McCann SJ, Pond SM, James KM, Le Couteur DG. The association between polymorphisms in the cytochrome P 450 2D6 gene and Parkinson's disease: a case control study and meta analysis. J Neurol Sci 1997; 153(1):50 53.

105. Funae Y, Kishimoto W, Cho T, Niwa T, Hiroi T. CYP2D in the brain. Drug Metab Pharmacokinet 2003; 18(6):337 349.
106. Schumacher M, Guennoun R, Robert F, Carelli C, Gago N, Ghoumari A, Gonzalez Deniselle MC, Gonzalez SL, Ibanez C, Labombarda F, Coirini H, Baulieu EE, De Nicola AF. Local synthesis and dual actions of progesterone in the nervous system: neuroprotection and myelination. Growth Horm IGF Res 2004; 14(Suppl A):S18 33.
107. Dorado P, Penas Lledo EM, Llerena A. CYP2D6 polymorphism: implications for antipsychotic drug response, schizophrenia and personality traits. Pharmacogenomics 2007; 8(11):1597 1608.
108. Crewe HK, Lennard MS, Tucker GT, Woods FR, Haddock RE. The effect of selective serotonin re uptake inhibitors on cytochrome P4502D6 (CYP2D6) activity in human liver microsomes. Br J Clin Pharmacol 1992; 34(3):262 265.
109. Alfaro CL, Lam YW, Simpson J, Ereshefsky L. CYP2D6 inhibition by fluoxetine, paroxetine, sertraline, and venlafaxine in a crossover study: intraindividual variability and plasma concentration correlations. J Clin Pharmacol 2000; 40(1):58 66.
110. Preskorn SH. Clinically relevant pharmacology of selective serotonin reuptake inhibitors. An overview with emphasis on pharmacokinetics and effects on oxidative drug metabolism. Clin Pharmacokinet 1997; 32(Suppl 1):1 21.
111. Nakamura K, Yokoi T, Inoue K, Shimada N, Ohashi N, Kume T, Kamataki T. CYP2D6 is the principal cytochrome P450 responsible for metabolism of the histamine H1 antagonist promethazine in human liver microsomes. Pharmacogenetics 1996; 6(5):449 457.
112. Yue J, Miksys S, Hoffmann E, Tyndale RF. Chronic nicotine treatment induces rat CYP2D in the brain but not in the liver: an investigation of induction and time course. J Psychiatry Neurosci 2008; 33(1):54 63.
113. Hedlund E, Wyss A, Kainu T, Backlund M, Köhler C, Pelto Huikko M, Gustafsson JA, Warner M. Cytochrome P4502D4 in the brain: specific neuronal regulation by clozapine and toluene. Mol Pharmacol 1996; 50(2):342 350.
114. Abraham BK, Adithan C, Shashindran CH, Vasu S, Alekutty NA. Genetic polymorphism of CYP2D6 in a keralite (South India) population. Br J Clin Pharmacol 2000; 49(3):285 286.
115. Bernard S, Neville KA, Nguyen AT, Flockhart DA. Interethnic differences in genetic polymorphisms of CYP2D6 in the U.S. population: clinical implications. Oncologist 2006; 11(2):126 135.
116. Pai HV, Kommaddi RP, Chinta SJ, Mori T, Boyd MR, Ravindranath V. A frameshift mutation and alternate splicing in human brain generate a functional form of the pseudogene cytochrome P4502D7 that demethylates codeine to morphine. J Biol Chem 2004; 279(26):27383 27389.
117. Gaedigk A, Gaedigk R, Leeder JS. CYP2D7 splice variants in human liver and brain: does CYP2D7 encode functional protein? Biochem Biophys Res Commun 2005; 336(4):1241 1250.
118. Bhathena A, Mueller T, Grimm DR, Idler K, Tsurutani A, Spear BB, Katz DA. Frequency of the frame shifting CYP2D7 138delT polymorphism in a large, ethnically diverse sample population. Drug Metab Dispos 2007; 35(8):1251 1253.
119. Pacini P, Orlandini GE, Gulisano M. Statistical study on the circumference of iliac arteries in man. Boll Soc Ital Biol Sper 1977; 53(1 2):93 96.
120. Boutelet Bochan H, Huang Y, Juchau MR. Expression of CYP2E1 during embryogenesis and fetogenesis in human cephalic tissues: implications for the fetal alcohol syndrome. Biochem Biophys Res Commun 1997; 238(2):443 447.
121. Song BJ. Ethanol inducible cytochrome P450 (CYP2E1): biochemistry, molecular biology and clinical relevance: 1996 update. Alcohol Clin Exp Res 1996; 20(8 Suppl):138A 146A.
122. Upadhya SC, Tirumalai PS, Boyd MR, Mori T, Ravindranath V. Cytochrome P4502E (CYP2E) in brain: constitutive expression, induction by ethanol and localization by fluorescence in situ hybridization. Arch Biochem Biophys 2000; 373(1):23 34.
123. Watts PM, Riedl AG, Douek DC, Edwards RJ, Boobis AR, Jenner P, Marsden CD. Co localization of P450 enzymes in the rat substantia nigra with tyrosine hydroxylase. Neuroscience 1998; 86(2):511 519.
124. Brzezinski MR, Boutelet Bochan H, Person RE, Fantel AG, Juchau MR. Catalytic activity and quantitation of cytochrome P 450 2E1 in prenatal human brain. J Pharmacol Exp Ther 1999; 289(3):1648 1653.

125. Nissbrandt H, Bergquist F, Jonason J, Engberg G. Inhibition of cytochrome P450 2E1 induces an increase in extracellular dopamine in rat substantia nigra: a new metabolic pathway? Synapse 2001; 40(4):294 301.
126. Gaedigk A, Baker DW, Totah RA, Gaedigk R, Pearce RE, Vyhlidal CA, Zeldin DC, Leeder JS. Variability of CYP2J2 expression in human fetal tissues. J Pharmacol Exp Ther 2006; 319(2): 523 532.
127. Roman RJ. P 450 metabolites of arachidonic acid in the control of cardiovascular function. Physiol Rev 2002; 82(1):131 185.
128. Saarikoski ST, Wikman HA, Smith G, Wolff CH, Husgafvel Pursiainen K. Localization of cytochrome P450 CYP2S1 expression in human tissues by in situ hybridization and immunohistochemistry. J Histochem Cytochem 2005; 53(5):549 556.
129. Smith G, Wolf CR, Deeni YY, Dawe RS, Evans AT, Comrie MM, Ferguson J, Ibbotson SH. Cutaneous expression of cytochrome P450 CYP2S1: individuality in regulation by therapeutic agents for psoriasis and other skin diseases. Lancet 2003; 361(9366):1336 1343.
130. Karlgren M, Miura S, Ingelman Sundberg M. Novel extrahepatic cytochrome P450s. Toxicol Appl Pharmacol 2005; 207(2 Suppl):57 61.
131. Chuang SS, Helvig C, Taimi M, Ramshaw HA, Collop AH, Amad M, White JA, Petkovich M, Jones G, Korczak B. CYP2U1, a novel human thymus and brain specific cytochrome P450, catalyzes omega and (omega 1) hydroxylation of fatty acids. J Biol Chem 2004; 279(8): 6305 6314.
132. McArthur AG, Hegelund T, Cox RL, Stegeman JJ, Liljenberg M, Olsson U, Sundberg P, Celander MC. Phylogenetic analysis of the cytochrome P450 3 (CYP3) gene family. J Mol Evol 2003; 57(2):200 211.
133. Corley Smith GE, Su HT, Wang Buhler JL, Tseng HP, Hu CH, Hoang T, Chung WG, Buhler DR. CYP3C1, the first member of a new cytochrome P450 subfamily found in zebrafish (Danio rerio). Biochem Biophys Res Commun 2006; 340(4):1039 1046.
134. Shimada T, Yamazaki H, Mimura M, Inui Y, Guengerich FP. Interindividual variations in human liver cytochrome P 450 enzymes involved in the oxidation of drugs, carcinogens and toxic chemicals: studies with liver microsomes of 30 Japanese and 30 Caucasians. J Pharmacol Exp Ther 1994; 270(1):414 423.
135. Krishna DR, Shekar MS. Cytochrome P450 3A: genetic polymorphisms and inter ethnic differences. Methods Find Exp Clin Pharmacol 2005; 27(8):559 567.
136. Eichelbaum M, Burk O. CYP3A genetics in drug metabolism. Nat Med 2001; 7(3):285 287.
137. McFayden MC, Melvin WT, Murray GI. Regional distribution of individual forms of cytochrome P450 mRNA in normal adult human brain. Biochem Pharmacol 1998; 55(6):825 830.
138. Pai HV, Upadhya SC, Chinta SJ, Hegde SN, Ravindranath V. Differential metabolism of alprazolam by liver and brain cytochrome (P4503A) to pharmacologically active metabolite. Pharmacogenomics J 2002; 2(4):243 258.
139. Schuetz JD, Beach DL, Guzelian PS. Selective expression of cytochrome P450 CYP3A mRNAs in embryonic and adult human liver. Pharmacogenetics 1994; 4(1):11 20.
140. Koch I, Weil R, Wolbold R, Brockmöller J, Hustert E, Burk O, Nuessler A, Neuhaus P, Eichelbaum M, Zanger U, Wojnowski L. Interindividual variability and tissue specificity in the expression of cytochrome P450 3A mRNA. Drug Metab Dispos 2002; 30(10):1108 1114.
141. Dragoni S, Bellik L, Frosini M, Matteucci G, Sgaragli G, Valoti M. Cytochrome P450 dependent metabolism of l deprenyl in monkey (Cercopithecus aethiops) and C57BL/6 mouse brain microsomal preparations. J Neurochem 2003; 86(5):1174 1180.
142. Sequeira DJ, Strobel HW. In vitro metabolism of imipramine by brain microsomes: effects of inhibitors and exogenous cytochrome P450 reductase. Brain Res 1996; 738(1):24 31.
143. Bhamre S, Anandatheerathavarada HK, Shankar SK, Boyd MR, Ravindranath V. Purification of multiple forms of cytochrome P450 from a human brain and reconstitution of catalytic activities. Arch Biochem Biophys 1993; 301(2):251 255.
144. Abel SM, Back DJ. Cortisol metabolism in vitro III. Inhibition of microsomal 6 beta hydroxylase and cytosolic 4 ene reductase. J Steroid Biochem Mol Biol 1993; 46(6): 827 832.

145. Waxman DJ, Attisano C, Guengerich FP, Lapenson DP. Human liver microsomal steroid metabolism: identification of the major microsomal steroid hormone 6 beta hydroxylase cytochrome P 450 enzyme. Arch Biochem Biophys 1988; 263(2):424 436.
146. Kerlan V, Dreano Y, Bercovici JP, Beaune PH, Floch HH, Berthou F. Nature of cytochromes P450 involved in the 2 /4 hydroxylations of estradiol in human liver microsomes. Biochem Pharmacol 1992; 44(9):1745 1756.
147. Niwa T, Yabusaki Y, Honma K, Matsuo N, Tatsuta K, Ishibashi F, Katagiri M. Contribution of human hepatic cytochrome P450 isoforms to regioselective hydroxylation of steroid hormones. Xenobiotica 1998; 28(6):539 547.
148. DeVane CL, Donovan JL, Liston HL, Markowitz JS, Cheng KT, Risch SC, Willard L. Comparative CYP3A4 inhibitory effects of venlafaxine, fluoxetine, sertraline, and nefazodone in healthy volunteers. J Clin Psychopharmacol 2004; 24(1):4 10.
149. Schmider J, Greenblatt DJ, von Moltke LL, Harmatz JS, Shader RI. Inhibition of cytochrome P450 by nefazodone in vitro: studies of dextromethorphan O and N demethylation. Br J Clin Pharmacol 1996; 41(4):339 343.
150. Greenblatt DJ, von Moltke LL, Schmider J, Harmatz JS, Shader RI. Inhibition of human cytochrome P450 3A isoforms by fluoxetine and norfluoxetine: in vitro and in vivo studies. J Clin Pharmacol 1996; 36(9):792 798.
151. Wilkinson GR. Drug metabolism and variability among patients in drug response. N Engl J Med 2005; 352(21):2211 2221.
152. Fichtenbaum CJ, Gerber JG. Interactions between antiretroviral drugs and drugs used for the therapy of the metabolic complications encountered during HIV infection. Clin Pharmacokinet 2002; 41(14):1195 1211.
153. Kerr BM, Thummel KE, Wurden CJ, Klein SM, Kroetz DL, Gonzalez FJ, Levy RH. Human liver carbamazepine metabolism. Role of CYP3A4 and CYP2C8 in 10,11 epoxide formation. Biochem Pharmacol 1994; 47(11):1969 1979.
154. Luo G, Cunningham M, Kim S, Burn T, Lin J, Sinz M, Hamilton G, Rizzo C, Jolley S, Gilbert D, Downey A, Mudra D, Graham R, Carroll K, Xie J, Madan A, Parkinson A, Christ D, Selling B, LeCluyse E, Gan LS. CYP3A4 induction by drugs: correlation between a pregnane X receptor reporter gene assay and CYP3A4 expression in human hepatocytes. Drug Metab Dispos 2002; 30(7):795 804.
155. Dimaraki EV, Jaffe CA. Troglitazone induces CYP3A4 activity leading to falsely abnormal dexamethasone suppression test. J Clin Endocrinol Metab 2003; 88(7):3113 3116.
156. Mouly S, Lown KS, Kornhauser D, Joseph JL, Fiske WD, Benedek IH, Watkins PB. Hepatic but not intestinal CYP3A4 displays dose dependent induction by efavirenz in humans. Clin Pharmacol Ther 2002; 72(1):1 9.
157. Willson TM, Kliewer SA. PXR, CAR and drug metabolism. Nat Rev Drug Discov 2002; 1(4):259 266.
158. Stanley LA, Horsburgh BC, Ross J, Scheer N, Wolf CR. PXR and CAR: nuclear receptors which play a pivotal role in drug disposition and chemical toxicity. Drug Metab Rev 2006; 38(3): 515 597.
159. Martínez C, Gervasini G, Agúndez JA, Carrillo JA, Ramos SI, García Gamito FJ, Gallardo L, Benítez J. Modulation of midazolam 1 hydroxylation activity in vitro by neurotransmitters and precursors. Eur J Clin Pharmacol 2000; 56(2):145 151.
160. Nakamura H, Nakasa H, Ishii I, Ariyoshi N, Igarashi T, Ohmori S, Kitada M. Effects of endogenous steroids on CYP3A4 mediated drug metabolism by human liver microsomes. Drug Metab Dispos 2002; 30(5):534 540.
161. Ozdemir V, Kalow W, Tang BK, Paterson AD, Walker SE, Endrenyi L, Kashuba AD. Evaluation of the genetic component of variability in CYP3A4 activity: a repeated drug administration method. Pharmacogenetics 2000; 10(5):373 388.
162. Thummel KE, Wilkinson GR. In vitro and in vivo drug interactions involving human CYP3A. Annu Rev Pharmacol Toxicol 1998; 38:389 430.
163. Huang W, Lin YS, McConn DJ 2nd, Calamia JC, Totah RA, Isoherranen N, Glodowski M, Thummel KE. Evidence of significant contribution from CYP3A5 to hepatic drug metabolism. Drug Metab Dispos 2004; 32(12):1434 1445.

164. Allqvist A, Miura J, Bertilsson L, Mirghani RA. Inhibition of CYP3A4 and CYP3A5 catalyzed metabolism of alprazolam and quinine by ketoconazole as racemate and four different enantiomers. Eur J Clin Pharmacol 2007; 63(2):173 179.
165. Domanski TL, Finta C, Halpert JR, Zaphiropoulos PG. cDNA cloning and initial character ization of CYP3A43, a novel human cytochrome P450. Mol Pharmacol 2001; 59(2):386 392.
166. Westlind A, Malmebo S, Johansson I, Otter C, Andersson TB, Ingelman Sundberg M, Oscarson M. Cloning and tissue distribution of a novel human cytochrome p450 of the CYP3A subfamily, CYP3A43. Biochem Biophys Res Commun 2001; 281(5):1349 1355.
167. Wang MH, Guan H, Nguyen X, Zand BA, Nasjletti A, Laniado Schwartzman M. Contribution of cytochrome P 450 4A1 and 4A2 to vascular 20 hydroxyeicosatetraenoic acid synthesis in rat kidneys. Am J Physiol 1999; 276(2 Pt 2):F246 F253.
168. Zhang F, Wang MH, Krishna UM, Falck JR, Laniado Schwartzman M, Nasjletti A. Modulation by 20 HETE of phenylephrine induced mesenteric artery contraction in spontaneously hypertensive and Wistar Kyoto rats. Hypertension 2001; 38(6):1311 1315.
169. Singh H, Cheng J, Deng H, Kemp R, Ishizuka T, Nasjletti A, Schwartzman ML. Vascular cytochrome P450 4A expression and 20 hydroxyeicosatetraenoic acid synthesis contribute to endothelial dysfunction in androgen induced hypertension. Hypertension 2007; 50(1):123 129.
170. Metea MR, Newman EA. Glial cells dilate and constrict blood vessels: a mechanism of neurovascular coupling. J Neurosci 2006; 26(11):2862 2870.
171. Roy CS, Sherrington CS. On the Regulation of the Blood supply of the Brain. J Physiol 1890; 11(1 2):85 158.17.
172. Iadecola C. Neurovascular regulation in the normal brain and in Alzheimer's disease. Nat Rev Neurosci 2004; 5(5):347 360.
173. Koehler RC, Gebremedhin D, Harder DR. Role of astrocytes in cerebrovascular regulation. J Appl Physiol 2006; 100(1):307 317.
174. Harder DR, Alkayed NJ, Lange AR, Gebremedhin D, Roman RJ. Functional hyperemia in the brain: hypothesis for astrocyte derived vasodilator metabolites. Stroke 1998; 29(1):229 234.
175. Anderson CM, Nedergaard M. Astrocyte mediated control of cerebral microcirculation. Trends Neurosci 2003; 26(7):340 344; author reply 344 345.
176. Chen L, Hardwick JP. Identification of a new P450 subfamily, CYP4F1, expressed in rat hepatic tumors. Arch Biochem Biophys 1993; 300(1):18 23.
177. Kawashima H, Strobel HW. cDNA cloning of three new forms of rat brain cytochrome P450 belonging to the CYP4F subfamily. Biochem Biophys Res Commun 1995; 217(3):1137 1144.
178. Kalsotra A, Strobel HW. Cytochrome P450 4F subfamily: at the crossroads of eicosanoid and drug metabolism. Pharmacol Ther 2006; 112(3):589 611.
179. Bylund J, Harder AG, Maier KG, Roman RJ, Harder DR. Leukotriene B4 omega side chain hydroxylation by CYP4F5 and CYP4F6. Arch Biochem Biophys 2003; 412(1):34 41.
180. Xu F, Falck JR, Ortiz de Montellano PR, Kroetz DL. Catalytic activity and isoform specific inhibition of rat cytochrome p450 4F enzymes. J Pharmacol Exp Ther 2004; 308(3):887 895.
181. Boehme CL, Strobel HW. In vitro metabolism of chlorpromazine by cytochromes P450 4F4 and 4F5 and the inhibitory effect of imipramine. Neurotox Res 2001; 3(4):329 337.
182. Kawashima H, Sequeira DJ, Nelson DR, Strobel HW. Genomic cloning and protein expression of a novel rat brain cytochrome P 450 CYP2D18* catalyzing imipramine N demethylation. J Biol Chem 1996; 271(45):28176 28180.
183. Kikuta Y, Kasyu H, Kusunose E, Kusunose M. Expression and catalytic activity of mouse leukotriene B4 omega hydroxylase, CYP4F14. Arch Biochem Biophys 2000; 383(2):225 232.
184. Cui X, Kawashima H, Barclay TB, Peters JM, Gonzalez FJ, Morgan ET, Strobel HW. Molecular cloning and regulation of expression of two novel mouse CYP4F genes: expression in peroxisome proliferator activated receptor alpha deficient mice upon lipopolysaccharide and clofibrate challenges. J Pharmacol Exp Ther 2001; 296(2):542 550.
185. Christmas P, Tolentino K, Primo V, Berry KZ, Murphy RC, Chen M, Lee DM, Soberman RJ. Cytochrome P 450 4F18 is the leukotriene B4 omega 1/omega 2 hydroxylase in mouse polymorphonuclear leukocytes: identification as the functional orthologue of human

polymorphonuclear leukocyte CYP4F3A in the down regulation of responses to LTB4. J Biol Chem 2006; 281(11):7189 7196.
186. Hashizume T, Imaoka S, Hiroi T, Terauchi Y, Fujii T, Miyazaki H, Kamataki T, Funae Y. cDNA cloning and expression of a novel cytochrome p450 (cyp4f12) from human small intestine. Biochem Biophys Res Commun 2001; 280(4):1135 1141.
187. Bylund J, Bylund M, Oliw EH. cDna cloning and expression of CYP4F12, a novel human cytochrome P450. Biochem Biophys Res Commun 2001; 280(3):892 897.
188. Hashizume T, Imaoka S, Mise M, Terauchi Y, Fujii T, Miyazaki H, Kamataki T, Funae Y. Involvement of CYP2J2 and CYP4F12 in the metabolism of ebastine in human intestinal microsomes. J Pharmacol Exp Ther 2002; 300(1):298 304.
189. Kalsotra A, Turman CM, Kikuta Y, Strobel HW. Expression and characterization of human cytochrome P450 4F11: Putative role in the metabolism of therapeutic drugs and eicosanoids. Toxicol Appl Pharmacol 2004; 199(3):295 304.
190. Lasker JM, Chen WB, Wolf I, Bloswick BP, Wilson PD, Powell PK. Formation of 20 hydroxyeicosatetraenoic acid, a vasoactive and natriuretic eicosanoid, in human kidney. Role of Cyp4F2 and Cyp4A11. J Biol Chem 2000; 275(6):4118 4126.
191. Ghahramani P, Ellis SW, Lennard MS, Ramsay LE, Tucker GT. Cytochromes P450 mediating the N demethylation of amitriptyline. Br J Clin Pharmacol 1997; 43(2):137 144.
192. Schmider J, Greenblatt DJ, von Moltke LL, Harmatz JS, Shader RI. N demethylation of amitriptyline in vitro: role of cytochrome P 450 3A (CYP3A) isoforms and effect of metabolic inhibitors. J Pharmacol Exp Ther 1995; 275(2):592 597.
193. Dahl ML, Johansson I, Palmertz MP, Ingelman Sundberg M, Sjöqvist F. Analysis of the CYP2D6 gene in relation to debrisoquin and desipramine hydroxylation in a Swedish population. Clin Pharmacol Ther 1992; 51(1):12 17.
194. Brosen K, Zeugin T, Meyer UA. Role of P450IID6, the target of the sparteine debrisoquin oxidation polymorphism, in the metabolism of imipramine. Clin Pharmacol Ther 1991; 49(6):609 617.
195. Koyama E, Chiba K, Tani M, Ishizaki T. Identification of human cytochrome P450 isoforms involved in the stereoselective metabolism of mianserin enantiomers. J Pharmacol Exp Ther 1996; 278(1):21 30.
196. Pfandl B, Mörike K, Winne D, Schareck W, Breyer Pfaff U. Stereoselective inhibition of nortriptyline hydroxylation in man by quinidine. Xenobiotica 1992; 22(6):721 730.
197. Spigset O, Axelsson S, Norström A, Hägg S, Dahlqvist R. The major fluvoxamine metabolite in urine is formed by CYP2D6. Eur J Clin Pharmacol 2001; 57(9):653 658.
198. Bloomer JC, Woods FR, Haddock RE, Lennard MS, Tucker GT. The role of cytochrome P4502D6 in the metabolism of paroxetine by human liver microsomes. Br J Clin Pharmacol 1992; 33(5):521 523.
199. Fang J, Baker GB, Silverstone PH, Coutts RT. Involvement of CYP3A4 and CYP2D6 in the metabolism of haloperidol. Cell Mol Neurobiol 1997; 17(2):227 233.
200. Sun YE. Neurogenic tumors of the mediastinum. Zhonghua Wai Ke Za Zhi 1984; 22(10):588 590, 637.
201. Shin JG, Soukhova N, Flockhart DA. Effect of antipsychotic drugs on human liver cytochrome P 450 (CYP) isoforms in vitro: preferential inhibition of CYP2D6. Drug Metab Dispos 1999; 27(9):1078 1084.
202. Dayer P, Desmeules J, Collart L. Pharmacology of tramadol. Drugs 1997; 53(suppl 2):18 24.
203. Related Articles, LinksShams ME, Arneth B, Hiemke C, Dragicevic A, Müller MJ, Kaiser R, Lackner K, Härtter S. CYP2D6 polymorphism and clinical effect of the antidepressant venlafaxine. J Clin Pharm Ther 2006; 31(5):493 502.
204. Fogelman SM, Schmider J, Venkatakrishnan K, von Moltke LL, Harmatz JS, Shader RI, Greenblatt DJ. O and N demethylation of venlafaxine in vitro by human liver microsomes and by microsomes from cDNA transfected cells: effect of metabolic inhibitors and SSRI antidepressants. Neuropsychopharmacology 1999; 20(5):480 490.
205. Fischer V, Vickers AE, Heitz F, Mahadevan S, Baldeck JP, Minery P, Tynes R. The polymorphic cytochrome P 4502D6 is involved in the metabolism of both 5 hydroxytrypt amine antagonists, tropisetron and ondansetron. Drug Metab Dispos 1994; 22(2):269 274.

206. Olesen OV, Linnet K. Identification of the human cytochrome P450 isoforms mediating in vitro N dealkylation of perphenazine. Br J Clin Pharmacol 2000; 50(6):563 571.
207. Bach MV, Coutts RT, Baker GB. Involvement of CYP2D6 in the in vitro metabolism of amphetamine, two N alkylamphetamines and their 4 methoxylated derivatives. Xenobiotica 1999; 29(7):719 732.
208. Liu Z, Mortimer O, Smith CA, Wolf CR, Rane A. Evidence for a role of cytochrome P450 2D6 and 3A4 in ethylmorphine metabolism. Br J Clin Pharmacol 1995; 39(1):77 80.
209. Desta Z, Wu GM, Morocho AM, Flockhart DA. The gastroprokinetic and antiemetic drug metoclopramide is a substrate and inhibitor of cytochrome P450 2D6. Drug Metab Dispos 2002; 30(3):336 343.
210. Caccia S. N dealkylation of arylpiperazine derivatives: disposition and metabolism of the 1 aryl piperazines formed. Curr Drug Metab 2007; 8(6):612 622.
211. Eap CB, Bertel Laubscher R, Zullino D, Amey M, Baumann P. Marked increase of venlafaxine enantiomer concentrations as a consequence of metabolic interactions: a case report. Pharmacopsychiatry 2000; 33(3):112 115.
212. Berecz R, Dorado P, De La Rubia A, Cáceres MC, Degrell I, LLerena A. The role of cytochrome P450 enzymes in the metabolism of risperidone and its clinical relevance for drug interactions. Curr Drug Targets 2004; 5(6):573 579.
213. Obach RS, Pablo J, Mash DC. Cytochrome P4502D6 catalyzes the O demethylation of the psychoactive alkaloid ibogaine to 12 hydroxyibogamine. Drug Metab Dispos 1998; 26(8): 764 768.
214. Related Articles, LinksGut I, Nedelcheva V, Soucek P, Stopka P, Vodicka P, Gelboin HV, Ingelman Sundberg M. The role of CYP2E1 and 2B1 in metabolic activation of benzene derivatives. Arch Toxicol 1996; 71(1 2):45 56.
215. Manyike PT, Kharasch ED, Kalhorn TF, Slattery JT. Contribution of CYP2E1 and CYP3A to acetaminophen reactive metabolite formation. Clin Pharmacol Ther 2000; 67(3):275 282.
216. Kharasch ED, Thummel KE. Identification of cytochrome P450 2E1 as the predominant enzyme catalyzing human liver microsomal defluorination of sevoflurane, isoflurane, and methoxyflurane. Anesthesiology 1993; 79(4):795 807.
217. Raijmakers PG, Groeneveld AB, Rauwerda JA, Schneider AJ, Teule GJ, Hack CE, Thijs LG. Transient increase in interleukin 8 and pulmonary microvascular permeability following aortic surgery. Am J Respir Crit Care Med 1995; 151(3 pt 1):698 705.
218. Gasche Y, Daali Y, Fathi M, Chiappe A, Cottini S, Dayer P, Desmeules J. Codeine intoxication associated with ultrarapid CYP2D6 metabolism. N Engl J Med 2004; 351(27): 2827 2831.
219. Wang JS, DeVane CL. Involvement of CYP3A4, CYP2C8, and CYP2D6 in the metabolism of (R) and (S) methadone in vitro. Drug Metab Dispos 2003; 31(6):742 747.
220. Kobayashi K, Yamamoto T, Chiba K, Tani M, Shimada N, Ishizaki T, Kuroiwa Y. Human buprenorphine N dealkylation is catalyzed by cytochrome P450 3A4. Drug Metab Dispos 1998; 26(8):818 821.
221. Labroo RB, Paine MF, Thummel KE, Kharasch ED. Fentanyl metabolism by human hepatic and intestinal cytochrome P450 3A4: implications for interindividual variability in disposition, efficacy, and drug interactions. Drug Metab Dispos 1997; 25(9):1072 1080.
222. Hirota N, Ito K, Iwatsubo T, Green CE, Tyson CA, Shimada N, Suzuki H, Sugiyama Y. In vitro/in vivo scaling of alprazolam metabolism by CYP3A4 and CYP3A5 in humans. Biopharm Drug Dispos 2001; 22(2):53 71.
223. Ono S, Hatanaka T, Miyazawa S, Tsutsui M, Aoyama T, Gonzalez FJ, Satoh T. Human liver microsomal diazepam metabolism using cDNA expressed cytochrome P450s: role of CYP2B6, 2C19 and the 3A subfamily. Xenobiotica 1996; 26(11):1155 1166.
224. Kronbach T, Mathys D, Umeno M, Gonzalez FJ, Meyer UA. Oxidation of midazolam and triazolam by human liver cytochrome P450IIIA4. Mol Pharmacol 1989; 36(1):89 96.
225. Reilly PE, Thompson DA, Mason SR, Hooper WD. Cytochrome P450IIIA enzymes in rat liver microsomes: involvement in C3 hydroxylation of diazepam and nordazepam but not N dealkylation of diazepam and temazepam. Mol Pharmacol 1990; 37(5):767 774.

226. Patki KC, Von Moltke LL, Greenblatt DJ. In vitro metabolism of midazolam, triazolam, nifedipine, and testosterone by human liver microsomes and recombinant cytochromes p450: role of cyp3a4 and cyp3a5. Drug Metab Dispos 2003; 31(7):938 944.
227. Renwick AB, Mistry H, Ball SE, Walters DG, Kao J, Lake BG. Metabolism of Zaleplon by human hepatic microsomal cytochrome P450 isoforms. Xenobiotica 1998; 28(4):337 348.
228. Pichard L, Gillet G, Bonfils C, Domergue J, Thénot JP, Maurel P. Oxidative metabolism of zolpidem by human liver cytochrome P450S. Drug Metab Dispos 1995; 23(11):1253 1262.
229. Von Moltke LL, Greenblatt DJ, Granda BW, Duan SX, Grassi JM, Venkatakrishnan K, Harmatz JS, Shader RI. Zolpidem metabolism in vitro: responsible cytochromes, chemical inhibitors, and in vivo correlations. Br J Clin Pharmacol 1999; 48(1):89 97.
230. Gorski JC, Jones DR, Wrighton SA, Hall SD. Characterization of dextromethorphan N demethylation by human liver microsomes. Contribution of the cytochrome P450 3A (CYP3A) subfamily. Biochem Pharmacol 1994; 48(1):173 182.
231. Nielsen KK, Flinois JP, Beaune P, Brøsen K. The biotransformation of clomipramine in vitro, identification of the cytochrome P450s responsible for the separate metabolic pathways. J Pharmacol Exp Ther 1996; 277(3):1659 1664.
232. Rotzinger S, Fang J, Baker GB. Trazodone is metabolized to m chlorophenylpiperazine by CYP3A4 from human sources. Drug Metab Dispos 1998; 26(6):572 575.
233. Zhu M, Zhao W, Jimenez H, Zhang D, Yeola S, Dai R, Vachharajani N, Mitroka J. Cytochrome P450 3A mediated metabolism of buspirone in human liver microsomes. Drug Metab Dispos 2005; 33(4):500 507.
234. Fabre G, Julian B, Saint Aubert B, Joyeux H, Berger Y. Evidence for CYP3A mediated N deethylation of amiodarone in human liver microsomal fractions. Drug Metab Dispos 1993; 21(6): 978 985.
235. Butler AM, Murray M. Biotransformation of parathion in human liver: participation of CYP3A4 and its inactivation during microsomal parathion oxidation. J Pharmacol Exp Ther 1997; 280(2):966 973.
236. Serkova NJ, Christians U, Benet LZ. Biochemical mechanisms of cyclosporine neurotoxicity. Mol Interv 2004; 4(2):97 107.
237. Kronbach T, Fischer V, Meyer UA. Cyclosporine metabolism in human liver: identification of a cytochrome P 450III gene family as the major cyclosporine metabolizing enzyme explains interactions of cyclosporine with other drugs. Clin Pharmacol Ther 1988; 43(6):630 635.
238. Pichard L, Fabre I, Fabre G, Domergue J, Saint Aubert B, Mourad G, Maurel P. Cyclosporin A drug interactions. Screening for inducers and inhibitors of cytochrome P 450 (cyclosporin A oxidase) in primary cultures of human hepatocytes and in liver microsomes. Drug Metab Dispos 1990; 18(5):595 606.
239. Yamaori S, Yamazaki H, Suzuki A, Yamada A, Tani H, Kamidate T, Fujita K, Kamataki T. Effects of cytochrome b(5) on drug oxidation activities of human cytochrome P450 (CYP) 3As: similarity of CYP3A5 with CYP3A4 but not CYP3A7. Biochem Pharmacol 2003; 66(12):2333 2340.
240. Matsunaga T, Kishi N, Higuchi S, Watanabe K, Ohshima T, Yamamoto I. CYP3A4 is a major isoform responsible for oxidation of 7 hydroxy Delta(8) tetrahydrocannabinol to 7 oxo delta(8) tetrahydrocannabinol in human liver microsomes. Drug Metab Dispos 2000; 28(11):1291 1296.
241. Watanabe K, Yamaori S, Funahashi T, Kimura T, Yamamoto I. Cytochrome P450 enzymes involved in the metabolism of tetrahydrocannabinols and cannabinol by human hepatic microsomes. Life Sci 2007; 80(15):1415 1419.
242. Hiratsuka M, Hinai Y, Sasaki T, Konno Y, Imagawa K, Ishikawa M, Mizugaki M. Characterization of human cytochrome p450 enzymes involved in the metabolism of cilostazol. Drug Metab Dispos 2007; 35(10):1730 1732.
243. Ríos C, Nader Kawachi J, Rodriguez Payán AJ, Nava Ruiz C. Neuroprotective effect of dapsone in an occlusive model of focal ischemia in rats. Brain Res 2004; 999(2):212 215.
244. Fleming CM, Branch RA, Wilkinson GR, Guengerich FP. Human liver microsomal N hydroxylation of dapsone by cytochrome P 4503A4. Mol Pharmacol 1992; 41(5):975 980.

245. Gentile DM, Tomlinson ES, Maggs JL, Park BK, Back DJ. Dexamethasone metabolism by human liver in vitro. Metabolite identification and inhibition of 6 hydroxylation. J Pharmacol Exp Ther 1996; 277(1):105 112.
246. Paquet Durand F, Gierse A, Bicker G. Diltiazem protects human NT 2 neurons against excitotoxic damage in a model of simulated ischemia. Brain Res 2006; 1124(1):45 54.
247. Sutton D, Butler AM, Nadin L, Murray M. Role of CYP3A4 in human hepatic diltiazem N demethylation: inhibition of CYP3A4 activity by oxidized diltiazem metabolites. J Pharmacol Exp Ther 1997; 282(1):294 300.
248. Chen J, Zhang C, Jiang H, Li Y, Zhang L, Robin A, Katakowski M, Lu M, Chopp M. Atorvastatin induction of VEGF and BDNF promotes brain plasticity after stroke in mice. J Cereb Blood Flow Metab 2005; 25(2):281 290.
249. Law M, Rudnicka AR. Statin safety: a systematic review. Am J Cardiol 2006; 97(8A):52C 60C.
250. Delanty N, Vaughan CJ, Sheehy N. Statins and neuroprotection. Expert Opin Investig Drugs 2001; 10(10):1847 1853.
251. Furuichi Y, Katsuta K, Maeda M, Ueyama N, Moriguchi A, Matsuoka N, Goto T, Yanagihara T. Neuroprotective action of tacrolimus (FK506) in focal and global cerebral ischemia in rodents: dose dependency, therapeutic time window and long term efficacy. Brain Res 2003; 965(1 2):137 145.
252. Iwasaki K. Metabolism of tacrolimus (FK506) and recent topics in clinical pharmacokinetics. Drug Metab Pharmacokinet 2007; 22(5):328 335.
253. Ha HR, Chen J, Krahenbuhl S, Follath F. Biotransformation of caffeine by cDNA expressed human cytochromes P 450. Eur J Clin Pharmacol 1996; 49(4):309 315.
254. Tassaneeyakul W, Birkett DJ, McManus ME, Tassaneeyakul W, Veronese ME, Andersson T, Tukey RH, Miners JO. Caffeine metabolism by human hepatic cytochromes P450: contributions of 1A2, 2E1 and 3A isoforms. Biochem Pharmacol 1994; 47(10):1767 1776.
255. Nakasa H, Nakamura H, Ono S, Tsutsui M, Kiuchi M, Ohmori S, Kitada M. Prediction of drug drug interactions of zonisamide metabolism in humans from in vitro data. Eur J Clin Pharmacol 1998; 54(2):177 183.
256. Stiff DD, Robicheau JT, Zemaitis MA. Reductive metabolism of the anticonvulsant agent zonisamide, a 1,2 benzisoxazole derivative. Xenobiotica 1992; 22(1):1 11.
257. Laurenzana EM, Owens SM. Metabolism of phencyclidine by human liver microsomes. Drug Metab Dispos 1997; 25(5):557 563.
258. Swainston Harrison T, Perry CM. Aripiprazole: a review of its use in schizophrenia and schizoaffective disorder. Drugs 2004; 64(15):1715 1736.
259. Ward BA, Morocho A, Kandil A, Galinsky RE, Flockhart DA, Desta Z. Characterization of human cytochrome P450 enzymes catalyzing domperidone N dealkylation and hydroxylation in vitro. Br J Clin Pharmacol 2004; 58(3):277 287.
260. Kalgutkar AS, Taylor TJ, Venkatakrishnan K, Isin EM. Assessment of the contributions of CYP3A4 and CYP3A5 in the metabolism of the antipsychotic agent haloperidol to its potentially neurotoxic pyridinium metabolite and effect of antidepressants on the bioactivation pathway. Drug Metab Dispos 2003; 31(3):243 249.
261. Yun CH, Okerholm RA, Guengerich FP. Oxidation of the antihistaminic drug terfenadine in human liver microsomes. Role of cytochrome P 450 3A(4) in N dealkylation and C hydroxylation. Drug Metab Dispos 1993; 21(3):403 409.
262. Bornheim LM. Effect of cytochrome P450 inducers on cocaine mediated hepatotoxicity. Toxicol Appl Pharmacol 1998; 150(1):158 165.
263. Garcion E, Wion Barbot N, Montero Menei CN, Berger F, Wion D. New clues about vitamin D functions in the nervous system. Trends Endocrinol Metab 2002; 13(3):100 105.
264. Gupta RP, He YA, Patrick KS, Halpert JR, Bell NH. CYP3A4 is a vitamin D 24 and 25 hydroxylase: analysis of structure function by site directed mutagenesis. J Clin Endocrinol Metab 2005; 90(2):1210 1219.

14
LC-MS Analysis in Drug Metabolism Studies

Stacy L. Gelhaus and Ian A. Blair
Centers for Cancer Pharmacology and Excellence in Environmental Toxicology, Department of Pharmacology, University of Pennsylvania, Philadelphia, Pennsylvania, U.S.A.

INTRODUCTION

New chemical entities (NCE) are constantly being developed as potential pharmaceuticals for the treatment of cardiovascular disease, cancer, and a variety of other developmental and hereditary diseases. Studies of drug absorption, distribution, metabolism, and excretion, (ADME) as well as drug metabolism and pharmacokinetic (DMPK) studies of NCEs require the use of sound analytical methodology that is sensitive, selective, accurate, precise, robust, and reproducible. Of the numerous, evolving bioanalytical methods for ADME and DMPK studies, liquid chromatography (LC) mass spectrometry (MS) has emerged as the preferred technique because it can fulfill all of these methodological criteria. More recently, LC-MS instrumentation has improved in an attempt to keep up with the demands of the pharmaceutical industry. Here we will review the most common instrumentation and ionization techniques used for analysis of drugs and their metabolites.

The use of MS as a detection technique coupled to LC requires that the analyte is first ionized in the gas phase. Therefore, early LC-MS analyses focused mainly on volatile organic compounds. Aqueous analytes had to be first extracted into organic solvents, which did not always result in acceptable ionization, and so methodology based on gas chromatography (GC)-MS was generally preferred in earlier studies of drug metabolism and disposition (1). Derivatization of polar functional groups, which was used to enhance extraction efficiency into organic solvents and/or to increase volatility, often resulted in enhanced MS sensitivity (2). Derivatization is time consuming and tedious, which often resulted in low sample throughput. These issues coupled with problems involved in analyzing thermally labile and involatile samples led to intense research into the use of LC-MS as a potentially more efficient alternative.

Coupling LC separation techniques to MS was more challenging than linking GC with MS because the analytes had to be ionized in the gas phase at room temperatures before entering the mass spectrometer. Therefore, the development of atmospheric pressure ionization (API) techniques, which moved away from low-pressure sources such as electron impact, chemical ionization, and fast atom bombardment, greatly aided in the development of LC-MS techniques. Since the mid-1980s, it has been possible to analyze

pharmaceutical compounds and their metabolites directly from biological matrices using LC-MS methodology. Aside from the lack of tedious derivatization and sample preparation of GC, LC separation does not expose samples to excessive heat, and sample throughput is generally higher (3). This is why LC-MS has become the method of choice for analyses of drugs and their metabolites (4).

LIQUID CHROMATOGRAPHY

LC separation techniques commonly used with MS are reversed-phase and normal phase. Ion exchange chromatography is often used as the first dimension in 2-D chromatography, which is employed in proteomics. Unfortunately, this methodology cannot be used as a separation phase alone because of the high salt content of the mobile phase. Reversed-phase is most common and can be used for a wide range of analytes including small molecules and biomolecules such as DNA and protein. Normal phase, or adsorption chromatography, is used to separate polar compounds where the strength of the interaction depends not only on the functional groups but also on steric factors; therefore, isomers are more easily separated using normal phase (5). Chiral chromatography, a branch of chromatography, is used to resolve optically pure substances, which has become extremely important for the pharmaceutical industry. Chiral stationary phases can be normal or reversed phase in nature. However, normal phase methods using cellulose-coated silica stationary phases tend to be more efficient for complex chiral separations (6).

IONIZATION METHODS FOR LC-MS

The ability of the source to sublimate incoming molecules is of utmost importance to the operation and success of LC-MS. An effective ion source should provide high sensitivity and reproducible spectra. A typical API source contains a probe, inert gas for solvent flow, evaporation and desolvation, a sampling cone, and transfer optics to the mass analyzer (7,8). The most commonly used sources are electrospray ionization (ESI) and atmospheric pressure chemical ionization (APCI) (9,10). This section will also touch on the offshoots of APCI, atmospheric pressure photo ionization (APPI) and atmospheric pressure laser ionization (APLI) (11).

Electrospray Ionization

ESI was first described in the mid-1980s (12,13) by John Fenn, who received the Nobel Prize in Chemistry in 2002 for his pioneering studies on proteins together with Koichi Tanaka and Kurt Wuthrich for their studies on macromolecules using matrix assisted laser desorption ionization (MALDI) and NMR, respectively. An aqueous LC effluent is transferred into the source through a metallic needle, which is surrounded by nitrogen gas. A voltage is also applied to the needle (2 8 kV), creating charged solution droplets. A heating device located within the source concentrates the droplets, which increases their charge density (14). The increase in charge to surface area due to evaporation results in a Coulombic explosion that affords vaporized analyte ions to enter the mass analyzer. The droplet charge can be positive or negative depending on the voltage polarity of the capillary. For macromolecules such as DNA and proteins, multiply charged ions can form, which makes it possible to conduct analyses with relatively low mass range instruments. Lower molecular weight drugs and their metabolites tend to form primarily singly charged ions corresponding either to protonated molecules in the positive mode or

to deprotonated molecules in the negative mode. The use of nanoliter flow rates using a nanospray methodology can significantly improve the efficiency of ionization, making it possible to significantly increase sensitivity of metabolite detection (15).

Atmospheric Pressure Chemical Ionization

APCI is probably the second most used API technique. In APCI, the aqueous phase enters the source through a glass capillary surrounded by carrier gas and encased within a heated block. The combination of high temperature (450 550°C) and carrier gas nebulizes both solvent and analyte molecules in the source, which envelop a corona discharge needle. The electrode, whose discharge causes the electrical breakdown of its adjacent atmosphere, otherwise known as the corona effect, ionizes the solution mist. The ionized droplets then react through acid-base chemistry with analyte molecules to form the ions that enter the mass analyzer (16). APCI requires thermally inert, volatile analytes and volatile HPLC mobile phases amendable to gas-phase acid-base reactions (17). This ionization technique is very well suited to neutral, nonpolar compounds. One advantage over ESI is the ability to use HPLC flow rates suited to analytical-size columns (4.6 mm I.D.). Ultrahigh sensitivity can be attained using electron capture APCI (18). This technique is useful for the analysis of drugs and their metabolites that are naturally electron capturing or after the attachment of an electron-capturing derivative such as a pentafluorobenzyl ester (19). The technique can also be employed in highly efficient chiral separations of trace amounts of analytes (6).

Atmospheric Pressure Photo Ionization

APPI is similar to APCI in that it uses a modified APCI source fitted with a heated nebulizer to facilitate LC effluent vaporization (9). Instead of ionizing the analyte using a corona discharge, APPI uses a krypton vacuum ultraviolet lamp as a source of 10-eV photons to ionize the analyte either directly or indirectly through an ionizable dopant. In APPI, the ionization potential remains below those of HPLC solvents, yet within the range of the majority of organic compounds. APPI is very sensitive and is noted for its ability to ionize compounds that have been hard to ionize or are characterized as poor ionizers in ESI and APCI sources.

Atmospheric Pressure Laser Ionization

APLI is the most recent API technique with potential utility for high-sensitivity drug metabolism studies (11). APLI replaces the krypton vacuum UV lamp in APPI with a stepwise two-photon ionization, greatly enhancing the selectivity of the ionization process. In addition, photo flux during an ionization event is drastically increased, leading to very low limits of detection. APLI operates directly on the analyte, allowing for efficient ionization of even the most nonpolar compounds.

MASS ANALYZERS FOR LC-MS

Quadrupole Mass Analyzers

The most commonly used quadrupole mass spectrometer for drug metabolism studies is the triple-stage quadrupole (TSQ). This mass analyzer was a much needed improvement over the single-stage quadrupole (SSQ), which contains a source, “Q0,” a lens that

Table 1 Comparison of a Triple Quadrupole Mass Spectrometer and 3D Ion Trap

QqQ	3D Ion trap
Advantages	Advantages
Selective MS/MS scans	MS^n capabilities
Mass range 30 Th to 1800/2000 Th	Excellent sensitivity in full scan and product ion scan
Fragmentation patterns include direct bond cleavage and metastable decay in a single spectrum	Very fast scan rates
Limitations	Limitations
Low duty cycle in full scan and product ion scan	1/3 mass range limit
Poor resolution	Fragmentation limited to lowest energy pathway
Poor mass accuracy	Space charge limitations
	Poor mass accuracy

transports the ions to the mass analyzer, and the single-quadrupole "Q1." The Q1 will work in full scan mode, scanning a range of *m/z* values or can perform selected ion monitoring (SIM), which filters ions for a specific *m/z*. TSQ can perform all of the scans that are available using SSQ; however, the data set is much richer because of the ability of TSQ to perform multiple reaction monitoring (MRM), precursor ion (PI), and constant neutral loss (CNL) scans (Table 1). Like the SSQ, the TSQ instrument contains the ion source, Q0, and Q1, but is also tandem to Q2, a collision chamber, and a second mass analyzer Q3. Ions are filtered in Q1 for the desired spectra and then fragmented by inert gas molecules (Ar or N_2) in Q2. The product ions are scanned in Q3 before reaching the detector. PI scans allow for the extraction of ions from the Q1 data set that contains a specific parent ion, which aids in the MS selection of drug-related ions. In PI scanning, Q1 scans a range of *m/z* values where Q3 filters for the specified product ion. Therefore, only Q1 ions that generate the specific product ion screened by Q3 will be recorded for data analysis. In a CNL scan, both Q1 and Q3 scan a range of *m/z* values with a mass offset equal to the mass of a designated uncharged fragment lost upon Q2 fragmentation. Only Q1 ions that produce a neutral loss are detected. These various TSQ scanning techniques provide much richer data sets for drug metabolism studies than can be obtained with SSQ instruments.

Ion Trap Mass Analyzers

Ion traps are composed of an ion source, a quadrupole ion trap, and a mass analyzer. Like the linear quadrupole, ion traps have great sensitivity, specificity, and scan speed, but they are not able to perform PI or CNL scanning (Table 1). The full scan of an ion trap is at least ten times more sensitive than that of a quadrupole. The increased sensitivity of the ion trap is a result of its ability to confine gaseous ions during a pulsed mode via changes in amplitude of radiofrequency potential, thus allowing the accumulation of ions within the trap without filtering. Conventional ion traps (LCQ) are known as 3D traps because of their hyperboloid geometry of the three-electrode ion trap. These traps have insufficient ion storage efficiency, capacity, and deterioration of the mass spectrum and dynamic response range (Table 1). In response to these shortcomings, the linear (or 2-D) ion trap (LIT) was developed, such as the LTQ (Thermo-Fisher, San Jose, California, U.S.). The

Table 2 QTrap Scan Modes

Q1 Scan	Q1 scan, q2 rf only, Q3 rf only
Q3 Scan	Q1 rf only, q2 rf only, Q3 scanning
Product ion	Q1 fixed, q2 fragmenting, Q3 scanning
Precursor ion	Q1 scanning, q2 fragmenting, Q3 fixed
Neutral loss	Q1 scanning, q2 fragmenting; Q3 scan linked to Q1 scan
Selected reaction monitoring	Q1 fixed, q2 fragmenting, q3 fixed
Enhanced MS	Q1 rf only, q2 rf only, Q3 LIT full scan
Enhanced resolution	Q1 rf only, q2 rf only, Q3 LIT narrow m/z range full scan
Enhanced product ion	Q1 fixed, q2 fragmenting, Q3 LIT full scan
MS^3	Q1 fixed, q2 fragmenting, Q3 LIT isolation, fragmentation
Enhanced multiply charged	Q1 rf only, q2 rf only, Q3 LIT time delayed scan
Time delayed fragmentation	Q1 scanning, q2 fragmenting, Q3 LIT time delayed trapping

LIT mass spectrometers are subdivided into those that mass-selectively eject stored ions to the mass detector either radially or axially, out of the trap. This allows the system to store more ions before space charge effects are encountered, making them much more sensitive. Depending on the molecular properties of the analyte and the optimization of instrumental parameters, MS^3 to MS^5 has been achieved with high confidence for structure elucidation. This design has lead to hybridization of the TSQ and ion trap, which combines the sensitivity of the TSQ and high ion capacity of the linear 2-D trap. An example of this is the MDS Sciex/Applied Biosystems 4000 QTrap. This type of platform allows for a wide range of analyses such as PI, CNL, or MRM scanning with sensitivity equivalent to the TSQ. Along with these scans, the Qtrap provides enhanced sensitivity of full scan and MS/MS data acquisition for metabolite identification studies as well as enhanced multiply charged ion scanning (20 22). As one can envision, this type of technology generates huge amounts of data that must be stored and properly analyzed (Table 2) (23).

LTQ-Orbitrap Mass Analyzer

The orbitrap consists of an inner and an outer electrode, which are shaped to create a quadro-logarithmic electrostatic potential (24). Ions generated by APCI or APPI rotate about the inner electrode and oscillate with a frequency characteristic of their *m/z* values. The LTQ-Orbitrap is a hybrid, high-resolution mass spectrometer that can typically operate at a resolution of 60,000. A transfer octapole delivers ions into a curved rf-only quadrupole whose central axis follows a C-shaped arc (C-trap) (25). The C-trap uses rods with hyperbolic surfaces, which are enclosed by two flat lenses with apertures to facilitate ion transport. The plate between the octapole and C-trap forms the gate electrode, and the other plate forms the trap electrode. After leaving the C-trap, ions pass through curved ion optics, are accelerated to high kinetic energies, and converge into a tight cloud, which is able to pass through a small entrance aperture and enter the orbitrap tangentially. The advantages of the LTQ-Orbitrap include high mass resolution, increased speed charge capacity compared with Fourier transform ion cyclotron resonance (FT-ICR) (see below), high mass accuracy, and dynamic range. These attributes have proved to be very useful for drug metabolite identification (26).

Quadrupole Time-of-Flight Mass Analyzer

Quadrupole time-of-flight mass spectrometers (QTOF-MS) are capable of recording all the ions produced in the source on a microsecond timescale, which leads to large duty

cycles, offering high sensitivity detection. Ions are accelerated from the source to a fixed kinetic energy and then allowed to pass down a field-free flight tube to the detector. The time it takes an ion to reach the detector is proportional to its *m/z* ratio; the higher the ratio, the longer the travel time. Quadrupole time-of-flight (QTOF) instruments are able to operate with medium mass resolution and to make accurate mass measurements, and are useful in metabolite structure elucidation (27). Because of the rapid data collection, QTOFs are amenable to high-speed chromatography such as ultra-performance liquid chromatography (UPLC). MS data can be collected over a chromatographic peak that is only 2*s* wide, which has proved to particularly useful for drug metabolomic profiling in biological fluids (28).

Fourier Transform Ion Cyclotron Resonance Mass Analyzer

FT-ICR is functionally a very different ion-trapping technique compared with quadrupole, time-of-flight, and magnetic sectors, which use ion transmission to separate masses. FT-ICR is based on the differing frequencies of circular motion (f_c) by ions with differing *m/z* ratios in a strong magnetic field (29). FT-ICR contains an ion source, an ion trap, and a Fourier transform (FT) for the conversion of the ion-generated frequency spectrum to a mass spectrum (29). Source-generated ions enter a source-trapping cell that is maintained at extremely low temperature and pressure and contained within a superconducting magnet. Ions in the cell are circularly rotated perpendicular to the magnetic field (B) produced by excitation plates. Varying radiofrequency pulses from the excitation plates form an alternating current between detector plates, and the frequency and intensity of the generated current are equal to the number of ions for a particular *m/z*, or $m/z = B/2f_c$. This process of stepped radiofrequency sweeps simultaneously quantifies all detected ions to afford a frequency versus time spectrum, which is deconvoluted by FT to generate a mass spectrum. FT-ICR is one of the most sensitive ion detection methods with resolution ranging from 10^5 to10^6 and mass accuracy of <1 ppm (30). Because of its great sensitivity and resolution analysis, it may be conducted on complex solutions even without chromatography. These qualities also make FT-ICR desirable for structure elucidation in drug metabolism studies (31). Unfortunately, the high costs of the ultrahigh vacuum system, superconducting magnet, and sophisticated data system make the FT-ICR out of the price range of many laboratories conducting ADME studies.

APPLICATIONS OF LC-MS IN DRUG METABOLISM STUDIES

The route by which a drug is metabolized plays important roles in its efficacy and safety. Interindividual differences in rates of metabolism can lead to significant changes in the concentrations of drugs and their metabolites in blood and tissues. Such differences are mediated by genetic polymorphisms in drug-metabolizing enzymes, particularly the cytochromes P-450 (CYPs). This causes interindividual differences in safety and efficacy, which is especially important for drugs with a narrow therapeutic range. Many aspects of ADME and DMPK are studied *in vitro* to potentially avoid adverse reactions in clinical trials. Unfortunately, there is often a poor correlation between in vitro testing and in vivo results. However, such studies are a useful mechanistic guide for potential safety and efficacy issues that might arise in vivo (32).

Metabolism is the aspect of ADME that is most amenable to in vitro study. The primary drug may be eliminated unchanged through urinary or fecal excretion or if it can go through one or more routes of metabolism. Therefore, metabolism is a major

contributor to drug clearance, the principle regulator of parent drug concentrations in plasma and tissues. Drug-drug interactions can also be established through in vitro studies. Even for drugs that are not metabolized substantially, their effect on the metabolism of a coadministered drug might be important as in the classic case of quinidine, which inhibits CYP3A4 even though it is not metabolized by this enzyme (33). Recombinant enzymes as well as sensitive and specific LC-MS assays greatly facilitate the in vitro studies that are conducted prior to clinical trials. LC-MS method development is the benchmark of drug development programs and will undoubtedly remain so for years to come.

Although in vitro testing cannot directly mimic in vivo pathways, the increase in high-throughput assays focusing on DMPK and ADME criteria of NCEs has decreased the failure rate of drug candidates associated with these characteristics from 40% in the 1990s to a current rate of approximately 10% (34). The development of high-throughput in vitro assays as part of the DMPK and ADME studies of drug candidates was driven by need to identify potential safety and efficacies as soon as possible in the drug development process (35). Advances in genomics, molecular biology, synthetic chemistry, and robotics have aided in the increase in NCEs. Numerous microsomal-, cell-, and tissue-based high-throughput in vitro models have been developed and added to the pharmacokinetic (PK) scientist's toolbox. Traditional high-throughput methods rely on fluorescent or radiolabeled reagents and/or coupling for quantification of enzymatic target inhibition or activation. Labeled substrates may not function exactly like unlabeled counterparts, and coupling reactions may cause interference (36). These added interactions can lead to false positives and false negatives. In addition, the synthesis of labeled substrates may add significantly to method development time. Alternatively, MS-based methodology provides a fast, sensitive, and selective method of analysis, which does not need require substrate labeling. For these reasons, LC-MS/MS has become the primary analytical tool for in vitro screening of NCEs.

CYP-Mediated Metabolism

In vitro drug metabolism studies also offer a way to explore and anticipate effects of test drug metabolites on other drugs and vice versa. CYPs are a family of heme-thiolate enzymes that play a major role in drug metabolism. This makes a substantial contribution to the "first pass effect" when drugs are transported into the liver from the portal system after oral dosing. To mimic potential in vivo situations, metabolism studies are normally conducted with hepatic microsomes from several donors along with known chemical inhibitors of the CYPs. Inhibition of one or more CYP by coadministered drugs is one of the major sources of drug-drug interactions. These interactions can drastically change the safety and efficacy of a drug, leading to adverse reactions and, in some instances, even fatalities. This is especially important in populations on multiple medications such as the elderly and those with chronic conditions. Therefore, enzyme inhibition studies are among the initial assays performed on NCEs. High-throughput drug-drug interaction assays are very valuable because they provide clear-cut results, allowing for easy go/no-go decisions for the NCE within drug development. Occasionally, an NCE that is the first drug in a class for previously untreated life-threatening disease is allowed to pass through, even though there may be drug-drug metabolic interactions.

One of the latest high-throughput approaches used by Chu and Nomeir at Schering-Plough Research (34) is to combine multiple CYP inhibition assays into a single incubation using human liver microsomes. This approach has been developed and validated by several laboratories (37 40). CYPs 3A4, 2D6, and 2C9 are responsible for

the bulk of adverse effects resulting from drug-drug interactions, so they are used as the first CYP inhibition screen, with the utilization of LC-MS/MS. If an NCE advances beyond this point, individual isoform testing including testing for CYP2C19 and 1A2 is also completed. Because of the well-documented substrate-dependent inhibition of CYP3A4, a second substrate such as testosterone or midazolam is generally used to evaluate the inhibition of CYP3A4 for the NCEs being recommended for drug development. In this assay, a 96-well plate format with robotic system is used, and incubation and analysis are performed in the same plates. For each compound, direct inhibition and metabolism/mechanism-based inhibition, which is caused by a metabolite of the NCE that is either a potent, direct reversible inhibitor (metabolism based) or a time-dependent irreversible inhibitor (mechanism based), are evaluated. Human liver microsomes from 10 to 20 donors are used along with the appropriate control reactions and probes at varying NCE concentrations. These reactions are quantified by LC-MS/MS in approximately one-minute run time. Chu and Nomeir, of Schering-Plough Research, use a Sciex API 3000 TSQ in positive-ion LC-ESI/MRM/MS mode (34). The column used for LC separation in this particular assay was a Develosil Combi-RP5, 5 μM, 3.5 × 20 mm (Phenomenex, Torrance, California, U.S.) with a flow rate of 1.1 mL/min. Since the same product was monitored for all NCEs, no method optimization was necessary, and the short run time was possible because of the selectivity and increased sensitivity gained from MRM/MS analysis.

One potential problem with short chromatographic run times is the potential for ion suppression or ion enhancement by the high concentrations of other components in the incubation mixtures. However, if ion suppression occurred, this would most likely be at high concentrations, thus generating high are IC_{50} values, which would not impact significantly on the false positive rate. Ion enhancement would result in an increase of metabolite concentration with an increase in NCE concentration, and could be easily identified. In these cases, a more rigorous LC-MS/MS approach could then be undertaken, and APCI, which is less susceptible to suppression effects than ESI, can be used (41,42). LC-MS/MS assays for metabolism by individual CYP isoforms are performed at later stages in the drug development process for compounds that have passed through several screening assays. An example is the CYP2C19 assay in which *S*-mephenytoin is used as the substrate. For CYP1A2, phenacetin is used as the specific substrate and, as mentioned above, midazolam for CYP3A4. The high throughput for this "3 in 1" assay is eight, 96-well plates/night/instrument. For instance, if 15 NCEs were being tested, four 96-well plates are used, two for preincubation and two for co-incubation. Eight plates/night/instrument would generate 180 IC_{50}s, which is ~100-fold increase in throughput compared with the HPLC-ultraviolet (UV) assay that was originally used by the Schering-Plough group (34).

Caco-2 Permeability

Drug absorption from the intestinal lumen can occur via four major pathways (43). However, the majority of drugs are absorbed via transcellular passive diffusion, a concentration gradient driven diffusion across the membrane of enterocytes, intestinal absorptive cells. Lipophilic compounds absorbed directly into the cell membrane, whereas hydrophilic small molecules may be absorbed via the paracellular route. Since these junctions are tight and represent a small surface area, this type of enterocyte absorption is slow and primarily for hydrophilic molecules with molecular weights <350 Da. Compounds may also be absorbed by a transmembrane transporter through facilitated diffusion or active transport. These two modes require the formation of a reversible drug carrier and may be more selective than transcellular passive diffusion.

The majority of NCEs are tested for potential oral absorption as this is the preferred route of administration for most drugs. A model to test oral absorption has been developed using CaCo-2 cells, an immortalized human colon adenocarcinoma cell line. This approach can only provide an approximation to the truth, and care has to be taken in interpreting the data. However, with this caveat, several studies have shown good correlation between Caco-2 permeability and oral absorption (44). Permeability and efflux transport (primarily via P-glycoprotein) utilize Caco-2 monolayers. Unlike the CYP assays, these screening assays are focused on the individual NCE; therefore, LC-MS/MS optimization may be necessary for each compound. The short run times are not feasible for this assay because of the unknown matrix effects. However, it is still possible to increase throughput through instrument design such as the multiplexed inlet system (MUX®, Waters Corporation, Milford, Massachusetts, U.S.), which allows for four or eight simultaneous data acquisitions (Fig. 1).

The MUX ion source interface is mounted directly onto the standard Z-spray source of a mass spectrometer. The MUX employs either four or eight nebulization-assisted electrospray probe tips arranged radially about the sampling cone. Samples are simultaneously introduced into the mass spectrometer, greatly reducing the time constraints of method development and sample analysis. Problems that can arise with this type of instrumental setup include interchannel variability and interchannel cross talk.

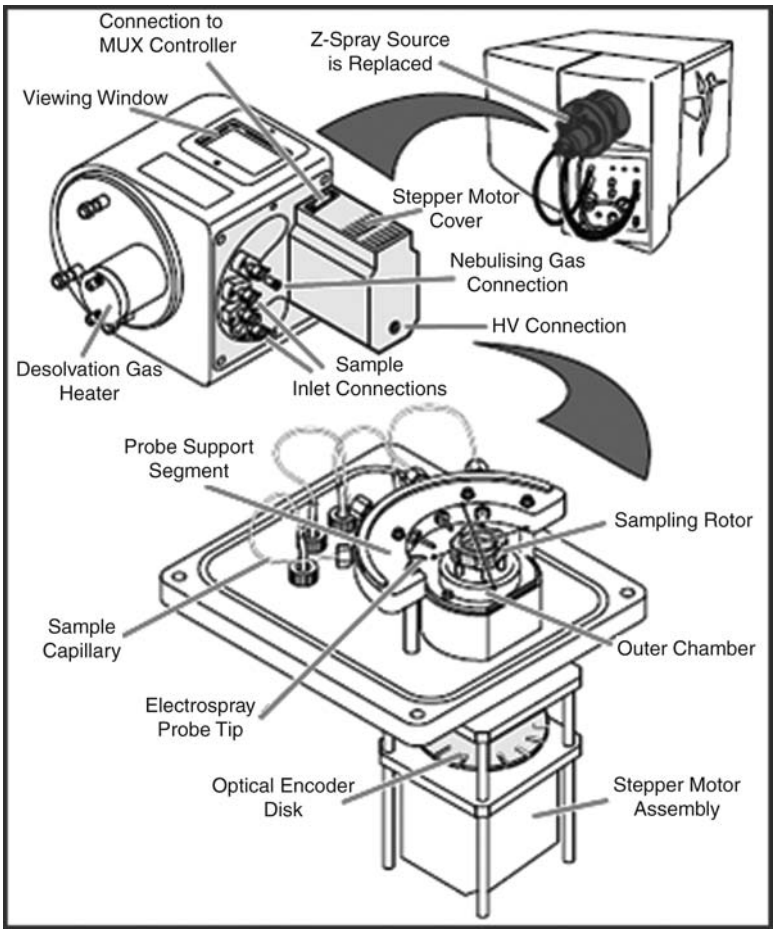

Figure 1 Schematic of Waters MUX system.

The MUX Exact interface, designed for time of flight (TOF) only, also provides a separate "reference spray" inlet in addition to the four or eight LC inlets on a standard MUX (45). Infusion of a known reference compound into the reference spray allows for the mass spectral data acquired from the LC inlet lines to be lock mass corrected, thus providing exact mass information. Mass interference, ion suppression/enhancement, and gradient effects are not an issue since the reference spray is independent of the LC sprays. The source provides a dramatic increase in sample throughput; however, a single-syringe system increases sample throughput time. When a single syringe based LC injector system, such as the CTC Pal, is used with the MUX system, the injection cycle time for four samples (including the time for washing the injectors and loading the samples) only provides a 2.4-fold increase in throughput compared with the theoretical 4-fold increase (45).

Hepatocyte Clearance

Hepatocyte clearance is evaluated using cryopreserved human tissues. As for drug-drug interaction studies described above, incubations are conducted using human hepatocytes that are typically pooled from several individuals in order to minimize the effects of interindividual variability in metabolizing enzymes. Incubations are typically performed using 24-well plates in a shaker at 37°C for two hours. This is followed by the removal of 100-μL aliquots that are mixed with two volumes of acetonitrile on a 96-well plate. Plates are then sonicated, vortex mixed, and centrifuged before LC-MS/MS analysis. Some fundamental assumptions made for this experimental design include the following: (*i*) in vitro enzyme kinetics are applicable to in vivo kinetic properties, (*ii*) intrinsic clearance follows first-order kinetics, and (*iii*) the liver is the major organ responsible for the clearance of test compounds (46,47).

Plasma Protein Binding

The free concentration of a drug is primarily responsible for its pharmacological activity, safety, and tissue distribution. In this regard, plasma protein binding may be useful in understanding the PKPD relationship of a drug candidate. During the lead characterization stage, protein binding is investigated in rat, dog, monkey, and human plasma. In vitro studies such as this one will help to characterize the therapeutic index for the selection of dose range in clinical trials (48). Examples of plasma protein binding assays include ultrafiltration and equilibrium dialysis. Samples are analyzed by LC-MS/MS, and the percentage of protein binding is calculated. For equilibrium dialysis, percent bound $= 100 \times (C_p - C_b)/C_p$, where C_p and C_b are the compound concentrations in plasma and buffer chambers, respectively. Recently, a new approach for screening plasma protein binding was reported (49). The method is based on equilibrium dialysis combined with rapid generic LC-MS analysis by using a sample pooling approach enabling high-throughput screening of protein binding in the drug discovery phase. The method was validated by a comparison of measured unbound free fractions between single and pooled compounds for a test set of structurally diverse compounds with a wide range of unbound fractions. Therefore, this new methodology provides an attractive method to conventional approaches during the drug candidate selection process.

CYP Isoform Profiling

Assays are performed in the lead characterization stage of drug development to identify the major CYP isoforms responsible for the metabolism of candidate drugs in humans.

These in vitro assays provide valuable information regarding bioavailability, potential interindividual variability, drug-drug interactions, and the polymorphic metabolism of drug candidates (50). For example, if a drug candidate is metabolized solely by a polymorphic CYP such as CYP2D6, in which only 7% of Caucasians are carriers, the decision to advance the drug may be considered (32). Human liver microsomes are incubated with the drug candidate in the presence of NADPH and with or without a selective CYP inhibitor. Microsomes from insect cells, such as SF9 cells, containing recombinant CYPs are also incubated with the drug candidate. The addition of cofactors is necessary when running experiments with microsomes. The other limitation is that microsomes do not contain other metabolizing enzymes. The most complete picture requires the use of intact liver systems. These systems also include self-sufficient cofactors, and the natural orientation of the enzyme is preserved. Unfortunately, the enzymes are not stable for more than 24 hours, and the livers are from organ donors who obviously died of one compromising cause or another (32).

If the metabolites are known from previous studies, the disappearance of substrate and appearance of product are monitored by LC-MS/MS. This allows for the assignment of metabolites to individual CYP metabolisms. Synthesis is an alternate route for metabolite preparation, especially for the development of standards and isotopically labeled internal standards, ^{2}H, ^{13}C, ^{15}N, or a combination of the above. Synthetic standards also provide a greater level of confidence in mass spectrometric analysis of metabolites, which is important for identification, characterization, and quantification.

Metabolite Structure Elucidation

Hydrogen-deuterium (H-D) exchange and derivatization methods in conjunction with MS facilitate structure elucidation and interpretation of MS/MS data (51,52). Deuterium labeling plays a role in MS studies of ionic reaction mechanisms in structural characterization applications. In this case, the number of active hydrogen atoms in groups such as OH, COOH, NH, or SH, by simple exchange with D_2O is widely used. H-D exchange was first reported by Henion, who obtained the chemical ionization mass spectrum of [$^{2}H_3$] dimethyl sulfoxide acquired by direct introduction using CD_3-CN-D_2O eluents with a microflow chromatography system (3). Solution and gas-phase H-D exchange have been used extensively to gain information on the mechanisms of ion formation as well (53). Chemical derivatization coupled with various ionization techniques can be useful for highly polar and unstable metabolites or for metabolites that have unusual structures (27,52).

Mechanistic Toxicology

Successful drug design requires the right combination of multiple drug properties such as activity, toxicity, and exposure. These properties encompass the “rule of three” for drug candidates, hence, their suitability for advancement in the drug pipeline. Toxicity issues are mainly a result of active metabolites that may cause idiosyncratic reactions. In the late states of drug development or even after a drug is on the market, these toxicity issues can surface and have a devastating impact on pharmaceutical companies. Examples of drugs taken off the market because of idiosyncratic reactions include Vioxx for mycocardial infarction, stroke, and liver damage, and fipexide, a nootropic drug derivative that was taken off the market for side effects such as fevers and hepatitis (54,55).

While medicinal chemistry and bioanalytical method development have kept pace with one another, biochemical toxicology has not. There is still much to be learned about

the biological mechanisms of reactive intermediates. There are indications that some substructures may be involved in toxicities in humans. These substructures include aryl acetic and aryl propionic acids, aryl hydroxamic acids, oxime, anilines, anilides, hydrazines, hydrazides, hydantoins, quinones, quinine methides, nitroaromatics, heteroaromatics, halogenated hydrocarbons, some halogenated aromatics, chemical groups that may be oxidized to acroleins, and medium-chain fatty acids (56). Although it is well established that some reactive intermediate formation results in toxicity, others formed, even those similar in structure, do not. Reactive intermediates are unstable, making direct detection highly improbable without the use of trapping techniques (57 59). Reactive metabolites can be trapped with nucleophilic scavengers such as glutathione (GSH) or N-acetyl cysteine. There is increasing appreciation for the role of glutathione *S*-transferases in the formation of drug metabolite derived GSH-adducts (60). CNL scans for glutamic acid (129 Da) is a characteristic decomposition pathway for GSH-adducts under tandem MS conditions and may also be used for detection of mercapturic acid derivatives (phase III). Another example is reactive iminium species, which may be generated through metabolic oxidation of cyclic and acyclic tertiary amines. These reactive intermediates may be trapped in vitro by the addition of cyanide ions to the incubation medium, resulting in the formation of stable α-cyanoamines (57). LC-MS/MS provides high sensitivity and selectivity for the analysis of these conjugates.

RECENT ADVANCES AND FUTURE DIRECTIONS

Samples from incubations conducted using in vitro methodology are thought to be relatively "clean" when compared with plasma, urine, and other biological samples. Therefore, it is often common practice to use SIM or shorten the HPLC run time to limit the method development and optimization. This may be true for the majority of in vitro analyses; however, there are several documented cases where this approach has not been adequate. Matrix effect and ion suppression/enhancement should always be investigated upon development of a novel assay.

The Waters MUX system was discussed previously, and this is one example of advances in instrumentation that have led to high-throughput analyses. Another advance introduced by Waters is UPLC-MS/MS, which has several advantages over conventional LC-MS/MS including increased resolution and sensitivity and decreased analysis time. UPLC instruments are able to work under pressures up to 14K psi, which allows for small particle sized columns and low dead volume. In a study by Pedraglio et al., a comparison between a previously validated LC-MS/MS on a proprietary preclinical antitumor candidate (NiK-12192) and the new UPLC-MS/MS method was made (61). The comparison of resolution power was performed on hepatocyte samples using the Acquity BEH C18 100 mm × 2.5 mm column with a particle size of 1.7 μm (UPLC) and the Xbridge C18 100 mm × 2.1 mm column with a 3.5-μm particle size (Fig. 2). In general, HPLC peaks were broader and less resolved than in the UPLC chromatogram, and peaks in the UPLC chromatogram were seen to coelute in the HPLC system. Overall, the UPLC system provides increased resolution and faster analysis. The increased chromatographic resolution will also allow for increased sensitivity and increased accurate mass analysis in full scan mode. Also, in vitro assays that only use SIM for analysis will have less matrix interference.

Despite these advances, LC-MS/MS is still not as "high throughput" as other developed techniques for PK and ADME analysis. A Novartis group has reported high-throughput screening techniques of 175K sample analyses using MUX-LC-MS/MS, four-way

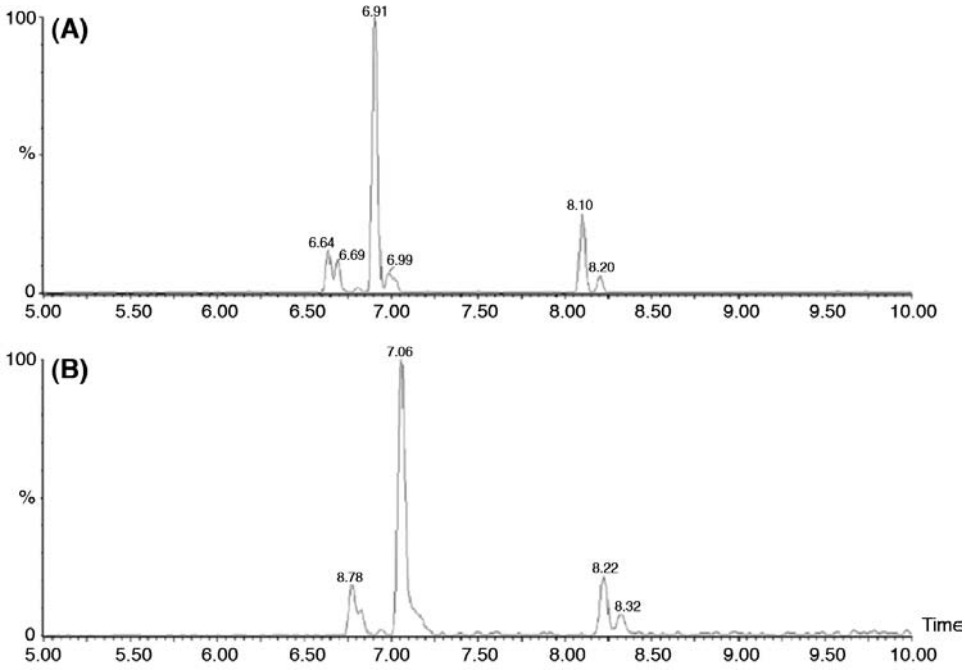

Figure 2 Reconstructed ion chromatograms obtained from fresh dog hepatocyte incubations analyzed on different columns. (**A**) Acquity BEH C18 100 mm × 2.5 mm column with a particle size of 1.7 μm (ultra performance liquid chromatography). (**B**) The Xbridge C18 100 mm × 2.1 mm column with a 3.5 μm particle size (conventional liquid chromatography). *Source*: From Ref. 61.

parallel staggered gradient liquid chromatography tandem MS, and eight-way staggered flow injection tandem MS following 384-well plate solid-phase extraction (SPE). These methods are capable of analyzing a 384-well plate in 37 minutes with typical analysis time of less than 2 hours. They were able to analyze 175K sample wells in either six weeks using parallel staggered gradients or four weeks using the four-way MUX on two LC-MS/MS instruments. The samples were previously analyzed using traditional methods, which generated relatively few hits (36).

Whalen et al. at Pfizer (62) published in 2006 a "centralized" approach to method development for drug screening. In this method, they use "Autoscan" and "Automation." These are two software products specific to MDS Sciex instruments. Both are able to quickly determine MRM transitions for hundreds of compounds per day, upward of 2000 compounds/week. This high-throughput ADME (HT-ADME) utilizes a compound management process that prepares 96- or 384-well plates for specific screening assays (63). Autoscan determines optimal polarity and collision energy (CE), while Automaton determines the optimal declustering potential (DP) as well as the CE. The optimized conditions are then loaded into a central database that can be accessed from all LC-MS/MS bioanalysis workstations. Specifically, the effects of DP and CE on sensitivity were investigated. It was found that the optimization of DP improved analyte response by 27% on average, while 10% of the analytes tested showed more than 50% improvement. However, it was determined that in most cases, the default setting of 25V for the DP could be used. Changes in CE greatly affected the sensitivity of the compounds tested, and it was determined that a minimum of three settings should be tested with 1V, 30V, and 45V providing adequate coverage for the majority of small-molecule drug discovery analytes.

Hybrid instrumentation, such as the QTrap, has also found a place in DMPK studies. As discussed earlier in the chapter, the main advantages of hybrid instrumentation are a result of combining the "best of both worlds." For example, the QTrap combines the sensitivity of MRM of the TSQ and the full scan of the ion trap. Many types of analyses can be performed on one instrument. Interestingly, each instrument's advantages are the others' limitations, making this combination particularly advantageous, especially for trace metabolite analysis. A thorough evaluation of the QTrap for metabolite identification was published in 2003 by Hopfgartner, University of Geneva, and Husser and Zell at Hoffmann-La Roche (64). This paper nicely describes how the QTrap technology fits in with other mass analyzers used in drug metabolism studies.

One of the earliest reported drug metabolism studies using the QTrap came from Xia et al. at Merck (65). This study demonstrated the flexibility of the instrument in qualitatively identifying metabolites from in vitro incubations of gemfibrozil. Phase I metabolites were identified using full scan in Q3 operated at the LIT as the survey scan for information-dependent data acquisition (IDA) of product ion spectra and MS^3 spectra. MS^2 data was generated by selecting the PI in Q1, affecting fragmentation by collision induced dissociation (CID), and trapping products in Q3. The trapped products were scanned out of the Q3 trap to generate the MS^2 product ion spectra. MS^3 spectra were obtained by isolating a single fragment from the MS^2 experiment in the trap and then applying auxiliary RF to excite the selected precursor. Collision with background N_2 that leaks into Q3 from the collision cell induces fragmentation, thus yielding the MS^3 spectrum. Phase II conjugates and phase I hydroxylations were identified using the CNL scan mode of the TSQ as the survey scan for the IDA of product ion spectra in the linear trap. The authors were able to show detection and structural characterization of all the in vitro metabolites identified by radiochemical detection for 25 μM gemfibrozil incubated in human liver microsomes with NADPH and UDPGA (65).

Although FT-ICR/MS instrumentation has been commercially available for over 20 years, cost, difficulty of use, and low throughput have prohibited ADME laboratories from taking advantage of its sensitivity, accuracy, and high mass resolution. Ion cyclotron resonance (ICR) alone was not compatible with the timescale of chromatographic separations, nor was the HPLC interface robust user friendly. The hybrid instruments provide the bridge between the excellent performance of the FTMS and the well-established and validated features of the TSQ and ion traps, making the LTQ-FT hybrid compatible with higher HPLC flow rates. However, most of the publications using the LTQ-FT are still focused on its application to proteomics. Some studies have been conducted in the area of metabonomics, but it has not been widely used for DMPK studies despite its excellent resolving power and mass accuracy (31). The LTQ-Orbitrap was also slow to start in the area of ADME for similar reasons to that of the LTQ-FT. The Orbitrap advantages include high mass resolution, increased space charge capacity compared with the FT-ICR, high mass accuracy and dynamic range, and upper mass limit. Again, like the LTQ-FT, few publications use the Orbitrap for in vitro DMPK studies. Schänzer's group at the German Sport University in Cologne have utilized the LTQ-Orbitrap for absolute determination of sports drug products (66). Another indication is that such powerful yet costly and low-throughput technology should be reserved for unambiguous identification of parent drug compounds and metabolites when absolutely necessary.

A new strategy for conducting label-free metabolite data was reported recently using a hybrid LIT/Orbitrap mass spectrometer (67). Multiple post-acquisition data-mining techniques were evaluated and applied to the detection and characterization of in vitro metabolites of indinavir. Extracted-ion chromatography (EIC) coupled with mass defect filter (MDF) was found to be highly effective in the detection of common

metabolites with predicted molecular weights. The MDF process, which searched for metabolites on the basis of the similarity of mass defects of metabolites to those of indinavir and its core substructures, was able to find uncommon metabolites not detected by normal EIC processing. As a result, a total of 15 metabolites including 2 new indinavir metabolites were detected and characterized in a rat liver S9 incubation sample. These data-mining techniques, which employed distinct metabolite search mechanisms, were complementary and effective in detecting both common and uncommon metabolites and should provide a useful approach for future studies of NCEs. This will most likely increase the use of the powerful LTQ/Orbitrap system for LC-MS studies of drug metabolism. The recent availability of ion mobility LC-MS systems may also have a significant impact on the field of ADME research (68).

ACKNOWLEDGMENTS

We acknowledge the support of NIH grants R01CA91016, U01ES016004, F32ES016683, and P30ES013508.

REFERENCES

1. Guetens G, De BG, Wood M, Maes RA, Eggermont AA, Highley MS, van Oosterom AT, de Bruijn EA, Tjaden UR. Hyphenated techniques in anticancer drug monitoring. I. Capillary gas chromatography mass spectrometry. J Chromatogr A 2002; 976(1 2):229 238.
2. Lehrer M. The role of gas chromatography/mass spectrometry. Instrumental techniques in forensic urine drug testing. Clin Lab Med 1998; 18(4):631 649.
3. Covey TR, Lee ED, Henion JD. High speed liquid chromatography/tandem mass spectrometry for the determination of drugs in biological samples. Anal Chem 1986; 58(12):2453 2460.
4. Blair IA, Tilve A. Analysis of anticancer drugs and their metabolites by mass spectrometry. Curr Drug Metab 2002; 3(5):463 480.
5. Meyer Veronika R. Practical High Performance Liquid Chromatography. New York: John Wiley and Sons, 1994.
6. Lee SH, Blair IA. Targeted chiral lipidomics analysis by liquid chromatography electron capture atmospheric pressure chemical ionization mass spectrometry (LC ECAPCI/MS). Methods Enzymol 2007; 433:159 174.
7. Munson MSB, Field FH. Chemical ionization mass spectrometry I. General introduction. J Am Chem Soc 1966; 88(12):2621 2630.
8. Horning EC, Horning MG, Carroll DI, Dzidic I, Stillweli RN. New picogram detection system based on a mass spectrometer with an external ionization source at atmospheric pressure. Anal Chem 1973; 45(6):936 943.
9. Robb DB, Covey TR, Bruins AP. Atmospheric pressure photoionisation: an ionization method for liquid chromatography mass spectrometry. Anal Chem 2000; 72(15):3653 3659.
10. Bruins AP. Mass spectrometry with ion sources operating at atmospheric pressure. Mass Spectrom Rev 1991; 10(1):53 77.
11. Constapel M, Schellentrager M, Schmitz OJ, Gab S, Brockmann KJ, Giese R, Benter T. Atmospheric pressure laser ionization: a novel ionization method for liquid chromatography/mass spectrometry. Rapid Commun Mass Spectrom 2005; 19(3):326 336.
12. Yamashita M, Fenn JB. Electrospray ion source another variation on the free jet theme. J Phys Chem 1984; 88(20):4451 4459.
13. Kebarle P, Tang L. From ions in solution to ions in the gas phase the mechanism of electrospray mass spectrometry. Anal Chem 1993; 65(22):A972 A986.

14. Ikonomou MG, Blades AT, Kebarle P. Investigations of the electrospray interface for liquid chromatography mass spectrometry. Anal Chem 1990; 62(9):957 967.
15. Hop CE. Use of nano electrospray for metabolite identification and quantitative absorption, distribution, metabolism and excretion studies. Curr Drug Metab 2006; 7(5):557 563.
16. Carroll DI, Dzidic I, Stillwell RN, Haegele KD, Horning EC. Atmospheric pressure ionization mass spectrometry corona discharge ion source for use in liquid chromatograph mass spectrometer computer analytical system. Anal Chem 1975; 47(14):2369 2373.
17. Schaefer WH, Dixon F. Effect of high performance liquid chromatography mobile phase components on sensitivity in negative atmospheric pressure chemical ionization liquid chromatography mass spectrometry. J Am Soc Mass Spectrom 1996; 7(10):1059 1069.
18. Singh G, Gutierrez A, Xu K, Blair IA. Liquid chromatography/electron capture atmospheric pressure chemical ionization/mass spectrometry: analysis of pentafluorobenzyl derivatives of biomolecules and drugs in the attomole range. Anal Chem 2000; 72(14):3007 3013.
19. Kamel A, Prakash C. High performance liquid chromatography/atmospheric pressure ionization/tandem mass spectrometry (HPLC/API/MS/MS) in drug metabolism and toxicology. Curr Drug Metab 2006; 7(8):837 852.
20. Lopez LL, Yu X, Cui DH, Davis MR. Identification of drug metabolites in biological matrices by intelligent automated liquid chromatography tandem mass spectrometry. Rapid Commun Mass Spectrom 1998; 12(22):1756 1760.
21. Li AC, Alton D, Bryant MS, Shou WZ. Simultaneously quantifying parent drugs and screening for metabolites in plasma pharmacokinetic samples using selected reaction monitoring information dependent acquisition on a QTrap instrument. Rapid Commun Mass Spectrom 2005; 19(14): 1943 1950.
22. Hager JW, Le Blanc JCY. Product ion scanning using a Q q Q (linear ion trap) (Q TRAP (TM)) mass spectrometer. Rapid Commun Mass Spectrom 2003; 17(10):1056 1064.
23. King R, Fernandez Metzler C. The use of Qtrap technology in drug metabolism. Curr Drug Metab 2006; 7(5):541 545.
24. Hu QZ, Noll RJ, Li HY, Makarov A, Hardman M, Cooks RG. The orbitrap: a new mass spectrometer. J Mass Spectrom 2005; 40(4):430 443.
25. Makarov A, Denisov E, Kholomeev A, Balschun W, Lange O, Strupat K, Horning S. Performance evaluation of a hybrid linear ion trap/orbitrap mass spectrometer. Anal Chem 2006; 78(7):2113 2120.
26. Lim HK, Chen J, Sensenhauser C, Cook K, Subrahmanyam V. Metabolite identification by data dependent accurate mass spectrometric analysis at resolving power of 60,000 in external calibration mode using an LTQ/Orbitrap. Rapid Commun Mass Spectrom 2007; 21(12):1821 1832.
27. Prakash C, Shaffer CL, Nedderman A. Analytical strategies for identifying drug metabolites. Mass Spectrom Rev 2007; 26(3):340 369.
28. Erve JC, Vashishtha SC, Ojewoye O, Adedoyin A, Espina R, Demaio W, Talaat RE. Metabolism of prazosin in rat and characterization of metabolites in plasma, urine, faeces, brain and bile using liquid chromatography/mass spectrometry (LC/MS). Xenobiotica 2008; 38(5): 540 558.
29. Marshall A. First North American Fourier transform ion cyclotron resonance mass spectrometry conference Tallahassee, Florida, March 13 15, 1997. J Am Soc Mass Spectrom 1997; 8(8):813.
30. Brown SC, Kruppa G, Dasseux JL. Metabolomics applications of FT ICR mass spectrometry. Mass Spectrom Rev 2005; 24(2):223 231.
31. Sanders M, Shipkova PA, Zhang HY, Warrack BM. Utility of the hybrid LTQ FTMS for drug metabolism applications. Curr Drug Metab 2006; 7(5):547 555.
32. DHHS, USDA, CDER, and CBER. Guidance for Industry: Drug Metabolism/Drug Interaction Studies in the Drug Development Process: Studies In Vitro. 1997. Available on: http://www.fda.gov/cder/guidance.htm.
33. Guengerich FP, Muller Enoch D, Blair IA. Oxidation of quinidine by human liver cytochrome P 450. Mol Pharmacol 1986; 30(3):287 295.

34. Chu I, Nomeir AA. Utility of mass spectrometry for in vitro ADME assays. Curr Drug Metab 2006; 7(5):467 477.
35. Baillie TA. Metabolism and toxicity of drugs. Two decades of progress in industrial drug metabolism. Chem Res Toxicol 2008; 21(1):129 137.
36. Roddy TP, Horvath CR, Stout SJ, Kenney KL, Ho PI, Zhang JH, Vickers C, Kaushik V, Hubbard B, Wang YK. Mass spectrometric techniques for label free high throughput screening in drug discovery. Anal Chem 2007; 79(21):8207 8213.
37. Bu HZ, Magis L, Knuth K, Teitelbaum P. High throughput cytochrome P450 (CYP) inhibition screening via a cassette probe dosing strategy. VI. Simultaneous evaluation of inhibition potential of drugs on human hepatic isozymes CYP2A6, 3A4, 2C9, 2D6 and 2E1. Rapid Commun Mass Spectrom 2001; 15(10):741 748.
38. Dierks EA, Stams KR, Lim HK, Cornelius G, Zhang HL, Ball SE. A method for the simultaneous evaluation of the activities of seven major human drug metabolizing cytochrome P450s using an in vitro cocktail of probe substrates and fast gradient liquid chromatography tandem mass spectrometry. Drug Metab Dispos 2001; 29(1):23 29.
39. Testino SA, Patonay G. High throughput inhibition screening of major human cytochrome P450 enzymes using an in vitro cocktail and liquid chromatography tandem mass spectrometry. J Pharm Biomed Anal 2003; 30(5):1459 1467.
40. Turpeinen M, Uusitalo J, Jalonen J, Pelkonen A. Multiple P450 substrates in a single run: rapid and comprehensive in vitro interaction assay. Eur J Pharm Sci 2005; 24(4):389.
41. Sunner J, Nicol G, Kebarle P. Factors determining relative sensitivity of analytes in positive mode atmospheric pressure ionization mass spectrometry. Anal Chem 1988; 60(13):1300 1307.
42. King R, Bonfiglio R, Fernandez Metzler C, Miller Stein C, Olah T. Mechanistic investigation of ionization suppression in electrospray ionization. J Am Soc Mass Spectrom 2000; 11(11): 942 950.
43. Stevenson CL, Augustijns PF, Hendren RW. Use of Caco 2 cells and LC/MS/MS to screen a peptide combinatorial library for permeable structures. Int J Pharm 1999; 177(1):103 115.
44. Polli JE, Ginski MJ. Human drug absorption kinetics and comparison to Caco 2 monolayer permeabilities. Pharm Res 1998; 15(1):47 52.
45. Fung EN, Chu IH, Li C, Liu TT, Soares A, Morrison R, Nomeir AA. Higher throughput screening for Caco 2 permeability utilizing a multiple sprayer liquid chromatography/tandem mass spectrometry system. Rapid Commun Mass Spectrom 2003; 17(18):2147 2152.
46. Lau YY, Sapidou E, Cui XM, White RE, Cheng KC. Development of a novel in vitro model to predict hepatic clearance using fresh, cryopreserved, and sandwich cultured hepatocytes. Drug Metab Dispos 2002; 30(12):1446 1454.
47. Komura H, Iwaki M. Usefulness of hepatocytes for evaluating the genetic polymorphism of CYP2D6 substrates. Xenobiotica 2005; 35(6):575 587.
48. Banker MJ, Clark TH, Williams JA. Development and validation of a 96 well equilibrium dialysis apparatus for measuring plasma protein binding. J Pharm Sci 2003; 92(5):967 974.
49. Wan H, Rchngren M. High throughput screening of protein binding by equilibrium dialysis combined with liquid chromatography and mass spectrometry, J Chromatogr A 2006; 1102(1 2): 125 134.
50. Linget JM, du Vignaud P. Automation of metabolic stability studies in microsomes, cytosol and plasma using a 215 Gilson liquid handler. J Pharm Biomed Anal 1999; 19(6):893 901.
51. Sidelmann UG, Bjornsdottir I, Shockcor JP, Hansen SH, Lindon JC, Nicholson JK. Directly coupled HPLC NMR and HPLC MS approaches for the rapid characterisation of drug metabolites in urine: application to the human metabolism of naproxen. J Pharm Biomed Anal 2001; 24(4):569 579.
52. Liu DQ, Hop CE. Strategies for characterization of drug metabolites using liquid chromatography tandem mass spectrometry in conjunction with chemical derivatization and on line H/D exchange approaches. J Pharm Biomed Anal 2005; 37(1):1 18.
53. Kamel AM, Munson B. Collision induced dissociation of purine antiviral agents: mechanisms of ion formation using gas phase hydrogen/deuterium exchange and electrospray ionization tandem mass spectrometry. Eur J Mass Spectrom 2004; 10(2):239 257.

54. FitzGerald GA. Coxibs and cardiovascular disease. N Engl J Med 2004; 351(17):1709 1711.
55. Guy C, Blay N, Rousset H, Fardeau V, Ollagnier M. [Fever caused by fipexide. Evaluation of the national pharmacovigilance survey]. Therapie 1990; 45(5):429 431.
56. Kalgutkar AS, Gardner I, Obach RS, Shaffer CL, Callegari E, Henne KR, Mutlib AE, Dalvie DK , Lee JS, Nakai Y, O'Donnell JP, Boer J, Harriman SP. A comprehensive listing of bioactivation pathways of organic functional groups. Curr Drug Metab 2005; 6(3):161 225.
57. Baillie TA. Future of toxicology metabolic activation and drug design: challenges and opportunities in chemical toxicology. Chem Res Toxicol 2006; 19(7):889 893.
58. Doss GA, Baillie TA. Addressing metabolic activation as an integral component of drug design. Drug Metab Rev 2006; 38(4):641 649.
59. Uetrecht J. Evaluation of which reactive metabolite, if any, is responsible for a specific idiosyncratic reaction. Drug Metab Rev 2006; 38(4):745 753.
60. Blair IA. Endogenous glutathione adducts. Curr Drug Metab 2006; 7(8):853 872.
61. Pedraglio S, Rozio MG, Misiano P, Reali V, Dondio G, Bigogno C. New perspectives in bio analytical techniques for preclinical characterization of a drug candidate: UPLC MS/MS in in vitro metabolism and pharmacokinetic studies. J Pharm Biomed Anal 2007; 44(3):665 673.
62. Gobey J, Janiszewski J. A centralized approach to tandem mass spectrometry method deve lopment for high throughput ADME screening. Rapid Commun Mass Spectrom 2006; 20(10): 1497 1503.
63. Whalen KM, Rogers KJ, Cole MJ, Janiszewski JS. AutoScan: an automated workstation for rapid determination of mass and tandem mass spectrometry conditions for quantitative bioanalytical mass spectrometry. Rapid Commun Mass Spectrom 14(21):2074 2079.
64. Hopfgartner G, Husser C, Zell M. Rapid screening and characterization of drug metabolites using a new quadrupole linear ion trap mass spectrometer. J Mass Spectrom 2003; 38(2): 138 150.
65. Xia YQ, Miller JD, Bakhtiar R, Franklin RB, Liu DQ. Use of a quadrupole linear ion trap mass spectrometer in metabolite identification and bioanalysis. Rapid Commun Mass Spectrom 2003; 17(11):1137 1145.
66. Thevis M, Thomas A, Schanzer W. Mass spectrometric determination of insulins and their degradation products in sports drug testing. Mass Spectrom Rev 2008; 27(1):35 50.
67. Ruan Q, Peterman S, Szewc MA, Ma L, Cui D, Humphreys WG, Zhu M. An integrated method for metabolite detection and identification using a linear ion trap/orbitrap mass spectrometer and multiple data processing techniques: application to indinavir metabolite detection. J Mass Spectrom 2008; 43(2):251 261.
68. Hatsis P, Brockman AH, Wu JT. Evaluation of high field asymmetric waveform ion mobility spectrometry coupled to nanoelectrospray ionization for bioanalysis in drug discovery. Rapid Commun Mass Spectrom 2007; 21(14):2295 2300.

15

The Practice of NMR Spectroscopy in Drug Metabolism Studies

Ian D. Wilson
Departments of Clinical Pharmacology, Drug Metabolism and Pharmacokinetics, AstraZeneca, Macclesfield, Cheshire, U.K.

John C. Lindon and Jeremy K. Nicholson
Department of Biomolecular Medicine, Imperial College London, South Kensington, London, U.K.

INTRODUCTION

Nuclear magnetic resonance (NMR) spectroscopy is employed in the study of drug metabolism and disposition in a variety of ways. There is of course the traditional use of the technique for structure determination following the isolation of pure, or relatively pure, metabolites from biofluids such as plasma, urine, and bile or solid material such as tissues or excreta. More recently, when hyphenated to liquid chromatography (LC), often in combination with mass spectrometry (MS), NMR has also been used for the structure elucidation of metabolites without the need for extensive pre-purification. The technique has also been used directly for the detection, identification, and quantitative determination of metabolites in intact biofluids and in excretion balance studies. NMR spectroscopy has also been extensively used for the determination of the reactivity of unstable metabolites such as ester glucuronide metabolites.

Here we review recent advances in such applications, thereby providing an overview of the current practice of NMR spectroscopy in drug metabolism studies.

NMR SPECTROSCOPY OF ISOLATED METABOLITES

"Classical" methods for isolating metabolites from biological fluids/extracts, etc., using, for example, liquid-liquid or solid phase extraction (LLE, SPE) (1) followed by further purification by LC if needed, or indeed direct isolation from the sample by "preparative" chromatography are well established and do not require further description here. The aim of such isolation procedures is to produce sufficient pure material for conventional NMR spectroscopy, and using modern NMR spectrometers operating at 600 MHz or above,

good one dimensional ^{1}H NMR spectra can be obtained on 10 to 50 μg of material in a reasonable time.

Most drug metabolism studies using NMR spectroscopy have concentrated on ^{1}H NMR, but in cases where a fluorine atom is present in the metabolite, ^{19}F NMR spectroscopy can be very useful for detection and quantification (1 3). Other nuclei can also be studied using NMR spectroscopy in special cases. These include ^{31}P NMR spectroscopy of phosphorus-containing drugs such as the anticancer drug ifosfamide (4) series or even ^{195}Pt NMR for cisplatin and analogues (5). Also, if drugs can be enriched in ^{13}C or ^{15}N, then use of these nuclei can aid both detection and identification (1). Most recent studies have concentrated on spectrometers operating at an observation frequency of 600 MHz, but nevertheless, a considerable number of studies have been performed using lower observation frequencies such as 400 or 500 MHz (with a corresponding lower sensitivity and spectral dispersion). Currently, based on the use of a 600-MHz NMR spectrometer, good-quality 1-D ^{1}H NMR spectra can be obtained on approximately 10 to 50 μg of material in a few minutes. For even better sensitivity and dispersion, instruments operating at higher observation frequencies are available, including 750, 800, and 900 MHz.

Another means of reducing the amounts of material required for analysis involves the use of cryogenic NMR probes, whereby the NMR detector coil and preamplifier are cooled to about 20K to reduce thermal electronic noise. These are commercially available and provide improvements in spectral signal-to-noise ratios of up to 500%, or a corresponding time saving of up to 25 times (6,7). This is of special advantage for 2-D NMR experiments, and such devices also permit the more routine use of natural-abundance ^{13}C NMR spectroscopy. In addition, a major improvement in the scope of NMR spectroscopy of small amounts of material has also been made possible by the commercialization of miniaturized NMR probes. Now it is possible to study substances by NMR in the low microliter range of sample sizes (8,9).

NMR spectroscopy provides detailed information on molecular structure, both for pure compounds and in complex mixtures, but can also be used to probe metabolite molecular dynamics and mobility through the interpretation of NMR spin relaxation times and by the determination of molecular diffusion coefficients (10).

NMR SPECTROSCOPY OF BIOFLUIDS

Direct NMR Spectroscopy of Biofluids

As indicated above, the use of NMR spectroscopy for structure determination of purified metabolites is well established. However, the improved sensitivity and dispersion of modern high-field NMR spectrometers means that it is often possible to obtain a great deal of information directly from biofluids such as urine and bile. The identification of metabolites detected in a biofluid NMR spectrum can involve the application of a number of other NMR techniques including 2-D experiments. Although the ^{1}H NMR spectra of urine and other biofluids are very complex, many resonances can be assigned directly on the basis of their chemical shifts, signal multiplicities, by adding authentic material, and remeasuring the spectrum. Indeed some of the earliest examples of the detection of xenobiotic metabolites in, for example, urine were performed using ^{1}H NMR spectroscopy directly on the untreated biofluid (11). Obviously 2-D NMR spectroscopy can also be useful for spreading the signals out and for working out the connectivities between signals, thereby enhancing the information content and helping to identify analytes [and once again such applications were reported for some of the earliest studies on

biofluids (12)]. These 2-D methods include the ^{1}H-^{1}H J-resolved experiment, which reduces the contribution of macromolecules and yields information on the multiplicity and coupling patterns of resonances (13). Other 2-D experiments such as correlation spectroscopy (COSY) and total correlation spectroscopy (TOCSY) provide ^{1}H-^{1}H spin-spin coupling connectivities. Use of other nuclei can be important to help assign NMR peaks, and here inverse-detected heteronuclear correlations, usually ^{1}H-^{13}C, can also be obtained by use of sequences such as heteronuclear single quantum coherence (HSQC) or heteronuclear multiple bond correlation (HMBC) (10).

As indicated above, NMR spectroscopy has been widely applied in drug metabolism studies involving fluorine-containing drugs and xenobiotics, with ^{19}F NMR spectroscopy of biofluids (e.g., urine) providing a relatively sensitive and highly specific means of determining the excretion and metabolic profiles of fluorinated compounds and their metabolites (2,3,14 18). ^{19}F NMR spectroscopy is particularly useful as resonances are usually well resolved as a result of the large chemical shift range for this nucleus. This makes ^{19}F NMR spectroscopy exquisitely sensitive to structural change, even many bonds away from the "reporter" fluorine substituent. However, while perfect for performing excretion balance and initial profiling studies, ^{19}F NMR spectra provide relatively little structural information, and metabolite characterization/identification generally requires additional studies.

A typical recent example from the literature is concerned with the detection and quantification of metabolites of a substituted aniline (19) where ^{19}F NMR was used to obtain metabolite profiles as an alternative to conventional [^{14}C]-labeling studies. This work was performed on samples derived from the earthworm *Eisenia veneta* following exposure to the model environmental toxin 2-fluoro-4-iodoaniline as part of a series of studies looking at the metabolic fate of fluorinated anilines in these worms (20,21). In this case, metabolism was studied using a range of tools including ^{19}F NMR spectroscopy, high performance liquid chromatography (HPLC)-MS, and iodine-specific detection via HPLC-ICPMS (inductively coupled plasma MS). Here ^{19}F NMR spectroscopy was used to provide quantitative and qualitative metabolite profiles with a total of some 13 ^{19}F-containing components detected (including unchanged parent). The presence of the fluorine substituent on the ring results in the coupling of the fluorine resonance to protons also present on the ring to give a characteristic multiplet (an apparent triplet due to the presence of *ortho* and *meta* protons). This meant that for the more abundant components, it was possible to use the fluorine as a "reporter" to show that metabolism had not occurred on the ring itself and must therefore have taken place on the aniline group. However, detection of proton-coupled ^{19}F NMR spectra ion this way does result in reduced sensitivity compared with proton-decoupled ^{19}F-$\{^{1}H\}$ NMR spectra. For this reason, quantification was performed on fully proton-decoupled spectra. Typical ^{19}F NMR and ^{19}F-$\{^{1}H\}$ NMR spectra from this study from whole-body worm extracts are shown in Figure 1A, B. LC-MS studies identified an N-glutamyl conjugate as the major metabolite with an N-glucoside also detected.

Statistical Total Correlation Spectroscopy

In addition to conventional NMR methods for the structure determination of metabolites, valuable structural data for drug metabolites in biological fluids can also be obtained via "statistical total correlation spectroscopy" (STOCSY) (22). This technique exploits the correlations seen between the intensities of spectral features over multiple spectra (e.g., obtained from a number of urine spectra from several subjects) so as to obtain a statistically derived spectrum. Thus, spectral features from the metabolite(s) of interest

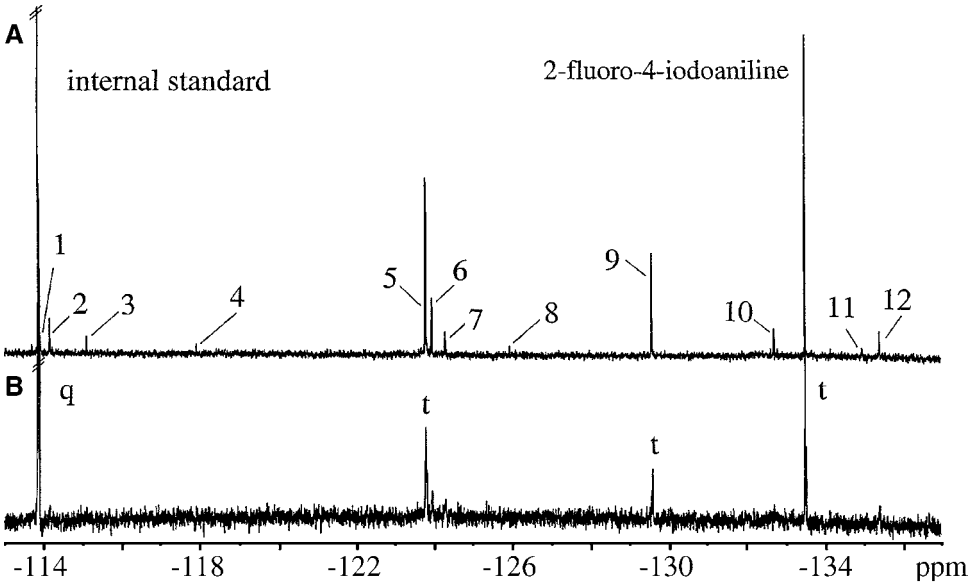

Figure 1 The ^{19}F $\{^{1}H\}$ (**A**) and ^{19}F NMR (**B**) spectra obtained from the combined methanolic extracts of four earthworms (*Eisenia veneta*) obtained following 72 hour exposure to 2 fluoro 4 iodoaniline impregnated filter papers (5μg/cm^2).

will show strong positive intensity correlations that can be used for structure determination. This technique is of particular value in metabolic profiling as this type of study typically generates numerous qualitatively similar, but quantitatively different, spectra for statistical analysis thereby providing the data needed to detect genuine structural correlations and reduce or eliminate spurious ones. STOCSY also, unlike conventional 2-D NMR spectroscopy, retains the spectral resolution of the original 1-D spectra. The conventional 2-D correlation NMR spectroscopic methods, in contrast, have certain practical limitations preventing the indirect dimension reaching the resolution of a directly acquired spectrum (important as there is usually significant spectral crowding/overlap in biofluid spectra). Metabolites are often present at relatively low concentrations compared with major endogenous metabolites, but STOCSY enables the better sensitivity of 1-D NMR over multidimensional NMR to be exploited, especially for long-range couplings. STOCSY, unlike the usual 2-D NMR experiments, which are limited by the strength of the scalar couplings or internuclear proximity, suffers no such reduction in sensitivity to these correlations as the distance between the relevant nuclei increases.

We have presented a strategy for directly detecting drugs and their metabolites in the biofluids of individuals on the basis of statistical correlation matrices calculated for individual spectral data points using urine samples collected as part of the INTERSALT and INTERMAP studies, which investigated the role of nutrition in adverse population blood pressure levels (23). Acetaminophen and ibuprofen were used to exemplify this method. To illustrate the approach, STOCSY was performed on the subset of samples from known acetaminophen users. Correlation matrices were calculated for data points selected to coincide with the peak maxima of acetaminophen-related NMR signals with a view to establishing correlations between the separate proton environments for each metabolite and generating molecular structural information. Because the intensities of different NMR peaks from the same molecule are directly related to the number of protons contributing to the signal, the relative intensity of signals from the same molecule

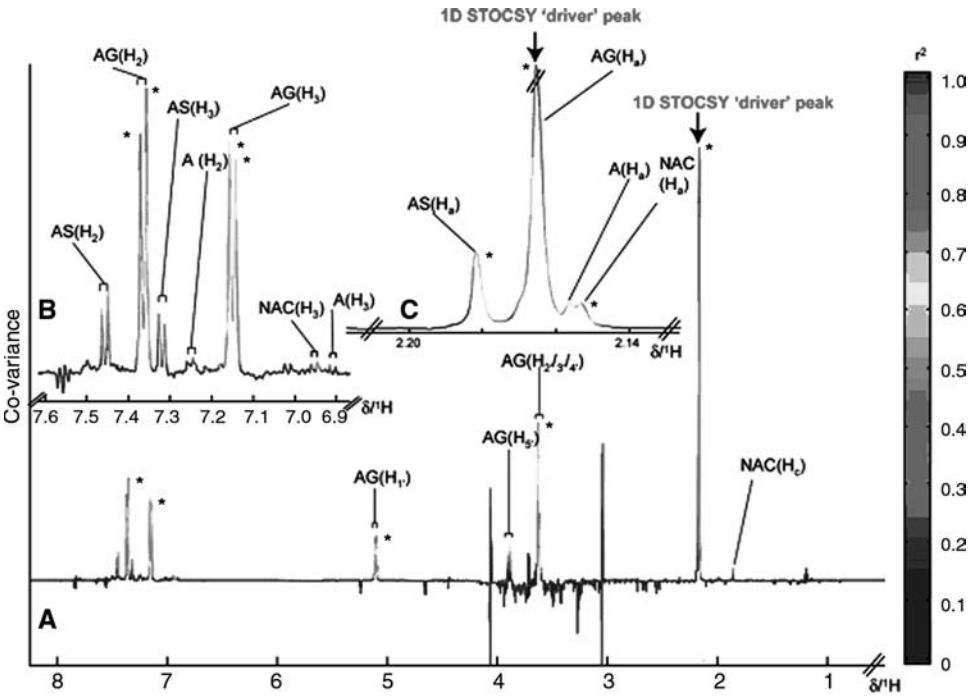

Figure 2 (**A**) statistical total correlation spectroscopy plot derived from the correlation matrix calculated between the data point at the peak maxima of the N acetyl proton signal of AG resonance (δ 2.17) and all other data points, as indicated by the arrow, showing strong correlation with resonances at δ 3.62, 3.89, 5.1, 7.13, and 7.36. Slightly weaker correlations are seen with A and AS. (**B**) Expansion for the aromatic region showing signals for acetaminophen and its related metabolites. (**C**) Expansions for the δ 2.17 N acetyl resonance of acetaminophen metabolites.

should in theory be highly correlated. Correlations between the selected resonance and all the other data points of the spectra can be presented using color coding (not shown here) for ease of visualization. The signal intensity and shape are used to represent the covariance matrix, which provides a graphical similarity to NMR spectra, thereby facilitating ease of interpretation by the NMR spectroscopist. The method is illustrated in Figure 2, which shows which peaks of acetaminophen metabolites show intensity correlations.

Importantly, the STOCSY application does not only provide structural information pertaining to protons on the same molecule but also connects signals for protons deriving from closely related molecules. For example, all metabolites derived from the same parent compound, for example, acetaminophen, acetaminophen glucuronide, acetaminophen sulfate, and *N*-acetyl cysteine acetaminophen, show correlations that vary in strength according to the degree of overlap with other endogenous or exogenous signals. This may prove a particularly useful feature in cases where the metabolism of a xenobiotic is not well characterized and may help to differentiate xenobiotic metabolites from drug-induced changes in endogenous molecules. STOCSY can differentiate between endogenous and exogenous signals on the basis of the structure of the pharmacological connections. The negative correlation matrix generated from any drug metabolite resonance will contain only endogenous responses to the drug. The positive correlation matrix will indicate either drug-related or endogenous correlations with drug metabolites. However, one would expect that in most cases the correlations between drug metabolites would be stronger than correlations observed between drug metabolites and endogenous

molecules. In the case of the positive correlation matrix, differentiation can be made on the basis of molecular structural information, since endogenous molecular structures will be largely implausible for drug biotransformations. It is also possible to draw inferences regarding the strength of intermolecular correlations. The correlation between acetaminophen and its sulfate conjugate is weaker than the correlation between the acetaminophen parent and the glucuronide. Factors that may influence drug metabolite ratios include saturation of metabolic pathways, interaction with other pharmaceuticals, nutritional status, and the time of administration of the drug in relation to sampling time. For example, acetaminophen sulfate is known to have a longer half-life than acetaminophen glucuronide, and the capacity for sulfation is more readily saturated.

A visualization of the connectivities that can be observed using STOCSY compared with conventional 2-D NMR spectroscopy for acetaminophen metabolites is shown in Figure 3.

While ^{1}H NMR spectra of biofluids are complex, containing much structural information, as discussed above, differentiating drug metabolite resonances is often complicated by the presence of large, overlapping resonances because of the endogenous

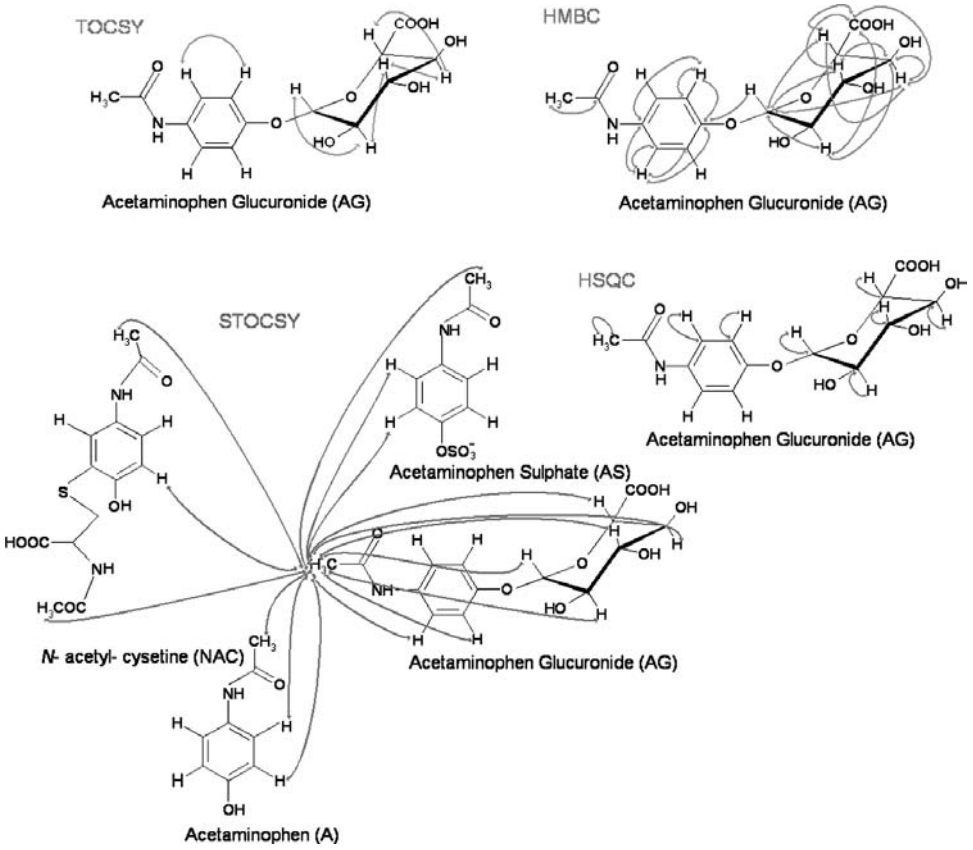

Figure 3 Schematic for acetaminophen glucuronide comparing the intramolecular ^{1}H ^{1}H and ^{1}H ^{13}C correlations detected in the TOCSY, HSQC, HMBC, and intra and intermolecular correlations given by statistical total correlation spectroscopy (STOCSY) analyses. Note that these are the actual observed, and not the theoretical correlations. Although the NMR parameters were optimized for this study by adjusting the acquisition/processing parameters, it may be possible to observe further correlation structures from each of these measurements.

compounds present in the sample. However, using a modified STOCSY approach with ^{1}H and X-nucleus (^{19}F) data sets, recorded in parallel and obtained for metabolites of, for example, the fluorinated antibiotic flucloxacillin (24), heteronuclear NMR spectra have been directly integrated by correlation analysis for drug metabolite analysis and show the novel use of statistically based heteronuclear editing of homonuclear correlation spectra to give a statistical equivalent of the 2-D-edited TOCSY-HSQC (10) experiment. This approach enables ^{19}F-^{1}H heteronuclear STOCSY to be used to exploit the resolution and specificity of ^{19}F NMR spectra for generating metabolite profiles and also enables access to the structurally rich ^{1}H NMR data. In addition, the resulting intermetabolite correlations can also provide information on the routes of biotransformation. This approach has advantages over traditional heteronuclear spectroscopy, particularly the preservation of spectroscopic resolution in 2-D spectra, and the detection of structural relationships across an effectively unlimited number of chemical bonds between nuclei. The examination of intermetabolite correlations can also aid in interpreting heteronuclear spectral correlations. Previous studies on flucloxacillin metabolism in the rat using ^{19}F-{^{1}H} NMR spectroscopy at 9.4 T (400 MHz ^{1}H resonance frequency, 376 MHz ^{19}F resonance frequency) detected 5′-hydroxymethylflucloxacillin and both 5R and 5S epimers of the β-lactam ring-opened penicilloic acid (25). In the more recent study in human, at a higher field strength (800 MHz ^{1}H frequency, 753 MHz ^{19}F frequency), these metabolites were readily observed following an oral administration of a normal therapeutic dose of 500 mg to five human volunteers. Urine samples were collected just prior to administration of the dose and then intermittently over a 72-hour period. On collection, samples were immediately frozen and stored at $-40^{\circ}C$. Typically, between four and six urine samples were collected from each volunteer during the course of the study. In addition, a further unknown metabolite was clearly visible by ^{19}F NMR spectroscopy (24). But even at this field strength, identifying compound-related signals, with the exception of the gem-methyl signals, in the corresponding ^{1}H spectra of the urine samples was not straightforward because of the large number of endogenous interferences.

However, examination of the correlation coefficient between the intensity of the parent ^{19}F resonance (I) with the values of each data point in the ^{1}H spectra, all of the characteristic resonances of flucloxacillin were identifiable (including resonances from protons up to 13 bonds from the F atom) (See figures in Ref. 24). This is also true for the major metabolite 5′-hydroxymethylflucloxacillin (III). In contrast, ^{1}H-^{19}F COSY experiments could only detect the cross peaks between aromatic ring protons, where there were significant scalar couplings ($J_{HF} > 2$ Hz). A further characteristic feature of flucloxacillin metabolites, such as the strongly correlated methyl resonances, was also highlighted via this STOCSY approach, which produced correlations that were dependent on the ^{19}F resonance selected to generate the 1-D correlations. In the case of 5S-flucloxicillin penicilloic acid, (IV) this method highlighted resonances originating from the parent and other metabolites with those to the gem-methyl resonances specific to the metabolite amongst the highest correlations ($R > 0.9$). In contrast, the correlation to the corresponding peak in the parent compound failed to highlight these resonances, showing that the underlying correlation structure of metabolite excretion was sufficiently different for the ^{1}H signals related to 5S-flucloxicillin penicilloic acid to be differentiated.

In addition to the peak-selective 1-D correlation analysis described above, the integration of both ^{19}F and ^{1}H data sets via statistical correlation is perfectly feasible. The most direct approach is to calculate the correlation coefficients between individual spectral points in the ^{1}H data set and those in the ^{19}F data set (22). This 2-D heteronuclear correlation analysis can be displayed as a conventional 2-D NMR data set with, for

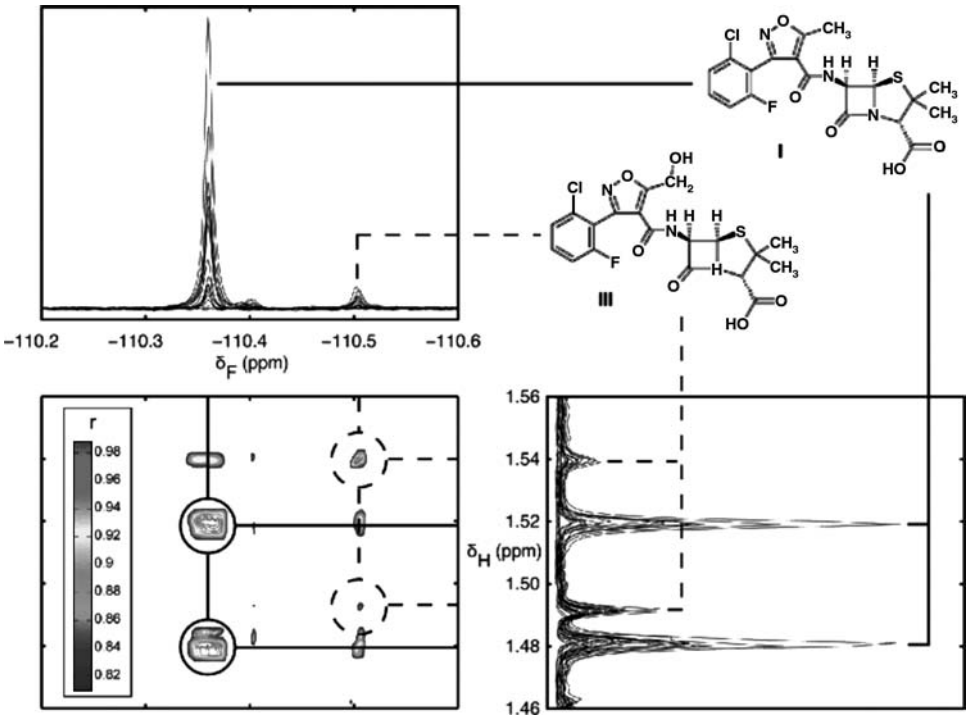

Figure 4 ^{19}F ^{1}H STOCSY analysis. Partial ^{19}F NMR, ^{1}H NMR, and ^{19}F ^{1}H heteronuclear STOCSY plots showing correlations between spectra, determined using the correlation between peak intensities in the two sets of spectra. Correlation cutoff set at $r > 0.8$. I, flucloxacillin; III, 5′ hydroxymethyl flucloxacillin. *Abbreviation*: STOCSY, statistical total correlation spectroscopy.

example, the gem-methyl resonances of flucloxacillin and its metabolite 5′-hydroxymethylflucloxacillin distinguished by the intensity level (degree of correlation) between the individual ^{19}F and ^{1}H resonances. This is illustrated in Figure 5 (For color representation See Ref. 24).

Statistical Integration of NMR and MS Data Sets

In an extension to the correlation approach for NMR spectra, a major extension has allowed the co-interrogation of NMR and MS data sets collected on the same cohort of samples. This provides a correlation connectivity between NMR peaks and corresponding MS ions, thus aiding the identification of both endogenous biomarkers of some perturbation and drug or other xenobiotic metabolites. The approach has been termed statistical heterospectroscopy (SHY) and applied to the biochemical effects of hydrazine toxicity in the rat (26). This method is extendable to any series of spectroscopic or indeed omics data sets recorded in series or in parallel on a group of samples. Also, it is possible to bridge from parent ion to fragment ion correlations (SHY-NMR-MS-MS) even by using ordinary LC-MS methods because there is always some fragmentation occurring in the ion source and this can be statistically recovered. The technique is particularly sensitive for biomarker mining because if there is one known disease biomarker in a given data set, then all correlated or anti-correlated biomarkers in the matrix can be detected and identified. The theory of SHY interactions and data recovery is shown in Figure 6 (below),

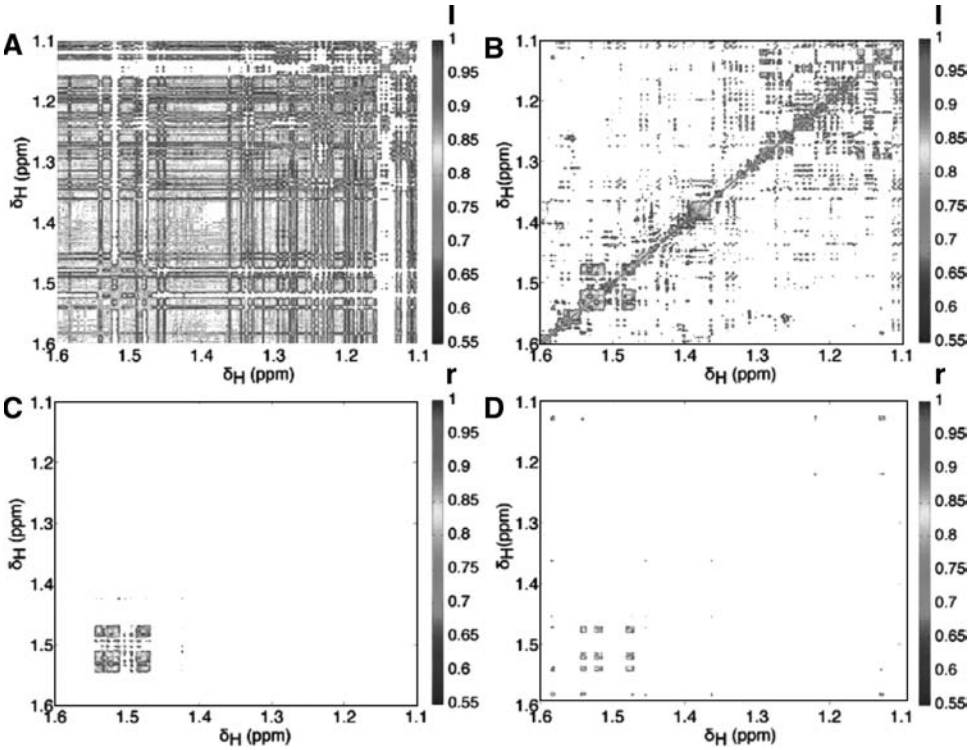

Figure 5 2 D ^{19}F edited ^{1}H ^{1}H statistical total correlation spectroscopy maps. (**A**) Unnormalized data; (**B**) normalized data; (**C**) normalized data, edited by correlation to the ^{19}F NMR peak of I (parent, δ_F 110.36 ppm); (**D**) normalized data edited by peak IV [(5S) flucloxacillin penicilloic acid, δ_F 110.07 ppm].

and a typical correlation map between MS and NMR data for hippurate is shown in Figure 6 (lower).

LC-NMR AND RELATED TECHNIQUES

NMR spectroscopic analysis need not require the time-consuming isolation and purification of metabolites given the efficient methods now available for "hyphenating" separations such as HPLC online with NMR (27,28). Indeed, even more efficient systems combining HPLC-NMR and HPLC-MS into a single "hypernated" system have been described for drug metabolite structure elucidation (29 31).

Obviously, when performing HPLC-NMR, it is necessary to detect signals from low concentrations of analytes in the presence of large ^{1}H NMR signals from the HPLC solvents. However, efficient solvent suppression methods are available, and these are more than capable of dealing with standard reversed-phase (RP) solvent NMR resonances arising from, for example, methanol/water or acetonitrile/water mixtures (including solvent gradients). For practical reasons, D_2O is generally used instead of H_2O for RP-solvent systems because this renders multiple solvent suppression easier. Indeed the use of D_2O, which is relatively inexpensive, in combination with deuterated organic solvents such as acetonitrile-d_3, is not uncommon in pharmaceutical laboratories given that the cost of the solvent is negligible compared with the costs of running the instrumentation,

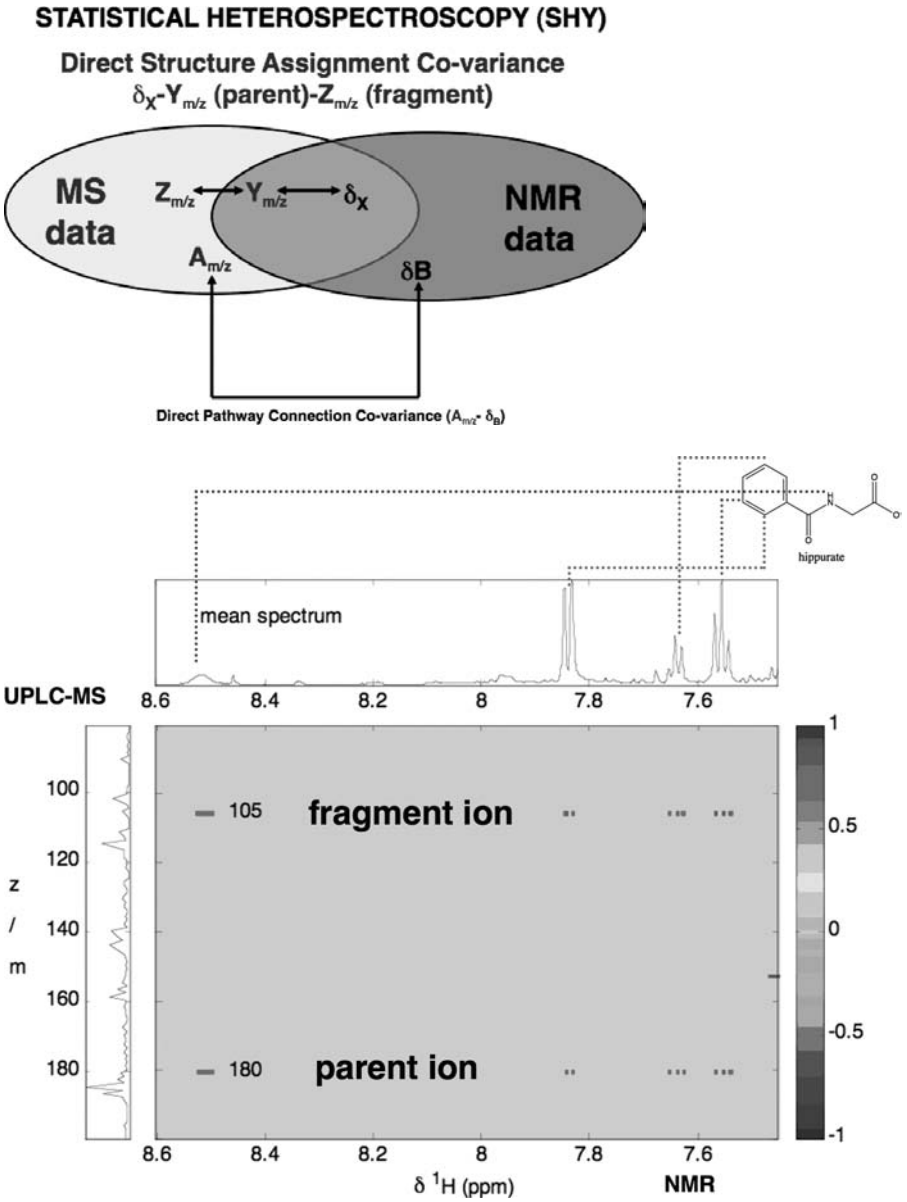

Figure 6 The concept of statistical heterospectroscopy for NMR and MS correlation analysis (*upper*), and a typical NMR/MS correlation data set indicating correlation between the NMR chemical shifts for hippurate (horizontal axis) and its related MS m/z values (vertical axis) (*lower*). *Abbreviation*: MS, mass spectrometry.

while a substantial gain in quality of the results is obtained. The use of elevated temperatures for LC has also been demonstrated (though not for drug metabolism studies) including the use of "superheated" D_2O, enabling the complete elimination of the organic modifier as a component of the mobile phase, thereby eliminating the need for dual solvent suppression (32).

In addition to a singlet methyl resonance in the ^1H NMR spectrum, both acetonitrile and methanol give rise to ^{13}C satellite peaks (caused by the one-bond ^1H-^{13}C spin

couplings resulting from the 1.1% of molecules containing the spin-active ^{13}C isotope in the methyl group). Because these satellite peaks can be larger than the signals for the trace analytes, they should also be suppressed. This can be accomplished in a variety of ways including setting a suppression irradiation frequency over the central peak and the two satellite peaks in a cyclical fashion, or if an inverse geometry probe with a ^{13}C coil is used, broadband ^{13}C decoupling can be performed to collapse the solvent satellite peaks under the central peak so that they are eliminated via conventional single frequency suppression.

Software provided by the NMR instrument manufacturers can be used for automatic solvent suppression, and this is especially valuable when gradient elution using organic modifiers such as acetonitrile is used as the NMR chemical shift for the methyl resonance will change with the solvent composition. In principle, it is possible to effect NMR detection for any of the magnetically active nuclei, but in practice, ^{1}H and ^{19}F have been studied most often. An obvious advantage of using ^{19}F NMR spectroscopy for detection of fluorine-containing molecules is, as in the case of biofluid analysis, the very low background and high specificity compared with detection by ^{1}H NMR spectroscopy.

The simplest method for LC-NMR is continuous-flow detection for ^{1}H (33,34) or ^{19}F NMR (35) spectroscopic detection of metabolites (though there are also a few examples of ^{2}H and ^{31}P NMR detection in the drug metabolism field) (4,36). If detailed studies on metabolites are required, stop-flow HPLC-NMR spectroscopy can be performed using all of the standard 2-D NMR techniques (e.g., COSY, TOCSY, etc.). Variations on the stop-flow experiment include the collection of fractions eluting from the column in capillary loops or on SPE phases (see below), for later off-line NMR study, or alternatively, the flow can be halted at short intervals as the eluted peak moves through the NMR flow cell, thereby obtaining spectra from various portions of the peak (useful for peaks containing several partially resolved components).

As indicated above, in addition to LC-NMR, it is also quite possible to perform the double hyphenation (or hypernation) of LC-NMR and MS. Generally, in LC-NMR, the spectrometers have been placed in parallel rather than in series, splitting the flow such that a minor fraction (approximately 5%) goes to the MS. Depending on the lengths of tubing used, it can be arranged that analytes are detected by the MS first allowing this to direct stopped-flow NMR experiments. For HPLC-NMR-MS, the principal MS ionization method used is electrospray (ESI) in positive- and negative-ion modes. MS can be used to search for particular diagnostic groups or fragments (e.g., an increase in m/z of 16 for hydroxylated metabolites or 176 for a glucuronide), and such data can then be used to aid the interpretation of the NMR spectroscopic data. There are now numerous examples of the use of LC-NMR-MS in drug metabolism studies [including the use of cryoprobes to increase sensitivity (45)] as well as a review (37). Selected applications include the human metabolism of the nonsteroidal inflammatory drug ibuprofen (38) and model compound metabolism in animals (15,16,39) illustrating the use of the technique.

Metabolite identification by LC-NMR in samples such as urine or bile is obviously complicated by the large number of endogenous components also present. However, a variety of strategies for metabolite detection enable the selective and specific detection of drug-related material. The classic approach is to employ radiolabels (^{3}H or ^{14}C), which provide a specific tracer for compound-related material. This approach, combined with both online NMR spectroscopy and MS, is exemplified by a study of the metabolism of the β-blocker practolol in the rat (40). Thus, on-flow radioactivity detection was used to monitor the eluent from the LC and quantify the metabolites present, while unequivocal metabolite identification was provided by online ^{1}H NMR and MS. The specifically detected [^{14}C]-radiolabeled peaks were subjected to stopped-flow ^{1}H NMR spectroscopy,

which was able to provide good-quality spectra for practolol, its ring-hydroxylated metabolite, and the corresponding glucuronide of this hydroxylated metabolite. These structures were confirmed by the complementary mass spectral data acquired at the same time. Concomitantly, the metabolic fate of practolol's N-acetyl group was also investigated via stable isotope labeling of the acetyl with [^{13}C]. This gave a diagnostic spin-spin coupling between the ^{13}C and the ^{1}H on the acetyl methyl as well as an increase of 1 mass unit in the mass spectra. This study demonstrated (by both NMR and MS) that a significant portion of the [^{13}C]-labeled acetyl was subject to a "futile" deacetylation-reacetylation cycle. Thus, this normally unobserved "silent" metabolism was found to have occurred to the extent of 7% to 10% of the total, including for the apparently "unchanged" parent compound. Indeed, the use of this type of stable isotope labeling is particularly useful for teasing out this type of metabolic information and has been used in several NMR-, LC-NMR-, and LC-NMR-MS-based studies of futile deacetylation for analytes such as acetaminophen and phenacetin in the rat (41,42) and human (43,44).

Obviously, isotopic labeling is not always an option, especially in the early stages of drug discovery, but other options for metabolite detection exist for LC-NMR-MS. At their simplest, these include screening for UV absorbing, or novel MS, peaks in the chromatogram that are not present in the pre-dose samples, and performing spectroscopy on them when the separation is transferred to the LC-NMR system. If LC-MS is used for the screening process, the presence of chlorine or bromine in the parent molecule can greatly aid this search. Alternatively, ^{19}F NMR spectroscopy can be used directly to monitor the LC eluent if one or more fluorine atoms are present in the drug. An illustrative example of the use of both approaches is the study of the metabolic fate of 2-bromo-4-trifluoromethyl-aniline in the rat (dosed at 50 mg/kg) (39) where both ^{19}F NMR and negative-ion ESI MS (for the bromine isotope pattern) were used to detect metabolites in the eluent. This showed that the major metabolite was 2-amino-3-bromo-5-trifluoromethylphenylsulfate (23%). In addition, 2-bromo-4-trifluoromethylphenyl-hydroxylamine-N-glucuronide and 2-amino-3-bromo-5-trifluoromethylphenyl-glucuronide were detected as minor metabolites (7% and 1.4% of the dose, respectively) together with numerous trace metabolites, detectable only by MS because of their low concentrations. Detection of low-abundance metabolites in LC eluents has been improved by the application of cryoprobes, as demonstrated by their use for acetaminophen metabolites present in urine (45) and detected on flow at 0.4 mL/min. In this study, 100-μL aliquots of human urine, obtained for the period zero to four hours post oral administration of 500 mg of the drug, were injected on to a conventional HPLC column (4.6 by 50 mm) and the metabolites eluted with a RP gradient of D_2O and acetonitrile-d_3 over a run time of 15 minutes. NMR and MS spectra for the unchanged parent, glucuronide, and sulfate were obtained together with previously unreported methoxy- and 3-methoxy-glucuronides (as well as an unidentified acetaminophen metabolite).

Another technical development for structure elucidation that combines LC and NMR involves trapping and concentrating peaks eluting from the column using online SPE (46). Isolated components are then eluted directly into the NMR flow probe, which can be done using a deuterated solvent, with the benefit that the composition of the solvent system with respect to, for example, mobile-phase additives used to optimize the separation is no longer an issue. Also, there is no longer any requirement to employ deuterated solvents for the chromatographic separation.

The SPE step can also be used to combine several runs to increase the amount of low-abundance metabolites for subsequent NMR spectroscopy. An example of the use of LC-SPE-NMR-MS approach is the determination of the metabolic fate of phenacetin in human (44). For this phenacetin study, a major focus was the determination of the degree of "futile deacetylation" undergone during metabolism of the drug (of interest because of

the analgesic nephropathy associated with phenacetin usage and the possible involvement of the potent nephrotoxin 4-aminophenol). Following a 150-mg oral dose of stable isotope labeled drug (phenacetin-C^2H_3), ^{1}H NMR spectroscopy directly on urine revealed the presence of acetaminophen metabolites (the glucuronide, sulfate, and N-acetyl-L-cysteinyl conjugates) with clear evidence from the presence of N-acetyl resonances for futile deacetylation (approximately 20%). However, partial overlap of the acetyl signals precluded an assessment of futile deacetylation for the N-acetyl-L-cysteinyl conjugate. LC-MS-SPE-NMR analysis of a urine extract from this study, with metabolites detected by MS and collected on the in-line SPE cartridges, was then performed (44). Metabolites of interest were eluted from the SPE phase using deuteromethanol directly into the flow probe of a 600-MHz NMR spectrometer. The futile deacetylation of the SPE-purified metabolites was found to be between 25% and 37% (by MS), depending on the structure, which is much higher than that observed when acetaminophen is administered to human. One point to note that came out of this study was partial chromatographic resolution of the deuterated and non-deuterated metabolites, which, because of the mass-directed SPE collection, resulted in the selective enrichment of the former. The consequence of this was that the amount of futile acetylation was underestimated by NMR spectroscopy compared with MS.

An approach to enhancing information recovery from cryogenic probe "on-flow" LC-NMR spectroscopic analyses of complex biological mixtures has been demonstrated using a variation on the STOCSY method (47). Cryoflow probe technology enables sensitive and efficient NMR detection of metabolites on flow, and the rapid spectral scanning allows multiple spectra to be collected over chromatographic peaks containing several species with similar, but nonidentical, retention times. This enables ^{1}H NMR signal connectivities between close-eluting metabolites to be identified, resulting in a "virtual" chromatographic resolution enhancement visualized directly in the NMR spectral projection. This method has been demonstrated for structure assignment of drug and endogenous metabolites in urine from HPLC of rat urine samples. An example is shown in Figure 7 for phenylglucuronide.

NMR AND LC-NMR SPECTROSCOPY APPLIED TO DRUG METABOLITE REACTIVITY

Reactive metabolites represent an ever-present concern for research programs seeking to discover and develop new drugs and NMR spectroscopy has contributions to make in determining the degree chemical reactivity of such species as part of the of risk assessment process (see chapter by Kumar and Baillie in this book). An example of this derives from the fact that many carboxylic acid containing drugs are metabolized to β-1-O-acyl glucuronides to a greater or lesser extent. It has long been appreciated that these ester glucuronides are both subject to base catalyzed hydrolysis, acyl migration and covalent adduct formation to proteins, with obvious potential for toxicological consequences, and the field has recently been reviewed (48). While hydrolysis is relatively easy to determine analytically, using, for example, HPLC-MS, acyl migration reactions result in a number of positional isomers (to the 2-, 3-, and 4-hydroxyl groups of the glucuronic acid moiety) with, in addition, production of the corresponding α- and β-anomers. An example of this type of application, to kinetic studies on the intramolecular acyl migration of the β-1-O-acyl glucuronides of ketoprofen (and metabolites) and tolmetin isolated from urine, is provided by a recent study (49). An example of the type of ^{1}H NMR spectra generated in this investigation is given in Figure 8. Another, more

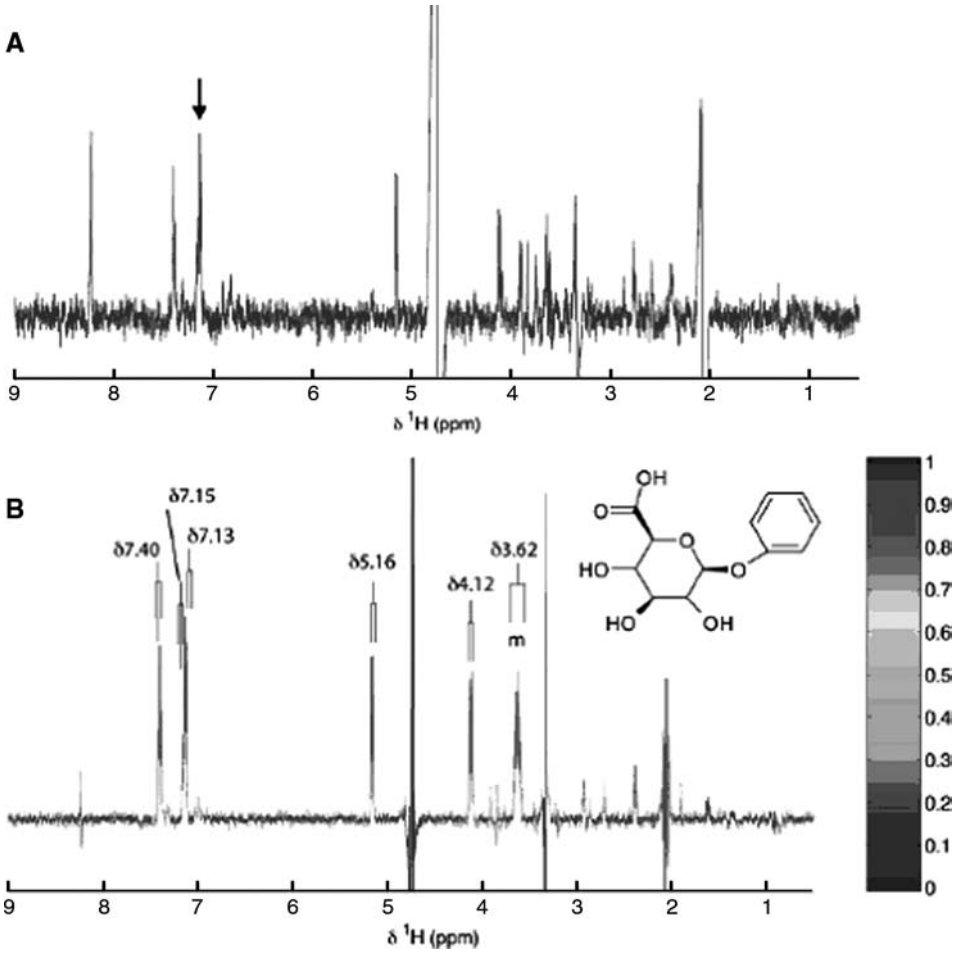

Figure 7 600 MHz 1 D ^{1}H NMR spectrum from an on flow chromatogram of rat urine, corresponding to a retention time of 54 minutes, showing the driver resonance marked with an arrow (**A**). (**B**) A 1 D STOCSY pseudo spectrum based on correlation to the driver chemical shift δ 7.13; the highlighted metabolite is phenylglucuronide, and resonances are indicate in (**B**) and resonances showing strong correlations to the driver peak are those with the assigned chemical shifts (δ).

recent, example of the use of the ^{1}H NMR spectroscopy based methodology on both the synthetic and urine-isolated ester glucuronides of ibuprofen and its metabolites illustrates the value of the approach (50). The results of these studies confirmed the different rates of acyl migration for R- and S-ibuprofen glucuronide (ca. 1.8 and 3.7 hours, respectively) but also revealed that the side chain oxidized ibuprofen metabolites (hydoxy- and carboxy-ibuprofen glucuronides) had surprising long transacylation half-lives (approximately 5 and 4.8 hours, respectively) compared with the glucuronides of the parent compound, given that the carboxyl and hydroxyl groups are far from the reactive carbonyl carbon in chemical bond terms and so do not exert a large electronic effect.

As well as the methods described above a variation the statistical spectroscopic method STOCSY has been applied to the recovery of structural information on unstable intermediates formed in reaction mixtures (51). This was exemplified with respect to the internal acyl migration reactions of the 1-β-O-acyl glucuronides. Multiple sequential

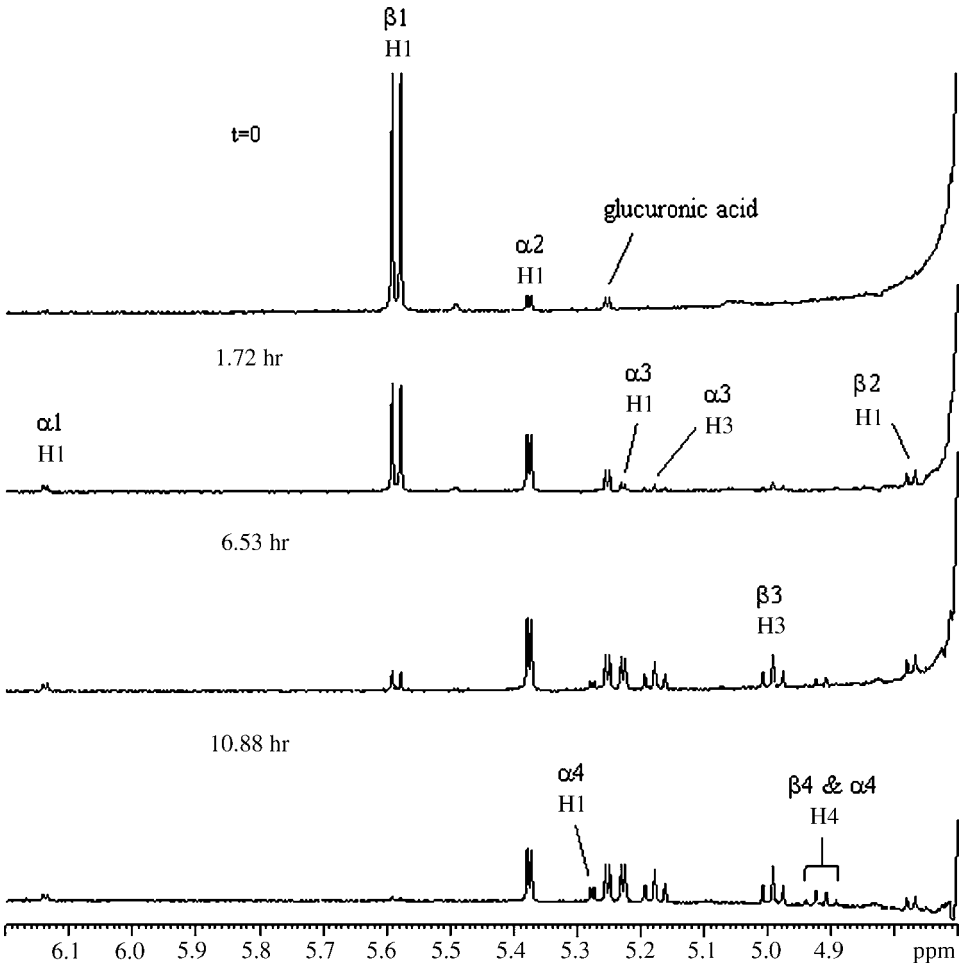

Figure 8 Degradation of (S) ketoprofen β 1 O acyl glucuronide and the appearance of positional isomers at pH 7.4 and 37°C as a function of time shown, as followed by ^{1}H NMR spectroscopy. The following example serves to show the NMR peak nomenclature: α2 H1 is the glucuronide H1 proton of the α form of the 2 O acyl isomer.

800 MHz cryoprobe ^{1}H NMR spectra [1-D and 2-D J-resolved (JRES)] were collected on a solution of a synthetic model drug glucuronide, 1-β-O-acyl (S)-α-methyl phenylacetyl glucuronide (MPG) over 18 hours to monitor the reaction which leads to the formation of the eight positional isomers and hydrolysis products. As the reaction proceeds and new isomers form, the NMR signal intensities vary accordingly allowing the application of a novel kinetic variant on statistical total correlation spectroscopy (K-STOCSY). This method can be used to recover the connectivities between proton signals on the same reacting molecule on the basis of their intensity covariance through standard 1-D NMR spectra and the skyline projected singlets of the ^{1}H-^{1}H JRES NMR spectra through time, that is, the K-JRES-STOCSY experimental variant, which increases the effective spectral dispersion. This method is ideally suited for the analysis of heavily overlapped spin systems. High statistical correlations were observed between mutarotated α- and β-anomers of individual positional isomers, as well as directly acyl migrated products and anticorrelation observed between signals from compounds that were being depleted as

others increased. This statistical kinetic approach enabled the recovery of structural connectivity information on all isomers allowing unequivocal resonance assignment, and this approach to spectroscopic information recovery has wider potential uses in the study of reactions that occur on the second-to-minute timescale in conditions where multiple sequential NMR spectra can be collected. JRES-STOCSY is also of potential use as a method for recovering spectroscopic information in highly overlapped NMR signals and spin systems in other types of complex mixture analysis.

As well as direct determination of these compounds in, for example, urine and the determination of their transacylation rates in aqueous solution or biological fluids LC-NMR has also been extensively used. For example, in the case of fluorobenzoic acid glucuronides, an HPLC-NMR method was used to separate 1-, 2-, 3-, and 4-positional isomers, and their α- and β-anomers, for 2-, 3-, and 4-fluorobenzoic acids together with the aglycones formed via hydrolysis on equilibrium mixtures of transacylated glucuronides, using continuous-flow LC (52). Each isomer was resolved chromatographically and identified via its NMR spectrum. Work of this type on a range of compounds showed that elution order of transacylated glucuronides was β-4-O-acyl-, α-4-O-acyl-, α-3-O-acyl-, β-3-O-acyl-, β-2-O-acyl-, and α-2-O-acyl- irrespective of the nature of the carboxylic acid containing moiety. Further applications of this approach to the study of kinetics of the acyl migration reaction for 2-, 3-, and 4-fluoro-, and 2- and 3-trifluoromethylbenzoyl-D-glucopyranuronic acids have been performed (53,54) using both continuous-flow HPLC-NMR and stopped-flow methods. For detailed studies the separated isomers were held in the flow probe and sequential ^{1}H NMR spectra collected, thus allowing the direct observation of the appearance of the glucuronide positional isomers as, for example, the β-4-O-acyl-glucuronides rearranged to the 3- and 2-positional isomers.

In this way, the acyl migration of the glucuronides of the model drug 6,11 dihydro-11-oxo-dibenz(b,e)oxepin-2-acetic acid (55), a novel retinoid known as CD271 (56), the glucuronides of enantiomeric 2-phenyl propionic acids (57), and S-naproxen glucuronide (58) has also been studied. Interestingly, work with HPLC-NMR demonstrated the presence of the α-1-O-acyl isomer of naproxen, formed via the back reaction from the α-2-O-acyl isomer, a reaction that had previously been thought unlikely (59).

Another example of the use of LC-NMR for the study of metabolite reactivity is provided by studies on the reactive intermediate of acetaminophen metabolism NAPQI. This metabolite can react with glutathione at the 2, 3, or ipso carbons. This reaction has been studied by mixing N-acetyl-p-benzo-quinone imine (NAPQI) and glutathione together with the product mixture then separated using directly coupled HPLC-NMR. In this work, all three isomers were detected with the ipso derivative being most abundant and the 2′-isomer, the least. The decomposition of the ipso-NAPQI-glutathione adduct to the other isomers over a period of an hour was then successfully studied in the flow probe of the NMR spectrometer (60).

CONCLUSIONS

NMR spectroscopy will continue to be a key part of any strategy for metabolite identification as, notwithstanding the great strides made in the application of LC-MS-based techniques for metabolite characterization, it is still the case that unambiguous identification of metabolites often requires NMR spectroscopy. The ability to use ^{19}F NMR spectroscopy to perform excretion balance and metabolite profiling studies without the need for radiolabels provides an interesting opportunity to obtain high-quality metabolic data either early in drug development or, alternatively, in patient populations where radiolabeled studies might not be

possible. Similarly, the use of statistical approaches in metabolite detection and structure determination such as STOCSY offers interesting possibilities for performing studies in human without the need for radiolabels. This may prove to be important given the need to determine the metabolic fate of candidate drugs with respect to the new guidance on safety testing of metabolites (see Chapter 22 in this book).

REFERENCES

1. Wilson ID, Nicholson JK, Lindon JC. The role of nuclear magnetic resonance spectroscopy in drug metabolism. In: Woolf TF, ed. Handbook of Drug Metabolism. New York: Marcel Dekker, 1999:523 550.
2. Malet Martino M, Bernadou J, Martino R, Armand JP. ^{19}F NMR spectrometry evidence for bile acid conjugates of alpha fluoro beta alanine as the main biliary metabolites of antineoplastic fluoropyrimidines in humans. Drug Metab Dispos 1988; 16:78 84.
3. Malet Martino M, Gilard V, Desmoulin F, Martino R. Fluorine nuclear magnetic resonance spectroscopy of human biofluids in the field of metabolic studies of anticancer and antifungal fluoropyrimidine drugs. Clin Chim Acta 2006; 366:61 73.
4. Foxall PJD, Lenz EM, Lindon JC, Neild GH, Wilson ID, Nicholson JK. NMR and HPLC NMR studies on the toxicity and metabolism of ifosfamide. Ther Drug Monit 1996; 18:498 505.
5. Gabano E, Marengo E, Bobba M, Robotti E, Cassino C, Botta M, Osella D. Pt 195 NMR spectroscopy: a chemometric approach. Coord Chem Rev 2006; 250:2158 2174.
6. Keun HC, Beckonert O, Griffin JL, Richter C, Moskau D, Lindon JC, Nicholson JK. Cryogenic probe C 13 NMR spectroscopy of urine for metabonomic studies. Anal Chem 2002; 74:4588 4593.
7. Losonczi J, Green I. Cryogenically cooled NMR probes: more information in less time. Am Lab 2004; 36:26.
8. Haner RL, Llanos W, Mueller L. Small volume flow probe for automated direct injection NMR analysis: design and performance. J Magn Reson 2000; 143:69 78.
9. Price KE, Vandaveer SS, Lunte CE, Larive CK. Tissue targeted metabonomics: metabolic profiling by microdialysis sampling and microcoil NMR. J Pharm Biomed Anal 2005; 38:904 909.
10. Keeler J. Understanding NMR Spectroscopy. Chichester, U.K.: J. Wiley and Sons Ltd, 2005.
11. Bales JR, Sadler PJ, Nicholosn JK, Timbrell JA. Urinary excretion of acetaminophen and its metabolites as studied by proton NMR spectroscopy. Clin Chem 1984; 30:1631 1636.
12. Bales JR, Nicholson JK, Sadler PJ. Two dimensional proton nuclear magnetic resonance "maps" of acetaminophen metabolites in human urine. Clin Chem 1985; 31:757 762.
13. Foxall PJD, Parkinson JA, Sadler IH, Lindon JC, Nicholson JK. Analysis of biological fluids using 600 MHz proton NMR spectroscopy: application of homonuclear two dimensional J resolved spectroscopy to urine and blood plasma for spectral simplification and assignment. J Pharm Biomed Anal 1993; 11:21 31.
14. Bollard ME, Holmes E, Blackledge CA, Lindon JC, Wilson ID, Nicholson JK. ^{1}H and ^{19}F NMR spectroscopic studies on the metabolism and urinary excretion of mono and disubstituted phenols in the rat. Xenobiotica 1996; 26:255 273.
15. Scarfe GB, Wright B, Clayton E, Taylor S, Wilson ID, Lindon JC, Nicholson JK. Quantitative studies on the urinary metabolic fate of 2 chloro 4 trifluoromethylaniline in the rat using ^{19}F NMR spectroscopy and directly coupled HPLC NMR MS. Xenobiotica 1999; 29:77 91.
16. Scarfe GB, Lindon JC, Nicholson JK, Wright B, Clayton E, Wilson ID. Investigation of the quantitative metabolic fate and urinary excretion of 3 methyl 4 trifluoromethylaniline and 3 methyl 4 trifluormethylacetanilide in the rat. Drug Metab Dispos 1999; 27:1171 1178.
17. Desmoulin F, Gilard V, Malet Martino MR, Martino. Metabolism of capecitabine, an oral fluorouracil prodrug: ^{19}F NMR studies in animal models and human urine. Drug Metab Dispos 2002; 30:1221 1229.
18. Tugnait M, Lenz EM, Phillips P, Hofmann M, Spraul M, Lindon JC, Nicholson JK, Wilson ID. The metabolism of 4 trifluoromethoxyaniline and [^{13}C] 4 trifluoromethoxyacetanilide in the

rat: detection and identification of metabolites excreted in the urine by NMR and HPLC NMR. J Pharm Biomed Anal 2002; 28:875 885.
19. Duckett CJ, Wilson ID, Douce DS, Walker HJ, Abou Shakra FR, Lindon JC, Nicholson JK. Metabolism of 2 fluoro 4 iodoaniline in the earthworm *Eisenia veneta* using ^{19}F NMR spectroscopy, HPLC MS, and HPLC ICPMS (^{127}I). Xenobiotica 2007; 37:1378 1393.
20. Bundy JG, Lenz EM, Osborn D, Weeks JM, Lindon JC, Nicholson JK. Metabolism of 4 fluoroaniline and 4 fluorobiphenyl in the earthworm *Eisenia veneta* characterised by high resolution NMR spectroscopy with directly coupled HPLC NMR and HPLC MS. Xenobiotica 2002; 32:479 470.
21. Lenz EM, Lindon JC, Nicholson JJ, Weeks JM, Osborn D. ^{19}F NMR and directly coupled ^{19}F/^{1}H HPLC NMR spectroscopic investigations of the model ecotoxin 3 trifluoromethylani line in the earthworm species *Eisenia veneta*. Xenobiotica 2002; 32:535 536.
22. Cloarec O, Dumas ME, Craig A, Barton RH, Trygg J, Hudson J, Blancher C, Gaugier D, Lindon JC, Holmes E, Nicholson JK. Statistical total correlation spectroscopy: an exploratory approach for latent biomarker identification from metabolic ^{1}H NMR data sets. Anal Chem 2005; 77:1282 1289.
23. Holmes E, Loo RL, Cloarec O, Coen M, Tang H, Maibaum E, Bruce S, Chan Q, Elliot P, Stamler J, Wilson ID, Lindon JC, Nicholson JK. Detection of urinary drug metabolite (xenometabolome) signatures in molecular epidemiology studies via statistical total correlation (NMR) spectroscopy). Anal Chem 2007; 79:2629 2640.
24. Keun HC, Athersuch TJ, Beckonert O, Wang Y, Shockcor JP, Wilson ID, Holmes E, Nicholson JK. Heteronuclear (^{19}F ^{1}H) statistical total correlation spectroscopy as a new tool in drug metabolism: a study of flucloxacillin biotransformation. Anal Chem 2008; 80:1073 1079.
25. Everett JR, Jennings K, Woodnutt G. ^{19}F NMR spectroscopy study of the metabolites of flucloxacillin in rat urine. J Pharm Pharmacol 1985; 37:869 873.
26. Crockford DJ, Holmes E, Lindon JC, Plumb RS, Zirah S, Bruce SJ, Rainville P, Stumpf CL, Nicholson JK. Statistical HeterospectroscopY (SHY), a new approach to the integrated analysis of NMR and UPLC MS datasets: application in metabonomic toxicology studies. Anal Chem 2006; 78:363 371.
27. Lindon JC, Nicholson JK, Wilson ID. Direct coupling of chromatographic separations to NMR spectroscopy. Prog NMR Spectrosc 1996; 29:1 49.
28. Lindon JC, Nicholson JK, Wilson ID. Development of directly coupled HPLC NMR and its application to drug metabolism. Drug Metab Rev 1997; 29:705 746.
29. Shockcor JP, Unger SE, Wilson ID, Foxall PJD, Nicholson JK, Lindon JC. Combined hyphenation of HPLC, NMR spectroscopy and ion trap mass spectrometry (HPLC NMR MS) with application to the detection and characterisation of xenobiotic and endogenous metabolites in human urine. Anal Chem 1996; 68:4431 435.
30. Lindon JC, Nicholson JK, Wilson ID. Directly coupled LC NMR MS for metabolite identification. Encylopedia of Mass Spectrometry 2007; 8:989 1008.
31. Wilson ID, Th Brinkman UA. Hype and hypernation: multiple hyphenation of column liquid chromatography and spectroscopy. Trends Anal Chem 2007; 26:847 854.
32. Louden D, Handley A, Taylor S, Sinclair I, Lenz E, Wilson ID. High temperature reversed phase HPLC using deuterium oxide as a mobile phase for the separation of model pharmaceuticals with multiple on line spectroscopic analysis (UV, IR, ^{1}H NMR and MS). Analyst 2001; 126:1625 1629.
33. Spraul M, Hofmann M, Dvortsack P, Nicholson JK, Wilson ID. Liquid chromatography coupled with high field proton NMR detection for profiling human urine for endogenous compounds and drug metabolites. J Pharm Biomed Anal 1992; 8:601 605.
34. Spraul M, Hofmann M, Dvortsack P, Nicholson JK, Wilson ID. High performance liquid chromatography coupled to high field proton nuclear magnetic resonance spectroscopy: a application to the urinary metabolites of ibuprofen. Anal Chem 1993; 65:327 330.
35. Spraul M, Hofmann M, Wilson ID, Lenz E, Nicholson JK, Lindon JC. Coupling of HLPC with ^{19}F and ^{1}H NMR spectroscopy to investigate the human urinary excretion of flurbiprofen metabolites. J Pharm Biomed Anal 1993; 11:1004 1015.

36. Farrant RD, Cupid BC, Nicholson JK, Lindon JC. Investigation of the feasibility of directly coupled HPLC NMR with ^{2}H detection with application to the metabolism of *N* dimethylformamide d_7. J Pharm Biomed Anal 1997; 16:1 5.
37. Lindon JC, Nicholson JK, Wilson ID. Directly coupled HPLC NMR and HPLC NMR MS in pharmaceutical research and development. J Chromatogr B Biomed Sci Appl 2000; 748:233 258.
38. Clayton E, Taylor S, Wright B, Wilson ID. The application of high performance liquid chromatography, coupled to nuclear magnetic resonance spectroscopy and mass spectrometry (HPLC NMR MS), to the characterisation of ibuprofen metabolites from human urine. Chromatographia 1997; 47:264 270.
39. Scarfe GB, Wright B, Clayton E, Taylor S, Wilson ID, Lindon JC, Nicholson JK. ^{19}F NMR and directly coupled HPLC NMR MS investigations into the metabolism of 2 bromo 4 trifluor omethylaniline in the rat: a urinary excretion balance study without the use of radiolabelling. Xenobiotica 1998; 28:373 388.
40. Scarfe GB, Lindon JC, Nicholson JK, Martin P, Wright B, Taylor S, Lenz E, Wilson ID. Investigation of the metabolism of $^{14}C/^{13}C$ practolol in rat using directly coupled radio HPLC NMR MS. Xenobiotica 2000; 30:717 729.
41. Nicholls AW, Caddick S, Wilson ID, Farrant DR, Lindon JC, Nicholson JK. High resolution NMR spectroscopic studies on the metabolism and futile deacetylation of 4 hydroxyacetanilde (paracetamol) in the rat. Biochem Pharmacol 1995; 49:1155 1164.
42. Nicholls AW, Lindon JC, Farrant RD, Shockcor JP, Wilson ID, Nicholson JK. Directly coupled HPLC NMR spectroscopic studies of metabolism and futile deacetylation of phenacetin in the rat. J Pharm Biomed Anal 1999; 20:865 873.
43. Nicholls AW, Farrant RD, Shockor JP, Unger S, Wilson ID, Lindon JC, Nicholson JK. NMR and HPLC NMR spectroscopic studies of futile deacetylation in paracetamol metabolites in rat and man. J Pharm Biomed Anal 1997; 15:901 910.
44. Nicholls AW, Wilson ID, Godejohann M, Nicholson JK, Shockcor JP. Identification of phenacetin metabolites in human urine after administration of phenacetin $C^{3}H_3$: measurement of futile metabolic deacetylation via HPLC/MS SPE NMR and HPLC ToF MS. Xenobiotica 2006; 36:615 629.
45. Spraul M, Freund AS, Nast RE, Withers RS, Maas WE, Corcoran O. Advancing NMR sensitivity for LC NMR MS using a cryoflow probe: application to the analysis of acetaminophen metabolites in urine. Anal Chem 2003; 75:1536 1541.
46. Griffiths L, Horton R. Optimization of LC NMR. III Increased signal to noise ratio through column trapping. Magn Reson Chem 1998; 36:104 109.
47. Cloarec O, Campbell A, Tseng LH, Braumann U, Spraul M, Scarfe G, Weaver R, Nicholson JK. Virtual chromatographic resolution enhancement in cryoflow LC NMR experiments via statistical total correlation spectroscopy. Anal Chem 2007; 79:3304 3311.
48. Stachulski AV, Harding JR, Lindon JC, Maggs JL, Park K, Wilson ID. Acyl glucuronides: biological activity, chemical reactivity, and chemical synthesis. J Med Chem 2006; 49:6931 6945.
49. Skordi E, Wilson ID, Lindon JC, Nicholson JK. Kinetic studies on the intramolecular acyl migration of β 1 O acyl glucuronides: application to the glucuronides of R and S ketoprofen, R and S hydroxy ketoprofen and tolmetin by ^{1}H NMR spectroscopy. Xenobiotica 2005; 35:715 725.
50. Johnson CH, Wilson ID, Harding JR, Stachulski AV, Iddon L, Nicholson JK, Lindon JC. NMR spectroscopic studies on the *in vitro* acyl glucuronide migration kinetics of ibuprofen ((+) (R,S) 2 (4 isobutylphenyl)propanoic acid), its metabolites and analogues. Anal Chem 2007; 79:8720 8727.
51. Johnson CH, Athersuch TJ, Wilson ID, Meng X, Iddon L, Stachulski AV, Lindon JC, Nicholson JK. Kinetic and J resolved statistical total correlation NMR spectroscopy (STOCSY) approaches to structural information recovery in complex reacting mixtures: application to acyl glucuronide intramolecular transacylation reactions. Anal Chem 2008; 80:4886 4895.
52. Sidelmann UG, Gavaghan C, Carless HJA, Spraul M, Hofmann M, Lindon JC, Wilson ID, Nicholson JK. 750 MHz directly coupled HPLC NMR: application to the sequential characterisation of the positional isomers and anomers of 2 , 3 , and 4 fluorobenzoic acid glucuronides in equilibrium mixtures. Anal Chem 1995; 67:4441 4445.

53. Sidelmann UG, Nicholls AW, Meadows PE, Gilbert JW, Lindon JC, Wilson ID, Nicholson JK. High performance liquid chromatography directly coupled to ^{19}F and ^{1}H NMR for the analysis of mixtures of isomeric ester glucuronide conjugates of trifluoromethyl benzoic acids. J Chromatogr 1996; 728:377 385.
54. Sidelmann UG, Hansen SH, Gavaghan C, Carless HJA, Lindon JC, Farrant RD, Wilson ID, Nicholson JK. Measurement of internal acyl migration reaction kinetics using directly coupled HPLC NMR: application for the positional isomers of synthetic (2 fluorobenzoyl) D glucopyranuronic acid. Anal Chem 1996b; 68:2564 2572.
55. Lenz EM, Greatbanks D, Wilson ID, Spraul M, Hofmann M, Troke J, Lindon JC, Nicholson JK. Direct characterisation of drug glucuronide isomers in human urine by HPLC NMR spectroscopy: application to the positional isomers of 6,11 dihydro 11 oxidibenz[b,e]oxepin 2 acetic acid glucuronide. Anal Chem 1996; 68:2832 2837.
56. Ruhl R, Thiel R, Lacker TS, Strohschein S, Albert K, Nau H. Synthesis, high performance liquid chromatography nuclear magnetic resonance characterization and pharmacokinetics in mice of CD271 glucuronide. J Chromatogr B Biomed Sci Appl 2001; 757:101 109.
57. Akira K, Hasegawa H, Shinohara Y, Imachi M, Hashimoto T. Stereoselective internal acyl migration of 1 beta O acyl glucuronides of enantiomeric 2 phenylpropionic acids. Biol Pharm Bull 2000; 23:506 510.
58. Mortensen RW, Corcoran O, Cornett C, Sidelmann UG, Lindon JC, Nicholson JK, Hansen SH. *S* Naproxen β 1 *O* acyl glucuronide degradation kinetic studies by stopped flow high perfor mance liquid chromatography ^{1}H NMR and high performance liquid chromatography UV. Drug Metab Dispos 2001; 29:375 380.
59. Corcoran O, Mortensen RW, Hansen SH, Troke J, Nicholson JK. HPLC/^{1}H NMR spectroscopic studies of the reactive α 1 *O* acyl isomer formed during acyl migration of S naproxen β 1 *O* acyl glucuronide. Chem Res Toxicol 2001; 14:1363 1370.
60. Chen W, Shockcor JP, Tonge R, Hunter A, Gartner C, Nelson SD. Protein and nonprotein cysteinyl thiol modification by *N* acetyl *p* benzoquinone imine via a novel *ipso* adduct. Biochemistry 1999; 38:8159.

16

Applications of Recombinant and Purified Human Drug-Metabolizing Enzymes: An Industrial Perspective

Ming Yao, Mingshe Zhu, Shu-Ying Chang, Donglu Zhang, and A. David Rodrigues

Pharmaceutical Candidate Optimization, Bristol-Myers Squibb, Princeton, New Jersey, U.S.A.

INTRODUCTION

It has become widely accepted that in vitro metabolism studies can play a useful role during the nonclinical testing of novel chemical entities (NCEs) (1 7). Therefore, most researchers have turned to various sources of human tissue and drug-metabolizing enzymes (DMEs). Because the liver has long been considered the major site of metabolism, typical in vitro studies have involved suspensions of primary hepatocytes, precision-cut liver slices, and various hepatic subcellular fractions (e.g., 9000 g supernatant fraction, microsomes, and cytosol) (5,7). With the realization that the gut can also play a role in first pass metabolism, increasing numbers of investigators have expanded their in vitro studies beyond the liver (8). For a given NCE, therefore, a substantial amount of in vitro data can be obtained relatively quickly prior to entry into late-stage nonclinical development or phase I clinical trials. This is important because such data allow one to anticipate drug interactions, inter-subject variability, polymorphic metabolism, pharmacologically active metabolites, human-specific metabolites, and metabolites that might exhibit off-target effects (1,5,9,10).

Most of the DME systems in various human tissues, such as cytochromes P450 (CYP; EC 1.14.14.1), UDP-glucuronosyltransferases (UGT; EC 2.4.17), *N*-acetyltransferases (NAT; EC 2.3.1.5), sulfotransferases (SULTs; EC 2.8.2), and NADPH-dependent flavin-containing monooxygenases (FMO; EC 1.14.13.8), are rather complex and comprise at least two different enzymes or "isoforms." In fact, many are representative of superfamilies, families, or subfamilies of genes (11 15). Members of each DME system, or "enzyme pool," can often interact differentially with any number of drugs or xenobiotics. Moreover, the expression of these proteins in different tissues is under the control of genetic factors and can vary with age, gender, disease, and medications. At the same time, there is a growing acceptance that individual enzyme systems (e.g., CYPs and UGTs) can

Figure 1 Summary of various models that enable in vitro metabolism studies.

interact with each other, and that one has to regard phase I (oxidative) and phase II (conjugation reactions) biotransformations coordinately with influx (phase zero) and efflux (phase III) transporter processes (16 18). Because of this interplay, investigators have sought to simplify in vitro metabolism models by opting to heterologously express individual human DMEs in cell types with low (background) levels of target enzyme and transporter activity (Fig. 1). The different cell types include, and are not limited to, yeast (e.g., *Saccharomyces cerevisiae*), bacteria (e.g., *Escherichia coli*), Chinese hamster (COS, CHO, V79), B-lymphoblast (AHH-1 TK+/−), human hepatoma (HepG2), and insect (e.g., *Spodoptera frugiperda*, Sf9 or Sf21; and *Trichoplusia ni*).

Researchers can now perform in vitro metabolism studies with commercially available preparations of heterologously expressed human DMEs such as CYP (various), cytochrome b_5, CYP reductase, FMO (e.g., forms 1, 3, and 5), NAT (forms 1 and 2), epoxide hydrolase, aldehyde oxidase (AO), monoamine oxidase (forms A and B), UGTs (various), SULTs (e.g., SULT1A1, SULT1A3, SULT1B1, SULT1E1, and SULT2A1), and glutathione *S*-transferases (various). Commercial sources include BD Gentest Corp. (Woburn, Massachusetts, U.S.), Invitrogen Corp. (Carlsbad, California, U.S.), Xenotech Plc (Lenexa, Kansas, U.S.), Cypex Ltd. (Dundee, Scotland, U.K.), Oxford Biomedical Research Inc. (Metamora, Michigan, U.S.), Abcam Plc (Cambridge, England, U.K.), Abnova Corp. (Taipei, Taiwan), and Sigma-Aldrich Corp. (St Louis, Missouri, U.S.). When necessary (e.g., CYP), it is possible to co-express partner proteins (e.g., CYP reductase and cytochrome b_5) to ensure catalytic activity and circumvent the need for enzyme reconstitution.

Cells expressing the human DME of choice can be used intact (as suspensions or plated on a substratum) or processed to generate enzyme-enriched membrane and cytosol fractions. Cells containing an individual recombinant (heterologously expressed) DME can also serve as a starting point for purifications, which yield electrophoretically homogenous enzyme using greatly simplified strategies (vs. native human tissue) (19,20). Once available, the purified protein can be used to prepare antibodies, or crystals for X-ray crystallography, and employed as a standard in quantitative and semiquantitative immunoassays (21–26). It may also be necessary to conduct reconstitution experiments when evaluating lipid-protein or protein-protein interactions. Availability of purified proteins enables such studies, because one can measure reaction rates at different molar ratios of constituent proteins, cofactors, lipids, and substrate. The following describes some of the current and potential applications of heterologously expressed or purified DMEs. Whenever possible, the discussion will not be limited to the human CYPs and will include examples of other DME systems (e.g., UGT, FMO, and SULT). In addition, both literature compounds and NCEs are discussed as much as possible.

An "Integrated Approach" to Studying In Vitro Drug Metabolism

Although heterologously expressed DMEs are useful, it is important that they should be used within the framework of an integrated approach. This is particularly true when attempting in vitro "reaction phenotyping" (enzyme mapping) and metabolic profiling on the run up to a regulatory submission (Fig. 2). Integration of the in vitro data set is important and enables improved in vitro-in vivo correlations and consolidation of nonclinical and clinical data sets (27,28).

Typically, integration involves the use of cDNA-expressed enzymes in conjunction with suspensions of primary human hepatocytes, precision-cut human liver tissue slices, and subcellular fractions like human liver microsomes (HLMs) (Fig. 1). Such an integrated approach allows one to exploit the strengths of each model system (5). It is imperative that an overall metabolic profile is initially obtained with intact cell models, especially when information concerning the metabolism of the drug in vivo is not available. In turn, the data that are obtained with either cDNA-expressed DMEs or subcellular fractions can be viewed in perspective. For instance, clozapine is metabolized in vitro by cDNA-expressed CYP2D6 (29), whereas in vivo there is no evidence that the enzyme plays a major role in the metabolism of the drug (30). Similarly, oxidation of (*S*)-nicotine to cotinine (via a $\Delta^{1'(5')}$iminium ion) is mediated by multiple cDNA-expressed CYP proteins (e.g., CYP2A6, CYP2D6, CYP2B6, and CYP2C9), although CYP2A6 is major in HLM (31–34). Likewise, most inhibitors of cyclooxygenase are metabolized by recombinant CYP2C9, and one might expect altered pharmacokinetics in subjects carrying variant alleles (e.g., *CYP2C9*3*). However, CYP2C9-dependent metabolism has to be viewed in light of all clearance pathways involving metabolism (e.g., direct glucuronidation, chiral inversion, CYP3A, CYP2C8, CYP1A, and FMO-catalyzed oxidation) and elimination of parent via renal and biliary routes (35).

It is advisable, therefore, to make full use of all in vitro models and not rely solely on cDNA-expressed and purified enzymes. Intact cell models, such as precision-cut liver slices, permit "coupled" (phases I and II) metabolism of drugs, in additon to minimizing the problems of excessive tissue disruption (5,7,8). Furthermore, one is able to study the effect of enzyme-inducing agents on the metabolism of a given NCE. Purified DMEs, either from native human tissue or heterologous expression systems, offer different advantages. First, one can study a given biotransformation event in the absence of competing reactions. This is especially important when trying to differentiate between

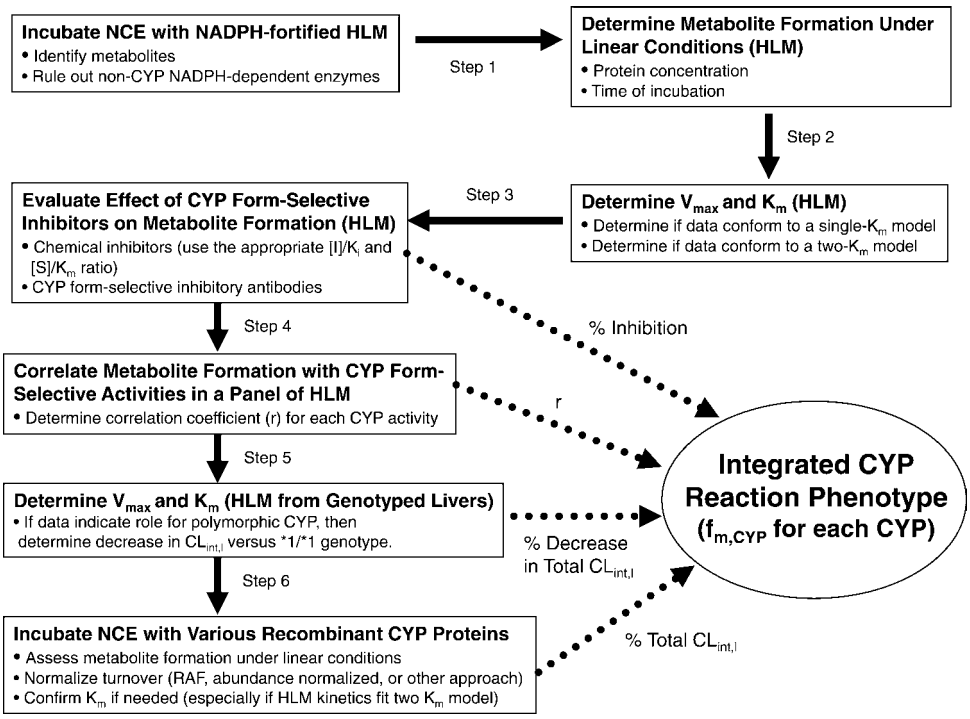

Figure 2 Schematic showing one possible cytochrome P450 (CYP) reaction phenotyping strategy. *Abbreviations*: CYP, cytochrome P450; HLMs, human liver microsomes; [S], substrate concentration; K_m, Michaelis constant; V_{max}, maximal rate of reaction; $f_{m,CYP}$, fraction of total CYP dependent metabolism catalyzed by individual CYP form; $CL_{int,l}$, total intrinsic clearance in liver; RAF, relative activity factor; NCE, new chemical entity; [I], inhibitor concentration; K_i, inhibition constant. *Source*: Adapted from Ref. 28.

CYP- and FMO-catalyzed *S*- and *N*-oxidations (36,37) or attempting to study oxidation of drugs in the absence of microsomal and cytosolic *N*-oxide, sulfoxide, or epoxide reductases (38 41). Conjugation reactions can also be studied unambiguously in the absence of sulfatases, hydrolases, and glucuronidases. Second, cDNA-expressed enzymes can be stored frozen and are a convenient source of human DMEs. Third, with the use of purified enzymes, concerns about the possible effects of proteolytic enzymes can be minimized. This is important to bear in mind when preparing subcellular fractions from native tissue. Most importantly, for enzyme systems such as FMOs, UGTs, and SULTs, recombinant proteins are the only tool available for reaction phenotyping studies. Unlike the human CYPs, selective inhibitors (chemical or antibodies) are not readily available, and reaction phenotyping approaches have yet to be standardized (28).

In the simplest case, a given drug or NCE is metabolized via one pathway involving a single DME. However, many metabolic profiles are complex and are generated by more than one DME in different organelles and tissues. For such drugs, it is essential to evaluate in vitro metabolism data carefully and view it holistically.

Case Study: Metabolism of 17α-Ethinylestradiol Involving CYP, SULT, and UGT

17α-Ethinylestradiol (EE) is a key active ingredient used in a variety of oral contraceptive (OC) formulations and its absorption, distrubution, metabolism, and excretion (ADME)

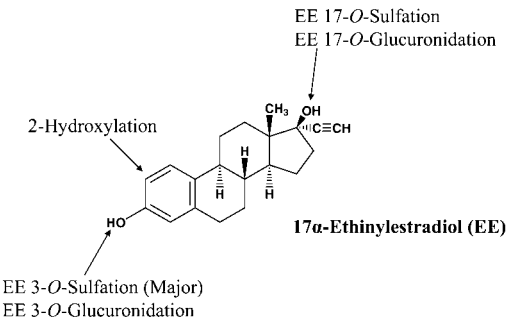

Model	Study	2-Hydroxylation	3-*O*-Sulfation	3-*O*-Glucuronidation	Reference
Ussing chamber	Gut tissue profile		+++	+	43,45
Human hepatocytes	Profile	+	+++	++	44
9000g supernatant	Liver profile	++	+++	++	44
Cytosol	Liver kinetics		+++		46, 47
Cytosol	Gut kinetics		+++		47
Recombinant SULTs	Phenotyping		+++		47
Recombinant UGTs	Phenotyping			+++	42
Recombinant CYPs	Phenotyping	+++			42

Figure 3 Study of 17α ethinylestradiol (EE) metabolism in vitro using different models. The extent to which the pathway in question is detected is indicated for each model system. *Abbreviations*: SULT, sulfotransferase; UGT, UDP glucuronosyltransferase; CYP, cytochrome P450.

profile in human subjects has been documented (42). EE is complex because its metabolism is extensive and involves CYPs, UGTs, and SULTs in both liver and intestine (Fig. 3). SULT-dependent (first pass) metabolism in the gut has received particular attention, because it is regarded as a major determinant of oral bioavailability (42). Therefore, one could not hope to evaluate the in vitro metabolic profile and reaction phenotype of EE without taking into account all three enzyme systems, their tissue expression, subcellular localization, and the low (clinically relevant) concentrations of EE (<10 nM) (43 47).

Fortunately, it is possible to evaluate EE metabolism in vitro using a number of model systems such as primary human hepatocytes, suitably fortified subcellular fractions (gut and liver), even whole tissue (e.g., intestine segments or slices), as well as recombinant DMEs (Fig. 3). Availability of such models is important because one is able to evaluate an NCE as an inhibitor of EE metabolism, and assess which one of the enzyme systems (UGT, SULT, and CYP) acts as the locus of a potential drug interaction prior to clinical trials (42). Clinical drug interaction studies with EE are commonplace and the majority of marketed drugs have labels (package inserts) that describe the results of such studies. From a marketing standpoint, it is advantageous to avoid having to restrict women of child-bearing potential that are taking OCs (42). If high-quality in vitro data are available early, one can anticipate an interaction with EE and prioritize the appropriate clinical drug interaction study. Because first pass sulfation is important, screening for inhibition of SULTs may be warranted in some cases.

Case Study: Metabolism of ABT-418 Involving AO, CYP, and FMO

A bio-isostere of (*S*)-nicotine, ABT-418 is a potent and selective neuronal nicotinic acetylcholine receptor ligand that has been in development for the treatment of attentional deficit disorder and Alzheimer's disease (48,49). In the course of preclinical studies, it was decided to study the metabolism of the drug in multiple species. Overall, the metabolism of ABT-418 was similar to that of nicotine, because the compound underwent CYP- and AO-dependent *C*-oxidation to the lactam and FMO-dependent *N*′-oxidation (Fig. 4). Owing to concerns about the stability of AO in both dog and human 9000 g supernatant fraction, initial studies were performed with precision-cut liver slices (48,49). The results showed that the rat, dog, and chimpanzee were efficient at catalyzing both *C*-oxidation and *N*′-oxidation of ABT-418 (Fig. 4). The formation of the two metabolites was confirmed in vivo, for both were detected in rat (*N*′-oxide C_{max}, 435 ng/mL; lactam $C_{max,}$ 131 ng/mL) and dog (*N*′-oxide C_{max}, 11.7 μg/mL; lactam C_{max}, 5.3 μg/mL) plasma. In contrast, only relatively low levels ($\leq$5.8% of total metabolism) of *N*′-oxide were detected in human liver slices after 24 hours of incubation.

Although it appeared that *C*-oxidation predominated in human liver slice incubates (Fig. 4), and because the product(s) of *N*′-oxidation might themselves be reduced back to parent drug in the presence of cytosolic or microsomal reductase(s) (48,49), it was important to show unambiguously that human liver microsomal FMO was able to catalyze the *N*′-oxidation of ABT-418. Toward this end, the drug was incubated with native HLM and *E. coli*-expressed FMO3 (48); FMO3 is considered to be the major FMO enzyme in native HLMs (14,36,48). The data indicated that ABT-418 was a substrate for human FMO3, present in native liver microsomes and in *E. coli* cell lysate (Fig. 4). Moreover, the rate of *N*′-oxidation was relatively low when compared with other sources of FMO. No reduction of ABT-418 *N*′-oxides *(cis* or *trans*) was detected in the presence of *E. coli*-expressed FMO3 (48). Therefore, it was concluded that *N*′-oxidation of ABT-418 did occur in humans, but that this was a relatively minor pathway, and that *C*-oxidation to

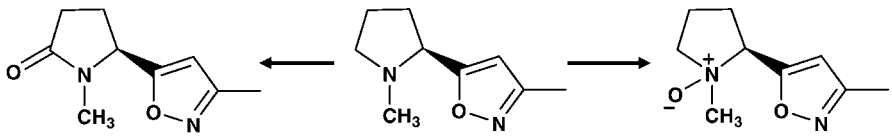

Species	Liver Slices (% Total Metabolism)		*N*-Oxide Formation (pmol/min/mg)			
	% Lactam	% *N*-Oxide	Liver Microsomes	Recombinant FMO1	Recombinant FMO2	Recombinant FMO3
Rat	21	44	237			
Dog	22	58	386			
Cynomolgus monkey	56	<1.0	84			
Chimpanzee	18	40	97			
Human	53	≤6.0	36	-	-	650
Rabbit	-	-	207	-	2556	-
Pig	-	-	-	2467	-	-

Figure 4 Metabolism of ABT 418 in vitro (48,49). *Abbreviation*: FMO, flavin containing monooxygenase.

lactam would be the major pathway. This observation was confirmed in subsequent clinical trials, because no *N*′-oxides were detected in either the plasma or urine of subjects receiving ABT-418, and the lactam was the major metabolite.

Case Study: Metabolism of Muraglitazar Involving CYP and UGT

Muraglitazar (Pargluva®), a dual α/γ-peroxisome proliferator-activated receptor activator, has been in development for the treatment of diabetes, and its ADME profile is known (50 52). Following oral administration of radiolabel, urinary excretion of radioactivity was low (<5% of the dose) in human subjects, and the majority of the dose was recovered in bile as a glucuronide of muraglitazar and oxidative metabolites (Fig. 5). The parent compound was a minor component in bile, suggesting extensive metabolism. In the presence of NADPH-fortified HLM, [^{14}C]muraglitazar formed multiple metabolites (e.g., hydroxylation and *O*-demethylation). After incubation with suspensions of human primary hepatocytes, both oxidative metabolites and direct glucuronide conjugate were identified as major metabolites. On the basis of the overall data package, therefore, muraglitazar was cleared metabolically via oxidative and conjugative pathways.

Additional studies were then conducted with commercially available recombinant human CYPs and UGTs in order to investigate the enzymes involved in metabolism (50 52). Upon initial screening with cDNA-expressed enzymes, multiple human CYPs (CYP2C8, CYP2C9, CYP2C19, CYP2D6, and CYP3A4) and UGTs (UGT1A1, UGT1A3, and UGT1A9) were found to metabolize muraglitazar. Furthermore, more than one enzyme was shown to catalyze the formation of several of the individual metabolites. Further studies with selective chemical inhibitors and HLM showed a complicated pattern of inhibition, although the profile was anticipated on the basis of the turnover observed with different recombinant CYPs. Since muraglitazar was oxidized by multiple CYP enzymes, the disappearance of the parent compound was monitored to evaluate the effect of inhibitors on the overall metabolism at a clinically relevant concentration of muraglitazar (2.5 μM). The results showed that both chemical inhibitors and immuno-inhibitory antibodies of CYP2C8, CYP2C9, CYP2D6, and CYP3A4 decreased the metabolism of muraglitazar in HLM.

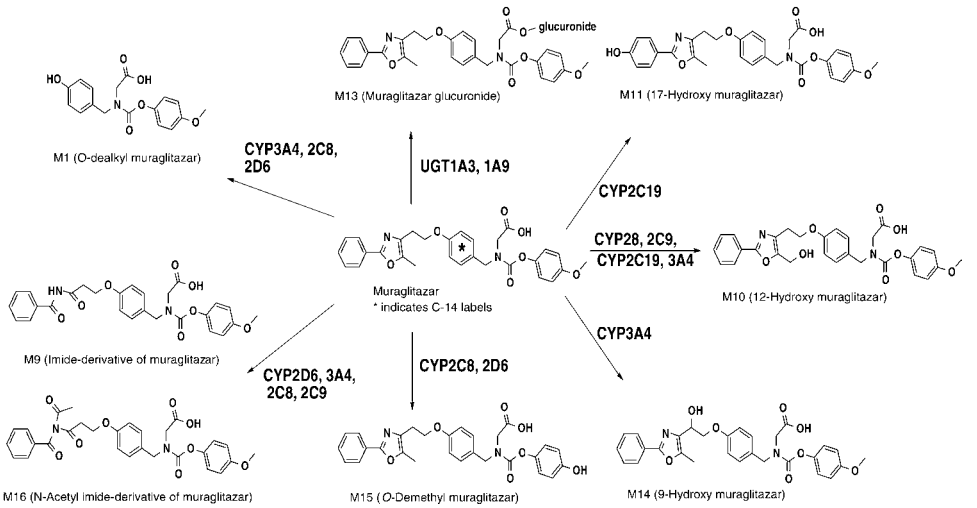

Figure 5 Biotransformation scheme for muraglitazar. *Abbreviations*: UGT, UDP glucuronosyl transferase; CYP, cytochrome P450.

The intrinsic clearance value of each individual CYP, defined as the ratio of V_{max}/K_m (V_{max}, maximal rate of reaction; K_m, Michaelis constant or concentration of substrate at half of V_{max}), was then used to estimate its contribution to the overall oxidative metabolism of muraglitazar and the formation of the oxidative metabolites. On the basis of the calculated intrinsic clearance and relative contribution values, CYP2C19 is predicted to be the major enzyme responsible for the 17-hydroxylation of muraglitazar (M11), and thus contributes to 36% of muraglitazar total oxidative metabolism. CYP2C8 was predicted to be the major enzyme responsible for *O*-demethylation of muraglitazar (12% of total oxidative metabolism; M15). CYP3A4 was predicted to be the major enzyme responsible for 9-hydroxylation of muraglitazar (M14) and to contribute up to 36% of total oxidative metabolism. CYP2C8, CYP2C9, CYP2C19, and CYP3A4 were involved in 12-hydroxylation of muraglitazar (M10). Although the predicted contribution of each CYP enzyme to the overall clearance of muraglitazar, based on the scaling of intrinsic clearance, did not fully match the prediction from inhibition studies measuring the disappearance of the parent compound in HLM, the combined results contributed to a better understanding of the clearance mechanisms of muraglitazar (50 52).

Glucuronidation of [^{14}C]muraglitazar was catalyzed by cDNA-expressed UGT1A1, UGT1A3, and UGT1A9, but not by UGT1A6, UGT1A8, UGT1A10, UGT2B4, UGT2B7, and UGT2B15. The enzyme kinetic parameters describing muraglitazar glucuronidation were determined with cDNA-expressed enzymes, and the apparent K_m values were similar among UGT1A1, UGT1A3, UGT1A9, and HLM ($\sim$3.0 μM). UGT1A1 probably did not contribute to the clearance of muraglitazar, because the rates of muraglitazar glucuronidation were not well correlated with the rates of bilirubin, EE, and estradiol glucuronidation in HLM. Overall, muraglitazar was metabolized by a number of DMEs and no one single enzyme was dominant. Such a profile was considered ideal because it diminished the likelihood of drug-drug interactions and intersubject variability related to polymorphic DMEs.

Case Study: Metabolism of Dasatinib Involving CYP and FMO

Dasatinib (SPRYCEL®), a potent inhibitor of the BCR-ABL (B-lymphocyte transcriptional regulator-Abelson murine leukemia) and *Src* family kinases, is currently marketed for the treatment of chronic myeloid leukemia (CML) and Philadelphia chromosome-positive acute lymphoblastic leukemia (Ph+ALL) that is resistant to imatinib (Gleevec®) treatment. Human ADME studies showed that the primary oxidative metabolites of dasatinib in humans resulted from *N*-dealkylation (M4), *N*-oxidation (M5), carboxylic acid formation (M6), aryl (M20), and benzylic (M24) hydroxylations (53 55). These various oxidative pathways represented approximately 81% of total dasatinib clearance (Fig. 6).

Reaction phenotyping of dasatinib was carried out with cDNA-expressed enzymes, followed by HLM with selective antibodies and chemical inhibitors (53 55). Upon initial screening with cDNA-expressed enzymes, multiple CYPs (CYP1A1, CYP1B1, CYP1A2, and CYP3A4/3A5) and FMO3 were found to be involved in the oxidation of dasatinib. CYP1A1, CYP1B1, and CYP3A4 were shown to catalyze the *N*-dealkylation, whereas CYP3A4 and CYP3A5 were the major enzymes catalyzing dasatinib aryl and benzylic hydroxylation. CYP1A1 and CYP1B1 are mainly expressed in the extrahepatic tissues with low levels detected in HLM (53 55). Therefore, these CYP enzymes were not expected to play a significant role in the hepatic clearance of dasatinib in humans. In the presence of cDNA-expressed CYP3A4, dasatinib *N*-dealkylation conformed to single-K_m Michaelis-Menten kinetics ($K_m \sim 90$ μM). This K_m was similar to that obtained with HLM. For both recombinant CYP3A4 and HLM, the estimated K_m values describing the

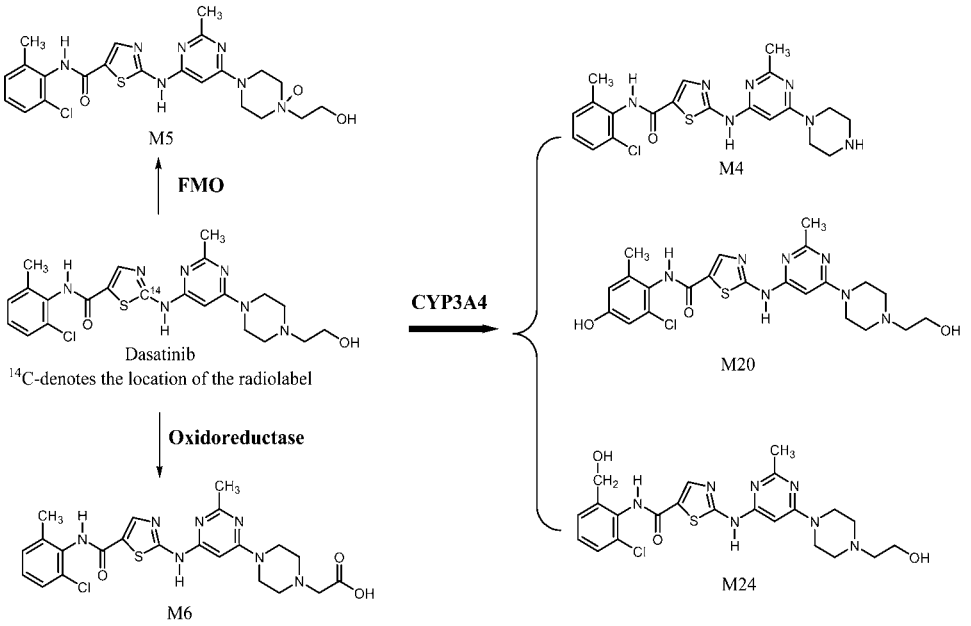

Figure 6 Biotransformation scheme for dasatinib. *Abbreviations*: FMO, flavin containing monooxygenase; CYP, cytochrome P450.

formation of the two major hydroxy metabolites were low (1.1 5.6 and 4.8 8.3 μM). The V_{max}/K_m ratios (recombinant CYP3A4) for the *N*-dealkylation, aryl hydroxylation, and benzylic hydroxylation reactions were 0.17, 1.98, and 0.17 μL/min/pmol, respectively, suggesting that the aryl hydroxylation in human liver was major. To complete the reaction phenotype, the activity of each recombinant CYP was normalized to its specific content in HLM (27,28). The results indicated that CYP3A4 was the major enzyme responsible for dasatinib *N*-dealkylation and hydroxylation. In agreement, troleandomycin (selective mechanism-based inhibitor of CYP3A enzymes) and CYP3A4 immuno-inhibitory antibodies inhibited both *N*-dealkylation and hydroxylation in HLM (53 55). Overall, the data supported the conclusion that the *N*-dealkylation and hydroxylation of dasatinib was catalyzed by CYP3A4. But what about the *N*-oxidation of dasatinib?

Dasatinib *N*-oxidation was evaluated after incubation with HLM and cDNA-expressed enzymes. Results generated from the incubations with expressed enzymes indicated that FMO3 was the most catalytically efficient enzyme, although CYP1A2, CYP1B1, CYP2C9, and CYP3A4 were also capable of catalyzing this reaction. Heat treatment of HLM (45°C for 5 min) significantly decreased the *N*-oxidation activity and was used as evidence to support the involvement of FMO. As expected, 1-aminobenzotriazole (broad spectrum CYP inhibitor) elicited a minimal effect on *N*-oxidation in HLM. The result was consistent with reports that FMO3 is major in HLM (Table 1). The relatively low rates of *N*-oxidation in the presence of cDNA-expressed CYPs, and the inhibition data, all provided confirmatory evidence that FMO3 played a major role in the *N*-oxidation reaction.

Once all of the in vitro and ADME data were integrated, it was estimated that a potent CYP3A4 inhibitor like ketoconazole would increase (~4-fold) the dasatinib area under the plasma concentration versus time curve (AUC) (53 55). Such a result was confirmed following a clinical drug interaction study with ketoconazole (4.5-fold increase in AUC). The significant fraction metabolized via CYP3A4 would also predict a

Table 1 Quantitation of Various Drug Metabolizing Enzymes in Human Liver and Intestine

	Specific content range (pmol/mg protein)	
	Liver	Intestine
Enzyme	Microsomes	
CYP reductase	47 103	Not available
Cytochrome b_5	157 569	Not available
CYP3A4	37 108	8.8 150
CYP3A5	1.0 117	4.9 25
CYP2D6	5.0 11	<0.2 3.1
CYP2A6	14 68	<1.0
CYP2E1	22 52	<1.0
CYP2C9	50 96	2.9 27
CYP2C8	12 64	Not detected
CYP2C19	8.0 20	<0.6 3.9
CYP1A2	19 67	Not detected
CYP1A1	Not detected	3.6 7.7
CYP2J2	Not detected	<0.2 3.1
FMO1	<1.0	1.1 6.4
FMO3	12.5 117	Not available
FMO5	3.5 34	Not available
	Cytosol	
SULT1A1 (ST1A3)	25 120	23 38
SULT1A3 (ST1A5)	2.6 6.4	44
SULT1E1 (ST1E4)	3.0 8.3	1.5 6.3
SULT2A1 (ST2A3)	29 190	4.4 28

Specific content for each protein has been reported in the literature (22,23,27,28,references therein, 56 62,76). If available, specific contents are from a range of different organ donors (see sect. "Abundance of Enzymes in Native Tissue"). Unless otherwise indicated, specific content was based on immunoassay employing recombinant (or purified) enzyme as standard. Specific content of cytochrome b_5 was determined spectrally. For the SULTs, expression levels are reported as μg/mg cytosol protein and have been converted to pmol/mg (monomeric molecular weight available in the references cited). CYP, cytochrome P450; SULT, sulfotransferase; FMO, NADPH flavin containing monooxygenase. All specific contents are reported as picomole of enzyme per milligram of total protein (microsomes or cytosol). For the sake of scaling and comparison across DME systems in the liver, one can assume that there are approximately 45 mg microsomal protein per gram of liver tissue and approximately 22 mg cytosol protein per gram of liver tissue.

substantial effect of enzyme inducers on dasatinib pharmacokinetics. Indeed, a decrease in dasatinib exposure (80% to 90%) was observed in subjects receiving rifampicin. In summary, incubation with human liver fractions generated all of the important metabolic clearance pathways of dasatinib. The studies with cDNA-expressed enzymes, CYP inhibitors (chemical and antibody), and kinetic analysis showed that dasatinib was mainly metabolized by CYP3A4.

PERSPECTIVE

Abundance of Enzymes in Native Tissue

Irrespective of the recombinant or purified DME being used in a study, it is imperative to have some idea of the expression level of each protein in native tissue. Such information allows one to "scale" turnover data and obtain estimates of reaction rate in different

tissues (see sect. "Bridging the Gap Between Recombinant and Purified Enzymes and Native Tissue"). Toward this end, the availability of recombinant and purified proteins has enabled the preparation of highly specific monoclonal and polyclonal antibodies. In turn, such reagents have allowed researchers to develop immunoassays that compliment other methodologies (e.g., reverse transcriptase-polymerase chain reaction for the quantitation of mRNA). For example, CYP, FMO, and SULT forms in different gene families and subfamilies have been immuno-quantitated (e.g., Western immunoblotting) in human liver and gut tissue (22,23,27,28,56 63). In most cases, recombinant and purified DMEs have been employed as standards (Table 1). Going forward, it is possible that novel approaches (e.g., matrix-assisted laser desorption/ionization-time of flight mass spectrometry) may enable more systematic quantitation of individual phases I and II DMEs in different tissues without the need for antibodies (64).

Specific Content of Heterologously Expressed or Purified Enzyme

It is highly likely that when experiments are performed with purified enzyme, the specific content of that enzyme will be known, because most investigators use this as one of the criteria for purification (19,20). However, when using whole cells, cell lysate, or subcellular fractions containing heterologously expressed DMEs, this is often not the case, and many investigators have had to express initial rates of reaction on a "per milligram (total) protein" basis. Fortunately, with the advent of high-level heterologous expression systems, it is now possible to express CYP (holoenzyme) at levels that can be detected spectroscopically as a ferrous-carbon monooxide complex (19,20,27). This means that one can determine the specific content of a recombinant human CYP, in membrane fractions of Sf9 and *T. ni* cells, and thus express the data on a "per nanomol CYP" basis (i.e., "turnover"). Similarly, it may be prudent to determine the specific content of an individual FMO (nanomol flavin adenine dinucleotide, FAD, per milligram of protein) and express catalytic activity on a per nanomol FAD basis.

Phase II enzymes are problematic because one has to conduct Western immunoblotting, or enzyme-linked immunosorbent assays, to ensure that all the recombinant isoforms are more or less expressed at equivalent levels of apoprotein. It follows that metabolism rates are normalized with respect to the levels of expressed apoprotein. In some instances, it may not be possible to determine V_{max} and the isoforms are differentiated in terms of K_m only (47).

Bridging the Gap Between Recombinant and Purified Enzymes and Native Tissue

As stated previouosly, one of the attractive features of heterologously expressed (or purified) DMEs is that one can greatly simplify drug metabolism studies and unambiguously assign the results to a particular enzyme. This is very important when attempting to study a particular biotransformation in the absence of competing enzymes and reactions. Although useful, it has to be acknowledged that systems containing recombinant (or purified) DMEs are artificial, because the enzyme is not present in its native environment and is often overexpressed (27). For the recombinant CYPs, in particular, this may be an important consideration. Membrane fractions containing recombinant CYPs can differ considerably from native HLM, and one has to consider differences in the lipid-to-protein ratio, nonspecific binding, and the ratio of CYP-to-CYP reductase (and cytochrome b_5) (27,56). Moreover, many CYPs (e.g., CYP2D6) are often heterologously expressed at levels that far exceed those present in native liver microsomes

(Table 1). Consequently, one has to use well-characterized recombinant CYPs (e.g., evaluate the level of expression and the CYP-to-CYP reductase ratio) and, as much as possible, relate the data to the levels of protein and activity in native tissue as part of an integrated reaction phenotyping strategy (27,28). The same can also be said for other DMEs like the FMOs, SULTs, and UGTs, although approaches (e.g., relative activity factor, RAF) for integrated reaction phenotyping of these enzymes are not well developed (28).

Human CYPs as an Example

Reaction-phenotyping studies employing recombinant CYPs are regularly conducted by monitoring either substrate depletion or metabolite formation (28). Reactions catalyzed by individual recombinant CYPs can be optimized and definitive kinetic parameters such as K_m, V_{max}, and k_{cat} (first-order rate constant that relates V_{max} to total enzyme concentration, E_o) can be determined. The choice of substrate concentration range is an important consideration, because one has to ensure that the experimental conditions enable the characterization of both low K_m (e.g., $\leq$5 μM) and high K_m CYPs, especially if the kinetic profile conforms to a two-K_m model in HLM (Fig. 2). When multiple CYP enzymes are involved, the relative contribution of each CYP can be estimated using a CYP abundance normalized approach (27,28), RAF (56), or intersystem extrapolation factors (65). Irrespective of the approach used, the reaction-phenotype based on the recombinant CYP profile should correspond as much as possible to that based on HLM data (27,28).

A number of examples are presented in Table 2, which describes HLM (correlation coefficient and inhibition) and abundance-normalized recombinant CYP data. In this instance, rates of metabolism for each recombinant CYP form were determined (pmol/min/pmol CYP) (27,28, references therein). For each recombinant CYP form, the normalized rate (NR, pmol/min per mg) was calculated by multiplying the turnover (pmol/min per pmol CYP) and the reported specific content of each CYP form in HLM (pmol/mg) (Table 1). The total normalized rate (TNR) was calculated as the sum of the NR values for each CYP. Finally, for each CYP form, the NR was expressed as a percent of the TNR. Using this approach it is possible to differentiate the role of different CYP forms (single reaction) or a single CYP (multiple reactions). In Table 2, the normalized recombinant data have been used to estimate the contribution of each CYP form in HLM only. Because the expression levels of each CYP in the gut are now known (Table 1), it is also possible to apply the approach to reaction phenotyping of human intestinal microsomes (HIM). Ultimately, the goal is to determine the contribution of each CYP (fraction of total intrinsic clearance, $f_{m,CYPn}$), and assess the likelihood of drug interactions or polymorphisms (27,28,35,66). Reaction phenotyping of HLM and HIM may be necessary for those NCEs that exhibit high intrinsic clearance and are predicted to undergo moderate to high extraction in both organs. Because of the high levels of CYP3A4 in the gut, as a percent of the total CYP pool, one cannot assume that the CYP reaction-phenotype obtained with HLM and HIM will be the same.

APPLICATIONS

Enzyme- and Isoform-Selective Biotransformations

The oxidative metabolism of a single drug can be catalyzed by multiple DME systems, such as cytosolic AO, microsomal CYP, and FMO. Although it is possible to differentially inhibit these various DMEs with selective agents, such as clotrimazole and 1-aminobenzotriazole (CYP selective), thiourea (FMO selective), and menadione (AO

Table 2 Examples of an Integrated In Vitro CYP Reaction Phenotype

			Human liver microsomes		
Compound	Reaction(s)	CYP form(s)	Correlation coefficient (r)[a]	% Inhibition[b]	% Total normalized rate (recombinant CYPs)[c]
Etoricoxib	Hydroxylation	3A4	0.64	65	58
		1A2	<0.40	5.0	2.0
		2C9	<0.40	10	6.0
		2D6	<0.40	10	26
"Compound A" (endothelin receptor antagonist)	Hydroxylation	2C8	0.91	>95	100
ABT 761	Hydroxylation	3A4	0.67	55	66
		2C9	0.40	20	19
Zileuton	Sulfoxidation	3A4	0.67	60	95
	Hydroxylation	1A2	0.58	45	57
Naproxen	*O* demethylation	2C9	0.67	50	56
		1A2	0.46	55	33
Clarithromycin	*N* demethylation	3A4	0.81	>95	100
	Hydroxylation	3A4	0.85	>95	100
Celecoxib	Hydroxylation	2C9	0.92	80	86
		3A4	0.55	20	6.0
L 771688	Multiple	3A4	0.98	95	100
(*R*) ( ) ibuprofen (500 μM)	2 Hydroxylation	2C9		50	32
		2C8		25	11
		3A4		32	42
	3 Hydroxylation	2C9		85	89
(*R*) ( ) ibuprofen (1 μM)	2 Hydroxylation	2C9		95	100
Dextromethorphan	*O* demethylation	2D6	0.93	90	82
Phenacetin	*O* deethylation	1A2	0.91	95	100
TPA 023	*N* deethylation	3A4		>90	100
	Hydroxylation	3A4		>90	100

The data have been reported in various references (27,28, references therein), except for ibuprofen, L 771688, and TPA023 (unpublished).

[a]Reaction rates were measured in a panel of human liver microsomes from at least 10 different organ donors. Rates were correlated with various CYP form selective activities.

[b]Reaction rates were measured in the presence of human liver microsomes co incubated with solvent or a CYP form selective inhibitor. Inhibition is expressed as percent loss of activity (solvent alone as reference).

[c]Reaction rate was determined after incubation with a panel of individual expressed recombinant CYP proteins. The rate for each CYP form was then normalized as described in Ref. 27 (see sect. "Bridging the Gap Between Recombinant and Purified Enzymes and Native Tissue").

selective in cytosol), the involvement of each enzyme can be unambiguously determined with the appropriate preparation of heterologously expressed or purified protein (48,49,67). As exemplified by the human CYPs, UGTs, and SULTs, the availability of recombinant DMEs becomes even more critical when one has to differentiate members of the same gene family and subfamily.

Biotransformations Involving Enzymes Belonging to Different Gene Families and Subfamilies

Differentiating CYP1, CYP2, and CYP3 Family Members and CYP2A, CYP2B, CYP2C, CYP2D, and CYP2E Subfamily Members. Customarily, the CYP forms involved in the metabolism of a given drug are determined using a combination of HLM (CYP-selective chemical inhibitors, inhibitory antibodies, correlation analyses) and heterologously expressed proteins (Fig. 2). The results in Table 2 show that it is possible to differentiate CYP1, CYP2, and CYP3 member forms using recombinant data (see sect. "Bridging the Gap Between Recombinant and Purified Enzymes and Native Tissue"). For example, naproxen *O*-demethylation is catalyzed by CYP1A2 and CYP2C9, etoricoxib hydroxylation is catalyzed by four CYPs (CYP3A4 > CYP2C9, CYP1A2, and CYP2D6), and celecoxib hydroxylation is catalyzed by CYP2C9 (major) and CYP3A4. Likewise, clarithromycin *N*-demethylation, L-771688 oxidation, TPA023 oxidation, and zileuton sulfoxidation are dominated by CYP3A4. In contrast, dextromethorphan *O*-demethylation, phenacetin *O*-deethylation, "compound A" hydroxylation, and (*R*)-(−)-ibuprofen (1 μM) 2-hydroxylation are dominated by CYP2D6, CYP1A2, CYP2C8, and CYP2C9, respectively. At least for the twelve compounds described in Table 2, other CYPs (e.g., CYP2E1, CYP2B6, and CYP2A6) play a very minor role.

Differentiating UGT1 and UGT2. In recent years, there has been an explosion in our knowledge of the human UGT family of enzymes (11,68 70). For example, at least 16 UGT isoforms have been identified in humans and, based on the sequence homology, they have been divided into two gene families (UGT1 and UGT2). The various forms of UGTs are now known to be expressed in numerous tissues, regulated transcriptionally, expressed polymorphically, and have been shown to exhibit some degree of selectivity toward different substrates. Toward this end, the availability of recombinant human UGTs has been very important. Such reagents have allowed different investigators to attempt reaction-phenotyping studies and classify different compounds as UGT1- or UGT2-selective substrates (68 70, references therein). Compounds such as bilirubin, estradiol, buprenorphine, trifluoperazine, serotonin, and propofol are glucuronidated by UGT1 forms, where agents such as morphine, (*S*)-oxazapam, and zidovudine are more UGT2 selective. Unfortunately, the majority of the reaction phenotype studies reported in the literature have relied heavily on recombinant UGTs, because of the lack of reagents selective enough to differentiate different UGTs in HLM preparations. With additional progress, it is very likely that new reagents (probe substrates and inhibitors) will enable the reaction phenotyping of different UGTs in HLMs (71,72).

Differentiating SULT1 and SULT2. The human cytosolic SULT superfamily comprises at least three gene families (SULT1, SULT2, and SULT4). Like the UGTs, members of these families are expressed in different tissues, are inducible, and often catalyze *N*- and *O*-sulfation in a substrate-dependent manner (15,22,73). Here also the availability of recombinant SULTs has enabled reaction-phenotyping studies, because selective inhibitors and immuno-inhibitory antibodies are not readily available. Despite the limitations, it has been possible to show that 4-nitrophenol, 2-aminophenol, dopamine, and estradiol are SULT1 selective, whereas steroids such as dehydroepiandrosterone and allopregnanolone are metabolized mainly by SULT2 forms (22,74). For the sake of illustration, EE sulfation is discussed.

As described previously, EE undergoes first pass 3-*O*-sulfation in the gut (major) and liver (42 47). Despite the importance of sulfation, however, it is only recently that the SULT forms involved have been characterized (47). In this instance, Schrag et al. were

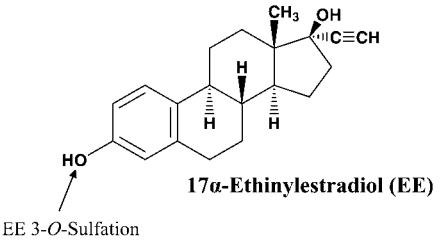

Preparation	K_m (nM)
Recombinant SULT1A1	890
Recombinant SULT2A1	239
Recombinant SULT1A3	18.9
Recombinant SULT1E1	6.7
Jejunum cytosol	24 (K_{m1})
	1206 (K_{m2})
Liver cytosol	8.0 (K_{m1})
	2407 (K_{m2})

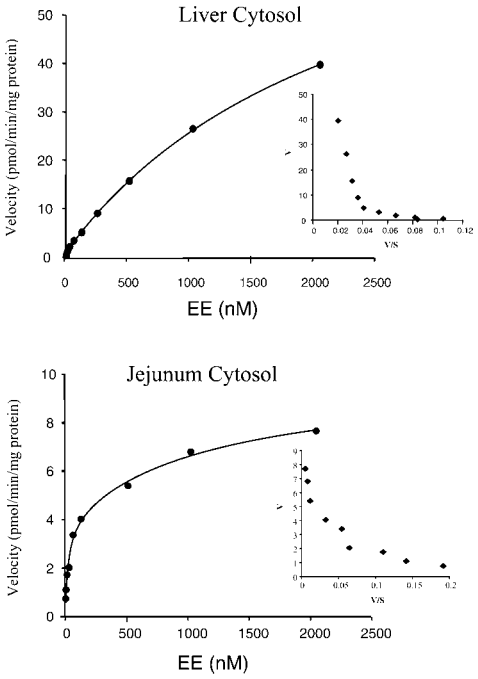

Figure 7 Sulfation of 17α ethinylestradiol (EE) in vitro by recombinant human sulfotransferases (SULTs) and human cytosol (liver and jejunum) (47).

able to assess the kinetics of 3-*O*-sulfation in vitro over a wide concentration of tritiated EE (1.0 2000 nM). The concentration range encompassed the known circulating EE concentrations ($\leq$10 nM) following OC dosing. In the presence of human liver and jejunum cytosol, the kinetic profile of EE 3-*O*-sulfation was biphasic and characterized by low and high K_m component (Fig. 7). With the availability of recombinant human SULTs, it was possible to show that two members of the SULT1 family (SULT1A3 and SULT1E1) served as low K_m enzymes, whereas a SULT2 form (SULT2A1) was a relatively high K_m enzyme. Further studies with chemical inhibitors such as quercetin (SULT1A1 and SULT1E1 inhibitor), estrone (SULT1A3 and SULT1E1 inhibitor), and 2,6-dichloro-4-nitrophenol (SULT1A1-selective inhibitor) showed that the low K_m component ($\sim$3 nM) in liver and gut cytosol was dominated by SULT1E1. Therefore, potent inhibitors of SULT1E1 could greatly impact the first pass 3-*O*-sulfation of EE (47). Although SULT1A1 and SULT2A1 were identified as high K_m EE SULTs, it is also possible that inducers of these enzymes can bring about reductions in circulating levels of EE and cause contraceptive failure (42,44). For example, rifampicin has been shown to increase the rates of EE sulfation in cultures of human primary hepatocytes, and so it cannot be assumed that induction involves CYP3A4 only (44). Interestingly, immuno-inhibition of EE 3-*O*-sulfation in human liver cytosol by anti-SULT1A antibodies has been reported, suggesting that inducible SULT1A1 contributes to approximately 40% of activity at a high concentration of EE (1000 nM) (Cypex Corp. website at www.cypex.co.uk).

Beyond EE, additional SULT substrates have been reaction phenotyped with recombinant proteins. For example, sulfation of troglitazone is dominated by SULT1A1, resveratrol is sulfated by SULT1A1 and SULT1E1, raloxifene by SULT2A1 and 4-hydroxytamoxifen by SULT1E1 (75,76). In most cases, investigators have evaluated

kinetics and focused on low K_m SULTs as much as possible. One laboratory has concluded that the sulfation of apomorphine is dominated by SULT1A1 in human cytosol, on the basis of correlation analysis and the use of inhibitory antibodies (78).

Differentiating Enzymes Within the Same Gene Subfamily

In many instances, a drug will be metabolized by multiple members of a single gene subfamily. This is apparent for CYP and UGTs, for which it may be difficult to differentiate between the various CYP2C, CYP3A, CYP1A, UGT1A, and UGT2B subfamily members using conventional correlation analyses and chemical inhibitors in HLM. Such differentiation is important, because metabolism by specific subfamily members often correlates with different clinical outcomes. For example, a drug cleared via CYP2C9, CYP2C8, or CYP2C19 will be prone to a different set of drug interactions and polymorphisms (35,66,79). This is also true for other gene subfamilies like CYP3A (3A4 and 3A5), CYP1A (CYP1A1 and CYP1A2), and UGT1A (UGT1A1, UGT1A4, UGT1A9, UGT1A10, etc.) (68 70,80,81).

Commercially available recombinant CYP and UGT preparations have enabled relatively easy assessment and differentiation of subfamily members. At the same time, the increased access to selective immuno-inhibitory CYP antibodies and chemical inhibitors has also allowed some labs to assess the role of different subfamily members in HLM (21,28,67,82,83). For example, the involvement of CYP2C8, CYP2C9, and CYP2C19 in HLM can now be determined with inhibitors like montelukast, sulfaphenazole, and (+)-*N*-3-benzyl-nirvanol, respectively (28, references therein). Likewise one can attempt to differentiate CYP3A4 from CYP3A5 by using HLM from genotyped subjects (e.g., individuals that are homozygous for the *CYP3A5*3* allele are "low CYP3A5 expressors") and chemical inhibitors like mifepristone, which appear to show selectivity toward CYP3A4 (vs. CYP3A5) (84,85).

CYP2C Subfamily as First Example. Availability of recombinant human CYP proteins has greatly increased our knowledge of the CYP2C subfamily. It is now known that there are three important members (CYP2C8, CYP2C9, and CYP2C19), each with a distinct profile in terms of polymorphic expression (e.g., allele frequency in different races), tissue expression, substrate, and inhibitor selectivity (21,60,66,79). Reaction phenotyping of CYP2C substrates has been facilitated, and the metabolism of drugs such as paclitaxel, (*S*)-(+)-mephenytoin, omeprazole, and (*S*)-warfarin has been assigned unambiguously to an individual subfamily member (66,79,82,86 88).

Paclitaxel 6α-hydroxylase and (*S*)-(+)-mephenytoin 4-hydroxylase, for example, are reactions known to be selective for CYP2C8 and CYP2C19, respectively. Likewise, (*S*)-warfarin 7-hydroxylase and tolbutamide hydroxylase are CYP2C9 selective in vitro. In all cases, the in vitro data have more or less correlated with clinical data (66,79). Some CYP2C substrates like ibuprofen have exhibited more complex profiles (89). Ibuprofen is dosed as a racemic mixture and each enantiomer is metabolized (hydroxylated) at two positions. As illustrated in Figure 8 (unpublished data), with recombinant CYP2Cs one is able to evaluate clearly the regio-selective hydroxylation of each enantiomer. Data for the (*R*)-(−)-enantiomer are presented and it is apparent that CYP2C8 favors the 2-hydroxylation reaction, whereas CYP2C9 exhibits a more balanced profile (ratio of 3-hydroxylation/2-hydroxylation ~ 1.0). Although CYP2C9 plays a major role in HLM, it is possible to discern the preference of CYP2C8 for 2-hydroxylation in the same preparations; montelukast (CYP2C8 selective) and anti-CYP2C8 inhibitory antibodies inhibit the 2-hydroxylation (11% to 24% inhibition) more so than 3-hydroxylation ($\leq$8% inhibition) reaction (unpublished data not shown).

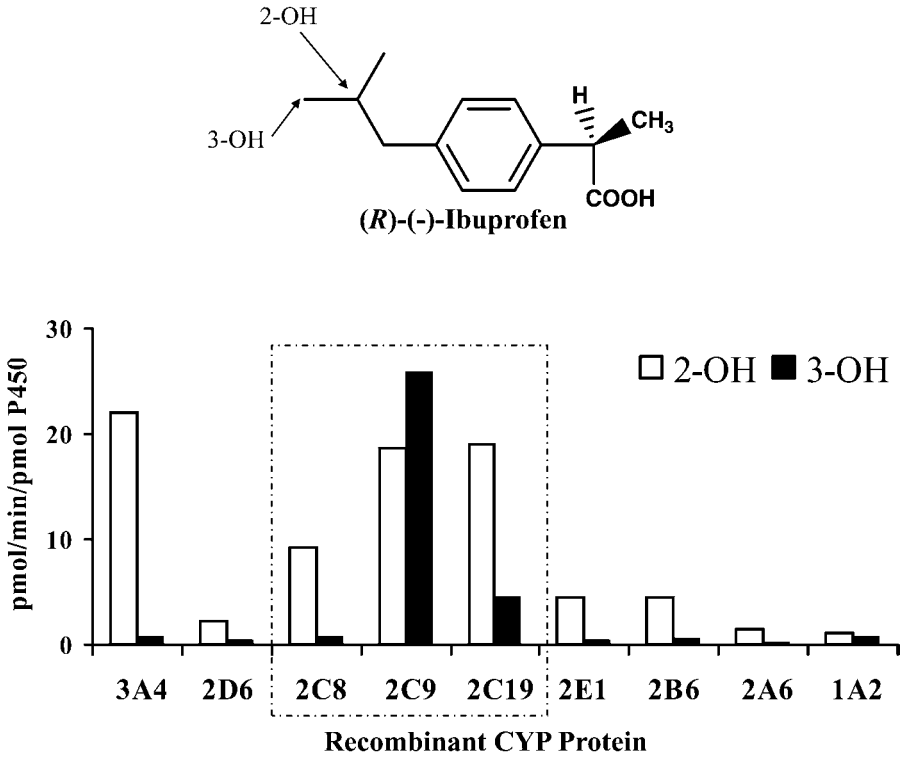

Figure 8 Hydroxylation (2 and 3 positions) of (*R*) ( ) ibuprofen in the presence of various recombinant human cytochrome P450 (CYP) proteins.

UGT1A Subfamily as Second Example. Members of the human UGT1A subfamily are numerous and are encoded by a complex gene locus, which is located on chromosome 2 (2q.37). The large UGT1A gene locus contains an array (exon 1) that is spliced onto four common exons (designated UGT1 exons 2 5) (68 70,90,91). Therefore, multiple UGT1A forms are constructed by linking different substrate binding sites (encoded by exon 1) to a constant portion of the enzyme (encoded by exons 2 5).

The various UGT1A subfamily members metabolize a diverse array of endogenous compounds, drugs, and other xenobiotics and more often than not exhibit overlapping substrate selectivity (68 70). This has made it difficult to develop selective UGT1A form probes (e.g., substrates and inhibitors) that afford reaction phenotyping of UGT1A1, UGT1A3, UGT1A4, UGT1A6, UGT1A7, UGT1A8, UGT1A9, and UGT1A10 in microsomes of different tissues. Typically, the substrate in question is incubated with a panel of different recombinant UGT1A forms, and the rates of metabolite formation are compared. If one or two UGT1A forms dominate, an attempt is made to correlate the metabolite formation with putative UGT1A form activities in a panel of HLM from different organ donors. Finally, chemical inhibitors are used when a particular UGT1A form appears to dominate in tissue microsomes (71,72).

In Figure 9, for example, tritiated EE (2 nM) has been incubated with a panel of UGTs and the rates of 3-*O*- and 17-*O*-glucuronide (EE 3-*O*-G and EE 17-*O*-G) formation determined. Activity is highest in the presence of UGT1A1, which favors the formation of EE 3-*O*-G. In agreement, EE 3-*O*-G formation correlates well with UGT1A1 protein levels ($r = 0.82$; $p < 0.05$), UGT1A1-selective estradiol 3-*O*-glucuronidation ($r = 0.87$; $p < 0.05$)

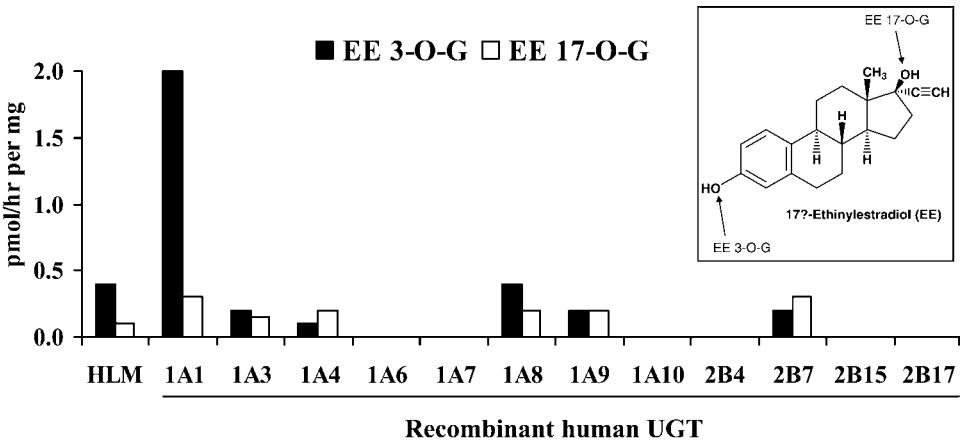

Figure 9 Glucuronidation of tritiated 17α ethinylestradiol (EE, 2 nM) in the presence of HLMs and various recombinant human UDP glucuronosyltransferases (42). *Abbreviations*: HLMs, human liver microsomes; UGT, UDP glucuronosyltransferase; EE 3 *O* G, EE 3 *O* glucuronide; EE 17 *O* G, EE 17 *O* glucuronide.

and bilirubin glucuronidation ($r = 0.95$; $p < 0.05$) in a bank of HLM (42). In contrast, correlations with UGT1A4 (trifluoperazine glucuronidation), UGT1A9 (propofol glucuronidation) and UGT2B7 (morphine glucuronidation) are weak ($r \leq 0.29$). In addition, EE 3-*O*-G formation is inhibited ($\sim$70%) by bilirubin. Obviously, the conclusion that EE 3-*O*-G formation is largely catalyzed by UGT1A1 in HLM is predicated on the utility of estradiol, trifluoperazine, and propofol as UGT1A1-, UGT1A4-, and UGT1A9-selective probes (92,93). This also extends to other substrates such as serotonin (UGT1A6 probe), 3′-azidothymidine (UGT2B7 probe), and (*S*)-oxazepam (UGT2B15 probe) (93,94).

Allelic Variant Forms

Our understanding of the molecular genetics of human DMEs has greatly increased in recent years (66,79, references therein, 95,96). For certain DMEs, the technology has reached a stage where it is now possible to prospectively determine the phenotypic or genotypic status of individuals involved in clinical trials. This is impressive, when one considers that changes in phenotype are more often than not the result of a single nucleotide polymorphism (SNP). The availability of heterologously expressed wild-type and variant forms of these different DMEs, in addition to the increased availability of tissue from genotyped subjects, has added an extra dimension to preclinical NCE-screening procedures (66).

For the sake of illustration, intrinsic clearance can be defined as the ratio of V_{max}/K_m (defined earlier, see sect. An "Integrated Approach" to Studying In Vitro Drug Metabolism) under first order conditions (where substrate concentration is well below the Michaelis constant, K_m). In turn, V_{max} is a composite term with enzyme concentration (E_o) being a variable, such that $V_{max} = k_{cat}\ E_o$ (28). Therefore, an SNP can alter the V_{max}/K_m ratio by affecting K_m (e.g., increase) and k_{cat} (e.g., decrease). Changes in k_{cat}/K_m ratio can be determined with recombinant DMEs, especially if the protein in question is electrophoretically homogeneous, or if one is able to get a specific measure of substrate turnover. It is worth pointing out that some allelic variant forms are unstable, and it is not possible to accurately assess changes in the k_{cat}/K_m ratio. Moreover, some SNPs give rise to changes

in E_o. For example, SNPs in the promoter region can bring about an increase, or decrease, in enzyme expression (E_o) with minimal impact on the k_{cat}/K_m ratio. In the most extreme cases, "null alleles" bring about a complete absence of protein, and it is not possible to obtain estimates of k_{cat}/K_m ratio. Overall, the impact of SNPs is reflected phenotypically as a change in the V_{max}/K_m ratio [$(k_{cat}\ E_o)/K_m$], leading to alterations in intrinsic clearance, organ clearance, and total clearance. Although CYP2C9 is discussed in detail, for brevity, the reader is advised to consult the literature for other examples (66,79,95–99).

CYP2C9. There are at least two clinically relevant allelic variant forms of CYP2C9 (35,66,79, references therein). The first (CYP2C9*2) results when an arginine at position 144 (Arg^{144}) is replaced by cysteine (Cys^{144}), whereas the second variant (CYP2C9*3) represents leucine (Leu^{359}) in place of an isoleucine (Ile^{359}) residue at position 359. Because these proteins have been heterologously expressed, it has been possible to directly investigate the effects of these point mutations on monooxygenase activity. For example, tolbutamide hydroxylase, phenytoin *p*-hydroxylase, and (*S*)-warfarin 7-hydroxylase V_{max}/K_m or k_{cat}/K_m are significantly reduced (>70%) in the presence of recombinant CYP2C9*3 (vs. wild-type CYP2C9*1), and in most cases, this has been associated with altered pharmacokinetics (trait measures and phenotype) in subjects genotyped *CYP2C9*1/*3* or *CYP2C9*3/*3* (35,66,79 references therein). In some instances, the impact of *CYP2C9* genotype is significant enough to warrant dose adjustment (79).

CYP2C9-catalyzed methyl hydroxylation of celecoxib, a cyclooxygenase-2 inhibitor, also illustrates the utility of recombinant CYP2C proteins (Fig. 10). The drug is known to be metabolized extensively, and in vitro reaction phenotype data support a major role for CYP2C9 in HLM, although CYP3A4 can play a role in some livers

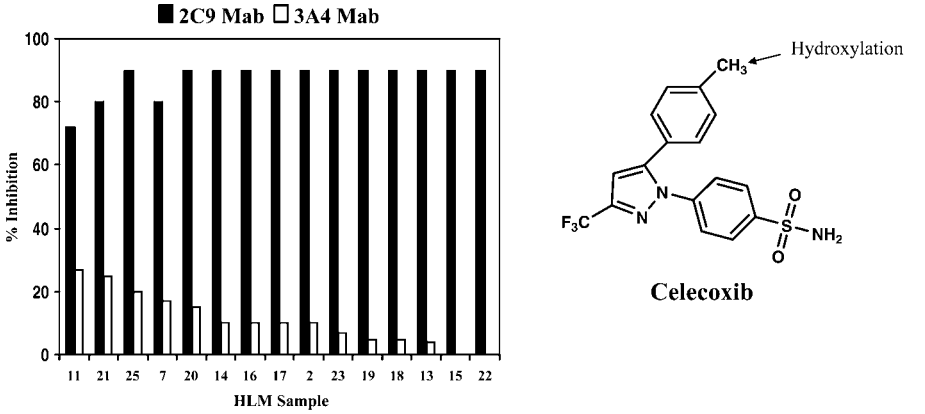

Recombinant CYP2C9 Protein	V_{max}/K_m (μL/min/nmol)
2C9*1 (Ile^{359})	2325 (100%)
2C9*3 (Leu^{359})	250 (11%)
2C9*1 + 2C9*3 (1:1)	1212 (52%)

Genotype (HLM Prep.)	CYP3A4/CYP2C9 Ratio	V_{max}/K_m (μL/min/mg)
CYP2C9*1/*1	1.0 to 7.9 (n = 8 livers)	4300 (pooled HLM)
CYP2C9*1/*3	3.5	4200
CYP2C9*1/*3	1.0 (n = 2 livers)	1800

Figure 10 Hydroxylation of celecoxib by HLMs and recombinant CYP2C9 variant forms (100,101). *Abbreviations*: HLMs, human liver microsomes; Mab, monoclonal antibodies.

(35,66,100,101). Upon incubation with recombinant CYP2C9*3, the k_{cat}/K_m ratio is reduced approximately 90% (vs. CYP2C9*1). Co-incubation of equimolar amounts of recombinant CYP2C9*1 and CYP2C9*3, to mimic the heterozygous genotype (*CYP2C9*1/*3*), results in an approximately 50% decrease in the k_{cat}/K_m ratio (100). In agreement, the V_{max}/K_m is decreased approximately 50% in HLM from a liver genotyped *CYP2C9*1/*3*. However, the impact of *CYP2C9* genotype may be offset in livers where the ratio of CYP3A4 to CYP2C9 is relatively high (>1.0) (Fig. 10). To date, clinical data confirm the association between celecoxib pharmacokinetics and *CYP2C9* genotype, although the impact of CYP3A4 on this association requires further study (35,66,100,102, references therein).

Structure-Function and Structure-Activity Studies

Nowhere has the impact of recombinant approaches been more evident than in the case of DME structure-function and structure-activity studies (103). In recent years, the ability to heterologously express, and purify, DMEs has enabled preparation of crystals for X-ray crystallography and structure elucidation. Therefore, high-resolution crystal structures for some ligand-bound SULTs, UGTs, and CYPs have been solved; the "ligand" in question is cofactor, inhibitor, or substrate (24 26,103). At the same time, it has been possible to conduct site-directed mutagenesis (SDM) employing bacteria (e.g., *E. coli*) that express the desired human DME. In this instance, the mutated DME is compared to wild-type form and, if needed, purified and also subjected to X-ray analysis. In toto, SDM of DMEs has provided useful information and enabled assessment of which amino acid residues are required for catalysis (e.g., binding of cofactor and substrate), protein folding, interaction with auxiliary proteins (e.g., CYP reductase and cytochrome b_5), and binding to inhibitor. For example, the amino acid residues of CYP2C9 and CYP2A6 that govern substrate binding have been determined (104 106). Likewise, the residues involved in the interaction of CYPs (e.g., 3A4 and 2E1) with CYP reductase and cytochrome b_5 have been investigated (107 109). Going beyond the human CYPs, other human DMEs such as SULT1A3 (110), UGT2B4 and UGT2B7 (111), and FMO3 (112) have also been subjected to SDM.

Integration of structural information garnered from crystal structures and SDM studies is very important because it allows one to build electron density maps, and atomic models, and enables computer-based ligand docking (103). For a given series of molecules, therefore, the structural features that govern binding at the active site (binding pocket) can be determined and structure-activity relationships (SARs) established. Such protein-based approaches can compliment more empirical physicochemico property (descriptor)-based and pharmacophore-based SAR approaches (113 115). As time has passed, the acceptance of such methods has increased as industrial scientists have turned to "in silico" methodologies that compliment existing assay based high-throughput screens (116,117). The ultimate goal is to screen out chemotypes that behave as potent inhibitors of CYP, while preserving potency and selectivity at the desired pharmacological target. Alternatively, one can dial in potency by optimizing the ligand-protein interaction.

Enzyme Kinetics

CYPs

It is now accepted widely that human CYPs do not always conform to classical single-K_m (hyperbolic) Michaelis-Menten kinetics. With the advent of improved software, it has been possible to fit experimental data (e.g., initial rate vs. substrate concentration) to

various kinetic models without the need for linear plots (118 120). As a result, CYP substrates have been shown to exhibit a number of profiles consistent with two-K_m (biphasic or nonasymptotic) kinetics, autoactivation (sigmoid) kinetics, heterotropic cooperativity (activation) kinetics, and substrate inhibition. Biphasic kinetics may result from two populations of CYPs (low K_m and high K_m) or biphasic binding of substrate to a single CYP. In addition, autoactivation and substrate inhibition can be reflective of multiple substrate molecules binding at the same site. Given the complex mixture of CYPs in HLM, it is often necessary to conduct kinetic studies with heterologously expressed or purified (reconstituted) CYPs and confirm the kinetic profile. For example, a sigmoidal kinetic profile has been observed for carbamazepine and diazepam (CYP3A4), naphthalene (CYP2B6, CYP2C8, CYP2C9, and CYP3A5), and dapsone (CYP2C9), whereas naphthalene (CYP3A4) and naproxen (CYP2C9) exhibit biphasic kinetics with the corresponding recombinant CYP (119,120).

Likewise, kinetic profiling also extends to NCEs that are in development. For instance, TPA023 is a potent human γ-aminobutyric $acid_A$ receptor agonist that has been in development for the treatment of anxiety (Fig. 11). When incubated with HLM, the compound undergoes *t*-butyl hydroxylation and *N*-deethylation; both reactions are catalyzed almost exclusively (>90%) by members of the CYP3A subfamily therein (121). Interestingly, TPA023 *N*-deethylation conforms to single-K_m (hyperbolic) Michaelis-Menten kinetics in the presence of recombinant CYP3A4. In contrast, a biphasic kinetic profile is evident with recombinant CYP3A5 (Fig. 11). In agreement, *N*-deethylation is described by two-K_m and single-K_m kinetics in the presence of CYP3A5-rich and CYP3A5-poor HLM preparations, respectively (121). These findings illustrate the utility of recombinant CYP preparations.

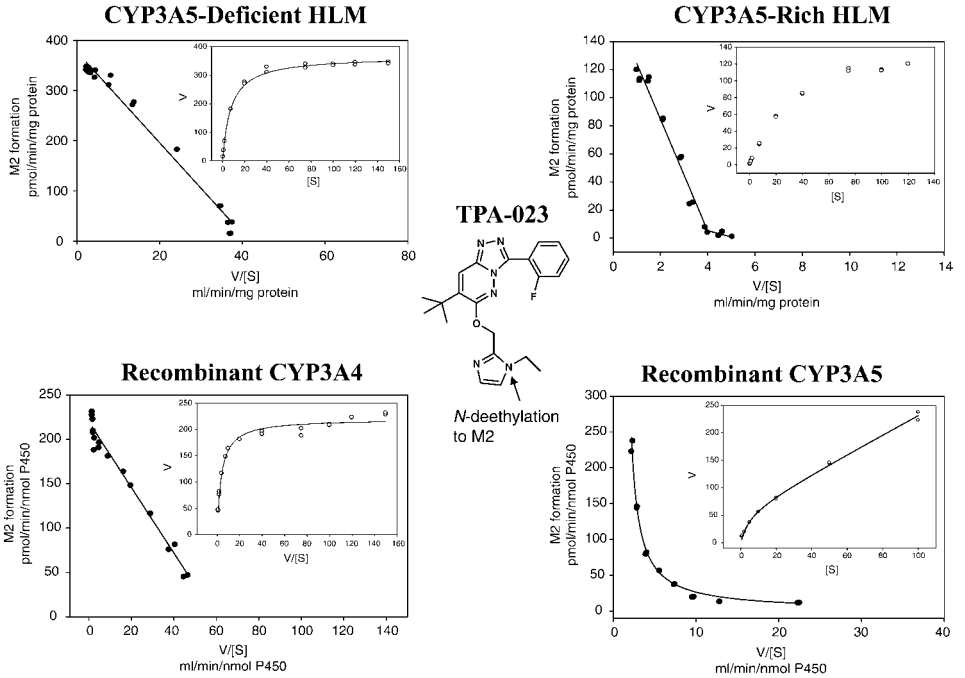

Figure 11 TPA023 *N* deethylation kinetics in the presence of recombinant CYP3A4 and CYP3A5, and CYP3A5, and human liver microsomes (HLMs) (121).

UGTs

Numerous laboratories have leveraged recombinant enzyme preparations to characterize the atypical kinetics of UGT-catalyzed reactions (122 127). In fact, data have suggested that UGT forms (e.g., UGT1A1, UGT1A4, and UGT1A6) may interact with each other and form heterodimers. This has the potential to further complicate kinetic analyses. For example, the co-expression of UGT1A1 and UGT1A4 increases the V_{max} of UGT1A6-catalyzed serotonin and diclofenac *O*-glucuronidation (122). Substrates of one UGT (e.g., propofol; UGT1A9) have been shown to stimulate (e.g., 4-methylumbelliferone) and inhibit (e.g., estradiol) glucuronidation catalyzed by a second UGT (e.g., UGT1A1) (123). A given substrate (e.g., morphine) might exhibit single-K_m Michaelis-Menten kinetics with one UGT form (UGT1A1-catalyzed 3-*O*-glucuronide formation) and atypical kinetics (3-*O*- and 6-*O*-glucuronide formation) with a second (e.g., UGT2B7) (124,127). Other substrates like resveratrol (UGT1A1, UGT1A9, and UGT1A10) and 4-methylumbelliferone (UGT1A9 and UGT2B7) exhibit atypical kinetics in the presence of a number of different UGTs (125,126).

SULTs

Cytosolic SULTs (monomeric molecular weight of 30 35 kDa) usually exist as homodimers and can exhibit atypical kinetics also (128 133). In fact, the phenomenon of substrate inhibition has been known for some time and attempts have been made to rationalize such findings on the basis of knowledge gleaned from the crystal structures and SDM of SULTs such as SULT1A1, SULT1A3, and SULT2A1 (130,133). For example, it has been possible to co-crystallize a SULT protein (e.g., SULT1A1) with two molecules of substrate (*p*-nitrophenol) and one of the cofactor (3′-phosphoadenosine 5′-phosphosulfate) per monomer. As observed with the UGTs, the same substrate (e.g., 1-OH pyrene) can exhibit single-K_m Michaelis-Menten kinetics with one form of recombinant SULT (e.g., SULT2A1) and atypical kinetics (e.g., substrate inhibition) with other forms of recombinant SULTs (e.g., SULT1A3 > SULT1A1 > SULT1E1) (132). Other substrates such as resveratrol are also characterized by a complex kinetic profile, because of sulfation at three different positions that are catalyzed by multiple SULT forms. Depending on the recombinant SULT in question (e.g., SULT1A1 vs. SULT1E1), each of the three-resveratrol sulfation reactions can conform to hyperbolic (single-K_m), substrate inhibition or sigmoid kinetics (75).

More recently, heterotrophic modulation of recombinant SULT2A1 by celecoxib has been reported by two different groups. Apparently, celecoxib is able to alter the regioselective sulfation (3-*O* vs. 17-*O* sulfation) of steroid substrates such as EE and β-estradiol (134,135). In both cases, the 3-*O*-sulfation dominates in the absence of celecoxib. However, the ratio of 17-*O*-sulfate to 3-*O*-sulfate is increased (>10) when celecoxib is added. A similar result can be obtained with human liver cytosol. The significance of this product switching is not known at the present time.

Enantio-, Regio-, and Stereoselective Biotransformations

Because enantiomers and stereomers can often exhibit markedly different pharmacological profiles, therapeutic indices, and metabolic profiles, most pharmaceutical companies have focused increasingly on enantio- and stereoselective drug-drug interactions and biotransformations (136,137). Armed with heterologously expressed and purified DMEs, investigators have been afforded the opportunity to unambiguously study the regio- and stereoselective oxidation (CYP and FMO catalyzed), glucuronidation and sulfation of the

racemic, pseudoracemic, and individual enantiomeric forms of numerous drugs (e.g., warfarin, ibuprofen, EE, oxazapam, omeprazole, resveratrol, morphine), steroids (e.g., β-estradiol), nonsteroid hormones (thyroxine), neurotransmitters (e.g., dopamine), and xenobiotics (32,36,42,75,89,93,134,138 144).

CYP-Dependent Metabolism of Zileuton as an Example

Zileuton, a racemic mixture of (*R*)-(+)- and (*S*)-(−)-*N*-(l-benz[*b*]thien-2-ylethyl)-*N*-hydroxyurea, is a 5-lipoxygenase inhibitor (145). During its development, in vitro metabolism data indicated that both enantiomers underwent CYP3A-dependent stereoselective sulfoxidation in the presence of native HLM (Fig. 12); (a) the formation of the (*R*)-(+)-enantiomer sulfoxide (S1) was highly correlated ($r = 0.995$; $p < 0.001$; $n = 11$) with the formation of the (*S*)-(−)-enantiomer sulfoxide (S2) in a panel of HLM; (b) the formation of both S1 and S2 was inhibited (∼60%) by troleandomycin, whereas inhibitors of other CYP forms were ineffective (≤5% inhibition); (c) S1 and S2 formation was stimulated (∼175%) by 7,8-benzoflavone; and (d) the formation of S1 ($r = 0.815$; $p < 0.01$) and S2 ($r = 0.794$; $p < 0.01$) was correlated with CYP3A-selective erythromycin *N*-demethylase activity. However, it appeared that the formation of S1 predominated over S2 (ratio = 2.1) in the presence of native HLM (0.62 ± 0.44 vs. 0.30 ± 0.21 nmol/hr/nmol CYP; mean ± SD; $n = 11$), which suggested that the (*R*)-(+)-enantiomer of zileuton was a better substrate for

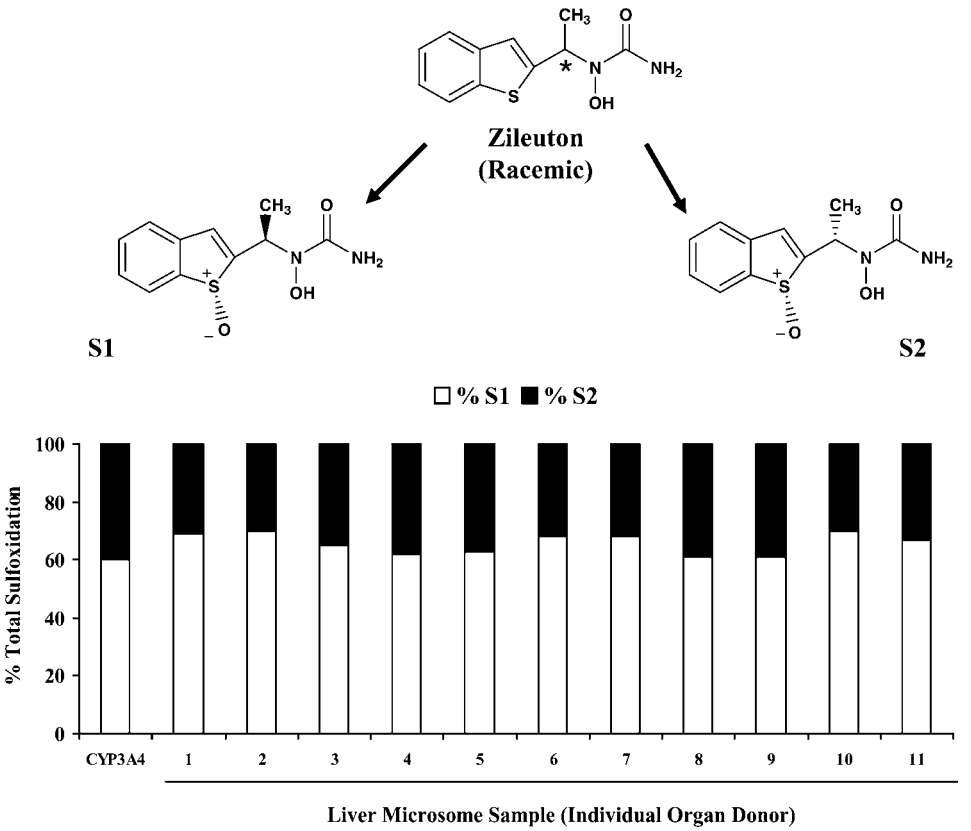

Figure 12 Sulfoxidation of zileuton catalyzed by human liver microsomes from various organ donors and fully reconstituted (purified) CYP3A4 (145).

CYP3A-catalyzed sulfoxidation (Fig. 12). With the availability of fully reconstituted (purified) CYP3A4, it was possible to unambiguously confirm that the formation of S1 predominated over S2 (ratio = 1.6).

FMO-Catalyzed cis- and trans-N′-Oxidation of ABT-418 as an Example

Depending on the enzyme source, FMO can often catalyze *N*- and *S*-oxidation reactions in a stereoselective manner (32,36,141 144). During the development of ABT-418 (single (*S*)-enantiomer), therefore, the possibility for stereoselective *N*′-oxidation had to be addressed. Earlier in vitro and in vivo experiments had revealed that the *N*′-oxidation of ABT-418 was stereoselective (100% *trans*) in the rat and dog (48,49). In contrast, ABT-418 *N*′-oxidation was not stereoselective when incubated with human (*trans*, ~50%; *cis*, ~50%), cynomolgus monkey (*trans*, 63%; *cis*, 37%), and chimpanzee (*trans*, 26%; *cis*, 74%) liver microsomes (Fig. 13). Interestingly, the *N*′-oxidation of ABT-418 in the presence of human kidney 9000 g supernant fraction was stereoselective (100% *trans*), which agreed with the observation that the kidney FMO pool (FMO1 > FMO3) differs from that present in HLM (FMO3 > FMO1) (48, references therein; Table 1). By using *E. coli*-expressed human FMO3, it was possible to confirm that the pattern of ABT-418 *N*′-oxidation was not stereoselective and was similar to that of native HLM (Fig. 13). On the other hand, purified pig liver microsomal FMO1 and rabbit lung microsomal FMO2 catalyzed the *N*′-oxidation of ABT-418 in a stereoselective (100% *trans*) manner (48). The availability of recombinant FMO3 was essential because ABT-418 *N*′-oxidation could be evaluated in the absence of competing *N*-oxide reductases.

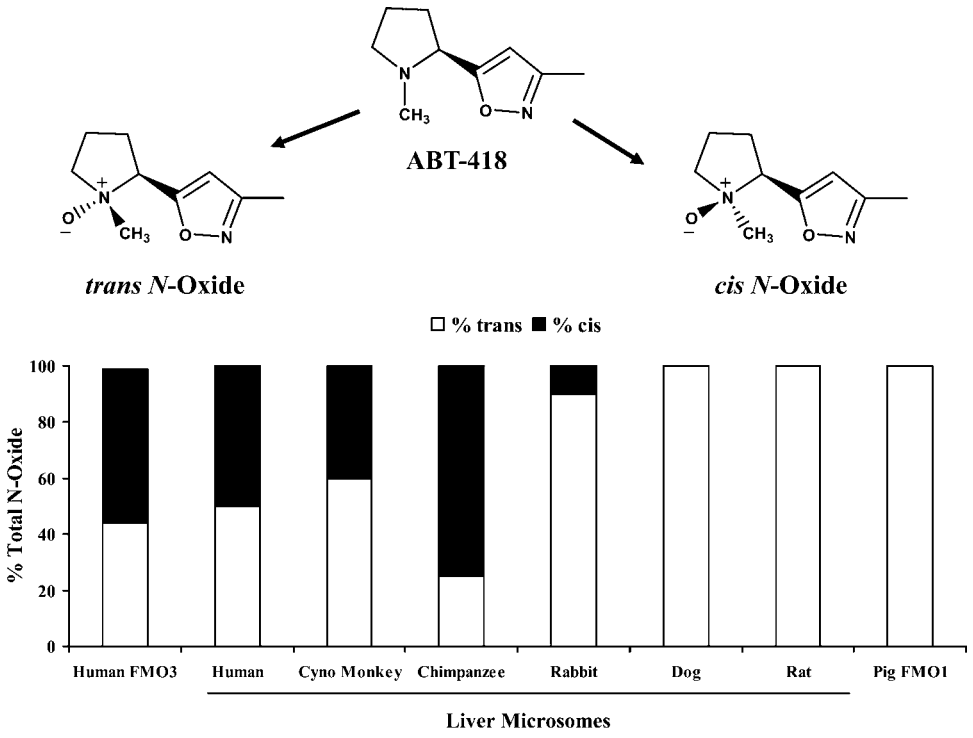

Figure 13 ABT 418 *N* oxidation (*cis* and *trans*) by human liver microsomes from various species and recombinant flavin containing monooxygenase (FMO) forms (FMO3, human; FMO1, pig) (48,49).

Stereoselective Glucuronidation of Oxazepam as an Example

Oxazepam is a 1,4-benzodiazepine derivative that is used as an anxiolytic, sedative, and anticonvulsant. The compound is administered as a racemic mixture and is known to be cleared almost exclusively via glucuronidation. Therefore, Court et al. (146) have described the glucuronidation of individual enantiomers by specific human UGT forms. Their data have shown that rates of (*S*)-oxazapam glucuronidation are highest with recombinant UGT2B15, whereas minimal to non-detectable activity is observed with other recombinant UGT forms such as UGT2B7 and UGT1As. In agreement, the kinetics of (*S*)-oxazapam glucuronidation (HLM and recombinant UGT2B15) were described by a single-K_m ($\sim$30 μM) and conformed to an uncompetitive substrate inhibition model. Interestingly, glucuronidation of the (*R*)-enantiomer was catalyzed by a different array of recombinant UGTs (UGT2B7 $\sim$ UGT1A9 >> UGT1A7). Therefore, UGT2B15 [(*S*)-enantiomer >> (*R*)-enantiomer], UGT1A9, and UGT2B7 [(*R*)-enantiomer>> (*S*)-enantiomer] exhibited considerable stereoselectivity. The result may be significant, because the same authors showed that the rates of (*S*)-oxazapam glucuronidation were reduced ($\sim$90%) in the presence of recombinant UGT2B15*2 variant form (vs. UGT2B15*1), and because certain subjects are known to carry the *UGT2B15*2* allele. More recently, the same group has confirmed that HLM preparations from organ donors genotyped *UGT2B15*2* do in fact exhibit reduced (*S*)-oxazapam glucuronidation (147). Furthermore, a second group has shown that an additional UGT2B15 and UGT1A9 substrate (e.g., 5-(4′-hydroxyphenyl)-5-phenylhydantoin) is also subject to stereoselective glucuronidation (148).

Drug-Drug Interaction (Inhibition) Studies

High-Throughput Inhibition Screening

Since the late 1990s, the availability of recombinant DMEs has facilitated the development of high-throughput inhibition assays (149 153). With the advent of nanodispensing technology, fully automated liquid handling devices, sophisticated robotics, and increased computing power, it has been possible to evolve from manual single test tube assays ($\sim$0.5 mL assay volume), through 96-well ($\sim$0.2 mL assay volume) and 384-well ($\sim$50 μL assay volume) formats, to miniaturized (<10 μL assay volume) fully automated 1536-well assay formats (154,155).

A wide range of CYP substrates are commercially available and include compounds such as 3-cyano-ethoxycoumarin (CEC) for CYP1A2 and CYP2C19, 3-[2-(*N*,*N*-diethyl-*N*-methyl-ammonium)ethyl]-7-methoxy-4-methyl-coumarin (AMMC) for CYP2D6, 7-methoxy-4-trifluoromethylcoumarin (MFC) for CYP2C9, and 7-benzyloxyquinoline (7-BQ) for CYP3A4 (149 155). Typically, such substrates are metabolized to fluorescent metabolites that are readily monitered with plate readers, so that time-consuming sample processing and liquid chromatography steps can be avoided. More often than not, however, such substrates are not selective for a given CYP form and one cannot conduct inhibition screening with HLM as the enzyme source. Nevertheless, recombinant CYP-based assays have proven extremely useful, and it is possible to rapidly screen out potent inhibitors and drive SAR campaigns (148 155).

One example of a fluorescence-based assay is presented in Figure 14. In this instance, 7-benzyloxy-4-(trifluoromethyl)-coumarin (BFC) is *O*-dealkylated by recombinant CYP3A4 to its fluorescent hydroxyl metabolite. The assay mix simply requires substrate (BFC), recombinant protein (CYP and CYP reductase) and buffer, and product formation is monitored after the addition of NADPH. For screening purposes, the inhibitor is added in the appropriate volume of solvent and an inhibition curve is

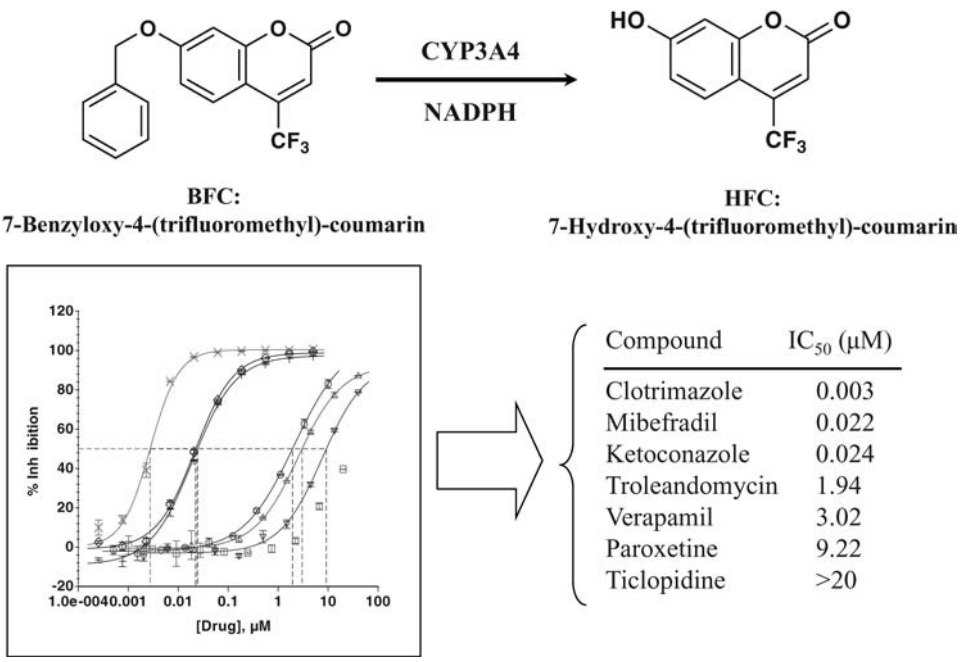

Figure 14 Example of a fluorescence based cytochrome P450 (CYP) inhibition assay. IC_{50}, concentration of inhibitor that gives rise to 50% inhibition.

generated. The concentration of inhibitor giving rise to 50% inhibition of BFC turnover (IC_{50}; substrate-to-K_m ratio $\sim$ 1.0) is determined, and the results are uploaded to a database. Typically, assays such as the one described are robust enough to enable screening of NCEs for reversible and time-dependent inhibition. The latter involves an enzyme-inhibitor preincubation step and monitering of IC_{50} shifts with time. If a time-dependent shift in IC_{50} is observed, then this may be indicative of a potent (reversible) inhibitory metabolite, or mechanism-based inhibition, and additional follow-up is required. It is also possible to determine the type of inhibition (e.g., competitive, noncompetitive, and mixed) and generate inhibition parameters such as K_i (inhibition constant), k_{inact} (maximal rate of inactivation), and K_I (half maximal rate of inactivation). Going forward, assay suites will likely be expanded to include other DMEs such as recombinant UGT1A1 and beyond (156).

Mechanistic Studies

In addition to high-throughput screening, recombinant DMEs have greatly facilitated the study of specific inhibitor-enzyme interactions. For the CYPs in particular, it has been possible to evaluate the isoform selectivity of a particular inhibitor (e.g., troleandomycin, 7,8-naphthoflavone, diethyldithiocarbamate, sulfaphenazole and furafylline, etc.) and determine IC_{50}, K_i, k_{inact}, and K_I (157 160). It has also been possible to generate visible difference spectra (380 600 nm wavelength range; type I, type II or reverse type I), determine spectral dissociation constants (K_s), and detect turnover-dependent (metabolite-inhibitor, "MI") spectral complexes (e.g., nitrosoalkane and carbene complex) (161 163). This is important, because spectra are impossible to generate when the CYP in question is expressed at low levels in HLM (Table 1).

As described previously (see sect. "Enzyme- and Isoform-Selective Biotransformations"), differentiation of CYP subfamily members has become the focus of numerous groups and many have attempted to evaluate specific inhibitor-CYP pairs. For example, Ha-Duong et al. (161) have shown that sulfaphenazole is a potent recombinant CYP2C9 inhibitor ($IC_{50} = 0.6$ μM) when compared with CYP2C8 ($IC_{50} = 130$ μM) and CYP2C19 ($IC_{50} > 500$ μM). Moreover, a Type II spectrum ($\lambda_{min} = 390$ nm; $\lambda_{max} = 425$ nm) can be obtained for sulfaphenazole with recombinant CYP2C9, and spectral titration yields a K_s (0.4 μM) consistent with the determined IC_{50}. Likewise, CYP3A subfamily members (CYP3A4 and CYP3A5) have received considerable attention also because of possible differences in pharmacokinetics, drug interactions, and efficacy related to *CYP3A5* genotype. (80,85,164 167). For most substrates, the k_{cat}/K_m ratio for CYP3A4 is similar to that of CYP3A5. However, where the two enzymes differ is in their sensitivity to reversible and time-dependent inhibitors (e.g., ketoconazole, fluconazole, indinavir, and diltiazem); greater inhibition is observed with recombinant CYP3A4 (85,164 167). This may be an important consideration because inhibition studies with HLM preparations from genotyped subjects (e.g., *CYP3A5*3/*3* and *CYP3A5*1/*3*, "non or low expressors"; vs. *CYP3A5*1/*1*, "expressors") corroborate the findings with recombinant CYP3A5 and CYP3A4 (168). In our hands, itraconazole is also a more potent inhibitor of recombinant CYP3A4 than CYP3A5 ($IC_{50} = 0.15$ μM vs. $IC_{50} = 2.1$ μM; ratio of substrate to $K_m \sim 1.0$) (unpublished results). Such a result may partly explain the reported impact of *CYP3A5* genotype on the interaction between itraconazole and clopidogrel. Efficacy of clopidogrel is dependent on CYP3A-catalyzed activation and CYP3A5 expressors (vs. non-expressors) appear to be less prone to the inhibitory effects of itraconazole (80). It is clear that the impact of *CYP3A5* genotype on the magnitude of drug interactions requires further study. Therefore, ready access to recombinant CYP3A proteins and genotyped HLM preparations will enable the comparison of different CYP3A substrate-inhibitor pairs and the prioritization of follow-up clinical studies.

It is worth noting that inhibition studies with recombinant DMEs can generate some unforeseen results. For example, ritonavir has been shown to be a more potent inhibitor of recombinant CYP2J2-catalyzed terfenadine oxidation than ketoconazole ($IC_{50} = 0.9$ μM vs. $IC_{50} = 2.8$ μM; ratio of substrate to $K_m \sim 1.0$) (unpublished observations). The availability of such a recombinant CYP2J2 preparation is important because enzyme-selective probes for use with HLM and HIM are not well validated yet. Such a result may be important because CYP2J2 is expressed in the gut (Table 1) and may contribute to the first pass extraction of drugs previously ascribed to CYP3A4 (e.g., ebastine and astemizole) (169,170). It is not known if CYP2J2 plays a role in the metabolism of HIV protease inhibitors (e.g., saquinavir), so booster therapy involving ritonavir inhibition of CYP2J2-dependent gut first pass cannot be ruled out at the present time.

Mechanistic studies should not be limited to the human CYPs, and it is hoped that progress will enable a better understanding of individual inhibitor-UGT, inhibitor-FMO, and inhibitor-SULT pairs. This is essential so that selective chemical inhibitors are developed as reaction-phenotyping tools.

Toxicity Testing and the Study of Reactive Intermediates

Xenobiotics are known to be metabolized to reactive metabolites that bind covalently to intracellular macromolecules (e.g., DNA or protein) (4,171 173). Such bioactivation can disrupt enzyme activity, DNA replication, mRNA processing, cell cycle kinetics, and bring about glutathione (GSH) depletion, mitochondrial arrest, and even cell death. With the advent of recombinant methodologies, it has been possible to heterologously express

individual human DMEs in "reporter" cells. Therefore, the metabolic activation of many procarcinogens and promutagens therein, as well as the toxicity of agents such as acetaminophen, has been attributed to specific human DMEs (e.g., NAT, SULT, CYP3A4, CYP1A2, CYP1A1, and CYP2E1) (174 183). Moreover, it is possible to develop high-throughput toxicity screens that support SAR campaigns in a discovery setting.

Mutagenicity and Toxicity Testing

As described above, many human DMEs are readily cloned and can be stably expressed in various cell lines. As a result, it is now possible to coordinately investigate the metabolic activation and appearance of cytotoxicity and mutagenicity as intracellular events. This is possible because many of the cell types in use (e.g., AHH-1 TK +/−, HepG2, and CHO) can be adapted for assaying the induction of micronuclei and chromosomal aberrations. In addition, these cells can be assayed for the induction of a variety of genotoxicity markers, including mutations at the thymidine kinase (*tk*) and hypoxanthine phosphoribosyl-transferase (*hprt*) loci or for gross cytotoxicity end points such as cell survival rates and enzyme leakage (174 188). Therefore, researchers are able to perform toxicity testing of NCEs with these transgenic cells alone, in parallel with conventional toxicity models (e.g., cultured primary hepatocytes and liver slices), or alongside genotoxicity assays employing tester strains of *Salmonella typhimurium* co-incubated with native HLM, 9000 g supernantant fraction, or purified (or heterologously expressed) DMEs. More recently, it has been possible to heterologously express individual human DMEs in the tester strains of bacteria themselves (189 191). For brevity, several examples of toxicity testing are listed in Table 3. Some researchers have managed to co-express two or more (phases I and II) DMEs in a single cell type. This is necessary when the bioactivation of a test compound requires CYP-dependent oxidation and secondary metabolism (e.g., *N*-acetylation or sulfation) to occur sequentially.

Mechanistic Studies

Upon incubation with recombinant and purified CYPs, most NCEs, drugs, and xenobiotics undergo "productive" catalysis, exemplified by reactions such as *S*- and *N*-oxidation, hydroxylations, *O*- and *N*-dealkylations, and epoxidations, etc. Depending on the actual site of metabolism, however, the particular CYP-substrate pair can also give rise to intermediates that can react with trapping agents (e.g., GSH; and potassium cyanide, KCN) (192,193, references therein). Some reactions also lead to increased levels of active oxygen species (e.g., superoxide anion) and H_2O_2, because of metabolites that redox cycle or because the reaction in question is characterized by a catalytic cycle that is extremely uncoupled. In most cases, it is possible to incubate a given compound with the desired recombinant CYP and measure the formation of an adduct (with GSH or KCN), or active oxygen species, in a time- and concentration-dependent manner. Covalent binding to total protein in the incubation can also be determined if radiolabel is used. If needed, one can attempt to isolate the actual adduct and determine its structure. Obviously, such an exercise would be more difficult if one was forced to use HLM. The approach is illustrated by the work of Lightning et al. (194,195), who were able to incubate a radiolabeled Merck compound (L-754,394) with cDNA-expressed CYP3A4. In this instance, the resulting incubates were subjected to protein hydrolysis, and the radioactive peptides were analyzed by mass spectrometry. The authors were then able to conclude that L-754,394, a CYP3A4 inactivator, was covalently bound to residue Glu^{307} of the enzyme. The residue is located within the active site of CYP3A4, and covalent binding involved activation of the furan moiety of L-754,394.

Table 3 Examples of In Vitro Toxicity Testing Employing Transgenic Cells Heterologously Expressing One or More Human Drug Metabolizing Enzymes

Cell type	Cell line	Test compound(s)	Expressed enzyme(s)	End point(s)	References
CHO	Various	PhIP, MeIQ, IQ	CYP1A2, NAT2	Cell survival	175
AHH 1 TK +/	1A2/Hyg 3A4/Hyg	Aflatoxin B_1	CYP1A2, CYP3A4	hprt, DNA binding, and cell survival	176
CHO	Various	IQ, MeIQ	CYP3A7, NAT2	Cell survival	177
HepG2	Mvh2E1 9	Acetaminophen	CYP2E1	LDH leakage and protein adducts	178
AHH 1 TK+/	Various	Tamoxifen	Epoxide hydrolase, CYP3A4, CYP2E1, CYP1A2, CYP1A1	Micronuclei test	185
V79	Various	Benzo[*a*]pyrene	CYP1A1	Cellular dye uptake and micronuclei test	186
AHH 1 TK+/	2D6/Hol	NNK	CYP2D6	Cell survival, hprt	187
CHO	AS52	NNK	CYP2A6	hprt	188
V79	XEMh1A2 MZ*1	MeAalphaC	CYP1A2 or NAT or SULT1A1	hprt	191
S. typhimurium	TA1538	MeAalphaC	SULT1A1, NAT1 or NAT2	his+ revertants	191

CYP, cytochrome P450; NAT, *N* acetyltransferase; SULT, sulfotransferase; IQ, 2 amino 3 methylimidazo[4,5 f] quinoline; MeIQ, 2 amino 3,8 dimethylimidazo[4,5 f]quinoline; PhIP, 2 amino 1 methyl 6 phenylimidazo[4,5 b] pyridine; NNK, 4 (methyl nitrosamino) 1 (3 pyridyl) 1 butanone; MeAalphaC, 2 amino 3 methyl 9H pyrido [2,3 b]indole; LDH, lactate dehydrogenase; hprt, hypoxanthine phosphoribosyltransferase mutation assay.

CYP2D6 Metabolism of the Trazodone Metabolite 1-(*m*-chlorophenyl)piperazine as Example. Trazodone and nefazodone are known to cause severe hepatic injury in certain individuals (196). Although the exact mechanisms of such hepatotoxicity are not clearly understood, CYP-dependent reactive metabolite formation is thought to be involved (4,197). Both trazodone and nefazodone undergo CYP3A4-catalyzed activation to form benzoquinone, quinone-imine, and/or epoxide intermediates that are trapped by GSH (198 200). The *N*-dealkylation of trazodone and nefazodone to 1-(*m*-chlorophenyl)piperazine (*m*-CPP), a major circulating metabolite, is also catalyzed by CYP3A4 (199,200).

Recently, Wen et al. (201) detected three novel *m*-CPP-derived GSH adducts (M3, M4, and M5) after incubation of trazodone with HLM (Fig. 15). The same three adducts were also observed when *m*-CPP itself was incubated with HLM. As a result, the authors then proceeded to conduct reaction-phenotyping studies with *m*-CPP and trazodone. Recombinant CYP2D6 was found to be the predominant enzyme involved in M4 formation from *m*-CPP. In agreement, formation of M4 from *m*-CPP in HLM was inhibited by quinidine, a potent and selective CYP2D6 inhibitor (Fig. 15). These data clearly suggested that the *N*-dealkylation of trazodone was mediated by CYP3A4/

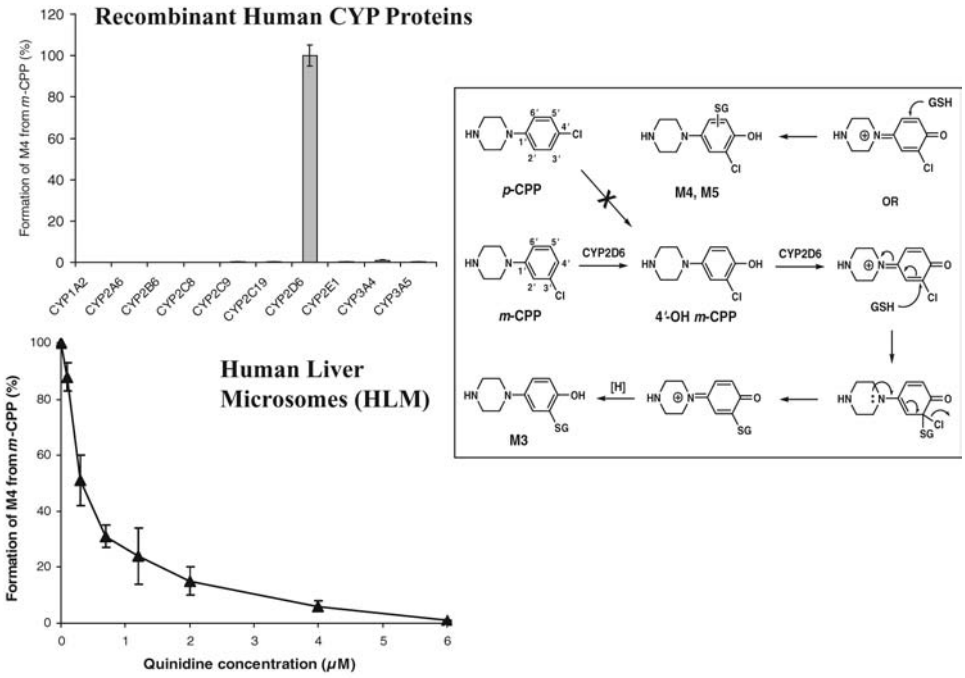

Figure 15 Metabolism of 1 (*m* chlorophenyl)piperazine (*m* CPP), a trazodone metabolite, in the presence of recombinant human cytochromes P450 (CYP). The effect of quinidine (a CYP2D6 inhibitor) on *m* CPP metabolism in human liver microsomes (HLMs) is shown also (201).

CYP3A5 and that bioactivation of *m*-CPP was mediated by CYP2D6. A two-step oxidation mechanism was proposed for the bioactivation of the 3-chlorophenylpiperazine ring of *m*-CPP; direct oxidation at the C-4′ position resulting in 4′-hydroxytrazodone, followed by further oxidation to form a quinone-imine reactive metabolite (Fig. 15). Trapping of the imine with GSH results in the formation of M4/M5 and M3. Incubations of *p*-CPP (regioisomer of *m*-CPP) with HLM and recombinant CYP2D6 did not lead to formation of M3, M4, and M5. Therefore, formation of M3, M4, and M5 may occur via a common reactive quinone imine intermediate involving two-electron oxidations (Fig. 15). CYP2D6 is polymorphically expressed and the significance of CYP2D6-dependent *m*-CPP metabolism requires further investigation.

CYP3A and CYP2C8-Catalyzed Formation of Troglitazone GSH Adduct as Example. Troglitazone (TGZ) was the first of the thiazolidinedione (TZD) class of drugs to be approved for the treatment of type II diabetes mellitus. However, an increased incidence of liver enzyme elevations was reported in 1% to 2% of patients receiving TGZ. Liver failure was documented in some cases (202). Multiple hypotheses have been proposed, including the formation of reactive metabolites (203). Therefore, various groups have attempted to elucidate the structures of TGZ reactive metabolites and the chemical mechanisms involved in their formation (204 209). For example, a major GSH adduct of TGZ (glutathionyl addition at the C-5 position of TZD ring) and several minor GSH adducts have been observed in HLM incubates and rat bile (207,209).

With the aid of a panel of human CYP proteins, Gan et al. (210) were able to assess which CYP(s) were involved in TGZ GSH adduct formation. The authors employed dansyl GSH (dGSH) as a trapping agent, which afforded the use of liquid chromatography

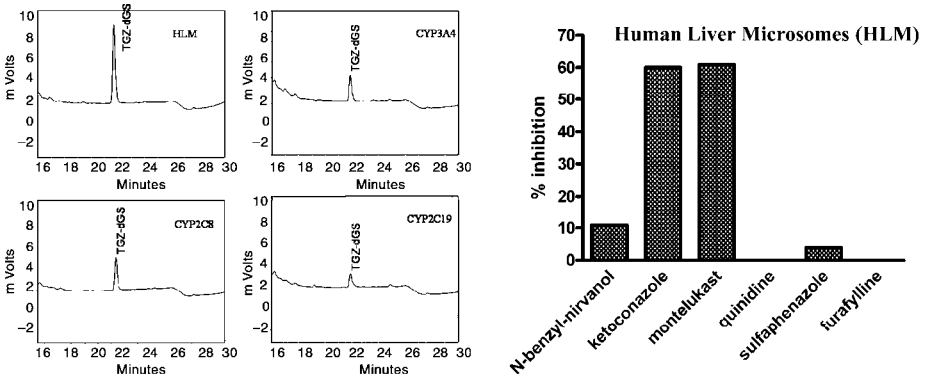

CYP	Turnover (min^{-1})	Mean CYP content in HLM (nmol CYP/mg protein)	NR (pmol/min/mg protein)	% TNR
3A4	1.1	0.108	0.119	49
2E1	0.0	0.049	0.00	0
2D6	0.1	0.01	0.00	0
2C19	0.6	0.019	0.01	5
1A2	0.1	0.045	0.00	2
2C9	0.1	0.096	0.01	4
2C8	1.4	0.064	0.09	37
2B6	0.2	0.039	0.01	3
		TNR (pmol/min/mg protein)	0.243	

Figure 16 Metabolism of troglitazone (TGZ) to a dansyl GSH adduct (TGZ dGS) in the presence of recombinant human cytochrome P450 proteins (CYP) and human liver microsomes. Human liver microsomes were co incubated with various inhibitors selective for different CYP forms (210). *Abbreviations*: NR, normalized rate; TNR, total normalized rate.

with fluorescence detection and circumvented the need for radiolabeled material and elaborate mass spectrometric determinations. As shown in Figure 16, a number of recombinant human CYPs were able to generate the TGZ-dansyl GSH (TGZ-dGS) adduct. In fact, it was possible to easily measure the rate of TGZ-dGS formation in each case, abundance normalize the data, and assess the contribution of each CYP. It was predicted that CYP3A4 (CYP3A5, data not shown) and CYP2C8 would play a major role in TGZ-dGS formation in HLM. In agreement, TGZ-dGS formation in HLM was inhibited by ketoconazole (CYP3A inhibitor) and montelukast (CYP2C8 inhibitor) (Fig. 16). Moreover, the results were consistent with reports of CYP3A4- and CYP2C8-dependent protein covalent binding (207). It is worth noting that CYP3A5 and CYP2C8 are expressed polymorphically, whereas CYP3A4 is the locus of numerous drug-drug interactions, so the levels of TGZ reactive metabolite(s) may be associated with *CYP* genotype and impacted by co-medications (210).

Bioreactors

In a drug discovery setting, medicinal chemists often generate many chemotypes with relatively complex structures and associated chemistries (211 214). Because of the fidelity and flexibility of DMEs, diverse and complex structures can yield equally diverse

and complex metabolites. In some instances, such metabolites are difficult to synthesize and investigators turn to "bioreactors." The goal is to harness the power of DMEs to exquisitely carry out regio-, stereo-, and enantioselective biotransformations and generate sufficient quantities of the desired product (215 218). This is useful because samples of metabolite are needed for structure determination by nuclear magnetic resonance (NMR), pharmacological (target and off target) testing, toxicity testing, and DME induction and inhibition screening (Table 4). Availability of a standard also enables quantitation of the metabolite in bio-fluids of animals and human subjects. This has become important, as regulatory agencies have focused increasingly on human circulating metabolites (9).

The concept of "cell-based" (free enzyme) or "immobilized enzyme based" (IEB) bioreactors is by no means novel, and different strategies have included (a) covalent attachment to solid supports, (b) adsorption on solid supports, (c) entrapment in polymeric gels, and (d) encapsulation (218 221). The potential advantages of IEB technology include ease of handling, facile separation of products from enzyme incubation mixtures, stabilization of the enzyme toward thermal and oxidative degradation, and the opportunity to recover and reuse the enzyme catalyst (218). For instance, immobilized thermolysin and penicillin amidase have been employed in the biosynthesis of aspartame and 6-aminopenicillanic acid, respectively (221, references therein). Whatever the strategy is, computer-controlled systems can permit online monitoring of oxygen tension, pH, temperature, and cofactor concentration within the bioreactor. Moreover, the rate of substrate delivery to the system can be controlled, in order to circumvent the problem of end product or substrate inhibition.

Cell-Based CYP Bioreactors

With the advent of recombinant technology, it is now possible to express human and other drug-metabolizing CYPs (e.g., *Bacillus megaterium*; CYP BM-3) in *E. coli* or insect (e.g., Sf21) cells (215 217). Once prepared, such cells can be used as bioreactors, either as intact cells in suspension (1 to 1000 mL) or as processed (enzyme-enriched) membrane fractions (Table 4). Bioreactors that employ human CYPs afford the generation of metabolites that are formed in vivo, in HLM, and precision-cut human liver slices, etc. On the other hand, it is possible to generate heme domain variants of baterial CYPs, such as CYP BM-3, that utilize H_2O_2 to drive biotransformation. This circumvents the need for costly cofactors such as NADPH (217). Therefore, each format has its advantages and disadvantages. For the purposes of illustration, here also, two examples are discussed in some detail.

Rushmore et al. (215) have utilized Sf21 insect cells (suspension culture) and generated several milligrams of testosterone, diazepam, and diclofenac metabolites. In this instance, SF21 cells (2×10^6 cells/mL; 250-mL spinner flasks) were co-infected with a virus encoding either CYP2C9 or CYP3A4 and a second virus encoding human CYP reductase. After maintaining the suspension cultures under optimum conditions for cell growth (27°C, 90 rpm, 2 days), substrates (100 μM) were added to the bioreactors. The expression of CYP3A4 and CYP2C9 in the bioreactors reached maximal levels at about 30 hours after the addition of tested substrates. Under optimal conditions, conversion of testosterone (12 hours), diazepam (48 hours), and diclofenac (12 18 hours) was 70%, 80%, and 82%, respectively. Likewise, Vail et al. (216) have used suspensions of *E. coli* cells (1 L) that express recombinant human CYP and CYP reductase. The authors were able to generate testosterone (CYP3A4), diclofenac (CYP2C9), and phenacetin (CYP1A2) metabolites (59 mg of 6β-hydroxytestosterone, 110 mg of 4′-hydroxydiclofenac and 88 mg of acetaminophen) with a conversion yield that ranged from 29% to 93% in 48 hours.

Table 4 Bioreactor Systems Expressing Individual Cytochrome P450 Enzymes and Their Applications

Purpose of biosynthesis	Scale of biosynthesis	CYP bioreactor system	Comments
Metabolite structure elucidation by NMR	0.1–50 μg for proton-NMR; up to 100 μg for two-dimensional NMR	Test tube incubations of microsomes from insect cells (or *E. coli*) expressing CYP and CYP reductase	Microsomes are commercially available and the incubations can be easily performed in any laboratory
In vitro testing of metabolite (bioassays, DME inhibition, toxicity, etc.)	1–5 mg for each assay	Incubations of cell membranes from *E. coli* co-expressing CYP and CYP reductase (50-mL scale)	Crude microsomes and cell membranes can be custom-ordered from venders. Optimization of incubation conditions is needed. Biosynthesis can be easily performed in any laboratory
		Suspension cultures of insect cells infected with baculovirus containing CYP and CYP reductase (100-mL scale)	Special facility for the large-scale cultures is needed. The large-scale cultures can be performed by venders or in-house if the preparations of baculovirus are available
Standard for quantitative analysis of metabolite using LC/MS (preclinical and clinical studies)	50–100 mg for assay development and analyses of samples from multiple studies	Suspension cultures of entire cells of *E. coli* expressing CYP and CYP reductase (1-Litre scale)	Special facility for the large-scale cultures is needed. The large-scale cultures can be performed by venders or in-house if preparations of *E. coli* are available
In vivo studies (PK, efficacy, and toxicological evaluation of metabolite)	200–800 mg for each study in animal species	Suspension cultures of *E. coli* overexpressing variants of CYP BM3 heme domain peroxygenase from *Bacillus megaterium* (10-L scale)	Screening of effective variant(s) for a specific compound is needed. Prepared 96-well plates containing variants for pre-screening are commercially available. Large-scale cultures are only performed by a vender

PK, pharmacokinetics; CYP, cytochrome P450; NMR, nuclear magnetic resonance Various CYP-based bioreactors have been described in the literature (215,216)

The Possibility of Using Immobilized Recombinant Human DMEs as Bioreactors

Development of IEB technology is more challenging, although various attempts have been made to immobilize native microsomes and solubilized (or purified) DMEs (222 227). These have included noncovalent immobilization in polymeric gels (e.g., gelatine, alginate; or κ-carrageenan), or covalent coupling onto column or beaded matrices containing cyanogen bromide activated Sepharose 4B or carbonyldi-imidazole-activated Sephadex G-150 (222 227). However, many of these methods in the past have relied on the availability of conventionally purified DMEs, such as rabbit CYP2B4 (P450 LM_2) and CYP reductase (226,228), while concerns about loss of activity after immobilization have also been reported (222,225,228), and it is not known if these bioreactors are robust enough to generate metabolites ($\geq$1 mg) over extended periods (>24 hours).

Advances in IEB technology will require (a) relatively large amounts of purified DMEs, (b) the development of gentle enzyme immobilization procedures, and (c) alternative (inexpensive) sources of reducing equivalents or cofactors. The first of these challenges may be met with currently available high-level heterologous expression systems. For instance, CYP-CYP reductase fusion proteins can be readily purified by affinity chromatography on 2′,5′-ADP Sepharose columns (19). Recombinant technology can also permit engineering of DMEs, to achieve strong noncovalent coupling of enzyme to solid supports using relatively mild conditions (230). For the human CYPs, reducing equivalents could be provided electrochemically, by oxygen surrogates (e.g., cumene hydroperoxide and iodosylbenzene) or by photoactive means (229,231,232). The possibilities are endless, and the development of this technology could be expanded to include the large-scale disposal of hazardous chemicals, the development of continuous-flow biosensors, or extracorporeal shunt systems for drug detoxification (218,226,229,233).

Miscellaneous

DMEs as Pharmacological Targets

It is now recognized that some human DMEs are expressed in numerous tissues and metabolize endogenous compounds (endobiotics). For example, members of the human CYP2C subfamily (e.g., CYP2C8 and CYP2C9) and CYP2J2 are expressed in the vasculature and metabolize arachidonic acid to various epoxyeicosatrienoic acids that may play a role in cardiovascular physiology and pathophysiology (234,235). In the future, therefore, it is possible that such enzymes will themselves be viewed as pharmacological targets. This would require access to sufficient quantities of the appropriate recombinant DME for (inhibition) screening, building of SARs, and support of crystal structure based active site modeling (235).

In some cases, organs like the liver are targeted for efficacy (e.g., treatment of metabolic diseases or viral infections), and "bioactivation" describes the DME-dependent activation of a non-active precursor (prodrug) to a pharmacologically active product (236,237). It is envisioned that the prodrug diffuses into the hepatocyte and undergoes DME-catalyzed metabolism to the desired product (237). Presumably, if the bioactivating enzyme is CYP3A4, then one would need ready access to the recombinant protein for screening purposes. Similarly, the observation that enzymes such as CYP1B1 are overexpressed in cancer cells raises the possibility that compound libraries could be screened for selective CYP-catalyzed bioactivation (e.g., heterologously expressed CYP1B1 vs. other human CYPs) with the goal of finding suitable chemotherapeutic agents (238).

Assessment of Species Differences in Metabolism

Pharmacokinetic, ADME, and toxicological testing of NCEs in various animal species is commonplace. In fact, such data are used to predict pharmacokinetics, dose, and set safety margins prior to human dosing (9,10,239). Despite their prominent role in drug testing, however, relatively little is known of the specific DMEs in different species. In most cases, the different gene family and subfamily members have been identified, but the actual proteins have not been expressed, characterized, and compared with those of human subjects. Therefore, one can only conduct rudimentary reaction-phenotyping studies with animal tissue preparations and subcellular fractions. More often than not, this means that species differences in vitro cannot be ascribed to a specific DME or combinations of DMEs. Over the years, this has hampered the development of animal models.

The CYP superfamily is perhaps the best studied. For example, various recombinant rat CYPs are commercially available (e.g., CYP1A1, CYP1A2, CYP3A1, CYP3A2, CYP2C11, CYP2C6, CYP2C12, CYP4A1, CYP2D2) (240). However, there are no commercial sources of recombinant forms of CYPs belonging to other species, such as the mouse, beagle dog and nonhuman primate. As a result, only a few groups have attempted to express, characterize, and compare these CYPs with their human counterparts (241 243). Reports of other DMEs, like monkey recombinant UGT2B10 and UGT2B9, dog UGT2B and SULT1A1, and monkey FMO2 are sporadic (244 249). In particular, information related to the DMEs of higher primates like the chimpanzee is almost nonexistent (48,250,251). In the future, it is hoped that recombinant forms of animal DMEs will become increasingly available. This will afford more direct comparisons of NCEs across species (e.g., k_{cat}/K_m ratio, K_i, K_s, k_{inact}/K_I ratio, IC_{50}, $f_{m,CYP}$, etc.), enable the development of animal-based drug interaction models, improve reaction-phenotyping tools, and establish more cross-species "DME-based" scaling approaches (252).

Interplay of DMEs with Drug Transporters

Many DME substrates and their metabolites (e.g., glucuronide and sulfate conjugates) are fluxed into and out of various cells by transporters. This has forced most investigators to view drug metabolism and transport more holistically (17,18,253,254). Therefore, it will become increasingly necessary to heterologously co-express various DMEs and transporters in different cell types and monitor drug uptake, metabolism, and efflux in a more integrated manner. For example, Liu et al. (255) have already described the "vectoral" transport of enalapril in Madin-Darby canine kidney (MDCK) II cells double-transfected with an uptake (organic anion-transporting polypeptide 1B1, OATP1B1) and efflux (multidrug resistance associated protein 2, MRP2) transporter. Similarly, Matsushima et al. (256) have evaluated vectoral transport of organic anions, such as estradiol 17-*O*-glucuronide, estrone 3-*O*-sulfate, pravastatin, and cerivastatin, employing double-transfected MDCKII cells expressing OATP1B1 with MDR1 (multidrug resistance 1) or OATP1B1 with BCRP (breast cancer resistance protein). It is only a matter of time before phases I and II enzymes are also expressed in such cell systems.

CONCLUSIONS

Advancements in recombinant gene technology have greatly increased our understanding of the complex DME systems present in human tissues (e.g., FMO, CYP, UGT, and SULT). One can now heterologously express many of these DMEs in various "non human" cell types so that minor (low abundance) enzymes can also be expressed at high

levels. If needed, the protein in question can be purified to electrophoretic homogeneity using relatively simplified procedures. Moreover, it is now recognized that strategies employing methods for investigating the metabolism and toxicity of drugs in vitro can play an important role in the discovery and development of NCEs, especially if the different models are used in an integrated fashion (1 5). Therefore, heterologously expressed human DMEs have become firmly established as reagents and have greatly facilitated the study of polymorphic biotransformations and reaction phenotyping, supported the generation of inhibition (e.g., IC_{50}, K_i, k_{inact}, K_I) and kinetic (e.g., K_m, V_{max}, k_{cat}/K_m) parameters, and enabled toxicity testing. Other applications have included the preparation of antibodies for DME immuno-inhibition and immuno-quantitation, preparation of protein crystals for X-ray crystallography, and the development of bioreactors for metabolite generation and testing (Table 5).

Table 5 Applications of Heterologously Expressed (Recombinant) and Purified Human Drug Metabolizing Enzymes: Summary

Application(s)	Comment(s)	References
Enzyme/isoform selective biotransformations	• Confirm involvement of particular DME (e.g., FMO vs. CYP) • Reaction phenotyping: distinguish between members of *different* gene families or subfamilies • Differentiate between members of the *same* gene subfamily • Compare kinetics of wild type vs. allele variant DME • Confirm selectivity of probe substrate	27, 28, 48, 66, 67, 71, 72, 79, 82, 86 88, 92 94, 100
Enzyme kinetics	• Confirm kinetic *profile* (vs. native human tissue); Michaelis Menten (monophasic, biphasic), sigmoid, substrate or product inhibition, and activation • Confirm apparent kinetic *parameters* obtained with native human tissue	118 133
Stereo , regio , and enantioselective biotransformations	• Confirm biotransformation in the absence of confounding reductases (*N* oxide, sulfoxide, and epoxide) or sulfatases and glucuronidases	32, 36, 42, 75, 89, 93, 134, 138 146
Inhibition studies	• High throughput DME inhibition screening • Confirmation of inhibition parameters obtained with native human tissue • Confirm selectivity of inhibitors (antibody or chemical)	149 167
Structure based studies	• Purified DME used to generate crystals for X ray crystallography studies • Confirm impact of site directed mutagenesis on catalytic activity • Spectroscopy (UV/visible): binding spectra and complex formation • Protein protein interactions	24 26, 62, 103 112

Table 5 Applications of Heterologously Expressed (Recombinant) and Purified Human Drug Metabolizing Enzymes: Summary (*Continued*)

Application(s)	Comment(s)	References
Toxicity testing	• Cell based testing: genotoxicity, cytotoxicity, and mutagenicity. • Genotoxicity testing: recombinant DME as activation system incubated with reporter strain of bacteria • Reporter bacteria engineered to express DME • Evaluation of reactive metabolite formation (kinetics, reaction phenotyping) • Adduct isolation and structure determination	174 191, 194, 195, 201, 210
Bioreactors (metabolite generation)	• Transgenic cells (insect or *E. coli*) expressing recombinant DME • Immobilized (purified) DME	215, 216
Antibody production	• DME as source of antigen for the production of monoclonal and polyclonal antibodies: quantitation, inhibition, precipitation, immunohistochemical assays	21 23, 56 61
Immunoassay	• Recombinant DME as a standard for immunoquantitation of protein in native human tissue	21 24, 56 63, 76
Comparison of DMEs across species	• Characterization of individual DME (kinetics, structure, etc.) • Comparison of substrate selectivity, inhibitor selectivity, kinetics (k_{cat} and K_m), enantio , regio , and stereoselectivity, etc. (e.g., CYPs, UGTs, SULTs, and FMOs)	240 249
DME as possible therapeutic target or DME enabled drug targeting	• Development of DME inhibitors because of "endobiotic" metabolism (e.g., arachidonic acid metabolism by CYP2Cs and CYP2J2) • Targeted drug delivery (e.g., CYP3A4 dependent metabolism in liver; CYP1B1 dependent metabolism in tumor cells, etc.)	234 238

DME, drug metabolizing enzyme; FMO, flavin containing monooxygenase; CYP, cytochrome P450.

Although considerable progress has been made with the human CYPs, the "tool kit" for other DMEs (e.g., SULTs, UGTs, FMOs, etc.) will need to be developed further. This should enable more complete reaction-phenotyping, drug interaction predictions, and prospective assessment of polymorphic metabolism. At the same time, it is very likely that newer technologies, models and reagents will come online also. For example, the number of citations describing studies with transgenic (humanized) mice, chimeric mice (humanized liver), new cell lines and culture formats, and formulations containing RNAi

(interfering ribonucleic acid) is increasing steadily (257 265). With time, many of these newer tools will be added to the existing repertoire of reagents and models (Figs. 1 and 2). If well-characterized (phenotyped and genotyped) human tissue continues to be available, then the next few years will see further advancements in the area of DME research. Such progress may reach a point when investigators realize the dream of greatly improved in vitro-in vivo correlations, robust drug interaction and pharmacokinetic predictions, fully coupled DME-transporter models, and, for a given NCE, the full integration of data across all of the individual DME systems in humans and animal species.

REFERENCES

1. Lin JH, Lu AY. Role of pharmacokinetics and metabolism in drug discovery and development. Pharmacol Rev 1997; 49(4):403 449.
2. White RE. Short and long term projections about the use of drug metabolism in drug discovery and development. Drug Metab Dispos 1998; 26(12):1213 1216.
3. Eddershaw PJ, Beresford AP, Bayliss MK. ADME/PK as part of a rational approach to drug discovery. Drug Discov Today 2000; 5(9):409 414.
4. Baillie TA. Metabolism and toxicity of drugs. Two decades of progress in industrial drug metabolism. Chem Res Toxicol 2008; 21(1):129 137.
5. Lin JH, Rodrigues AD. In vitro models for early studies of drug metabolism. In: Testa B, van de Waterbeemd H, Folkers G, and Guy R, eds. Pharmacokinetic Optimization in Drug Research: Biological, Physiochemical, and Computational Strategies. New York: Wiley VCH, 2001:217 243.
6. Soars MG, McGinnity DF, Grime K, Riley RJ. The pivotal role of hepatocytes in drug discovery. Chem Biol Interact 2007; 168(1):2 15.
7. Graaf IA, Groothuis GM, Olinga P. Precision cut tissue slices as a tool to predict metabolism of novel drugs. Expert Opin Drug Metab Toxicol 2007; 3(6):879 898.
8. van de Kerkhof EG, de Graaf IA, Groothuis GM. In vitro methods to study intestinal drug metabolism. Curr Drug Metab 2007; 8(7):658 675.
9. Smith DA, Obach RS. Metabolites and safety: what are the concerns, and how should we address them? Chem Res Toxicol 2006; 19(12):1570 1579.
10. Roffey SJ, Obach RS, Gedge JI, Smith DA. What is the objective of the mass balance study? A retrospective analysis of data in animal and human excretion studies employing radiolabeled drugs. Drug Metab Rev 2007; 39(1):17 43.
11. Mackenzie PI, Bock KW, Burchell B, Guillemette C, Ikushiro S, Iyanagi T, Miners JO, Owens IS, Nebert DW. Nomenclature update for the mammalian UDP glycosyltransferase (UGT) gene superfamily. Pharmacogenet Genomics 2005; 15(10):677 685.
12. Nelson DR, Koymans L, Kamataki T, Stegeman JJ, Feyereisen R, Waxman DJ, Waterman MR, Gotoh O, Coon MJ, Estabrook RW, Gunsalus IC, Nebert DW. P450 superfamily: update on new sequences, gene mapping, accession numbers and nomenclature. Pharmacogenetics 1996; 6(1):1 42.
13. Vatsis KP, Weber WW, Bell DA, Dupret JM, Evans DA, Grant DM, Hein DW, Lin HJ, Meyer UA, Relling MV. Nomenclature for *N* acetyltransferases. Pharmacogenetics 1995; 5(1):1 17.
14. Lawton MP, Cashman JR, Cresteil T, Dolphin CT, Elfarra AA, Hines RN, Hodgson E, Kimura T, Ozols J, Phillips IR. A nomenclature for the mammalian flavin containing monooxygenase gene family based on amino acid sequence identities. Arch Biochem Biophys 1994; 308(1): 254 257.
15. Blanchard RL, Freimuth RR, Buck J, Weinshilboum RM, Coughtrie MW. A proposed nomenclature system for the cytosolic sulfotransferase (SULT) superfamily. Pharmacoge netics 2004; 14(3):199 211.
16. Fremont JJ, Wang RW, King CD. Coimmunoprecipitation of UDP glucuronosyltransferase isoforms and cytochrome P450 3A4. Mol Pharmacol 2005; 67(1):260 262.

17. Benet LZ, Cummins CL, Wu CY. Transporter enzyme interactions: implications for predicting drug drug interactions from in vitro data. Curr Drug Metab 2003; 4(5):393 398.
18. Zamek Gliszczynski MJ, Hoffmaster KA, Nezasa K, Tallman MN, Brouwer KL. Integration of hepatic drug transporters and phase II metabolizing enzymes: mechanisms of hepatic excretion of sulfate, glucuronide, and glutathione metabolites. Eur J Pharm Sci 2006; 27(5):447 486.
19. Shet MS, Fisher CW, Holmans PL, Estabrook RW. Human cytochrome P450 3A4: enzymatic properties of a purified recombinant fusion protein containing NADPH P450 reductase. Proc Natl Acad Sci U S A 1993; 90(24):11748 11752.
20. Gillam EM, Guo Z, Martin MV, Jenkins CM, Guengerich FP. Expression of cytochrome P450 2D6 in *Escherichia coli*, purification, and spectral and catalytic characterization. Arch Biochem Biophys 1995; 319(2):540 550.
21. Krausz KW, Goldfarb I, Buters JT, Yang TJ, Gonzalez FJ, Gelboin HV. Monoclonal antibodies specific and inhibitory to human cytochromes P450 2C8, 2C9, and 2C19. Drug Metab Dispos 2001; 29(11):1410 1423.
22. Fujita K, Nagata K, Yamazaki T, Watanabe E, Shimada M, Yamazoe Y. Enzymatic characterization of human cytosolic sulfotransferases; identification of ST1B2 as a thyroid hormone sulfotransferase. Biol Pharm Bull 1999; 22(5):446 452.
23. Shimada T, Yamazaki H, Mimura M, Inui Y, Guengerich FP. Interindividual variations in human liver cytochrome P 450 enzymes involved in the oxidation of drugs, carcinogens and toxic chemicals: studies with liver microsomes of 30 Japanese and 30 Caucasians. J Pharmacol Exp Ther 1994; 270(1):414 423.
24. Pedersen LC, Petrotchenko EV, Negishi M. Crystal structure of SULT2A3, human hydroxysteroid sulfotransferase. FEBS Lett 2000; 475(1):61 64.
25. Miley MJ, Zielinska AK, Keenan JE, Bratton SM, Radominska Pandya A, Redinbo MR. Crystal structure of the cofactor binding domain of the human phase II drug metabolism enzyme UDP glucuronosyltransferase 2B7. J Mol Biol 2007; 369(2):498 511.
26. Williams PA, Cosme J, Vinkovic DM, Ward A, Angove HC, Day PJ, Vonrhein C, Tickle IJ, Jhoti H. Crystal structures of human cytochrome P450 3A4 bound to metyrapone and progesterone. Science 2004; 305(5684):683 686.
27. Rodrigues AD. Integrated cytochrome P450 reaction phenotyping: attempting to bridge the gap between cDNA expressed cytochromes P450 and native human liver microsomes. Biochem Pharmacol 1999; 57(5):465 480.
28. Zhang H, Davis CD, Sinz MW, Rodrigues AD. Cytochrome P450 reaction phenotyping: an industrial perspective. Expert Opin Drug Metab Toxicol 2007; 3(5):667 687.
29. Fischer V, Vogels B, Maurer G, Tynes RE. The antipsychotic clozapine is metabolized by the polymorphic human microsomal and recombinant cytochrome P450 2D6. J Pharmacol Exp Ther 1992; 260(3):1355 1360.
30. Dahl ML, Llerena A, Bondesson U, Lindström L, Bertilsson L. Disposition of clozapine in man: lack of association with debrisoquine and *S* mephenytoin hydroxylation polymorphisms. Br J Clin Pharmacol 1994; 37(1):71 74.
31. Flammang AM, Gelboin HV, Aoyama T, Gonzalez FJ, McCoy, GD. Nicotine metabolism by cDNA expressed human cytochrome P450s. Biochem Arch 1992; 8:1 8.
32. Cashman JR, Park SB, Yang ZC, Wrighton SA, Jacob P 3rd, Benowitz NL. Metabolism of nicotine by human liver microsomes: stereoselective formation of *trans* nicotine *N′* oxide. Chem Res Toxicol 1992; 5(5):639 646.
33. McCracken NW, Cholerton S, Idle JR. Cotinine formation by cDNA expressed human cytochromes P450. Med Sci Res 1992; 20:877 878.
34. Berkman CE, Park SB, Wrighton SA, Cashman JR. In vitro in vivo correlations of human (*S*) nicotine metabolism. Biochem Pharmacol 1995; 50(4):565 570.
35. Rodrigues AD. Impact of *CYP2C9* genotype on pharmacokinetics: are all cyclooxygenase inhibitors the same? Drug Metab Dispos 2005; 33(11):1567 1575.
36. Lomri N, Yang Z, Cashman JR. Regio and stereoselective oxygenations by adult human liver flavin containing monooxygenase 3. Comparison with forms 1 and 2. Chem Res Toxicol 1993; 6(6):800 807.

37. Yanni SB, Annaert PP, Augustijns P, Bridges A, Gao Y, Benjamin DK Jr, Thakker DR. Role of Flavin containing monooxygenase in oxidative metabolism of voriconazole by human liver microsomes. Drug Metab Dispos 2008; 36(6):1119 1125.
38. Douch PG, Buchanan LL. Some properties of the sulphoxidases and sulphoxide reductases of the cestode *Moniezia expansa*, the nematode *Ascaris suum* and mouse liver. Xenobiotica 1979; 9(11):675 679.
39. Tatsumi K, Kitamura S, Yamada H. Sulfoxide reductase activity of liver aldehyde oxidase. Biochim Biophys Acta 1983; 747(1 2):86 92.
40. Kitamura S, Tatsumi K. Reduction of tertiary amine *N* oxides by liver preparations: function of aldehyde oxidase as a major *N* oxide reductase. Biochem Biophys Res Commun 1984; 121(3):749 754.
41. Hirao Y, Kitamura S, Tatsumi K. Epoxide reductase activity of mammalian liver cytosols and aldehyde oxidase. Carcinogenesis 1994; 15(4):739 743.
42. Zhang H, Cui D, Wang B, Han YH, Balimane P, Yang Z, Sinz M, Rodrigues AD. Pharmacokinetic drug interactions involving 17α ethinylestradiol: a new look at an old drug. Clin Pharmacokinet 2007; 46(2):133 157.
43. Rogers SM, Back DJ, Orme ML. Intestinal metabolism of ethinyloestradiol and paracetamol in vitro: studies using Ussing chambers. Br J Clin Pharmacol 1987; 23(6):727 734.
44. Li AP, Hartman NR, Lu C, Collins JM, Strong JM. Effects of cytochrome P450 inducers on 17α ethinyloestradiol (EE_2) conjugation by primary human hepatocytes. Br J Clin Pharmacol 1999; 48(5):733 742.
45. Back DJ, Bates M, Breckenridge AM, Ellis A, Hall JM, Maciver M, Orme ML, Rowe PH. The in vitro metabolism of ethinyloestradiol, mestranol and levonorgestrel by human jejunal mucosa. Br J Clin Pharmacol 1981; 11(3):275 278.
46. Shiraga T, Niwa T, Ohno Y, Kagayama A. Interindividual variability in 2 hydroxylation, 3 sulfation, and 3 glucuronidation of ethynylestradiol in human liver. Biol Pharm Bull 2004; 27 (12):1900 1906.
47. Schrag ML, Cui D, Rushmore TH, Shou M, Ma B, Rodrigues AD. Sulfotransferase 1E1 is a low K_m isoform mediating the 3 *O* sulfation of ethinyl estradiol. Drug Metab Dispos 2004; 32 (11):1299 1303.
48. Rodrigues AD, Kukulka MJ, Ferrero JL, Cashman JR. In vitro hepatic metabolism of ABT 418 in chimpanzee (*Pan troglodytes*). A unique pattern of microsomal flavin containing monooxygenase dependent stereoselective *N*′ oxidation. Drug Metab Dispos 1995; 23(10): 1143 1152.
49. Rodrigues AD, Ferrero JL, Amann MT, Rotert GA, Cepa SP, Surber BW, Machinist JM, Tich NR, Sullivan JP, Garvey DS. The in vitro hepatic metabolism of ABT 418, a cholinergic channel activator, in rats, dogs, cynomolgus monkeys, and humans. Drug Metab Dispos 1994; 22(5):788 798.
50. Zhang D, Zhang H, Aranibar N, Hanson R, Huang Y, Cheng PT, Wu S, Bonacorsi S, Zhu M, Swaminathan A, Humphreys WG. Structural elucidation of human oxidative metabolites of muraglitazar: use of microbial bioreactors in the biosynthesis of metabolite standards. Drug Metab Dispos, 2006; 34(2):267 280.
51. Wang L, Zhang D, Swaminathan A, Xue Y, Cheng PT, Wu S, Mosqueda Garcia R, Aurang C, Everett DW, Humphreys WG. Glucuronidation as a major metabolic clearance pathway of 14C labeled muraglitazar in humans: metabolic profiles in subjects with or without bile collection. Drug Metab Dispos 2006; 34(3):427 439.
52. Zhang D, Wang L, Chandrasena G, Ma L, Zhu M, Zhang H, Davis CD, Humphreys WG. Involvement of multiple cytochrome P450 and UDP glucuronosyltransferase enzymes in the in vitro metabolism of muraglitazar. Drug Metab Dispos 2007; 35(1):139 149.
53. Christopher LJ, Cui D, Li W, Barros A Jr, Arora VK, Zhang H, Wang L, Zhang D, Manning JA, He K, Fletcher AM, Ogan M, Lago M, Bonacorsi SJ, Humphreys WG, Iyer RA. Biotransformation of [^{14}C]dasatinib: In vitro studies in rat, monkey and human and disposition after administration to rats and monkeys. Drug Metab Dispos 2008; 36(7):1341 1356.

54. Christopher LJ, Cui D, Wu C, Luo R, Manning JA, Bonacorsi SJ, Lago M, Allentoff A, Lee FY, McCann B, Galbraith S, Reitberg DP, He K, Barros A Jr, Blackwood Chirchir A, Humphreys WG, Iyer RA. Metabolism and disposition of dasatinib after oral administration to humans. Drug Metab Dispos 2008; 36(7):1357 1364.
55. Wang L, Christopher LJ, Cui D, Li W, Iyer R, Humphreys WG, Zhang D. Identification of the human enzymes involved in the oxidative metabolism of dasatinib: an effective approach for determining metabolite formation kinetics. Drug Metab Dispos 2008; 36(9):1828 1839.
56. Venkatakrishnan K, von Moltke LL, Court MH, Harmatz JS, Crespi CL, Greenblatt DJ. Comparison between cytochrome P450 (CYP) content and relative activity approaches to scaling from cDNA expressed CYPs to human liver microsomes: ratios of accessory proteins as sources of discrepancies between the approaches. Drug Metab Dispos 2000; 28(12):1493 1504.
57. McManus ME, Hall PD, Stupans I, Brennan J, Burgess W, Robson R, Birkett DJ. Immunohistochemical localization and quantitation of NADPH cytochrome P 450 reductase in human liver. Mol Pharmacol 1987; 32(1):189 194.
58. Overby LH, Carver GC, Philpot RM. Quantitation and kinetic properties of hepatic microsomal and recombinant flavin containing monooxygenases 3 and 5 from humans. Chem Biol Interact 1997; 106(1):29 45.
59. Yeung CK, Lang DH, Thummel KE, Rettie AE. Immunoquantitation of FMO1 in human liver, kidney, and intestine. Drug Metab Dispos 2000; 28(9):1107 1111.
60. Läpple F, von Richter O, Fromm MF, Richter T, Thon KP, Wisser H, Griese EU, Eichelbaum M, Kivistö KT. Differential expression and function of CYP2C isoforms in human intestine and liver. Pharmacogenetics 2003; 13(9):565 575.
61. Teubner W, Meinl W, Florian S, Kretzschmar M, Glatt H. Identification and localization of soluble sulfotransferases in the human gastrointestinal tract. Biochem J 2007; 404(2):207 215.
62. Dajani R, Cleasby A, Neu M, Wonacott AJ, Jhoti H, Hood AM, Modi S, Hersey A, Taskinen J, Cooke RM, Manchee GR, Coughtrie MW. X ray crystal structure of human dopamine sulfotransferase, SULT1A3. Molecular modeling and quantitative structure activity relation ship analysis demonstrate a molecular basis for sulfotransferase substrate specificity. J Biol Chem 1999; 274(53):37862 37868.
63. Barker EV, Hume R, Hallas A, Coughtrie WH. Dehydroepiandrosterone sulfotransferase in the developing human fetus: quantitative biochemical and immunological characterization of the hepatic, renal, and adrenal enzymes. Endocrinology 1994; 134(2):982 989.
64. Alterman MA, Kornilayev B, Duzhak T, Yakovlev D. Quantitative analysis of cytochrome P450 isozymes by means of unique isozyme specific tryptic peptides: a proteomic approach. Drug Metab Dispos 2005; 33(9):1399 1407.
65. Proctor NJ, Tucker GT, Rostami Hodjegan A. Predicting drug clearance from recombinantly expressed CYPs: intersystem extrapolation factors. Xenobiotica 2004; 34(2):151 178.
66. Rodrigues AD, Rushmore TH. Cytochrome P450 pharmacogenetics in drug development: in vitro studies and clinical consequences. Curr Drug Metab 2002; 3(3):289 309.
67. Ogilvie BW, Usuki E, Yerino P, Parkinson A. In vitro approaches for studying the inhibition of drug metabolizing enzymes and identifying the drug metabolizing enzymes responsible for the metabolism of drugs (reaction phenotyping) with emphasis on cytochrome P450. In: Rodrigues AD, ed. Drug Drug Interactions, 2nd ed. New York: Informa Healthcare, 2008:231 358.
68. Remmel RP, Zhou J, Argikar UA. UDP glucuronosyltransferases. In: Rodrigues AD, ed. Drug Drug Interactions, 2nd ed. New York: Informa Healthcare, 2008:87 133.
69. Clarke DJ, Burchell B. The uridine diphosphate glucuronosyltransferase multigene family: function and regulation in conjugation deconjugation reactions. In: Kauffman FC, ed. Drug Metabolism and Toxicity. New York: Springer Verlag, 1994:3 43.
70. Radominska Pandya A, Czernik PJ, Little JM, Little JM, Battaglia E, Mackenzie PI. Structural and functional studies of UDP glucuronosyltransferases. Drug Metab Rev 1999; 31(4):817 899.
71. Katoh M, Matsui T, Yokoi T. Glucuronidation of antiallergic drug, Tranilast: identification of human UDP glucuronosyltransferase isoforms and effect of its phase I metabolite. Drug Metab Dispos 2007; 35(4):583 589.

72. Mano Y, Usui T, Kamimura H. The UDP glucuronosyltransferase 2B7 isozyme is responsible for gemfibrozil glucuronidation in the human liver. Drug Metab Dispos 2007; 35(11):2040 2044.
73. Blanchard RL. Nomenclature and molecular biology of the human sulfotransferase family. In: Pacifici GM, Coughtrie MWH, eds. Human Cytosolic Sulfotransferases. Boca Raton: CRC Press, 2005:1 25.
74. Riches Z, Bloomer JC, Coughtrie MW. Comparison of 2 aminophenol and 4 nitrophenol as in vitro probe substrates for the major human hepatic sulfotransferase, SULT1A1, demonstrates improved selectivity with 2 aminophenol. Biochem Pharmacol 2007; 74(2): 352 358.
75. Miksits M, Maier Salamon A, Aust S, Thalhammer T, Reznicek G, Kunert O, Haslinger E, Szekeres T, Jaeger W. Sulfation of resveratrol in human liver: evidence of a major role for the sulfotransferases SULT1A1 and SULT1E1. Xenobiotica 2005; 35(12):1101 1119.
76. Honma W, Shimada M, Sasano H, Ozawa S, Miyata M, Nagata K, Ikeda T, Yamazoe Y. Phenol sulfotransferase, ST1A3, as the main enzyme catalyzing sulfation of troglitazone in human liver. Drug Metab Dispos 2002; 30(8):944 949.
77. Falany JL, Pilloff DE, Leyh TS, Falany CN. Sulfation of raloxifene and 4 hydroxytamoxifen by human cytosolic sulfotransferases. Drug Metab Dispos 2006; 34(3):361 368.
78. Thomas NL, Coughtrie MW. Sulfation of apomorphine by human sulfotransferases: evidence of a major role for the polymorphic phenol sulfotransferase, SULT1A1. Xenobiotica 2003; 33(11):1139 1148.
79. Gardiner SJ, Begg EJ. Pharmacogenetics, drug metabolizing enzymes, and clinical practice. Pharmacol Rev 2006; 58(3):521 590.
80. Suh JW, Koo BK, Zhang SY, Park KW, Cho JY, Jang IJ, Lee DS, Sohn DW, Lee MM, Kim HS. Increased risk of atherothrombotic events associated with cytochrome P450 3A5 polymorphism in patients taking clopidogrel. CMAJ 2006; 174(12):1715 1722.
81. Melkersson KI, Scordo MG, Gunes A. Impact of CYP1A2 and CYP2D6 polymorphisms on drug metabolism and on insulin and lipid elevations and insulin resistance in clozapine treated patients. J Clin Psychiatry 2007; 68(5):697 704.
82. Lasker JM, Wester MR, Aramsombatdee E, Raucy JL. Characterization of CYP2C19 and CYP2C9 from human liver: respective roles in microsomal tolbutamide, *S* mephenytoin, and omeprazole hydroxylations. Arch Biochem Biophys 1998; 353(1):16 28.
83. Wang RW, Newton DJ, Liu NY, Shou M, Rushmore T, Lu AY. Inhibitory anti CYP3A4 peptide antibody: mapping of inhibitory epitope and specificity toward other CYP3A isoforms. Drug Metab Dispos 1999; 27(2):167 172.
84. Khan KK, He YQ, Correia MA, Halpert JR. Differential oxidation of mifepristone by cytochromes P450 3A4 and 3A5: selective inactivation of P450 3A4. Drug Metab Dispos 2002; 30(9):985 990.
85. Huang W, Lin YS, McConn DJ 2nd, Calamia JC, Totah RA, Isoherranen N, Glodowski M, Thummel KE. Evidence of significant contribution from CYP3A5 to hepatic drug metabolism. Drug Metab Dispos 2004; 32(12):1434 1445.
86. Goldstein JA, Faletto MB, Romkes Sparks M, Sullivan T, Kitareewan S, Raucy JL, Lasker JM, Ghanayem BI. Evidence that CYP2C19 is the major (*S*) mephenytoin 4′ hydroxylase in humans. Biochemistry 1994; 33(7):1743 1752.
87. Rahman A, Korzekwa KR, Grogan J, Gonzalez FJ, Harris JW. Selective biotransformation of taxol to 6α hydroxytaxol by human cytochrome P450 2C8. Cancer Res 1994; 54(21): 5543 5546.
88. Hall SD, Hamman MA, Rettie AE, Wienkers LC, Trager WF, Vandenbranden M, Wrighton SA. Relationships between the levels of cytochrome P4502C9 and its prototypic catalytic activities in human liver microsomes. Drug Metab Dispos 1994; 22(6):975 978.
89. Hamman MA, Thompson GA, Hall SD. Regioselective and stereoselective metabolism of ibuprofen by human cytochrome P450 2C. Biochem Pharmacol 1997; 54(1):33 41.
90. Ritter JK, Chen F, Sheen YY, Tran HM, Kimura S, Yeatman MT, Owens IS. A novel complex locus UGT1 encodes human bilirubin, phenol, and other UDP glucuronosyltransferase isozymes with identical carboxyl termini. J Biol Chem 1992; 267(5):3257 3261.

91. Owens IS, Ritter JK. Gene structure at the human UGT1 locus creates diversity in isozyme structure, substrate specificity, and regulation. Prog Nucleic Acid Res Mol Biol 1995; 51:305 338.
92. Uchaipichat V, Mackenzie PI, Elliot DJ, Miners JO. Selectivity of substrate (trifluoperazine) and inhibitor (amitriptyline, androsterone, canrenoic acid, hecogenin, phenylbutazone, quinidine, quinine, and sulfinpyrazone) "probes" for human UDP glucuronosyltransferases. Drug Metab Dispos 2006; 34(3):449 456.
93. Court MH. Isoform selective probe substrates for in vitro studies of human UDP glucuronosyltransferases. Methods Enzymol 2005; 400:104 116.
94. Krishnaswamy S, Hao Q, Von Moltke LL, Greenblatt DJ, Court MH. Evaluation of 5 hydroxytryptophol and other endogenous serotonin (5 hydroxytryptamine) analogs as substrates for UDP glucuronosyltransferase 1A6. Drug Metab Dispos 2004; 32(8):862 869.
95. Ingelman Sunberg M, Johansson I. The molecular genetics of the human drug metabolizing cytochrome P450s. In: Pacifici GM, Fracchia GN, eds. Advances in Drug Metabolism in Man. Brussels: European Commission, 1995:545 585.
96. Gonzalez FJ, Idle JR. Pharmacogenetic phenotyping and genotyping. Present status and future potential. Clin Pharmacokinet 1994; 26(1):59 70.
97. Guillemette C. Pharmacogenomics of human UDP glucuronosyltransferase enzymes. Pharmacogenomics J 2003; 3(3):136 158.
98. Nowell S, Falany CN. Pharmacogenetics of human cytosolic sulfotransferases. Oncogene. 2006; 25(11):1673 1678.
99. Koukouritaki SB, Hines RN. Flavin containing monooxygenase genetic polymorphism: impact on chemical metabolism and drug development. Pharmacogenomics 2005; 6(8):807 822.
100. Tang C, Shou M, Rushmore TH, Mei Q, Sandhu P, Woolf EJ, Rose MJ, Gelmann A, Greenberg HE, De Lepeleire I, Van Hecken A, De Schepper PJ, Ebel DL, Schwartz JI, Rodrigues AD. In vitro metabolism of celecoxib, a cyclooxygenase 2 inhibitor, by allelic variant forms of human liver microsomal cytochrome P450 2C9: correlation with *CYP2C9* genotype and in vivo pharmacokinetics. Pharmacogenetics 2001; 11(3):223 235.
101. Tang C, Shou M, Mei Q, Rushmore TH, Rodrigues AD. Major role of human liver microsomal cytochrome P450 2C9 (CYP2C9) in the oxidative metabolism of celecoxib, a novel cyclooxygenase II inhibitor. J Pharmacol Exp Ther 2000; 293(2):453 459.
102. Rodrigues AD, Yang Z, Chen C, Pray D, Kim S, Sinz M. Is celecoxib an inducer of cytochrome P450 3A4 in subjects carrying the *CYP2C9*3* allele? Clin Pharmacol Ther 2006; 80(3):298 301.
103. Feenstra KA, de Graaf C, Vermeulen NPE. Cytochrome P450 protein modeling and ligand docking. In: Rodrigues AD, ed. Drug Drug Interactions 2nd ed. New York: Informa Healthcare, 2008:435 470.
104. Davies C, Witham K, Scott JR, Pearson A, DeVoss JJ, Graham SE, Gillam EM. Assessment of arginine 97 and lysine 72 as determinants of substrate specificity in cytochrome P450 2C9 (CYP2C9). Drug Metab Dispos 2004; 32(4):431 436.
105. Melet A, Assrir N, Jean P, Pilar Lopez Garcia M, Marques Soares C, Jaouen M, Dansette PM, Sari MA, Mansuy D. Substrate selectivity of human cytochrome P450 2C9: importance of residues 476, 365, and 114 in recognition of diclofenac and sulfaphenazole and in mechanism based inactivation by tienilic acid. Arch Biochem Biophys 2003; 409(1):80 91.
106. Sansen S, Hsu MH, Stout CD, Johnson EF. Structural insight into the altered substrate specificity of human cytochrome P450 2A6 mutants. Arch Biochem Biophys 2007; 464(2): 197 206.
107. Wen B, Lampe JN, Roberts AG, Atkins WM, David Rodrigues A, Nelson SD. Cysteine 98 in CYP3A4 contributes to conformational integrity required for P450 interaction with CYP reductase. Arch Biochem Biophys 2006; 454(1):42 54.
108. Gao Q, Doneanu CE, Shaffer SA, Adman ET, Goodlett DR, Nelson SD. Identification of the interactions between cytochrome P450 2E1 and cytochrome b5 by mass spectrometry and site directed mutagenesis. J Biol Chem 2006; 281(29):20404 20417.
109. Yamaguchi Y, Khan KK, He YA, He YQ, Halpert JR. Topological changes in the CYP3A4 active site probed with phenyldiazene: effect of interaction with NADPH cytochrome P450

reductase and cytochrome b5 and of site directed mutagenesis. Drug Metab Dispos 2004; 32(1): 155 161.
110. Dajani R, Hood AM, Coughtrie MW. A single amino acid, glu146, governs the substrate specificity of a human dopamine sulfotransferase, SULT1A3. Mol Pharmacol 1998; 54(6): 942 948.
111. Barre L, Fournel Gigleux S, Finel M, Netter P, Magdalou J, Ouzzine M. Substrate specificity of the human UDP glucuronosyltransferase UGT2B4 and UGT2B7. Identification of a critical aromatic amino acid residue at position 33. FEBS J 2007; 274(5):1256 1264.
112. Adali O, Carver GC, Philpot RM. The effect of arginine 428 mutation on modulation of activity of human liver flavin monooxygenase 3 (FMO3) by imipramine and chlorpromazine. Exp Toxicol Pathol 1999; 51(4 5):271 276.
113. Gleeson MP, Davis AM, Chohan KK, Paine SW, Boyer S, Gavaghan CL, Arnby CH, Kankkonen C, Albertson N. Generation of in silico cytochrome P450 1A2, 2C9, 2C19, 2D6, and 3A4 inhibition QSAR models. J Comput Aided Mol Des 2007; 21(10 11):559 573.
114. Jensen BF, Vind C, Padkjaer SB, Refsgaard HH. In silico prediction of cytochrome P450 2D6 and 3A4 inhibition using Gaussian kernel weighted k nearest neighbor and extended connectivity fingerprints, including structural fragment analysis of inhibitors versus noninhibitors. J Med Chem 2007; 50(3):501 511.
115. Maréchal JD, Sutcliffe MJ. Insights into drug metabolism from modelling studies of cytochrome P450 drug interactions. Curr Top Med Chem 2006; 6(15):1619 1626.
116. Stoner CL, Gifford E, Stankovic C, Lepsy CS, Brodfuehrer J, Prasad JV, Surendran N. Implementation of an ADME enabling selection and visualization tool for drug discovery. J Pharm Sci 2004; 93(5):1131 1141.
117. Yamashita F, Hashida M. In silico approaches for predicting ADME properties of drugs. Drug Metab Pharmacokinet 2004; 19(5):327 338.
118. Tracy TS, Hummel MA. Modeling kinetic data from in vitro drug metabolism enzyme experiments. Drug Metab Rev 2004; 36(2):231 242.
119. Shou M, Mei Q, Ettore MW Jr, Dai R, Baillie TA, Rushmore TH. Sigmoidal kinetic model for two co operative substrate binding sites in a cytochrome P450 3A4 active site: an example of the metabolism of diazepam and its derivatives. Biochem J 1999; 340(pt 3):845 853.
120. Korzekwa KR, Krishnamachary N, Shou M, Ogai A, Parise RA, Rettie AE, Gonzalez FJ, Tracy TS. Evaluation of atypical cytochrome P450 kinetics with two substrate models: evidence that multiple substrates can simultaneously bind to cytochrome P450 active sites. Biochemistry 1998; 37(12):4137 4147.
121. Ma B, Polsky Fisher SL, Vickers S, Cui D, Rodrigues AD. Cytochrome P450 3A dependent metabolism of a potent and selective gamma aminobutyric acid Aalpha2/3 receptor agonist in vitro: involvement of cytochrome P450 3A5 displaying biphasic kinetics. Drug Metab Dispos 2007; 35(8):1301 1307.
122. Fujiwara R, Nakajima M, Yamanaka H, Katoh M, Yokoi T. Interactions between human UGT1A1, UGT1A4, and UGT1A6 affect their enzymatic activities. Drug Metab Dispos 2007; 35(10):1781 1787.
123. Mano Y, Usui T, Kamimura H. Substrate dependent modulation of UDP glucuronosyltransferase 1A1 (UGT1A1) by propofol in recombinant human UGT1A1 and human liver microsomes. Basic Clin Pharmacol Toxicol 2007; 101(3):211 214.
124. Ohno S, Kawana K, Nakajin S. Contribution of UDP glucuronosyltransferase 1A1 and 1A8 to morphine 6 glucuronidation and its kinetic properties. Drug Metab Dispos 2008; 36(4):688 694.
125. Tsoutsikos P, Miners JO, Stapleton A, Thomas A, Sallustio BC, Knights KM. Evidence that unsaturated fatty acids are potent inhibitors of renal UDP glucuronosyltransferases (UGT): kinetic studies using human kidney cortical microsomes and recombinant UGT1A9 and UGT2B7. Biochem Pharmacol 2004; 67(1):191 199.
126. Iwuchukwu OF, Nagar S. Resveratrol (trans resveratrol, 3,5,4′ trihydroxy *trans* stilbene) glucuronidation exhibits atypical enzyme kinetics in various protein sources. Drug Metab Dispos 2008; 36(2):322 330.

127. Stone AN, Mackenzie PI, Galetin A, Houston JB, Miners JO. Isoform selectivity and kinetics of morphine 3 and 6 glucuronidation by human UDP glucuronosyltransferases: evidence for atypical glucuronidation kinetics by UGT2B7. Drug Metab Dispos 2003; 31(9):1086 1089.
128. Taskinen J, Coughtrie MWH. Structure and function of sulfotransferases. In: Pacifici GM, Coughtrie MWH, eds. Human Cytosolic Sulfotransferases. Boca Raton: CRC Press, 2005:27 42.
129. Gamage N, Barnett A, Hempel N, Duggleby RG, Windmill KF, Martin JL, McManus ME. Human sulfotransferases and their role in chemical metabolism. Toxicol Sci 2006; 90(1):5 22.
130. Lu LY, Hsieh YC, Liu MY, Lin YH, Chen CJ, Yang YS. Identification and characterization of two amino acids critical for the substrate inhibition of human dehydroepiandrosterone sulfotransferase (SULT2A1). Mol Pharmacol 2008; 73(3):660 668.
131. Gamage NU, Tsvetanov S, Duggleby RG, McManus ME, Martin JL. The structure of human SULT1A1 crystallized with estradiol. An insight into active site plasticity and substrate inhibition with multi ring substrates. J Biol Chem 2005; 280(50):41482 41486.
132. Ma B, Shou M, Schrag ML. Solvent effect on cDNA expressed human sulfotransferase (SULT) activities in vitro. Drug Metab Dispos 2003; 31(11):1300 1305.
133. Barnett AC, Tsvetanov S, Gamage N, Martin JL, Duggleby RG, McManus ME. Active site mutations and substrate inhibition in human sulfotransferase 1A1 and 1A3. J Biol Chem 2004; 279(18):18799 18805.
134. Cui D, Booth Genthe CL, Carlini E, Carr B, Schrag ML. Heterotropic modulation of sulfotransferase 2A1 activity by celecoxib: product ratio switching of ethynylestradiol sulfation. Drug Metab Dispos 2004; 32(11):1260 1264.
135. Wang LQ, James MO. Sulfotransferase 2A1 forms estradiol 17 sulfate and celecoxib switches the dominant product from estradiol 3 sulfate to estradiol 17 sulfate. J Steroid Biochem Mol Biol 2005; 96(5):367 374.
136. Gibaldi M. Stereoselective and isozyme selective drug interactions. Chirality 1993; 5(6):407 413.
137. Brocks DR, Jamali F. Stereochemical aspects of pharmacotherapy. Pharmacotherapy 1995; 15(5):551 564.
138. Oguri K, Yamada H, Yoshimura H. Regiochemistry of cytochrome P450 isozymes. Annu Rev Pharmacol Toxicol 1994; 34:251 279.
139. Daikh BE, Lasker JM, Raucy JL, Koop DR. Regio and stereoselective epoxidation of arachidonic acid by human cytochromes P450 2C8 and 2C9. J Pharmacol Exp Ther 1994; 271(3):1427 1433.
140. Mautz DS, Nelson WL, Shen DD. Regioselective and stereoselective oxidation of metoprolol and bufuralol catalyzed by microsomes containing cDNA expressed human P4502D6. Drug Metab Dispos 1995; 23(4):513 517.
141. Sadeque AJ, Eddy AC, Meier GP, Rettie AE. Stereoselective sulfoxidation by human flavin containing monooxygenase. Evidence for catalytic diversity between hepatic, renal, and fetal forms. Drug Metab Dispos 1992; 20(6):832 839.
142. Rettie AE, Lawton MP, Sadeque AJ, Meier GP, Philpot RM. Prochiral sulfoxidation as a probe for multiple forms of the microsomal flavin containing monooxygenase: studies with rabbit FMO1, FMO2, FMO3, and FMO5 expressed in *Escherichia coli*. Arch Biochem Biophys 1994; 311(2):369 377.
143. Park SB, Jacob P 3rd, Benowitz NL, Cashman JR. Stereoselective metabolism of (*S*) ( ) nicotine in humans: formation of *trans* (*S*) ( ) nicotine *N* 1′ oxide. Chem Res Toxicol 1993; 6 (6):880 888.
144. Damani LA, Pool WF, Crooks PA, Kaderlik RK, Ziegler DM. Stereoselectivity in the *N*′ oxidation of nicotine isomers by flavin containing monooxygenase. Mol Pharmacol 1988; 33(6):702 705.
145. Machinist JM, Mayer MD, Shet MS, Ferrero JL, Rodrigues AD. Identification of the human liver cytochrome P450 enzymes involved in the metabolism of zileuton (ABT 077) and its *N* dehydroxylated metabolite, Abbott 66193. Drug Metab Dispos 1995; 23(10):1163 1174.
146. Court MH, Duan SX, Guillemette C, Journault K, Krishnaswamy S, Von Moltke LL, Greenblatt DJ. Stereoselective conjugation of oxazepam by human UDP glucuronosyltrans ferases (UGTs): *S* oxazepam is glucuronidated by UGT2B15, while *R* oxazepam is glucuronidated by UGT2B7 and UGT1A9. Drug Metab Dispos 2002; 30(11):1257 1265.

147. Court MH, Hao Q, Krishnaswamy S, Bekaii Saab T, Al Rohaimi A, von Moltke LL, Greenblatt DJ. UDP glucuronosyltransferase (UGT) 2B15 pharmacogenetics: UGT2B15 D85Y genotype and gender are major determinants of oxazepam glucuronidation by human liver. J Pharmacol Exp Ther 2004; 310(2):656 665.
148. Nakajima M, Yamanaka H, Fujiwara R, Katoh M, Yokoi T. Stereoselective glucuronidation of 5 (4′ hydroxyphenyl) 5 phenylhydantoin by human UDP glucuronosyltransferase (UGT) 1A1, UGT1A9, and UGT2B15: effects of UGT UGT interactions. Drug Metab Dispos 2007; 35(9):1679 1686.
149. Miller VP, Stresser DM, Blanchard AP, Turner S, Crespi CL. Fluorometric high throughput screening for inhibitors of cytochrome P450. Ann N Y Acad Sci 2000; 919:26 32.
150. Yamamoto T, Suzuki A, Kohno Y. High throughput screening for the assessment of time dependent inhibitions of new drug candidates on recombinant CYP2D6 and CYP3A4 using a single concentration method. Xenobiotica 2004; 34(1):87 101.
151. Yan Z, Rafferty B, Caldwell GW, Masucci JA. Rapidly distinguishing reversible and irreversible CYP450 inhibitors by using fluorometric kinetic analyses. Eur J Drug Metab Pharmacokinet 2002; 27(4):281 287.
152. Naritomi Y, Teramura Y, Terashita S, Kagayama A. Utility of microtiter plate assays for human cytochrome P450 inhibition studies in drug discovery: application of simple method for detecting quasi irreversible and irreversible inhibitors. Drug Metab Pharmacokinet 2004; 19(1):55 61.
153. Di L, Kerns EH, Li SQ, Carter GT. Comparison of cytochrome P450 inhibition assays for drug discovery using human liver microsomes with LC MS, rhCYP450 isozymes with fluores cence, and double cocktail with LC MS. Int J Pharm 2007; 335(1 2):1 11.
154. Trubetskoy OV, Gibson JR, Marks BD. Highly miniaturized formats for in vitro drug metabolism assays using vivid fluorescent substrates and recombinant human cytochrome P450 enzymes. J Biomol Screen 2005; 10(1):56 66.
155. Kariv I, Fereshteh MP, Oldenburg KR. Development of a miniaturized 384 well high throughput screen for the detection of substrates of cytochrome P450 2D6 and 3A4 metabolism. J Biomol Screen 2001; 6(2):91 99.
156. Trubetskoy OV, Finel M, Kurkela M, Fitzgerald M, Peters NR, Hoffman FM, Trubetskoy VS. High throughput screening assay for UDP glucuronosyltransferase 1A1 glucuronidation profiling. Assay Drug Dev Technol 2007; 5(3):343 354.
157. Chang TK, Gonzalez FJ, Waxman DJ. Evaluation of triacetyloleandomycin, alpha naphthoflavone and diethyldithiocarbamate as selective chemical probes for inhibition of human cytochromes P450. Arch Biochem Biophys 1994; 311(2):437 442.
158. Ching MS, Blake CL, Ghabrial H, Ellis SW, Lennard MS, Tucker GT, Smallwood RA. Potent inhibition of yeast expressed CYP2D6 by dihydroquinidine, quinidine, and its metabolites. Biochem Pharmacol 1995; 50(6):833 837.
159. Tassaneeyakul W, Birkett DJ, Veronese ME, McManus ME, Tukey RH, Quattrochi LC, Gelboin HV, Miners JO. Specificity of substrate and inhibitor probes for human cytochromes P450 1A1 and 1A2. J Pharmacol Exp Ther 1993; 265(1):401 407.
160. Newton DJ, Wang RW, Lu AY. Cytochrome P450 inhibitors. Evaluation of specificities in the in vitro metabolism of therapeutic agents by human liver microsomes. Drug Metab Dispos 1995; 23(1):154 158.
161. Ha Duong NT, Marques Soares C, Dijols S, Sari MA, Dansette PM, Mansuy D. Interaction of new sulfaphenazole derivatives with human liver cytochrome P450 2Cs: structural determinants required for selective recognition by CYP 2C9 and for inhibition of human CYP 2Cs. Arch Biochem Biophys 2001; 394(2):189 200.
162. Rodrigues AD, Roberts EM. The in vitro interaction of dexmedetomidine with human liver microsomal cytochrome P4502D6 (CYP2D6). Drug Metab Dispos 1997; 25(5):651 655.
163. Ahlström MM, Zamora I. Characterization of type II ligands in CYP2C9 and CYP3A4. J Med Chem 2008; 51(6):1755 1763.
164. McConn DJ 2nd, Lin YS, Allen K, Kunze KL, Thummel KE. Differences in the inhibition of cytochromes P450 3A4 and 3A5 by metabolite inhibitor complex forming drugs. Drug Metab Dispos 2004; 32(10):1083 1091.

165. Allqvist A, Miura J, Bertilsson L, Mirghani RA. Inhibition of CYP3A4 and CYP3A5 catalyzed metabolism of alprazolam and quinine by ketoconazole as racemate and four different enantiomers. Eur J Clin Pharmacol 2007; 63(2):173 179.
166. Soars MG, Grime K, Riley RJ. Comparative analysis of substrate and inhibitor interactions with CYP3A4 and CYP3A5. Xenobiotica 2006; 36(4):287 299.
167. Granfors MT, Wang JS, Kajosaari LI, Laitila J, Neuvonen PJ, Backman JT. Differential inhibition of cytochrome P450 3A4, 3A5 and 3A7 by five human immunodeficiency virus (HIV) protease inhibitors in vitro. Basic Clin Pharmacol Toxicol 2006; 98(1):79 85.
168. Gibbs MA, Thummel KE, Shen DD, Kunze KL. Inhibition of cytochrome P 450 3A (CYP3A) in human intestinal and liver microsomes: comparison of K_i values and impact of CYP3A5 expression. Drug Metab Dispos 1999; 27(2):180 187.
169. Matsumoto S, Hirama T, Kim HJ, Nagata K, Yamazoe Y. In vitro inhibition of human small intestinal and liver microsomal astemizole *O* demethylation: different contribution of CYP2J2 in the small intestine and liver. Xenobiotica 2003; 33(6):615 623.
170. Hashizume T, Imaoka S, Mise M, Terauchi Y, Fujii T, Miyazaki H, Kamataki T, Funae Y. Involvement of CYP2J2 and CYP4F12 in the metabolism of ebastine in human intestinal microsomes. J Pharmacol Exp Ther 2002; 300(1): 298 304.
171. Guengerich FP. Bioactivation and detoxication of toxic and carcinogenic chemicals. Drug Metab Dispos 1993; 21(1):1 6.
172. Guengerich FP. Metabolic activation of carcinogens. Pharmacol Ther 1992; 54(1):17 61.
173. Guengerich FP, Shimada T. Oxidation of toxic and carcinogenic chemicals by human cytochrome P 450 enzymes. Chem Res Toxicol 1991; 4(4):391 407.
174. Gonzalez FJ, Crespi CL, Gelboin HV. DNA expressed human cytochrome P450s: a new age of molecular toxicology and human risk assessment. Mutat Res 1991; 247(1):113 27.
175. Thompson LH, Wu RW, Felton JS. Genetically modified Chinese hamster ovary (CHO) cells for studying the genotoxicity of heterocyclic amines from cooked foods. Toxicol Lett 1995; 82 83:883 889.
176. Crespi CL, Penman BW, Steimel DT, Gelboin HV, Gonzalez FJ. The development of a human cell line stably expressing human CYP3A4: role in the metabolic activation of aflatoxin B1 and comparison to CYP1A2 and CYP2A3. Carcinogenesis 1991; 12(2):355 359.
177. Hashimoto H, Yanagawa Y, Sawada M, Itoh S, Deguchi T, Kamataki T. Simultaneous expression of human CYP3A7 and *N* acetyltransferase in Chinese hamster CHL cells results in high cytotoxicity for carcinogenic heterocyclic amines. Arch Biochem Biophys 1995; 320(2): 323 329.
178. Dai Y, Cederbaum AI. Cytotoxicity of acetaminophen in human cytochrome P4502E1 transfected HepG2 cells. J Pharmacol Exp Ther 1995; 273(3):1497 1505.
179. Hawksworth GM. Advantages and disadvantages of using human cells for pharmacological and toxicological studies. Hum Exp Toxicol 1994; 13(8):568 573.
180. Ulrich RG, Bacon JA, Cramer CT, Peng GW, Petrella DK, Stryd RP, Sun EL. Cultured hepatocytes as investigational models for hepatic toxicity: practical applications in drug discovery and development. Toxicol Lett 1995; 82 83:107 115.
181. Yamazaki H, Inui Y, Wrighton SA, Guengerich FP, Shimada T. Procarcinogen activation by cytochrome P450 3A4 and 3A5 expressed in *Escherichia coli* and by human liver microsomes. Carcinogenesis 1995; 16(9):2167 2170.
182. Yamazaki H, Mimura M, Oda Y, Inui Y, Shiraga T, Iwasaki K, Guengerich FP, Shimada T. Roles of different forms of cytochrome P450 in the activation of the promutagen 6 aminochrysene to genotoxic metabolites in human liver microsomes. Carcinogenesis 1993; 14 (7):1271 1278.
183. Aoyama T, Yamano S, Guzelian PS, Gelboin HV, Gonzalez FJ. Five of 12 forms of vaccinia virus expressed human hepatic cytochrome P450 metabolically activate aflatoxin B1. Proc Natl Acad Sci U S A 1990; 87(12):4790 4793.
184. Shimada T, Gillam EM, Sandhu P, Guo Z, Tukey RH, Guengerich FP. Activation of procarcinogens by human cytochrome P450 enzymes expressed in *Escherichia coli*. Simplified bacterial systems for genotoxicity assays. Carcinogenesis 1994; 15(11):2523 2529.

185. Styles JA, Davies A, Lim CK, De Matteis F, Stanley LA, White IN, Yuan ZX, Smith LL. Genotoxicity of tamoxifen, tamoxifen epoxide and toremifene in human lymphoblastoid cells containing human cytochrome P450s. Carcinogenesis 1994; 15(1):5 9.
186. Schmalix WA, Mäser H, Kiefer F, Reen R, Wiebel FJ, Gonzalez F, Seidel A, Glatt H, Greim H, Doehmer J. Stable expression of human cytochrome P450 1A1 cDNA in V79 Chinese hamster cells and metabolic activation of benzo[a]pyrene. Eur J Pharmacol 1993; 248(3):251 261.
187. Crespi CL, Penman BW, Gelboin HV, Gonzalez FJ. A tobacco smoke derived nitrosamine, 4 (methylnitrosamino) 1 (3 pyridyl) 1 butanone, is activated by multiple human cytochrome P450s including the polymorphic human cytochrome P4502D6. Carcinogenesis 1991; 12(7):1197 1201.
188. Tiano HF, Wang RL, Hosokawa M, Crespi C, Tindall KR, Langenbach R. Human CYP2A6 activation of 4 (methylnitrosamino) 1 (3 pyridyl) 1 butanone (NNK): mutational specificity in the gpt gene of AS52 cells. Carcinogenesis 1994; 15(12):2859 2866.
189. Fujita K, Kamataki T. Genetically engineered bacterial cells co expressing human cytochrome P450 with NADPH cytochrome P450 reductase: prediction of metabolism and toxicity of drugs in humans. Drug Metab Pharmacokinet 2002; 17(1):1 22.
190. Yamazaki Y, Fujita K, Nakayama K, Suzuki A, Nakamura K, Yamazaki H, Kamataki T. Establishment of ten strains of genetically engineered *Salmonella typhimurium* TA1538 each co expressing a form of human cytochrome P450 with NADPH cytochrome P450 reductase sensitive to various promutagens. Mutat Res 2004; 562(1 2):151 162.
191. Glatt H, Pabel U, Meinl W, Frederiksen H, Frandsen H, Muckel E. Bioactivation of the heterocyclic aromatic amine 2 amino 3 methyl 9H pyrido [2,3 b]indole (MeAalphaC) in recombinant test systems expressing human xenobiotic metabolizing enzymes. Carcinogenesis 2004; 25(5):801 807.
192. Argoti D, Liang L, Conteh A, Chen L, Bershas D, Yu CP, Vouros P, Yang E. Cyanide trapping of iminium ion reactive intermediates followed by detection and structure identification using liquid chromatography tandem mass spectrometry (LC MS/MS). Chem Res Toxicol 2005; 18 (10):1537 1544.
193. Samuel K, Yin W, Stearns RA, Tang YS, Chaudhary AG, Jewell JP, Lanza T Jr, Lin LS, Hagmann WK, Evans DC, Kumar S. Addressing the metabolic activation potential of new leads in drug discovery: a case study using ion trap mass spectrometry and tritium labeling techniques. J Mass Spectrom 2003; 38(2):211 221.
194. Lightning LK, Trager WF. Characterization of covalent adducts to intact cytochrome P450s by mass spectrometry. Methods Enzymol 2002; 357:296 300.
195. Lightning LK, Huang H, Moenne Loccoz P, Loehr TM, Schuller DJ, Poulos TL, de Montellano PR. Disruption of an active site hydrogen bond converts human heme oxygenase 1 into a peroxidase. J Biol Chem 2001; 276(14): 10612 10619.
196. Beck PL, Bridges RJ, Demetrick DJ, Kelly JK, Lee SS. Chronic active hepatitis associated with trazodone therapy. Ann Intern Med 1993; 118(10):791 792.
197. Nelson SD. Structure toxicity relationships: how useful are they in predicting toxicities of new drugs? Adv Exp Med Biol 2001; 500:33 43.
198. Bauman JN, Frederick K, Sawant A, Walsky RL, Cox LM, Obach RS, Kalgutkar AS. Comparison of the bioactivation potential of the antidepressant and Hepatotoxin Nefazodone with Aripiprazole, a Structural Analog and Marketed Drug. Drug Metab Dispos 2008; 36(6): 1016 1029.
199. Kalgutkar AS, Henne KR, Lame ME, Vaz AD, Collin C, Soglia JR, Zhao SX, Hop CE. Metabolic activation of the nontricyclic antidepressant trazodone to electrophilic quinone imine and epoxide intermediates in human liver microsomes and recombinant P4503A4. Chem Biol Interact 2005; 155(1 2):10 20.
200. Kalgutkar AS, Vaz AD, Lame ME, Henne KR, Soglia J, Zhao SX, Abramov YA, Lombardo F, Collin C, Hendsch ZS, Hop CE. Bioactivation of the nontricyclic antidepressant nefazodone to a reactive quinone imine species in human liver microsomes and recombinant cytochrome P450 3A4. Drug Metab Dispos 2005; 33(2):243 253.

201. Wen B, Ma L, Rodrigues AD, Zhu M. Detection of novel reactive metabolites of trazodone: evidence for CYP2D6 mediated bioactivation of *m* chlorophenylpiperazine. Drug Metab Dispos 2008; 36(5):841 850.
202. Watkins PB, Whitcomb RW. Hepatic dysfunction associated with troglitazone. N Engl J Med 1998; 338(13):916 917.
203. Watkins PB. Idiosyncratic liver injury: challenges and approaches. Toxicol Pathol 2005; 33(1):1 5.
204. Kassahun K, Pearson PG, Tang W, McIntosh I, Leung K, Elmore C, Dean D, Wang R, Doss G, Baillie TA. Studies on the metabolism of troglitazone to reactive intermediates in vitro and in vivo. Evidence for novel biotransformation pathways involving quinone methide formation and thiazolidinedione ring scission. Chem Res Toxicol 2001; 14(1):62 70.
205. Yan Z, Maher N, Torres R, Caldwell GW, Huebert N. Rapid detection and characterization of minor reactive metabolites using stable isotope trapping in combination with tandem mass spectrometry. Rapid Commun Mass Spectrom 2005; 19(22):3322 3330.
206. Park BK, Kitteringham NR, Maggs JL, Pirmohamed M, Williams DP. The role of metabolic activation in drug induced hepatotoxicity. Annu Rev Pharmacol Toxicol 2005; 45:177 202.
207. He K, Talaat RE, Pool WF. Metabolic activation of troglitazone: identification of a reactive metabolite and mechanisms involved. Drug Metab Dispos 2004; 32(6):639 646.
208. Prabhu S, Fackett A, Lloyd S, McClellan HA, Terrell CM, Silber PM, Li AP. Identification of glutathione conjugates of troglitazone in human hepatocytes. Chem Biol Interact 2002; 142 (1 2):83 97.
209. Tettey JN, Maggs JL, Rapeport WG, Pirmohamed M, Park BK. Enzyme induction dependent bioactivation of troglitazone and troglitazone quinone in vivo. Chem Res Toxicol 2001; 14(8): 965 974.
210. Gan J, Qu Q, He B, Shyu WC, Rodrigues AD, He K. Troglitazone thiol adduct formation in human liver microsomes: enzyme kinetics and reaction phenotyping. Drug Metab Letts 2008; 2(3):184 189.
211. Gordon EM, Barrett RW, Dower WJ, Fodor SP, Gallop MA. Applications of combinatorial technologies to drug discovery. Combinatorial organic synthesis, library screening strategies, and future directions. J Med Chem 1994; 37(10):1385 1401.
212. Kyranos JN, Cai H, Zhang B, Goetzinger WK. High throughput techniques for compound characterization and purification. Curr Opin Drug Discov Devel 2001; 4(6):719 728.
213. Ley SV, Baxendale IR. New tools and concepts for modern organic synthesis. Nat Rev Drug Discov 2002; 1(8):573 586.
214. Alcázar J, Dielsb G, Schoentjes B. Applications of the combination of microwave and parallel synthesis in medicinal chemistry. Comb Chem High Throughput Screen 2007; 10(10):918 932.
215. Rushmore TH, Reider PJ, Slaughter D, Assang C, Shou M. Bioreactor systems in drug metabolism: synthesis of cytochrome P450 generated metabolites. Metab Eng 2000; 2(2):115 125.
216. Vail RB, Homann MJ, Hanna I, Zaks A. Preparative synthesis of drug metabolites using human cytochrome P450s 3A4, 2C9 and 1A2 with NADPH P450 reductase expressed in *Escherichia coli*. J Ind Microbiol Biotechnol 2005; 32(2):67 74.
217. Otey CR, Bandara G, Lalonde J, Takahashi K, Arnold FH. Preparation of human metabolites of propranolol using laboratory evolved bacterial cytochromes P450. Biotechnol Bioeng 2006; 93(3):494 499.
218. Dulik DM, Fenselau C. Use of immobilized enzymes in drug metabolism studies. FASEB J 1988; 2(7):2235 2240.
219. Kierstan M, Bucke C. The immobilization of microbial cells, subcellular organelles, and enzymes in calcium alginate gels. Biotechnol Bioeng 1977; 19(3):387 397.
220. Klibanov AM. Enzyme stabilization by immobilization. Anal Biochem 1979; 93(1):1 25.
221. Katchalski Katzir E. Immobilized enzymes: learning from past successes and failures. Trends Biotechnol 1993; 11(11):471 478.
222. Ibrahim M, Decolin M, Batt AM, Dellacherie E, Siest G. Immobilization of pig liver microsomes. Stability of cytochrome P 450 dependent monooxygenase activities. Appl Biochem Biotechnol 1986; 12(3):199 213.

223. Alebic Kolbah T, Wainer IW. Microsomal immobilized enzyme reactor for on line production orf glucuronides in a HPLC column. Chromatographia 1993; 37:608 612.
224. Pallante SL, Lisek CA, Dulik DM, Fenselau C. Glutathione conjugates. Immobilized enzyme synthesis and characterization by fast atom bombardment mass spectrometry. Drug Metab Dispos 1986; 14(3):313 318.
225. Schubert F, Scheller F, Mohr P. Application of cytochrome P 450 in enzyme reactors and enzyme electrodes. Pharmazie 1985; 40(4):235 239.
226. King DJ, Azari MR, Wiseman A. Immobilization of a cytochrome P 450 enzyme from *Saccharomyces cerevisiae*. Methods Enzymol 1988; 137:675 686.
227. Brunner G, Holloway CJ, Lösgen H. The application of immobilized enzymes in an artificial liver support system. Artif Organs 1979; 3(1):27 30.
228. Brunner G, Losgen H, Gawlik B, Belsner K. Immobilization of solubilized cytochrome P450 and NADPH cytochrome P450 (*c*) reductase. In: Gustafsson J A, Carlstedt Duke J, Mode A, et al., eds. Biochemistry, Biophysics and Regulation of Cytochrome P450. New York: Elsevier/North Holland, 1980:573 576.
229. Shumyantseva VV, Bulko TV, Archakov AI. Electrochemical reduction of cytochrome P450 as an approach to the construction of biosensors and bioreactors. J Inorg Biochem 2005; 99(5):1051 1063.
230. Stempfer G, Höll Neugebauer B, Kopetzki E, Rudolph R. A fusion protein designed for noncovalent immobilization: stability, enzymatic activity, and use in an enzyme reactor. Nat Biotechnol 1996; 14(4):481 484.
231. Yamazaki H, Ueng YF, Shimada T, Guengerich FP. Roles of divalent metal ions in oxidations catalyzed by recombinant cytochrome P450 3A4 and replacement of NADPH cytochrome P450 reductase with other flavoproteins, ferredoxin, and oxygen surrogates. Biochemistry 1995; 34(26):8380 8389.
232. Hara M, Iazvovskaia S, Ohkawa H, Asada Y, Miyake J. Immobilization of P450 monooxygenase and chloroplast for use in light driven bioreactors. J Biosci Bioeng 1999; 87(6):793 797.
233. Murachi T, Tabata M. Use of immobilized enzyme column reactors in clinical analysis. Methods Enzymol 1988; 137:260 271.
234. Gauthier KM, Yang W, Gross GJ, Campbell WB. Roles of epoxyeicosatrienoic acids in vascular regulation and cardiac preconditioning. J Cardiovasc Pharmacol 2007; 50(6):601 608.
235. Lafite P, Dijols S, Buisson D, Macherey AC, Zeldin DC, Dansette PM, Mansuy D. Design and synthesis of selective, high affinity inhibitors of human cytochrome P450 2J2. Bioorg Med Chem Lett 2006; 16(10):2777 2780.
236. Erion MD, Bullough DA, Lin CC, Hong Z. HepDirect prodrugs for targeting nucleotide based antiviral drugs to the liver. Curr Opin Investig Drugs 2006; 7(2):109 117.
237. Erion MD, van Poelje PD, Mackenna DA, Colby TJ, Montag AC, Fujitaki JM, Linemeyer DL, Bullough DA. Liver targeted drug delivery using HepDirect prodrugs. J Pharmacol Exp Ther 2005; 312(2):554 560.
238. Bruno RD, Njar VC. Targeting cytochrome P450 enzymes: a new approach in anti cancer drug development. Bioorg Med Chem 2007; 15(15):5047 5060.
239. Huang C, Zheng M, Yang Z, Rodrigues AD, Marathe P. Projection of exposure and efficacious dose prior to first in human studies: how successful have we been? Pharm Res 2008; 25(4):713 726.
240. Kobayashi K, Urashima K, Shimada N, Chiba K. Selectivities of human cytochrome P450 inhibitors toward rat P450 isoforms: study with cDNA expressed systems of the rat. Drug Metab Dispos 2003; 31(7):833 836.
241. McLaughlin LA, Dickmann LJ, Wolf CR, Henderson CJ. Functional expression and comparative characterisation of nine murine cytochrome P450s by fluorescent inhibition screening. Drug Metab Dispos 2008; 36(7):1322 1331.
242. Carr B, Norcross R, Fang Y, Lu P, Rodrigues AD, Shou M, Rushmore T, Booth Genthe C. Characterization of the rhesus monkey CYP3A64 enzyme: species comparisons of CYP3A

substrate specificity and kinetics using baculovirus expressed recombinant enzymes. Drug Metab Dispos 2006; 34(10):1703 1712.
243. Shou M, Norcross R, Sandig G, Lu P, Li Y, Lin Y, Mei Q, Rodrigues AD, Rushmore TH. Substrate specificity and kinetic properties of seven heterologously expressed dog cytochromes P450. Drug Metab Dispos 2003; 31(9):1161 1169.
244. Girard C, Barbier O, Turgeon D, Bélanger A. Isolation and characterization of the monkey UGT2B30 gene that encodes a uridine diphosphate glucuronosyltransferase enzyme active on mineralocorticoid, glucocorticoid, androgen and oestrogen hormones. Biochem J 2002; 365 (pt 1):213 222.
245. Green MD, Bélanger G, Hum DW, Bélanger A, Tephly TR. Glucuronidation of opioids, carboxylic acid containing drugs, and hydroxylated xenobiotics catalyzed by expressed monkey UDP glucuronosyltransferase 2B9 protein. Drug Metab Dispos 1997; 25(12):1389 1394.
246. Soars MG, Fettes M, O'Sullivan AC, Riley RJ, Ethell BT, Burchell B. Cloning and characterisation of the first drug metabolising canine UDP glucuronosyltransferase of the 2B subfamily. Biochem Pharmacol 2003; 65(8):1251 1259.
247. Soars MG, Smith DJ, Riley RJ, Burchell B. Cloning and characterization of a canine UDP glucuronosyltransferase. Arch Biochem Biophys 2001; 391(2):218 224.
248. Krueger SK, Yueh MF, Martin SR, Pereira CB, Williams DE. Characterization of expressed full length and truncated FMO2 from rhesus monkey. Drug Metab Dispos 2001; 29(5):693 700.
249. Tsoi C, Morgenstern R, Swedmark S. Canine sulfotransferase SULT1A1: molecular cloning, expression, and characterization. Arch Biochem Biophys 2002; 401(2):125 133.
250. Williams ET, Rodin AS, Strobel HW. Defining relationships between the known members of the cytochrome P450 3A subfamily, including five putative chimpanzee members. Mol Phylogenet Evol 2004; 33(2):300 308.
251. Wong H, Grossman SJ, Bai SA, Diamond S, Wright MR, Grace JE Jr, Qian M, He K, Yeleswaram K, Christ DD. The chimpanzee (*Pan troglodytes*) as a pharmacokinetic model for selection of drug candidates: model characterization and application. Drug Metab Dispos 2004; 32(12):1359 1369.
252. Marathe PH, Rodrigues AD. In vivo animal models for investigating potential CYP3A and Pgp mediated drug drug interactions. Curr Drug Metab 2006; 7(7):687 704.
253. Ho RH, Kim RB. Transporters and drug therapy: implications for drug disposition and disease. Clin Pharmacol Ther 2005; 78(3):260 277.
254. Tsuji A. Impact of transporter mediated drug absorption, distribution, elimination and drug interactions in antimicrobial chemotherapy. J Infect Chemother 2006; 12(5):241 250.
255. Liu L, Cui Y, Chung AY, Shitara Y, Sugiyama Y, Keppler D, Pang KS. Vectorial transport of enalapril by Oatp1a1/Mrp2 and OATP1B1 and OATP1B3/MRP2 in rat and human livers. J Pharmacol Exp Ther 2006; 318(1):395 402.
256. Matsushima S, Maeda K, Kondo C, Hirano M, Sasaki M, Suzuki H, Sugiyama Y. Identification of the hepatic efflux transporters of organic anions using double transfected Madin Darby canine kidney II cells expressing human organic anion transporting polypeptide 1B1 (OATP1B1)/multidrug resistance associated protein 2, OATP1B1/multidrug resistance 1, and OATP1B1/breast cancer resistance protein. J Pharmacol Exp Ther 2005; 314(3):1059 1067.
257. Gonzalez FJ, Kimura S. Study of P450 function using gene knockout and transgenic mice. Arch Biochem Biophys 2003; 409(1):153 158.
258. Felmlee MA, Lon HK, Gonzalez FJ, Yu AM. Cytochrome P450 expression and regulation in CYP3A4/CYP2D6 double transgenic humanized mice. Drug Metab Dispos 2008; 36(2):435 441.
259. Katoh M, Tateno C, Yoshizato K, Yokoi T. Chimeric mice with humanized liver. Toxicology 2008; 246(1):9 17.
260. Katoh M, Sawada T, Soeno Y, Nakajima M, Tateno C, Yoshizato K, Yokoi T. In vivo drug metabolism model for human cytochrome P450 enzyme using chimeric mice with humanized liver. J Pharm Sci 2007; 96(2):428 437.
261. Yu AM. Small interfering RNA in drug metabolism and transport. Curr Drug Metab 2007; 8(7):700 708.

262. Kanebratt KP, Andersson TB. Evaluation of HepaRG cells as an in vitro model for human drug metabolism studies. Drug Metab Dispos 2008; 36(7):1444 1452.
263. Sivaraman A, Leach JK, Townsend S, Iida T, Hogan BJ, Stolz DB, Fry R, Samson LD, Tannenbaum SR, Griffith LG. A microscale in vitro physiological model of the liver: predictive screens for drug metabolism and enzyme induction. Curr Drug Metab 2005; 6(6):569 591.
264. Kosuge M, Takizawa H, Maehashi H, Matsufuji S. A comprehensive gene expression analysis of human hepatocellular carcinoma cell lines as components of a bioartificial liver using a radial flow bioreactor. Liver Int 2007; 27(1):101 108.
265. Ruhnke M, Nussler AK, Ungefroren H, Hengstler JG, Kremer B, Hoeckh W, Gottwald T, Heeckt P, Fandrich F. Human monocyte derived neohepatocytes: a promising alternative to primary human hepatocytes for autologous cell therapy. Transplantation 2005; 79(9):1097 1103.

17
In Vitro Metabolism: Subcellular Fractions

Michael A. Mohutsky, Steven A. Wrighton, and Barbara J. Ring
Lilly Research Laboratories, Eli Lilly & Company, Indianapolis, Indiana, U.S.A.

INTRODUCTION

Over the past 30 years, there has been an increase in the use of in vitro systems for the study of xenobiotic metabolism in the pharmaceutical and toxicological sciences. This is mainly due to the development and optimization of such systems by numerous groups to be used as tools to rapidly evaluate the metabolism of pharmacologically active compounds and toxicity endpoints. The commercial availability of subcellular fractions along with characterization and enrichment of fractions for specific enzyme(s) to answer targeted questions has also increased the use of these methodologies. Further, in vitro studies also decrease the use of animals in drug discovery and development.

In vitro models used for metabolism studies can be broadly separated into two groups. The first group consists of subcellular fractions usually from the liver, including microsomes [vesicles of endoplasmic reticulum (ER)], cytosol, and S-9 (liver homogenate after removal of nuclei and mitochondria) and occasionally erythrocyte membranes, mitochondria, lysosomes, and nuclear fractions. This group also contains purified or isolated enzymes that metabolize drugs after reconstitution with appropriate cofactors and coenzymes. The second group of in vitro systems includes intact cells, incorporating freshly isolated and cultured hepatocytes, cryopreserved hepatocytes, liver slices, the isolated perfused liver, and cell lines. Unlike the subcellular fractions, none of these whole-cell models require cofactors for enzymatic activity. However, culturing of hepatocytes can lead to decreased levels of some enzymes such as the cytochromes P450 (P450) (1). In addition, cryopreservation of hepatocytes can lead to depletion of certain cofactors such as reduced glutathione (2) for conjugation. The advantages and disadvantages of all cellular models for drug metabolism have been extensively reviewed (3 8) and are discussed elsewhere in this text. As the use of subcellular fractions for metabolism studies has been a popular approach for many years, this review, although not exhaustive, describes the preparation techniques for the subcellular fraction from various tissues and the applications of subcellular fractions to drug metabolism.

SUBCELLULAR SYSTEMS

Overview

Both hepatic and extrahepatic cells contain a multitude of xenobiotic- and endobiotic-metabolizing enzymes that are usually localized to specific organelles within the cell (Tables 1 and 2), although some of these enzymes may also be expressed in an organ-specific manner. Hence, individual subcellular fractions can be thought of as highly concentrated enzyme sources, with the cytosol, microsomes, and mitochondria containing most drug-metabolizing enzymes. The major enzymes involved in drug metabolism (9), P450s and UDP-glucurono-syltransferases (UGTs), along with flavin-containing monooxygenases (FMOs), carboxylesterases (CESs), and epoxide hydrolases (EHs), are predominantly localized within the ER (Tables 1 and 2). Consequently, microsomes isolated from multiple organs and species are the most popular subcellular fractions for use in in vitro metabolism studies. Normally, the liver is considered the major drug-metabolizing organ, although, depending on the specific enzyme and xenobiotic, other organs may also be important for metabolism; for example, UGT1A7, 1A8, and 1A10 are expressed predominantly in the gastrointestinal (GI) tract (10).

Advantages of subcellular fractions for xenobiotic metabolism include their ease of preparation, flexibility of incubation conditions [cofactor(s), buffer, pH, and temperature for optimum catalysis], and simple long-term storage protocols (discussed later). Disadvantages of subcellular fractions include lability of some enzymes during preparation (e.g., FMO), loss of cellular heterogeneity (where the organ consists of multiple cell types), and limitation of sequential metabolism that requires multiple cofactors or multiple subcellular components to be complete. However, the flexibility of

Table 1 Characteristics of Major Phase I Enzymes

Enzyme	Reaction	Cofactor	Location
Cytochromes P450	Oxidation Reduction	NADPH	Endoplasmic reticulum
Flavin containing monooxygenase	Oxidation	NADPH	Endoplasmic reticulum
Monoamine oxidases	Oxidation		Mitochondria
Alcohol or aldehyde dehydrogenases	Oxidation	NAD	Cytosol
Reductases	Reduction		Cytosol
Esterases and amidases	Hydrolysis		Cytosol Endoplasmic reticulum
Epoxide hydrolase	Hydration		Cytosol Endoplasmic reticulum

Table 2 Characteristics of Major Phase II Enzymes

Enzyme	Reaction	Cofactor	Location
UDP glucuronosyltransferases	Transferase	UDPGA	Endoplasmic reticulum
Sulfotransferases	Transferase	PAPS	Cytosol
Methyltransferases	Transferase	SAM	Endoplasmic reticulum Cytosol
N acetyltransferase	Transferase	Acetyl CoA	Cytosol
Glutathione *S* transferase	Transferase	GSH	Cytosol Endoplasmic reticulum

the incubation conditions and the ability to test different fractions are key strengths of subcellular fraction use, allowing for incubation conditions to help determine which drug-metabolizing enzymes are involved in a drug's clearance. Data generated with the subcellular fractions from multiple cell types have helped in understanding the relations between metabolism and target organ toxicity.

In the crudest sense, isolation of multiple subcellular fractions requires disruption of the cell by homogenization (scissor mince followed by use of Waring blender, then Ultra Turrax or Potter Elvehjem homogenizers) in a suitable buffer, followed by differential centrifugation (using differences in density and size of particles), and finally, resuspension of the pellet in a suitable storage buffer or isolation of a soluble fraction (Fig. 1). It is possible to use variations of this technique with many organs with the minimal of changes to the method. Although extrahepatic organs are suggested as more difficult to fractionate, it has been possible to obtain the desired fraction from numerous

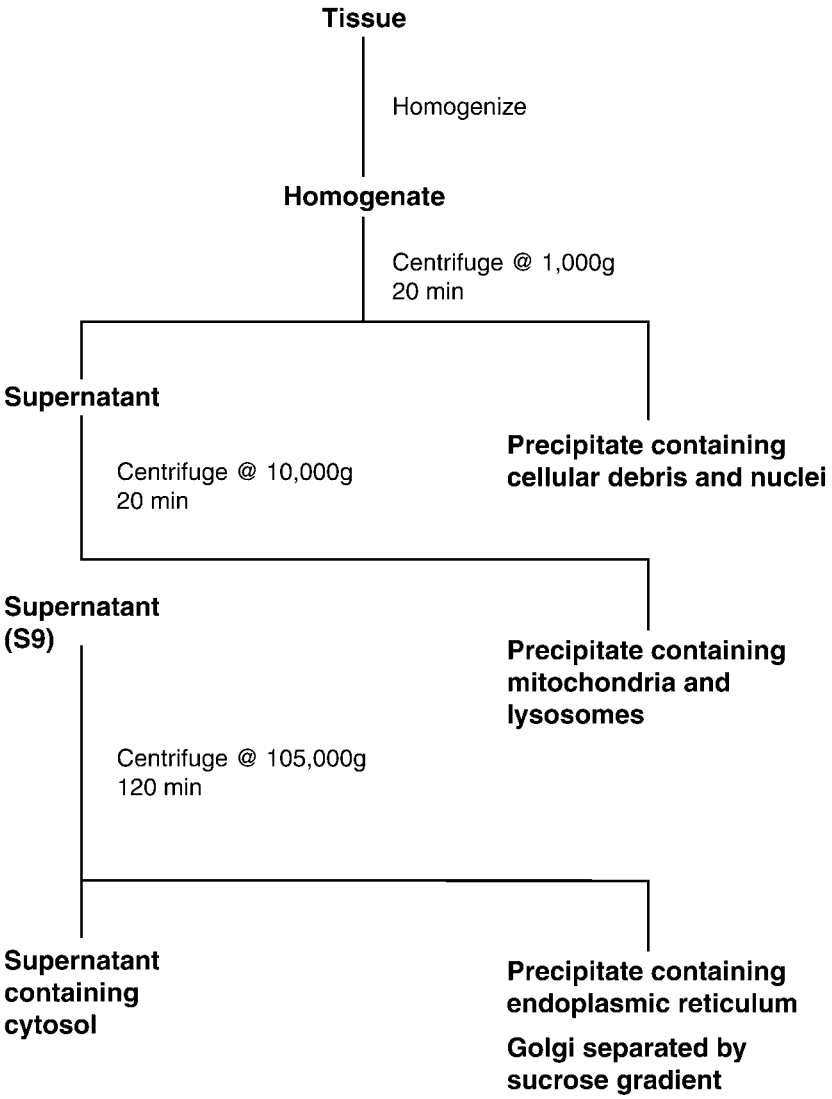

Figure 1 Generalized subcellular fractionation scheme.

Table 3 Selected Enzyme Markers of Subcellular Fractions

Subcellular location	Marker	Ref.
Microsomal	Glucose 6 phosphatase	13
	Cytochrome *c* reductase	14
Mitochondrial	Succinic INT reductase	15
	Cytochrome *c* oxidase	16
	Succinate dehydrogenase	17
	Xanthine oxidase	18
	Glutamate dehydrogenase	19
	Monoamine oxidase	20
Cytosol	Lactate dehydrogenase	21
	Glutathione *S* transferase	22
	Alcohol dehydrogenase	23
Golgi	Galactosyltransferase	24
Lysosomal	Acid phosphatase	25
	β glucuronidase	26
	N acetyl β glucuronidase	26
Peroxisomes	Catalase	27
Plasma membrane	Alkaline phosphatase	28
	Alkaline phosphodiesterase	28

tissues (11,12), which is exemplified by the commercial availability of these fractions from different tissues. Assurance that the isolated fractions represent the organelle of interest can be obtained through checking that the fraction is enriched for enzymes that are markers for that organelle (Table 3).

One of the most frequently used fractionation systems for hepatic microsomes is outlined in Figure 1 (29). Although there have been many variations of this method for the liver and extrahepatic organs, including different buffers, and centrifugation time and speeds, the end products appear to be similar. The principles behind homogenization and centrifugal fractionation have been reviewed by others (30) and will not be discussed here, other than to say that there is a choice of methods and buffers available to be used for the isolation of any one particular fraction.

Review of Protocols for Preparation

A previous extensive review on subfractionation of the liver cell discussed isolation techniques for each component and linked these with morphometry and biochemical analyses (30). These authors discussed the impurities in each subcellular fraction, the artificial nature of in vitro studies that complicate correlating biochemical data with specific organelles, and then concluded with the disclaimer that in vitro models may not reliably predict the in vivo situation. While the techniques used to isolate the subcellular fractions have been used in the decades since this review, the disclaimer has been repeatedly discredited with multiple examples of good in vitro to in vivo correlations as covered later in this chapter.

There have been many other early reviews of subcellular fractionation that describe different protocols for preparation of these fractions from many organs. One of the earliest protocols for liver microsomal preparation (31) suggests microsomes should be prepared from the livers of fasted animals to eliminate contamination of the fraction with glycogen particles, and it also suggested that a single microsome preparation method may not be

universally applicable across all organs. This has been further qualified by the definition of microsomal fractions as consisting of rough and smooth microsomes (with and without ribosomes, respectively) (32). Separation of both types of microsomes from different animals and across organs may necessitate modifications in the method for successful isolation. Initially, the investigator must choose between high recovery and high impurity or lower recovery and higher purity of a specific fraction. In addition, excessive homogenization damages rough microsomes and decreases enzyme activity. To try and solve this problem, alternative methods were developed. A method using puromycin and potassium chloride has been used for the nondestructive preparation of rat liver rough microsomes, characterization, and separation into ribosomal and membranous, smooth, components (33).

Rabbit hepatic microsomes have been separated into three fractions following the initial centrifugation: heavy, medium, and light fractions (34). Total and specific enzyme contents of these three fractions were determined using esterase, glucose-6-phosphatase, ATPase, arylsulfatase, aniline hydroxylase, NADH-cytochrome-*c* reductase, NADPH-cytochrome-*c* reductase, cytochrome b_5, and P450. The P450 and all other enzymes requiring electron transport reactions were more concentrated in the light fraction. The authors located additional enzymes in other fractions and concluded that microsomal fractions contained several types of vesicles.

Subfractionation of rat liver microsomes using 0.26% sodium deoxycholate in a 1/10 ratio with microsomes yields smooth ER with no ribosomes (35). Following this procedure, electron microscopy and enzyme analysis were used to characterize fractions. Membrane-bound enzymes reacted differently to storage and dilution, indicating that an enzyme activity could be controlled by external agents acting on the subcellular structure (35). Schenkman and Cinti (36) described another method for rat liver microsome preparation using calcium, which binds the microsomal fraction, negating the need for an ultracentrifuge and decreasing preparation time. Many enzyme activities were stable using this method, although some actvities may decrease. Furthermore, this technique is also not universally applicable to other organs and species.

The subcellular fractionation of rat liver homogenates into all the major organelles has been described using countercurrent partition or sucrose density centrifugation (37). The countercurrent partition technique enhances the separation of lysosomes and ER from the plasma membrane by separation of particles on the basis of their surface properties. Further isolations of various minor subcellular fractions, such as endosomes and Golgi fractions, have been documented. Endosomes are the membrane vacuoles where endogenous ligands are located following transfer from the plasma membrane (38). Endosomes rapidly hydrolyze these ligands, recycle receptors, and amplify cell-cell signals, although the mechanism is not fully characterized. To prepare Golgi fractions, liver homogenates were fractionated to obtain microsomes. Then the pellet was gently resuspended and fractionated by sucrose gradient centrifugation. Each fraction was collected and washed in sucrose. Further fractionation of the Golgi illustrated that the light and intermediate fractions possessed highest galactosyltransferase activities. Microsomal enzymes also demonstrated lower activities in Golgi fractions (39). Purity of these fractions was checked by electron microscopy to assess for contaminating organelles. Administration of cycloheximide to rats intravenously depletes the liver of secretory products, allowing Golgi membranes to be isolated in a purer form, free of internal contents (40).

Important considerations required for successful subcellular fractionation from any organ or species include the use of optimal conditions throughout the procedure. Not only do microsomal membranes have a negative surface charge that can be used to aid in

fractionation but also proteins present during subfractionation have an intrinsic pH-buffering capacity. However, despite this intrinsic-buffering capacity, it is necessary to use sucrose medium in buffer for homogenization and centrifugation. As mentioned previously, the generalized protocol for microsomal preparation from common laboratory species may also include fasting the animal for 20 hours to reduce glycogen contamination. Other additions to the preparation protocol include using the serine protease or esterase inhibitor, phenylmethylsulfonylfluorine (PMSF), in the homogenization buffer and the chelating agent antioxidant ethylenediaminetetraacetic acid (EDTA), the thiol-protecting agent dithiothreitol, and the antioxidant butylated hydroxytoluene as additives in the microsomal buffer to retard lipid peroxidation and protein degradation. A second high-speed centrifugation step uses pyrophosphate buffer to remove hemoglobin and nucleic acids from the microsomal or subcellular fraction preparation (41). High concentrations of PMSF during microsome isolation can limit the use of the subcellular fraction to study enzymes such as the CESs.

One of the most-studied enzymes systems found in liver microsomal fractions are the hemethiolate proteins known as the P450s. These enzymes were first recognized in the seminal studies, demonstrating that an enzyme was responsible for the demethylation of azo dyes (42,43) localized within microsomes (44). This finding was years before identification of these enzymes as P450s in Wistar rat liver microsomes (45), pig liver microsomes (46), and rabbit liver microsomes (47). The early work by Garfinkel (46) also suggested that additional washing of the microsomes with Ringer's solution was necessary to remove hemoglobin interference with the spectral measurements undertaken. The effect of washing rat hepatic microsomes with sucrose solutions, with or without EDTA, has also been evaluated using xenobiotic metabolism as a marker (48). EDTA prevented the decrease in metabolism of some substrates after washing with sucrose alone, stimulating metabolism of other substrates.

Characterization

The unique localization of particular enzymes to specific, different organelles allows their use as characteristic markers (Table 3). Various reactions by the particular enzymes allow for the characterization of the preparations and the determination of contamination by different subcellular fractions. For general characterization of the microsomal fraction, glucose-6-phosphatase (13) and cytochrome *c* reductase (14) are often used. Because of the various enzymes necessary for the tricarboxylic acid (TCA) cycle and other processes in mitochondria, numerous enzymes can be used for characterization of the mitochondrial fraction, including succinic INT reductase (15), cytochrome *c* oxidase (16), succinate dehydrogenase (17), xanthine oxidase (18), glutamate dehydrogenase (19), and monoamine oxidase (20). The several enzyme markers of the cytosolic fraction include lactate dehydrogenase (LDH) (21), glutathione-*S*-transferase (GST) (22), and alcohol dehydrogenase (23). Golgi fractions are monitored with galactosyltransferase (24). Enzymes used to characterize lysosomes are acid phosphatase (25), along with β-glucuronidase and *N*-acetyl-β-glucuronidase (26); peroxisomes are evaluated via catalase (27) and plasma membranes via alkaline phosphatase and alkaline phosphodiesterase (28).

The use of electron microscopy is the ultimate method to characterize subcellular organelle fractions based purely on morphology and contamination with other organelles. Ribosome preparation from guinea pig liver microsomes by extraction with deoxycholate has been described (49), and the final fraction is analyzed by electron microscopy to demonstrate a relatively pure preparation. In a further example of fractionation characterization by electron microscopy, isolated guinea pig brain nerve endings, myelin

fragments, and mitochondria were prepared by sucrose density gradient centrifugation from an initial homogenate, along with nuclei and cell debris, microsomes, and ribosomes (50). Morphological studies may also be carried out using electron micrographs, which are additionally useful in understanding organelle surface area/volume ratios of the whole cell and how these can be related to enzyme activity. The importance of the hepatic ultrastructure has been recognized since the early stereological morphometric studies of rat liver (51,52). These studies indicated that rough ER and mitochondria both possessed the largest surface areas of all the subcellular components in liver parenchymal cells, and these morphometric data allowed correlation with biochemical studies of phenobarbital induction of microsomal P450 (53).

Storage

One of the advantages of subcellular fractions is their ability to be frozen and easily stored. Because of the valuable nature of human liver for in vitro metabolism studies, numerous groups have examined the effects of storage of human livers at $-80^{\circ}C$ as homogenates, cytosol, microsomal pellets, microsomal suspensions, or snap-frozen pieces. Although some had suggested storage at $-80^{\circ}C$ has little effect on drug metabolism (54) and activities can be well maintained for years with only slight changes (55), in 1996, these statements were rigorously tested. In this evaluation, the effects of freezing, thawing, and time in storage (up to 2 years at $-80^{\circ}C$) of human liver microsomes was examined. The results indicated no change in CYP1A2, CYP2A6, CYP2C9, CYP2C19, CYP2D6, CYP2E1, CYP3A4/5, or CYP4A9/11 catalytic activities (56). In contrast, an earlier study of a number of human hepatic xenobiotic-metabolizing enzymes stored for various lengths of time as pieces, microsomes, or homogenates showed conjugating enzymes were stable and P450 behavior was unpredictable (57). An even earlier study using human liver microsomes and frozen liver cubes stored at $-80^{\circ}C$ for six months found little effect on various enzyme activities when compared with fresh tissue, for P450 activities were stable, although glutathione conjugation declined by 20% (58). Without a doubt it is acknowledged that to ensure successful storage of human livers as either subcellular fractions or whole-cell preparation, the starting quality of the tissue should be as high as possible. In the early years of drug metabolism research with human liver, tissue quality was questionable, as demonstrated by enzyme activities (55,57). The overall quality and availability of human tissue available for drug metabolism research has improved, owing to the increasing network of nonprofit organizations across the United States and Europe that coordinate and distribute donated human tissues under strict ethical committee guidelines. For the liver and kidney specifically, factors such as perfusion with University of Wisconsin buffer have allowed adequate storage time for transportation of viable tissue around the world within 24 hours of removal from the donor.

Extrahepatic Fractions

As described earlier, many organs and cell types may be subfractionated using various methods. However, sedimentation of ER into the final 100,000-g pellets is variable with different extrahepatic tissues (59). The preparation differences and P450 activities in many extrahepatic microsomal fractions obtained from multiple species have been thoroughly reviewed by Burke and Orrenius (11). Along with this chapter, the metabolism by the lung, gut, kidney, and brain are covered in chapters 10 to 13 of this text and will only be covered here briefly.

Localization of enzymes, particularly CYP3A4, within the GI tract has been identified as important in the metabolism of orally administered drugs, owing to a major role in first-pass metabolism. GI homogenates were originally used for drug metabolism, because stable microsomal preparations were hard to obtain; however, this problem was rectified by the addition of a trypsin inhibitor and glycerol (20%) in isotonic potassium chloride, which act as stabilizers of enzymatic activity (60). S-9 supernatant of intestinal biopsy tissue has been used along with midazolam 1′-hydroxylation to demonstrate an 11-fold variation in CYP3A4 in human intestine (61). The isolation of microsomes from intestinal tissue has been shown to be dependent on the method of tissue isolation, and the differences observed between hepatic and intestinal activities have often been accredited to the method of isolation. For example, a report of greater than 10-fold V_{max} values were found with microsomes isolated from eluted enterocytes compared with mucosal scraping (62). The amount of enzyme present in the fraction is also dependent on the portion of intestine from where the microsomes were isolated. CYP3A4, for example, was found in greater quantities in the proximal than distal intestinal sections (63). As a result, in vitro activities with high variability have been reported with different preparations of intestinal microsomes. The study of metabolism by human intestinal tissue has recently been reviewed (64) and is covered elsewhere in this text. Further down the GI tract subcellular fractions from human colon have also been used to assay 1-naphthol conjugation activity, with subcellular fractions demonstrating more sulfation than glucuronidation. The higher sulfation activity observed could likely be due to experimental design since nothing, such as adding detergent or sonication, was done to overcome the latency of the UGT enzymes (65).

When used as a source of subcellular fractions, the kidney is particularly complex to subfractionate, because it consists of localized multiple cell types that themselves must first be isolated to provide any meaningful data on cell-specific metabolism. The standard differential centrifugation technique yields microsomal fractions contaminated with other cellular fragments (11). Enzyme activities are also localized to areas within the kidney, such as the loop of Henle or the proximal tubule, where they are involved in xenobiotic and endobiotic metabolism. P450, GST, and UGT activities were lower in microsomes from the whole kidney than from hepatic microsomes from the rat, rabbit, mouse, hamster, and guinea pig (38). However, recent evidence has shown the importance of the kidney in drug metabolism, especially through glucuronidation. For example, it has been shown that a substantial part of the glucuronide metabolite of the anesthetic propofol is formed in the kidney (66), and this has also been shown using kidney microsomes (67).

The lung is exposed to high blood flow, and enzymes are localized to various cell types. A recent review has focused on the lung and summarizes the different drug-metabolizing enzymes found in the organ and, where available, their location within the tissue (68). Besides the high content of connective tissue, which makes homogenization difficult, the preparation of microsomal fractions from rat lungs requires extensive washing to remove hemoglobin. Compared with the liver, rabbit lung contains relatively little ER (69). Consequently, lung P450 activities are also much lower than the liver (70). This difference is similar for GST, *N*-acetyl transferase (NAT), and UGT activities between pulmonary and hepatic microsomes of rat, mouse, hamster, guinea pig, and humans (71). However, even with the fairly low levels of P450 compared with the liver, the lung does contain several preferentially expressed P450 forms, including CYP1A1, 1B1, 2A13, 2F1, 2S1, and 4B1 (68). The lung is metabolically active for xenobiotics, which enter the lung via inhalation but can also metabolize xenbiotics, which enter the lung through systemic circulation, though at a much lower extent than the liver (72).

Few drug metabolism studies use subcellular fractions derived from the heart. One example focused on quinone metabolism in rat and guinea pig cardiac subcellular fractions found to be localized to the mitochondrial and soluble fraction (73). Another

study showed different stereoselectivity of reduction of oracin by microsomes and S-9 from various tissues, including the heart (74).

The epidermis is exposed to numerous cosmetics, toxicants, and environmental xenobiotics and is one of the largest organs of the body owing to surface area considerations. Because of these properties, the skin has enzyme activity toward many chemicals (75). The skin has been shown to have relatively good P450 (76) and hydrolase activities (77), which are important in the skin's role as a barrier to entrance of xenobiotics. A recent review has covered metabolism by the skin more extensively (78).

The use of nasal tissue from many laboratory animal species has been reviewed relative to metabolic activation by P450 and other drug-metabolizing enzymes (79,80). While the levels of drug-metabolizing enzymes and activities (especially, phenacetin and chlorzoxazone metabolism) are high in the rat nasal cavity (81), overall these would be relatively minor contributors to the disposition of the drug compared with the liver because of the liver's much greater tissue mass. However, the enzymes appear to play a role in local bioactivation and toxicity in the nasal tissue (82,83).

Although not as widely used as other tissues for in vitro metabolism, reproductive tissues are important for investigating metabolites of xenobiotics that are likely to result in teratogenesis (84). Siekevitz (31) used a method similar to that used with the liver for the preparation of microsomes from the placenta. Placental tissue subcellular fractions have also been prepared and acetylcholinesterase (microsomal) and butyrylcholinesterase (cytosolic) activities measured (85). The standard microsomal preparation protocol is less effective with placental than with liver tissue. The addition of glycerol and heparin in homogenization solutions improves catalytic properties of placental microsomes (86,87). Human placenta expresses several P450s, although many catalytic activities are low compared with liver tissue (87,88). Mouse mammary gland subcellular fractions exhibit EH and GST activities at much lower levels than in liver subcellular fractions (89). Rat testicular subcellular fractions can be prepared and used to study metabolism, as demonstrated using the Sertoli cell toxicant 1,3-dinitrobenzene, which is reductively metabolized by this S-9 fraction (90).

Several studies have used brain tissue from various species for the preparation of subcellular fractions for use in metabolic studies. The metabolism in this tissue will be covered more extensively in chapter 13 and has been reviewed elsewhere (91 93). Rat brain subcellular fractions have been prepared in a method described by Alivisatos et al. (94). Brain subcellular fractions have been obtained and have demonstrated higher mitochondrial P450 than microsomal P450 in humans (95). Also, rat brain subcellular fractions have been isolated as described by Hillard et al. (96) and used to study anandamide hydrolysis, with the highest activity in microsomes and myelin. Specific brain subcellular fractions have also been isolated and analyzed for the presence of numerous enzymatic activities. A protocol for mitochondrial preparation from homogenized brain tissue in sucrose/EDTA/heparin has also been detailed (97). Esterase activity in rat brain has been measured in subcellular fractions and in synaptosomes that were isolated by Ficol gradient centrifugation of the crude mitochondrial pellet (98).

USE OF SUBCELLULAR FRACTIONS

Metabolite Identification

Initial metabolism screening is often performed using microsomes supplemented with NADPH or an NADPH-regenerating system, since the major route of metabolism for a majority of new chemical entities is through the P450s. Along with the P450s, this incubation system will allow metabolism by the FMOs along with the CESs. In addition,

inclusion of alamethicin and uridine 5′-diphosphoglucuronic acid (UDPGA) (99) along with the NADPH will allow for the study of the major phase I and phase II enzymes, the P450s and the UGTs, involved in drug metabolism; however, UGT2B7 has been found to have very little activity in this system (100). An advantage of subcellular fractions early in drug discovery is that unlike intact cell methods (hepatocytes and tissue slices) drug uptake is not an issue.

The metabolites generated by subcellular systems can then be rapidly identified using modern, highly sensitive analytical techniques as reviewed previously (101 103). The identity of metabolites formed by microsomes can be determined when this in vitro model is used in conjunction with liquid chromatography mass spectrometry using various ionization methods, including electrospray ionization (ESI), atmospheric pressure chemical ionization (APCI), atmospheric pressure ionization (API), and various mass analyzers, including triple quadrupole, quadrupole time of flight (Q-Tof), and quadrupole ion trap mass analyzers. For example, a recently published example showed the tentative identification of metabolites of an anxiolytic agent using API-MS and MS/MS of relatively small amounts of metabolites generated in vitro. Several demethylation metabolites, hydroxyl phenyl, hydroxyl and oxo-pyrido, along with a dehydration product, all were observed in the in vitro system (104). As seen from the example, the increasing sensitivity and automation of mass spectrometry and related technology has had considerable effect on early drug development by providing an initial read on the potential metabolic profile of the compound. In addition, the subcellular fractions are powerful tools that can be used to biosynthesize metabolites that are either too difficult or too expensive to generate via chemical synthesis.

Species Comparisons of Xenobiotic Metabolism

Since the adoption and use of in vitro techniques, such as subcellular fractions, there have been numerous reports of drug metabolism studies with many different species. Therefore, it is not surprising that comprehensive reviews of multiple enzyme-multiple species and sex difference comparisons in metabolism exist. One such study compared numerous enzyme-specific phases I and II activities in human and rhesus monkey microsomes and cytosol (105). More recently, this work has been expanded to include dog and cynomolgus monkey (106). The importance of understanding species differences in the metabolism of xenobiotics has become more obvious with the necessity to test metabolites for safety in accordance with the Food and Drug Administration's (FDA's) guidance on "Metabolites in Safety Testing" as covered in chapter 24. Subcellular fractions are a very useful tool to study the differences in metabolism between species (including humans) early in drug discovery and development to begin to determine metabolite coverage in preclinical toxicology studies. Species differences (most often in rate or extent of formation) are observed in metabolism of drugs by virtually all enzyme systems using subcellular fractions. For example, species differences were observed for sulfoxidation of 4-hydroxypropranolol (107), carboxyl-glucuronidation of mitiglinide (108), NAT metabolism of a selective androgen receptor modulator (109), and numerous others.

Xenobiotic Activation

Activation of xenobiotics to potential reactive species by subcellular fractions has been recognized as a very common occurrence, and it is accepted practice to include this fraction in mutagenicity assays. For example, the classic Ames mutagenicity assay uses S-9 fraction from arochlor-induced rats to activate xenobiotics prior to testing for mutagenicity to a salmonella strain (110).

Interspecies comparisons have also been used to study carcinogen activation by hepatic microsomes, and these have been highly useful in explaining differential susceptibility to such xenobiotic agents. One example is the considerably higher *N*-hydroxylation of the food-borne carcinogen 2-amino-l-methyl-6-phenylimidazo[4,5-*b*] pyridine (PhIP) in human, rather than in rat and mouse in vitro. Whereas the rodent species detoxify PhIP by 4-hydroxylation to an equal extent, humans have little of this activity (111). The activation of xenobiotics by subcellular fractions will also be covered more extensively in chapter 23.

In Vitro Model Comparisons from Multiple Organs

There are several studies comparing subcellular fractions with other models of in vitro drug metabolism, although there are surprisingly fewer cases for which subcellular fractions from multiple organs are used to study one or more metabolic pathways. Some examples of the latter comparisons will be briefly described. Tissue homogenates (of rat liver, lung, skin, and blood), mitochondria, nuclei, microsomes, and cytosol from these tissues (111) were used to compare esterase activities. The esterase activities were found to be the highest in the liver and plasma. Additionally, esterase activity in human liver cytosol and microsomes has been compared with plasma esterase activity (112). A comparison of glucuronidation of thyroxine with microsomes from the liver, jejunum, and kidney showed that the jejunum had the lowest K_m and highest V_{max} of all the three systems (113). Styrene metabolism by P450 and EH has been measured in microsomes from the liver, heart, lungs, spleen, and kidneys obtained from rat, mouse, guinea pig, and rabbit (114). Another group assessed EH in microsomes and GST activity in cytosol of the liver, kidney, and lungs from mouse, hamster, rat, guinea pig, rabbit, dog, pig, baboon, and human (115). EH was highest in baboon liver and GST was highest in guinea pig liver when compared with the other tissues and species. Liver and lung interspecies comparisons of P450 and EH in microsomes and GST in cytosol indicated considerable differences in enzyme activities among species and higher activities in the lung than the liver (116).

In Vitro-In Vivo Pharmacokinetic Predictions

Because of the increasing pressure to reduce the cost and time to bring a product to market, significant research effort has gone into using in vitro microsomal data prior to first human dose for increasingly quantitative predictions of human P450 inhibitory potential and pharmacokinetics for new drug entities. Thus, in vitro microsomal models of drug metabolism and P450 inhibition have been incorporated into the drug development paradigm from early discovery into the development stages. Applications in early discovery are primarily focused around identification of potential metabolic liabilities of drug platforms using high-throughput absorption, distribution, metabolism, and excretion (ADME) screening (117,118) with a goal of reducing these liabilities with structural modification. As clinical candidates are identified, in-depth in vitro analyses of the candidates potential to cause drug-drug interactions and their metabolic fate are performed, with human microsomes following guidelines set by regulatory agencies (119) and recommendations of Pharmaceutical Research and Manufacturers of America (PhRMA) (120) resulting in an assessment of possible metabolic liabilities, which are further examined in the clinic.

P450 Inhibition

Definitive in vitro studies with human liver microsomes evaluate the possibility that use of a new chemical entity may inhibit the metabolism of coadministered drugs, which

could lead to serious side effects. For these studies, varying concentrations of both probe substrates of each of the P450s and possible inhibitor are incubated with human liver microsomes. The resultant inhibition profile results are used to calculate a K_i or IC_{50} of reversible inhibition. The maximal expected concentration of inhibitor in human plasma (C_{max}) is often used to determine a C_{max}/K_i ratio. This ratio can then be used to predict the clinical relevance of this inhibition, where $C_{max}/K_i > 1$, between 1 and 0.1, and <0.1 predicts inhibition of likely, possible, and remote, respectively (120). Time-dependent inhibition or mechanism-based inhibition can be similarly evaluated following preincubation of the new chemical entity with human liver microsomes and NADPH prior to incubations with probe P450 substrates.

The use of in vitro study results in the design and interpretation of clinical studies, and some of the complexities involved are exemplified by studies performed with tadalafil (121). Tadalafil was examined as a reversible and mechanism-based inhibitor of CYP3A using in vitro incubations with human liver microsomes. A low potential to reversibly inhibit CYP3A, with an I/K_i ratio of 0.05, was predicted; however, additional studies showed that tadalafil had a moderate potential to exhibit mechanism-based inhibition of CYP3A. These data were complemented by in vitro induction studies in human hepatocytes where induction and mechanism-based inhibition of CYP3A activity were observed as simultaneously occurring and essentially balancing each other's effect. Two clinical studies with different CYP3A substrates, midazolam and lovastatin, showed that the pharmacokinetics of these CYP3A probes were essentially unchanged after tadalafil administration, suggesting that inhibition and induction were indeed offset in vivo (121).

Prediction of Exposure and Pharmacokinetic Variability of New Chemical Entities

In vitro studies are performed to predict drug exposure in the human population and to understand the metabolic basis of variability in this exposure (reaction phenotyping). Prior to human exposure, there has been an increasing reliance on in vitro microsomal techniques to predict clearance when oxidative metabolism and/or direct glucuronidation are the primary clearance routes (122 124). Using in vitro human microsomal data, the value termed "the human in vitro intrinsic clearance" ($Cl_{int,h,in\ vitro}$), an estimate of in vivo intrinsic hepatic clearance ($Cl_{int,h,in\ vivo}$), can be determined either through a determination of K_m and V_{max} of the metabolic pathways responsible for clearance or through examination of the rate of loss (k_{loss}) of compound (125). Using physiologically based scaling factors (PB-SF), $Cl_{int,h,in\ vitro}$ is scaled to $Cl_{int,h,in\ vivo}$ [$Cl_{int,h,in\ vivo}$=$Cl_{int,h,in\ vitro}$(mL/min/mg protein)*PB-SF], where PB-SF is the product of the microsomal protein content per gram of the liver and the average liver weight in humans. The $Cl_{int,h,in\ vivo}$ is then scaled to total hepatic Cl_h, most often by using the well-stirred model in which hepatic blood flow (Q_h) and, often, plasma protein binding (fu_p), microsomal protein binding (fu_{mic}), and blood/plasma (R_B) partitioning terms are included.

$$Cl_h = \frac{\frac{Cl_{int,h,invitro}}{fu_{mic}} * Q_h * \left(\frac{fu_p}{R_B}\right)}{Q_h + \left(\frac{Cl_{int,h,invitro}}{fu_{mic}} * \left(\frac{fu_p}{R_B}\right)\right)}$$

The resultant predictions of clearance exhibit a two- to threefold prediction error and a systemic underprediction bias, which has been corrected by some groups with an empirical scaling factor (124). These data, with the uncertainty around the prediction, can be used in context to that obtained preclinically to calculate efficacious or safe first human doses prior to human dosing for hepatically cleared drugs, thus hopefully focusing

these initial studies in a dosing range on the basis of data obtained in a human system versus that empirically derived from purely preclinical sources.

Related to predictions of clearance are questions as to what factors, such as environmental or genetic, influence in vivo metabolic clearance in the general population. This information relies on an understanding of the enzymes involved in the routes of metabolism of a new chemical entity and major or active metabolites (>25 30% of drug clearance), which impact the compounds clearance and/or efficacy (120). Since the realization that P450 was not a single enzyme but a multigene family composed of multiple enzymes with distinct (and in some cases overlapping) substrate specificities (126), it has been possible to identify, quantify, and characterize individual P450s in a tissue using specific probe substrates (127), inhibitors (120), or immunoquantification (128). This approach is useful in the development of a human liver "microsome bank" (129) that contains numerous microsomal preparations that have been characterized for their expression of drug-metabolizing enzymes, including phase II enzymes (130). Microsomes from these characterized liver banks are used to answer these questions of clearance when oxidative and/or direct UGT-mediated metabolism is involved. The major focus for reaction phenotyping are the P450s; however, other drug-metabolizing enzymes can be evaluated such as UGTs, sulfotransferases (SULTs), FMOs, and hydrolysis enzymes if the pathways are important in a compound's clearance, often using subcellular systems other than microsomes (120). Further, the study of effects of genetics and other factors on xenobiotic metabolism is performed in vitro because of the ease of use and long-term stability of the subcellular fractions.

As an example, duloxetine reaction phenotyping studies show the use of this approach (131). Results from in vitro studies with duloxetine using human liver microsomes and microsomes prepared from human β-lymphoblastoid cells expressing human P450s found that the clearance of duloxetine via three hydroxylated routes was related to CYP1A2 and CYP2D6. Clinical studies found that paroxetine (CYP2D6 inhibitor) increased the C_{max} and AUC of duloxetine moderately (about 60% for both) (132), and fluoxamine (CYP1A2 inhibitor) increased the AUC and C_{max} by 460% and 141%, respectively (131). Thus, the in vitro studies allowed focused clinical studies to be performed, which concluded that duloxetine is predominantly metabolized by CYP1A2 and to a lesser extent CYP2D6.

SUMMARY AND CONCLUSION

The information discussed in this chapter indicates that subcellular fractions can be prepared from many different cell types, organs, and species and may be stored for a number of years at 80°C and still retain their enzymatic activity reflective of fresh tissue. The unique organ architectures, however, may complicate use of a standard method for preparation of a single subcellular fraction; and this may partially explain the numerous combinations of buffer constituents, homogenization conditions, and centrifugation protocols available both for the same organ as well as across-species studies. Therefore, it is recommended that some form of characterization be performed to ensure that the isolated fraction is essentially from a single organelle. Characterization techniques include enzymatic, electron microscopic, or immunochemical techniques. For in vitro drug metabolism studies, microsomes are clearly the most widely used subcellular fraction, and the liver is the most extensively studied organ. There is a reasonable relationship using microsomes for in vitro-in vivo correlation of xenobiotic metabolism, although it is not perfect owing to confounding factors present within this system. The use

of other fractions, such as cytosol or whole-cell models, may be necessitated if the xenobiotic undergoes metabolism mediated by enzymes found outside the ER fraction. With reference to multiple metabolic pathways in numerous organelles, a single subcellular system will not allow sequential metabolism unless the whole pathway is catalyzed by enzymes found solely in the single preparation. Depending on the enzyme(s) involved, cofactors are required to facilitate metabolism, and this requires prior knowledge of the identity and the amounts of the cofactors necessary for optimal turnover. This represents one of the disadvantages of using this system.

The use of subcellular fractions to determine interspecies differences in metabolism is a useful tool to help in the design of toxicology studies. Using microsomes, S-9, and/or cytosol from preclinical species along with those from humans early will allow for choice of optimal toxicology species with coverage of prominent metabolites in humans or, barring this, allow for the synthesis and toxicology testing of unique human metabolites in the animals. When human tissue is available, the formation of a phenotyped bank is possible, which is of enormous value for early definition of metabolic routes for new drugs and ultimately useful to screen out molecules that may present problems to some or all potential patients. If the bank is significantly large, it may also give some idea of the variability in metabolism that may be present in the patient population. Subcellular fractions are also useful to predict hepatic clearance, which can be used to help choose first human dose. In addition, microsomes are used to determine the P450 inhibition liability of a new chemical entity and may preclude the need for a clinical drug interaction study.

In conclusion, subcellular systems when supplemented with the required cofactors are a sophisticated representation of only part of the whole cell. The ability to control the enzyme system studied by use of specific conditions and subcellular fractions make this system extremely powerful. However, such systems do not take into account the regulatory effects of cell-cell contact communication, the heterogeneous cellular nature of many organs, or the interplay between different enzymes and transporters within a cell or tissue. These considerations aside, it is clear that subcellular fractions have many useful roles in the pharmaceutical industry, and their niche in the future seems assured.

ACKNOWLEDGMENTS

The authors wish to thank Jukka Mäenpää and Sean Ekins for their contributions to the initial version.

REFERENCES

1. Silva JM, Morin PE, Day SH, et al. Refinement of an in vitro cell model for cytochrome P450 induction. Drug Metab Dispos 1998; 26(5):490 496.
2. Sohlenius Sternbeck AK, Schmidt S. Impaired glutathione conjugating capacity by cryopre served human and rat hepatocytes. Xenobiotica 2005; 35(7):727 736.
3. Ekins S. Past, present, and future applications of precision cut liver slices for in vitro xenobiotic metabolism. Drug Metab Rev 1996; 28(4):591 623.
4. Jia L, Liu X. The conduct of drug metabolism studies considered good practice (II): in vitro experiments. Curr Drug Metab 2007; 8(8):822 829.
5. Li AP. Human hepatocytes: isolation, cryopreservation and applications in drug development. Chem Biol Interact 2007; 168(1):16 29.
6. Vermeir M, Annaert P, Mamidi RN, et al. Cell based models to study hepatic drug metabolism and enzyme induction in humans. Expert Opin Drug Metab Toxicol 2005; 1(1):75 90.

7. Hariparsad N, Sane RS, Strom SC, et al. In vitro methods in human drug biotransformation research: implications for cancer chemotherapy. Toxicol In Vitro 2006; 20(2):135 153.
8. Wienkers LC, Heath TG. Predicting in vivo drug interactions from in vitro drug discovery data. Nat Rev Drug Discov 2005; 4(10):825 833.
9. Williams JA, Hyland R, Jones BC, et al. Drug drug interactions for UDP glucuronosyltransferase substrates: a pharmacokinetic explanation for typically observed low exposure (AUCi/AUC) ratios. Drug Metab Dispos 2004; 32(11):1201 1208.
10. Strassburg CP, Nguyen N, Manns MP, et al. Polymorphic expression of the UDP glucuronosyltransferase UGT1A gene locus in human gastric epithelium. Mol Pharmacol 1998; 54(4):647 654.
11. Burke MD, Orrenius S. Isolation and comparison of endoplasmic reticulum membranes and their mixed function oxidase activities from mammalian extrahepatic tissues. Pharmacol Ther 1979; 7(3):549 599.
12. Bend JR, Serabjit Singh CJ. Xenobiotic metabolism by extrahepatic tissues: Relationship to target organ and cell toxicity. In: Mitchell JR, Horning MG, eds. Drug Metabolism and Drug Toxicity. New York: Raven Press, 1984:99.
13. Arion WJ, Wallin BK, Lange AJ, et al. On the involvement of a glucose 6 phosphate transport system in the function of microsomal glucose 6 phosphatase. Mol Cell Biochem 1975; 6(2): 75 83.
14. Masters BSS Jr., William CH, Kamin H. The preparation and properties of microsomal NADPH cytochrome *c* reductase from pig liver. Methods Enzymol 1967; 10:565 573.
15. Pennington RJ. Biochemistry of dystrophic muscle. Mitochondrial succinate tetrazolium reductase and adenosine triphosphatase. Biochem J 1961; 80:649 654.
16. Wikstrom MK. Proton pump coupled to cytochrome c oxidase in mitochondria. Nature 1977; 266(5599):271 273.
17. Gutman M. Modulation of mitochondrial succinate dehydrogenase activity, mechanism and function. Mol Cell Biochem 1978; 20(1):41 60.
18. Hille R, Nishino T. Flavoprotein structure and mechanism. 4. Xanthine oxidase and xanthine dehydrogenase. FASEB J 1995; 9(11):995 1003.
19. Schmidt E. Glutamate dehydrogenase. In: Bergmeyer HU, ed. Methods of Enzymatic Analysis. New York: Academic Press, 1974; 650 656.
20. Schnaitman C, Erwin VG, Greenawalt JW. The submitochondrial localization of monoamine oxidase. An enzymatic marker for the outer membrane of rat liver mitochondria. J Cell Biol 1967; 32(3):719 735.
21. Bergmeyer HU, Bernt E. Lactate dehydrogenase. In: Bergmeyer HU ed. Methods of enzymatic analysis. New York: Academic Press, 1974: 574 79.
22. Habig WH, Pabst MJ, Jakoby WB. Glutathione S transferases. The first enzymatic step in mercapturic acid formation. J Biol Chem 1974; 249(22):7130 7139.
23. Wynne HA, Wood P, Herd B, et al. The association of age with the activity of alcohol dehydrogenase in human liver. Age Ageing 1992; 21(6):417 420.
24. Baxter A, Durham JP. A rapid, sensitive disk assay for the determination of glycoprotein glycosyltransferases. Anal Biochem 1979; 98(1):95 101.
25. Drexler HG, Gignac SM. Characterization and expression of tartrate resistant acid phosphatase (TRAP) in hematopoietic cells. Leukemia 1994; 8(3):359 368.
26. Lombardo A, Caimi L, Marchesini S, et al. Enzymes of lysosomal origin in human plasma and serum: assay conditions and parameters influencing the assay. Clin Chim Acta 1980; 108(3): 337 346.
27. Chance B, Herbert D. The enzyme substrate compounds of bacterial catalase and peroxides. Biochem J 1950; 46(4):402 414.
28. Emmelot P, Bos CJ, Benedetti EL, et al. Studies on Plasma Membranes. I. Clinical composition and enzyme content on plasma membranes isolated from rat liver. Biochim Biophys Acta. 1964, 90, 126 145.
29. van der Hoeven TA, Coon MJ. Preparation and properties of partially purified cytochrome P 450 and reduced nicotinamide adenine dinucleotide phosphate cytochrome P 450 reductase from rabbit liver microsomes. J Biol Chem 1974; 249(19):6302 6310.

30. Moulé Y, Chauveau J. The cell components of the liver. Isolation, morphology, bio chemistry. In: Rouiller C, ed. The Liver, Morphology, Biochemistry, Physiology. New York: Academic Press, 1963:379.
31. Siekevitz P. Preparation of microsomes and submicrosomal fractions: Mammalian. Methods Enzymol 1962; 5:61 68.
32. Dallner G. Isolation of microsomal subfractions by use of density gradients. Methods Enzymol 1978; 52:71 83.
33. Adelman MR, Blobel G, Sabatini DD. Nondestructive separation of rat liver rough microsomes into ribosomal and membranous components. Methods Enzymol 1974; 31:201 215.
34. Imai Y, Ito A, Sato R. Evidence for biochemically different types of vesicles in the hepatic microsomal fraction. J Biochem 1966; 60(4):417 428.
35. Ernster L, Siekevitz P, Palade GE. Enzyme structure relationships in the endoplasmic reticulum of rat liver: A Morphological and Biochemical Study. J Cell Biol 1962; 15(3):541 562.
36. Schenkman JB, Cinti DL. Preparation of microsomes with calcium. Methods Enzymol 1978; 52:83 89.
37. Morris WB, Smith GD, Peters TJ. Subcellular fractionation of liver organelles from phenobarbital treated rats by counter current partition and sucrose gradient centrifugation. Biochem Pharmacol 1986; 35(13):2187 2191.
38. Evans WH. Hepatic endosomes: preparation, properties and roles in receptor recycling. Biochem Soc Trans 1986; 14(1):170 172.
39. Bergeron JJ. Golgi fractions from livers of control and ethanol intoxicated rats. Enzymic and morphologic properties following rapid isolation. Biochim Biophys Acta 1979; 555(3): 493 503.
40. Taylor JA, Limbrick AR, Allan D, et al. Isolation of highly purified Golgi membranes from rat liver. Use of cycloheximide in vivo to remove Golgi contents. Biochim Biophys Acta 1984; 769(1):171 178.
41. Guengerich FP, Analysis and characterisation of enzymes. In: Hayes AW ed. Principles and Methods of Toxicology. New York: Raven Press, 1994: 1259.
42. Brown RR, Miller JA, Miller EC. The metabolism of methylated aminoazo dyes. IV. Dietary factors enhancing demethylation in vitro. J Biol Chem 1954; 209(1):211 222.
43. Conney AH, Miller EC, Miller JA. The metabolism of methylated aminoazo dyes. V. Evidence for induction of enzyme synthesis in the rat by 3 methylcholanthrene. Cancer Res 1956; 16(5): 450 459.
44. Conney AH, Brown RR, Miller JA, et al. The metabolism of methylated aminoazo dyes. VI. Intracellular distribution and properties of the demethylase system. Cancer Res 1957; 17(6): 628 633.
45. Klingenberg M. Pigments of rat liver microsomes. Arch Biochem Biophys 1958; 75(2): 376 386.
46. Garfinkel D. Studies on pig liver microsomes. I. Enzymic and pigment composition of different microsomal fractions. Arch Biochem Biophys 1958; 77(2):493 509.
47. Omura T, Sato R. The carbon monoxide binding pigment of liver microsomes. I. Evidence for its hemoprotein nature. J Biol Chem 1964; 239:2370 2378.
48. Powis G, Boobis AR. Effect of washing the hepatic microsomal fraction in sucrose solutions and in sucrose solution containing EDTA upon the metabolism of foreign compounds. Biochem Pharmacol 1975; 24(19):1771 1776.
49. Kirsch JF, Siekevitz P, Palade GE. Amino acid incorporation in vitro by ribonucleoprotein particles detached from guinea pig liver microsomes. J Biol Chem 1960; 235:1419 1424.
50. Gray EG, Whittaker VP. The isolation of nerve endings from brain: an electron microscopic study of cell fragments derived by homogenization and centrifugation. J Anat 1962; 96:79 88.
51. Loud AV. A quantitative stereological description of the ultrastructure of normal rat liver parenchymal cells. J Cell Biol 1968; 37(1):27 46.
52. Weibel ER, Stäubli W, Gnägi HR, et al. Correlated morphometric and biochemical studies on the liver cell. I. Morphometric model, stereologic methods, and normal morphometric data for rat liver. J Cell Biol 1969; 42(1):68 91.

53. Stäubli W, Hess R, Weibel ER. Correlated morphometric and biochemical studies on the liver cell. II. Effects of phenobarbital on rat hepatocytes. J Cell Biol 1969; 42(1):92 112.
54. Wrighton SA, Vandenbranden M, Stevens JC, et al. In vitro methods for assessing human hepatic drug metabolism: their use in drug development. Drug Metab Rev 1993; 25(4): 453 484.
55. Chapman DE, Christensen TA, Michener SR, et al. Xenobiotic metabolism studies with human liver. In: Jeffery EH, ed. Human Drug Metabolism from Molecular Biology to Man. Boca Raton: CRC Press, 1993:53.
56. Pearce RE, McIntyre CJ, Madan A, et al. Effects of freezing, thawing, and storing human liver microsomes on cytochrome P450 activity. Arch Biochem Biophys 1996; 331(2):145 169.
57. Powis G, Jardine I, Van Dyke R, et al. Foreign compound metabolism studies with human liver obtained as surgical waste. Relation to donor characteristics and effects of tissue storage. Drug Metab Dispos 1988; 16(4):582 589.
58. von Bahr C, Glaumann H, Mellström B, et al. In vitro assessment of hepatic drug metabolism in man: a clinical pharmacological perspective. In: Lamble JW, ed. Drug Metabolism and Distribution. Amsterdam: Elsevier Biomedical Press, 1983:152.
59. Raunio H, Pasanen M, Mäenpää J., et al. Expression of extrahepatic cytochrome P450 in humans. In: Pacifici GM, ed. Advances in Drug Metabolism. Brussels: European Commission, 1995:233.
60. Stohs SJ, Grafström RC, Burke MD, et al. The isolation of rat intestinal microsomes with stable cytochrome P 450 and their metabolism of benzo(alpha) pyrene. Arch Biochem Biophys 1976; 177(1):105 116.
61. Lown KS, Kolars JC, Thummel KE, et al. Interpatient heterogeneity in expression of CYP3A4 and CYP3A5 in small bowel. Lack of prediction by the erythromycin breath test. Drug Metab Dispos 1994; 22(6):947 955.
62. Galetin A, Houston JB. Intestinal and hepatic metabolic activity of five cytochrome P450 enzymes: impact on prediction of first pass metabolism. J Pharmacol Exp Ther 2006; 318(3): 1220 1229.
63. Paine MF, Khalighi M, Fisher JM, et al. Characterization of interintestinal and intraintestinal variations in humanCYP3A dependent metabolism. J Pharmacol Exp Ther 1997; 283(3): 1552 1562.
64. Fisher MB, Labissiere G. The role of the intestine in drug metabolism and pharmacokinetics: an industry perspective. Curr Drug Metab 2007; 8(7):694 699.
65. Gibby EM, Cohen GM. Conjugation of 1 naphthol by human colon and tumour tissue using different experimental systems. Br J Cancer 1984; 49(5):645 651.
66. Takizawa D, Hiraoka H, Goto F, et al. Human kidneys play an important role in the elimination of propofol. Anesthesiology 2005; 102(2):327 330.
67. Al Jahdari WS, Yamamoto K, Hiraoka H, et al. Prediction of total propofol clearance based on enzyme activities in microsomes from human kidney and liver. Eur J Clin Pharmacol 2006; 62(7):527 533.
68. Zhang JY, Wang Y, Prakash C. Xenobiotic metabolizing enzymes in human lung. Curr Drug Metab 2006; 7(8):939 948.
69. Philpot RM. Modulation of the pulmonary cytochrome P450 system as a factor in pulmonary selective toxic responses: fact and fiction. Am J Respir Cell Mol Biol 1993; 9(4):347 349.
70. Matsubara T, Prough RA, Burke MD, et al. The preparation of microsomal fractions of rodent respiratory tract and their characterization. Cancer Res 1974; 34(9):2196 2203.
71. Litterst CL, Mimnaugh EG, Reagan RL, et al. Comparison of in vitro drug metabolism by lung, liver, and kidney of several common laboratory species. Drug Metab Dispos 1975; 3(4): 259 265.
72. Borlak J, Blickwede M, Hansen T, et al. Metabolism of verapamil in cultures of rat alveolar epithelial cells and pharmacokinetics after administration by intravenous and inhalation routes. Drug Metab Dispos 2005; 33(8):1108 1114.
73. Floreani M, Carpenedo F. Metabolism of simple quinones in guinea pig and rat cardiac tissue. Gen Pharmacol 1995; 26(8):1757 1764.

74. Szotáková B, Skálová L, Jílek P, et al. Stereospecific reduction of the original anticancer drug oracin in rat extrahepatic tissues. J Pharm Pharmacol 2003; 55(7):1003 1011.
75. Bickers DR, Dutta Choudhury T, Mukhtar H. Epidermis: a site of drug metabolism in neonatal rat skin. Studies on cytochrome P 450 content and mixed function oxidase and epoxide hydrolase activity. Mol Pharmacol 1982; 21(1):239 247.
76. Ahmad N, Agarwal R, Mukhtar H. Cytochrome P 450 dependent drug metabolism in skin. Clin Dermatol 1996; 14(4):407 415.
77. Jewell C, Ackermann C, Payne NA, et al. Specificity of procaine and ester hydrolysis by human, minipig, and rat skin and liver. Drug Metab Dispos 2007; 35(11):2015 2022.
78. Oesch F, Fabian E, Oesch Bartlomowicz B, et al. Drug metabolizing enzymes in the skin of man, rat, and pig. Drug Metab Rev 2007; 39(4):659 698.
79. Reed CJ. Drug metabolism in the nasal cavity: relevance to toxicology. Drug Metab Rev. 1993; 25(1 2):173 205.
80. Sarkar MA. Drug metabolism in the nasal mucosa. Pharm Res 1992; 9(1):1 9.
81. Minn AL, Pelczar H, Denizot C, et al. Characterization of microsomal cytochrome P450 dependent monooxygenases in the rat olfactory mucosa. Drug Metab Dispos 2005; 33(8): 1229 1237.
82. Brittebo EB. Metabolism dependent activation and toxicity of chemicals in nasal glands. Mutat Res 1997; 380(1 2):61 75.
83. Ding X, Kaminsky LS. Human extrahepatic cytochromes P450: function in xenobiotic metabolism and tissue selective chemical toxicity in the respiratory and gastrointestinal tracts. Annu Rev Pharmacol Toxicol 2003; 43:149 173.
84. Wells PG, Winn LM. Biochemical toxicology of chemical teratogenesis. Crit Rev Biochem Mol Biol 1996; 31(1):1 40.
85. Simone C, Derewlany LO, Oskamp M, et al. Acetylcholinesterase and butyrylcholinesterase activity in the human term placenta: implications for fetal cocaine exposure. J Lab Clin Med 1994; 123(3):400 406.
86. Pelkonen O, Pasanen M. Effect of heparin on the subcellular distribution of human placental 7 ethoxycoumarin O deethylase activity. Biochem Pharmacol 1981; 30(23):3254 3256.
87. Pasanen M, Pelkonen O. The expression and environmental regulation of P450 enzymes in human placenta. Crit Rev Toxicol 1994; 24(3):211 229.
88. Hakkola J, Pasanen M, Hukkanen J, et al. Expression of xenobiotic metabolizing cytochrome P450 forms in human full term placenta. Biochem Pharmacol 1996; 51(4):403 411.
89. Silva MH, Wixtrom RN, Hammock BD. Epoxide metabolizing enzymes in mammary gland and liver from BALB/c mice and effects of inducers on enzyme activity. Cancer Res 1988; 48(6):1390 1397.
90. Ellis MK, Foster PM. The metabolism of 1,3 dinitrobenzene by rat testicular subcellular fractions. Toxicol Lett 1992; 62(2 3):201 208.
91. Woodland C, Huang TT, Gryz E, et al. Expression, activity and regulation of CYP3A in human and rodent brain. Drug Metab Rev 2008; 40(1):149 168.
92. Meyer RP, Gehlhaus M, Knoth R, et al. Expression and function of cytochrome p450 in brain drug metabolism. Curr Drug Metab 2007; 8(4):297 306.
93. Haining RL, Nichols Haining M. Cytochrome P450 catalyzed pathways in human brain: metabolism meets pharmacology or old drugs with new mechanism of action? Pharmacol Ther 2007; 113(3):537 545.
94. Alivisatos SG, Ungar F, Parmar SS, et al. Monoamine oxidase dependent labeling in vivo of mouse brain by 14C serotonin. Biochem Pharmacol 1968; 17(9):1993 1995.
95. Ghersi Egea JF, Perrin R, Leininger Muller B, et al. Subcellular localization of cytochrome P450, and activities of several enzymes responsible for drug metabolism in the human brain. Biochem Pharmacol 1993; 45(3):647 658.
96. Hillard CJ, Wilkison DM, Edgemond WS, et al. Characterization of the kinetics and distribution of N arachidonylethanolamine (anandamide) hydrolysis by rat brain. Biochim Biophys Acta 1995; 1257(3):249 256.

97. Basford RE. Preparation and properties of brain mitochondria. Methods Enzymol 1967; 10:96 101.
98. Durrer A, Walther B, Racciatti A, et al. Structure metabolism relationships in the hydrolysis of nicotinate esters by rat liver and brain subcellular fractions. Pharm Res 1991; 8(7):832 839.
99. Fisher MB, Campanale K, Ackermann BL, et al. In vitro glucuronidation using human liver microsomes and the pore forming peptide alamethicin. Drug Metab Dispos 2000; 28(5): 560 566.
100. Engtrakul JJ, Foti RS, Strelevitz TJ, et al. Altered AZT (3′ azido 3′ deoxythymidine) glucuronidation kinetics in liver microsomes as an explanation for underprediction of in vivo clearance: comparison to hepatocytes and effect of incubation environment. Drug Metab Dispos 2005; 33(11):1621 1627.
101. Baranczewski P, Stańczak A, Kautiainen A, et al. Introduction to early in vitro identification of metabolites of new chemical entities in drug discovery and development. Pharmacol Rep 2006; 58(3):341 352.
102. Prakash C, Shaffer CL, Nedderman A. Analytical strategies for identifying drug metabolites. Mass Spectrom Rev 2007; 26(3):340 369.
103. Castro Perez JM. Current and future trends in the application of HPLC MS to metabolite identification studies. Drug Discov Today 2007; 12(5 6):249 256.
104. Wu WN, McKown LA, Reitz AB. Metabolism of the new anxiolytic agent, a pyrido[1,2] benzimidazole (PBI) analog (RWJ 53050), in rat and human hepatic S9 fractions, and in dog; identification of cytochrome p450 isoforms mediated in the human microsomal metabolism. Eur J Drug Metab Pharmacokinet 2006; 31(4):277 283.
105. Stevens JC, Shipley LA, Cashman JR, et al. Comparison of human and rhesus monkey in vitro phase I and phase II hepatic drug metabolism activities. Drug Metab Dispos 1993; 21(5): 753 760.
106. Sharer JE, Shipley LA, Vandenbranden MR, et al. Comparisons of phase I and phase II in vitro hepatic enzyme activities of human, dog, rhesus monkey, and cynomolgus monkey. Drug Metab Dispos 1995; 23(11):1231 1241.
107. Narimatsu S, Kobayashi N, Asaoka K, et al. High performance liquid chromatographic analysis of the sulfation of 4 hydroxypropranolol enantiomers by monkey liver cytosol. Chirality 2001; 13(3):140 147.
108. Yu L, Lu S, Lin Y, et al. Carboxyl glucuronidation of mitiglinide by human UDP glucuronosyltransferases. Biochem Pharmacol 2007; 73(11):1842 1851.
109. Gao W, Johnston JS, Miller DD, et al. Interspecies differences in pharmacokinetics and metabolism of S 3 (4 acetylamino phenoxy) 2 hydroxy 2 methyl N (4 nitro 3 trifluoromethylphenyl) propionamide: the role of N acetyltransferase. Drug Metab Dispos 2006; 34(2):254 260.
110. McCann J, Choi E, Yamasaki E, et al. Detection of Carcinogens as Mutagens in the Salmonella/Microsome Test: Assay of 300 Chemicals. Proc Natl Acad Sci U S A 1975; 72(12):5135 5139.
111. McCracken NW, Blain PG, Williams FM. Nature and role of xenobiotic metabolizing esterases in rat liver, lung, skin and blood. Biochem Pharmacol 1993; 45(1):31 36.
112. McCracken NW, Blain PG, Williams FM. Human xenobiotic metabolism in esterases in liver and blood, Biochem. Pharmacol 1993; 46(7):125 129.
113. Yamanaka H, Nakajima M, Katoh M, et al. Glucuronidation of thyroxine in human liver, jejunum, and kidney microsomes. Drug Metab Dispos 2007; 35(9):1642 1648.
114. Cantoni L, Salmona M, Facchinetti T, et al. Hepatic and extrahepatic formation and hydration of styrene oxide in vitro in animals of different species and sex. Toxicol Lett 1978; 2(3): 179 186.
115. Pacifici GM, Boobis AR, Brodie MJ, et al. Tissue and species differences in enzymes of epoxide metabolism. Xenobiotica 1981; 11(2):73 79.
116. Lorenz J, Glatt HR, Fleischmann R, et al. Drug metabolism in man and its relationship to that in three rodent species: monooxygenase, epoxide hydrolase, and glutathione S transferase activities in subcellular fractions of lung and liver. Biochem Med 1984; 32(1):43 56.

117. Yu H, Adedoyin A. ADME Tox in drug discovery: integration of experimental and computational technologies. Drug Discov Today 2003; 8(18):852 861.
118. Kassel DB. Applications of high throughput ADME in drug discovery. Curr Opin Chem Biol 2004; 8(3):339 345.
119. Guidance for Industry; drug interaction studies study design, data analysis, and implications for dosing and labeling DRAFT. 2006. Food and Drug Administration, Clinical Pharmacology. Avilable at: http://www.fda.gov/cder/guidance/6695dft.pdf
120. Bjornsson TD, Callaghan JT, Einolf HJ, et al. Pharmaceutical Research and Manufacturers of America (PhRMA) Drug Metabolism/Clinical Pharmacology Technical Working Group; FDA Center for Drug Evaluation and Research (CDER). The conduct of in vitro and in vivo drug drug interaction studies: a Pharmaceutical Research and Manufacturers of America (PhRMA) perspective. Drug Metab Dispos 2003; 31(7):815 832.
121. Ring BJ, Patterson BE, Mitchell MI, et al. Effect of tadalafil on cytochrome P450 3A4 mediated clearance: studies in vitro and in vivo. Clin Pharmacol Ther 2005; 77(1):63 75.
122. Mohutsky MA, Chien JY, Ring BJ, et al. Predictions of the in vivo clearance of drugs from rate of loss using human liver microsomes for phase I and phase II biotransformations. Pharm Res 2006; 23(4):654 662.
123. Obach RS. Prediction of human clearance of twenty nine drugs from hepatic microsomal intrinsic clearance data: An examination of in vitro half life approach and nonspecific binding to microsomes. Drug Metab Dispos 1999; 27(11):1350 1359.
124. Ito K, Houston JB. Prediction of human drug clearance from in vitro and preclinical data using physiologically based and empirical approaches. Pharm Res 2005; 22(1):103 112.
125. Obach RS, Baxter JG, Liston TE, et al. The prediction of human pharmacokinetic parameters from preclinical and in vitro metabolism data. J Pharmacol Exp Ther 1997; 283(1):46 58.
126. Nelson DR. Cytochrome P450 nomenclature, 2004. Methods Mol Biol 2006; 320:1 10.
127. Walsky RL, Obach RS. Validated assays for human cytochrome P450 activities. Drug Metab Dispos 2004; 32(6):647 660.
128. Guengerich FP, Wang P, Davidson NK. Estimation of isozymes of microsomal cytochrome P 450 in rats, rabbits, and humans using immunochemical staining coupled with sodium dodecyl sulfate polyacrylamide gel electrophoresis. Biochemistry 1982; 21(7):1698 1706.
129. von Bahr C, Groth CG, Jansson H, et al. Drug metabolism in human liver in vitro: establishment of a human liver bank. Clin Pharmacol Ther 1980; 27(6):711 725.
130. Iyer KR, Sinz MW. Characterization of Phase I and Phase II hepatic drug metabolism activities in a panel of human liver preparations. Chem Biol Interact 1999; 118(2):151 169.
131. Lobo ED, Bergstrom RF, Reddy S, et al. In Vitro and In Vivo Evaluations of Cytochrome P450 1A2 Interactions with Duloxetine. Clin Pharmacokinet 2008; 47(3):191 202.
132. Skinner MH, Kuan HY, Pan A, et al. Duloxetine is both an inhibitor and a substrate of cytochrome P4502D6 in healthy volunteers. Clin Pharmacol Ther 2003; 73(3):170 177.

18
In Vitro Metabolism: Hepatocytes

Michael W. Sinz
Bristol-Myers Squibb Co., Wallingford, Connecticut, U.S.A.

INTRODUCTION

The liver is predominately responsible for metabolism of carbohydrates, proteins, lipids, porphyrins, and bile acids. In addition, the liver serves a significant role in the detoxification, metabolism, and elimination of xenobiotics. The main architectural features of the liver include blood supply (portal vein and hepatic artery), bile canaliculi, phagocytic Kupffer cells, fat-storing stellate cells, Pit cells (lymphocytes) and the major cell type, hepatocytes. Hepatocytes are polarized cells with a sinusoidal membrane (basolateral or blood side) and a canalicular membrane (apical or bile side) with multiple tight and gap junctions between each of the cells. Hepatocytes or parenchymal cells are the functional units of the liver and the major site for biotransformation of xenobiotic and endogenous substrates. Hepatocytes contain the majority of phases I and II drug metabolizing enzymes, as well as several active transport mechanisms (uptake and efflux transporters) (1). Figure 1 illustrates the drug-metabolizing enzymes and transporters found within the hepatocytes and associated with the cell membrane, respectively.

When using hepatocytes as a model system, studies are conducted within a setting that contains physiological concentrations of enzymes and cofactors, as well as the cellular machinery necessary to regulate synthesis and trafficking of new proteins (e.g., enzyme induction). Similar to the hepatocyte found in vivo, xenobiotics must cross biological membranes, interact with cellular organelles/proteins and receptors, and compete with endogenous substrates. In comparison to many other in vitro techniques, such as isolated enzymes, subcellular fractions, or liver homogenates, hepatocytes are clearly more akin to the in vivo environment. Suspensions or primary cultures of hepatocytes have a multitude of applications in the field of drug metabolism from an industrial perspective where they are used as a model system to study drugs in discovery and development as well as use in the pursuit of basic research issues (2 5). In addition, given the extensive number of transporters found associated with hepatocytes, they are often used to assess drug and metabolite transport (6,7). Hepatocytes are also a useful tool for studying the detoxification or toxicity of xenobiotics either directly or derived via metabolism. Finally, the hepatocyte model can be useful in studying liver diseases, such as viral and parasitic infections (8).

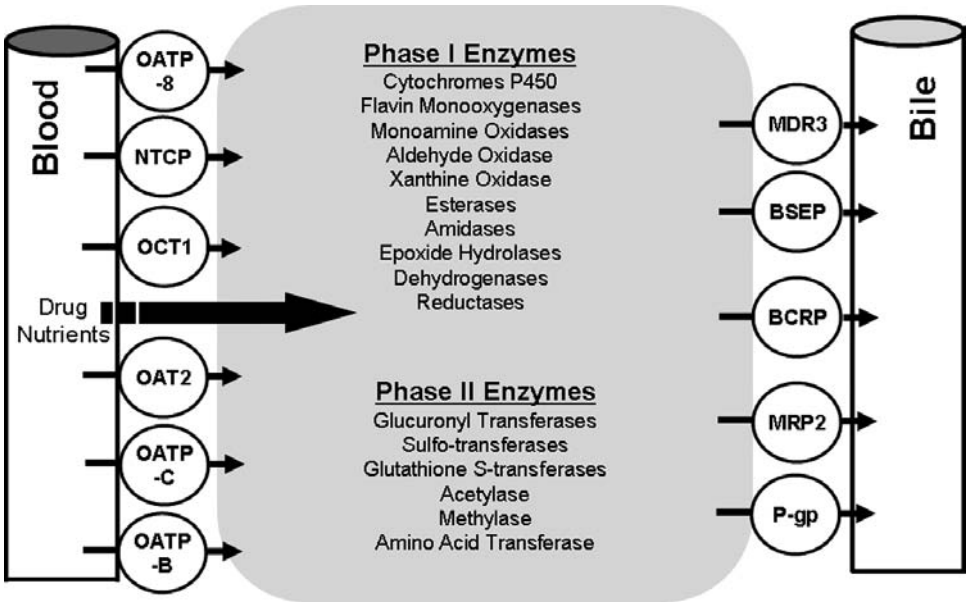

Figure 1 Drug transporters (uptake and efflux) and drug metabolizing enzymes (phases I and II) of the human hepatocyte.

HEPATOCYTE ISOLATION

Historically, cells from liver tissue were isolated as early as the 1940s (9). The early methods typically involved some form of mechanical isolation, which resulted in mostly dead cells or cells so severely damaged that they were unable to survive or maintain normal physiological functions. The discovery of proteolytic enzymes, such as collagenase (EC 3.4.24.3 from *Clostridium hystoliticum*) and hyaluronidase resulted in the development of a new generation of hepatocyte isolation procedures, which were superior to the mechanical methods. The original enzyme procedure involved slicing the liver tissue followed by incubation in buffer containing collagenase and hyaluronidase (10), which was later improved by Fry and Belleman in the 1970s (11 13). In 1969, Berry and Friend established the first protocol involving a liver perfusion technique employing collagenase (2,14). This new perfusion method, commonly referred to as the one-step perfusion method, more efficiently exposed the cells and extracellular matrices to the dissociation buffer and resulted in improved cell yields and viability. Several years later, Seglen refined the perfusion method by introducing the two-step perfusion method (15). The first step involved perfusing the liver with a medium devoid of Ca^{2+} to irreversible cleave desmosomal cell-cell contacts. The second perfusion medium contained collagenase to digest the extracellular matrix (ECM). Only minor changes have been made to the original two-step isolation method over the past 30 years, and it still remains the most common isolation procedure used today.

Isolation of Rat Hepatocytes

The following is a description of the current two-step perfusion method of Seglen employed in many laboratories (2,16 18). Several buffers or media are necessary at

different stages of the isolation and incubation steps, these include (*i*) first perfusion buffer (wash buffer), (*ii*) second perfusion buffer (collagenase buffer), (*iii*) cell wash or isolation buffer, and (*iv*) incubation buffer or media. The initial perfusion buffer is used to remove blood from the liver and deplete the liver of Ca^{2+}. The lack of Ca^{+2} is responsible for the cleavage of desmosomes or zonulae adherens. Desmosomes are adhering junctions on cell membranes that bind cells tightly together and impart strength to the overall tissue. Irreversible desmosomal cleavage is the first important event in hepatocyte isolation. In order to irreversibly cleave the desmosomal contacts, the first buffer should be perfused for a minimum of 10 minutes. Shorter perfusions may result in the desmosomes repairing themselves that can lead to poor cell yields. In order to remove Ca^{2+} ions from the liver, investigators use a wash buffer devoid of Ca^{2+} with or without EGTA [ethylene glycol-bis (beta-aminoethyl ether)-N,N,N′,N′-tetraacetic acid] as a calcium ion chelator. However, it has been found that the addition of 0.1 mM EGTA can prevent the loss of reduced glutathione from the cells (19). The choice of buffering system is also variable among investigators. The two most commonly used buffering systems are HEPES and bicarbonate. The bicarbonate system (e.g., Krebs-Henseleit bicarbonate, KH) is more physiological, but requires continuous bubbling of oxygen and carbon dioxide throughout both perfusion steps to maintain the appropriate pH. HEPES [N-(2-hydroxyethyle) piperazine-N′-(4-butanesulfonic acid)] (10 100 mM), a synthetic buffering system, is more convenient and for some experimental setups may be more appropriate.

Preparation of Buffers

The composition of wash buffer is as follows: NaCl, 120 mM; KCl, 5.3 mM; $NaHCO_3$, 7.4 mM; Na_2HPO_4, 0.3 mM; glucose, 5.6 mM; HEPES, 10 mM; EGTA, 0.5 mM (final pH 7.4). Typically 400 mL of this buffer is prepared for each isolation experiment. The buffer can also be prepared as a 10× solution and stored at 4°C after sterile filtration. The collagenase buffer is similar to that of the wash buffer, except for the addition of calcium chloride and collagenase and omission of EGTA. The composition of collagenase buffer is as follows: NaCl, 120 mM; KCl, 5.3 mM; $NaHCO_3$, 7.4 mM; Na_2HPO_4, 0.3 mM; glucose, 5.6 mM; HEPES, 10 mM; $CaCl_2$, 2.5 mM; 0.04% collagenase, type IV, Sigma Chemical Co., (final pH 7.4). The activities of various collagenases are known to vary, and it is appropriate to evaluate the amount of collagenase necessary for satisfactory liver digestion. Typically 400 mL of this buffer is prepared for each isolation experiment. The buffer can also be prepared as a 10× solution (without addition of $CaCl_2$ and collagenase) and stored at 4°C after sterile filtration. The $CaCl_2$ should be added after the 10× concentrate has been diluted to prevent precipitation of calcium salts, and collagenase should be added just prior to the start of each experiment.

Both perfusion buffers should be well oxygenated prior to the start of experiment and during the experiment if possible to prevent cellular hypoxia. The buffers should also be immersed in a water bath set at approximately 40°C. The actual water bath temperature should be predetermined so that the temperature of the perfusion buffer at the cannula is between 36 to 39°C, the optimal temperature for collagenase activity.

The choice of isolation/wash buffer or media employed to isolate hepatocytes from the digested tissue are quite varied. Commonly, a complete media, such as William's E (WE) or Dulbecco's modified Eagle's medium (DMEM) for both the isolation of cells and incubation medium is used, although simple buffers, such as KH or Hank's balanced salt solution (HBSS), can also be used. In general, for incubations of short duration (30 90 min) a simple buffer may be adequate to maintain cell viability and biotransformation reactions, but for longer incubations (2 4 hours) it is recommended that a more complete media containing essential amino acids and nutrients be employed.

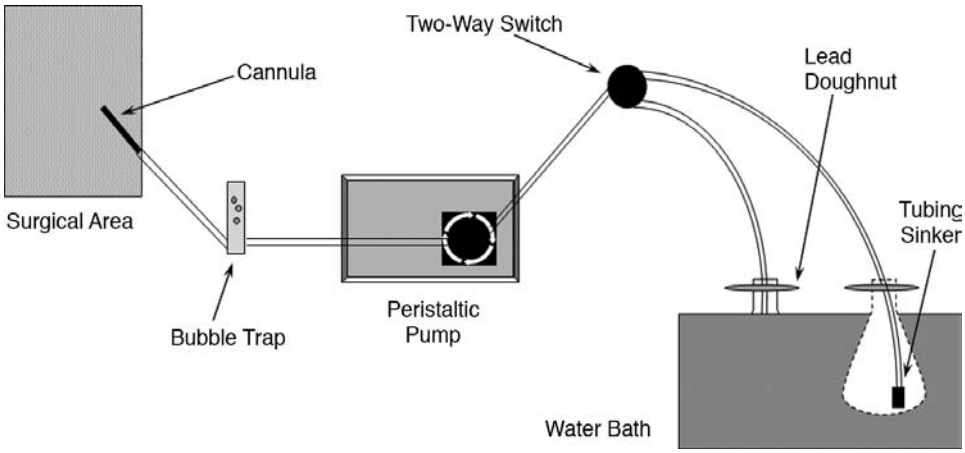

Figure 2 A schematic diagram of the equipment setup for rat hepatocytes.

Equipment and Supplies

The equipment and instruments necessary to perform the isolation are as follows: water bath, peristaltic pump, tubing, tubing end sinkers, bubble trap, two-way switch, lead doughnuts, 20 gauge IV catheter/trocar (catheter and needle assembly, 32 mm) or 18 gauge needle, operating board or grate placed over a drain pan, 3-O surgical silk, surgical scissors (large and small), fine and coarse forceps, sterile saline, cotton-tipped swaps, cotton gauze, stainless steel dog comb (or surgical rake), Erlenmeyer flasks, large glass crystallizing dish ($\sim$125 mL), 50 mL centrifuge tubes, centrifuge, nylon filters (250 and 125 μm), trypan blue solution (0.4%), hemocytometer, and a light microscope.

Oxygenated wash and collagenase buffers are poured into separate 500 mL Erlenmeyer flasks that are placed in the water bath with lead doughnuts. Tubing from the peristaltic pump (with attached end sinkers) is placed in each of the flasks and the catheter placed on the opposite end of the tubing. Figure 2 illustrates the entire apparatus setup.

Surgical Procedure Whole Liver In Situ Perfusion

Rats between 150 to 200 g are optimal for good cell yields and viability. The animal is anesthetized with sodium pentobarbital (60 mg/kg, IP) or isofluorane inhalation. The unconscious animal is placed on an operating board ventral side up. A large U-shaped incision is made on the ventral surface exposing the abdominal cavity all the way to the diaphragm. The cut begins at the midsection of the lower abdomen and progresses up toward the right foreleg. The second portion of the U-shape again starts at the same midsection cut and progresses upward toward the left foreleg. The incisions are best made by first cutting through the skin followed by a second U-shaped incision through the muscle layer. The intestines are gently lifted and moved over and out of the body cavity to the right side of the animal. This exposes the portal vein that is then gently teased away from the surrounding fascia with cotton-tipped swaps and forceps. Three ligatures (3-O silk) are then placed around the portal vein. One ligature is placed near the entrance to the liver, the second approximately 1.0 cm below the first, and the third ligature 1.5 cm below the second. Tie loops are prepared on the first pair of ligatures, but are not tied down. Figure 3 indicates the correct placement of ligatures and cannula. The portal vein is carefully cannulated with the 20 gauge catheter by gently pulling back on the third ligature to straighten and hold in place the portal vein. The cannula/needle assembly is

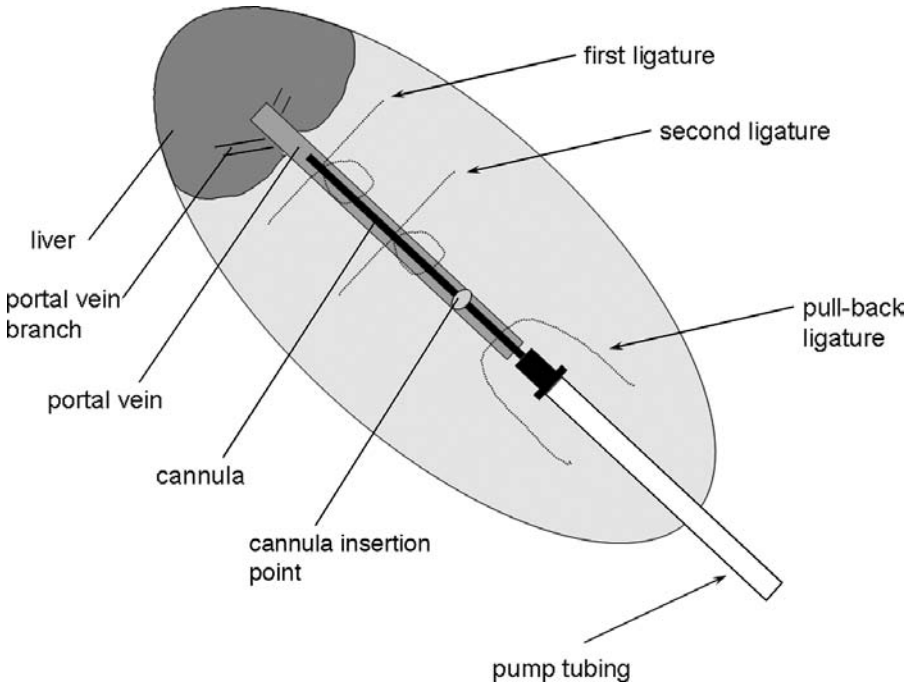

Figure 3 Diagram of rat portal vein cannulation.

inserted into the portal vein at a 25° angle, and the cannula angle immediately reduced to avoid puncture of the underside of the portal vein as the assembly is pushed forward approximately 2 to 3 cm. Once inserted, the needle portion of the assembly is carefully removed. After the needle is removed, blood will begin to flow from the back end of the cannula. The pump tubing is reconnected to the cannula after blood has completely filled the cannula connector so as to prevent an air bubble. The final position of the cannula end should be just below the first venous branch into a liver lobe. The catheter is immediately secured into place by tightening the first and second ligatures around the catheter and the wash buffer started at a flow rate of 15 to 20 mL/min. On starting the wash buffer, the superior vena cava is severed by plunging a pair of fine surgical scissors through the diaphragm and severing the vena cava. The wash buffer will exit the vena cava and drain from the animal. During the perfusion, the liver tissue is kept moist and warm at all times by bathing the tissue with warm saline. The wash buffer is perfused for approximately 10 to 15 min. While the liver is perfused with wash buffer, collagenase (0.04%, w/v) is added to the second perfusion (collagenase) buffer. The collagenase buffer perfusion is initiated by switching the two-way valve, and the liver is perfused for an additional 10 to 20 min. The liver is then carefully removed from the body cavity and placed in a dish containing 50 mL of oxygenated WE. The dog comb is then raked through the tissue to release cells, connective tissue, and any undigested liver tissue. The cells are then placed in a shaking water bath for 15 min at 37°C to allow damaged cells to either repair themselves or expire ($\sim$20 50 rpm). The entire cell suspension is then strained through cheese cloth and centrifuged at 50 $\times$ *g* for 5 min to sediment parenchymal cells from nonparenchymal and dead cells. The supernatant is then carefully removed, the cells gently resuspended in media, and recentrifuged for a total of 3 centrifugation steps. The final cell pellet is resuspended in 40 to 50 mL of WE, which is filtered through 250 and 105 μm nylon

filters. Smaller filters, 60 to 80 μm, may also be used to remove cell aggregates. The final cell suspension is used to determine both viability and cell number. Viability of the initial cell suspension is determined by trypan blue exclusion that determines the integrity of the cell membrane. Only cell suspensions with a percent viability of >85% are deemed acceptable for drug metabolism studies (typical cell viability will range from 90% to 100%). The cells are then diluted to approximately $(0.5-2) \times 10^6$ cells/mL in WE (final cell concentration based on the number of live cells present in the suspension) and used immediately for suspension experiments or placed into primary culture.

Isolation of Human Hepatocytes

The following is a description of the two-step perfusion method for the isolation of human hepatocytes and is based on the biopsy perfusion method with an encapsulated liver lobe of 5 to 50 g (5,20 22). The final viability and cell yield from such an experiment are dependent on the medical/social history of the individual donor, the conditions under which the tissue was removed, preserved, and shipped, as well as the conditions under which the cells are isolated (5,22,23). We have found that freshly excised human livers perfused and shipped with University of Wisconsin or histidine-tryptophan-ketoglutarate solutions on wet ice within 24 hours of tissue harvest result in isolations of viable cells. Isolation of cells from livers that are grossly cirrhotic or have a fat content >50% result in lower cell yields, viability, and attachment efficiency (22).

Preparation of Buffers/Equipment

The perfusion buffers can either be the same as those described for the in situ rat perfusion method or a simpler buffer system containing NaCl, KCl, and HEPES may be substituted. The composition of the simple buffer system is as follows: 5 L of stock buffer are prepared by dissolving 2.5 g of KCl, 41.5 g of NaCl, and 12.0 g of HEPES and adjusting the pH to 7.4 with HCl. The wash buffer is prepared by adding 1.14 g EGTA to 2 L of stock buffer and adjusting the pH to 7.4. The collagenase buffer is prepared by adding 4.0 mL of a 0.37 g/mL solution of calcium chloride to 2 L of the stock buffer and adjusting the pH to 7.4 with NaOH. Collagenase ($\sim$500 mg/1000 mL) is added to the collagenase buffer prior to the start of the experiment. Approximately 100 mL of each buffer are required for each 10 g of liver tissue. Both buffers should be well oxygenated prior to the start of the isolation procedure and during the perfusions if logistics permit. The supplies necessary for the biopsy (encapsulated lobe) perfusion are similar to those already described, except that a multichannel perfusion pump is used and the collagenase buffer is recirculated.

Encapsulated Lobe Perfusion

Both the wash and collagenase buffers are prewarmed in a 45°C water bath. The encapsulated lobe is placed on the operating board (screen) with a drain pan below. Several perfusion lines (1 5) are connected to various sizes of mouse and/or rat oral gavage needles, which are placed into exposed vascular openings on the single cut surface of the encapsulated lobe. Alternatively, 16 to 22 gauge Teflon cannulas, 200 μL pipette tips, or serological pipettes (1 10 mL) can be used in place of gavage needles (5,23). Whatever the choice, each needle/cannula/tip should be sutured or glued into place (Loctite®) to securely attach the needle/cannula to the exposed vessel(s), and the remaining open face of the liver lobe is covered with a thin layer of adhesive. If more than one face of the liver tissue is exposed, the second face should be covered with a layer of adhesive glue. The use of glue serves two purposes: (*i*) hold the cannula in place with a

tight seal and (*ii*) restore the liver capsule to ensure a good perfusion of the tissue. Eventually the perfusate will need to escape the liver; therefore, one to three cuts are made on the capsule opposite the exposed face, thus allowing proper perfusion of the majority of the tissue.

Perfusion of the wash buffer is started at 20 to 30 mL/min/line with a multichannel peristaltic pump and continued for 15 to 20 minutes at which time the wash buffer is replaced with the collagenase buffer, which is perfused for an additional 20 to 25 minutes. The wash buffer is not recirculated, but the collagenase buffer is recirculated to conserve collagenase. It is important that the tissue be warmed to 37 to 38°C as quickly as possible and that as much of the UW (University of Wisconsin) solution be removed from the tissue for maximum effect of buffers and collagenase. The tissue is kept moist and warm at all times by bathing with warm saline, except during the perfusion of the collagenase buffer where additional saline will dilute and contaminate the buffer. Alternatively, submerging the liver tissue in calcium-free and then collagenase buffers during perfusion will help maintain the proper temperature (5). After perfusion, the liver is placed in a glass dish and cut into small sections to disperse digested portions of the tissue. Tissue sections are also further disintegrated with a dog comb or tissue rake. Isolated hepatocytes are washed with freshly oxygenated WE and separated from undigested tissue by filtration through cheese cloth. The hepatocytes are further purified as previously described with rat hepatocytes. Although cell yields will depend on the quality of the donor liver and vary between laboratories, several researches have reported cell yields of 7 20 $\times$ 10^6 cells/g tissue and 1 15 $\times$ 10^6 cells/g tissue (mean of 6 $\times$ 10^6 cells/g tissue) (21,24).

Isolation from Other Species, Sterile Isolation, Percoll Isolation Procedure, and Cryopreservation

Isolation of Hepatocytes from Other Animal Species

Hepatocytes have been isolated from a variety of animal species. The most common species are those associated with the pharmaceutical industry, such as rat, mouse, dog, monkey, rabbit, as well as human (5,16 18,21 23,25 31). Hepatocytes have also been isolated from a number of agricultural species, such as cow, pig, horse, sheep, chicken, duck, goat, and deer (32 38). Various other species include guinea pig, hamster, gerbil, cat, amphibians, and fish (39 47). The rat in situ or human biopsy perfusion methods are readily adaptable to the isolation of hepatocytes from many different animal species. Whole liver perfusions are most common with smaller animals, such as mouse, hamster, guinea pig, monkey, or rabbit, and the wedge biopsy or single-lobe perfusion methods employed for larger species, such as the dog. Whole liver perfusions can be performed on larger species, albeit they are much more expensive in terms of collagenase, and for most experimental needs the large number of cells isolated from a single liver is not immediately necessary. However, cryopreservation methods have improved so that unused cells can be properly frozen and stored for future experiments. Finally, several detailed experimental protocols are noted for the isolation of mouse, rabbit, guinea pig, hamster, dog, monkey, horse, cow, pig, and fish hepatocytes (25,27,28,30 33,35,40,45,48).

Sterile Isolation

Hepatocytes that are to be used in suspension generally do not require aseptic isolation; however, hepatocytes placed in primary culture do require special treatment in the preparation of buffers and equipment as well as the actual isolation procedure. Some details are listed below that should be considered when isolating cells for primary culture.

In all cases, it is best to work in a sterile environment as much as possible, and all solutions should be filtered through a 0.2 μm filter. All surgical apparatus and pump tubing should be sterilized prior to use. Generally, penicillin (100 U/mL) and streptomycin (100 μg/mL) should be used in the cell isolation and culture media. Prior to surgery, it is recommended to shave and clean the rat abdomen with 70% ethanol or Betadine to prevent contamination from the outer surface of the animal. Once the cells have been isolated, all centrifugation steps and any additional procedures should be done with sterile tubes and dishes. All of the remaining isolation steps (tissue disintegration, filtration, and plating) should be conducted in a sterile environment.

Percoll Isolation Procedure

In instances where cell viability is low (<85%), more elaborate means of cell isolation in addition to centrifugation are necessary. Normally, this additional isolation procedure is unnecessary with rat hepatocytes; however, the use of Percoll is often necessary when isolating human hepatocytes, which often results in the isolation of significant numbers of unviable cells. Cells with damaged membranes when incubated in suspension or primary culture will release proteolytic enzymes that can be detrimental to intact surrounding cells; therefore, removal of damaged cells is beneficial. The use of Percoll, a colloidal suspension of silica particles coated with polyvinylpyrrolidine, has been shown to effectively separate damaged hepatocytes and other nonparenchymal cells from intact hepatocytes. The procedure involves centrifuging the cell suspension through a Percoll medium with a density of 1.06 g/mL. The resulting cell pellet contains predominately viable hepatocytes while damaged cells, cellular debris, cell aggregates, and non-parenchymal cells remain suspended in the Percoll medium. Hepatocytes isolated by the Percoll method have been shown to exhibit superior characteristics (longer viability, CYP450 maintenance, membrane transport, and drug metabolism capacity) compared with cells isolated by low-speed centrifugation (49,50). An isotonic solution of Percoll is prepared with KH, HBSS, or PBS to give a density of 1.06 g/mL and mixed with cells [(1 3) $\times$ 10^6 cells per total volume] in a 50-mL centrifuge tube. The mixture is then centrifuged at (50 70) $\times$ g for 10 min. If the hepatocytes do not sediment after centrifugation, either dilute the Percoll media and centrifuge a second time, centrifuge the cells at a slightly higher g-force, or centrifuge the cells for a longer period of time. Finally, wash the cells with culture media once or twice $\times$ (50 $\times$ g for 3 min) to remove any remaining Percoll before use.

Cryopreservation

There are times when the numbers of cells isolated from a single liver are so great or the cells are of such significance that long-term storage of unused freshly isolated cells would be advantageous. The ability to cryopreserve hepatocytes for long periods of time and utilize them when needed would be beneficial particularly with human hepatocytes where there is difficulty in obtaining tissue and controlling the frequency at which tissue becomes available.

There are many methods for cryopreserving cells, but all utilize penetrating and nonpenetrating cryoprotectants. For example, DMSO and glycerol are common penetrating cryoprotectants while dextran and polyvinylprrolidine (PVP) are non-penetrating cryoprotectants. When cryopreserving hepatocytes, 10% DMSO is commonly used along with the addition of optional cryoprotectants, such as fetal calf serum or PVP to enhance viability, plating efficiency, or enzyme function after thawing (51 53). In the presence of cryoprotectant, the cells undergo controlled freezing down to -80 to -196°C

(liquid nitrogen). In general, the freezing rate is slow enough to reduce the formation of ice crystals, which will damage the cells, as well as minimize the release of heat (heat of fusion) when crystals start to form (52). When the cells are needed for use in experiments, they are rapidly thawed at 37°C over one to two minutes and the cryoprotectant immediately diluted in media to prevent cell toxicity. Once diluted, it is advisable to further isolate intact hepatocytes using Percoll, which has been shown to improve plating efficiency and drug metabolism (52).

The optimal scenario would be the ability to freeze hepatocytes and retrieve them from storage with similar viability and cellular function as freshly isolated cells. For the most part, cryopreserved hepatocytes function in a similar manner as freshly isolated cells, albeit some loss of total cell viability is expected and can be managed by Percoll. After cryopreservation, CYP450-mediated oxidation, glucuronidation, sulfation, and epoxide hydrolase activities are similar to fresh hepatocytes; however, glutathione conjugation was found to be significantly decreased (52,54,55). Sohlenius-Sternbeck determined that glutathione transferase activity was unaffected by cryopreservation, but that glutathione levels were dramatically decreased (>90%) (55). In addition, when cryopreserved hepatocytes are plated in a sandwich culture, multiple uptake and efflux transporter were found to be functional (NTCP, OATP, MDR1, MRP2, BSEP, and BCRP) (56). These data would indicate that cryopreserved hepatocytes are functionally capable for use in drug metabolism and transporter studies, albeit glutathione conjugation is not represented in the overall metabolic profile, and fresh hepatocytes should be used for this purpose.

Attachment or plating efficiency is somehow compromised even when cryopreserved cells are properly frozen and thawed. Attachment of cells is batch (donor) dependent and only some donor hepatocytes sufficiently attach after cryopreservation. One important factor in the plating efficiency of cryopreserved hepatocytes is the quality of the cells prior to freezing. Damaged cells are unlikely to survive the osmotic changes that occur during freezing and thawing and therefore do not recover appropriately after thawing. In recent years, methods to improve the plating efficiency after cryopreservation have been proposed; these generally include a brief incubation time in which the cells repair themselves prior to freezing. Techniques such as incubating cells in media at 37°C for 30 minutes prior to freezing or plating the cells as a monolayer or sandwich culture on collagen-coated dishes prior to freezing have been shown to increase the plating efficiency of cryopreserved hepatocytes (51,57,9).

Hepatocyte Viability and Functional Assessment

After the isolation of cells, functional capabilities and viability of each preparation should be examined. Depending on the type of experiment to be performed, different types of functional assays may be necessary. In all cases, the viability of the preparation should be evaluated by one or more techniques. The most common methods of assessing hepatocyte viability are cell membrane integrity (trypan blue, lactate dehydrogenase, visual inspection) and cellular or enzyme function (ATP content, MTT, CYP450 activity). Trypan blue dye exclusion is by far the most popular method for assessing cell viability. This assay measures the integrity of the cell membrane by excluding trypan blue dye, which binds to nuclear DNA if the membrane is damaged. Trypan blue is a fast and simple assay and is generally coupled to the determination of cell number. Lactate dehydrogenase enzyme leakage and visual inspection of the cell membrane under a light microscope are alternative methods to assess cell viability (58). Cell blebbing (small extrusions or extension of the cell membrane) are often observed and are indicative of membrane damage. Often these blebs will contract and the membrane will repair itself,

other times the damage is too great and the cells will die. Additional methods to assess viability or cytotoxicity include measuring ATP content or mitochondrial function with the tetrazolium dye MTT (54,59). For drug metabolism studies, measurement of total CYP450 content or specific drug-metabolizing enzyme activities (phases I and II) can be useful to assess metabolic capability (60 62). In general, it is best to use at least one test for cell viability and one for functionality with each hepatocyte preparation. In all instances, the data obtained from hepatocyte experiments need to be normalized to some factor that allows interpretation of data between different cell preparations. Normalizing the data to the number of cells present, typically "per 10^6 cells," is the most common approach. Quantitation of protein content, cellular DNA, or total spectral CYP450 are other common method of normalizing hepatocyte data (27,63 65).

Hepatocytes in Suspension or Primary Culture

Isolated hepatocytes in suspension are a uniquely simple drug-metabolizing system requiring no additional cofactors, except for an adequate buffer system for incubations. Commonly a complete media, such as WE or DMEM, which contain many of the nutrients necessary for cell survival are used; however simple buffers, such as phosphate buffer or HBSS, can be employed for short-term incubations. Experiments performed in hepatocyte suspensions are initiated by the addition of a substrate after which sample aliquots are removed at appropriate time points. Hepatocytes survive in suspension for three to four hours with gentle agitation and oxygenation, after which significant cell death begins to occur. Sample preparation and extraction are similar to those employed with other in vitro methods, except that higher protein and salt content of hepatocyte suspensions can cause greater problems with extraction, reconstitution, and detection of parent drug or metabolites.

Hepatocytes by nature survive only when attached to a substratum (anchorage dependent); therefore, suspension experiments are considered short-term experiments, whereas hepatocytes in culture attached to an ECM are considered long-term experiments. A major advantage of employing hepatocytes in primary culture is the ability to study drug metabolism, pharmacological, or toxicological events that take longer than three to four hours to manifest themselves. However, to better understand the application of hepatocytes in cell culture, one must appreciate the cellular events that occur during cell isolation, and how they subsequently affect the hepatocyte in culture. During the process of cell isolation, cellular contacts are disrupted between cells and multiple phenotypic and gene expression changes begin to occur. The cellular changes arise from three identified area: (*i*) oxidative stress, (*ii*) contaminants in collagenase, and (*iii*) disruption of cell contacts (66,67). Oxidative stress or ischemia-reperfusion-induced stress during cell isolation occurs when the tissue is deprived of oxygen for a period of time and then is reoxygenated (66). Also, endotoxins present in the crude preparations of collagenase can elicit a cascade of events that disrupt cell homeostasis, such as inflammation and cytokine release. Finally, destruction of the cellular architecture, cell contacts, and detachment from an ECM during the cell isolation procedure activate apoptotic signals leading to cell death. All or any one of these insults to the hepatocyte place it on a road to dedifferentiation or cell death. Elaut et al. provides an excellent review of these topics as they relate to hepatocyte isolation and culture (66).

The most significant change that occurs when hepatocytes are placed in culture is the loss of differentiated function (cellular dedifferentiation, i.e., loss of liver-specific functions). The most dramatic phenotypic change observed in culture is the rapid decline in CYP450 levels, that is, significant loss of CYP450 gene expression immediately after

cell isolation followed by a subsequent loss of enzymatic activity. Several investigators have shown that with rat hepatocytes in culture, total CYP450 levels decrease by 50% to 80% in the first 24 hours and continue to fall significantly through 72 hours (28,38,68 71). Each of the CYP450 isoenzymes appears to have its own half-life with some decreasing rapidly while others remain reasonably stable. For example, with human hepatocytes CYP1A2, CYP2A6, and CYP2B6 decline very rapidly, while CYP2C9, CYP2E1, and CYP3A4 decline at a modest rate, and CYP2D6 falls to about 50% and then remains constant when measured over three days (72,73). In some situations, human CYP450 enzymes have shown an initial decline in activity over the first three days in culture but then demonstrate an increase in activity over days 3 to 6. In particular CYP3A4 was shown to return to a level similar to fresh hepatocytes on day 4 in culture, while the CYP2Cs increased to levels at day 4 that were greater than fresh hepatocytes (4,74). Total CYP450 levels in primary cultures of rat, monkey, and mouse hepatocytes appear to decline rapidly (60 80% loss in 24 hours), whereas CYP450 levels in hamster hepatocytes fall moderately (50% loss in 24 hours) and CYP450 levels in rabbit and human cells decline at a slower rate ($\sim$35% loss in 24 hours) (28,38,69,73,75 78). The rate and extent of CYP450 loss is dependent on the species as indicated above, but also on the culture conditions (such as monolayer vs. sandwich culture or the addition of supplements to the media). In general, the conditions which best retain CYP450 function are sandwich culture with serum-free media containing dexamethasone (3). Ultimately, if the objective of a hepatocyte culture experiment is dependent on the enzymatic capacity of one or more drug-metabolizing enzymes, then these activities should be measured over the time course of the experiment under the culture conditions employed to ensure adequate expression and activity.

Suitable cell culture methods are those that maintain the original differentiated state, for example, cell morphology, cell polarity, cell-cell contacts, expression and induction of enzymatic activity/transporters, and metabolism of xenobiotics. The main factors that have significant bearing on this maintenance are: type and format of the ECM on which the cells attach, media supplements, and plating density. When first placed in culture, some of the architectural components of liver structure are restored, such as attachment to a basement membrane, cell-cell contacts, and regeneration of membrane receptors that may have been removed or internalized during cell isolation. The currently used ECM materials are collagen (rigid or gelled) and Matrigel. When human hepatocytes are attached to a rigid collagen monolayer, they have a flattened appearance and will spread out until the plate becomes confluent, and cell-cell contacts are reestablished. When human hepatocytes are plated as a monolayer on Matrigel, they tend to form clusters and aggregates and retain a more rounded appearance. In addition to the type of ECM, the three-dimensional structure or geometry of the ECM surrounding the cells also plays an important role. Some methods use cells attached to a substratum of ECM in monolayer culture; however, a useful technique that results in improved cell morphology and function is the sandwich technique with either collagen, Matrigel, or a combination of both ECMs (4,56,79,80). When cells are plated in sandwich culture (hepatocytes plated on a basement ECM and overlaid with ECM) of either collagen-collagen or collagen-Matrigel, they establish a cuboidal shape similar to that found in the liver. Hepatocytes in sandwich culture (collagen-collagen or collagen-Matrigel) will also spread out and reestablish cell-cell contacts, whereas cells plated in a sandwich of gelled collagen will form cord-like arrays (4). Cells in the sandwich culture reestablish normal morphology, reform tight/gap junctions, have better cell viability and attachment efficiency, and display hepatocyte-specific functions for longer periods of times. In addition, they reestablish normal cell polarity, express drug transporters, and reform bile canaliculi providing the opportunity to measure hepatic uptake and biliary clearance (4,56). LeCluyse et al. provides an excellent methodology for

establishing human hepatocytes in sandwich culture (5). Interestingly, metabolism studies with rat hepatocytes demonstrate a greater responsiveness to inducers and improved cell viability if the cells are plated in sandwich culture and do not perform as well as human hepatocytes in monolayer (79,81,82).

Different culture media have been employed over the years, such as DMEM, Chee's, and WE, and they all appear to perform in a similar fashion, although the supplements or additives to each of these base media can have profound effects on the viability and response of hepatocytes in culture. For most short-term cell culture experiments ($\sim$1 2 weeks), a base medium supplemented with insulin, transferrin, selenium, and dexamethasone appears to provide optimal cell culture conditions and is most often employed when culturing human hepatocytes (4). Alternatively, for longer-term cultures, Yamamoto has demonstrated that an optimized media can retain hepatocyte-like function for up to two to four weeks (83). Often, cells are plated in serum containing media and allowed to attach for several hours; however, at the first media change, serum-free media is used. Serum aids in the attachment of cells; however, it has detrimental effects on the expression of hepatocyte-like function over time. For example, serum has been shown to inhibit the reformation of bile canaliculi (3,84).

In addition to ECM and media, cell-plating density can have a dramatic effect on cell morphology and function. Cells are plated at or near confluency, which minimizes cell flattening and spreading (both of which disrupt normal cell architecture) and help maintain normal cell function (4,85). The optimal seeding density for human hepatocytes has been determined to be (1.25 1.5) $\times$ 10^5 cells/cm^2 (5). This seeding density is similar for rat hepatocytes that are approximately the same size as human hepatocytes ($\sim$17 22 μm); however, the seeding density should be adjusted slightly up and down for monkey (10 μm) and mouse ($\sim$30 μm) hepatocytes, respectively because of their differences in cell size (2).

DRUG METABOLISM–RELATED STUDIES WITH ANIMAL AND HUMAN HEPATOCYTES

Metabolite Identification and Species Differences

When one begins to examine the vast number of research articles describing various techniques and methods of employing hepatocytes, it becomes apparent that an enormous amount of research has been conducted in this area. Early publications on hepatocytes described methodologies to isolate intact cells and their use in the evaluation of hepatic biochemistry. Subsequent to these earlier studies, hepatocytes were used to study multiple aspects of drug metabolism, transport, and toxicity (3,21,54,86 89). Hepatocytes were first employed as a model of drug metabolism as early as 1969 when Henderson and Dewaide examined the metabolism of aminopyrine, aniline, and *para*-nitrophenol in rat hepatocytes (90). Freshly isolated hepatocytes contain physiological levels of all hepatic drug metabolizing enzymes and cofactors making them suitable for a myriad of drug metabolism studies. By employing hepatocytes in metabolite identification, there exists the ability to assess both phases I and II reactions that can occur sequentially or independently, for example, phase I hydroxylation followed by sulfation or direct phase II glucuronidation of a molecule. An example of this integrated metabolism is illustrated with the metabolism of CI-976 in rat hepatocytes (Fig. 4). CI-976 is metabolized predominately by ω-hydroxylation at the terminal carbon of the long alkyl chain in liver microsomes. However, in vivo the major metabolite is a six-carbon chain shortened carboxylic acid derivative (65). In this instance, hepatocytes were able to recapitulate the

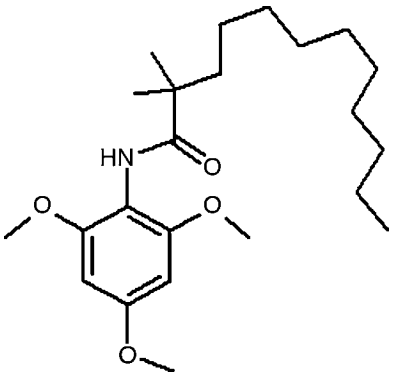

Figure 4 Structure of CI 976.

integrated metabolism of CYP450-mediated oxidation followed by β-oxidation, while the microsomal metabolism provided an incomplete picture of overall metabolism. During the course of such metabolite identification experiments, reaction phenotyping (identification of the enzyme involved in metabolic pathways) is often conducted with the use of specific enzyme inhibitors and inducing agents. Such was the case with CI-976 reaction phenotyping when several inhibitors/inducers of CYP450 and β-oxidation were employed to elucidate the enzymes and organelles involved in metabolism of the fatty acid like alkyl chain (65).

Human hepatocytes offer a distinct advantage over other models in that they provide a comprehensive human metabolic profile well in advance of clinical studies. In addition, they provide information on metabolites that are often difficult to identify or ascertain, such as those that are not found in the systemic circulation but are eliminated predominately in human bile. In a very unique experiment, Ponsoda et al. was able to evaluate the in vitro metabolism of accelofenac in human hepatocytes obtained from liver biopsies of patients who subsequently received an oral dose of accelofenac shortly after the biopsy (91). The in vitro metabolism of accelofenac in hepatocytes was very similar to the urine metabolite profile for each patient, and the inter-individual differences observed in each of the patient profiles was reflected in the hepatocyte profiles. These results indicate that hepatocytes placed in culture have the ability to accurately represent human metabolism as well as the phenotypic variability between individuals. In addition, the metabolic profile obtained from human hepatocytes can be compared with the in vitro hepatocyte and in vivo profiles from multiple animals species, that is, cross-species metabolic profiling. This type of comparison (animal in vitro and in vivo) provides greater confidence that the in vitro human hepatocyte metabolite profile will be similar to the human in vivo metabolism.

Metabolic Stability and Prediction of Hepatic Clearance

In general, low to moderate clearance drugs are desired in order to achieve once or twice a day dosing of new medications and most often, the predominant clearance pathway is metabolic clearance. Liver microsomes and hepatocytes are routinely used to make early assessments of metabolic stability in drug discovery and, with more detailed experiments, can be used to predict animal or human hepatic metabolic clearance. In both cases, the in vitro models can be used to assess metabolic stability or predict clearance, rank order compounds, and construct structure-metabolism relationships to block metabolic soft

spots and increase metabolic stability. Although microsomes are a good initial high-throughput screen to assess metabolic stability, they only represent the majority of oxidative pathways and not phase II reactions. Whereas the hepatocytes offer a wide range of integrated drug-metabolizing pathways, they often predict in vivo hepatic clearance better than liver microsomes (92,93).

A great deal of literature discusses the use of fresh versus cryopreserved hepatocytes and suspension versus cultured hepatocytes for the assessment of metabolic stability (3,54,94 96). Overall there appears to be little difference in rates of metabolism between fresh and cryopreserved hepatocytes with the exception that cryopreserved hepatocytes do contain lower concentrations of glutathione, and this pathway may be underrepresented (55). However, cryopreserved hepatocytes offer the advantage of availability and routine screening compared with fresh hepatocytes (96). Regarding suspension versus cultured hepatocytes, both methods are employed, and it has been shown that compounds with rapid turnover are better represented in fresh hepatocytes, and low-turnover compounds are better represented in cultured hepatocytes (94 96). Most often fresh or cryopreserved hepatocytes in suspension are considered to be more appropriate as they contain physiological levels of drug-metabolizing enzymes and cofactors and should therefore identify high to moderate clearance compounds quite well. However, if an accurate prediction of hepatic clearance is needed for a low-turnover compound, cultured hepatocytes where longer incubation times are possible may be appropriate.

The general procedure for assessing metabolic stability or clearance involves incubating the compound of interest and removing aliquots of drug and/or metabolites at various time points. Linearity with respect to time and cell density are important and that the drug concentration be low (often below the K_m) to ensure first order kinetics. This can be assessed by either measuring formation of metabolite(s) or more often by measuring the depletion of substrate. The two most common methods of determining hepatic intrinsic clearance (CL_i) are: determination of K_m and V_{max} kinetic parameters ($CL_i = V_{max}/K_m$) or metabolic half-life ($CL_i = 0.693/\text{half-life} \times 10^6$ cells/mL). In both situations, the resulting units are μL/min/10^6 cells, which can be scaled to whole liver intrinsic clearance by using scaling factors, such as "10^6 cells/g liver tissue" known as the hepatocellularity and "g liver tissue/kg body weight," which convert in vitro CL_i to an in vivo clearance value (mL/min/kg). Table 1 contains various constants used when scaling rate of hepatocyte metabolism to in vivo hepatic clearance (CL_H) by using the equation: $CL_H = Q_H \times F_{ub} \times CL_i/Q_H + F_{ub} \times CL_i$ (where Q_H is the hepatic blood flow and F_{ub} is the fraction drug unbound).

The two most commonly scaled species are rat and human, and considerable effort has gone into determining the hepatocellularity of these two species. Reviewing numerous references describing rat hepatocellularity, the numbers vary from (97 167) $\times 10^6$ cells/g liver; however, the average and most often cited value is 120 $\times 10^6$ cells/g liver. For

Table 1 Hepatocellularity and Scaling Factors for Hepatic Clearance Determination

Species	Hepatocellularity (10^6 cells/g liver)	Grams liver/kg body weight (97)	Liver blood blow (mL/min/kg) (97)
Mouse	135 (98)	87.5	90
Rat	120, 117 (98)	40.0	55.2
Rabbit	114 (98)	30.8	70.8
Dog	240 (99), 215 (98)	32.0	30.9
Monkey	135 (100)	30.0	43.6
Human	139 (98), 99 (101)	25.7	20.7

humans, the two most recent publications indicate 99×10^6 cells/g liver (geometric mean with a 95% CI: 74 131) and 139×10^6 cells/g liver (101,98).

It should be noted that these clearance predictions represent metabolic hepatic clearance and will not represent total body clearance when considerable extrahepatic metabolism occurs or when renal/biliary elimination of the parent drug is significant. In the end, it is prudent to develop a correlation between in vitro hepatocyte clearance and in vivo animal clearance in order to build confidence that the hepatocytes are representing the major pathway of elimination. For example, if rat hepatocytes do not correlate with rat in vivo clearance, then there would be little reason to believe that the human hepatocyte clearance would be predictive of drug clearance in patients (assuming similar metabolic and elimination profiles between rats and humans).

Drug-Drug Interactions

Inhibition of drug-metabolizing enzymes has serious consequences when co-administered drugs lead to harmful or sometimes fatal increases in drug exposure. Most often inhibition of CYP450 enzymes is the culprit in drug-drug interactions, and screening or characterization of enzyme inhibition has routinely been assessed using human liver microsomes. Liver microsomes are readily accessible for routine experiments, amenable to high-throughput methodologies, easy to use, and have established a wealth of comparative and correlative data with clinical drug interactions. However, theoretically hepatocytes should provide an improved model to predict human-drug interactions due to several key features, which are similar to the in vivo environment where drug and hepatocyte interact. For example, hepatocytes have a cell membrane, which drugs must pass through either by passive diffusion or transport (efflux and uptake), and contain drug-metabolizing enzymes, intracellular proteins, and organelles in which the drug must interact. All of these aspects can affect the drug concentration inside the cell and at the enzyme site. Unfortunately, the methods for employing hepatocytes for routine enzyme inhibition studies are not completely understood or consistent between laboratories. For example, the omission or addition of serum to hepatocyte incubations, increased nonspecific binding to hepatocytes, or the use of suspension versus cultured hepatocytes are all variables that are not well understood (87,89,102 104). In addition, there is not an extensive database of information on enzyme inhibition in hepatocytes to actual in vivo drug-drug interactions. In general, inhibitory constants (IC_{50} or K_i) tend to be higher using hepatocytes compared with recombinant CYP450 systems or liver microsomes. This shift toward lower inhibition potential is probably due to increased nonspecific binding or metabolism of the drug both of which can effect drug concentration (87,89). Nonetheless, with further evaluation and standardization, human hepatocytes may become the next enzyme inhibition model with greater accuracy and predictive power in the assessment of drug-drug interactions. Several laboratories have begun to establish the necessary correlations between hepatocytes, recombinant enzymes, microsomes, and clinical data to better understand the predictive power of human hepatocytes in estimating enzyme inhibition (87,89,102). In addition to reversible inhibition of CYP450 enzymes, hepatocytes have also been utilized to evaluate time-dependent or irreversible inactivation of CYP450 enzymes (89,105,106).

In contrast to the limited use of hepatocytes to assess enzyme inhibition, the cultured primary human hepatocyte model is the most common and widely accepted means to predict drug-drug interactions mediated by enzyme induction (21,89). In addition to the host of drug-metabolizing enzymes, hepatocytes also contain physiological concentrations of nuclear hormone receptors and transcription factors necessary to initiate

and mediate induction of drug-metabolizing enzymes and drug transporters (107,108). In addition, extensive research and literature has solidified the general methodology of hepatocyte culture and the in vitro-in vivo correlation between induction response in hepatocytes and drug-drug interactions in patients (4,109,110). In general, hepatocytes (fresh or cryopreserved) are plated as a monolayer on collagen or sandwiched between collagen and Matrigel and allowed to adapt (recover) for one to two days. After this adaptation period, the cells are treated for three days with varying concentrations of test compound, refreshing the media and test compound each day. At the end of three days, the enzyme activity of CYP450 isoforms is measured either in situ or from microsomes prepared from hepatocytes. In addition to enzyme activity, RNA expression of drug-metabolizing enzymes and transporters can also be measured, as well as the protein level by SDS-PAGE Western blotting. When assessing the actual drug interaction potential of a test compound, the U.S. FDA has indicated that enzyme activity is the most relevant parameter to predict enzyme induction potential in humans, albeit quantitation of RNA expression changes or protein levels can be helpful in uncovering effects that may influence the overall induction response (111). For example, measuring RNA expression in addition to enzyme activity is especially important when evaluating the induction potential of a compound, which is also an inhibitor of the same enzyme.

The most common inducing agents employed as positive controls are: omeprazole, β-naphthoflavone, or 3-methylcholanthrene for CYP1A2; phenobarbital for CYP2B6; and rifampicin for CYP3A4, as well as their enzyme activity probes: phenacetin O-deethylation for CYP1A2; efavirenz hydroxylation, or bupropion hydroxylation for CYP2B6; and midazolam 1′-hydroxylation or testosterone 6β-hydroxylation for CYP3A4 (3,111). At the time of this writing, the most commonly accepted quantitative measure to predict enzyme induction mediated drug interactions was the following: when a test compound, at or near therapeutic drug concentrations, increases the enzyme activity of a particular CYP450 enzyme greater than 40% of the positive control for that CYP450 enzyme, then the test compound is anticipated to cause drug interactions due to enzyme induction. However, other evaluations that involve efficacy and potency measures, such as E_{max} and EC_{50}, as well as no effect level (NOEL) are being proposed and evaluated (112). All of these semiquantitative measures appear to work well for known enzyme inducers, in particular those mediated through CYP3A4 where the greatest number of clinical drug-drug interactions are known.

Drug Transporters and Hepatotoxicity

The transport of xenobiotics into (uptake) and out (efflux) of hepatocytes can be studied with suspensions and cultures of fresh and cryopreserved hepatocytes (3,21,89). Several laboratories have established the presence of transporters on hepatocytes, such as the uptake transporters sodium taurocholate cotransporting protein (NTCP) and organic anion transporting proteins (OATP1B1/1B3), as well as efflux transporters, such as multidrug-resistance protein (MDR1, P-gp), multidrug resistance associated protein (MRP2), bile salt export protein (BSEP), and breast cancer resistance protein (BCRP) (Fig. 1) (7,56). Hepatocyte uptake studies can be conducted in cell suspension or monolayer culture often by measuring uptake of a radiolabeled substrate or in the presence of specific transport inhibitors (3). When hepatocytes are placed in a sandwich format, they repolarize and reestablish vectoral excretion of substrates (i.e., uptake on the basolateral surface coupled with efflux on the canalicular surface) (7,56). In addition, they reform bile canaliculi as described previously, which provides the means to study biliary

excretion (56). Also, drug-drug interactions (inhibition and induction) related to transporters can be evaluated in hepatocytes (113). For example, Shitara et al. were able to elucidate the mechanism behind the clinically relevant drug-drug interaction between cerivastatin and cyclosporine A using human hepatocytes indicating that the interaction was due to inhibition of cerivastatin uptake by cyclosporine A (114).

Hepatotoxicity can be mediated by the drug itself or by metabolism to reactive or toxic metabolites. Suspensions or cultures of hepatocytes provide an opportunity to evaluate many of the aspects involved in hepatotoxicity, with integration of metabolism, drug transport, and toxicity. Although hepatocytes do not represent the entire organ due to the absence of many other cell types (e.g., Kupffer cells), which may participate in the overall toxic mechanism or response, they do represent the majority of processes involved in hepatotoxicity. Cells in both suspension and culture are employed throughout drug discovery and development as screening models, as well as mechanistic models to investigate in vivo hepatotoxicity or idiosyncratic toxicities (115 117). As described previously, cells in suspension contain physiological concentrations of drug-metabolizing enzymes but can only be incubated for short periods of time, and cells in culture allow for longer drug exposures and the participation of drug transporters but will generally have lower levels of enzymes; hence, the most appropriate hepatocyte model configuration will depend on the nature of the toxic event.

NOVEL HEPATOCYTE–LIKE MODELS

Immortalized Hepatocytes

Primary human hepatocytes are commonly used in drug metabolism related studies; however, their limited supply, decline in expression of drug-metabolizing enzymes, and significant donor-to-donor variation complicate their use in early drug discovery. Hence, there is a need to generate human immortalized cell lines that provide a continuous supply of cells while maintaining stable expression of necessary enzymes, transporters, and nuclear hormone receptors for routine screening of metabolism and enzyme induction. Immortalized cells are defined as cells that can grow and divide indefinitely under optimal culture conditions (118). Immortalized cells can occur naturally (e.g., hepatocarcinoma) or by converting primary hepatocytes into nontumorigenic immortalized cells (119). There are many different approaches employed to immortalize primary hepatocytes, but the most common methods of immortalization are overexpression of SV-40 large T antigen (viral oncogene) or expression of telomerase reverse transcriptase (TERT). With any of the immortalized cell lines, the goal is to identify a line that maintains the phenotypic characteristics of hepatocytes and provides an unlimited, stable supply of cells. Several reviews have compared the most recent cell lines as to their expression patterns and utility in drug metabolism (3,120,121). The following sections describe some of the most commonly cited immortalized cell lines.

The most well-characterized and widely used immortalized cell line is the HepG2 cell line (established in 1979). While retaining some liver-specific functions, HepG2 cells have low expression and activity of CYP450 and phase II enzymes (122). Mostly, fetal isoforms, such as CYP1A1 and CYP3A7, are expressed in high levels; however, compared with the expression levels in cryopreserved human hepatocytes, HepG2 cells expresses much lower levels of all major CYP450s (CYP1A1, CYP1A2, CYP2A6, CYP2B6, CYP2C8, CYP2C9, CYP2C19, CYP2D6, CYP2E1 and CYP3A4) as well as phase II enzymes (UGT1A1 and CYP1A6) (123 125). However, the expression levels of

sulfotransferases (SULTs), glutathione-*S*-transferases (GSTs), *N*-acetylytransferases (NATs), and epoxide hydrolase were similar to those in human hepatocytes. Moreover, the expression levels of several CYP450s and phase II enzymes were increased in response to model inducers (126 128). Nonetheless, due to the low basal expression of enzymes and low-moderate induction responses, HepG2 cells are not considered an appropriate model to study metabolism or drug-drug interactions.

The BC2 cell line when seeded at confluency undergoes a differentiation process resulting in the expression of liver-specific functions as well as drug-metabolizing enzymes (129,130). Gomez-Lechon et al. performed an extensive analysis of the biotransformation properties of BC2 cells by measuring basal and inducible expression of phases I and II enzymes (131). The analysis revealed lower but measurable activities of CYP1A1/2, -2A6, -2B6, -2C9, and -3A4. Upon treatment of the cells with enzyme inducers, the activity of CYP1A1/2 was greatly increased while marginal induction was observed for CYP2B6 and CYP3A4.

The HepaRG cell line was isolated from a resected liver tumor of a female patient suffering from hepatitis C related hepatocellular carcinoma (132). When cells are cultured to confluency for several weeks in the presence of 2% DMSO and hydrocortisone, a highly differentiated hepatocyte-like cell line develops. A comprehensive expression analysis performed by Aninat et al. showed that RNA expression of various transcription factors (PXR, AhR, CAR), CYP450s (CYP1A2, 2C9, 2D6, 2E1, 3A4), and phase II enzymes (UGT1A1 and GSTs) were expressed, for most of them, at comparable levels to cultured primary human hepatocytes (133). However, in the presence of DMSO, HepaRG cells were refractory to rifampicin (CYP3A4) induction, and it was postulated that DMSO treatment alone induced the expression of CYP3A4 to the maximum level achievable. Le Vee et al. examined the expression of hepatic transporters in HepaRG cells where the transcript levels of OCT-1, OATP-C, NTCP, OATP-8, BSEP, and MRP-2 were approximately 10% to 55% of those found in primary human hepatocytes while the expression of OATP-B, MDR-1, and MRP-3 were higher in HepaRG than in primary human hepatocytes (134). The evaluation of uptake transporter activities showed that OCT-1, OATP/OAT2, and NTCP activities were detectable but lower than primary human hepatocytes; however, the activities of efflux transporters such as MDR-1 and MRP were similar or higher than those in human hepatocytes. The treatment of HepaRG cells with known inducers of transporters such as rifampicin, phenobarbital, and chenodeoxycholic acid significantly increased the mRNA expression of MDR-1, MRP2, and BSEP, respectively. Overall, the HepaRG cell line could represent a reliable surrogate in vitro model to primary human hepatocytes as an unlimited source of hepatocyte-like cells for evaluating drug metabolism (135 137).

The Fa2N-4 cell line is derived from primary hepatocytes (12-year-old female donor) through immortalization using the SV-40 large T antigen. Fa2N-4 cells retain expression and inducibility of several drug-metabolizing enzymes and transporters. Generally, the activities of CYP450 enzymes were much lower than those found in primary hepatocytes. However, using known inducers of CYP enzymes, Mills et al. reported concentration-dependent increases in both transcript levels and enzyme activities of CYP3A4, -2C9, and -1A2 (138). These changes were comparable to the induction responses observed in primary human hepatocytes. In addition, UGT1A and MDR-1 were also induced by rifampicin treatment in this cell line. However, the Fa2N-4 cells have very low expression of CAR; therefore, induction of CYP2B6 cannot be evaluated, and the induction of CYP3A4 may be attenuated in this cell line (139). In addition, the expression of several drug transporters (OATP, NTCP, OCT1, and BSEP) were shown to be low when compared with human hepatocytes (139).

While no one immortalized cell line affords an exact reproduction of hepatocyte function, several cell types, such as HepaRG and Fa2N-4, do replicate the majority of hepatocyte-like characteristics. These characteristics combined with the attributes of continuous supply and consistent drug response provide the opportunity to establish routine and high-throughput models to evaluate drug metabolism at any stage of drug discovery or development. For example, Ripp et al. developed a high-throughput induction assay using Fa2N-4 cells in 96-well plates and produced detailed concentration-response curves for known inducers of CYP3A4 (140).

Stem Cell–Derived Hepatocytes

Stem cells are defined as omnipotent progenitor cells that retain the ability to replicate indefinitely in vitro or in vivo as undifferentiated cells and under appropriate conditions, differentiate into specialized cell types, such as hepatocytes. Stem cells offer a potential unlimited source of functional human hepatocyte-like cells. Hepatocyte-like cells have been differentiated from a variety of origins, both embryonic and adult stem cells (bone marrow, umbilical cord blood, amniotic fluid, placenta, adipose, and liver tissue) (141). A comprehensive analysis of expression and induction of drug-metabolizing enzymes from hepatocyte-like cells derived from human stem cells was reported by Ek et al. (142). These cells expressed CYP1A2, CYP3A4/7, and low levels of CYP1A1 and CYP2C proteins. Generally, the activities of CYP1A1 and CYP3A4 were much lower than those found in primary hepatocytes. When treated with a cocktail of known CYP450 inducers, the protein expressions of CYP1A2 and CYP3A4 were increased. Stem cell derived hepatocytes are not widely used in drug metabolism research because they are not fully characterized, and at the present time do not represent an equivalent model to isolated hepatocytes (6,127). However, further research and refinement in stem cell technology as well as extensive characterization of cellular functions could greatly advance and expand their utility in drug metabolism.

SUMMARY

Advancement in cell culture and cryopreservation has improved our ability to employ human and animal hepatocytes in drug metabolism. Also, our understanding of gene expression changes that occur during and after cell isolation have increased our awareness of how best to utilize hepatocyte models for different applications. Additional development or refinement of hepatocyte-like cell models (immortalized or stem cell derived) that recapitulate the function of isolated hepatocytes will enhance our ability to more routinely employ hepatocyte models in all stages of drug discovery and development. Furthermore, unique applications of hepatocytes continue to emerge, such as the chimeric mouse, which involves transplanting human hepatocytes into a mouse liver thus creating an in vivo model capable of assessing human drug metabolism/disposition and enzyme regulation by xenobiotics (143,144).

The preceding description and application of hepatocytes and hepatocyte-like cells has attempted to demonstrate the versatility and utility of hepatocytes as an in vitro model of drug metabolism. The hepatocyte as a model of drug metabolism with its complement of enzymes, regulatory elements, and intact cell membrane is a close approximation to the in vivo functioning liver. In conclusion, the hepatocyte serves as an excellent model system for evaluating drug metabolism, pharmacology, and toxicology and will continue to advance and improve in its ability to accurately predict xenobiotic disposition and effects in humans.

ACKNOWLEDGMENTS

The author wishes to thank Dr. Kenneth Santone, Dr. Susan Jenkins, and Ms. Zuzana Haarhoff for their thoughtful comments during the review of this chapter.

REFERENCES

1. Oswald S, Grube M, Siegmund W, Kroemer HK. Transporter mediated uptake into cellular compartments. Xenobiotica 2007; 37(10 11):1171 1195.
2. Berry M, Edwards A, Barritt G. Isolated Hepatocytes Preparation, Properties, and Applications. Vol. 21. New York: Elsevier, 1991.
3. Hewitt NJ, Lechon MJ, Houston JB, Hallifax D, Brown HS, Maurel P, Kenna JG, Gustavsson L, Lohmann C, Skonberg C, Guillouzo A, Tuschl G, Li AP, LeCluyse E, Groothuis GM, Hengstler JG. Primary hepatocytes: current understanding of the regulation of metabolic enzymes and transporter proteins, and pharmaceutical practice for the use of hepatocytes in metabolism, enzyme induction, transporter, clearance, and hepatotoxicity studies. Drug Metab Rev 2007; 39(1):159 234.
4. LeCluyse EL. Human hepatocyte culture systems for the in vitro evaluation of cytochrome P450 expression and regulation. Eur J Pharm Sci 2001; 13(4):343 368.
5. LeCluyse EL, Alexandre E, Hamilton GA, Viollon Abadie C, Coon DJ, Jolley S, Richert L. Isolation and culture of primary human hepatocytes. Methods Mol Biol 2005; 290:207 229.
6. Turncliff RZ, Hoffmaster KA, Kalvass JC, Pollack GM, Brouwer KL. Hepatobiliary disposition of a drug/metabolite pair: comprehensive pharmacokinetic modeling in sandwich cultured rat hepatocytes. J Pharmacol Exp Ther 2006; 318(2):881 889.
7. Hoffmaster KA, Turncliff RZ, LeCluyse EL, Kim RB, Meier PJ, Brouwer KL. P glycoprotein expression, localization, and function in sandwich cultured primary rat and human hepatocytes: relevance to the hepatobiliary disposition of a model opioid peptide. Pharm Res 2004; 21(7):1294 1302.
8. Glebe D. Attachment sites and neutralising epitopes of hepatitis B virus. Minerva Gastroenterol Dietol 2006; 52(1):3 21.
9. Schneider W, Potter V. The assay of animal tissues for respiratory enzymes. J Biol Chem 1943; 149(1):217 227.
10. Howard RB, Pesch LA. Respiratory activity of intact, isolated parenchymal cells from rat liver. J Biol Chem 1968; 243(11):3105 3109.
11. Bellemann P, Gebhardt R, Mecke D. An improved method for the isolation of hepatocytes from liver slices. Selective removal of trypan blue dyeable cells. Anal Biochem 1977; 81(2): 408 415.
12. Fry JR. Preparation of mammalian hepatocytes. Methods Enzymol 1981; 77:130 137.
13. Fry JR, Jones CA, Wiebkin P, Bellemann P, Bridges JW. The enzymic isolation of adult rat hepatocytes in a functional and viable state. Anal Biochem 1976; 71(2):341 350.
14. Berry MN, Friend DS. High yield preparation of isolated rat liver parenchymal cells: a biochemical and fine structural study. J Cell Biol 1969; 43(3):506 520.
15. Seglen PO. Preparation of isolated rat liver cells. Methods Cell Biol 1976; 13:29 83.
16. Gebhardt R, Hengstler JG, Muller D, Glockner R, Buenning P, Laube B, Schmelzer E, Ullrich M, Utesch D, Hewitt N, Ringel M, Hilz BR, Bader A, Langsch A, Koose T, Burger HJ, Maas J, Oesch F. New hepatocyte in vitro systems for drug metabolism: metabolic capacity and recommendations for application in basic research and drug development, standard operation procedures. Drug Metab Rev 2003; 35(2 3):145 213.
17. Neufeld DS. Isolation of rat liver hepatocytes. Methods Mol Biol 1997; 75:145 151.
18. Papeleu P, Vanhaecke T, Henkens T, Elaut G, Vinken M, Snykers S, Rogiers V. Isolation of rat hepatocytes. Methods Mol Biol 2006; 320:229 237.
19. Vina J, Hems R, Krebs HA. Maintenance of glutathione content is isolated hepatocyctes. Biochem J 1978; 170(3):627 630.

20. Allen K, Green CE. Isolation of human hepatocytes by biopsy perfusion methods. In: Tyson CA, Frazier J, eds. Methods in Toxicology. New York: Academic Press, 1993:262.
21. Li AP. Human hepatocytes: isolation, cryopreservation and applications in drug development. Chem Biol Interact 2007; 168(1):16 29.
22. Mitry RR, Hughes RD, Dhawan A. Progress in human hepatocytes: isolation, culture and cryopreservation. Semin Cell Dev Biol 2002; 13(6):463 467.
23. Richert L, Alexandre E, Lloyd T, Orr S, Viollon Abadie C, Patel R, Kingston S, Berry D, Dennison A, Heyd B, Mantion G, Jaeck D. Tissue collection, transport and isolation procedures required to optimize human hepatocyte isolation from waste liver surgical resections. A multilaboratory study. Liver Int 2004; 24(4):371 378.
24. Alexandre E, Viollon Abadie C, David P, Gandillet A, Coassolo P, Heyd B, Mantion G, Wolf P, Bachellier P, Jaeck D, Richert L. Cryopreservation of adult human hepatocytes obtained from resected liver biopsies. Cryobiology 2002; 44(2):103 113.
25. Dirven HA, van den Broek PH, Peeters MC, Peters JG, Mennes WC, Blaauboer BJ, Noordhoek J, Jongeneelen FJ. Effects of the peroxisome proliferator mono(2 ethylhexyl) phthalate in primary hepatocyte cultures derived from rat, guinea pig, rabbit and monkey. Relationship between interspecies differences in biotransformation and peroxisome prolifer ating potencies. Biochem Pharmacol 1993; 45(12):2425 2434.
26. Elaut G, Papeleu P, Vinken M, Henkens T, Snykers S, Vanhaecke T, Rogiers V. Hepatocytes in suspension. Methods Mol Biol 2006; 320:255 263.
27. Gee SJ, Green CE, Tyson CA. Comparative metabolism of tolbutamide by isolated hepatocytes from rat, rabbit, dog, and squirrel monkey. Drug Metab Dispos 1984; 12(2):174 178.
28. Maslansky CJ, Williams GM. Primary cultures and the levels of cytochrome P450 in hepatocytes from mouse, rat, hamster, and rabbit liver. In Vitro 1982; 18(8):683 693.
29. Oldham HG, Standring P, Norman SJ, Blake TJ, Beattie I, Cox PJ, Chenery RJ. Metabolism of temelastine (SK&F 93944) in hepatocytes from rat, dog, cynomolgus monkey and man. Drug Metab Dispos 1990; 18(2):146 152.
30. Reese JA, Byard JL. Isolation and culture of adult hepatocytes from liver biopsies. In Vitro 1981; 17(11):935 940.
31. Sacci JB Jr. Hepatocyte perfusion, isolation, and culture. Methods Mol Med 2002; 72:503 505.
32. Bakala A, Karlik W, Wiechetek M. Preparation of equine isolated hepatocytes. Toxicol In Vitro 2003; 17(5 6):615 621.
33. Forsell JH, Jesse BW, Shull LR. A technique for isolation of bovine hepatocytes. J Anim Sci 1985; 60(6):1597 1609.
34. Kitos TE, Tyrrell DL. Intracellular metabolism of 2′,3′ dideoxynucleosides in duck hepatocyte primary cultures. Biochem Pharmacol 1995; 49(9):1291 1302.
35. Sielaff TD, Hu MY, Rao S, Groehler K, Olson D, Mann HJ, Remmel RP, Shatford RA, Amiot B, Hu WS, Cerra FB. A technique for porcine hepatocyte harvest and description of differentiated metabolic functions in static culture. Transplantation 1995; 59(10):1459 1463.
36. Skalova L, Szotakova B, Lamka J, Kral R, Vankova I, Baliharova V, Wsol V. Biotransformation of flobufen enantiomers in ruminant hepatocytes and subcellular fractions. Chirality 2001; 13(10):760 764.
37. Tachibana S, Sato K, Cho Y, Chiba T, Schneider WJ, Akiba Y. Octanoate reduces very low density lipoprotein secretion by decreasing the synthesis of apolipoprotein b in primary cultures of chicken hepatocytes. Biochim Biophys Acta 2005; 1737(1):36 43.
38. van't Klooster GA, Woutersen van Nijnanten FM, Blaauboer BJ, Noordhoek J, van Miert AS. Applicability of cultured hepatocytes derived from goat, sheep and cattle in comparative drug metabolism studies. Xenobiotica 1994; 24(5):417 428.
39. Fentem JH, Hammond AH, Fry JR. Maintenance of monooxygenase activities and detection of cytochrome P 450 mediated cytotoxicity in Mongolian gerbil hepatocyte cultures. Xenobio tica 1991; 21(10):1363 1370.
40. Ferraris M, Radice S, Catalani P, Francolini M, Marabini L, Chiesara E. Early oxidative damage in primary cultured trout hepatocytes: a time course study. Aquat Toxicol 2002; 59 (3 4):283 296.

41. Mommsen TP, Storey KB. Hormonal effects on glycogen metabolism in isolated hepatocytes of a freeze tolerant frog. Gen Comp Endocrinol 1992; 87(1):44 53.
42. Naicker D, Myburgh JG, Botha CJ. Establishment and validation of primary hepatocytes of the African sharptooth catfish (*Clarias gariepinus*). Chemosphere 2007; 68(1):69 77.
43. Peyon P, Baloche S, Burzawa Gerard E. Synthesis of vitellogenin by eel (*Anguilla anguilla* L.) hepatocytes in primary culture: requirement of 17 beta estradiol priming. Gen Comp Endocrinol 1993; 91(3):318 329.
44. Prelovsek PM, Batista U, Bulog B. Isolation and primary culture of *necturus maculosus* (amphibia: Urodela) hepatocytes. In Vitro Cell Dev Biol Anim 2006; 42(8 9):255 262.
45. Remmel RP, Sinz MW. A quaternary ammonium glucuronide is the major metabolite of lamotrigine in guinea pigs. In vitro and in vivo studies. Drug Metab Dispos 1991; 19(3):630 636.
46. Silva SV, Mercer JR. The effect of lysosomal inhibitors on protein degradation in cat hepatocyte monolayers. Int J Biochem 1991; 23(5 6):525 529.
47. Smith DJ, Grossbard M, Gordon ER, Boyer JL. Isolation and characterization of a polarized isolated hepatocyte preparation in the skate raja erinacea. J Exp Zool 1987; 241(3):291 296.
48. Ulrich RG, Aspar DG, Cramer CT, Kletzien RF, Ginsberg LC. Isolation and culture of hepatocytes from the cynomolgus monkey (*macaca fascicularis*). In Vitro Cell Dev Biol 1990; 26(8):815 823.
49. Dalet C, Fehlmann M, Debey P. Use of percoll density gradient centrifugation for preparing isolated rat hepatocytes having long term viability. Anal Biochem 1982; 122(1):119 123.
50. Kreamer BL, Staecker JL, Sawada N, Sattler GL, Hsia MT, Pitot HC. Use of a low speed, iso density percoll centrifugation method to increase the viability of isolated rat hepatocyte preparations. In Vitro Cell Dev Biol 1986; 22(4):201 211.
51. Gomez Lechon MJ, Lahoz A, Jimenez N, Vicente Castell J, Donato MT. Cryopreservation of rat, dog and human hepatocytes: influence of preculture and cryoprotectants on recovery, cytochrome P450 activities and induction upon thawing. Xenobiotica 2006; 36(6):457 472.
52. Hengstler JG, Utesch D, Steinberg P, Platt KL, Diener B, Ringel M, Swales N, Fischer T, Biefang K, Gerl M, Bottger T, Oesch F. Cryopreserved primary hepatocytes as a constantly available in vitro model for the evaluation of human and animal drug metabolism and enzyme induction. Drug Metab Rev 2000; 32(1):81 118.
53. Rijntjes PJ, Moshage HJ, Van Gemert PJ, De Waal R, Yap SH. Cryopreservation of adult human hepatocytes. The influence of deep freezing storage on the viability, cell seeding, survival, fine structures and albumin synthesis in primary cultures. J Hepatol 1986; 3(1):7 18.
54. Li AP, Lu C, Brent JA, Pham C, Fackett A, Ruegg CE, Silber PM. Cryopreserved human hepatocytes: characterization of drug metabolizing enzyme activities and applications in higher throughput screening assays for hepatotoxicity, metabolic stability, and drug drug interaction potential. Chem Biol Interact 1999; 121(1):17 35.
55. Sohlenius Sternbeck AK, Schmidt S. Impaired glutathione conjugating capacity by cryopre served human and rat hepatocytes. Xenobiotica 2005; 35(7):727 736.
56. Bi YA, Kazolias D, Duignan DB. Use of cryopreserved human hepatocytes in sandwich culture to measure hepatobiliary transport. Drug Metab Dispos 2006; 34(9):1658 1665.
57. Koebe HG, Muhling B, Deglmann CJ, Schildberg FW. Cryopreserved porcine hepatocyte cultures. Chem Biol Interact 1999; 121(1):99 115.
58. Chao ES, Dunbar D, Kaminsky LS. Intracellular lactate dehydrogenase concentration as an index of cytotoxicity in rat hepatocyte primary culture. Cell Biol Toxicol 1988; 4(1):1 11.
59. Page RA, Stowell KM, Hardman MJ, Kitson KE. The assessment of viability in isolated rat hepatocytes. Anal Biochem 1992; 200(1):171 175.
60. Lahoz A, Donato MT, Montero S, Castell JV, Gomez Lechon MJ. A new in vitro approach for the simultaneous determination of phase I and phase II enzymatic activities of human hepatocyte preparations. Rapid Commun Mass Spectrom 2008; 22(2):240 244.
61. Lahoz A, Donato MT, Picazo L, Gomez Lechon MJ, Castell JV. Determination of major human cytochrome P450s activities in 96 well plates using liquid chromatography tandem mass spectrometry. Toxicol In Vitro 2007; 21(7):1247 1252.

62. Paine AJ, Hockin LJ, Legg RF. Relationship between the ability of nicotinamide to maintain nicotinamide adenine dinucleotide in rat liver cell culture and its effect on cytochrome P 450. Biochem J 1979; 184(2):461 463.
63. Chenery RJ, Ayrton A, Oldham HG, Standring P, Norman SJ, Seddon T, Kirby R. Diazepam metabolism in cultured hepatocytes from rat, rabbit, dog, guinea pig, and man. Drug Metab Dispos 1987; 15(3):312 317.
64. Kraner JC, Lasker JM, Corcoran GB, Ray SD, Raucy JL. Induction of P4502E1 by acetone in isolated rabbit hepatocytes. Role of increased protein and mRNA synthesis. Biochem Pharmacol 1993; 45(7):1483 1492.
65. Sinz MW, Black AE, Bjorge SM, Holmes A, Trivedi BK, Woolf TF. In vitro and in vivo disposition of 2,2 dimethyl N (2,4,6 trimethoxyphenyl)dodecanamide (CI 976). Identification of a novel five carbon cleavage metabolite in rats. Drug Metab Dispos 1997; 25(1):123 130.
66. Elaut G, Henkens T, Papeleu P, Snykers S, Vinken M, Vanhaecke T, Rogiers V. Molecular mechanisms underlying the dedifferentiation process of isolated hepatocytes and their cultures. Curr Drug Metab 2006; 7(6):629 660.
67. Paine AJ, Andreakos E. Activation of signalling pathways during hepatocyte isolation: relevance to toxicology in vitro. Toxicol In Vitro 2004; 18(2):187 193.
68. Croci T, Williams GM. Activities of several phase I and phase II xenobiotic biotransformation enzymes in cultured hepatocytes from male and female rats. Biochem Pharmacol 1985; 34(17):3029 3035.
69. Paine AJ. The maintenance of cytochrome P 450 in rat hepatocyte culture: some applications of liver cell cultures to the study of drug metabolism, toxicity and the induction of the P 450 system. Chem Biol Interact 1990; 74(1 2):1 31.
70. Steward AR, Dannan GA, Guzelian PS, Guengerich FP. Changes in the concentration of seven forms of cytochrome P 450 in primary cultures of adult rat hepatocytes. Mol Pharmacol 1985; 27(1):125 132.
71. Wortelboer HM, de Kruif CA, van Iersel AA, Falke HE, Noordhoek J, Blaauboer BJ. The isoenzyme pattern of cytochrome P450 in rat hepatocytes in primary culture, comparing different enzyme activities in microsomal incubations and in intact monolayers. Biochem Pharmacol 1990; 40(11):2525 2534.
72. Rodriguez Antona C, Donato MT, Boobis A, Edwards RJ, Watts PS, Castell JV, Gomez Lechon MJ. Cytochrome P450 expression in human hepatocytes and hepatoma cell lines: molecular mechanisms that determine lower expression in cultured cells. Xenobiotica 2002; 32(6):505 520.
73. Strom SC, Pisarov LA, Dorko K, Thompson MT, Schuetz JD, Schuetz EG. Use of human hepatocytes to study P450 gene induction. Methods Enzymol 1996; 272:388 401.
74. Morel F, Beaune PH, Ratanasavanh D, Flinois JP, Yang CS, Guengerich FP, Guillouzo A. Expression of cytochrome P 450 enzymes in cultured human hepatocytes. Eur J Biochem 1990; 191(2):437 444.
75. Blaauboer BJ, van Holsteijn I, van Graft M, Paine AJ. The concentration of cytochrome P 450 in human hepatocyte culture. Biochem Pharmacol 1985; 34(13):2405 2408.
76. Guillouzo A, Morel F, Fardel O, Meunier B. Use of human hepatocyte cultures for drug metabolism studies. Toxicology 1993; 82(1 3):209 219.
77. Mennes WC, van Holsteijn CW, Timmerman A, Noordhoek J, Blaauboer BJ. Biotransforma tion of scoparone used to monitor changes in cytochrome P450 activities in primary hepatocyte cultures derived from rats, hamsters and monkeys. Biochem Pharmacol 1991; 41(8): 1203 1208.
78. Schwarz L, Wiebel F. Cytochrome P450 in primary and permanent liver cell cultures. In: Schenkman J, Grein H, eds. Handbook of Experimental Pharmacology. Vol. 105. New York: Springer Verlag, 1993:399.
79. LeCluyse E, Bullock P, Madan A, Carroll K, Parkinson A. Influence of extracellular matrix overlay and medium formulation on the induction of cytochrome P 450 2B enzymes in primary cultures of rat hepatocytes. Drug Metab Dispos 1999; 27(8):909 915.

80. LeCluyse E, Madan A, Hamilton G, Carroll K, DeHaan R, Parkinson A. Expression and regulation of cytochrome P450 enzymes in primary cultures of human hepatocytes. J Biochem Mol Toxicol 2000; 14(4):177 188.
81. Davila JC, Morris DL. Analysis of cytochrome P450 and phase II conjugating enzyme expression in adult male rat hepatocytes. In Vitro Cell Dev Biol Anim 1999; 35(3): 120 130.
82. Sidhu JS, Liu F, Omiecinski CJ. Phenobarbital responsiveness as a uniquely sensitive indicator of hepatocyte differentiation status: requirement of dexamethasone and extracellular matrix in establishing the functional integrity of cultured primary rat hepatocytes. Exp Cell Res 2004; 292(2):252 264.
83. Yamamoto N, Wu J, Zhang Y, Catana AM, Cai H, Strom S, Novikoff PM, Zern MA. An optimal culture condition maintains human hepatocyte phenotype after long term culture. Hepatol Res 2006; 35(3):169 177.
84. Terry TL, Gallin WJ. Effects of fetal calf serum and disruption of cadherin function on the formation of bile canaliculi between hepatocytes. Exp Cell Res 1994; 214(2):642 653.
85. Hamilton GA, Jolley SL, Gilbert D, Coon DJ, Barros S, LeCluyse EL. Regulation of cell morphology and cytochrome P450 expression in human hepatocytes by extracellular matrix and cell cell interactions. Cell Tissue Res 2001; 306(1):85 99.
86. Gomez Lechon MJ, Castell JV, Donato MT. Hepatocytes the choice to investigate drug metabolism and toxicity in man: in vitro variability as a reflection of in vivo. Chem Biol Interact 2007; 168(1):30 50.
87. Gomez Lechon MJ, Donato MT, Castell JV, Jover R. Human hepatocytes in primary culture: the choice to investigate drug metabolism in man. Curr Drug Metab 2004; 5(5):443 462.
88. Ito K, Iwatsubo T, Kanamitsu S, Nakajima Y, Sugiyama Y. Quantitative prediction of in vivo drug clearance and drug interactions from in vitro data on metabolism, together with binding and transport. Annu Rev Pharmacol Toxicol 1998; 38:461 499.
89. Soars MG, McGinnity DF, Grime K, Riley RJ. The pivotal role of hepatocytes in drug discovery. Chem Biol Interact 2007; 168(1):2 15.
90. Henderson PT, Dewaide JH. Metabolism of drugs in isolated rat hepatocytes. Biochem Pharmacol 1969; 18(9):2087 2094.
91. Ponsoda X, Pareja E, Gomez Lechon MJ, Fabra R, Carrasco E, Trullenque R, Castell JV. Drug biotransformation by human hepatocytes. In vitro/in vivo metabolism by cells from the same donor. J Hepatol 2001; 34(1):19 25.
92. Hewitt NJ, Buhring KU, Dasenbrock J, Haunschild J, Ladstetter B, Utesch D. Studies comparing in vivo in vitro metabolism of three pharmaceutical compounds in rat, dog, monkey, and human using cryopreserved hepatocytes, microsomes, and collagen gel immobilized hepatocyte cultures. Drug Metab Dispos 2001; 29(7):1042 1050.
93. Miners JO, Knights KM, Houston JB, Mackenzie PI. In vitro in vivo correlation for drugs and other compounds eliminated by glucuronidation in humans: pitfalls and promises. Biochem Pharmacol 2006; 71(11):1531 1539.
94. Blanchard N, Alexandre E, Abadie C, Lave T, Heyd B, Mantion G, Jaeck D, Richert L, Coassolo P. Comparison of clearance predictions using primary cultures and suspensions of human hepatocytes. Xenobiotica 2005; 35(1):1 15.
95. Griffin SJ, Houston JB. Comparison of fresh and cryopreserved rat hepatocyte suspensions for the prediction of in vitro intrinsic clearance. Drug Metab Dispos 2004; 32(5):552 558.
96. McGinnity DF, Soars MG, Urbanowicz RA, Riley RJ. Evaluation of fresh and cryopreserved hepatocytes as in vitro drug metabolism tools for the prediction of metabolic clearance. Drug Metab Dispos 2004; 32(11):1247 1253.
97. Davies B, Morris T. Physiological parameters in laboratory animals and humans. Pharm Res 1993; 10(7):1093 1095.
98. Sohlenius Sternbeck AK. Determination of the hepatocellularity number for human, dog, rabbit, rat and mouse livers from protein concentration measurements. Toxicol In Vitro 2006; 20(8):1582 1586.

99. Bayliss MK, Bell JA, Jenner WN, Park GR, Wilson K. Utility of hepatocytes to model species differences in the metabolism of loxtidine and to predict pharmacokinetic parameters in rat, dog and man. Xenobiotica 1999; 29(3):253 268.
100. Luttringer O, Theil FP, Poulin P, Schmitt Hoffmann AH, Guentert TW, Lave T. Physiolog ically based pharmacokinetic (PBPK) modeling of disposition of epiroprim in humans. J Pharm Sci 2003; 92(10):1990 2007.
101. Barter ZE, Bayliss MK, Beaune PH, Boobis AR, Carlile DJ, Edwards RJ, Houston JB, Lake BG, Lipscomb JC, Pelkonen OR, Tucker GT, Rostami Hodjegan A. Scaling factors for the extrapolation of in vivo metabolic drug clearance from in vitro data: reaching a consensus on values of human microsomal protein and hepatocellularity per gram of liver. Curr Drug Metab 2007; 8(1):33 45.
102. Brown HS, Chadwick A, Houston JB. Use of isolated hepatocyte preparations for cytochrome P450 inhibition studies: comparison with microsomes for Ki determination. Drug Metab Dispos 2007; 35(11):2119 2126.
103. Lu C, Hatsis P, Berg C, Lee FW, Balani SK. Prediction of pharmacokinetic drug drug interactions using human hepatocyte suspension in plasma and CYP phenotypic data. Part II. In vitro in vivo correlation with ketoconazole. Drug Metab Dispos 2008; 36(7):1255 1260 [Epub April 1, 2008].
104. Lu C, Miwa GT, Prakash SR, Gan LS, Balani SK. A novel model for the prediction of drug drug interactions in humans based on in vitro cytochrome P450 phenotypic data. Drug Metab Dispos 2007; 35(1):79 85.
105. Zhao P. The use of hepatocytes in evaluating time dependent inactivation of P450 in vivo. Expert Opin Drug Metab Toxicol 2008; 4(2):151 164.
106. Zhao P, Lee CA, Kunze KL. Sequential metabolism is responsible for diltiazem induced time dependent loss of CYP3A. Drug Metab Dispos 2007; 35(5):704 712.
107. Nakata K, Tanaka Y, Nakano T, Adachi T, Tanaka H, Kaminuma T, Ishikawa T. Nuclear receptor mediated transcriptional regulation in phase I, II, and III xenobiotic metabolizing systems. Drug Metab Pharmacokinet 2006; 21(6):437 457.
108. Timsit YE, Negishi M. CAR and PXR: the xenobiotic sensing receptors. Steroids 2007; 72(3): 231 246.
109. Hewitt NJ, de Kanter R, LeCluyse E. Induction of drug metabolizing enzymes: a survey of in vitro methodologies and interpretations used in the pharmaceutical industry do they comply with FDA recommendations? Chem Biol Interact 2007; 168(1):51 65.
110. Kafert Kasting S, Alexandrova K, Barthold M, Laube B, Friedrich G, Arseniev L, Hengstler JG. Enzyme induction in cryopreserved human hepatocyte cultures. Toxicology 2006; 220(2 3): 117 125.
111. FDA draft guideline: drug interaction studies study design, data analysis, and implications for dosing and labeling, 2006.
112. Hewitt NJ, Lecluyse EL, Ferguson SS. Induction of hepatic cytochrome P450 enzymes: methods, mechanisms, recommendations, and in vitro in vivo correlations. Xenobiotica 2007; 37(10 11):1196 1224.
113. Nishimura M, Koeda A, Suzuki E, Kawano Y, Nakayama M, Satoh T, Narimatsu S, Naito S. Regulation of mRNA expression of MDR1, MRP1, MRP2 and MRP3 by prototypical microsomal enzyme inducers in primary cultures of human and rat hepatocytes. Drug Metab Pharmacokinet 2006; 21(4):297 307.
114. Shitara Y, Itoh T, Sato H, Li AP, Sugiyama Y. Inhibition of transporter mediated hepatic uptake as a mechanism for drug drug interaction between cerivastatin and cyclosporin A. J Pharmacol Exp Ther 2003; 304(2):610 616.
115. Dambach DM, Andrews BA, Moulin F. New technologies and screening strategies for hepatotoxicity: use of in vitro models. Toxicol Pathol 2005; 33(1):17 26.
116. Liguori MJ, Waring JF. Investigations toward enhanced understanding of hepatic idiosyncratic drug reactions. Expert Opin Drug Metab Toxicol 2006; 2(6):835 846.
117. O'Brien PJ, Siraki AG. Accelerated cytotoxicity mechanism screening using drug metabolising enzyme modulators. Curr Drug Metab 2005; 6(2):101 109.

118. Hahn WC. Immortalization and transformation of human cells. Mol Cells 2002; 13(3):351 361.
119. Sinz MW, Kim S. Stem cells, immortalized cells and primary cells in ADMET assays. Drug Discov Today: Technol 2006; 3(1):79 85.
120. Castell JV, Jover R, Martinez Jimenez CP, Gomez Lechon MJ. Hepatocyte cell lines: their use, scope and limitations in drug metabolism studies. Expert Opin Drug Metab Toxicol 2006; 2(2):183 212.
121. Donato MT, Lahoz A, Castell JV, Gomez Lechon MJ. Cell lines: a tool for in vitro drug metabolism studies. Curr Drug Metab 2008; 9(1):1 11.
122. Vermeir M, Annaert P, Mamidi RN, Roymans D, Meuldermans W, Mannens G. Cell based models to study hepatic drug metabolism and enzyme induction in humans. Expert Opin Drug Metab Toxicol 2005; 1(1):75 90.
123. Westerink WM, Schoonen WG. Cytochrome P450 enzyme levels in HepG2 cells and cryopreserved primary human hepatocytes and their induction in HepG2 cells. Toxicol In Vitro 2007; 21(8):1581 1591 [Epub June 8, 2007].
124. Westerink WM, Schoonen WG. Phase II enzyme levels in HepG2 cells and cryopreserved primary human hepatocytes and their induction in HepG2 cells. Toxicol In Vitro 2007; 21(8): 1592 1602 [Epub July 18, 2007].
125. Wilkening S, Stahl F, Bader A. Comparison of primary human hepatocytes and hepatoma cell line HepG2 with regard to their biotransformation properties. Drug Metab Dispos 2003; 31(8): 1035 1042.
126. Bapiro TE, Andersson TB, Otter C, Hasler JA, Masimirembwa CM. Cytochrome P450 1A1/2 induction by antiparasitic drugs: dose dependent increase in ethoxyresorufin O deethylase activity and mRNA caused by quinine, primaquine and albendazole in HepG2 cells. Eur J Clin Pharmacol 2002; 58(8):537 542.
127. Iwanari M, Nakajima M, Kizu R, Hayakawa K, Yokoi T. Induction of CYP1A1, CYP1A2, and CYP1B1 mRNAs by nitropolycyclic aromatic hydrocarbons in various human tissue derived cells: chemical , cytochrome P450 isoform , and cell specific differences. Arch Toxicol 2002; 76(5 6):287 298.
128. Baliharova V, Skalova L, Maas RF, De Vrieze G, Bull S, Fink Gremmels J. The effects of benzimidazole anthelmintics on P4501A in rat hepatocytes and HepG2 cells. Res Vet Sci 2003; 75(1):61 69.
129. Le Jossic C, Glaise D, Corcos L, Diot C, Dezier JF, Fautrel A, Guguen Guillouzo C. Trans acting factors, detoxication enzymes and hepatitis B virus replication in a novel set of human hepatoma cell lines. Eur J Biochem 1996; 238(2):400 409.
130. O'Connor JE, Martinez A, Castell JV, Gomez Lechon MJ. Multiparametric characterization by flow cytometry of flow sorted subpopulations of a human hepatoma cell line useful for drug research. Cytometry A 2005; 63(1):48 58.
131. Gomez Lechon MJ, Donato T, Jover R, Rodriguez C, Ponsoda X, Glaise D, Castell JV, Guguen Guillouzo C. Expression and induction of a large set of drug metabolizing enzymes by the highly differentiated human hepatoma cell line BC2. Eur J Biochem 2001; 268(5): 1448 1459.
132. Gripon P, Rumin S, Urban S, Le Seyec J, Glaise D, Cannie I, Guyomard C, Lucas J, Trepo C, Guguen Guillouzo C. Infection of a human hepatoma cell line by hepatitis B virus. Proc Natl Acad Sci U S A 2002; 99(24):15655 15660.
133. Aninat C, Piton A, Glaise D, Le Charpentier T, Langouet S, Morel F, Guguen Guillouzo C, Guillouzo A. Expression of cytochromes P450, conjugating enzymes and nuclear receptors in human hepatoma HepaRG cells. Drug Metab Dispos 2006; 34(1):75 83.
134. Le Vee M, Jigorel E, Glaise D, Gripon P, Guguen Guillouzo C, Fardel O. Functional expression of sinusoidal and canalicular hepatic drug transporters in the differentiated human hepatoma HepaRG cell line. Eur J Pharm Sci 2006; 28(1 2):109 117.
135. Josse R, Aninat C, Glaise D, Dumont J, Fessard V, Morel F, Poul JM, Guguen Guillouzo C, Guillouzo A. Long term functional stability of human HepaRG hepatocytes and use for chronic toxicity and genotoxicity studies. Drug Metab Dispos 2008; 36(6):1111 1118 [Epub March 17, 2008].

136. Kanebratt KP, Andersson TB. Evaluation of HepaRG cells as an in vitro model for human drug metabolism studies. Drug Metab Dispos 2008; 1444 1452 [Epub, April 2, 2008].
137. Kanebratt KP, Andersson TB. HepaRG cells as an in vitro model for evaluation of cytochrome P450 induction in humans. Drug Metab Dispos 2008; 36(1):137 145.
138. Mills JB, Rose KA, Sadagopan N, Sahi J, de Morais SM. Induction of drug metabolism enzymes and MDR1 using a novel human hepatocyte cell line. J Pharmacol Exp Ther 2004; 309(1):303 309.
139. Hariparsad N, Carr BA, Evers R, Chu X. Comparison of immortalized Fa2N 4 cells and human hepatocytes as in vitro models for cytochrome P450 induction. Drug Metab Dispos 2008, 1046 1055 [Epub March 10, 2008].
140. Ripp SL, Mills JB, Fahmi OA, Trevena KA, Liras JL, Maurer TS, de Morais SM. Use of immortalized human hepatocytes to predict the magnitude of clinical drug drug interactions caused by CYP3A4 induction. Drug Metab Dispos 2006; 34(10):1742 1748.
141. Banas A, Yamamoto Y, Teratani T, Ochiya T. Stem cell plasticity: learning from hepatogenic differentiation strategies. Dev Dyn 2007; 236(12):3228 3241.
142. Ek M, Soderdahl T, Kuppers Munther B, Edsbagge J, Andersson TB, Bjorquist P, Cotgreave I, Jernstrom B, Ingelman Sundberg M, Johansson I. Expression of drug metabolizing enzymes in hepatocyte like cells derived from human embryonic stem cells. Biochem Pharmacol 2007; 74(3):496 503.
143. Nishimura M, Yokoi T, Tateno C, Kataoka M, Takahashi E, Horie T, Yoshizato K, Naito S. Induction of human CYP1A2 and CYP3A4 in primary culture of hepatocytes from chimeric mice with humanized liver. Drug Metab Pharmacokinet 2005; 20(2):121 126.
144. Tateno C, Yoshizane Y, Saito N, Kataoka M, Utoh R, Yamasaki C, Tachibana A, Soeno Y, Asahina K, Hino H, Asahara T, Yokoi T, Furukawa T, Yoshizato K. Near completely humanized liver in mice shows human type metabolic responses to drugs. Am J Pathol 2004; 165(3):901 912.

19

Drug Interaction Studies in the Drug Development Process: Studies In Vitro

R. Scott Obach and Robert L. Walsky
Department of Pharmacokinetics, Pharmacodynamics, and Drug Metabolism, Pfizer Global Research and Development, Groton, Connecticut, U.S.A.

INTRODUCTION: IN VITRO INHIBITION IN DRUG DEVELOPMENT

Determination of the potential effects of new molecules on the activities of drug-metabolizing enzymes in vitro can be useful in several areas of drug research. The data can serve as an indicator of whether a new compound could cause pharmacokinetic-based drug-drug interactions (DDIs). In early research, such assays can be conducted using high-throughput approaches to accommodate the large numbers of compounds synthesized and tested for pharmacological activity (Fig. 1). To be fit for purpose (i.e., development of structure-activity relationships, driving compound design), these assays require high capacity and sacrifice some aspects of assay performance to allow for this capacity. Miniaturized methods that use fluorogenic substrates and plate reader platforms (1,2) or cocktail methods [in which multiple substrates are mixed and the assays done simultaneously (3 9)] are well suited for these needs.

The focus of this chapter is on in vitro methods used during the later development phase of drug research (Fig. 1). The purposes of the in vitro inhibition data gathered during this phase are (*i*) determining which drug-metabolizing enzymes are unaffected by the drug candidate, (*ii*) planning a clinical DDI strategy (i.e., which, if any, drug interactions should be anticipated and explored), and (*iii*) product labeling used to advise prescribing physicians whether certain drug combinations should be avoided. Because conclusions are drawn from these in vitro data regarding the potential safety of human study subjects and patients and potentially forgoing clinical DDI studies, it is of utmost importance that the data be unassailable there is no room for error. Thus, unlike the aforementioned assay approaches appropriate for early drug research, in vitro inhibition studies done in support of compounds in the development phase must be done with a high degree of accuracy and no chance of false negative results. While it has not been mandated from government drug regulatory agencies that such assays be done under the guidances of Good Laboratory Practices, some have suggested that this be considered (10,11).

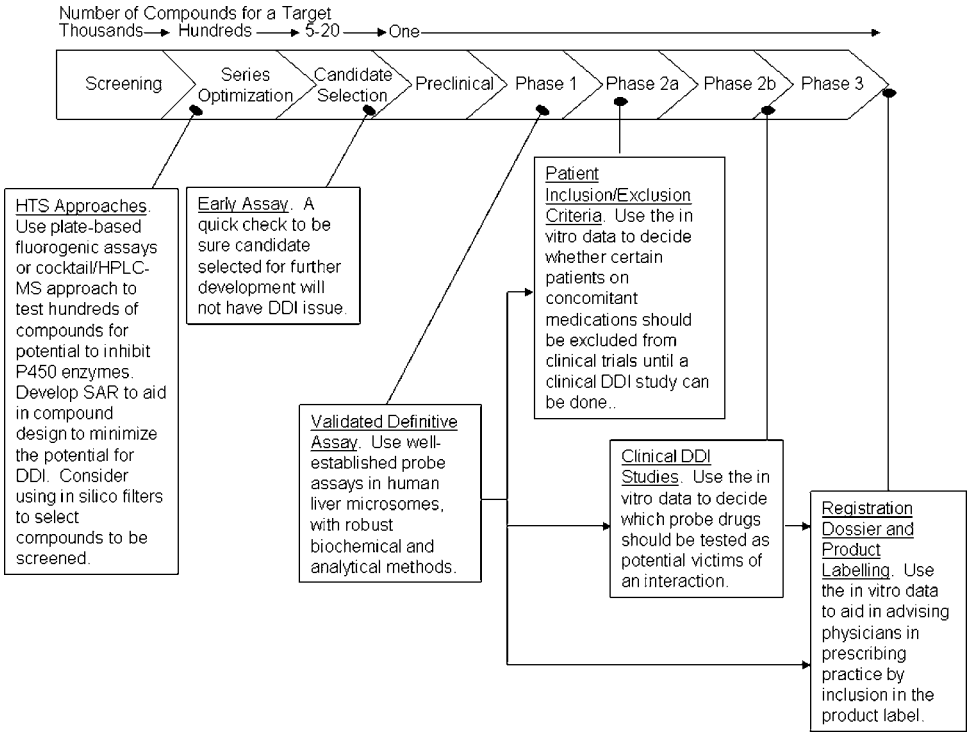

Figure 1 Strategy for placement of in vitro inhibition studies in the drug discovery and development processes.

This chapter describes the assays used for testing new compounds as inhibitors of drug-metabolizing enzymes during the later phases of drug research and how the data can be used in drug development. It will not cover the aforementioned high-throughput methods applied in early drug research, and readers are directed to other reviews of that topic (12). Also, this chapter addresses the testing of new drugs as potential "perpetrators" or "precipitants" of drug interactions. Focus on new compounds as "victims" or "objects" of drug interactions using in vitro data that aim to identify the enzyme(s) involved in the metabolism of a new drug is in chapter 16 in this volume.

ELEMENTS OF ASSAY DESIGN AND PERFORMANCE

Biochemical Elements

The possible sources of drug-metabolizing enzymes for determination of enzyme kinetics and inhibition data include pure enzymes, enzymes expressed in heterologous systems from recombinant DNA, tissue subcellular fractions, or whole cell assays. Pros and cons can be derived for each of these systems. The focus of this chapter will be on the most frequently used system (liver microsomes) to address the potential for DDI with the most important drug-metabolizing enzymes [cytochrome P450s (CYPs)].

The collection of accurate in vitro inhibition data requires that fundamentally sound enzyme kinetic practices be employed. To ensure this, reaction characteristics must be well defined. The most important experimental variables for drug metabolism reactions are substrate concentration, incubation time, and protein concentration. Other important

parameters such as temperature, pH, and buffer strength are usually set to match or mimic in vivo conditions. [It should be noted that a temperature of 37°C and a pH of 7.4 are routinely used as standard since these are appropriate for human liver. However, there is variability around buffers used. Effects of different buffers and concentrations on drug-metabolizing enzymes have been noted (13), and this should be an area of further research and systematic evaluation.] The incubation time needs to be long enough such that adequate product is formed for precise quantitation, but it also must be within a linear range so that reaction velocities are accurate. Likewise, the protein concentration must be high enough to permit formation of an adequate amount of product to be measured, but must not be so high as to consume too much substrate or show a nonlinear relationship between reaction velocity and protein concentration. An initial experiment is required in which product formation is measured at multiple time points in incubations containing different concentrations of protein. A lack of velocity linearity with time can arise from two sources: autoinactivation of the enzyme or too much substrate depletion. The substrate concentration chosen for this determination of linearity should be the lowest one anticipated to be used in substrate saturation experiments. A depiction of a linearity experiment is illustrated in Figure 2A. From this experiment, an incubation time and protein concentration can be selected for all subsequent experiments using the reaction and enzyme source. The lowest protein concentration that still yields adequate product formation should be selected. The use of high microsomal protein concentrations has been demonstrated to cause an alteration of inhibition constants for highly lipophilic drugs due to nonspecific binding (14). The incubation time used can be the longest one feasible that is still linear (i.e., the reaction velocity does not fall below 95% of what is measured using earlier incubation time points) (Fig. 2B). The linear formation of metabolite with increasing microsomal protein concentration should be verified at the chosen incubation time (Fig. 2C). When the enzyme source is changed (e.g., one lot of liver microsomes to another, from liver microsomes to heterologously expressed recombinant enzymes, etc.), this linearity determination must be redone.

After appropriate incubation conditions are established, a substrate saturation experiment is conducted to establish the enzyme kinetic parameters for the reaction in that system. The kinetic parameters, especially K_M, should be within the range of those reported in the scientific literature. The enzyme kinetic behavior for drug metabolism reactions may not follow the simple hyperbolic relationship defined by the basic Michaelis-Menten equation (Fig. 3A,B). Other common kinetic phenomena include activation kinetics, substrate inhibition kinetics, or two-enzyme kinetics (Fig. 3C H). The kinetic behavior can be diagnosed using linearized plots of the data (e.g., Eadie-Hofstee plots), and the data fit using nonliear regression and statistical criteria, such as the Aikake information criteria, to select the most appropriate fit of the data.

The enzyme kinetic data are subsequently used to select the most appropriate substrate concentrations for routine testing of new compounds as inhibitors of drug-metabolizing enzymes. A three-step testing paradigm of

1. single inhibitor concentration,
2. IC_{50} determination, and
3. K_i determination

can be resource sparing and yet provide data needed for decision making in drug development. Initial testing should be done at a single concentration of test compound, using a substrate concentration at or below K_M, such that the large number of compounds that will show no effect can be adequately addressed with minimal yet appropriate resources (i.e., single concentration of test compound). For compounds that demonstrate

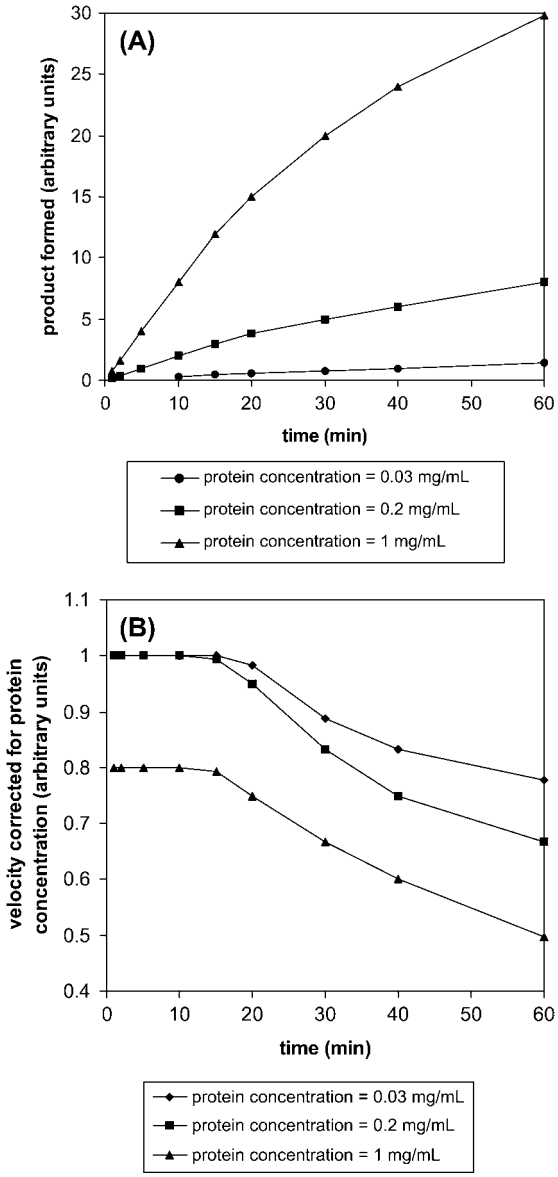

Figure 2 Demonstration of linearity of enzymatic reactions. In plot A, the product formed is measured over incubation time at three different protein concentrations. The limit of detection in this example is 0.25, so the incubation conducted at 0.03 mg/mL has too low a protein concentration because 95% inhibition would yield an amount of product that would be below the lower limit of quantitation of the assay. In plot B, the data from plot A are converted to velocity values to determine the longest incubation time for which linearity is demonstrated. In this example, a maximum incubation time of 15 minutes should not be exceeded. In plot C, the velocity at 15 minutes is plotted versus the protein concentration, which shows that the reaction is linear for the 0.03 and 0.2 mg/mL concentrations, but not the 1 mg/mL concentration. Therefore, a protein concentration of 0.2 mg/mL should not be exceeded.

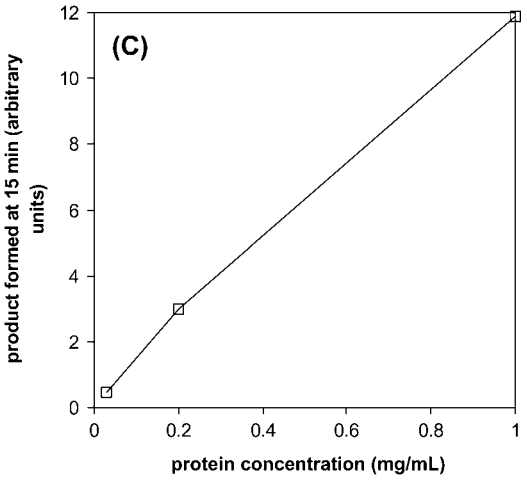

Figure 2 (*Continued*)

some degree of inhibition, a follow-up in rapid succession can be done to measure IC_{50}, again using a substrate concentration at or below K_M. (If $[S] = K_M$, then it can be inferred that $IC_{50} = 2X\ K_i$ for a competitive inhibitor. The utility of such an approach is described in the section "Interpretation of Inhibition Data in Drug Development.") Later on, a K_i can be determined using multiple substrate and inhibitor concentrations, which will define the enzyme kinetic mechanism of inhibition. However, whether a compound is a competitive, noncompetitive, or uncompetitive inhibitor is not known to impact decision making around the potential for clinical relevance for DDI.

Testing whether a new compound can cause time-dependent inhibition is also important, as some of the most important clinical DDIs are caused by drugs that are mechanism-based inactivators. Initial experiments in which the test compound is incubated with enzyme and cofactors in the absence of substrate, followed by addition of the substrate, or dilution into an incubation mixture containing substrate, can be done to detect whether a new compound is a time-dependent inhibitor. Follow-up experiments for those compounds demonstrating that this activity can include the measurement of inactivation parameters k_{inact} and K_I (the maximum inactivation rate constant and the inactivator concentration that provides half of this rate), which can be used in prediction of DDI. However, specifics around the conduct of these experiments are described in chapter 21 and will not be discussed in detail here.

Analytical Elements

High-quality in vitro inhibition data requires not only sound enzyme kinetic practice, but also robust quantitative methods to analyze the incubation samples. In this case, the assay is designed to quantitate the product of the reaction. Almost all standard assays used in the drug development phase utilize a chromatographic separation step in-line with either ultraviolet (UV)/visible (VIS), fluorescence, or mass spectrometric (MS) detectors. While the early assays for P450 enzymes commonly used the two former techniques, more recent assays typically use tandem quadrupole MS/MS instrumentation using selected

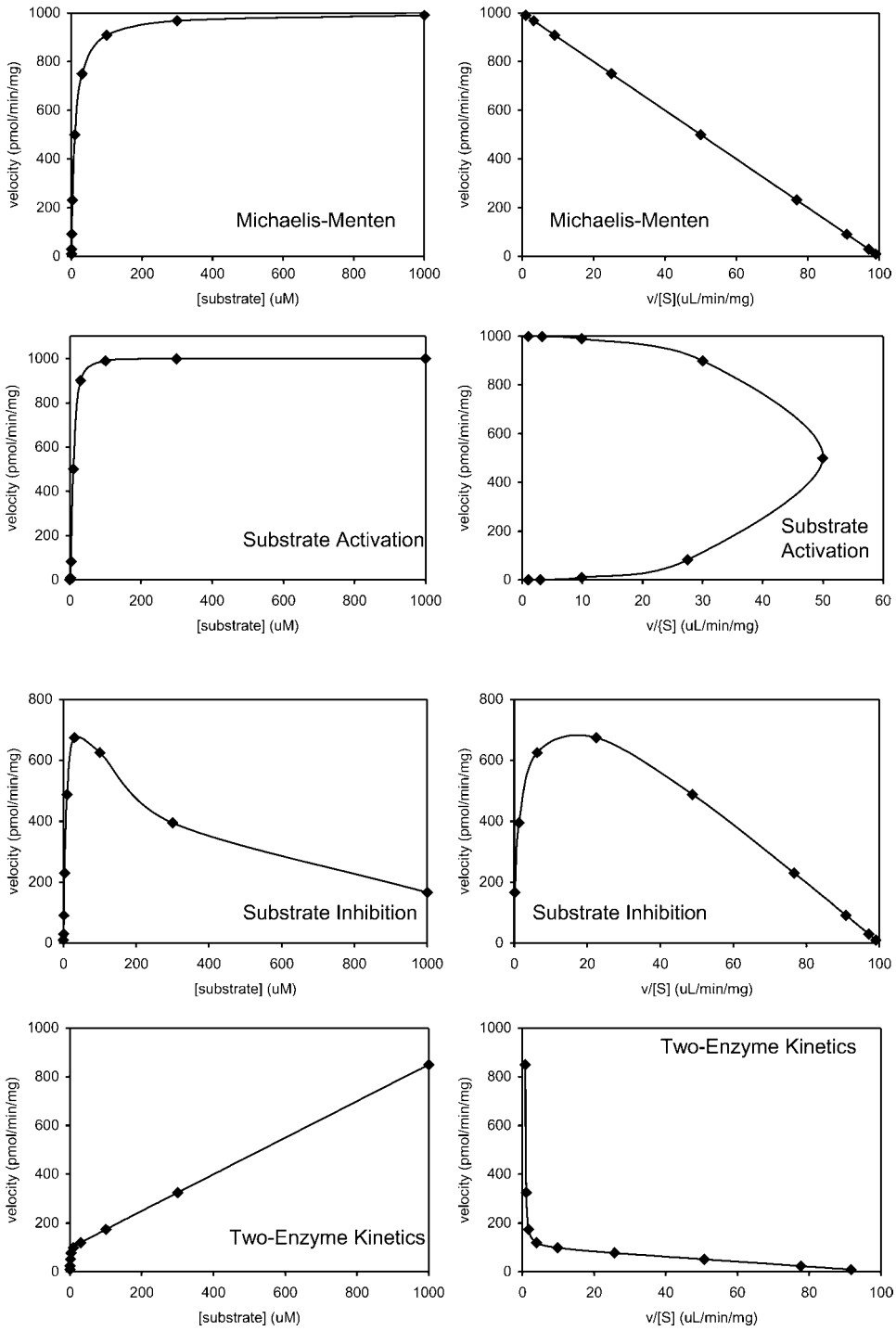

Figure 3 Four common enzyme kinetic models for cytochrome P450 catalyzed reactions in human liver microsomes. Substrate saturation curves (*left*). Eadie Hofstee transformed plots of the data on the left (*right*).

reaction monitoring. The sensitivity and specificity of this approach makes it the preferred standard for simple, robust assays (15 17).

For in vitro samples, the sample work-up needed prior to sample analysis is generally simple, as compared with procedures usually required for other more complex biological matrices. For UV/VIS and fluorescence detection based methods, some sample work-up may be required to remove interfering endogenous materials or to concentrate the sample for effective detection. Samples will have required termination of the reaction, which is usually done by addition of miscible organic solvent, acid, or base. For more robust assays, a suitable internal standard will be added to account for intersample variability in analyte recovery and HPLC injector variability. Internal standards for UV/VIS and fluorescence methods should be structural analogues of the analytes that behave similarly throughout the sample processing technique, have similar detection properties, and are adequately resolved from the analyte (as well as the substrate) on HPLC. For MS detection, internal standards that are identical to the analyte except that at least three atoms are replaced with stable isotopes (i.e., ^{2}H, ^{13}C, or ^{15}N) to allow for an isotopic dilution approach to quantitation. Liquid and solid-phase extraction techniques are typical for UV/VIS and fluorescence methods. For MS detection, a simple filtration of the samples is all that is needed so that protein that can clog HPLC columns is removed.

There are several standard criteria that must be met for an acceptable analytical method. These are:

1. Assay interferences eliminated. The method used, typically HPLC, should be free of interferences from the matrix. In the case of in vitro assays, the matrix is usually a terminated incubation mixture containing a source of enzyme (e.g., liver microsomes), buffer, and other cofactors, and compared with most biological matrices, this is fairly clean. To avoid problems, the analyte needs to be eluted from the column at a retention time after the time when the void volume elutes since this time is when most potential interferences will elute (i.e., absorbing materials for UV/VIS detection or ion-suppressing materials for MS detection). Thus, control samples in which the in vitro matrix lacking analyte should be run.
2. Definition of a standard curve range. The lower limit of quantitation (LLOQ) should be such that an uninhibited reaction should yield an amount of product that is 20-fold greater than the LLOQ, thus allowing for the accurate determination of up to 95% inhibition. The upper limit of quantitation (ULOQ) should be high enough such that the concentration of product formed does not exceed the ULOQ when the substrate incubations are done at saturating conditions (e.g., at $[S] \geq 9X\ K_M$). The standard curve should contain a blank and at least four other points residing between LLOQ and ULOQ.
3. Quality control (QC) standards. Separately prepared QC standards at concentrations within the standard curve range should be analyzed and measured in each assay run, and the measured concentrations should be within 15% of the nominal value for the run to be considered acceptable.
4. Stability of standards and stock solutions. In most cases, the analytes for these assays are valuable materials, and for cost and convenience, it is advantageous to prepare stock solutions from which standard curve and QC samples can be made, and to store these solutions for extended periods (e.g., months). Therefore, conditions under which such solutions can be stored (e.g., solution strength, solvent, temperature) need to be established, and stock solutions that exceed this expiry need to be discarded and prepared fresh. The initial potency

of standard solid materials needs to be established; if purchased from a vendor, this should be provided as part of the analytical specifications datasheet. Furthermore, storage stability of the standard solid materials needs to be established, using standard analytical methods (e.g., HPLC-UV). The solid material may need to be stored in a dry box containing desiccant and may require refrigeration.

In addition to these analytical assay characteristics, there are a couple of others that are unique to in vitro incubation mixtures:

5. Interference by the test compound. In rare instances, the compound being tested can share detection features of the analyte (i.e., absorbance in the same wavelength range for UV/VIS assays, same ions for MS assays) or interfere with the analyte response (i.e., coelution with the analyte and suppression of its signal in MS). This could yield misleading results such that the inhibition by a compound could be overlooked or a compound could be concluded to be an inhibitor when it is not. Therefore, the test compound at the highest concentration tested should be spiked into a low-level QC sample to ensure that the QC response is minimally affected.
6. Interference by contamination in the substrate. For some assays, the substrate material can contain the product (analyte) as a trace contaminant. This is particularly common for P450 reactions in which the reaction is one where some low level of spontaneous oxidation is energetically favorable (e.g., N-dealkylations; aromatizations). Since good enzyme kinetic practice demands that substrate turnover is kept to a minimum, even a very small level of impurity of the substrate by the product can confound inhibition assays. This needs to be tested when characterizing the assay and should be monitored in assay runs by including injection of the unincubated substrate at the highest concentration used. When unavoidable, a correction for this contamination can be applied, but this represents another source of variability that can confound an assay.

INDIVIDUAL ENZYMES AND SUBSTRATES

Among the many drug-metabolizing enzymes that could be potentially inhibited by new drugs, the ones of greatest focus are the CYP enzymes. It is an expectation that the effects of new agents on common P450 activities be studied and included in the government regulatory agency registration dossiers (18). This is not yet the case for other families of drug-metabolizing enzymes as these are less well characterized, cases of clinically meaningful DDI are considerably rarer, and in vitro approaches (e.g., well-characterized specific probe reactions and inhibitors) are not well developed.

The ideal reactions to use as probes for P450 activities will have the following characteristics: (*i*) selectivity for one enzyme, (*ii*) high reaction rate, (*iii*) readily available substrate, metabolite standard, and internal standard for the metabolite from common commercial suppliers at reasonable costs, (*iv*) one metabolite product with unique spectral properties, (*v*) metabolite with high responsivity and selectivity in UV, fluorescence, or MS detectors, (*vi*) substrate, metabolite, and internal standard with stability as dry materials and in concentrated stock solutions, (*vii*) substrate with high solubility in aqueous solution, (*viii*) easy-to-handle substrate (does not bind nonspecifically to laboratory ware or microsomes), (*ix*) materials that are not US Drug Enforcement Agency-controlled substances, and (*x*) materials with safety characteristics for routine use

in the laboratory. None of the P450 probe substrates possess all of these properties, but the most important attribute is selectivity for one enzyme, and other attributes are sacrificed to varying extents to ensure that selectivity meets the needs of the analysis. The substrates and reactions described in the following sections are depicted in Figure 4.

Cytochrome P4501A2

CYP1A2 is responsible for the clearance of numerous drugs. For clinical DDI, the most studied drugs that have a high dependence on CYP1A2 for clearance are theophylline and caffeine. Theophylline has a fairly low therapeutic index, and some notable DDIs arising

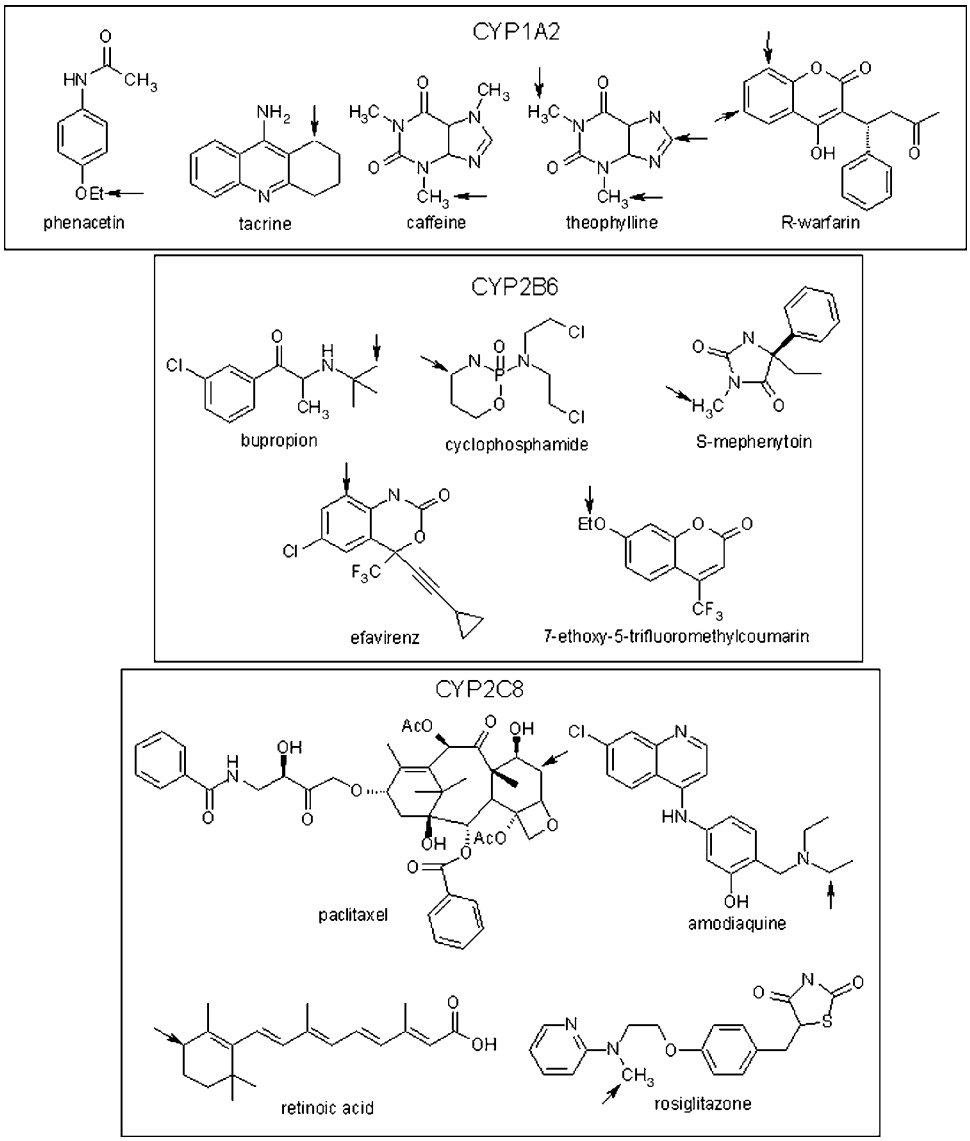

Figure 4 Structures of substrates used in measurement of cytochrome P450 activities and sites of metabolism.

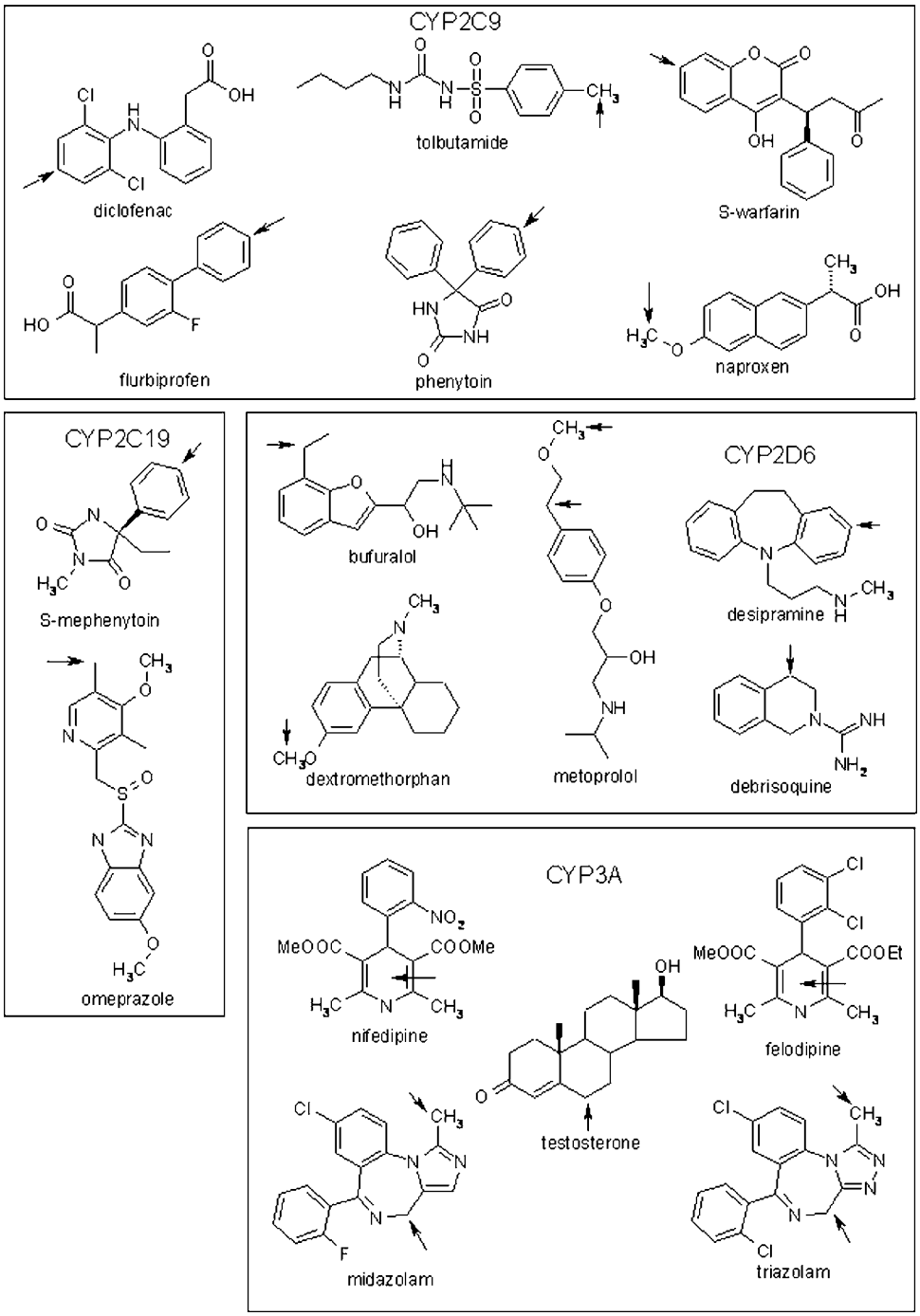

Figure 4 (*Continued*)

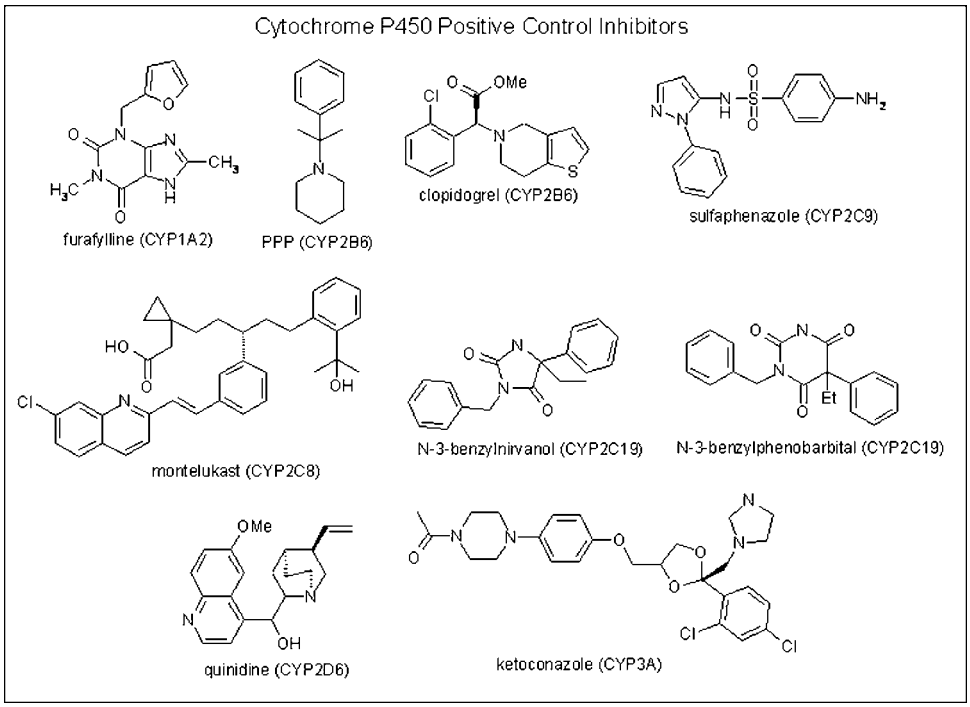

Figure 4 (*Continued*)

from CYP1A2 inhibition were observed when enoxacin was prescribed to patients with bacterial infection who were already on chronic theophylline regimens to control asthma (19). However, theophylline clearance is partially mediated by renal secretion, limiting the maximum DDI to about fivefold, whereas caffeine has a much greater dependence on CYP1A2 for clearance (20). More recently, two other drugs have been noted to have very high dependence on CYP1A2 for clearance: tizanidine and ramelteon (21,22).

The main vitro assay to test for CYP1A2 inhibition in drug development is the phenacetin *O*-deethylase assay. The assay offers the advantage that the metabolite, acetaminophen, is readily available, inexpensive, and chemically stable. The earlier HPLC assays for measuring phenacetin *O*-deethylase activity in human liver microsomes involved the use of UV detection (23). These have been adapted for MS detection, and preparation of stable isotope labeled acetaminophen is facile, to provide a robust assay (16,17). Also, a radiometric assay was described, in which [^{14}C-ethyl]phenacetin was used as substrate and the radioactive acetaldehyde quantitated after separation from the unreacted substrate (24). Phenacetin O-deethylation demonstrates linearity out to relatively long incubation times, allowing for the use of lower protein concentrations to still yield enough product formation for measurement. Interestingly, a wide range of K_M values have been reported for phenacetin *O*-deethylase, emphasizing the need that individual laboratories should determine their own enzyme kinetic parameters before conducting inhibition studies. Other enzymes besides CYP1A2 have been shown to catalyze phenacetin *O*-deethylase, but with high K_M values (25 27), thus it is important that assays testing for CYP1A2 inhibition keep substrate concentrations within an appropriate range (i.e., <200 μM).

CYP1A2 activity has also been assayed using other reactions. Tacrine is hydroxylated to four regioisomeric products (28), the major product being the 1-hydroxytacrine isomer. To accurately quantify this activity, 1-hydroxytacrine must be chromatographically separated from the 2-, 4-, and 7-hydroxytacrine minor products. While theophylline has been a commonly used in vivo probe for CYP1A2 activity, its use as an in vitro probe is limited by the very slow turnover to its N-demethylated products. Other less frequently used reactions for CYP1A2 have been caffeine N-demethylation to paraxanthine (23,29) and (*R*)-warfarin 6- and 8-hydroxylation (30), which also require chromatographic resolution of other isomeric metabolites. Many of the assays used for CYP1A2 have cross talk with CYP1A1, although expression of the latter in liver is very low.

Inhibitors that can be used as positive controls for CYP1A2 inhibition include furafylline and fluvoxamine. The former is a mechanism-based inactivator and should be incubated prior to addition of the substrate (31,32). The latter is a potent reversible inhibitor (33,34) that also has activity against CYP2C19. Other inactivators include zileuton and rofecoxib (35,36).

Cytochrome P4502B6

Relative to the other P450s discussed in this chapter, CYP2B6 is of generally lower importance in drug metabolism, but it has been gaining in importance in recent years (37,38). It is important in the bioactivation of the cytotoxic anticancer agent cyclophosphamide (39). It has also been shown to be involved in the clearance of efavirenz and a contributing enzyme in the clearance of sertraline and bupropion among others (40 43).

A commonly used in vitro probe reaction specific for CYP2B6 is bupropion hydroxylation. While bupropion is primarily cleared in vivo by reduction of the ketone (44), the hydroxylation reaction on the *t*-butyl group has been shown to be mediated by CYP2B6 in vitro (45,46) and affected by CYP2B6 inhibitors in vivo (47). The hydroxybupropion metabolite forms a stable six-membered cyclic ketal, which is likely what is detected on HPLC. The early HPLC-UV assays utilized a low wavelength to detect hydroxybupropion; greater selectivity was afforded by the use of MS detection, and stable isotope labeled hydroxybupropion is now commercially available for use as an internal standard.

Other assays that have been used to measure CYP2B6 activity have included cyclophosphamide 4-hydroxylation (48), *S*-mephenytoin N-demethylation (49), efavirenz 8-hydroxylation (50), and 7-ethoxytrifluoromethylcoumarin *O*-deethylase (51). The former three are HPLC-UV assays, and the latter a plate-based method using fluorescence detection. The mephenytoin N-demethylation reaction suffers from the fact that CYP2B6 is a high K_M component and that CYP2C9 also catalyzes the reaction with a lower K_M, thus requiring great care in selection of appropriate substrate concentrations. Inhibitors used as positive controls have included thioTEPA, clopidogrel, phenylethyl piperidine ("PPP"), and orphenadrine. The latter is a reversible inhibitor with low potency and selectivity (52), while the former three are mechanism-based inactivators (53 55). Clopidogrel can be challenging to use because the ester group in it can be readily hydrolyzed and the resulting acid does not appear to inactivate, while thioTEPA is not selective for CYP2B6 (56).

Cytochrome P4502C8

While there are not many DDIs caused by inhibition of CYP2C8, there have been a few notable ones, including the inhibition of clearance of cerivastatin and repaglinide by gemfibrozil (57,58). There is experimental evidence to suggest that the mechanism of

DDIs caused by gemfibrozil may be mediated by inactivation by the gemfibrozil glucuronide metabolite, and part of the effect can be attributed to hepatic transport mechanisms (59,60). Nevertheless, with a growing list of drugs with clearance dependent on the activity of CYP2C8, measurement of the potential for inhibition of this enzyme is important.

Over the years, CYP2C8 activity has been measured in vitro using paclitaxel 6α-hydroxylase or retinoic acid 4-hydroxylase activities (61 64). However, the cost of reagents for paclitaxel (drug, metabolite) and challenges in handling for retinoic acid reagents (instability), along with the discovery that CYP2C8 was the predominant enzyme in the catalysis of the N-deethylation of the antimalarial agent amodiquine, has led to the adoption of the latter activity as a facile CYP2C8 marker activity (65). The initial report utilized an HPLC-UV assay, and this has been converted to a MS-based assay (16). Rosiglitazone N-demethylation has also been shown to be catalyzed by CYP2C8. However, this reaction also has a significant contribution by CYP2C9, making it a less optimal marker activity (66). The most potent in vitro inhibitor of CYP2C8 is montelukast, with a potency in the nM range, with the caveat that the apparent potency is dependent on protein concentration used as montelukast demonstrates nonspecific binding (67). Trimethoprim has also been shown to selectively inhibit CYP2C8, although with much lower potency (68). Quercetin has also been used but is not specific for CYP2C8 (67).

Cytochrome P4502C9

CYP2C9 is one of the most important of the human P450s in DDI since it metabolizes hundreds of drugs, and in some instances, its contribution to the clearance of some drugs predominates to such a large extent that inhibition of the enzyme in vivo can result in substantial DDI (69). The CYP2C9 substrate of greatest clinical concern is warfarin, since CYP2C9-catalyzed 7-hydroxylation contributes around 90% of the clearance of the pharmacologically potent *S*-isomer. Other drugs cleared by CYP2C9 include many NSAIDs and agents involved in regulation of glucose in diabetic patients, and CYP2C9 plays a contributory role in the clearance of some members of many other classes of drugs (e.g., benzodiazepine anxiolytic agents, antidepressants, etc.).

The three most commonly used assays to measure CYP2C9 activity in in vitro inhibition studies are diclofenac 4′-hydroxylase, tolbutamide methyl hydroxylase, and (*S*)-warfarin 7-hydroxylase. Diclofenac 4′-hydroxylation is an easy assay to conduct since the rate is very high relative to other P450 assays. In the past, the challenge was obtaining suitable authentic standard for the 4′-hydroxy metabolite, and the material was expensive, however, biosynthetic methods have been developed that can yield gram quantities and have reduced the cost (70). Early methods used HPLC-UV (71,72), while later, the assay was adapted for MS-based detection (16,17). Tolbutamide hydroxylase has also been used as a CYP2C9 marker activity, earlier with HPLC-UV assays and later on with MS-based assays (73,16). A portion of this activity can be attributed to CYP2C19 (74,75). (S)-warfarin 7-hydroxylase is selective for CYP2C9, however, use of this substrate in human liver microsomes requires that the regioisomeric metabolites (e.g., 6- and 8-hydroxywarfarin) be chromatographically resolved (76,77). Other assays that have been used for CYP2C9 include flurbiprofen 4′-hydroxylase (78), naproxen *O*-demethylase (79,80) and phenytoin *p*-hydroxylase (81), although care must be taken when using naproxen or phenytoin since other P450 enzymes can contribute to metabolism of these substrates (79,80,82). Recent evidence suggests that inhibitors of CYP2C9 will have different effects on different CYP2C9 reactions and different genetic variants of the enzyme (81,83). The activities of a large panel of CYP2C9 inhibitors showed that there appear to be at least three classes of substrate for CYP2C9: *S*-warfarin is one class,

flurbiprofen is a second, and a third that has diclofenac, tolbutamide, and phenytoin. For example, indomethacin inhibited CYP2C9 warfarin 7-hydroxylase activity with a potency (K_i) of 0.66 μM while inhibiting tolbutamide or diclofenac hydroxylase activities at 14 μM and inhibiting flurbiprofen hydroxylase at 53 μM. Such different potency values would lead to different conclusions to be made regarding the potential importance of the finding. There was no pattern regarding which activity would be most potently inhibited, and some inhibitors demonstrated activities that did not depend on the specific substrate used, so for new compounds, it presently cannot be predicted which substrate activity will be most potently inhibited. Furthermore, the carrier solvent can have an effect on the metabolism of some substrates but not others (81). As a positive control inhibitor, sulfaphenazole has been shown to be selective (84) and consistently used, and even the recent data regarding substrate classes have not altered the usefulness of this compound as a suitable, selective, positive control inhibitor.

Cytochrome P4502C19

CYP2C19 has been the focus of considerable attention over the years, although there are actually very few drugs that have this enzyme as such a large contributor to clearance that substantial DDI can be observed by inhibiting this enzyme. The 4′-hydroxylation of (S)-mephenytoin and the use of metabolite/parent ratios in urine have been the most studied experimental endpoints to measure CYP2C19 activity in vivo [for both enzyme activity and effects of genotype polymorphisms (85,86)]. However, mephenytoin is not a therapeutically used drug. Omeprazole metabolism, specifically the hydroxylation of the methyl group on the 5-position of the pyridine ring, is a CYP2C19 selective activity, and omeprazole demonstrates marked differences in pharmacokinetics in CYP2C19 extensive and poor metabolizers (87).

The most frequently used assay for CYP2C19 is *S*-mephenytoin 4′-hydroxylase. Analysis of 4′-hydroxymephenytoin originated as an HPLC-UV method but has since been converted to a MS-based method as well as a tritium release approach (15 17,88,89). The assay suffers from a slow turnover rate and possesses challenges in detection of the product as it neither absorbs UV light particularly strongly nor at long wavelengths. It also does not strongly ionize in HPLC-MS as compared with other compounds. Fortunately, the CYP2C19 mephenytoin 4′-hydroxylase activity appears to be linear out to long (relative to other P450s) incubation times (e.g., >40 min), and the substrate does not bind to microsomes so that higher enzyme concentrations can be used compared with other activities. The only other activity widely used to measure CYP2C19 activity is omeprazole 5-hydroxylase. Selective positive control inhibitors for CYP2C19 are rare. Benzyl-substituted nirvanol and phenobarbital have been fairly recently prepared and shown to be selective inhibitors for CYP2C19 (90). Ticlopidine had been reported to inactivate CYP2C19, but it also significantly affects other P450s (54,91,92), and fluvoxamine is a potent reversible inhibitor, which also affects CYP1A2.

Cytochrome P4502D6

One of the most important drug-metabolizing enzymes is CYP2D6. Compared with the other P450 enzymes, CYP2D6 tends to have a high affinity for many of its substrates and inhibitors and is thus frequently involved as an underlying mechanism for DDI. It is involved in the metabolism of many basic amine-containing compounds including neuroleptics, antidepressants, and cardiovascular agents. Testing new experimental drugs for their potential to inhibit CYP2D6 is important because of the number of drugs cleared

by this enzyme. However, it is noteworthy that many drugs that are cleared primarily by CYP2D6 have relatively large therapeutic indices because of the naturally occurring genetic polymorphisms that result in such a wide range of enzyme activities across the population. If a CYP2D6-cleared compound were to have a low therapeutic index, it would be very challenging to use in clinical practice because the same dose level would be ineffective in many patients and toxic to many others. Personalized medicine would need to be applied such that patients would need to be tested with CYP2D6 genotyping before drug administration. Since such an approach has not become part of clinical practice, new drugs that are cleared by CYP2D6 will continue to need wide therapeutic indices.

While there are many possible selective substrates that could be used to measure CYP2D6 activity (93), the most commonly used ones have been bufuralol 1′-hydroxylase, dextromethorphan *O*-demethylase, debrisoquine 4-hydroxlase (94), and other activities have included metoprolol [both O-demethylation and α-hydroxylation (95)], desipramine 2-hydroxylation (96), and sparteine dehydrogenation. Bufuralol 1′-hydroxylase was originally run as an HPLC assay with fluorescence detection since the benzofuran ring system is highly fluorescent. The activity is almost exclusively dependent on CYP2D6, especially at concentrations <10 μM. Some contribution by CYP2C19, particularly when stereochemical considerations are made, is evident at higher concentrations (97,98), but racemic bufuralol can be used reliably at an appropriate concentration range (<100 μM). Debrisoquine 4-hydroxylation has also been used as a selective probe activity for CYP2D6 using GC-MS methods (99,100).

Dextromethorphan *O*-demethylase has been a widely utilized CYP2D6 probe substrate, and this probe also possesses the advantage over bufuralol and debrisoquine activities of being used easily in clinical studies. (Neither bufuralol or debrisoquine is available clinically in the United States.) The dextrorphan/dextromethorphan urinary ratio has been a common CYP2D6 phenotyping tool in humans [provided that urinary pH is not aberrant, (101)]. Likewise, the conversion of dextromethorphan to dextrorphan has been a commonly employed assay to measure the potential for new drugs to inhibit CYP2D6, with early assays employing HPLC with fluorescence detection (94) or radiometric detection using [O-methyl^{14}C]dextromethorphan as substrate (102) and later assays using MS detection (16,17). Dextromethorphan can also be N-demethylated to methoxymorphinan by CYP3A, so care needs to be taken to resolve these two demethylated metabolites by HPLC, and trace quantities of the *N*-desmethyl metabolite can be present as a contaminant in commercial samples of dextromethorphan. Otherwise, this assay is a robust and facile method for making this measurement. There are several compounds that could be potentially used as positive control inhibitors, however, the most regularly used one is quinidine.

Cytochrome P4503A

CYP3A poses the greatest complexities when attempting to measure the potential effect of a new drug as an inhibitor. First, the term "CYP3A" refers to two very related enzymes CYP3A4 and CYP3A5, which have some subtle differences with regard to substrate and inhibitor specificities (103 107), but with exception to, perhaps, vincristine, none large enough to permit measuring their activities independently in liver microsomes. CYP3A5 possesses a common genetic polymorphism, with possession of two copies of genes coding for functional enzyme highly dependent on the ethnicity of the population (108). Second, CYP3A4 is present in both liver and intestine, and the enzyme in both of these tissues plays a substantial role in the pharmacokinetcs and DDI for CYP3A-cleared drugs

[reviewed in (109)]. Third, CYP3A, more often than other P450s, demonstrates atypical enzyme kinetic behaviors including autoactivation, substrate inhibition kinetics, and heterotropic activation. These can be affected by cytochrome b_5 as well as buffer and Mg^{2+} (110 114). Finally, CYP3A4 appears to possess different substrate classes (like CYP2C9 above) such that a new drug can show inhibition against some substrates but not others (115). The in vivo relevance of these various phenomena are not known.

Assays to measure the effect on CYP3A in liver microsomes essentially measure the effect on CYP3A4 and 3A5 simultaneously. In liver microsome samples *pooled* from multiple individual donors, the amount of CYP3A4 should exceed the amount of CYP3A5 and dominate the activity, however, in individual samples, the opposite can be true. With the observation of different effects of inhibitors on different activities, measurement of the effect of new drugs on CYP3A involves the operation of three different assays. One substrate class is well represented by imidazobenzodiazepine drugs (e.g., midazolam, triazolam, etc.), a second by dihydropyridine calcium channel blockers (e.g., nifedipine, felodipine), and a third by steroids and macrolide antibiotics (e.g., testosterone, erythromycin, etc.). The three most commonly used assays are midazolam 1′-hydroxylase, testosterone 6β-hydroxylase, and nifedipine or felodipine dehydrogenase.

Midazolam is metabolized at two positions by both CYP3A4 and 3A5: the 1′-methyl group and the 4-position on the diazepine ring. The 1′-hydroxylase assay is more commonly used. Measurement of the 4-hydroxymidazolam product can be challenging because the product demonstrates some instability. Midazolam also demonstrates time-dependent inhibition (116), forcing the use of relatively quick incubation times (i.e., <5 min). Substrate inhibition kinetics are observed for midazolam 1′-hydroxylation, which requires that additional substrate concentrations be used when determining K_M values (16).

Testosterone is hydroxylated at several positions by several P450 enzymes, however, the hydroxylation at the 6-position in the β orientation predominates and is catalyzed by CYP3A4. Early assays utilized long HPLC-UV runs developed for rat metabolism experiments to permit resolution of the many regioisomers (117); optimization of the assay chromatography has resulted in more rapid HPLC-MS assays (16).

The third class of substrate represented by the dihydropyridine calcium channel blockers is the one that more often demonstrates the outlier behavior compared with the other two, with test compounds either inhibiting the other two and not affecting the dihydropyridine metabolic activity [e.g., cyclosporine (118)] or potently inhibiting the nifedipine dehydrogenation and affecting the others much less [e.g., haloperidol (119)]. The use of nifedipine can be particularly challenging because of the instability of this compound with VIS light. Felodipine does not have this problem to the same degree. In both cases, since dihydropyridines can spontaneously oxidize in air, obtaining substrates that are free of the metabolites is challenging. This requires the use of corrections for formation of dehydrogenated products in control incubations in which NADPH is not included.

Despite these complexities with CYP3A assays, ketoconazole can serve adequately as a positive control inhibitor. Ketoconazole is a potent inhibitor that binds by forming a tight ligand interaction with the heme iron and the imidazole, and does not appear to be influenced by substrate. When CYP3A inhibition is observed in pooled human liver microsomes, it is advisable to test the effect on CYP3A4 and 3A5 separately. This can be accomplished by using recombinant enzymes, or by testing in liver microsome samples from different individual donors in which the amounts of CYP3A4 and 3A5 show considerable differences.

INTERPRETATION OF INHIBITION DATA IN DRUG DEVELOPMENT

Collection of in vitro data on the ability of experimental drugs to inhibit P450 enzymes is important to drug development because the information is used both in the design of clinical DDI studies and in determining enzymes requiring no further evaluation. Through the extensive amount of research conducted on P450 enzymes and their role in drug metabolism over the years, there is enough confidence to utilize in vitro information to make predictions of DDI without necessarily requiring clinical DDI studies. In the drug development phase, in vitro inhibition data collected using the definitive methods described above need to be available before patients in phase 2 and 3 studies are dosed with the new compound. Without this information, patient recruitment may need to be limited to exclude patients on concomitant medications, because it would not be known whether the new compound could affect the clearance of the concomitant drugs. (Note that in some target indications, such as cancer, phase 1 study subjects are also patients on other medications, so the in vitro data should be gathered before administration of the new compound.) Two approaches to utilizing in vitro inhibition data for the P450 enzymes to predict DDI are described below.

Prediction of DDI

Although some of the fundamental principles describing the relationship between inhibitory potency and magnitude of DDI have been available for over three decades, the use of these relationships to predict DDI has only been reduced to practice over the past five years or so. Application of these principles required the knowledge obtained over the past ten years regarding the substrate selectivity of the P450 enzymes for various drugs.

Predicting in vivo DDI from in vitro inhibition data begins with the Rowland-Matin equation (120), which describes the relationship between the magnitude of the DDI for a hepatically cleared orally administered drug and the inhibitory potency.

$$\text{Fold change in exposure} = \frac{CL_{po,control}}{CL_{po,inhibited}} = \frac{AUC_{inhibited}}{AUC_{control}} = \frac{1}{\frac{f_{CL_h,CYP}}{\left(1+\frac{[I]_{hepatic}}{K_i}\right)} + (1 - f_{CL_h,CYP})}$$

$AUC_{inhibited}$ and $AUC_{control}$ are the exposure values to the affected drug in the presence and absence of the inhibiting drug, respectively, and $CL_{po,inhibited}$ and $CL_{po,control}$ are the oral clearance values for the affected drug in the presence and absence of the inhibiting drug, respectively. K_i is the inhibitory potency of the inhibiting drug against the P450 enzyme that clears the affected drug, and $[I]_{hepatic}$ is the intrahepatic concentration of the inhibiting drug that is available to bind to the P450 enzyme. The value $f_{CL_h,CYP}$ is the fraction of the affected drug that is cleared by the P450 enzyme in the liver that is the target for inhibition. The value of $f_{CL_h,CYP}$ is important and provides a ceiling on the magnitude of the interaction; when this parameter is ignored, the predictions of DDI will almost always be overestimates. For example, if $f_{CL_h,CYP}$ is 0.5, then no matter how extensively the affected enzyme is inhibited, the largest interaction can be twofold. For $f_{CL_h,CYP}$ values of 0.8 and above, larger interactions can theoretically be observed (Fig. 5). Values of $f_{CL_h,CYP}$ for victim drugs in which high confidence can be placed are not commonly available, and estimates of these can be made from EM/PM pharmacokinetic studies (for CYP2C9-, 2C19-, and 2D6-cleared drugs) or from combining in vitro reaction phenotyping data with radiolabel ADME studies in humans. (Some examples of these are in Fig. 5.) The value for K_i is the value measured from the in vitro study. In the case where just an IC_{50} is measured,

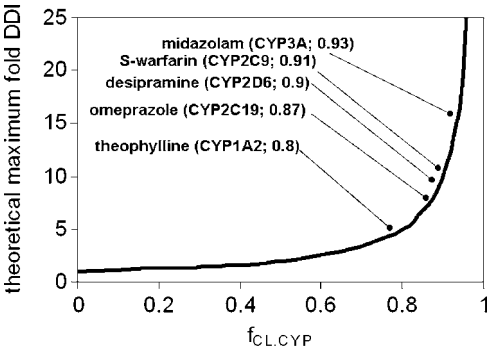

Figure 5 Theoretical maximum magnitude of a drug interaction versus the fraction of the victim drug cleared by the affected enzyme.

competitive inhibition can be assumed and the value converted to a K_i using the Cheng-Prusoff equation (121).

$$K_i = \frac{IC_{50}}{1 + \frac{[S]}{K_M}}$$

(If the incubations are run at $[S] = K_M$, then $K_i = 0.5 \times IC_{50}$.) These values refer to free values, assuming that all of the inhibitor in the in vitro incubation is free in solution to bind the enzyme. In some cases, this may not be true, especially for lipophilic cationic compounds that are known to bind nonspecifically to phospholipid membranes in microsomes. In these instances, the free fraction of the inhibitor should be measured using mock incubation conditions (14). The value for $[I]_{hep}$ represents an in vivo concentration that is unmeasurable and must be estimated. Assumptions that unbound inhibitor concentrations in the plasma are equal to those in the liver and that only unbound inhibitor can bind the enzyme (consistent with the free drug hypothesis) are needed. For this, the inhibitor must be able to freely diffuse across the cell membrane, and there can be no active transport processes altering the ratio of free inhibitor concentration inside and outside the cell from the value of unity. Clearly, there are some drugs for which this assumption will not be valid, and there are in vitro methods available to better understand whether new compounds are substrates for hepatic transporters. Finally, for liver, the concentrations occurring during absorption can be considerably greater than those in the systemic circulation. To deal with this factor, the value used for $[I]_{hep}$ is estimated from the following equation (122):

$$[I]_{hepatic} = f_u \bullet \left(C_{max} + \frac{\text{Dose} \bullet F_{abs} \bullet k_{abs}}{Q_h} \right)$$

in which F_{abs} and k_{abs} are estimates of the fraction absorbed and the absorption rate constant for the inhibitor, respectively, C_{max} is the systemic maximum concentration of inhibitor, f_u is the unbound fraction of the inhibitor in plasma, and Q_h is hepatic blood flow ($\sim$21 mL/min/kg body weight). (If the blood/plasma ratio for the inhibitor is substantially different from unity, f_u will need to be corrected for this factor.) For drugs that inhibit hepatic P450 enzymes (CYP1A2, 2C9, 2C19, and 2D6), this approach predicts the magnitude of DDI with mean-fold error of 1.7X for victim drugs that are affected by twofold or more (118).

For CYP3A, an additional consideration for the effect on the intestinal extraction during first pass must also be considered. A similar equation is used to account for this.

$$\frac{\mathrm{AUC_{inhibited}}}{\mathrm{AUC_{control}}} = \frac{1}{\frac{f_{\mathrm{CL_h,CYP3A}}}{\left(1+\frac{[\mathrm{I}]_{\mathrm{hepatic}}}{K_\mathrm{i}}\right)} + (1 - f_{\mathrm{CL_h,CYP3A}})} \bullet \frac{1}{F_\mathrm{g} + (1 - F_\mathrm{g}) \bullet \left(\frac{1}{1+\frac{[\mathrm{I}]_{\mathrm{gut}}}{K_\mathrm{i}}}\right)}$$

The first term is the same and accounts for the effect on hepatic CYP3A. The second term addresses the effect in the intestine during first pass. The parameter F_g is the fraction of the victim drug that ordinarily evades first-pass extraction by the intestine in the control state. It can be estimated from the CYP3A4 in vitro intrinsic clearance combined with the knowledge of the ratio of CYP3A4 in the liver and the intestine [approximately 100:1 (123)], the free fraction in plasma of the victim drug, and the in vivo oral clearance (assuming complete absorption). Or it can be obtained for drugs for which a pharmacokinetic study was done with liver transplant patients during the anhepatic phase of the procedure [e.g., midazolam, cyclosporine (124,125)]. In many cases, the value of F_g can drive the prediction of DDI because the $[\mathrm{I}]_{\mathrm{gut}}/K_\mathrm{i}$ ratio will be very high (109). $[\mathrm{I}]_{\mathrm{gut}}$ is the concentration of the inhibitor in the intestinal enterocytes. It is estimated from (126) that

$$[\mathrm{I}]_{\mathrm{gut}} = \frac{\mathrm{Dose} \bullet F_{\mathrm{abs}} \bullet \mathrm{k_{abs}}}{Q_\mathrm{g}}$$

in which Q_g is the intestinal flow (ca. 3.5 mL/min/kg body weight). Using this equation, the mean-fold error for CYP3A inhibitors that caused at least a twofold increase in a CYP3A-cleared compound was 1.87 (118).

This sort of approach requires application of a static situation with the system fully at equilibrium. It thus uses some simplifications, and recently, more sophisticated software packages that are based on this fundamental physiological approach but can better model the dynamic situation that occurs in vivo have been developed.

For time-dependent inhibitors, equations similar in structure can be used to make predictions of DDI, but with in vitro inactivation parameters (K_I and $\mathrm{k_{inact}}$) in place of reversible K_i values and inclusion of in vivo degradation rate constants for the enzymes (105,131).

$$\frac{\mathrm{AUC_{inhibited}}}{\mathrm{AUC_{control}}} = \frac{1}{\frac{f_{\mathrm{CL_h,CYP}}}{\left(1+\frac{\mathrm{k_{inact}} \bullet [\mathrm{I}]_{\mathrm{hepatic}}}{\mathrm{k_{deg(CYP)}} \bullet ([\mathrm{I}]_{\mathrm{hepatic}}+K_\mathrm{I})}\right)} + (1 - f_{\mathrm{CL_h,CYP}})}$$

is for hepatic enzymes, and

$$\frac{\mathrm{AUC_{inhibited}}}{\mathrm{AUC_{control}}} = \frac{1}{\frac{f_{\mathrm{CL_h,CYP3A}}}{\left(1 + \frac{\mathrm{k_{inact}} \bullet [\mathrm{I}]_{\mathrm{hepatic}}}{\mathrm{k_{deg(CYP3A,hepatic)}} \bullet ([\mathrm{I}]_{\mathrm{hepatic}} + K_\mathrm{I})}\right)} + (1 - f_{\mathrm{CL_h,CYP3A}})} \bullet \frac{1}{F_\mathrm{g} + (1 - F_\mathrm{g}) \bullet \left(\frac{1}{1+\frac{\mathrm{k_{inact}} \bullet [\mathrm{I}]_{\mathrm{gut}}}{\mathrm{k_{deg(CYP3A,gut)}} \bullet ([\mathrm{I}]_{\mathrm{gut}}+K_\mathrm{I})}}\right)}$$

is for CYP3A that also incorporates the effect in the intestine. The other parameters are as described above. Values for in vivo degradation rate constants for P450 enzymes can be estimated from clinical inactivation and induction data (131). Half-lives of 39, 51, 36, and 24 hours have been estimated for CYP1A2, CYP2D6, hepatic CYP3A4, and intestinal CYP3A4, respectively. Data needed to calculate these values for the other important P450

enzymes are not available, but since the values for the hepatic enzymes are fairly similar to each other, it might be assumed that degradation half-lives for CYP2B6, 2C8, 2C9, and 2C19 may be in the same range. The value for intestinal CYP3A4 is similar to the half-life for enterocytes, which are constantly sloughing off and being replenished. In general, this approach tends to overpredict the magnitude of DDI, even when using unbound systemic C_{max} for the value for $[I]_{hep}$.

The Rank-Order Approach

A more cautious approach to using in vitro inhibition data to predict clinical DDI is the use of the "rank-order" approach, in which at least one clinical DDI study is run irrespective of the potency of the K_i values (127 129). Since the prediction methods described above require acceptance of some assumptions and estimates for input parameters (e.g., $[I]_{hep}$), the fundamental assumption underlying the rank-order approach is that the drugs most likely to be subject to the largest DDI will be the ones cleared by the P450 enzyme most potently inhibited in vitro. A clinical DDI study for a new compound as a potential perpetrator of an interaction would be run using a good probe substrate for the most potently inhibited P450 in vitro (i.e., $f_{CL,CYP} > 0.85$). If this study shows that no interaction occurs (i.e., <twofold increase in AUC), then it can be assumed that there will be no interaction for drugs cleared by the other less potently inhibited P450 enzymes, and this conclusion can be claimed in the product labeling. It must be assured that a probe substrate with a very high $f_{CL,CYP}$ value is the one selected for the clinical DDI study. Some cautions while using this approach must be exhibited.

1. Applying the rank-order approach for a new drug that reversibly inhibits one enzyme but irreversibly inactivates a second enzyme should not be done. Reversible and irreversible inhibitors cannot be compared since the irreversible effect also depends on k_{inact}.
2. Applying the approach for CYP3A4 should be done cautiously. A new compound that inhibits CYP3A less potently than another P450 may show an interaction with a CYP3A-cleared probe and not a probe for the other enzyme, if the CYP3A probe has a high intestinal extraction.

However, if used thoughtfully and with an understanding of the fundamentals behind the mechanisms of DDI, the rank-order approach can be an effective method to leverage in vitro inhibition data to gain an understanding of DDI potential for a new compound without having to empirically run multiple clinical studies. A test of this approach using retrospective data yielded a favorable outcome, with only a very small percentage of DDI being missed, and of those missed, the magnitude of the interaction was just over 2 times. No major DDIs were missed (128).

CONCLUSIONS

Our understanding of the P450 enzymes involved in drug metabolism coupled with pharmacokinetic theory and physiological underpinnings has led us to an era of possessing an ability to fully leverage in vitro inhibition data to reliably predict clinical DDI. This provides a great advantage to clinical DDI strategies that can be mechanistically based rather than the empirical approaches that needed to be used in the past. In vitro experimental approaches to P450 inhibition studies have matured to the point that they have become a routine part of drug discovery and development. In early drug discovery research, the experimental approaches have been modified to high-throughput

platforms that can accommodate the thousands of new chemical entities synthesized for each new pharmacological target. In the drug development phase, the P450 assays have become such a routine part of the safety characterization process that it is not unreasonable to place particular expectations around assay characteristics and robustness (11,18,130). The more recent advances have shown that in vitro data, if properly obtained, can be used for predicting the magnitude of DDI in the clinic and can also be used in lieu of conducting clinical DDI studies when it is shown that there is no inhibition. This provides a boost to the efficiency of an already costly drug development process and will ensure that medications get to patients with the information required to prescribe them safely in combination with other medications as needed.

ACKNOWLEDGEMENT

Critical review of this chapter from Dr. Larry M. Tremaine is gratefully acknowledged.

REFERENCES

1. Crespi CL. Higher throughput screening with human cytochromes P450. Curr Opin Drug Disc Dev 1999; 2(1):15 19.
2. Crespi CL, Miller VP, Penman BW. Microtiter plate assays for inhibition of human, drug metabolizing cytochromes P450. Anal Biochem 1997; 248(1):188 190.
3. Bu HZ, Magis L, Knuth K, Teitelbaum P. High throughput cytochrome P450 (CYP) inhibition screening via cassette probe dosing strategy. I. Development of direct injection/on line guard cartridge extraction/tandem mass spectrometry for the simultaneous detection of CYP probe substrates and their metabolites. Rapid Commun Mass Spectrom 2000; 14(17):1619 1624.
4. Dierks EA, Stams KR, Lim H Kg Cornelius, G, Zhang H, Ball SE. A method for the simultaneous evaluation of the activities of seven major human drug metabolizing cytochrome P450s using an in vitro cocktail of probe substrates and fast gradient liquid chromatography tandem mass spectrometry. Drug Metab Dispos 2001; 29(1):23 29.
5. Testino AS, Patonay G. High throughput inhibition screening of major human cytochrome P450 enzymes using an in vitro cocktail and liquid chromatography tandem mass spectrometry. J Pharm Biomed Anal 2003; 30(5):1459 1467.
6. Turpeinen M, Jouko U, Jorma J, Olavi P. Multiple P450 substrates in a single run: rapid and comprehensive in vitro interaction assay. Eur J Pharm Sci 2005; 24(1):123 132.
7. Di L, Kerns EH, Li SQ, Carter GT. Comparison of cytochrome P450 inhibition assays for drug discovery using human liver microsomes with LC MS, rhCYP450 isozymes with fluores cence, and double cocktail with LC MS. Int J Pharm 2007; 335(1 2):1 11.
8. Smith D, Sadagopan N, Zientek M, Reddy A, Cohen L. Analytical approaches to determine cytochrome P450 inhibitory potential of new chemical entities in drug discovery. J Chromatogr B Analyt Technol Biomed Life Sci 2007; 850(1 2):455 463.
9. Dixit V, Hariparsad N, Desai P, Unadkat JD. In vitro LC MS cocktail assays to simultaneously determine human cytochrome P450 activities. Biopharm Drug Dispos 2007; 28(5):257 262.
10. Bajpai M, Esmay JD. In vitro studies in drug discovery and development: an analysis of study objectives and application of good laboratory practices (GLP). Drug Metab Rev 2002; 34(4): 679 689.
11. Tucker GT, Houston JB, Huang SM. Optimizing drug development: strategies to assess drug metabolism/transporter interaction potential toward a consensus. Pharm Res 2001; 18(8):1071 1080.
12. Zlokarnik G, Grootenhuis PDJ, Watson JB. High throughput P450 inhibition screens in early drug discovery. Drug Discov Today 2005; 10(21):1443 1450.
13. Hutzler JM, Powers FJ, Wynalda MA, and Wienkers LC. Effect of carbonate anion on cytochrome P450 2D6 mediated metabolism in vitro: the potential role of multiple oxygenating species. Arch Biochem Biophys 2003; 417(2):165 175.

14. Margolis JM, Obach RS. Impact of nonspecific binding to microsomes and phospholipid on the inhibition of cytochrome P4502D6: implications for relating in vitro inhibition data to in vivo drug interactions. Drug Metab Dispos 2003; 31(5):606 611.
15. Ayrton J, Plumb R, Leavens WJ, Mallett D, Dickins M, Dear GJ. Application of a generic fast gradient liquid chromatography tandem mass spectrometry method for the analysis of cytochrome P450 probe substrates. Rapid Commun Mass Spectrom 1998; 12(5):217 224.
16. Walsky RL, Obach RS. Validated assays for human cytochrome P450 activities. Drug Metab Dispos 2004; 32(6):647 660.
17. Yao M, Zhu M, Sinz MW, Zhang H, Humphreys WG, Rodrigues AD, Dai R. Development and full validation of six inhibition assays for five major cytochrome P450 enzymes in human liver microsomes using an automated 96 well microplate incubation format and LC MS/MS analysis. J Pharm Biomed Anal 2007; 44(1):211 223.
18. http://www.fda.gov/cder/drug/drugInteractions/default.htm. Accessed December 28, 2007.
19. Wijnands WJ, Vree TB, van Herwaarden CL. The influence of quinolone derivatives on theophylline clearance. Br J Clin Pharmacol 1986; 22(6):677 683.
20. Culm Merdek KE, von Moltke LL, Harmatz JS, Greenblatt DJ. Fluvoxamine impairs single dose caffeine clearance without altering caffeine pharmacodynamics. Br J Clin Pharmacol 2005; 60(5):486 493.
21. Granfors MT, Backman JT, Neuvonen M, Ahonen J, Neuvonen PJ. Fluvoxamine drastically increases concentrations and effects of tizanidine: a potentially hazardous interaction. Clin Pharmacol Ther 2004; 75(4):331 341.
22. http://www.fda.gov/cder/foi/label/2005/021782lbl.pdf. Accessed January 1, 2008.
23. Butler MA, Iwasaki M, Guengerich FP, Kadlubar FF. Human cytochrome P 450PA (P 450IA2), the phenacetin O deethylase, is primarily responsible for the hepatic 3 demethylation of caffeine and N oxidation of carcinogenic arylamines. Proc Nat Acad Sci U S A 1989; 86 (20):7696 7700.
24. Rodrigues AD, Surber BW, Yao Ye, Wong SL, Roberts EM. [O Ethyl 14C]phenacetin O deethylase activity in human liver microsomes. Drug Metab Dispos 1997; 25(9):1097 1100.
25. Kobayashi K, Nakajima M, Oshima K, Shimada N, Yokoi T, Chiba K. CYP2C9 is a principal low affinity phenacetin O deethylase: fluvoxamine is not a specific CYP1A2 inhibitor. Reply to comments. Drug Metab Dispos 1999; 27(12):1521 1522.
26. Kobayashi K, Nakajima M, Oshima K, Shimada N, Yokoi T, Chiba K. Involvement of CYP2E1 as a low affinity enzyme in phenacetin O deethylation in human liver microsomes. Drug Metab Dispos 1999; 27(8):860 865.
27. Venkatakrishnan K, von Moltke LL, Greenblatt DJ. Human cytochromes P450 mediating phenacetin O deethylation in vitro: validation of the high affinity component as an index of CYP1A2 activity. J Pharm Sci 1998; 87(12):1502 1507.
28. Spaldin V, Madden S, Adams DA, Edwards RJ, Davies DS, Park BK. Determination of human hepatic cytochrome P4501A2 activity in vitro use of tacrine as an isoenzyme specific probe. Drug Metab Dispos 1995; 23(9):929 934.
29. Berthou F, Flinois JP, Ratanasavanh D, Beaune P, Riche C, Guillouzo A. Evidence for the involvement of several cytochromes P 450 in the first steps of caffeine metabolism by human liver microsomes. Drug Metab Dispos 1991; 19(3):561 567.
30. Kaminsky LS, Zhang ZY. Human P450 metabolism of warfarin. Pharmacol Ther 1997; 73(1): 67 74.
31. Kunze KL, Trager WF. Isoform selective mechanism based inhibition of human cytochrome P450 1A2 by furafylline. Chem Res Toxicol 1993; 6(5):649 656.
32. Clarke SE, Ayrton AD, Chenery RJ. Characterization of the inhibition of P4501A2 by furafylline. Xenobiotica 1994; 24(6):517 526.
33. Gjervig J, Klaus EPH, Doehmer J, Loft S. Kinetics and inhibition by fluvoxamine of phenacetin O deethylation in V79 cells expressing human CYP1A2. Pharmacol Toxicol 1995; 76(4):286 287.
34. Brosen K, Skjelbo E, Fasmussen BB, Poulsen HE, Loft S. Fluvoxamine is a potent inhibitor of cytochrome P4501A2. Biochem Pharmacol 1993; 45(6):1211 1214.

35. Lu P, Schrag ML, Slaughter DE, Raab CE, Shou M, Rodrigues AD. Mechanism based inhibition of human liver microsomal cytochrome P450 1A2 by zileuton, a 5 lipoxygenase inhibitor. Drug Metab Dispos 2003; 31(11):1352 1360.
36. Karjalainen MJ, Neuvonen PJ, Backman JT. Rofecoxib is a potent, metabolism dependent inhibitor of CYP1A2: implications for in vitro prediction of drug interactions. Drug Metab Dispos 2006; 34(12):2091 2096.
37. Zanger UM, Klein K, Saussele T, Blievernicht J, Hofmann MH, Schwab M. Polymorphic CYP2B6: molecular mechanisms and emerging clinical significance. Pharmacogenomics 2007; 8(7):743 759.
38. Turpeinen M, Raunio H, Pelkonen O. The functional role of CYP2B6 in human drug metabolism: substrates and inhibitors in vitro, in vivo and in silico. Curr Drug Metab 2006; 7(7):705 714.
39. Xie HJ, Yasar U, Lundgren S, Griskevicius L, Terelius Y, Hassan M, Rane A. Role of polymorphic human CYP2B6 in cyclophosphamide bioactivation. Pharmacogenomics J 2003; 3(1):53 61.
40. Desta Z, Saussele T, Ward B, Blievernicht J, Li L, Klein K, Flockhart DA, Zanger UM. Impact of CYP2B6 polymorphism on hepatic efavirenz metabolism in vitro. Pharmacogenomics 2007; 8(6):547 558.
41. Obach RS, Cox LM, Tremaine LM. Sertraline is metabolized by multiple cytochrome P450 enzymes, monoamine oxidases, and glucuronyl transferases in human: an in vitro study. Drug Metab Dispos 2005; 33(2):262 270.
42. Kobayashi K, Ishizuka T, Shimada N, Yoshimura Y, Kamijima K, Chiba K. Sertraline N demethylation is catalyzed by multiple isoforms of human cytochrome P 450 in vitro. Drug Metab Dispos 1999; 27(7):763 766.
43. Turpeinen M, Nieminen R, Juntunen T, Taavitsainen P, Raunio H, Pelkonen O. Selective inhibition of CYP2B6 catalyzed bupropion hydroxylation in human liver microsomes in vitro. Drug Metab Dispos 2004; 32(6):626 631.
44. Schroeder DH. Metabolism and kinetics of bupropion. J Clin Psychiatry 1983; 44(5 pt 2): 79 81.
45. Hesse LM, Venkatakrishnan K, Court MH, Von Moltke LL, Duan SX, Shader RI, Greenblatt DJ. CYP2B6 mediates the in vitro hydroxylation of bupropion: potential drug interactions with other antidepressants. Drug Metab Dispos 2000; 28(10):1176 1183.
46. Faucette SR, Hawke RL, Lecluyse EL, Shord SS, Yan B, Laethem RM, Lindley CM. Validation of bupropion hydroxylation as a selective marker of human cytochrome P450 2B6 catalytic activity. Drug Metab Dispos 2000; 28(10):1222 1230.
47. Turpeinen M, Tolonen A, Uusitalo J, Jalonen J, Pelkonen O, Laine K. Effect of clopidogrel and ticlopidine on cytochrome P450 2B6 activity as measured by bupropion hydroxylation. Clin Pharmacol Ther 2005; 77(6):553 559.
48. Chang TKH, Weber GF, Crespi CL, Waxman DJ. Differential activation of cyclophosphamide and ifosphamide by cytochromes P 450 2B and 3A in human liver microsomes. Cancer Res 1993; 53(23):5629 5637.
49. Heyn H, White RB, Stevens JC. Catalytic role of cytochrome P4502B6 in the N demethylation of S mephenytoin. Drug Metab Dispos 1996; 24(9):948 954.
50. Ward BA, Gorski JC, Jones DR, Hall SD, Flockhart DA, Desta Z. The cytochrome P450 2B6 (CYP2B6) is the main catalyst of efavirenz primary and secondary metabolism: implication for HIV/AIDS therapy and utility of efavirenz as a substrate marker of CYP2B6 catalytic activity. J Pharmacol Exp Ther 2003; 306(1):287 300.
51. Chang TKH, Crespi CL, Waxman DJ. Determination of CYP2B6 component of 7 ethoxy 4 trifluoromethylcoumarin O deethylation activity in human liver microsomes. Methods Mol Biol 2006; 320:97 102.
52. Guo Z, Raeissi S, White RB, Stevens JC. Orphenadrine and methimazole inhibit multiple cytochrome P450 enzymes in human liver microsomes. Drug Metab Dispos 1997; 25(3):390 393.

53. Rae JM, Soukhova NV, Flockhart D, Desta Z. Triethylenethiophosphoramide is a specific inhibitor of cytochrome P450 2B6: implications for cyclophosphamide metabolism. Drug Metab Dispos 2002; 30(5):525 530.
54. Richter T, Murdter TE, Heinkele G, Pleiss J, Tatzel S, Schwab M, Eichelbaum M, Zanger UM. Potent mechanism based inhibition of human CYP2B6 by clopidogrel and ticlopidine. J Pharmacol Exp Ther 2004; 308(1):189 197.
55. Richter T, Schwab M, Eichelbaum M, Zanger UM. Inhibition of human CYP2B6 by N,N′,N″ triethylenethiophosphoramide is irreversible and mechanism based. Biochem Pharmacol 2005; 69(3):517 524.
56. Walsky RL, Obach RS. A comparison of 2 phenyl 2 (1 piperidinyl)propane (PPP), 1,1′,1″ phosphinothioylidynetrisaziridine (thioTEPA), clopidogrel, and ticlopidine as selective inactivators of human cytochrome P450 2B6. Drug Metab Dispos 2007; 35(11):2053 2059.
57. Niemi M, Backman JT, Neuvonen M, Neuvonen PJ. Effects of gemfibrozil, itraconazole, and their combination on the pharmacokinetics and pharmacodynamics of repaglinide: potentially hazardous interaction between gemfibrozil and repaglinide. Diabetologia 2003; 46(3): 347 351.
58. Backman JT, Kyrklund C, Neuvonen M, Neuvonen PJ. Gemfibrozil greatly increases plasma concentrations of cerivastatin. Clin Pharmacol Ther 2002; 72(6):685 691.
59. Shitara Y, Hirano M, Sato H, Sugiyama Yi. Gemfibrozil and its glucuronide inhibit the organic anion transporting polypeptide 2 (OATP2/OATP1B1:SLC21A6) mediated hepatic uptake and CYP2C8 mediated metabolism of cerivastatin: analysis of the mechanism of the clinically relevant drug drug interaction between cerivastatin and gemfibrozil. J Pharmacol Exp Ther 2004; 311(1):228 236.
60. Ogilvie BW, Zhang D, Li W, Rodrigues AD, Gipson AE, Holsapple J, Toren P, Parkinson A. Glucuronidation converts gemfibrozil to a potent, metabolism dependent inhibitor of CYP2C8: implications for drug drug interactions. Drug Metab Dispos 2006; 34(1):191 197.
61. Walle T. Assays of CYP2C8 and CYP3A4 mediated metabolism of taxol in vivo and in vitro. Methods Enzymol 1996; 272:145 151.
62. Desai PB, Duan JZ, Zhu YW, Kouzi S. Human liver microsomal metabolism of paclitaxel and drug interactions. Eur J Drug Metab Pharmacokinet 1998; 23(3):417 424.
63. Fujino H, Yamada I, Shimada S, Yoneda M. Simultaneous determination of taxol and its metabolites in microsomal samples by a simple thin layer chromatography radioactivity assay inhibitory effect of NK 104, a new inhibitor of HMG CoA reductase. J Chrom B 2001; 757(1): 143 150.
64. Nadin L, Murray M. Participation of CYP2C8 in retinoic acid 4 hydroxylation in human hepatic microsomes. Biochem Pharmacol 1999; 58(7):1201 1208.
65. Liee XQ, Bjorkman A, Andersson TB, Ridderstrom M, Masimirembwa CM. Amodiaquine clearance and its metabolism to N desethylamodiaquine is mediated by CYP2C8: a new high affinity and turnover enzyme specific probe substrate. J Pharmacol Exp Ther 2002; 300(2): 399 407.
66. Baldwin SJ, Clarke SE, Chenery RJ. Characterization of the cytochrome P450 enzymes involved in the in vitro metabolism of rosiglitazone. Br J Clin Pharmacol 1999; 48(3): 424 432.
67. Walsky RL, Obach RS, Gaman EA, Gleeson JPR, Proctor WR. Selective inhibition of human cytochrome P4502C8 by montelukast. Drug Metab Dispos 2005; 33(3):413 418.
68. Wen X, Wang JS, Backman JT, Laitila J, Neuvonen PJ. Trimethoprim and sulfamethoxazole are selective inhibitors of CYP2C8 and CYP2C9, respectively. Drug Metab Dispos 2002; 30(6):631 635.
69. Rettie AE, Jones JP. Clinical and toxicological relevance of CYP2C9: drug drug interactions and pharmacogenetics. Annu Rev Pharmacol Toxicol 2005; 45:477 494.
70. Webster R, Pacey M, Winchester T, Johnson P, Jezequel S. Microbial oxidative metabolism of diclofenac: production of 4′ hydroxydiclofenac using Epiccocum nigrum IMI354292. Appl Microbiol Biotechnol 1998; 49(4):371 376.

71. Leemann T, Transon C, Dayer P. Cytochrome P450TB (CYP2C): a major monooxygenase catalyzing diclofenac 4′ hydroxylation in human liver. Life Sci 1993; 52(1):29 34.
72. Crespi CL, Chang TKH, Waxman DJ. Determination of CYP2C9 catalyzed diclofenac 4′ hydroxylation by high performance liquid chromatography. Methods Mol Biol 1998; 107:129 133.
73. Miners JO, Birkett DJ. Use of tolbutamide as a substrate probe for human hepatic cytochrome P450 2C9. Methods Enzymol 1996; 272:139 145.
74. Lasker JM, Wester MR, Aramsombatdee E, Raucy JL. Characterization of CYP2C19 and CYP2C9 from human liver: respective roles in microsomal tolbutamide, S mephenytoin, and omeprazole hydroxylations. Arch Biochem Biophys 1998; 353(1):16 28.
75. Wester MR, Lasker JM, Johnson EF, Raucy JL. CYP2C19 participates in tolbutamide hydroxylation by human liver microsomes. Drug Metab Dispos 2000; 28(3):354 359.
76. Zhang ZY, King BM, Wong YN. Quantitative liquid chromatography/mass spectrometry/mass spectrometry warfarin assay for in vitro cytochrome P450 studies. Anal Biochem 2001; 298(1):40 49.
77. Fasco MJ, Piper LJ, Kaminsky LS. Biochemical applications of a quantitative high pressure liquid chromatographic assay of warfarin and its metabolites. J Chrom 1977; 131:365 373.
78. Hutzler JM, Hauer MJ, Tracy TS. Dapsone activation of CYP2C9 mediated metabolism: evidence for activation of multiple substrates and a two site model. Drug Metab Dispos 2001; 29(7):1029 1034.
79. Rodrigues AD, Kukulka MJ, Roberts EM, Ouellet D, Rodgers TR. [O Methyl 18C] naproxen O demethylase activity in human liver microsomes. Evidence for the involvement of cytochrome P4501A2 and P4502C9/10. Drug Metab Dispos 1996; 24(1):126 136.
80. Miners JO, Coulter S, Tukey RH, Veronese ME, Birkett DJ. Cytochromes P450, 1A2, and 2C9 are responsible for the human hepatic O demethylation of R and S naproxen. Biochem Pharmacol 1996; 51(8):1003 1008.
81. Tang C, Shou M, Rodrigues AD. Substrate dependent effect of acetonitrile on human liver microsomal cytochrome P450 2C9 (CYP2C9) activity. Drug Metab Dispos 2000; 28(5): 567 572.
82. Giancarlo GM, Venkatakrishnan K, Granda BW, von Moltke LL, Greenblatt DJ. Relative contributions of CYP2C9 and 2C19 to phenytoin 4 hydroxylation in vitro: inhibition by sulfaphenazole, omeprazole, and ticlopidine. Eur J Clin Pharmacol 2001; 57(1):31 36.
83. Kumar V, Wahlstrom JL, Rock DA, Warren CJ, Gorman LA, Tracy TS. CYP2C9 inhibition: impact of probe selection and pharmacogenetics on in vitro inhibition profiles. Drug Metab Dispos 2006; 34(12):1966 1975.
84. Newton DJ, Wang RW, Lu AYH. Cytochrome P450 inhibitors: evaluation of specificities in the in vitro metabolism of therapeutic agents by human liver microsomes. Drug Metab Dispos 1995; 23(1):154 158.
85. Shimada T, Shea JP, Guengerich FP. A convenient assay for mephenytoin 4 hydroxylase activity of human liver microsomal cytochrome P 450. Anal Biochem 1985; 147(1):174 179.
86. Ward SA, Goto F, Nakamura K, Jacqz E, Wilkinson GR, Branch RA. S mephenytoin 4 hydroxylase is inherited as an autosomal recessive trait in Japanese families. Clin Pharmacol Ther 1987; 42(1):96 99.
87. Furuta T, Shirai N, Sugimoto M, Nakamura A, Hishida A, Ishizaki T. Influence of CYP2C19 pharmacogenetic polymorphism on proton pump inhibitor based therapies. Drug Metab Pharmacokinet 2005; 20(3):153 167.
88. Chiba K, Manabe K, Kobayashi K, Takayama Y, Tani M, Ishizaki T. Development and preliminary application of a simple assay of S mephenytoin 4 hydroxylase activity in human liver microsomes. Eur J Clin Pharmacol 1993; 44(6):559 562.
89. Di Marco A, Cellucci A, Chaudhary A, Fonsi M, Laufer R. High throughput radiometric CYP2C19 inhibition assay using tritiated (S) mephenytoin. Drug Metab Dispos 2007; 35(10): 1737 1743.

90. Suzuki H, Kneller MB, Haining RL, Trager WF, Rettie AE. (+) N 3 benzyl nirvanol and ( ) N 3 benzyl phenobarbital: new potent and selective in vitro inhibitors of CYP2C19. Drug Metab Dispos 2002; 30(3):235 239.
91. Donahue SR, Flockhart DA, Abernethy DR, Ko JW. Ticlopidine inhibition of phenytoin metabolism mediated by potent inhibition of CYP2C19. Clin Pharmacol Ther 1997; 62(5):572 577.
92. Mankowski DC. The role of CYP2C19 in the metabolism of (+/) bufuralol, the prototypic substrate of CYP2D6. Drug Metab Dispos 1999; 27(9):1024 1028.
93. Zanger UM, Raimundo S, Eichelbaum M. Cytochrome P450 2D6: overview and update on pharmacology, genetics, biochemistry. Naunyn Schmiedebergs Arch Pharmacol 2004; 369(1): 23 37.
94. Kronbach T, Mathys D, Gut J, Catin T, Meyer UA. High performance liquid chromatographic assays for bufuralol 1′ hydroxylase, debrisoquine 4 hydroxylase, and dextromethorphan O demethylase in microsomes and purified cytochrome P 450 isozymes of human liver. Anal Biochem 1987; 162(1):24 32.
95. Belpaire FM, Wijnant P, Temmermann A, Rasmussen BB, Brosen K. The oxidative metabolism of metoprolol in human liver microsomes: inhibition by the selective serotonin reuptake inhibitors. Eur J Clin Pharmacol 1998; 54(3):261 264.
96. Henthorn TK, Spina E, Dumont E, von Bahr C. In vitro inhibition of a polymorphic human liver P 450 isozyme by narcotic analgesics. Anesthesiology 1989; 70(2):339 342.
97. Dayer P, Gasser R, Gut J, Kronbach T, Robertz GM, Eichelbaum M, Meyer UA. Characterization of a common genetic defect of cytochrome P 450 function (debrisoquine sparteine type polymorphism) increased Michaelis constant (Km) and loss of stereoselectivity of bufuralol 1′ hydroxylation in poor metabolizers. Biochem Biophys Res Commun 1984; 125(1):374 380.
98. Narimatsu S, Takemi C, Tsuzuki D, Kataoka H, Yamamoto S, Shimada N, Suzuki S, Satoh T, Meyer UA, Gonzalez FJ. Stereoselective metabolism of bufuralol racemate and enantiomers in human liver microsomes. J Pharmacol Exp Ther 2002; 303(1):172 178.
99. Boobis AR, Murray S, Kahn GC, Robertz GM, Davies DS. Substrate specificity of the form of cytochrome P 450 catalyzing the 4 hydroxylation of debrisoquine in man. Mol Pharmacol 1983; 23(2):474 481.
100. Murray S, Kahn GC, Boobis AR, Davies DS. Molecular aspects of debrisoquine metabolism studied by gas chromatography mass spectrometry with electron capture negative ion chemical ionization. Int J Mass Spec Ion Phys 1983; 48:89 92.
101. Ozdemir M, Crewe KH, Tucker GT, Rostami Hodjegan A. Assessment of in vivo CYP2D6 activity: differential sensitivity of commonly used probes to urine pH. J Clin Pharmacol 2004; 44(12):1398 1404.
102. Rodrigues AD, Kukulka MJ, Surber BW, Thomas SB, Uchic JT, Rotert GA, Michel G, Thome Kromer B, Machinist JM. Measurement of liver microsomal cytochrome P450 (CYP2D6) activity using [O methyl 14C]dextromethorphan. Anal Biochem 1994; 219(2):309 320.
103. Gorski JC, Hall SD, Jones DR, Vandenbranden M, Wrighton SA. Regioselective biotransformation of midazolam by members of the human cytochrome P450 3A (CYP3A) subfamily. Biochem Pharmacol 1994; 47(9):1643 1653.
104. Gibbs MA, Thummel KE, Shen DD, Kunze KL. Inhibition of cytochrome P 450 3A (CYP3A) in human intestinal and liver microsomes: comparison of KI values and impact of CYP3A5 expression. Drug Metab Dispos 1999; 27(2):180 187.
105. Wang YH, Jones DR, Hall SD. Differential mechanism based inhibition of CYP3A4 and CYP3A5 by verapamil. Drug Metab Dispos 2005; 33(5):664 671.
106. Dennison JB, Kulanthaivel P, Barbuch RJ, Renbarger JL, Ehlhardt WJ, Hall SD. Selective metabolism of vincristine in vitro by CYP3A5. Drug Metab Dispos 2006; 34(8):1317 1327.
107. Pearson JT, Wahlstrom JL, Dickmann LJ, Kumar S, Halpert JR, Wienkers LC, Foti RS, Rock DA. Differential time dependent inactivation of P450 3A4 and P450 3A5 by raloxifene: a key role for C239 in quenching reactive intermediates. Chem Res Toxicol 2007; 20(12):1778 1786.
108. Xiee HG, Wood AJJ, Kim RB, Stein CM, Wilkinson GR. Genetic variability in CYP3A5 and its possible consequences. Pharmacogenomics 2004; 5(3):243 272.

109. Galetin A, Hinton LK, Burt H, Obach RS, Houston JB. Maximal inhibition of intestinal first pass metabolism as a pragmatic indicator of intestinal contribution to the drug drug interactions for CYP3A4 cleared drugs. Curr Drug Metab 2007; 8(7):685 693.
110. Maenpaa J, Hall SD, Ring BJ, Strom SC, Wrighton SA. Human cytochrome P450 3A (CYP3A) mediated midazolam metabolism: the effect of assay conditions and regioselective stimulation by a naphthoflavone, terfenadine and testosterone. Pharmacogenetics 1998; 8(2): 137 155.
111. Yamazaki H, Nakajima M, Nakamura M, Asahi S, Shimada N, Gillam EMJ, Guengerich FP, Shimada T, Yokoi T. Enhancement of cytochrome P 450 3A4 catalytic activities by cytochrome b5 in bacterial membranes. Drug Metab Dispos 1999; 27(9):999 1004.
112. Schrag ML, Wienkers LC. Topological alteration of the CYP3A4 active site by the divalent cation Mg (2+). Drug Metab Dispos 2000; 28(10):1198 1201.
113. Yamaori S, Yamazaki H, Suzuki A, Yamada A, Tani H, Kamidate T, Fujita K I, Kamataki T. Effects of cytochrome b5 on drug oxidation activities of human cytochrome P450 (CYP) 3As: similarity of CYP3A5 with CYP3A4 but not CYP3A7. Biochem Pharmacol 2003; 66 (12):2333 2340.
114. Jushchyshyn MI, Hutzler JM, Schrag ML, Wienkers LC. Catalytic turnover of pyrene by CYP3A4: evidence that cytochrome b5 directly induces positive cooperativity. Arch Biochem Biophys 2005; 438(1):21 28.
115. Kenworthy KE, Bloomer JC, Clarke SE, Houston JB. CYP3A4 drug interactions: correlation of 10 in vitro probe substrates. Br J Clin Pharmacol 1999; 48(5):716 727.
116. Khan KK, He YQ, Domanski TL, Halpert JR. Midazolam oxidation by cytochrome P450 3A4 and active site mutants: an evaluation of multiple binding sites and of the metabolic pathway that leads to enzyme inactivation. Mol Pharmacol 2002; 61(3):495 506.
117. Sonderfan AJ, Arlotto MP, Dutton DR, McMillen SK, Parkinson A. Regulation of testosterone hydroxylation by rat liver microsomal cytochrome P 450. Arch Biochem Biophys 1987; 255 (1):27 41.
118. Obach RS, Walsky RL, Venkatakrishnan K, Gaman EA, Houston JB, Tremaine LM. The utility of in vitro cytochrome P450 inhibition data in the prediction of drug drug interactions. J Pharmacol Exp Ther 2006; 316(1):336 348.
119. Galetin A, Clarke SE, Houston JB. Quinidine and haloperidol as modifiers of CYP3A4 activity: multisite kinetic model approach. Drug Metab Dispos 2002; 30(12):1512 1522.
120. Rowland M, Matin SB. Kinetics of drug drug interactions. J Pharmacokinet Biopharm 1973; 1(6):553 567.
121. Cheng YC, Prusoff WH. Relation between the inhibition constant K1 and the concentration of inhibitor which causes fifty per cent inhibition (I50) of an enzymic reaction. Biochem Pharmacol 1973; 22(23):3099 3108.
122. Kanamitsu SI, Ito K, Sugiyama Y. Quantitative prediction of in vivo drug drug interactions from in vitro data based on physiological pharmacokinetics: use of maximum unbound concentration of inhibitor at the inlet to the liver. Pharm Res 2000; 17(3):336 343.
123. Thummel KE, Kunze KL, and Shen DD. Enzyme catalyzed processes of first pass hepatic and intestinal drug extraction. Adv Drug Deliv Rev 1997; 27:99 127.
124. Paine MF, Shen DD, Kunze KL, Perkins JD, Marsh CL , McVicar JP, Barr DM, Gillies BS, Thummel KE. First pass metabolism of midazolam by the human intestine. Clin Pharmacol Ther 1996; 60(1):14 24.
125. Kolars JC, Awni WM, Merion RM, Watkins PB. First pass metabolism of cyclosporin by the gut. Lancet 1991; 338(8781):1488 1490.
126. Rostami Hodjegan A, Tucker G. 'In silico' simulations to assess the 'in vivo' consequences of 'in vitro' metabolic drug drug interactions. Drug Disc Today Tech 2004; 1(4):441 448.
127. Huang SM, Lesko LJ, Williams RL. Assessment of the quality and quantity of drug drug interaction studies in recent NDA submissions: study design and data analysis issues. J Clin Pharmacol 1999; 39(10):1006 1014.
128. Obach RS, Walsky RL, Venkatakrishnan K, Houston JB, and Tremaine LM. In vitro cytochrome P450 inhibition data and the prediction of drug drug interactions: qualitative

relationships, quantitative predictions, and the rank order approach. Clin Pharmacol Ther 2005; 75(6):582 592.
129. Rodrigues AD. Prioritization of clinical drug interaction studies using in vitro cytochrome P450 data: proposed refinement and expansion of the "rank order" approach. Drug Metab Lett 2007; 1(1):31 35.
130. Bjornsson TD, Callaghan JT, Einolf HJ, Fischer V, Gan L, Grimm S, Kao J, King SP, Miwa G, Ni L, Kumar G, McLeod J, Obach RS, Roberts S, Roe A, Shah A, Snikeris F, Sullivan JT, Tweedie D, Vega JM, Walsh J, Wrighton SA. The conduct of in vitro and in vivo drug drug interaction studies: a pharmaceutical research and manufacturers of America (PhRMA) perspective. Drug Metab Dispos 2003; 31(7):815 832.
131. Obach RS, Walsky RL, Venkatakrishnan K. Mechanism based inactivation of human cytochrome P450 enzymes and the prediction of drug drug interactions. Drug Metab Dispos 2007; 35(2):246 255.

20

Enzyme Induction Studies in Drug Discovery & Development

J. Greg Slatter and Leslie J. Dickmann
Pharmacokinetics and Drug Metabolism, Amgen Inc., Seattle, Washington, U.S.A.

INTRODUCTION

Central to the problem of metabolism- or transport-driven drug-drug interactions (DDIs) are the opposite concepts of inhibition and induction of drug-metabolizing enzymes or transporters (DMETs), each arising from the action of a perpetrator of an interaction on a victim of the interaction.[1] Induction of DMET is generally perceived to be an adaptive response that lowers drug exposure and facilitates excretion of molecules that resemble dietary toxins (1).

Induction of DMET by a perpetrating drug can subtly or profoundly decrease exposure to the drug itself after one or several doses (auto-induction) or decrease exposure to another drug whose rate-limiting clearance steps are mediated by the induced enzyme(s). The clinical importance of the induction will depend on several factors, including the therapeutic window of the victim of the interaction, the pharmacology or toxicology of the victims' metabolite(s), the magnitude of the decrease in exposure (highlighting the importance of alternate clearance pathways), the consequences of lost therapeutic effect, and nascent pharmacokinetic variability. These effects appear and disappear slowly, predicated on the half-life of the inducer and victim and rates of synthesis and degradation of the induced enzyme(s). Upward dose adjustment of the victim and therapeutic efficacy monitoring are the most common clinical consequences of induction, and these figure prominently in the drug label.

SCOPE OF THE REVIEW

Enzyme induction, as it applies to metabolism and pharmacokinetics in drug discovery and development, has been well reviewed in the recent literature. Practical reviews emphasizing industrial in vitro approaches and in vitro-in vivo correlations (IVIVC) have been done by several researchers (2 5). This chapter will therefore focus on recent

[1] Victim and perpetrator refer to the effect of one drug (the perpetrator) on the pharmacokinetics of another (the victim). Drug interaction studies typically assess a drug candidate's potential to be victim, perpetrator, or both.

literature and practical aspects of enzyme induction and rely on reference to recent reviews for detailed discussions.

THE WORK PROCESS IN INDUSTRIAL DRUG DISCOVERY AND DEVELOPMENT

A high-level view of industrial approaches to ADME (absorption, distribution, metabolism and excretion) enzyme induction is shown in Figure 1 (5). During drug discovery, active leads may be assessed by reporter gene assays for PXR (pregnane X receptor) transactivation. At this stage, an induction hit should trigger lead redesign discussions to remove functional groups associated with induction. To avoid the consequences of coadministration with enzyme inducers, drug candidates that are cleared by more than one metabolism or clearance pathway are preferred.

Potential candidates are then subjected to induction studies in primary human hepatocytes. This is largely focused on CYP3A4 because of its role in the metabolism of the majority of marketed drugs (6). CYP1A2, 2B6, 2C9, and 2C19 are also commonly assessed. Induction of CYP isoform proteins is measured using isoform-specific marker assays and LCMS (liquid chromatography mass spectrometry) (7) or luminographic assays (8) and/or by western blots. At the gene expression level, induction of P450 messenger RNA (mRNA) is assessed with bDNA kits, RT-PCR, or multiplexed PCR-based methods. Message and protein are both measured, so the induction effect is not obscured by coincident time-dependent P450 inhibition (2,9).

Induction in preclinical species is also assessed in early multiple dose safety studies, especially when decreases in AUC occur at steady state, relative to the first dose. This may be evidence of auto-induction, and tissues are collected proactively for marker assay and/or RT-PCR assessment of hepatic P450 isoforms. Auto-induction may be problematic if it limits exposure to the parent drug and suitable exposure-based safety margins for

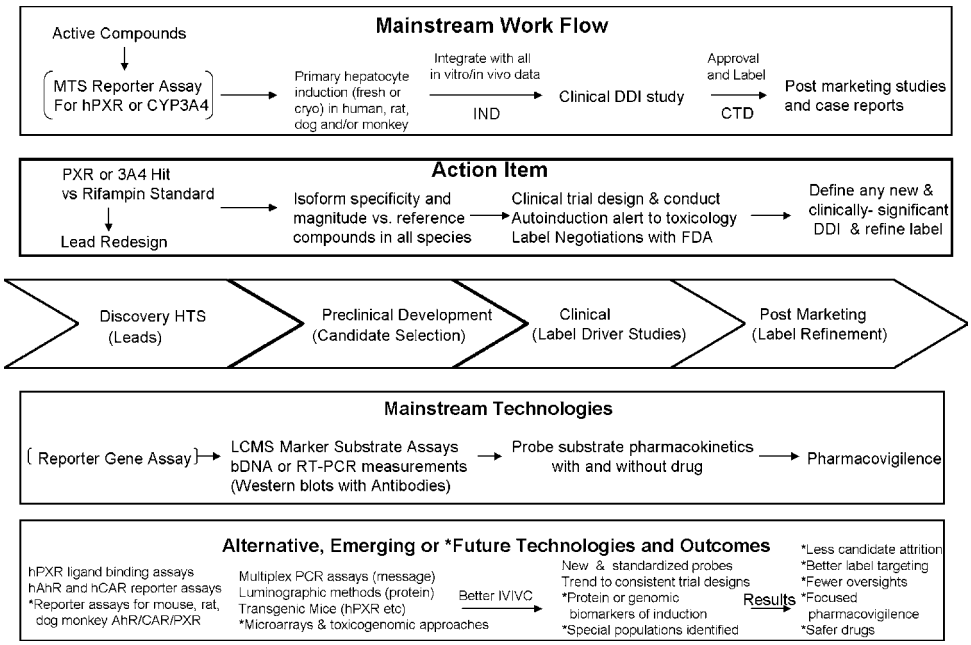

Figure 1 Overview schematic of induction related activities. *Abbreviations*: MTS, moderate through put screening; HTS, high through put screening; IND, investigational new drug application; CTD, common technical document of a new drug application. *Source*: From Ref. 5.

human clinical trials cannot be attained. Induction data can also be used to differentiate mechanism when liver weight/body weight increases occur. P450 inducer-related liver weight increases typically manifest ultrastructurally as endoplasmic reticulum (ER) proliferation and can be differentiated from other causes related to overt damage and repair, proliferation, and lipid or peroxisome proliferation by robust increases in message or marker enzymes in the CYP1A, 2B, 3A, or 4A families.

Human hepatocyte induction data are typically expressed for each isoform as a percentage of positive control inducers at relevant concentrations. Positive signals of induction in human hepatocytes are combined with other metabolism and pharmacology data to make candidate go-no go decisions and to help design appropriate label-driver clinical DDI studies.

REGULATORY GUIDANCE

Enzyme induction is dealt with in the 2006 draft guidance for industry: "*Drug Interaction Studies-Study Design, Data Analysis and Implications for Dosing and Labeling*" (10). In vitro techniques for induction assessment are summarized in the 2006 draft guidance and define primary hepatocyte experiment design and appropriate positive controls and concentrations. A decision tree defines responses to positive data, and the guidance tabulates favored marker substrates and other factors for assessing the clinical magnitude of induction. The 2006 draft guidance also defines inducible drug classes most likely to incur a restrictive label, dose adjustment, and patient-monitoring recommendations.

DRUG LABELING RELATED TO INDUCTION

The clinical consequences of induction can include oral contraceptive failure (estrogens or progestins), transplant rejection (cyclosporine A, tacrolimus), anti-infective failure and resistance (saquinavir), tumor progression (paclitaxel), anticoagulant failure (warfarin), cardiac problems (amiodarone), seizure (phenytoin, mephenytoin), and psychosis (thioridazine).

Some examples of induction warning language in drug labels are as follows: "Drugs whose efficacy is impaired by Drug X include: corticosteroids, coumarin anticoagulants, digitoxin, doxycycline, estrogens, furosemide, oral contraceptives, quinidine, rifampin, theophylline, vitamin D"; "Administration of Drug X may reduce the efficacy of hormonal contraceptives. Patients should be advised to use alternative or back-up methods of contraception during treatment with Drug X and for 1 month following the last dose of Drug X" (11).

In the United States, data showing lack of a drug interaction risk are also allowed in the drug label and provide an incentive to conduct studies that clearly define the clinical interaction profile of the product. Some drug labels specify procedures to be undertaken for inducible narrow therapeutic window agents, such as dose adjustment, drug concentration monitoring, efficacy, and side effect monitoring, both when the inducer is introduced and when it is withdrawn. Ensuring patient compliance becomes a key issue for clinicians in these instances.

MECHANISMS OF INDUCTION AND GENE REGULATION BY THE NUCLEAR RECEPTORS PXR, CAR, AND AHR

Regulation

Induction of ADME genes is commonly mediated at the transcriptional level in the intestine and liver by key members of the nuclear receptor (NR) family. Regulation mechanisms of drug-metabolizing enzymes, in particular CYP2A, 2B, 2C, and 3A induction by the pregnane

X receptor (PXR, NR1i2), CYP2B induction by the constitutive androstane receptor (CAR, NR1i3), and CYP1A induction by the aryl hydrocarbon receptor (AhR) have been the subject of many recent reviews (12 16). Some older in vitro preclinical reports discuss slow CYP3A or CYP2E1 degradation as an alternative induction mechanism (17,18).

PXR

PXR and CAR are ligand-activated transcription factors formerly considered to be "orphan" NRs but are now known to be metabolic and xenobiotic sensors involved in rapid-response regulation of a variety of endogenous pathways involved in energy metabolism and bile acid homeostasis. Unlike the steroid NRs, precise endogenous ligand(s) for PXR and CAR are not defined. PXR contains a carboxy terminal, helical AF-2 domain that changes conformation to recruit coactivators in response to events at the adjacent, hydrophobic, and flexible ligand-binding domain (LBD), as well as a hinge region and a conserved DNA-binding domain (DBD) containing a xenobiotic response sequence (XRS) that modulates target gene transcription by interacting with the target gene upstream response elements (REs) (16,19).

PXR, like CAR, resides as a CAR cytoplasmic retention protein (CCRP) and heat-shock chaperone (HSP90) complex in cytoplasm. Events relating to its ligand-activated dissociation and nuclear translocation are still being elucidated. In the nucleus, ligand-bound PXR activates transcription as a heterodimer with RXRα and recruits transcriptional co-regulators, including members of the p160 family. The complex binds to the IR-6 and DR-3 REs of the xenobiotic responsive enhancer module (XREM) in the 5′ regulatory region of target genes (16).

As a frontline xenosensor, PXR is an important regulator of CYP3A4 and regulates many other phases 1, 2, and 3 ADME genes.[2] PXR's endogenous functions include protective farnesoid X receptor (FXR)-independent transcriptional regulation of bile acid metabolism. Bile acids stimulate PXR to upregulate genes that extract (OATP1A4), metabolize (CYP3A4) and excrete (MRP2) bile acids, and also downregulate CYP7A1 to decrease bile acid production (20,21).

CAR

In addition to genes involved in cholesterol metabolism, cholestasis, thyroid hormone homeostasis, nutritional stress (fasting), hyperbilirubinemia, and energy metabolism, CAR regulates a variety of P450s, SULTs, UGTs, GSTs, MRPs, and OATPs involved in drug metabolism, notably bellwether ADME genes CYP2B6, 2B10, and 2B15 in humans, mice, and rats, respectively (22). The sequence of nuclear translocation and heterodimerization with RXR has high-level similarity to PXR but can proceed either with direct binding of a ligand such as TCPOBOP in mouse or, because CAR is constitutively active, by indirect activation of signaling cascades involving protein phosphatase 2A (PP-2A) by ligands such as phenobarbital, bilirubin, bile acids, or steroids (23). Transcriptional activation can be inhibited by androstanes, such as inverse agonists androstanol and androstenol. Binding of CAR REs such as the phenobarbital RE (PBRE) or retinoic acid RE (RARE) in target genes initiates transcription (24).

AhR

AhR is a ligand-activated, basic helix-loop-helix, PER ARNT SIM (PAS) transcription factor that resides primarily in cytosol. When ligand is not present, inactive AhR

[2] CYP1A1, CYP1A2, CYP2A6, CYP2B6, CYP2C8, CYP2C9, CYP2C19, CYP3A4, CYP3A7, CYP24A1, SULT2A1, UGT1A1, UGT1A3, UGT1A4, ABCB1 (MDR1, P glycoprotein), ALAS1, PAPS2, AHR, CAR, PXR, iNOS, MSX2.

associates with a 90-kDa heat-shock protein p23 and X-associated protein (XAP2). Ligand binding results in nuclear translocation and heterodimerization with the AhR nuclear translocator (ARNT). The AhR-ARNT dimer initiates transcription by binding to xenobiotic REs (XREs) in target genes such as CYP1A1 and CYP1A2 and a network of other genes that mediate diverse biological effects (25,26). Microarrays have been used to discern the hepatic gene networks in rodents that respond to prototypical and atypical AhR ligands (27,28).

Two target genes of AhR, CYP1A1 and 1A2, are involved in the oxidation of planar aromatic substrates/autoinducers like benzo[a]pyrene and 3-methylcholanthrene. Prototypical inducers include dioxin (TCDD) and arochlor 1254. Clinical interest is historically related to the bioactivation of environmental and dietary pro-carcinogens, toxins, and metabolism-related protection against chemical carcinogens.

CYP450 Induction and Liver Weight Increases

A key manifestation of enzyme induction in preclinical toxicology studies is liver weight gain (hepatic hypertrophy and hepatomegaly), which is often associated with alanine aminotransferase (ALT) elevations when potent inducers are given at higher doses. Mechanisms underlying the consequences of ER overload because of P450 overproduction involve ER stress response signal transduction pathway components of the unfolded protein response (UPR) and the ER overload response (EOR). These pathways include ER proliferative effects of IRE1 activation and subsequently NFkB activation that is anti-apoptotic and may aid survival of hepatic cells with P450-induced ER stress (29).

NR Cross Talk

Cross talk is common among key members of the 48 human NRs, GR, FXR, LXR, ER, AR, PR, VDR, RAR[3], hepatocyte nuclear factor-4a (HNF4a), small heterodimer partner (SHP) etc., coactivators and corepressors such as the nuclear receptor corepressor (NCoR), and silencing mediator for retinoid and thyroid hormone receptor (SMRT) that are all involved in the regulation of both drug disposition genes and biochemical homeostasis of intermediary metabolism (30). This is most interesting to the drug developer when CAR and PXR effects overlap to reciprocally activate both of their respective bellwether genes, CYP2B6 and CYP3A4. In rats and mice, preclinical in vivo studies have shown that potency differences in the induction of the expression of bellwether genes across dose can be used to define some ligands as CAR or PXR predominant (28).

Interplay among bile acid and steroid metabolism and xenobiotic metabolism functions of CAR and PXR have been reviewed by Eloranta and Kullack-Ublick (31). Kretschmer and Baldwin (32) have discussed the role of CAR ligands in endocrine disruption on the basis of cross talk between CAR and sex steroid metabolism. Zhai et al. (33) proposed similar disruption of glucocorticoid and mineralocorticoid homeostasis from PXR activation. Supply limitations of shared coactivators and corepressors such as GRIP1 have been proposed to result in cross talk among sex steroids and CAR (34).

As microarray-based technologies, transgenic animals, and gene network mapping have become more prevalent, broad questions are now being asked about the networks of genes involved in cross talk among AhR, CAR, and PXR and other NRs[3] (28,35,36). Lim and Huang have listed target genes of PXR and defined when ADME gene responses are also under the control of other NRs (21).

[3] GR, glucocorticoid receptor; FXR, farnesoid X receptor; LXR, liver X receptor; ER, estrogen receptor; AR, androgen receptor; PR, progesterone receptor; VDR vitamin D receptor; RAR, retinoic acid receptor.

Genetic Factors

Polymorphisms in inducible ADME target genes and NRs may contribute to the risk of induction-related DDI. Lamba et al. have defined genetic variations within the NRs PXR and CAR and have identified human polymorphisms, which may have effects on the function of CYP3A4 and other target genes (37,38). Tissue-specific splice variants of CAR may explain gene expression differences in certain tissues, and ethnic differences in CAR target gene transcription have been described in Hispanic subjects (39). Posttranscriptional regulation of human PXR by micro-RNA and correlations with effects on CYP3A4 expression were also recently reported to be a potential missing component in understanding the large interindividual variability in CYP3A4 expression (40).

THE OPPOSITE OF INDUCTION: TRANSCRIPTIONAL SUPPRESSION OF P450 EXPRESSION

Proactive collection of P450 marker activity data and RT-PCR data for key P450 genes in early multiple dose toxicology studies, after a single dose and at steady state, is done routinely to give context to pharmacokinetic evidence of auto-induction. Occasionally, suppression of both P450 transcript and protein expression is observed. The mechanisms underlying P450 suppression are not as well understood as induction, in part because mixed inducer/inhibitors such as the non-nucleaside reverse transcriptose inhibitors (NNRTIs) and time-dependent inhibitors can afford contradictory P450 protein expression data. Transcriptional suppression appears to be mechanistically related to inflammatory responses, originally manifesting clinically as increased phenytoin plasma concentrations in patients treated the with influenza vaccine (41). Assenat et al. reviewed the role of the NF-kB pathway and GR cross talk with CAR and PXR that were observed along with decreases in P450 expression in cancer-related inflammation (42). A variety of pro-inflammatory cytokines reduce the expression of CAR and PXR, and inflammation-related decreases in CAR and PXR decrease both constitutive and inducible P450s. P450 suppression is also observed clinically as a consequence of liver disease, with P450 expression trending downward as Child-Pugh score increases (43). Related mechanisms may underlay the problem of gradual loss of P450 expression in hepatocyte culture (44).

Recently, a novel HIV protease inhibitor was shown to functionally antagonize PXR in human hepatocytes in vitro, resulting in suppression of a panel of PXR-responsive genes, the opposite effect of other drugs in its class, adding this compound to a short list of PXR antagonists that include ketoconazole, ET-743 (trabectidin), sulforaphane (45), and some PCBs (32).

There is current interest in the role of TLR-4 in mediating JNK and NF-kB activation and inflammation-related ADME gene suppression (46). Roth et al. have studied lipid accumulation effects on interactions between SREBP-1 and P450 regulators and found that SREBP-1 blocks PXR and CAR interaction with key cofactors such as SRC1 and impairs induction of P450 enzymes (47).

TOOLS OF THE INDUCTION TRADE

Reporter Gene Assays for NR Activation by Inducers

During drug discovery, active leads may be screened for induction by a variety of reporter gene assays for PXR transactivation (48 51). Immortalized cells are transfected transiently or stably with two DNA vectors, one containing a reporter gene construct and the other

containing the NR gene, such as AhR or PXR. The reporter gene construct contains a NR RE of the target metabolism gene fused to a reporter gene such as luciferase, chloramphenicol acetyl transferase (CAT), or alkaline phosphatase to allow monitoring using luminescent or colorimetric assays in 96- or 384-well format. Transfected cells are treated with relevant concentrations of drug or positive controls and compared to a vehicle response (52). A critical component of these assays is the NR RE. This is exemplified in PXR reporter assays where the choice of regulatory element and the reporter gene gave a maximal-fold induction by rifampicin ranging between 3- and 40-fold across five different laboratories using different PXR reporter assays (49,53 56). Accordingly, cross validation of NR activation assays to hepatocyte and clinical induction data is a focus of several recent studies. Using a PXR gene reporter assay containing the CYP3A4 proximal promoter, El-Sankary rank ordered the induction potential of 17 compounds, 7 of which were known CYP3A4 inducers in vivo (49). Luo et al. correlated hepatocyte CYP3A4 activity and mRNA induction with PXR activation and obtained r values of 0.864 and 0.643, respectively, when CYP3A4 mechanism-based inhibitors were excluded (50). Persson et al. and Zhu et al. compared EC_{50} values from PXR reporter gene assays in HepG2 cells with induction in human liver slices and with a SPA-based PXR-binding assay, respectively (57,58). Sinz et al. correlated hPXR transactivation data for 170 xenobiotics with available data on the magnitude of clinical CYP3A4 induction (59).

Attempts to create a CAR gene reporter assay have been largely unsuccessful because CAR accumulates in the nucleus of transfected cell lines where it is constitutively active (60). In assays using full-length CAR, most compounds decreased CAR constitutive transcriptional activity (61 63). High concentrations of inverse agonists like androstanol or androstenol can be used to antagonize the constitutive activity of CAR; however, atypical ligands such as phenobarbital work by promoting CAR translocation from the cytoplasm to the nucleus (64), rather than by binding to the NR.

Primary Hepatocytes

The use of cultured human primary hepatocytes in drug interaction studies is the gold standard for studying the induction of drug-metabolizing enzymes by drug candidates (10). Although there are many vendors for fresh human hepatocytes, sporadic availability can make accrual of replicate donors time consuming. The time commitment for an induction study is five to seven days, encompassing plating of cells, multiple dosing, viability measurement, and protein and RNA measurements. Because of low throughput, this is likely carried out at or near candidate selection, or earlier if induction is being designed out of a chemical scaffold. The recent availability of high-quality, cryopreserved, plateable human hepatocytes has made hepatocyte induction studies more convenient. Advantages include the ability to perform replicate donor incubations simultaneously, to initiate studies at any time, and to prescreen donors for cells that plate well and exhibit solid induction. The disadvantage is cost, which may be up to five times higher than for fresh hepatocytes. Cryopreserved hepatocytes also afford reproducible induction data across time (65).

In 2007, Hewitt et al. surveyed how researchers at pharmaceutical companies carry out in vitro induction studies (66). Select results of this survey are compared to the FDA guidance in Table 1. There is no industry standard method or evaluation criteria for in vitro assays, and most researchers do not follow the FDA draft guidance closely. The draft guidance has a P450 focus and defines which positive controls should be used (Table 2). Several researchers were interested in phase II enzymes; however, the dilemma in examining phase II and phase III enzymes or the less-common P450 isoforms is the loose

Table 1 A Comparison of In Vitro Enzyme Induction Methodologies Between FDA Recommendations and Those Surveyed Among Pharmaceutical Researchers

Methodology	FDA guidelines (2006)	Pharmaceutical industry practice[a]
Enzymes to evaluate	CYP1A2 CYP3A4[c]	CYP3A4 100%[b], CYP1A2 93% CYP2C9 67%, CYP2C19 33%, CYP2B6 37%, CYP2C8 10%, CYP2D6 20%, CYP2A6 3%, CYP2E1 30%, UGT 33%, SULT 17%.
Type of hepatocytes	Fresh or cryopreserved human	23% fresh human only 37% cryopreserved human only 40% both
Number of donors	$\geq$3 donors for primary human hepatocytes. Immortalized human liver cells may be used if positive controls demonstrate CYP1A2 and CYP3A4 induction.	1 for screening $\geq$3 for further testing
Culture Type	No recommendation	73% use conventional monolayer 27% use sandwich culture
Use of sub μM amounts of dexamethasone in media	No recommendation	70% use dexamethasone 30% do not supplement
Pre incubation culture time before addition of compounds	No recommendation	3% incubated for 3 hr 52% incubated for 24 hrs 73% incubated 24 48 hr
Induction period	48 72 hr	7% induced for 24 hr (for mRNA) 59% induced for 48 hr 34% induced for 72 hr 14% induced up to 8 days
Number of test article concentrations tested	$\geq$3 concentrations spanning the anticipated therapeutic range with 1 concentration an order of magnitude greater than the average expected plasma concentration.	10% used 2 concentrations 60% used 3 concentrations 6% used 2 6 concentrations 23% used $>$ 4 concentrations
End points	Enzyme activity Protein, mRNA, and reporter gene assay results as a compliment	100% measure enzyme activity 40% measure mRNA 23% measure protein 40% measure toxicity 67% measure a combination

Table 1 A Comparison of In Vitro Enzyme Induction Methodologies Between FDA Recommendations and Those Surveyed Among Pharmaceutical Researchers (*Continued*)

Methodology	FDA guidelines (2006)	Pharmaceutical industry practice[a]
Data interpretation	If enzyme activity of cells treated with test article is ≥40% of positive control, the test article is considered an in vitro inducer.	46% considered a positive response to be a ≥2 fold increase over VC[d] 32% used FDA criteria of ≥40% of PC 11% used ≥3 fold increase over VC

[a]Data taken from Ref. 66.
[b]Indicates the percentage of industry researchers who tested this particular enzyme.
[c]If induction studies with a test drug confirm that it is not an inducer of CYP3A4, then it can be assumed that the test drug will not be an inducer of CYP2C8, CYP2C9, and CYP2C19.
[d]VC, vehicle control; PC, positive control.
[e]2003 FDA guidelines recommend the use of sandwich culture to improve cell morphology and survival, but the 2004 and 2006 guidelines do not specify either way. Sandwich culture is not necessary for an induction response (Ref. 102).

Table 2 FDA Preferred and Acceptable Chemical Inducers for In Vitro Experiments Using Primary Human Hepatocytes

Cytochrome P450	Preferred inducer	Inducer concentration (μM)	Acceptable inducer	Inducer concentration (μM)
CYP1A2	Omeprazole	25 100	Lansoprazole	10
	β naphthoflavone	33 50		
	3 methylcholanthrene	1 2		
CYP2A6	Dexamethasone	50	Pyrazole	1000
CYP2B6	Phenobarbital	500 1000	Phenytoin	50
CYP2C8	Rifampicin	10	Phenobarbital	500
CYP2C9	Rifampicin	10	Phenobarbital	100
CYP2C19	Rifampicin	10		
CYP2D6	None identified			
CYP3A4	Rifampicin	10 50	Phenobarbital	100 2000
			Phenytoin	50
			Rifapentine	50
			Troglitazone	10 75
			Taxol	4
			Dexamethasone	33 250

Source: From Ref. 10.

connection between an in vitro induction event and a measurable, clinically significant outcome. Therefore, enzyme selection at individual companies may vary and be drug or drug class dependent. LeCluyse has proposed a marker gene screening paradigm with CYP1A2, 2B6, and 3A4 representing enzymes induced through the AhR, CAR, and PXR pathways, respectively (67). The decision tree in Figure 2 shows an experimental paradigm wherein both enzyme activity and mRNA levels are determined. Measuring mRNA ensures that mechanism-based inhibitors do not obscure an induced enzyme activity. mRNA can also be interrogated for induction of many genes by RT-PCR or microarray approaches.

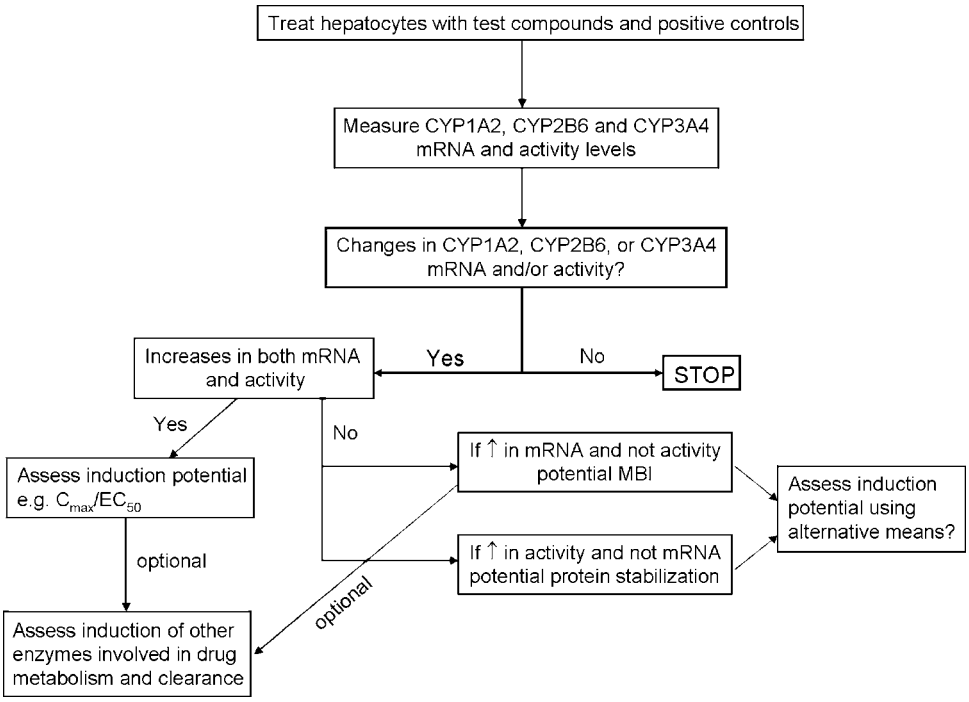

Figure 2 A flowchart decision tree for hepatocyte induction studies.

The FDA draft guidance recommends at least three drug concentrations with two concentrations spanning the anticipated therapeutic range, and one concentration an order of magnitude greater. If a drug produces an induction response that is 40% of positive control or greater, a clinical study is warranted. Several laboratories have evaluated the use of an induction EC_{50} value and whether the C_{max}/EC_{50} ratio would be more predictive of clinical induction. The approach is similar to the [I]/K*i* ratio for clinically relevant inhibitors (3). A C_{max}/EC_{50} ratio greater than 1 indicates that the compound is likely to cause clinical induction, 0.1 to 1.0 indicates a potential for clinical induction, and a value less than 0.1 indicates that a clinical induction study is not necessary. The in vitro C_{max} (or C_{ss})/EC_{50} value was used to correctly rank order clinical induction by 11 compounds (3).

Because induction is a receptor-mediated process, the law of mass action should relate ligand binding to activity. Kato et al. proposed the following equation:

$$\text{Induction response} = E_{max} * C_{ss}(f_u)/EC_{50} + C_{ss}(f_u) \quad \text{(Eq. 1)}$$

where E_{max} is the maximum induction response (68). Quantitative predictions of clinical induction were made by applying Eq. 1 to in vitro human hepatocyte data on seven CYP3A4 and CYP1A2 inducers. The predicted induction response for all but omeprazole correlated well with the clinical literature, and application of this equation to CYP3A4 induction response was proposed.

Hewitt et al. calculated an induction risk factor by incorporating the no observable effect level (NOEL) for induction into Eq. 1 to give Eq. 2, reasoning that both the onset concentration and the concentration-response window are compound specific and important (3):

$$\text{Induction risk factor} = [E_{max} * C_{max}(f_u)/EC_{50} + C_{max}(f_u)] * [NOEL/C_{max}(f_u)] \quad \text{(Eq. 2)}$$

It has not been thoroughly investigated whether the use of free versus total drug concentration is necessary, although Ripp et al. found that better predictions of clinical induction were obtained using free drug plasma concentrations (69).

As quality public data on preclinical and clinical induction expands, modeling and simulation approaches will improve the ability to quantitatively predict the clinical pharmacokinetic behavior of inducible compounds from hepatocyte data. Present approaches are promising for simple cases, and the greater than 40% in vitro induction signal will always trigger a clinical study.

Model Cell Lines

Model cell lines are used as a surrogate for primary hepatocytes, but all have pros and cons. The human hepatocellular carcinoma cell line, HepG2, has very low levels of CAR, PXR, CYP3A4, and other phase I and phase II enzymes, but relatively high levels of CYP3A7, indicative of a fetal expression profile (70 73). Low levels of NRs limit the use of HepG2 cells in induction studies because of a muted induction response. However, HepG2 cells are useful for NR gene reporter assays.

The Fa2N-4 immortalized hepatocyte cell line has been used to assess PXR- and AhR-mediated ADME gene induction (69,74). Fa2N-4 cells are not suitable for the study of CAR agonists since they possess low levels of CAR (75) but are suitable for screening purposes since FDA guidelines require only CYP1A2 and CYP3A4 assessment.

The human hepatoma cell line, HepaRG, when differentiated by 2% DMSO, expresses many NRs and phase I and phase II and transporter enzymes (76,77). However, P450 mRNA levels were generally less than 10%, except CYP2C9 (50%) when compared to primary human hepatocytes. HepaRG cells have been used for the evaluation of P450 induction. Exposure to prototypical inducers increased CYP1A1, CYP1A2, CYP2B6, CYP2C8, CYP2C19, and CYP3A4 mRNA and activity (78). Using nine CYP3A4 inducers, there was a good correlation between CYP3A4 mRNA induction in HepaRG cells and the percentage decrease in AUC for CYP3A probe substrates in human clinical studies. This cell line could be used to complement the use of primary human hepatocytes for induction studies.

Humanized Mouse Models

Species differences in PXR- and CAR-mediated ADME gene induction make extrapolations of preclinical species induction data to human induction misleading. Mouse PXR (mPXR), mouse CAR (mCAR), P450 knockout mice, and humanized transgenic mice with knock-in human CAR (hCAR) and PXR (hPXR), both with and without human CYP3A4 and CYP2B6, are recently available (79 82). Both hPXR and hCAR mouse models exhibit induction of PXR and CAR target genes when dosed with human-specific inducing agents (83,84). These models are still expensive and are not well validated as predictive tools for drug development. Currently, they are being used to understand ADME-related gene expression networks and cross talk related to CAR and PXR activation and may someday be useful in cases where major human metabolites are not significantly produced by standard preclinical species.

Chimeric mice with humanized liver have also been generated by transplanting human hepatocytes into mouse liver. Tateno et al. replaced more than 80% of mouse liver with human hepatocytes (85). CYP3A4 and CYP1A2 were induced by rifampicin and 3-methylcholanthrene, respectively, with only moderate induction of Cyp3a11, the major mouse Cyp3a isoform. The authors advocated the chimeric mouse model as a low-cost source of human hepatocytes.

SPECIES DIFFERENCES IN INDUCTION RESPONSE

There are marked species differences in response to inducers among humans and preclinical species. Although the main functions of AhR, CAR, and PXR are conserved, genetic differences and cross talk among diverse other NRs, cofactors, and coregulators translate into differences in both endogenous and xenobiotic ligand specificity. Some industrially important differences are that rifampicin induces rabbit and human but not rat CYP3A, while pregnenolone-16α-carbonitrile (PCN) induces rat but not human or rabbit CYP3A (86,87). Hyperforin, the active component in St. John's Wort, is a well-known human-specific PXR ligand that is responsible for a number of drug interactions with CYP3A4 substrates (88). The antiemetic, meclizine, is an agonist for mCAR but is an inverse agonist to hCAR, and inhibits the phenobarbital-induced expression of CAR target genes (89). Species differences in PXR and CAR activation may in part be related to limited homology of the LBD, relative to the conserved DBD (2).

Microarrays are a powerful way to compare the in vivo potency of inducer ligands in liver from preclinical species. For example, 26 well-known ADME gene inducers were compared across six doses in rats and mice (28). Over 600 genes in key ADME gene families were assessed on 25K Agilent microarrays. Dose-response relationships differentiated the induction potencies of strong inducers at AhR, CAR, and PXR by the responses of bellwether genes CYP1A1 (AhR), CYP2B10 and 2B15 (CAR in mouse and rat), and CYP3A1 (PXR in rat) across dose. Some ligands like TCPOBOP were more potent in mice than rats, though pharmacokinetics may underlay cross-species potency differences. Furthermore, signature gene sets were derived for AhR, CAR, and PXR responses using groups of prototypical inducers for each NR, and cross talk across the ADME transcriptome was qualitatively defined by overlaps among these gene sets (28).

Induction in dog and monkey species is relatively less studied. Rifampicin is a potent inducer of CYP1A2 in dog hepatocytes but causes only moderate induction in monkey hepatocytes and no induction of CYP1A2 in human hepatocytes (3). Recent work on ADME gene induction in dog and monkey hepatocytes and phase II enzymes in monkeys is beginning to fill this gap in the literature (90,91).

CLINICAL ASPECTS OF INDUCTION

Some Basic Tenets

The clinical aspects of enzyme induction have been reviewed by several authors (2,19,26). Because CYP3A4 mediates the metabolism of approximately 50% of marketed drugs and because assessing patient CYP3A4 status is not commercially viable, induction and inhibition of CYP3A4 is one of the more significant problems in drug development. Zhou et al. have compiled a list of 408 known CYP3A4 substrates, inhibitors, and inducers (6). Of these, 24 (5.9%) were classified as having a strong inducing effect and 31 (7.6%) had a weak inducing effect.[4] Dose-related hepatic exposure, PXR/CAR activation potency, route of administration, and tissue-specific induction are among the many factors that may modulate

[4] Strong and weak CYP3A4 inducer designations do not necessarily denote major or minor role of the feature in clinical drug interactions. The list is not comprehensive of all CYP3A4 inducers.
Strong: aminoglutethimide; atorvastatin; bosentan; carbamazepine; dapsone; dexamethasone; (benchmark, rat); efavirenz; fluvastatin; hyperforin; (benchmark, human); lopinavir; lovastatin; nevirapine; oxcarbazepine; pentobarbitol; phenobarbitol; phenytoin; primidone; rifabutin; rifampin; (benchmark, human); rifapentine; simvastatin; valproic; Acid.
Weak: aprepitant; bexarotene; calcitriol; chlorpromazine; clofibrate; clonazepam; colchicine; cortisol; cyclophosphamide; diazepam; dicloxacillin; estradiol; estrogens; conjugated; exemestane; felbamate; hydrocortisone; ifosfamide; medroxyprogesterone; modafenil; moricizine; nafcillin; oxazepam; paclitaxel; pantoprazol; pioglitazone; prednisolone; prednisone; ritonavir; rofecoxib; sulfinpyrazone; terbinafine; topiramate; troglitazone.

the magnitude of clinical induction. Lin (2) has done an excellent review of related clinical and preclinical data that illustrate some basic tenets of clinical induction, which are extracted and augmented as follows: (*i*) Multiple P450s and multiple tissues may contribute to induction; (*ii*) High and moderate hepatic clearance drugs have the largest induction-related fold decreases in AUC after oral administration, but have negligible changes after intravenous administration; (*iii*) Low hepatic clearance drugs, with less first-pass clearance, have lower fold decreases in AUC, but induction is observed after either intravenous or oral administration; (*iv*) Liver trumps small intestine in terms of overall contribution to induction-related fold decrease in the AUC of inducible oral drugs; (*v*) Variability in the fold range of induction lies mainly in basal levels of expression, since the maximum amount of induction in vitro is relatively similar across individual hepatocyte donors; (*vi*) The magnitude of fold induction of message in vitro is generally larger when basal expression is low or negligible (i.e., CYP1A). Nonetheless, overall changes in metabolic clearance will be predicated on net change in the active P450 protein responsible for a rate-limiting clearance step. As such, induction of enzymes with high basal expression, such as CYP2E1, will afford modest fold increases in protein in vitro, but may afford significant increases in protein mass in vivo with concomitant decreases in victim AUC; (*vii*) In vitro fold change data for individual-induced P450 isoforms are benchmarked to an isoform-specific positive control, whereas clinical induction is typically expressed as fold decrease in victim AUC on the basis of measurement of the plasma AUC before and after a multiple dose regimen of the inducer; (*viii*) Fold decrease in AUC may or may not correlate with fold increase in active protein or message, especially if alternate metabolic or transport pathways are contributing to clearance.

Magnitude of Clinical Induction of Key Substrates

Lin surveyed CYP3A4 and CYP2C clinical induction studies to illustrate the relationship between rate of oral clearance and clinical fold induction because of rifampin coadministration. Select examples are *R*-verapamil (high clearance, 52-fold AUC decrease); midazolam (moderate clearance, 24-fold AUC decrease), and cyclosporine A, tacrolimus, methadone, alprazolam, diazepam, and zolipidem (low clearance, 3.1 8.0-fold AUC decrease). The inducible CYP2C8 and 2C9 substrates surveyed were low clearance and had fold decreases in AUC after oral rifampicin in the range 1.5 (glimepiride) to 3.7 (*S*-warfarin) (2).

Time Course of Induction

CYP1A2 activity measured in smokers using the probe substrate caffeine declined to a nadir at days 6 to 8 after smoking cessation with a CYP1A2 degradation half-life of 36 hours (92). Induction of *R*- and *S*-verapamil clearance by rifampicin was maximal by approximately day 8 with a half-life of 1 day. Upon discontinuation of rifampicin, return to baseline verapamil C_{min} occurred over about 8 plus days with a half-time of approximately 1.5 to 2 days (93). On the basis of these data, typical clinical steady-state one- to two-week long dosing regimens of an inducer will allow new enzyme synthesis to reach steady state. After discontinuation, a comparable time period passes before enzyme levels return to baseline. Dose adjustments and monitoring of clinical efficacy for low therapeutic index victims of enzyme induction such as warfarin can therefore be a protracted process.

Clinical Tools

At the heart of all clinical induction studies are a probe substrate and ideally a positive control inducer. Liu et al. lists clinically useful probe drugs for CYP3A4 and/or CYP3A5 status. These are midazolam (3A4/5), triazolam (3A4/5), alfentanil (miosis biomarker,

3A4/5), testosterone 6-β hydroxylation (3A4/5), cortisol (6-β hydroxyl, 3A4/5, urine biomarker), alprazolam (α-hydroxylation, CYP3A5), tacrolimus (demethylation, CYP3A5), vincristine (CYP3A5), and erythromycin demethylation (IV ^{14}C breath test for hepatic CYP3A4 and oral for intestinal CYP3A4/P-gp and hepatic CYP3A4) (94).

The CDER guidances also specify preferred inducible probe drugs that should be used in clinical studies. These include theophylline or caffeine for CYP1A2, efavirenz for CYP2B6, repaglinide or rosiglitazone for CYP2C8, S-warfarin or tolbutamide for CYP2C9, omeprazole, esoprazole, lansoprazole, or pantoprazole for CYP2C19, and midazolam, buspirone, felodipine, lovastatin, eletriptan, sildenafil, simvastatin, or triazolam for CYP3A4. Midazolam (a selective CYP3A4 substrate) and oral contraceptives (chosen due to probable concomitant use and clinical consequence) are the most common probes used during the clinical development of potential inducers.

Clinical positive controls for induction perpetrators are smokers versus nonsmokers for CYP1A2, rifampin covers CYP2B6, 2C8, 2C9, and 2C19 and CYP3A4, with carbamazepine as a CYP3A4 alternative. These inducers decrease the plasma AUC of their respective P450 substrates by 30% or more (95).

Drug Labels of Prototypical Inducers

The Drugdex monograph for the protoypical PXR activator rifampin has 31 "major" induction-based drug interactions, all related to CYP3A4 (96). There are relatively few induced CYP2C substrates in the rifampin monograph and all are weak or moderate (ambrisentan, losartan, pioglitazone, rosiglitazone, and ramelteon). There are no interactions attributed specifically to CYP2B or 2A. P-glycoprotein induction is also co-implicated in the induction mechanism of maraviroc, ambrisentan, ranolazine, and tacrolimus.

In contrast, the atypical CAR activator, phenobarbital, has a surprisingly short victim list, mainly including CYP3A4 substrates aprenavir, armodafanil, bexarotene, clozepine (1A2/3A4), ritonavir, and tiranavir (96). Methadone appears to be the only victim listed where induction of metabolism by CYP2B6 is co-implicated in the drug label along with CYP2C19 and CYP3A4. Induction of CYP2B6 by ritonavir results in small increases in the *R*- and *S*- bupropion clearance (97), but both CYP2B6 interactions are complicated by activity of the perpetrator at other isoforms. CYP2B6 seems rarely to be rate limiting in the clearance of known drugs.

CYP1A2 induction by omeprazole was a development issue in the early 1990s because CYP1A induction was traditionally viewed as a liability because of associations of induced CYP1A enzymes with bioactivation of dietary pro-carcinogens (26). However, the commercial success, safety, and efficacy of omeprazole have done much to allay this concern. A therapeutic dose of omeprazole induced the clearance of the probe substrate caffeine, but only in CYP2C19 poor metabolizers exposed to higher concentrations of omeprazole and not in extensive metabolizers (98). There is no mention of CYP1A2 induction in the omeprazole label (11). Like CYP2B6, there appear to be relatively few drugs that undergo rate-limiting metabolism by CYP1A2.

NEW TECHNOLOGIES

New Hepatocyte Model

Limitations of sandwiched monolayer hepatocyte culture with respect to maintenance of liver architecture and ADME gene expression were recently highlighted in a paper by Khetani and Bhatia who developed a microscale multiwell human liver cell/fibroblast

coculture system that maintains cell morphology and ADME gene functions for four to six weeks (99). Microarray assessment of diverse ADME genes, NRs, and liver-enriched transcription factors showed impressive gene expression at day 42.

Gene Expression Microarrays

Drug metabolism induction is largely a CYP3A4-centric problem, and simple multiplexed gene expression approaches comprising just a few dozen ADME genes can cover most commercially important ADME genes from a regulatory and PKDM development perspective. However, cross talk among NRs in health and disease and the overlaps of the disciplines of drug metabolism with mechanistic toxicology make microarray-based methods an obvious next step in the timely dissection of subtle metabolism/toxicology problems on a mechanistic level. Using 25,000 gene microarrays, variability in ADME gene expression in 75 human livers was measured across 553 members of the ADME gene transcriptome. For inducible genes, expression frequency distributions were usually skewed, and many inducible ADME genes had large fold-range variability relative to non-ADME genes. This combination of frequency distribution asymmetry and large fold range allowed identification of co-expressed or co-regulated genes for CYP3A4, 2B6, and 1A2. The goal was to find secretable protein products corresponding to correlated genes that may be biomarkers of CYP3A4 phenotype (36).

Microarrays have also been used to develop a transcriptome-wide understanding of ADME gene induction in rats and mice. Microarray compendia of in vivo liver gene expression for 500 to 800 ADME genes were developed across a wide dose range for a library of 26 of the world's best-known inducers (28). This work applied toxicogenomic strategy to a drug resource sparing model developed by Meador et al. for discovery toxicology studies (100). The cross talk of strong AhR, CAR, and PXR ligands was evident in the dose response of target genes and was able to differentiate ligands that were predominantly CAR or predominantly PXR. Consensus gene sets were developed for each NR.

Microarray applications to ADME are still daunting to many non-practitioners. However, user-friendly data visualization tools such as Ingenuity™, public domain gene expression compendia, falling costs, regulatory safe harbor provisions for toxicogenomic data, and regulatory success stories will eventually enable more frequent applications of microarrays to mechanistic drug metabolism and toxicology investigations.

CONCLUSION

Since attrition of clinical candidates due to metabolism-related factors has decreased significantly since the early 1990s, (101) future improvements in predicting and quantifying clinically significant enzyme induction are likely to be incremental. At present, validation of correlations between in vitro and in vivo data and modeling of anticipated clinical data from in vitro DDI data are progressing. The genetics, gene expression, and proteomics of biochemical cross talk in induction mechanisms are active research areas. Ultimately, less expensive human cell culture techniques, accessible toxicogenomic toolsets, and cost-effective, peripherally accessible biomarkers of induction status will advance our ability to predict and monitor the clinical impact of ADME gene induction.

REFERENCES

1. Reschly EJ, Krasowski MD. Evolution and function of the NR1I nuclear hormone receptor subfamily (VDR, PXR, and CAR) with respect to metabolism of xenobiotics and endogenous compounds. Curr Drug Metab 2006; 7(4):349 365.
2. Lin JH. CYP induction mediated drug interactions: in vitro assessment and clinical implications. Pharm Res 2006; 23(6):1089 1116.
3. Hewitt NJ, Lecluyse EL, Ferguson SS. Induction of hepatic cytochrome P450 enzymes: methods, mechanisms, recommendations, and in vitro in vivo correlations. Xenobiotica 2007; 37(10 11):1196 1224.
4. Grover GS, Brayman TG, Voorman RL, Ware JA. Development of in vitro methods to predict induction of CYP1A2 and CYP3A4 in humans. Assay Drug Dev Technol 2007; 5(6):793 804.
5. Wahlstrom L, Rock D, Slatter J, Wienkers L. Advances in predicting CYP mediated drug interactions in the drug discovery setting. Expert Opin Drug Discov 2006; 1(7):15.
6. Zhou SF, Xue CC, Yu XQ, Li C, Wang G. Clinically important drug interactions potentially involving mechanism based inhibition of cytochrome P450 3A4 and the role of therapeutic drug monitoring. Ther Drug Monit 2007; 29(6):687 710.
7. Walsky RL, Obach RS. Validated assays for human cytochrome P450 activities. Drug Metab Dispos 2004; 32(6):647 660.
8. Cali JJ, Ma D, Sobol M, Simpson DJ, Frackman S, Good TD, Daily WJ, Liu D. Luminogenic cytochrome P450 assays. Expert Opin Drug Metab Toxicol 2006; 2(4):629 645.
9. McGinnity DF, Berry AJ, Kenny JR, Grime K, Riley RJ. Evaluation of time dependent cytochrome P450 inhibition using cultured human hepatocytes. Drug Metab Dispos 2006; 34(8):1291 1300.
10. FDA. Drug Interaction Studies: Study Design, Data Analysis, and Implications of Dosing and Labeling http://www.fda.gov/cder/guidance/6695dft.pdf. 2006.
11. Staff TH. Physicians Desk Reference. 62 ed. Thompson Healthcare, 2008.
12. Xu C, Li CY, Kong AN. Induction of phase I, II and III drug metabolism/transport by xenobiotics. Arch Pharm Res 2005; 28(3):249 268.
13. Jana S, Paliwal J. Molecular mechanisms of cytochrome p450 induction: potential for drug drug interactions. Curr Protein Pept Sci 2007; 8(6):619 628.
14. Tompkins LM, Wallace AD. Mechanisms of cytochrome P450 induction. J Biochem Mol Toxicol 2007; 21(4):176 181.
15. Pavek P, Dvorak Z. Xenobiotic induced transcriptional regulation of xenobiotic metabolizing enzymes of the cytochrome p450 superfamily in human extrahepatic tissues. Curr Drug Metab 2008; 9(2):129 143.
16. Timsit YE, Negishi M. CAR and PXR: the xenobiotic sensing receptors. Steroids 2007; 72(3):231 246.
17. Watkins PB, Wrighton SA, Schuetz EG, Maurel P, Guzelian PS. Macrolide antibiotics inhibit the degradation of the glucocorticoid responsive cytochrome P 450p in rat hepatocytes in vivo and in primary monolayer culture. J Biol Chem 1986; 261(14):6264 6271.
18. Koop DR, Crump BL, Nordblom GD, Coon MJ. Immunochemical evidence for induction of the alcohol oxidizing cytochrome P 450 of rabbit liver microsomes by diverse agents: ethanol, imidazole, trichloroethylene, acetone, pyrazole, and isoniazid. Proc Natl Acad Sci U S A 1985; 82(12):4065 4069.
19. Urquhart BL, Tirona RG, Kim RB. Nuclear receptors and the regulation of drug metabolizing enzymes and drug transporters: implications for interindividual variability in response to drugs. J Clin Pharmacol 2007; 47(5):566 578.
20. Kullak Ublick GA, Becker MB. Regulation of drug and bile salt transporters in liver and intestine. Drug Metab Rev 2003; 35(4):305 317.
21. Lim YP, Huang JD. Interplay of pregnane X receptor with other nuclear receptors on gene regulation. Drug Metab Pharmacokinet 2008; 23(1):14 21.
22. Meyer UA. Endo xenobiotic crosstalk and the regulation of cytochromes P450. Drug Metab Rev 2007; 39(2 3):639 646.

23. Goodwin B, Moore JT. CAR: detailing new models. Trends Pharmacol Sci 2004; 25(8): 437 441.
24. Xie W, Barwick JL, Simon CM, Pierce AM, Safe S, Blumberg B, Guzelian PS, Evans RM. Reciprocal activation of xenobiotic response genes by nuclear receptors SXR/PXR and CAR. Genes Dev 2000; 14(23):3014 3023.
25. Monteiro P, Gilot D, Le Ferrec E, Rauch C, Lagadic Gossmann D, Fardel O. Dioxin mediated up regulation of aryl hydrocarbon receptor target genes is dependent on the calcium/ calmodulin/CaMKIalpha pathway. Mol Pharmacol 2008; 73(3):769 777.
26. Ma Q, Lu AY. CYP1A induction and human risk assessment: an evolving tale of in vitro and in vivo studies. Drug Metab Dispos 2007; 35(7):1009 1016.
27. Coe KJ, Nelson SD, Ulrich RG, He Y, Dai X, Cheng O, Caguyong M, Roberts CJ, Slatter JG. Profiling the hepatic effects of flutamide in rats: a microarray comparison with classical aryl hydrocarbon receptor ligands and atypical CYP1A inducers. Drug Metab Dispos 2006; 34(7): 1266 1275.
28. Slatter JG, Cheng O, Cornwell PD, de Souza A, Rockett J, Rushmore T, Hartley D, Evers R, He Y, Dai X, Hu R, Caguyong M, Roberts CJ, Castle J, Ulrich RG. Microarray based compendium of hepatic gene expression profiles for prototypical ADME gene inducing compounds in rats and mice in vivo. Xenobiotica 2006; 36(10 11):902 937.
29. Szczesna Skorupa E, Chen CD, Liu H, Kemper B. Gene expression changes associated with the endoplasmic reticulum stress response induced by microsomal cytochrome p450 overproduction. J Biol Chem 2004; 279(14):13953 13961.
30. Dixit SG, Tirona RG, Kim RB. Beyond CAR and PXR. Curr Drug Metab 2005; 6(4):385 397.
31. Eloranta JJ, Kullak Ublick GA. Coordinate transcriptional regulation of bile acid homeostasis and drug metabolism. Arch Biochem Biophys 2005; 433(2):397 412.
32. Kretschmer XC, Baldwin WS. CAR and PXR: xenosensors of endocrine disrupters? Chem Biol Interact 2005; 155(3):111 128.
33. Zhai Y, Pai HV, Zhou J, Amico JA, Vollmer RR, Xie W. Activation of pregnane X receptor disrupts glucocorticoid and mineralocorticoid homeostasis. Mol Endocrinol 2007; 21(1):138 147.
34. Min G, Kemper JK, Kemper B. Glucocorticoid receptor interacting protein 1 mediates ligand independent nuclear translocation and activation of constitutive androstane receptor in vivo. J Biol Chem 2002; 277(29):26356 26363.
35. Yang Y, Blomme EA, Waring JF. Toxicogenomics in drug discovery: from preclinical studies to clinical trials. Chem Biol Interact 2004; 150(1):71 85.
36. Slatter JG, Templeton IE, Castle JC, Kulkarni A, Rushmore TH, Richards K, He Y, Dai X, Cheng OJ, Caguyong M, Ulrich RG. Compendium of gene expression profiles comprising a baseline model of the human liver drug metabolism transcriptome. Xenobiotica 2006; 36(10 11):938 962.
37. Lamba J, Lamba V, Strom S, Venkataramanan R, Schuetz E. Novel single nucleotide polymorphisms in the promoter and intron 1 of human pregnane X receptor/NR1I2 and their association with CYP3A4 expression. Drug Metab Dispos 2008; 36(1):169 181.
38. Lamba JK, Lamba V, Yasuda K, Lin YS, Assem M, Thompson E, Strom S, Schuetz E. Expression of constitutive androstane receptor splice variants in human tissues and their functional consequences. J Pharmacol Exp Ther 2004; 311(2):811 821.
39. Finkelstein D, Lamba V, Assem M, Rengelshausen J, Yasuda K, Strom S, Schuetz E. ADME transcriptome in Hispanic versus white donor livers: evidence of a globally enhanced NR1I3 (CAR, constitutive androstane receptor) gene signature in Hispanics. Xenobiotica 2006; 36(10 11):989 1012.
40. Takagi S, Nakajima M, Mohri T, Yokoi T. Post transcriptional regulation of human pregnane X receptor by micro RNA affects the expression of cytochrome P450 3A4. J Biol Chem 2008; 283(15):9674 9680.
41. Grabenstein JD. Drug interactions involving immunologic agents. Part I. Vaccine vaccine, vaccine immunoglobulin, and vaccine drug interactions. DICP 1990; 24(1):67 81.
42. Assenat E, Gerbal chaloin S, Maurel P, Vilarem MJ, Pascussi JM. Is nuclear factor kappa B the missing link between inflammation, cancer and alteration in hepatic drug metabolism in patients with cancer? Eur J Cancer 2006; 42(6):785 792.

43. Frye RF, Zgheib NK, Matzke GR, Chaves Gnecco D, Rabinovitz M, Shaikh OS, Branch RA. Liver disease selectively modulates cytochrome P450 mediated metabolism. Clin Pharmacol Ther 2006; 80(3):235 245.
44. Paine AJ, Andreakos E. Activation of signalling pathways during hepatocyte isolation: relevance to toxicology in vitro. Toxicol In Vitro 2004; 18(2):187 193.
45. Healan Greenberg C, Waring JF, Kempf DJ, Blomme EA, Tirona RG, Kim RB. A human immunodeficiency virus protease inhibitor is a novel functional inhibitor of human pregnane X receptor. Drug Metab Dispos 2008; 36(3):500 507.
46. Ghose R, White D, Guo T, Vallejo J, Karpen SJ. Regulation of hepatic drug metabolizing enzyme genes by Toll like receptor 4 signaling is independent of Toll interleukin 1 receptor domain containing adaptor protein. Drug Metab Dispos 2008; 36(1):95 101.
47. Roth A, Looser R, Kaufmann M, Meyer UA. Sterol regulatory element binding protein 1 interacts with pregnane X receptor and constitutive androstane receptor and represses their target genes. Pharmacogenet Genomics 2008; 18(4):325 337.
48. Chang TK, Waxman DJ. Pregnane X receptor mediated transcription. Methods Enzymol 2005; 400:588 598.
49. El Sankary W, Gibson GG, Ayrton A, Plant N. Use of a reporter gene assay to predict and rank the potency and efficacy of CYP3A4 inducers. Drug Metab Dispos 2001; 29(11):1499 1504.
50. Luo G, Cunningham M, Kim S, Burn T, Lin J, Sinz M, Hamilton G, Rizzo C, Jolley S, Gilbert D, Downey A, Mudra D, Graham R, Carroll K, Xie J, Madan A, Parkinson A, Christ D, Selling B, LeCluyse E, Gan LS. CYP3A4 induction by drugs: correlation between a pregnane X receptor reporter gene assay and CYP3A4 expression in human hepatocytes. Drug Metab Dispos 2002; 30(7):795 804.
51. Noracharttiyapot W, Nagai Y, Matsubara T, Miyata M, Shimada M, Nagata K, Yamazoe Y. Construction of several human derived stable cell lines displaying distinct profiles of CYP3A4 induction. Drug Metab Pharmacokinet 2006; 21(2):99 108.
52. Luo G, Guenthner T, Gan LS, Humphreys WG. CYP3A4 induction by xenobiotics: biochemistry, experimental methods and impact on drug discovery and development. Curr Drug Metab 2004; 5(6):483 505.
53. Bertilsson G, Heidrich J, Svensson K, Asman M, Jendeberg L, Sydow Backman M, Ohlsson R, Postlind H, Blomquist P, Berkenstam A. Identification of a human nuclear receptor defines a new signaling pathway for CYP3A induction. Proc Natl Acad Sci U S A 1998; 95(21):12208 12213.
54. Blumberg B, Sabbagh W, Jr., Juguilon H, Bolado J, Jr., van Meter CM, Ong ES, Evans RM. SXR, a novel steroid and xenobiotic sensing nuclear receptor. Genes Dev 1998; 12(20):3195 3205.
55. Lehmann JM, McKee DD, Watson MA, Willson TM, Moore JT, Kliewer SA. The human orphan nuclear receptor PXR is activated by compounds that regulate CYP3A4 gene expression and cause drug interactions. J Clin Invest 1998; 102(5):1016 1023.
56. Goodwin B, Hodgson E, Liddle C. The orphan human pregnane X receptor mediates the transcriptional activation of CYP3A4 by rifampicin through a distal enhancer module. Mol Pharmacol 1999; 56(6):1329 1339.
57. Persson KP, Ekehed S, Otter C, Lutz ES, McPheat J, Masimirembwa CM, Andersson TB. Evaluation of human liver slices and reporter gene assays as systems for predicting the cytochrome p450 induction potential of drugs in vivo in humans. Pharm Res 2006; 23(1):56 69.
58. Zhu Z, Kim S, Chen T, Lin JH, Bell A, Bryson J, Dubaquie Y, Yan N, Yanchunas J, Xie D, Stoffel R, Sinz M, Dickinson K. Correlation of high throughput pregnane X receptor (PXR) transactivation and binding assays. J Biomol Screen 2004; 9(6):533 540.
59. Sinz M, Kim S, Zhu Z, Chen T, Anthony M, Dickinson K, Rodrigues AD. Evaluation of 170 xenobiotics as transactivators of human pregnane X receptor (hPXR) and correlation to known CYP3A4 drug interactions. Curr Drug Metab 2006; 7(4):375 388.
60. Willson TM, Kliewer SA. PXR, CAR and drug metabolism. Nat Rev Drug Discov 2002; 1(4):259 266.
61. Sueyoshi T, Kawamoto T, Zelko I, Honkakoski P, Negishi M. The repressed nuclear receptor CAR responds to phenobarbital in activating the human CYP2B6 gene. J Biol Chem 1999; 274(10):6043 6046.

62. Tzameli I, Moore DD. Role reversal: new insights from new ligands for the xenobiotic receptor CAR. Trends Endocrinol Metab 2001; 12(1):7 10.
63. Moore LB, Parks DJ, Jones SA, Bledsoe RK, Consler TG, Stimmel JB, Goodwin B, Liddle C, Blanchard SG, Willson TM, Collins JL, Kliewer SA. Orphan nuclear receptors constitutive androstane receptor and pregnane X receptor share xenobiotic and steroid ligands. J Biol Chem 2000; 275(20):15122 15127.
64. Swales K, Negishi M. CAR, driving into the future. Mol Endocrinol 2004; 18(7):1589 1598.
65. Hewitt NJ, Lechon MJ, Houston JB, Hallifax D, Brown HS, Maurel P, Kenna JG, Gustavsson L, Lohmann C, Skonberg C, Guillouzo A, Tuschl G, Li AP, LeCluyse E, Groothuis GM, Hengstler JG. Primary hepatocytes: current understanding of the regulation of metabolic enzymes and transporter proteins, and pharmaceutical practice for the use of hepatocytes in metabolism, enzyme induction, transporter, clearance, and hepatotoxicity studies. Drug Metab Rev 2007; 39(1):159 234.
66. Hewitt NJ, de Kanter R, LeCluyse E. Induction of drug metabolizing enzymes: a survey of in vitro methodologies and interpretations used in the pharmaceutical industry do they comply with FDA recommendations? Chem Biol Interact 2007; 168(1):51 65.
67. LeCluyse E. Assessing enzyme induction in vitro: a scientific and regulatory perspective. Presented at: the 10th International Conference on Drug Drug Interactions; 2007; Seattle, WA.
68. Kato M, Chiba K, Horikawa M, Sugiyama Y. The quantitative prediction of in vivo enzyme induction caused by drug exposure from in vitro information on human hepatocytes. Drug Metab Pharmacokinet 2005; 20(4):236 243.
69. Ripp SL, Mills JB, Fahmi OA, Trevena KA, Liras JL, Maurer TS, de Morais SM. Use of immortalized human hepatocytes to predict the magnitude of clinical drug drug interactions caused by CYP3A4 induction. Drug Metab Dispos 2006; 34(10):1742 1748.
70. Pascussi JM, Jounaidi Y, Drocourt L, Domergue J, Balabaud C, Maurel P, Vilarem MJ. Evidence for the presence of a functional pregnane X receptor response element in the CYP3A7 promoter gene. Biochem Biophys Res Commun 1999; 260(2):377 381.
71. Vyhlidal CA, Gaedigk R, Leeder JS. Nuclear receptor expression in fetal and pediatric liver: correlation with CYP3A expression. Drug Metab Dispos 2006; 34(1):131 137.
72. Wilkening S, Stahl F, Bader A. Comparison of primary human hepatocytes and hepatoma cell line Hepg2 with regard to their biotransformation properties. Drug Metab Dispos 2003; 31(8): 1035 1042.
73. Maruyama M, et al. Comparison of basal gene expression and induction of CYP3As in HepG2 and human fetal liver cells. Biol Pharm Bull 2007; 30(11):2091 2097.
74. Mills JB, Rose KA, Sadagopan N, Sahi J, de Morais SM. Induction of drug metabolism enzymes and MDR1 using a novel human hepatocyte cell line. J Pharmacol Exp Ther 2004; 309(1):303 309.
75. Hariparsad N, Carr BA, Evers R, Chu X. Comparison of immortalized Fa2N 4 cells and human hepatocytes as in vitro models for cytochrome P450 induction. Drug Metab Dispos 2008; 36:1046 1055. [Epub 2008, Mar 10].
76. Aninat C, Piton A, Glaise D, Le Charpentier T, Langouet S, Morel F, Guguen Guillouzo C, Guillouzo A. Expression of cytochromes P450, conjugating enzymes and nuclear receptors in human hepatoma HepaRG cells. Drug Metab Dispos 2006; 34(1):75 83.
77. Guillouzo A, Corlu A, Aninat C, Glaise D, Morel F, Guguen Guillouzo C. The human hepatoma HepaRG cells: a highly differentiated model for studies of liver metabolism and toxicity of xenobiotics. Chem Biol Interact 2007; 168(1):66 73.
78. Kanebratt KP, Andersson TB. HepaRG cells as an in vitro model for evaluation of cytochrome P450 induction in humans. Drug Metab Dispos 2008; 36(1):137 145.
79. Stanley LA, Horsburgh BC, Ross J, Scheer N, Wolf CR. PXR and CAR: nuclear receptors which play a pivotal role in drug disposition and chemical toxicity. Drug Metab Rev 2006; 38(3):515 597.
80. Katoh M, Yokoi T. Application of chimeric mice with humanized liver for predictive ADME. Drug Metab Rev 2007; 39(1):145 157.
81. Gonzalez FJ. CYP3A4 and pregnane X receptor humanized mice. J Biochem Mol Toxicol 2007; 21(4):158 162.

82. Gong H, Sinz MW, Feng Y, Chen T, Venkataramanan R, Xie W. Animal models of xenobiotic receptors in drug metabolism and diseases. Methods Enzymol 2005; 400:598 618.
83. Xie W, Barwick JL, Downes M, Blumberg B, Simon CM, Nelson MC, Neuschwander Tetri BA, Brunt EM, Guzelian PS, Evans RM. Humanized xenobiotic response in mice expressing nuclear receptor SXR. Nature 2000; 406(6794):435 439.
84. Zhang J, Huang W, Chua SS, Wei P, Moore DD. Modulation of acetaminophen induced hepatotoxicity by the xenobiotic receptor CAR. Science 2002; 298(5592):422 424.
85. Tateno C, Yoshizane Y, Saito N, Kataoka M, Utoh R, Yamasaki C, Tachibana A, Soeno Y, Asahina K, Hino H, Asahara T, Yokoi T, Furukawa T, Yoshizato K. Near completely humanized liver in mice shows human type metabolic responses to drugs. Am J Pathol 2004; 165(3):901 912.
86. Wrighton SA, Schuetz EG, Watkins PB, Maurel P, Barwick J, Bailey BS, Hartle HT, Young B, Guzelian P. Demonstration in multiple species of inducible hepatic cytochromes P 450 and their mRNAs related to the glucocorticoid inducible cytochrome P 450 of the rat. Mol Pharmacol 1985; 28(3):312 321.
87. Barwick JL, Quattrochi LC, Mills AS, Potenza C, Tukey RH, Guzelian PS. Trans species gene transfer for analysis of glucocorticoid inducible transcriptional activation of transiently expressed human CYP3A4 and rabbit CYP3A6 in primary cultures of adult rat and rabbit hepatocytes. Mol Pharmacol 1996; 50(1):10 16.
88. Madabushi R, Frank B, Drewelow B, Derendorf H, Butterweck V. Hyperforin in St. John's wort drug interactions. Eur J Clin Pharmacol 2006; 62(3):225 233.
89. Huang W, Zhang J, Wei P, Schrader WT, Moore DD. Meclizine is an agonist ligand for mouse constitutive androstane receptor (CAR) and an inverse agonist for human CAR. Mol Endocrinol 2004; 18(10):2402 2408.
90. Graham RA, Tyler LO, Krol WL, Silver IS, Webster LO, Clark P, Chen L, Banks T, LeCluyse EL. Temporal kinetics and concentration response relationships for induction of CYP1A, CYP2B, and CYP3A in primary cultures of beagle dog hepatocytes. J Biochem Mol Toxicol 2006; 20(2):69 78.
91. Nishimura M, Koeda A, Shimizu T, Nakayama M, Satoh T, Narimatsu S, Naito S. Comparison of inducibility of sulfotransferase and UDP glucuronosyltransferase mRNAs by prototypical microsomal enzyme inducers in primary cultures of human and cynomolgus monkey hepatocytes. Drug Metab Pharmacokinet 2008; 23(1):45 53.
92. Faber MS, Fuhr U. Time response of cytochrome P450 1A2 activity on cessation of heavy smoking. Clin Pharmacol Ther 2004; 76(2):178 184.
93. Fromm MF, Busse D, Kroemer HK, Eichelbaum M. Differential induction of prehepatic and hepatic metabolism of verapamil by rifampin. Hepatology 1996; 24(4):796 801.
94. Liu YT, Hao HP, Liu CX, Wang GJ, Xie HG. Drugs as CYP3A probes, inducers, and inhibitors. Drug Metab Rev 2007; 39(4):699 721.
95. FDA. Drug Development and Drug Interactions: Table of Substrates, Inhibitors and Inducers. 2006. Available at: http://www.fda.gov/cder/drug/drugInteractions/tableSubstrates.htm#4.
96. Rifampin. Drug Information for the Health Care Professional. In: 26 Ed., Thomson Micromedex, 2006; 2595 2604.
97. Kharasch ED, Mitchell D, Coles R, Blanco R. Rapid clinical induction of hepatic cytochrome P4502B6 activity by ritonavir. Antimicrob Agents Chemother 2008; 52(5):1663 1669.
98. Rost KL, Brosicke H, Scheffler M, Roots I. Dose dependent induction of CYP1A2 activity by omeprazole (Antra). Int J Clin Pharmacol Ther Toxicol 1992; 30(11):542 543.
99. Khetani SR, Bhatia SN. Microscale culture of human liver cells for drug development. Nat Biotechnol 2008; 26(1):120 126.
100. Meador V, Jordan W, Zimmermann J. Increasing throughput in lead optimization in vivo toxicity screens. Curr Opin Drug Discov Devel 2002; 5(1):72 78.
101. Kola I, Landis J. Can the pharmaceutical industry reduce attrition rates? Nat Rev Drug Discov 2004; 3(8):711 715.
102. LeCluyse E, Madan A, Hamilton G, Carroll K, DeHaan R, Parkinson A. Expression and regulation of cytochrome P450 enzymes in primary cultures of human hepatocytes. J Biochem Mol Toxicol 2000; 14(4):177 188.

21

Experimental Characterization of Cytochrome P450 Mechanism Based Inhibition

Dan Rock,[1] Michael Schrag,[2] and Larry C. Wienkers[1]
[1]*Department of Pharmacokinetics and Drug Metabolism, Amgen Inc., Seattle, Washington, U.S.A.*
[2]*Department of Drug Metabolism, Array BioPharma Inc., Boulder, Colorado, U.S.A.*

INTRODUCTION

Oxidative metabolism mediated by the superfamily of heme enzymes known as the cytochromes P450 represents an important elimination pathway for the majority of drugs prescribed today (1). In general, the enzymes catalyze the oxidative metabolism of a wide range of drugs and endogenous compounds to yield products (e.g., metabolites) that are usually more hydrophilic through the addition of a polar functional group, which may then serve as a reactive site for conjugating enzymes to enhance the rate of clearance and excretion of the products further by the addition of a yet more polar moiety (1). For the most part, cytochrome P450 mediated reactions are typically considered to reflect detoxification pathways of xenobiotics as the hydrophilic metabolites are rapidly excreted from the body. In some instances, however, P450 metabolism results in the formation of reactive intermediates that can react with cellular macromolecules such as DNA, RNA, and proteins, and lead to toxicity (2). Given the chemical nature of these reactive intermediates, it is not surprising then that the same enzymes responsible for their formation are also susceptible to modification by these bioactivated species (3). Compounds that are transformed by the P450 enzymes into reactive intermediates, which then react with active-site moieties leading to inactivation of the enzyme, are referred to as mechanism-based inactivators (4).

Cytochrome P450 mechanism-based inhibitors (MBIs) have been identified across multiple therapeutic areas including antiarrhythmics [e.g., amiodarone (5)], antibacterials [e.g., clarithromycin (6) and troleandomycin (7)], antidepressants [e.g., fluoxetine (8) and paroxetine (9)], anti-HIV agents [e.g., ritonavir (10) and delavirdine (11)], antihypertensives [e.g., diltiazem (12) and verapamil (13)], nonsteroidal anti-inflamatory drugs

(NSAIDs) [suprofen (14) and zileuton (15)], steroids/receptor modulators [e.g., gestodene (16) and raloxifene (17)], methylenedioxymethamphetamine [(MDMA) (18)], and oncology drugs [e.g., tamoxifen (19) and irinotecan (20)]. In addition, P450 MBIs can be found in environmental sources such as: illicit drugs [e.g., phencyclidine (PCP) (21) and various dietary constituents (e.g., bergamottin (22), resveratrol (23), and 8-methoxypsoralen (24)]. Consistent with the concepts outlined previously for a reversible inhibitor, the severity of the observed drug-drug interactions (DDIs) encountered with P450 MBIs is primarily dependent on two factors: (*i*) the number of relevant clearance pathways associated with the victim drug's clearance and (*ii*) how well the increase in victim drug concentration is tolerated by the system (25). In response to the observed safety risks associated with P450 inhibition (reversible or irreversible), global regulatory agencies now require a robust understanding of the potential for drug inhibition of P450 enzymes for any new drug application (26).

MBIs are a class of enzyme inhibitors, which contain a latent functional group that is by itself chemically unreactive, but can become activated to a highly reactive intermediate upon metabolism (27). The activated species then binds irreversibly to the enzyme-active site and thereby inactivates the enzyme.

Given that the reactive groups present within the active site of the enzyme are nucleophiles (such as hydroxyl or sulfhydryl groups), irreversible inhibition via covalent addition of reactive species to the enzymes requires that the reactive species be some form of electrophilic moiety. For many enzymes, the formation of a reactive species (using the catalytic mechanism of the enzyme) falls into a few distinct categories, such as the generation of Michael acceptors, haloalkyl derivatives, and rearrangements leading to an acyl-enzyme intermediate (e.g., proteases). For P450 MBIs, several structural moieties can serve as latent chemical groups associated with enzyme activation (Fig. 1).

CRITERIA FOR CYTOCHROME P450 MECHANISM-BASED INHIBITION

Characterization of MBIs follows intuitive kinetic and chemical criteria (28,29). In short, a MBI is required to be a substrate, where physical binding to the enzyme-active site precedes catalysis. The interaction between substrate and enzyme needs to reflect a binding equilibrium followed by first-order chemical process leading to inactivation. To this end, as inhibitor concentration is increased, a greater fraction of the total enzyme will be occupied with inhibitor and the saturation of enzyme with inhibitor will be consistent with the kinetic specificity of the initial binding step. In addition, if covalent modification of the enzyme is a mechanism-based process, which proceeds via adduct formation to a key amino acid residue within the enzyme-active site, the chemical stoichiometry of modification should be unity (1:1 adduct/enzyme ratio) (30).

Today there exist well-defined criteria to assess whether a substrate is a P450 mechanism-based inactivator. Briefly, the inhibition must include the following:

1. The loss of enzyme activity must exhibit time dependence.
2. Enzyme inactivation should exhibit saturation kinetics with respect to the concentration of the inhibitor.
3. The inactivation occurs in a catalytically competent system (e.g., necessary cofactors are present and metabolism is occurring).
4. The enzyme should be protected from inactivation upon co-incubation with a competitive substrate/inhibitor.
5. Lack of suppression of inactivation by reactive intermediate scavengers.

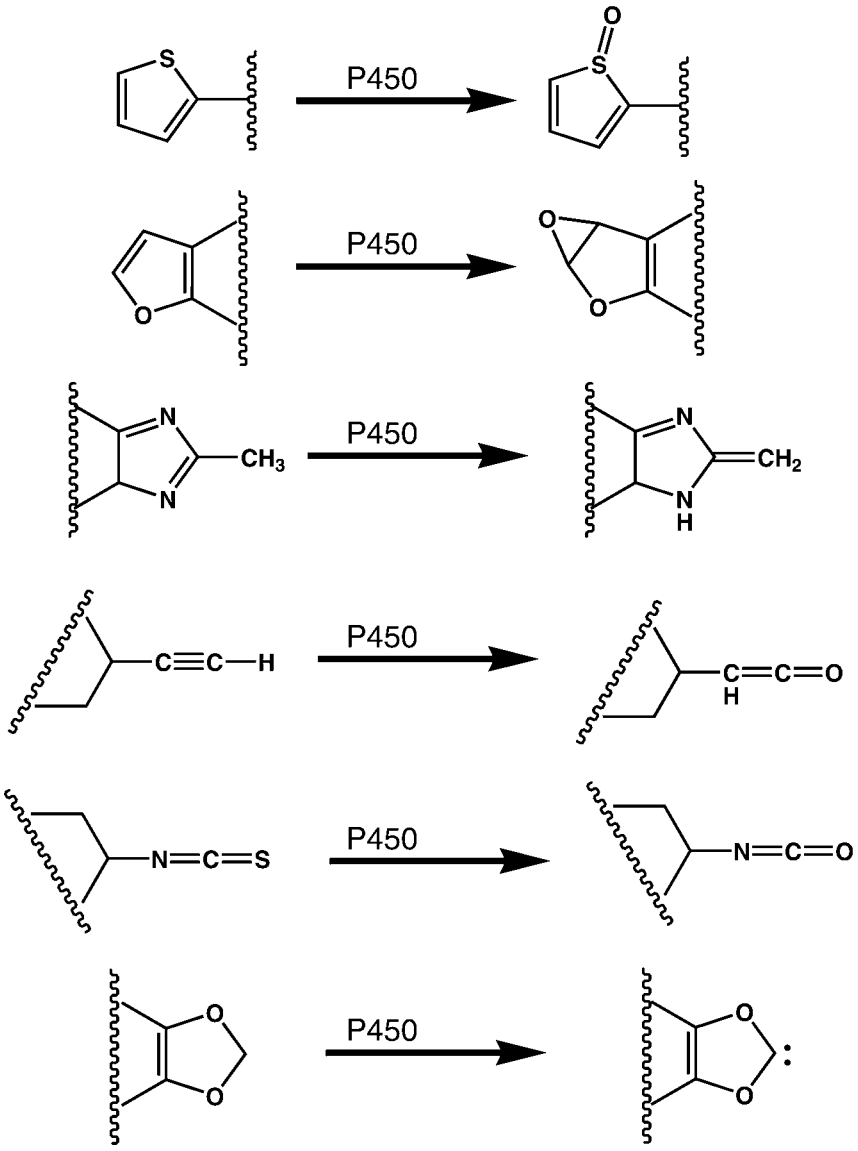

Figure 1 A listing of common P450 bioactivation reactions.

6. The inactivation should be irreversible, and activity should not return upon dialysis or gel filtration.
7. Following inactivation, it should be possible to demonstrate a 1:1 stoichiometry of inactivator to enzyme molecule inactivated.

Interestingly, while metabolic intermediates (MIs) associated with many P450 MBIs are quite reactive, the rate of P450 enzyme inactivation for many MBIs is quite slow. The apparent discrepancy between the robust chemical reactivity of the activated species and the rate of enzyme inactivation is a reflection of the multiple metabolic pathways typically associated with P450 substrates. For non-P450 MBIs, the mechanism of enzyme inactivation takes advantage of a highly ordered catalytic mechanism between

substrate and enzyme. As stated earlier, P450 enzymes have large active sites, which allow for multiple substrate orientations and thus are susceptible to multiple oxidative reactions (31). A second feature that adds to the complexity of understanding P450 mechanism-based inhibition is the fact that in some cases the underlying mechanism of enzyme inactivation for one P450 enzyme does not extrapolate to a different P450 enzyme. For instance, while there are only subtle sequence differences between P450 3A4 and P450 3A5 (e.g., these enzymes share >95% amino acid homology), there are profound differences in susceptibility to mechanism-based inhibition by raloxifene (32).

CHARACTERIZATION OF CYTOCHROME P450 MECHANISM-BASED INHIBITION

In general, there are three types of P450 enzyme mechanism-based inactivators, which can be refined into two classes: *irreversible MBIs,* inhibitors which, upon activation, bind covalently to the apoprotein or cause destruction of the prosthetic heme group; and *pseudo-irreversible MBIs,* inhibitors which, upon activation, coordinate with the heme iron.

Irreversible P450 Inactivation

As mentioned above, there are a handful of structural features that serve as latent chemical groups associated with enzyme activation; these include substituted imidazoles, furan rings, thiophenes, and acetylenes (Fig. 2). Below is a listing of the types of P450 mechanism-based inhibition and the chemistry associated with the latent chemical moieties, which lead to irreversible enzyme inactivation.

Substituted Imidazoles

Putative bioactivation of this latent group requires formation of an imidazomethide, as the electrophilic species (33). The mechanism(s) for the generation of this reactive species involves initial P450-mediated electron abstraction leading to the formation of a radical intermediate that can undergo oxygen rebound to form the hydroxyl metabolite. Alternatively, the radical may proceed through a second electron or hydrogen atom abstraction to form a reactive imidazomethide species, which can adduct to nucleophilic sites within the P450 enzyme-active site or react with water (34).

Furans

Furans are electron-rich aromatic groups that are readily oxidized by P450 enzymes to form electrophilic species, which have been linked to drug-related toxicities (35) as well as serve as MBIs (36). The current hypothesis regarding P450-mediated bioactivation of furan rings involves epoxide formation that could either be deactivated via hydrolysis to yield the diol (37) or react irreversibly with the P450 enzyme either through direct adduction of the epoxide or through an intramolecular rearrangement of the epoxide to form an α, β-unsaturated carbonyl, which serves as a Michael acceptor for protein adduction (38).

Thiophenes

Currently, the cytochrome P450 mediated bioactivation of thiophene-containing drugs is thought to proceed via two possible mechanisms. The first mechanism proceeds via P450

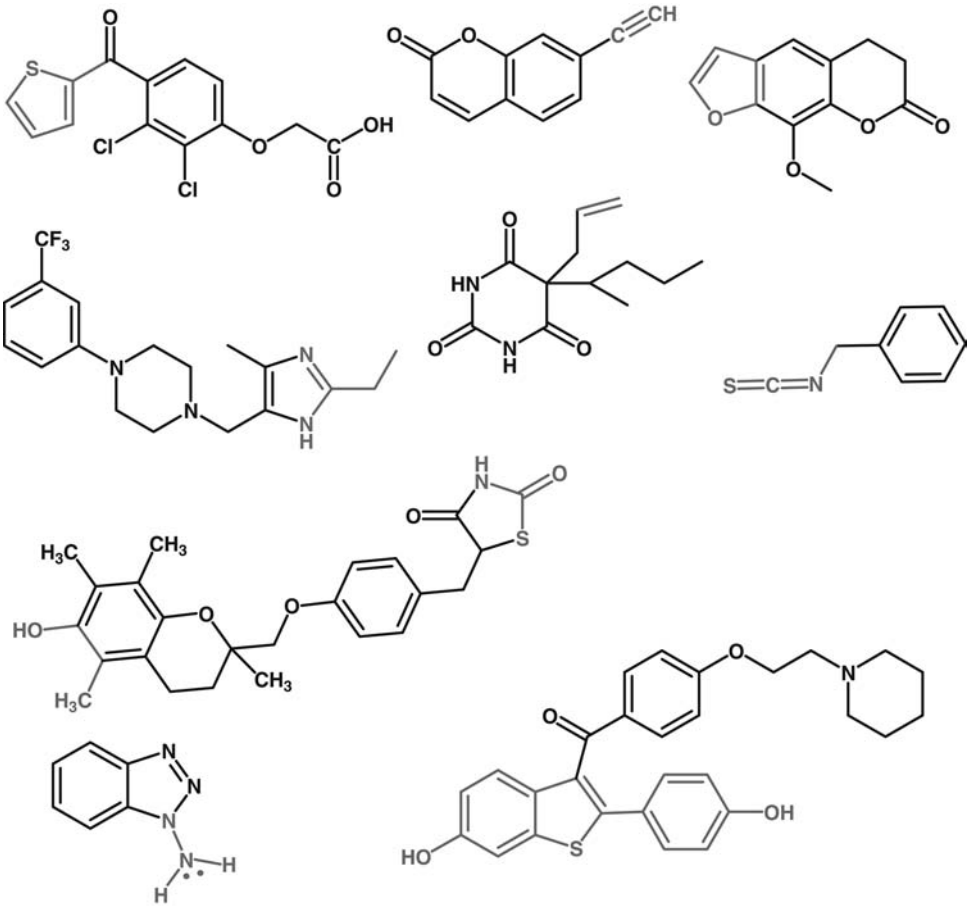

Figure 2 Known cytochrome P450 mechanism based inhibitors with highlighted latent chemistry groups.

oxidation of the thiophene sulfur atom leading to formation of a reactive thiophene-S-oxide intermediate. The thiophene-S-oxide is susceptible to a Michael-type addition with nucleophilic amino acids within the P450-active site (39). The second mechanism stems from a P450-mediated oxidation of the thiophene ring to form a reactive thiophene epoxide metabolite, which may react directly with the P450 enzyme (40). Alternatively, the epoxide in a mechanism analogous to furan bioactivation generates a cis-2-butene-1,4-dialdehyde reactive intermediate. In this instance, the thioketo-α,β-unsaturated aldehyde serves as the electrophilic intermediate that covalently binds to P450 enzyme (14).

Acetylenes

Many compounds containing an acetylenic group have been shown to be mechanism-based inactivators of P450 enzymes (41). For this functional moiety, two mechanisms for the inactivation of P450 have been described in detail (42). In this mechanism (Fig. 2), the transfer of the oxygen from the activated oxygen intermediate of the P450 to the terminal carbon of the acetylene results in an intermediate that is able to rearrange via a 1,2 shift of the terminal hydrogen to the vicinal carbon to generate a ketene. The reactive ketene species produced by this rearrangement can then be hydrolyzed to produce the carboxylic

acid product, or it can acylate nucleophilic residues within the P450-active site and inactivate the protein. Alternatively, the transfer of the oxygen from the P450-activated oxygen intermediate to the internal carbon of the acetylene would generate a reactive intermediate that leads to heme alkylation.

As discussed above, modification of the P450 apoprotein by reactive species typically involves covalent binding to an active-site nucleophilic amino acid residue such as lysine, serine, threonine, tyrosine, or cysteine (17,43,44). In contrast, the chemistry associated with modification of the heme moiety by a MBI is more complex. There are two potential mechanisms of cytochrome P450 self-inactivation during catalytic turnover that can be considered. The first is via the formation of active substrate intermediates that are capable of covalently modifying the heme. Direct heme adduction has been demonstrated for many compounds (45). For example, norethisterone, a steroid with an ethynyl substitution, diminishes the drug-metabolizing activity of the liver via a time- and dose-dependent inactivation of cytochrome P450 both in vitro and in vivo (46). For this type of inactivation, P450 heme loss occurs only in the presence of NADPH and oxygen and can be inhibited by carbon monoxide (47). Additional experimental evidence that implicates P450 oxidation as a requisite in heme destruction is the presence of a green-brown pigment (48).

The second mechanism is postulated to arise from the uncoupled cytochrome P450 catalyzed monooxygenase reactions. Specifically, the mechanism involves formation of hydrogen peroxide (H_2O_2) within the enzyme-active site, which interacts with the enzyme associated Fe^{2+}, thereby generating hydroxyl radicals that ultimately bleach the heme. This mechanism operates unlike enzymatic degradation, which specifically attacks the α-methene bridge, as reactive oxygen species are able to randomly attack all the carbon methene bridges of the tetrapyrrole rings, producing various pyrrole products in addition to releasing iron (49). For example, it was found that H_2O_2-mediated P450 self-inactivation during benzphetamine oxidation is accompanied by heme degradation (50). In this instance, the P450 heme modification involves heme release from the enzyme because of H_2O_2 formation within the P450 enzyme-active site via the peroxycomplex decay. The inactivation of cytochrome P450 by H_2O_2 is distinct from heme destruction via adduct formation as the destruction of heme does not mediate cytochrome P420 formation (51).

Characterization of Irreversible MBIs

Cytochrome P450 apoprotein adducts are characterized by the covalent labeling of a bioactivated drug reacting with a surrounding P450 active-site nucleophile. Typically, the drug-P450 adducts represent a mechanism of P450 inactivation and reduces the metabolic capacity of the adducted protein. When feasible, characterizing the chemical composition of the resultant adducts provides detailed information required to eliminate the structural motif responsible for inactivation from future chemical leads. Techniques that facilitate the speed and detail of the analysis of the chemical mechanism leading to adduct formation may readily reduce cost and time that it takes to develop novel therapeutics.

Radiolabel drug provides a quantitative tool to rapidly assess irreversible binding of protein and locate peptides that have radiolabel drug incorporated, and serves as a tool to determine binding stoichiometry (2). Covalent-binding assays often serve as a part of the final safety assessment for a lead compound prior to development (2,52,53). The strategies for covalent binding in drug discovery and the imposed limits will be reviewed in subsequent chapters. Irreversible covalent binding experiments do not distinguish adduction of the P450 versus other hepatic proteins, without further isolation of the

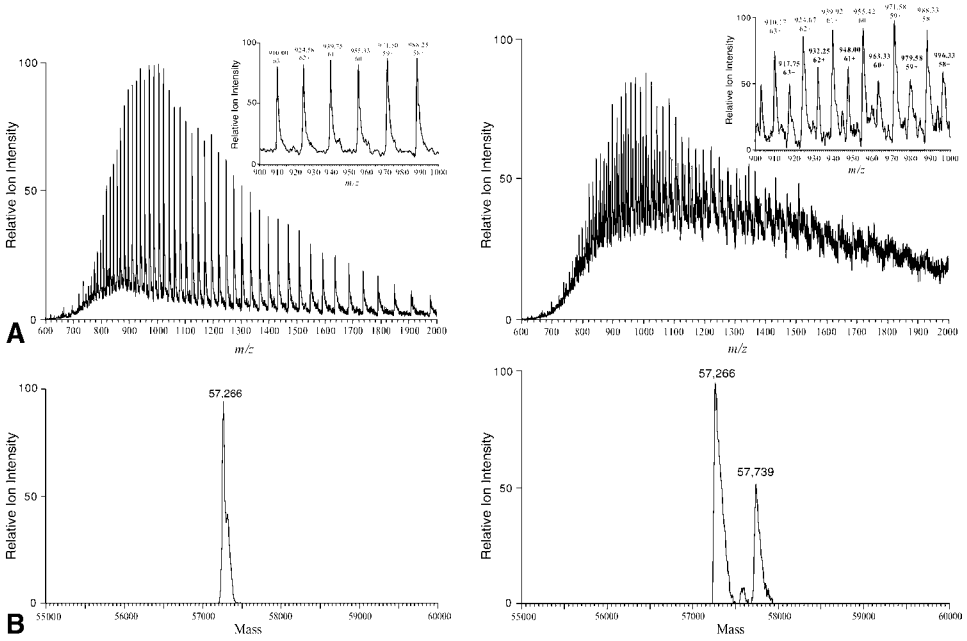

Figure 3 ESI MS spectrum of P450 3A4 (**A**) control incubation with NADPH and no raloxifene and (**B**) incubated in the presence of raloxifene. Deconvoluted mass is consistent with parent mass of raloxifene.

protein adduct sample from the in vitro incubation with additional techniques such as separation by HPLC-size exclusion chromatography or gel electrophoresis (41,54 56).

The use of mass spectrometry to elucidate P450-drug adducts is an attractive approach given its ability to yield molecular weight changes to the protein as a result of the drug adduct and simultaneously provides the adduct stoichiometry and proof of irreversibility of the drug-P450 complex (17,57,58). Adducts to several of the major hepatic P450s have been observed using intact protein mass spectrometry and will be briefly reviewed. Figure 3 illustrates an example of P450 3A4 incubated with the MBI raloxifene (17). The protein envelop of P450 3A4 dominates the chromatogram; however, at lower abundance, a new envelop representing a new protein entity is observed. The new species is right-shifted from the native protein envelop. Deconvulation of the protein envelope reveals two species present in the chromatogram. The smaller envelop corresponds to the 472-Da adducted P450 3A4 implicating the reactive diquinone methide of raloxifene as the reactive intermediate responsible P450 3A4 inactivation. Glutathione adducts of raloxifene include *m/z* of 779, 795 and 1050. Without protein mass spectrometry of the P450 3A4 adduct it would be impossible to know which reactive species inactivates P450 3A4. This information could be used to generate raloxifene analogs void of the capacity to form the diquinone methide, as was observed with the close analog arzoxifene (59).

Adducts with P450 3A4 and 3A5 have also been observed with 17α-ethynyl estradiol (EE). Using mass spectrometry which aided in the elucidated of the mechanism of MBI formation (60,61). With P450 3A5, the inactivation by EE was also dependent on the presence of cytochrome b5. This example also provides a unique case where inactivation was well characterized to implicate that the inactivation occurs through both heme and apoprotein adduction presumably through the formation of a 17α-oxirene-related reactive

metabolite that partitions the oxygen between the internal and terminal carbons of the ethynyl group dictating the mode of inactivation.

Tienilic acid is a MBI of P450 2C9 (39,62). When tienilic acid is incubated with P450 2C9, two tienilic acid adducts are observed (Fig. 4A), whereas in the presence of glutathione, the adduct formation is reduced to a 1:1 stoichiometry (Fig. 4B). This indicates that in addition to MBI, the reactive metabolite(s) from tienilic acid can adduct with an alternate amino acid of the enzyme that is not associated with MBI. The mass spectral chromatogram indicates the formation of both apo adducts arising from the oxidation of tienilic acid. Two mechanisms were proposed: (*i*) direct sulfur oxidation where, upon covalent adduction, the oxidation does not dehydrate and (*ii*) through a thiophene epoxide, which could undergo nucleophilic ring opening. Both mechanisms could result in the observed P450 2C9 adduct of tienilic acid shown in Figure 4. Interestingly, despite the direct evidence for apoprotein adduction, CO difference spectra indicate a loss of >60% of the P-450, which has been a technique used to implicate heme adducts by P450. This brings into question the use of CO binding as a diagnostic to differentiate heme adducts from apo adducts.

1-[(2-ethyl-4-methyl-1H-imidazol-5-yl)methyl]-4-[4-(trifluoromethyl)-2-pyridinyl] piperazine (EMTPP) was demonstrated to produce an adduct with P450 2D6 by mass spectrometry (34). The mass difference from the unlabeled P450 was 353 Da, consistent with addition of the parent compound (Fig. 5). Metabolism data from NMR and CID mass spectrometry complimented the protein adduct mass spectrometry data in showing that adduct formation potentially resulted from multiple oxidations of the drug to form a dehydrated methide of EMTPP, similar to that proposed for 3-methylindole (63). The EMTPP-P450 2D6 example illustrates the challenges with identifying the nature of MBI and the potential resolution limitations of intact protein mass spectrometry when trying to identify the molecular entity responsible for inactivation.

At present, most laboratory instruments cannot distinguish a difference of 2 Da for proteins >50 kDa (resolution = 100,000 Da). This becomes especially difficult with the increasing level of heterogeneity observed in P450 enzymes after in vitro incubations. This has been well documented by Bateman et al., who illustrated the effect of incubation time on the quality of the P450 3A4 protein envelope and the difficulty that arises with protein deconvolution from heterogeneous samples (57). Several factors can be employed to minimize sample degradation, including short incubation times, limiting oxygen to the incubation sample or using subsaturating amounts of NADPH, and through the addition of reactive oxygen scavenger to reduce protein oxidation (superoxide dismutase and catalase). The latter point, protein oxidation, highlights a potential pitfall of protein mass spectrometry for determining the MBI precursor because of the potential for misinterpretation of mass differences upon adduct formation. Despite the theoretical possibility, no examples of direct P450 oxidation have been described. Overall, the detection of intact P450-protein adducts has been met with variable success and, on the basis of the limited number of protein adducts identified to this point, may indicate a number of factors that contribute to the success of protein adduct detection, such as the composition of the chemical moiety undergoing bioactivation and the kinetics of its formation.

The resolution limitations of intact protein mass spectrometry can be circumvented by proteolytic digestion of the adducted protein (64,65). This added step has the potential to provide greater detail with respect to the structural composition of the protein adduct and the chemistry resulting in the irreversible binding of the drug to the protein. The adducted peptide is easily tracked through the numerous steps of isolation and purification by the use of radiolabel. Through CID spectral characterization, analytical digests of the protein adduct also provide an opportunity to unambiguously identify the adducted amino acid residue The ability to elucidate the covalently bound drug adducts of P450 enzymes

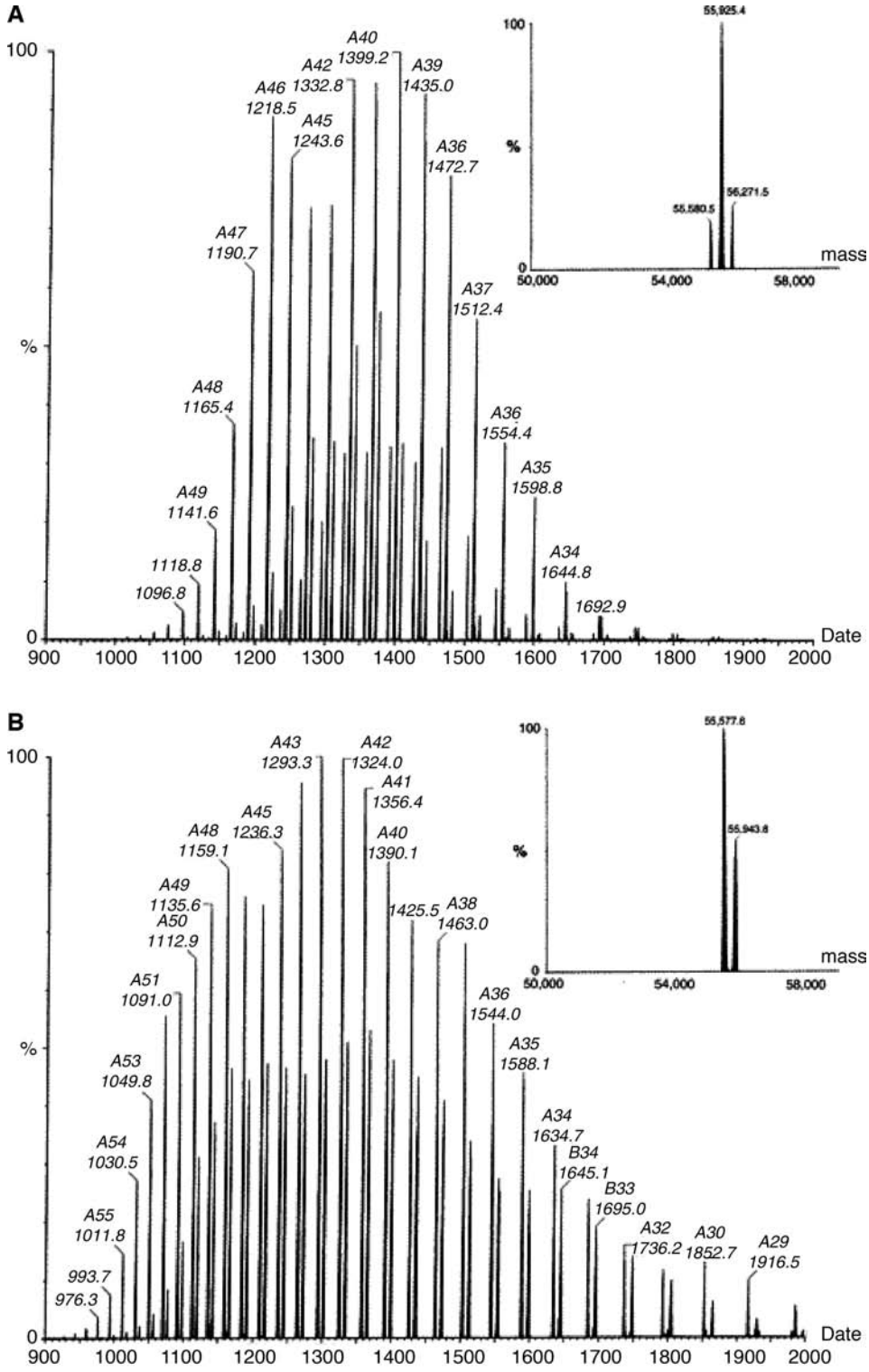

Figure 4 ESI MS spectrum of P450 2C9 (**A**) after incubation with NADPH and tienilic acid and (**B**) incubated with NADPH tienilic acid and glutathione. Deconvoluted mass is consistent with single oxidized product of tienilic acid responsible for adduct formation.

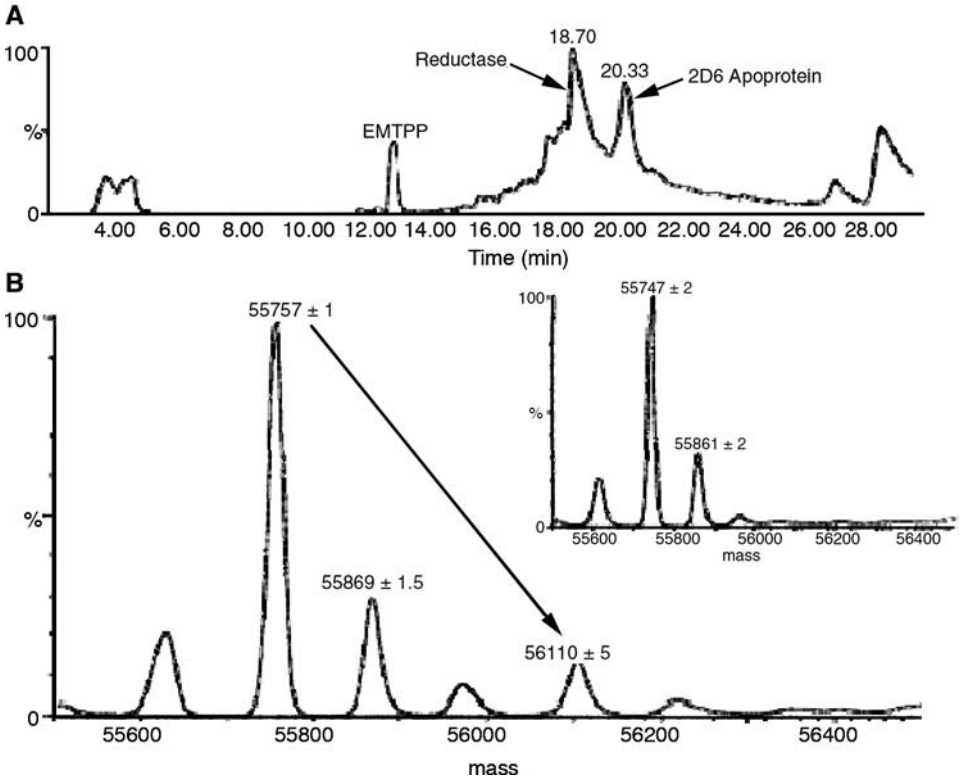

Figure 5 (**A**) Representative chromatogram illustrating separation of components (reductase and apoprotein) from an incubation containing recombinant P450 2D6. (**B**) Deconvoluted mass spectrum of EMTPP inactivated P450 2D6 illustrating an EMTPP adduct with a mass shift consistent with the mass of EMTPP. Inset shows the absence of this additional mass in control incubations (NADPH). *Abbreviation*: EMTPP, 1 [(2 ethyl 4 methyl 1H imidazol 5 yl)methyl] 4 [4 (trifluoromethyl) 2 pyridinyl]piperazine.

is filled with technical challenges stemming from the difficulty in isolating the membrane-associated enzymes themselves and from the innate difficulty in obtaining sufficient sequence coverage from the digests necessary to characterize the location and nature of MBI adduct (66). Cytochrome P450 2C9 adducts with tienilic acid were identified as mentioned above with intact protein mass spectrometry. Subsequent tryptic digests were used to identify the site of adduction but failed to yield the location of the drug adduct (67). The lack of adduct was attributed to the potential instability of the covalent linkage. This phenomenon is not specific to P450 2C9 and tienilic acid. For example, L-754,394 was found to be an MBI of P450 3A4 observable by intact protein mass spectrometry, but upon digestion, no adduct was identified (66).

The difficulty in observing direct structural information from peptide adducts has lead several investigators to probe various P450-active sites for nucleophilic residues susceptible to covalent adduction by electophilic species. Tools including photoaffinity labeling (68,69), alkylation with xenobiotic linked to biotin (70), and direct alkylation of purified P450 with reactive electrophiles like iodoacetamide (17) have been investigated. In combination with the nucleophilicity of active-site amino acid residues, these tools provide a focal point for locating drug-P450 adducts and may simplify data mining by narrowing in on specific "soft spots" of the P450, which favor adduction by MBI.

Photoaffinity labels have long been used to probe enzyme structure function of cytosolic and transmembrane proteins (71,72). The use of photoaffinity probes in P450 labeling has also been explored. Initial efforts were performed with 1-(4-azidophenyl) imidazole with soluble, bacterial P450cam (73). Recently, lapachenole was selected to investigate the alkylation of P450 3A4 (69). The photoactivation of lapachenole produced two distinct peptide adducts at Cys98 and Cys468. Cys98 is in close proximity to the B-B′ loop region, which is located near the substrate recognition site 1 (SRS-1) and is postulated to form part of the access channel to the heme iron (74). On the basis of the crystal structure, the second adducted species, Cys468, appears to be a solvent-accessible cysteine on the exterior of the protein and thus less informative with regard to prospective MBI adducts. The ability of these tools to locate reactive nucleophilic residues is well established and may be used to provide information regarding solvent-accessible nucleophiles in other P450 enzymes.

Alternatively, the use of biotin-linked electrophiles holds promise for use in identifying key enzyme electrophiles with the added benefit of having a selective isolation tool when combined with streptavidin for isolation. Proof of concept was explored by linking biotin with raloxifene and subsequently used to illustrate binding of the activated raloxifene moiety to Cys47 of GST P1-1 (70). When employed against a dexamethasone-treated preparation of rat liver microsomes, five adducts were identified, none of which, however, corresponded to P450. This capture and isolation technique illustrates how labeling of an MBI with biotin can be accomplished without inhibiting its bioactivation, and therefore, this technique could be amenable to isolating adducted P450 enzymes from catalytically active systems such as reconstituted enzymes or insect membrane preparations.

Direct alkylation with reactive electrophiles offers the simplest method in an attempt to locate solvent-accessible nucleophilic amino acid residues. A diverse set of electrophilic reagents can be utilized to label both the soft and hard protein nucleophiles. The use of maleimide as a soft electrophile to covalently label cysteines has long been used in protein biochemistry. With respect to P450 enzymes, maleimide has a detrimental effect on the integrity of the protein and results in inactive protein after labeling occurs (75). Iodoactemide (IA) derivatives are also commonly used and have a variety of chemistries linked to them including fluorescent tags, biotin for capturing, and spin-trapping reagents (www.invitrogen.com). Interestingly, in P450 3A4, the use of IA or PIA resulted in single stoichiometric reactions when run for one hour (76). Upon digestion with proteinase K, the alkylated residue was identified by LC-MS/MS as Cys239. Upon analysis of the crystal structure of P450 3A4 (www.rcsb.org, 1TQN.pdb), Cys239 resides between the G and G′ helices and may serve a perfect hook for electrophilic residues as they egress the active site of P450 3A4. Surprisingly, the label of P450 3A4 by photoaffinity label lapachenole and that of IA provide unique sites of reactivity. Further, investigation of the regioselectivity differences between these electrophilic agents may help to determine if the reactive metabolic species produce structural alteration of the enzyme leading to unique accessibility to the different protein nucleophiles or if the reactivities of Cys239 and Cys98 differ in their microenvironments (pKa) within the P450 such that their inherent nucleophilic properties differ substantially so as to favor unique electrophiles.

Detailed characterization of the amino acid residues involved in protein adduct formation requires protein digestion for analysis. The use of different digesting reagents can provide a unique series of fragments, which may help to visualize the adducted protein. Cyanogen bromide is a chemical agent used to digest proteins and produces large peptide fragments. Given the size of fragments generated, this agent typically works well when interfaced with a MALDI-TOF instrument, but is limited because of the lack of

MS/MS capabilities. Lysyl endopeptidase also generates rather large fragments as this protease cleaves at the c-terminus of lysine residues. Lysyl endopeptidase digestions are also very amenable to TOF technology given their large molecular weights and the generation of limited protein fragments of the protein to be searched. Trypsin digests are most commonly employed and serve to digest proteins at the c-terminus of lysine and arginine residues. The fragments produced from trypsin are very suitable for LC-MS/MS using a variety of mass spectrometry platforms largely because of their tendency to carry $[M+2H]^{+2}$ since the end caps are both capable of carrying a charge. Recently, proteinase K has been used to exploit its lack of discrimination in protein cleavage sites to generate small peptide fragments (17). When separating a proteinase K digested sample on a reverse phase column, the bulk of peptides elute quickly, with the more hydrophobic drug-based adduct retaining on the column, providing easy identification of the adducted peptide. This is not the case with larger peptides, where the physical properties of the drug have minimal impact on the chromatographic properties of the peptide adduct. In addition, the use of proteinase K should improve ionization efficiencies by reduced hydrophobic aggregation and less ion suppression from the reduced number of coeluting peptides. The tools described for identifying active-site nucleophiles provide a focal point for future studies aimed at locating drug-based peptide adducts and should ultimately lead to our improved ability to generate high-quality structural data in a more timely fashion.

Pseudo-Irreversible P450 Inactivation

These classes of MBI represent molecules that are transformed by P450 enzymes into MI products, which are able to coordinate with the heme iron. The interaction between MI product and heme iron is extremely strong, however, not covalent, as the MI/heme complex can be displaced under extreme experimental conditions (e.g., potassium ferricyanide), as a consequence, the inactivation is described as pseudo-irreversible.

Methylenedioxy Compounds

The effects of methylenedioxyphenyl (MDP) compounds on P450 may be traced back to early observations that sesame oil could synergize the effects of the insecticide pyrethrum. Early investigators noted that "the inhibition of biological oxidation of methyl parathion and of aldrin to dieldrin leads to the speculation that pyrethrin may also be detoxified by biological oxidations and that the synergism produced by pyrethrins and synergists may be due to the inhibition of such oxidation." This initial suggestion by Hodgson and Casida was followed by the observation that both piperonyl butoxide and sesamex inhibited the oxidation of N,N-dimethyl-p-nitro-phenyl carbamate and the corresponding diethyl compound in rat microsomes (77,78). MDP compounds are not only inhibitors of oxidation but they are also P450 substrates. Metabolism of piperonyl butoxide has been studied extensively and in vivo mouse studies have demonstrated that the methylene bridge carbon is metabolized to carbon dioxide (79,80). In vitro it has also been shown that the bridge carbon is metabolized to carbon monoxide and formate (81). Moreover, the cleavage of the methylenedioxy ring to yield catechol metabolites was also documented for 6-nitro-3,4-methlyenedioxybenzene (80) and 1,2,5,6-tetrachloro-3,4-methylenedioxy-benzene (82).

The contemporary view of MDP compounds is that the class is characterized by metabolism-dependent noncompetitive inhibition. Clearly, the extent of observed noncompetitive inhibition depends on the compound being metabolized, and so MDP compounds as a whole will contain examples of a variety of inhibition types. However,

early studies involving metabolism and inhibition of MDP compounds contained conflicting reports of both competitive and noncompetitive inhibition. In a review by Hodgson and Philpot, it was noted that in many of these studies, nicotinamide was added to in vitro incubations because it was thought to be a requirement for microsomal reactions (inhibition of pyridine nucleotidase) (81). Schenkman et al. reported that nicotinamide was not required and that, furthermore, it was an inhibitor of several oxidative reactions (83). Thus, the inclusion of nicotinamide in early experiments may have been a confounding influence on data interpretation. As an alternative explanation, Franklin showed that when piperonyl butoxide was incubated with microsomes (plus NADPH), the inhibition of N-demethylation of ethylmorphine was at first competitive but then was noncompetitive after the formation of an observable complex. The complex that was formed is now known as a MI complex. This complex has been shown to be formed in a manner that is dependent on time, NADPH, and oxygen, consistent with the requirement of cytochrome P450 oxidation to uncover the latent ability of MDP compounds to complex with the heme (84).

The method used to detect MI complex formation is difference spectroscopy and the Soret region of absorbance (blue wavelength) is the region of interest. When the iron of P450 is in the reduced state (ferrous), these complexes show absorbance maxima similar to those of well-documented ligands such as carbon monoxide (450 nm) and ethylisocyanate (455 nm) (85,86). MI complexes from a number of MDP compounds are characterized by an absorbance maximum at both 455 nm and 427 nm (84). The intensity of these peaks depends on both pH and the substrate involved. In the ferric state, the absorbance maximum is found at a single absorption spectrum of 437 to 438 nm (84,85). It is an interesting observation that when an MDP compound is administered in vivo, the resulting in vitro ferrous spectra are often not observed until after the addition of a reducing agent such as dithionate. Not only can reducing agents help visualize the complex, but the 455-nm absorbance is resistant to oxidative agents such as potassium ferricyanide. When added, potassium ferricyanide will diminish the 455-nm absorbance, but subsequent addition of dithionite will regenerate the peak (87). It is also worth noting that the ferric state is less stable, and some ligands can be displaced by incubation with lipophilic compounds, with the subsequent regeneration of P450 activity (41). In contrast, the ferrous state is unaffected by such incubations, but it can be dissociated by irradiation at 400 to 500 nm as shown by Ullrich and Schnabel (42).

In early studies, the nature of the mechanism leading to MI complex formation was the subject of much speculation. Several mechanisms were proposed, which involved either carbocation (88), free radical, (42) or carbanion intermediates. Using fluorine as a model, Ullrich and Schnabel produced a convincing argument for the binding of carbanions to P450 (42). In this instance, the authors noted that when fluorine was added to NADPH-supplemented microsomes from phenobarbitol-treated rats, a difference spectrum was produced with an absorbance at 446 nm. It was then observed that neither anaerobic conditions nor the addition of NADH under aerobic conditions could reproduce the absorbance at 446 nm. This suggested to the investigators that a mono-oxidation product of fluorine was responsible for complex formation, although incubating known oxidative metabolites with microsomes could not reproduce the effect (fluorenol and fluorenonone). In addition, the incubation time used in this experiment was very short, only 10 to 20 seconds, so it was not likely that enough time had passed for the accumulation of significant amounts of oxidation products to potentially complex with the enzyme.

Fluorine is a very simple structure, and the methylene bridge is the most likely moiety to form a reactive species. Moreover, one chemical feature of this group is the

acidity of its hydrogens (pKa value of 22 in aprotic solutions) (42). Ullrich and Schnabel noted that the dissociation of this proton yielded a species with increased resonance and it had an absorption maximum at 373 nm (42). When they examined the difference spectra of a reduced microsomal suspension after incubation of fluorene with NADPH, a peak at 374 nm was observed, which they postulated was due to a species similar to the fluorine anion. The free electron pair of the fluorine could potentially interact with the ferrous iron in the same way as carbon monoxide or ethylisocyanide. Thus, in principle, the binding of fluorene or MDP compounds would be similar to carbon monoxide, and consequently, one might expect that a photodissociation of the complex with light could be achieved. As noted above, these investigators were able to partially decrease the inhibition of ethylmorphine demethylation caused by piperonyl butoxide by irradiation with high-intensity light between 400 and 500 nm. This experiment provided evidence for the ligand binding nature of piperonyl butoxide. The only questions remaining were what "mono-oxidation" product of fluorene (or piperonyl butoxide) was involved and how that gave rise to MI complex formation.

Although the evidence for a carbanion presented by Ullrich and Schnabel is compelling, the exact mechanism by which cytochrome P450 would produce this species is not clear. An additional mechanism proposed by Ullrich and Schnabel showed that a carbene could be produced from MDP compounds by hydroxylation of the methylene bridge followed by elimination of water (Fig. 6) (89). Like the carbanion proposed above, the carbene would also have free electrons available for coordination to the heme. The

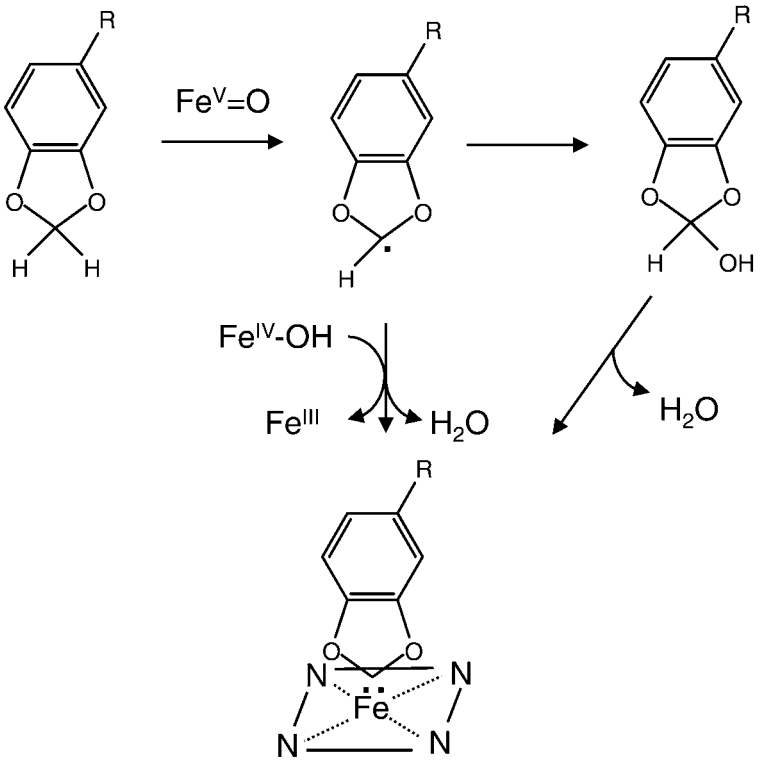

Figure 6 Proposed mechanism for the formation of an metabolic intermediate complex from the metabolism of methylenedioxy compounds.

metabolism of the methylene bridge to form a carbene is most consistent with the data reported in the literature. For example, it has been shown that when the methylene group hydrogens are substituted with methyl groups, there is an almost complete loss in P450-complex formation (82). In addition, a deuterium isotope effect of similar magnitude has been reported for both the formation rate of carbon monoxide in vitro and attenuation of in vivo insecticide effects (90). These observations coupled with the fact that MDP compounds labeled with isotopes have shown that carbon monoxide derives directly from the methylene carbon indicates that the reaction appears to involve the cleavage of the C-H bond with the subsequent formation of a species that can then complex with cytochrome P450, or the form of a variety of oxidative metabolites.

In Figure 6, two pathways are shown that could result in carbene formation. In the first pathway (path A), initial hydrogen abstraction leaves a carbon-centered radical on the methylene bridge, which (without oxygen rebound), if oxidized further, will yield a cationic species that can then deprotenate to form a carbene. The second pathway involves the elimination of water after hydroxylation of the methylene bridge, which could then directly form a carbene (path B). However, it is likely that the elimination of water in this mechanism is more complex and may involve cationic intermediates such as an oxonium ion, which, upon further deprotenation, could yield a carbene (91). As an example of how metabolites could arise from this mechanism, one possibility is the rearrangement of the methylenic hydroxyl-MDP intermediate to 2-hydroxyphenylformate and hydrolysis to the subsequent catechol and carbon monoxide or formate metabolites (92).

Amine Compounds

In the 1950s, a number of reports were published that showed that a new compound, diehtylamonoethyl-2,2,-diphenylvalerate HCl (SKF 525-A), potentiated the pharmacology of drugs such as methodone and morphine (93), some hypnotic drugs, (94) and nervous system stimulants such as amphetamine (95). Like the observation of Hodgson and Casida regarding MDP compounds and their mode of action on insecticides, the potentiating effect of SKF 525-A was reported to result from decreased biotransformation of these drugs and therefore decreased clearance (96,97). Castro and Sasame observed that irreversible inhibition of drug metabolism occurred when microsomes were preincubated in vitro with (*i*) NADPH, (*ii*) SKF 525-A, and (*iii*) oxygen (98). Further studies with this compound and others showed not only that MDP compounds could form an observable MI complex but also that SKF 525-A (99) and benzphetamine (100) could yield absorption bands in the 455-nm region. One moiety that was common to many of these compounds including SKF 525-A was a substituted amine. It is now generally understood that substituted amines must first be dealkylated to primary amines before heme coordination can take place (Fig. 7A). It was also found that an MI complex could be formed from hyroxylamines or by reduction of some nitroalkanes (101). These observations suggested that a species intermediate to a hydroxylamine and the nitro-oxidation state was involved in P450 complex formation. Consequently, it was proposed and widely accepted that a nitrosoalkane was the iron ligand producing the 455 nm absorbing complex (Fig. 7A). In iron-porphyrin model studies, a crystal structure between a nitroso ligand in a tetraphenylporphyrin-iron complex showed that the nitroso ligand was bound to the iron by its nitrogen atom and that the resulting bond was very stable (e.g., could not be displaced by strong ligands such as carbon monoxide) (102).

In general, MI complexes derived from amines differ from those formed from MDP compounds. The wavelength that characterizes the absorbance maxima for amine complexes is in a wider range than that observed for MDP compounds (446 455 nm). One

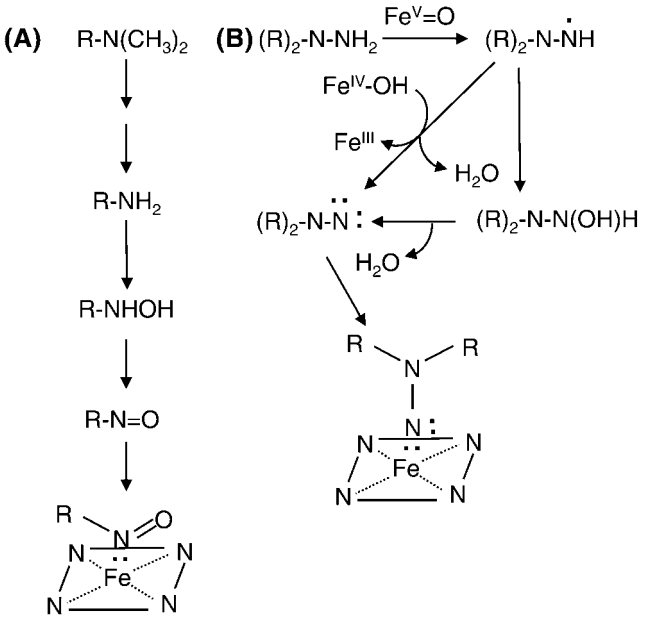

Figure 7 Proposed pathways for formation of metabolic intermediate complexes from oxidation of (**A**) amines and (**B**) hydrazines.

of the primary differences between MDP-P450 complexes and amine-P450 complexes is their instability in the ferric state. When potassium ferricyanide is added to an in vitro incubation, the ferrous 455-nm peak of the nitroso complex is diminished presumably as the complex is shifted to the ferric state. However, the 455-nm peak cannot be regenerated by the addition of dithionite, as can be observed with MDP complexes (99). It is also worth noting that some complexes are unstable in the presence of dithionite and it appears that many aryl amines yield complexes that are characterized by this instability (103). Finally, in contrast to MDP compounds, when amine-containing compounds form complexes in vivo, they are immediately observed in the resulting microsomes without the addition of dithionite (99), thus showing that in vivo nitroso complexes stabilize P450 in the ferrous state.

Hydrazines

The incubation of microsomes with 1,1-disubstituted hydrazines in the presence of NADPH and oxygen reveals a spectral complex that can be observed in the Soret region with a maximum at 438 nm and a minimum at 414 nm (ferric state). Under anaerobic conditions, the minimum shifts to 407 nm and the maxima shifts to 449 nm (ferrous state). It has also been shown that to produce an observable complex, hydrazines should be 1, 1-disubstituted and cannot be monosubstituted or 1,2-disubstituted (104). An exception to this rule is some acyl hydrazines such as isoniazid (INH). INH was introduced as a drug in the 1950s and has been reported to decrease the clearance of several other drugs including phenytoin (105). When INH is incubated with microsomes, NADPH, and oxygen, a complex is formed that has an absorption maximum at 449 nm (ferrous state) (106). This result is in contrast with the 1,1-disubstituted hydrazine spectrum that is visualized in the

ferric state. In addition, when potassium ferricyanide is added, the complex dissociates, thus demonstrating that the INH complex is stable only in the ferrous form, similar to the nitroso complexes discussed *vida supra* (107).

It has been proposed that INH and 1,1-disubstituted hydrazines can be metabolized to a nitrene, which can then coordinate with cytochrome P450 both in vivo and in vitro (Fig. 7B) (104). Studies with porphyrin systems indicate that the nitrene formed coordinates with the iron via the terminal nitrogen (104,106). It is likely that both acyl hydrazines and 1,1-disubstituted hydrazines are oxidized in a stepwise fashion by cytochrome P450 to produce an aminonitrene-iron complex as shown in Figure 7B.

KINETICS OF CYTOCHROME P450 MECHANISM-BASED INHIBITION

The structural and functional characterization to this point has been focused on the structural identification and characterization employed to develop the most appropriate clinical candidate. If MBI persists in the lead candidate, the potential impact on the exposure of other medications is required to clearly define the clinical limitations of the therapeutic agent including defining drugs susceptible to drug interaction upon coadministration of the MBI, defining at-risk patient population (e.g., age or pharmacogenetics), and the duration of treatment (acute or chronic) to properly context all the potential safety concerns. This requires the combination of much of the data already accumulated including the K_I and k_{inact}, with the endogenous enzyme degradation rate to describe the extent of drug interaction that could result on the basis of irreversible inhibition kinetics. Additional information regarding the expected metabolism and disposition of the substrate responsible for producing irreversible inhibitor will typically serve to increase the predictive power of the estimated changes expected in AUC and includes an understanding of the overall metabolic pathway, potential for gut metabolism, and the existence of multiple inactivation pathways including those produced from metabolites may also be incorporated in an attempt to refine in vivo extrapolations. Furthermore, when possible, the fraction of total hepatic metabolism due to the affected P450 should be considered for improved predictability of the magnitude of the drug interaction (108).

When a cytochrome P450 enzyme converts a nonreactive molecule into a species that is reactive, there are several general outcomes. The reactive species can be released as some form of product (where it can potentially react with water), or it can react with the P450 apoprotein structure or the active-site heme moiety.

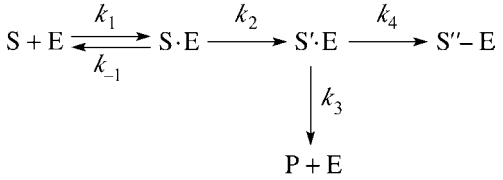

The above scheme illustrates the possible outcomes by depicting two separate pathways described by the rate constants k_4 and k_3. Subsequent to the formation of a reactive species (S′-E), the substrate is shown forming product (P) or reacting with the enzyme (S″-E). These two pathways and associated rate constants are the basis for an important descriptive parameter in mechanism-based inactivation the partition ratio. This term was introduced by Walsh in an effort to describe the number of inactivator

molecules released as product versus those that reacted with the enzyme to form an inactivated complex (109). It is apparent that very efficient enzyme inactivators would lead to very little product formation and greater enzyme inactivation, and the converse would be true for inefficient inactivation. Therefore, efficient enzyme inactivation would be described by a low partition ratio (k_3/k_4). The most efficient inactivation would produce no product and only inactivated enzyme and thus be characterized by a partition ratio of zero. No molecules have been described to inactivate P450 with a partition ratio of 0, however, a Merck compound L-754,394 has been reported to have a partition ratio for P450 3A4 of approximately 1.34 (110).

Another important parameter is k_{inact}, which is the rate of inactivation. If one examines scheme 1, it is tempting to conclude that k_{inact} and k_2 are the same. However, this is not the case. The term k_{inact} is more complex and is comprised of rate constants k_2, k_3, and k_4, and only under specific conditions (i.e., $k_2 \ll k_4$, k_3 is very slow or equal to zero), $k_{inact} = k_2$ (110). Early work of Kitz and Wilson and subsequent derivations of Jung and Metcalf provide the following expression, which relates active enzyme concentration to k_{inact}.

$$\frac{d[\mathrm{E}]_t}{dt} = \frac{-k_{inact}[\mathrm{I}]}{K_\mathrm{I} + [\mathrm{I}]}[\mathrm{E}]_t \qquad \text{(Eq. 1)}$$

where $[\mathrm{E}]_t$ is the concentration of active enzyme at time t, K_I is the concentration of inhibitor at which half-maximal inactivation occurs, and I is the concentration of inhibitor (111,112). Experimentally, k_{inact} and K_I are most often determined from a dilution assay where aliquots of enzyme incubated with inhibitor in a primary incubation are then transferred at different time intervals to a secondary incubation that contains a reporter substrate (i.e., testosterone for P450 3A4). To reflect this type of experiment, the relationship in eq. 1 can be integrated.

$$\frac{[\mathrm{E}]}{[\mathrm{E}]_{total}} = e^{\frac{k_{inact}[\mathrm{I}]t}{K_\mathrm{I}+[\mathrm{I}]}} \qquad \text{(Eq. 2)}$$

or

$$\ln\frac{[\mathrm{E}]}{[\mathrm{E}]_{total}} = \frac{-k_{inact}[\mathrm{I}]t}{K_\mathrm{I} + [\mathrm{I}]} \qquad \text{(Eq. 3)}$$

In the experiment described above, the aliquots from a primary incubation are taken at various time points, and the amount of enzyme activity remaining (e.g., fractional activity) is reported in the secondary incubation by a reporter substrate. This data is then plotted on a semilogarithmic plot as the natural log of fractional activity versus time (Fig. 8). When the reporter substrate is at a concentration of approximately 5 $\times$ its k_m value, then the velocity of product formation is approximated by

$$Vel \approx V_{max}$$

or

$$Vel \approx [\mathrm{E}]k_{cat}$$

Therefore, under these conditions, the velocity of product formation is proportional to the enzyme concentration, and the natural log of fractional activity is essentially given by eq. 3. The slope of this data is then given by

$$\frac{-k_{inact}[\mathrm{I}]}{K_\mathrm{I} + [\mathrm{I}]} \qquad \text{(Eq. 4)}$$

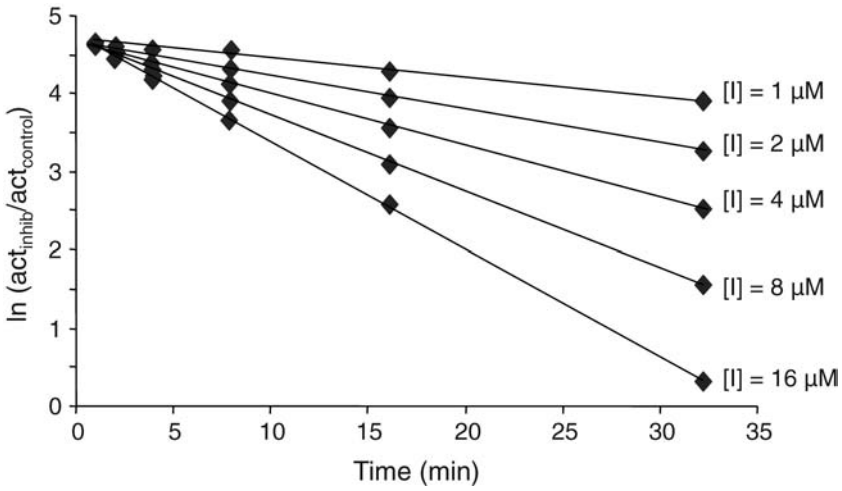

Figure 8 Slopes of the natural log of fractional activity yield k_{obs} values for varying concentrations of inhibitor.

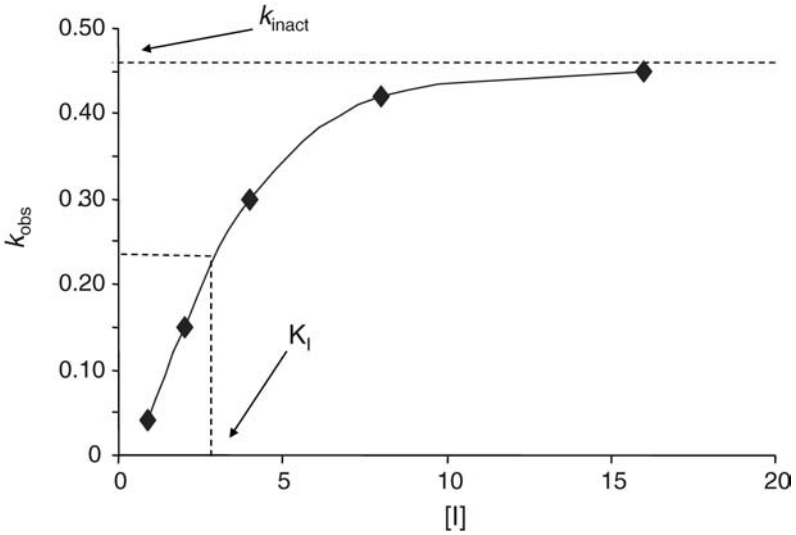

Figure 9 Determination of k_{inact} and K_I from a plot of k_{obs} versus inhibitor concentration.

This is a hyperbolic relationship similar to the familiar Michaelis-Menten kinetics where the "velocity" of inactivation or k_{obs} is equal to

$$k_{obs} = \frac{k_{inact}[I]}{K_I + [I]} \quad \text{(Eq. 5)}$$

Therefore, when the absolute value of the slopes from the experimental data shown in Figure 8 are plotted versus inhibitor concentration, the resulting graph should obey a hyperbolic relationship as shown in Figure 9. As such, this data is akin to Michaelis-Menten kinetics, and the resulting parameters (K_I and k_{inact}) may be determined in a manner that is analogous to the parameter determination for standard hyperbolic enzyme kinetics. Before the advent of computers, this was most easily achieved through linear transformation, but

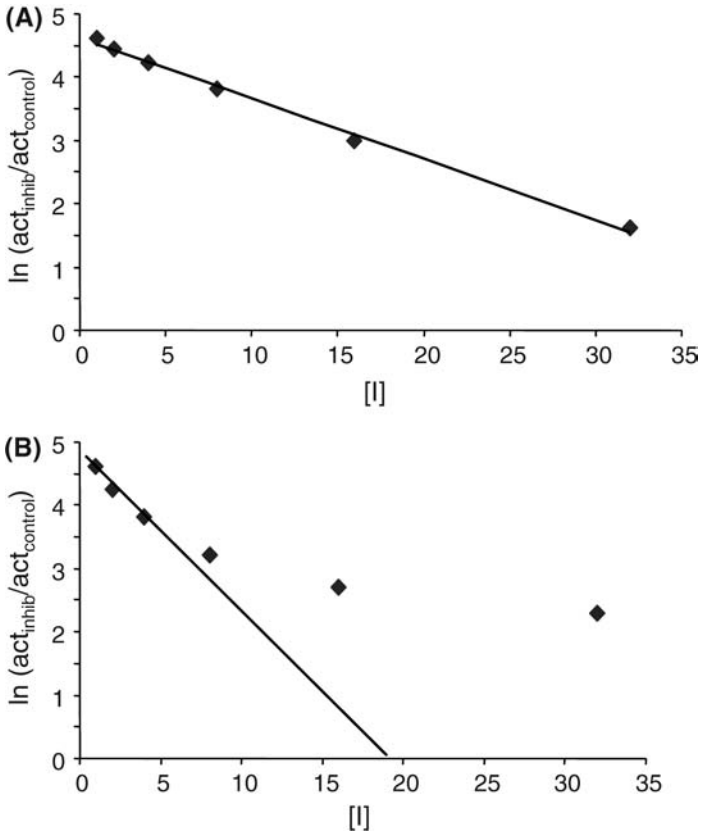

Figure 10 Determining kobs where (**A**) inactivation is linear with time and (**B**) inactivation is non linear with time possibly due to significant inhibitor depletion.

today the slope data from eq. 3 (or slopes of the experimental data in Fig. 9) can be fitted to a hyperbolic curve by any number of commercially available programs, and the values of K_I and k_{inact} can be readily determined.

Examination of eq. 3 suggests that the rate of inactivation for a given inhibitor concentration should be linear with time (Fig. 10A). However, this may not be the case, and it is often observed that the data becomes nonlinear with time (Fig. 10B). One explanation for this nonlinearity is that significant inhibitor depletion may have occurred in the primary incubation prior to dilution into the secondary-reporter assay. It is apparent from examination of the relationship in eq. 3 that no change in the inhibitor concentration is assumed. Therefore, assay conditions that minimize inhibitor depletion should be used. These conditions can include shorter assay time or a reduction in the temperature of the assay to slow down inhibitor metabolism (58).

As an alternative, it may also be possible that several mechanisms of inactivation are occurring simultaneously and that the passage of time serves to unmask the slower rate of inactivation. The result would be apparent nonlinearity in the data similar to inhibitor depletion. In such cases of nonlinearity, it is the best practice to take the slope of early time points to determine parameters such as K_I and k_{inact} (Fig. 10B).

Experimentally, determination of the partition ratio can be accomplished in two ways. The first method is by titration; the use of this method involves increasing amounts of inhibitor that is added to a known, fixed amount of enzyme, and the reaction is allowed

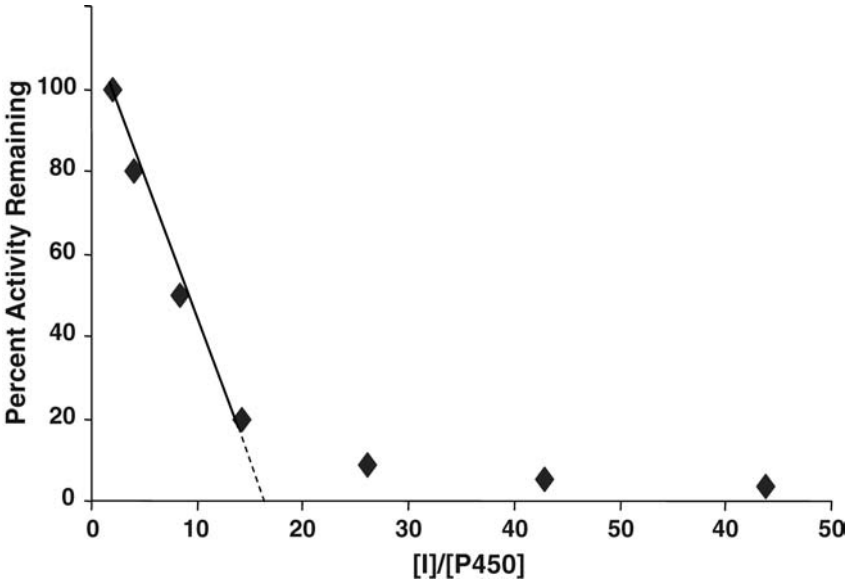

Figure 11 Estimation of the partition ratio.

to go to completion (50). The enzyme is then dialyzed, or diluted sufficiently in a secondary reaction with a reporter substrate, and a plot is constructed of remaining enzyme activity versus moles of inhibitor divided by moles of enzyme (see Fig. 11). Theoretically, this plot should yield a straight line. However, in practice, this does not often occur, and the data must be extrapolated to the x-axis, which gives the ratio of inhibitor to enzyme needed for complete inactivation of enzyme activity. When extrapolation to the x-axis is performed, the intersection of the line and the axis yields the turnover number. It is important to note that this number or ratio includes the amount of inhibitor required to inactivate the enzyme, and if one assumes a 1:1 stoichiometry, then the partition ratio is the turnover number minus one.

A second and more direct method involves determination of the molar amount of products formed from reaction of the inhibitor with P450 and an assessment of the amount of P450 enzyme inactivated. This may be accomplished in several ways. In microsomes a high concentration of inhibitor can be used along with an appropriate incubation period to insure complete inactivation of the enzyme. The resulting decrease in the carbon monoxide binding spectrum can be used to quantitate the amount of enzyme inactivated. Once this value is established, a separate incubation containing enzyme and inhibitor is assayed with the dilution method, and this can be used to estimate the molar amount of enzyme inactivated. In the same incubation, product formation of the reaction is then measured (or inhibitor depletion is measured), and the ratio of product formed versus enzyme inactivated directly yields the partition ratio. Alternatively, the experiment can be performed with expressed enzyme, which has the advantage of containing only one P450, and in this case, the confounding influences of other P450 enzymes on carbon monoxide binding and inhibitor metabolism are not present. These methods were used by Kunze and Trager to estimate the partition ratio of furafylline for P450 1A2 inactivation (33). The obvious drawback to this approach is that it is necessary to have a method to quantitate all of the products formed (radio label or synthetic standards). Therefore, in the absence of a radiolabel or metabolite standard(s), the titration method is often used to estimate the partition ratio.

PREDICTING IN VIVO CYTOCHROME P450 MECHANISM-BASED INHIBITION

The accurate in vivo extrapolation of irreversible (MBI) inhibition based on in vitro DDI data requires two key elements; the ability to differentiate reversible from irreversible inhibition (MBI) and, thereafter, to correctly express the impact of the irreversible mechanisms in vivo. In practice, MBI is the result of a chemical transformation of an inhibitor to an intermediate that irreversibly binds to and inactivates the P450 prior to exiting the active site (113). The impact of this mechanism is distinct from competitive inhibition. Foremost, when a competitive inhibitor is eliminated, the potential for a drug interaction is gone, whereas for MBI, the potential persists well after the compound has been eliminated (114). This relates to the second difference, which is that the MBI perturbs the steady-state levels of the P450 it inactivates and levels recover only with the natural synthesis rate within the organism (115). Numerous mechanistic models have been developed to describe this relationship (116 118).

The synergy between *in silico* and experimental data is enabled by the ability to approximate the expected clinical impact on AUC on the basis of in vitro DDI data (119). The most visible program Simcyp has gained popularity amongst pharmaceutical companies and the FDA (www.simcyp.com). The underlying drug interaction predictions are based on the equations described by Brown et al. (120,121). The in vivo extrapolations can be determined from a variety of in vitro systems including human liver microsomes (HLMs), hepatocytes, or recombinant P450 (rP450). The relative activities of the latter system often vary kinetically from HLM and hepatocytes and, therefore, need to be corrected with the use of scaling factors. The intersystem extrapolation factor (ISEF) is used to normalize in vitro data generated from rP450s (122). Simcyp also has the unique ability to represent the patient-variable response to drugs in clinical trials by using Monte Carlo simulations to vary patient demographics, genetics, and physiology to introduce "typical" population variance (123). Within Simcyp, inhibition and induction parameters can be included with the intrinsic clearance for a given compound to predict its in vivo exposure. One area of interest regarding the predictive capacity of Simcyp is the consistent overprediction of the Rss (AUC change due to the addition of inhibitor) for inhibitors that proceed through mechanism-based inhibition. This overprediction could be due to variability in the k_{degrad} rate constants reported for various P450 isoforms. Most commonly, the data from in vitro human hepatocytes as well as the data generated from rats in vivo are used despite their disparate half-lives, 14 to 44 hours, respectively. Experimental evidence suggests the homeostasis of a hepatocyte is disrupted precluding the accurate half-life determination of P450 enzymes within in vitro experiments (115), while the rat determined values clearly have limited human physiological relevance. Despite the k_{degrad} being an attractive target for potential error in Rss estimates, it must be tempered with the potential error associated with the additional in vitro measurements that are used in predicting the in vivo clearance, and thus, any combination of inaccurate in vitro data could skew the Rss predictions. As computational tools like Simcyp become more commonly used for predicting DDI, the predictive limitations will be more readily identified, leading to improved strategies for in vitro to in vivo predictions of drug pharmacokinetics and possible MBI-based DDIs.

CONCLUSION

Mechanism-based inhibition of cytochrome P450 enzyme activity is an important factor in clinically relevant DDIs. Over the past 30 years, our knowledge of the structure and associated chemistry of P450 mechanism-based inhibition has increased immensely. Our

ability to elucidate the nature of MBI and potentially avoid key structural drug features in drug candidate selection. Moreover, the magnitude of P450 MBI is now predictable in a manner that patient risk for serious DDIs is minimized.

REFERENCES

1. Wienkers LC, Heath TG. Predicting in vivo drug interactions from in vitro drug discovery data. Nat Rev Drug Discov 2005; 4:825 833.
2. Evans DC, Watt AP, Nicoll Griffith DA, Baillie TA. Drug protein adducts: an industry perspective on minimizing the potential for drug bioactivation in drug discovery and development. Chem Res Toxicol 2004; 17:3 16.
3. Kent UM, Juschyshyn MI, Hollenberg PF. Mechanism based inactivators as probes of cytochrome P450 structure and function. Curr Drug Metab 2001; 2:215 243.
4. Kalgutkar AS, Obach RS, Maurer TS. Mechanism based inactivation of cytochrome P450 enzymes: chemical mechanisms, structure activity relationships and relationship to clinical drug drug interactions and idiosyncratic adverse drug reactions. Curr Drug Metab 2007; 8:407 447.
5. Polasek TM, Elliot DJ, Lewis BC, Miners JO. Mechanism based inactivation of human cytochrome P4502C8 by drugs in vitro. J Pharmacol Exp Ther 2004; 311:996 1007.
6. Ito K, Ogihara K, Kanamitsu S, Itoh T. Prediction of the in vivo interaction between midazolam and macrolides based on in vitro studies using human liver microsomes. Drug Metab Dispos 2003; 31:945 954.
7. Yamazaki H, Shimada T. Comparative studies of in vitro inhibition of cytochrome P450 3A4 dependent testosterone 6beta hydroxylation by roxithromycin and its metabolites, troleando mycin, and erythromycin. Drug Metab Dispos 1998; 26:1053 1057.
8. Murray M, Murray K. Mechanism based inhibition of CYP activities in rat liver by fluoxetine and structurally similar alkylamines. Xenobiotica 2003; 33:973 987.
9. Hara Y, Nakajima M, Miyamoto KI, Yokoi T. Inhibitory effects of psychotropic drugs on mexiletine metabolism in human liver microsomes: prediction of in vivo drug interactions. Xenobiotica 2005; 35:549 560.
10. von Moltke LL, Durol AL, Duan SX, Greenblatt DJ. Potent mechanism based inhibition of human CYP3A in vitro by amprenavir and ritonavir: comparison with ketoconazole. Eur J Clin Pharmacol 2000; 56:259 261.
11. Voorman RL, Maio SM, Payne NA, Zhao Z, Koeplinger KA, Wang X. Microsomal metabolism of delavirdine: evidence for mechanism based inactivation of human cytochrome P450 3A. J Pharmacol Exp Ther 1998; 287:381 388.
12. Jones DR, Gorski JC, Hamman MA, Mayhew BS, Rider S, Hall SD. Diltiazem inhibition of cytochrome P 450 3A activity is due to metabolite intermediate complex formation. J Pharmacol Exp Ther 1999; 290:1116 1125.
13. Wang YH, Jones DR, Hall SD. Differential mechanism based inhibition of CYP3A4 and CYP3A5 by verapamil. Drug Metab Dispos 2005; 33:664 671.
14. O'Donnell JP, Dalvie DK, Kalgutkar AS, Obach RS. Mechanism based inactivation of human recombinant P450 2C9 by the nonsteroidal anti inflammatory drug suprofen. Drug Metab Dispos 2003; 31:1369 1377.
15. Lu P, Schrag ML, Slaughter DE, Raab CE, Shou M, Rodrigues AD. Mechanism based inhibition of human liver microsomal cytochrome P450 1A2 by zileuton, a 5 lipoxygenase inhibitor. Drug Metab Dispos 2003; 31:1352 1360.
16. Guengerich FP. Mechanism based inactivation of human liver microsomal cytochrome P 450 IIIA4 by gestodene. Chem Res Toxicol 1990; 3:363 371.
17. Baer BR, Wienkers LC, Rock DA. Time dependent inactivation of P450 3A4 by raloxifene: identification of Cys239 as the site of apoprotein alkylation. Chem Res Toxicol 2007; 20: 954 964.

18. Van LM, Swales J, Hammond C, Wilson C, Hargreaves JA, Rostami Hodjegan A. Kinetics of the time dependent inactivation of CYP2D6 in cryopreserved human hepatocytes by methylenedioxymethamphetamine (MDMA). Eur J Pharm Sci 2007; 31:53 61.
19. Zhao XJ, Jones DR, Wang YH, Grimm SW, Hall SD. Reversible and irreversible inhibition of CYP3A enzymes by tamoxifen and metabolites. Xenobiotica 2002; 32:863 878.
20. Hanioka N, Ozawa S, Jinno H,,o M, Saito Y, Sawada J. Human liver UDP glucuronosyl transferase isoforms involved in the glucuronidation of 7 ethyl 10 hydroxycamptothecin. Xenobiotica 2001; 31: 687 699.
21. Crowley JR, Hollenberg PF. Mechanism based inactivation of rat liver cytochrome P4502B1 by phencyclidine and its oxidative product, the iminium ion. Drug Metab Dispos 1995; 23: 786 793.
22. He K, Iyer KR, Hayes RN, Sinz MW, Woolf TF, Hollenberg PF. Inactivation of cytochrome P450 3A4 by bergamottin, a component of grapefruit juice. Chem Res Toxicol 1998; 11:252 259.
23. Chan WK, Delucchi AB. Resveratrol, a red wine constituent, is a mechanism based inactivator of cytochrome P450 3A4. Life Sci 2000; 67:3103 3112.
24. Koenigs LL, Trager WF. Mechanism based inactivation of cytochrome P450 2B1 by 8 methoxypsoralen and several other furanocoumarins. Biochemistry 1998; 37:13184 13193.
25. Bertz RJ, Granneman GR. Use of in vitro and in vivo data to estimate the likelihood of metabolic pharmacokinetic interactions. Clin Pharmacokinet 1997; 32:210 258.
26. Bjornsson TD, Callaghan JT, Einolf HJ, Fischer V, Gan L, Grimm S, Kao J, King SP, Miwa G, Ni L, Kumar G, McLeod, J., Obach SR, Roberts S, Roe A, Shah A, Snikeris F, Sullivan JT, Tweedie D, Vega JM, Walsh J, Wrighton SA. The conduct of in vitro and in vivo drug drug interaction studies: a PhRMA perspective. J Clin Pharmacol 2003; 43:443 469.
27. Walsh CT. Suicide substrates, mechanism based enzyme inactivators: recent developments. Annu Rev Biochem 1984; 53:493 535.
28. Shannon P, Marcotte P, Coppersmith S, Walsh C. Studies with mechanism based inactivators of lysine epsilon transaminase from Achromobacter liquidum. Biochemistry 1979; 18:3917 3920.
29. Walsh C. Suicide substrates: mechanism based inactivators of specific target enzymes. Mol Biol Biochem Biophys 1980; 32:62 77.
30. Wang EA, Kallen R, Walsh C. Mechanism based inactivation of serine transhydroxymethy lases by D fluoroalanine and related amino acids. J Biol Chem 1981; 256:6917 6926.
31. Desta Z, Ward BA, Soukhova NV, Flockhart DA. Comprehensive evaluation of tamoxifen sequential biotransformation by the human cytochrome P450 system in vitro: prominent roles for CYP3A and CYP2D6. J Pharmacol Exp Ther 2004; 310:1062 1075.
32. Pearson JT, Wahlstrom JL, Dickmann LJ, Kumar S, Halpert JR, Wienkers LC, Foti RS, Rock DA. Differential time dependent inactivation of P450 3A4 and P450 3A5 by raloxifene: a key role for C239 in quenching reactive intermediates. Chem Res Toxicol 2007; 20:1778 1786.
33. Kunze KL, Trager WF. Isoform selective mechanism based inhibition of human cytochrome P450 1A2 by furafylline. Chem Res Toxicol 1993; 6:649 656.
34. Hutzler JM, Steenwyk RC, Smith EB, Walker GS, Wienkers LC. Mechanism based inactivation of cytochrome P450 2D6 by 1 [(2 ethyl 4 methyl 1H imidazol 5 yl)methyl] 4 [4 (trifluoromethyl) 2 pyridinyl] piperazine: kinetic characterization and evidence for apo protein adduction. Chem Res Toxicol 2004; 17:174 184.
35. Kouzi SA, McMurtry RJ, Nelson SD. Hepatotoxicity of germander (Teucrium chamaedrys L.) and one of its constituent neoclerodane diterpenes teucrin A in the mouse. Chem Res Toxicol 1994; 7:850 856.
36. Sahali Sahly Y, Balani SK, Lin JH, Baillie TA. In vitro studies on the metabolic activation of the furanopyridine L 754,394, a highly potent and selective mechanism based inhibitor of cytochrome P450 3A4. Chem Res Toxicol 1996; 9:1007 1012.
37. Khojasteh Bakht SC, Chen W, Koenigs LL, Peter RM, Nelson SD. Metabolism of (R) (+) pulegone and (R) (+) menthofuran by human liver cytochrome P 450s: evidence for formation of a furan epoxide. Drug Metab Dispos 1999; 27:574 580.
38. Chen LJ, Hecht SS, Peterson LA. Characterization of amino acid and glutathione adducts of cis 2 butene 1,4 dial, a reactive metabolite of furan. Chem Res Toxicol 1997; 10:866 874.

39. Lopez Garcia MP, Dansette PM, Mansuy D. Thiophene derivatives as new mechanism based inhibitors of cytochromes P 450: inactivation of yeast expressed human liver cytochrome P 450 2C9 by tienilic acid. Biochemistry 1994; 33:166 175.
40. Dansette PM, Bertho G, Mansuy D. First evidence that cytochrome P450 may catalyze both S oxidation and epoxidation of thiophene derivatives. Biochem Biophys Res Commun 2005; 338:450 455.
41. Dickins M, Elcombe CR, Moloney SJ, Netter KJ, Bridges JW. Further studies on the dissociation of the isosafrole metabolite cytochrome P 450 complex. Biochem Pharmacol 1979; 28:231 238.
42. Ullrich V, Schnabel KH. Formation and binding of carbanions by cytochrome P 450 of liver microsomes. Drug Metab Dispos 1973; 1:176 183.
43. Lin HL, Hollenberg PF. The inactivation of cytochrome P450 3A5 by 17alpha ethynylestradiol is cytochrome b5 dependent: metabolic activation of the ethynyl moiety leads to the formation of glutathione conjugates, a heme adduct, and covalent binding to the apoprotein. J Pharmacol Exp Ther 2007; 321:276 287.
44. Yukinaga H, Takami T, Shioyama SH, Tozuka Z, Masumoto H, Okazaki O, Sudo K. Identification of cytochrome P450 3A4 modification site with reactive metabolite using linear ion trap Fourier transform mass spectrometry. Chem Res Toxicol 2007; 20:1373 1378.
45. Ortiz de Montellano PR, Kunze KL, Yost GS, Mico BA. Self catalyzed destruction of cytochrome P 450: covalent binding of ethynyl sterols to prosthetic heme. Proc Natl Acad Sci U S A 1979; 76:746 749.
46. Reilly PE, Gomi RJ, Mason SR. Mechanism based inhibition of rat liver microsomal diazepam C3 hydroxylase by mifepristone associated with loss of spectrally detectable cytochrome P450. Chem Biol Interact 1999; 118:39 49.
47. De Matteis F, Sparks RG. Iron dependent loss of liver cytochrome P 450 haem in vivo and in vitro. FEBS Lett 1973; 29:141 144.
48. Correia MA, Farrell GC, Olson S, Wong JS, Schmid R, Ortiz de Montellano PR, Beilan HS, Kunze KL, Mico BA. Cytochrome P 450 heme moiety. The specific target in drug induced heme alkylation. J Biol Chem 1981; 256: 5466 5470.
49. Karuzina II and Archakov AI. The oxidative inactivation of cytochrome P450 in monooxygenase reactions. Free Radic Biol Med 1994; 16:73 97.
50. Karuzina II, Zgoda VG, Kuznetsova GP, Samenkova NF, Archakov AI. Heme and apoprotein modification of cytochrome P450 2B4 during its oxidative inactivation in monooxygenase reconstituted system. Free Radic Biol Med 1999; 26:620 632.
51. Barr DP, Mason RP. Mechanism of radical production from the reaction of cytochrome c with organic hydroperoxides. An ESR spin trapping investigation. J Biol Chem 1995; 270: 12709 12716.
52. Baillie TA. Future of toxicology metabolic activation and drug design: challenges and opportunities in chemical toxicology. Chem Res Toxicol 2006; 19:889 893.
53. Williams DP, Antoine DJ, Butler PJ, Jones R, Randle L, Payne A, Howard M, Gardner I, Blagg J, Park BK. The metabolism and toxicity of furosemide in the Wistar rat and CD 1 mouse: a chemical and biochemical definition of the toxicophore. J Pharmacol Exp Ther 2007; 322:1208 1220.
54. Buckpitt AR, Bahnson LS, Franklin RB. Hepatic and pulmonary microsomal metabolism of naphthalene to glutathione adducts: factors affecting the relative rates of conjugate formation. J Pharmacol Exp Ther 1984; 231:291 300.
55. Buckpitt AR, Warren DL. Evidence for hepatic formation, export and covalent binding of reactive naphthalene metabolites in extrahepatic tissues in vivo. J Pharmacol Exp Ther 1983; 225:8 16.
56. Kent UM, Bend JR, Chamberlin BA, Gage DA, Hollenberg PF. Mechanism based inactivation of cytochrome P450 2B1 by N benzyl 1 aminobenzotriazole. Chem Res Toxicol 1997; 10:600 608.
57. Bateman KP, Baker J, Wilke M, Lee J, Leriche T, Seto C, Day S, Chauret N, Ouellet M, Nicoll Griffith DA. Detection of covalent adducts to cytochrome P450 3A4 using liquid chromatography mass spectrometry. Chem Res Toxicol 2004; 17:1356 1361.

58. Regal KA, Schrag ML, Kent UM, Wienkers LC, Hollenberg PF. Mechanism based inactivation of cytochrome P450 2B1 by 7 ethynylcoumarin: verification of apo P450 adduction by electrospray ion trap mass spectrometry. Chem Res Toxicol 2000; 13:262 270.
59. Liu H, Liu J, van Breemen RB, Thatcher GR, Bolton JL. Bioactivation of the selective estrogen receptor modulator desmethylated arzoxifene to quinoids: 4′ fluoro substitution prevents quinoid formation. Chem Res Toxicol 2005; 18:162 173.
60. Kent UM, Lin HL, Mills DE, Regal KA, Hollenberg PF. Identification of 17 alpha ethynylestradiol modified active site peptides and glutathione conjugates formed during metabolism and inactivation of P450s 2B1 and 2B6. Chem Res Toxicol 2006; 19:279 287.
61. Kent UM, Mills DE, Rajnarayanan RV, Alworth WL, Hollenberg PF. Effect of 17 alpha ethynylestradiol on activities of cytochrome P450 2B (P450 2B) enzymes: characterization of inactivation of P450s 2B1 and 2B6 and identification of metabolites. J Pharmacol Exp Ther 2002; 300:549 558.
62. Melet A, Assrir N, Jean P, Pilar Lopez Garcia M, Marques Soares C, Jaouen M, Dansette PM, Sari MA, Mansuy D. Substrate selectivity of human cytochrome P450 2C9: importance of residues 476, 365, and 114 in recognition of diclofenac and sulfaphenazole and in mechanism based inactivation by tienilic acid. Arch Biochem Biophys 2003; 409:80 91.
63. Skiles GL, Yost GS. Mechanistic studies on the cytochrome P450 catalyzed dehydrogenation of 3 methylindole. Chem Res Toxicol 1996; 9: 291 297.
64. Dooley GP, Prenni JE, Prentiss PL, Cranmer BK, Andersen ME, Tessari JD. Identification of a novel hemoglobin adduct in Sprague Dawley rats exposed to atrazine. Chem Res Toxicol 2006; 19:692 700.
65. Guengerich FP, Arneson KO, Williams KM, Deng Z, Harris TM. Reaction of aflatoxin B(1) oxidation products with lysine. Chem Res Toxicol 2002; 15:780 792.
66. Lightning LK, Jones JP, Friedberg T, Pritchard MP, Shou M, Rushmore TH, Trager WF. Mechanism based inactivation of cytochrome P450 3A4 by L 754,394. Biochemistry 2000; 39:4276 4287.
67. Koenigs LL, Peter RM, Hunter AP, Haining RL, Rettie AE, Friedberg T, Pritchard MP, Shou M, Rushmore TH, Trager WF. Electrospray ionization mass spectrometric analysis of intact cytochrome P450: identification of tienilic acid adducts to P450 2C9. Biochemistry 1999; 38:2312 2319.
68. Wen B, Lampe JN, Roberts AG, Atkins WM, David Rodrigues A, Nelson SD. Cysteine 98 in CYP3A4 contributes to conformational integrity required for P450 interaction with CYP reductase. Arch Biochem Biophys 2006; 454:42 54.
69. Gartner CA, Wen B, Wan J, Becker RS, Jones G, 2nd, Gygi SP, Nelson SD. Photochromic agents as tools for protein structure study: lapachenole is a photoaffinity ligand of cytochrome P450 3A4. Biochemistry 2005; 44:1846 1855.
70. Liu J, Li Q, Yang X, van Breemen RB, Bolton JL, Thatcher GR. Analysis of protein covalent modification by xenobiotics using a covert oxidatively activated tag: raloxifene proof of principle study. Chem Res Toxicol 2005; 18:1485 1496.
71. Wang J, Bauman S, Colman RF. Photoaffinity labeling of rat liver glutathione S transferase, 4 4, by glutathionyl S [4 (succinimidyl) benzophenone]. Biochemistry 1998; 37:15671 15679.
72. Tessier S, Boivin S, Aubin J, Lampron P, Detheux M, Fournier A. Transmembrane domain V of the endothelin A receptor is a binding domain of ETA selective TTA 386 derived photoprobes. Biochemistry 2005; 44:7844 7854.
73. Swanson RA, Dus KM. Specific covalent labeling of cytochrome P 450CAM with 1 (4 azidophenyl)imidazole, an inhibitor derived photoaffinity probe for P 450 heme proteins. J Biol Chem 1979; 254:7238 7246.
74. Williams PA, Cosme J, Vinkovic DM, Ward A, Angove HC, Day PJ, Vonrhein C, Tickle IJ, Jhoti H. Crystal structures of human cytochrome P450 3A4 bound to metyrapone and progesterone. Science 2004; 305:683 686.
75. Paul H, Illing A, Netter KJ. The effects of sulphydryl reagents on the binding and mixed function oxidation of hexobarbital in rat hepatic microsomes. Xenobiotica 1975; 5:1 15.

76. Baer BR, Wienkers LC, Rock DA. Time dependent inactivation of P450 3A4 by raloxifene: identification of Cys239 as the site of apoprotein alkylation(1). Chem Res Toxicol 2007; 20:954 964.
77. Hodgson E, Casida JE. Biological oxidation of N, N dialkyl carbamates. Biochim Biophys Acta 1960; 42:184 186.
78. Hodgson E, Casida JE. Metabolism of N:N dialkyl carbamates and related compounds by rat liver. Biochem Pharmacol 1961; 8:179 191.
79. Casida JE, Engel JL, Essac EG, Kamienski FX and Kuwatsuka S. Methylene C14 dioxyphenyl compounds: metabolism in relation to their synergistic action. Science 1966; 153:1130 1133.
80. Kamienski FX, Casida JE. Importance of demethylenation in the metabolism in vivo and in vitro of methylenedioxyphenyl synergists and related compounds in mammals. Biochem Pharmacol 1970; 19:91 112.
81. Hodgson E, Philpot RM. Interaction of methylenedioxyphenyl (1,3 benzodioxole) compounds with enzymes and their effects on mammals. Drug Metab Rev 1974; 3:231 301.
82. Wilkinson GR, Way EL. Sub microgram estimation of morphine in biological fluids by gas liquid chromatography. Biochem Pharmacol 1969; 18:1435 1439.
83. Schenkman JB, Ball JA, Estabrook RW. On the use of nicotinamide in assays for microsomal mixed function oxidase activity. Biochem Pharmacol 1967; 16:1071 1081.
84. Casida JE. Mixed function oxidase involvement in the biochemistry of insecticide synergists. J Agric Food Chem 1970; 18:753 772.
85. Franklin MR. The enzymic formation of methylenedioxyphenyl derivative exhibiting an isocyanide like spectrum with reduced cytochrome P 450 in hepatic microsomes. Xenobiotica 1971; 1:581 591.
86. Philpot RM, Hodgson E. A cytochrome P 450 piperonyl butoxide spectrum similar to that produced by ethyl isocyanide. Life Sci II 1971; 10:503 512.
87. Philpot RM, Hodgson E. The production and modification of cytochrome P 450 difference spectra by in vivo administration of methylenedioxyphenyl compounds. Chem Biol Interact 1972; 4:185 194.
88. Hansch C. The use of homolytic, steric, and hydrophobic constants in a structure activity study of 1,3 benzodioxole synergists. J Med Chem 1968; 11:920 924.
89. Ullrich V, Schnabel KH. Formation and ligand binding of the fluorenyl carbanion by hepatic cytochrome P 450. Arch Biochem Biophys 1973; 159:240 248.
90. Yu LS, Wilkinson CF, Anders MW. Generation of carbon monoxide during the microsomal metabolism of methylenedioxyphenyl compounds. Biochem Pharmacol 1980; 29:1113 1122.
91. Anders MW, Sunram JM, Wilkinson CF. Mechanism of the metabolism of 1,3 benzodioxoles to carbon monoxide. Biochem Pharmacol 1984; 33:577 580.
92. Dahl AR, Brezinski DA. Inhibition of rabbit nasal and hepatic cytochrome P 450 dependent hexamethylphosphoramide (HMPA) N demethylase by methylenedioxyphenyl compounds. Biochem Pharmacol 1985; 34:631 636.
93. Cook L, Navis G, Fellows EJ. Enhancement of the action of certain analgetic drugs by beta diethylaminoethyldiphenyl propylacetate hydrochloride. J Pharmacol Exp Ther 1954; 112:473 479.
94. Cook L, Macko E, Fellows EJ. The effect of beta diethylaminoethyldiphenyl propylacetate hydrochloride on the action of a series of barbiturates and C.N.S. depressants. J Pharmacol Exp Ther 1954; 112:382 386.
95. Jonsson KH, Lindeke B. Cytochrome P 455 nm complex formation in the metabolism of phenylalkylamines. XII. Enantioselectivity and temperature dependence in microsomes and reconstituted cytochrome P 450 systems from rat liver. Chirality 1992; 4:469 477.
96. Axelrod J, Reichenthal J, Brodie BB. Mechanism of the potentiating action of beta diethylaminoethyl diphenylpropylacetate. J Pharmacol Exp Ther 1954; 112:49 54.
97. Cooper JR, Axelrod J, Brodie BB. Inhibitory effects of beta diethylaminoethyl diphenylpro pylacetate on a variety of drug metabolic pathways in vitro. J Pharmacol Exp Ther 1954; 112:55 63.

98. Castro JA, Sasame HA, Sussman H, Gillette JR. Diverse effects of SKF 525 A and antioxidants on carbon tetrachloride induced changes in liver microsomal P 450 content and ethylmorphine metabolism. Life Sci 1968; 7:129 136.
99. Schenkman JB, Wilson BJ, Cinti DL. Dimethylaminoethyl 2,2 diphenylvalerate HCl (SKF 525 A) in vivo and in vitro effects of metabolism by rat liver microsomes formation of an oxygenated complex. Biochem Pharmacol 1972; 21:2373 2383.
100. Werringloer J, Estabrook RW. Evidence for an inhibitory product cytochrome P 450 complex generated during benzphetamine metabolism by liver microsomes. Life Sci 1973; 13:1319 1330.
101. Mansuy D, Beaune P, Chottard JC, Bartoli JF, Gans P. The nature of the "455 nm absorbing complex" formed during the cytochrome P450 dependent oxidative metabolism of amphet amine. Biochem Pharmacol 1976; 25:609 612.
102. Franklin MR. The influence of cytochrome P 450 induction on the metabolic formation of 455 NM complexes from amphetamines. Drug Metab Dispos 1974; 2:321 326.
103. Mansuy D, Rouer E, Bacot C, Gans P, Chottard JC, Leroux JP. Interaction of aliphatic N hydroxylamines with microsomal cytochrome P450: nature of the different derived complexes and inhibitory effects on monoxygenases activities. Biochem Pharmacol 1978; 27: 1129 1137.
104. Hines RN, Prough RA. The characterization of an inhibitory complex formed with cytochrome P 450 and a metabolite of 1,1 disubstituted hydrazines. J Pharmacol Exp Ther 1980; 214:80 86.
105. Kutt H, Brennan R, Dehejia H, Verebely K. Diphenylhydantoin intoxication. A complication of isoniazid therapy. Am Rev Respir Dis 1970; 101:377 384.
106. Muakkassah SF, Yang WC. Mechanism of the inhibitory action of phenelzine on microsomal drug metabolism. J Pharmacol Exp Ther 1981; 219:147 155.
107. Muakkassah SF, Bidlack WR, Yang WC. Reversal of the effects of isoniazid on hepatic cytochrome P 450 by potassium ferricyanide. Biochem Pharmacol 1982; 31:249 251.
108. Wang YH, Jones DR, Hall SD. Prediction of cytochrome P450 3A inhibition by verapamil enantiomers and their metabolites. Drug Metab Dispos 2004; 32:259 266.
109. Walsh C, Cromartie T, Marcotte P, Spencer R. Suicide substrates for flavoprotein enzymes. Methods Enzymol 1978; 53:437 448.
110. Chiba M, Nishime JA, Lin JH. Potent and selective inactivation of human liver microsomal cytochrome P 450 isoforms by L 754,394, an investigational human immune deficiency virus protease inhibitor. J Pharmacol Exp Ther 1995; 275:1527 1534.
111. Jung MJ, Metcalf BW. Catalytic inhibition of gamma aminobutyric acid alpha ketoglutarate transaminase of bacterial origin by 4 aminohex 5 ynoic acid, a substrate analog. Biochem Biophys Res Commun 1975; 67:301 306.
112. Kitz R, Wilson IB. Esters of methanesulfonic acid as irreversible inhibitors of acetylcholines terase. J Biol Chem 1962; 237:3245 3249.
113. Silverman RB. Mechanism based enzyme inactivators. Methods Enzymol 1995; 249:240 283.
114. Waley SG. Kinetics of suicide substrates. Practical procedures for determining parameters. Biochem J 1985; 227:843 849.
115. Correia MA. Cytochrome P450 turnover. Methods Enzymol 1991; 206:315 325.
116. Waley SG. Kinetics of suicide substrates. Biochem J 1980; 185:771 773.
117. Funaki T, Takanohashi Y, Fukazawa H, Kuruma I. Estimation of kinetic parameters in the inactivation of an enzyme by a suicide substrate. Biochim Biophys Acta 1991; 1078:43 46.
118. Mayhew BS, Jones DR, Hall SD. An in vitro model for predicting in vivo inhibition of cytochrome P450 3A4 by metabolic intermediate complex formation. Drug Metab Dispos 2000; 28:1031 1037.
119. Rostami Hodjegan A, Tucker GT. 'In silico' simulations to assess the 'in vivo' consequences of 'in vitro' metabolic drug drug interactions. Drug Discov Today Technol 2004; 1:441 448.
120. Brown HS, Galetin A, Hallifax D, Houston JB. Prediction of in vivo drug drug interactions from in vitro data: factors affecting prototypic drug drug interactions involving CYP2C9, CYP2D6 and CYP3A4. Clin Pharmacokinet 2006; 45:1035 1050.
121. Brown HS, Ito K, Galetin A, Houston JB. Prediction of in vivo drug drug interactions from in vitro data: impact of incorporating parallel pathways of drug elimination and inhibitor absorption rate constant. Br J Clin Pharmacol 2005; 60:508 518.

122. Proctor NJ, Tucker GT, Rostami Hodjegan A. Predicting drug clearance from recombinantly expressed CYPs: intersystem extrapolation factors. Xenobiotica 2004; 34:151 178.
123. Howgate EM, Rowland Yeo K, Proctor NJ, Tucker GT, Rostami Hodjegan A. Prediction of in vivo drug clearance from in vitro data. I: impact of inter individual variability. Xenobiotica 2006; 36:473 497.

22
Clinical Drug Metabolism

Kirk R. Henne,[1] George R. Tonn,[1] William F. Pool,[2] and Bradley K. Wong[1]
[1]*Department of Pharmacokinetics and Drug Metabolism, Amgen Inc., South San Francisco, California, U.S.A.*
[2]*Department of Pharmacokinetics, Dynamics, and Metabolism, Pfizer Global Research and Development, San Diego, California, U.S.A.*

INTRODUCTION

Clinical drug metabolism studies provide definitive characterization of the metabolic fate of drug candidates. Frequently, the human absorption, distribution, metabolism, and excretion (ADME) study will be the only clinical study of a new chemical entity (NCE) designed specifically to characterize metabolism and disposition. In addition to fulfilling a regulatory requirement for registration of a new drug, a main purpose of these studies is to support qualitative extrapolation of the preclinical animal toxicology results to humans by demonstrating that the metabolites formed by humans are also formed by animals. Until recently, clinical drug metabolism studies have been conducted late in the development time line, however, a changed regulatory environment and improvements in technology are driving the early conduct of human ADME studies. Advances in the mechanistic knowledge of drug metabolism enzymology are enabling the early-stage understanding of clearance pathways, which can be applied in designing clinical pharmacology programs. With the current generation of mass spectrometry instrumentation, it is now possible to routinely profile major metabolites in the earliest first-in-human (FIH) studies without being limited by method sensitivity. Accelerator mass spectrometry (AMS) is emerging as an enabling technology for assessing mass balance with very low doses of radioactivity, with potential application in very early, if not the earliest, human trials. This chapter focuses on clinical drug metabolism studies using labeled or unlabeled materials to assess disposition pathways and excretion routes of development-stage candidates.

Evolving Regulatory Environment and Clinical Drug Metabolism

The U.S. Food and Drug Administration (FDA) recently (February 2008) issued a guidance for industry entitled "Safety Testing of Drug Metabolites" that may impact the timing and

conduct of human ADME studies (1). Under a traditional paradigm, metabolites do not undergo separate toxicity testing, and the safety margins derived from parent drug exposure in animals at the no adverse effect dose level (NOAEL) and in humans at the clinically relevant dose are sufficient to support registration. On a compound-specific basis, a metabolite could be subject to separate toxicological testing if it contributes substantially to total pharmacological activity, it is present in preclinical species at low or no systemic exposure, or there is a specific concern about toxic potential. The new FDA guidance defines conditions in which a metabolite will need to undergo additional toxicity evaluation (1) (see chap. 24). The regulatory impetus behind it is to understand the specific contribution of metabolites to the toxicity of an investigational drug. The guidance defines a quantitatively "disproportionate metabolite" that may be subject to separate toxicology studies involving administration of the metabolite itself. Disproportionate metabolites are defined as those with steady-state systemic exposure in humans that exceeds 10% of the parent drug exposure. The new guidance provides additional decision criteria for requiring toxicity testing if the steady-state metabolite exposure in animal studies is less than the corresponding exposure in humans, then nonclinical toxicology testing will be needed (Fig. 1). The type of toxicology studies that are recommended include those conducted for parent drug: general toxicity, genotoxicity, embryo-fetal development, and carcinogenicity (1). A disproportionate metabolite whose exposure in animals is equal to or higher than that in humans would not require further testing and would be considered qualified, in-line with current practice. A change from existing practice is that the decision criteria within the guidance do not consider the pharmacological activity of the metabolite, recognizing the potential for toxicities which are mediated by off-target actions of the NCE. It does recognize that separate toxicity testing of certain types of metabolites (ether glucuronides and some

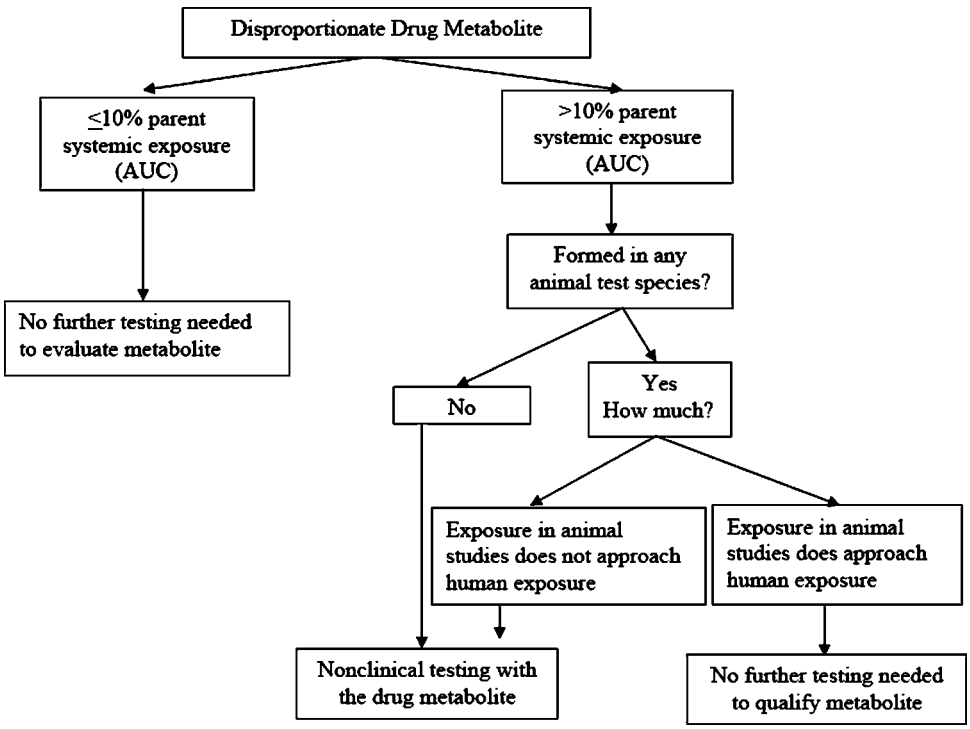

Figure 1 Decision tree flow diagram from FDA guidance "Safety Testing of Drug Metabolites." *Source*: From Ref. 1.

phase II conjugates) does not add to the understanding of the risk associated with the parent drug. The guidance does not apply to cancer therapies where different risk-benefit considerations apply. A consequence of implementation of the guidance is that earlier and more detailed characterization of metabolite exposure in toxicology studies and humans will be required.

Extrapolating the toxicological significance of synthetic metabolites to risk assessments of parent drug is complicated by the potential kinetic differences in the behavior of the metabolite after administration of the parent drug and the metabolite itself (2). Physical properties (e.g., lipophilicity), metabolizing enzyme distribution, and effects of transporters can result in substantially different metabolite concentrations in tissue despite the same systemic exposure. The biological complexity associated with separate administration of metabolites is illustrated by the case of simvastatin, which is administered in its inactive lactone form and undergoes enzymatic and chemical hydrolysis in vivo to the pharmacologically active acid metabolite (2). Administration of the lactone form produces concentrations of the acid metabolite in brain and muscle that are two- to threefold higher than those achieved after giving the acid itself. This different metabolite pharmacokinetic behavior is attributable to the greater passive permeability and absence of P-gp-mediated efflux, which increases availability of the precursor lactone (3). Interestingly, despite the substantially differing tissue exposures, administration of simvastatin lactone and acid metabolite results in comparable plasma concentrations of the acid metabolite. A possible consequence of the evolving regulatory environment is that the need to interpret metabolite toxicology studies may stimulate research interest in the determinants of metabolite pharmacokinetics, especially as related to tissue exposure.

Impact of FDA Guidance for Industry "Safety Testing of Drug Metabolites" on Clinical Drug Metabolism Studies

Implementation of the FDA "Safety Testing of Drug Metabolites" guidance will affect the timing of preclinical and clinical ADME studies because the potential need for additional toxicology studies of metabolites could delay time lines and require the commitment of additional company resources (4,5). Minimizing the risk of late identification of a disproportionate metabolite would include a full preclinical characterization of metabolites by knowledgeable scientists using modern technologies. These studies will need to be completed well in advance of the initiation of registration-enabling toxicology studies. As the guidance dictates that the metabolite toxicology studies should be conducted to GLP standards, synthetic metabolite material would have to be qualified and bioanalytical methods validated with defined storage conditions for maintaining metabolite integrity (which may differ from those for parent drug). Another implication is that sufficient time must be allowed for follow-up studies that could be required for a proper scientific perspective of the metabolite toxicity evaluations (2). The use of low-dose radioactivity regimens and accelerator mass spectrometric detection to characterize human metabolism during phase I multiple-dose studies is one possible means to obtain steady-state drug metabolism information at the earliest stages of clinical development. As with other issues encountered during the registration process, discussions between the sponsor and agency are a means of arriving at scientifically and technically based resolutions.

Rationale for Conducting Clinical Drug Metabolism Studies Early in the Drug Development Time Line

Changes in regulatory requirements along with significant advances in the molecular understanding of the enzymology related to drug metabolism provide a strong rationale

for conducting human drug metabolism studies early in the NCE development time line. Commercially available, well-characterized human-derived subcellular fractions (microsomes, cytosol), whole cells (hepatocytes) and recombinant enzymes [cytochrome P450 (CYP), UDP-glucuronosyltransferases (UGT)s] of documented quality are routinely used to generate human-based metabolites. The availability of highly specific monoclonal inhibitory CYP antibodies and selective chemical inhibitors used in combination with human hepatic subcellular systems facilitates phenotyping studies that lead to the identification of enzymes involved in metabolic clearance (6,7). Consequently, by the start of human studies, a reasonable scientific foundation can be available for rational design of clinical pharmacology programs. These data along with information from clinical drug metabolism studies may provide the basis for the conduct of specific drug-drug interaction (DDI) studies and the characterization of the pharmacokinetics in special populations. For example, in vitro phenotyping studies may implicate a particular CYP isozyme (e.g., 3A4 or 2D6) as a major contributor to the metabolism of an NCE. Early clinical drug metabolism studies showing that elimination of a drug proceeds primarily via these oxidative pathways justifies the early clinical evaluation of coadministration of clinically significant CYP inhibitors (e.g., ketoconazole or quinidine) in DDI studies. A clinical drug metabolism study suggesting a low risk of DDIs may justify a minimal set of clinical pharmacology studies, while an unfavorable DDI profile could lead to project termination, depending on the risk-benefit associated with the therapeutic indication. The benefits of reaching the latter decision before the initiation of large-scale clinical trials are substantial. Conversely, establishing that glucuronidation or renal excretion was quantitatively most important could lead to clinical studies assessing the effect on drug clearance of coadministration of valproic acid (a UGT inhibitor) or of renal impairment (8).

While solid directional data on clearance mechanism(s) are obtained from preclinical animal and in vitro studies, an in vivo clinical drug metabolism study is needed for definitive characterization of human clearance pathways. These definitive data are usually obtained from a human ADME study conducted with radiolabeled drug. However, evaluation of drug metabolism during early clinical studies (e.g., FIH) conducted with unlabeled material can provide a valuable opportunity to explore human drug disposition. Information regarding circulating levels of key metabolites (major or active), metabolic pathways, and, in certain instances, insight into the elimination pathways of an NCE may be obtained from these experiments.

Administration of a radiolabeled drug candidate to human subjects affords a unique opportunity to determine quantitatively the in vivo disposition and metabolism of a molecule. When mass balance is achieved, the clearance mechanisms of an NCE can be fully elucidated through characterization of the excretion profile of parent drug and associated metabolites. Routes of clearance determined through the course of a study may validate previous insights made on the basis of in vitro human data, preclinical interspecies extrapolations, or early clinical metabolism studies conducted without radiolabel. Alternatively, results from the radiolabel study may highlight unforeseen ADME knowledge gaps requiring additional research efforts to support advancement of a potential drug. Efficacy- and safety-related concerns are also addressed in the context of the radiolabel human ADME study, as metabolites present in circulation are identified and quantified to evaluate their possible contribution to pharmacological or toxicological effects (in accordance with recent FDA guidance). Given the relative ease with which radiolabeled molecules and their metabolites are identified and quantified amidst complex endogenous background components, radioisotopes are an essential tool in the assessment of the in vivo fate of drug candidates.

CLINICAL DRUG METABOLISM WITH NON-RADIOLABELED DRUG

Qualitative Approaches

In the absence of quantitative tools (i.e., radiolabeled material or synthetic standards), useful information regarding in vivo metabolic pathways of an NCE can be obtained via qualitative means. Exploratory analysis of human plasma, urine, and bile may reveal important details concerning the biotransformation of an investigational drug. Generally, in vitro human data provide a framework for conduct of exploratory investigations of biological samples. Usually, these data demonstrate reasonable concordance between in vitro and in vivo metabolic profiles; however, there are cases where in vitro data is of limited value. Piperaquine (PQ) is an antimalarial agent initially synthesized in the 1960s. In combination with dihydroartemisinin, use of PQ in malaria treatment has increased recently because of its efficacy and tolerability (9). Despite PQ's lengthy clinical use, little is known about the biotransformation of this drug in humans. The low turnover rate in standard in vitro systems limits the formation of metabolites, which complicates the study of PQ biotransformation. Following oral administration of PQ (960 mg) to human volunteers, five oxidative metabolites were detected in urine at quantities sufficient to permit structural elucidation by liquid chromatography (LC)-tandem mass spectrometry (MS/MS) and nuclear magnetic resonance (NMR) analyses (10). Information derived from early studies using unlabeled drug can also identify differences in biotransformation profiles between humans and preclinical species. Analysis of urine samples collected from subjects receiving a 1000-mg oral dose of indinavir (Crixivan®), an HIV protease inhibitor, revealed the formation of several prominent oxidative metabolites including a novel quaternary *N*-glucuronide (11). While good agreement was observed across species (rat, dog, monkey, and human) for oxidative metabolites, the quaternary *N*-glucuronide was observed only in human and nonhuman primates (12,13).

When measurement of biliary secretion of parent drug or metabolites is warranted, bile can be collected from either patients undergoing certain surgical procedures (e.g., cholecystectomy, temporary bile shunt, and nasobiliary drainage) or healthy subjects, using either duodenal perfusion or oroentric tubes (14). A recent study applied oroentric tubes to collect bile for the evaluation of metabolites of piperacillin [2 g intravenous (IV) dose] in normal volunteers (15). Piperacillin was excreted predominantly into urine, while its metabolites desethylpiperacillin and desethylpiperacillin glucuronide were excreted predominantly in bile. The glucuronide conjugate of desethylpiperacillin was a novel metabolite previously undescribed, potentially because it was subject to hydrolysis by intestinal β-glucuronidases. The bile collection method involves the oral insertion of a customized multiluminal oroentric tube that is modified for the aspiration of gastric and duodenal contents (16). A small balloon is inflated on the distal end of the tube to prevent the loss of biliary secretions into the lower GI tract, which facilitates quantitative bile collection. In addition, administration of cholecystokinin-8 to stimulate gall bladder contraction improves recovery of bile (16). This technique may provide a less invasive method of bile collection from human volunteers for purposes of clinical drug metabolism studies.

Quantitative Analysis of Plasma and Excreta

The availability of synthetic standards of key metabolites allows for a more quantitative understanding of the human biotransformation of an NCE during early clinical studies. Timely data on the role of circulating metabolites can be instrumental in understanding the pharmacological response of a new agent, since active metabolites can significantly

impact the intensity, duration, and spectrum of pharmacological activity (17). In early clinical development, often the challenge is the lack of definitive data on which to base selection of relevant metabolite(s) to be synthesized and measured. In vitro data using human-derived tissue, qualitative metabolite identification (ID) from preclinical or clinical studies, or a priori knowledge as to the potential for pharmacological activity of a given metabolite may aid this decision. In addition, the complexity of biotransformation often impacts the ease with which these decisions can be made. Circumstances where only a limited number of metabolites are formed make this approach more feasible.

This was the case with AMG487, an investigational CXCR3 antagonist[Chemokine (C-X-C) motif receptor], where analysis of in vitro human microsomal and hepatocyte incubations showed that only three primary metabolites were formed: a pyridyl *N*-oxide (M1 major) and two minor metabolites (O-deethylated AMG 487 and O-deethylated AMG 487 *N*-oxide). Evaluation of synthetic M1 demonstrated similar potency for CXCR3 inhibition as parent. Quantitation of M1 in human plasma samples collected from FIH studies showed that this metabolite circulated at levels two- to six-fold greater than AMG 487 (18). These data highlighted the need to evaluate both AMG 487 and M1 concentrations to understand the Pharmacokinetic/Pharmacodynamic (PK/PD) properties of parent, and to ensure the selection of appropriate doses in preclinical safety testing for coverage of M1 concentrations across preclinical species. The latter posed a considerable challenge since M1 concentrations were considerably lower in the species used for safety testing than in humans. Predicting plasma metabolite concentrations on the basis of in vitro data is not straightforward. This is because plasma metabolite levels are a function of formation rate, elimination rate, sequential metabolism (i.e., the availability of the metabolite to blood from the site of formation), and volume of distribution (19).

Quantitation of parent and/or metabolites in excreta (urine, bile, feces) provides useful information about the routes of elimination of an NCE. This information can be helpful in designing key clinical experiments (e.g., DDI trials or studies in special populations). The contribution of metabolism to the overall elimination of a drug can often be inferred by measuring the excretion of parent drug in the urine. High recovery of parent drug in urine indicates that renal excretion, rather than metabolism and/or biliary secretion pathways (or others), will dominate the elimination of an NCE. The urinary recoveries of atenolol, many cephalosporin antibiotics, hydrochlorothiazide, and lisinopril are $>90\%$, suggesting that biotransformation of these agents plays only a minor role, while renal excretion is dominant in their elimination (20).

Efforts to determine mass balance of an NCE solely on the basis of parent drug recovery in excreta would be expected to yield incomplete recovery for most drug candidates. Therefore, measuring both parent drug and metabolite(s) in excreta provides considerably more insight as to the elimination routes of an NCE. In the optimal case of quantitative mass balance, a more detailed description of the elimination pathways emerges. This was the case with acetaminophen. Following a 1000-mg oral dose of acetaminophen, essentially complete (100%) recovery was obtained by measurement of the acetaminophen, phase I oxidative metabolites, and phase II conjugates (glucuronide, sulfate, and glutathione conjugates) excreted in urine over a 24-hour period (21). In the case of this drug, the complete accounting of the dose was aided by the historical understanding of the major metabolites of this compound and their excretion profile. Unfortunately, quantification of drug-related material using cold assay techniques rarely results in complete recovery; however, important information can still be obtained from early clinical studies. In phase I studies of maribavir, a novel antiviral agent, $<2\%$ of the dose was excreted in urine as parent drug, while 30% to 40% of the dose was recovered as the corresponding N-dealkylated metabolite (22). In vitro based phenotyping

demonstrated that formation of this N-dealkylated metabolite was mediated almost exclusively by CYP3A4 (23). Despite the incomplete recovery of material in this study, it was clear that CYP3A4-mediated biotransformation contributed significantly to the overall elimination of the drug. Although the exact extent to which the elimination of maribavir was dependent on CYP3A4 could not be determined from these data, prioritization of CYP3A4-oriented DDI studies may be warranted (24). Classically, urinary excretion of parent drug and metabolites has formed the basis of phenotyping humans for polymorphic CYP enzymes. For example, urinary ratios of 4-hydroxydebrisoquine to debrisoquine or dextrorphan to dextromethorphan are often used as a means of determining CYP2D6 phenotype (25,26). In a recent example, the key metabolite of atomoxetine, 4-hydroxyatomoxetine, was shown to be the result of CYP2D6-mediated biotransformation (27). A 90-mg oral dose of atomoxetine (Strattera®), a blocker of the presynaptic norepinephrine transporter, was administered to "extensive" and "poor" CYP2D6 metabolizers (EMs and PMs, respectively). In EMs, the oral dose was recovered in urine over 24 hours as parent, *N*-desmethylatomoxetine, 4-hydroxyatomoxetine and the glucuronide conjugate of 4-hydroxyatomoxetine (28), of which the latter two accounted for the majority (60%) of the administered dose. This suggested that oxidative metabolism of atomoxetine to 4-hydroxyatomoxetine was a key elimination pathway for this drug. In PMs, the total recovery was much lower (11%), and the pattern of metabolites recovered was different, that is, there was a greater dependence on the formation of *N*-desmethylatomoxetine and excretion of parent drug (28). The impact of CYP2D6 phenotype on the biotransformation of atomoxetine was confirmed subsequently in a radiolabel mass balance study (29). It is also important to point out that low recovery of parent and known metabolites may preclude the collection of any useful information regarding the disposition of an NCE. The low recovery may be due to incomplete absorption of the compound following oral administration, incomplete understanding of the elimination routes in humans, and drug-related material being excreted in another matrix.

Application of ^{19}Fluorine NMR Spectroscopy

Fluorine (^{19}F) NMR provides an alternate means for metabolite quantitation without the prerequisite of synthetic reference standards or radiolabeled material. ^{19}F NMR shares some attributes of radiochemical analysis because the method is highly selective for drug-related material because of the low background of endogenous fluorine, and the NMR signal is directly proportional to the number of fluorine nuclei in a molecule (30). The large range of chemical shifts and the high sensitivity of the fluorine nuclei to its environment allows for the differentiation of the various chemical species within a biological sample, often without prior chromatographic separation (30,31). Depending on the sample matrix, only limited sample workup is generally required. Exceptions are matrices prone to macromolecular binding (e.g., plasma) and micellar substructures (e.g., bile), which can obscure the NMR signal (30). The key limitations of ^{19}F NMR compared with LC-MS/MS and radiochemical techniques are related to access to equipment, lower sensitivity, and increased sample volume. In addition, not all metabolites produce a discernible shift in the NMR signal. Nevertheless, this technique is powerful in selected instances for studying clinical drug metabolism.

Using ^{19}F NMR analysis, a total of eight metabolites were detected in human urine following oral administration of 150 and 800 mg flurbiprofen (32). Base hydrolysis abolished the major putative metabolite peaks while increasing those corresponding to parent drug and another metabolite, suggesting that these were acyl glucuronide conjugates. Further characterization of the second metabolite led to its assignment as the

glucuronide of 4-hydroxyflurbiprofen. Another case demonstrated the utility of LC-^{19}F/^{1}H NMR-MS to identify a novel metabolite of the experimental reverse transcriptase inhibitor BW935U83 in human urine (33). Analysis of urine samples collected following oral administration of a 1000-mg dose detected parent drug, a known glucuronide conjugate, and a second unknown metabolite. The latter metabolite was not detected using LC-MS/MS or ^{1}H NMR methods because of background interference from endogenous components. Subsequent structural characterization using LC-^{19}F/^{1}H NMR coupled with tandem MS analysis identified this metabolite as 3-fluoro-ribolactone, a metabolite believed to be derived from the CYP-mediated cleavage of the nucleoside-sugar bond of the parent molecule (33). In the presence of a known concentration of standard (e.g., trifluoromethylbenzoic acid, fluoroacetate, trifluoroacetic acid, etc.), quantitation of the ^{19}F signal is also possible (30). A mass balance study of an experimental HIV-1 integrase inhibitor conducted in rats demonstrated comparable total recoveries determined by standard radiometric and ^{19}F NMR methods (34). A good correlation was also observed for the recovery in urine and bile of individual metabolite components (e.g., parent, the glucuronide conjugate, and an N-demethylated metabolite). Provided the fluorine substituent is metabolically stable within the molecule of interest, ^{19}F NMR represents a useful technique for the quantification of drug metabolites without reference standards or radiolabel. For additional information on this technique, the reader is referred to an excellent review describing ^{19}F NMR application to drug disposition (30).

RADIOLABEL HUMAN ADME STUDY: BACKGROUND

Exploratory analyses of clinical samples from standard, non-radiolabel phase I dose escalation studies can provide valuable information about metabolite exposure in certain instances, where in vivo metabolism closely follows in vitro prediction and is not overly complicated (see sect. “Clinical Drug Metabolism with Non-Radiolabeled Drug”). In cases where metabolism is not completely understood or may be more extensive in vivo than in vitro, the obvious concern centers around which metabolites are potentially missed in the absence of a detection method specific for exogenous drug-related material. Scenarios involving complex metabolic pathways or unknown clearance mechanisms highlight the value of radiolabel when dosed in vivo radioisotopes can be used to identify and quantify *all* drug-related material without the need for metabolite standards and standard curves. These benefits are brought about by the fact that the decay of a radioactive isotope, and thus the ability to detect and quantitate radiolabeled material, is independent of molecular structure. Quantitation of the radioisotope requires only a simple measurement of disintegrations per minute (dpm) by liquid scintillation counting (LSC) and the specific activity of the radiolabel dose, which is known at the outset of the study. Furthermore, given the very low background of naturally occurring radioisotopes in vivo, unchanged drug and its metabolites are readily distinguished from components of the complicated and diverse biological matrices in which they reside.

Drug candidates are most commonly labeled with low-energy radioisotopes of carbon (Carbon-14, ^{14}C) or hydrogen (Tritium, ^{3}H) to enable characterization of their in vivo ADME properties in humans (35,36) as well as preclinical species (36,37). Between these two radioisotopes, ^{14}C is generally preferred because of its relatively high degree of chemical stability and detection efficiency by standard LSC when compared with ^{3}H. A potential advantage of ^{3}H is the relative ease with which it may be incorporated into an investigational drug, however, the possibility of isotope exchange with water must be carefully investigated through additional experimental efforts (38). Whether ^{14}C or ^{3}H is utilized as an isotopic label, specific attention must be paid to placement of the label within

the molecule. Incorporation of the label at a position of chemical or metabolic instability that results in the formation of a very low molecular weight entity (i.e., tritiated water) or volatile entity (i.e., $^{14}CO_2$) may easily confound interpretation of results or lead to poor radiolabel recovery. At a minimum, it is prudent to utilize in vitro cross-species metabolic stability data together with chemical stability information and chemical synthesis feasibility assessments to optimize placement of the radiolabel.

The dosing of radioisotopes to humans is done with the proper oversight with regard to the safety of the study participants. Guidance on the appropriate conduct of studies involving the administration of radiolabeled drugs to humans is set forth by 21 CFR § 361.1, which mandates protocol review by both an FDA-approved Radioactive Drug Research Committee (comprised of a physician specializing in nuclear medicine, a specialist in radiation dosimetry and/or safety, and at least three other medical experts) and an Institutional Review Board (39). Radiolabel studies are most frequently conducted in healthy volunteers, however, those where narrow therapeutic index agents (i.e., anticancer agents) are administered are generally conducted in patients (40). The amount of radioactivity given to subjects in a single dose must be as low as feasible to achieve study objectives without exceeding 3-rem exposure for whole body, active blood-forming organs, lens of the eye, and gonads; and 5-rem exposure for all other organs. Annually, these limits increase to 5 rem and 15 rem, respectively, for sponsors planning multiple-dose administration (which is less common than single-dose studies). Exposure to radioactivity in human is estimated by means of a dosimetry experiment using preclinical models, most often rat (35). In a dosimetry experiment, radioactivity exposure is measured for each tissue type either by direct quantitation in dissected organs (41) or whole-body autoradioluminography imaging techniques (41 45). A survey of major pharmaceutical companies (*circa* 1994) revealed that these guidelines translate to radioisotope doses ranging from 10 to 300 μCi for ^{14}C (100 μCi most commonly) and 50 to 1000 μCi for ^{3}H (35). Administration of a radiolabel dose is most often by the oral route, since the intended clinical route of dosing is oral for most small molecule drugs. Examples of IV (46 51) and dermal (52) administration are also present in the literature.

Though the data generated from a radiolabel human ADME study are key to understanding human disposition and metabolism of a drug candidate in vivo, the investments required to synthesize radiolabeled material and to perform the requisite dosimetry analysis are not trivial. Therefore, the timing of the radiolabel ADME study with respect to development stage may vary depending on the need to address scientific questions early (phase I) or the philosophy that the conduct of the study can be performed later (phase II). Purely from a scientific perspective, earlier would be ideal to utilize ADME data to design the development plan prospectively in terms of clinical DDI studies and metabolite monitoring strategies for toxicology and clinical studies. However, resource limitations or lower confidence in a high-risk (i.e., unvalidated) therapeutic target may dictate a later human ADME study (53). Naturally, the decision to collect in vivo human ADME data later in phase II carries with it a risk that unexpected findings may arise, resulting in program delays or termination of the candidate after more costly proof-of-concept clinical trials.

KEY DELIVERABLES OF THE RADIOLABEL HUMAN ADME STUDY AND EXAMPLES

Radiolabel human ADME studies provide insight into the disposition and metabolism of a drug candidate in three primary ways: (*i*) determination of mass balance of the drug and drug-related material; (*ii*) characterization of routes of elimination and clearance

mechanisms of the drug; and (*iii*) identification and quantitation of drug metabolites in circulatory and excretory matrices. Each element of the study is discussed in detail in this section with specific examples to highlight both typical findings and unexpected outcomes at the conclusion of the study. Details and recommendations regarding the design and conduct of the studies, with specifics about sample workup and analysis, are reviewed elsewhere (40,53).

Mass Balance

The most straightforward human ADME deliverable is the determination of mass balance. Careful characterization of the dose administered to each subject measured against the total recovery of radioactivity in excretory matrices from each subject determines this outcome. If total recovery approaches or exceeds 85% to 90% of dose, the consensus in the ADME discipline would be that mass balance is complete (40,53,54). Celecoxib (Celebrex®), a well-known cyclooxygenase-2 inhibitor, was administered to eight healthy volunteers at a 300-mg dose containing approximately 100 μCi of ^{14}C-labeled drug (55). Total recovery of dose was an acceptable 85%, with 27% excreted in urine and 58% excreted in feces. Profiling of these matrices revealed metabolism as the major clearance route with only three major metabolites. In the case of valdecoxib (Bextra®), a closely related analog with similar pharmacology, a 50-mg dose containing 100 μCi of ^{14}C-labeled drug was administered as a single dose to eight volunteers, and 94% recovery was achieved (76% in urine and 18% in feces). Valdecoxib exhibited more extensive metabolism than celecoxib, with $>$10 metabolites observed; nonetheless, complete recovery was achieved. Therefore, in the absence of other factors, the degree of metabolism is not necessarily a determinant of recovery (note: for valdecoxib the majority of radioactivity in the form of metabolites was excreted in urine). Together, celecoxib and valdecoxib are representative of a large number of human ^{14}C mass balance studies with successful recoveries (36).

Potential reasons for lower recovery in a human radiolabel ADME study include limitations brought about by the excretion profile of the investigational drug and the pharmacology related to the drug and its target. Imatinib (Gleevec®), a tyrosine kinase inhibitor effective in the treatment of certain cancers, was administered at a 200-mg dose (free base equivalent) containing 32 μCi of ^{14}C drug (56). Recovery of radiolabeled dose hit a plateau by day 7, and continued collections through day 11 resulted in little additional radioisotope retrieval. At the end of the study, approximately 68% of drug-related material was found in feces and approximately 13% in urine, with total recovery lower than the consensus 85% goal. Investigators hypothesized that recovery was limited by a slow terminal elimination half-life in feces estimated at three weeks. A likely driving force behind the prolonged fecal elimination was the concurrent observation that the terminal half-life of radioactivity in plasma was 57 hours, suggesting that excretion would continue via the fecal route for a protracted period. This is consistent with data tabulated from a review of radiolabeled ADME studies that demonstrated an inverse relationship between plasma half-life and recovery of total dose (36). It was shown that compounds exhibiting radioactivity plasma half-lives of $<$50 hours achieved mass balance (defined as $>$85% recovery) about 80% of the time, meaning those compounds with radioactivity half-lives in plasma exceeding 50 hours (like imatinib) were much less likely to achieve full recovery.

Aside from technical challenges associated with recovery in the fecal matrix (e.g., intersubject variability in time course of excretion, high sample mass, sample consistency, etc.), additional reasons cited for low mass balance recoveries were tissue sequestration,

phospholipid affinity, and subject compliance. Alendronate (Fosamax®), a bisphosphonate inhibitor of osteoclast-mediated bone resorption used in the treatment of osteoporosis, provides a good example of tissue sequestration limiting recovery of a radiolabeled dose as a result of pharmacology (51). Clinically relevant alendronate doses given in animal models revealed unsaturable uptake in bone tissue, the site of action, with estimated elimination half-lives of >200 days in rats and 1000 days in dogs (57). In these species, approximately half of the administered dose was excreted unchanged in urine. In human, a pharmacokinetic study at a 30 mg/kg IV dose (7.5 mg/day × 4 consecutive days; unlabeled drug) revealed prolonged urinary excretion similar to preclinical species with detectable drug 18 months after dosing (58). A follow-on clinical investigation was subsequently carried out in the context of a ^{14}C ADME study (performed in oncology patients), where a 10-mg IV dose containing 26 μCi ^{14}C-labeled alendronate was administered to 12 subjects (51). Observations from the earlier pharmacokinetic study were confirmed, as 47% of the radiolabeled dose was recovered in urine within three days and negligible dose was excreted in feces. Incomplete recovery was attributed to a high degree of distribution to bone. In comparison with alendronate, tigecycline (Tygacil®), a first-in-class glycylcycline antibiotic, distributed extensively to bone in rats after a single IV dose (59). A human tigecycline ADME study was subsequently conducted with a radiolabeled dose (50 μCi IV) administered to six study subjects who had been previously given non-labeled compound to reach steady state (49). In this case, recovery was considered complete (excluding two subjects who had incomplete fecal sample collection), with 92% of total dose excreted predominantly in feces and more sparingly in urine. These findings demonstrate that, in contrast to alendronate, saturable tissue distribution of tigecycline may be overcome by dosing to steady state prior to administration of the labeled dose to improve mass balance recovery.

Molecules that form covalent bonds with their therapeutic target, or other proteins nonspecifically, may represent a challenge in terms of definitive mass balance. As a class, thiol-containing angiotensin-converting enzyme (ACE) inhibitors generally exhibit lower recoveries than other non-thiol compounds. The free thiol present in this group of ACE inhibitors binds to the zinc atom at the active site of the enzyme and is important with respect to mechanism of action. However, free thiols also react with sulfur-containing moieties present in other proteins and small molecules, which serves as the basis for concern in terms of recovery of drug-related material. With no requirement for bioactivation processes, the entire dose is available to form disulfide linkages or react with endogenous molecules in other ways (i.e., nucleophilic addition reactions). The investigational drug gemopatrilat, a more recent entry to the thiol-containing ACE inhibitor class, was dosed orally to humans at a dose of 50 mg containing 112 μCi of ^{14}C-labeled drug (60). A sustained presence of total radioactivity was observed in plasma (half-life of 85 hours), and only 77% of the administered dose was recovered. Investigators specified that approximately half of the drug-derived radioactivity in circulation was bound via disulfide bonds to protein, as determined by extraction recovery experiments in the presence and absence of reducing equivalents. This was likely the main cause for low recovery of gemopatrilat, and was also suspected to limit recovery of omapatrilat (61) and captopril (Capoten®) (62). In contrast to free thiol-containing pharmaceutical agents, compounds that require metabolic bioactivation to generate thiol-containing metabolites that bind to proteins in circulation (or in tissues) tend to exhibit much higher recoveries. Clopidogrel (Plavix®) is a thienopyridine compound that antagonizes platelet aggregation by means of binding to the platelet $P2Y_{12}$ receptor via disulfide linkage (63). Unlike gemopatrilat, clopidogrel requires CYP-mediated biotransformation to convert the thienopyridine moiety to one exhibiting a free thiol

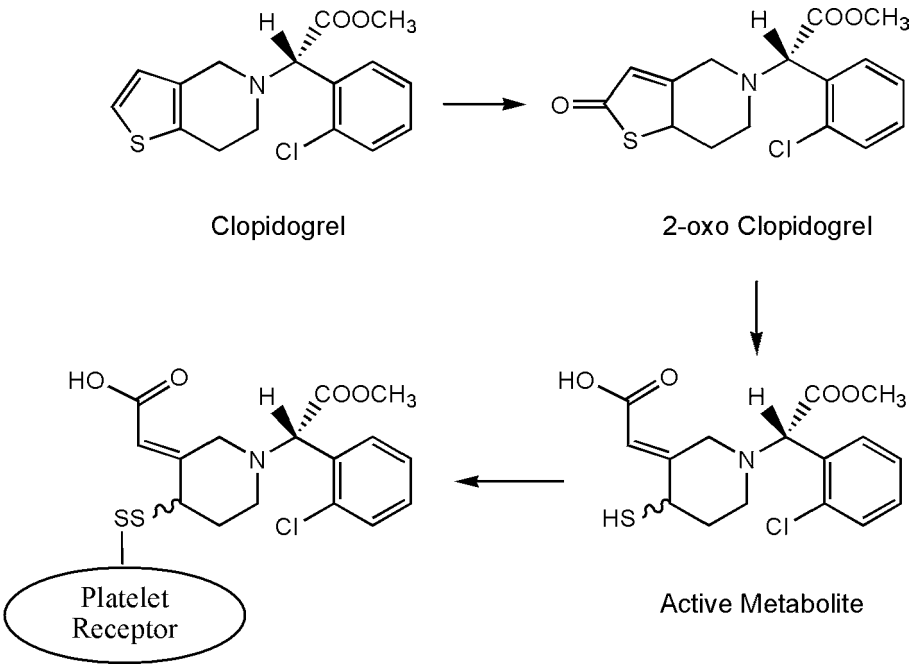

Figure 2 Formation of the active metabolite of clopidogrel and disulfide bond formation with the target receptor on platelets. *Source*: From Ref. 63.

the active form of the drug (Fig. 2). [^{14}C]Clopidogrel human ADME studies were conducted in six healthy volunteers at a dose of 75 mg containing 76 μCi radiolabeled drug (64). Despite the established on-mechanism covalent binding to $P2Y_{12}$ receptor (and presumably other circulatory components), mass balance was achieved at a level of 92% of dose, excreted almost equally in urine and feces. Terminal half-life in plasma was a prolonged 338 hours. Prasugrel (Effient®), an irreversible $P2Y_{12}$ inhibitor very similar in nature to clopidogrel, is also essentially a prodrug that requires both hydrolysis and CYP activity to transform it into a free thiol (65,66). In a study utilizing [^{14}C]prasugrel administered as an oral dose of 15 mg (containing 100 μCi radioactivity), 95% mass balance was achieved with the majority of recovery occurring in urine. Like clopidogrel, a substantial fraction of radioactivity in plasma was covalently bound to protein and the terminal radioactivity half-life in plasma was $>$180 hours.

Aside from thiol-containing compounds, the investigational drug maxipost (BMS-204352) for treatment of ischemic stroke serves as an example of metabolic activation involving covalent bond formation to plasma proteins via a mechanism other than disulfide bond formation. CYP-mediated O-demethylation of maxipost forms a phenol that undergoes subsequent CYP-mediated bioactivation to generate a quinone methide, which was shown to bind covalently to macromolecules in rats (67), as shown in Figure 3. In humans, IV dosing of 10 mg of maxipost containing 50 μCi ^{14}C-labeled drug resulted in 97% recovery over 14 days (37% in urine and 60% in feces) (68). In this case, significant covalent binding to plasma protein (particularly at later time points) coincided with a terminal plasma half-life in excess of 250 hours, which together did not limit radioactivity excretion to the extent it would cause low mass balance recovery. Overall, compounds that initially contain a protein-reactive functional group (e.g., thiol) tend to stand a poor chance of achieving mass balance, perhaps because of the high fraction of

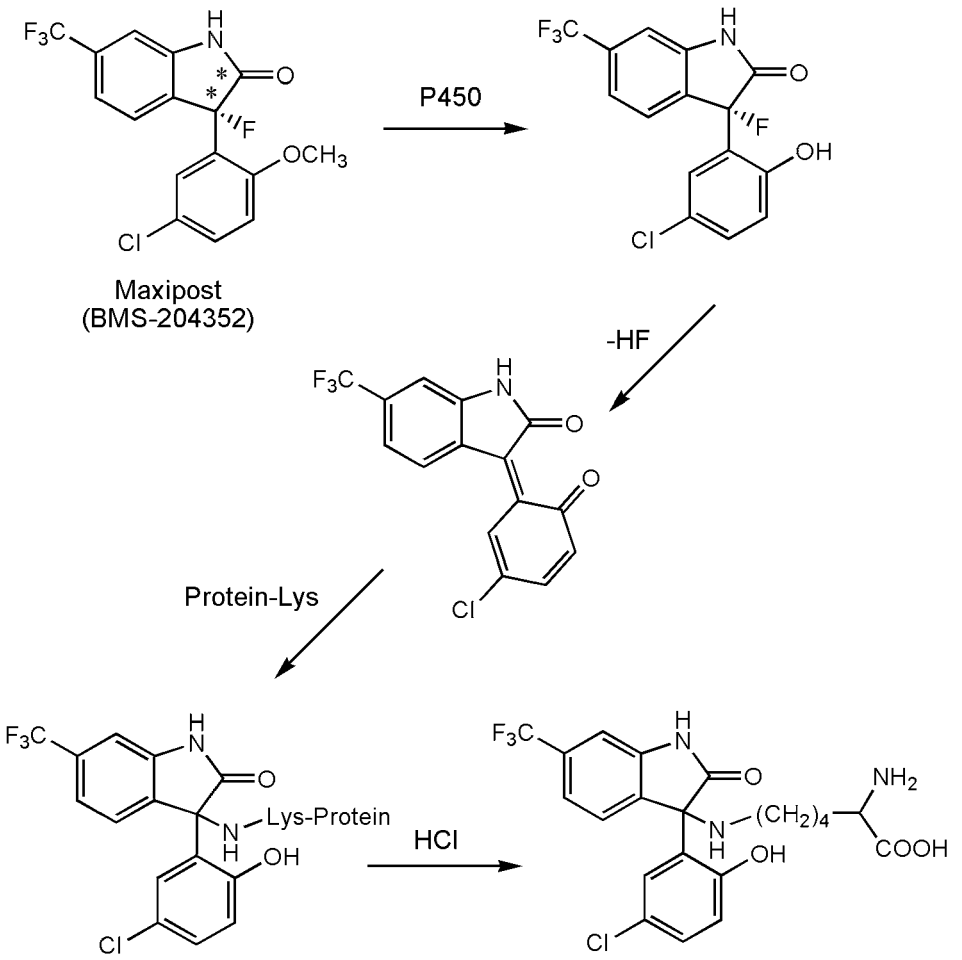

Figure 3 Proposed bioactivation of maxipost (BMS 204352) via cytochrome P450 mediated oxidation and covalent binding to protein lysine residues in vivo. *Source*: From Ref. 67.

dose available for covalent binding. Conversely, for compounds where bioactivation is a prerequisite for covalent binding, it is more likely that a lower fraction of dose is cleared exclusively via bioactivation and complete recovery is commonly observed. Additional examples of compounds known to undergo bioactivation (and exhibit toxicity) are summarized in a comprehensive review focusing on mass balance outcomes in preclinical and human species (36). A consensus view is that low recovery in a mass balance study is not a reliable indicator of an in vivo bioactivation clearance pathway.

Characterization of Drug Clearance

A second major deliverable from the radiolabel human ADME study is the characterization of drug clearance. This assessment mainly involves the quantitative determination of whether the administered dose is primarily excreted unchanged, or whether the majority of dose is excreted in the form of metabolites. When metabolism is a primary clearance route, the identity of the metabolites is expected to provide insight into the classes of enzymes responsible. A thorough example of the characterization of metabolic

clearance in the design and conduct of a radiolabel human ADME study can be seen with the investigational drug traxoprodil, a potential treatment for the prevention of neuronal death associated with brain injury (48). Typical of CNS drugs, traxoprodil contains a tertiary basic amine as part of a lipophilic scaffold a common feature in CYP2D6 substrates. In light of this and the intersubject variability in pharmacokinetic behavior observed during early phase I clinical trials, the investigators chose to examine the role of CYP2D6 in the metabolic clearance of traxoprodil in vitro and in vivo, enrolling both PM and EM CYP2D6 phenotypes in a ^{14}C ADME study. In vitro data showed a relatively low microsomal K_m of 1.7 μM (V_{max} of 0.66 nmol/nmolP450/min), and confirmation of a major contribution to in vitro metabolism by CYP2D6 was made on the basis of correlation analyses, inhibition of microsomal turnover by quinidine, and traxoprodil metabolism by recombinant enzyme. In vivo data generated from a single IV infusion of a 50-mg (100 μCi) dose revealed lower mass balance recovery in EM subjects when compared with PM subjects (61% and 89%, respectively), with the majority of drug-related material excreted in urine. Metabolite profiling in urine from PM subjects revealed predominantly parent drug and its direct glucuronide conjugate (M6), while EM subjects displayed only low levels of unchanged parent drug accompanied by two major metabolites (M7 and M14) formed via CYP-mediated oxidation and subsequent phase II metabolic processes (Fig. 4). Plasma and fecal matrices further demonstrated an abundance of phase I metabolites (and their conjugates) in EMs, while metabolites in PMs arose mainly from phase II conjugation of traxoprodil itself. Quantitative recovery of individual metabolites as a percentage of dose in EM and PM subjects is summarized in Table 1. With regard to persistence of drug in circulation, traxoprodil had a 3-hour half-life in EM subjects and a much longer 27-hour half-life in PM subjects. Interestingly, in EMs, plasma half-life of total radioactivity was estimated to be >140 hours, which by comparison with other previously mentioned examples may partly explain the low recovery in these subjects. Overall, the results of the in vivo study highlighted the role of metabolism in the clearance of traxoprodil, most importantly contributions by CYP2D6 as a key enzyme in the metabolic pathway.

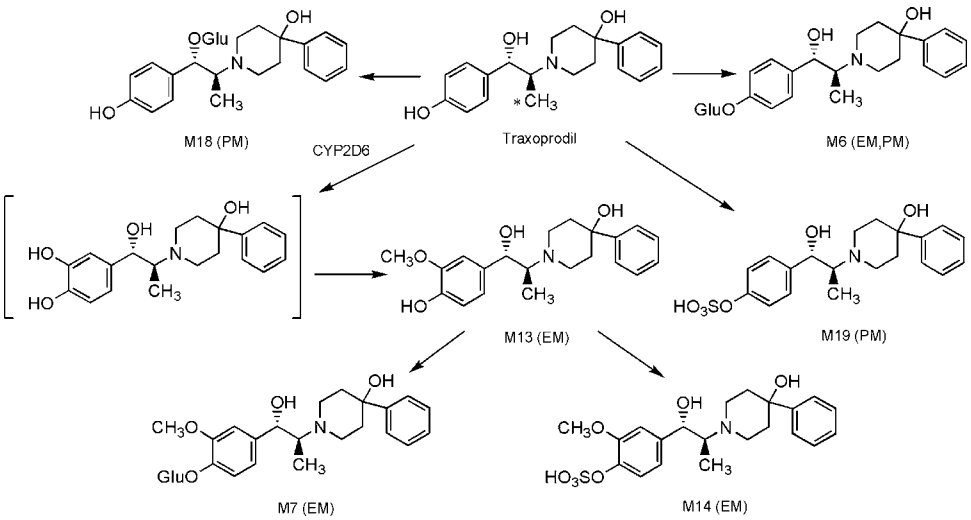

Figure 4 Metabolism of traxoprodil in human CYP2D6 extensive metabolizer (EM) and poor metabolizer (PM) phenotypes. *Abbreviation*: CYP, cytochrome P450. *Source*: From Ref. 48.

Table 1 Mean Recoveries of Traxoprodil and Its Metabolites in Human Cytochrome P4502D6 Extensive Metabolizer (EM) and Poor Metabolizer (PM) Phenotypes

	Mean recovery (% administered dose)	
Components	EM subjects ($n = 4$)	PM subjects ($n = 2$)
M6	0.68	25
M7	8.8	ND
M13	2.8	ND
M14	39	ND
M18	ND	1.4
M19	ND	12
Traxoprodil	7.1	50

Abbreviation: ND, not detected.
Source: Adapted from Ref. 48.

A heavy reliance on any single clearance pathway increases the risk of a pharmacokinetic DDI (69). The traxoprodil example further serves to demonstrate the added value of the ^{14}C ADME study where, in the absence of a specific clinical DDI study, insight may be gained into the potential for a meaningful DDI. As a comparison of the PM and EM data indicated, reduced capacity for CYP2D6-mediated metabolism was directly linked to increased traxoprodil exposure in circulation for the PM subjects (48). Therefore, coadministered agents with a more potent CYP2D6 interaction (with respect to K_m) may be expected to affect traxoprodil exposure similarly. Such data are very valuable in the development process as they are an important factor in assessing the clinical utility of a compound with regard to the kinds of therapeutic agents likely to be coadministered. In the case of traxoprodil and at least one other investigational agent (70), enrollment of a special population in the radiolabel study (CYP2D6 PMs) allowed for a quantitative assessment of the role of a specific enzyme and its potential for pharmacokinetic DDI in human.

Biliary excretion and its contribution to clearance is directly measurable in radiolabel ADME studies in preclinical species because of the availability of bile duct cannulated animals. In human, this information is far more challenging to obtain, leaving investigators to infer human biliary clearance on the basis of cross-species extrapolation and/or characterization of drug-related material in feces collected during a standard radiolabel human ADME study. While this method is potentially simplified when dosing occurs through the IV route, most compounds are dosed orally where it is impossible to distinguish unabsorbed dose in feces from that excreted unchanged in bile or that secreted in the intestine. Recent advances in medical technology involving the use of oroentric or modified nasogastric tubes (14), however, have led to a nonsurgical method of obtaining bile from healthy subjects participating in radiolabel studies (see sect. "Clinical Drug Metabolism with Non-Radiolabeled Drug"). Such a technique was applied to the investigation of montelukast (Singulair®) (71). Two cohorts were enrolled in a ^{14}C radiolabel study; one was orally administered a 102-mg dose (84 μCi) and another was orally administered a 55-mg dose (122 μCi). The first cohort was studied in accordance with a "typical" protocol, while the second underwent bile collection for either a 2- to 8-hour interval post dose (fasted) or a 6- to 12-hour interval postdose (fed). Results from the second cohort demonstrated little biliary excretion of parent drug with much more significant levels of oxidative montelukast metabolites in bile, thereby confirming metabolism as the primary contributor to clearance of absorbed dose. Results from the

"typical" study design followed in the first cohort showed trace recovery of dose in urine and 86% recovery in feces, consistent with biliary excretion of absorbed dose (in the form of metabolites) and fecal excretion of unabsorbed drug. By collecting bile in the second cohort, investigators were also able to characterize biliary metabolites in the absence of any influence from metabolism by intestinal microbes. Though similar data may have been obtained by utilizing surgical cholecystectomy candidates or patients with biliary T-tubes [as in the case of atorvastatin (Lipitor®) (72) and irinotecan (73)], these special patient populations may present additional challenges due to either enrollment difficulty or the nature of their preexisting conditions.

Another example of a radiolabel human ADME study that included bile collection utilizing a method similar to the montelukast study involved the investigational dual PPARα/γ activator, muraglitazar (74,75). In the case of muraglitazar, radiolabel ADME studies in preclinical species showed a significant role for glucuronidation in the clearance of the drug, as evidenced by high levels of glucuronides in bile from these species. Interestingly, fecal extracts showed little in the way of glucuronides, presumably as a result of gluronidase activity present in gut microbes or chemical instability. Of particular interest was acyl glucuronide formation at the carboxylic acid moiety, which was readily detected in bile but proved elusive in the fecal matrix. Investigators sought confirmation of in vivo acyl glucuronide formation in humans, choosing to sample bile during the course of a [^{14}C]muraglitazar study. A single 20-mg (103 μCi) oral dose was administered to study participants, with collection of bile, urine, feces, and plasma. Feces was determined to be the major route of elimination of drug-related material (>90%), with urine playing only a very minor role (<5%). Total recovery of radiolabeled dose was approximately 94% in both bile-sampled subjects and those with conventional collection. Human bile contained a substantial fraction of administered dose (40%), and many of these components were found to be acyl glucuronides. These data confirmed a role for glucuronidation in the clearance of muraglitazar that may otherwise have gone underestimated if fecal elimination had been relied upon solely, as feces contained either low or undetectable levels of these metabolites.

Identification of Circulating Metabolites

The third major deliverable derived from radiolabel human ADME data is the identification and quantitation of drug metabolites in systemic circulation. As mentioned in the previous section, the identity of metabolites present in any matrix provides essential information about the biotransformation pathways involved in the clearance of an NCE. However, circulating metabolites in plasma (or blood) generally receive a higher degree of attention as they contribute to systemic exposure. If active, metabolites in circulation may help drive the intended pharmacological effect, or cause toxicity by exaggeration of on-target pharmacology. Conversely, toxicity may be the result of unintended off-target pharmacology or chemical toxicity. Recent FDA guidance focusing specifically on metabolite-related toxicity (described in detail in sect. "Introduction" and see chap. 24) sets forth the expectation that any metabolite in circulation at levels exceeding 10% of parent drug exposure must be independently evaluated for toxicity *unless* coverage can be verified in preclinical toxicology studies. The value of radiolabel in this regard is that contributions of each metabolite to circulating radioactivity can be quantitatively assessed cross species to distinguish any metabolites in human that are not adequately covered in preclinical toxicology studies. Upon confirmation of structural identity, metabolites can be synthesized, if necessary, and tested in accordance with FDA guidance. CP-122721, an investigational neurokinin-1 (NK1) receptor antagonist evaluated for the treatment of

various neurological conditions, was administered to healthy volunteers as part of a radiolabel human ADME study (70). A 30-mg (100 μCi) [^{14}C]CP-122721 dose was extensively metabolized, with recovery of radiolabeled drug primarily in urine (>70%) in the form of several oxidative metabolites. One of these, a carboxylic acid cleavage product (5-trifluoromethoxy salicylic acid) formed via O-demethylation, N-dealkylation, and subsequent oxidation, was only a minor component accounting for <5% of the administered dose. A potentially unimportant metabolite at first glance, investigators determined that this low level excretory component was present in circulation as a major contributor to circulating radioactivity (>50% in EM subjects and 29% in PM subjects), far exceeding parent drug levels. Complete mass spectral and NMR characterization definitively established the identity of this important metabolite, which was subsequently confirmed with synthetic standard. Though inactive in terms of NK1 antagonism, off-target toxicity associated with this metabolite could not be excluded since it was not observed in preclinical toxicology species (76). In the case of CP-122721, the radiolabel human ADME study led to the discovery of a significant human-specific metabolite due to its systemic exposure in circulation. Such a finding would likely require further evaluation according to current FDA guidance.

CURRENT AND EMERGING TECHNOLOGIES APPLIED IN CLINICAL DRUG METABOLISM STUDIES

Current practice for the quantification of unlabeled analytes and the structure elucidation of metabolites employs the use of LC coupled with atmospheric pressure ionization (API) MS/MS, collectively abbreviated LC-API/MS/MS. Where radioisotopes are assayed, in-line radiochemical flow detectors are readily integrated into these analytical systems to aid in metabolite identification efforts. High performance liquid chromatography (HPLC) is the most common front-end LC separation technology used for small molecules in combination with MS analysis, with ultrahigh performance liquid chromatography (UPLC) gaining favor in applications where better peak resolution and shorter analysis times (via higher pressures) are preferred. The most widely used API technique for drug-like analytes is electrospray ionization (ESI), since it is well suited for ionization of molecules in the liquid state as they exit the LC system and enter the ion source of the MS instrument. In addition to ESI, atmospheric pressure chemical ionization (APCI) is important for certain analytes (most notably steroids), where ionization occurs by chemical reaction in the gas phase. Tandem MS experiments following ion formation can be performed in a variety of ways, as advances in technology relating to ion optics continue to introduce powerful new MS instruments to the ADME laboratory. Perhaps the most versatile and ubiquitous platform is the triple quadrupole mass spectrometer (TQMS), which is both an exemplary quantitative instrument and a qualitative metabolite ID cornerstone. Recently developed linear ion trap instruments like the Q-Trap™ and LTQ™ are ideal for metabolite identification applications given their MS^3 and MS^n and capabilities, respectively. Finally, quadrupole time-of-flight (Q-TOF) and Orbitrap™ instruments bring high-resolution MS capabilities to bear when more definitive elemental composition data for metabolites and their fragment ions are required. Interestingly, high-resolution instruments are also being utilized to more selectively distinguish drug-related material from biological background by means of mass defect filtering techniques (77 80), and therefore may become more widely utilized in earlier FIH exploratory applications in addition to later definitive studies. More detailed reviews of these technologies, and others, associated with drug metabolism studies have been published recently (81 83). Overall,

LC-API/MS/MS technology encompasses a variety of instrument platforms and experimental approaches that may be viewed as complimentary to one another. The specialized ADME analytical laboratory is best served if all these tools are available and applied according to the needs of the challenge at hand.

Despite the availability of numerous MS platforms ranging from unit mass to high resolution, the ability to unequivocally identify metabolites using MS technology is ultimately limited by the nature of the metabolite and the extent to which its tandem MS (or MS^n) fragments are informative with respect to structure. Definitive structure elucidation often requires NMR spectroscopy for correct assignment of stereochemical or isomeric configurations, which are rarely readily apparent on the basis of MS data alone. ^1H and ^{13}C nuclei are among the more common targets for NMR experiments, which by virtue of either homonuclear or heteronuclear design are well suited to establish bond connectivity and molecular structure if adequate sample is available. Particularly in cases where metabolites are of high interest either because of their relative abundance or potential for toxicity, definitive structure assignment is critical and underlies the importance of close alignment between ADME scientists and the NMR spectroscopist. For additional discussion, the reader is directed to chap. 15.

When the use of radiolabel is employed in clinical ADME studies, quantitation of drug-related material in biological matrices is most commonly performed by standard LSC techniques. Using traditional LSC methodologies, detection and quantification of radioisotope is a function of radioactive decay (disintegrations), and robust measurements require a reasonable quantity of material (doses in the μCi range) and/or sufficiently long counting times to accurately determine disintegrations per minute. Though history has proven this approach to be widely successful, continued efforts to reduce the levels of radioactivity dosed to humans (and to minimize radioactive waste) have recently led to the utilization of a technology platform new to the ADME field. With its roots in carbon dating and varied earth science applications, AMS directly measures $^{14}C/^{12}C$ radioisotope ratios at the atomic level with no dependence on isotope decay for detection (84,85). Biological samples are oxidized completely to CO_2, which may be analyzed directly or subsequently reduced to solid carbon prior to being subjected to ionization by a cesium sputter source, mass selection, collision at high voltage to break down carbon hydride isobars (e.g., $^{12}CH_2$, ^{13}CH), and detection. Using AMS, samples containing approximately 1 mg of carbon can be reliably assayed for ^{14}C at attomole (10^{-18}) levels with good accuracy and precision. At such low isotope levels, LSC detection would not be a viable option, since decay of ^{14}C nuclei would occur less frequently than 1/hr (85). This enhanced sensitivity relative to conventional radiometric detection has allowed for administration of ^{14}C doses on the order of 100 nCi in preclinical and human radiolabel ADME studies, which is far below doses used in conventional ADME experiments (84). The benefit of lower, "trace" level doses is that they are similar to the naturally occurring ^{14}C levels in human (84) and generally do not require dosimetry calculations (86). Therefore, these truly minimal radiolabel doses facilitate earlier timing for definitive ADME studies in human, if desired. In addition to ^{14}C, AMS has also been adapted to measure trace quantities of other radioisotopes like ^3H (87,88), making it a versatile technology for many biopharmaceutical and toxicological applications.

AMS validation studies and applications in ADME and toxicology experiments have been described in the literature regularly in the past several years. A comparison of conventional LSC analysis and AMS detection of [^{14}C]fluconazole (Diflucan®) and [^{14}C] fluticasone (Flonase®) in circulatory, urinary, and fecal matrices from human and rat revealed good agreement between the two approaches (89). In one experiment, samples analyzed by LSC required nearly 12,000-fold dilution prior to AMS analysis, where a

similar result was achieved. AMS was subsequently used in a clinical study to establish a 94% mass balance recovery of an investigational farnesyl transferase inhibitor, R115777, administered at a dose of 50 mg containing only 34 nCi of radioactivity (90). Profiles of drug and human metabolites (reconstructed from LC fractions) were also obtained in urine, feces, and plasma. Similar success was observed with ixabepilone (Ixempra®), a microtubule stabilizing agent, which achieved a recovery of 77% dose after administration of only 80 nCi of radiolabel (70 mg) (91). Investigators measured total plasma ^{14}C pharmacokinetics by AMS and ixabepilone pharmacokinetics by LC-MS/MS to establish a major contribution to circulating ^{14}C by yet unidentified metabolites. AMS was also successfully utilized in the determination of nelfinavir (Viracept®) bioavailability in humans (92), and for the quantitation of in vivo DNA adduct formation in human colon tissue after administration of tamoxifen (Nolvadex®) (93). DNA adducts were also observed in rodents using AMS technology after the dosing of various halogenated hydrocarbons (94).

Looking forward, both regulatory drivers (FDA guidance on "Safety Testing of Metabolites") and technology developments (LC-MS/MS and AMS) continue to provide added impetus for early human ADME studies through implementation of microdosing strategies. While drug metabolism scientists working within this environment recognize the need for high quality, progressive science and push for rigorous characterization of NCEs on the registration pathway, caveats remain to the general application of microdosing in clinical drug metabolism studies. Firstly, administration of microdose quantities of an NCE may only provide insight into pharmacokinetic behavior and metabolism characteristics of a molecule that are relevant at very low (i.e., non-pharmacological) doses. Without a complete understanding of whether clearance processes are linear or nonlinear across a wide dose range, there are risks associated with heavy reliance on microdose data in early development. Recent studies have been conducted to evaluate dose linearity between microdoses and more pharmacologically relevant doses (95 97), and though for some compounds linearity has been demonstrated, it is likely that this evaluation will need to be made on a compound-by-compound basis to provide proper context for microdose data. Secondly, enabling AMS technology is not widely available commercially and lacks an LC interface, making routine analyses cumbersome because of the need for fraction collection and sample shipment. Whether or not microdoses will routinely provide sufficient metabolite quantities for more definitive metabolite characterization by standard LC-MS/MS techniques or NMR is also unclear. What remains certain is that clinical drug metabolism studies provide key information about the disposition of potential drug molecules that may impact the evaluation of their safety and efficacy. Earlier characterization of human ADME properties, perhaps even in the context of exploratory Investigational New Drug Application (IND) (eIND) filings, may ultimately become routine for compounds or programs where this information forms the basis of critical success factors.

REFERENCES

1. Guidance for Industry Safety Testing of Drug Metabolites, Center for Drug Evaluation and Research (CDER), Food and Drug Administration, U.S. Department of Health and Human Services, 2008:1 14. Available at: http://www.fda.gov/cder/guidance/6897fnl.pdf. Accessed April 2008.
2. Prueksaritanont T, Lin JH, Baillie TA. Complicating factors in safety testing of drug metabolites: kinetic differences between generated and preformed metabolites. Toxicol Appl Pharmacol 2006; 217(2):143 152.

3. Hochman JH, Pudvah N, Qiu J, Yamazaki M, Tang C, Lin JH, Prueksaritanont T. Interactions of human P glycoprotein with simvastatin, simvastatin acid, and atorvastatin. Pharm Res 2004; 21(9):1686 1691.
4. Baillie TA, Cayen MN, Fouda H, Gerson RJ, Green JD, Grossman SJ, Klunk LJ, LeBlanc B, Perkins DG, Shipley LA. Drug metabolites in safety testing. Toxicol Appl Pharmacol 2002; 182 (3):188 196.
5. Smith DA, Obach RS. Metabolites and safety: what are the concerns, and how should we address them? Chem Res Toxicol 2006; 19(12):1570 1579.
6. Mei Q, Tang C, Assang C, Lin Y, Slaughter D, Rodrigues AD, Baillie TA, Rushmore TH, Shou M. Role of a potent inhibitory monoclonal antibody to cytochrome P 450 3A4 in assessment of human drug metabolism. J Pharmacol Exp Ther 1999; 291(2):749 759.
7. Mei Q, Tang C, Lin Y, Rushmore TH, Shou M. Inhibition kinetics of monoclonal antibodies against cytochromes P450. Drug Metab Dispos 2002; 30(6):701 708.
8. Lin JH, Wong BK. Complexities of glucuronidation affecting in vitro in vivo extrapolation. Curr Drug Metab 2002; 3(6):623 646.
9. Davis TM, Hung TY, Sim IK, Karunajeewa HA, Ilett KF. Piperaquine: a resurgent antimalarial drug. Drugs 2005; 65(1):75 87.
10. Tarning J, Bergqvist Y, Day NP, Bergquist J, Arvidsson B, White NJ, Ashton M, Lindegardh N. Characterization of human urinary metabolites of the antimalarial piperaquine. Drug Metab Dispos 2006; 34(12):2011 2019.
11. Balani SK, Arison BH, Mathai L, Kauffman LR, Miller RR, Stearns RA, Chen IW, Lin JH. Metabolites of L 735,524, a potent HIV 1 protease inhibitor, in human urine. Drug Metab Dispos 1995; 23(2):266 270.
12. Balani SK, Woolf EJ, Hoagland VL, Sturgill MG, Deutsch PJ, Yeh KC, Lin JH. Disposition of indinavir, a potent HIV 1 protease inhibitor, after an oral dose in humans. Drug Metab Dispos 1996; 24:(12):1389 1394.
13. Lin JH, Chiba M, Balani SK, Chen IW, Kwei GY, Vastag KJ, Nishime JA. Species differences in the pharmacokinetics and metabolism of indinavir, a potent human immunodeficiency virus protease inhibitor. Drug Metab Dispos 1996; 24(10):1111 1120.
14. Ghibellini G, Leslie EM, Brouwer KL. Methods to evaluate biliary excretion of drugs in humans: an updated review. Mol Pharm 2006; 3(3):198 211.
15. Ghibellini G, Bridges AS, Generaux CN, Brouwer KL. In vitro and in vivo determination of piperacillin metabolism in humans. Drug Metab Dispos 2007; 35(3):345 349.
16. Ghibellini G, Johnson BM, Kowalsky RJ, Heizer WD, Brouwer KL. A novel method for the determination of biliary clearance in humans. AAPS J 2004; 6(4):e33.
17. Fura A. Role of pharmacologically active metabolites in drug discovery and development. Drug Discov Today 2006; 11(3 4):133 142.
18. Floren LC, Berry K, Tonn GR, Ye Q, Wright M, Huang AX, Wang X, Marcus A, Johnson M, Collins T, Medina J, Kersey K. T0906487 (T487), a novel CXCR3 antagonist: first time in human study of safety and pharmacokinetics. In: 6th Annual World Congress of Inflammation, Vancouver, B.C., Canada, 2003.
19. Houston JB. Drug metabolite kinetics. Pharmacol Ther 1981; 15(3):521 552.
20. Benet LZ, Oie S, Schwartz JB. Design and optimization of dosage regimens: pharmacokinetic data. In: Hardman JG, Limbird LE, Molinoff PB, et al., eds. The Pharmcological Basis of Therapeutics. 9th ed. New York: McGraw Hill, 1995:1707 1792.
21. Slattery JT, Wilson JM, Kalhorn TF, Nelson SD. Dose dependent pharmacokinetics of acetaminophen: evidence of glutathione depletion in humans. Clin Pharmacol Ther 1987; 41 (4):413 418.
22. Wang LH, Peck RW, Yin Y, Allanson J, Wiggs R, Wire MB. Phase I safety and pharmacokinetic trials of 1263W94, a novel oral anti human cytomegalovirus agent, in healthy and human immunodeficiency virus infected subjects. Antimicrob Agents Chemother 2003; 47 (4):1334 1342.
23. Koszalka GW, Johnson NW, Good SS, Boyd L, Chamberlain SC, Townsend LB, Drach JC, Biron KK. Preclinical and toxicology studies of 1263W94, a potent and selective inhibitor

of human cytomegalovirus replication. Antimicrob Agents Chemother 2002; 46(8): 2373 2380.
24. Goldwater DR, Dougherty C, Schumacher M, Villano SA. Effect of ketoconazole on the pharmacokinetics of maribavir in healthy adults. Antimicrob Agents Chemother 2008; 52(5): 1794 1798.
25. Chladek J, Zimova G, Beranek M, Martinkova J. In vivo indices of CYP2D6 activity: comparison of dextromethorphan metabolic ratios in 4 h urine and 3 h plasma. Eur J Clin Pharmacol 2000; 56(9 10):651 657.
26. Christensen M, Andersson K, Dalen P, Mirghani RA, Muirhead GJ, Nordmark A, Tybring G, Wahlberg A, Yasar U, Bertilsson L. The Karolinska cocktail for phenotyping of five human cytochrome P450 enzymes. Clin Pharmacol Ther 2003; 73(6):517 528.
27. Ring BJ, Gillespie JS, Eckstein JA, Wrighton SA. Identification of the human cytochromes P450 responsible for atomoxetine metabolism. Drug Metab Dispos 2002; 30(3):319 323.
28. Mullen JH, Shugert RL, Ponsler GD, Li Q, Sundaram B, Coales HL, Yakupkovic JE, Lelacheur RM, Wheeler WJ, Belas FJ, Sauer JM. Simultaneous quantification of atomoxetine as well as its primary oxidative and O glucuronide metabolites in human plasma and urine using liquid chromatography tandem mass spectrometry (LC/MS/MS). J Pharm Biomed Anal 2005; 38(4):720 733.
29. Sauer JM, Ponsler GD, Mattiuz EL, Long AJ, Witcher JW, Thomasson HR, Desante KA. Disposition and metabolic fate of atomoxetine hydrochloride: the role of CYP2D6 in human disposition and metabolism. Drug Metab Dispos 2003; 31(1):98 107.
30. Martino R, Gilard V, Desmoulin F, Malet Martino M. Fluorine 19 or phosphorus 31 NMR spectroscopy: a suitable analytical technique for quantitative in vitro metabolic studies of fluorinated or phosphorylated drugs. J Pharm Biomed Anal 2005; 38(5):871 891.
31. Bernadou J, Martino R, Malet Martino MC, Lopez A, Armand JP. Fluorine 19 NMR: a technique for metabolism and disposition studies of fluorinated drugs. Trends Pharmacol Sci 1985; 6 (3):103 105.
32. Wade KE, Wilson ID, Troke JA, Nicholson JK. 19F and 1H magnetic resonance strategies for metabolic studies on fluorinated xenobiotics: application to flurbiprofen [2 (2 fluoro 4 biphenylyl)propionic acid]. J Pharm Biomed Anal 1990; 8(5):401 410.
33. Shockcor JP, Unger SE, Savina P, Nicholson JK, Lindon JC. Application of directly coupled LC NMR MS to the structural elucidation of metabolites of the HIV 1 reverse transcriptase inhibitor BW935U83. J Chromatogr B Biomed Sci Appl 2000; 748(1):269 279.
34. Monteagudo E, Pesci S, Taliani M, Fiore F, Petrocchi A, Nizi E, Rowley M, Laufer R, Summa V. Studies of metabolism and disposition of potent human immunodeficiency virus (HIV) integrase inhibitors using 19F NMR spectroscopy. Xenobiotica 2007; 37(9):1000 1012.
35. Dain JG, Collins JM, Robinson WT. A regulatory and industrial perspective of the use of carbon 14 and tritium isotopes in human ADME studies. Pharm Res 1994; 11(6):925 928.
36. Roffey SJ, Obach RS, Gedge JI, Smith DA. What is the objective of the mass balance study? A retrospective analysis of data in animal and human excretion studies employing radiolabeled drugs. Drug Metab Rev 2007; 39(1):17 43.
37. Marathe PH, Shyu WC, Humphreys WG. The use of radiolabeled compounds for ADME studies in discovery and exploratory development. Curr Pharm Des 2004; 10(24):2991 3008.
38. Shaffer CL, Langer CS. Metabolism of a 14C/3H labeled GABAA receptor partial agonist in rat, dog and human liver microsomes: evaluation of a dual radiolabel strategy. J Pharm Biomed Anal 2007; 43(4):1195 1205.
39. 21 CFR 361.1. Food and Drug Administration, Department of Health and Human Services. Revised April 2001. Available at: http://www.access.gpo.gov/nara/cfr/waisidx 01/21cfrv5 01 .html. Accessed April 2008.
40. Beumer JH, Beijnen JH, Schellens JH. Mass balance studies, with a focus on anticancer drugs. Clin Pharmacokinet 2006; 45(1):33 58.
41. Potchoiba MJ, West M, Nocerini MR. Quantitative comparison of autoradioluminographic and radiometric tissue distribution studies using carbon 14 labeled xenobiotics. Drug Metab Dispos 1998; 26(3):272 277.

42. Potchoiba MJ, Nocerini MR. Utility of whole body autoradioluminography in drug discovery for the quantification of tritium labeled drug candidates. Drug Metab Dispos 2004; 32(10): 1190 1198.
43. Potchoiba MJ, Tensfeldt TG, Nocerini MR, Silber BM. A novel quantitative method for determining the biodistribution of radiolabeled xenobiotics using whole body cryosectioning and autoradioluminography. J Pharmacol Exp Ther 1995; 272(2):953 962.
44. Solon EG, Kraus L. Quantitative whole body autoradiography in the pharmaceutical industry: survey results on study design, methods, and regulatory compliance. J Pharmacol Toxicol Methods 2001; 46(2):73 81.
45. Sonada M, Takana M, Miyahara J, KAto H. Computed radiography utilising scanning laser stimulated luminescence. Radiology 1983; 148:833 838.
46. Vree TB, Waitzinger J, Hammermaier A, Radhofer Welte S. Absolute bioavailability, pharmacokinetics, renal and biliary clearance of distigmine after a single oral dose in comparison to i.v. administration of 14C distigmine bromide in healthy volunteers. Int J Clin Pharmacol Ther 1999; 37(8):393 403.
47. Nave R, Bethke TD, van Marle SP, Zech K. Pharmacokinetics of [14C]Ciclesonide after oral and intravenous administration to healthy subjects. Clin Pharmacokinet 1994; 43(7):479 486.
48. Johnson K, Shah A, Jaw Tsai S, Baxter J, Prakash C. Metabolism, pharmacokinetics, and excretion of a highly selective N methyl D aspartate receptor antagonist, traxoprodil, in human cytochrome P450 2D6 extensive and poor metabolizers. Drug Metab Dispos 2003; 31(1):76 87.
49. Hoffmann M, DeMaio W, Jordan RA, Talaat R, Harper D, Speth J, Scatina J. Metabolism, excretion, and pharmacokinetics of [14C]tigecycline, a first in class glycylcycline antibiotic, after intravenous infusion to healthy male subjects. Drug Metab Dispos 2007; 35(9): 1543 1553.
50. Harrison MP, Haworth SJ, Moss SR, Wilkinson DM, Featherstone A. The disposition and metabolic fate of 14C meropenem in man. Xenobiotica 1993; 23(11):1311 1323.
51. Cocquyt V, Kline WF, Gertz BJ, Van Belle SJ, Holland SD, DeSmet M, Quan H, Vyas KP, Zhang KE, De Greve J, Porras AG. Pharmacokinetics of intravenous alendronate. J Clin Pharmacol 1999; 39(4):385 393.
52. Weichers JW, Herder RE, Drenth BFH, de Zeeuw RA. Percutaneous absorption, disposition, metabolism, and excretion of 14C labelled Cyoctol in humans after a single dermal application. Int J Pharm 1990; 65(1 2):77 84.
53. Rohatagi S, Wang Y, Argenti D. Mass balance studies. Pharmacokinet Drug Dev 2004; 1:121 148.
54. Sunzel M. Studies of the basic pharmacokinetic properties of a drug: a regulatory perspective. In: Sahajwalla CG, ed. New Drug Development, Regulatory Paradigms for Clinical Pharmacology and Biopharmaceutics. Vol. 141. New York: Marcel Decker, 2004:187 212.
55. Paulson SK, Hribar JD, Liu NW, Hajdu E, Bible RH Jr, Piergies A, Karim A. Metabolism and excretion of [(14)C]celecoxib in healthy male volunteers. Drug Metab Dispos 2000; 28(3): 308 314.
56. Gschwind HP, Pfaar U, Waldmeier F, Zollinger M, Sayer C, Zbinden P, Hayes M, Pokorny R, Seiberling M, Ben Am M, Peng B, Gross G. Metabolism and disposition of imatinib mesylate in healthy volunteers. Drug Metab Dispos 2005; 33(10):1503 1512.
57. Lin JH, Duggan DE, Chen IW, Ellsworth RL. Physiological disposition of alendronate, a potent anti osteolytic bisphosphonate, in laboratory animals. Drug Metab Dispos 1991; 19(5): 926 932.
58. Khan SA, Kanis JA, Vasikaran S, Kline WF, Matuszewski BK, McCloskey EV, Beneton MN, Gertz BJ, Sciberras DG, Holland SD, Orgee J, Coombes GM, Rogers SR, Porras AG. Elimination and biochemical responses to intravenous alendronate in postmenopausal osteoporosis. J Bone Miner Res 1997; 12(10):1700 1707.
59. Tombs NI. Tissue distribution of Gar 936, a broad spectrum antibiotic, in male rats. Abstr Intersci Conf Antimicrob Agents Chemother 1999; 39:302.
60. Wait JC, Vaccharajani N, Mitroka J, Jemal M, Khan S, Bonacorsi SJ, Rinehart JK, Iyer RA. Metabolism of [14C]gemopatrilat after oral administration to rats, dogs, and humans. Drug Metab Dispos 2006; 34(6):961 970.

61. Iyer RA, Mitroka J, Malhotra B, Bonacorsi S Jr, Waller SC, Rinehart JK, Roongta VA, Kripalani K. Metabolism of [(14)C]omapatrilat, a sulfhydryl containing vasopeptidase inhibitor in humans. Drug Metab Dispos 2001; 29(1):60 69.
62. Kripalani KJ, McKinstry DN, Singhvi SM, Willard DA, Vukovich RA, Migdalof BH. Disposition of captopril in normal subjects. Clin Pharmacol Ther 1980; 27(5):636 641.
63. Savi P, Pereillo JM, Uzabiaga MF, Combalbert J, Picard C, Maffrand JP, Pascal M, Herbert JM. Identification and biological activity of the active metabolite of clopidogrel. Thromb Haemost 2000; 84(5):891 896.
64. Lins R, Broekhuysen J, Necciari J, Deroubaix X. Pharmacokinetic profile of 14C labeled clopidogrel. Semin Thromb Hemost 1999; 25(suppl 2):29 33.
65. Farid NA, Smith RL, Gillespie TA, Rash TJ, Blair PE, Kurihara A, Goldberg MJ. The disposition of prasugrel, a novel thienopyridine, in humans. Drug Metab Dispos 2007; 35(7): 1096 1104.
66. Rehmel JL, Eckstein JA, Farid NA, Heim JB, Kasper SC, Kurihara A, Wrighton SA, Ring BJ. Interactions of two major metabolites of prasugrel, a thienopyridine antiplatelet agent, with the cytochromes P450. Drug Metab Dispos 2006; 34(4): 600 607.
67. Zhang D, Ogan M, Gedamke R, Roongta V, Dai R, Zhu M, Rinehart JK, Klunk L, Mitroka J. Protein covalent binding of maxipost through a cytochrome P450 mediated ortho quinone methide intermediate in rats. Drug Metab Dispos 2003; 31(7):837 845.
68. Zhang D, Krishna R, Wang L, Zeng J, Mitroka J, Dai R, Narasimhan N, Reeves RA, Srinivas NR, Klunk LJ. Metabolism, pharmacokinetics, and protein covalent binding of radiolabeled MaxiPost (BMS 204352) in humans. Drug Metab Dispos 2005; 33(1): 83 93.
69. Ito K, Hallifax D, Obach RS, Houston JB. Impact of parallel pathways of drug elimination and multiple cytochrome P450 involvement on drug drug interactions: CYP2D6 paradigm. Drug Metab Dispos 2005; 33(6):837 844.
70. Colizza K, Awad M, Kamel A. Metabolism, pharmacokinetics, and excretion of the substance P receptor antagonist CP 122,721 in humans: structural characterization of the novel major circulating metabolite 5 trifluoromethoxy salicylic acid by high performance liquid chromatography tandem mass spectrometry and NMR spectroscopy. Drug Metab Dispos 2007; 35(6):884 897.
71. Balani SK, Xu X, Pratha V, Koss MA, Amin RD, Dufresne C, Miller RR, Arison BH, Doss GA, Chiba M, Freeman A, Holland SD, Schwartz JI, Lasseter KC, Gertz BJ, Isenberg JI, Rogers JD, Lin JH, Baillie TA. Metabolic profiles of montelukast sodium (Singulair), a potent cysteinyl leukotriene1 receptor antagonist, in human plasma and bile. Drug Metab Dispos 1997; 25(11): 1282 1287.
72. Pool WF. Clinical drug metabolism studies. In: Woolf TF, ed. Handbook of Drug Metabolism. New York: Marcel Dekker, Inc., 1999:577 587.
73. Slatter JG, Schaaf LJ, Sams JP, Feenstra KL, Johnson MG, Bombardt PA, Cathcart KS, Verburg MT, Pearson LK, Compton LD, Miller LL, Baker DS, Pesheck CV, Lord RS 3rd. Pharmacokinetics, metabolism, and excretion of irinotecan (CPT 11) following I.V. infusion of [(14)C]CPT 11 in cancer patients. Drug Metab Dispos 2000; 28(4):423 433.
74. Wang L, Zhang D, Swaminathan A, Xue Y, Cheng PT, Wu S, Mosqueda Garcia R, Aurang C, Everett DW, Humphreys WG. Glucuronidation as a major metabolic clearance pathway of 14c labeled muraglitazar in humans: metabolic profiles in subjects with or without bile collection. Drug Metab Dispos 2006; 34(3):427 439.
75. Zhang D, Wang L, Raghavan N, Zhang H, Li W, Cheng PT, Yao M, Zhang L, Zhu M, Bonacorsi S, Yeola S, Mitroka J, Hariharan N, Hosagrahara V, Chandrasena G, Shyu WC, Humphreys WG. Comparative metabolism of radiolabeled muraglitazar in animals and humans by quantitative and qualitative metabolite profiling. Drug Metab Dispos 2007; 35(1):150 167.
76. Kamel A, Davis J, Potchoiba MJ, Prakash C. Metabolism, pharmacokinetics and excretion of a potent tachykinin NK1 receptor antagonist (CP 122,721) in rat: characterization of a novel oxidative pathway. Xenobiotica 2006; 36(2 3):235 258.
77. Ruan Q, Peterman S, Szewc MA, Ma L, Cui D, Humphreys WG, Zhu M. An integrated method for metabolite detection and identification using a linear ion trap/Orbitrap mass spectrometer and

multiple data processing techniques: application to indinavir metabolite detection. J Mass Spectrom 2008; 43(2):251 261.
78. Zhang D, Cheng PT, Zhang H. Mass defect filtering on high resolution LC/MS data as a methodology for detecting metabolites with unpredictable structures: identification of oxazole ring opened metabolites of muraglitazar. Drug Metab Lett 2007; 1(4):287 292.
79. Zhu M, Ma L, Zhang D, Ray K, Zhao W, Humphreys WG, Skiles G, Sanders M, Zhang H. Detection and characterization of metabolites in biological matrices using mass defect filtering of liquid chromatography/high resolution mass spectrometry data. Drug Metab Dispos 2006; 34 (10):1722 1733.
80. Zhu M, Ma L, Zhang H, Humphreys WG. Detection and structural characterization of glutathione trapped reactive metabolites using liquid chromatography high resolution mass spectrometry and mass defect filtering. Anal Chem 2007; 79(21):8333 8341.
81. Kamel A, Prakash C. High performance liquid chromatography/atmospheric pressure ioniza tion/tandem mass spectrometry (HPLC/API/MS/MS) in drug metabolism and toxicology. Curr Drug Metab 2006; 7(8):837 852.
82. Papac DI, Shahrokh Z. Mass spectrometry innovations in drug discovery and development. Pharm Res 2001; 18(2):131 145.
83. Prakash C, Shaffer CL, Nedderman A. Analytical strategies for identifying drug metabolites. Mass Spectrom Rev 2007; 26(3):340 369.
84. Lappin G, Garner RC. The use of accelerator mass spectrometry to obtain early human ADME/ PK data. Expert Opin Drug Metab Toxicol 2005; 1(1):23 31.
85. Vogel J. Accelerator mass spectrometry for quantitative in vivo tracing. Biotechniques 2005; 38:S25 S29.
86. Turteltaub KW, Vogel JS. Bioanalytical applications of accelerator mass spectrometry for pharmaceutical research. Curr Pharm Des 2000; 6(10):991 1007.
87. Chiarappa Zucca ML, Dingley KH, Roberts ML, Velsko CA, Love AH. Sample preparation for quantitation of tritium by accelerator mass spectrometry. Anal Chem 2002; 74(24): 6285 6290.
88. Vogel JS, Love AH. Quantitating isotopic molecular labels with accelerator mass spectrometry. Methods Enzymol 2005; 402:402 422.
89. Garner RC, Barker J, Flavell C, Garner JV, Whattam M, Young GC, Cussans N, Jezequel S, Leong D. A validation study comparing accelerator MS and liquid scintillation counting for analysis of 14C labelled drugs in plasma, urine and faecal extracts. J Pharm Biomed Anal 2000; 24(2):197 209.
90. Garner RC, Goris I, Laenen AA, Vanhoutte E, Meuldermans W, Gregory S, Garner JV, Leong D, Whattam M, Calam A, Snel CA. Evaluation of accelerator mass spectrometry in a human mass balance and pharmacokinetic study experience with 14C labeled (R) 6 [amino (4 chlorophenyl)(1 methyl 1H imidazol 5 yl)methyl] 4 (3 chlorophenyl) 1 methyl 2(1H) quinolinone (R115777), a farnesyl transferase inhibitor. Drug Metab Dispos 2002; 30(7):823 830.
91. Beumer JH, Garner RC, Cohen MB, Galbraith S, Duncan GF, Griffin T, Beijnen JH, Schellens JH. Human mass balance study of the novel anticancer agent ixabepilone using accelerator mass spectrometry. Invest New Drugs 2007; 25(4):327 334.
92. Sarapa N, Hsyu PH, Lappin G, Garner RC. The application of accelerator mass spectrometry to absolute bioavailability studies in humans: simultaneous administration of an intravenous microdose of 14C nelfinavir mesylate solution and oral nelfinavir to healthy volunteers. J Clin Pharmacol 2005; 45(10):1198 1205.
93. Brown K, Tompkins EM, Boocock DJ, Martin EA, Farmer PB, Turteltaub KW, Ubick E, Hemingway D, Horner Glister E, White IN. Tamoxifen forms DNA adducts in human colon after administration of a single [14C] labeled therapeutic dose. Cancer Res 2007; 67(14):6995 7002.
94. Watanabe K, Liberman RG, Skipper PL, Tannenbaum SR, Guengerich FP. Analysis of DNA adducts formed in vivo in rats and mice from 1,2 dibromoethane, 1,2 dichloroethane, dibromomethane, and dichloromethane using HPLC/accelerator mass spectrometry and relevance to risk estimates. Chem Res Toxicol 2007; 20(11):1594 1600.

95. Balani SK, Nagaraja NV, Qian MG, Costa AO, Daniels JS, Yang H, Shimoga PR, Wu JT, Gan LS, Lee FW, Miwa GT. Evaluation of microdosing to assess pharmacokinetic linearity in rats using liquid chromatography tandem mass spectrometry. Drug Metab Dispos 2006; 34(3):384 388.
96. Lappin G, Kuhnz W, Jochemsen R, Kneer J, Chaudhary A, Oosterhuis B, Drijfhout WJ, Rowland M, Garner RC. Use of microdosing to predict pharmacokinetics at the therapeutic dose: experience with 5 drugs. Clin Pharmacol Ther 2006; 80(3):203 215.
97. Sandhu P, Vogel JS, Rose MJ, Ubick EA, Brunner JE, Wallace MA, Adelsberger JK, Baker MP, Henderson PT, Pearson PG, Baillie TA. Evaluation of microdosing strategies for studies in preclinical drug development: demonstration of linear pharmacokinetics in dogs of a nucleoside analog over a 50 fold dose range. Drug Metab Dispos 2004; 32(11):1254 1259.

23

Minimizing Metabolic Activation in Drug Discovery

Sanjeev Kumar
Department of Drug Metabolism and Pharmacokinetics, Merck Research Laboratories, Rahway, New Jersey, U.S.A.

Thomas A. Baillie
Department of Drug Metabolism and Pharmacokinetics, Merck Research Laboratories, Rahway, New Jersey, and West Point, Pennsylvania, U.S.A.

OVERVIEW: RELEVANCE OF METABOLIC ACTIVATION PHENOMENON IN DRUG DISCOVERY

Today's pharmaceutical industry is under a tremendous amount of pressure to cut operating costs, reduce cycle times for drug discovery and development, and deliver safe and effective medicines to treat unmet medical needs or improve upon existing therapies in terms of efficacy and safety. One significant challenge to the industry meeting these demands is the unpredictable nature of most forms of drug toxicity. This lack of predictability frequently leads to failure of new drug candidates during low throughput and relatively expensive preclinical toxicity testing, with the cost of this failure being directly related to the stage at which the toxicities manifest (e.g., during acute, subchronic, or chronic toxicity testing). Further, this necessitates that pharmaceutical companies invest costly resources into backup compounds/programs to increase the number of "shots on goal" and increase the probability of success. These factors, along with the poor success rate at which new biological targets yield clinical efficacy for human disease conditions, add tremendously to the cost of drug development, which according to some estimates now exceeds ~$800 million for each new drug introduced onto the market (1,2). An even more serious issue relates to the fact that while the potential for many target organ toxicities can be identified during preclinical safety evaluation, some adverse effects (that are many times mediated via the immune system) fail to manifest in animals. These toxicities (often described as idiosyncratic) generally have a low incidence (1 in 5000 or more) and may only become apparent during large scale clinical trials when a significant resource investment has already been made into the drug candidate or, even worse, after a compound has been introduced onto the market and needs to be withdrawn. This unpredictable nature of drug toxicity thus represents an issue

of great significance both in terms of patient safety and economic loss to the sponsor company, as has been well illustrated by the recent high-profile drug withdrawals for troglitazone (Rezulin®), fenfluramine (Fen-Phen®), and rofecoxib (Vioxx®).

While there can be many possible mechanisms of drug-induced toxicity, it appears that biotransformation of drugs to reactive, electrophilic metabolites that bind covalently to cellular macromolecules is the initial step in many drug-induced adverse events, including direct target organ damage and immune-mediated idiosyncratic toxicity (3 8). There is strong indirect evidence from research conducted over the last 40 years that some, but not all, reactive metabolites can result in toxicity. Most marketed drugs that have been associated with idiosyncratic toxicity are known to form reactive metabolites that are capable of covalently modifying proteins in vitro and/or in vivo (9 12). Although it is now possible, in most cases, to identify the structures of reactive metabolites of drug candidates using modern analytical technologies, it is not possible to predict a priori which of these electrophiles would produce adverse events, since the current knowledge on the downstream biochemical/physiological events remains sparse. In general, it would appear that covalent binding of reactive drug metabolites to critical cellular macromolecules, when combined with certain host-specific genetic, environmental, or disease factors, can render certain individuals more susceptible to drug-induced idiosyncratic toxicity. Since it is not possible to identify these individual-specific factors during preclinical safety testing and map their relationship to drug-induced idiosyncratic toxicity, our ability to predict the potential for these toxicities is limited. Because of this inability to predict and quantify the risk for idiosyncratic drug toxicities, the strategy of attempting to minimize the formation of reactive metabolites via informed structural modification during drug discovery represents a prudent approach to mitigate the risk for these toxicities.

As opposed to the difficult challenges in correlating metabolic activation with low-incidence and human-specific idiosyncratic toxicities mediated by the immune system, it seems likely that a closer relationship exists, at least for certain compounds, between bioactivation and target organ toxicity. For example, studies in animals have established a clear dose-response relationship for acetaminophen hepatotoxicity following depletion of protective glutathione (GSH) stores, and the degree of covalent binding to liver tissues in these experiments correlates well with the severity of the resulting lesions (13,14). In this regard, efforts to understand mechanisms of metabolic activation can be of value in rationalizing foreign compound-mediated toxicities, especially when these toxicities are species-specific. Such understanding can, in turn, provide a framework for assessing risk of certain toxicities in humans that may be mediated through metabolic activation phenomena. An elegant illustration of this is provided by studies with the non-nucleoside HIV reverse transcriptase inhibitor, efavirenz, which causes renal tubular epithelial cell necrosis in rats but not in cynomolgus monkeys or humans at equivalent or greater systemic exposures (15,16). The sulfate conjugate of hydroxylated efavirenz is metabolized to a cyclopropanol metabolite via oxidation at the methine position of the cyclopropane moiety that is linked to an alkyne functionality (Fig. 1). This cyclopropanol metabolite likely serves as a substrate for a *rat-specific* glutathione-*S*-transferase(s) and results in the addition of GSH to the alkyne moiety of efavirenz in rats but not in other species. This GSH conjugate of efavirenz is processed further in the rat kidney to a cysteinylglycine conjugate via γ-glutamyl transpeptidase-catalyzed removal of the glutamic acid residue, and the cysteinylglycine conjugate is either excreted in rat urine or is involved in further bioactivation events that eventually lead to nephrotoxicity in the rat. Strong evidence was obtained for this hypothesis where a decrease in the formation of the cysteinylglycine conjugate, either via interfering with the formation of the

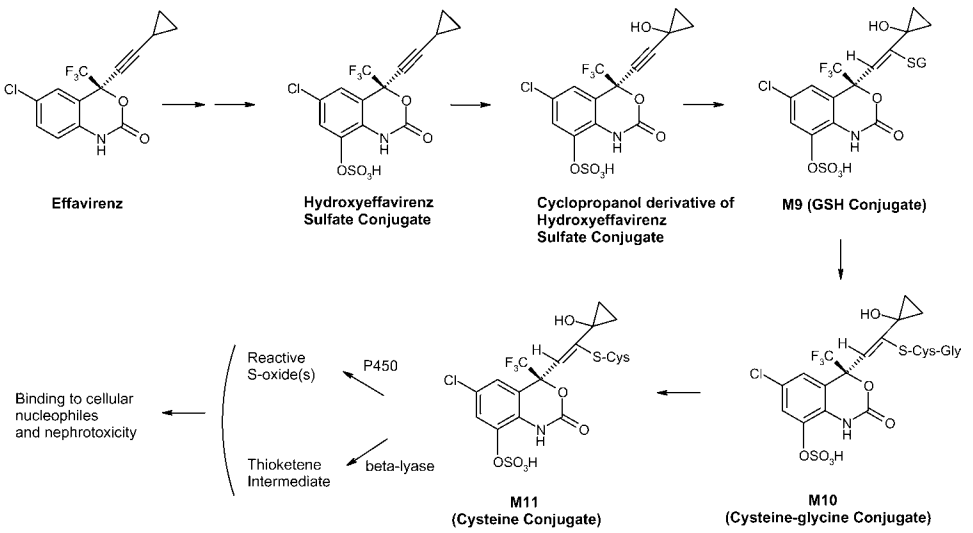

Figure 1 Proposed mechanism for the rat specific metabolic activation of efavirenz and its role in nephrotoxicity in the rat. *Source*: Adapted from Refs. 15, 16.

cyclopropanol metabolite or via inhibition of γ-glutamyl transpeptidase, led to reductions in the incidence and severity of nephrotoxicity. This example clearly demonstrates the value of understanding bioactivation mechanisms and their relationship to toxicity findings in preclinical species for a more rational assessment of risk in humans.

In addition to acting as a potential trigger for many idiosyncratic or target organ toxicities, the role of chemically reactive metabolites in genotoxicity and carcinogenesis has been well established [e.g., polycyclic aromatic hydrocarbons and aromatic amines (17,18)]. For example, a number of quinone- or quinone methide reactive intermediates derived from estrogens and tamoxifen have been shown to bind to DNA bases and induce DNA damage (19 22). Thus, efforts at minimizing metabolic activation can help in screening out candidates that may prove to be mutagenic in downstream preclinical safety assessment studies.

Another area of interest to pharmaceutical industry is the mechanism-based irreversible inhibition of P450 enzymes by chemically reactive metabolites via alkylation of either the heme or the P450 apoprotein (23,24) and the consequent potential for serious clinical drug-drug interaction liabilities, as was illustrated by the withdrawal of mibefradil (Posicor®) from the market. As an example, the grapefruit juice constituent bergamottin is a mechanism-based inhibitor of CYP3A4, CYP1A2, 2B6, 2C9, 2C19, and 2D6, but not of 2E1, in human liver microsomes (25 27). When [^{14}C]bergamottin is incubated with membrane preparations of individual human recombinant P450 enzymes, the covalent binding of radioactivity, or a lack thereof, correlates well with the inhibitory potential of bergamottin for these enzymes (the covalent binding values were 575, 152, 214, 263, 593, 166, and <5 pmol Eq/nmol P450 over one-hour incubation for CYP3A4, 1A2, 2B6, 2C9, 2C19, 2D6, and 2E1, respectively; S. Kumar, unpublished data). Thus, minimizing the formation of chemically-reactive metabolites represents a direct strategy for dialing out potential for mechanism-based P450 inhibition during pharmaceutical lead optimization.

Overall, it would appear that the relatively modest investment of resources early in the lead optimization phase to minimize the formation of chemically reactive metabolites

has the potential to offer large returns in terms of enhancing the overall quality of drug candidates that are advanced into development and reducing the overall risk of failure due to a variety of reasons outlined above. This view is accepted by many pharmaceutical companies who have incorporated minimization of metabolic activation as an integral part of the drug discovery process (7,10,11,28 30). In the following sections of this chapter, we review the various approaches that are available for minimizing metabolic activation and propose a logical roadmap to deal with this issue during pharmaceutical lead optimization. Limitations of various approaches and future scientific developments that have the potential to address these limitations will also be discussed.

APPROACHES FOR MINIMIZING METABOLIC ACTIVATION IN DRUG DISCOVERY

Approaches for addressing bioactivation issues during drug discovery need to rely on both, a quantitative, and a quantitative assessment of the potential for formation of reactive intermediates. The qualitative assessment entails the identification of the reactive metabolite(s) in question, with particular attention to the substructural motif that is involved in bioactivation so that appropriate chemical modifications can be made by medicinal chemists to block the undesired metabolic pathway(s). Since pharmaceutical lead optimization invariably is a balancing act that strives to achieve the best possible combination of numerous desirable attributes in a drug candidate (e.g., physicochemical properties, potency at the target, on- and off-target pharmacology, pharmacokinetics, and metabolism to name a few), a quantitative assessment of bioactivation liabilities also is important so that appropriate comparisons among different lead candidates can be made.

The most direct approach to assessing the potential (both qualitative and quantitative) for bioactivation is the identification and quantification of the actual adduct of the chemically reactive species with protein or DNA, the macromolecules considered most relevant to toxicological consequences of bioactivation. However, the throughput and speed of currently available technologies for this purpose is not adequate for a fast-paced drug discovery setting. Hence, industrial drug metabolism scientists need to rely on more rapid and higher-throughput surrogate approaches, such as those described below, to identify and measure the bioactivation potential of pharmaceutical lead candidates.

Chemical Structural Alerts

It is widely appreciated that certain chemical substructures are particularly prone to forming reactive electrophilic metabolites that are capable of covalently binding to cellular macromolecules. Examples of these include anilines (unmasked), hydrazines, nitroarenes, α,β-unsaturated carbonyls, thiophenes, terminal alkenes or alkynes, etc. A large body of circumstantial evidence exists in the literature linking bioactivation of these functional groups to various forms of toxicity observed with drugs that contain these substructures (e.g., ticlodipine, tienilic acid, and zileuton for thiophene; carbutamide, procainamide, and tocainide for aniline; phenelzine, hydralazine, dihydralazine, and isoniazid for hydrazine; chloramphenicol, tolcapone, flutamide, and metronidazone for nitroaromatics, etc.) (9 11). At least in some cases, replacement of the *offending* substructure with a more *metabolically benign* one has indeed led to a safer and less toxic second-generation agent. For example, the antidiabetic agent carbutamide was withdrawn from the market due to severe bone marrow toxicity; however, replacement of the aniline moiety of carbutamide with a toluene substituent led to the discovery of tolbutamide,

which is devoid of this toxicity. Similarly, the antiarrhythmics procainamide and tocainide contain an aniline substructure and cause bone marrow aplasia and lupus syndrome, while a closely related congener, flecainide, lacks the aniline motif and is devoid of these toxicities. This subject has been reviewed in depth in several recent articles and we refer the reader to these papers for additional information (10,11,31,32). In addition to the above more widely appreciated structural alerts, information on novel pathways of bioactivation of other substructures continues to emerge on a constant basis and adds to this list of potentially troublesome functional groups; examples of this include thiazolidinedione (TZD), pyrazinone, furan, piperazine, and N-substituted piperidines, etc. (33 37). Thus, it should be emphasized that while awareness of bioactivation structural alerts certainly should be part of the strategy to address this issue during pharmaceutical lead optimization, and replacement with metabolically benign substructures should be explored, an approach that altogether avoids all potential structural alerts would neither be possible nor appropriate; such a strategy would severely limit medicinal chemists' exploration of the full chemical space for structure-activity relationship (SAR) and fails to take into account the fact that metabolism of the offending functionality needs to occur before reactive intermediates are formed. The focus of the strategy should, in fact, be on minimizing the metabolism of the potential structural alert to reactive species, either via *masking* the offending motif within the overall structure of the molecule or by incorporating alternative clearance/metabolism pathways into the chemical class.

LC-MS-Based Identification of Chemically Reactive Metabolites via "Trapping" Studies

Liquid chromatography mass spectrometry (LC-MS)-based approaches likely represent the single most important tool and the first step for assessing the bioactivation liabilities in a drug discovery setting and for identifying the metabolic pathways that result in the formation of reactive species. The latter usually is accomplished via in vitro metabolism studies where a select number of drug candidates of interest are incubated with appropriately cofactor-fortified liver preparations (e.g., hepatocytes, microsomes, or S9) from selected preclinical species and humans. The reactive electrophilic species formed from drug candidates generally do not exhibit sufficient stability to allow their direct detection and identification via LC-MS and need to be detected following adduction with small molecule nucleophiles that are included as "traps" in the incubation; some exceptions to this are acyl glucuronides or CoA thioesters, and rarely some epoxides. This approach obviously inherently assumes that the covalent binding of compounds to biological macromolecules and to the surrogate small molecule trapping agents involves the same bioactivation mechanism. The tripeptide glutathione (γ-glutamylcysteinylglycine, GSH) is the most common trapping agent used in such applications where its cysteinyl thiol nucleophilic center reacts covalently with the electrophilic reactive intermediate. As an extension of this approach, other thiols, such as *N*-acetylcysteine, cysteine, and 2-mercaptoethanol, also have been used in such studies; however, when the reaction between the thiol nucleophile and the reactive species can be catalyzed enzymatically (e.g., by glutathione-*S*-transferases), GSH may appear more efficient at trapping the relevant reactive species. Interestingly, cysteine has been shown to react with its both thiol and amine functional groups to trap bifunctional electrophiles. For example, the enedial intermediate from the furan-containing compound, ipomeanine, is trapped by cysteine to form a cyclic adduct (Fig. 2) (38). It is to be noted that these thiol derivatives are "soft" nucleophiles and react readily with soft electrophiles (e.g., quinones, epoxides;

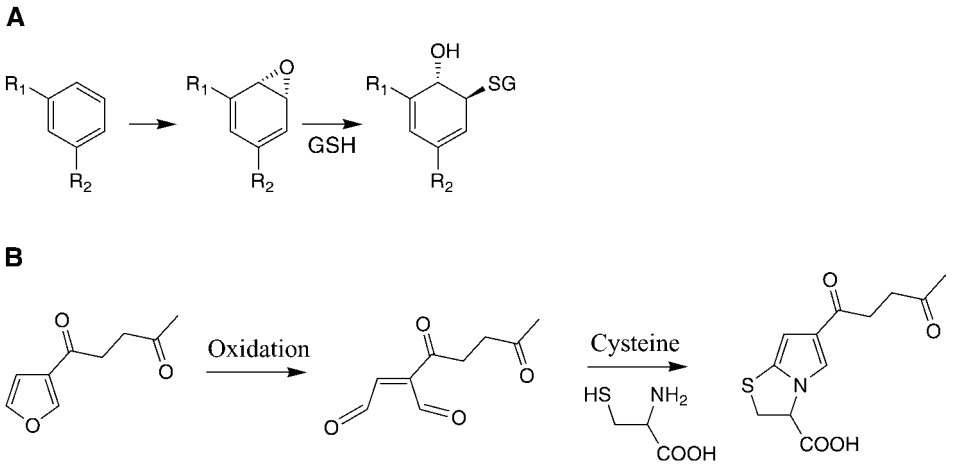

Figure 2 (**A**) Trapping of an arene oxide by glutathione and (**B**) trapping of enedial intermediate from ipomeanine by cysteine.

Fig. 2), but they are not efficient at trapping "hard" electrophilic intermediates such as iminium ions and other reactive species such as electrophilic carbonyls (e.g., aldehydes and ketones). These latter reactive intermediates are more efficiently trapped by the non-thiol hard nucleophiles such as cyanide, semicarbazide, methoxylamine, and DNA bases (e.g., guanine).

The LC-MS analysis of adducts of drug candidates with trapping agents typically involves two steps; in the first step, the molecular mass of the adduct is determined via identification of the molecular ion and in the second, product ion spectra are generated by collision-induced dissociation (CID) of the parent ion to determine the substructural motif(s) involved in bioactivation. Advances in mass spectrometry and separation technologies over the last decade have provided drug metabolism scientists with extremely sensitive and reliable tools for detecting low-level metabolites in complex biological matrices. Neutral loss and precursor ion scans are the most commonly employed modes for the detection of molecular ions of adducts. The neutral loss scan mode has found particularly wide applicability for the detection of GSH adducts that frequently lose a neutral fragment of 129 Da (in positive ion mode), corresponding to the loss of pyroglutamic acid from the protonated GSH adduct (39). This methodology can be adapted to screen for reactive intermediates in a relatively high-throughput assay in a drug discovery setting (40). In recent years, a number of refinements of the classical neutral loss assay for the detection of GSH adducts of drug candidates have been published that enhance the reliability of this approach. Soglia et al. (41) demonstrated a much greater sensitivity for the detection of thiol adducts via the use of the glutathione ethyl ester as the trapping agent. Castro-Perez et al. (42) reported a "pseudo" neutral loss scan corresponding to the exact mass of pyroglutamic acid (129.0426 Da) by alternating low and high collision energy scans on a high-resolution Q-Tof mass spectrometer and triggering a product ion scan of the relevant precursor ion when a difference of 129.0426 Da is detected (within preset mass error windows). This approach significantly enhances the selectivity of detection and reduces the number of false positives. However, it should be appreciated that not all GSH adducts lose a neutral fragment of 129 Da upon CID (e.g., aliphatic and benzylic thioethers frequently eliminate the intact GSH molecule corresponding to a neutral loss of 307 Da), and awareness of bioactivation chemistry is necessary while

employing these screening methodologies. Recently, Dieckhaus et al. (43) investigated the MS/MS behavior of intact GSH and GSH adducts of xenobiotics in the negative ion mode and demonstrated that these produce an abundant anion at *m/z* 272 corresponding to deprotonated γ-glutamyl dehydroalanyl glycine (loss of the elements of hydrogen sulfide from glutathione). Thus, scanning for precursors of this specific anion can provide sensitive and selective detection of GSH adducts (43). It is important to note that when an unknown conjugate is detected via the above neutral loss or negative ion precursor scan methods, a positive ion CID experiment is usually necessary to elucidate the substructure involved in GSH adduction. The neutral loss scans also have been used to detect adducts of drug candidates with other nucleophiles; for example, a high-throughput method that employs the neutral loss of 27 Da to detect cyanide adducts of a series of compounds forming iminium ions has been reported (44).

In addition to the above methods, another commonly used approach for the identification of molecular ion(s) of adducts is a knowledge-based search for the expected masses from full scan MS data. This has traditionally been done manually but more recently, facility of rule-based algorithms has become available within the LC-MS software that allows automated generation of exhaustive lists of masses of expected metabolites the detection of which, in turn, can be used to trigger further CID scans. As an example of such an approach, Samuel et al. (45) used lists of expected masses to trigger MS^n scans on an ion trap mass spectrometer and gain insights into the structures of reactive species involved in GSH adduction. A further interesting application of a similar concept is found in a recent study where up to 100 possible Multiple reaction monitoring (MRM) transitions corresponding to expected GSH adducts were included in a single run on an API4000 Q-Trap® mass spectrometer, and a positive signal in an MRM channel was used to trigger a full product ion scan for that particular precursor ion, resulting in an overall enhanced sensitivity for detection of GSH adducts (46).

Several investigators have focused their efforts on enhancing the ease and reliability with which often very small amounts of adducts of various nucleophiles with reactive species generated from the drug candidate(s) can be detected in the presence of a complex biological matrix. For example, some studies have used equimolar mixtures of naturally occurring and stable isotope labeled GSH (which incorporates [1,2-$^{13}C_2$, ^{15}N]glycine) as a trapping agent in microsomal incubations and identification of adducts by the readily detectable isotopic "signature" of a doublet of molecular ions that are separated by 3 Da (47 49). Similar methods also have been employed with stable isotope labeled cyanide as the trapping agent to detect adducts of iminium ions (Merck Research Laboratories, unpublished data).

The widespread availability of high-resolution mass spectrometers in the past three to four years has provided new avenues for rapid and unbiased identification of drug-related components in complex biological matrices using so-called mass defect filter-based approaches (50 52). These approaches capitalize on the similarity of the mass defects between the parent molecule and its metabolites and on the fact that most xenobiotics exhibit negative mass defects relative to endogenous materials; thus, by defining preset filter windows, ions that fall outside the defect range can be filtered out, and compound-related ions are selected over those from the matrix. Recently, application of the mass defect filtering technique to the identification of the GSH adducts of reactive intermediates from a series of model compounds was illustrated nicely by scientists at Bristol Myers Squibb (46). The use of such approaches for assessing the formation of reactive metabolites in drug discovery is likely to grow rapidly in the near future as high-resolution mass spectrometry instrumentation and software tools for mass defect filtering become more widely available.

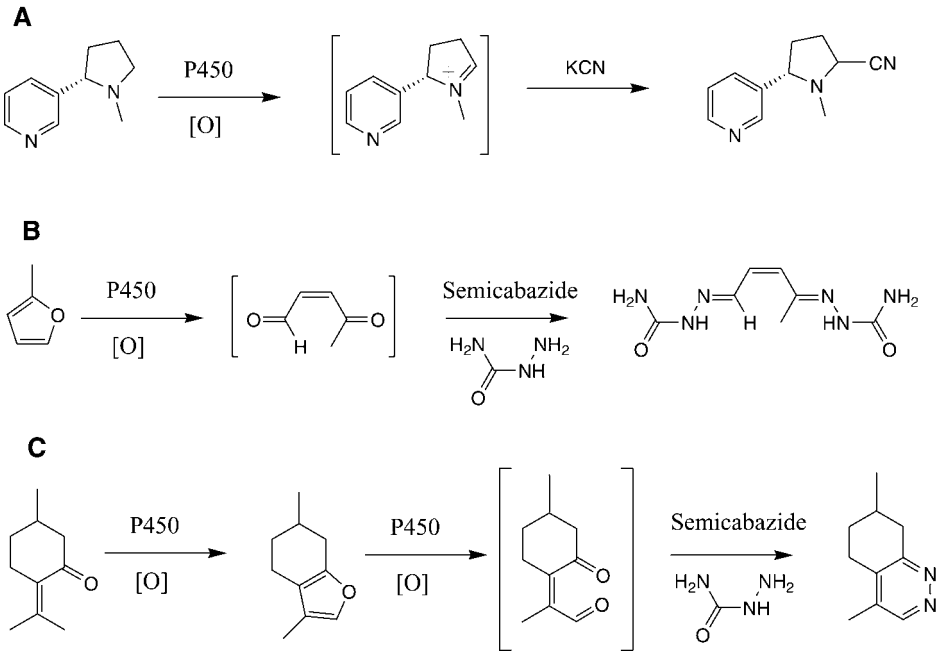

Figure 3 (**A**) Cyanide trapping of (*S*) nicotine, (**B**) semicarbazide trapping of 1 methylfuran, and (**C**) semicarbazide trapping of pulegone.

The above-discussed trapping assays with GSH generally provide only qualitative information on the formation, or a lack thereof, of a reactive intermediate when a drug candidate is incubated with metabolically competent tissue preparations. Several attempts have been made to tailor these approaches to provide semiquantitative data for decision-making in drug discovery. One such approach is the use of a quaternary ammonium derivative of GSH that carries a fixed positive charge, thus reducing differences in ionization efficiency between adducted versus non-adducted trapping agent and allowing for the latter to be used as a calibration standard for measuring the amounts of thiol adduct(s) formed (53). Another elegant method was developed by utilizing fluorescent dansylated glutathione as the trapping agent and employing fluorescent detection in combination with LC-MS/MS for the detection, structure elucidation, and quantification of relevant thiol adduct peaks (54).

Cyanide has been used to trap "hard" electrophiles such as iminium ions resulting from metabolic activation of compounds such as *S*-nicotine (Fig. 3A) and other alicyclic tertiary amines (55). For compounds suspected to yield aldehydes as reactive intermediates, the most commonly used trapping agents are semicarbazide and methoxylamine. For example, furan-containing compounds undergo ring opening to form aldehyde intermediates that can be trapped by methoxylamine and semicarbazide (Fig. 3B) (31,56). An interesting product from semicarbazide trapping of the furan-derived intermediate of pulegone is the tetrahydrocinnoline derivative that supposedly arises from condensation of one molecule of semicarbazide with the γ-ketoenal intermediate of furan ring metabolism as shown in Figure 3C (57).

The discussion above has focused on the identification of reactive intermediates formed from drug candidates via (P450-mediated) oxidative metabolism. While oxidative metabolism represents the most prolific pathway for the generation of reactive species,

other metabolic routes also can generate reactive species capable of covalent binding to macromolecules. For example, several drugs containing the carboxylic acid moiety form conjugates with amino acids such as glycine, taurine, and glutamine, and this is presumed to involve an electrophilic coenzyme A (CoA) thioester intermediate (58 60). The potential for these electrophilic CoA thioester intermediates to covalently modify nucleophilic sites on proteins has been demonstrated clearly in vivo in the rat (61). In a drug discovery setting, CoA adduct formation can be investigated in freshly isolated hepatocytes or in hepatic microsomes supplemented with CoA, Mg^{2+}, and ATP as cofactors (58 60). While the LC-MS detection of CoA adducts is relatively straightforward due to their relatively large molecular mass (addition of 749 Da to the carboxylic acid) and characteristic CID fragmentation, these conjugates tend to be labile, and special precautions need to be taken during sample handling.

Metabolism of carboxylic acid containing compounds can also lead to the formation of reactive acyl glucuronide conjugates that can covalently modify proteins either via a transacylation process or by forming reactive aldehyde species via migration of the acyl moiety around the hydroxyl groups of the glucuronic acid core (62 64). Hepatocytes or liver microsomes supplemented with uridine 5′-diphosphoglucuronic acid (UDPGA) serve as excellent models to screen for the bioactivation of carboxylate-containing drug candidates via acyl glucuronidation where the key parameters to identify acyl glucuronide reactivity are the stability of the conjugate and its propensity to form isobaric rearrangement products via acyl migration.

In addition to proteins, low molecular weight electrophiles formed from xenobiotics can also bind to DNA, with the potential consequences of mutagenicity and carcinogenesis. DNA modifications generally are detected as adducts to individual bases following digestion of the adducted DNA strands. Common examples of such adducts are from the selective estrogen modulator class of molecules (SERMs); for example, guanine adducts of tamoxifen, which are postulated to be formed via transient carbocation, quinone, or quinone methide intermediates, have been observed in endometrial tissues from patients taking the drug (65). Chemically prepared quinone methides of desmethyl arzoxifene and acolbifene, two newer SERMs, have been shown to form adducts in vitro when incubated with deoxynucleosides (66,67). In drug discovery, there are frequent situations when drug candidates turn out to be positive in early mutagenicity testing in a metabolism-dependent manner (Ames bacterial mutagenicity assay in the presence of liver S9 fractions). At Merck Research Laboratories, attempts have been made to use DNA bases (e.g., guanine) as trapping agents for the reactive species generated in such systems in order to explore SAR for guanine adduct formation and Ames assay results (Merck Research Laboratories, unpublished data). The limited experience with this strategy suggests that it has the potential to guide rational SAR for eliminating mutagenicity potential, at least in some chemical series, and needs to be further evaluated.

Covalent Binding Studies with Radiolabeled Drug Candidates

Application of Covalent Binding Studies in Drug Discovery

The above-discussed LC-MS-based approaches aimed at evaluating the potential for bioactivation currently provide, at best, qualitative or semiquantitative information and are not likely to be applicable universally for trapping all types of reactive intermediates. The current "gold standard" approach for reliably quantifying the extent of bioactivation remains the traditional covalent binding studies that are conducted with radiolabeled analogs of drug candidates. However, the requirement for synthesis of a radiolabeled

analog of the drug candidate makes these studies low throughput, costly, and not amenable to the rapid screening strategies desired in a drug discovery setting. Thus, covalent binding studies generally are conducted as a second step in the lead optimization process following synthesis of radiolabeled analogs of a limited number of more mature lead candidates. At Merck Research Laboratories, the approach that has been adopted involves measuring the extent of covalent binding of drug-related material to rat and human liver microsomal protein in vitro (or to hepatocytes when the major metabolic routes involve cytosolic and/or phase II enzymes) and to liver and plasma proteins in rats in vivo under standardized conditions via semiautomated methods that allow rapid generation of data for comparison of different lead compounds/series (68,69). The covalent binding data (expressed as pmol Eq/mg protein) obtained from these assays are indicative of the propensity of the drug candidate to form reactive species that are capable of covalent adduction to proteins under both in vitro and in vivo conditions. The in vivo assay allows factors such as dose, systemic exposure, blood-to-liver partitioning, plasma protein binding, and native protective mechanisms (e.g., GSH conjugation, quinone reductases) that can modulate metabolism and reactive metabolite exposure, to be taken into account. It should be stressed that because of the significance of the aforementioned factors, more emphasis should be placed on the in vivo data (which can only be generated routinely in rodents for reasons of practicality) for assessing risk from covalent binding-related liabilities. Furthermore, the key to correct interpretation of the covalent binding data is the qualitative and quantitative understanding of metabolic and bioactivation routes of the drug candidate in liver preparations from the rat and human, and in rats in vivo. This information serves to "bridge" the preclinical data to man and helps project potential exposure of humans to chemically reactive metabolites after administration of the drug candidate at a clinically relevant dose. These covalent binding studies, albeit somewhat crude in terms of their relevance to predicting toxicological outcomes, afford a means during drug discovery to differentiate lead candidates in terms of their potential to generate reactive species in animal safety testing and eventually in humans. Over the past five to seven years, this approach has been adopted in multiple drug discovery programs at Merck in order to measure and minimize the potential for metabolic activation in lead candidates before they are advanced into development (33,35,45,54,70–72).

Challenges in Interpreting Data from Covalent Binding Studies

Since metabolic activation is only one aspect of the overall risk/benefit assessment for advancing a particular lead candidate into development, it has been advocated previously (68,72,73) that covalent binding data should be interpreted in a broader context that includes factors such as: Is the drug intended to treat a disabling or life-threatening unmet medical need? Will the drug be used acutely, chronically, or prophylactically? Is the drug aimed at a novel biological target awaiting clinical proof of concept? Does the mechanism of biological action of the drug involve bioactivation and covalent binding to its target? (covalent binding studies for antimicrobials from the β-lactam class and for many cytotoxic anticancer agents that act via alkylation of cellular macromolecules would not be relevant for risk/benefit assessment). What is the intended patient population (pediatric, elderly)? Is the clinical dose likely to be low ($\leq$10 mg/day)? How tractable is the chemical lead with respect to modification at the site of bioactivation? Because such a diverse range of factors must be taken into account, the lead optimization process involves frequent comparison of multiple compounds in regard to their metabolic activation potential (along with other properties) in order to make a risk/benefit assessment. The following section discusses the attributes and limitations of the experimental models and

approaches used to measure covalent binding so that these data can be interpreted in an appropriate context.

Covalent Binding Targets. There has been much debate within the pharmaceutical industry as to what constitutes an acceptable level of covalent binding for a drug candidate. Considering the limitations of our understanding of the biochemical mechanisms by which reactive intermediates cause toxicities, a simple answer to this question remains elusive. It has been proposed that a value of 50 pmol Eq/mg protein [under well-defined experimental conditions (68)] be used as an upper-end target for advancing drug candidates into development. This target is based primarily on the observation that the extent of covalent binding of a number of known hepatotoxins (e.g., acetaminophen, bromobenzene, furosemide, and 4-ipomeanol) in animal liver, under conditions where they cause liver necrosis, is of the order of $\sim$1 nmol Eq/mg protein. Thus, the 50 pmol Eq/mg protein value provides an $\sim$20-fold margin over the levels of binding that typically are associated with frank hepatic necrosis. A second (practical) reason for the selection of $<$50 pmol Eq/mg protein as the target for covalent binding is that this figure is $\sim$10-fold higher than the limit of quantification of the liquid scintillation counting assays when typical levels of radioactivity are employed in the covalent binding study.

Covalent Binding in Relation to Drug Exposure. An additional point of discussion is the assay conditions under which the extent of covalent binding is measured including considerations such as the concentration of the drug candidate in incubations with liver preparations in vitro and the dose, formulation, bioavailability, and systemic exposure in studies in vivo. To a certain extent, optimal conditions to allow estimation of the maximal extent of bioactivation are expected to vary for every drug candidate due to differing kinetics of their metabolism, variable absorption and pharmacokinetic properties, and tissue (liver) partitioning, etc. However, since a key goal of the lead optimization process is to be able to make comparisons across multiple compounds, it is important to perform measurements under carefully standardized conditions, which may be less than optimal for individual compounds or may not be entirely physiologically relevant. For these reasons, at Merck Research Laboratories, we have adopted a strategy of measuring the extent of covalent binding somewhat arbitrarily at a drug concentration of 10 μM in the in vitro studies and at an oral dose of 20 mg/kg in rats in vivo (68). Due to the arbitrary nature of the assay conditions chosen, the target value of 50 pmol Eq/mg protein covalent binding value mentioned above should not be used as a cutoff criterion to make decisions on advancing or terminating compounds. Indeed, the optimum use of these data is to drive modifications to the chemical structure to minimize the potential for covalent modification of protein. However, if this is not possible due to tractability issues within the chemical lead class or other competing factors, the covalent binding data should be assessed within a broader context that takes into account the totality of the data available on the compound/program (68,72,73).

Low Metabolic Turnover. For a substantial fraction of drug candidates, the extent of metabolic turnover during the typical incubation time period (1 2 hour) employed for in vitro covalent binding studies is quite low because a key goal of many drug discovery programs is to decrease rates of metabolism and thereby extend elimination half-life in order to achieve once-a-day dosing regimen. The low metabolic turnover presents challenges in fully assessing the bioactivation potential of lead candidates and makes identification of the "trapped" reactive species more difficult. This also results in a

reduced confidence in the understanding of qualitative and quantitative similarities and differences in various metabolic pathways (including those involved in bioactivation) across species leading to a less robust "bridging" of preclinical data to the human situation (72).

Relationship between Overall Metabolic Turnover and Bioactivation. The rate and quantitative importance of the metabolic pathway(s) that leads to covalent binding to protein correlates with the overall metabolic turnover of the compound in the in vitro covalent binding assay systems in some cases, but not in others. Thus, it is not advisable to universally normalize the extent of the observed covalent binding of drug-related material to microsomal/hepatocyte protein to the overall turnover of the compound. This makes comparison of bioactivation liabilities of compounds or lead series with differing rates and extent of metabolic turnover in vitro more difficult and necessitates an understanding of the relationship of the overall metabolic turnover to the extent of covalent binding for risk assessment.

Interspecies Differences in Metabolism. While qualitative species differences in the metabolism of xenobiotics across mammalian species are relatively uncommon, differences in the quantitative contribution of various metabolic pathways to drug disposition, including those involved in the formation of chemically reactive metabolites, are almost always apparent. Thus, it is important to understand the disposition of the drug candidate(s) and gain a mechanistic view of the pathways involved in bioactivation and covalent binding for accurate assessment of the relevance of covalent binding data generated in animals (rats) to humans.

In summary, the discussion above supports the notion that rigid "cutoff" values for the extent of covalent binding to protein for decision making in drug discovery are inappropriate and should be avoided. The extent of covalent binding should be interpreted in light of knowledge of the overall metabolic turnover of the compounds and systemic exposure to drug-related material in relation to the target clinical exposure, and species differences in metabolism should be taken into account when extrapolating covalent binding risk to humans.

Higher-Throughput Surrogate Assays for Quantifying the Potential for Bioactivation

Because of the fact that covalent binding studies with radiolabeled analogs of drug candidates are low throughput and costly, there is tremendous interest within the pharmaceutical industry to develop higher-throughput approaches for quantitatively assessing bioactivation potential. In situations where a correlation can be established between the extent of covalent binding of drug-related material to protein and the amount of adduct(s) detected in LC-MS-based trapping assays (i.e., when the identity of the reactive species binding to protein and to the trapping agent is presumed to be the same), we and others have explored the use of radiolabeled trapping agents (such as [^{3}H]GSH, [^{35}S]GSH, [^{35}S]β-mercaptoethanol, and [^{14}C]CN) for the capture of reactive intermediates; the resulting radioactive adduct can then be separated from the excess trapping agent by appropriate extraction procedures and quantified using plate-based radioactivity detection methods (74). This assay format is easily amenable to automation, thus dramatically increasing the speed and throughput of data generation. An example of this application is provided by Meneses-Lorente et al. (74) who demonstrated that the extent of covalent binding of a series of piperidine-containing drug candidates measured using radiolabeled analogs of individual compounds was reduced substantially by the

inclusion of KCN in incubations. Further, formation of the radiolabeled cyanide adducts of these compounds in liver microsomal incubations supplemented with $K^{14}CN$ correlated reasonably well with the covalent binding of these analogs to liver microsomal protein. These data suggest that, for this series of compounds, iminiun ions are the likely *culprit* species involved in covalent binding of drug-related material to microsomal protein, and a strategy based on screening for metabolic activation potential with radiolabeled cyanide is a viable option. In contrast, the extent of covalent binding of another class of compounds from a Merck drug discovery program was attenuated significantly with inclusion of GSH (but not cyanide) in incubations, and a number of thiol adducts that were postulated to be formed via trapping of arene oxide and quinone intermediates were identified in these incubations (45). For this class of compounds, we explored the use of [^{35}S]β-mercaptoethanol (as a substitute for [^{35}S]GSH that tends to have issues with stability) as a trapping agent and observed a good correlation between the extent of covalent binding of compounds measured previously (45) with the amount of [^{35}S]β-mercaptoethanol adducts formed in human liver microsomes (Merck Research Laboratories, unpublished data). Similarly, Masubuchi et al. (75) demonstrated a good correlation between the amount of GSH conjugates formed (using both unlabeled and [^{35}S]-labeled GSH) from a set of 10 model compounds with the extent of covalent binding of radiolabeled drug-related material to human and rat liver microsomal protein, and to rat liver protein in vivo when systemic exposure [plasma AUC (area under the curve)] and plasma free fraction were taken into account. These limited number of studies that describe application of variations of trapping assays for quantitative assessment of bioactivation liabilities suggest that a judicious selection of the trapping agent(s) for reactive intermediate screening that is based on a sound understanding of the metabolic pathways involved in bioactivation/covalent binding can help increase the speed, efficiency and throughput, and lower the overall cost of bioactivation studies by significantly reducing the number of radiolabeled drug candidates that need to be synthesized for this purpose.

PROPOSED ROADMAP FOR ADDRESSING METABOLIC ACTIVATION IN DRUG DISCOVERY

On the basis of the currently available approaches discussed above, we propose a four-tier roadmap outlined in Figure 4 as a general strategy for addressing metabolic activation issues in drug discovery. The first step of this strategy (that preferably occurs at an early

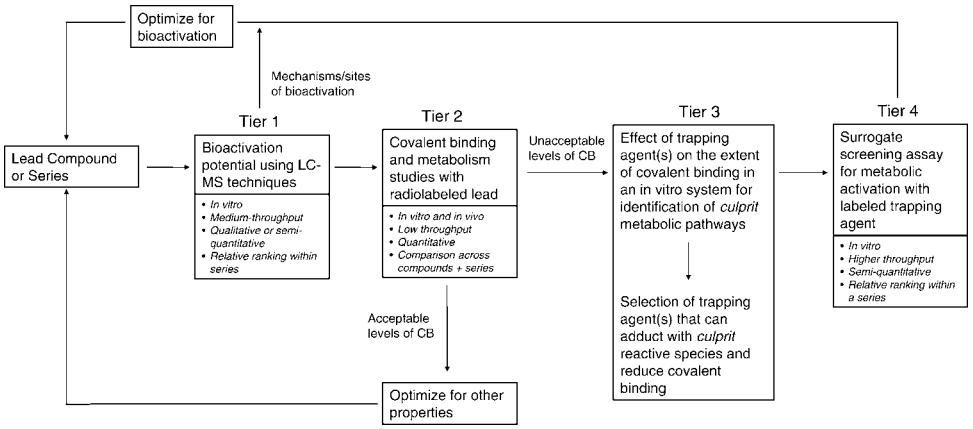

Figure 4 Proposed roadmap for addressing metabolic activation issues in drug discovery.

stage in the program) involves qualitative (or possibly semiquantitative) evaluation of the pathways involved in metabolic activation of several representative chemical lead structures via LC-MS-based trapping assays (using a variety of trapping agents) in liver preparations from appropriate species (usually rat and human). These studies can be used to drive structural modification, in parallel with overall program SAR, to block these metabolic pathways at an early stage. As the program and the leads mature and as a tier 2 strategy in the proposed roadmap, radiolabeled analogs of a select number of more advanced lead candidates should be synthesized and in vitro and in vivo covalent binding and metabolism studies conducted to quantitatively assess the bioactivation liabilities and to guard against potential reactive intermediates that may not be efficiently scavenged by the trapping reagent(s) employed in tier 1. If these studies reveal minimal potential for metabolic activation, the program can progress toward optimization of other desired properties. However, if significant covalent binding is observed in tier 2 studies, effort should be made to identify the mechanisms of bioactivation and covalent binding by examining the effect of various trapping agents on the extent of covalent binding (tier 3 studies), and identification of the adducts formed (with the trapping agent(s) that results in reductions in covalent binding) via LC-MS studies similar to those in tier 1. If these studies clearly reveal the identity of the reactive species that are involved in covalent binding, higher-throughput surrogate screening assays that employ appropriate radiolabeled or fluorescent trapping agent can be used as a tier 4 strategy to develop quantitative SAR for bioactivation. As the chemical lead evolves in response to this screening process, these surrogate screening assays should be interfaced with additional tier 1 studies to monitor for potential switch in the mechanisms of bioactivation. For this four-tier cycle to be most effective, a close and iterative collaboration between Medicinal Chemistry and Drug Metabolism scientists should begin as early as possible in the life cycle of the drug discovery program.

Although relatively costly and low-throughout, the covalent binding studies of protein using radiolabeled drug candidates currently play a central and indispensable role in this proposed roadmap for quantifying the extent of metabolic activation and in the selection of appropriate trapping agent(s) for understanding and addressing the mechanisms involved in bioactivation. This is underscored by the following two examples from drug discovery programs at Merck.

In the first case study, a lead candidate **1** (Fig. 5) was assessed for its potential to form reactive metabolites in LC-MS-based trapping assays using a variety of trapping agents. There were no indications of the formation of any thiol or cyanide adducts when GSH, *N*-acetylcysteine, or cyanide were included in incubations of **1** with human liver microsomes. However, when a tritium-labeled derivative of **1** was incubated with human liver microsomes under standard conditions (68), the extent of covalent binding of

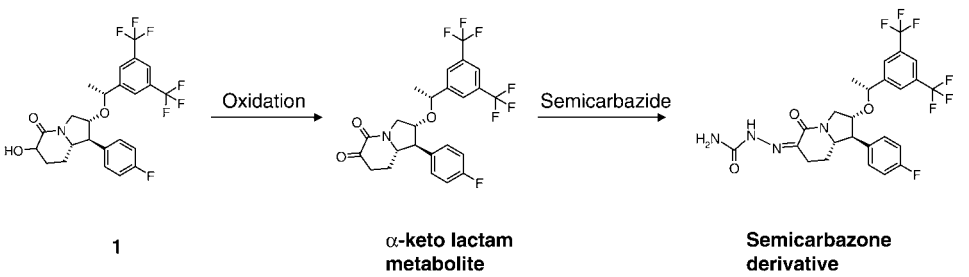

Figure 5 Metabolism of compound **1** to an α ketolactam metabolite that can be trapped as the corresponding semicarbazone derivative by reaction with semicarbazide.

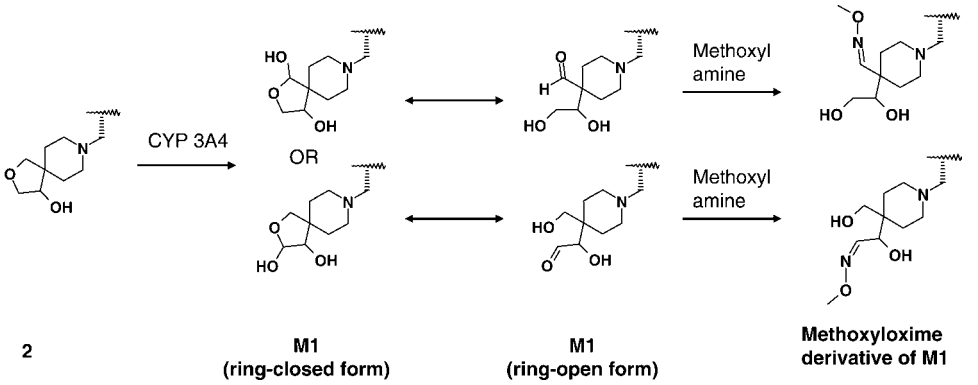

Figure 6 Metabolism of compound **2** to aldehyde metabolites via oxidation of the tetrahydrofuran ring and identification of these reactive species via trapping with methoxylamine.

radioactivity to protein was ~500 pmol Eq/mg liver microsomal protein over a one-hour incubation time. Further, the major metabolite of [^{3}H]**1** in human liver microsomal incubations was the oxidized α-keto lactam derivative. This α-keto lactam metabolite underwent facile condensation with semicarbazide, and essentially all of the metabolite formed in human liver microsomal incubations could be trapped as the corresponding semicarbazone derivative when semicarbazide was included in the incubation. This finding possibly implicated this metabolite as a culprit in the covalent binding of [^{3}H]**1**-associated radioactivity to human liver microsomal protein via its reaction with basic amino acid residues. However, the inclusion of semicarbazide in the incubations led to very small (<20%) reductions in the extent of covalent binding of [^{3}H]**1**-associated radioactivity to protein, suggesting that the α-keto lactam is likely not the major reactive species of concern. This case study stresses the point that mere detection of an adduct with a trapping agent does not necessarily provide a true indication of the metabolic activation and covalent protein-binding liability of a particular chemical substructure and SAR driven on this basis only, without appropriately interfacing with covalent binding studies, has the potential to lead to misguided medicinal chemistry efforts.

In the second case study, compound **2** contained a spirocyclic motif with tetrahydrofuran and piperidine moieties (Fig. 6). Similar to compound **1** in the previous case study, **2** also did not yield any thiol or cyanide adducts when incubated with human liver microsomes in the presence of thiol or cyanide trapping agents. However, extent of covalent binding of a radiolabeled analog of this compound ([^{3}H]**2**) to human liver microsomal protein in vitro and to rat liver protein in vivo was ~400 and ~50 to 60 pmol Eq/mg protein, respectively, under the standard assay conditions described earlier (68). The covalent binding of radioactivity to human liver microsomal protein was not reduced significantly by the inclusion of GSH or cyanide in incubations but was suppressed nearly completely (>90%) with methoxylamine. This led to the hypothesis that oxidation at the carbons α- to the oxygen of the tetrahydrofuran ring or nitrogen of the piperidine ring could lead to the formation of corresponding hemiacetal or hemiaminal metabolites, respectively, which could exist in equilibrium with their ring-opened and reactive aldehyde form; one or more of these aldehyde derivatives could then react covalently with basic amino acid residues and lead to the covalent binding observed with this drug candidate. At least one of these aldehyde intermediates could be trapped with methoxylamine as its corresponding oxime derivative, the mass spectral fragmentation of which corresponded to a condensation product of methoxylamine with a ring-opened aldehyde intermediate formed following oxidation of the tetrahydrofuran ring (Fig. 6).

Although two different adducts are possible with this chemical structure, the aldehyde intermediate depicted in the top row of Figure 6 would bind with amine nucleophiles (e.g., lysine residues) to form an imine that would generally be unstable toward hydrolysis in biological environment whereas the α-hydroxy imine derivative formed from the α-hydroxy aldehyde intermediate depicted in the bottom row could rearrange in an Amadori-like process to form a stable β-keto amine adduct that would result in measurable covalent binding of drug-related material to protein. In agreement with this hypothesis, the corresponding cyclopentane analog of **2**, where the oxygen of the tetrahydrofuran ring was replaced by a carbon in order to block ring opening and formation of aldehyde intermediates, displayed greatly reduced levels of covalent binding to human liver microsomal protein ($\sim$100 pmol Eq/mg protein/1-hour incubation) (68). This example highlights the critical role that covalent binding studies play in the selection of the correct trapping agent for understanding the bioactivation/covalent binding mechanism(s) involved in protein modification so that medicinal chemistry efforts can be focused in a productive fashion.

MINIMIZING METABOLIC ACTIVATION IN DRUG DISCOVERY: FUTURE DIRECTIONS

In spite of the progress made in recent years in our ability to address metabolic activation issues in drug discovery, it should be acknowledged that our scientific approach to addressing this issue remains rudimentary both in terms of the quality of models that are employed for measuring the extent of metabolic activation for human risk assessment and in our understanding of the biological mechanisms that result in toxic insult following exposure to some, but not all, chemically reactive metabolites. It can perhaps be argued that the inability to understand risk with specific reactive species formed from individual drug candidates forces the pharmaceutical industry to adopt a conservative approach where attempts are made to minimize metabolic activation recognizing that, in the process, many molecules may be eliminated from consideration that could be developed as safe drugs in spite of their metabolic activation potential. In the past two to three years, several exciting scientific breakthroughs have occurred that have the potential to address the above gap areas and transform the process of minimizing metabolic activation during drug discovery from a crude empirical approach to a much more rational one. These breakthroughs include developments in the systems biology-based "omic" approaches including toxicogenomics and proteomics that investigate early patterns of change across a broad range of biological networks in response to toxicants and offer the promise of identifying the trigger mechanisms that lead to toxic insult. Microarray-based toxicogenomic technologies already have matured to a point where they can be applied routinely in a drug discovery environment to aid in the rapid development of predictive tools for assessing the toxicity potential of drug candidates (via metabolic activation or other mechanisms) (76,77). From a purely metabolic activation perspective, it is evident that the most promising avenue for predictive differentiation between *benign* versus *toxic* reactive intermediates is likely to come from the identification of the cellular macromolecules that are targeted by a diverse array of reactive metabolites. However, until recently, progress in this area has been very slow due to the lack of adequate analytical tools to detect sub-stoichiometric protein modifications in a complex biological matrix where the abundance of different proteins can vary by a million-fold or more; this has resulted in the identification of only a limited number of protein targets for a few model compounds in over two to three decades of research [Reactive Metabolite Target

Protein Database, http://tpdb.medchem.ku.edu/tpdb.html (78)]. However, recent advances in high-resolution mass spectrometry technology and intelligent data analysis software tools show tremendous promise in tackling this problem (79 82). Because of the complex and multifactorial nature of drug toxicity, these "shotgun" type genomic and proteomic technologies and powerful network integration and pattern recognition tools offer great promise to provide a detailed elucidation of the biochemical and cellular processes by which certain chemically reactive metabolites trigger toxicity, while others activate cellular defense mechanisms and thus represent a benign form of bioactivation.

As has been discussed earlier in this chapter, the current experimental models for assessing the potential for metabolic activation (liver microsomes and hepatocytes in vitro, rodents in vivo) are far from ideal and enable only an empirical approach to addressing the issue of metabolic activation. However, significant progress has been made recently in the development of improved preclinical models for predicting human drug metabolism, including the propensity for metabolic activation. These include, on the one hand, better in vitro tools such as engineered micropatterned human liver tissue that is closer in three-dimensional structure and function to the native human liver (83,84) and, on the other hand, even more ambitious and promising genetically engineered and chimeric animals that express single, multiple, or the entire complement of human drug metabolizing enzymes and transporters (85 88). These animal models should offer unparalleled opportunities to explore a variety of variables of interest to drug discovery scientists, including the potential for metabolic activation as a function of dose and exposure and under "human-like" in vivo conditions that take into account important variables such as plasma protein binding, tissue partitioning, and a more complete set of protective and clearance mechanisms. These models will also allow investigation of the link between metabolic activation of established human toxicants (that are suspected to elicit toxicity via covalent binding to macromolecules) to changes in the genomic and the proteomic signature of the target tissues (liver in particular). The hope is that patterns of change will emerge from these investigations that will yield predictive biomarkers for human toxicity which, in turn, will aid in assessing the toxicological significance, or lack thereof, of metabolic activation of a particular drug candidate before it is advanced into development or introduced onto the market.

REFERENCES

1. Adams CP, Brantner VV. Estimating the cost of new drug development: is it really 802 million dollars? Health Aff (Millwood) 2006; 25:420 428.
2. DiMasi JA, Hansen RW, Grabowski HG. The price of innovation: new estimates of drug development costs. J Health Econ 2003; 22:151 185.
3. Baillie TA. Future of toxicology metabolic activation and drug design: challenges and opportunities in chemical toxicology. Chem Res Toxicol 2006; 19:889 893.
4. Park K, Williams DP, Naisbitt DJ, Kitteringham NR, Pirmohamed M. Investigation of toxic metabolites during drug development. Toxicol Appl Pharmacol 2005; 207:425 434.
5. Park KB, Dalton Brown E, Hirst C, Williams DP. Selection of new chemical entities with decreased potential for adverse drug reactions. Eur J Pharmacol 2006; 549:1 8.
6. Uetrecht J. Evaluation of which reactive metabolite, if any, is responsible for a specific idiosyncratic reaction. Drug Metab Rev 2006; 38:745 753.
7. Nassar AE, Lopez Anaya A. Strategies for dealing with reactive intermediates in drug discovery and development. Curr Opin Drug Discov Devel 2004; 7:126 136.
8. Uetrecht J. Idiosyncratic drug reactions: current understanding. Annu Rev Pharmacol Toxicol 2007; 47:513 539.

9. Boelsterli UA, Ho HK, Zhou S, Leow KY. Bioactivation and hepatotoxicity of nitroaromatic drugs. Curr Drug Metab 2006; 7:715 727.
10. Kalgutkar AS, Soglia JR. Minimising the potential for metabolic activation in drug discovery. Expert Opin Drug Metab Toxicol 2005; 1:91 142.
11. Kalgutkar AS, Gardner I, Obach RS, Shaffer CL, Callegari E, Henne KR, Mutlib AE, Dalvie DK, Lee JS, Nakai Y, O'Donnell JP, Boer J, Harriman SP. A comprehensive listing of bioactivation pathways of organic functional groups. Curr Drug Metab 2005; 6:161 225.
12. Zhou S, Chan E, Duan W, Huang M, Chen YZ. Drug bioactivation, covalent binding to target proteins and toxicity relevance. Drug Metab Rev 2005; 37:41 213.
13. Potter WZ, Thorgeirsson SS, Jollow DJ, Mitchell JR. Acetaminophen induced hepatic necrosis. V. Correlation of hepatic necrosis, covalent binding and glutathione depletion in hamsters. Pharmacology 1974; 12:129 143.
14. Tarloff JB, Khairallah EA, Cohen SD, Goldstein RS. Sex and age dependent acetaminophen hepato and nephrotoxicity in Sprague Dawley rats: role of tissue accumulation, nonprotein sulfhydryl depletion, and covalent binding. Fundam Appl Toxicol 1996; 30:13 22.
15. Mutlib AE, Chen H, Nemeth GA, Markwalder JA, Seitz SP, Gan LS, Christ DD. Identification and characterization of efavirenz metabolites by liquid chromatography/mass spectrometry and high field NMR: species differences in the metabolism of efavirenz. Drug Metab Dispos 1999; 27:1319 1333.
16. Mutlib AE, Gerson RJ, Meunier PC, Haley PJ, Chen H, Gan LS, Davies MH, Gemzik B, Christ DD, Krahn DF, Markwalder JA, Seitz SP, Robertson RT, Miwa GT. The species dependent metabolism of efavirenz produces a nephrotoxic glutathione conjugate in rats. Toxicol Appl Pharmacol 2000; 169:102 113.
17. Miller JA. Brief history of chemical carcinogenesis. Cancer Lett 1994; 83:9 14.
18. Miller JA. The metabolism of xenobiotics to reactive electrophiles in chemical carcinogenesis and mutagenesis: a collaboration with Elizabeth Cavert Miller and our associates. Drug Metab Rev 1998; 30:645 674.
19. Bolton JL, Trush MA, Penning TM, Dryhurst G, Monks TJ. Role of quinones in toxicology. Chem Res Toxicol 2000; 13:135 160.
20. Kolbanovskiy A, Kuzmin V, Shastry A, Kolbanovskaya M, Chen D, Chang M, Bolton JL, Geacintov NE. Base selectivity and effects of sequence and DNA secondary structure on the formation of covalent adducts derived from the equine estrogen metabolite 4 hydroxyequilenin. Chem Res Toxicol 2005; 18:1737 1747.
21. Liu X, Pisha E, Tonetti DA, Yao D, Li Y, Yao J, Burdette JE, Bolton JL. Antiestrogenic and DNA damaging effects induced by tamoxifen and toremifene metabolites. Chem Res Toxicol 2003; 16:832 837.
22. Zhang F, Swanson SM, van Breemen RB, Liu X, Yang Y, Gu C, Bolton JL. Equine estrogen metabolite 4 hydroxyequilenin induces DNA damage in the rat mammary tissues: formation of single strand breaks, apurinic sites, stable adducts, and oxidized bases. Chem Res Toxicol 2001; 14:1654 1659.
23. Kalgutkar AS, Obach RS, Maurer TS. Mechanism based inactivation of cytochrome P450 enzymes: chemical mechanisms, structure activity relationships and relationship to clinical drug drug interactions and idiosyncratic adverse drug reactions. Curr Drug Metab 2007; 8: 407 447.
24. Masubuchi Y, Horie T. Toxicological significance of mechanism based inactivation of cytochrome p450 enzymes by drugs. Crit Rev Toxicol 2007; 37:389 412.
25. He K, Iyer KR, Hayes RN, Sinz MW, Woolf TF, Hollenberg PF. Inactivation of cytochrome P450 3A4 by bergamottin, a component of grapefruit juice. Chem Res Toxicol 1998; 11:252 259.
26. Lin HL, Kent UM, Hollenberg PF. The grapefruit juice effect is not limited to cytochrome P450 (P450) 3A4: evidence for bergamottin dependent inactivation, heme destruction, and covalent binding to protein in P450s 2B6 and 3A5. J Pharmacol Exp Ther 2005; 313:154 164.
27. Tassaneeyakul W, Guo LQ, Fukuda K, Ohta T, Yamazoe Y. Inhibition selectivity of grapefruit juice components on human cytochromes P450. Arch Biochem Biophys 2000; 378:356 363.

28. Erve JC. Chemical toxicology: reactive intermediates and their role in pharmacology and toxicology. Expert Opin Drug Metab Toxicol 2006; 2:923 946.
29. Tang W. Drug metabolite profiling and elucidation of drug induced hepatotoxicity. Expert Opin Drug Metab Toxicol 2007; 3:407 420.
30. Baillie TA. Metabolism and toxicity of drugs. Two decades of progress in industrial drug metabolism. Chem Res Toxicol 2008; 21:129 137.
31. Dalvie DK, Kalgutkar AS, Khojasteh Bakht SC, Obach RS, O'Donnell JP. Biotransformation reactions of five membered aromatic heterocyclic rings. Chem Res Toxicol 2002; 15:269 299.
32. Nelson SD. Structure toxicity relationships how useful are they in predicting toxicities of new drugs? Adv Exp Med Biol 2001; 500:33 43.
33. Doss GA, Miller RR, Zhang Z, Teffera Y, Nargund RP, Palucki B, Park MK, Tang YS, Evans DC, Baillie TA, Stearns RA. Metabolic activation of a 1,3 disubstituted piperazine derivative: evidence for a novel ring contraction to an imidazoline. Chem Res Toxicol 2005; 18:271 276.
34. Kassahun K, Pearson PG, Tang W, McIntosh I, Leung K, Elmore C, Dean D, Wang R, Doss G, Baillie TA. Studies on the metabolism of troglitazone to reactive intermediates in vitro and in vivo. Evidence for novel biotransformation pathways involving quinone methide formation and thiazolidinedione ring scission. Chem Res Toxicol 2001; 14:62 70.
35. Singh R, Silva Elipe MV, Pearson PG, Arison BH, Wong BK, White R, Yu X, Burgey CS, Lin JH, Baillie TA. Metabolic activation of a pyrazinone containing thrombin inhibitor. Evidence for novel biotransformation involving pyrazinone ring oxidation, rearrangement, and covalent binding to proteins. Chem Res Toxicol 2003; 16:198 207.
36. Yin W, Doss GA, Stearns RA, Chaudhary AG, Hop CE, Franklin RB, Kumar S. A novel P450 catalyzed transformation of the 2,2,6,6 tetramethyl piperidine moiety to a 2,2 dimethyl pyrrolidine in human liver microsomes: characterization by high resolution quadrupole time of flight mass spectrometry and 1H NMR. Drug Metab Dispos 2003; 31:215 223.
37. Yin W, Mitra K, Stearns RA, Baillie TA, Kumar S. Conversion of the 2,2,6,6 tetramethylpiperidine moiety to a 2,2 dimethylpyrrolidine by cytochrome P450: evidence for a mechanism involving nitroxide radicals and heme iron. Biochemistry 2004; 43:5455 5466.
38. Chen LJ, DeRose EF, Burka LT. Metabolism of furans in vitro: ipomeanine and 4 ipomeanol. Chem Res Toxicol 2006; 19:1320 1329.
39. Baillie TA, Davis MR. Mass spectrometry in the analysis of glutathione conjugates. Biol Mass Spectrom 1993; 22:319 325.
40. Chen WG, Zhang C, Avery MJ, Fouda HG. Reactive metabolite screen for reducing candidate attrition in drug discovery. In: Dansette PM, Snyder R, Delaforge M, et al., eds. Biological Reactive Intermediates VI: Chemical and Biological Mechanisms in Susceptibility to and Prevention of Environmental Diseases. New York: Kluwer Academic/Plenum Press, 2001: 521 524.
41. Soglia JR, Harriman SP, Zhao S, Barberia J, Cole MJ, Boyd JG, Contillo LG. The development of a higher throughput reactive intermediate screening assay incorporating micro bore liquid chromatography micro electrospray ionization tandem mass spectrometry and glutathione ethyl ester as an in vitro conjugating agent. J Pharm Biomed Anal 2004; 36:105 116.
42. Castro Perez J, Plumb R, Liang L, Yang E. A high throughput liquid chromatography/tandem mass spectrometry method for screening glutathione conjugates using exact mass neutral loss acquisition. Rapid Commun Mass Spectrom 2005; 19:798 804.
43. Dieckhaus CM, Fernandez Metzler CL, King R, Krolikowski PH, Baillie TA. Negative ion tandem mass spectrometry for the detection of glutathione conjugates. Chem Res Toxicol 2005; 18:630 638.
44. Argoti D, Liang L, Conteh A, Chen L, Bershas D, Yu CP, Vouros P, Yang E. Cyanide trapping of iminium ion reactive intermediates followed by detection and structure identification using liquid chromatography tandem mass spectrometry (LC MS/MS). Chem Res Toxicol 2005; 18:1537 1544.
45. Samuel K, Yin W, Stearns RA, Tang YS, Chaudhary AG, Jewell JP, Lanza T, Jr., Lin LS, Hagmann WK, Evans DC, Kumar S. Addressing the metabolic activation potential of new leads

in drug discovery: a case study using ion trap mass spectrometry and tritium labeling techniques. J Mass Spectrom 2003; 38:211 221.
46. Zhu M, Ma L, Zhang H, Humphreys WG. Detection and structural characterization of glutathione trapped reactive metabolites using liquid chromatography high resolution mass spectrometry and mass defect filtering. Anal Chem 2007; 79:8333 8341.
47. Mutlib A, Lam W, Atherton J, Chen H, Galatsis P, Stolle W. Application of stable isotope labeled glutathione and rapid scanning mass spectrometers in detecting and characterizing reactive metabolites. Rapid Commun Mass Spectrom 2005; 19:3482 3492.
48. Yan Z, Caldwell GW. Stable isotope trapping and high throughput screenings of reactive metabolites using the isotope MS signature. Anal Chem 2004; 76:6835 6847.
49. Yan Z, Maher N, Torres R, Caldwell GW, Huebert N. Rapid detection and characterization of minor reactive metabolites using stable isotope trapping in combination with tandem mass spectrometry. Rapid Commun Mass Spectrom 2005; 19:3322 3330.
50. Bateman KP, Castro Perez J, Wrona M, Shockcor JP, Yu K, Oballa R, Nicoll Griffith DA. MSE with mass defect filtering for in vitro and in vivo metabolite identification. Rapid Commun Mass Spectrom 2007; 21:1485 1496.
51. Ruan Q, Peterman S, Szewc MA, Ma L, Cui D, Humphreys WG, Zhu M. An integrated method for metabolite detection and identification using a linear ion trap/Orbitrap mass spectrometer and multiple data processing techniques: application to indinavir metabolite detection. J Mass Spectrom 2007.
52. Zhu M, Ma L, Zhang D, Ray K, Zhao W, Humphreys WG, Skiles G, Sanders M, Zhang H. Detection and characterization of metabolites in biological matrices using mass defect filtering of liquid chromatography/high resolution mass spectrometry data. Drug Metab Dispos 2006; 34:1722 1733.
53. Soglia JR, Contillo LG, Kalgutkar AS, Zhao S, Hop CE, Boyd JG, Cole MJ. A semiquantitative method for the determination of reactive metabolite conjugate levels in vitro utilizing liquid chromatography tandem mass spectrometry and novel quaternary ammonium glutathione analogues. Chem Res Toxicol 2006; 19:480 490.
54. Gan J, Harper TW, Hsueh MM, Qu Q, Humphreys WG. Dansyl glutathione as a trapping agent for the quantitative estimation and identification of reactive metabolites. Chem Res Toxicol 2005; 18:896 903.
55. Kalgutkar AS, Dalvie DK, O'Donnell JP, Taylor TJ, Sahakian DC. On the diversity of oxidative bioactivation reactions on nitrogen containing xenobiotics. Curr Drug Metab 2002; 3:379 424.
56. Peterson LA. Electrophilic intermediates produced by bioactivation of furan. Drug Metab Rev 2006; 38:615 626.
57. Khojasteh Bakht SC, Chen W, Koenigs LL, Peter RM, Nelson SD. Metabolism of (R) (+) pulegone and (R) (+) menthofuran by human liver cytochrome P 450s: evidence for formation of a furan epoxide. Drug Metab Dispos 1999; 27:574 580.
58. Li C, Olurinde MO, Hodges LM, Grillo MP, Benet LZ. Covalent binding of 2 phenylpropionyl S acyl CoA thioester to tissue proteins in vitro. Drug Metab Dispos 2003; 31:727 730.
59. Olsen J, Li C, Bjornsdottir I, Sidenius U, Hansen SH, Benet LZ. In vitro and in vivo studies on acyl coenzyme A dependent bioactivation of zomepirac in rats. Chem Res Toxicol 2005; 18:1729 1736.
60. Olsen J, Li C, Skonberg C, Bjornsdottir I, Sidenius U, Benet LZ, Hansen SH. Studies on the metabolism of tolmetin to the chemically reactive acyl coenzyme A thioester intermediate in rats. Drug Metab Dispos 2007; 35:758 764.
61. Li C, Grillo MP, Benet LZ. In vivo mechanistic studies on the metabolic activation of 2 phenylpropionic acid in rat. J Pharmacol Exp Ther 2003; 305:250 256.
62. Grillo MP, Hua F, Knutson CG, Ware JA, Li C. Mechanistic studies on the bioactivation of diclofenac: identification of diclofenac S acyl glutathione in vitro in incubations with rat and human hepatocytes. Chem Res Toxicol 2003; 16:1410 1417.
63. Grillo MP, Knutson CG, Sanders PE, Waldon DJ, Hua F, Ware JA. Studies on the chemical reactivity of diclofenac acyl glucuronide with glutathione: identification of diclofenac S acyl glutathione in rat bile. Drug Metab Dispos 2003; 31:1327 1336.

64. Stachulski AV. The chemistry and biological activity of acyl glucuronides. Curr Opin Drug Discov Devel 2007; 10:58 66.
65. Shibutani S, Ravindernath A, Suzuki N, Terashima I, Sugarman SM, Grollman AP, Pearl ML. Identification of tamoxifen DNA adducts in the endometrium of women treated with tamoxifen. Carcinogenesis 2000; 21:1461 1467.
66. Liu H, Liu J, van Breemen RB, Thatcher GR, Bolton JL. Bioactivation of the selective estrogen receptor modulator desmethylated arzoxifene to quinoids: 4′ fluoro substitution prevents quinoid formation. Chem Res Toxicol 2005; 18:162 173.
67. Liu J, Liu H, van Breemen RB, Thatcher GR, Bolton JL. Bioactivation of the selective estrogen receptor modulator acolbifene to quinone methides. Chem Res Toxicol 2005; 18:174 182.
68. Evans DC, Watt AP, Nicoll Griffith DA, Baillie TA. Drug protein adducts: an industry perspective on minimizing the potential for drug bioactivation in drug discovery and development. Chem Res Toxicol 2004; 17:3 16.
69. Day SH, Mao A, White R, Schulz Utermoehl T, Miller R, Beconi MG. A semi automated method for measuring the potential for protein covalent binding in drug discovery. J Pharmacol Toxicol Methods 2005; 52:278 285.
70. Tang C, Subramanian R, Kuo Y, Krymgold S, Lu P, Kuduk SD, Ng C, Feng DM, Elmore C, Soli E, Ho J, Bock MG, Baillie TA, Prueksaritanont T. Bioactivation of 2,3 diaminopyridine containing bradykinin B1 receptor antagonists: irreversible binding to liver microsomal proteins and formation of glutathione conjugates. Chem Res Toxicol 2005; 18:934 945.
71. Zhang Z, Chen Q, Li Y, Doss GA, Dean BJ, Ngui JS, Silva EM, Kim S, Wu JY, Dininno F, Hammond ML, Stearns RA, Evans DC, Baillie TA, Tang W. In vitro bioactivation of dihydrobenzoxathiin selective estrogen receptor modulators by cytochrome P450 3A4 in human liver microsomes: formation of reactive iminium and quinone type metabolites. Chem Res Toxicol 2005; 18:675 685.
72. Kumar S, Kassahun K, Tschirret Guth RA, Mitra K, Baillie TA. Minimizing metabolic activation during pharmaceutical lead optimization: progress, knowledge gaps and future directions. Curr Opin Drug Discov Devel 2008; 11:43 52.
73. Evans DC, Baillie TA. Minimizing the potential for metabolic activation as an integral part of drug design. Curr Opin Drug Discov Devel 2005; 8:44 50.
74. Meneses Lorente G, Sakatis MZ, Schulz Utermoehl T, De Nardi C, Watt AP. A quantitative high throughput trapping assay as a measurement of potential for bioactivation. Anal Biochem 2006; 351:266 272.
75. Masubuchi N, Makino C, Murayama N. Prediction of in vivo potential for metabolic activation of drugs into chemically reactive intermediate: correlation of in vitro and in vivo generation of reactive intermediates and in vitro glutathione conjugate formation in rats and humans. Chem Res Toxicol 2007; 20:455 464.
76. Gatzidou ET, Zira AN, Theocharis SE. Toxicogenomics: a pivotal piece in the puzzle of toxicological research. J Appl Toxicol 2007; 27:302 309.
77. Woods CG, Heuvel JP, Rusyn I. Genomic profiling in nuclear receptor mediated toxicity. Toxicol Pathol 2007; 35:474 494.
78. Hanzlik RP, Koen YM, Theertham B, Dong Y, Fang J. The reactive metabolite target protein database (TPDB) a web accessible resource. BMC Bioinformatics 2007; 8:95.
79. Dennehy MK, Richards KA, Wernke GR, Shyr Y, Liebler DC. Cytosolic and nuclear protein targets of thiol reactive electrophiles. Chem Res Toxicol 2006; 19:20 29.
80. Liebler DC, Guengerich FP. Elucidating mechanisms of drug induced toxicity. Nat Rev Drug Discov 2005; 4:410 420.
81. Shin NY, Liu Q, Stamer SL, Liebler DC. Protein targets of reactive electrophiles in human liver microsomes. Chem Res Toxicol 2007; 20:859 867.
82. Liebler DC. Protein damage by reactive electrophiles: targets and consequences. Chem Res Toxicol 2008; 21:117 128.
83. Khetani SR, Bhatia SN. Microscale culture of human liver cells for drug development. Nat Biotechnol 2008; 26:120 126.

84. Sivaraman A, Leach JK, Townsend S, Iida T, Hogan BJ, Stolz DB, Fry R, Samson LD, Tannenbaum SR, Griffith LG. A microscale in vitro physiological model of the liver: predictive screens for drug metabolism and enzyme induction. Curr Drug Metab 2005; 6:569 591.
85. Azuma H, Paulk N, Ranade A, Dorrell C, Al Dhalimy M, Ellis E, Strom S, Kay MA, Finegold M, Grompe M. Robust expansion of human hepatocytes in Fah / /Rag2 / /Il2rg / mice. Nat Biotechnol 2007; 25:903 910.
86. Katoh M, Sawada T, Soeno Y, Nakajima M, Tateno C, Yoshizato K, Yokoi T. In vivo drug metabolism model for human cytochrome P450 enzyme using chimeric mice with humanized liver. J Pharm Sci 2007; 96:428 437.
87. Senekeo Effenberger K, Chen S, Brace Sinnokrak E, Bonzo JA, Yueh MF, Argikar U, Kaeding J, Trottier J, Remmel RP, Ritter JK, Barbier O, Tukey RH. Expression of the human UGT1 locus in transgenic mice by 4 chloro 6 (2,3 xylidino) 2 pyrimidinylthioacetic acid (WY 14643) and implications on drug metabolism through peroxisome proliferator activated receptor alpha activation. Drug Metab Dispos 2007; 35:419 427.
88. van Herwaarden AE, Smit JW, Sparidans RW, Wagenaar E, van der Kruijssen CM, Schellens JH, Beijnen JH, Schinkel AH. Midazolam and cyclosporin a metabolism in transgenic mice with liver specific expression of human CYP3A4. Drug Metab Dispos 2005; 33:892 895.

24

Kinetic Differences between Generated and Preformed Metabolites: A Dilemma in Risk Assessment

Thomayant Prueksaritanont and Jiunn H. Lin
Department of Drug Metabolism and Pharmacokinetics, Merck Research Laboratories, West Point, Pennsylvania, U.S.A.

SUMMARY

The main objective of this chapter is to examine the kinetic differences between preformed and generated metabolites and highlight potential complications associated with the approaches in risk assessment of drug metabolites by dosing preformed metabolites. To illustrate the kinetic differences between preformed and generated metabolites, theoretical considerations and specific examples are presented. The kinetic behavior of several preformed metabolites given exogenously is shown to differ significantly from that of the corresponding metabolites generated endogenously from the parent compound in vivo. Demonstrated differences exist in the accumulation of the preformed versus generated metabolites in specific tissues, and in sequential metabolism to downstream products. In such cases, a "bridging study" performed by dosing the preformed metabolite in animals would fail to characterize the true toxicological contribution of the metabolite generated from its parent and complicate the toxicity evaluation of the metabolite. It is recommended that the kinetic behavior of a metabolite generated in vivo versus that given exogenously be assessed before conducting the so-called bridging study. Given recent advancements in transgenic animal models, it is conceivable that sometime in the future humanized mouse lines expressing specific drug transporters and metabolizing enzymes may serve as valuable tools for risk assessment of drug metabolites that are disproportionately higher in humans than in animal species used for toxicity studies.

INTRODUCTION

During the drug development process, monitoring plasma profiles of parent drug and its metabolites in the nonclinical toxicology studies are required to ensure adequate systemic exposure to characterize organ toxicity and to cover the expected plasma profiles in

clinical studies. In some cases, however, significant qualitative or quantitative differences in metabolite profiles occur between the test animal species and humans because of species differences in drug metabolism. Concerns have arisen regarding potential inadequacy of the animal toxicology studies with only parent drugs. In the past few years, the issue of drug metabolites in safety testing and the role of metabolites as potential mediators of the toxicity of new drug products have gained increased attention by both pharmaceutical companies and regulatory agencies (1 4). After much debate, the Food and Drug Administration (FDA) has issued in February 2008 the *Guidance for Industry on Safety Testing of Drug Metabolites*, which outlines recommendations on when and how to characterize and evaluate the safety of "disproportionate" metabolites of small molecule drug products (5). Metabolites are defined as disproportionate if they present only in humans or present at higher plasma concentrations in humans than in the animals used in nonclinical studies. In cases where a relevant animal species that forms the metabolites at adequate exposure cannot be identified, a bridging study will be required to evaluate safety of the specific metabolite by dosing preformed metabolite(s) in animals. The risk assessment of drug metabolites is considered to be part of an investigational new drug (IND) application and recommended to be completed before beginning large-scale clinical trials prior to new drug application (NDA) in the United States.

The main objective of this review article is to examine the kinetic differences between preformed and generated metabolites and highlight potential complications associated with the approaches in risk assessment of drug metabolites by dosing preformed metabolites. We hope to convey that considerations to conduct the metabolite testing be based on knowledge and understanding of the kinetic behavior of a metabolite generated in vivo versus that given exogenously, and that this chapter would promote continued discussions on finding alternatives/approaches to the proposed nonclinical testing of drug metabolites to better ensure the clinical safety of new therapeutic agents.

THEORETICAL CONSIDERATIONS

From a pharmacokinetic viewpoint, in order to achieve the goals set forth by FDA Guidance, two key assumptions have to be met: (*i*) the kinetic behavior, with respect to the relationship between systemic exposure and tissue distribution, of a preformed (synthesized) metabolite administered exogenously is the same as that of the metabolite formed in vivo following administration of the parent compound and (*ii*) the kinetics of a preformed metabolite in an animal species selected for nonclinical testing reflect those of the corresponding metabolite formed in vivo in humans following administration of its parent. While these two assumptions may be valid for many drug metabolites, there are cases that the assumptions may not be valid, so that the results of toxicity testing of a drug metabolite can be misleading, or fail to characterize the true toxicological contribution of the metabolite when formed from the parent.

The processes of absorption, distribution, metabolism, and excretion (ADME) of a compound are known to be influenced by (*i*) the specific characteristics of the compound, including its physicochemical properties and ability to interact with transporters, drug-metabolizing enzymes, and binding proteins, and (*ii*) physiological factors, which govern the exposure of the compound to those proteins, such as distribution, tissue localization, and organ blood flow (6,7). While the pharmacokinetics of a preformed metabolite, measured as systemic or tissue concentrations as a function of time, will depend largely on the ADME properties of the synthesized metabolite per se, the kinetics of a metabolite generated in vivo also are influenced by the ADME properties of the parent compound, in

addition to its own (6,8). Therefore, differences between the kinetic behavior of a preformed metabolite and the metabolite generated from the parent drug could arise because of intrinsic differences between the parent and its metabolite in physicochemical properties and/or the nature of their interactions with transporters, drug-metabolizing enzymes, and/or binding proteins. Moreover, the kinetics of a preformed metabolite in an animal species selected for nonclinical testing may not be the same as those of a metabolite formed in vivo, either in that animal species or humans, following administration of the parent, due to species differences in the interaction of a compound with transporters, enzymes, or plasma/tissue-binding proteins, and intrinsic activities or distribution across organs (9).

There are many physicochemical and biological factors that may contribute to the kinetic differences between preformed and generated metabolites (10,11). This paper focuses mainly on three major factors, namely physicochemical properties, drug transporters, and drug-metabolizing enzymes. In addition, species differences in transporters and drug-metabolizing enzymes and the interplay between transporter and metabolizing enzyme are also discussed.

Physicochemical Factors

Lipophilicity is generally considered as a key determinant of permeability across tissue membranes, and consequently in determining the extent of drug absorption, distribution to tissues (particularly brain), and elimination processes such as hepatic transport and renal reabsorption (10). Uptake of lipophilic compounds across the basolateral membrane usually is very efficient as compared with that of hydrophilic molecules. Since metabolites are generally more polar than their parent compounds, they commonly experience much greater diffusional barriers to tissues (11,12). Consequently, the distribution of a preformed metabolite to organs and tissues may be more limited than when the metabolite is formed in vivo, thus may restrict potential toxicities to somewhat limited tissues, as compared with that generated from the parent. Additionally, because of the larger permeability barrier to transverse out of cells, the metabolite, once formed in vivo, also has a greater potential to accumulate inside the cells. If the site of metabolite formation is tissue specific, the difference in polarity between a metabolite and its parent could lead to differences in tissue-specific distribution or retention between the generated versus preformed metabolite and, hence, in their tissue-specific toxicity profiles.

Other physicochemical properties that may impact the disposition of a compound include chemical stability (13). If a metabolite is less stable chemically than its parent, administration of the preformed metabolite may lead to more limited distribution of the metabolite than is the case when the parent is dosed. The distribution of a metabolite formed in vivo is expected to be dependent on the tissue distribution of both the parent drug and the metabolizing enzymes responsible for the parent-to-metabolite conversion. Furthermore, there are cases when the generated metabolite, because of its instability, leads to regeneration of the precursor within the body ("futile cycling"). Many conjugated metabolites (e.g., glucuronides) can be hydrolyzed back to their corresponding aglycones either chemically or, more commonly, via the action of β-glucuronidase enzymes (14 16). In such cases, the exposure ratio between a metabolite and its parent in the systemic circulation and/or in a given organ following administration of a preformed metabolite may differ appreciably from that following administration of the parent, depending on the interconversion rate and the efficiency of competing pathways. Additionally, if the locus of formation of a labile metabolite differs from that at which it causes toxicity, the tissue distribution (and hence toxic effects) of the preformed metabolite would be anticipated to

be quite distinct from those of the corresponding metabolite generated endogenously. For example, hydroxylamine metabolites of certain carcinogenic aromatic amines are themselves carcinogenic. However, when given as the parent aromatic amines, the hydroxylamine metabolites are subject to efficient hepatic glucuronidation and subsequent "transport" from the liver to the kidney in the form of labile *N*-glucuronide conjugates. Upon exposure of these conjugates to the acidic urinary pH in the bladder, reactive intermediates are generated which cause bladder-specific tumors (17). It is very likely that the toxicity profiles would be quite different when the parent aromatic amines or *N*-glucuronides of hydroxylamine are given.

Transporter Factors

The results of a large number of in vivo and in vitro studies indicate that transporters represent an important determinant of drug disposition (10). Drug transporters generally can be separated into two major classes uptake and efflux transporters. Several of these transporters have been demonstrated to possess substrate specificities and are known to localize in different tissues/organs (18). For example, the ABC-B family (P-glycoprotein, P-gp, and its relatives) mediates ATP-driven efflux transport of cationic and neutral xenobiotics (19), while the ABC-C family (the multidrug resistance associated proteins, MRPs) is ATP-driven drug pumps that handle anionic compounds (20,21). Both are highly expressed in brain and several peripheral tissues, particularly excretory organs. A family of polyspecific uptake transporters, the organic anion transporting polypeptides, or OATPs (22), which also are prominent in excretory organs and barrier epithelia, handle somewhat large hydrophobic organic anions. Human OATP1B1, OATP1B3, and rat Oatp1b2, which are known to be expressed exclusively in liver, have been shown to be responsible for the selective liver uptake of pravastatin (23,24). The organic cation and anion transporters, OCTs and OATs, respectively, accommodate relatively small molecular weight molecules and exhibit tissue-specific expression (25,26). In humans, OCT1 is expressed ubiquitously with relatively robust expression in the liver, and OCT2 is highly expressed in the kidney (27). In rodents, Oct1 is expressed in both the liver and kidney, whereas Oct2 is expressed mainly in the kidney. Recently, the high levels of Oct1/2 in kidney have been reported to be responsible for selective tissue retention of tetraethylammonium (TEA) in mouse kidney (kidney/plasma ratio ~80) (28), while that of Oct1 has been shown to be associated with high intra-hepatic concentrations of metformin, resulting in a known potentially lethal side effect, lactic acidosis (29). Similarly, OAT1 and OAT3 are known to be expressed exclusively in kidney tissue. Indeed, OAT1-mediated renal uptake has been implicated as a contributing factor in the intracellular accumulation of adefovir and cidofovir, leading to the nephrotoxicity of these agents (30). Conceivably, differences in tissue-selective exposure or accumulation between a metabolite formed in vivo versus given exogenously would ensue if the metabolite and its parent are substrates of different uptake transporters, which exhibit tissue selectivity. Similarly, there may be differences in excretory profiles or tissue localization/exposure between preformed and generated metabolites when the metabolite and its parent are substrates of different excretory transporters, which are located in different tissues.

It is noteworthy that transporter-mediated drug disposition reflects the dynamic interplay between uptake and efflux transporters within any given epithelial cell, in which the translocation of drugs across membranes may be impeded or facilitated by the presence of transporters on apical or basolateral membranes (31,32). Therefore, for many drugs, the combined and sometimes complementary actions of transporters expressed

within specific membrane domains of epithelial cells determine the extent and direction of drug movement across organs such as the liver, kidney, and brain. It is to be expected that differences between a metabolite and its parent in their interactions with uptake and efflux transporters would lead to differences in disposition between a preformed metabolite and a metabolite generated in vivo.

Compounding this issue further is the question of species differences in the expression level, functional activity, and tissue distribution of transporters. Recent data have revealed that rat liver contains much more (~10-fold) Mrp2 protein resulting in a much higher capacity for the biliary excretion of organic anions in rats than in humans or other preclinical species (32). Species differences between rat and human OATs also have been reported; hOAT1 accepts cimetidine as a substrate, whereas rOat1 does not interact with cimetidine (33 35). These differences have been associated with species differences in the renal elimination of cimetidine, as well as a number of organic anions and cations (34). Similarly, OCTs expressed in the kidney differ between rodents and humans. Both Oct1 (Slc22a1) and Oct2 (Slc22a2) are involved in the renal uptake of organic cations on the basolateral membrane of the proximal tubules in rodents, whereas OCT2, but not OCT1, is abundant in the human kidney (36). As a result of species differences in drug- and metabolite-transporter interactions, it is conceivable that the disposition of a preformed metabolite in animals may differ substantially from that of the corresponding metabolite formed in vivo in humans following administration of its parent.

Metabolizing Enzyme Factors

Drug-metabolizing enzymes have been shown to exhibit heterogeneity in distribution within an organ. An enrichment of cytochromes (CYPs), glutathione-S-transferases (GSTs), carboxylesterases, and UDP-glucuronyltransferases (UGTs) was demonstrated in the perihepatic venous region of the liver, while sulfotransferases (SULTs) were found predominantly in the periportal region (11,37 39). This zonal distribution of enzymes has been proposed, both on theoretical and experimental grounds, to represent one determinant of metabolite disposition, resulting in differences in the fate of a preformed metabolite entering the liver from the circulation relative to that of the same metabolite formed within the liver. In-depth reviews of this topic with specific examples are provided in Pang et al. (11) and Abu-Zahra and Pang (38).

In theory, differences in the disposition between a preformed versus an in vivo generated metabolite, especially with respect to formation of downstream metabolites, may result from differences in tissue distribution or exposure between the preformed and generated metabolite (as a consequence of the aforementioned physicochemical and/or transporter factors). This potential difference in the formation of downstream metabolites could be complicated further by the fact that some drug-metabolizing enzymes, as is the case with transporters, exhibit tissue-specific expression. Although most CYPs are found in the liver, some CYPs are expressed preferentially in extrahepatic tissues, which may lead to unique extrahepatic metabolites and tissue-specific consequences in terms of cellular toxicity and organ pathology. Among those in the CYP2 gene family, CYP2A6, 2B6, 2C18, and 2J2 are expressed preferentially in extrahepatic tissues, including epithelial tissues at the environmental interface such as skin, nasal, respiratory, and digestive systems (40,41). Similarly, UGT1A8 and UGT1A10 are expressed exclusively in gastrointestinal tissues, each with a unique distribution pattern (42,43). SULT1A1 is the major adult liver SULT1A subfamily member, whereas SULT1A3 is barely detectable in the adult human liver but is highly expressed in jejunum and intestine (44). In the brain, the cellular and regional distribution of drug-metabolizing enzymes is known to be

heterogeneous, with the blood brain interfaces bearing special drug-metabolic capacities; MAO-B and class III alcohol dehydrogenase (ADH) appear to be highly expressed and active at the blood CSF barrier in rat and human choroid plexuses (45).

Additionally, species differences in drug-metabolizing enzyme activities are well recognized and the reader is referred to reviews on this topic (9). These differences may lead to the formation of species-selective metabolites, and consequently to species-selective toxicity. An increase in CYP-mediated hydroxylation, low esterase activity, and relatively high aldehyde dehydrogenase activity in rats relative to humans have been linked to the characteristic toxic effects of felbamate in humans, which are not seen in rats (46). Also, as is the case for the drug transporters, several enzymes are known to exhibit species differences in tissue distribution, including acylases (*N*-acetyl-L-cysteine-deacetylating enzyme) and GSTs (47,48). In rats, e.g., a cysteinylglycine adduct formed by renal γ-glutamyltranspeptidase-mediated cleavage of a GSH adduct of efavirenz (generated by a species-specific GST) was demonstrated to be associated with nephrotoxicity. This kidney toxicity was observed only in rats, and not in cynomulgus monkeys or humans (49). Moreover, some drug-metabolizing enzymes have been shown to exhibit species differences in intracellular distribution. In guinea pig, as in humans, the liver ciprofibroyl-CoA hydrolase is localized in the mitochondrial and soluble fractions of cells, while in rats, the enzyme has a microsomal localization (50). In principle, these differences could contribute to tissue-selective exposure and species differences in toxicity profiles between the preformed and generated metabolite.

Interplay Between Membrane Permeability/Transporters and Drug-Metabolizing Enzymes

As will be evident from the above discussion, the disposition of a compound is dependent on a number of factors, including membrane permeability, drug transporters, and drug-metabolizing enzymes. These factors work either in concert with or competitively against each other, and it is reasonable to expect that differences in the interplay between a metabolite and its parent with these systems would lead to differences in the disposition of a preformed metabolite relative to its counterpart generated in vivo. Using computer modeling, Miyauchi and coworkers (51) demonstrated that when there is no diffusional barrier for the metabolite, differences in the extraction ratio between the preformed and generated metabolite are dependent on enzyme activity and could be as large as fivefold. In cases where a diffusional barrier exists for the metabolite, a much higher hepatic extraction ratio (up to 10-fold) is observed for the endogenously generated metabolite relative to the exogenously dosed preformed metabolite (51). Recent studies (7,52) also have demonstrated the importance of the interplay of uptake and efflux transporters with metabolic enzymes in drug disposition as the access of drug molecules to the enzymes is controlled by drug transporters. Both transporter activities and localization of enzymes in the liver influenced the mean hepatic residence time of a metabolite formed in vivo (53). In the case of CPT-11, the interplay between esterases, UGTs, β-glucuronidases, and the efflux transporter MRP2, has been implicated in the localization of its active metabolite, SN-38, in the intestinal tract, leading to diarrhea, the dose-limiting toxicity of CPT-11 (54,55). SN-38 is formed by esterases from CPT-11, deactivated by UGTs, excreted via MRP2- and/or P-gp-mediated biliary excretion, and deconjugated by β-glucuronidases in the intestinal lumen.

The interplay discussed above also has been shown to impact the metabolic pattern and extraction ratio of compounds given orally. Thus, luminal administration of phenol yielded phenol glucuronide as the primary metabolite, while following vascular

administration, sulfation represented the primary metabolic pathway of phenol (56). A much greater overall extraction also was obtained following luminal than following vascular administration (56). This was attributed to a greater and/or more prolonged exposure of the perorally administered phenol to the apically placed UGTs. Phenol required more time to diffuse across the lipid-rich barrier of the ER to access the active site of the UGTs, as compared with the readily accessible cytosolic SULTs, whereas the phenol glucuronide, being more polar and much larger than its aglycone, experienced a greater diffusional barrier to its efflux from the ER lumen. Similar route-of-administration-dependent metabolism, resulting from a dynamic interplay between UGTs and efflux transporters, has been reported for morphine and its glucuronide metabolite (57). A logical extension of these observations is that the route of administration may have a significant effect on the toxicity profile of a drug metabolite, such that the findings from a study in which the preformed metabolite is dosed may not reflect those of a study in which the metabolite is generated from the parent.

SPECIFIC EXAMPLES

In the section that follows, examples are provided to illustrate the differences in the disposition kinetics of a preformed metabolite versus the same metabolite generated in vivo from the parent, either within a given animal species or between animals and humans. Where applicable, the consequences of these differences in disposition, either pharmacological or toxicological, are highlighted.

Acetaminophen and Phenacetin

Quantitative differences in the sequential metabolism of a preformed metabolite and its counterpart generated by metabolism are best exemplified by the case of acetaminophen. Both phenacetin and acetaminophen (the O-de-ethylated metabolite of phenacetin) distribute equally and rapidly from blood to hepatocytes; i.e., there is little, if any, diffusional barrier in the process (58). Using the rat isolated liver perfusion technique, Pang and Gillette (59) demonstrated that the hepatic extraction ratio (the fraction of dose metabolized by the liver during each passage) of [^{14}C]acetaminophen derived from [^{14}C] phenacetin was lower than that of preformed [^{3}H]acetaminophen when given exogenously (0.50 versus 0.68). These results suggest that the hepatic exposure to acetaminophen formed in vivo would be higher than that when preformed acetaminophen is given exogenously, assuming an equimolar molar dose of the two species. This lower extraction ratio of generated [^{14}C]acetaminophen was proposed to be due to the uneven distribution of the corresponding enzyme systems responsible for the metabolism of phenacetin (CYPs) and acetaminophen (UGTs and SULTs). The CYP-mediated O-deethylation of phenacetin occurred predominantly in the centrilobular region, while a sequential metabolic step, sulfate conjugation, occurred predominantly in the periportal region (58,60). This hypothesis is consistent with computer simulations under various patterns of enzyme distribution and membrane permeability (51,60). It is noteworthy that acetaminophen undergoes oxidative metabolism to a product, namely *N*-acetyl-*p*-benzoquinone imine (NAPQI), that is toxic to the liver (61,62). Therefore, the hepatic exposure to the hepatotoxic intermediate, and consequently hepatotoxicity, would conceivably be significantly greater, as a result of greater hepatic exposure to acetaminophen, in animals dosed with acetaminophen than in animals given an equimolar amount of phenacetin itself.

Enalaprilat and Enalapril

Unlike the acetaminophen/phenacetin pair, differential effects of a diffusional barrier on generated and preformed metabolite kinetics have been reported to be important factors in the disposition of enalaprilat, an ACE inhibitor employed for the treatment of hypertension. In animals and humans, enalapril, an inactive prodrug, is hydrolyzed completely by carboxylesterases to its polar dicarboxylic acid metabolite, enalaprilat (63,64). Studies in the perfused rat liver with simultaneous delivery of [^{14}C]enalapril and its active metabolite, [^{3}H]enalaprilat, revealed a marked difference in the biliary recovery of the generated [^{14}C]enalaprilat (18% dose) and the preformed [^{3}H]enalaprilat (5% dose). A higher hepatic exposure (>3-fold) of enalaprilat was obtained when the compound was generated from the parent drug than when given as the preformed metabolite (63). In a subsequent study using a perfused rat liver preparation, these authors showed that the biliary clearance of generated [^{14}C]enalaprilat was 15-fold higher than the biliary clearance of the preformed [^{3}H]enalaprilat (65). Similarly, a significant difference in the urinary clearance for the generated versus preformed enalaprilat was reported in studies using the isolated perfused rat kidney (66). Collectively, these results suggest that a diffusional barrier for enalaprilat served to limit entry of the preformed enalaprilat into hepatocytes or renal epithelium cells, thereby decreasing biliary or urinary excretion. This differential diffusional barrier between enalapril and enalaprilat is consistent with differences in their physical properties; under physiological pH, the dicarboxylic acid metabolite is present in ionized form, which is very polar in nature. Both compounds also differ in their ability to interact with OATP1, a drug transporter; thus, enalapril, but not enalaprilat, has been shown to be taken up by rat Oatp1a1 and human OATP1B1 and OATP1B3 in the liver (67,68).

Dopamine and L-Dopa

In addition to the liver, a profound difference in tissue-specific distribution and retention between a preformed metabolite and the metabolite generated from the parent drug also may occur as a result of the presence of a diffusional barrier or specific influx transporters in extrahepatic tissues, as illustrated by the penetration of dopamine into the central nervous system (CNS). Many transport systems, which play an important role in the uptake of water-soluble nutrients from the blood circulation into the brain, are known to be present at the blood brain barrier (BBB) (69). The large neutral amino acid carrier (LAT) mediates the uptake of phenylalanine and other neutral amino acids from the circulation into the brain. L-dopa, used for the treatment of Parkinson's disease, is a neutral amino acid analog that traverses the BBB via the LAT into the brain, where it is decarboxylated to the pharmacologically active metabolite, dopamine (70). Since dopamine is not a substrate for the LAT and is highly water soluble, it does not cross the BBB. When given exogenously, dopamine has no therapeutic effect in the treatment of Parkinson's disease.

Nucleotides, Nucleosides, and Nucleoside Prodrugs

Similar to L-dopa, an active uptake system (adenosine nucleoside transporter) is involved in the uptake of nucleosides into various tissues where they are converted to the corresponding pharmacologically active nucleotides. Since nucleotides are not substrates for adenosine nucleoside transporter and are very water soluble, they usually do not cross cell membranes by passive diffusion. Consequently, the tissue exposure of nucleotides

would be expected to be much higher when given as nucleosides than when dosed exogenously as the preformed metabolites (nucleotides). Indeed, following oral administration of MRL111, a nucleoside analog, in rats, mice, dogs, and monkeys, the AUC of the active triphosphate metabolite in the liver was ~25- to 30-fold higher than the plasma AUC of the parent nucleoside (data on file, Merck Research Laboratories). In rat hepatocyte studies, MRL111 showed time- and temperature-dependent uptake, consistent with the involvement of equilibrative transport into hepatocytes, commonly mediated by nucleoside transporters (71).

Tenofovir, a dianion at physiological pH, belongs to a class of nucleotide analogs that exhibit prolonged intracellular half-lives (72). The long intracellular half-life of tenofovir is a result of rapid metabolism within the cell to the nucleotide diphosphate, the active metabolite. The low cellular permeability of the nucleotide metabolite limits its efflux from cells. The amidate prodrug GS 7340 was designed to overcome the permeability limitations of tenofovir by masking the dianion with a neutral promoiety and increasing the plasma stability of the prodrug relative to its intracellular stability. In vivo administration of GS 7340 to dogs resulted in an enhanced distribution to lymphatic tissue compared with tenofovir; concentrations of tenofovir in peripheral blood mononuclear cells (PBMCs) versus plasma were much higher (>10-fold) following GS 7340 than following tenofovir (73). Consistent with this finding, GS 7340 also was found to distribute widely to lymphatic tissues (73). This expanded distribution and the higher intracellular levels of tenofovir after administration of GS 7340 than after tenofovir raises the possibility of safety issues that may not be observed with tenofovir itself.

Statin Acids and Lactones

HMG-CoA reductase inhibitors, or "statins," which target HMG-CoA reductase, the rate-limiting enzyme in cholesterol biosynthesis, are used widely for the treatment of hypercholesterolemia and hypertriglyceridemia. Except for simvastatin and lovastatin, which are administered in the inactive lactone forms, all currently available statins are administered as the pharmacologically active ^{TM}−hydroxy acids. The statin lactones are hydrolyzed to their open acids chemically or enzymatically by esterases or paraoxonases (16). The major physicochemical difference between the lactone and acid form for each statin is that the lactone has a higher partition coefficient (log P) or lipophilicity (log D), compared with the acid (74,75). The acid versus lactone forms of statins, including atorvastatin, lovastatin, and simvastatin, also have differential activities toward several transporters, including P-gp (76,77).

Simvastatin is not a P-gp substrate, whereas the acid form of both simvastatin and atorvastatin exhibit a moderate level of P-gp-mediated transport (76). Therefore, it is possible that the superior membrane permeability of the statin lactone (due to increased lipophilicity) and its inability to interact with P-gp may allow ready access of the lactone form to tissues. Indeed, the acid form of simvastatin accumulated in muscle and brain to a greater degree (2-3-fold) when given to dogs as the lactone than as the open acid, even though plasma levels of the open acid were comparable in each case (data on file, Merck Research Laboratories). In an earlier dog study, the disposition of simvastatin lactone also was found to be more hepatoselective than that of simvastatin acid; thus, simvastatin lactone exhibited a higher hepatic extraction ratio than simvastatin acid (93% vs. 80%), resulting in a lower systemic burden of prodrug and active drug after administration of simvastatin lactone versus simvastatin acid (78). Evidently, treatment with simvastatin lactone is more selective with respect to inhibition of hepatic versus extrahepatic HMG-CoA reductase. This was substantiated further by the finding that plasma levels of active

drug equivalents, after administration of simvastatin acid and lactone to dogs at doses which produced a similar degree of cholesterol lowering, are approximately 10-fold higher when simvastatin acid is given (78). Hence, the safety or toxicity profile of simvastatin acid in dogs may be different when the open acid is given exogenously as compared with when it is formed in vivo from the lactone.

Interestingly, the above observation was found to be species specific. As shown in an earlier study (78), the half-life of simvastatin in rodent plasma is approximately four minutes due to very rapid hydrolysis of the lactone, while essentially no hydrolysis occurs in human or dog plasma. Consistent with this observation, the oral bioavailability of the lactone was essentially zero when simvastatin was dosed to rodents (78). Studies on the disposition and metabolism of simvastatin lactone and open acid in rodents revealed that the systemic levels of the acid form, active or total HMG-CoA inhibitory activity, and total radioactivity following administration of simvastatin acid were similar to those observed following dosing with simvastatin lactone in the same species and gender (data on file, Merck Research Laboratories). Tissue distribution patterns of radioactivity following a dose of [^{14}C]simvastatin acid to rats also were similar to those found after [^{14}C]simvastatin lactone was given (78). Thus, the safety or toxicity profile of preformed and metabolically generated simvastatin acid in rodents would be expected to be similar. However, this is not likely to be the case in dogs, and possibly also in humans.

Morphine and Its Glucuronides

In mammals, morphine, a potent analgesic, is metabolized mainly by glucuronidation to yield morphine-3-glucuronide (M3G) and morphine-6-glucuronide (M6G). Because of their greater polarity relative to the parent aglycone, these conjugates are subject to significant diffusional barriers. Studies using the isolated perfused rat liver demonstrated that the hepatic disposition of the pharmacologically inactive metabolite M3G is indeed membrane permeability-rate limited; the biliary excretion and extraction ratio of hepatically generated M3G is much more efficient ($>$10-fold) than that of M3G given exogenously (79,80). Additionally, using a loading wash-out design and a physiologically based pharmacokinetic model, the volume of distribution of hepatically generated M3G was found to be approximately 50 times the intracellular space of the rat liver, suggesting that the generated M3G accumulates within hepatocytes, consistent with its poor membrane permeability (81).

Unlike M3G, M6G is an opioid agonist that plays a role in the clinical effects of morphine. M6G has been shown to exhibit much lower BBB permeability than morphine, as supported by studies showing lower brain penetration with M6G than morphine (82). Also consistent with the limited membrane permeability, plasma M6G, unlike morphine, was below detection limits after intracerebroventricular injection of M6G, and the apparent elimination clearance of M6G from the cerebrospinal fluid was 10 times lower than that of morphine after central administration of morphine to rats (83). Using a brain slice uptake method, the same authors showed that morphine was distributed in the brain parenchyma cells, whereas M6G was located in the extracellular fluid. It has been suggested recently that morphine is a substrate for P-gp (84), but M6G may be a substrate for an active uptake transporter and MRP (80,85). This difference may account for the differential brain distribution between morphine and M6G, given that P-gp is expressed mainly in the cerebral capillary endothelium, whereas MRP is expressed predominantly elsewhere in the brain (86).

To complicate the matter further, brain UGT(s) is capable of catalyzing the conjugation of morphine (87), and exhibits a regioselectivity toward morphine that is

different from the liver enzyme. M6G is the primary metabolite in brain, whereas M3G is the major conjugate in liver (88). Additionally, human kidney preferentially forms M3G (M3G/M6G ratio ~20) relative to human liver (M3G/M6G ratio ~5) (89). Furthermore, the metabolism of morphine also differs markedly between animal species, and between animals and humans (89,90). Whereas in human and guinea pig liver microsomes fortified with UDPGA, both the M3G and M6G are generated, with M3G being the major product, in rat and mouse liver microsomes, morphine forms almost exclusively M3G (M3G/M6G ratio ~90). Consequently, the distribution of the two isomeric glucuronides to various brain regions or tissues following administration of preformed M6G or M3G may be different in animals and humans.

Acyl Glucuronides and Aglycones

Acyl glucuronides are a unique class of electrophilic metabolites, capable of hydrolysis to reform the parent aglycone and also of intramolecular rearrangement. Both intra- and extrahepatic exposure to acyl glucuronides depends not only on the efficiency of competing glucuronidation and hydrolysis processes in the liver, but also on the efficiency of the hepatic membrane transport systems. Sallustio et al. (91) used the isolated perfused liver preparation to examine the hepatic disposition of the fibrate hypolipidemic agent gemfibrozil and its acyl glucuronide metabolite, 1-*O*-gemfibrozil-β-*D*-glucuronide (GG). Unlike observations with morphine, acetaminophen or 4-nitrophenol and their respective ether glucuronide conjugates (79,92), the hepatic extraction ratio of gemfibrozil was found to be lower than that of GG (0.09 vs. 0.65, respectively), consistent with its lower unbound fraction in perfusate (0.004), compared with that of GG (0.018). The fraction of gemfibrozil excreted in bile as the glucuronide conjugate also was lower (0.35 vs. 0.53, respectively) after administration of gemfibrozil than after GG. The relatively lower biliary excretion of the hepatically generated GG was attributed to the more efficient sinusoidal efflux into perfusate. On the basis of the finding of high concentration gradients (>40) for GG between the liver and perfusate and between bile and the liver (93), it was also suggested that the movement of GG from perfusate into bile is a two-step concentrative process involving carrier-mediated systems at both the sinusoidal and canalicular membranes of hepatocytes, possibly via OATP2 and MRP2, respectively (14,94). Similarly, naproxen acyl glucuronide was excreted in bile in much higher quantities (~25% vs. 4% of the dose) following administration of naproxen acyl glucuronide than after dosing with naproxen (95). In addition, rearranged isomers of naproxen acyl glucuronide were not observed following naproxen administration, whereas they were detected in significant levels in bile (3% of the dose) after naproxen acyl glucuronide administration (95).

Acyl glucuronides are intrinsically reactive; following rearrangement, positional isomers can react with amino acids of macromolecules to form protein adducts, potentially contributing to hepatotoxicity. Dipeptidylpeptidase IV, UGTs, and tubulin have been identified as intra-hepatic targets of adduct formation by acyl glucuronides (94,96). The concentrative effect of carrier-mediated hepatic membrane transport observed following dosing with preformed acyl glucuronides, together with the detection of their rearranged isomers, suggests that significantly higher intra-hepatic protein adduct formation would follow, even in the absence of detectable plasma acyl glucuronide concentrations, after administration of the preformed acyl glucuronides than after the corresponding aglycones. Thus, it may be anticipated that the toxicity profile obtained following administration of preformed acyl glucuronides could be different from (in this case more toxic) that following the respective aglycones, even with comparable systemic

exposure of the glucuronides. Consistent with this hypothesis, increased covalent naproxen-protein adducts in the liver were observed following perfusion of naproxen acyl glucuronide, as compared with perfusion with naproxen (0.34 0.20% of the doses, respectively) in an isolated rat liver perfusion system (95). Similar findings also have been reported with diflunisal and diflunisal acyl glucuronide (97).

CONCLUSIONS AND PERSPECTIVES

Risk assessment of drug metabolites is a complex issue that has been discussed extensively by pharmaceutical, academic, and regulatory scientists (1 4,98). As aforementioned, the kinetic behavior of a preformed metabolite given exogenously may differ significantly from that of the corresponding metabolite generated endogenously from the parent compound in animals or humans. In some cases, this complication may be overcome by administering high doses of preformed metabolites to generate sufficient systemic and tissue exposure. However, for hydrophilic metabolites, it may not readily be overcome by giving high doses of preformed metabolites because of poor passive permeability and/or interactions with specialized transporters and/or drug-metabolizing enzymes. Additionally, potential differences in physiological factors such as tissue-selective distribution and species differences in transporters and/or metabolizing enzymes also could contribute to differences in tissue- and species-specific toxicities depending on the compound administered (preformed metabolite vs. metabolite generated from the parent drug). It is, therefore, important to better understand the kinetic behavior of a metabolite generated in vivo versus that given exogenously before conducting the so-called bridging study to evaluate the safety of the drug metabolite.

Over the past few decades, considerable progress has been made in the generation of transgenic animal models for drug metabolism studies (99). Significant qualitative or quantitative differences in metabolite profiles between the test animal species and humans could theoretically be addressed by these animal models. To date, at least six mouse models expressing human CYP1A1, CYP1A2, CYP2D6, CYP2E1, and CYP3A4 have been generated and characterized (99 101). The usefulness of these mouse models is, however, still limited because of variable expression levels and erroneous localization of CYP enzymes. More recently, transgenic mouse models expressing human CYP3A4 in a tissue-specific expression manner (particularly liver vs. intestine) have been established and initial characterization showed promising results (102). Additionally, a chimeric mouse model with approximately 80% replacement by humanized liver has been reported to express functionally active, although not quantitatively as compared to, results obtained with human livers, human drug-metabolizing enzymes, and transporters (103). Conceivably, in the next decade humanized mouse lines expressing selected drug transporters and metabolizing enzymes in specific tissues could be available for use in risk assessment of drug metabolites that are disproportionately higher in humans than in animal species used for toxicity studies.

ACKNOWLEDGMENTS

The authors would like to thank Dr. Thomas A. Baillie of the Department of Global Drug Metabolism and Pharmacokinetics, Merck Research Laboratories, for his careful review and valuable suggestions.

REFERENCES

1. Baillie TA, Cayen MN, Fouda H, Gerson RJ, Green JD, Grossman SJ, Klunk LJ, LeBlanc B, Perkins DC, and Shipley LA. Drug metabolites in safety testing. Toxicol Appl Pharmacol 2002; 182:188 196.
2. Smith DA, Obach RS. Seeing through the MIST: abundance versus percentage. Drug Metab Dispos 2005; 33:1409 1417.
3. Davis Bruno KL, Atrakchi A. A regulatory perspective on issues and approaches in characterizing human metabolites. Chem Res Toxicol 2006; 19:1561 1563.
4. Prueksaritanont T, Lin JH, Baillie TA. Complicating factors in safety testing of drug metabolites: kinetic differences between generated and preformed metabolites. Toxicol Appl Pharmacol 2006; 217:143 152.
5. US Food and Drug Administration (2008) Guidance to Industry Safety Testing of drug Metabolites. Available at: www.fda.gov/cder/guidance.
6. Rowland M, Tozer TN. Clinical Pharmacokinetics: Concepts and Applications. 3rd ed. New York: Lee & Febiger, 1995.
7. Liu LC, Pang KS. The roles of transporters and enzymes in hepatic drug processing. Drug Metab Dispos 2005; 33:1 9.
8. Houston JB. Drug metabolite kinetics. Pharmacol Ther 1982; 15:521 552.
9. Lin JH. Species similarities and differences in pharmacokinetics. Drug Metab Dispos 1995; 23:1008 1021.
10. Lin JH. Tissue distribution and pharmacodynamics: a complicated relationship. Curr Drug Metab 2006; 7:39 65.
11. Pang KS, Xin X, Stpierre MV. Determinants of metabolite disposition. Annu Rev Pharmacol Toxicol 1992; 32:623 669.
12. Evans AM. Membrane transport as a determinant of the hepatic elimination of drugs and metabolites. Clin Exp Pharmacol Physiol 1996; 23:970 974.
13. Dell D. Labile metabolites. Chromatographia 2004; 59(suppl):S139 S148.
14. Sallustio BC, Fairchild BA, Shanahan K, Evans AM, and Nation RL. Disposition of gemfibrozil and gemfibrozil acyl glucuronide in the rat isolated perfused liver. Drug Metab Dispos 1996; 24:984 989.
15. Tan E, Lu T, Pang KS. Futile cycling of estrone sulfate and estrone in the recirculating perfused rat liver preparation. J Pharmacol Exp Ther 2001; 297:423 436.
16. Prueksaritanont T, Subramanian R, Fang X, Ma B, Qiu Y, Lin JH, Pearson PG, Baillie TA. Glucuronidation of statins in animals and humans: a novel mechanism of statin lactonization. Drug Metab Dispos 2002; 30:505 512.
17. Kadlubar FF, Unruh LE, Flammang TJ, Sparks D, Mitchum RK, and Mulder GJ. Alteration of urinary levels of the carcinogen, N hydroxy 2 naphthylamine, and its N glucuronide in the rat by control of urinary pH, inhibition of metabolic sulfation, and changes in biliary excretion. Chem Biol Interact 1981; 33:129 147.
18. Maher JM, Slitt AL, Cherrington NJ, Cheng X, Klaassen CD. Tissue distribution and hepatic and renal ontogeny of the multidrug resistance associated protein (MRP) family in mice. Drug Metab Dispos 2005; 33:947 955.
19. Schinkel AH, Jonker JW Mammalian drug efflux transporters of the ATP binding cassette (ABC) family: an overview. Adv Drug Deliv Rev 2003; 55:3 29.
20. Kruh GD, Belinsky MG. The MRP family of drug efflux pumps. Oncogene 2003; 22:7537 7552.
21. Haimeur A, Conseil G, Deeley RG, Cole SPC. The MRP related and BCRP/ABCG2 multidrug resistance proteins: biology, substrate specificity and regulation. Curr Drug Metab 2004; 5:21 53.
22. Hagenbuch B, Meier PJ. The superfamily of organic anion transporting polypeptides. Biochim Biophys Acta 2003; 1609:1 18.
23. Yamazaki M, Tokui T, Ishigami M, Sugiyama Y. Tissue selective uptake of pravastatin in rats: contribution of a specific carrier mediated uptake system. Biopharm Drug Dispos 1996; 17:775 789.

24. Hirano M, Maeda K, Shitara Y, Sugiyama Y. Contribution of OATP2 (OATP1B1) and OATP8 (OATP1B3) to the hepatic uptake of pitavastatin in humans. J Pharmacol Exp Ther 2004; 311:139 146.
25. Koepsell H, Endou H. The SLC22 drug transporter family. Pflugers Arch 2004; 447:666 676 (epub 2003, Jul 19).
26. You GF. The role of organic ion transporters in drug disposition: an update. Curr Drug Metab 2004; 5:55 62.
27. Ito S, Alcorn J. Xenobiotic transporter expression and function in the human mammary gland. Adv Drug Deliv Rev 2003; 55:653 665.
28. Jonker JW, Wagenaar F, Mol CA, Buitelaar M, Koepsell H, Smit JW, Schinkel AH. Deficiency in the organic cation transporters 1 and 2 (Oct1/Oct2 [Slc22a1/Slc22a2]) in mice abolishes renal secretion of organic cations. Mol Cell Biol 2001; 23:7902 7908.
29. Wang DS, Kusuhara H, Kato Y, Jonker JW, Schinkel AH, Sugiyama Y. Involvement of organic cation transporter 1 in the lactic acidosis caused bv metformin. Mol Pharmacol 2003; 63:844 848.
30. Ho ES, Lin DC, Mendel DB, Cihlar T. Cytotoxicity of antiviral nucleotides adefovir and cidofovir is induced by the expression of human renal organic anion transporter 1. J Am Soc Nephrol 2000; 11:383 393.
31. Kusuhara H, Sugiyama Y. Role of transporters in the tissue selective distribution and elimination of drugs: transporters in the liver, small intestine, brain and kidney. J Control Release 2002; 78:43 54.
32. Zamek Gliszczynski MJ, Hoffmaster KA, Nezasa K, Tallman MN, Brouwer KLR. Integration of hepatic drug transporters and phase II metabolizing enzymes: mechanisms of hepatic excretion of sulfate, glucuronide, and glutathione metabolites. Eur J Pharm Sci 2006; 27:447 486.
33. Nagata Y, Kusuhara H, Endou H, Sugiyama Y. Expression and functional characterization of rat organic anion transporter 3 (rOat3) in the choroid plexus. Mol Pharmacol 2002; 61: 982 988.
34. Tahara H, Kusuhara H, Endou H, Koepsell H, Imaoka T, Fuse E, Sugiyama Y. A species difference in the transport activities of H 2 receptor antagonists by rat and human renal organic anion and cation transporters. J Pharmacol Exp Ther 2005; 315:337 345.
35. Tahara H, Shono M, Kusuhara H, Kinoshita H, Fuse E, Takadate A, Otagiri M, Sugiyama Y. Molecular cloning and functional analyses of OAT1 and OAT3 from cynomolgus monkey kidney. Pharm Res 2005; 22:647 660.
36. Wright SH, Dantzler WH. Molecular and cellular physiology of renal organic cation and anion transport. Physiol Rev 2004; 84:987 1049.
37. Tirona RG, Pang KS. Sequestered endoplasmic reticulum space for sequential metabolism of salicylamide coupling of hydroxylation and glucuronidation. Drug Metab Dispos 1996; 24:821 833.
38. Abu Zahra TN, Pang KS. Effect of zonal transport and metabolism on hepatic removal: enalapril hydrolysis in zonal, isolated rat hepatocytes in vitro and correlation with perfusion data. Drug Metab Dispos 2000; 28:807 813.
39. Schwab AJ, Tao L, Kang M, Meng L, Pang KS. Moment analysis of metabolic heterogeneity: conjugation of benzoate with glycine in rat liver studied by multiple indicator dilution technique. J Pharmacol Exp Ther 2003; 305:279 289.
40. Ding XX, Kaminsky LS. Human extrahepatic cytochromes P450: function in xenobiotic metabolism and tissue selective chemical toxicity in the respiratory and gastrointestinal tracts. Annu Rev Pharmacol Toxicol 2003; 43:149 173.
41. Du LP, Hoffman SMG, Keeney DS. Epidermal CYP2 family cytochromes P450. Toxicol Appl Pharmacol 2004; 195:278 287.
42. Gregory PA, Lewinsky RH, Gardner Stephen DA, Mackenzie PI. Regulation of UDP glucuronosyltransferases in the gastrointestinal tract. Toxicol Appl Pharmacol 2004; 199:354 363.
43. Kiang TKL, Ensom MHH, Chang TKH. UDP glucuronosyltransferases and clinical drug drug interactions. Pharmacol Ther 2005; 106:97 132.

44. Gamage N, Barnett A, Hempel N, Duggleby RG, Windmill KF, Martin JL, McManus ME. Human sulfotransferases and their role in chemical metabolism. Toxicol Sci 2006; 90:5 22.
45. Strazielle N, Khuth ST, Ghersi Egea JF. Detoxification systems, passive and specific transport for drugs at the blood CSF barrier in normal and pathological situations. Adv Drug Deliv Rev 2004; 56:1717 1740.
46. Dieckhaus CM, Miller TA, Sofia RD, Macdonald TL. A mechanistic approach to understanding species differences in felbamate bioactivation: relevance to drug induced idiosyncratic reactions. Drug Metab Dispos 2000; 28:814 822.
47. Urrea R, Bronfman M. Species differences in the intracellular distribution of ciprofibroyl CoA hydrolase. Implications for peroxisome proliferation. FEBS Lett 1996; 389:219 223.
48. Their R, Wiebel FA, Hinkel A, Burger A, Brüning T, Morgenroth K, Senge T, Wilhelm M, Schulz TG. Species differences in the glutathione transferase GSTT1 1 activity towards the model substrates methyl chloride and dichloromethane in liver and kidney. Arch Toxicol 1998; 72:622 629.
49. Mutlib AE, Chen H, Nemeth GA, Markwalder JA, Seitz SP, Gan LS, Christ DD. Identification and characterization of efavirenz metabolites by liquid chromatography/mass spectrometry and high field NMR: species differences in the metabolism of efavirenz. Drug Metab Dispos 1999; 27:1319 1333.
50. Yamauchi A, Ueda N, Hanafusa S, Yamashita E, Kihara M, Naito, S. Tissue distribution of and species differences in deacetylation of N acetyl L cysteine and immunohistochemical localization of acylase I in the primate kidney. J Pharm Pharmacol 2002; 54:205 212.
51. Miyauchi S, Sugiyama Y, Sato H, Sawada Y, Iga T, Hanano M. Effects of a diffusional barrier to a metabolite across hepatocytes on its kinetics in "enzyme distributed" model a computer aided simulation study. J Pharmacokinet Biopharm 1987; 15:399 421.
52. Benet LZ, Cummins CL, Wu CY. Unmasking the dynamic interplay between efflux transporters and metabolic enzymes. Int J Pharm 2004; 277:3 9.
53. Schwab AJ, Pang KS. The multiple indicator dilution method for the study of enzyme heterogeneity in liver: theoretical basis. Drug Metab Dispos 1999; 27:746 755.
54. Mathijssen RHJ, van Alphen RJ, Verweij J, Loos WJ, Nooter K, Stoter G, Sparreboom, A. Clinical pharmacokinetics and metabolism of irinotecan (CPT 11). Clin Cancer Res 2001; 7:2182 2194.
55. Ma MK, McLeod HL. Lessons learned from the irinotecan metabolic pathway. Curr Med Chem 2003; 10:41 49.
56. Kothare PA, Zimmerman CL. Intestinal metabolism: the role of enzyme localization in phenol metabolite kinetics. Drug Metab Dispos 2002; 30:586 594.
57. Doherty MM, Pang KS. Route dependent metabolism of morphine in the vascularly perfused rat small intestine preparation. Pharm Res 2000; 17:291 298.
58. Pang KS, Waller L, Horning MG, Chan KK. Metabolite kinetics formation of acetaminophen from dueterated and non dueterated phenacetin and acetanilide on acetaminophen sulfation kinetics in the perfused rat liver preparation. J Pharmacol Exp Ther 1982; 222:14 19.
59. Pang KS, Gillette JR. Kinetics of metabolite formation and elimination in the perfused rat liver preparation: differences between elimination of preformed acetaminophen and acetaminophen formed from phenacetin. J Pharmacol Exp Ther 1978; 207:178 194.
60. Pang KS, Terrell A. Conjugation kinetics of acetaminophen by the perfused rat liver preparation. Biochem Pharmacol 1981; 30:1959 1965.
61. James LP, Mayeux PR, Hinson JA. Acetaminophen induced hepatotoxicity. Drug Metab Dispos 2003; 31:1499 1506.
62. Bender RP, Lindsey RH, Burden DA, Osheroff, N. N acetyl p benzoquinone imine, the toxic metabolite of acetaminophen, is a topoisomerase II poison. Biochemistry 2004; 43:3731 3739.
63. Pang KS, Cherry WF, Terrell JA, Ulm EH. Disposition of enalapril and its diacid metabolite, enalaprilat, in a perfused rat liver preparation. Presence of a diffusional barrier into hepatocytes. Drug Metab Dispos 1984; 12:309 313.
64. Pang KS, Baker F, Cherry WF, Goresky CA. Esterases for enalapril hydrolysis are concentrated in the perihepatic venous region of the rat liver. J Pharmacol Exp Ther 1991; 257:294 301.

65. de Lannoy IAM, Baker F, Pang KS. Formed and preformed metabolite excretion clearances in liver, a metabolite formation organ: studies on enalapril and enalaprilat in the single pass and recirculating perfused rat liver. J Pharmacokint Biopharm 1993; 21:395 422.
66. de Lannoy IAM, Nespeca R, Pang KS. Renal handling of enalapril and enalprilat: studies in the isolated red blood cell perfused rat kidney. J Pharmacol Exp Ther 1989; 251:1211 1222.
67. Pang KS, Wang PJ, Chung AYK, Wolkoff AW. The modified dipeptide, enalapril, an angiotensin converting enzyme inhibitor, is transported by the rat liver organic anion transport protein. Hepatology 1998; 28:1341 1346.
68. Liu LC, Cui YH, Chung AY, Shitara Y, Sugiyama Y, Keppler D, Pang KS. Vectorial transport of enalapril by Oatp1a1/Mrp2 and OATP1B1 and OATP1B3/MRP2 in rat and human livers. J Pharmacol Exp Ther 2006; 318:395 402.
69. Pardridge WM. Recent advances in blood brain barrier transport. Annu Rev Pharmacol Toxicol 1988; 28:25 39.
70. Nutt JG, Woodward WR, Hammerstad JP, Carter MN, Anderson JL. The "on off" phenomenon in Parkinson's disease. Relation to levodopa absorption and transport. N Engl J Med 1984; 310:483 488.
71. Pastor Anglada M, Cano Soldado P, Molina Arcas M, Pilar Lostaob M, Larráyozb I, Martínez Picadoc J, Casado FJ. Cell entry and export of nucleoside analogues. Virus Res 2005; 107:151 164.
72. Pauwels R, Baba M, Balzarini J, Herdewijn P, Desmyter J, Robins MJ, Zou R, Madej D, de Clercq, E. Investigations on the anti HIV activity of 2′,3′ dideoxyadenosine analogs with modification in either the pentose or purine moiety potent and selective anti HIV activity of 2,6 diaminopurine 2′,3′ dideoxyriboside. Biochem Pharmacol 1988; 37, 1317 1325.
73. Lee WA, He GX, Eisenberg E, Cihlar T, Swaminathan S, Mulato A, Cundy KC. Selective intracellular activation of a novel prodrug of the human immunodeficiency virus reverse transcriptase inhibitor tenofovir leads to preferential distribution and accumulation in lymphatic tissue. Antimicrob Agents Chemother 2005; 49:1898 1906.
74. Serajuddin AT, Ranadive SA, Mahoney EM. Relative lipophilicities, solubilities, and structure pharmacological considerations of 3 hydroxy 3 methylglutaryl coenzyme A (HMG CoA) reductase inhibitors pravastatin, lovastatin, mevastatin, and simvastatin. J Pharm Sci 1991; 80:830 834.
75. Ishigami M, Honda T, Takasaki W, Ikeda T, Komai T, Ito K, Sugiyama Y. A comparison of the effects of 3 hydroxy 3 methylglutaryl coenzyme A (HMG CoA) reductase inhibitors on the CYP3A4 dependent oxidation of mexazolam in vitro. Drug Metab Dispos 2001; 29:282 288.
76. Hochman JH, Pudvah NT, Qiu Y, Yamazaki M, Tang C, Lin JH, Prueksaritanont T. Interactions of human P glycoprotein with simvastatin, simvastatin acid, and atorvastatin. Pharm Res 2004; 21:1688 1693.
77. Chen C, Mireles RJ, Campbell SD, Lin J, Mills JB, Xu JJ, Smolarek TA. Differential interaction of 3 hydroxy 3 methylglutaryl coenzyme A reductase inhibitors with ABCB1, ABCC2, and OATP1B1. Drug Metab Dispos 2005; 33:537 546.
78. Vickers S, Duncan CA, Chen, I. W, Rosegay A, Duggan DE. Metabolic disposition studies of simvastatin, a cholesterol lowering prodrug. Drug Metab Dispos 1990; 18:138 145.
79. Evans AM, Shanahan K. Biliary excretion of hepatically generated and pre formed morphine 3 glucuronide (M 3 G) in the isolated perfused rat liver: evidence for a diffusional barrier. Clin Exp Pharmacol Physiol 1993; 10(suppl 1):S22.
80. Doherty MM, Poon IM, Tsang C, Pang KS. Transport is not rate limiting in morphine glucuronidation in the single pass perfused rat liver preparation. J Pharmacol Exp Ther 2006; 317:890 900.
81. Evans AM, O'Brien J, Nation RL. Application of a loading wash out method for investigating the hepatocellular efflux of a hepatically generated metabolite morphine 3 glucuronide. J Pharm Pharmacol 1999; 51:1289 1297.
82. Wu DF, Kang YS, Bickel U, Pardridge WM. Blood brain barrier permeability to morphine 6 glucuronide is markedly reduced compared with morphine. Drug Metab Dispos 1997; 25:768 771.

83. Okura T, Saito M, Nakanishi M, Komiyama N, Fujii A, Yamada S, Kimura R. Different distribution of morphine and morphine 6 β glucuronide after intracerebroventricular injection in rats. Br J Pharmacol 2003; 140:211 217.
84. Cisternino S, Rousselle C, Debray M, and Scherrmann JM. In situ transport of vinblastine and selected P glycoprotein substrates: implications for drug drug interactions at the mouse blood brain barrier. Pharm Res 2004; 21:1382 1389.
85. Bourasset F, Cisternino S, Temsamani J, Scherrmann, JM. Evidence for an active transport of morphine 6 beta D glucuronide but not P glycoprotein mediated at the blood brain barrier. J Neurochem 2003; 86:1564 1567.
86. Regina A, Koman A, Piciotti M, El Hafny B, Center MS, Bergmann R, Couraud PO, Roux F. Mrp1 multidrug resistance associated protein and P glycoprotein expression in rat brain microvessel endothelial cells. J Neurochem 1998; 71:705 715.
87. Wahlström A, Winblad B, Bixo M, Rane A. Human brain metabolism of morphine and naloxone. Pain 1998; 35:121 127.
88. Nagano W, Yamada H, Oguri K. Characteristic glucuronidation pattern of physiologic concentration of morphine in rat brain. Life Sci 2000; 67:2453 2464.
89. Coughtrie MWH, Ask B, Rane A, Burchell B, Hume R. The enantioselective glucuronidation of morphine in rats and humans. Biochem Pharmacol 1989; 19:3273 3280.
90. Kuo CK, Hanioka N, Hoshikawa Y, Oguri K, Yoshimura H. Species difference of site selective glucuronidation of morphine. J Pharmacobiodyn 1991; 14:187 193.
91. Sallustio BC, Sabordo L, Evans AM, Nation RL. Hepatic disposition of electrophilic acyl glucuronide conjugates. Curr Drug Metab 2000; 1:163 180.
92. Watari N, Iwai M, Kaneniwa N. Pharmacokinetic study of the fate of acetaminophen and its conjugates in rats. J Pharmacokinet Biopharm 1983; 11:245 272.
93. Sabordo L, Sallustio BC, Evans AM, Nation RL. Hepatic disposition of the acyl glucuronide1 O gemfibrozil β D glucuronide: effects of dibromosulfophthalein on membrane transport and aglycone formation. J Pharmacol Exp Ther 1999; 288:414 420.
94. Sallustio BC, Sabordo L, Evans AM, Nation RL. Hepatic disposition of electrophilic acyl glucuronide conjugates. Curr Drug Metab 2000; 1:163 180.
95. Lo A, Addison RS, Hooper WD, Dickinson RG. Disposition of naproxen, naproxen acyl glucuronide and its rearrangement isomers in the isolated perfused rat liver. Xenobiotica 2001; 31:309 319.
96. Wang M, Gorrell MD, McCaughan GW, Dickinson RG. Dipeptidyl peptidase IV is a target for covalent adduct formation with the acyl glucuronide metabolite of the anti inflammatory drug zomepirac. Life Sci 2001; 68:785 797.
97. Wang M, Dickinson RG. Disposition and covalent binding of diflunisal and diflunisal acyl glucuronide in the isolated perfused rat liver. Drug Metab Dispos 1998; 26:98 104.
98. Naito S, Furuta S, Yoshida T, Kitada M, Fueki O, Unno T, Ohno Y, Onodera H, Kawamura N, Kurokawa M, Sagami F, Shinoda K, Nakazawa T. Yamazaki T. Current opinion: Safety evaluation of drug metabolites in development of pharmaceuticals. J Toxicol Sci 2007; 32: 329 341.
99. Gonzalez FJ, Yu A M. Cytochrome P450 and xenobiotic receptor humanized mice. Annu Rev Pharmacol Toxicol 2006; 46:41 64.
100. Gonzalez FJ. CYP3A4 and pregnane X receptor humanized mice. J Biochem Mol Toxicol 2007; 21:158 162.
101. Dragin N, Uno S, Wang B, Dalton TP Nebert DW. Generation of humanized hCYP1A1 1A2 Cyp1a1/1a2 (/) mouse line. Biochem Biophys Res Commun 2007; 359:635 642.
102. Van Herwaarden AE, Wagenaar E, van der Kruijssen CMM, van Waterschoot RAB, Smit JW, Song JY, van der Valk MA, van Tellingen O, van der Hoorn JWA, Rosing H, Beijnen JH, Schinkel AH. Knockout of cytochrome P450 3A yields new mouse models for understanding xenobiotic metabolism. J Clin Invest 2007; 117:3583 3592.
103. Okumura H, Katoh M, Sawada T, Nakajima M, Soeno Y, Yabuuchi H, Ikeda T, Tateno C, Yoshizato K, Yokoi T. Humanization of excretory pathway in chimeric mice with humanized liver. Toxicol Sci 2007; 97:533 538.

25

The Use of Transgenic Animals to Study Drug Metabolism

Colin J. Henderson and C. Roland Wolf
Cancer Research UK Molecular Pharmacology Unit, Biomedical Research Institute, University of Dundee, Ninewells Hospital and Medical School, Dundee, Scotland, U.K.

Nico Scheer
TaconicArtemis GmbH, Cologne, Germany

INTRODUCTION

As with many other areas of biological science, the field of toxicology and molecular pharmacology has been revolutionized by transgenic technology over the past two decades. The ability to express foreign genes, delete specifically, in certain tissues or at defined times or globally in all cells or mutate specific endogenous genes in a living multicellular organism, has vastly added to our knowledge of drug-metabolizing enzymes how they are expressed and regulated, how they function, and how they interact with each other. The majority of this work has been done in the mouse, and gene knockouts/knock-ins almost exclusively so, for both historical and technological reasons.

BACKGROUND TO TRANSGENIC TECHNOLOGY

Although transgenics the (random) insertion of a foreign gene into the genome of an animal was first demonstrated using viral vectors in the 1970s, the area really took off during the 1980s with pronuclear microinjection, whereby the DNA construct is injected in very small volumes typically picoliters into the pronucleus of an embryo, and it integrates into the host genome. The disadvantages of this technique lie both in the random integration the foreign DNA sequence may integrate into a region of chromosomal DNA, which is transcriptionally silent, or may interrupt the function of an endogenous gene and in the fact that multiple copies of the inserted DNA may result. These factors mean that it is often essential to create a number of independent transgenic lines from each DNA construct to ensure the generation of an animal that has suitable expression of the inserted transgene, which can be costly both in terms of effort and resources.

Targeted transgenesis became possible in the late 1980s with the development of cultured embryonic stem (ES) cells initially from the 129 mouse strain which retained their pluripotency in culture, i.e., the ability to differentiate into any cell type including, crucially, germ cells. The process underlying targeted transgenesis is called homologous recombination, whereby DNA fragments of similar sequence are aligned, leading to a crossover between the pieces of DNA and subsequent exchange of genetic material at a specified part of the genome. Correctly targeted ES cells are identified by the inclusion of a selectable marker in the targeting construct and are injected into the inner cell mass of a developing blastocyst from a different mouse genetic background (usually C57BL/6), where they will subsequently differentiate into a range of cell lineages, including the germ line. The resultant mouse referred to as a chimera owing to the presence of two ES cell lineages is then crossed to propagate the genetic change(s). Although ES cells were originally isolated from the 129 mouse line an inbred strain, which is subject to breeding difficulties ES cells have recently been derived from the C57BL/6 mouse, considered by many to be the "gold standard" among laboratory mice. Although it has been known for many years that the genetic background of genetically manipulated mice could significantly alter the phenotype, it is only recently that steps have been taken to address this in a systematic manner, and this theme will be addressed later in this article.

The major advantage of targeted transgenesis through homologous recombination is that there is absolute control on the DNA inserted, both in terms of copy number and location in the genome. Although initially a specialized technique, in recent years, the generation of gene-targeted mice has become almost routine, particularly following the sequencing of the mouse genome. By 2004, only around 10% of all known mouse genes had been knocked out, and a major international collaborative program the Knockout Mouse Project has been initiated to produce and phenotype a knockout for every mouse gene (1).

Over the past few years, gene-targeting techniques have been such refined that it is possible to conditionally delete or alter genes in a spatiotemporal manner (Fig. 1). This has employed a number of different techniques, although the majority involve the flanking of the gene of interest with DNA sequences, which are recognized by recombinase enzymes from either a bacteriophage (*Cre*/loxP) or yeast (*FLP*/FRT) (2). This has greatly enhanced the utility of gene targeting and allows, for instance, the circumvention of embryonic lethality encountered in some cases of genetic manipulation. Further development of these conditional gene-targeting techniques has resulted in recombinase-mediated cassette exchange (RMCE), where the use of heterologous pairs of loxP or FRT sites allow the efficient exchange of large regions of genomic DNA (3,4). As a consequence of this technology, genes may now be deleted or altered in a specific tissue, and/or at a specific time in the development of an animal, greatly enhancing the utility of genetic manipulation.

CYTOCHROME P450

The cytochrome P450 superfamily contains 57 genes in humans and around 103 in mice (http://drnelson.utmem.edu/CytochromeP450.html) (5). There have been a number of recent reviews in many areas of P450 research (6,7), including the generation and use of transgenic mice (8 11). Table 1 summarizes the cytochrome P450 gene knockouts to date.

Cyp1a

Knockout mice for the Cyp1a subfamily were first described by (12) for Cyp1a2 and were found to suffer from severe respiratory distress, lethality occurring in the neonatal period.

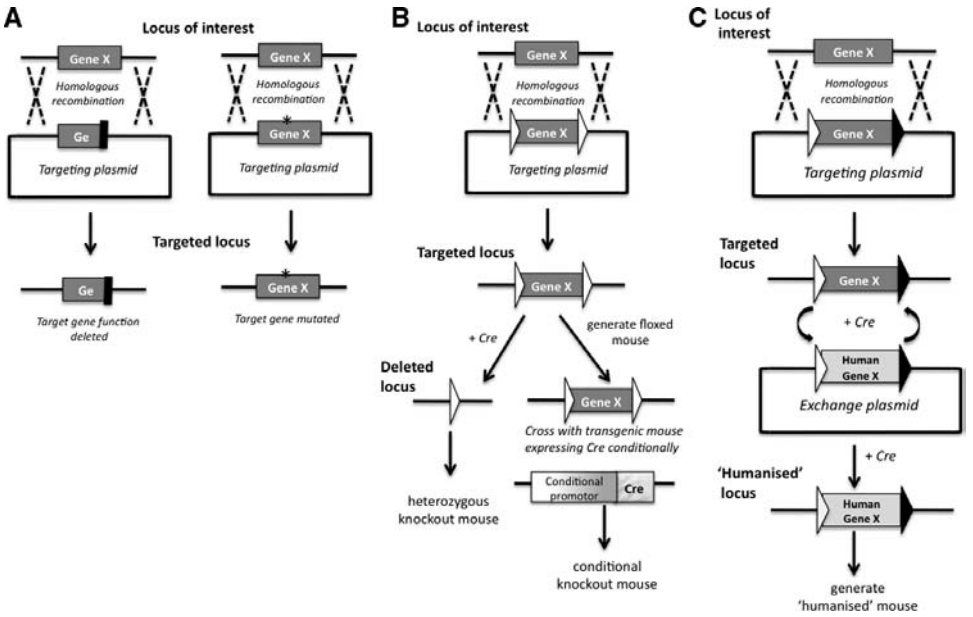

Figure 1 Principles of gene targeting. (**A**) Deletion (*left*) or mutation (*) of gene function (*right*) by homologous recombination. Note that this illustrates a "replacement" targeting approach and that several other strategies are available. (**B**) Conditional deletion of gene function. Target gene is flanked"floxed" by loxP sites (*white triangles*). Subsequent expression of *Cre* recombinase and deletion of target gene can be carried out either in ES cells, and a mouse lacking the gene then generated, or in vivo by crossing the floxed mouse to a line in which the *Cre* recombinase is under the control of an inducible or tissue specific promotor. Activation of the *Cre* recombinase then generates a conditional knockout mouse. Note that if the loxP sites were placed in an opposite orientation to each other, *Cre* recombinase would invert the flanked DNA. It is also possible to use the *Flp*/FRT system instead of, or in addition to, the *Cre*/loxP. (**C**) Recombinase mediated cassette exchange. Homologous recombination is used to flank the target gene with heterologous lox sites, i.e., loxP and lox511 (*white and black triangles*). Subsequently, *Cre* recombinase is used to exchange the target gene with the modified, or the humanized, gene.

However, the phenotype appeared to be incompletely penetrant, with approximately 3% of mutant pups surviving to adulthood, apparently normal and able to reproduce. Subsequently, another group (13) deleted *Cyp1a2* and found no overt phenotype, and described how the absence of *Cyp1a2* significantly increased the paralysis time in a zoxazolamine paralysis test compared with wild-type mice, demonstrating unequivocally a role for Cyp1a2 in the metabolism of this drug in vivo. It is interesting to note the different phenotypes generated in these two studies; Liang et al. (13) speculated on a number of reasons for these differences, which encapsulate neatly some of the problems that may be encountered when working with genetically altered mouse lines. Genetic background may play a role, with the *Cyp1a2*$^{-/-}$ mice of Liang et al. on either a 129 × CF-1 or 129 × Swiss Black background, whereas those of Pineau et al. were 129 × C57BL/6. Alternatively, it is possible that environmental differences could be involved, for example, the presence of respiratory pathogens in one of the animal facilities. A further possibility lies in the targeting construct used in each case Pineau et al. disrupted the *Cyp1a2* gene by placing a selectable marker into exon 2, while Liang et al. employed a strategy whereby most of exon 2, plus all of exons 3 5, were deleted.

Table 1 Drug-Metabolizing Cytochrome P450 Genes in Knockout Mice

Deleted gene	Genetic background	Strategy	Phenotype	Reference	Comment
Cyp1a1	129 × C57BL/6	All coding sequences deleted	No overt phenotype	Dalton et al. (19)	Use of Cre/loxP
	C57BL/6 (94%)		Decreased BaP hepatotoxicity	Uno et al. (20)	
	C57BL/6 (>99.8%)		Decreased uroporphyria and TCDD toxicity	Uno et al. (21)	
Cyp1a2	129 × C57BL/6	Disrupt exon 2 with *neo*	Severe respiratory distress, neonatal lethality	Pineau et al. (12)	Incompletely penetrant
			No hepatic sequestration of TCDD	Diliberto et al. (14)	
	129 × CF-1 or 129 ×	Delete part exons 2, 35	Increased zoxazolamine paralysis time	Liang et al. (13)	
	Swiss Black		No change in acetaminophen metabolism	Tonge et al. (15)	
	C57BL/6 (87.5%)		Cyp1a2 essential for uroporphyria	Sinclair et al. (16)	
	C57BL/6 (87.5%)		Cyp1a2 involved in bilirubin degradation	Zaccaro et al. (18)	
Cyp1b1	129/Sv	Disrupt exon 3 with *neo*	Decreased tumorigenic response to DMBA	Buters et al. (30)	
Cyp1a1/1b1	C57BL/6 (>99.8%)	Breed Cyp1b1 null with Cyp1a1 or Cyp1a2 null	Increased blood BaP levels	Uno et al. (22)	
Cyp1a2/1b1	C57BL/6 (>99.8%)		Increased BaP-DNA adducts	Uno et al. (22)	

Cyp1a1/1a2/1b1	C57BL/6 (>99.8%)	Interchromosomal excision and breeding with Cyp1b1 null	Slower weight gain and increased risk of embryonic lethality, hydrocephalus, hermaphroditism, and cystic ovaries	Dragin et al. (24)	Incompletely penetrant Birth defects lost by C57BL/6 (N10)
Cyp2e1	129/Sv × C57BL/6	Replace intron 1/exon 2/intron 3 with *neo*	Decreased acetaminophen hepatotoxicity	Lee et al. (36)	
	129/Sv		Decreased carbon tetrachloride toxicity	Wong et al. (38)	
	129/Sv		Decreased chloroform toxicity	Constan et al. (39)	
Cyp1a2/2e1	129/Sv × C57BL/6	Breed Cyp1a2 null with Cyp2e1 null	Further decreased acetaminophen hepatotoxicity	Zaher et al. (37)	
Cyp2g1	129 × C57BL/6	Replace exon 3 with *neo*	Decreased progesterone, testosterone & coumarin metabolism in olfactory mucosa	Zhuo et al. (43)	Highly expressed in olfactory mucosa
POR	129 × C57BL/6	Delete exons 5-15	Altered lipid homeostasis	Henderson et al. (45)	Conditional – liver
	129 × C57BL/6	Delete exons 3-15	Increased pentobarbital sleeping time	Gu et al. (46)	Conditional – liver
		Delete exons 3-15	Limited embryonic lethality, altered lipid homeostasis, reduced drug metabolism	Wu et al. (51)	Hypomorphic- 74–95% *Por* knockdown in all tissues tested
	129 × C57BL/6	Delete exons 5-15	Lethal E9-10	Otto et al. (2003)	Complete deletion
		Delete exon 2	Lethal E10-11	Shen et al. (2002)	Complete deletion

Abbreviations: TCDD, 2,3,7,8-tetrachlorodibenzo-*p*-dioxin; DMBA, 12-dimethylbenz[a]anthracene; BaP, benzo[a]pyrene

Both of these *Cyp1a2* null mouse lines were subsequently used to investigate the role of this enzyme in dioxin metabolism. Diliberto et al. (14) showed that in mice lacking Cyp1a2 there was essentially no hepatic sequestration of 2,3,7,8-tetrachlorodibenzo-*p*-dioxin (TCDD) and other related polychlorinated biphenyls, strongly supporting the hypothesis that this enzyme was responsible for binding and localizing TCDD in the liver. Liang et al. (13) investigated the effect of *Cyp1a2* deletion on the inducibility by TCDD of the other member of the Cyp1a subfamily, Cyp1a1, and found no effect over a wide range of concentrations, suggesting that the degree of hepatic TCDD sequestration was not related to the regulation of Cyp1a1 expression in the liver. The *Cyp1a2*$^{-/-}$ mice were subsequently used to determine the role of the enzyme in acetaminophen metabolism, and it was concluded that Cyp1a2 played no significant role in the hepatotoxicity of this drug (15), whereas it was deemed to be essential for the generation of uroporphyria by (16,17) and involved in microsomal bilirubin degradation (18).

Cyp1a1 null mice were generated by Dalton et al. and shown to be viable with no obvious phenotype (19). Further study found that mice lacking Cyp1a1 were protected against the hepatotoxic effects of benzo[a]pyrene (BaP), although somewhat unexpectedly the *Cyp1a1* null mice were found to have a fourfold higher level of BaP-DNA adducts compared with wild-type animals (20,21). This work was extended further by the use of a number of Cyp1 knockout mice where *Cyp1a1* or *Cyp1a2* null mice, either alone or in combination with a *Cyp1b1* deletion (see below for detail on *Cyp1b1* deletion alone), were treated orally with BaP and assessed for toxicity (22). It was reported that BaP toxicity, and potentially carcinogenicity, was dependent on a balance between the tissue-specific activity of Cyp1a1 and Cyp1b1, the route of administration of the compound, and location and extent of phase II metabolizing enzymes (22,23).

A triple-knockout mouse *Cyp1a1/Cyp1a2/Cyp1b1* null has also been reported, with a number of phenotypic consequences, some of which are variably penetrant (Table 1) (24). Although the creation of *Cyp1a1/Cyp1b1* or *Cyp1a2/Cyp1a2* double-null mice was achieved by conventional crossing of the single knockout lines, the proximity of the *Cyp1a1* and *Cyp1a2* genes arranged head-to-head with a shared $\sim$14 kb bidirectional promotor on chromosome 9 meant that it had proved impossible to generate a Cyp1a1/Cyp1a2 double-knockout mouse simply by breeding. By employing an interchromosomal excision mediated by Cre/loxP, Dragin et al. (25) deleted both *Cyp1a* genes and were able to create a mouse line in which all the *Cyp1* genes were removed by crossing the *Cyp1a1/Cyp1a2* null mice with those lacking *Cyp1b1* (24). *Cyp1a1/Cyp1a2/Cyp1b1* null mice were able to reproduce, although with smaller litter sizes; treatment of the *Cyp1a1/Cyp1a2/Cyp1b1* null mice with BaP resulted in serum BaP levels around 90-fold higher than in wild-type animals, similar to those found in the *Cyp1a1/Cyp1b1* double-null mice (22).

Cyp1b1

CYP1B1 was first identified and purified from mouse embryo fibroblasts (26) and is capable of metabolizing polycyclic aromatic hydrocarbons, similar to CYP1A1 and CYP1A2, but is expressed in a different distribution pattern being mainly found in steroidogenic tissues and at low levels in the liver, kidney, and lungs (27). Mutations in CYP1B1 have also been linked to primary congenital glaucoma in humans (28), and CYP1B1 has also been considered as a drug target because of its elevated expression in a range of different tumors (29). *Cyp1b1* null mice are phenotypically normal, but when challenged with 7,12-dimethylbenz[a]anthracene (DMBA) developed almost 10-fold less lymphomas than wild-type mice, and significantly lower numbers of skin tumors, strongly supporting the view that CYP1B1 was responsible for mediating between DMBA toxicity (30) and immunosuppression (31). These findings were further bolstered by a study in

which another polycyclic aromatic hydrocarbon, dibenzo[a,l]pyrene, was found to cause a range of benign and malignant tumors in all wild-type mice treated, whereas only 62% of *Cyp1b1* null mice formed tumors, exclusively adenomas of the lung, and endometrial hyperplasia (32,33).

Cyp2e1

Cyp2e1 is a highly conserved cytochrome P450 enzyme, which metabolizes ethanol and other low molecular weight toxins it is inducible by ethanol and also by disease states such as starvation, obesity, and diabetes (34,35). *Cyp2e1* null mice displayed no overt phenotype, and no compensatory changes in the hepatic expression of other P450s were noted (36). When challenged with acetaminophen, mice lacking the *Cyp2e1* gene were significantly more resistant to the hepatotoxic effects of this drug than wild-type mice, with 50% of treated animals dying at 400 mg/kg acetaminophen, whereas all *Cyp2e1* null mice survived at this dose (36). Since CYP1A2 has also been implicated in the activation of acetaminophen, Zaher et al. created a double-knockout mouse, nulled for both *Cyp1a2* and *Cyp2e1*, which further increased the resistance to acetaminophen hepatotoxicity such that mice lacking both P450 genes could be treated with 1200 mg/kg acetaminophen before low levels of toxicity became evident (37).

Cyp2e1 null mice have also been used to investigate the role of this enzyme in the hepatotoxicity of carbon tetrachloride (38) and chloroform (39).

Cyp2g1

CYP2G1, which is a highly conserved P450 expressed at high levels in the olfactory mucosa of mice and rabbits (40,41), has been found to be polymorphic in humans (42) and metabolizes a number of steroid hormones. *Cyp2g1* null mice were phenotypically normal, with apparently normal olfactory ability (43). However, microsomes from the olfactory mucosa of *Cyp2g1* null mice were found to have significantly lower activity toward the metabolism of progesterone, testosterone, and coumarin.

Cytochrome P450 Reductase

The size of the P450 supergene family and the overlapping substrate specificities exhibited by individual enzymes mean that although it might be desirable to delete P450 genes in greater numbers to overcome potential redundancy issues, this is practically difficult, although the use of RMCE (see above) is now allowing the deletion and manipulation of increasingly large segments of the genome (3,44).

Microsomal cytochromes P450s are supplied with reducing equivalents from the reduced form of nicotinamide adenine dinucleotide phosphate (NADPH) via a single electron donor, NADPH-cytochrome P450 oxidoreductase (POR). The unique nature of this enzyme has allowed two groups to delete this enzyme in a conditional manner specifically in the liver, using the Cre/loxP system (see above) and essentially ablate all hepatic P450 functions. Henderson et al. (45) and Gu et al. (46) found that mice lacking hepatic *Por* hepatic reductase null (HRN) and thus P450 function, were viable and developed and bred normally. The only phenotypic characteristic evident in the HRN mice was altered lipid homeostasis, such that the mice had an enlarged, fatty liver and significant reductions (>50%) in serum cholesterol and triglycerides.

The HRN mouse has been used to investigate the relationship between drug metabolism and disposition and toxicokinetics, using the anticancer prodrug cyclophosphamide as a model example (47,48). A variation of the HRN line has been reported, in which the rat CYP1A1 promotor (See sect. “Reporter Mice”) was used to drive Cre

expression and conditionally delete POR in a regulatable manner; by altering the CYP1A1 inducing agent administered, it was possible to delete POR (and thus P450 function) in the liver or the liver and gut, thus defining the relative contribution of these organs to drug metabolism (49).

Interestingly, although the group of Ding et al. (46,50) used a similar approach to that of Henderson et al. (45) in generating their conditional POR deletion by placing the neomycin gene in intron 15 as a selectable marker, the former oriented the neomycin gene transcriptionally in the opposite direction to that of the POR gene. The result was a hypomorphic POR mouse model where POR expression was decreased by between 74% and 95% in all tissues examined (51). This mouse displayed a degree of embryonic lethality, fertility problems, and range of other significant phenotypic issues, including decreased body and organ weights and reduced metabolism of a number of common drugs.

GLUTATHIONE TRANSFERASES

A recent review of glutathione transferase (GST), was done by Hayes et al. (52). The principal function of GST is to catalyze the conjugation of reduced glutathione (a tripeptide, glu-cys-gly) to an electrophilic carbon, sulfur, or nitrogen atom on nonpolar compounds. GST nomenclature is summarized in Mannervik et al. (53). Table 2 summarizes the GST knockout mice generated to date.

GST Alpha

The only member of this subfamily that has been deleted to date is GSTA4 (54). GSTA4 null mice are overtly normal, but were found to have a reduced litter size, higher fat content in the bones, and a greater susceptibility to bacterial infection than wild-type mice. Mice lacking GSTA4 also had a significantly reduced capacity for the conjugation of the lipid peroxidation product 4-hydroxynon-2-enal, a reaction known to be catalyzed by GSTA4 (55), and were more susceptible to the toxic effects of paraquat (54). Further study of this mouse line found that GSTA4 also played a role in protecting against carbon tetrachloride toxicity, at least during the early stages of the oxidative stress response (56).

GST Pi

The first GST gene deletion reported in the late 1990s was that of *Gstp* (57). GSTP has been reported to be significantly elevated in a range of tumors, both in animals and humans, although the mechanism by which this enzyme may be involved in the tumorigenic process is still unclear; indeed, the endogenous role(s) of GSTP has yet to be fully elucidated. Cell lines that have been engineered to over-express human GSTP also develop resistance to a range of drugs (58 60), although many of these compounds are not known to be substrates of the enzyme, and thus, it is becoming increasingly clear that GSTP may have actions that do not involve its primary catalytic function (61).

The mouse is unusual in that it possesses two GSTP genes, *Gstp1* and *Gstp2*, arranged in tandem on chromosome 1, whereas most other species have a single GSTP gene. Although GSTP is found almost ubiquitously in all tissues, in humans the expression of GSTP is restricted in the liver to the biliary epithelium (62,63), whereas in the mouse it is found in hepatocytes and expressed in a sexually differentiated manner, with GSTP1 at higher levels in males than females (and *Gstp1* at $\sim$10-fold higher levels

Table 2 Glutathione Transferase Genes in Knockout Mice

Class	Gene	Phenotype	Reference	Comment
Alpha	*GSTA4*	Reduced litter size Increased susceptibility to infection Higher lipid content in bones Reduced metabolism of 4 hydroxynonenal More susceptible to paraquat and CCl_4 toxicity	Engle et al. (54) Dwivedi et al. (56)	
Omega	*GSTO1*	(MMA) (V) reductase activity down by 80%	Chowdhury et al. (77)	Encodes MMA (V) reductase
Pi	*GSTP1/2*	Increased papilloma formation in skin tumorigenesis bioassay Increased adenoma formation in lung tumorigenesis bioassay Increased resistance to acetaminophen hepatotoxicity Regulation of JNK	Henderson et al. (57); Adler et al. (69); Henderson et al. (68); Elsby et al. (70); Ritchie et al. (66)	
Sigma	*Ptgds2*	Reduced allergic reactivity	Urade et al. (78)	Encodes hematopoietic prostaglandin D2 synthase
Theta	*GSTT1*	Reduced GST activity toward 1,2 epoxy 3 (*p* nitrophenoxy)propane dichloromethane 1,3 *bis*(2 chloroethyl) 1 nitrosourea	Fujimoto et al. (80)	Encodes MAAI,
Zeta	*GSTZ1*	Accumulation of urinary fumarylacetoacetate and succinylacetone	Fernandez Canon et al. (81)	Phenotypic variability with genetic background

Abbreviations: GST, glutathione S transferase; MMA, monomethylarsenate; JNK, Jun N terminal kinase; MAAI, maleylacetoacetate isomerase.

than *Gstp2* in both sexes) (64). No null mutation has been described for GSTP in humans, although a number of polymorphic variants have been described, with differing catalytic activities that have been correlated with altered disease susceptibility (65). The GstP null mouse has no overt phenotype; however, significantly increased papilloma formation was observed when exposed to a two-stage skin tumorigenesis test involving the use of dimethylbenz[a]anthracene as initiator and the phorbol ester TPA as promotor (57). Interestingly, no significant changes were found in the formation of DNA adducts in skin

from mice lacking *Gstp* (CJ Henderson, unpublished data), suggesting that the role of GstP in protecting against skin tumorigenesis may involve more than just the catalytic function of the enzyme. In a further carcinogenesis study, the lung tumor bioassay, GstP null mice were again found to be significantly more susceptible to chemically induced tumorigenesis when treated with polycyclic aromatic hydrocarbons, chemicals known to induce lung adenoma formation (66). Intriguingly, when BaP was used to induce lung tumors, there was a significant increase in pulmonary DNA adducts in *Gstp* null mice; however, although *Gstp* null mice treated with 3-methylcholanthrene had more lung adenomas than wild-type animals, there was no difference in DNA adducts, once again implying a role for GstP in addition to its detoxification function.

In a further phenotypic characterization of the *Gstp* null mouse, Henderson et al. administered acetaminophen in the expectation that those animals lacking GstP would be more sensitive to the hepatotoxic effects of the drug, since literature reports suggested GstP to be involved in conjugating and detoxifying the active metabolite of acetaminophen, *N*-acetylbenzoquinonimine (67). However, diametrically opposite results were found, such that $GstP^{-/-}$ mice were highly resistant to acetaminophen hepatotoxicity, despite no significant differences between GstP null and wild-type mice in terms of acetaminophen metabolism or the binding of reactive acetaminophen intermediates to cellular proteins (68). This resistance to acetaminophen hepatotoxicity appeared to be related to the increased ability of the *Gstp* null mice to regenerate glutathione following drug treatment. The mechanism behind this remains unclear, but may be related to a proposed function for GstP in the regulation of Jun N-terminal kinase (JNK), whereby GstP binds to JNK and inhibits its activity in embryonic fibroblasts (69). Cells isolated from *Gstp* null mice had a higher basal level of JNK activity and thus greater activation of the transcription factor c-jun, part of the AP-1 complex, which regulates the expression of a number of genes involved in mediating both cell survival and apoptosis. The fact that AP-1 binding to DNA is induced by acetaminophen would support the premise that this pathway is crucial in providing protection against acetaminophen cytotoxicity (70). It is possible that under normal conditions, GstP inhibits JNK, thus preventing c-jun activity as part of the AP-1 complex and so potentiating the toxicity of acetaminophen by preventing the expression of cytoprotective genes. In the absence of GstP, JNK activity is not restrained, and *Gstp* null mice are thus more resistant to acetaminophen toxicity. Other studies have also shown a link between GstP, JNK, and apoptosis, with GstP inhibiting JNK, and thus preventing apoptosis in dopaminergic neurons (71), while in a Jurkat human leukemia or SH-SY5Y human neuroblastoma, cell line treatment with etoposide resulted in dimerization of GSTP and release of JNK from inhibition, leading to increased apoptosis (72,73).

GST Omega

GSTO was first reported in 2000 and was found to be widely expressed in different tissues and organisms, and in humans, it is also found with a nuclear localization in a number of different cell types (74,75). GSTO1 possesses glutathione-dependent thiol transferase and dehydroascorbate reductase activities characteristic of the glutaredoxins and is unusual among GSTs in that it has an active site cysteine capable of forming a disulfide bond with glutathione. A second member of this subfamily has been identified, GSTO2, which is mainly expressed in the testes (76). GSTO1 is identical to monomethylarsenate (MMA) (V) reductase, and the knockout of this gene in mice by the deletion of 222bp in exon 3 was reported in 2006, although it is worth noting that *Gsto1* transcript levels were only decreased by 3.3-fold (77).

GST Sigma

The cytosolic enzyme hematopoietic prostaglandin D2 synthase is encoded by the sigma class GST, and a gene knockout for this enzyme has been reported (78). Little is known about the phenotype of such mice, other than that they have a reduced allergic reaction relative to wild-type mice.

GST Theta

GSTT is considered to be one of the oldest forms of GST, being found in bacteria and throughout the animal and plant kingdoms, and appears to have undergone an early gene duplication event to generate two forms, GSTT1 and GSTT2. *GSTT1* is polymorphic in humans, with 20% of Caucasian and 80% of Asian populations being nulled for the gene, which epidemiological studies have shown alters susceptibility to various cancers, dependent on the tissue and environmental exposure to halogenated solvents (79).

Fujimoto et al. reported the deletion of the *Gstt1* gene; no overt phenotypic differences were observed between *Gstt1* null and wild-type mice, although activity toward a range of known GSTT substrates was significantly lower in the *Gstt1* null mice (80).

Gst Zeta

The murine *Gstz1* gene encodes maleylacetoacetate isomerase (MAAI), which catalyzes the *cis-trans* isomerization of maleylacetoacetate to fumarylacetoacetate in the tyrosine/phenylalanine catabolic pathway. The *Gstz1* gene was disrupted in mice with no obvious phenotype, although detailed analysis found an accumulation of fumarylacetoacetate and succinylacetone in the urine of these mice, indicating that intermediates of tyrosine metabolism were accumulating (81). Another *Gstz1* knockout mouse model was generated by Lim et al. (82), and again displayed no obvious phenotype, although further examination revealed enlarged liver and kidneys and atrophy of the spleen, and dietary phenyalanine supplementation was rapidly lethal.

NUCLEAR RECEPTORS

Nuclear receptors (NRs) are a family of ligand-activated transcription factors, comprising a DNA-binding domain and containing two zinc finger complexes and a ligand-binding domain, which also mediates dimerization of the NR with a binding partner and which is involved in regulating a wide range of physiological processes. A review of this field and associated nomenclature was done by Germain et al. (83). In terms of the regulation of expression of drug metabolizing enzymes and transporters, two key NRs are the constitutive androstane receptor (CAR; NR1I3) and the pregnane X receptor (PXR; NR1I2), which are the subject of a recent review (84). Within the NR family, those members for which an endogenous ligand has not been identified are often referred to as "orphan" NRs, and both CAR and PXR would fall into this category, although CAR and PXR have also been classified as xenobiotic sensors because of their role in mediating the cell's response to chemical challenge. It is important to note that this NR-mediated induction of gene expression can be subjected to a degree of species specificity, probably because of structural differences in the NR and also cross talk, because of many genes possessing regulatory elements that can respond to both CAR and PXR.

A gene knockout for PXR was first reported by Staudinger et al. (85), who replaced the first coding exon of the PXR gene with a cassette containing a neomycin selectable

marker. It is important to note that although one of the two zinc finger DNA binding domains in PXR was thus deleted, a truncated transcript was still produced in PXR null mice; however, even if this transcript was translated, it would be nonfunctional. The PXR null mice, on a 129 × C57BL/6 genetic background, displayed no overt phenotype, but were used to demonstrate that PXR plays a pivotal role in protecting against the hepatotoxic effects of lithocholic acid as well as being central to xenobiotic homeostasis (86).

Wei et al. reported a mouse line in which CAR had been deleted (on a 129 × C57BL/6 background) and the β-galactosidase gene "knocked-in" to the CAR locus, allowing not only an assessment of the phenotypic consequences of the absence of this gene (overtly none) but also providing a mechanism to define the pattern of CAR expression in vivo (87). These CAR null mice exhibited significantly increased sensitivity to zoxazolamine, failing to recover from the paralysis induced by this drug, and also displayed increased cocaine hepatotoxicity as a consequence of their inability to upregulate expression of the P450 enzymes, which would normally metabolically inactivate these drugs.

Crossing the CAR and PXR null mice yielded a double-knockout line in which both NRs were absent, and once again no overt phenotype was evident under basal conditions; however, a detailed characterization found both specific and overlapping responses mediated by CAR and PXR in protecting the cell against exogenous and endogenous stresses (88).

REPORTER MICE

A number of reporter mice have been generated to facilitate investigation of the expression and function of drug-metabolizing enzymes, as illustrated by Wei et al. using β-galactosidase knocked into the murine CAR locus (above) and demonstrating expression of CAR in the liver and also in the epithelial cells of the small intestinal villi (89). Using random transgenesis, Robertson et al. placed a 13-kb fragment of the CYP3A4 promotor upstream of the *lacZ* gene and generated a reporter mouse in which constitutive and inducible CYP3A4 expression was found to reflect that found in humans (90). This model was further employed to investigate the adaptive physiological expression of CYP3A4 following cholestasis (induced by ligation of the bile duct) (91).

Campbell et al. used a portion of the rat CYP1A1 promotor to drive a *lacZ* reporter and illustrated the tightly regulated nature of this system in a transgenic mouse line, where no constitutive expression of β-galactosidase was detected but administration of the CYP1A1 inducer 3-methylcholanthrene caused a significant (>1000-fold) induction of transgene expression in several tissues, including the liver and intestine (92). This reporter system not only provided a model system with which to establish those environmental and hormonal factors regulating expression of CYP1A1 but could be used to drive expression of heterologous genes in a truly on/off manner. The CYP1A1/*lacZ* system was subsequently adapted to express Cre recombinase and used to conditionally delete β-catenin in a regulatable manner (93) and was also employed in a similar manner in the deletion of POR (see sect. "P450 Reductase") (49).

More recently, in another targeted approach, β-galactosidase has been knocked-in to the endogenous murine P450 reductase locus, replacing one copy of the POR gene and generating a mouse line in which constitutive and induced expression of POR can be investigated in a developmental-, tissue-, and cell-specific manner (CJ Henderson, H Wolf, unpublished).

HUMANIZATION

The genes involved in drug metabolism provide an adaptive response to environmental challenge and, as a consequence, these detoxifying mechanisms have diverged between species in evolution. Therefore, a compound can be metabolized differentially in different species, making it difficult to extrapolate data from animals to humans. These differences can occur at all stages of the drug metabolism pathway. For example, the NRs PXR, CAR, and PPARα and the basic-helix-loop-helix transcription factor AHR of different species bind to distinct ligands as well as with different binding affinities to the same ligand, leading to species-specific induction profiles of drug-metabolizing enzymes (DMEs). Not only the factors that regulate their expression but also the DMEs themselves vary in their catalytic activities and their multiplicity markedly between species. A prominent case in the group of phase I enzymes is the CYP2D family, for which only one functional gene, *CYP2D6*, exists in humans, while there are, for example, nine functional genes in the mouse. Similar differences do exist for other DMEs, for example, the CYP3A family. Accordingly, a lot of effort has been made in recent years to generate humanized mouse models for drug metabolism studies. With regard to humanization, mice are preferred model organisms because of their short generation times, convenience in handling, frequent use in pharmacological studies, and particularly their accessibility to genetic manipulation.

Different xenobiotic receptor humanized mice for *PXR*, *CAR*, *PPARα,* and *AHR* have been generated. In case of *PXR*, *CAR*, and *PPARα*, the common approach from different groups was to knockout the corresponding mouse receptor and to insert a human expression cassette by random transgenesis into the mouse genome. By making use of this approach, *PXR* and *CAR* humanized mice have been generated, in which cDNAs of the human receptors are expressed by the liver-specific albumin promote (94,95). In these mice, the human receptors restore the xenobiotic response in the mouse liver, but with a humanized response profile (96). In another approach, a *PXR*-humanized mouse model containing a genomic fragment with the entire human *PXR* gene and its promoter was created by random integration on a *Pxr* null background (97). Pretreatment of these mice with the human-specific PXR agonist rifampicin led to a faster metabolism of midazolam, while no change in midazolam metabolism was observed in wild-type mice. Therefore, the *PXR*-humanized mice reflect the common drug-drug interaction found in humans cotreated with rifampicin and midazolam more accurately. Two *PPARα*-humanized mice on a mouse *PPARα* null background have been described. In the first model, the human PPARα was expressed with a tetracycline-responsive system (98), and in the second model, a genomic fragment comprising the human *PPARα* promoter and gene sequences were introduced (99). Both models responded to PPARα ligands by the induction of known PPARα downstream genes; however, similar to the situation in humans, the humanized mice did not exhibit the hepatocellular proliferation that is observed in wild-type mice upon Pparα activation. The humanized mice therefore can help to assess the human risk of PPARα ligands to non-genotoxic liver tumor promotion more accurately than wild-type mice. In case of AHR, transgenic mice have been generated in which the human AHR cDNA is knocked into the mouse *Ahr* gene locus so that the mouse promoter controls the expression of the human receptor (99). On treatment with AHR ligands, these mice do show induction of typical AHR target genes, but in agreement with in vitro studies, they are functionally less responsive to the environmental toxicant TCDD. In the light of drug metabolism studies, the xenobiotic receptor-humanized mice can be of critical importance because the species-specific interaction of a compound with these

receptors will alter the expression of DMEs and this in turn can affect the metabolism and therefore the drug bioavailability, toxicity, and efficacy of the compound itself.

Because of species-specific differences of DMEs, cytochrome P450 (CYP)-humanized mice can be valuable tools for drug metabolism studies. Many transgenic mice expressing human CYPs have become available in recent years, including mice expressing human CYP2D6, CYP3A4, CYP2E1, CYP1A1, CYP1A2, CYP1B1, and others (100). Mice expressing human CYP2D6 efficiently metabolized debrisoquine, which is used as a probe substrate of CYP2D6 activity in humans (101), and CYP3A4 transgenic mice showed a higher rate of midazolam metabolism and clearance after oral administration (102). However, most of the current transgenic mouse models expressing human CYPs have the disadvantage that the homologous mouse genes are still present. This drawback is overcome in mouse lines expressing human CYP1A1/1A2 on a mouse *Cyp1a1/1a2* null background (25) and CYP3A4 on a mouse *Cyp3a* cluster knockout background (103). In the latter case, eight mouse *Cyp3a* genes have been functionally replaced with a human CYP3A4 cassette expressed either in the liver or in the intestine. CYP3A4 expression in the intestine decreased the absorption of docetaxel into the bloodstream, while hepatic expression increased the systemic docetaxel clearance, showing the utility of these mice to analyze the relative contribution of the liver and intestine to the CYP3A4-mediated metabolism of a drug. A mouse model representing a phase II humanization was generated by random integration of the human *UGT1* locus into the mouse genome (104), which could be a useful tool to study human UGT1 metabolism of a drug.

In summary, humanized mouse models are becoming valuable tools to study the in vivo metabolism of compounds and in addition to the existing in vitro and in vivo assays can help to better predict the pathways of drug disposition and toxicity in humans. In order that the models become widely accepted in this field, a number of obvious improvements will have to be accomplished. First of all, it has to be ensured that the models provide the bona fide expression of the human proteins, both in terms of expression level and tissue distribution. Usually this can be achieved by using the corresponding human or appropriate mouse promoters. Besides this, the expression of genomic sequences instead of cDNAs can be beneficial in those cases where human splice variants are known to be important for the normal function of a gene. Second, in models expressing human proteins, the deletion of the corresponding homologous mouse gene(s) is advantageous in order to achieve a true humanlike profile of drug metabolism. And finally, the utility of humanized models would be greatly increased by the combination of the most relevant humanizations of xenobiotic receptors and DMEs in a single mouse model. This would allow the establishment of a complete human pathway of drug metabolism and would supersede the necessity of multiple tests in different mouse models.

GENETIC BACKGROUND

As intimated earlier in this chapter, the genetic background of a genetically altered mouse strain may play a significant role in modifying the resulting phenotype. The generation of two *Cyp1a2* null mouse lines with dramatically different phenotypes (see above) on different genetic backgrounds reflects this, and there are other examples, for instance, the deletion of the epidermal growth factor (EGF) receptor (105) results in embryonic lethality at mid-gestation on a pure 129 genetic background, while pups survive until birth on a 129 × C57BL/6 background or live for up to three weeks on a mixed 129 × C57BL/6 × MF1 background. This illustrates the importance of controlling the genetic

background in genetic manipulation experiments, either by crossing into a pure genetic background or by ensuring a mixed genetic background is maintained by truly random breeding. It should also be clear from the foregoing that many of the genetically altered mouse lines generated in the field of drug metabolism have been created on a range of mixed genetic backgrounds, although in recent times there have been concerted efforts to address this issue. The recent generation of ES cells from C57BL/6 mice capable of germ line transmission of genetic alterations should be an extremely useful development and should allow generation of genetically manipulated mouse lines on this commonly used genetic background. However, C57BL/6 is not an ideal background for all experimental purposes in many tumorigenesis protocols, it is "resistant" to tumor formation, spontaneous or chemically induced and it is clear that the process of backcrossing to a defined genetic background will have to continue, while the creation and deployment of ES cells from different genetic backgrounds are undertaken. The reader is referred to an excellent recent commentary which covers the issue of genetic background and suggests potential solutions in more detail (106).

SUMMARY

The use of genetically manipulated mice in the area of drug metabolism has yielded many useful insights into the expression and function of drug-metabolizing enzymes. As with studies in other fields, which employ genetically altered animals, it is crucial to take full account of genetic background when interpreting experimental results and be aware of the potential for confounding of data when using conditional deletions or alterations. The recent trend toward "humanization" should be welcomed as a significant step forward in this area, and this has already begun to yield valuable information on the role of human drug-metabolizing enzymes in vivo.

REFERENCES

1. Austin CP, Battey JF, Bradley A, Bucan M, Capecchi M, Collins FS, Dove WF, Duyk G, Dymecki S, Eppig JT, Grieder FB, Heintz N, Hicks G, Insel TR, Joyner A, Koller BH, Lloyd KC, Magnuson T, Moore MW, Nagy A, Pollock JD, Roses AD, Sands AT, Seed B, Skarnes WC, Snoddy J, Soriano P, Stewart DJ, Stewart F, Stillman B, Varmus H, Varticovski L, Verma IM, Vogt TF, von Melchner H, Witkowski J, Woychik RP, Wurst W, Yancopoulos GD, Young SG, Zambrowicz B. The knockout mouse project. Nat Genet 2004; 36(9):921 924.
2. Lewandoski M. Conditional control of gene expression in the mouse. Nat Rev Genet 2001; 2(10):743 755.
3. Baer A, Bode J. Coping with kinetic and thermodynamic barriers: RMCE, an efficient strategy for the targeted integration of transgenes. Curr Opin Biotechnol 2001; 12(5):473 480.
4. Wong ET, Kolman JL, Li YC, Mesner LD, Hillen W, Berens C, Wahl GM. Reproducible doxycycline inducible transgene expression at specific loci generated by Cre recombinase mediated cassette exchange. Nucleic Acids Res 2005; 33(17):e147.
5. Nelson DR. Cytochrome P450 nomenclature, 2004. Methods Mol Biol 2006; 320:1 10.
6. Bernhardt R. Cytochromes P450 as versatile biocatalysts. J Biotechnol 2006; 124(1):128 145.
7. Nebert DW, Russell DW. Clinical importance of the cytochromes P450. Lancet 2002; 360 (9340):1155 1162.
8. Fernandez Salguero PM, Gonzalez FJ. Targeted disruption of specific cytochromes P450 and xenobiotic receptor genes. Methods Enzymol 1996; 272:412 430.
9. Gonzalez FJ, Kimura S. Understanding the role of xenobiotic metabolism in chemical carcinogenesis using gene knockout mice. Mutat Res 2001; 477(1 2):79 87.

10. Henderson CJ, Otto DM, McLaren AW, Carrie D, Wolf CR. Knockout mice in xenobiotic metabolism. Drug Metab Rev 2003; 35(4):385 392.
11. Henderson CJ, Wolf CR. Transgenic analysis of human drug metabolizing enzymes: preclinical drug development and toxicology. Mol Interv 2003; 3(6):331 343.
12. Pineau T, Fernandez Salguero P, Lee SS, McPhail T, Ward JM, Gonzalez FJ. Neonatal lethality associated with respiratory distress in mice lacking cytochrome P450 1A2. Proc Natl Acad Sci U S A 1995; 92(11):5134 5138.
13. Liang HC, McKinnon RA, Nebert DW. Sensitivity of CYP1A1 mRNA inducibility by dioxin is the same in Cyp1a2(+/+) wild type and Cyp1a2(/) null mutant mice. Biochem Pharmacol 1997; 54(10):1127 1131.
14. Diliberto JJ, Burgin D, Birnbaum LS. Role of CYP1A2 in hepatic sequestration of dioxin: studies using CYP1A2 knock out mice. Biochem Biophys Res Commun 1997; 236(2): 431 433.
15. Tonge RP, Kelly EJ, Bruschi SA, Kalhorn T, Eaton DL, Nebert DW, Nelson SD. Role of CYP1A2 in the hepatotoxicity of acetaminophen: investigations using Cyp1a2 null mice. Toxicol Appl Pharmacol 1998; 153(1):102 108.
16. Sinclair PR, Gorman N, Dalton T, Walton HS, Bement WJ, Sinclair JF, Smith AG, Nebert DW. Uroporphyria produced in mice by iron and 5 aminolaevulinic acid does not occur in Cyp1a2(/) null mutant mice. Biochem J 1998; 330(pt 1):149 153.
17. Sinclair PR, Gorman N, Walton HS, Bement WJ, Dalton TP, Sinclair JF, Smith AG, Nebert DW. CYP1A2 is essential in murine uroporphyria caused by hexachlorobenzene and iron. Toxicol Appl Pharmacol 2000; 162(1):60 67.
18. Zaccaro C, Sweitzer S, Pipino S, Gorman N, Sinclair PR, Sinclair JF, Nebert DW, De Matteis F. Role of cytochrome P450 1A2 in bilirubin degradation studies in Cyp1a2 (/) mutant mice. Biochem Pharmacol 2001; 61(7):843 849.
19. Dalton TP, Dieter MZ, Matlib RS, Childs NL, Shertzer HG, Genter MB, Nebert DW. Targeted knockout of Cyp1a1 gene does not alter hepatic constitutive expression of other genes in the mouse [Ah] battery. Biochem Biophys Res Commun 2000; 267(1):184 189.
20. Uno S, Dalton TP, Shertzer HG, Genter MB, Warshawsky D, Talaska G, Nebert DW. Benzo [a]pyrene induced toxicity: paradoxical protection in Cyp1a1(/) knockout mice having increased hepatic BaP DNA adduct levels. Biochem Biophys Res Commun 2001; 289(5): 1049 1056.
21. Uno S, Dalton TP, Sinclair PR, Gorman N, Wang B, Smith AG, Miller ML, Shertzer HG, Nebert DW. Cyp1a1(/) male mice: protection against high dose TCDD induced lethality and wasting syndrome, and resistance to intrahepatocyte lipid accumulation and uroporphyria. Toxicol Appl Pharmacol 2004; 196(3):410 421.
22. Uno S, Dalton TP, Dragin N, Curran CP, Derkenne S, Miller ML, Shertzer HG, Gonzalez FJ, Nebert DW. Oral benzo[a]pyrene in Cyp1 knockout mouse lines: CYP1A1 important in detoxication, CYP1B1 metabolism required for immune damage independent of total body burden and clearance rate. Mol Pharmacol 2006; 69(4):1103 1114.
23. Nebert DW, Dalton TP. The role of cytochrome P450 enzymes in endogenous signalling pathways and environmental carcinogenesis. Nat Rev 2006; 6(12):947 960.
24. Dragin N, Shi Z, Madan R, Karp CL, Sartor MA, Chen C, Gonzalez FJ, Nebert D. Phenotype of the Cyp1a1/1a2/1b1(/) triple knockout mouse. Mol Pharmacol 2008; 73(6):1844 1856. [Epub 2008, Mar 27].
25. Dragin N, Uno S, Wang B, Dalton TP, Nebert DW. Generation of 'humanized' hCYP1A1 1A2 Cyp1a1/1a2(/) mouse line. Biochem Biophys Res Commun 2007; 359(3): 635 642.
26. Pottenger LH, Jefcoate CR. Characterization of a novel cytochrome P450 from the transformable cell line, C3H/10T1/2. Carcinogenesis 1990; 11(2):321 327.
27. Savas U, Bhattacharyya KK, Christou M, Alexander DL, Jefcoate CR. Mouse cytochrome P 450EF, representative of a new 1B subfamily of cytochrome P 450s. Cloning, sequence determination, and tissue expression. J Biol Chem 1994; 269(21):14905 14911.

28. Stoilov I, Akarsu AN, Sarfarazi M. Identification of three different truncating mutations in cytochrome P4501B1 (CYP1B1) as the principal cause of primary congenital glaucoma (Buphthalmos) in families linked to the GLC3A locus on chromosome 2p21. Hum Mol Genet 1997; 6(4):641 647.
29. Murray GI, Taylor MC, McFadyen MC, McKay JA, Greenlee WF, Burke MD, Melvin WT. Tumor specific expression of cytochrome P450 CYP1B1. Cancer Res 1997; 57(14): 3026 3031.
30. Buters JT, Sakai S, Richter T, Pineau T, Alexander DL, Savas U, Doehmer J, Ward JM, Jefcoate CR, Gonzalez FJ. Cytochrome P450 CYP1B1 determines susceptibility to 7, 12 dimethylbenz[a]anthracene induced lymphomas. Proc Natl Acad Sci U S A 1999; 96(5): 1977 1982.
31. Gao J, Lauer FT, Dunaway S, Burchiel SW. Cytochrome P450 1B1 is required for 7,12 dimethylbenz(a) anthracene (DMBA) induced spleen cell immunotoxicity. Toxicol Sci 2005; 86(1):68 74.
32. Buters JT, Mahadevan B, Quintanilla Martinez L, Gonzalez FJ, Greim H, Baird WM, Luch A. Cytochrome P450 1B1 determines susceptibility to dibenzo[a,l]pyrene induced tumor formation. Chem Res Toxicol 2002; 15(9):1127 1135.
33. Shimada T, Fujii Kuriyama Y. Metabolic activation of polycyclic aromatic hydrocarbons to carcinogens by cytochromes P450 1A1 and 1B1. Cancer Sci 2004; 95(1):1 6.
34. Cederbaum AI. CYP2E1 biochemical and toxicological aspects and role in alcohol induced liver injury. Mt Sinai J Med 2006; 73(4):657 672.
35. Gonzalez FJ. The 2006 Bernard B. Brodie Award Lecture. Cyp2e1. Drug Metab Dispos 2007; 35(1):1 8.
36. Lee SS, Buters JT, Pineau T, Fernandez Salguero P, Gonzalez FJ. Role of CYP2E1 in the hepatotoxicity of acetaminophen. J Biol Chem 1996; 271(20):12063 12067.
37. Zaher H, Buters JT, Ward JM, Bruno MK, Lucas AM, Stern ST, Cohen SD, Gonzalez FJ. Protection against acetaminophen toxicity in CYP1A2 and CYP2E1 double null mice. Toxicol Appl Pharmacol 1998; 152(1):193 199.
38. Wong FW, Chan WY, Lee SS. Resistance to carbon tetrachloride induced hepatotoxicity in mice which lack CYP2E1 expression. Toxicol Appl Pharmacol 1998; 153:109 118.
39. Constan AA, Sprankle CS, Peters JM, Kedderis GL, Everitt JI, Wong BA, Gonzalez FL, Butterworth BE. Metabolism of chloroform by cytochrome P450 2E1 is required for induction of toxicity in the liver, kidney, and nose of male mice. Toxicol Appl Pharmacol 1999; 160(2): 120 126.
40. Ding X, Dahl A. Olfactory mucosa:composition, enzymatic localisation and metabolism. In: Doty R, ed. Handbook of Olfaction and Gustation. New York: Marcel Dekker, 2003:51 73.
41. Zhuo X, Schwob JE, Swiatek PJ, Ding X. Mouse cyp2g1 gene: promoter structure and tissue specific expression of a cyp2g1 lacz fusion gene in transgenic mice. Arch Biochem Biophys 2001; 391(1):127 136.
42. Sheng J, Guo J, Hua Z, Caggana M, Ding X. Characterization of human CYP2G genes: widespread loss of function mutations and genetic polymorphism. Pharmacogenetics 2000; 10(8): 667 678.
43. Zhuo X, Gu J, Behr MJ, Swiatek PJ, Cui H, Zhang QY, Xie Y, Collins DN, Ding X. Targeted disruption of the olfactory mucosa specific Cyp2g1 gene: impact on acetaminophen toxicity in the lateral nasal gland, and tissue selective effects on Cyp2a5 expression. J Pharmacol Exp Ther 2004; 308(2):719 728.
44. Toledo F, Liu CW, Lee CJ, Wahl GM. RMCE ASAP: a gene targeting method for ES and somatic cells to accelerate phenotype analyses. Nucleic Acids Res 2006; 34(13):e92.
45. Henderson CJ, Otto DM, Carrie D, Magnuson MA, McLaren AW, Rosewell I, Wolf CR. Inactivation of the hepatic cytochrome P450 system by conditional deletion of hepatic cytochrome P450 reductase. J Biol Chem 2003; 278(15):13480 13486.
46. Gu J, Weng Y, Zhang QY, Cui H, Behr M, Wu L, Yang W, Zhang L, Ding X. Liver specific deletion of the NADPH cytochrome P450 reductase gene: impact on plasma cholesterol

homeostasis and the function and regulation of microsomal cytochrome P450 and heme oxygenase. J Biol Chem 2003; 278(28):25895 25901.
47. Henderson CJ, Pass GJ, Wolf CR. The hepatic cytochrome P450 reductase null mouse as a tool to identify a successful candidate entity. Toxicol Lett 2006; 162(1):111 117.
48. Pass GJ, Carrie D, Boylan M, Lorimore S, Wright E, Houston B, Henderson CJ, Wolf CR. Role of hepatic cytochrome p450s in the pharmacokinetics and toxicity of cyclophosphamide: studies with the hepatic cytochrome p450 reductase null mouse. Cancer Res 2005; 65(10): 4211 4217.
49. Finn RD, McLaren AW, Carrie D, Henderson CJ, Wolf CR. Conditional deletion of cytochrome P450 oxidoreductase in the liver and gastrointestinal tract: a new model for studying the functions of the p450 system. J Pharmacol Exp Ther 2007; 322(1):40 47.
50. Wu L, Gu J, Weng Y, Kluetzman K, Swiatek P, Behr M, Zhang QY, Zhuo X, Xie Q, Ding X. Conditional knockout of the mouse NADPH cytochrome P450 reductase gene. Genesis 2003; 36(4):177 181.
51. Wu L, Gu J, Cui H, Zhang QY, Behr M, Fang C, Weng Y, Kluetzman K, Swiatek PJ, Yang W, Kaminsky L, Ding X. Transgenic mice with a hypomorphic NADPH cytochrome P450 reductase gene: effects on development, reproduction, and microsomal cytochrome P450. J Pharmacol Exp Ther 2005; 312(1):35 43.
52. Hayes JD, Flanagan JU, Jowsey IR. Glutathione transferases. Annu Rev Pharmacol Toxicol 2005; 45:51 88.
53. Mannervik B, Board PG, Hayes JD, Listowsky I, Pearson WR. Nomenclature for mammalian soluble glutathione transferases. Methods Enzymol 2005; 401:1 8.
54. Engle MR, Singh SP, Czernik PJ, Gaddy D, Montague DC, Ceci JD, Yang Y, Awasthi S, Awasthi YC, Zimniak P. Physiological role of mGSTA4 4, a glutathione S transferase metabolizing 4 hydroxynonenal: generation and analysis of mGsta4 null mouse. Toxicol Appl Pharmacol 2004; 194(3):296 308.
55. Singh SP, Janecki AJ, Srivastava SK, Awasthi S, Awasthi YC, Xia SJ, Zimniak P. Membrane association of glutathione S transferase mGSTA4 4, an enzyme that metabolizes lipid peroxidation products. J Biol Chem 2002; 277(6):4232 4239.
56. Dwivedi S, Sharma R, Sharma A, Zimniak P, Ceci JD, Awasthi YC, Boor PJ. The course of CCl4 induced hepatotoxicity is altered in mGSTA4 4 null (/) mice. Toxicology 2006; 218(1): 58 66.
57. Henderson CJ, Smith AG, Ure J, Brown K, Bacon EJ, Wolf CR. Increased skin tumorigenesis in mice lacking pi class glutathione S transferases. Proc Natl Acad Sci U S A 1998; 95(9): 5275 5280.
58. Black SM, Beggs JD, Hayes JD, Bartoszek A, Muramatsu M, Sakai M, Wolf CR. Expression of human glutathione S transferases in Saccharomyces cerevisiae confers resistance to the anticancer drugs adriamycin and chlorambucil. Biochem J 1990; 268(2):309 315.
59. Black SM, Wolf CR. The role of glutathione dependent enzymes in drug resistance. Pharmacol Ther 1991; 51(1):139 154.
60. Townsend DM, Tew KD. The role of glutathione S transferase in anti cancer drug resistance. Oncogene 2003; 22(47):7369 7375.
61. Tew KD. Redox in redux: emergent roles for glutathione S transferase P (GSTP) in regulation of cell signaling and S glutathionylation. Biochem Pharmacol 2007; 73(9):1257 1269.
62. Hayes JD, Pulford DJ. The glutathione S transferase supergene family: regulation of GST and the contribution of the isoenzymes to cancer chemoprotection and drug resistance. Crit Rev Biochem Mol Biol 1995; 30(6):445 600.
63. Hayes PC, Harrison DJ, Bouchier IA, McLellan LI, Hayes JD. Cytosolic and microsomal glutathione S transferase isoenzymes in normal human liver and intestinal epithelium. Gut 1989; 30(6):854 859.
64. Bammler TK, Smith CA, Wolf CR. Isolation and characterization of two mouse Pi class glutathione S transferase genes. Biochem J 1994; 298(pt 2):385 390.

65. Harries LW, Stubbins MJ, Forman D, Howard GC, Wolf CR. Identification of genetic polymorphisms at the glutathione S transferase Pi locus and association with susceptibility to bladder, testicular and prostate cancer. Carcinogenesis 1997; 18(4):641 644.
66. Ritchie KJ, Henderson CJ, Wang XJ, Vassieva O, Carrie D, Farmer PB, Gaskell M, Park K, Wolf CR. Glutathione transferase pi plays a critical role in the development of lung carcinogenesis following exposure to tobacco related carcinogens and urethane. Cancer Res 2007; 67(19):9248 9257.
67. Coles B, Wilson I, Wardman P, Hinson JA, Nelson SD, Ketterer B. The spontaneous and enzymatic reaction of N acetyl p benzoquinonimine with glutathione: a stopped flow kinetic study. Arch Biochem Biophys 1988; 264(1):253 260.
68. Henderson CJ, Wolf CR, Kitteringham N, Powell H, Otto D, Park BK. Increased resistance to acetaminophen hepatotoxicity in mice lacking glutathione S transferase Pi. Proc Natl Acad Sci U S A 2000; 97(23):12741 12745.
69. Adler V, Yin Z, Fuchs SY, Benezra M, Rosario L, Tew KD, Pincus MR, Sardana M, Henderson CJ, Wolf CR, Davis RJ, Ronai Z. Regulation of JNK signaling by GSTp. EMBO J 1999; 18(5):1321 1334.
70. Elsby R, Kitteringham NR, Goldring CE, Lovatt CA, Chamberlain M, Henderson CJ, Wolf CR, Park BK. Increased constitutive c Jun N terminal kinase signaling in mice lacking glutathione S transferase Pi. J Biol Chem 2003; 278(25):22243 22249.
71. Ishisaki A, Hayashi H, Suzuki S, Ozawa K, Mizukoshi E, Miyakawa K, Suzuki M, Imamura T. Glutathione S transferase Pi is a dopamine inducible suppressor of dopamine induced apoptosis in PC12 cells. J Neurochem 2001; 77(5):1362 1371.
72. Bernardini S, Bellincampi L, Ballerini S, Ranalli M, Pastore A, Cortese C, Federici G. Role of GST P1 1 in mediating the effect of etoposide on human neuroblastoma cell line Sh Sy5y. J Cell Biochem 2002; 86(2):340 347.
73. Bernardini S, Bernassola F, Cortese C, Ballerini S, Melino G, Motti C, Bellincampi L, Iori R, Federici G. Modulation of GST P1 1 activity by polymerization during apoptosis. J Cell Biochem 2000; 77(4):645 653.
74. Board PG, Coggan M, Chelvanayagam G, Easteal S, Jermiin LS, Schulte GK, Danley DE, Hoth LR, Griffor MC, Kamath AV, Rosner MH, Chrunyk BA, Perregaux DE, Gabel CA, Geoghegan KF, Pandit J. Identification, characterization, and crystal structure of the Omega class glutathione transferases. J Biol Chem 2000; 275(32):24798 24806.
75. Yin ZL, Dahlstrom JE, Le Couteur DG, Board PG. Immunohistochemistry of omega class glutathione S transferase in human tissues. J Histochem Cytochem 2001; 49(8):983 987.
76. Whitbread AK, Masoumi A, Tetlow N, Schmuck E, Coggan M, Board PG. Characterization of the omega class of glutathione transferases. Methods Enzymol 2005; 401:78 99.
77. Chowdhury UK, Zakharyan RA, Hernandez A, Avram MD, Kopplin MJ, Aposhian HV. Glutathione S transferase omega [MMA(V) reductase] knockout mice: enzyme and arsenic species concentrations in tissues after arsenate administration. Toxicol Appl Pharmacol 2006; 216(3):446 457.
78. Urade Y, Eguchi N, Aritake K, Hayaishi O. [Functional analyses of lipocalin type and hematopoietic prostaglandin D synthases]. Nippon Yakurigaku Zasshi 2004; 123(1):5 13.
79. Landi S. Mammalian class theta GST and differential susceptibility to carcinogens: a review. Mutat Res 2000; 463(3):247 283.
80. Fujimoto K, Arakawa S, Watanabe T, Yasumo H, Ando Y, Takasaki W, Manabe S, Yamoto T, Oda S. Generation and functional characterization of mice with a disrupted glutathione S transferase, theta 1 gene. Drug Metab Dispos 2007; 35(12):2196 2202.
81. Fernandez Canon JM, Baetscher MW, Finegold M, Burlingame T, Gibson KM, Grompe M. Maleylacetoacetate isomerase (MAAI/GSTZ) deficient mice reveal a glutathione dependent nonenzymatic bypass in tyrosine catabolism. Mol Cell Biol 2002; 22(13):4943 4951.
82. Lim CE, Matthaei KI, Blackburn AC, Davis RP, Dahlstrom JE, Koina ME, Anders MW, Board PG. Mice deficient in glutathione transferase zeta/maleylacetoacetate isomerase exhibit a range of pathological changes and elevated expression of alpha, mu, and pi class glutathione transferases. Am J Pathol 2004; 165(2):679 693.

83. Germain P, Staels B, Dacquet C, Spedding M, Laudet V. Overview of nomenclature of nuclear receptors. Pharmacol Rev 2006; 58(4):685 704.
84. Stanley LA, Horsburgh BC, Ross J, Scheer N, Wolf CR. PXR and CAR: nuclear receptors which play a pivotal role in drug disposition and chemical toxicity. Drug Metab Rev 2006; 38(3):515 597.
85. Staudinger JL, Goodwin B, Jones SA, Hawkins Brown D, MacKenzie KI, LaTour A, Liu Y, Klaassen CD, Brown KK, Reinhard J, Willson TM, Koller BH, Kliewer SA. The nuclear receptor PXR is a lithocholic acid sensor that protects against liver toxicity. Proc Natl Acad Sci U S A 2001; 98(6):3369 3374.
86. Staudinger J, Liu Y, Madan A, Habeebu S, Klaassen CD. Coordinate regulation of xenobiotic and bile acid homeostasis by pregnane X receptor. Drug Metab Dispos 2001; 29(11): 1467 1472.
87. Wei P, Zhang J, Egan Hafley M, Liang S, Moore DD. The nuclear receptor CAR mediates specific xenobiotic induction of drug metabolism. Nature 2000; 407(6806):920 923.
88. Zhang J, Huang W, Qatanani M, Evans RM, Moore DD. The constitutive androstane receptor and pregnane X receptor function coordinately to prevent bile acid induced hepatotoxicity. J Biol Chem 2004; 279(47):49517 49522.
89. Wei P, Zhang J, Dowhan DH, Han Y, Moore DD. Specific and overlapping functions of the nuclear hormone receptors CAR and PXR in xenobiotic response. Pharmacogenomics J 2002; 2(2):117 126.
90. Robertson GR, Field J, Goodwin B, Bierach S, Tran M, Lehnert A, Liddle C. Transgenic mouse models of human CYP3A4 gene regulation. Mol Pharmacol 2003; 64(1):42 50.
91. Stedman C, Robertson G, Coulter S, Liddle C. Feed forward regulation of bile acid detoxification by CYP3A4: studies in humanized transgenic mice. J Biol Chem 2004; 279(12): 11336 11343.
92. Campbell SJ, Carlotti F, Hall PA, Clark AJ, Wolf CR. Regulation of the CYP1A1 promoter in transgenic mice: an exquisitely sensitive on off system for cell specific gene regulation. J Cell Sci 1996; 109(11):2619 2625.
93. Ireland H, Kemp R, Houghton C, Howard L, Clarke AR, Sansom OJ, Winton DJ. Inducible Cre mediated control of gene expression in the murine gastrointestinal tract: effect of loss of beta catenin. Gastroenterology 2004; 126(5):1236 1246.
94. Xie W, Barwick JL, Downes M, Blumberg B, Simon CM, Nelson MC, Neuschwander Tetri BA, Brunt EM, Guzelian PS, Evans RM. Humanized xenobiotic response in mice expressing nuclear receptor SXR. Nature 2000; 406(6794):435 439.
95. Zhang J, Huang W, Chua SS, Wei P, Moore DD. Modulation of acetaminophen induced hepatotoxicity by the xenobiotic receptor CAR. Science 2002; 298(5592):422 424.
96. Xie W, Evans RM. Orphan nuclear receptors: the exotics of xenobiotics. J Biol Chem 2001; 276(41):37739 37742.
97. Ma X, Shah Y, Cheung C, Guo GL, Feigenbaum L, Krausz KW, Idle JR, Gonzalez FJ. The PREgnane X receptor gene humanized mouse: a model for investigating drug drug interactions mediated by cytochromes P450 3A. Drug Metab Dispos 2007; 35(2):194 200.
98. Cheung C, Akiyama TE, Ward JM, Nicol CJ, Feigenbaum L, Vinson C, Gonzalez FJ. Diminished hepatocellular proliferation in mice humanized for the nuclear receptor peroxisome proliferator activated receptor alpha. Cancer Res 2004; 64(11):3849 3854.
99. Yang Q, Nagano T, Shah Y, Cheung C, Ito S, Gonzalez FJ. The PPAR alpha humanized mouse: a model to investigate species differences in liver toxicity mediated by PPAR alpha. Toxicol Sci 2008; 101(1):132 139.
100. Gonzalez FJ, Yu AM. Cytochrome P450 and xenobiotic receptor humanized mice. Annu Rev Pharmacol Toxicol 2006; 46:41 64.
101. Corchero J, Granvil CP, Akiyama TE, Hayhurst GP, Pimprale S, Feigenbaum L, Idle JR, Gonzalez FJ. The CYP2D6 humanized mouse: effect of the human CYP2D6 transgene and HNF4alpha on the disposition of debrisoquine in the mouse. Mol Pharmacol 2001; 60(6): 1260 1267.

102. Granvil CP, Yu AM, Elizondo G, Akiyama TE, Cheung C, Feigenbaum L, Krausz KW, Gonzalez FJ. Expression of the human CYP3A4 gene in the small intestine of transgenic mice: in vitro metabolism and pharmacokinetics of midazolam. Drug Metab Dispos 2003; 31(5): 548 558.
103. van Herwaarden AE, Wagenaar E, van der Kruijssen CM, van Waterschoot RA, Smit JW, Song JY, van der Valk MA, van Tellingen O, van der Hoorn JW, Rosing H, Beijnen JH, Schinkel AH. Knockout of cytochrome P450 3A yields new mouse models for understanding xenobiotic metabolism. J Clin Invest 2007; 117(11):3583 3592.
104. Chen S, Beaton D, Nguyen N, Senekeo Effenberger K, Brace Sinnokrak E, Argikar U, Remmel RP, Trottier J, Barbier O, Ritter JK, Tukey RH. Tissue specific, inducible, and hormonal control of the human UDP glucuronosyltransferase 1 (UGT1) locus. J Biol Chem 2005; 280(45):37547 37557.
105. Threadgill DW, Dlugosz AA, Hansen LA, Tennenbaum T, Lichti U, Yee D, LaMantia C, Mourton T, Herrup K, Harris RC, Barnard, JA, Yuspa, SH, Coffey, RJ, Magnuson, T. Targeted disruption of mouse EGF receptor: effect of genetic background on mutant phenotype. Science 1995; 269(5221):230 234.
106. Ridgway WM, Healy B, Smink LJ, Rainbow D, Wicker LS. New tools for defining the 'genetic background' of inbred mouse strains. Nat Immunol 2007; 8(7):669 673.

26

Preclinical Pharmacokinetic Models for Drug Discovery and Development

Kevin L. Salyers
Pharmacokinetics and Drug Metabolism, Amgen Inc., Thousand Oaks, California, U.S.A.

INTRODUCTION

In today's drug discovery paradigm, pharmacokinetics and drug metabolism (PKDM) play an integral role in the process of compound optimization and progression to candidate selection. The traditional focus of PKDM was to support lead optimization and drug development. But, support widened to include drug discovery, as it became clear that selection of candidates with suitable absorption, distribution, metabolism, and elimination (ADME) characteristics was critical to their success in development.

The nature and extent of ADME/PK studies for lead optimization are determined by the available in vitro and in vivo tools, capacity of the selected assays, and the target product profile. ADME screens are generally the in vitro methods used to measure permeability, specific enzyme activity, or metabolic stability and are amendable to automation-maximizing capacity. A major advantage for the ADME screens is the availability of human-derived tissues and the view of likely behavior to the targeted species. The use of the ADME screens is not to reject compounds but to rank order them for further studies. To ensure ADME screens are yielding accurate ranking information, it is important to validate in vitro data with in vivo results on a regular basis.

In this chapter, we will review animal models used in discovery PKDM and discuss some of the challenges that remain. The chapter is divided into three major sections: systemic metabolism and excretion, absorption, and distribution models. For the most part, the animal models discussed are those that help identify ADME liabilities. Many of the models require basic surgical resources to allow access to vasculature sites for sampling of various biological matrices in preclinical species.

METABOLISM AND EXCRETION MODELS

The metabolic clearance of compounds is most often studied with a combination of in vitro and in vivo methods. There are several in vivo models in preclinical species to identify systemic clearance liabilities and poor oral exposure due to first-pass metabolism.

Together with in vitro results on specific mechanisms for rapid systemic clearance, they provide the tools needed to devise rapid techniques to screen for the specific liability. Ideally, the discovery chemist needs to know the metabolically vulnerable moieties within a molecule. This information is essential to determine what structural changes can be made that retain potency and enhance metabolic stability. Metabolic liabilities resulting in high clearance are often identified by the metabolic stability in vitro screens described in previous chapters in this book. Importantly, the in vitro-screening results need to be validated by in vivo studies. Metabolism and other determinates of systemic exposure are listed in Figure 1. The decision-tree arrangement provides a useful tool in teasing out factors responsible for poor systemic exposure.

Hepatic Extraction

Identifying the cause of poor systemic exposure is crucial to understanding ADME liabilities and is necessary to direct in vitro-screening efforts. There are a couple of different study designs commonly used to determine hepatic extraction in rodents. In the simplest design, the dose is administered via the portal vein, and the systemic drug concentration is measured over time. Cassidy and Houston (1) used this method to assess the hepatic metabolism of phenol in the rat. Portal vein infusions can be carried out in conscious rat, dog, and nonhuman primate (NHP) to measure the fraction of drug extracted by the liver. In the dog and NHP, vascular access ports can be installed that allow access to the portal vein in a conscious animal. One potential drawback of this technique is that it may be possible to saturate liver metabolism and thus underestimate the extent of hepatic metabolism at lower, often clinically relevant concentrations. To avoid possible saturation, a high and low dose of investigational compound should be infused over 30 to 60 minutes. The area under the plasma concentration versus time curves (AUCs) from this treatment should be compared to that of an equivalent systemic infusion dose. The concentration range of linear pharmacokinetics can be determined by running multiple doses and comparing dose-normalized AUCs or by an accelerated infusion technique described by Ward and colleagues (2). Another consideration for this technique is that the portal vein cannula may alter the blood flow to the liver. To minimize the impairment of blood flow in the portal vein, Kim et al. (3) cannulated the pyloric vein, a tributary flowing directly into the hepatic portal vein.

Hepatic extraction can also be determined following oral administration. In this design, an oral dose is administered and blood samples measured from the portal vein and systemic circulation. Iwamoto and colleagues (4) used this method to examine gut versus liver first-pass effects of salicylamide in the rat. The assumption in this model is that hepatic blood flow is high enough to dilute absorbed drug to systemic circulation levels. Basically, the AUC obtained from systemic circulation is divided by the AUC from the portal vein concentrations to yield hepatic extraction.

In Vivo Drug Interactions

Enzyme Inhibitors

The coadministration of an enzyme inhibitor can be used as a tool to identify enzymes involved in the metabolism and excretion of the test compound and to predict potential drug interactions. However, if an enzyme inhibitor is required to get systemic drug exposure, the compound is likely to have limited clinical utility because of poor PK

properties. Although advances in in vitro methodologies have obviated the need for many in vivo studies, nonclinical animal studies are very necessary for drug development. Early on it was recognized that 1-aminobenzotriazole could be administered to animals before drug treatment to inhibit P450 enzymes (5). Results following treatment with inhibitor should indicate a decrease in metabolic clearance, and increased exposure should translate to an increase in pharmacological activity. If drug clearance is not changed with administration of 1-aminobenzotriazole, then cytochromes P450 are not responsible for the majority of drug metabolism. Ketoconazole is a commercially available antifungal agent and is widely used as a CYP3A and P-glycoprotein (Pgp) inhibitor (6). Salphati et al. (7) demonstrated the effects of ketoconazole on digoxin absorption and disposition in the rat. The authors showed that concomitant ketoconazole increases digoxin plasma concentrations, AUC, rate of absorption, and oral bioavailability. However, this model does not differentiate the effects of ketoconazole on metabolism versus Pgp inhibition on digoxin absorption and clearance (7).

Motivated by species-specific poor oral bioavailability and no specific in vitro tool to directly address the problem, Ward et al. (8) developed a screening model using ketoconazole to determine the role of Pgp and CYP3A in limiting oral exposure in the NHP. The authors developed an in vivo screen in the NHP that uses ketoconazole, a dual inhibitor of Pgp and CYP3A (9,10), to assess their effects on absorption and first-pass extraction. The model requires surgical resources to install vascular access ports to allow access to portal vein sampling and intraduodenal dosing. In this model, the authors used erythromycin, a known substrate for Pgp and CYP3A, and propranolol as the negative control (6). The authors were able to overcome the species-specific absorption liability with active lead optimization, in vitro permeability assays, and the ketoconazole in vivo screen as described by Ward and colleagues (8).

Enzyme Induction

Induction of drug-metabolizing enzymes can have a significant impact on the disposition, toxicology, and metabolic profile of the pharmaceutical agent or other drugs taken concomitantly. Enzyme induction in animals can be assessed usually by one of two ways: the animals can be induced in vivo followed by organ removal or dosing with probe substrates, or cells or slices can be prepared from normal animal tissues and treated in culture to induce enzymatic activity in vitro. Induction in animals does not always correlate with induction in humans. Thus, methodologies using human hepatocytes are often used to predict potential clinical effects. For example, Pichard et al. (11) used cultured human hepatocytes to screen a series of 59 xenobiotics for their potential to induce or inhibit CYP3A. If induction is suspected, dosing with probe substrates can be used in humans for a definitive assessment.

Early multiple dose pharmacology or toxicology studies may reveal the potential for induction of metabolic enzymes. If induction or inhibition of in vivo metabolism is suspected, the liver is typically removed and its metabolic capacity assessed with in vitro methods (see chapter 20). Induction of CYP enzymes can sometimes explain observations from nonclinical toxicology studies, such as increased liver weights in the absence of marked liver enzyme elevation. In vivo studies may be necessary to determine the metabolic mechanism involved. Pretreatment of preclinical animals with inducing agents such as phenobarbital (CYP2B) (12,13), β-naphthoflavone (CYP1A) (13), clofibrate (CYP4A) (14), and ethanol (CYP2E1) (15) can alter the metabolic capacity of animals and allows for examination of the role particular cytochromes P450 in in vivo metabolism.

Genetic Knockout Models

Recently, several useful mouse models that target the cytochrome P450 enzyme system or the *Cpr* locus have been established. The activities of cytochrome P450 enzymes are dependent on a redox partner, the NADPH cytochrome P450 reductase (CPR), for their monooxygenase function. In the first of these models, the *Cpr*-low (CL) mouse, *Cpr* expression is decreased by greater than 70% in all tissues examined, including the liver, kidney, heart, adrenal glands, olfactory mucosa, testis, ovary, lung, and brain (16). However, the decreased *Cpr* expression is accompanied by compensatory increases in hepatic and renal microsomal P450 content (16). In another model, the liver-specific *Cpr*-null (LCN) mouse, *Cpr* expression is absent in hepatocytes, but at normal levels in other tissues (17). In the CL-LCN mouse, which combines the phenotypes of the CL and LCN mice, *Cpr* expression is absent in hepatocytes and substantially decreased in other tissues. These mouse models have made it possible to determine the relative contribution of liver and extrahepatic tissue P450 enzymes in the disposition and bioactivation of drugs.

ABSORPTION/PK MODELS

There is a growing consensus within the pharmaceutical industry that bioavailability in human in excess of 30% is usually desired to facilitate clinical development. Issues associated with low bioavailability drugs include high inter-and intrasubject variability and high-dose requirement. Absorption is affected by a compound's physiochemical properties, which affect its dissolution and transmembrane permeability as well as its presystemic interactions with drug-metabolizing enzymes and transporters.

During the lead optimization process, unless a species-specific liability has been identified, drug discovery teams will typically assess oral bioavailability in the rat because of the relatively low compound requirement. Teams will typically set a goal of 20% oral bioavailability from suspension formulation at a pharmacological dose in the rat. These in vivo bioavailability determinations will be supplemented with mechanistic investigations, including in vitro determinations of metabolic stability, cytochrome P450 inhibition liabilities, passive permeability, and active transport processes. Absorption and other determinates of systemic exposure are listed in Figure 1.

"Higher-Throughput" PK Screening

Although in vitro assays can provide information on enzyme kinetics and other key parameters, in vivo studies provide the definitive assessment of overall drug ADME. The focus for the in vivo-screening models is to assess the exposure and PK estimates following intravenous, oral, or other routes of administration. Automatic blood-sampling devices are commercially available and can reduce resources necessary to conduct PK studies. Various devices are available for rodents, and a few that are amendable to nonrodent species. These devices automate blood sampling and cannula maintenance, along with temperature-controlled blood storage.

Cassette dosing is where multiple compounds (typically about 10) are coadministered to an animal model. Blood samples are collected, drug concentrations determined by liquid chromatography-mass spectrometry (LC-MS) and multiple PK profiles are obtained. Cassette dosing is a means to improve in vivo throughput and has been described in the literature (18,19) and provides a relatively quick way of ranking compounds according to PK properties. Molecules with attractive PK properties in a cassette study would be analyzed in a more definitive study design. Cassette dosing is amendable to rodent and nonrodent species and can significantly reduce the use of animals, especially nonrodent

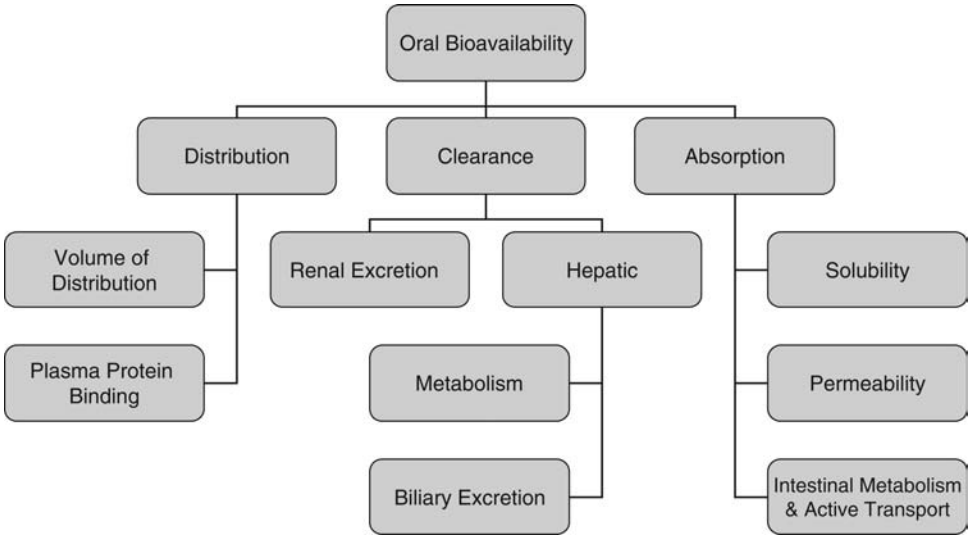

Figure 1 Relationship between the many determinants of oral bioavailability. The decision tree format can be helpful in teasing out the underlying factors that are responsible for the poor oral bioavailability.

species. Other advantages to cassette dosing include reduction in interanimal variability, reduced analysis time, and condensed report format. Disadvantages of cassette dosing include difficulties in preparing the dose formulation of a mixture of compounds, excessive set-up time required for analysis, and the potential for drug-drug interactions (20). The following suggestions may decrease the risk of drug-drug interactions: exclude compounds with P450 inhibition liabilities, include benchmark probe substrates in each cassette, reduce the dose of each compound in the mixture, and reduce the number of compounds per cassette. For example, cassettes usually contain about 10 compounds each administered at 1 to 2 mg/kg; the dose of each compound could be decreased to 0.5 mg/kg, and the number of compounds could be decreased to 5 and still retain much of the higher throughput. Depending on analytical resources, more time may be required for the enhanced analytical sensitivity required for the lower doses. Cassette dosing, which is often referred to as "cocktail dosing," is also being used in humans. The purpose of such a study is to identify drug-drug interactions; an example of this approach was recently published by Zhou et al. (21). The potential for drug-drug interactions and other disadvantages of cassette dosing need to be considered against the advantage of higher throughput.

Oral Exposure

Oral delivery of drugs along with once-a-day dosing is often crucial to patient compliance and successful development of a new therapeutic. The oral performance of a drug is regulated mainly by absorption and first-pass hepatic extraction; these processes have been shown to be modulated by Pgp and CYP3A (9,10). A combination of in vitro and in vivo studies is often employed to understand factors that affect oral bioavailability. In vitro assays include determinations of membrane permeability, solubility, and stability in subcellular fractions. The most common in vivo method for estimation of intestinal absorption is to measure the fraction of dose entering the portal vein following oral administration. The method has been described in the literature (22) and requires basic surgical resources to cannulate the portal vein. The cannulation of the portal vein may

alter blood flow to the liver, and the impact needs to be considered. The model is often used to determine if poor absorption or high hepatic extraction is responsible for low systemic exposure following oral administration. The model is robust in conscious animals, and many discovery programs routinely use it as an effective screening strategy. However, it does not distinguish between gut metabolism and poor absorption of the drug.

Occasionally, in lead optimization, species-specific liabilities are identified, for example, low oral bioavailability in NHP. Often times, the in vitro tools pertain to human and rodent absorption and are not available for NHP. However, improvement in bioavailability in this species may be desirable if the species is to be used further in safety assessment. This scenario requires the PK scientist to develop a screen to evaluate compounds in the species that is problematic. Ward et al. (23) identified an increased-throughput in vivo screen that estimates absorption and first-pass hepatic extraction in the NHP. The model requires surgical resources to install vascular access ports to allow access to portal vein sampling and intraduodenal dosing. The authors studied over 200 structurally diverse compounds, evaluated in cassettes of five compounds each, administered to a single monkey followed by simultaneous portal and systemic sampling. Follow-up definitive studies to determine absolute bioavailability were carried out on 14 selected compounds; these molecules represented the range of absorption and bioavailability from the original set. The screen correctly categorized 71% of the compounds evaluated in the definitive studies. Further, none of the compounds incorrectly categorized were false negatives. The authors suggest that the false positives may be due to coadministration of a P450 inhibitor within the cassette mixture (23).

Models That Assess Transporter Involvement

Genetic knockout animal models can be used to evaluate the role of transporter interactions in vivo. Through the combination of knockout animal data and in vitro studies in cell lines expressing mouse and human transporters, we can better predict the consequences of the many transporters on drug disposition in man. Transporters can affect drug absorption in the small intestine and drug elimination in the liver and kidney. The inhibition or lack of transporter functions can significantly increase or decrease exposure of drugs to tissues and result in either no efficacy or increased toxicity. Pgp is encoded by the *MDR1* gene and is partially responsible for the multidrug resistance observed with chemotherapeutic agents. It is a drug efflux transporter localized on the mucosal membrane of the intestines. The role of Pgp in drug absorption, disposition, and elimination has been well documented using mdr1 knockout mice (24,25).

GF120918A has been used as a P-glycoprotein/breast cancer-resistant protein (Pgp/Bcrp) inhibitor both in vitro and in vivo. Recently, Ward and colleagues have characterized Pgp/Bcrp inhibition by GF120918A in the mouse, rat, dog, and NHP (26). In this study, coadministration of GF120918A with erythromycin, a known substrate for Pgp and CYP3A4 (6), resulted in about a 10-fold increase in the AUC of erythromycin. Interestingly, GF120918A is not a CYP3A4 inhibitor at concentrations examined in this in vivo model; the authors suggest that erythromycin exposure following oral administration in preclinical species may be dependent on Pgp/Bcrp activity and not Pgp/CYP3A, as has been suggested in the literature (27).

To estimate the contribution of Bcrp and multidrug resistance protein 2 (Mrp2) transporters in the biliary clearance of pitavastatin, Hirano et al. (28) used a combination of genetic knockout animals. The authors demonstrated that the Bcrp transporter was responsible for the majority of biliary excretion in mice, and to a lesser extent, the Mrp2 transporter played a role in rats (28). Because deletion of one transporter can cause altered

expression of other transporters or enzymes in knockout animals (29), caution needs to be taken when using these models to determine dispositional changes, especially when extrapolating across species.

Renal Impairment Models

The kidney plays an important role in the elimination of drugs and their water-soluble metabolites. There are several models of acute and chronic kidney failure. Methods commonly used to induce renal failure include ischemia caused by reduced or total occlusion of the renal artery, ureteral ligation, which causes urine to collect in the kidney, administration of nephrotoxins (i.e., uranyl nitrate), and partial and complete surgical removal.

These models can be very useful in predicting changes in renal excretion of drugs in acute and chronic kidney failure. The acute kidney failure model is where both kidneys are surgically removed and is referred to as binephrectomized rats. These animals are severely compromised and have minimal survival time, usually 24 to 48 hours, depending on food and water consumption pre- and postsurgery (30). A widely used model for chronic renal failure is the 5/6 nephrectomy. This model involves the surgical removal of two poles on the left kidney, and one week later, the right kidney is excised as previously described (31). The animals recover well from the surgeries, and rats can be studied for up to 24 weeks following surgery (32). These models allow PK scientist to evaluate the impact of renal clearance in acute and chronic renal failure.

PK/PD-Concentration-Effect Relationship

Often, it is valuable to characterize the concentration-effect or the pharmacokinetic/pharmacodynamic (PK/PD) relationship in animal models. A common challenge early in lead optimization is a discrepancy between the in vitro potency (usually IC_{50} values) and the efficacious dose in the pharmacology model (usually an ED_{50} value). This is why PKDM scientists support and work directly with the pharmacologist to determine systemic drug exposure-response relationship in the animal model. If activity is poor or absent in the animal model and little or no drug is measurable, then metabolic stability and/or absorption should be investigated. However, if drug is present at efficacious levels in the systemic circulation, then lack of drug at the effector site or protein binding may be the issue. Generally, the concentration of the drug at the effector site, on-target or off-target, should drive efficacy and toxicity. If protein binding is not the problem, then differences in target binding may be occurring. In some instances, the in vivo activity may be greater than predicted from the in vitro-derived IC_{50} values; this suggests that an active metabolite may be formed and is responsible for enhanced pharmacological activity. In vitro metabolism studies can confirm formation of the metabolite, and further in vivo studies can confirm that circulating levels may be responsible for the additional activity. If competitor molecules are available, they are often used to help validate the pharmacology model and in vitro assays. If an animal model for efficacy can be successfully validated, the model can be used to explore PK/PD relationship.

DISTRIBUTION MODELS

The rate of drug distribution to organs or tissues is determined primarily by blood flow and the rate of diffusion out of the capillary bed into the cells of a particular organ or tissue. In general, the initial phase of distribution is dominated by blood flow, so that highly perfused

organs and tissues initially receive most drug, while drug to muscle, fat, and skin may take several hours to reach steady state. Distribution also depends on the affinity of the drug for various tissues. Lipid-soluble compounds move readily into cells by diffusion. In contrast, hydrophilic and ionized drugs are largely restricted to the extracellular space, unless a transport system is available to transport them into the cell. Drug distribution may also be limited by drug binding to plasma proteins. A highly bound drug has limited access to cellular sites of action. Drug may also accumulate in tissues because of binding to intracellular constituents, pH gradients, or partitioning into lipids. However, in the absence of active transport, unbound concentration should be equal in plasma and tissue at steady state. Termination of drug effect usually is by metabolism and excretion, but it may also result from redistribution of the drug from its site of action into other tissues or sites. Distribution and other determinates of systemic exposure are listed in Figure 1.

In general, the extent of distribution of a compound depends on its physiochemical properties and its affinity for a transporter system. In vitro models to predict drug distribution are generally lacking. However, one example is the prediction of brain-to-plasma ratio by measuring brain and plasma unbound fraction in vitro (33). Since distribution of compounds may significantly affect their efficacy and/or toxicity, direct sampling at the effector site, or as close as possible for drug concentrations, can be important to a good understanding of the PK/PD relationship.

Radiolabeled ADME Studies

The major objective of in vivo metabolism studies is to determine the distribution, metabolic profile, and elimination of the drug candidate. It is important that circulating metabolites are identified in selected toxicology species and to verify that these metabolites are also formed in humans at appropriate levels. When these profiles are significantly different, additional studies may be required to assess the risk of first in human (FIH) studies. Definitive metabolic profiling may not be necessary to advance a drug candidate into phase I clinical trials, but it is very important to select the appropriate animal models for more-advanced safety studies. ADME studies are generally conducted in the same animal species selected for safety assessment studies, generally a rodent (rat or mouse) and nonrodent (dog, NHP, or rabbit). ADME studies can be performed on nonradiolabeled compounds. However, the availability of radiolabeled compounds greatly simplifies the ability to monitor the formation and excretion of metabolites. The most common isotopes used in metabolism studies are tritium (^{3}H) and carbon 14 (^{14}C). A major concern in preparing the radiolabeled compound is the introduction of the radiolabel into the molecule in a position that is metabolically stable (i.e., it will not lead to loss of radiolabel upon metabolism of the test compound).

Initial drug disposition studies commonly focus on mass balance or recovery of a radioactive dose in the rat. Results from in vitro metabolism studies, elimination half-life, bioavailability, and other PK properties are used to determine the radiochemical dose and duration of sampling. Blood, urine, and feces are collected throughout the study, usually greater than 5 plasma half-life of parent. Often, selected target tissues and/or organs are collected to quantify total radiolabel concentration and to determine a metabolic profile for some tissues or organs. For many drugs, metabolism by the liver followed by biliary excretion plays a major role in their disposition. Therefore, many ADME studies have intact and bile duct-cannulated animals, where bile is collected and replaced with bile salts throughout the study. These studies are routinely carried out in rat (34), dog, and monkey for 24 to 72 hours; however, the model does require significant surgical capabilities. In the nonrodent species, sometimes a chronic model can be used

and access ports installed in the bile duct; in this manner, animals can be used again following proper washout period. Metabolic profiles of plasma, urine, and fecal samples are generated at various time points by high performance liquid chromatography (HPLC) separation followed by flow-through scintillation detection. Often, the flow of mobile phase from the LC is split to feed the flow-through scintillation detector and mass detector simultaneously. Results generated are used to determine metabolic profiles and excretion routes of parent and metabolites. Significant levels of radioactivity observed in the feces following oral administration suggest either lack of drug absorption or biliary excretion. To address the issue between absorption and biliary excretion, bile can be collected and feces and bile can be profiled for parent and metabolites. Another approach to distinguish absorption from biliary excretion is to perform the study following intravenous administration; biliary excretion is responsible for all test compounds and metabolites in feces.

Whole-Body Autoradiography

Quantitative whole-body autoradiography (QWBA) is a useful nonspecific technique for assessing the tissue distribution of radiolabel in animals. For a radiolabel human ADME study, regulatory agencies require tissue distribution study in pigmented animals, usually Long Evans rat, to provide dosimetry to various tissues and organs (35). Briefly, the proposed clinical route of administration should be used for radiolabel dose, animals sacrificed and immediately frozen at predetermined times, and carcasses of the whole animals cut into thin sections (30 40 uM) and exposed to phosphorimaging plates, and QWBA images are acquired from these imaging plates. With the help of imaging analysis software and a standard curve, exposure of radiolabel can be quantified in each tissue. On the basis of body weight and surface area, exposure of tissues to radiolabel in the rat can be extrapolated to humans and used to estimate whole-body exposure. QWBA is a very useful tool for distribution studies in preclinical animals; however, it does not provide information on the chemical identity of the radioactivity.

Microdialysis

Microdialysis sampling has become a standard technique in the neurosciences, and its success has led to its use in pharmacokinetic, toxicology, and ADME studies. Microdialysis sampling is accomplished by implanting a probe through which the sampling solution, termed "the perfusate," is slowly pumped. The perfusate is an aqueous solution, which closely matches the pH and ionic composition of the surrounding sample matrix, usually extracellular fluid. Microdialysis is a diffusion-controlled process, and the driving force for mass transport is the concentration gradient between the extracellular fluid and the perfusate. Microdialysis sampling in tissues (36) and sampling for PKDM studies (37) have been reviewed. Also, a recent American Association of Pharmaceutical Scientist-Food Drug Administration (AAPS-FDA) workshop produced a white paper on the principles and application of microdialysis (38). A major advantage of microdialysis sampling is the exclusion of proteins, resulting in sampling of the free fraction of drug and/or metabolite. In vivo microdialysis sampling has been conducted in freely moving rats dosed at steady state with a melatonin analog and compared with the results from equilibrium dialysis method (39). Good agreement was found between the in vivo free fraction and the in vitro value of rat plasma. Drug discovery teams often rely on plasma concentrations of drugs to estimate the drug concentration in peripheral tissues. Otherwise, absolute tissue levels are obtained by sacrificing one or more animals per time point. Microdialysis sampling allows direct access to the extracellular fluid of peripheral tissues. Drug levels in rat muscle tissue

obtained by microdialysis sampling correlated well with unbound plasma levels determined in serial blood samples for two fluoroquinolones, pazufloxacin and ofloxacin (40).

Models of CNS Distribution

Brain exposure of drugs is critical in many therapeutic areas within the pharmaceutical industry. Many neuroscience programs require drug delivery to the central nervous system (CNS), while other programs monitor brain exposure because of potential CNS toxicity or adverse events. The ability of a drug to cross the blood-brain barrier (BBB) is related to the drug's molecular weight, lipid solubility, degree of ionization, protein and tissue binding, and its affinity for specific active transporters. Generally, increased lipid solubility enhances the rate of penetration of drugs into the CNS, whereas ionization greatly diminishes it. The reader is referred to reviews describing in silico approaches to estimate physicochemical properties such as cLogP and polar surface area (PSA) (41,42). Common lead optimization strategies often combine in silico, in vitro, and in vivo methods. The strategies employed will depend on the specific needs of the program in a given phase of drug discovery. CNS exposure potential is best assessed using data from multiple and complementary assay systems. Because brain penetration can be affected by the free fraction of compound in the systemic circulation, assessment of plasma protein binding in the relevant species is also critical. Species differences in plasma protein binding can greatly affect the PK and tissue distribution behavior of drugs.

Many active transporters have been identified in the BBB and include several members of the ATP-binding cassette (Pgp, Bcrp, and Mrp1) and many from the solute carrier family (amino acid, organic cation, and organic anion). The reader is referred to a recent review of transporters (43). The in vitro tools to assess the role of many of these active transport systems are available or being developed for mouse and human, but generally, many are not available for other preclinical species such as dog and primate. Currently, transfected epithelial cell lines (Caco-2, MDCK, or LLC-PK1) that express a given transporter, such as mouse (mdr1a) and human (MDR1) transporters, are accepted by the draft of FDA guidance on drug-drug interaction studies as models to evaluate Pgp substrates or inhibitors. From these assays, an efflux ratio calculated as the quotient of the basolateral-to-apical (B-A) and the apical-to-basolateral (A-B) rates of transfer is determined (44). In general, molecules that exhibit high efflux ratios (>5) have poor CNS penetration in vivo.

The role of Pgp and Bcrp tansporters in restricting CNS distribution of drugs has been extensively studied in mdr1a (/) and Bcrp (/) knockout mouse models. Recently, Yamazaki et al. (45) demonstrated a good correlation between efflux ratios in mouse Pgp-expressing LLC-PK1 cells and CNS levels in mdr1a (/) knockout mouse model. Although in vitro assay for mouse Pgp can predict in vivo brain penetration in Pgp knockout mice and the efflux ratios between mouse and human transfected cells roughly correlate, the potential species difference in Pgp can be significant enough that the knockout mouse can not be used alone to predict human Pgp activity and human CNS penetration.

The most common in vivo method for assessing CNS exposure in rodents is a single measurement of plasma and CNS levels, usually a terminal time point, where the brain is removed and homogenized and drug levels quantified. Direct measurement in this manner is often criticized because it assesses only total brain levels (i.e., blood-brain partitioning), whereas free drug exposure in brain interstitial fluid is deemed biologically relevant. Whenever possible, exposure in plasma and brain should be determined as part of pharmacological (i.e., pharmacodynamic) studies in order to build some understanding of PK/PD relationhips on the basis of in vitro compound properties, including potency.

Other commonly used in vivo models include cerebrospinal fluid (CSF) concentrations, in situ perfusion, microdialysis, and ex vivo receptor occupancy. Brain perfusion in rodent is useful to measure the permeability of compounds across the BBB (46); the technique requires surgical resources for cannulation of the carotid artery. For instance, this approach was used to study the influence of plasma protein binding on BBB permeability of organic acids (47). Dagenais et al. applied the technique to *mdr1a* mutant mice to study the influence of Pgp on the brain uptake of synthetic opioids and other compounds (48). BBB active transport mechanisms can be explored by the use of chemical inhibitors in the perfusate (49). This technique is not routinely applied to CNS drug discovery, but can be useful to answer specific mechanistic questions about BBB transport. Some academic laboratories and a limited number of contract research organizations (CROs) may conduct brain perfusion studies for a fee.

For microdialysis sampling in the CNS, the reader is directed to an excellent review that discusses the literature on its use (50) and another review of microdialysis in the study of drug transporters in the CNS (51). In a study to measure the concentration of anticancer agents into rat brain tumors, microdialysis was used to obtain concentration time profiles of methotrexate in tumor-bearing rats (52). In another study, simultaneous microdialysis sampling from the blood and brain was used to determine the concentration of experimental *N*-methyl-D-aspartic acid (NMDA) antagonist and resulted in good agreement between microdialysis- based pharmacokinetics parameters and those based on conventional blood sampling (53). In a microdialysis study of rabbit brain, probenecid-administered IV was found to decrease the brain plasma transport rate and elimination clearance from the CNS of zidovudine, administered by intracerebroventricular infusion (54). Recently, Marchand et al. (2003) examined the linearity of the CNS distribution of norfloxacin over a wide range of IV doses (12.5 150 mg/kg), using intracerebral microdialysis to conscious freely moving rats. The authors concluded that the CNS distribution of norfloxacin was linear over the range of doses tested, but its systemic exposure was not linear (55). Despite its high content value in measuring drug exposure in the most relevant biophase within the CNS, microdialysis tends to be used very selectively in drug discovery, often in synergy with neurochemistry groups that routinely measure neurotransmitter release as a pharmacodynamic endpoint. The methodology remains time consuming and technically demanding, especially with regard to properly estimating probe recovery to derive meaningful data. A number of CROs specialize in microdialysis services in the context of CNS drug discovery.

Because the CSF is in relatively close anatomical proximity to the brain extracellular cerebral fluid (BECF) compartment, many investigators suggest that CSF levels may be the best surrogate measure of free concentrations of compound in the brain (41,56). Some empirical observations support the view that exposure in the CSF is a better approximation of BECF than plasma-free concentration. For instance, CSF exposure appears to more closely approximate BECF than plasma-free concentrations for efflux substrates (56). Currently, CSF sampling serves as the most readily available means of characterizing the PK behavior of CNS-targeted drugs. The total volume of CSF sample(s) should be limited to only a fraction of the total volume and take into account turnover rate if repeated sampling is desired. CSF samples are easily contaminated by blood and should be free of such contamination to yield useful information. Test articles should be administered to conscious animals and allowed to circulate as long as possible before sampling to minimize the potential effect of anesthetic agents on cerebral blood flow, protein binding, and CSF composition. The ability to do repeat sampling in a nonanesthetized animal, with minimal discomfort to the animal, makes this a good example of refinement and reduction of research animals.

There are a number of published methods for collecting CSF in dogs. The collection sites are different between the models and include cisterna magna (57), lateral cerebral ventricles, and the subarachnoid space of the cervical or lumbar vertebrae (58). Some methods use a local analgesia (59) for CSF collection, while other methods describe serial sampling of CSF in conscious, sling-restrained dogs, with the access port placed beneath the skin surface (58). Many of these models can be used to deliver test compounds to specific areas of the CNS via the collection cannula. Success rates of the CSF collection models are based on length of cannula patency, and many dog collection models have cannula patency that ranges from six weeks to six years. As stated above, species differences in efflux and other BBB properties are poorly understood.

Most CSF sampling in NHP has been in ketamine-anesthetized animals with direct sampling from the cisterna magna, which has its drawbacks. Recently, chronic models of CSF collection have been established in the NHP; many of these models implement stainless steel cannulas into the lateral or fourth ventricles or catheters into the cerebral or spinal subarachnoid space. These methods require invasive techniques to pass through the skull and may require highly specialized stereotaxic equipment. Recently, Gilberto et al. (60) developed a method that allows direct CSF sampling from the cisterna magna in a nonanesthetized chaired rhesus monkey. The method uses a silicone catheter inserted into the cisterna magna and connected to a titanium port placed beneath the skin between the scapulae to permit easy access for CSF sampling in a conscious chaired NHP. The model is difficult, and the authors suggest a success rate of about 60%. Success is defined as consistent patency for CSF collection for longer than two weeks postoperatively. Gilberto et al. (60) instrumented rhesus monkeys from which they have consistently sampled CSF for over 18 months.

LC-MS-based determination of ex vivo receptor occupancy as determined by displacement of a tracer in a region of interest is gaining popularity in CNS drug discovery organizations (61,62). This is an indirect means of measuring target coverage in the brain. The requirements for a successful tracer (high affinity, minimal nonspecific binding, and sufficient receptor density in a large enough area of the brain) are more stringent as compared with a drug candidate. Noninvasive imaging techniques such as positron emission tomography (PET) and single-photon emission computed tomography (SPECT) find little use in routine drug discovery. However, their application in primates can play an important translational role once candidate drugs are identified. If the target is amenable to receptor occupancy, tracers may be identified from early lead optimization efforts within the project. Molecules should be selected on the basis of their compatibility for direct and rapid labeling with short-lived positron emitters such as ^{18}F and ^{11}C.

CONCLUSIONS

A well-designed set of PK studies in a preclinical species can identify ADME liabilities of early lead molecules. Once identified, appropriate in vitro screens can focus on a specific ADME property. A good understanding of these liabilities is the cornerstone of a rational PKDM lead optimization strategy. Screening results need to be delivered to the medicinal chemist in a timely manner to influence the next round in the synthetic program. Moreover, it is important that in vitro screens are regularly validated against in vivo data to ensure proper ranking of compounds for further study. Overall, the types of PKDM studies are determined by the available in vitro and in vivo tools, the number of compounds, and the capacity of the selected assay. The goal of this chapter has been to provide insights into the role that preclinical animal models have in optimizing pharmacokinetic parameters.

REFERENCES

1. Cassidy MK, Houston JB. In vivo assessment of extrahepatic conjugative metabolism in first pass effects using the model compound phenol. J Pharm Pharmacol 1980; 32:57 59.
2. Ward KW, Griffiths R, Levy MA, Smith BR. Evaluation of the utility of accelerated infusions for the determination of pharmacokinetic linearity. J Pharmacol Exp Ther 2000; 293:468 479.
3. Kim J, Kim SH, Lee MG. Liver and gastrointestinal first pass effects of azosemide in rats. J Pharm Pharmacol 1997; 49:878 883.
4. Iwamoto K, Arakawa Y, Watanabe J. Gastrointestinal and hepatic first pass effects of salicylamide in rats. J Pharm Pharmacol 1983; 35:687 689.
5. Mugford CA, Mortillo M, Mico BA, Tarloff JB. 1 Aminobenzoletriazole induced destruction of hepatic and renal cytochromes P450 in male Sprague Dawley rats. Fundam Appl Toxicol 1992; 19:43 49.
6. Wacher VJ, Wu CY, Benet LZ. Overlapping substrate specificities and tissues distribution of cytochrome P450 3A and P glycoprotein: implications for drug delivery and activity in cancer chemotheraphy. Mol Carcinog 1995; 13:129 134.
7. Salphati L, Benet LZ. Effects of ketoconazole on digoxin absorption and disposition in rat. Pharmacology 1998; 56:308 313.
8. Ward KW, Stelman GJ, Morgan JA, Zeigler KS, Azzarano LM, Kehler JR, McSurdy Freed JE, Proksch JW, Smith BR. Development of an in vivo preclinical screen model to estimate absorption and first pass hepatic extraction of Xenobiotics. II. Use of ketoconazole to identify P glycoprotein/CYP3A limited bioavailability in the monkey. Drug Metab Dispos 2004a; 32:172 177.
9. Benet LZ, Wu CY, Herbert MF, Wacher VJ. Intestinal drug metabolism and antitransport processes: a potential paradigm shift in oral drug delivery. J Control Release 1996; 39:139 143.
10. Wacher VJ, Salphati L, Benet LZ. Active secretion and enterocytic drug metabolism barriers to drug absorption. Adv Drug Deliv Rev 2001; 46:89 102.
11. Pichard L, Fabre JM, Domergue J, Fabre G, Saint Aubert B, Mourad G, Maurel P. Molecular mechanism of cyclosporine A drug interactions: inducers and inhibitors of cyctochrome P450 screening in primary cultures of human hepatocytes. Transplant Proc 1991; 23:978 979.
12. Waxman DJ, Azaroff L. Phenobarbital induction of cytochrome P 450 gene expression. Biochem J 1992; 281:577 592.
13. Tuntaterdtum S, Chaudhary IP, Cibull M, Robertson LW, Blouin RA. Acetaminophen hepatotoxicity: influence of phenobarbital and B naphthoflavone treatment in obese and lean Zucker rats. Toxicol Appl Pharmacol 1993; 123:219 225.
14. Bars RG, Bell DR, lcombe CR. Induction of cytochrome P450 and peroximal enzymes by clofibric acid in vivo and in vitro. Biochem Pharmacol 1993; 45:2045 2053.
15. Tsutsumi M, Lasker JM, Takahashi T, Lieber CS. In vivo induction of hepatic P4502E1 by ethanol: role of increased enzyme synthesis. Arch Biochem Biophys 1993; 304:209 218.
16. Wu L, Gu J, Cui H, Zhang Q, Behr M, Fang C, Weng Y, Kluetzman K, Swiatek PJ, Yang W, Kaminsky L, Ding X. Transgenic mice with a hypomorphic NADPH cytochrom P450 reductase gene: effects on development, reproduction, and microsomal cytochrome P450. J Pharm Exper Ther 2005; 312:35 43.
17. Gu J, Chen C, Wei Y, Fang C, Xie F, Kannan K, Yang W, Waxman DJ, Ding X. A mouse model with liver specific deletion and global suppression of the NADPH cytochrome P450 reductase gene: characterization and utility for in vivo studies of cyclophosphamide disposition. J Pharmacol Exp Ther 2007; 321:9 17.
18. Frick LW, Adkison KK, Wells Knecht KJ, Woollard P, Higton DM. Rapid in vivo assessment of pharmacokinetics. Pharm Sci Tech Today 1998; 1:12 18.
19. Shaffer JE, Adkison KK, Halm K, Hedeen K, Berman J. Use of "N in one" dosing to create an in vivo pharmacokinetics database for use in developing structure pharmacokinetic relation ships. J Pharm Sci 1999; 88:313 318.
20. White RE, Manitpistkul P. Pharmacokinetic theory of cassette dosing in drug discovery screening. Drug Metab Dispos 2001; 29:957 966.

21. Zhou H. 'Cocktail' approaches and strategies in drug development: valuable tool or flawed science? J Clin Pharmacol 2004; 44:120 134.
22. Hoffman DJ, Seifert T, Borre A, Nellans HN. Method to estimate the rate and extent of intestinal absorption in conscious rats using an absorption probe and portal blood sampling. Pharm Res 1995; 12:889 894.
23. Ward KW, Proksch JW, Levy MA, Smith BR. Development of an in vivo preclinical screen model to estimate absorption and bioavailability of xenobiotics. Drug Metab Dispos 2001; 9:82 88.
24. Schinkel AH, Wagenaar E, van Deemter L. P glycoprotein in the blood brain barrier of mice influences the brain penetration and pharmacological activity of many drugs. J Clin Invest 1996; 97:2517 2524.
25. Schinkel AH, Mayer U, Wagenaar E, van Deemter L, Smit JJ, van der Valk MA, Voordouw AC, van Tellingen O. Normal and altered pharmacokinetics in mice lacking Mdr1 type (drug transporting) P glycoproteins. Proc Natl Acad Sci U S A 1997; 94:4028 4033.
26. Ward KW, Azzarano LM. Preclinical pharmacokinetic properties of the P glycoprotein inhibitor GF 120918A (HCl salt of GF 120918, 9, 10 dihydro 5 methoxy9 oxo N [4 [2 (1,2,3,4 tetrahydro 6,7 dimethoxy 2 isoquinolinyl)ethyl]phenyl] 4 acridine carboxamide) in the mouse, rat, dog, and monkey. J Pharmacol Exp Ther 2004b; 310:703 709.
27. Mather LE, Austin KL, Philpot CR, McDonald PJ. Absorption and bioavailability of oral erythromycin. Br J Clin Pharmacol 12; 1981:131 140.
28. Hirano M, Maeda K, Matsushima S, Nozaki Y, Kusuhara H, Sugiyama Y. Involvement of BCRP (ABCG2) in the biliary excretion of pitavastatin. Mol Pharmacol 2005; 68:800 807.
29. Ogawa K, Suzuki H, Hirohashi T, Ishikawa T, Meier PJ, Hirose K, Akizawa T, Yoshioka M, Sugiyama Y. Characterization of inducible nature of MRP3 in rat liver. Am J Physiol 2000; 278:438 446.
30. Zurovsky Y, Eligal Z. The effects of food and drink on the survival of binephrectomized rats. Exp Toxicol Pathol 1995; 47:293 297.
31. MacLaughlin M, Monserrat AJ, Muller A, Matoso M, Amorena C. Role of kinins in the renoprotective effect of angiotensin converting enzyme inhibitors in experimental chronic renal failure. Kidney Blood Press Res 1998; 21:329 334.
32. Torres AM, MacLaughlin M, Muller A, Brandoni A, Anzai N, Endou H. Altered renal elimination of organic anions in rats with chronic renal failures. Biochim Biophys Acta 2005; 1740:29 37.
33. Kalvass JC, Maurer TS. Influence of nonspecific brain and plasma binding on CNS exposure: implications for rational drug discovery. Biopharm Drug Dispos 2002; 23:327 338.
34. Xu ZX, Melethil S. Simultaneous sampling of blood, bile and urine in rats for pharmacokinetics studies. J Pharmacol Methods 1990; 24:203 208.
35. Solon EG, Kraus L. Quantitative whole body autoradiography in the pharmaceutical industry. Survey results on study design, methods, and regulatory compliance. J Phamacol Toxicol Methods 2001; 46:73 81.
36. de la Pena A, Liu P, Derendorf H. Microdialysis in peripheral tissues. Adv Drug Deliv Rev 2000; 45:189 216.
37. Verbeeck RK. Blood microdialysis in pharmacokinetic and drug metabolism studies. Adv Drug Deliv Rev 2000; 45:217 228.
38. Chaurasia CS, Muller M, Bashaw ED, Benfeldt E, Bolinder J, Bullock R, Bungay PM, deLange CM, Derendorf H, Elmquist WF, Hammarlund Udenaes M, Joukhadar C, Kellogg DL, Lunte CE, Nordstrom CH, Rollema H, Sawchuk RJ, Cheung BW, Shah VP, Stahle L, Ungerstedt U, Welty DF, Yeo H. AAPS FDA Workshop white paper: microdialysis principles, application and regulatory perspectives. Pharm Res 2007; 24(5):1014 1025.
39. LeQuellec A, Dupin S, Tufenkji A, Genissel P, Houin G. In vivo microdialysis of melatonin analog in the freely moving rat. Pharm Res 1994; 11:935 838.
40. Araki H, Ogake N, Minami S, Watanabe Y, Narita H, Tamai I, Tsuji A. Application of muscle microdialysis to evaluate the concentrations of the fluoroquinolones pazufloxacin and ofloxacin in the tissue interstitial fluids of rats. J Pharm Pharmacol 1997; 49:1141 1144.
41. Martin P. Prediction of blood brain barrier penetration: are we missing the point? Drug Discov Today 2004; 9:161 162.

42. Clark DE. In silico prediction of blood brain barrier permeation. Drug Discov Today 2003; 8:927 933.
43. Loescher W, Potschka H. Role of drug efflux transporters in the brain for drug disposition and treatment of brain diseases. Prog Neurobiol 2005; 76:22 76.
44. Polli JW, Wring SA, Humphreys JE, Huang L, Morgan JB, Webster LO, Serabjit Singh CS. Rational use of in vitro P glycoprotein assays in drug discovery. J Pharmacol Exp Ther 2001; 299:620 628.
45. Yamazaki M, Neway WE, Ohe T, Chen I, Row JF, Hochman JH, Chiba M, Lin JH. In vitro substrate studies for p glycoprotein mediated transport: species difference and predictability of in vivo results. J Pharmacol Exp Ther 2001; 296:723 735.
46. Smith QR. A review of blood brain barrier transport techniques. Methods Mol Med 2003; 89:193 208.
47. Mandula H, Parepally JM, Feng R, Smith QR. Role of site specific binding to plasma albumin in drug availability to brain. J Pharmacol Exp Ther 2006; 317:667 675.
48. Dagenais C, Rousselle C, Pollack GM, Scherrmann JM. Development of an in situ mouse brain perfusion model and its application to mdr1a P glycoprotein deficient mice. J Cereb Blood Flow Metab 2000; 20(2):381 386.
49. Dagenais C, Ducharme J, Pollack GM. Uptake and efflux of the peptidic delta opioid receptor agonist. Neurosci Lett 2001; 301(3):155 158.
50. Hammarlund Udenaes M. The use of microdialysis in CNS drug delivery studies pharmacokinetic perspectives and results with analgesics and antiepileptics. Adv Drug Deliv Rev 2000; 45:283 294.
51. Sawchuk RJ, Elmquist WF. Microdialysis in the study of drug transporters in the CNS. Adv Drug Deliv Rev 2000; 45:295 307.
52. deLange E, deVries J, Zurcher C, Danhof M, deBoer A, Breimer D. The use of intracerebral microdialysis for the determination of pharmacokinetic profiles of anticancer drugs in tumor bearing rat brain. Pharmacol Res 1995; 12:1924 1931.
53. Malhotra B, Lemaire M, Brouillard J, Sawchuck R. High performance liquid chromatographic analysis of (S) α amino 5 phosphonomethyl[1,1′ biphenyl] 3 propanoic acid (EAB 515) in brain and blood microdialysate and in plasma ultrafiltrate of freely moving rats. J Chromatogr 1996; 679:167 176.
54. Wang Y, Wei Y, Sawchuck R. Zidovudine transport within the rabbit brain during intra cerebroventricular administration and the effect of probenecid. J Pharm Sci 1997; 86:1484 1490.
55. Marchand S, Chenel M, Lamarche I, Pariat C, Couet W. Dose ranging pharmacokinetic and brain distribution of Norfloxacin using microdialysis in rats. J Pharm Sci 2003; 92:2458 2465.
56. Liu X, Smith BJ, Chen C, Callegari E, Becker SL, Chen X, Cianfrogna J, Doran AC, Doran SD, Gibbs JP, Hosea N, Liu J, Neson FR, Szewc MA, Deusen JV. Evaluation of cerebrospinal fluid concentration and plasma free concentration as a surrogate measurement for brain free concentration. Drug Metab Dispos 2006; 34:1443 1447.
57. Suzuki H, Ferrario CM. New method for the collection of cerebrospinal fluid from the cisterna magna of conscious dogs. Am J Physiol 1984; 246:H551 H558.
58. Rockar RA, Sadanaga KK, Burkett DE, Mitroka JG, Boner RA, Weinstein MJ. Cerebrospinal fluid retrieval in the conscious dog: a methods development study. J Invest Surg 1995; 9:85 94.
59. Wilsson Rahmberg M, Olovson SG, Forshult E. Method for long term cerebrospinal fluid collection in the conscious dog. J Invest Surg 1998; 11:207 214.
60. Gilberto DB, Zeoli AH, Szczerba PJ, Gehret JR, Holahan MA, Sitko GR, Johnson CA, Cook JJ, Motzel SL. An alternative method of chronic cerebrospinal fluid collection via cisterna magna in conscious rhesus monkeys. Contemp Top Lab Anim Sci 2003; 42(4):53 59.
61. Chernet E, Martin LJ, Li D, Need AB, Barth VN, Rash KS, Phebus LE. Use of LC/MS to assess brain tracer distribution in preclinical, in vivo receptor occupancy studies: dopamine D2, serotonin 2A and NK 1 receptors as examples. Life Sci 2005; 78:340 346.
62. Barth VN, Chernet E, Martin LJ, Need AB, Rash KS, Morin M, Phebus LE. Comparison of rat dopamine D2 receptor occupancy for a series of antipsychotic drugs measured using radiolabel or nonlabeled raclopride tracer. Life Sci 2006; 78:3007 3012.

Index

Pharmaceutical Science

about the book...

This timely and expanded new edition is the definitive handbook for experienced drug metabolism and pharmaceutical scientists, as well as those new to the field.

Written by internationally renowned authors, it provides integrated, comprehensive coverage of the fundamental aspects of drug metabolism and the practical applications that help guide researchers through key challenges in modern drug discovery and development.

The ***Second Edition*** covers the many recent scientific and technical advances in the field and is organized into four sections—ideal for use in undergraduate and graduate programs in Drug Metabolism and Clinical Pharmacology:

- fundamental aspects of drug metabolism
- factors that affect drug metabolism
- new enabling technologies to study drug metabolism
- applications of metabolism studies in drug development and drug discovery

about the editors...

PAUL G. PEARSON is President and CEO, Pearson Pharma Partners, Westlake Village, California, USA. Dr. Pearson received his Ph.D. in Pharmaceutical Sciences from Aston University, Birmingham, UK. He has had an extensive and successful career in pharmaceutical science, previously serving as Vice President of Pharmacokinetics and Drug Metabolism at Amgen, Inc. and Executive Director of Preclinical Drug Metabolism at Merck & Co, Inc. He is an active member of several international and national professional organizations, including the International Society for the Study of Xenobiotics and the American Society for Clinical Pharmacology and Therapeutics. Dr. Pearson has contributed to numerous peer-reviewed publications and has been an honored invited lecturer at conferences, society meetings, and symposia on drug development, drug metabolism, and drug discovery.

LARRY C. WIENKERS is Executive Director of the Department of Pharmacokinetics and Drug Metabolism, Amgen, Inc., Seattle, Washington, USA. His other notable professional experience includes roles as Senior Director of Pharmacokinetics, Dynamics, and Metabolism at Pfizer and Director of Drug Metabolism and Disposition Research at Pharmacia & Upjohn. He obtained his Ph.D. in Medicinal Chemistry from the University of Washington, Seattle, Washington, USA. Dr. Wienkers is a member of numerous professional societies, such as the International Society for the Study of Xenobiotics, the American Association of Pharmaceutical Scientists, and the American Society for Pharmacology and Experimental Therapeutics. He is Associate Editor for the journal *Advances in Pharmacological Sciences* and is on the editorial board for the journals *Drug Metabolism and Disposition* and *Open Medicinal Chemistry Letters*.

Printed in the United States of America

H7647

ISBN 978-142007647-9

9 781420 076479 90000

informa
healthcare
www.informahealthcare.com

52 Vanderbilt Avenue
New York, NY 10017

Telephone House
69-77 Paul Street
London EC2A 4LQ, UK